



## 4. SEERC Conference Proceeding e-Book

**ELECTRIC MACHINES AND  
POWER ELECTRONICS**



**ELECTRIC  
TRANSMISSION**



**AUTOMATION AND  
CONTROL**

**POWER  
GENERATION**



**ENERGY  
TRANSITION**



**DISTRIBUTION SYSTEMS  
AND SMART GRIDS**



[www.seercturkiye2023.com](http://www.seercturkiye2023.com)



<https://www.linkedin.com/company/cigre-seerc/>

**11-12 OCTOBER 2023**



**TÜRKİYE ELEKTRİK SANAYİ BİRLİĞİ TİCARİ İŞLETMESİ**  
Mustafa Kemal Mahallesi Dumlupınar Bulvarı 7. Km No: 166  
Çankaya - Ankara / TÜRKİYE  
Yayıncı Sertifika No: 53255  
[www.cigreturkiye.org.tr](http://www.cigreturkiye.org.tr)  
[www.cigre-seerc.org](http://www.cigre-seerc.org)

**4. SEERC Conference Proceeding e-Book**  
ISBN: 978-605-63465-1-4

**Editors**  
Ayten Sümer

**Prepared for Publication**  
CIGRE Türkiye

**Design**  
Alp Ofset Matbaacılık Ltd. Şti.  
Ali Suavi Sok. No.60 Maltepe - Ankara  
Tel. : 0.535. 443 72 33 • Faks: 0.312. 230 76 29  
[www.alpofset.com.tr](http://www.alpofset.com.tr)  
Matbaa Sertifika No: 47917

All rights of this publication are reserved.

© 2023, TESAB

No part of this publication may be sold or reproduced for sale in any form without permission.

However, this publication can be quoted without permission, provided that the source is provided.



# PREFACE



In the year 2023, which marks the 100th anniversary of our Republic, we organized a highly significant event. The 4th Conference of the Southeast Europe Regional Council (SEERC) of The International Council on Large Electric Systems (CIGRE), for which our country held the presidency from 2021 to 2023, took place in Istanbul from October 11th to 13th. This conference saw valuable contributions from the 17 member countries of SEERC, with presentations, special sessions, and the participation of esteemed sector representatives in our exhibition area. With this valuable conference, which showcased that the heart of the power systems sector beats in Turkey, international public representatives, academics, and industry stakeholders came together. Our main goal was to provide an attractive platform where participants from around the world, including the public sector, private sector, students, researchers, and academics, could discuss new ideas and share their areas of interest with delegates from different parts of the world. Our conference covered papers and special sessions encompassing the main themes of Automation and Control, Electric Machines and Power Electronics, Electric Transmission, Energy Transformation, Distribution Systems, and Smart Grids, as well as Energy Production.

We received more than 120 paper submissions for our conference, and after the review process, 80 papers were selected for poster and oral presentations. With these valuable papers, expert industry representatives, researchers, and academics in the field engaged in discussions with international delegates. Accepted papers from 20 countries and 25 different international private sector, public sector, and university entities were presented in oral and poster ses-

sions across 10 different sessions. Also, special sessions were held to discuss new and innovative developments in power systems. The conference exhibition served as a showcase for more than 50 companies and sponsors. Additionally, with over 500 participants, our conference garnered significant interest in the energy sector. Public institutions and private companies in the energy sector engaged with academics, experts, and other firms over two days, providing information about their services and products. Private sector representatives, public sector officials, and academics attending the conference had the opportunity not only for scientific interaction but also to access the latest technical developments in the energy sector.

The 4th SEERC Conference in Istanbul became one of the internationally recognized gatherings in the energy sector. The conference provided an excellent opportunity for academics, experts, and companies to exchange ideas, opinions, products, and services. We worked hard to ensure the conference ran smoothly, and we hope it met expectations. We are grateful to the paper presenters and the exhibition participants for their valuable contributions that shaped the direction of the industry. We hope that this conference booklet, containing the full texts of the 80 papers reflecting the uniqueness of the congress, will be useful to our esteemed readers. We extend heartfelt thanks to the academics who contributed to the conference and to all public and private sector representatives who supported it.

**Assoc.Prof.Dr.Tuğçe DEMİRDELEN**

*CIGRE SEERC TAC CHAIR*

# EXECUTIVE COMMITTEE





# 4<sup>th</sup> SEERC CONFERENCE ISTANBUL

WOW İSTANBUL HOTEL and CONVENTION CENTER

11-12 OCTOBER 2023

## CONFERENCE PROGRAMME



ELECTRIC MACHINES AND  
POWER ELECTRONICS



ELECTRIC  
TRANSMISSION



AUTOMATION AND  
CONTROL

POWER  
GENERATION



ENERGY  
TRANSITION



DISTRIBUTION SYSTEMS  
AND SMART GRIDS



[www.seercturkiye2023.com](http://www.seercturkiye2023.com)



<https://www.linkedin.com/company/cigre-seerc/>



SCAN ME



**4th SEERC CONFERENCE İSTANBUL-TÜRKİYE**

WOW HOTELS and CONGRESS CENTER

OCTOBER 11, 2023 - First Day of Conference

08.30-10.00	REGISTRATION	
	HALL-1	ARTEMIS-1 HALL
10.00 -10.45	<b>OPENING SESSION</b> <b>Zafer Benli</b> Chair of SEERC  <b>Philippe Adam</b> General Secretary of CIGRE  <b>Dr. Alparslan Bayraktar</b> Minister of Energy and Natural Resources of Republic of Türkiye	
10.45 - 11.00	<b>Handover Ceremony of SEERC Chair to Bosnia and Herzegovina</b>	
11.00 - 11.45	<b>COFFEE BREAK</b>	
11.45-12.15	<b>Keynote Speech</b> <b>Eleni Charpantidou</b> – ENTSO-E Board Member <b>Serhat Metin</b> – Med-TSO Vice President	
12.15-12.25	<b>Main Sponsor Welcome Speech</b>  <b>ASTOR®</b> <b>Hakan Ünsal</b> – Astor Energy General Manager	
12.25-13.30	<b>LUNCH</b>	
13.30 - 15.00	<b>Earthquake in Türkiye and Electric Power System Resilience</b> <b>Chair: Muhammer Nuri Aslan</b> Deputy General Manager (TEİAŞ)  <b>Speakers:</b> <b>Ahmet Suat Üstün</b> – Deputy General Manager (EÜAŞ) <b>Ömer Baydilli</b> – Head of Operation and Maintenance Department (TEİAŞ) <b>Lale Yılmaz</b> – Coordinator of Corporate Communication (ELDER) <b>Özgün Ersoyoğlu</b> – Regional Manager of Distribution Operations (TOROSLAR EDAS)	
15.00 - 15.30	<b>COFFEE BREAK</b>	





4th SEERC CONFERENCE İSTANBUL-TÜRKİYE

WOW HOTELS and CONGRESS CENTER


OCTOBER 11, 2023 - First Day of Conference

HALL-1	HALL-2	ARTEMIS-1	ARTEMIS-2	ARTEMIS-3
<p><b>EURELECTRIC SESSION (15.30-16.15)</b>                      -----                      "Decarbonisation Speedways – Achieving Europe’s 2050 Decarbonisation Objectives"  <i>Cillian O’Donoghue</i>  <i>Eurelectric</i>  <i>Policy Director</i></p> <p><b>CIGRE TUTORIAL WG C1.45 (16.15-17.30)</b>                      -----                      Cost-Benefit Analysis Metrics for New Interconnections  <i>Piertuigi Vicini</i>  <i>Convener WG C1.45</i>  <i>Fabio D’Agostino</i>  <i>Secretary WG C1.45</i></p>	<p><b>DISTRIBUTION SYSTEMS AND SMART GRIDS</b>  <i>Croatia - Goran Spilac (Chair)</i>  <i>Slovenia - Uros Kerin (Co-chair)</i>                      -----  <b>ID: 132</b>                      Estimation of Georgian Power System flexibility and adequacy  <i>Archil Kokhtashvili</i>                      -----  <b>ID: 133</b>                      A clustering and benchmarking based monthly electricity consumption analysis for creating energy efficiency insights for the utility end-users  <i>Hakan Demirer</i>                      -----  <b>ID: 143</b>                      The feasibility of frequency stabilization using battery energy storage system (BESS) in 400 kV power systems  <i>Ergin Kayar</i>                      -----  <b>ID: 153</b>                      Distribution management system (DMS) integration in distribution network of Kosovo  <i>Turan Kocabayraktar</i>                      -----  <b>ID: 156</b>                      Challenges of protection system of Kosovo Distribution Network  <i>Nezir Nezir</i>                      -----  <b>ID: 170</b>                      Integration of solar power plants in distribution network - examples from Bosnia and Herzegovina  <i>Seila Gruhonjic Ferhatbegovic</i></p>	<p><b>ELECTRIC TRANSMISSION</b>  <i>Austria - Klemens Reich (Chair)</i>  <i>Greece - Dionysios Stamatiadis (Co-chair)</i>                      -----  <b>ID: 90</b>                      Transmission capacity maximization using dynamic thermal rating in Croatian Power System  <i>Zoran Bunce</i>                      -----  <b>ID: 101</b>                      Impact of the hydrological risk on the power grid: a case study on a portion of the Italian Transmission Power System exposed to the hazard of flooding  <i>Silverio Casulli</i>                      -----  <b>ID: 125</b>                      Fault detection in power transmission lines with artificial intelligence  <i>Büşra Töre</i>                      -----  <b>ID: 126</b>                      FACTS for improved controllability of high voltage power transmission network in Georgia  <i>Teona Elizarashvili</i>                      -----  <b>ID: 129</b>                      Challenges and opportunities for multipurpose interconnectors and wind off-shore generation  <i>Arman Derviskadic</i>                      -----  <b>ID: 161</b>                      Comparative performance analysis of network reduction on the transmission expansion planning  <i>Ahmet Ova</i></p>	<p><b>POSTER SESSION</b>  <b>ELECTRIC MACHINES AND POWER ELECTRONICS / ENERGY TRANSITION</b>  <i>Türkiye - Mikail Pürü (Chair)</i>  <b>(15.30-16.15)</b>                      -----  <b>ID: 106</b>                      Short circuit analytical prediction for transformer winding  <i>Mattia Medini</i>                      -----  <b>ID: 118</b>                      Optical current transformers  <i>Melis Aliefendioğlu</i>                      -----  <b>ID: 157</b>                      Instrument Transformers using alternative and eco-friendly high voltage insulation systems  <i>Umut Babur Elik</i>                      -----  <b>ID: 160</b>                      Reliability analysis and condition monitoring of power transformers from the Romanian Power Grid  <i>Bogdan Lev</i>  <b>(16.15-17.00)</b>                      -----  <b>ID: 171</b>                      Reliability of transformers  <i>Anatoly Shkolnik</i>                      -----  <b>ID: 162</b>                      Protection and metering solutions for transmission tie lines in the Romanian power systems  <i>Iulia Cristina Constantin</i>                      -----  <b>ID: 225</b>                      Algorithm for calculation of line distance protection settings  <i>Vladimer Popkhadze</i>                      -----  <b>ID: 112</b>                      Insuring power system reliability under high renewables penetration with energy storages - a case for Ukraine  <i>Sergii Shulzhenko</i></p>	<p><b>SPECIAL WORKSHOP</b>    <b>(15.30-16.30)</b>                      Overcoming challenges in DGA monitoring through innovative solutions  <i>Eliel Kouvalainen</i></p> <p><b>(16.30-17.30)</b>                      Testing Protection Relays with Superimposed-Quantities and Traveling-Wave based Elements  <i>Thomas Hensler</i></p>
15.30-17.30				
19.00-23.00				
Gala Dinner - Bosphorus Tour				

4th SEERC CONFERENCE İSTANBUL-TÜRKİYE

WOW HOTELS and CONGRESS CENTER

OCTOBER 12, 2023 - Second Day of Conference

	HALL-1	HALL-2	ARTEMIS-1	ARTEMIS-2	ARTEMIS-3
9.30-11.15	<p><b>ELECTRIC TRANSMISSION</b> <i>Türkiye - Deniz Çoşkun - TEİAŞ (Chair)</i> <i>Kosovo - Kadri Kadriu (Co-chair)</i></p> <p>-----</p> <p><b>ID: 95</b> Classification of power quality events in the transmission grid: comparative evaluation of different machine learning models <i>Umut Güvengir</i></p> <p>-----</p> <p><b>ID: 191</b> Strategic positioning of transmission system operators to achieve long-term goals and sustainability of the green transition - Analysis and case study <i>Igor Ivankovic</i></p> <p>-----</p> <p><b>ID: 192</b> An innovative solution for reducing EMFs: the "5-phases" pylons <i>Maria Rosaria Guarniere</i></p> <p>-----</p> <p><b>ID: 195</b> A compact 24-pulses converter for overhead lines de-icing and reactive power compensation <i>Roberto Spezie</i></p> <p>-----</p> <p><b>ID: 193</b> An innovative OHL design for renewable energy harvesting and transmission: the "5-phases" pylons <i>Maria Rosaria Guarniere</i></p>	<p><b>DISTRIBUTION SYSTEMS AND SMART GRIDS</b> <i>Greece - Emmanouil Voumvoulakis (Chair)</i> <i>Kosovo - Avni Alidemaj (Co-chair)</i></p> <p>-----</p> <p><b>ID: 172</b> Imputation and forecasting of energy consumption data collected by smart meters using big data technologies in the distribution system operator <i>Andrej Somrak</i></p> <p>-----</p> <p><b>ID: 181</b> Low voltage direct current distribution roadmap of Türkiye <i>Deniz Kartal</i></p> <p>-----</p> <p><b>ID: 187</b> Analysis of loads during the summer-winter season in Substation (SS) 35/10 kV Gjilani I <i>Eliona Aliju</i></p> <p>-----</p> <p><b>ID: 205</b> Under-frequency load shedding based on Huang's Empirical Model Decomposition approach for estimation of df/dt and artificial neural networks <i>Maja Murtic Dedovic</i></p> <p>-----</p> <p><b>ID: 221</b> The impact of renewable resources on the improvement of frequency and voltage value in the distribution network of Kosovo <i>Avni Alidemaj</i></p>	<p><b>SPONSORED WORKSHOP</b> <b>Prysmian Group</b> <b>(10.15 - 10.55)</b> Reducing losses and increasing ampacity of overhead conductor - Bringing Sustainability for Grid <i>Vitthal Sawant</i></p> <p>-----</p> <p><b>(10.55 - 11.15)</b> Cable Production / Using Big Data and AI for Predictive Quality and Maintenance <i>Erdinc Yüksel</i></p>	<p><b>POSTER SESSION</b> <b>DISTRIBUTION SYSTEMS AND SMART GRIDS / ENERGY TRANSITION</b> <i>Türkiye - Mikail Pürü (Chair)</i> <b>(09.30 - 10.15)</b></p> <p>-----</p> <p><b>ID: 131</b> Smart metering benefits for costumers and distribution system <i>Hamnijete Qorolli</i></p> <p>-----</p> <p><b>ID: 138</b> The impact of wind park plants on mitigation of energy crisis (2022) in Kosovo's Power System <i>Rexhep Selimi</i></p> <p>-----</p> <p><b>ID: 176</b> Prevention of high voltage network disturbance propagation by on-line monitoring and diagnostic of relay protection <i>Janez Zakonjsek</i></p> <p>-----</p> <p><b>ID: 186</b> A novel method for short circuit calculation <i>Giorgi Arziani</i></p> <p>-----</p> <p><b>(10.15-11.00)</b></p> <p>-----</p> <p><b>ID: 189</b> An innovative metric for evaluating operational resilience of the high-voltage grid <i>Chiara Vergine</i></p> <p>-----</p> <p><b>ID: 190</b> Smart grid project GreenSwitch <i>Goran Levacic</i></p> <p>-----</p> <p><b>ID: 233</b> The caterpillar and the butterfly the experience of Italian engineering <i>M. Celozzi</i></p> <p>-----</p> <p><b>ID: 109</b> Optimization module and auction mechanism for trading of guarantees of origin <i>Milan Josifovic</i></p>	<p><b>SPONSORED WORKSHOP</b> <b>ASTOR®</b> <b>(09.30-10.30)</b> The Silent Power Player: Leakage Reactance's Impact on Transformers <i>Dr. Kamran Dawood</i></p> <p>-----</p> <p> Maschinenfabrik Reinhausen GmbH Germany <b>(10.45-11.15)</b> The innovative future-oriented pioneer of on-load tap-changers ECOTAP®VI <i>Gunter Panzer</i></p>
	11.15-11.30	<b>COFFEE BREAK</b>			

4th SEERC CONFERENCE İSTANBUL-TÜRKİYE

WOW HOTELS and CONGRESS CENTER

OCTOBER 12, 2023 - Second Day of Conference

HALL-1	HALL-2	ARTEMIS-1	ARTEMIS-2	ARTEMIS-3
<p><b>AUTOMATION AND CONTROL</b> <i>Serbia – Ninel Cukalevski (Chair)</i> <i>Türkiye – Benan Başoğlu (Co-chair)</i> ----- <b>ID: 86</b> Dynamic tariffs and smart electric vehicle charging infrastructure <i>Andreja Ivartnik Kanduc</i> ----- <b>ID: 100</b> Application for optimization of capacity reserve trading auctions <i>Goran Jakupovi</i> ----- <b>ID: 108</b> Autonomous mobile robot for warehouse logistics <i>Şeyma Tuğba Ayrancıoğlu</i> ----- <b>ID: 110</b> Central dispatching and generation control system for Electric Power Industry of Serbia <i>Goran Jakupovic</i> ----- <b>ID: 111</b> Emerging problems in system operator training and possible training simulator solutions <i>Ninel Cukalevski</i> ----- <b>ID: 124</b> The system split and blackout detection application <i>Igor Bundalo</i></p>	<p><b>ELECTRIC MACHINES AND POWER ELECTRONICS/ ELECTRIC TRANSMISSION</b> <i>Georgia – Giorgi Amuzashvili (Chair)</i> <i>Türkiye – Kerem Küseoğlu (Co-chair)</i> ----- <b>ID: 174</b> Impact of renewable generation on distance protection and adaptive algorithms to optimise performance <i>Rajesh Ananth</i> ----- <b>ID: 178</b> Analysing electromagnetic and thermal effects of using aluminium shield and magnetic shunt combinations at high-voltage level autotransformers <i>Necmettin Mert Koçanalı</i> ----- <b>ID:197</b> A modular design for OHL grounding systems based on deep electrodes <i>Maria Rosaria Guarniere</i> ----- <b>ID: 210</b> Adriatic Corridor: A step towards deployment of Italian multiterminal HVDC systems <i>Enrico Maria Carlini</i> ----- <b>ID: 213</b> Hybrid high voltage AC and DC system strength evaluation with large penetration of renewable energy sources <i>Enrico Maria Carlini</i></p>	<p><b>WIE SESSION</b> <b>THE ROLE OF WOMEN IN THE FUTURE OF ENERGY SECTOR</b> <i>Kosovo – Pranvera Dobruna Kryeziu (Chair)</i> <b>(11.30-12.30)</b> ----- <i>Philippe Adam</i> <i>Karolin Ersöz</i> <i>Teona Elizashvili</i> ----- <b>ENERGY SECTOR FROM THE PERSPECTIVE OF YOUNG WOMEN</b> <i>Türkiye – Hayriye Gürbüz (Chair)</i> <b>(12.30-13.00)</b> ----- <i>Beril Bulut</i> <i>Özlem Taşçı</i> <i>Sonnur Erdem</i></p>	<p><b>POSTER SESSION</b> <b>AUTOMATION AND CONTROL /ENERGY TRANSITION</b> <i>Türkiye – Burak Esenboğa (Chair)</i> <b>(11.30-12.15)</b> ----- <b>ID: 105</b> Electricity tampering detection system project <i>Muna Saleh Al Jabri</i> ----- <b>ID: 116</b> ADMS for planning and der control in distribution network <i>Boris Njavro</i> ----- <b>ID: 122</b> Power Quality System within Romanian TSO <i>Ciprian Diaconu</i> ----- <b>ID: 147</b> Monitoring and management of ambient conditions of the electrical grid with sensor network system <i>Büşra Töre</i> <b>(12.15-13.00)</b> ----- <b>ID: 169</b> Digitization of DSO business processes based on the agnostic relational model of process flows on the example of Public Enterprise Electric Utility of Bosnia and Herzegovina <i>Jasmin Heljić</i> ----- <b>ID: 207</b> The concept of Ukraine's power system development taking into account the impact of the pumped-storage power plant in modern conditions <i>Oleksandr Ryabenko</i> ----- <b>ID: 214</b> The role of PSPP in the implementation of strategy of accelerated development of RES in the countries of South-Eastern Europe <i>Yuriy Landau</i> ----- <b>ID: 229</b> The implementation of intraday auctions and its impact on the Croatian Electricity Market <i>Martina Vajdić</i></p>	<p><b>SPONSORED WORKSHOP</b> <b>ENPAY</b> Transformer Components <b>(11.30 – 12.15)</b> Sustainability in the supply of transformer components <i>Emrah Yürekten</i> <i>Gülsün Alkan Çolak</i>  <b>MİTAŞ ENERGY</b> <b>(12.15-13.00)</b> Mitaş' Sustainability in Overhead Transmission Line Industry and Construction <i>Ahmet Acet</i> <i>Neşri Murat Bingöl</i> <i>Osman Fakoğlu</i></p>
11.30-13.00				
13.00-14.00	<b>LUNCH</b>			

4th SEERC CONFERENCE İSTANBUL-TÜRKİYE

WOW HOTELS and CONGRESS CENTER

OCTOBER 12, 2023 - Second Day of Conference

	HALL-1	HALL-2	ARTEMIS-1	ARTEMIS-2	ARTEMIS-3	
14.00 - 15.45	<p><b>AUTOMATION AND CONTROL</b> <i>Italy – Massimo Pompili (Chair)</i> <i>Greece – Dionysios Stamatiadis (Co-chair)</i></p> <p><b>ID: 128</b> Automatic generation control working scheme in Georgia, under the liberalized energy market <i>Mikheil Odisharia</i></p> <p><b>ID: 134</b> A dynamic thermal rating architecture for thermal monitoring and congestion management in the Italian Grid <i>Enrico Maria Carlini</i></p> <p><b>ID: 136</b> Challenges and the role of the dispatch center in the management and control of the power transmission system – a summary analysis <i>Vezir Rexhepi</i></p> <p><b>ID: 155</b> The relationships between concentrations of particulate matter (PM2.5 and PM10) and meteorological parameters in the Sarajevo Canton: seasonal variations <i>Sabina Dacic Lepara</i></p> <p><b>ID: 173</b> The impact of interconnection line synchronization on power system dynamic stability <i>Giorgi Erikashvili</i></p> <p><b>ID: 180</b> Investigation of the effect of batteries on frequency control in power system <i>Muhammet Furkan Yilmaz</i></p>	<p><b>ELECTRIC MACHINES AND POWER ELECTRONICS</b> <i>Türkiye – Tuğçe Demirdelen (Chair)</i> <i>Georgia – Giorgi Amuzashvili (Co-chair)</i></p> <p><b>ID: 87</b> Determination of the L-location of partial discharges in the power transformer model using UHF sensors <i>Djordje Radmilo Dukanac</i></p> <p><b>ID: 98</b> Pressboard barriers in smart connection systems for high voltage power transformers <i>Hakan Coşer</i></p> <p><b>ID: 102</b> Istanbul: City centre infeed with voltage source converter-based HVDC <i>Arman Derviskadic</i></p> <p><b>ID: 107</b> Coupled numerical electromagnetic-structural simulation for transformer winding <i>Mattia Medini</i></p> <p><b>ID: 152</b> Current transformers dimensioning in the context of digital substations <i>Anamaria Iamandi</i></p>	<p><b>NGN SESSION</b> <b>“NGN FEATURES: WHAT CAN NGN PROVIDE US”</b> <i>Türkiye – Ahmet Kerem Köseoğlu (Chair)</i> <i>Drenusha Gashi</i> <i>Bogdan Lev</i> <i>Michael Schrammel</i></p>			<p><b>SPONSORED WORKSHOP</b></p> <p><b>PSCAD</b> LEAN POWER</p> <p><b>(14.00-14.45)</b> Lessons Learned: TSO Experiences from EMT Studies <i>Türkiye – Gökhan Önal (Chair)</i> <i>Ümit Çetinkaya</i> <i>Yahya Mrabti</i> <i>Öner Alican</i></p> <p><b>ŞA-RA GROUP</b> <b>(15.00-15.45)</b> Overhead transmission towers: An overview of loading test, design and strain gauge correlation <i>Selahattin Selçuk Çıplak</i> <i>Yılmaz Erdiç Saçılık</i></p>
	15.45-16.00 <b>COFFEE BREAK</b>					



4th SEERC CONFERENCE İSTANBUL-TÜRKİYE

WOW HOTELS and CONGRESS CENTER

OCTOBER 12, 2023 - Second Day of Conference

	HALL-1	HALL-2	ARTEMIS-1	ARTEMIS-2	ARTEMIS-3	
14.00 - 15.45	<p><b>AUTOMATION AND CONTROL</b> <i>Italy – Massimo Pompili (Chair)</i> <i>Greece – Dionysios Stamatiadis (Co-chair)</i></p> <p><b>ID: 128</b> Automatic generation control working scheme in Georgia, under the liberalized energy market <i>Mikheil Odisharia</i></p> <p><b>ID: 134</b> A dynamic thermal rating architecture for thermal monitoring and congestion management in the Italian Grid <i>Enrico Maria Carlini</i></p> <p><b>ID: 136</b> Challenges and the role of the dispatch center in the management and control of the power transmission system – a summary analysis <i>Vezir Rexhepi</i></p> <p><b>ID: 155</b> The relationships between concentrations of particulate matter (PM2.5 and PM10) and meteorological parameters in the Sarajevo Canton: seasonal variations <i>Sabina Dacic Lepara</i></p> <p><b>ID: 173</b> The impact of interconnection line synchronization on power system dynamic stability <i>Giorgi Erikashvili</i></p> <p><b>ID: 180</b> Investigation of the effect of batteries on frequency control in power system <i>Muhammet Furkan Yilmaz</i></p>	<p><b>ELECTRIC MACHINES AND POWER ELECTRONICS</b> <i>Türkiye – Tuğçe Demirdelen (Chair)</i> <i>Georgia – Giorgi Amuzashvili (Co-chair)</i></p> <p><b>ID: 87</b> Determination of the L-location of partial discharges in the power transformer model using UHF sensors <i>Djordje Radmilo Dukanac</i></p> <p><b>ID: 98</b> Pressboard barriers in smart connection systems for high voltage power transformers <i>Hakan Coşer</i></p> <p><b>ID: 102</b> Istanbul: City centre infeed with voltage source converter-based HVDC <i>Arman Derviskadic</i></p> <p><b>ID: 107</b> Coupled numerical electromagnetic-structural simulation for transformer winding <i>Mattia Medini</i></p> <p><b>ID: 152</b> Current transformers dimensioning in the context of digital substations <i>Anamaria Iamandi</i></p>	<p><b>NGN SESSION</b> <b>“NGN FEATURES: WHAT CAN NGN PROVIDE US”</b> <i>Türkiye – Ahmet Kerem Köseoğlu (Chair)</i> <i>Drenusha Gashi</i> <i>Bogdan Lev</i> <i>Michael Schrammel</i></p>			<p><b>SPONSORED WORKSHOP</b></p> <p><b>PSCAD</b> LEAN POWER</p> <p><b>(14.00-14.45)</b> Lessons Learned: TSO Experiences from EMT Studies <i>Türkiye – Gökhan Önal (Chair)</i> <i>Ümit Çetinkaya</i> <i>Yahya Mrabti</i> <i>Öner Alican</i></p> <p><b>ŞA-RA GROUP</b> <b>(15.00-15.45)</b> Overhead transmission towers: An overview of loading test, design and strain gauge correlation <i>Selahattin Selçuk Çıplak</i> <i>Yılmaz Erdinç Saçılık</i></p>
	15.45-16.00	<b>COFFEE BREAK</b>				





# CONTENTS

## AUTOMATION AND CONTROL

### Oral Presentation

Article ID: 86	Dynamic Network Tariffs Electric Vehicle Smart Charging Infrastructure.....	17
Article ID: 100	Application for Optimization of Capacity Reserve Trading Auctions.....	25
Article ID: 108	Autonomous Mobile Robot for Warehouse Logistics.....	36
Article ID: 110	Central Dispatching and Generation Control System for Electric Power Industry of Serbia.....	47
Article ID: 111	Emerging Problems in System Operator Training and Possible Training Simulator Solutions.....	58
Article ID: 124	The System Split and Blackout Detection Application.....	68
Article ID: 128	Automatic Generation Control Working Scheme in Georgia, Under the Liberalized Energy Market.....	74
Article ID: 134	A Dynamic Thermal Rating Architecture for Thermal Monitoring and Congestion Management in the Italian Grid.....	81
Article ID: 136	Challenges and the Role of the Dispatch Centre in the Management of the Power Transmission System – A Summary Analysis.....	89
Article ID: 155	The Relationships Between Concentrations of Particulate Matter (Pm2.5 And Pm10) and Meteorological Parameters in the Sarajevo Canton: Seasonal Variations.....	99
Article ID: 173	The Impact of Interconnection Line Synchronization on Power System Dynamic Stability.....	108
Article ID: 180	Investigation of The Effect of Batteries on Frequency Control in Power System.....	119
Article ID: 198	Development of Energy Monitoring System for Sustainable Production in the Textile Industry.....	128
Article ID: 217	The First Lessons from Rocket Attacks on the Ukrainian Power System Relatively Power Unit's Automation and Control Systems.....	140
Article ID: 218	Hypergrid: Coordination and Control of Different HVDC Links.....	146

### Poster Presentation

Article ID: 105	Electricity Tampering Detection System Project.....	157
Article ID: 116	ADMS for Planning And Der Control in Distribution Network.....	161
Article ID: 122	Power Quality System within Romanian TSO.....	169
Article ID: 147	Monitoring and Management of Ambient Conditions of the Electrical Grid with Sensor Network System.....	175
Article ID: 169	Digitization of DSO Business Processes Based on the Agnostic Relational Model of Process Flows on the Example of Public Enterprise Electric Utility of Bosnia and Herzegovina.....	184

## ELECTRIC MACHINES AND POWER ELECTRONICS

### Oral Presentation

Article ID: 87	Determination of the Location of Partial Discharges in the Power Transformer Model Using UHF Sensors.....	192
Article ID: 98	Pressboard Barriers in Smart Connection Systems for High Voltage Power Transformers.....	203
Article ID: 102	Istanbul: City Centre Infeed with Voltage Source Converter-Based HVDC.....	213
Article ID: 107	Coupled Numerical Electromagnetic-Structural Simulation For Transformer Winding.....	226
Article ID: 152	Current Transformers Dimensioning in the Context of Digital Substations.....	236
Article ID: 174	Impact of Renewable Generation on Distance Protection and Adaptive Algorithms to Optimise Performance.....	246
Article ID: 178	Prevention of High Voltage Network Disturbance Propagation by On-Line Monitoring and Diagnostic of Relay Protection.....	255

### Poster Presentation

Article ID: 106	Short Circuit Analytical Prediction for Transformer Winding.....	262
Article ID: 118	Optical Current Transformers.....	273
Article ID: 157	Instrument Transformers Using Alternative and Eco-Friendly High Voltage Insulation Systems .....	279
Article ID: 160	Reliability Analysis and Condition Monitoring of Power Transformers from the Romanian Power Grid .....	285
Article ID: 171	Reliability of Transformers .....	291
Article ID: 178	Analysing Electromagnetic and Thermal Effects of Using Aluminium Shield and Magnetic Shunt Combinations at High-Voltage Level Autotransformers .....	297

## ELECTRIC TRANSMISSION

### Oral Presentation

Article ID: 90	Transmission Capacity Maximization Using Dynamic Thermal Rating in Croatian Power System .....	306
Article ID: 95	Classification of Power Quality Events in the Transmission Grid: Comparative Evaluation of Different Machine Learning Models .....	316
Article ID: 101	Impact of the Hydrological Risk on the Power Grid: A Case Study on a Portion of the Italian Transmission Power System Exposed to the Hazard of Flooding.....	322
Article ID: 125	Fault Detection in Power Transmission Lines with Artificial Intelligence .....	336
Article ID: 126	FACTS for Improved Controllability of High Voltage Power Transmission Network in Georgia .....	343
Article ID: 129	Challenges and Opportunities for Multi-Purpose Interconnectors and Wind Offshore Generation .....	351
Article ID: 161	Comparative Performance Analysis of Network Reduction on the Transmission Expansion Planning .....	363
Article ID: 191	Strategic Positioning of Transmission System Operators to Achieve Long-Term Goals and Sustainability of the Green Transition - Analysis and Case Study.....	372
Article ID: 192	An Innovative Solution for Reducing Emfs: The "5-Phases" Pylons.....	384
Article ID: 193	An Innovative OHL Design for Renewable Energy Harvesting and Transmission: The "5-Phases" Pylons .....	393
Article ID: 195	A Compact 24-Pulses Converter for Overhead Lines De-Icing and Reactive Power Compensation .....	402
Article ID: 197	A Modular Design for OHL Grounding Systems Based on Deep Electrodes.....	410
Article ID: 210	Adriatic Corridor: A Step Towards Deployment of Italian Multiterminal HVDC Systems .....	419
Article ID: 213	Hybrid High Voltage AC and DC System Strength Evaluation With Large Penetration of Renewable Energy Sources .....	432

### Poster Presentation

Article ID: 162	Protection and Metering Solutions for Transmission Tie Lines in the Romanian Power Systems .....	443
Article ID: 225	Algorithm for Calculation of Line Distance Protection Settings.....	451

## ENERGY TRANSITION

### Oral Presentation

Article ID: 234	Geopolitics Impact on Electrical Grids during Energy Transition .....	464
Article ID: 166	Short-Term Solar Radiation Prediction Based on Long Short-Term Memory for Çukurova Region.....	482

### Poster Presentation

Article ID: 109	Optimization Module and Auction Mechanism for the Trading of Guarantees of Origin.....	489
Article ID: 112	Insuring Power System Reliability Under High Renewables Penetration with Energy Storages - A Case for Ukraine.....	497

Article ID: 207	The Concept of Ukraine’s Power System Development Taking into Account the Impact of the Pumped-Storage Power Plant in Modern Conditions .....	<b>496</b>
Article ID: 214	The Role of PSPP in the Implementation of Strategy of Accelerated Development of RES in the Countries of South-Eastern Europe .....	<b>511</b>
Article ID: 229	The Implementation of Intraday Auctions and its Impact on the Croatian Electricity Market .....	<b>517</b>

## **DISTRIBUTION SYSTEMS AND SMART GRIDS**

### **Oral Presentation**

Article ID: 088	Effective Lightning Mitigation Method on Unshielded Distribution Line by Using High Charge Ratings Externally Gapped Line Arresters .....	<b>527</b>
Article ID: 099	An Ai-Based Scalable and Integrated Monitoring System for the Electrical Grid .....	<b>535</b>
Article ID: 120	Implementation of Artificial Neural Networks in Conductor Tension Calculations.....	<b>541</b>
Article ID: 127	Short Circuit Studies with the Presence of Fault Current Limiter Reactor Installed at the Transmission Line Terminals or at the Neutral Point of the Transformer .....	<b>548</b>
Article ID: 130	Impacts of Variable Renewable Energy on new Wholesale Market in Georgia.....	<b>559</b>
Article ID: 132	Estimation of Georgian Power System Flexibility and Adequacy .....	<b>568</b>
Article ID: 133	A Clustering and Benchmarking Based Monthly Electricity Consumption Analysis for Creating Energy Efficiency Insights to the Utility End-Users.....	<b>587</b>
Article ID: 143	The Frequency Stabilization Using Battery Energy Storage System (BESS) in 400 kV Power Systems: a simulation study.....	<b>595</b>
Article ID: 153	Distribution Management System (DMS) Integration in Distribution Network of Kosovo .....	<b>604</b>
Article ID: 156	Challenges of Protection System of Kosovo Distribution Network.....	<b>614</b>
Article ID: 170	Integration of Solar Power Plants in Distribution Network – examples from Bosnia and Herzegovina .....	<b>622</b>
Article ID: 172	Imputation and Forecasting of Energy Consumption data collected by smart meters using Big Data Technologies in the Distribution System Operator.....	<b>632</b>
Article ID: 181	Preparation of a Road Map for DC Transformation of the Turkish Electricity Distribution Grid.....	<b>648</b>
Article ID: 187	Analysis of Loads During the Summer-Winter Season in Substation (SS) 35/10 kV Gjilani I .....	<b>656</b>
Article ID: 205	Under-Frequency Load Shedding Based on Huang’s Empirical Model Decomposition Approach for Estimation of $df/dt$ and Artificial Neural Networks.....	<b>666</b>
Article ID: 221	The Impact of the Connection of Renewable Resources in the Distribution Network - The Case of Hydro Power Plants in Kosovo.....	<b>674</b>

### **Poster Presentation**

Article ID: 131	Smart Metering Benefits for Customers and Distribution System.....	<b>687</b>
Article ID: 138	The Impact of Wind Farm Parks on Mitigation of Energy Crisis (2022) in Kosovo’s Power System .....	<b>693</b>
Article ID: 176	Prevention of High Voltage Network Disturbance Propagation By On-Line Monitoring and Diagnostic of Relay Protection .....	<b>701</b>
Article ID: 186	A Novel Method for Short Circuit Calculation .....	<b>707</b>
Article ID: 189	An Innovative Metric for Evaluating Operational Resilience of the High-Voltage Grid.....	<b>715</b>
Article ID: 190	Smart Grid Project GreenSwitch.....	<b>721</b>
Article ID: 233	The Caterpillar and the Butterfly the Experience of Italian Engineering.....	<b>729</b>

**AUTOMATION AND  
CONTROL**

**ORAL PRESENTATION**



ELECTRIC MACHINES AND  
POWER ELECTRONICS



ELECTRIC  
TRANSMISSION



AUTOMATION AND  
CONTROL

POWER  
GENERATION



ENERGY  
TRANSITION



DISTRIBUTION SYSTEMS  
AND SMART GRIDS



**11-12 OCTOBER 2023**



# Dynamic Network Tariffs and Electric Vehicle Smart Charging Infrastructure

[andreja.kanduc@eimv.si](mailto:andreja.kanduc@eimv.si)

**ANDREJA I. KANDUČ, MSC\*, IGOR PODBELŠEK, MSC, AMILA D. KALOPER, MEE**  
*EIMV*

**JANEZ HUMAR, PHD**  
*ELES*

**SIMEON LISEC**  
*Telekom Slovenije*

*Slovenia*

## SUMMARY

By 2025 Istanbul is expected to become Europe's largest urban area. The fast-growing population trends suggest that it very likely will be the only European urban area to reach a population of 20 million inhabitants. Furthermore, the rise of EU industrial reshoring opportunities will most probably lead to subsequent extensions of organized industrial zones (in Turkish "Organize Sanayi Bölgesi"). Urban electrical power systems with steep demand increases need innovative technical solutions that can address several challenges simultaneously. As power loads in Istanbul are increasing, the metropolitan power network will continuously be upgraded in order to meet the demand for huge amount of power. In most crowded areas land space is becoming scarce and expensive, and therefore, substantial difficulties arise whenever new right-of-way must be secured to carry additional power over traditional transmission lines. As power transmission levels increase, the risk of exceeding the short-circuit capability of existing switchgear equipment, as well as other network components, becomes another real threat to the further expansion of power networks. Strategies to develop urban power networks must also address issues like power congestion, pollution, acoustic and electrical noise, electromagnetic fields, power quality and control, and permits, among others.

With HVDC technology all the above issues can be overcome. The HVDC converter stations based on Voltage Source Converters with small footprint are ideal for infeed to city centres. To reduce the visual impact and to increase resilience to different environmental conditions, the converter station may be built as an enclosed building containing all equipment. To minimize the footprint and the total volume, the converter station may be built on two or more floors. This design principle gives a station design suitable for high power handling on a compact site that would be useful where land area is at a premium.

In addition, several system benefits can be achieved by Voltage Source Converter (VSC) technology which makes it easy to apply in heavily loaded grids, such as independent full active and reactive power control, no added contribution to the short-circuit levels, the balance of power flows on multiple urban infeeds, enhanced grid stability, etc.

Finally, the use of VSC-HVDC enables long underground transmission distances and high transmission capacity through XLPE DC cables as compared to equivalent AC cables. The DC cables can easily be installed using existing right-of-ways and the capacity can thus be significantly increased on existing power corridors. In addition to the mentioned benefits, an advantage would be the possibility of removing obsolete and polluting generating plants from the city centre, improving the air quality and allowing for a clean-air breath-taking view of Sultanahmet across the Bosphorus.

A number of different topologies are possible for single or multi-infeed, giving large freedom of design to adapt to the specific network situation. Design and technical analysis of an HVDC transmission system, capable to feed more than 1'000 MW to Istanbul city is presented in this paper.

## KEYWORDS

Electric vehicle charging, storage, dynamic tariff system, network usage charging, flexibility, green transformation





## 1. INTRODUCTION

Building upon the progress made through the ‘Clean Energy Package’ (CEP) for all Europeans’ initiative, the plan emphasizes the utilization of diverse renewable energy sources and emphasizes the active role of consumers in the transition. One of the key conditions for this is the supportive regulatory environment. With this goal in mind, the Slovenian Energy Market Regulator adopted a new methodology for network tariff calculations for transmission and distribution system operators, which entered into force at the end of year 2022 by adopting the Act on the Methodology for Determining the Network Charges for the Electricity System Operators (hereinafter referred to as the Act) [1]. The network charge under this Act shall apply in the beginning of 2024.

The newly introduced methodology brings forth a more dynamic tariff system, empowering users to assume a proactive role. Under this framework, network tariffs are designed to provide users with dynamically variable prices that reflect the impact of their electricity consumption or generation on future network upgrade costs. This system aims to encourage more efficient utilization of the network by shifting the load from peak periods to the periods with lower consumption. Users who effectively manage their electricity consumption and contribute to load balancing are rewarded with lower network charges. Conversely, those with higher capacity consumption during peak load times may incur higher network charges. Moreover, the Act also ensures fairness to the users in the energy communities and active network users who provide flexibility as a service to the system. All network users are treated equally and contribute to the network costs according to its use. Electric charging stations for electric vehicles (hereinafter referred to as EVs) will rise a demand for the energy, which will further burden the electricity system and have a significant impact on future network cost so it is very important that the network charging system steers the increased energy consumption.

## 2. BENEFITS OF THE EV IMPLEMENTATION

One of the major benefits of the mass use of EVs is the reduction of the adverse effects of transport on the environment, space, and health by reducing greenhouse gas emissions, noise pollution, and air pollution. Transport accounts for almost a third of Slovenia’s greenhouse gas emissions and is an important cause of urban air pollution. A shift towards sustainable, low-carbon mobility is essential to address this challenge. Slovenia has set a target of reducing emissions by at least 50% as outlined in its Operational Programme for Reducing Greenhouse Gas Emissions by 2050. Beginning in 2025, restrictions on the first registration of passenger cars and light goods vehicles in categories M1, MG1, and N1 have been implemented. These restrictions target vehicles with CO<sub>2</sub> emissions exceeding 100 g/km and aim to further reduce the limit to 50 g/km by 2030. On 14 February 2023, the European Parliament took a step further by voting against the sale of passenger cars and light commercial vehicles with internal combustion, which will enter into force in 2035. These European objectives will drive the prominence of alternative fuel vehicles, including electric, hydrogen and gas vehicles. Slovenia has committed to introducing a minimum of 200,000 EVs and an ample number of other alternative fuel vehicles by 2030. In 2021, in Slovenia 5,400 electric vehicles were registered, marking a 47% increase compared to the previous year. An even higher growth was registered in the segment of hybrid vehicles. Trend shows growth, but it is still far from the goal. One of the reasons is also the lack of charging stations infrastructure.

Partners ELES and Telekom Slovenije, as prominent and influential Slovenian companies, have demonstrated their commitment to sustainability and ethical practices. Recognizing the importance of environmental responsibility, both companies have taken an active role in integrating electric mobility into their business operations and have even encouraged their employees to embrace it. In pursuit of this objective, they have jointly launched the E8 [3] initiative. E8 is the concept of integral development of infrastructure for mass charging of EVs. The purpose of this paper is to analyze the effects of the infrastructure required for EVs charging on the company cost (network charges for electricity system operators) and explore the methods for effective control.

### DYNAMIC TARIFFS

With the adoption of the Act, the Slovenian Energy Market Operator has introduced a novel approach to charging network fees. The dynamic tariff system is putting in place a pricing mechanism that rewards adjustment of charging based on grid conditions, aiming to optimize resource utilization. The act is centered around network charging that relies on 15-minute data from smart meters at the final network user. The network charge is applicable for the transmission and distribution system independently from the geographical location (postage stamp principle) and it varies based on multiple factors such as season, time of use (network load in each season, intraday network load), and the level of connection of the user (depending on the share of total network load). Consequently, network tariff rates fluctuate at different times, actively encouraging system users to utilize the network during periods of reduced consumption. Conversely, users of the system are not encouraged to use the network during times of high demand as this may lead to potential network overload.

		Time block					
		period	B1	B2	B3	B4	B5
SEASON	HIGH	Work day (from November to February)	From 7.00 to 14.00 From 16.00 to 20.00	From 6.00 do 7.00 From 14.00 to 16.00 From 20.00 to 22.00	From 0.00 to 6.00 From 22.00 to 24.00		
	Holidays and weekends			From 7.00 to 14.00 From 16.00 to 20.00	From 6.00 do 7.00 From 14.00 to 16.00 From 20.00 to 22.00	From 0.00 to 6.00 From 22.00 to 24.00	
LOW	Work day (from March to October)		From 7.00 to 14.00 From 16.00 to 20.00	From 6.00 do 7.00 From 14.00 to 16.00 From 20.00 to 22.00	From 0.00 to 6.00 From 22.00 to 24.00		
	Holidays and weekends			From 7.00 to 14.00 From 16.00 to 20.00	From 6.00 do 7.00 From 14.00 to 16.00 From 20.00 to 22.00	From 0.00 to 6.00 From 22.00 to 24.00	From 0.00 to 6.00 From 22.00 to 24.00

Table 1: New tariff system time segmentation [4, Attachment 2].

Another significant advancement in the new methodology is the increased emphasis on capacity rather than energy in determining network charges, as the demand for higher capacity is the driver of new investments. Under the new approach, the aim is for users to evenly distribute their energy consumption within the agreed contracted capacity. This shift recognizes the importance of managing capacity demand efficiently to optimize network utilization and minimize potential overload situations. By encouraging users to maintain a more balanced energy consumption pattern, the new methodology promotes a more effective and sustainable use of network resources.

EVs are poised to become significant electricity consumers in the near future. However, by being able to align their charging patterns (considering also the individual requirements of EV owners) this presents the advantage to the needs of the overall network capacity. In the following discussion, we will highlight the impact of the growing number of electric vehicles on the demand for network capacity and how it subsequently affects the increased network charging costs for companies. Furthermore, we will delve into how companies can further mitigate network charges by integrating smart charging stations and leveraging the benefits from local photovoltaic (PV) installations on network charging costs.

### 3. IMPACT OF EVS ON NETWORK CHARGES

One of the primary challenges faced by companies opting to purchase EVs is that they have to subsequently provide the charging infrastructure. Consequently, the network capacity needs and costs are increased. However, the cost of network fees for connection power is not the only significant hurdle. The existing network often imposes limitations that prevent immediate increases in network capacity when users require it. The Slovenian distribution network struggles to keep pace with the growing demands of electrification, necessitating new investments in network upgrades, which often involve construction interventions and require comprehensive documentation and approvals. In this paper, we assume that the distribution operator can meet the user’s capacity requirements.

#### 3.1. Connection capacity charge

In Slovenia, there are two types of charges related to the capacity for EV charging. The first is the network connection charge, which customers are required to pay for any increase in capacity. The second charge is a monthly fee, which is determined based on the contracted capacity for each specific time block.

For the purposes of this paper, based on data from year 2019 [5], we have calculated simulated tariff rates for connection power for the year 2024, considering the voltage level of the system user. (User on HV - EUR 42.20/kW, user on MV - EUR 81.71/kW, and user on LV - EUR 97.43/kW).

### 3.2. Network charges for capacity and energy

Network users in Slovenia are categorized into different segments based on their connection to the network, specifically their voltage level. Each group contributes to the overall network costs based on the impact they have on a particular voltage level. It's important to note that network costs are primarily covered by consumers, while producers are not obligated to bear these costs under the existing and new methodology. The network charges are structured in two components: the transmission operator charging fee and the distribution operator charging fee. The final cost for consumers depends on their energy consumption and the contracted capacity, which can vary for different time blocks. Equation 1 presents the condition for contracted capacity for each block ( $Cc_b$ ).

$$Cc_b \leq Cc_{b+1}$$

Equation 1

The contracted capacity should be equal or higher in off-peak periods with respect to peak periods. In the case that the actual measured 15-min consumption exceeds the contracted capacity, an additional cumulative excess demand charge would be applied. This charge provides the incentive to adjust consumption to the contracted capacity.

$$OMR_b^{Cex} = \mathcal{F}_{ex} \times T_{i,b}^c \times Cex_b = \begin{cases} 0 & ; Cm_{k,b} \leq Cc_b \\ \mathcal{F}_{ex} \times T_{i,b}^c \times \sqrt{\sum_{k=1}^n (Cm_{k,b} - Cc_b)^2} & ; Cm_{k,b} \geq Cc_b \end{cases} \quad (\text{EUR})$$

$$OMRd^c \sum_h OMRd_b^c \quad (\text{EUR})$$

Equation 2

**Where:**

$OMR_b^{Cex}$  : excess demand charge at time-block b (€/kW),

$T_{i,b}^c$  : tariff for capacity charge at time-block b (€/kW), which is equal to the capacity charge for time block b and voltage level I,

$Cex_b$  : excess consumed capacity by the customer, in kW, in time-block b

$Cm_{k,b}$  : maximum demand consumed by the customer, in kW, for each 15-min sample when contracted capacity is exceeded in time-block b

$Cc_b$  : contracted capacity by the customer, in kW, in time-block b

$k$  : total number of 15-min samples when contracted capacity is exceeded.

$\mathcal{F}_{ex}$ : weight factor

### 3.3. Impact of the new methodology for network charging with and without EVs

For the impact analysis, we have selected two company locations of Telekom Slovenija that fall into different customer categories:

1. Location A, which operates at the medium voltage level with a contracted capacity of 900 kW and falls under customers with more than 2500 operating hours.
2. Location B, which operates at the low voltage network with a contracted capacity of 86 kW and falls under customers with less than 2500 operating hours.

Initially, we conducted an analysis to assess the impact of the new Act at each location, assuming that the consumption and the load profile remained unchanged. To perform the simulations, tariffs were calculated based on 15-minute interval network data from 2020. By using this data and considering the changes introduced by the new Act, we were able to estimate the potential network charges for the specified locations in 2024. This allowed us to evaluate the potential cost implications for Telekom Slovenija.

Table 2: Network charges under the old methodology (2022) and the new methodology (2024).

Network charges	A		B	
	Energy [€/year]	Capacity [€/year]	Energy [€/year]	Capacity [€/year]
2022	7,472	8,593	1,218	1,115
2024	9,306	12,466	709	539
Factor	1.25	1.45	0.58	0.48

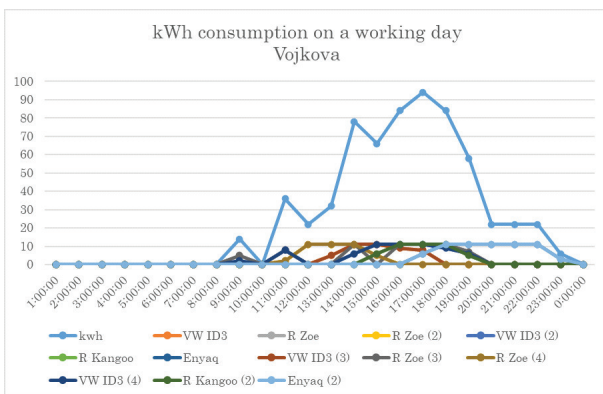


Figure 1: Load profile EV loc. A.

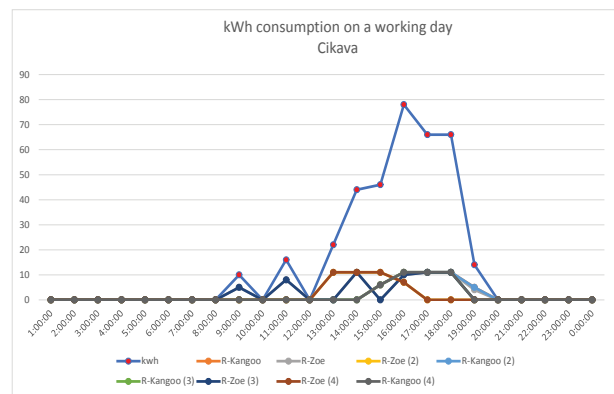


Figure 2: Load profile EV loc. B.

In the next step, we assessed the potential changes in energy and power demands resulting from the installation of charging infrastructure for electric vehicles at both locations. Specifically, we projected that twelve EVs would be charged at the location A, while the location B would have ten EVs for charging. This analysis allows us to understand the additional capacity and energy requirements for Telekom Slovenije at those two locations.

With the EVs, there is an increase in energy consumption and power demand during peak load periods. This means that the need for capacity is the highest in the time block with the highest network tariff. The increased adoption of EV charging will result in higher network charging costs for companies. Additionally, at locations with current low connection power, the needed capacity increases significantly, which exceeds the currently contracted capacity at the location.

Companies will have to purchase additional capacities from the network provider, which can be costly. Furthermore, it can be, that the DSO does not have available capacities on that location. In this paper, we assume that the DSO can meet the user's capacity requirements.

To mitigate these issues, smart charging solutions and load management techniques were examined. Additionally, a study has been conducted to explore the implementation of PV systems, considering the current charging habits of EV owners, who predominantly charge their vehicles during the daytime. The simulations and findings related to both areas are presented below.

## 4. NETWORK COST MITIGATION

### 4.1. Smart Charging and Load Management Solutions

The examination of smart charging solutions and load management techniques has yielded promising results. By implementing advanced algorithms and intelligent charging infrastructure, it is possible to optimize charging loads, considering factors such as grid capacity, electricity demand patterns, and network tariffs and driver needs. These solutions can effectively mitigate strain on the grid and help distribute the charging demands more efficiently.

Table 3: Network charge with and without EVs

Network charges (simulations for 2024)	A		B	
	Energy [€/year]	Capacity [€/year]	Energy [€/year]	Capacity [€/year]
without EV	9,306	12,466	709	539
with EV	11,126	14,007	2,102	2,031
increase %	19.56%	12.36%	196.47%	276.81%

In the case of location B, the increased need for additional network capacity due to EV charging necessitates an upgrade in connection power capacity. This upgrade incurs an additional one-off cost for the network charge, totaling EUR 5,066.36.

As we see, the cost of network charges increases greatly, as car charging is not managed. Thus, we charge the EV with the highest power during the most expensive tariff. In one day, during the high season, at the location A, 1,700 kWh is consumed in the most expensive tariff with the peak capacity 196 kW. 667 kWh is consumed during the second most expensive tariff with the peak capacity 189 kW, and 668 kWh is consumed at the minimum tariff with the peak capacity 109 kW. Let us observe the same day for the location B. At this location, 363 kWh are consumed within the highest tariff with the peak capacity 83 kW, 122 kWh are consumed during the second most expensive tariff with the peak capacity 56 kW, and 40 kWh are consumed during the lowest tariff with the peak capacity 5 kW. No EV charging happened during the lowest tariff period. These values include the regular consumption of the company on that day with added EV consumption.

As observed, the network charges increase significantly when EV charging is unmanaged. To address this issue, we have examined a scenario where EV charging is controlled and optimized using software-controlled smart charging. In this controlled charging scenario, EV batteries are charged to the same capacity, but instead of using “dummy” charging, the charging process is dynamically adjusted based on capacity cost and availability, thereby distributing the power curve more efficiently.

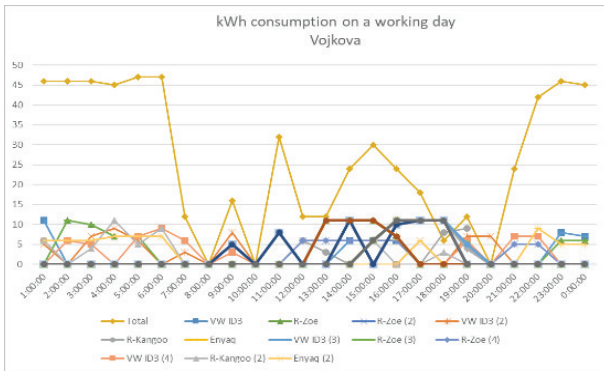


Figure 3: Regulated load profile EV loc. A

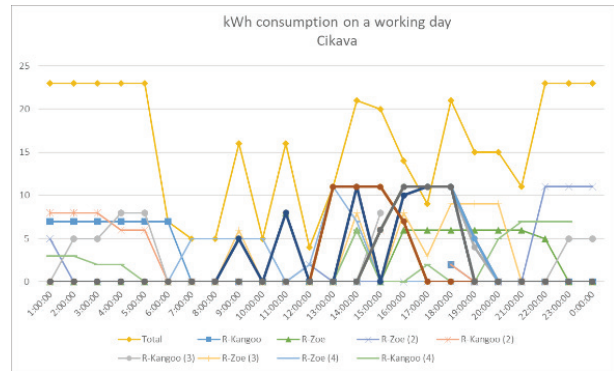


Figure 4: Regulated load profile EV loc. B.

Table 4: Network charge with and without load management

Network charges (simulations for 2024) with EV	A		B	
	Energy [€/year]	Capacity [€/year]	Energy [€/year]	Capacity [€/year]
without load management	11,126	14,007	2,102	2,031
with load management	11,061	13,365	2,076	883
decrease %	0.58%	4.58%	1.24%	56.52%



By managing EV charging the consumption during the tariff blocks has changed. The same day during high season is used to observe the impact of smart charging. At the location A, 1,420 kWh is consumed in the most expensive tariff with the peak capacity 169 kW. 605 kWh are consumed during the second most expensive tariff with the peak capacity 142 kW, and 1010 kWh are consumed at the minimum tariff with the peak capacity 131 kW. At the location B 212 kWh are consumed within the highest tariff with the peak capacity 29 kW, 105 kWh are consumed during the second most expensive tariff with the peak capacity 31 kW, and 208 kWh are consumed during the lowest tariff with the peak capacity 26 kW. These values include the regular consumption of the company on that day and the EV consumption with load management.

### 4.2. Integration of PV systems with EV charging

PV systems can play a significant role in charging EVs by providing renewable and sustainable energy directly from the sun. By utilizing solar energy for EV charging, carbon emissions associated with traditional grid electricity are reduced, leading to a greener and more sustainable charging process. But how much can PV systems contribute to the cost savings on network charging?

For research purposes in this article we have simulated the installation of one PV system at both locations and tested its performance by using the PVGIS online tool [6]. The characteristics of each PV are shown in the table below.

Table 5: PV system characteristics

Characteristics	A	B
Solar radiation database	PVGIS-SARAH 2	PVGIS-SARAH 2
PV technology	Crystalline silicon	Crystalline silicon
Installed peak power[kWp]	50	66
System loss [%]	14	14
Mounting type	Fixed	Fixed

Power flows for different scenarios are shown in Figure 5 and 6. The same date during high season was chosen for both locations. As expected, the impact of PVs during the higher season is quite low, as solar irradiation during November, December, January, and February is reduced.

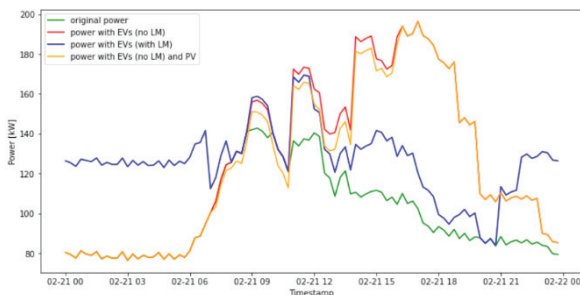


Figure 5: Power flow scenarios, location A

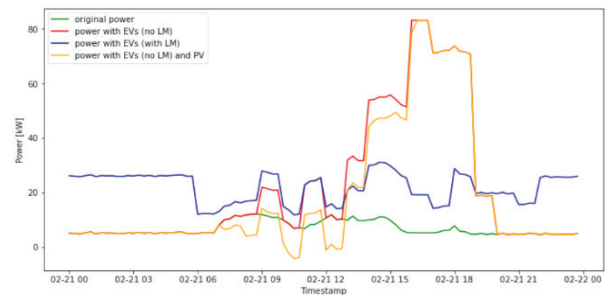


Figure 6: Power flow scenarios, location B.

Table 6 shows network charges with and without PVs while having EV charging without load management (LM) usage.

Table 6: Network charge with and without PV

Network charges (simulations for 2024) with EVs	A		B	
	Energy [€/year]	Capacity [€/year]	Energy [€/year]	Capacity [€/year]
without PV	11,126	14,007	2,102	2,031
with PV	11,102	13,862	1,868	2,031
decrease %	0.22%	1.04%	11.13%	0.00%

Figures 7 and 8 compare network charges for all mentioned scenarios. For both locations, A at MV and B at LV, the most profitable scenario is achieved using EV charging with LM.

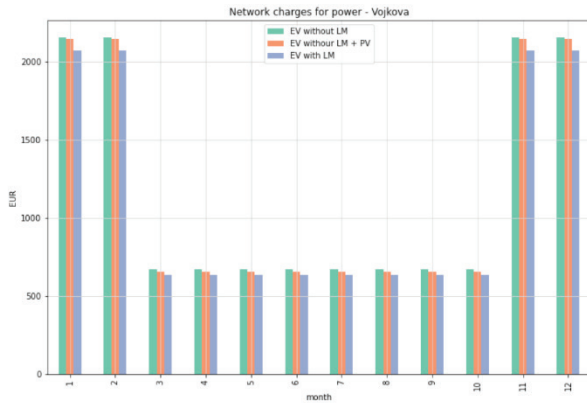


Figure 7: Network charges, location A.

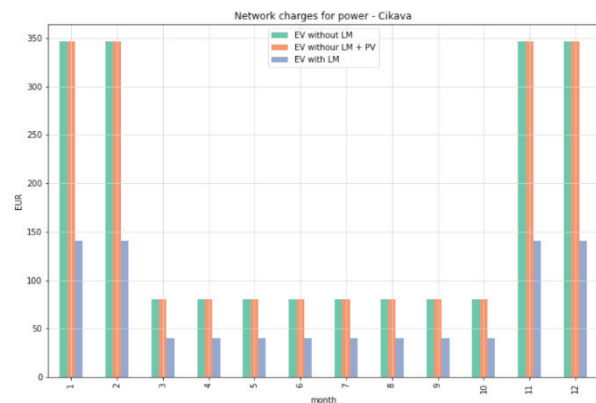


Figure 8: Network charges, location B.

## 5. CONCLUSION

The simulations have shown that the green transition objectives can be supported by utilizing 15 minutes consumption meter data available in a process of managing our patterns of electricity consumption. We have shown how quickly, with simple measures of time-planned EV charging process and shifting charging from hours of high network loads to hours of lower load, we can achieve savings in the network charge. As the number of EVs at the company and among employees increases, the importance of managing EVs charging becomes even more significant. In addition to controlling peak load and charging times, integrating a fleet management program into the charging system will become necessary. By connecting a fleet management program to the charging infrastructure, valuable information can be obtained regarding planned business trips and vehicle availability. This data can then be used to prioritize electric vehicles charging.

Our research shows that the use of PVs does not have any significant influence on network charging costs. At the location B, with and without a PV, the network charges remained the same. Network costs are the highest in the winter, when there are not enough sunny days in Slovenia, to make a significant difference in the amount of energy needed from the network. Therefore, network charges show only small improvement. Even so, PVs can still show its costs benefits if one would take into consideration electricity energy costs<sup>1</sup>.

The next step would certainly be the introduction of battery storage system that would allow even smarter load shifting between tariff blocks.

## BIBLIOGRAPHY

- [1] 'Directive 2003/87/EC of the European Parliament and of the Council of 13 October 2003 establishing a system for greenhouse gas emission allowance trading within the Union and amending Council Directive 96/61/EC (Text with EEA relevance)', <https://web.archive.nationalarchives.gov.uk/eu-exit/https://eur-lex.europa.eu/legal-content/EN/TXT/?uri=CELEX:02003L0087-20200101>. <https://www.legislation.gov.uk/eu/2003/87/article/30> (accessed 24 June 2022).
- [2] 'Portal Energetika - Nacionalni energetski in podnebni načrt'. <https://www.energetika-portal.si/dokumenti/strateski-razvojni-dokumenti/nacionalni-energetski-in-podnebni-na crt/> (accessed 14 May 2020).
- [3] 'E8 - koncept celostnega razvoja infrastrukture za masovno polnjenje e-vozil'. <https://www.e8concept.com/sl> (accessed 30 March 2023).
- [4] 'Akt o metodologiji za obračunavanje omrežnine za elektrooperaterje - Javna obravnava aktov - Agencija za energijo'. [https://www.agen-rs.si/javna-obravnav-aktov/-/asset\\_publisher/M2GdU2jRtCxV/content/akt-o-metodologiji-za-obracunavanje-omreznine-za-elektrooperaterje?inheritRedirect=false&redirect=https%3A%2F%2Fwww.agen-rs.si%2Fjavna-obravnav-aktov%3Fp\\_id%3D101\\_INSTANCE\\_M2GdU2jRtCxV%26p\\_p\\_lifecycle%3D0%26p\\_p\\_state%3Dnormal%26p\\_p\\_mode%3Dview%26p\\_p\\_col\\_id%3Dcolumn-1%26p\\_p\\_col\\_count%3D1](https://www.agen-rs.si/javna-obravnav-aktov/-/asset_publisher/M2GdU2jRtCxV/content/akt-o-metodologiji-za-obracunavanje-omreznine-za-elektrooperaterje?inheritRedirect=false&redirect=https%3A%2F%2Fwww.agen-rs.si%2Fjavna-obravnav-aktov%3Fp_id%3D101_INSTANCE_M2GdU2jRtCxV%26p_p_lifecycle%3D0%26p_p_state%3Dnormal%26p_p_mode%3Dview%26p_p_col_id%3Dcolumn-1%26p_p_col_count%3D1) (accessed 8 June 2022).
- [5] 'Prenova metodologije obračunavanja omrežnine in tarifnega sistema št.2507' (accessed 20 April 2022) [Online]. Available: [https://www.agen-rs.si/docu-ments/10926/283610/D7\\_AGEN\\_Reforma\\_Obra%C4%8DunOMR-TarifniSistem\\_SLO\\_V4\\_nerevidirana.pdf/e4e1465d-79d4-4adc-b15c-546ab085a387](https://www.agen-rs.si/documents/10926/283610/D7_AGEN_Reforma_Obra%C4%8DunOMR-TarifniSistem_SLO_V4_nerevidirana.pdf/e4e1465d-79d4-4adc-b15c-546ab085a387)
- [6] 'PVGIS online tool'. [Online]. Available: [https://joint-research-centre.ec.europa.eu/pvgis-online-tool\\_en](https://joint-research-centre.ec.europa.eu/pvgis-online-tool_en)

<sup>1</sup> This paper is focused only on network charging costs



# Application for Optimization of Capacity Reserve Trading Auctions

[goran.jakupovic@pupin.rs](mailto:goran.jakupovic@pupin.rs)

**GORAN JAKUPOVIC\***, MILAN JOSIFOVIC, PAVLE LUCIC, NIKOLA STOJAKOVIC  
*Institute "Mihajlo Pupin", University of Belgrade*

**DEJAN STOJCEVSKI, ALEKSANDAR PETKOVIC**  
*SEEPEX a.d. Beograd (SEEPEX)*

**SIMEON LISEC**  
*Telekom Slovenije*

**Serbia**

## SUMMARY

In this paper, we present the operation of the optimization module of the Capacity Reserve Market application. First, we present a brief overview of the entire application and its business process, as well as the software architecture, and then we present a description of algorithms, i.e., a mathematical model of the optimization process. After, we give a functional description of the optimization module software, as well as a description of the software technologies used. Finally, a brief overview of the user interface is shown. The optimization module was developed using the C++ programming language on the Linux platform (specifically Oracle Linux 7.9). The basic optimization problem comes down to the linear programming problem, and open-source libraries, specifically the GNU Linear Programming Toolkit, are used to solve this problem. Data on auctions, participants, CZC/ATC, and other data are stored in a relational database on a MySQL-compatible MariaDB platform.

This module, which serves to procure capacities for the needs of the balancing system, is a regionally market-based tool in the process of procuring regional reserve capacities on a weekly basis through an auction mechanism. It enables the procurement of reserves as close as possible to real-time, considering the state of the system, the procurement time period, the location of capacities that provide balancing services, and the increase in the number of participants that will lead to increased competition and obtaining a real market value for capacity reservations.

The described module was developed within the HORIZON 2020 project TRINITY (H2020-863874 Transmission system enhancement of regional borders by means of Intelligent market technology).

## KEYWORDS

Capacity reserve trading, Optimization, Linear programming.



### 1. INTRODUCTION

The TRINITY (*TR*ansmission system enhancement of *regio*Nal borders by means of *IntelligenT* market technology) project deals with topics from the European Union's research program called Research Horizon Framework 2020 Programme, within the field of "Building a low-carbon future resilient to climate change: secure, clean, and efficient energy"[1].

The main goal of the Trinity project is to enhance coordination and strengthen cooperation between transmission system operators (TSOs) in Southeast Europe (SEE), market operators, electricity producers, and market participants to support the integration of the electricity market in this region, with maximum utilization of "green" energy sources. Additionally, this project aims to harmonize cross-border services between the EU and non-EU countries.

The three main pillars on which the mentioned project objectives are based are: Market coupling, Coordination of transmission system operators, and Integration of renewable energy sources (RES). They are directly covered by three TRINITY products, which are interconnected thanks to the fourth product, the T-coordination platform. This project is implemented in cooperation with 19 companies from 11 European countries.

One of the products being developed within this project is the Market Coupling Platform, which consists of four independent modules that will enable cross-border trading of electricity and the integration of national markets into a regional market as a first step towards creating a single European electricity market. The modules comprising this product are intended for:

- Intraday market coupling through an auction mechanism
- Trading of capacity reserves for system balancing purposes
- Bilateral trading
- Trading of Guarantees of Origin.

The demonstration of these modules was scheduled for 2022 and 2023.

The Capacity Reserves Trading module, jointly developed by IMP (Mihajlo Pupin Institute), EKC (Electricity Coordination Center), and SEEPEX (Electricity Market Operator), represents one of the most significant tools for increasing system operational security, reducing costs, and enhancing cross-border cooperation among transmission system operators. This module, which serves for procuring capacity reserves for system balancing purposes, is a regionally market-based tool in the process of procuring regional capacity reserves on a weekly basis through an auction mechanism. It enables the procurement of reserves as close to real-time as possible, taking into account the system's state, the procurement time frame, the location of capacity providers offering balancing services, and the increase in the number of participants, which will lead to an increased competition and obtaining a realistic market value for capacity reservation.

Capacity reserves for balancing are used to raise the system frequency (positive services) or lower the system frequency (negative services). A provider of positive services will either increase production or reduce electricity consumption, while a provider of negative services will do the opposite. Transmission system operators must maintain a balance between electricity production and consumption within their control areas at all times. To perform this task, transmission system operators require different types of capacity reserves: frequency containment reserve (**FCR**), automatic frequency restoration reserve (**aFRR**), manual frequency restoration reserve (**mFRR**), and replacement reserve (**RR**). These types differ based on the activation principle and their response to activation [2-4].

The collaboration between transmission system operators in a region contributes to minimizing the overall requirements for regulating reserves without compromising system security. These regulating reserves differ in terms of the speed at which they can be activated. FCR and mFRR are automatic regulations, where FCR must be available within 30 seconds, while aFRR must be available within 5 minutes. In contrast, mFRR, which should be available within 5 - 15 minutes, is activated manually (individual activation is sent to the service provider, phone delivery, and email), as well as RR, which must be available within 15 - 60 minutes.

This module enables the organization and procurement of all aforementioned types of capacity reserves depending on the needs of transmission system operators.

In Figure 1, a simplified business process of the Capacity Reserves Trading module is presented.

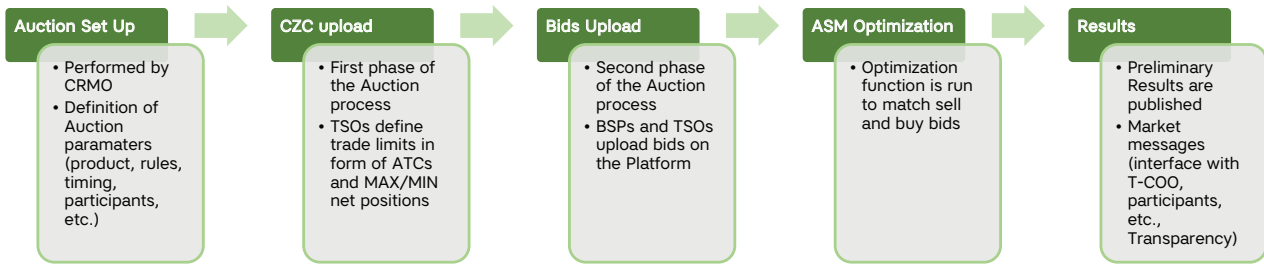


Figure 1. Simplified business process

The procurement procedure is based on auctions, applied at the regional level (and also at the national level), enabling increased competition and reducing the obligations of transmission system operators to hold capacity reserves at the national level.

The module allows for conducting weekly auctions for each defined reserve type and includes 42 four-hour blocks covering the upcoming week. Before the start of the auction, the auction administrator inserts cross-zonal capacities (CZC) and maximum/minimum net values for each participating control zone. The auction for the respective reserve type begins with the opening of the bidding process for buying and selling. Transmission system operators submit linear orders, while registered balancing service providers submit block orders. After the gate closure time, the algorithm calculates the results, which are then sent to the TSOs for verification. Upon a positive response, the auction results are delivered to the participants and published on the website. Relevant operational messages (OMMs) during the auction process are created and published on the T-coordination platform and the website.

## 2. GENERAL OVERVIEW OF ARCHITECTURE

The capacity reserves trading application consists of two components that utilize a shared database:

- The “back-end” part, which includes the **scheduler** and **auction optimizer**.
- The “front-end” part, which consists of the WEB HMI interface and the *GlassFish* application server.

The MySQL compatible MariaDB database is another part of the system which contains all the necessary tables for storing results and communication between front-end and back-end.

The general simplified structure of the system is shown in Figure 2.

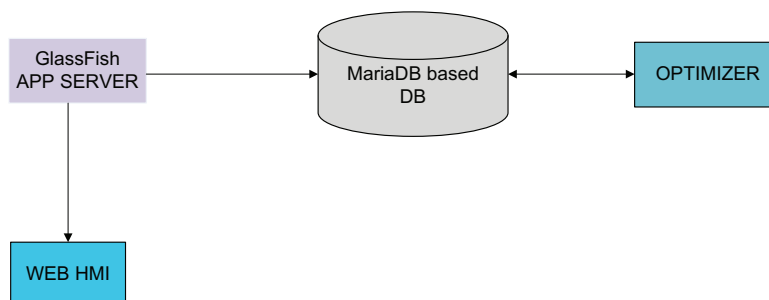


Figure 2. Simplified structure of the system

The purpose of the auction optimizer is to find an optimal solution using linear programming for a defined objective function with constraints.

For each product, optimization is performed separately, meaning that an auction for each product represents an optimization problem that needs to be solved. Within one auction, one of the four different types of products can occur:

- FCR** (Frequency Containment Reserve) - reserve for frequency containment, i.e., primary regulation.
- mFRR** (Manual Frequency Restoration Reserve) - reserve for manual frequency restoration, mFRR up and mFRR down.



- **aFRR** (Automatic Frequency Restoration Reserve) - reserve for automatic frequency restoration, i.e., secondary regulation, aFRR up and aFRR down.
- **RR** (Replacement Reserve) - tertiary reserve, RR up and RR down.

### OPTIMIZATION ALGORITHM

For each of the defined products (mFRRup, mFRRdown, aFRRup, aFRRdown, RRup, RRdown), separate optimization is performed using the optimization algorithm described in the following text. However, it should be noted that in the case of the FCR product, the same optimization algorithm described below is applied, with the difference that in this case, there are no transmission network constraints (ATC/CZC). It is assumed that the corresponding capacities are unlimited due to the fact that the appropriate transmission capacity is already implicitly allocated (within TRM) in the transmission capacity calculation process.

The objective function of the optimization algorithm is the total welfare, which needs to be maximized over the considered time interval. Welfare is defined as the difference between the cumulative amount of money that buyers (TSOs) are willing to pay and the cumulative amount of money that sellers (BSPs) are willing to sell for a certain quantity of the product (which lies between zero and the maximum offered quantity for each market participant) for all trading time intervals (T). It can be shown that this defined difference represents the sum of the surplus of TSO, the surplus of BSP, and congestion revenue. The objective function is as follows:

$$\max \sum_{a \in A} \sum_{t \in T} \left( \sum_{i=1}^{n_a} q_{a,i,t}^B \cdot (p_{a,i,t}^B + \varepsilon) - \sum_{j=1}^{m_a} q_{a,j,t}^S \cdot (p_{a,j,t}^S - \varepsilon) - \delta \cdot \sum_{l=1}^b (P_{l,t}^+ + P_{l,t}^-) \right) \quad (1)$$

where  $A$  is the set of all areas,  $T$  is the set of all time intervals (hours) for which the auction is conducted,  $n_a$  is the total number of buy bids in area  $a$ ,  $m_a$  is the total number of sell bids in area  $a$ ,  $b$  is the total number of boundaries (all possible combinations<sup>1</sup>), while on the other hand:

- $p_{a,i,t}^B$  - the price at which the  $i$ -th buyer (TSO) from the area  $a$  is willing to purchase the offered quantity of reserve in time interval  $t$  (constant)
- $p_{a,j,t}^S$  - the price at which the  $j$ -th seller (BSP) from the area  $a$  is willing to sell the offered quantity of reserve in time interval  $t$  (constant)
- $q_{a,i,t}^B$  - the accepted quantity by the  $i$ -th buyer from the area  $a$  in the time interval  $t$  (variable)
- $q_{a,j,t}^S$  - the accepted quantity by the  $j$ -th seller from the area  $a$  in the time interval  $t$  (variable)
- $P_{l,t}^+$  - the flow on the  $l$ -th boundary in the forward direction in the time interval  $t$  (variable)
- $P_{l,t}^-$  - the flow on the  $l$ -th boundary in the reverse direction in the time interval  $t$  (variable)

It should be noted that two additional terms dependent on parameters  $\varepsilon$  and  $\delta$  have been introduced in the objective function in order to maximize the traded quantity in case of uncertainty in quantity and prevent the occurrence of circular flows (multiple solutions to the optimization problem regarding flows between areas). The values of parameters  $\varepsilon$  and  $\delta$  in the objective function can be arbitrarily small, depending on the price resolution applied in the observed market. If the offered prices are given with precision up to two decimal places, the following parameter values can be adopted in the objective function:  $\varepsilon = 10^{-3}$  and  $\delta = 10^{-6}$ .

Within the optimization problem, which involves maximizing the previously defined objective function, the following linear constraints need to be respected and can be divided into five categories.

**C1:** Since bids can be accepted in whole or in part, the accepted quantities of bids for buying/selling must satisfy the following linear constraints:

$$\begin{aligned} 0 &\leq q_{a,i,t}^B \leq Q_{a,i,t}^B \\ 0 &\leq q_{a,j,t}^S \leq Q_{a,j,t}^S \end{aligned} \quad (2)$$

where:

$Q_{a,i,t}^B$  - the submitted quantity of the  $i$ -th buyer from the area  $a$  in the time interval  $t$

$Q_{a,j,t}^S$  - the submitted quantity of the  $j$ -th seller from the area  $a$  in the time interval  $t$

<sup>1</sup>  $b = \frac{n(n-1)}{2}$ , where  $n$  is the total number of areas.

The previous two variables are entered by the TSO/BSP participants during the bid loading phase.

**C2:** The selection of bids is done in such a way that bilateral exchanges between neighboring areas, i.e., flows across boundaries between areas, match the level of reserve import/export. For this reason, the following balancing constraint is introduced for each area  $a$  in the time interval  $t$ :

$$\sum_{j=1}^{m_a} q_{a,j,t}^S - \sum_{i=1}^{n_a} q_{a,i,t}^B = \sum_{l=1}^b k_{a,l} \cdot (P_{l,t}^+ - P_{l,t}^-) \quad (3)$$

where  $k_{a,l}$  is the corresponding element of the boundary-to-area incidence matrix, whose value is 1 if boundary  $l$  is directed from the area  $a$ , -1 if boundary  $l$  is directed towards area  $a$ , and 0 if boundary  $l$  and area  $a$  are not incident.

Additionally, it is necessary to ensure the following balancing constraint for a closed system, i.e., for each individual area  $a$  in every time interval  $t$ :

$$\sum_{a \in A} \left( \sum_{j=1}^{m_a} q_{a,j,t}^S - \sum_{i=1}^{n_a} q_{a,i,t}^B \right) = 0 \quad (4)$$

**C3:** All cross-border exchanges must satisfy the constraints imposed by the transmission network (ATC/CZC). Therefore, inequality constraints are defined that must be satisfied by the flow on each defined boundary and direction in every time interval  $t$ :

$$\begin{aligned} 0 &\leq P_{l,t}^+ \leq ATC_{l,t}^+, \text{ for each } l = 1, 2, \dots, b \\ 0 &\leq P_{l,t}^- \leq ATC_{l,t}^-, \text{ for each } l = 1, 2, \dots, b \end{aligned} \quad (5)$$

where  $ATC_{l,t}^+$  and  $ATC_{l,t}^-$  are the corresponding values of the cross-border capacities (ATC) in time interval  $t$ , for boundary  $l$  in the forward and reverse direction, respectively. These values are entered by the TSO. However, it should be emphasized that the initial values of ATC for all boundaries are set to 0. If there is no defined boundary between two areas, or the corresponding values are not entered by the TSO, the given ATC values remain equal to the initial values, and the corresponding flows ( $P_{l,t}^+$  and  $P_{l,t}^-$ ), based on constraint C3, are equal to zero.

**C4:** On the other hand, each TSO can define the maximum and minimum net position for its control area  $a$ , in each considered time interval  $t$ :

$$-MAX NET_{a,t}^- \leq \sum_{j=1}^{m_a} q_{a,j,t}^S - \sum_{i=1}^{n_a} q_{a,i,t}^B \leq MAX NET_{a,t}^+ \quad (6)$$

where:

$MAX NET_{a,t}^+$  - maximum reserve export of area  $a$  in the time interval  $t$

$MAX NET_{a,t}^-$  - maximum reserve import of area  $a$  in the time interval  $t$

The values of  $MAX NET_{a,t}^+$  and  $MAX NET_{a,t}^-$  are read from files provided by TSO, or entered by TSO within the CZC HMI tab.

**C5:** In addition to constraint C4, a net position constraint is introduced for each LFC block  $z$  in time interval  $t$ :

$$-MAX LFC_{z,t}^- \leq \sum_{a \in Z} \left( \sum_{j=1}^{m_a} q_{a,j,t}^S - \sum_{i=1}^{n_a} q_{a,i,t}^B \right) \leq MAX LFC_{z,t}^+ \quad (7)$$

where:

$MAX LFC_{z,t}^+$  - maximum export of reserve for LFC block  $z$  in time interval  $t$

$MAX LFC_{z,t}^-$  - maximum import of reserve for LFC block  $z$  in time interval  $t$

The values of  $MAX LFC_{z,t}^+$  and  $MAX LFC_{z,t}^-$  are read from files provided by the TSO or entered by the TSO within the CZC HMI tab.

### 3. OPERATION OF THE OPTIMIZATION MODULE

The Optimization module represents a separate unit whose logic is depicted in Figure 3. The Process Scheduler waits for data related to a specific auction, and when the auction is completed (after the data entry period and before the calculation period), it forwards it to the optimizer for further processing.

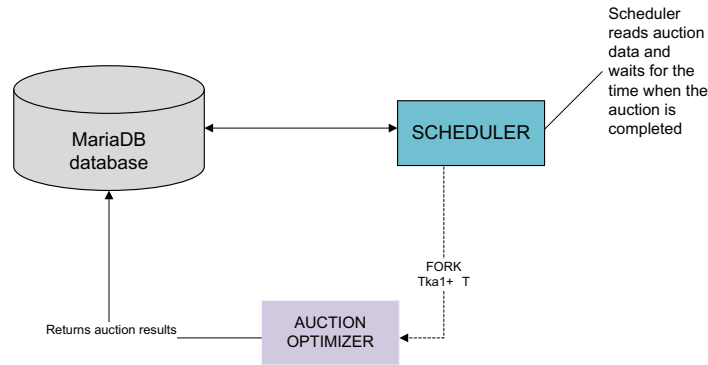


Figure 3. Scheduler and optimizer

After accepting the auction, the optimizer creates a linear problem structure in CPLEX format and solves it using the GNU Linear Programming Toolkit (GLPK) library for linear programming [5]. The optimization is performed independently for each time period (e.g., if the period is 1 hour, each hour will have a separate optimization).

The solutions are then stored in a database for further processing and display through a web interface. The obtained solutions represent the optimal values of bids (buy and sell) and their initial prices, as well as the allocated capacities and congestion prices in case the entire transmission capacity (CZC) is utilized. The complete procedure is illustrated in Figure 4.

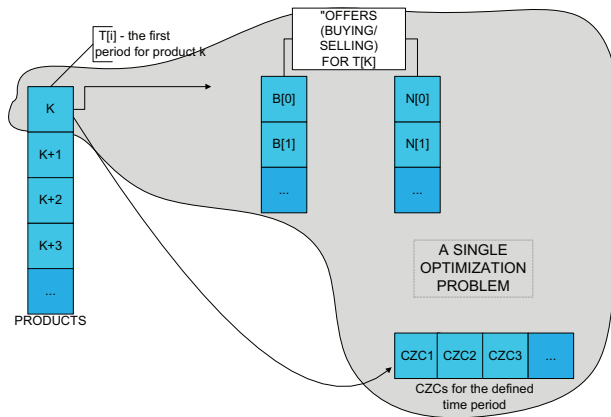


Figure 4. A single optimization problem

For each area, their final prices are calculated based on their belonging to the price zone.

In the beginning, in the first iteration, an initial price zone is created by solving the optimization problem. Then, for that area, the following calculations are performed on the buying offers:

$$p_1 = \min(\text{completely accepted buying offers})$$

$$p_3 = \max(\text{unaccepted buying offers})$$

Then, a pass is made through the selling offers, and the following calculations are performed:

$$p_2 = \min(\text{unaccepted selling offers})$$

$$p_4 = \max(\text{completely accepted selling offers})$$



Oral Presentation: Application for Optimization of Capacity Reserve Trading Auctions

Finally, their minimum and maximum values are calculated:

$$p_a = \min(p_1, p_2)$$

$$p_b = \max(p_3, p_4)$$

For the subsequent areas, a check is performed to determine if they belong to the same price zone (i.e., if the initial price is equal to the final price of that area). If they belong to the same price zone, the values of  $p_a$  and  $p_b$  are calculated. If an area does not belong to the same price zone, it is added to a new price zone, and the values of  $p_a$  and  $p_b$  are calculated. The next areas are compared to the existing price zones, and if they belong, they are associated with the corresponding price zone; otherwise, a new price zone is created.

Finally, the calculation of the final prices is performed. If there were partially accepted offers within the price zone, the initially obtained price is retained. Otherwise, the final price is obtained using the following formula:

$$F_c = \frac{p_a + p_b}{2} \quad (8)$$

#### 4. SOFTWARE IMPLEMENTATION OF OPTIMIZATION MODULE

The optimization algorithm is implemented in the C++ programming language using the GLPK library for linear programming. GLPK (Gnu Linear Programming Toolkit) is designed for solving large-scale linear programming (LP) problems, mixed integer programming (MIP), and other related problems. GLPK provides a set of routines written in ANSI C (which means it can be used within C/C++ applications) and is organized in the form of a library [5]. In our solution, this library is called from a C++ application.

The applications are developed for Linux (primarily supported on CentOS, Oracle Enterprise Linux, and Red Hat Enterprise Linux, but can also be used on other Linux platforms) on a 64-bit platform.

As the database platform, we used MariaDB 5.5, which is compatible with MySQL. The optimization module utilizes ODBC and the native MySQL C-API for connecting to the database.

#### 5. WEB USER INTERFACE AND APPLICATIONS

Web user interface and applications provide the following main functions:

- defining the auction
- uploading input data (CZC, Area limits, Block limits)
- uploading bids
- auction monitoring
- checking published results
- user administration

Users of the platform are assigned to specific user types by which they are enabled or restricted to access different functions of the Ancillary Services Market (ASM). There are 5 types of users:

- **Market participant** – BSP/Trader, placing orders to offer different balancing reserve products.
- **TSO** - Upload/change the ATC values and place orders for the purchase of different balancing reserve products.
- **National regulatory authorities (NRA)** – supervision of ASM/CRM platform and process. The supervisory role can be appointed to Regulators to follow the auction process and to observe the auction results.
- **Capacity Reserve Market Operator (CRMO)** – has the role of Administrator, platform configuration and auction settings are editable only for CRMO.
- **Guest** – can view the auction results.

The *GlassFish* application server is used as the platform for web applications. The architecture of the GlassFish application server is based on the Java EE (Enterprise Edition) standard. It is divided into several layers, each serving a specific purpose. The layers are as follows:

- **Presentation layer:** This layer is responsible for presenting the user interface to the client.
- **Web layer:** This layer handles web-based requests and provides web services.
- **Business logic layer:** This layer provides the core functionality of the application and implements the business logic.
- **Data layer:** This layer manages the connection to the database and handles data access.

The web application designed for end users is developed in the Java programming language. The applications are accessed from a web browser using the appropriate web address. Since the application is fully web-based, no additional software is required to run it apart from a standard web browser (*IE, Edge, Firefox, Chrome, Opera*). This means that the application can be launched from any operating system that has a compatible web browser.

As an interface with MariaDB based database JDBC is used. Examples of web-based HMI are shown in the following figures:

Home ▾ Auction ▾ Trading ▾ Results ▾ Logs ▾

**Trading/Dashboard**

Current Auction: TRINITY\_FCR\_260523  
 Product: FCR  
 Process Stage: Czc Upload/Bids Upload

Area/Region: BIH-Bugaria-Montenegro-N.Macedonia-Serbia  
 Date: 2023-05-26  
 Time: 00:00:00

Min quantity per bid: 0  
 Max quantity per bid: 999

Min price per bid: 0  
 Max price per bid: 999

Product	Area/Region	Date and Time	Phase	Ongoing Process
FCR	RS-ME-MK-BH-BG	2023-05-26 00:00:00	New	czc-upload: <b>in progress</b> bids-upload: <b>in progress</b>

Figure 5. Trading/Dashboard

Home ▾ Auction ▾ Trading ▾ Results ▾ Logs ▾ crmo Logout

**Auction/Registry**

Participate	Area	Area Code	EIC Y Code	TSO	LFC Block	Edit	Delete
<input checked="" type="checkbox"/>	Serbia	RS	10XCS-SBRBAT.S0B	EMS	SMM	<input type="checkbox"/>	<input type="checkbox"/>
<input checked="" type="checkbox"/>	Montenegro	ME	10XCS-CG.TSO-5	CGES	SMM	<input type="checkbox"/>	<input type="checkbox"/>
<input checked="" type="checkbox"/>	N.Macedonia	MK	10XMK-MEP30-M	MEP30	SMM	<input type="checkbox"/>	<input type="checkbox"/>
<input checked="" type="checkbox"/>	BIH	BH	10XBA-IPCZK.K	NOSEBH	SHD	<input type="checkbox"/>	<input type="checkbox"/>
<input checked="" type="checkbox"/>	Bugaria	BG	bg_etc_code	ESO	ESO	<input type="checkbox"/>	<input type="checkbox"/>

Add New Area

Participate	Area1	Area2	Edit	Delete
<input checked="" type="checkbox"/>	RS	ME	<input type="checkbox"/>	<input type="checkbox"/>
<input checked="" type="checkbox"/>	RS	MK	<input type="checkbox"/>	<input type="checkbox"/>
<input checked="" type="checkbox"/>	RS	BH	<input type="checkbox"/>	<input type="checkbox"/>
<input checked="" type="checkbox"/>	ME	BH	<input type="checkbox"/>	<input type="checkbox"/>
<input checked="" type="checkbox"/>	RS	BG	<input type="checkbox"/>	<input type="checkbox"/>
<input checked="" type="checkbox"/>	MK	BG	<input type="checkbox"/>	<input type="checkbox"/>

Add New Border

Participate	HSP	Area	FCR	aF-RN	mF-RN	NR	Trade Limit	Approved by ISO	Appr. by CRMO	Edit	Delete
<input checked="" type="checkbox"/>	RS_BSP1	RS	<input checked="" type="checkbox"/>	<input checked="" type="checkbox"/>	<input checked="" type="checkbox"/>	<input checked="" type="checkbox"/>	100000	<input checked="" type="checkbox"/>	<input checked="" type="checkbox"/>	<input type="checkbox"/>	<input type="checkbox"/>
<input checked="" type="checkbox"/>	RS_BSP2	RS	<input checked="" type="checkbox"/>	<input checked="" type="checkbox"/>	<input checked="" type="checkbox"/>	<input checked="" type="checkbox"/>	100000	<input checked="" type="checkbox"/>	<input checked="" type="checkbox"/>	<input type="checkbox"/>	<input type="checkbox"/>

Time	Log Message
2023-05-22 14:50:14	TRINITY_mFRRDown_260523: CZC-s uploaded by user crmo.
2023-05-22 14:50:03	TRINITY_mFRRUp_260523: CZC-s uploaded by user crmo.
2023-05-22 14:49:50	TRINITY_FCR_260523: CZC-s uploaded by user crmo.

Figure 6. Auction/Registry





Oral Presentation: Application for Optimization of Capacity Reserve Trading Auctions

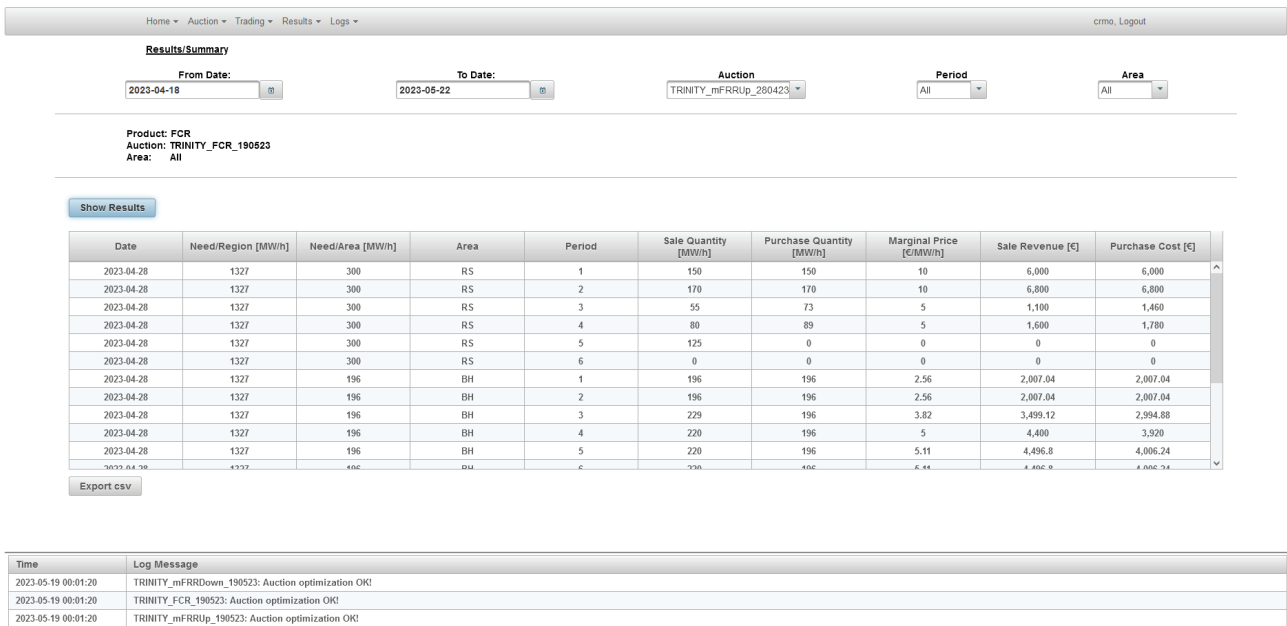


Figure 7. Results/Summary

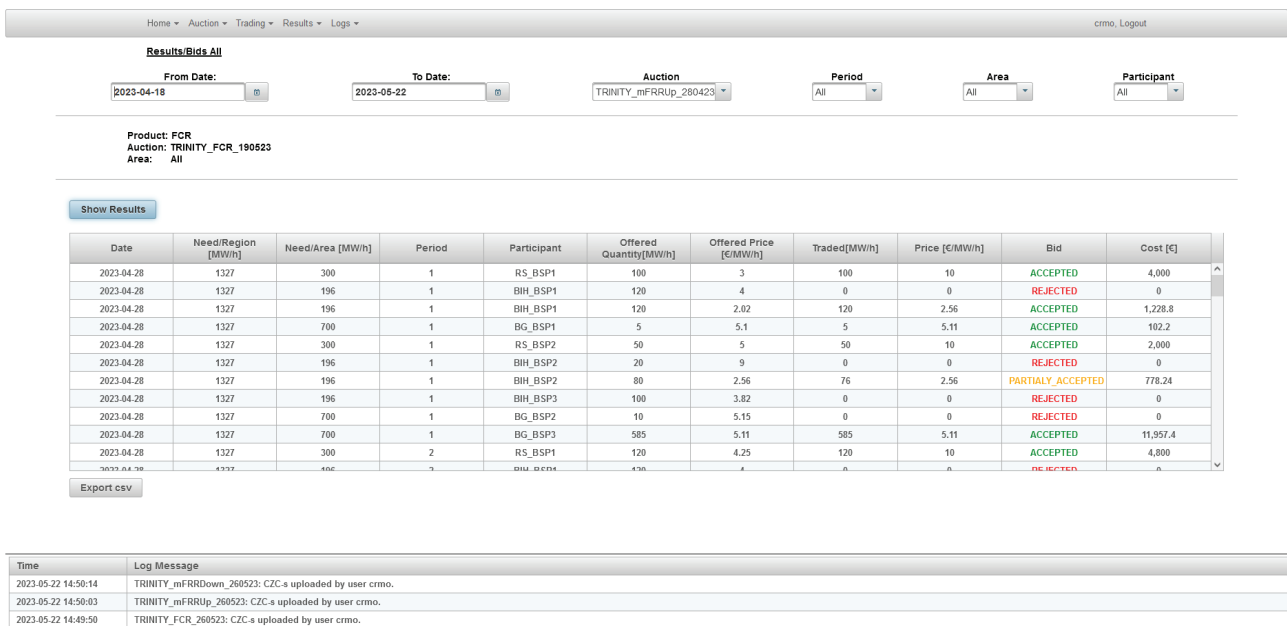


Figure 8. Results/Bids All

In addition to the web interface intended for use by auction platform end-users, as part of the optimization module development, an auxiliary tool for auction input has been developed. Within this testing tool, it is possible to generate and display auction results. Java 1.8 JDK and Swing GUI framework were used for the testing tool development. In Figure 9, a part of the user interface of the testing tool is shown.



Oral Presentation: Application for Optimization of Capacity Reserve Trading Auctions

CRM AUCTION GENERATOR

Menu Auction

Auction	Control Blocks	Areas	Area Connectivity	TSOS	BSPS	Area exchange limits	CZC	Bids	
Area name	BSP name	Product type	Sale/Purchase	Period	Period date	Period time	Quantity	Price	Status
	EPS	mFRR	sale	60	2021-07-07	16:00:00	200	2.5	NEW
	EPS	mFRR	sale	60	2021-07-07	16:00:00	100	3.2	NEW
	EPS	mFRR	sale	60	2021-07-07	16:00:00	100	4.5	NEW
	EPCG	mFRR	sale	60	2021-07-07	16:00:00	100	3.5	NEW
	EPCG	mFRR	sale	60	2021-07-07	16:00:00	80	4.8	NEW
	EPCG	mFRR	sale	60	2021-07-07	16:00:00	50	5.5	NEW
	EPBIH	mFRR	sale	60	2021-07-07	16:00:00	180	4.4	NEW
	EPBIH	mFRR	sale	60	2021-07-07	16:00:00	50	5	NEW
	EPBIH	mFRR	sale	60	2021-07-07	16:00:00	30	6	NEW
Serbia		mFRR	purchase	60	2021-07-07	16:00:00	150	9	NEW
Serbia		mFRR	purchase	60	2021-07-07	16:00:00	100	4.2	NEW
Serbia		mFRR	purchase	60	2021-07-07	16:00:00	150	2.2	NEW
Montenegro		mFRR	purchase	60	2021-07-07	16:00:00	120	8.5	NEW
Montenegro		mFRR	purchase	60	2021-07-07	16:00:00	50	4.1	NEW
Montenegro		mFRR	purchase	60	2021-07-07	16:00:00	50	2.2	NEW
BIH		mFRR	purchase	60	2021-07-07	16:00:00	200	9.5	NEW
BIH		mFRR	purchase	60	2021-07-07	16:00:00	150	6.2	NEW
BIH		mFRR	purchase	60	2021-07-07	16:00:00	40	3.8	NEW

Figure 9. Testing tool example - Auction Generator

6. EXAMPLE OF AUCTION

For the validation of the optimization module, a sample with three areas defined in Figure 3 was used. The transmission capacity constraint (CZC/ATC) is 50MW between all areas, while there is only a constraint between the third and second areas. The selected product is up mFRR (manual Frequency Restoration Reserve). Based on the results shown in Figure 10, it can be seen that there are: 9 fully accepted offers, 3 partially accepted offers, and 6 rejected offers.

CRM AUCTION GENERATOR

Menu Auction

Auction Results

TEST AUCTION 2021-07-15 16:14

Auction name	Auction Assigned	Auction Completed	Auction Status
TEST AUCTION 2021-07-15 16:14	yes	yes	success

Bids

Area	BSP	Type	Date	Time	Quantity	Accepted quantity	Price	Settled price	Surplus	Status
BIH	BIH TSO	mFRRup purchase	2021-07-07	16:00:00	200	200	9.50	6.00	700.00	ACCEPTED
BIH	BIH TSO	mFRRup purchase	2021-07-07	16:00:00	150	150	6.20	6.00	30.00	ACCEPTED
BIH	BIH TSO	mFRRup purchase	2021-07-07	16:00:00	40	0	3.80	0.00	0.00	REJECTED
BIH	EPBIH	mFRRup sale	2021-07-07	16:00:00	30	20	6.00	6.00	0.00	PARTIALLY_ACCEP...
BIH	EPBIH	mFRRup sale	2021-07-07	16:00:00	180	180	4.40	6.00	288.00	ACCEPTED
BIH	EPBIH	mFRRup sale	2021-07-07	16:00:00	50	50	5.00	6.00	50.00	ACCEPTED
Montenegro	Montenegro TSO	mFRRup purchase	2021-07-07	16:00:00	50	0	4.10	0.00	0.00	REJECTED
Montenegro	Montenegro TSO	mFRRup purchase	2021-07-07	16:00:00	50	0	2.20	0.00	0.00	REJECTED
Montenegro	Montenegro TSO	mFRRup purchase	2021-07-07	16:00:00	120	120	8.50	4.80	444.00	ACCEPTED
Montenegro	EPCG	mFRRup sale	2021-07-07	16:00:00	100	100	3.50	4.80	130.00	ACCEPTED
Montenegro	EPCG	mFRRup sale	2021-07-07	16:00:00	80	20	4.80	4.80	0.00	PARTIALLY_ACCEP...
Montenegro	EPCG	mFRRup sale	2021-07-07	16:00:00	50	0	5.50	0.00	0.00	REJECTED
Serbia	Serbia TSO	mFRRup purchase	2021-07-07	16:00:00	150	150	9.00	4.20	720.00	ACCEPTED
Serbia	Serbia TSO	mFRRup purchase	2021-07-07	16:00:00	100	50	4.20	4.20	0.00	PARTIALLY_ACCEP...
Serbia	Serbia TSO	mFRRup purchase	2021-07-07	16:00:00	150	0	2.20	0.00	0.00	REJECTED
Serbia	EPS	mFRRup sale	2021-07-07	16:00:00	100	100	3.20	4.20	100.00	ACCEPTED
Serbia	EPS	mFRRup sale	2021-07-07	16:00:00	100	0	4.50	0.00	0.00	REJECTED
Serbia	EPS	mFRRup sale	2021-07-07	16:00:00	200	200	2.50	4.20	340.00	ACCEPTED

Figure 10. Auction Results - Offers and Prices

In Figure 11, the allocated CZC results and congestion revenues are provided for both directions.

CRM AUCTION GENERATOR

Menu Auction

Auction Results

TEST AUCTION 2021-07-15 16:14

Auction name	Auction Assigned	Auction Completed	Auction Status
TEST AUCTION 2021-07-15 16:14	yes	yes	success

Bids

Border/direction	Date	Time	CZC [MW]	Allocated CZC [MW]	Congestion Price [EUR/MW]	Congestion Income [EUR]
Serbia->Montenegro	2021-07-07	16:00:00	50	50	0.60	29.99
Serbia->BIH	2021-07-07	16:00:00	50	50	1.80	89.99
Montenegro->Serbia	2021-07-07	16:00:00	50	0	-0.60	0.00
Montenegro->BIH	2021-07-07	16:00:00	50	50	1.20	60.00
BIH->Serbia	2021-07-07	16:00:00	50	0	-1.80	0.00
BIH->Montenegro	2021-07-07	16:00:00	50	0	-1.20	0.00

Figure 11. The auction results - allocated capacities.



## 7. CONCLUSION

The current trends in Europe and the world are driving the implementation of renewable energy sources, demand response, and the use of electric vehicles through market mechanisms in the organization of the electricity market. This has led to an increased importance of providing balancing energy to ensure the continuous and secure operation of the power system while maintaining appropriate power quality. To engage in balancing energy, it is necessary to pre-book sufficient capacity for all products used for system balancing.

The capacity reserves trading platform, which is necessary to provide reserves for balancing the power system, represents a software solution that enables regional collaboration for the exchange of balancing reserves (FCR, aFRR, mFRR, RR). It allows the inclusion of multiple control areas from different control blocks in the SEE region. As such, the platform uses an optimization algorithm that combines different sets of trading constraints that differentiate the treatment of reserve exchanges between control areas within the same control block and between control areas from different control blocks. This represents a unique solution compared to the previous cooperation in the Continental Europe Synchronous Area.

This platform is a regional market-based tool in the process of procuring regional capacity reserves on a weekly basis through an auction mechanism. It enables the procurement of reserves as close as possible to real-time, taking into account the system's condition, the procurement time frame, the location of capacity providers offering balancing services, and increasing the number of participants, which will lead to increased competition and obtaining the real market value for capacity reservations. The regional approach to reserve procurement allows for the sharing of reserves within the region, reduces the overall costs for individual TSOs, increases the security of power system operation, optimizes the use of generation capacity, and enhances cross-border cooperation between TSOs.

## 8. ACKNOWLEDGEMENTS

The work described in this paper has been conducted within the HORIZON 2020 TRINITY project (*H2020-863874 Transmission system enhancement of regional borders by means of Intelligent market technology*). The research and development described in this paper have been produced with the financial assistance of the European Union. The contents of this document are the sole responsibility of the authors and can under no circumstances be regarded as reflecting the position of the European Union. Additionally, the research described in this paper was funded by the Ministry of Education, Science, and Technological Development of Serbia.

## BIBLIOGRAPHY

- [1] T-MARKET COUPLING FRAMEWORK, <http://trinityh2020.eu/>
- [2] "ELECTRICITY BALANCING IN EUROPE, AN OVERVIEW OF THE EUROPEAN BALANCING MARKET AND ELECTRICITY BALANCING GUIDELINE", European Network of Transmission System Operators for Electricity (ENTSO-E), November 2018
- [3] Goran Jakupović, Nikola Stojaković, Zoran Vujasinović, Nebojša Jović, Dušan Vlaisavljević, Jasmina Trhulj, "SOFTWARE ENVIRONMENT (SIMULATOR) FOR TECHNICAL SUPPORT OF CROSS-BORDER ELECTRIC ENERGY BALANCING IN WB6 REGION", 3rd SEERC Conference Vienna 2021 (online), 30th November 2021
- [4] Goran Jakupović, Ninel Čukalevski, Nikola Obradović, Duško Aničić, "Implementation of Reserve Trading in SMM ENTSO-E Control Block", SEERC Power Conference, Portoroz, Slovenia, 7th-8th June 2016
- [5] Andrew Makhorin, "GNU Linear Programming Kit – Reference Manual for GLPK Version 4.58", Free Software Foundation, Inc., February 2016



# Autonomous Mobile Robot for Warehouse Logistics

[tayrancioglu@teknokaucuk.com.tr](mailto:tayrancioglu@teknokaucuk.com.tr)**CEMİL ŞEN\*, SELİN MİNA KÜTÜK**  
*Yildiz Technical University***ŞEYMA TUĞBA AYRANCIOĞLU**  
*Tekno Kauçuk Sanayii A.Ş.***Türkiye**

## SUMMARY

In warehouse logistic, there is various methods to supply the logistics. In generally, logistics is held by the manual workers and several forklifts. However, manual logistics need more cost and there is non-acceptable high level of accident rate. Therefore, factories need to eliminate the risk of accidents and reduce the unit operation time with the cost-effective way.

Within the industrialization, warehouse logistics sector tends to apply more autonomous and intelligent solutions to their operations. Due to this orientation, unit logistic cost and operation duration is decreasing.

In industry manual labor replacing with autonomous mobile robot. In addition to this, mobile robot has been seen in the other sectors and with respect the value of mobile robot, investments on that ascends.

There is different type of mobile robots. Most prior ones on the industrial usage sorting, pick and place and service robots. In "Autonomous Mobile Robot for Warehouse Logistic" project, designed robot is aimed to execution of lifting operation with the help of the dynamic mapping and localization package. Within this package, system becomes more dynamic and collision avoidance. For mapping laser scanner based 2-D mapping has been chosen.

In that project mobile robot differs from the others. It has additional proactive cautions. One of them is for flood and other is risk of fire detections. In addition to this, workers can observe and call the mobile robot from any location on the warehouse via the designed guided user interface.

## 1. INTRODUCTION

### 1.1. Motivation

Nowadays, in the manufacturing and warehouse area autonomous mobile robots (AMR) are helping to transport many products which play an important role in the development of humanity. In this project improved AMRs are used in the smart warehouses. The robots minimize driver errors in human-driven transport systems. The field workers can be direct to the tasks which require complex human skills. It adapts to changing environments in warehouse area dynamically. It provides not interrupt the production line and minimize occupational injury, so it helps to be fast storage. Considering all these, autonomous mobile robots bring a new breath to the warehouse technology and support sustainable transportation process.

## KEYWORDS

Warehouse – autonomous – SLAM – Lidar – logistic – ROS



AMR which is aimed to be built a prototype in this project is intended to move in the area with mechatronic system equipment. Equipped with sensors the robot will prevent the pre-specified dangers while driving around the area, also inform the user about the danger which may occur (fire, flood, etc.) in the area. Thus, it will help not to interrupt the production in the manufacturing area (lean manufacturing).

Dangerous situations in storage areas cause both material and nonmaterial losses. For this reason, the developed robot is requested to be safer, more efficient, and cost-effective as compared to other robots in the market. Within the framework of these purposes and motivation, a domestic autonomous mobile robot has been designed, which will be offered to the user at a friendly cost and where after-sales engineering services will be provided domestically.

1.2. Literature Review

Warehouse automation splits into four main headings:

- Basic Warehouse Automation: This automation type is the simplest technology. It refers manual labor which is assisted by people.
• Warehouse System Automation: This automation type uses software for machine learning and data analytics. It generally does automation for the repeated activities. Therefore, it saves the time and reduce cost due to the traverse.
• Mechanized Warehouse Automation: This warehouse automation generally uses robotic systems and its' equipment to assist humans and with respect to them warehouse.
• Advanced Warehouse Automation: Advanced warehouse automation is the combination of the mechanized warehouse robotics and automation systems. As a result of this combination, robotic system which equipped intelligent and proactive systems make autonomous operation in contrast with the manual type.

Warehouse automation technology includes various type of product options which are:

- Goods-to-Person (GTP)
• Automated Storage and Retrieval Systems (AS/RS)
• Automatic Guided Vehicles (AGVs)
• Autonomous Mobile Robots (AMRs)
• Pick-to-Light and Put-to-Light Systems
• Automated Sortion Systems [1]

Table 1: Autonomous Mobile Robot at Sector

Table with 4 columns: Product Name, AMB-J 150 [2], LD-60 [3], Mir-100 [4]. Rows include Load Capacity, Weight, Operation Time, Recharging Time, Operation Speed, Navigation Method, Ambient Humidity, Safety Precautions, Battery Type, and Floor Incidence.



## 2. REQUIREMENTS

The Table:4 was established for aimed specifications according obtained from the literature review. the specifications are aimed, and they have added the table obtained data in the realization.

**Table 2:** Technical Specifications

Technical Requirements	Target	Realized
Navigation method	LIDAR SLAM	LIDAR SLAM
Navigation Speed [m/s]	~ 0.7	0.3
Mapping Algorithm	Gmapping	HectorSlam
LxWxH [mm]	~ 800x600x300	820x620x236
Weight (with battery, no load) [kg]	~ 25	32
Load capacity [kg]	15	5
Lifting platform dimensions [mm]	550x380	595x385
Operation Time (minute)	~ 60	60

### 2.1. Mechanical Calculations

#### 2.1.1. Required Torque

In a first-place calculation of required force and with respect to the composition of the required force we need to obtain appropriate torque and power quantity.

To obtain the result we need to modelling the system for the specific operation medium. With respect to the system assumption corresponding to the environment, maximum slope on the warehouse is 3 degrees. [7]

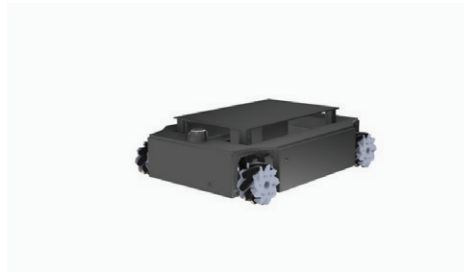


**Figure 1:** Mobile Robot 3D Model

#### 2.1.2. Aerodynamic Drag Force

In the defined mobile robot project, it is aimed to modelling system which moves at relatively low speeds in the range of 0-1 m/s. In reality, there is more intense relation with velocity and aerodynamic drag. However, at that speed aerodynamic drag force which effects on load and body relatively small. To obtain more precise modelling, aerodynamic force has been included the modelling phase.

$$F_{ad} = \frac{1}{2} \cdot p \cdot A \cdot C_d \cdot V^2 \quad (\text{Eq. 3.1})$$

As an interpretation of calculations; medium and operation conditions and geometry of whole system has priority impact on the aerodynamic drag force.

$$F_{ad} = \frac{1}{2} \cdot 1.225 \cdot (7,2 \cdot 10^{-5} + 1,8 \cdot 10^{-4}) \cdot 0.35 \cdot (1.8)^2$$

$$F_{ad} = 1.75 \cdot 10^{-4} [N]$$

### 2.1.3. Climbing Force

As mentioned on the assumptions and environment properties, mobile robot will be on the effect on maximum 3-degree incline. With respect to that incline climbing force should be calculated.

$$F_{cf} = m \cdot g \cdot \sin(\theta) \quad (\text{Eq 3.2})$$

$$\theta = 3^\circ \text{ (Maximum)}$$

$$F_{cf} = m \cdot g \cdot \sin(3^\circ)$$

$$F_{cf} = (25 + 15) \cdot 9.81 \cdot \sin(3^\circ) = 20.53 \text{ [N]}$$

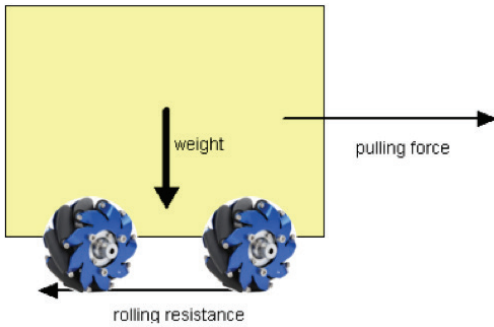


Figure 1: Free Body Of Mobile Robot

### 2.1.4. Wheel Rolling Force

In the real world, there is no system which is perfect. When wheel is rolling there is force between the ground and wheel. It is most critical point which needs to know about calculation, rolling coefficient is significantly less than friction force.

$$F_r = \mu_{rr} \cdot m \cdot g \cdot \cos(\theta) \quad (\text{Eq 3.3})$$

$$m = 25 \text{ (mobile robot)} + 15 \text{ (payload)} = 40 \text{ [kg]}$$

$$g = 9.81 \text{ [m/s}^2\text{]}$$

$$\mu_{rr} = 0.015$$

$$F_r = \mu_{rr} \cdot m \cdot g \cdot \cos(\theta) = 0.015 \cdot 40 \cdot 9.81 \cdot \cos(3^\circ) = 5.877 \text{ [N]}$$

### 2.1.5. Accelerating Force

$$\int_{s_0}^s ds = \int_{t_0}^t (v_0 + a \cdot t) dt = 5 \text{ m} \quad (\text{Eq 3.4})$$

$$v_0 \cdot t + a \frac{t^2}{2} = 5$$

**The time duration** : 5 seconds

**Initial Conditions** :

$$v_0 : 0$$

$$a : 0.4 \text{ [m/s}^2\text{]}$$

$$F_a = m \cdot a = 40 \cdot 0.4 = 16 \text{ [N]} \quad (\text{Eq 3.5})$$

### 2.1.6. Total Force Acting On the System

$$F_{total} = F_a + F_r + F_{ad} + F_{cf} \quad (\text{Eq 3.6})$$

$$F_{total} = 16 + 5.877 + 1.75 \cdot 10^{-4} + 20.53 = 42.407 \text{ [N]}$$

### 2.1.7. Torque Calculations

$$T = F_{total} \cdot r \quad (\text{Eq 3.7})$$

$$\text{Required Torque} = 42.407 \times 0.076 = 3.223 \text{ [N.m]}$$

Therefore, we can define the number of drive motors to find the appropriate motor and drive system for the solution [8].



$$\text{Required unit motor torque} = \frac{\text{Required total torque}}{\text{Number of Drive motor}}$$

$$\text{Required unit motor torque} = \frac{3.223}{4} = \mathbf{0.8057 [N.m]}$$

Within the result of calculation, project is planned to use 4 motors. Therefore, each motor should be capable to supply **0.8057 [N.m]** torque value.

### 2.1.8. Required Power Calculations

$$\text{Power} = \text{Torque} \cdot \text{Angular Velocity} = \mathbf{T \cdot \omega} \quad (\text{Eq 3.8})$$

In the scope of the Project, fixed linear velocity is 0.7 m/s and it is already known the relation of linear velocity equals to the radius and angular velocity's multiplication;

$$\mathbf{V = w \cdot r} \quad (\text{Eq 3.9})$$

$$0.7 = w \times 0.076 \text{ and we can find that } \mathbf{w = 9.21 \text{ rad/s}}$$

Motor rpm calculation:

$$\frac{2 \cdot \pi \cdot rpm}{60} = \text{rad/s}$$

Motor speed is: 88 rpm

$$\text{Power for each motor: } 0.8057 [N.m] \times 9.21 = \mathbf{7.4205 [W]}$$

Total system power needs:

$$\text{Each motor power needs} \times \text{Number of motor} = 7.4205 \times 4 = \mathbf{29.682[W]}$$

### 2.1.9. Battery Calculation

Chosen motor has a peak current of **5.5 A** and rated current of **2 A** with the rated voltage of **12 Volts** each motor. Since there are 4 motors, continuous current  $A_c$  and peak current  $A_p$  needed is

$$\mathbf{A_c = 2 A \cdot 4 = 8 A}$$

$$\mathbf{A_p = 5.5 A \cdot 4 = 22 A}$$

Therefore, the Li-po batteries of 4S 10000 mAh 25C Li-po Battery pack will give 10A/hour as,

The motors are needed continuous current as 8A. It is assumed that other electronic components will draw 2A current,

$$10000 \text{ mAh} / 10A = 1/h$$

Which allows system to work for at least 1 hours under normal load conditions.

## 3. MECHANICAL DESIGN

The model of the robot is designed by using the Solidworks program by looking at some designs in the market and desired technical specifications. Material assignment, weight and dimensions of the design have been big important before the assembly phase. The material was chosen to carry the useful loads and be durable to impact.

## 4. ANALYSIS

In this project, Static deformation analysis is simulated via Solidworks Simulation Add-in.

Load surface stress analysis use von Misses method to determine if a given material will yield or fracture. The external force is defined as 150 N according to the specifications, and the material is 5754 aluminium alloy. As seen in Figure:2, there is stress just on the bending edge.

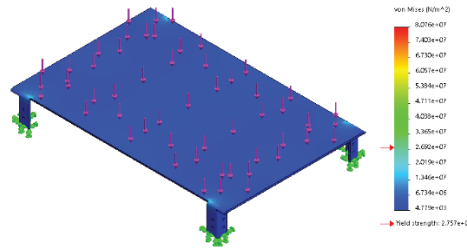


Figure 2: Stress Results of Load Surface

Displacement analysis is made for measuring surface failure after putting the load. The maximum displacement for the load surface is  $4.45675 \cdot 10^{-4}$  m.

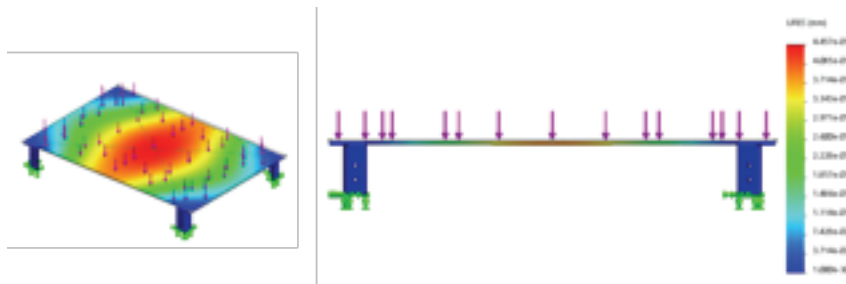


Figure 3: Displacement Result of Load Surface

## 5. ELECTRICAL DESIGN

### 5.1. Controller

Development cards or microcontrollers work like a computer of an electronic circuit. They are electronic cards with hardware such as processor, storage and memory. They process the data they receive according to the written code and output them; they allow the outside element to perform its function. With the renewal of their software, they can do this over and over again. In this project, Arduino Mega development kit will be used for motor driving operations.

### 5.2. Control Of Motor

A DC motor cannot be controlled by itself like a servo or stepper motor. With an added encoder, you can follow the motor revolutions, the distance travelled, and in this way, a nice feedback system can be made that can be used to control the DC motor. To read data coming from encoder, a controller is needed. Since controller cannot provide large amount of power to the motor, a driver must be placed between controller and motor. Controller applies instructions that determined by programming, to the driver and driver runs the motor.

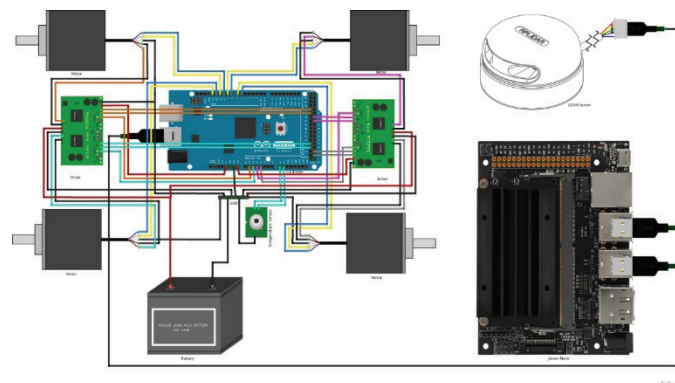


Figure 4: Schema of the Electric Components



## 6. SOFTWARE

### 1.1. Mapping Method

During the operation, the autonomous mobile robot must map the environment that it did not know before, and accordingly, determine its location simultaneously. In this context, the mobile robot should use SLAM algorithms, which means simultaneous localization. Landmark extraction, data association, state estimation, state and landmark update create SLAM.

Visual Slam uses images which are supplied from the cameras and other image sensors. Wide angle, fisheye, spherical, RGB-D cameras are the basic camera types which are currently used in VSLAM. Monocular SLAM is used for the situation when there is only one camera is used for the VSLAM. Due to the problems of detecting depth with one camera, these systems use another sensor such as inertial measurement units (IMUs), which can measure physical quantities such as velocity and orientation.

Algorithms which have been used for VSLAM can be classified into mainly two categories. Sparse methods match feature points of images, and they use algorithms which are PTAM and ORB-SLAM. Dense methods use the overall brightness of images, and they use algorithms which named DTAM, LSD-SLAM, DSO, and SVO. [3]

The main other SLAM method is Lidar SLAM. When compared with the VSLAM, this method can work at various working conditions and gives precise solutions. Laser scanning-based SLAM method especially common applications which are mainly;

- High-Speed vehicles
- Self - driving cars
- Drones

In literature, mapping which the output of the SLAM can be composed in a form generally 2D (x, y) or 3D (x, y, z) point cloud data. The laser sensor point cloud provides high-precision distance measurements and works very effectively for map construction with SLAM. For lidar point cloud matching, registration algorithms such as iterative closest point (ICP) and normal distributions transform (NDT) algorithms are used. 2D or 3D point cloud maps can be represented as a grid map or voxel map. [3]

On the other hand, point clouds are not as finely detailed as images in terms of density and do not always provide sufficient features for matching. For example, in places where there are few obstacles, it is difficult to align the point clouds, and this may result in losing track of the vehicle location. In addition, point cloud matching generally requires high processing power, so it is necessary to optimize the processes to improve speed. Due to these challenges, localization for autonomous vehicles may involve fusing other measurement results such as wheel odometry, global navigation satellite system (GNSS), and IMU data.

In the proposed project, there is certain restriction due to the dynamic structures. Especially, for the dynamic obstacles, mapping capability of JETSON NANO for the large area is limited. As a consequent, 2D LIDAR mapping has been chosen.

### 5.2. LIDAR SLAM Methods

2D mapping has been established. Within the project scope and literature research intersection, there is prior algorithms to use mapping

- 1) GMapping
- 2) Hector SLAM
- 3) Cartographer [4]

Within the project scope, there is 2D Mapping has been processed. As a result of literature review, Gmapping has been decided to use.



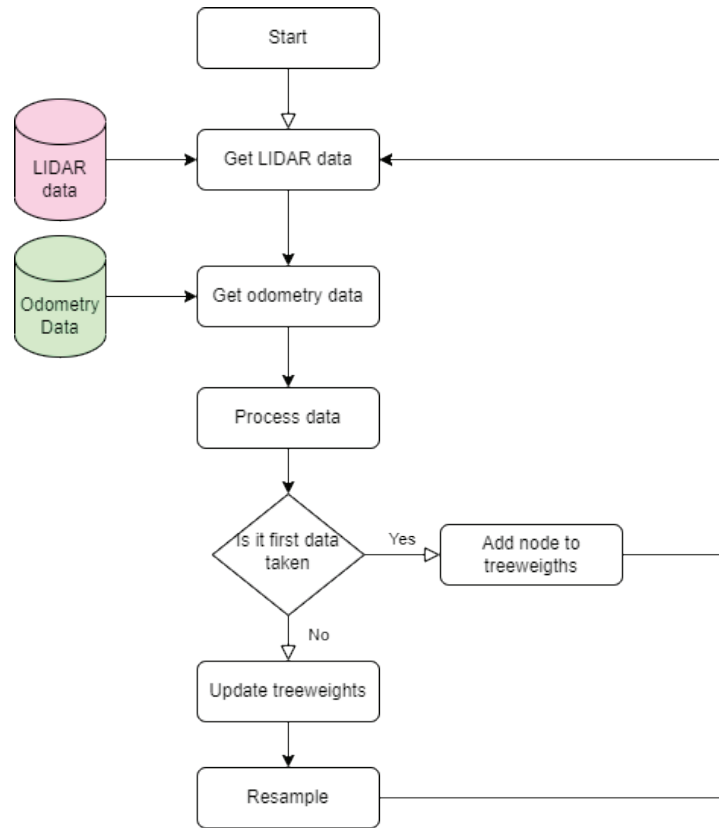


Figure 5: Flowchart of GMapping Algorithm

### 5.3. Mapping

#### 5.3.1. Map With LIDAR

System has been controlled at a 0.11 m/s to provide stable and accurate map. In the mapping process, Rplidar A2M8 LIDAR has been used.

As a result of mapping process of E2 Block of Yildiz Technical University Mechatronics Engineering Laboratory; cabinet, chairs, doors, and walls are seen obviously and accurate position.

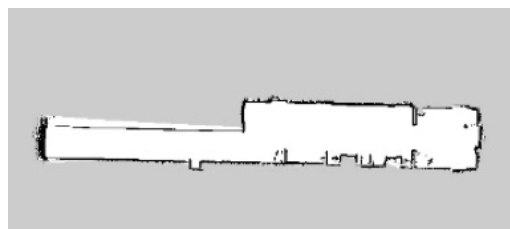


Figure 6: PGM File of Corridor of Laboratory

### 5.4. Localization

There are many localization methods used in the industrial applications. The oldest one of these is GPS. Although this system is useful in outdoor, it is inefficient in closed areas, underground or near high-rise buildings. So nowadays different methods are used for localization in the literature. The following systems have been studied to be used in this project.

- AMCL
- Hector-Slam

Among these systems, AMCL's position error rate (0.20 cm) will be chosen because it is less than Hector-Slam's (0.35 cm) error rate. [5]

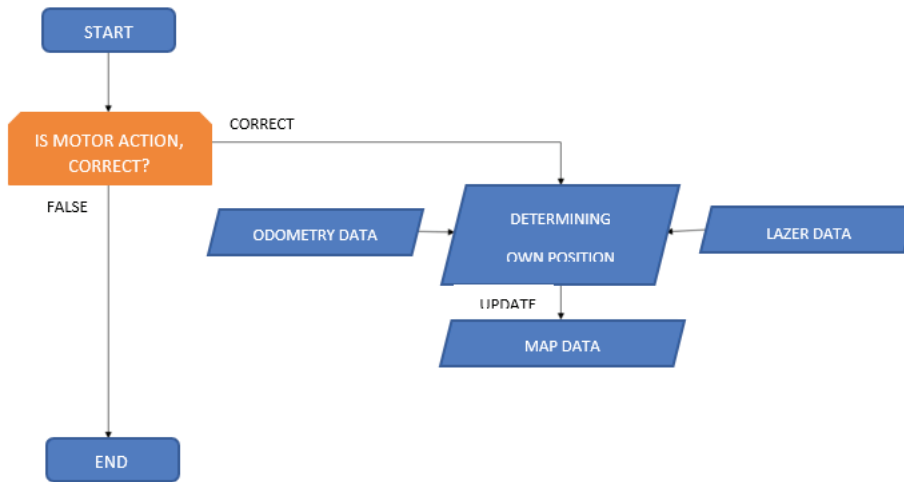


Figure 7: Block Diagram of Positioning Algorithm

AMCL positioning is obtained as follows;

The map will be created in the first place. Secondly, this map is divided into matrices. They recognize each other by the triangular matching method with the positioning in the matrices. Each of these positions is assigned an ID, and each of these IDs has a weight. These weights are calculated as orientation and positioning weights. Lastly, these calculated weights are converted into position matrix and determine the position of the vehicle. [6]

Two important data will be used while collecting location information: odometry data and laser data. Laser data from LIDAR will be the most important data of the system.

Odometry data is IMU and Encoder information. Since IMU is generally used in unmanned aerial vehicles, the vehicle to be integrated as odometry data will have encoder information. Laser data is the distance information of the beam coming from LIDAR. Thus, by taking both data, positioning will be done without hitting obstacles.

### 6.4.1. Localization Results

AMCL works with LIDAR, transform messages and as a output, it provides estimation of location. AMCL subscribe :

- Scan
- Tf
- Initial pose
- Map messages

After bein subscriber to them, AMCL also pusblish these :

- AMCL pose
- Particle Cloud
- Tf

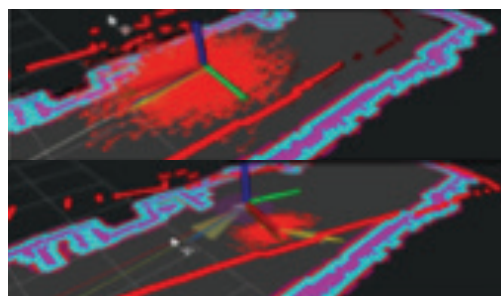


Figure 8: AMCL Results

As a result of the AMCL data, it is seen that, dimension and scattering of particle cloud is less in below image. That scattering is decreased because, below image pose estimate has been created after navigating on the test environment. Due to that reason, estimation parameter accuracy is increased.

## 6.5. Path Planning

In the project, the transactions were made over ROS. ROS packages are also used for route planning algorithms. The ROS Navigation Stack uses two cost maps to store information about obstacles in the world.

### Global Costmap

A configuration file created for global costmap.

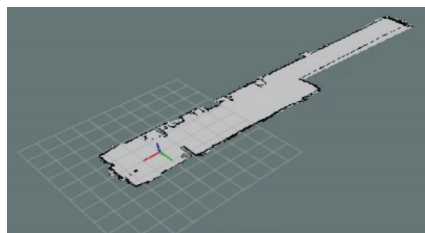


*Figure 9: Global Costmap of Mapped Place*

### Local Costmap

Created a configuration file that will house parameters for the local costmap.

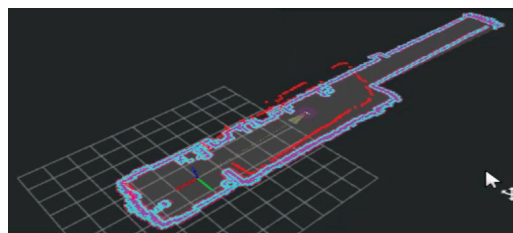


*Figure 10: Local Costmap of the Mapped Area*

### Base Local Planner Configuration and Move Base Node

In addition to the cost map configurations made in the previous section, it is necessary to configure the basic local planner of the ROS Navigation Stack. Base local planner calculates velocity commands sent to robot base controller.

Now that the configuration files have been created, it is necessary to add them to the initialization file. Configuration files will be used by the move\_base node of the ROS Navigation Stack. The move\_base node is the backstage workhorse responsible for planning a collision-free path for a mobile robot from a start location to a target location.

After the navigation goal estimation command, algorithms are completed and a route planning is assigned between the target point and the robot's point. The route is shown green line in the figure below.

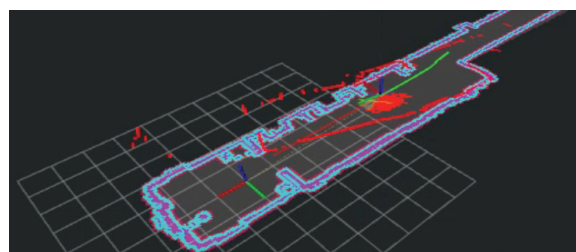


*Figure 11: Path Planning (Green Line)*



## 7. CONCLUSION

Within the effectuation of the project, it is aimed to use the human factor more efficiently in the production and storage areas. As a result of execution of autonomous mobile robot project, it is aimed to design and realize mobile robot which capable for indoor warehouse logistics with the help of its dynamic mapping feature. As a whole product, it is capable to execute mapping, lifting, transportation any location through the factory. All feature and operation cycle of mobile robot can be observed and controlled via designed graphical user interface.

Mechanical design, algorithm and compatible platforms has been decided. As next studies, it is planned to execute the assembly all set components of parts and also realize system work and test it.

This project is supported by the Tekno Kauçuk company financially and by giving the opportunity to test it in the production area. The product is requested to be used by this company at the end of project.

Another financial sponsor, TÜBİTAK, expects to contribute to the national literature with the articles to be written.

As future works of the project, it is planned to merge additional duties for robot to execute. These properties are, communication with the doors and elevators, adding arm mechanism to use different purposes.

## BIBLIOGRAPHY

- [1] "Netsuite," [Online]. Available: <https://www.netsuite.com/portal/resource/articles/inventory-management/warehouse-automation.shtml>.
- [2] "Seer-group," [Online]. Available: <https://www.seer-group.com/agvs/amr-robots/AMB-J>.
- [3] "Assets," [Online]. Available: [https://assets.omron.eu/downloads/datasheet/en/v16/i828\\_id-series\\_mobile\\_robot\\_datasheet\\_en.pdf](https://assets.omron.eu/downloads/datasheet/en/v16/i828_id-series_mobile_robot_datasheet_en.pdf).
- [4] "Mobile-industrial-robots," [Online]. Available: <https://www.mobile-industrial-robots.com/solutions/robots/mir100/>.
- [5] "Globenewswire," [Online]. Available: <https://www.globenewswire.com/news-release/2021/11/15/2334194/0/en/Autonomous-Mobile-Robots-Market-Size-Share-Business-Insights-Vital-Challenges-and-Forecast-Analysis-by-2028.html>.
- [6] "fortune business insights," [Online]. Available: <https://www.fortunebusinessinsights.com/autonomous-mobile-robots-market-105055>.
- [7] "Servo magazin," [Online]. Available: [https://www.servomagazine.com/uploads/issue\\_downloads/pdf/Tips%20For%20Selecting%20DC%20Motors%20For%20Your%20Mobile%20Robot.pdf](https://www.servomagazine.com/uploads/issue_downloads/pdf/Tips%20For%20Selecting%20DC%20Motors%20For%20Your%20Mobile%20Robot.pdf).
- [8] A. Habibov, "Simultaneous Positioning and Mapping with Mobile Robots, Yıldız Technical University Institute of Science and Technology, Fbe Computer Engineering Department," *Istanbul, Türkiye*, vol. Yıldız Technical University Institute of Science and Technology, 2011.



# Central Dispatching and Generation Control System for Electric Power Industry of Serbia

[goran.jakupovic@pupin.rs](mailto:goran.jakupovic@pupin.rs)

**GORAN JAKUPOVIC\*, TAMARA JELIC, PAVLE LUCIC, GORDAN KONECNI**  
*Institute "Mihajlo Pupin", University of Belgrade*

**DRAGAN SURUDZIC, ZLATKO MITROVIC, MIODRAG VULIC**  
*Electric Power Industry of Serbia (EPS)*

Serbia

## SUMMARY

With the development of the electricity market, there is a need to improve the existing active power management systems, both in the world and in the region and specifically in the Electric Power Industry of Serbia (EPS).

To improve the process of managing production capacities, Elektroprivreda Srbije has launched the projects Central Planning System (CPS) and Central Dispatch System (CDS). The CPS is essentially a software platform for short-term and long-term planning (optimization) of production. CDS is a "real-time" system SCADA / GMS (Generation Management System) type that provides monitoring of the operation of production capacities and real-time control of those units where such a possibility exists, based on schedules from the CPS. A GMS is a remote control of the active power component of a CDS system. The generation control system additionally relies on local active power control systems in production facilities.

Additional motivations for the introduction of a new SCADA/GMS system are changes resulting from new cross-border processes like PICASSO, and the introduction of multiple providers of secondary (aFRR) and tertiary (mFRR, RR) reserve, which will put EPS in a position of one of the multiple providers of those services for Serbian TSO, where services will be provided based on both maintaining system security and optimal economical allocation of EPS resources.

This paper will present the Generation Management System (GMS) of the new central dispatch system (CDS) for the Electric Power Industry of Serbia. First, a brief overview of the logical architecture and functionality of the CDS as a whole is given. Next, an overview of the functions provided by the SUP, primarily remote automatic active power control (base, secondary and tertiary control of active power). Further described are the algorithms of active power control on the CDS/GMS side and a description of the logic of resolving control responsibilities between EPS and Serbian TSO (EMS ad) on the side of EPS power plants that are in the remote-control system. Additionally, an overview of the plant's local active power joint control will be given. Then an overview of the software implementation and software platform of GMS applications on the CDS side is given. In the end, conclusions and possible directions for further development of the GMS will be presented.

## KEYWORDS

Generation control, Secondary control, AGC, Basepoint, Tertiary control, Active power, aFRR, mFRR



### 1. INTRODUCTION

In order to improve the management process of production capacities, Public Enterprise Electric Power Industry of Serbia (EPS) initiated development, implementation, and integration projects for two interconnected systems in 2018:

- Central Dispatching System (CDS)
- Central Planning System (CPS)

CPS is responsible for production optimization and provides production plans (schedules) for CDS.

CDS is a real-time supervision and control system for EPS production units of the SCADA/GMS (*Generation Management System*) type. The Generation Management System (GMS) is a component of CDS responsible for providing ancillary services and various aspects of remote control of production units, which are further discussed in this paper.

These two systems were developed, implemented, integrated, and tested at the EPS Dispatch Center from 2019 to 2022. In parallel with activities at the central location (DC EPS), upgrades to local control systems of EPS production units were carried out to integrate them into the EPS remote control system [1].

By implementing CPS and CDS projects, EPS achieves the possibility to participate in the balancing market, as well as the opportunity to reduce costs resulting from imbalances within its balancing group.

### 2. FUNCTIONALITY AND ORGANISATION

The Generation Management System is an integral part of the Central Dispatching System and together they enable the following:

- Real-time monitoring of the generation process,
- Availability of relevant data at a centralized level,
- Remote automatic and manual change of active power of the grid-connected generator from the dispatch center of Public Enterprise Electric Power Industry of Serbia (JP EPS),
- Graphic interfaces are provided at the central location, intended for technical personnel, to display selected real-time production values from power plants,
- Real-time integration with the Central Planning System (CPS),
- Management of ancillary services provided by the Serbian Transmission System Operator (TSO) in generation units where feasible,
- Automatic generation control through economic dispatching of generation units that do not participate in ancillary services (based on manually inputted cost curves of generation and realized in CPS),
- Different modes of operation for secondary regulation (uniform load distribution, proportional load distribution based on remaining reserves, load distribution according to a priority list - merit order list),
- Long-term database for analytical purposes with a reporting system.

The simplified conceptual block diagram of the entire CDS/GMS system and its connections with other systems is shown in Figure 1. In Figure 1, "NDC EMS" represents the national dispatch center of the transmission system operator in Serbia (Elektromreža Srbije), "Power Plant Gateway" denotes the communication-acquisition equipment that enables telemetry acquisition from the power plants and transmission of commands/setpoints to the power plants, "DCS" represents the Distributed Control System of the power plants, and "JAPC" stands for the Power Plant Joint Active Power Controller.



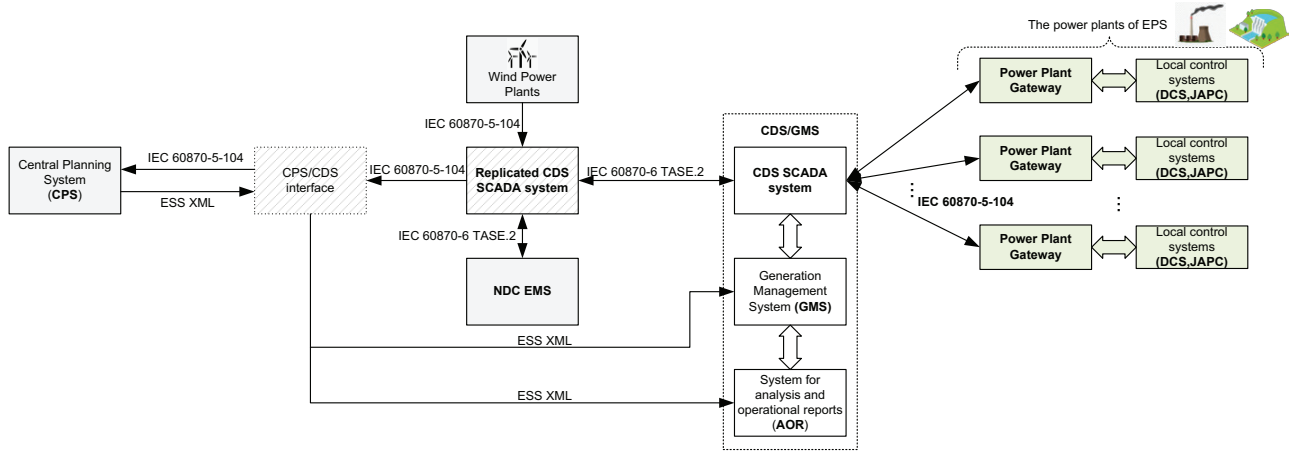


Figure 1. Simplified conceptual block diagram of the entire CDS/GMS system

More detailed overview of CDS/GMS system architecture is given at figure 2.

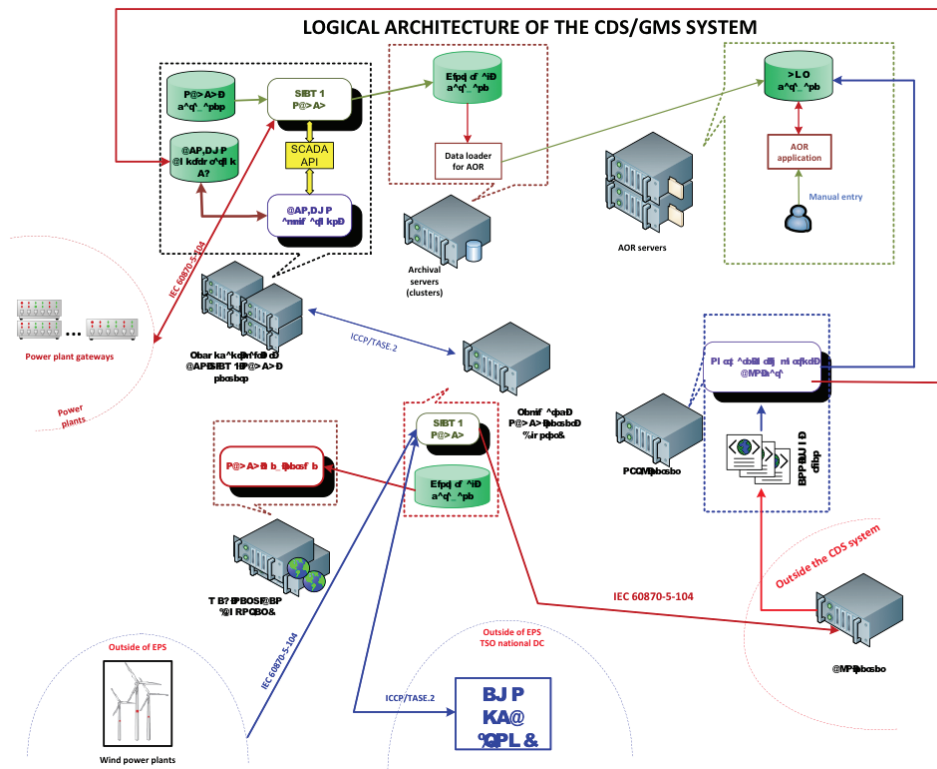


Figure 2. Conceptual logical representation of the CDS/GMS architecture

### 3. ACTIVE POWER CONTROL ALGORITHMS

The Generation Management System supports the following types of remote active power control:

- Basepoint regulation
- Balancing regulation
- Secondary (AGC) regulation of EPS
- Tertiary regulation

These types of remote active power control are further described in the text of the paper.

The Generation Management System (GMS) defines “controlled units” as control objects. Controlled units are virtual software entities within the context of the Generation Management System (CDS/GMS) that define the objects to which commands (setpoints) are sent. A controlled unit consists of one or more generators/units of a power plant. Various parameters related to regulation (such as PI controller parameters, etc.) are associated with the controlled unit. Typically, all generators of a power plant are associated with a controlled unit (typical for hydroelectric plants) or a single generator is associated (typical for thermal power plants). In real-time, the statuses and telemetry obtained from the power plant are checked, and the generators that meet the conditions are dynamically activated. The same generator can statically belong to two controlled units of different types, but it cannot be simultaneously active in both units in real-time (this is automatically resolved based on the statuses and telemetry obtained from the power plant).

The GMS utilizes two types of controlled units:

- Basepoint controlled units used for basepoint and tertiary regulation
- AGC (LFC) controlled units used for the implementation of AGC performed by EPS

#### 4 BASEPOINT CONTROL

Remote automatic control of the base active power of generators (production units) is performed based on schedules (dispatch orders) obtained from CPS (Central Planning System) or manually set desired power of the production unit by the EPS dispatcher. All available generators/power plants for remote control, not currently included in Automatic Generation Control (Load-Frequency Control), can be automatically adjusted to the specified (scheduled) values provided by CPS or manually set by the dispatcher. For production units that cannot be automatically remotely controlled, the planned base power value obtained from CPS is simply forwarded for display to the plant operator on the local SCADA/DCS system. Basepoint control is carried out independently for each power plant participating in basepoint control. Semi-automatic tertiary regulation and balancing regulation are achieved by incorporating corrective terms to the calculated effective base power value.

When a unit is initially included in regulation or there are changes in the units involved in regulation, the system automatically enters a ‘tracking’ mode as follows:

- The manually set base power is automatically adjusted to match the net power of the unit at the time of inclusion.
- The unit is automatically switched to the mode of manually setting the base power, which remains until action is taken by the dispatcher.

The block diagram of the basepoint control is shown in Figure 3.

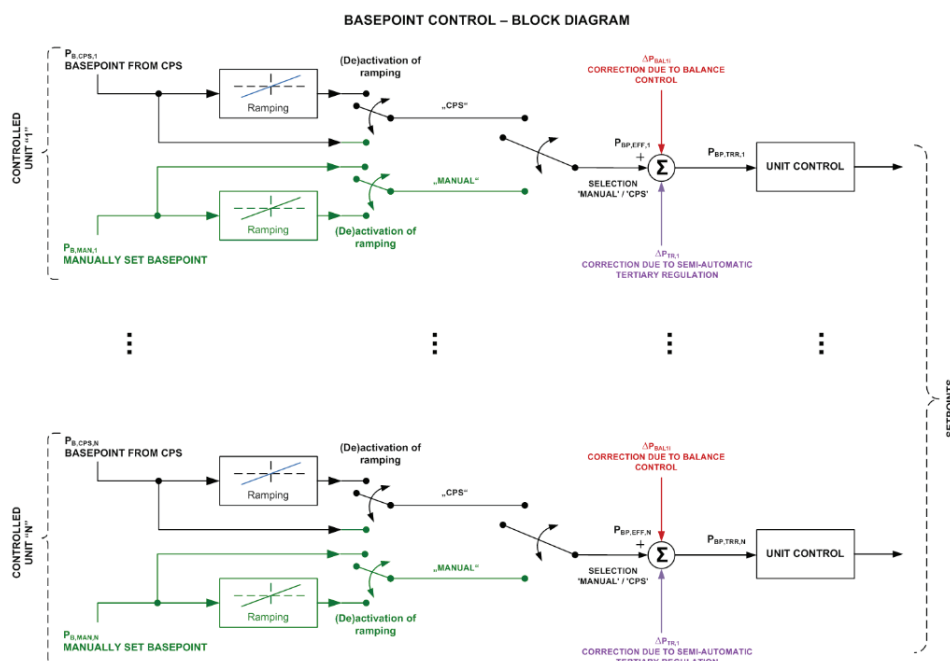


Figure 3. Simplified block diagram of basepoint control

The block diagram of control for an individual unit in basepoint regulation is shown in Figure 4.

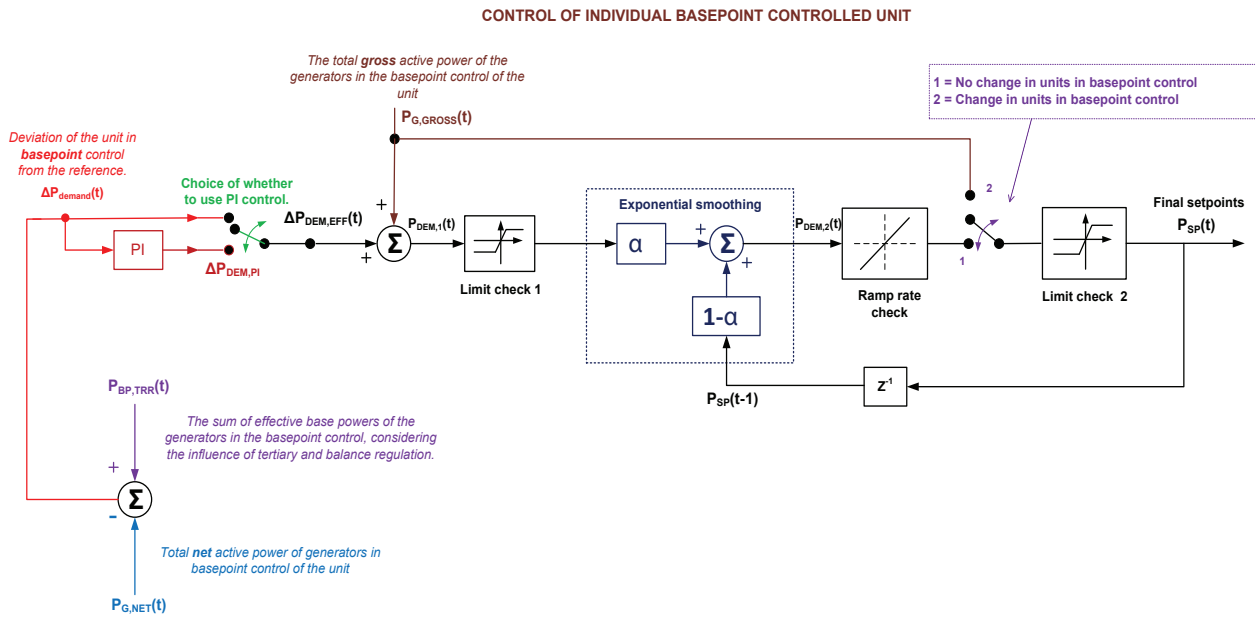


Figure 4. Block diagram of control for an individual unit in basepoint regulation

Basepoint control adjusts the net power (net power output) of the generating units to the desired value (basepoint). However, since local regulators control the gross active power, the final setpoint is the gross value.

### 5. BALANCE CONTROL

The purpose of the balance control loop is to maintain the total sum of active powers of units operating in base power mode at the desired value.

Only remotely controllable units that are currently active in base control and not included in AGC control can participate in balancing.

Balance control can affect the operation of secondary control and is therefore normally disabled and must be activated by a conscious action of the EPS dispatcher using the appropriate user interface.

The balance controller calculates the sum of net active powers of all units operating in base power mode and the sum of desired (base) powers of the same units. The difference between these two values represents the current balance error. The balance error is distributed among the units active in base control proportionally to the available reserve (correction factor  $\Delta P_{BAL,i}$  in Figures 3 and 5).

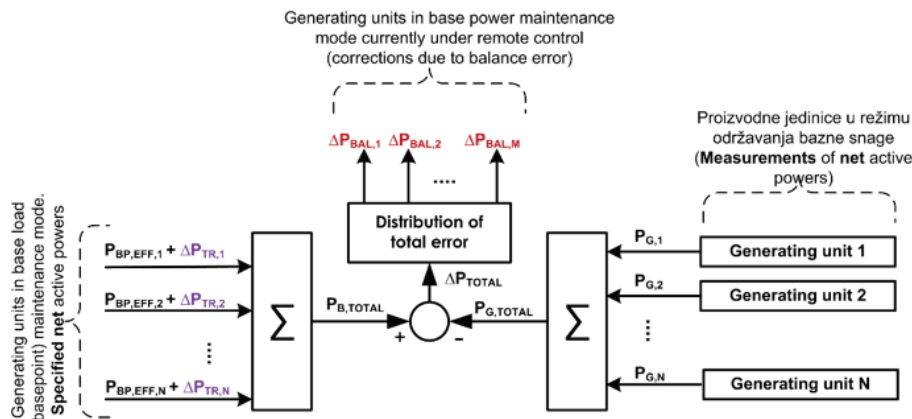


Figure 5. Balancing regulation - block diagram

### 6. SEMIAUTOMATIC TERTIARY REGULATION

Semiautomatic tertiary regulation enables the activation and distribution of tertiary reserve among power plants currently participating in the base regulation of EPS. Activation is performed by adding the component due to tertiary regulation to the base power  $\Delta P_{TR}$  of the base-controlled units currently under remote control. The total demand for activating the tertiary reserve (PTR) can be sent from the transmission system operator’s dispatch center ( $P_{TR,TSO}$ ) via ICCP/TASE.2 or manually set by the EPS dispatcher ( $P_{TR,EPS}$ ) through the semiautomatic tertiary regulation configuration HMI form.

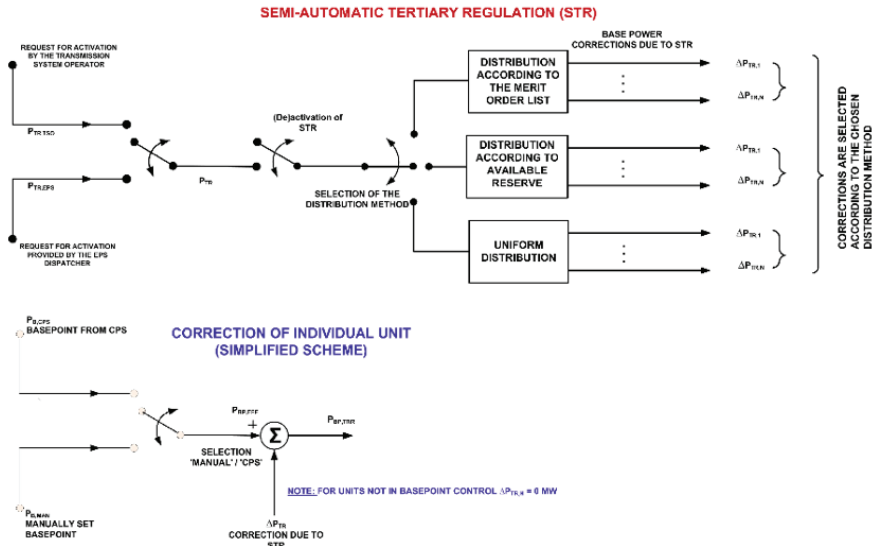


Figure 6. Conceptual block diagram of semi-automatic tertiary regulation

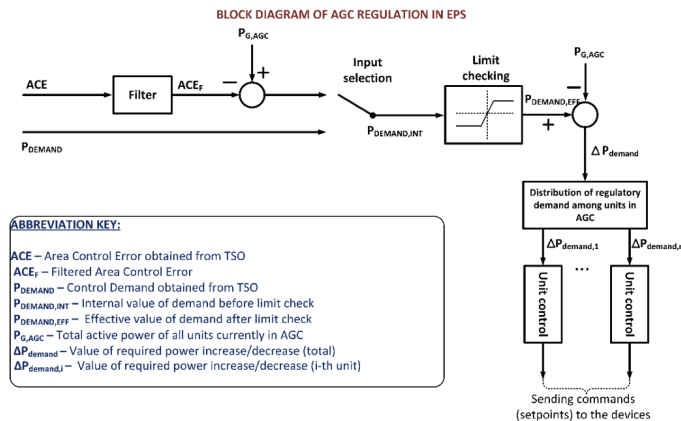
A conceptual block diagram describing the operation of semiautomatic tertiary regulation is shown in Figure 6.

For the purposes of tertiary regulation, three methods of distributing the required activation of the tertiary reserve are supported:

- Distribution proportional to the remaining reserve
- Distribution based on a merit order list
- Equal (uniform) distribution

### 7. SECONDARY (AGC) REGULATION OF EPS

Standard solution implies that the system service of the secondary regulation (AGC/LFC) is provided directly to the Transmission System Operator (TSO). In this mode, the TSO has direct access to the regulating units (HPP Đerdap 1, HPP Bajina Bašta, RPH Bajina Bašta, HPP Bistrica, TPP Nikola Tesla A3-A6) and controls them by sending regulating signals in form of raise/lower pulses [2].



**ABBREVIATION KEY:**  
 ACE – Area Control Error obtained from TSO  
 ACE<sub>F</sub> – Filtered Area Control Error  
 P<sub>DEMAND</sub> – Control Demand obtained from TSO  
 P<sub>DEMAND,INT</sub> – Internal value of demand before limit check  
 P<sub>DEMAND,EFF</sub> – Effective value of demand after limit check  
 P<sub>G,AGC</sub> – Total active power of all units currently in AGC  
 ΔP<sub>demand</sub> – Value of required power increase/decrease (total)  
 ΔP<sub>demand,i</sub> – Value of required power increase/decrease (i-th unit)

Figure 7. Conceptual block diagram of AGC regulation in EPS

AGC regulation of EPS is a mode of secondary regulation in which EPS directly controls its own objects in AGC. The TSO views EPS objects as a single “virtual power plant” to which it forwards the total regulating requirement  $P_{DEMAND}$  (desired total output power of the generating units currently included in AGC) or the regulation area error ACE. The conceptual block diagram of AGC regulation of EPS is shown in Figure 7.

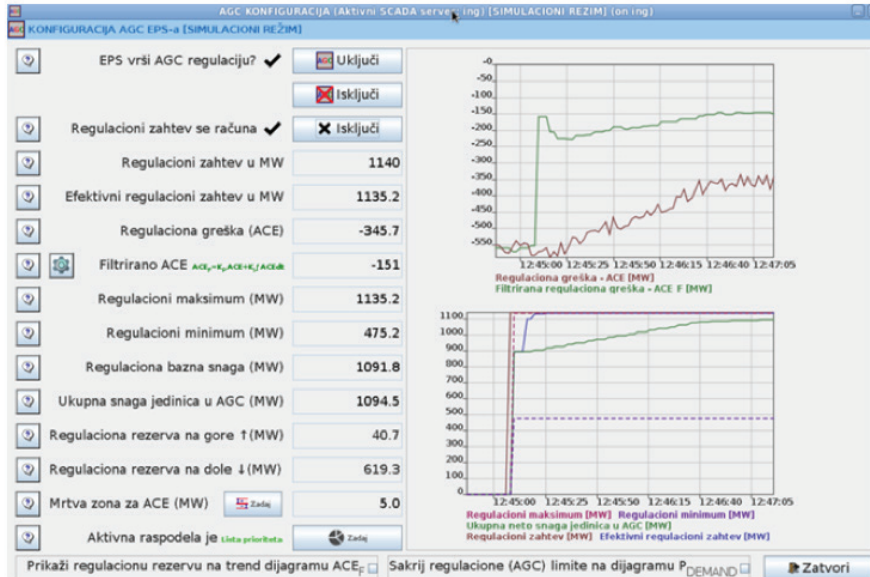


Figure 8. HMI Configuration Form for AGC in EPS (The form is in Serbian)

EPS dispatchers can enable or disable AGC regulation of EPS, select what serves as the input to the controller, choose the method of regulation error filtering, and so on using the AGC configuration form (Figure 8). The same display can be used to monitor the regulating reserve, ACE, regulating requirement, and regulating limits in the form of trend diagrams.

When the Area Control Error (ACE) provided by the Transmission System Operator (TSO) is used as the input to the AGC controller, via the ICCP/TASE.2 protocol, the raw ACE is always filtered to remove fast-changing components. The block diagram of the ACE filtering algorithm is shown in Figure 9.

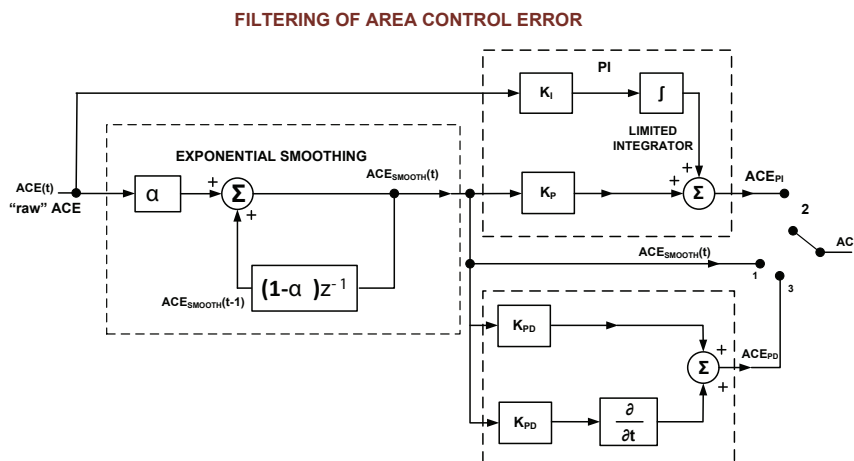


Figure 9. Block diagram of ACE filter

The block diagram of the algorithm for controlling an individual AGC-controlled unit is shown in Figure 10.

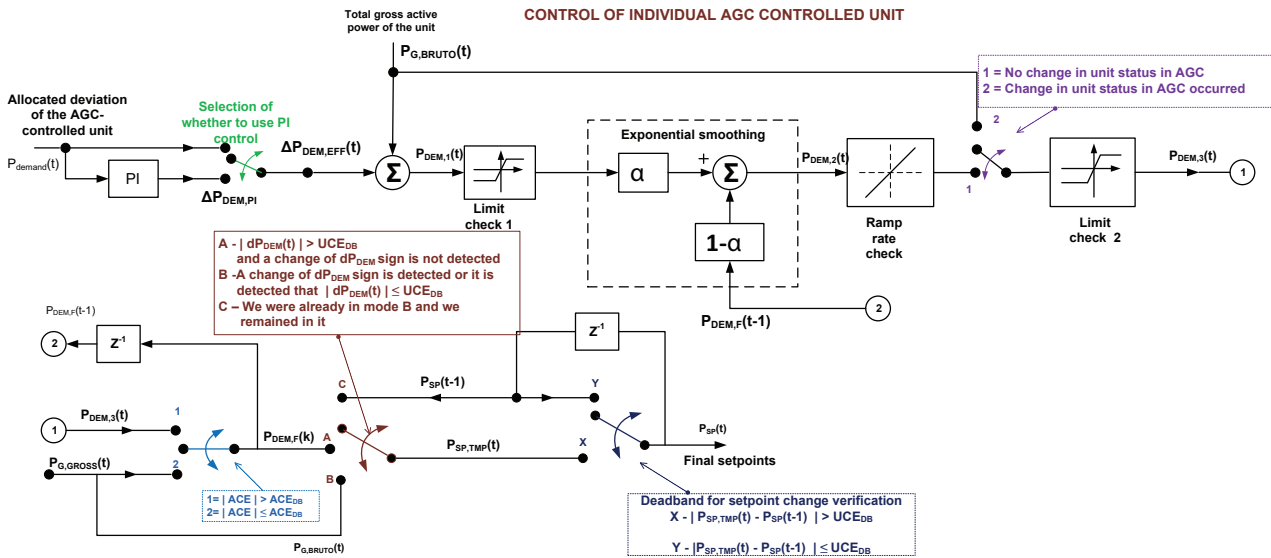


Figure 10. Block diagram of the algorithm for controlling an individual AGC regulated unit

Allocation of desired power change (distribution of control work), i.e., determining the value of  $\Delta P_{DEMAND}(t)$  for individual controlled units can be performed using one of the four supported methods:

- Allocation proportional to remaining secondary reserve
- Allocation based on merit order list
- Uniform allocation
- Allocation proportional to unit speed (ramp rate)

## 8. CONTROL LOGIC AND RESOLUTION OF CONTROL AUTHORITY AT POWER PLANTS

Central regulators within the Supervisory Control and Data Acquisition (SCADA) system generate setpoints or desired values for the total gross active power of the generators involved in the respective control. Specifically, the final adjustment of the units to the desired power levels is performed by local regulators at the power plants. At hydroelectric power plants, automatic adjustment of the units to the required active power values is carried out by Power Plant Joint Active Power Controllers (JAPC). At thermal power plants, individual units are always directly controlled, and the local regulation is implemented through the control logic integrated within the SCADA/DCS system of the units. Modifications to local regulators for integration into the remote-control system were implemented as part of a separate parallel project [1].

At power plants participating in the secondary (AGC) control, which can also be directly controlled by the Transmission System Operator (TSO), additional logic is implemented to resolve the issue of current control authority.

The fundamental logic for resolving control authority (EPS↔TSO) is shown in Figure 11. The labels in Figure 11 are as follows:

- $I_L$  - local signal for remote control permission (set by the power plant operator)
- $I_R$  - request for inclusion in remote control (set by the EPS dispatcher)
- $I_{AGC}$  - request for inclusion in AGC control (set by the EPS dispatcher)
- $I_{EPSTSO}$  - signal by which the SCADA defines whether AGC control should be performed by EPS (1) or TSO (0)
- $I_{EPS}$  - feedback signal defining whether EPS has control authority for AGC
- $I_{TSO}$  - feedback signal defining whether TSO has control authority for AGC. This signal is transmitted to the RTU gateway of the TSO instead of the existing signal that indicates the unit's availability for remote control.



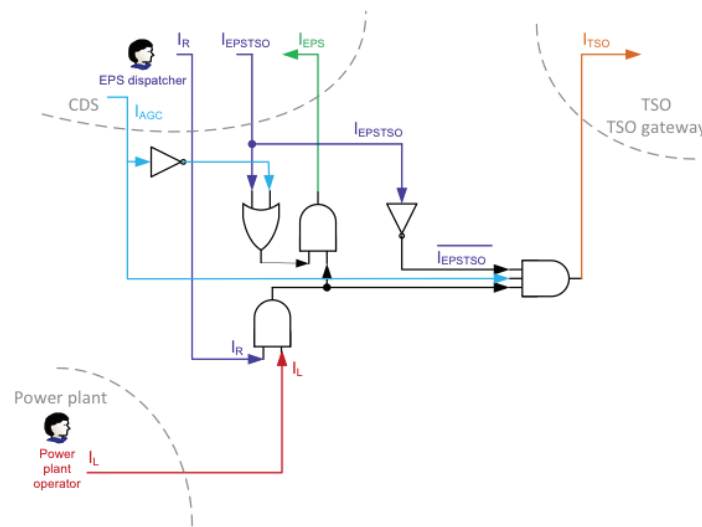


**Figure 11.** Logic for resolving control authority

The signals  $I_{EPS}$  and  $I_{TSO}$  will never have a simultaneous value of 1 for the same generator. The CDS ensures that there is no unauthorized situation where some power plants participating in AGC are marked to be controlled by EPS and others by TSO (Transmission System Operator). Power plants that do not participate in secondary (AGC) regulation do not require this authority resolution (there,  $I_{EPS}$  is always equal to  $I_R \cdot I_L$ ).

In principle, the logic works as follows:

- If a generator is not currently remotely controlled, neither the EPS dispatch center nor the TSO dispatch center have control authority over that generator.
- If a generator is currently remotely controlled but not included in AGC, the EPS dispatch center has control authority over that generator.
- If a generator is included in AGC, the following applies:
  - If the AGC regulation of EPS is disabled (default state), the TSO has control authority over the generator.
  - If the AGC regulation of EPS is enabled, the EPS has control authority over the generator.
- In case of communication loss between a power plant and the EPS dispatch center, the logic is as follows:
  - If EPS had control authority over the generator, the generator is automatically excluded from remote regulation.
  - If TSO had control authority over the generator, there is no automatic change in the generator's status regarding availability for AGC.

In case of communication loss with the EPS dispatch center, the operator at the power plant can manually assign control authority to TSO for the generator in AGC.

## 9. SOFTWARE TECHNOLOGIES USED

Control applications of the central generation management system are implemented in the C++ programming language. The applications are developed for the Linux platform (CentOS, Oracle Enterprise Linux, and Red Hat Enterprise Linux are supported) 64-bit architecture. User interfaces are implemented using the Java programming language. Since they are developed in Java, they are compatible with all operating systems that support Java. The MySQL-compatible MariaDB 5.1 is used as the database platform. Control components for database connectivity utilize ODBC and native MySQL C-API. Java applications use JDBC. The operational report viewing application (AOR) is powered by the Glassfish 4 application server running on an Oracle Linux 7.x operating system. The solution is based on the Java EE 7 platform and utilizes PrimeFaces 5.2 libraries for web page generation. The data used for generating reports is stored in the MariaDB 5.1 database. Users access the application through a web browser (MS Internet Explorer, MS Edge, Mozilla Firefox, Google Chrome).

## 10. TESTING

As part of the overall testing of CDS/GMS [3], special attention was given to the testing of control loops. The testing was conducted by first coordinating with the parallel project, which involved modifying the control algorithms at power plants, and performing testing of local algorithms and logic by manually inputting signals and setpoints from the central system at the TSO dispatch center. Once the modifications at the power plants were initially verified, the testing of central control algorithms for SUP regulation was conducted. The basepoint, semi-automatic tertiary, and secondary (AGC) regulation of the TSO were tested.

The testing of the basepoint regulation was performed at HPP Djerdap 1, HPP Bajina Bašta, and HPP Zvornik. All tests of the basepoint regulation were successfully completed. For the purposes of testing the semi-automatic tertiary regulation, the TSO dispatchers manually set the desired activation of power in the tertiary STR regulation using a dedicated SCADA interface. During testing, various distributions of activated tertiary reserves (uniform distribution, distribution based on available reserve, and distribution based on priority list) were successfully tested. The same power plants used during the basepoint regulation tests were used for testing. The testing of the EPS secondary (AGC) regulation was performed based on the Area Control Error (ACE) provided by the TSO via the TASE.2 link. Testing of control based on the regulation requirement was not possible as, during the testing period, the TSO had not yet configured the “virtual EPS power plant.” The primary power plant used during testing was primarily HE Djerdap 1, as it is the most important control unit in the system. During these tests, the EPS performed AGC regulation based on the ACE provided by the TSO, while the AGC regulator in the TSO dispatching center (NDC EMS) was suspended. Satisfactory controller performance was achieved during the final testing. Figure 12 shows the response of HE Djerdap to control actions during testing, and Table I shows the average 15-minute ACE values during testing.

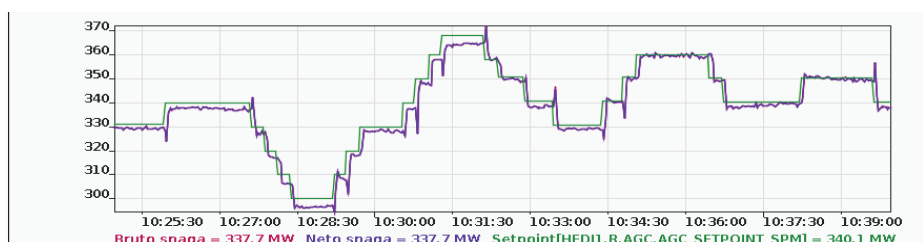


**Figure 12.** HPP Djerdap I response during AGC tests. Red is gross power; Blue is net power and green is setpoint (desired power).

**Table 1.** ACE during testing of EPS AGC controller

Time interval	Average ACE (MW)	Comment
10:15-10:30	11.91	The AGC regulation of the EPS was activated at 10:26
10:30-10:45	8.64	
10:45-11:00	4.5	
11:00-11:15	28.34	The AGC control was not active due to a lack of secondary (aFRR) reserve
11:15-11:30	-7.34	
11:30-11:45	-5.39	

## 11. CONCLUSIONS

The paper provides a brief overview of the control components (Generation Control System - GCS) of the new Central Dispatching System (CDS) of EPS. It describes the algorithms, technologies, and testing procedures. The current solution is primarily designed for remote control of conventional sources (conventional hydroelectric and thermal power plants). However, considering the proliferation and increasing significance of renewable and distributed energy sources, the system is designed to be expandable through mechanisms of “virtualization” of power sources, namely, the creation of Virtual Power Plants (VPPs) that aggregate multiple distributed sources into one or more virtual entities. These virtual entities can participate more easily, compared to individual “physical” objects, in providing services related to ancillary services and system management/balancing, which represents a potential direction for future development.



### BIBLIOGRAPHY

- [1] J. Car, N. Radmilović, G. Jakupović, E. Veljković-Grbić, T. Jelić, D. Bojanić, D. Dimitrijević, M. Bogdanović, A. Latinović, D. Surudžić, Z. Bojanić, "Modifications of the local control system and group regulator of HPP Đerdap 1 in order to integrate them into the central control system (CDS) of EPS", 19th CIGRE Symposium Serbia - Control, Telecommunications, and Protection in Power Systems, Serbia, October 20-23, 2020.
- [2] M. Đurđević, Z. Rudić, N. Obradović, G. Jakupović, N. Čukalevski, "Implementation and Testing of AGC SMM Control Block in NDC in Serbian TSMO within the Project of Modernization and Upgrading of Existing SCADA/EMS System", DEMSEE 2015, 10th Jubilee International Conference on Deregulated Electricity Market Issues in South Eastern Europe, Budapest, Hungary, 24-25 September 2015.
- [3] T. Jelić, G. Jakupović, P. Lučić, G. Konečni, D. Surudžić, D. Komatina, Z. Mitrović, "Testing of the central dispatching system and generation management system of EPS", 20th Symposium CIGRE Serbia - Control, Telecommunications, and Protection in Power Systems, Bajina Bašta, Serbia, October 10-13, 2022.



# Emerging Problems in System Operator Training and Possible Training Simulator Solutions

[ninel.cukalevski@pupin.rs](mailto:ninel.cukalevski@pupin.rs)**NINEL ČUKALEVSKI***Mihajlo Pupin Institute***Serbia**

## SUMMARY

The electric power industry is currently undergoing important changes, mainly due to the society-initiated decarbonization efforts aimed at the integration of large amounts of renewable energy sources. New developments in energy transmission technology can solve some of the challenges. Many of these new resources and devices are typically power-electronic (PE) interfaced with the system, with a sizable negative impact on system dynamic performance, strength, and power quality.

To cope with the increasing system complexity, utilities are expanding the scale and intensity of automation/control and ICT (information and communication technology) solutions use. Those solutions although enabling easier system control/operation are adding a layer of complexity. That all together creates a situation that asks for new planning, operation, and regulatory approaches, that are in parallel with research and development, going worldwide.

In this paper, based on the author's previous work in the domain of operator training and operator/dispatcher training simulators (OTS/DTS) use, and data acquired through CIGRE surveys and their analysis, the current domain situation is described and solutions needed are proposed.

Firstly, key electricity sector challenges that might impact system operation will be outlined. Secondly, emerging control center operator training challenges that the power system operators are likely to experience will be examined. Those identified will be shortly presented along with the necessary improvements in existing training facilities and practices. It was concluded that in a grid operation domain, a more systematic approach to operator training design, implementation, and execution, including more coordination, and more advanced training tools like OTS/DTS, is necessary to cope with increasing system complexity. A few illustrations will be given here. Thirdly, existing operator training tools and methods used, together with identified OTS/DTS limitations will be presented shortly.

The possible future developments needed in the domain of operator training tools needed to support new training requirements that stem from the utility industry transformation process will be presented. As it was concluded that an environment that exhibits many new phenomena and changed dynamic behavior, requires operator training that should also include all the information, control, and decision support means available and used by different parties. This fully applies to the future Advanced OTS (AOTS) but only partially to the existing OTS/DTS solutions. The architecture of the advanced OTS/DTS proposed will be outlined here.

## KEYWORDS

Power system emerging problems; operator training; operator training simulator; AOTS



### 1. INTRODUCTION

The actual energy transformation of the electricity sector was globally initiated a few years ago with the main goal to enable the sustainable development of energy and other related industries, through decarbonization initiatives, i.e. through a decreased use of fossil fuels. Decarbonization is to be achieved mainly through the massive introduction of renewable energy sources (RES), mainly from wind and solar, in electricity generation, but also through the transport electrification expansion, industry, and communal sphere, and increase of energy efficiency of all the processes in the chain from generation to the end use.

The existing RES, but also many other devices in the grid (like HVDC, SVC, STATCOM, and BESS) based on modern energy technologies, are connected to the power grid employing power electronic interface (PEI) devices, and the same holds for the increasing number of advanced customers (like modern regulated drives). As their numbers increase, within the generation (PEI Generation-PEIG) in the first place, power system behavior is more and more different from those with conventional generation sources (based on synchronous generators), especially in the dynamic respect.

The consequences of the above said on power system depend mostly on the level of RES penetration, and they are system specific, and thoroughly analyzed in numerous systems, probably first in Ireland [1]. Impacts and consequences on the power system can be aggregated into several main groups:

- RES generation variability and uncertainty make system operational planning more difficult
- system balancing
- provision of system services
- impact on the short circuit currents/powers levels in the network, protection
- system stability
- power quality

Also, we should keep in mind that for some time intensive research and attempts, with the corresponding solutions on the service market, are going on to use RES and other PEID, to provide balancing and system services [2,3].

On the other side, power system monitoring and control digitalization, in power plants (PP) and substations (SS), as well, combined in parallel with informatization of all the electricity sector segments (generation, transmission, and distribution), although intending to handle the existing complexity, is introducing an additional layer of interrelations and constraints in the decision-making process at all the hierarchical levels, especially at the control centers (CC).

The consequences of the increased complexity are visible during large disturbances and power system blackouts, especially when operator errors or omissions (or more widely human factors) are contributing factors, which come under scrutiny. Although large disturbances and power system blackouts worldwide are far from rare, available data [4,5,6] indicate that the share of human factors within the large cascading disturbance/blackout causes or important influencing factors, looking globally is almost stable and is not negligible (10-30% from all causes), and typically ranks on the third place of causes (after natural causes and equipment failures), no matter the overall increased level of ICT use. This might imply the possibility that the existing operator training methods and tools are not fully adequate for the existing challenges and associated risks.

Based on the results [7] of the recent international CIGRE survey (in which the author took part), and on the author's earlier research [8,9] in the domain of modern/perspective operator requirements and training tools, in this paper's innovative architecture of the advanced OTS/DTS (AOTS) is defined and proposed, one which enables simulation of the wider range of the power system dynamic phenomena than that is the case with the majority of conventional operator training simulators in utility use. The power system models and simulation algorithms of AOTS should enable not only the long-term dynamic of current and voltage and faster electro-mechanical phenomena simulation, but also electro-magnetic transient phenomena, that manifest themselves with stability loss, and a trip of the converters of PEI connected devices (generators/batteries, HVDC, STATCOM, or customer loads). To satisfy numerous new operator requirements, the AOTS proposed must replicate also all other information and control systems that are used in CC at the specific (usually the highest one) hierarchical level.

After the introduction, in section 2 characteristics of electricity sector transformation and decarbonization efforts with their impact on power system operation, control centers, and their personnel are outlined. Section 3 shortly describes existing approaches to training and related tools. Based on the results of the recent international survey between the TSOs, section 4 identifies current challenges in the operator training domain together with the new OTS-related requirements. An attempt to satisfy these new requirements is presented in section 5 which shortly describes innovative architecture and functions of the advanced OTS (AOTS). In the end, the paper's conclusions and bibliography are presented too.



## 2. ELECTRICITY SECTOR TRANSFORMATION AND ITS CONSEQUENCES

All around the world, from the moment power systems were established almost a century ago they change and evolve permanently, no matter in different speeds and forms, mainly due to the growing need for electric energy from consumers, and with generation, transmission, and distribution technology improvements. As such, changes and associated challenges so far were always successfully solved. During the last decade, especially in highly developed countries, energy transformation was focused on decarbonization, i.e. on reduction of use and on accelerated plans to eliminate fossil fuels (coal, oil, gas) use as a primary energy resource, that is conducted through massive introduction of RES, wind and solar at first. The main goal of this transformation is the creation of conditions that enable the electricity sector's sustainable development and functioning, where an important role has multi-decade efforts to improve energy efficiency, within the sector, but also the energy use domain in other sectors.

In parallel, further PP and SS monitoring and control digitalization processes are going on, as it is going on intensive informatization of numerous business processes (technical and commercial) that are performed in the electricity sector, by using business/technical information systems.

During the last couple of years, within the professional and research community and literature worldwide, interest to understand consequences and challenges that accompany the electricity sector transformation, and finding possible solutions, or at least relief of unwanted consequences, has grown sizably

### 2.1. Challenges related to power system operation

With the increase of RES share in the companies' generation portfolio, and thus in the system generation, numerous consequences arise, for example:

- increased generation variability and uncertainty
- increased volatility and transmission distance of power transits
- changes in the power system dynamic behavior

The level of expression/manifestation of these consequences is dependent on several factors, but from the level of the RES share in the overall generation balance, is it small (10-15%), moderate (20-30%), or high (50-60%), not to mention about 90-100% levels, although, in some systems, such regimes of generation are also possible for a short time.

Both variability and uncertainty of generation from renewables are a result of the quality of their primary resource (wind speed and sun irradiation). Having in mind typical RES locations (especially of the offshore wind parks) and the changing disposition of areas with currently high RES generation, it is clear that the power flows through the power system will vary considerably, as well as their direction through transmission, from or towards the distribution network in a specific area. Many actual projects of the RES integration just increase these distances.

The majority of modern RES to connect to the transmission or distribution network has a converter that is made from power electronic components, i.e. has a PEI to the network connection point. Finally, an increase of the RES power share in the overall generation balance provokes changes in power system dynamic behavior and the emergence of new dynamic phenomena, that greatly expand the range of relevant dynamics, from the traditional one, where mid-term and long-term lasting processes (electro-mechanical and thermo-dynamic) are of interest, to those of short and very short duration (electro-magnetic and wave phenomena) as depicted at Fig.1 [10] below.



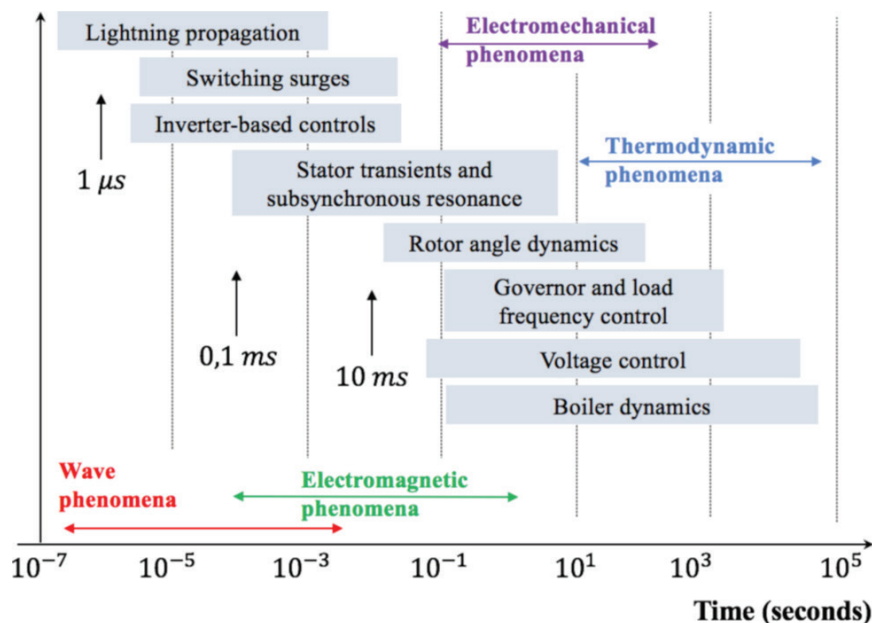


Figure 1. Power system time scales, source [10]

Also, with the RES share increase, problems associated with all types of system stability (frequency, voltage, rotor angle, convertor, resonance) get worsen, i.e. typically stability reserves are reduced. It should be noted that the PEID (like SVC, STATCOM, and HVDC) have the influence and enable control of many of the dynamic phenomena.

## 2.2. Challenges related to control centers and their operators

As the result of changes that are going on in the system from the operational side, apart from those already mentioned, many other challenges exist, with the details in [11], while from the side of CC and operational personnel, it is possible to identify, especially actual today, the following issues:

- Increased congestion in the network and decrease of re-dispatch capabilities
- Operation of hybrid HVAC-HVDC systems
- Observability and controllability of RES
- Increased vertical coordination TSO-DSO
- Increased horizontal coordination TSO-TSO
- Power system restoration services
- Operators need to be better equipped and have more skills

These challenges have a global character and their importance will increase in pace with the decarbonization programs implementation.

As a result of RES generation growth worldwide, especially those from the offshore wind parks, more and more far away from the load centers, cross-border flows grow, often close to the security limits. Thus network congestions are on the rise, which combined with decreased redistribution capabilities results in congestion re-dispatch cost increase.

To enable long-distance transmission, usually of large amounts of power, and connection of the rising numbers of offshore wind parks, the numbers of new HVDC lines/cables increase fast, generating new challenges associated with their control, protection, and reaction in case of faults in the close HVAC networks. That makes CC operator work, due to the HVDC systems' many new functionalities and phenomena, more demanding and error-prone. The same is relevant for operator control of many other PEI devices in the grid, that all together impact system dynamic behavior and system services.

Within conventional power systems with generation concentrated in several power plants, observability, and controllability issues are more or less practically solved. The massively "green" power system with large numbers of distributed renewable generation



sources (especially those of PV type) integrated into the distribution network makes the above issues more difficult and costly to solve. Often RES with capacity over some threshold (like 5 MW) must provide for two-way data transmission with the CC that might be separate from or integrated with TSOs CC. This is partly solved through the better vertical TSO-DSO coordination that at the same time enables the use of system services from the RES connected to a distribution network.

For highly meshed networks, in conditions of variable flows and transits, it is important to enhance regional TSO cooperation and coordination of all relevant TSO's operational processes, on all the time scales, typically by establishing Reliability Coordinator (in North America) or Regional Security Coordinators-RSC (in Europe).

Within the same context, of increased DG/RES contribution and associated closing or conservation of classical PP with synchronous generators, a lack of frequency and voltage support emerges, as well as a lack of black-start capabilities in the system, creating the general situation of insufficient restoration services and other system services as well. But, with adequate market solutions (DG aggregators), legal framework, and technical preconditions (ICT support), RES at the distribution level (mostly PV) might be an important source of system services.

All these indicate the high need for ISO/TSO for new or improved existing procedures and tools to monitor, control, and support decision-making by the operators in the power system/grid control center/room. Namely, there is a stronger need for:

- RES generation (wind, PV) forecast tools
- Wider use of the tools for stability analysis and monitoring (like DSA, and VSA)
- On-line calculation and monitoring of system inertia and short circuit power levels
- PMU/WAMS data processing and better visualization in CC
- Power quality and dynamic performance monitoring (using PMU) at the RES connection points
- More profound training of operational personnel and more adequate training tools

That requires the development of new or improved existing processes, systems, and tools, to handle challenges that rise with the increased numbers and amounts of RES. This will be the subject of future work, from here on focus is only on control center operational personnel and tools for their training (initial and ongoing).

### 3. CONTROL CENTERS OPERATOR TRAINING TODAY

As a result of the numerous changes that took place in the electricity sector worldwide, from those provoked by energy transformation and DG/RES introduction to those that emerged from the development and use of advanced energy, information, and communication technologies, power system complexity has grown up considerably, especially in the domain of system control and decision making by the system operators. That, among other, raise several questions related to operator training and related tools.

#### 3.1. Operator training methodology

Until about a decade ago numerous utility companies around the world approached the problem of power system operator training program development and implementation without the use of any formal methodology, favoring a practical approach of "on the job training".

Numerous power system large disturbances and system blackouts around the world (only in the last 20 years) influenced largely to regulatory bodies and technical organizations (like FERC/NERC in North America and ENTSO-E in Europe) to require operator certification to be allowed for daily shift work in the CC, as well as the accreditation of the operator training programs. Namely, it is required that the operator's knowledge and control skills are confirmed, and typically time-constrained, thus requiring periodic recertification. The specific country's situation in respect of the certification, training requirements, and conformance depends also on the local regulatory environment.

State of the art framework for the development and use of operator training programs, based on a formal SAT (Systems Approach to Training) methodology, was proposed and explained in detail within the CIGRE TB [8], and its basic methodological statements are still valid today. But, due to the emergence of new processes and market participants/actors, tools, phenomena, and system procedures, it is necessary to regularly update the operator activity lists, as well as other program elements. That said is more so relevant for the training tools and training simulators in the first place.

### 3.2. Operator training tools

Although today numerous means and tools for the initial and refresher operator training exist, the key training tool, that has the broadest functionality, is the power system operator/dispatcher training simulator. Its basic structure is depicted in Fig.2.

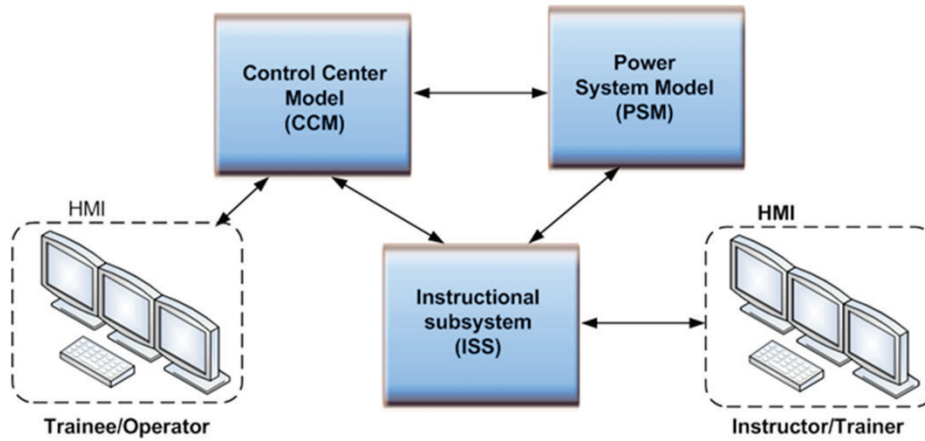


*Figure 2. Traditional OTS/DTS basic architecture [8]*

Due to the need that operators trained, should use and inter-react in the same manner as with the identical decision support/control tools they use in their daily work, it is necessary to have (at least) a replica of the CC basic monitoring and control system (traditionally SCADA/EMS), or more precisely, with the CCM subsystem that models CC basic control system (Control Center Model, on Fig.2).

Due to the need instructor (trainer) has to monitor and control the OTS training session, including his actions on scenario events, and the trainee's reactions, necessarily within the OTS there is an instructional subsystem (ISS-Instructors Sub System, in Fig.2), aimed at the instructor.

Finally, the central part regarding its importance is the OTS subsystem that models power system dynamic response, the so-called PSM (Power System Model, in Fig.2), on changes in load, topology, and other activities that the operator might initiate through its HMI/CCM. The PSM response for the specific power system modeled, as defined by the ISO/TSO service territory and neighboring systems should be maximally realistic which is dependent on model quality, implying the need for calibration of all the model parameters. Numerous other details and constraints, as well as other possible architectures, are given and explained in [8]. The majority of existing OTS simulates just mid-term and long-term dynamic phenomena, typically as a sequence of power system quasi-stationary states, while just a few of them include also short-term dynamic phenomena (of electro-mechanical type), i.e. enable calculation of rotor angle stability.

The existing training simulators have numerous and different constraints, some generic some specific to the supplier, which trainee operators should be aware off to have the maximal effect from the OTS training. Typically, within the traditional OTS, modeling shortcomings or infidelities are "solved" with the introduction of the discrete events in a scenario by the instructor, thus degrading the realism of the simulation.

Some of the newly emerged OTS constraints will be identified and analyzed in the next section.

## 4. OPERATOR TRAINING CHALLENGES AND OTS/DTS REQUIREMENTS

It is understandable that important changes that are currently undergoing within the electricity sector, apart from their impact on the power system and human operators, also have an influence on the existing training methods and tools, once again raising a question about their effectiveness and adequacy.

Before all, we consider training challenges generated by:

- The massive introduction of RES, and more DER at the distribution level
- Use of PEI to connect different devices (RES, DER, HVDC, SVC, STATCOM,...) to the network

Oral Presentation: Emerging Problems in System Operator Training and Possible Training Simulator Solutions

- Use of DER in the system restoration process
- The presence of energy accumulation devices of different types (like BESS, EV)
- The presence of HV DC lines (HVDC)
- Introduction of monitoring systems (like WAMS) based on phase angle measurement units (PMU)
- More often use of different system protection schemes (SPS)
- Numerous new stand-alone systems and applications that support CC operators in decision making

The evaluation of the influence of the above challenges on existing operator training processes and tools, including OTS, was based on the analysis of individual answers from ISO/TSOs, acquired during the recent CIGRE international survey [7], in which the author took part, and with summary results to be published soon as CIGRE technical brochure. To illustrate the above, in the sequel just a small part of the survey analysis findings will be addressed.

Regarding the **RES and distributed energy resources**, the recent survey revealed that most system operator (85.7%) training programs include operator actions with RES, whereas the majority (65%) of TSOs in their training scenarios include events related to RES production changes and RES plant limit violations. Half of the respondents stated that RES is implemented in their training simulator; with RES injections represented in OTS, where in some cases wind power plants are modeled in OTS as hydropower plants. As a rule, current OTS/DTS is not widely used for operator training in handling RES-provided system services (like restoration). The representation of RES in OTS varies from TSO to TSO, however, it is concluded that there is a problem to represent RES production from DG.

In respect of power **system restoration operator training** and its participants, as in Fig.3, it is possible to notice that conventional generators and DSOs are the primary external participants that are involved in restoration OTS-based training, while the **DER operator's participation** in joint system restoration training, so far is modest (18%), although many TSOs also include significant TSO customers, Aggregated Generator Units (AGU), and Demand Side Units (DSU).

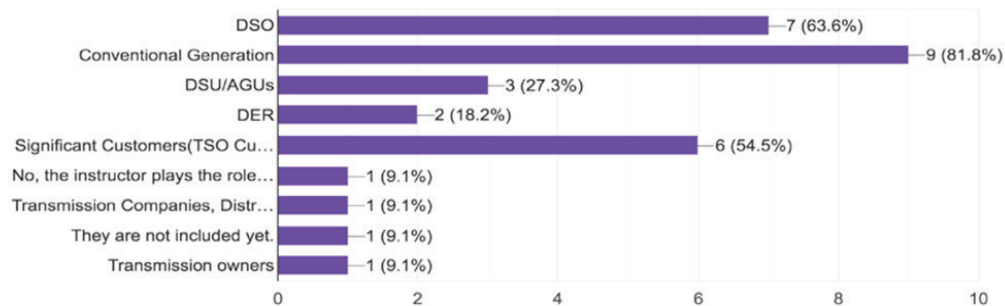


Figure 3. External participants involved in OTS/DTS restoration training [7]

The importance of OTS-based operator training for the control of the PEI devices, such are **HVDC lines**, is also noticeable, as illustrated by the fact that all the survey participating TSOs (100%), that have one or more HVDC lines, model them in OTS/DTS, as in Fig.4.



Figure 4. Possibility for OTS/DTS to represent HVDC lines [7]

The situation is quite different with another category of PEI devices, those of **energy accumulators**, especially of modern **BESS type** (Battery Energy Storage System) usually with Li-ion batteries, probably as a consequence of the early stage of their use. Thus it is understandable that the majority of the TSOs (83%) currently don't model BESS in their OTS. But still the majority of responding TSOs can model in their OTS/DTS their pump-storage hydro (PSH) units/plants, as presented in Fig.5.

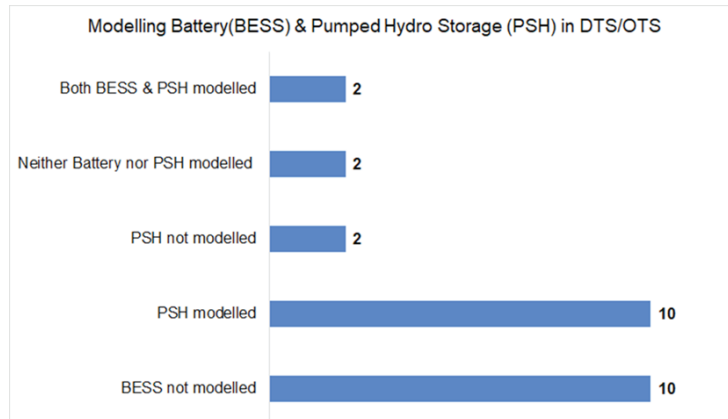


Figure 5. Possibility for OTS/DTS to model BESS and PSH [7]

Regarding the consequences of the introduction of **new monitoring systems** (like WAMS), **based on the phase angle measurement units** (PMU), the survey demonstrated that a large majority of TSOs (91%) use PMU data in their CC and that those data are mainly used within the three application areas: visualization and real-time situational awareness enhancement; identification of undamped oscillation modes; after the event analysis (post mortem/post-dispatch) as in Fig.6:

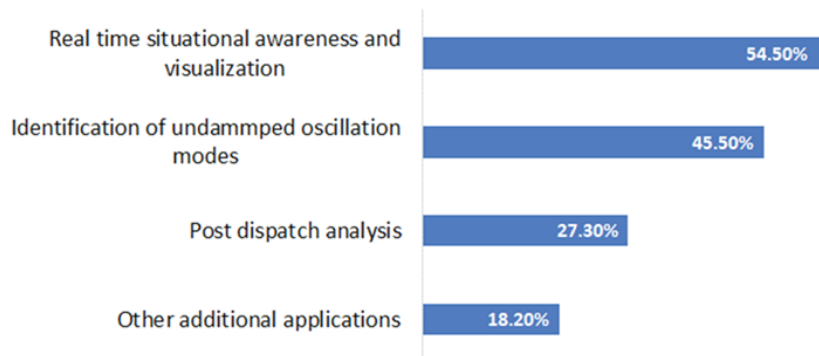


Figure 6. Use of PMU data within the ISO/TSO control center [12]

The **training of operators for stand-alone/loosely coupled support ICT tools use** (like DLR, LDS, WAMS, etc.), where it exists is mainly done separately from the OTS. Those (42%) who consider current operator training for stand-alone or loosely coupled ICT systems use do represent a problem; have identified several, where the main one is an unsatisfactory level of ICT tools integration with the SCADA/EMS.

Based on the insight attained by the survey analysis it is possible to conclude that power system current operator training worldwide, as well as its main training tool OTS/DTS, are not fully effective and adequate for the integrated simulation/visualization of new power system dynamic phenomena and devices, especially those with PEI.

## 5. ADVANCED OPERATOR TRAINING SIMULATOR

To enable, power system operator training and different post-operational analyses as well, in the current and more so under the fast-approaching future with the high-level RES/PEID system conditions, it is necessary to possess an advanced operator training simulator (AOTS/ADTS) with the following capabilities:

- To realistically model all power system relevant elements and devices, not only those traditional (generators, lines, transformers), but also FACTS, HVDC, BESS devices, and DG/RES that are PEI system connected.



- To represent, the best as a replica, all the existing monitoring and control systems in relevant CC (like SCADA/EMS, SCADA/DMS, or SCADA/GMS, depending on who is participating in the joining training), as well as others, usually stand-alone applications/systems intended for operator decision support (like DSA-dynamic security analysis, PMU/WAMS, DLR-dynamic line rating, LDS-lightning detection systems, at transmission level).
- To support the instructor in scenario building; insight and control during the training session; and evaluation of training results.
- To enable team training of operators/shifts inside a company (like NCC, RCC), and joint training with other TSOs and other entities (Reliability coordinators, DSO, GenCo).
- To simulate in parallel, disturbance development within the individual electrical islands.
- To have the capability to simulate an event/disturbance with the cascading development.
- To have the capability to use during the simulation several power system models that have different levels of detail.

The proposed architecture of the advanced operator training simulator, intended at first place for power system operator initial and refresher type training, but also for other operational personnel dealing with operational planning and post-operative analysis, is depicted in Fig.7. As many other software systems intended for operator training (like in nuclear PP, aircraft simulators, military systems), AOTS system should consist of the three basic subsystems: **Power system model (PSM)**-Power System Model, in Fig.7), **control center model (CCM)**-Control Center Model, in Fig.7) and instructional sub-system (**ISS**-Instructional Sub System, Fig.7), but with the characteristics and performances which are much higher than those of the existing operator training simulators (Fig.2).

**The power system model** within the AOTS must have a much wider scope, as in equipment modeled and in simulated phenomena as well, in comparison with PSM of conventional existing OTS/DTS. Regarding the equipment, advanced PSM must encircle both traditional basic equipment and those new energy technologies are bringing (like DG/RES, DER), especially ones connected to the network with the help of PEI (like BESS, HVDC, SVC, STATCOM), and specific customer load categories. Depending on the type of analysis, phenomena, and time scales of interest for the training of today’s power system operators, and more so of future power systems, two basic types of models are needed, dynamic models with effective values of variables, i.e. **RMS models** (RMS-Root Mean Square) and dynamic models of electromagnetic transients, i.e. **EMT Model** (EMT-Electro Magnetic Transient) which enable hybrid dynamic simulation, that uses advantages of both type of models.

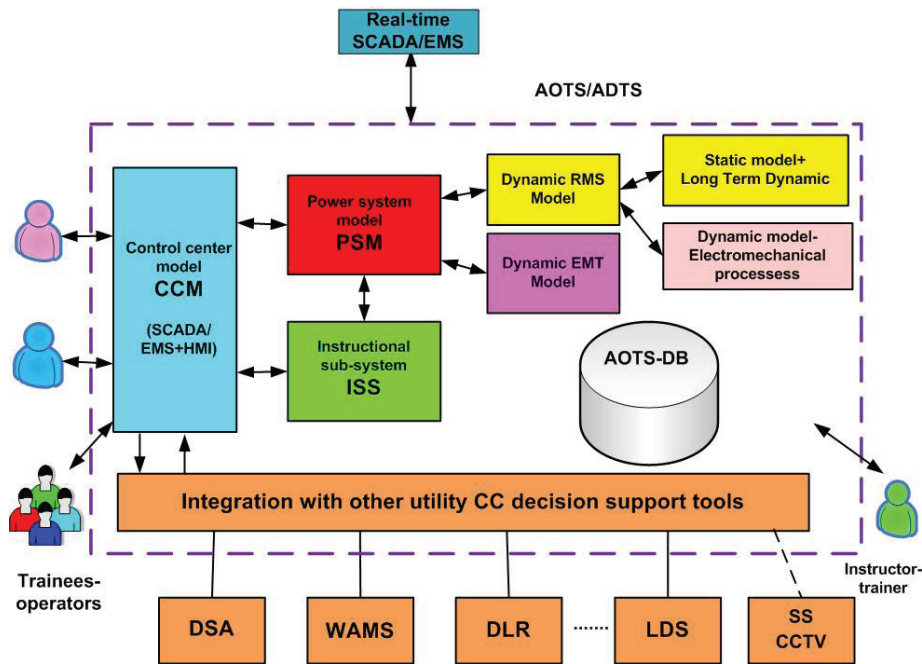


Figure 7. The architecture of the advanced operator training simulator (AOTS/ADTS)

The RMS-type models for a long time were quite satisfactory for the analysis and simulation in the time domain of frequency, voltage, and angle stability, and thus are still used in power system transient processes of short-term, mid-term, and long-term duration, i.e. in the time interval from 100 ms up to several hours (Fig. 1). Although in power engineering, and especially in equipment design, EMT





analysis is done for a long time, while just the massive introduction of RES and other PEI devices has raised the question of the EMT software and models used in the domain of operation control. Namely, the EMT models are needed for resonance stability analysis (both electrical and torsional) and convertor-driven stability analysis, due to the possible influence FACT/HVDC might have on torsional resonance stability, and due to the fast/slow dynamic interactions of the PEI control systems with power system slow/fast response components and other PEID, respectively. Here phenomena of very short duration are of interest, within the time interval from 0.1 ms to 1s, but practically important as might result in converter fault out and loss of associated services. More details about when and how to use RMS and/or EMT models can be found in [13].

**Control center model (CCM)** within the AOTS, besides the standard software for data acquisition, monitoring, and control (i.e. SCADA/EMS, in case of TSO/ISO type companies) must also include all the IT decision support tools that CC operators use, that is typically stand-alone or loosely coupled with the SCADA/EMS, like the: dynamic OH line rating/loading (DLR), lightning detection systems (LDS), dynamic security analysis (DSA), wide area voltage phase angle monitoring systems (PMU/WAMS), and different forecasting systems (load, RES generation). It should be noted that the integration of those systems in the proposed architecture represents a nontrivial technical (development and implementation) problem and as such subject of the future papers.

**The instructional sub-system (ISS)** within the proposed AOTS/ADTS should possess, not only the OTS standard trainer functions for the simulation session control (such as: start, stop, pause, resume, repeat, etc.) and training session execution but also the instructors' capability to: Change the relevant power system model parameters to better suite specific training program/session/scenario goals; Change the relevant CCM parameters that impact the monitoring/control system behavior; Introduce the information which the trainees-operators should react on; Emulate other operators within/outside the CC, other CC or companies; Create or edit simulation training scenario; Have the tools for individual and group training results evaluation (session, program).

## 6.CONCLUSION

The power systems are permanently under development and change of basic technologies, in parallel with operation and control tools and procedures which become more and more complex. All these make the work of system operators, in CC of all power system domains and at all hierarchical levels, more difficult, making existing training methods and tools insufficiently effective. To improve the existing state, in the first place training content should be modified, in a way to include new phenomena and procedures, and then the training tools, before all the training simulators. It is predicted that, regarding the actual training needs and technological capabilities, there is a right moment to start development of the new generation of advanced OTS, with the architecture and functionality described in the paper.

## BIBLIOGRAPHY

- [1] EIRGRID-All Island TSO Facilitation of Renewables Studies, Eirgrid, Dublin, 2010.
- [2] M. Power et al., Challenge in the Control Centre (EMS) due to Distributed Generation and Renewables, CIGRE TB-700, September 2017.
- [3] Abhimanyu Kaushal, Dirk Van Hertem, An Overview of Ancillary Services and HVDC Systems in European Context, *Energies* 2019, 12, 3481; doi: 10.3390/en12183481
- [4] Ben Li, N. Cukalevski, et al., Lessons Learnt from Recent Emergencies and Blackout Incidents, CIGRE TB-608, Paris, France, January 2015. ISBN: 978-2-85873-309-5
- [5] Krzysztof Sroka, Daria Złotecka, The risk of large blackout failures in power systems, *ARCHIVES OF ELECTRICAL ENGINEERING*, VOL. 68(2), pp. 411–426 (2019)
- [6] Hassan H. Alhelou, et al, A Survey on Power System Blackout and Events: Research motivations and Challenges, *Energies* 2019, 12, 682;
- [7] N. Cukalevski, A.P. Das, J. D. Macedo, Power System Operator Training and Training Tools for Future Sustainable Grid Operation, Kyoto, Japan, 3-8 April 2022
- [8] N. Cukalevski, et al, CIGRE TB-524, "Control Centre Operator Requirements, Selection, Training and Certification", Paris, France, 2013, ISBN: 978-2-85873-217-3
- [9] A. Stanković, N. Čukalevski, et al., Methods for Analysis and Quantification of Power System Resilience, DOI 10.1109/TPWRS.2022.3212688, *IEEE Trans. Power Syst.* 2022, 1–4.
- [10] Nikos Hatziaargyriou, Jovica Milanovic, et al., Definition and Classification of Power System Stability – Revisited & Extended, *IEEE TRANSACTIONS ON POWER SYSTEMS*, VOL. 36, NO. 4, JULY 2021, pp.3271–3281
- [11] Vinay Sewdien, et al., System Operational Challenges from the Energy Transition, CIGRE S&E, No.17, February 2020
- [12] N.Cukalevski, A.Das et al, CIGRE WG C2.39, Topic1 and Topic 6 survey preliminary analysis, 2021
- [13] B.Badrzadeh, et al., The Need for Enhanced Power System Modeling Techniques and Simulation Tools, CIGRE S&E, No17, February 2020



# The System Split and Blackout Detection Application

[igor.bundalo@pupin.rs](mailto:igor.bundalo@pupin.rs)**IGOR BUNDALO, GORAN JAKUPOVIC, MARKO BATIC***Institute "Mihajlo Pupin", University of Belgrade***SRDJAN SUBOTIC***Elektromreza Srbije JSC***DUSAN PRESIC***Security Coordination Centre SCC Ltd. Belgrade***Serbia**

## SUMMARY

The system split and blackout detection application was developed as part of the Emergency and Restoration (ER) module of the HORIZON 2020 project called TRINITY (H2020-863874, *Transmission system enhancement of Regional borders by means of Intelligent market Technology*). The main purpose of the ER module is operational resilience enhancement. The module also includes a network topology modelling software (database editor), as well as a messaging and coordination platform. This paper aims to describe all components of the ER module with a focus on the system split and blackout detection application. The application was developed based on a topology processor, a standard component of network applications. The Linux platform and C++ as a programming language were used for the development of this application. A relational MySQL database is used to store system models and other data. The messaging and coordination platform is based on OperatorFabric technology. In conclusion, the paper discusses the improvements achieved and the release plans for further development, as a part of the new Horizon Europe project called R<sup>2</sup>D<sup>2</sup> (HORIZON-101075714, *Reliability, Resilience and Defense technology for the grid*).

## KEYWORDS

System split, blackout, topology processor, electrical islands, coordination platform

## 1. INTRODUCTION

The unification of the electricity market into a single entity is a significant barrier that Europe must overcome. While Northern and Western Europe have made progress in recent years, the Southern and Eastern regions (SEE) still face significant obstacles to catch up with their more experienced EU counterparts. To address this challenge and improve the current situation, HORIZON 2020 project called TRINITY aims to facilitate the interconnection of South-Eastern electricity markets within the Multi Regional Coupling area (MRC). The project developed a set of solutions to enhance cooperation and coordination among transmission system operators in the SEE region. This will support the integration of electricity markets and promote the adoption of clean energy sources.[1]

As part of the TRINITY project, an Emergency and Restoration (ER) module has been developed. The main purpose of this module is, firstly, to detect a disturbance or blackout of the system based on measurements in the SCADA system, and then to initiate guided communication at the SEE regional level. This communication should follow certain predefined disturbance or blackout scenarios and guide dispatchers through all the steps provided by applicable rules and procedures, as well as help them make operational decisions based on the characteristics of the disturbance. The second motivation for creating this tool arose from a major system disturbance that happened on November 4, 2006, which proved that coordination among TSOs is necessary [2]. The similar thing happened on January 8, 2021, after work on the ER module began, so we can now confidently say that the idea for its development was justified. It has also been shown that the current tool for exchanging global system status information (European Awareness System – EAS) is not sufficient in such disruptions. On the other hand, it should be noted that disruption from January 8, 2021 was successfully resolved, despite all detected problems, as assessed by ENTSO-E experts.[3]

The ER module is installed at SCC, Regional Security Coordinator (RSC) and a member of the TRINITY consortium located in Belgrade. The SCADA system performs the necessary operations, while system operators utilize workstations for communication, resembling the EAS. Currently, RSCs lack the authority to participate in real-time processes. However, it has been observed that Europe is moving towards expanding RSC responsibilities, as seen in the Clean Energy Package, making it likely that their authority will eventually include the domain of transmission system management.

## 2. ALGORITHMS OF THE SYSTEM SPLIT AND BLACKOUT DETECTION APPLICATION

The system split and blackout detection application consists of three basic modules:

1. Network Topology Processor (NTP);
2. Application Database Editor (ADB Editor);
3. Coordination platform.

In addition, the application includes two auxiliary modules for appropriate data conversion: XML2ADB, which imports manually entered data from an XML file into ADB, and ADB2NTP, which converts data from ADB to a text format used as input to NTP. The algorithm of the system split and blackout detection application is shown in Figure 1.

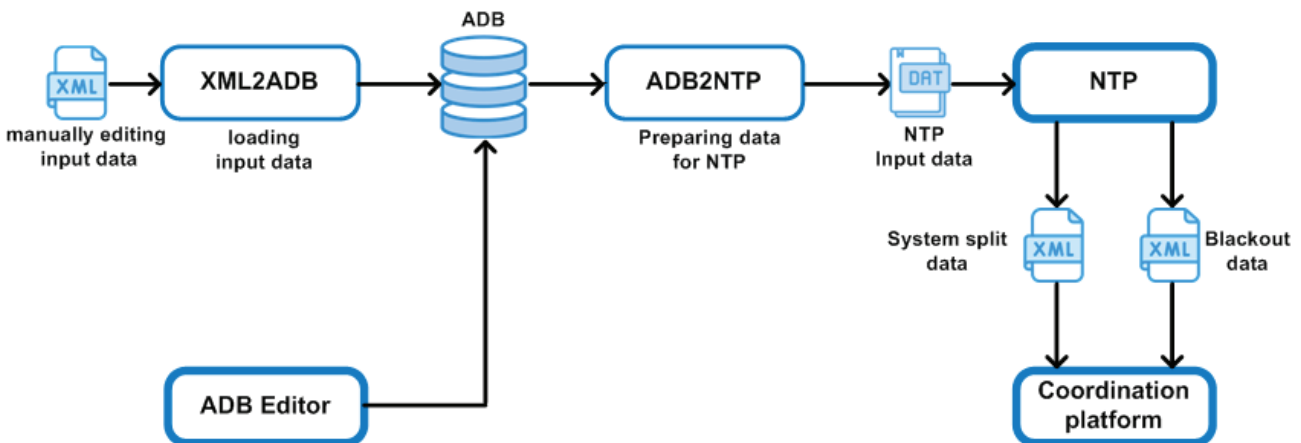


Figure 1. Algorithm of the system split and blackout detection application



### 3. NETWORK TOPOLOGY PROCESSOR (NTP)

Based on static equipment connectivity and switching equipment statuses, NTP determines network topology and identifies electrical islands. The NTP generates a bus-branch equivalent network model with branch parameters determined from actual equipment parameters. Measurements from the SCADA system are further associated to this bus-branch model. The NTP model is entirely bus-branch oriented, so all equipment must be represented with no more than two terminals. In cases where equipment has more than two terminals, such as three-winding transformers, a single-branch representation is no longer possible, resulting in more than one equivalent branch. Three-winding transformers must be decomposed into three two-winding transformers in order to represent them with no more than two terminals.

Topology is processed in two stages: identification of the buses and identification of the islands. First stage identifies buses through processing of switching equipment statuses. Determination of energized electrical islands is performed after measurements allocation. An electrical island is energized if there is at least one voltage measurement above a certain threshold. [4][5]

In every execution cycle, NTP generates an XML file with a temporary list of islands. Each island is assigned a temporary ID that corresponds only to that cycle of the topology processor. Each island has an energization status indicating whether it is energized and a list of nodes. At any given time, there may be islands in the network that have been split or have become de-energized. Any changes in the energization status of islands are detected, and some may be declared as split or in a blackout state. The algorithm considers only 220 kV and 400 kV nodes by default for input data. Users have the possibility to define voltage levels of interest for analysis.

In each processing cycle, topology processor data from the current and previous cycle are used. There are theoretically three situations:

1. Pure system split - an energized island is split into two or more smaller islands that are still energized;
2. System splitting with blackout- an energized island is split into two or more smaller islands, where some of the smaller islands are de-energized;
3. System blackout- the previously energized island becomes completely de-energized.

System split detection is performed as follows:

- A check is performed for each 400kV and 220kV nodes to see if it exists in the list of nodes from the parent island of the previous cycle. If a node did not belong to any island, for example, because it was isolated, it will not be analyzed in the next cycle.
- By comparing the IDs of the parent island in the current cycle, each node is checked to see if it remains in the same island. If a node from the list belongs to a different island, a system split is declared if the observed node that changed islands is in an island that is larger than or equal to the electric island threshold, which is user-configurable. To prevent a branch failure from being misinterpreted as a network split, this threshold is set to 3.
- The islands in which node splitting occurred in the latest cycle are marked as new split islands. These islands, as well as all nodes that belong to them, are assigned the "split" status.

The blackout detection algorithm is performed by iterating through all connected electrical islands. When an electrical island is de-energized, its list of corresponding nodes is checked to see if any were energized in the previous cycle. If the number of such nodes is greater than a user-configurable threshold, the entire island and all nodes within it are marked with a blackout status.

Islands can be classified as:

- Splitting island - all nodes of such islands have the status "split" and do not have the status "blackout";
- Island entered a blackout state - all nodes in such islands have the status blackout and do not have the status "split";
- Splitting island entered a blackout state – all nodes of such islands have the status "split" and have the status "blackout".

Following the final classification, the system stores the following data:

- Time of the previous and current cycle;
- List of all connected islands in the current and previous cycle;
- If an island was formed by splitting, information about the original island is kept, as well as a list of all islands that were split from the same island as the current one;
- Information about the status of the island.

### 4 APPLICATION DATABASE EDITOR

The ADB is implemented as a relational database and serves as a central repository of data on the power system elements (generators, transmission lines, transformers, loads), as well as all necessary data for determining the static topology of the network (element connectivity, bus structure, busbar field descriptions, circuit breaker descriptions...). The static connectivity of the power system elements is described by their terminal connections to the nodes. Apart from static, relatively unchanging data, the application database contains dynamic data on analog measurement values and the status of switchgear obtained from the SCADA system. The application database also contains system parameters necessary for the operation of network applications, as well as corresponding data required for the connection with the SCADA system.

The ADB Editor (shown on Figure 2) is a tool for viewing and editing ADB content. The network model is visually represented in the form of a hierarchical tree. The hierarchical levels are: company, area, substation, and voltage level. Although the Network topology processor algorithm treats all nodes identically, the ADB editor classifies and represents them visually with different colours based on their type:

1. NODE - a type of topological node used exclusively for connecting switchgear devices (●);
2. ENODE - a type of topological node in the busbar field that connects power lines and transformers (◐);
3. GNODE - a type of topological node used for connecting generators with a block transformer or a busbar field (◑);
4. PNODE – a type of topological node used for connecting consumers (◒);
5. BUS - busbars or busbar sections (—).

The ADB editor has a database validation functionality. This functionality involves a series of tests to determine the correctness of the static network model. These tests are classified into three categories:

1. Critical tests that will definitely create issues in operation - “red messages”;
2. Alerts for potential issues - “orange messages”;
3. Information on potential issues with real-time measurements (with measurement signs) - “blue messages”.

The content of the ADB can be saved in the form of a study case on which various analyses can be performed, such as turning on/off breakers, which could result in the network being split into multiple islands.

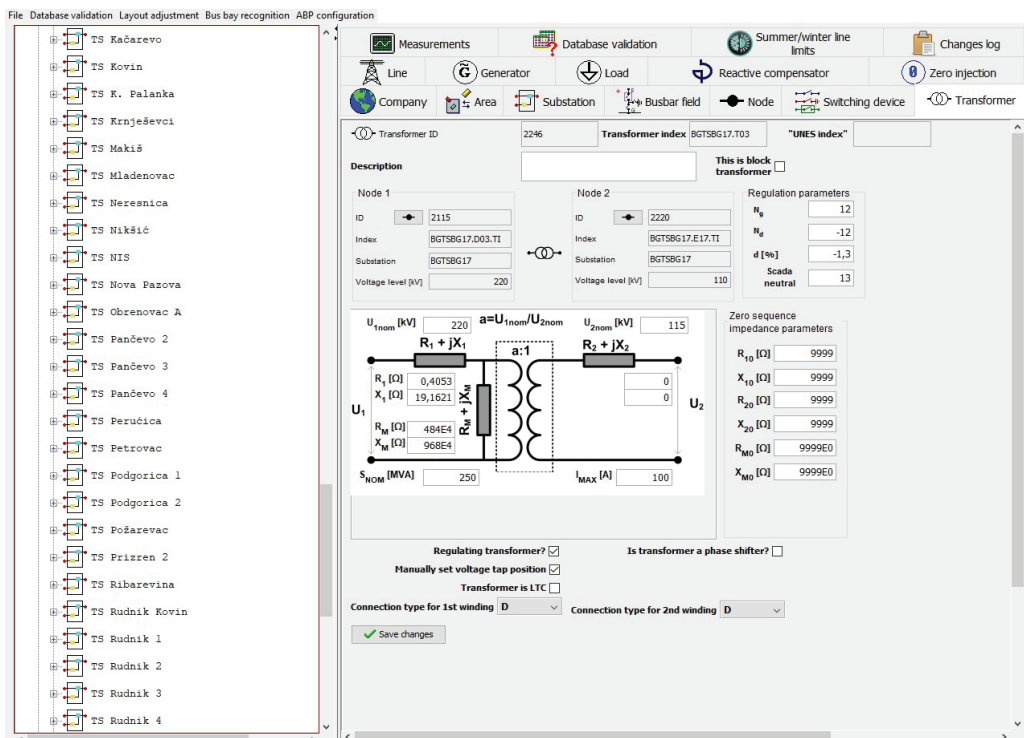


Figure 2. Application database editor

## 5. COORDINATION PLATFORM

Based on the results of the system split and blackout detection application, reports are created on the coordination platform. This platform serves as a means of communication between participants in the process and for coordinating their actions. It is based on the *OperatorFabric* platform which is a modular, extensible, industrial-strength platform for use in electricity, water, and other utility operations [6]. This platform is developed by the Linux Foundation and with publicly available code. Communication through the coordination platform is based on a notification system in the form of cards that are displayed to users. There are four types of cards:

1. Informative cards notify the operator of an event or convey a message from other participants in the system, without requiring a response from the operator.
2. Active notifications require some action from the operator, such as confirming or rejecting a proposed power outage plan, requesting an increase in production, and so on. Active cards are also used when coordinating multiple users to align the plan of action, such as when a part of the system fails, multiple participants in the power system need to coordinate their work to safely restore the system to a stable state.
3. Alarm cards are similar to active cards, but additionally indicate that an urgent response from the operator is required.
4. Alignment cards indicate that some coordination has been completed and send the results of that coordination.

Figure 3 provides an example of an active card from the coordination platform. This figure also depicts main screen of coordination platform, which includes: timeline with indications (top of the window), list of received cards (left side of the window) and content of the selected card (central and right part of the window).

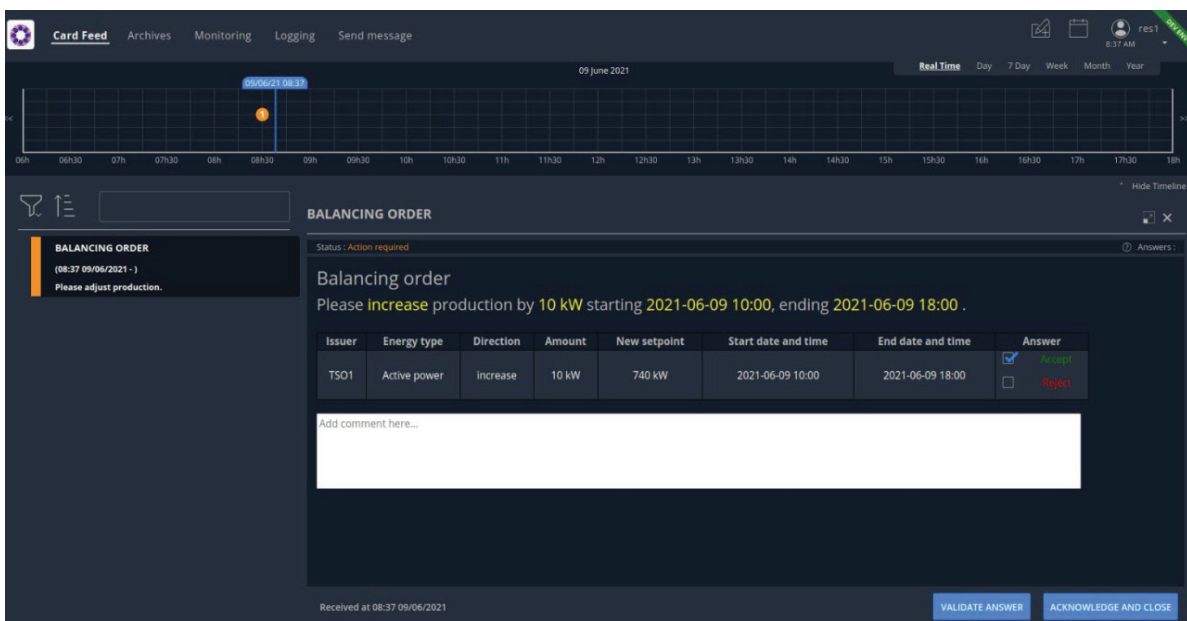


**Figure 3.** Example of a card in a coordination platform - Active card

The coordination platform provides a fast and reliable way of communication and coordination that allows all users to monitor the status of a process, the progress of coordination, and similar information at any time. It allows for a review of the coordination process and exchanged messages if there is a need to rectify any issues in the problem-solving process.

## 6. CONCLUSION

As a part of the Emergency and Restoration (ER) module in the TRINITY project, a study version of the system split and blackout detection application was developed. In order to facilitate the successful implementation, testing, and future improvements of the ENTSO-E ER procedure in a practical setting, the ER module that was originally developed in the TRINITY project and integrated into the SCC (RSC from Belgrade, Serbia) infrastructure will be expanded with SCADA (Supervisory Control and Data Acquisition) system and a historical database. It will also establish appropriate APIs between the ER module and future SCADA system as well as external





telemetry providers (use of IEC 60870-6-505 TASE.2 is planned). Customizations to the ER module and the application database will be made as needed to ensure proper storage of real-time data acquired by the SCADA system, as well as enabling manual input and intervention in case of any missing data.

The proposed ER module enhancement with SCADA system will also include modules for visual presentation of the acquired real-time data as well as the ER module outputs. Moreover, there are ongoing amendments to the Emergency and Restoration procedures that are in force in Continental Europe. Therefore, these improvements and updates are scheduled to be implemented as part of the R<sup>2</sup>D<sup>2</sup> project [7]. Alongside the enhancements that are part of the R<sup>2</sup>D<sup>2</sup> project, one of the next steps is to improve the algorithm to include frequency-based verification. If there is a low-voltage part of the network that is not included in the model, the existing algorithm could, theoretically, falsely report the occurrence of an islanding event even if it does not exist (islands connected at lower voltages). Additional frequency-based verification would improve the algorithm and prevent such errors from occurring.

## 7. ACKNOWLEDGMENTS

The paper is part of the HORIZON 2020 TRINITY project (*H2020-863874 Transmission system enhancement of regional borders by means of Intelligent market technology*). This document has been produced with the financial assistance of the European Union. The contents of this document are the sole responsibility of the authors and can under no circumstances be regarded as reflecting the position of the European Union. Additionally, the research described in this paper was funded by the Ministry of Education, Science, and Technological Development of Serbia.

## BIBLIOGRAPHY

- [1] <http://trinityh2020.eu/download/8267/>
- [2] [http://ecolo.org/documents/documents\\_in\\_english/blackout-nov-06-UCTE-report.pdf](http://ecolo.org/documents/documents_in_english/blackout-nov-06-UCTE-report.pdf)
- [3] [https://eepublicdownloads.azureedge.net/clean-documents/SOC%20documents/SOC%20Reports/entso-e\\_CESysSep\\_Final\\_Report\\_210715.pdf](https://eepublicdownloads.azureedge.net/clean-documents/SOC%20documents/SOC%20Reports/entso-e_CESysSep_Final_Report_210715.pdf)
- [4] Goran Stefanović, Milos Stojic, Ivana Kršenkovic, Goran Jakupovic, Ninel Cukalevski, Igor Bundalo, "Dynamic Coloring of Power System Elements on SCADA/EMS Displays Based on Topological Analysis" V Conference CG KO CIGRE, Budva, May 2017
- [5] Igor Bundalo, Milos Stojic, Goran Jakupovic, Nina Stojanović, Ninel Cukalevski, "SCADA/EMS Network Applications Of Regional Dispatch Centers Within Elektromreža Srbije JSC", VII Conference CG KO CIGRE, Budva 28-30 September 2021
- [6] <https://opfab.github.io>
- [7] <https://r2d2project.eu>



# Automatic Generation Control Working Scheme in Georgia, Under the Liberalized Energy Market

[Mikheil.Odisharia@gse.com.ge](mailto:Mikheil.Odisharia@gse.com.ge)

**MIKHEIL ODISHARIA**  
*Georgian State Electrosystem*

**Georgia**

## SUMMARY

During the last decade, the energy system of Georgia has undergone drastic changes. Under the ten-year network development plan, many projects have been introduced, such as the first HVDC substation in the region, transmission lines, and substations, which enabled the power system to integrate new generation units into the grid.

Because Georgia was a member of the extensive energy system of the Soviet Union, its topology and planning are not adapted to today's reality, and its operation is related to technical/economic problems. Nevertheless, the transmission system operator of Georgia is trying to implement n-1 criteria and take system operation to the next level.

The proof of the above-mentioned proposition is the implementation of Automatic Generation Control (AGC) in Georgian power system. The mentioned project was implemented with the help of SIEMENS, and the activation of reserves became partially automated.

But as we have already mentioned, due to the peculiarities of the energy system of Georgia, it was necessary to implement AGC in a nonstandard way (Only one unit was participating in joint control, and it was activated based on central dispatch principles), as it is not presented in Europe and worldwide. This article will be dedicated to the implementation of Automatic Generation Control in the energy system of Georgia and its transition based on the new market model. The paper aims to share the experience that the Georgian Transmission system operator has accumulated during this process. For stakeholders who want to change their automatic generation control scheme from a basepoint to Basepoint free scheme, this article will help them navigate the process from the TSO to BSP.

These topics will be most relevant in countries where Automatic Generation Control is based on non-market principles.

The article shows in detail how the old AGC worked, how the new model is managed under the self-dispatching scheme, which scheme is more acceptable in terms of system operation, and what challenges we face when working on the new model.

During the development of the article, the best practices from around the world were used, as well as the knowledge and experience of the experts involved in the project.

At this point, the energy system of Georgia operates in central dispatching mode, which means that the Transmission system operator plans the system based on its calculations, but with the liberalization of the energy markets, the energy system must move to a self-dispatch mode, where TSOs have to make a lot of changes in automation and daily processes.

## KEYWORDS

Georgia, Automatic Generation Control (AGC), Transmission System Operator (TSO), Balancing Service Provider (BSP)



Liberalization of energy markets implies the creation of balancing products to balance the system in real-time, for Georgia it is the following:

- Frequency Containment Reserve (Primary Regulation)
- Automatic Frequency Restoration Reserve (Secondary Reserve)
- Manual Frequency Restoration Reserve (Tertiary reserve)
- Emergency Fast reserve (Emergency reserve)
- Emergency Slow reserve (Emergency reserve)

In this article, we will focus on the Automatic Frequency Restoration Reserve which directly refers to the activation of Automatic Generation Control.

### 1. INTRODUCTION

The power system must maintain a balance between generation and consumption at every moment, this ensures that 50 hertz is retained and electricity is supplied to consumers uninterapidly. Back in the early days, very simple control systems were used to adjust generation to consumption. The generator’s output may have been increased or decreased by the plant operator using a straightforward dial control, which was hand-adjusted until it was matched to the load. With the change of time and technology, it becomes crucial to adjust generation to load more sophisticatedly, as power systems have expanded and consumer expectations of power system performance have risen. To achieve the desired balance between generation and load, advanced control systems have been designed and one of them is Automatic Generation Control, which makes the activation of reserves automatic and precise.

Georgian Transmission system operator in 2013 introduced Automatic Generation Control and with this, the operation of the power grid has moved to a new stage and significantly improved the following components:

- Stability of the power grid and maintaining frequency within the nominal value
- Strict adherence to agreed schedules with neighboring countries and reduction of cross-border deviations
- The possibility that the activation of reserves is based on the principle of minimum price and that the system is balanced in the most efficient way

### 2. AUTOMATIC FREQUENCY RESTORATION RESERVE (AFRR)

After signing the Association Agreement between Georgia and the European Union, the third energy package was obligated to be transferred into the legislative framework. Georgia adopted the best European practices and created new market segments: day-ahead, intraday, forward, and balancing markets. The most crucial market segment for the power grid is the balancing market, where system balance takes place in real time. This market segment ensures that all balancing products are purchased and ready to use by the National Control Center. One of these balancing products is the Automatic Frequency Restoration Reserve, which we will explain in detail in this chapter.

Table1: Requirements for AFRR provider unit

Characteristics of Automatic Frequency Restoration Reserve	
Availability duration for AFRR provider unit	Not less then 15 minutes
Response on Setpoint	After new setpoint not more than 10 seconds,
Full activation and deactivation time	Full activation 5 minutes
	Full deactivation 5 minutes
Permissible deviation	Permissible deviation not more than 10% of provided bid amount
Accuracy	In every 10 seconds, two deviations are permissible
Balancing product period	4 hourly blocks (00-04 h; 04-08 h; 08-12 h; 12-16 h; 16-20 h; 20-24 h)

Automatic Frequency Restoration Reserve is a symmetrical product, Balancing Service provider (BSP) must provide reserve on upward and downward regulation at the same time. Balancing Service Provider through Market Management System (MMS) provides bids on tenders and afterward, based on minimal price principle merit order list is generated and sent to SCADA, AGC module.

The above-mentioned process is visible in Figure 1;

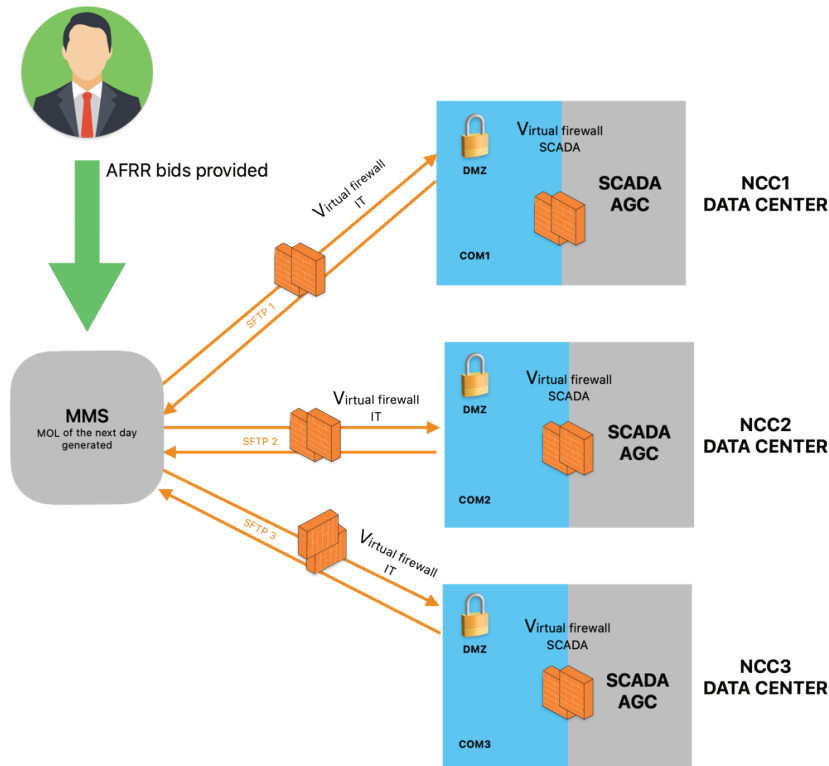


Figure 1: Information flow from MMS to SCADA/AGC

With the introduction of the Automatic Frequency Restoration Reserve (aFRR), there was a need for the Georgian TSO to change its AGC system based on market principles. The merit order list generated from the tendering procedures of MMS needed to be entered into the SCADA system and then the Automatic Generation Control (AGC) would work based on the merit order list.

Along with the liberalization of the markets and the introduction of aFRR product, the TSO has faced the following challenges, the solution of which is a long-term process. These are:

- Technical ability to provide aFRR product only on one unit
- Not readiness of the current AGC system to market liberalization
- Interest new BSPs to comply with the requirements of aFRR balancing product, to increase market liquidity and system security

### 3. AUTOMATIC GENERATION CONTROL PRINCIPLES

A system called Automatic Generation Control (AGC) is used in power plants to control the active power output of generators in response to fluctuations in electricity demand. AGC’s major objective is to keep the power grid’s generation and consumption into account while ensuring that the frequency or interchange schedule remains constant and within acceptable limits.

AGC regulates the output of the generators in real-time in accordance with changing demand for electricity using a combination of control algorithms and communication technologies. The power output of the generators is adjusted by the control algorithms using information about the power demand that is currently present and anticipated in the future.

The power grid’s frequency or cross-border deviation is continuously measured by the AGC system, and it is compared to a predetermined nominal frequency or schedule. The AGC system regulates the output of the generators to return the frequency or the

load on the cross-border line to the nominal value. While adjusting the active power output, the AGC system also takes into account additional elements like the availability of generators, fuel prices, and transmission limitations.

AGC commonly functions in three different modes, especially:

- Constant Frequency Control (Flat Frequency Control)
- Constant Net Interchange Control (Flat Tie-Line Control)
- Tie Line Bias Control

Georgian Transmission System Operator operates in Constant Net Interchange Control (Flat Tie-Line Control), Because Georgia works for the most part in a parallel synchronous mode with the Russian power grid, due to the large size of the Russian system, the frequency in Georgia is always within the nominal range, therefore it is more important to control the interchange on the cross-border line and strictly follow the schedule agreed with the neighboring country.

A flat tie line control (FTLC) model is employed in multi-area power systems to keep the power balance between connected control areas. FTLC is one of the modes of AGC, which is the closed-loop control system to balance the output of generators to power system demand. Depending on the specific needs of the power grid and the operating conditions, several control modes can be used within the FTLC mode, these modes consist of:

- Active power control
- Reactive power control
- Combination mode of active and reactive power control
- AGC with DC tie-line control

The power grid's characteristics and control requirements will influence the mode selection within FTLC. Using one or more of these FTLC schemes, the AGC system will continually monitor the power flow across the interconnecting tie-lines and adjust the power output of generators in the proper control areas to maintain the scheduled power flow within the permissible range.

Georgian TSO conducted tests in the Constant Frequency Control and Tie line Bias Control mode but the regulation of frequency was too rough, the reason is that in the Georgian power grid, few power plants are regulating frequency and there is a small chance to have smooth frequency regulation.

If we take a good look at the graph below, which clearly shows the cross-border deviations with the neighboring country with and without AGC, we will be convinced of the importance of the Constant Net Interchange Control mode for Georgia.

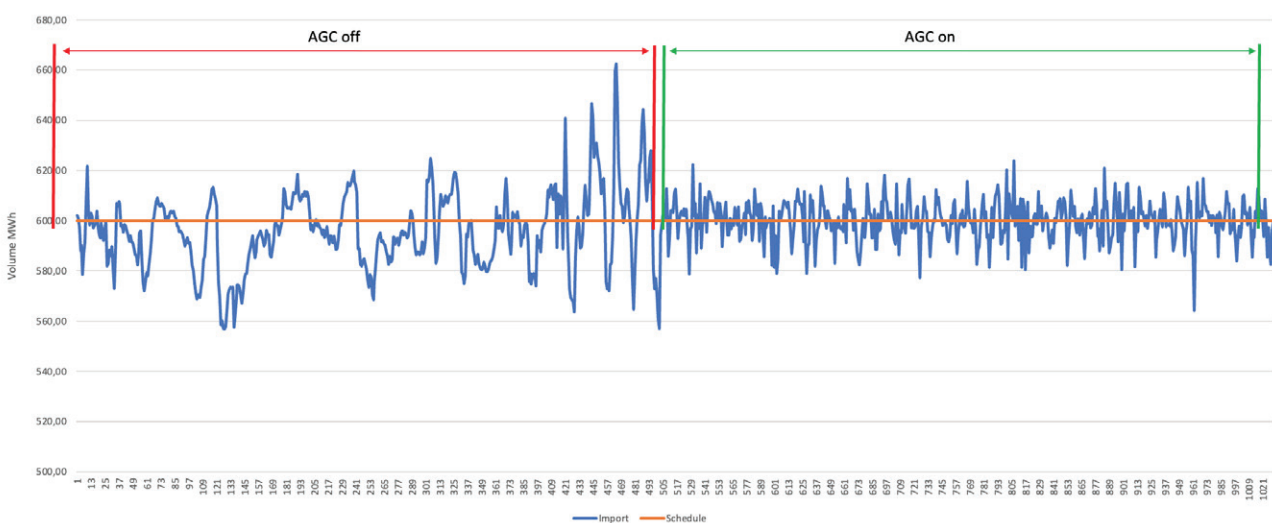


Figure 2: Cross-border deviations during AGC turn-off and turn-on in Flat Tie-Line Control.

The main reason for big deviations on cross-border lines during the AGC turned-off occurred because of steel factories. Steel factories deviate their load drastically and instant load drop can reach 50 MW, which is a big volume for the Georgian power grid.

Oral Presentation: Automatic Generation Control Working Scheme in Georgia, Under the Liberalized Energy Market

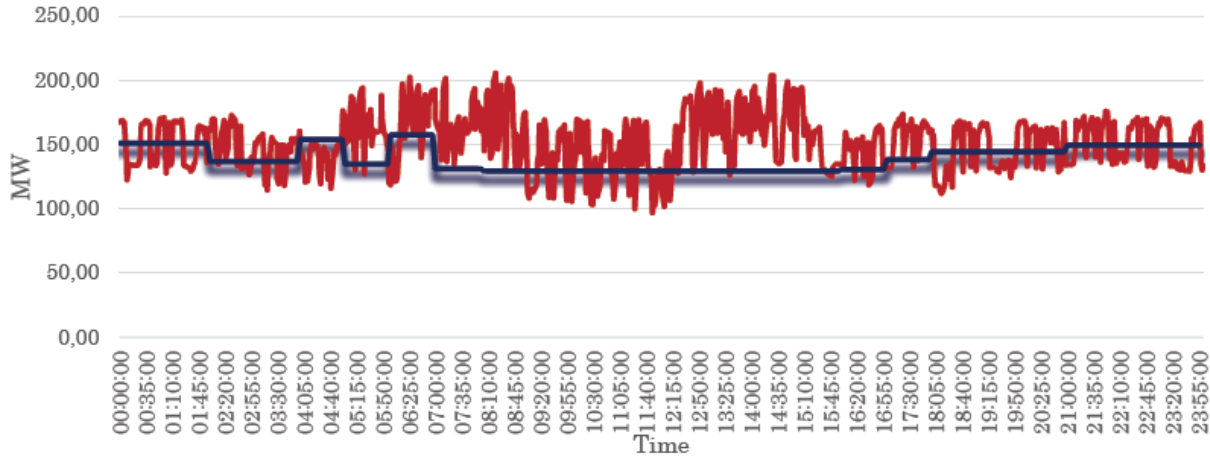


Figure 3: Steel factories' deviations from their schedule.

#### 4. MOVING FROM BASEPOINT TO BASEPOINT FREE SCHEME

As we mentioned, AGC's work had to move to a new level, which should be complied with the new market model. The main requirement was that AGC could work on the merit order list.

In the first stage, the internal system scheme change was carried out with the help of SIEMENS, and all the details were fixed before it came to the generation units, despite the integration of the new scheme, GSE has retained the scheme of the old model, the so-called room to move option, which will be used during the emergency mode in the power grid. GSE set new requirements for BSPs to be able to harmonize with the new AGC scheme.

Requirements and the working scheme is explained in the 4 figure.

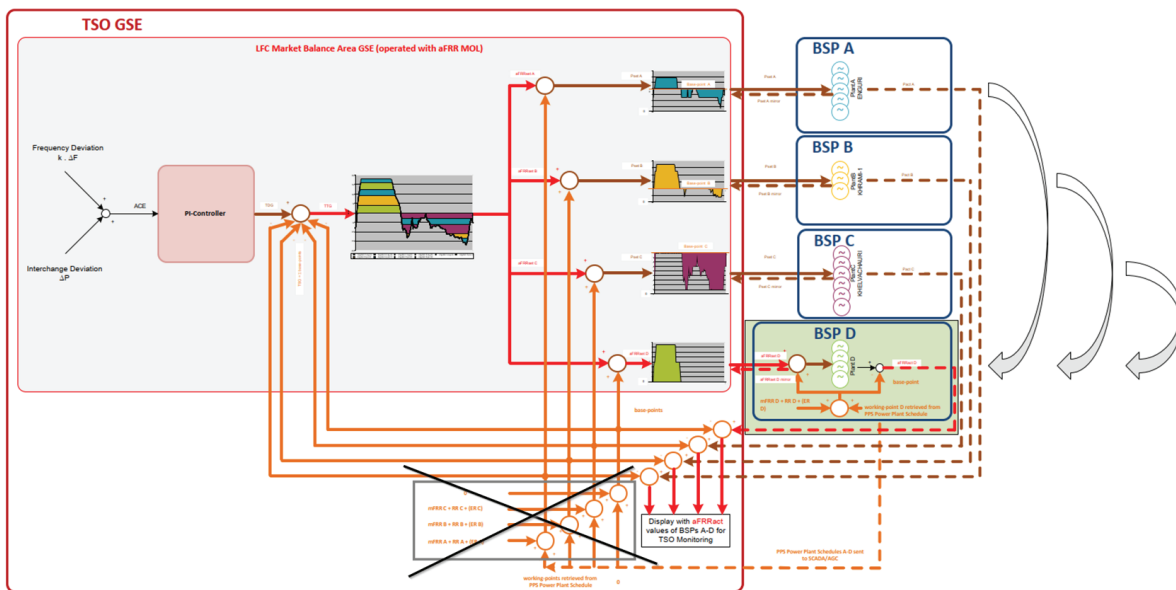


Figure 4: Working scheme of new AGC

Figure 4 shows that with the new scheme, there won't be the capability to work AGC only in absolute setpoint, it should be moved to AGC relative setpoint. this combination of algorithms required very complex adaptations of the controller program (database + source code) in the SCADA AGC system.



In the figure, BSP D presents, how the data are processed in the Basepoint free AGC and how JC shall process its data.

After the successful implementation of the mentioned model in TSO, it was necessary to make all modifications on the Joint Controller(JC), on the BSP side. Therefore the most advanced power plant was selected, in terms of JC and it was Enguri HPP with the installed capacity of 1300 MW.

The power plant implemented Basepoint free solution, after which it could enter the schedule and activated mFRR from the plant side. From the TSO setpoint was sent and BSP's unit performed ramping up or down with requirements of the aFRR qualification document. In the process of changing the scheme at the station, it was necessary to add a field in JC where volumes activated from last-resort instruction would be entered. Dispatcher during the winter period when there is a lack of reserves in the Market Management System (MMS), most of the time uses last resort instructions, which means that the powerplant is activated despite not being in the merit order list. Mentioned activation affects generator output so this activation volume also should be reflected in the JC.

After the implementation of the new scheme, one problem occurred which was related to the response of the generator on the processed setpoint.

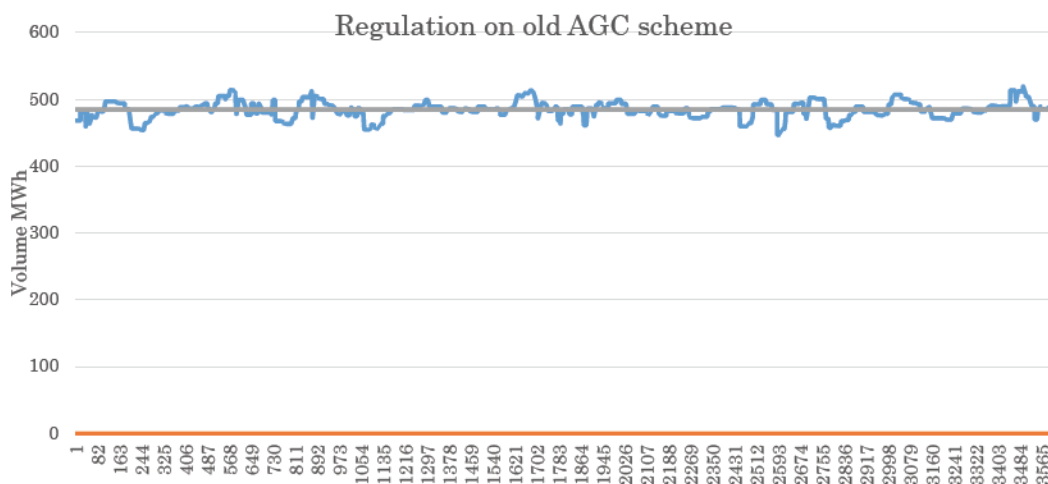


Figure 5: Old AGC regulation vs New AGC regulation

As the 5 graph shows old AGC scheme response on ACE is faster than the new AGC model, this challenge was solved with ramping time entering in JC, 1MW per second. With the mentioned action AGC became quite fast and practice showed that it is possible to solve a similar problem by referring to ramping time.

## 5. CONCLUSION

At the end of the issue, I would like to summarize the events that were discussed in the article, based on the experience of Georgia, all parties, such as the regulatory, ministry, etc. must be involved in such processes from the beginning, this will bring the issue and its importance to the fore. The main problem the TSO may face is a lack of interest from generation companies in the change of the new AGC scheme, in this case, there are two ways to solve this problem, one is to make them financially interested, which did not work In case of Georgia, due too much-regulated market, and the second is to become it mandatory at the legislative level.

Countries, where it becomes necessary to change the mentioned scheme, should consider the following topics:

- Participating in the aFRR balancing product should be financially attractive, so there won't be problems with liquidity on this product;
- Changing the scheme should start with the most advanced powerplant and then share that experience with other generation companies.
- At the initial stage, the TSO should help the generation companies' representatives understand the requirements of the new model and conduct close working meetings with them.
- All the power systems are different, so depending on the specifics of the system, do not hesitate to adjust the scheme to the AGC system and make non-standard decisions



Oral Presentation: Automatic Generation Control Working Scheme in Georgia, Under the Liberalized Energy Market

### BIBLIOGRAPHY

- [1] EPRI Power System Dynamics tutorial (July 2009, 1010 pages 40-58)  
<https://www.epri.com/research/products/00000000001016042>
- [2] H.Bevrani, T.Hiyama, Intelligent Automatic Generation Control (2011, pages 11-35)  
<https://www.routledge.com/Intelligent-Automatic-Generation-Control/Bevrani-Hiyama/p/book/9781138076235>
- [3] GSE FS Basepoint-free\_AGC manual (2015, pages 1-12)
- [4] Commission Regulation (EU) 2017/2195 of 23 November 2017 establishing a guideline on electricity balancing EBGL (2017, pages 1-48)  
<https://eur-lex.europa.eu/legal-content/EN/TXT/?uri=CELEX%3A32017R2195>



# A Dynamic Thermal Rating Architecture for Thermal Monitoring and Congestion Management in the Italian Grid

[enricomaria.carlini, giorgio.giannuzzi, fabio.bassi, cosimo.pisani, guido.coletta]@terna.it

**ENRICO MARIA CARLINI, GIORGIO MARIA GIANNUZZI, FABIO BASSI, COSIMO PISANI,  
GUIDO COLETTA\***

*Terna Rete Italia S.p.a.*

*Italy*

## SUMMARY

The large-scale diffusion of non-predictable renewable power generation and the efficiency policies introduced through the constant evolution in the power markets are rapidly pushing power systems to operate closer to their technical limits. To fully exploit the advantages introduced by these new scenarios, the TSOs need to remove technical constraints by implementing appropriate network expansion plans that allow to solve network congestion and transfer energy between different areas without impacting market price equilibria. However, the typical time for the construction of new transmission assets is far longer than those characterizing the renewable resources diffusion. To fill this gap, the adoption of methodologies for maximizing the transmission capacity of the existing networks becomes crucial.

One of these is the Dynamic Thermal Rating (DTR) paradigm, which allows the on-line estimation of the actual capability margin of monitored constrained lines by exploiting the knowledge of boundary conditions influencing their thermal state. Indeed, overhead transmission lines (OHL) operation requires the minimization of the risk of excessive elongation and lifetime reduction. Both these factors are strictly related to the conductor operating temperature, which is usually limited in function of conductor type and clearance constraints. Traditionally, this limit is translated into a maximum current limit, assuming worst-case conditions for the variables influencing the conductor thermal exchange process (e.g., low wind speed, hot air temperature, maximum solar irradiation, etc.). However, these are very conservative assumptions, which make the line limits underestimated for most of their operating life. Hence, the possibility to on-line monitor the conductor temperature allow a radical change of paradigm, passing from a current-based to a temperature-based dispatching.

The application of DTR methodologies requires the measurement or the estimation of the conductor temperature at least in the most critical spans of the line. This can be achieved following two different approaches, namely direct and indirect methods. The first ones involve the measurement of the conductor temperature itself or its estimation based on the measurement of quantities directly related to it, e.g. sag, oscillations frequency, ecc. On the other hand, indirect methods involve the temperature estimation based on the measurement of environmental quantities influencing the conductor thermal exchange process, e.g. wind speed and direction, air temperature and humidity, solar irradiation and line current.

The Italian Transmission System Operator, Terna, has started a large implementation of DTR all over the national transmission and sub-transmission grids. The approach is based on a mix of temperature estimations based on short-term forecasts of meteorological variables and direct measures coming from temperature sensors installed in the critical spans.

## KEYWORDS

Dynamic Thermal Rating, Congestion Management, Overhead Lines, Thermal monitoring

**Oral Presentation:** A Dynamic Thermal Rating Architecture for Thermal Monitoring and Congestion Management in the Italian Grid

With this in mind, the aim of this paper is to describe the DTR architecture deployed by Terna and present its main applications to solve congestion among market zones, local congestion caused by renewable generators overproduction and their beneficial effects for system operation. Moreover, a focus will be put on the ongoing R&D activities and future developments in the field. In particular, some algorithm possible improvements and new applications for rating estimation some hours ahead will be shortly described.

## 1. INTRODUCTION

During the last years, the EU Commission is pushing member Countries towards carbon neutrality by 2050. To achieve this ambitious objective, in 2021 within the *Green Deal* the EU Council settled a roadmap through the *Fit for 55* for reducing carbon emissions by at least 55% with respect to 1990 levels up to 2030 and laying the foundation for the decarbonization of the entire economy by 2050 [2]. After Russia-Ukraine war and consequent energy crisis, EU published the *RePowerEU* plan to further push energy efficiency and speed up the reduction of fossil fuels dependency [3].

The electric power sector will be profoundly affected by these politics, since the decarbonization of several sectors will be based on their electrification, which in turn requires electric power being produced by renewable energy sources [1]. As a consequence, 592 GW of solar PV and 510 GW of wind power are expected to be connected during the next 5-7 years [4]. In Italy, the projection scenarios suggest that more than 70 GW new installed capacity are necessary to meet the 2030 goals.

In this context, national transmission networks will play a crucial role, since it will be required to transmit power from areas with high density of renewable power production to the main consumption poles. Moreover, these energy flows can deeply change on season and year basis due to the variability of RES and their geographical dispersion, following the availability of the primary energy sources (e.g. solar in southern Europe and wind in northern Europe and North Sea). Transmission System Operators (TSOs) need to intercept in advance the evolution of the generation capacity in certain areas and plan network expansions accordingly [5]. However, the process of building new infrastructures has characteristic times far longer than those of new renewable generation plants: this means that there may be a gap between the connection of new generators and the strengthening of the network necessary to the proper dispatch the energy they produce. In this context, measures that allow to maximize the carrying capacity of the existing interconnections become crucial to remove power transfer capacity constraints between market zones and maximize renewable energy exploitation [6].

The power transfer capacity of a transmission corridor is constrained by three factors, namely stability constraints, voltage constraints, and thermal limits.

Stability and voltage constraints are usually limiting for long, high-voltage, interconnection lines, especially on the primary network. On the other hand, shorter over-head sub-transmission lines are often limited by thermal constraints: they express the maximum operating temperature at which a line can be operated without violating safety and reliability requirements [7]. The primary concerns for limiting transmission line operating temperature are to respect line clearance limits and to avoid conductor annealing. Thus, the maximum operating temperature becomes a maximum operating current limit by considering a pre-defined *worst-case* evaluation of boundary variables influencing the heat transfer between the conductor and the surrounding, e.g. solar irradiation, wind speed, wind direction, air temperature, and so on. This approach is usually addressed as Static Thermal Rating (STR) or Static Line Rating (SLR) [8]. This means that most of the time the interconnection limits are set lower than their real capability [9, 10]. A different approach, namely the Dynamic Thermal Rating (DTR) or Dynamic Line Rating (DLR), can be used, which aims at estimating line ampacity based on real-time information about weather variable and its actual loading conditions [11, 12]. This means that, at each time the loadability of the line is maximized, while still guaranteeing the same reliability and security margins [13, 14].

## 2. DYNAMIC THERMAL RATING

The model describing a transmission line span thermal behavior is based on a first order ordinary differential equation:

$$mC_p \dot{T}_c = P_s + I^2 R(T_c) - P_c - P_r \quad (1)$$

where  $T_c$  and  $I$  are the conductor temperature and current, respectively;  $R$  is the AC resistance of the conductor at  $T_c$ ;  $mC_p$  is the total heat capacity of the conductor; and the remaining terms are defined by a set of non-linear algebraic equations that rule the main heat exchange phenomena affecting the conductor thermal state, i.e. convection ( $P_c$ ), radiation ( $Q_r$ ) and solar heating ( $Q_s$ ) (see Figure 1). The set of parameters included in these equations depend on both external weather variables, such as wind speed and direction, environmental temperature, and several physical factors, including conductor material, line geometry, span location. A detailed description of this model can be found in [15, 16].

**Oral Presentation:** A Dynamic Thermal Rating Architecture for Thermal Monitoring and Congestion Management in the Italian Grid

The reliable estimation of real time conductor operating temperature in the most critical spans is crucial to define reliable overloading policies for the considered line. To get this information, several methodologies exist, usually classified as direct and indirect methods. The first ones aim at directly measuring temperature or some other quantity that can be directly related to it, while the other produce estimation of the conductor temperature by means of a conductor thermal model as the one introduced above. Based on knowledge of the critical conductor temperature, it is possible to define a dynamic capability curve. This is a time vs current curve, which provides for the maximum current that bring the conductor to operate at its rated temperature after a defined time horizon. This is a key information for Control Room operators, which can exploit it even to solve short duration contingencies taking advantage from thermal inertia of the conductor (typical time constant about 10÷15 minutes) [16].

### 3. TERNA'S DTR ARCHITECTURE

Terna has been using DTR information for real-time operation for several years now [17, 18, 19, 20]. The DTR architecture is based on a hybrid framework, which includes sensors directly installed on the conductors of critical spans, weather stations installed on towers on the line route and takes advantage of high resolution forecasts and a distributed weather station network owned by the national Air Force department [21].

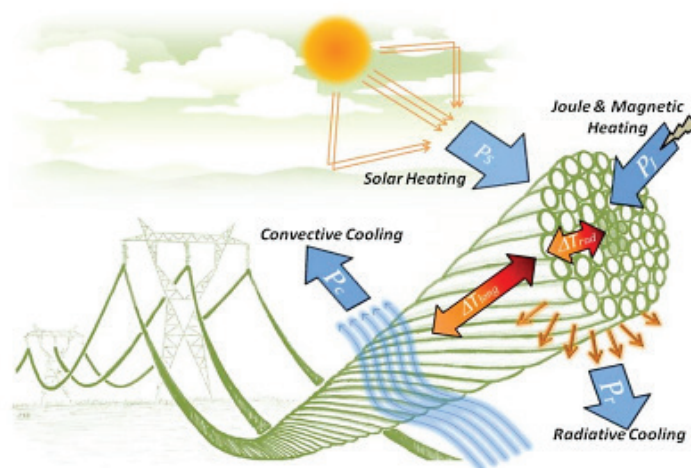


**Figure 1:** OHL heat transfer process [22].

The conductor temperature monitoring is the key process for a reliable application of DTR – based overloading policies. This is a very complex spatial-temporal problem, since different environmental condition insist on the conductor surrounding along line's route. The idealistic approach to the problem would be measuring the conductor temperature at all line spans, so to produce a spatial reconstruction of the thermal state of the entire line [23, 24]. On the other extreme, a *sensor-less* approach, based on conductor temperature estimation starting from weather forecast only, would benefit of no costs for installing equipment uses a thermal, but could be not enough accurate and reliable due to uncertainties affecting weather variables [18].

To take benefits of both these approaches, Terna followed a mixed approach to design its DTR architecture: a thermo-mechanical model [17, 18] was developed for estimating the main conductor parameters (sag, temperature, stress) at each line span starting from short-term weather forecasts and some monitoring systems have been installed to validate and continuously calibrating the model for the most critical spans in terms of clearance.

Wind intensity and direction have a relevant sensitivity on total cooling of the conductor, so also relatively small errors in forecast can impact in a sensible way the ampacity.

Meteo providers usually give data on a fixed mesh so values have to be interpolated to real span positions: wind values, for example, vice versa have high variability depending on local orography so at least for most critical spans only direct measures can guarantee an adequate accuracy.

The model considers as inputs conductor parameters, georeferenced position of the spans, available thanks to a wide LIDAR scan of the EHV/HV network performed in last years, actual line current and maximum span temperatures to respect the clearance limits.

Oral Presentation: A Dynamic Thermal Rating Architecture for Thermal Monitoring and Congestion Management in the Italian Grid

Sometimes DTR ampacity is capped by the presence of hard constraints given by rated limits of substation bay elements which don't provide any temporary overload capacity.

These conductor temperature estimations are corrected using real-time temperature measures in the critical spans.

In particular, the thermo-mechanical model produces a spatial and temporal estimation of conductor sag and temperature along the entire line route and maximum ampacity for the next 30 minutes. This time horizon has been chosen in coherence with the timing for re-dispatching orders to conventional power plants in Ancillary Service Market and for RES curtailments.

Ampacity results are sent both to control room operators via HMI and to OPF procedures as time varying constraints in place of STR limits, as clearly depicted in Figure 2 and Figure 3.

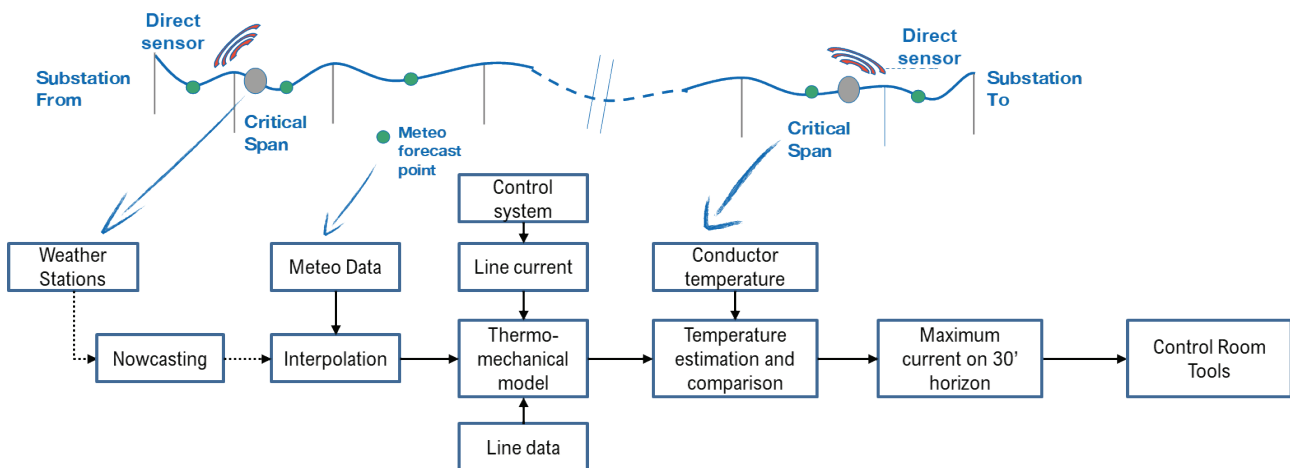


Figure 2. DTR architecture.

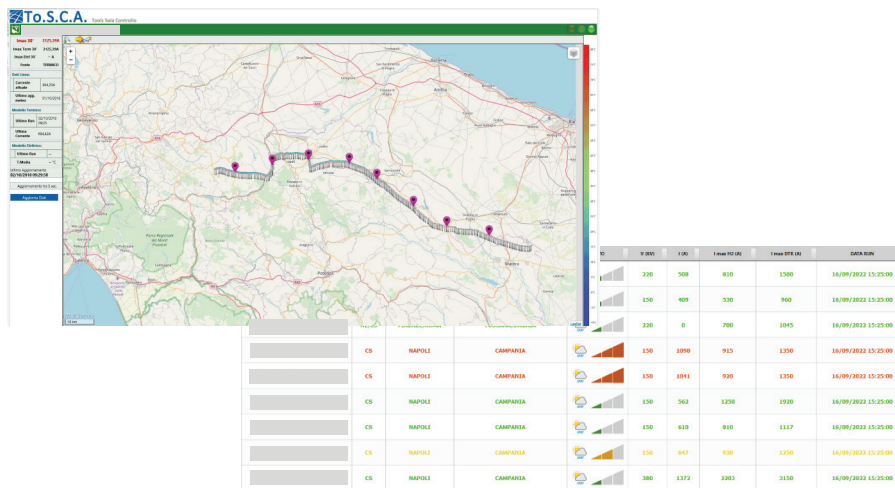


Figure 3. HMI screenshots.

#### 4. DTR APPLICATIONS IN THE ITALIAN TRANSMISSION SYSTEM

In recent years, DTR application perimeter has been extended with the aim not only of punctually mitigating possible congestion conditions but also of using it, with priority on the critical sections of the Italian system, as a new asset management paradigm, moving from traditional static limit-based management towards a temperature-based management much closer to and adhering to the real capabilities in terms of capacity ("ampacity") of the lines.

The application is currently already used on more than 70 OHLs in EHV/HV with a relevant extension plan for next years.

DTR allows to relax constraints on maximum power flowing through thermal-constrained lines. However, it is important to highlight that increased DTR limit is used only for managing possible congestions in N-1 conditions, while in N conditions the usual static limits



**Oral Presentation:** A Dynamic Thermal Rating Architecture for Thermal Monitoring and Congestion Management in the Italian Grid

are used for grid operation. This means that overloading policies are used for managing N-1 contingencies, so that the conductor is used close to its thermal limit just for the time strictly necessary for re-dispatching actions (few minutes).



**Figure 4.** DTR current application

On the other way round, DTR is used in the Italian Network also to solve local congestion caused by high-RES power injection. One example is the management of 150 kV sub-transmission grid lines connecting large wind farms in Southern regions of Italy, where in very windy conditions their STR limits can be reached. In this case, the positive correlation between high line loading due to high wind power generation and high convective conductor cooling due to high wind speed can be reliably exploited in order to avoid RES power curtailment.

Another similar example is the application of DTR policies to lines collecting power generated by hydro units in the Alpine valleys. In this case, the orographic characteristics of the area prevent the construction of new lines due to the high investment costs needed and environmental impacts.

This application has been implemented on 132 kV lines of the mountain areas in North Italy characterized by high hydroelectric production, which often cause grid congestions in spring and early summer with ice melting and consequent high hydraulicity.

The presence of limited loads in the surrounding areas and the distributed generation (hydroelectric and photovoltaic) connected in MV and LV networks, often lead to an inversion of power flow from the MV distribution networks towards HV ones. These phenomena moreover happen in correspondence with lower seasonal static current limits (summer limits from May to September) so grid congestions are sometimes recorded. Their containment is only possible adopting radial configurations of the grid and/or through limitation of the Production Units (Hydroelectric plants) with consequent economic impacts in terms of dispatching costs and/or increased risk of Energy Not Supplied and Non-Withdrawal Energy from the System Operator.

The application of the DTR guarantees good results in terms of increased transport capacity, despite the limited section conductor used in those lines, often quite old, as it can take advantage from environmental conditions typical of mountain areas (almost all the pylons are above 1000m of altitude) with ambient temperatures more favourable than the standard conservative one used in the calculation of static limits.

## 5. RESULTS

DTR approach guarantees for most of the time ratings beyond static limits. The weather conditions used to assess the limit almost always are better than the standard ones used for STR calculation (0,6 m/s, 1000 W/m<sup>2</sup>, 30°C in summer period, 10°C in winter period). Moreover, for short term (30') thermal inertia of conductors makes possible to carry supplementary overload current.

**Oral Presentation:** A Dynamic Thermal Rating Architecture for Thermal Monitoring and Congestion Management in the Italian Grid

Among the applications described in previous paragraph, the best in terms of ampacity increase are the ones for lines connecting areas with high concentration of wind farms because of the positive correlation between line load and wind cooling effect. In Figure 5, some examples of duration curves of DTR ampacity are reported. Statistic curves are built for 3 different 150 kV lines with ACSR 585 mm<sup>2</sup> conductors considering one year 15' data. Values are normalized to respective STR values for summer and winter period. Considering that summer STR limits are lower than winter ones, higher rating increases are possible until almost 2 times the STR. Winter cases are limited by the presence of substation bay hard limits. Depending on different routes and angles respect prevalent wind direction, DTR limits are smaller than STR ones only for 2% to 9% of the samples.

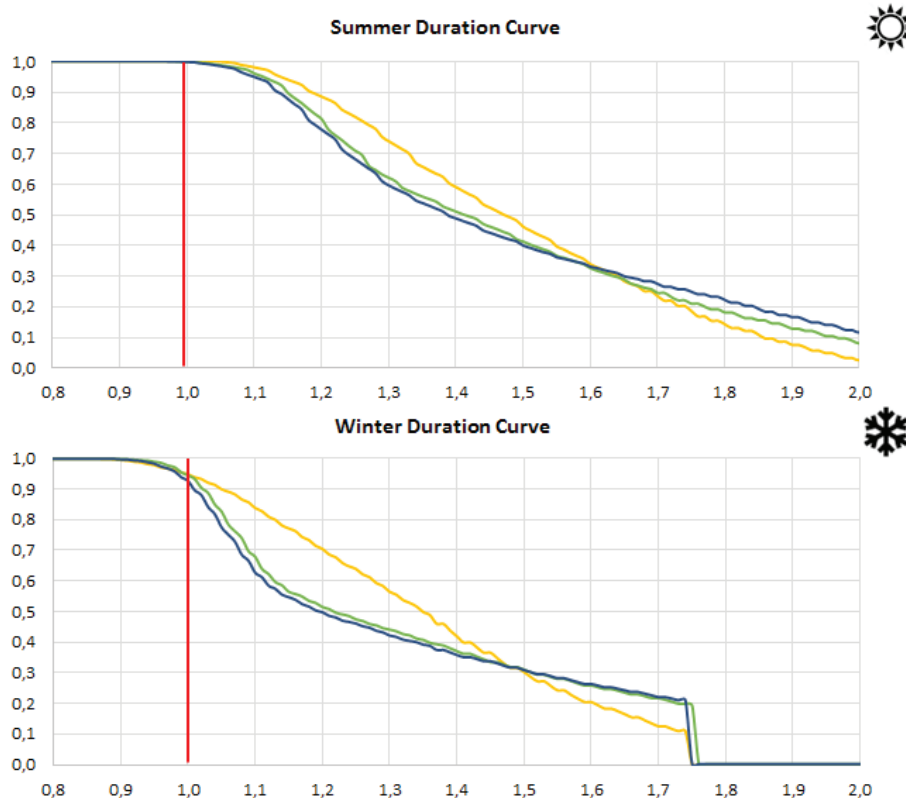


**Figure 5:** Examples of DTR application to connection lines for wind power plants

In other cases, as happens for 380 kV of the critical sections between market bidding zones vice versa there's no direct correlation between power flow and favourable ambient conditions. Flows depends on market outcomes and on RES production but in this case high wind conditions could be in very distant areas and for these reasons this type of application gives not the same percentual rating increase compared to the previous one.

On the other hand, also a marginal increase in rating creates a relevant benefit for the general dispatching cost of the system.

Dynamic rating cap is given by bay limits, which in these lines is often close to winter STR. So in lines where these limits can cause an important constraint, some capital light interventions for uprating of bay elements must be performed in order to fully exploit the DTR.

In Figure 6, some examples of duration curves of DTR ampacity are reported. Statistic curves are built for 4 different 380 kV lines with ACSR 3x585 mm<sup>2</sup> conductors considering one year 15' data. Values are normalized to respective STR values for summer and winter period.

Oral Presentation: A Dynamic Thermal Rating Architecture for Thermal Monitoring and Congestion Management in the Italian Grid

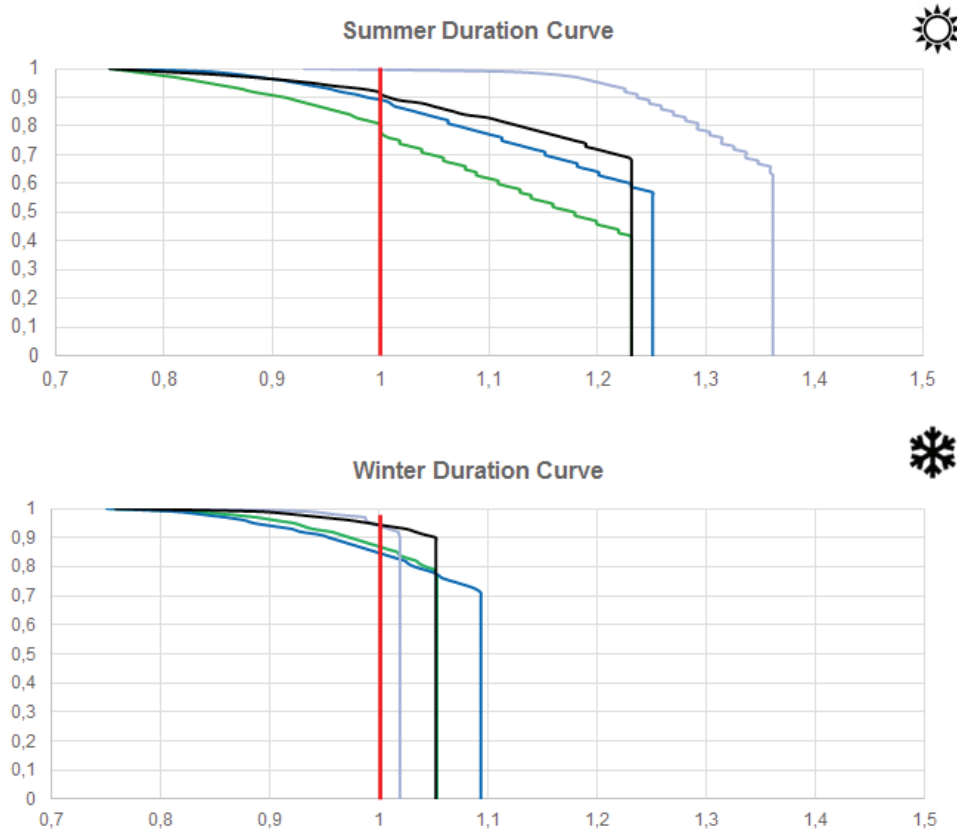


*Figure 6: Examples of DTR application to 380 kV of critical sections*

## 6. FUTURE DEVELOPMENTS

Terna, taking advantage from the current experience gained in some years of operational use of DTR, is committed in a continuous improvement process.

Two main topics are under investigation and in first development phase:

- weather parameters forecast improvements;
- algorithm extension to evaluate ratings in next few hours (up to 24h).

First topic is useful both for current real time use (30') and future approach with a wider ampacity forecast range.

Improvements in weather parameters estimation, in particular wind, guarantees a relevant increase in model accuracy in particular in low wind speed conditions.

Terna is investigating a nowcast approach using statistical models considering also as input real measurements from own weather stations installed on pylons.

The current DTR calculation core model will be adapted to fit also for hours-ahead ampacity forecast adding appropriate de-rating margins evaluated on statistical basis, using historical data collected, in order to guarantee a preset confidence level.

## 7. CONCLUSIONS

The application of overloading policies based on the DRT approach is a key tool for unlocking additional transfer capacity while guaranteeing the same grid operation security and safety levels. Terna implemented advanced technologies and methodologies for estimating conductor temperature on critical lines route. The main applications of DTR in the Italian grid concern N-1 congestion management, local sub transmission grid congestion management related to RES and mitigation of constraints between market zones. The applications to lines collecting power from wind power plants can reach up a significative (more than 150%) ampacity



Oral Presentation: A Dynamic Thermal Rating Architecture for Thermal Monitoring and Congestion Management in the Italian Grid

increase in respect to summer and winter SLR rating. On the other hand, for main 380 kV lines the DTR additional ampacity is more limited and can reach at maximum 130% and 110% of their summer and winter rating, respectively. The operation experience demonstrates that the application of this approach is extremely beneficial for the secure and economic operation of the transmission grid.

## BIBLIOGRAPHY

- [1] IEA, World Energy Outlook 2023, IEA, 2023.
- [2] European Commission, Fit for 55.
- [3] European Commission, REPowerEU Plan, 2022.
- [4] European Commission, Implementing the REPower EU Action Plan: Investment Needs, Hydrogen Accelerator and Achieving the Bio-Methane Targets.
- [5] Terna, Piano di Sviluppo 2023, 2023.
- [6] "On-line control of ders to enhance the dynamic thermal rating of transmission lines," *IEEE Transactions on Sustainable Energy*, vol. 11, no. 4, pp. 2836--2844, 2020.
- [7] E. M. Carlini, C. Pisani, A. Vaccaro and D. Villacci, "Dynamic Line Rating Monitoring in WAMS: Challenges and Practical Solutions," in *2015 IEEE 1st International Forum on Research and Technologies for Society and Industry Leveraging a better tomorrow (RTSI)*, 2015.
- [8] J. Iglesias, G. Watt, D. Douglass, V. Morgan, R. Stephen, M. Bertinat, D. Muftic, R. Puffer, D. Guery, S. Ueda and others, Guide for Thermal Rating Calculations of Overhead Lines, Cigré, 2014.
- [9] D. Poli, P. Pelacchi, G. Lutzemberger, T. B. Scirocco, F. Bassi and G. Bruno, "The possible impact of weather uncertainty on the Dynamic Thermal Rating of transmission power lines: A Monte Carlo error-based approach," *Electric Power Systems Research*, vol. 170, p. 338-347, 2019.
- [10] D. Villacci, F. Gasparotto, L. Orrù, P. Pelacchi, D. Poli, A. Vaccaro, G. Lisciandrello and G. Coletta, "Congestion Management in Italian HV grid using novel Dynamic Thermal Rating methods: first results of the H2020 European project Osmose," in *2020 AEIT International Annual Conference (AEIT)*, 2020.
- [11] O. A. a. T. J. Lawal, "Dynamic Thermal Rating Forecasting Methods: A Systematic Survey," *IEEE Access*, vol. 10, pp. 65193--65205, 2022.
- [12] C.-M. a. T. J. Lai, "Comprehensive review of the dynamic thermal rating system for sustainable electrical power systems," *Energy Reports*, vol. 8, 2022.
- [13] D. Fang, M. Zou, . , A. Vaccaro and S. Z. Djokic, "Handling uncertainties with affine arithmetic and probabilistic OPF for increased utilisation of overhead transmission lines," *Electric Power Systems Research*, vol. 170, p. 364-377, 2019.
- [14] S. C. E. Jupe, M. Bartlett and K. Jackson, "Dynamic Thermal Ratings: The State of The Art," in *21st Int. Conf. on Electricity Distribution*, 2011.
- [15] W. CIGRE, "The thermal behaviour of overhead conductors," *Electra*, vol. 144, p. 107-125, 1992.
- [16] "IEEE Standard for Calculating the Current-Temperature Relationship of Bare Overhead Conductors," *IEEE Std 738-2012 (Revision of IEEE Std 738-2006 - Incorporates IEEE Std 738-2012 Cor 1-2013)*, pp. 1-72, December 2013.
- [17] F. Bassi, G. Giannuzzi, M. Giuntoli, P. Pelacchi and D. Poli, "Mechanical behaviour of multi-span overhead transmission lines under dynamic thermal stress of conductors due to power flow and weather conditions," *International Review on Modelling and Simulations, IREMOS*, vol. 6, 2013.
- [18] F. Bassi, G. Giannuzzi, M. Giuntoli, P. Pelacchi and D. Poli, "Thermomechanical dynamic rating of OHTL: applications to Italian lines," *CIGRE Session 2014*, 2014.
- [19] F. Bassi, G. M. Giannuzzi, M. Giuntoli, G. Lutzemberger, P. Pelacchi, A. Piccinin and D. Poli, "A novel HTLS thermo-mechanical model: applications to Italian OHTL," in *CIGRE Session*, 2016.
- [20] F. Massaro, M. G. Ippolito, E. M. Carlini and F. Bassi, "Maximizing energy transfer and RES integration using dynamic thermal rating: Italian TSO experience," *Electric Power Systems Research*, vol. 174, p. 105864, 2019.
- [21] A. Bosisio, A. Berizzi, D.-D. Le, F. Bassi and G. Giannuzzi, "Improving DTR assessment by means of PCA applied to wind data," *Electric Power Systems Research*, vol. 172, p. 193-200, 2019.
- [22] CIGRE, *TB 601. Guide for Thermal Rating Calculations of Overhead Lines*, 2012.
- [23] K. Morozovska and P. Hilber, "Study of the Monitoring Systems for Dynamic Line Rating," *Energy Procedia*, vol. 105, p. 2557 - 2562, 2017.
- [24] A. Pavlinic and V. Komen, "Direct Monitoring Methods of Overhead Line Conductor Temperature," *Engineering Review : International journal for publishing of original researches from the aspect of structural analysis, materials and new technologies in the field of mechanical engineering, shipbuilding, fundamental engineering sciences, computer sciences, electrical engin*, vol. 37, p. 134-146, 2017.



# Challenges and the Role of the Dispatch Centre in the Management of the Power Transmission System – A Summary Analysis

[vezir.rexhepi@uni-pr.edu](mailto:vezir.rexhepi@uni-pr.edu) / [rrahman\\_p@hotmail.com](mailto:rrahman_p@hotmail.com)

**VEZIR REXHEPI<sup>1\*</sup>, RRAHMAN PËRVETICA<sup>1</sup> AND MUHAMET PURELLKU<sup>2</sup>**

*University of Prishtina "Hasan Prishtina" Faculty of Electrical and Computer Engineering, Kosovo*

*<sup>1,2</sup>Transmission System and Market Operator of Kosovo – KOSTT, Kosovo*

**Kosovo**

## SUMMARY

Transmission system operators play a very significant and essential role in the functioning of the power system as a whole. Considering technological advances and economic development trends, especially the integration of renewable sources and continuous energy transition, constitutes a great challenge in the complexity of properly managing the electrical subsystems. However, the energy balance between production and consumption remains one of the most important factors. This means continuous management and security of electrical energy systems, such as production, distribution, large consumers, and also those of households. The coordination and management of the energy balance include a multitude of components and methods to keep the synchronous frequency in its reliable bandwidth. The management and coordination of the hierarchy and the chain include, among others, also important parameters such as the flows of active and reactive power, currents, and voltages of the primary components (transformers and lines). Monitoring and coordinating the reliability of these parameters requires an organized and advanced structure. Another aspect of the preservation and reliability of the transmission system remains the continuity of safe operation within the regulatory block/zone and neighboring interconnected systems for balance and market transactions between European countries through transmission networks within the ENTSO-e synchronous zone. The purpose of the paper includes an overview of the role of the dispatch center in the management, control, monitoring, and measures that must be taken to maintain the transmission system's stability, security, and reliability. This means proper management of various failures and unplanned outages, safe operations during emergencies as well as contingencies in real time.

The paper presents an overview of the power system management by the Dispatch Center and its responsibility during the operation in real time.

## KEYWORDS

Dispatch Center, Transmission System Operator, Energy balance, Management, Monitoring and Control, Contingencies.

Oral Presentation: Challenges and the Role of the Dispatch Centre in the Management of the Power Transmission System – A Summary Analysis

### 1. INTRODUCTION

The power system plays a fundamental role in development progress, people’s lives, and the country’s economy in general. The rapid development trends and the energy transition require proper preparation and management of the power systems, respectively the transmission systems. Therefore, the role of the national dispatch center in a transmission system is very significant, but also the challenges faced by the systems remain a key factor that requires management from the national center and the professional skills of operators for the operation and coordination of the power system. All stakeholders in the power industry, including society, government, electricity providers, consumers, and power transmission and distribution operators, are desperate for a much more efficient operating system to mitigate the burden and pressure of rapid demand growth. Meanwhile, regulation and customer demand for higher service quality and system reliability also become important considerations of the stakeholders.

Global initiation of environment protection and carbon dioxide emission reduction substantially constrain the development of conventional power systems based on fossil energy, while promoting the utilization of renewable energy sources [1].

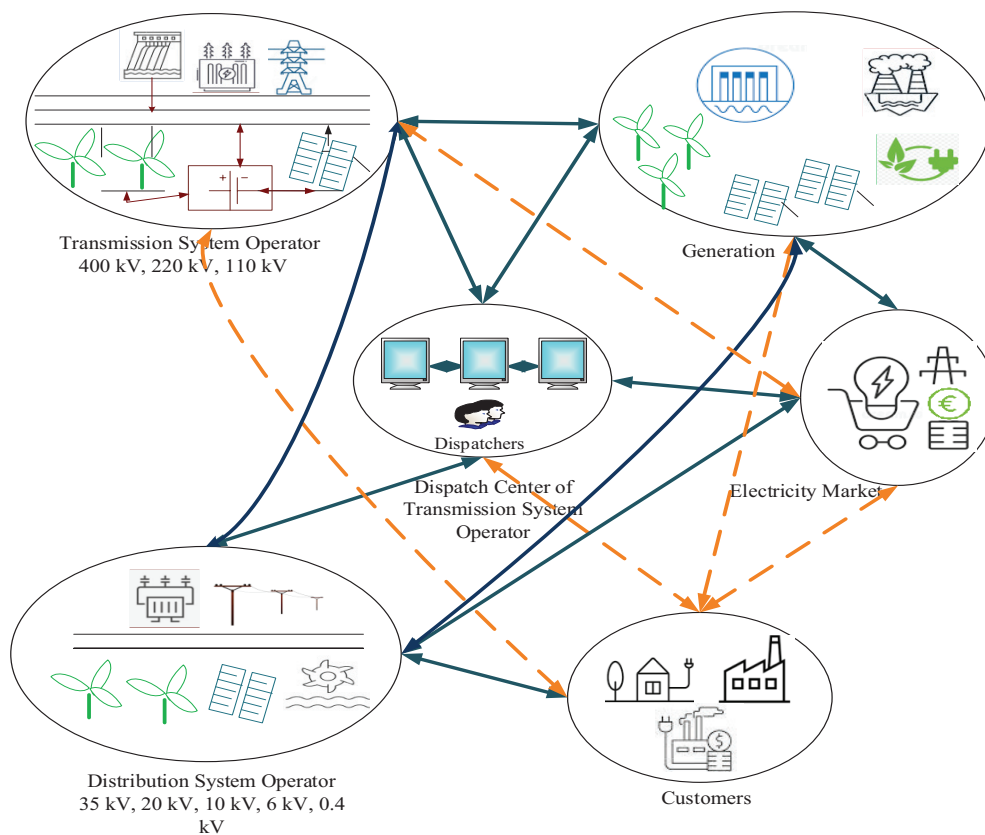


Figure 1. Dispatch center role in the control and managing of the power system [2]

Thus, transmission emerges as a key factor in this energy transition and power grid evolution, necessary to achieve higher levels of renewable energy penetration. Improvements to existing transmission networks, including their planning and operation, are crucial to a broader acceleration of grid decarbonization [3], [4]. The rapid development of enhanced economic integration in today’s power industry and other related industries, especially with the coal industry and other energy resources is inextricably linked. In energy resource depletion, concerns about the deteriorating natural environment background, how to make effective energy resources, and produce the greatest benefits becomes a hot issue [5]. An overview of the Dispatch Center’s role is predicted in Figure 1.

### 2. THE ROLE OF THE DISPATCH CENTER IN THE CONTROL AND MANAGEMENT OF THE POWER SYSTEM

Nowadays, electricity is a necessity for all economic, health, educational, and industrial development. Electricity is involved in everyday human activity, either directly or indirectly. But sometimes can be occurred unpredicted outages or blackouts caused by



Oral Presentation: Challenges and the Role of the Dispatch Centre in the Management of the Power Transmission System – A Summary Analysis

a variety of factors such as transmission line overloads, high demand levels with low energy production, mistakes in load forecast, meteorological events, maintenance problems, cyber-attacks, terrorist or criminal actions, and dispatching mistakes [6]. Given the increased reliance on electricity, in the event of a blackout, a great number of everyday human activities are affected [6].

The power system mainly relies on two aspects, i.e. reliability and safety. Reliability means that an analysis should be made of the stationary operation of the power system when all the components are in operation and meet the consumer demand and all transactions of the electricity market. [7]. Also, the integration of renewable energy sources, battery storage, as well as operation of the power distribution network close to the load centers is increasing to meet the continuously growing power demands, so it is necessary to analyze the reliability and make a risk assessment of these systems to assure balanced operation of the power transmission system [8], [9].

The purpose of the energy control system is to ensure the quality and security of the operation of the power system covering a defined geographical area. The performance that the power system is intended to control has been planned according to a well-defined philosophy and lends itself to reliable and optimum operation [10].

### 3. POWER SYSTEM STABILITY AND CONTROL

To operate a power system in a reliable and efficient manner, different parameters must be within an acceptable limit. Among the numerous parameters, stable frequency is one that plays an essential role in the proper operation of a power system [11]. Basically, the frequency of a system should be maintained within an acceptable range, thereby preventing issues such as the total generation capacity trying to balance the total load. However, both generation and demand change dynamically, which may lead to an imbalance between the total generation and total demand within that system for an instant of time. This imbalance creates a frequency deviation. If the deviation is within an acceptable range, there will be no significant impact; however, if it crosses a certain threshold, it will affect the power system’s operation, reliability, efficiency, and security, as well as degrade load performance, overload transmission lines, and lead to protection failures [12]. Figure 2 shows the power system components reliability and control by Dispatch Center.

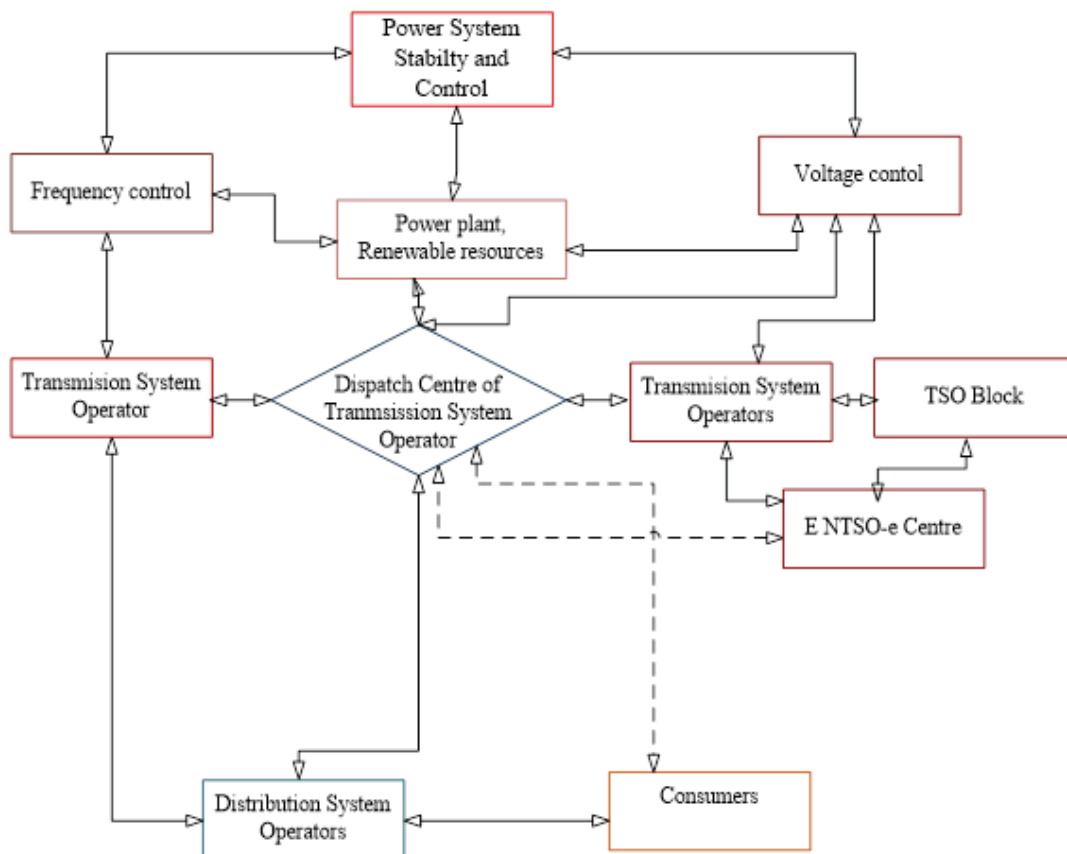


Figure 2. Power system components reliability and control by Dispatch Center

Oral Presentation: Challenges and the Role of the Dispatch Centre in the Management of the Power Transmission System – A Summary Analysis

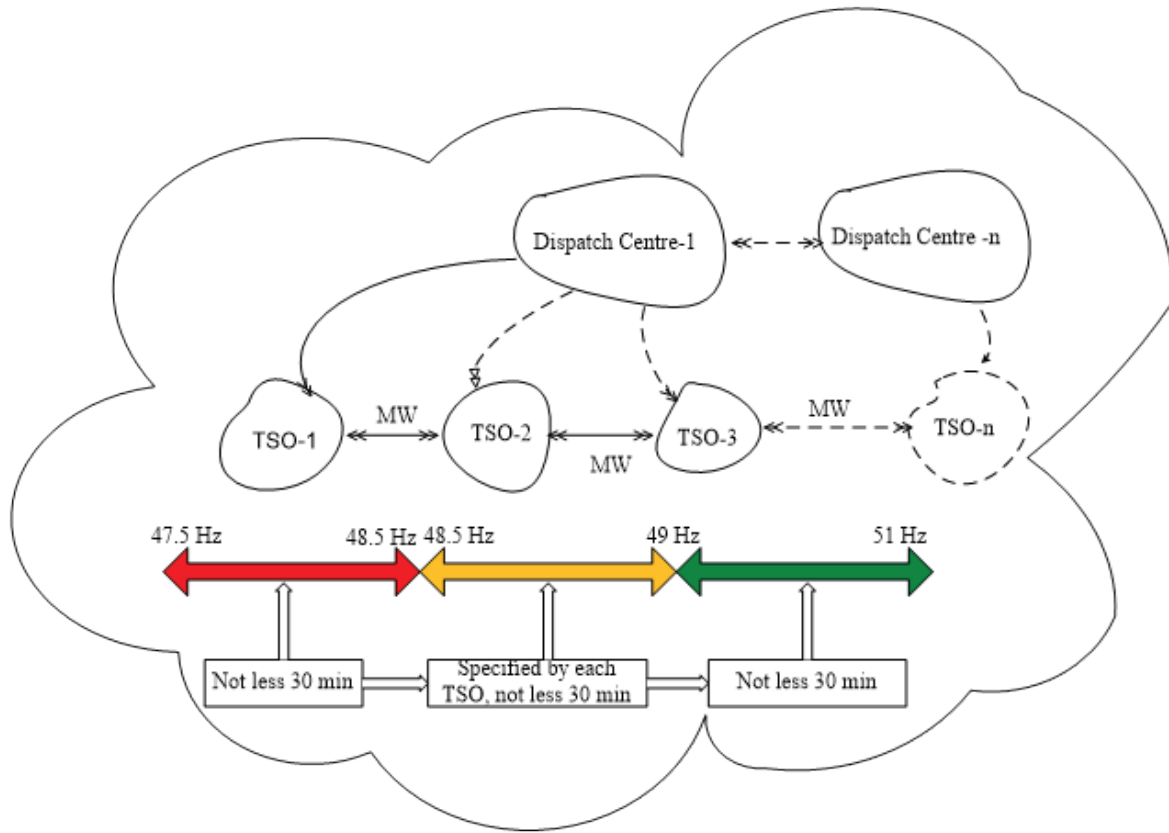


Figure 3. Stability classification of a power system [6]

Any power system’s ability can be described from a power system reliability evaluation. Adequacy

and security are the main two aspects of any power system reliability analysis [6]. Adequacy can be expressed as the availability of adequate amenities to convince the consumer’s demand. The adequacy of a power system is associated to conditions that are static and can be analyzed in the study of power flow simulation [13]. Other important factors are the static and dynamic stability as well as the economic dispatch of the generating and transmitting system. This makes the national center responsible and decision-maker in management, whose primary role is to maintain the frequency and voltages in the allowed operating band [14]. It is known that, among other things, the dispatch center has its role in the coordination and support of the secondary and tertiary reserve according to the need and demand of the energy balance and stability of the power systems, the block, and the synchronous zone of the ENTSO transmission networks. Above all, the role of the center consists in keeping the frequency and voltages stable according to the expected electrical norms (Figure 3).

*The role of the frequency on the control of the power system* – the role of frequency is fundamental in the smooth running and safe operation of the electric power system. The frequency has a primary impact on the safety of the electrical system and depends on several factors, such as production and consumption, therefore large imbalances in the electrical systems can cause significant deviations and with very serious consequences for the electrical systems up to the zero point. According to the standards, there are operating frequency bands that the operators of the electrical systems, where the national centers have a role in the operational and continuous work and their coordination among themselves and with the transmission systems and generally with the synchronous area (Table 1).



Oral Presentation: Challenges and the Role of the Dispatch Centre in the Management of the Power Transmission System – A Summary Analysis

Table 1. Range operation of the frequency in the different synchronous areas [15]

Ranges	Synchronous area				
	GB	IE/NI	Baltic	Nordic	CE
47.0Hz-47.5Hz	20 seconds	.....	.....	.....	.....
47.5Hz-48.5Hz	90 minutes	90 minutes	To be specified by each TSO , but not less than 30 minutes	30 minutes	To be specified by each TSO , but not less than 30 minutes
48.5Hz-49.0Hz	To be specified by each TSO , but not less than 90 minutes	To be specified by each TSO , but not less than 90 minutes	To be specified by each TSO , but not less than period for 47.5Hz-48.5Hz	To be specified by each TSO , but not less than 30 minutes	To be specified by each TSO , but not less than period for 47.5Hz-48.5Hz
49.0Hz-51.0Hz	Unlimited	Unlimited	Unlimited	Unlimited	Unlimited
51.0Hz-51.5Hz	90 minutes	90 minutes	To be specified by each TSO , but not less than 30 minutes	30 minutes	30 minutes
51.5Hz-52.0Hz	15 minutes	.....	.....	.....	.....

Frequency stability depends on the ability to restore the equilibrium between system generation and load demand with minimum loss of loads. Various reasons can lead to a loss of system frequency stability, like loss of generation which may result from a sudden imbalance between system generation and load demand [16]. Therefore, frequency instability is due to electrical power deficiency. Large deviations of both system frequency and voltage, in addition to power flow and other system parameters generally lead to severe system blackouts. The interconnected power systems can be commonly associated with splitting systems into islands with different capacities of generation and certain loads [17]. Anc case of the frequency deviations during he day is shown in Figure 4.

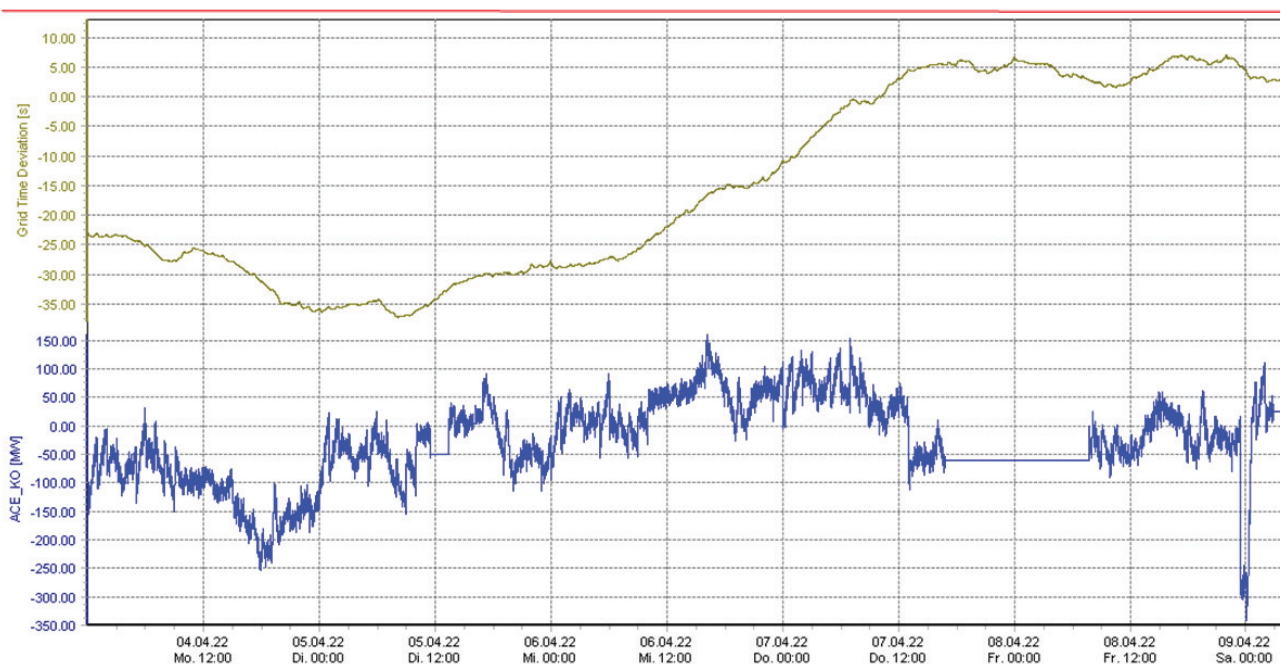


Figure 4. Frequency deviations and stability during a day (KOSTT) [18]



Oral Presentation: Challenges and the Role of the Dispatch Centre in the Management of the Power Transmission System – A Summary Analysis

Frequency in a power system is a real-time changing variable that indicates the balance between generation and demand. In Great Britain, the National Grid is the system operator that is responsible for maintaining the frequency response of the power system within acceptable limits. Two main levels define these limits: the operational limit, which is equal to ± 0.2 Hz (i.e. 49.8 Hz to 50.2 Hz), and the statutory limit, which is equal to ± 0.5 Hz (i.e. 49.5 Hz and 50.5 Hz). Under a significant drop in the frequency (i.e. below 49.2 Hz), a disconnection by low-frequency relays is provided for frequency control of both the generators and demand [11].

As a task, it remains for the Dispatch Center within the Power Systems, in cases of deviations above or below the operating range, to take corrective actions for the energy balance by putting into action the support reserve according to the need and deviating values.

Impact of the voltage on power system – the voltages in the power transmission systems are defined as one of the most fundamental parameters in the overall functioning of the power system.

The voltage stability problem in power systems is attracting more attention from researchers around the world mainly because of several voltage collapse incidents in recent history]. It is widely felt that the uncertainties of power system restructuring efforts as well as utility economics have led many companies to operate their systems close to the maximum liability limits thereby unwittingly pushing their systems toward the brink of collapse. There are several definitions of voltage stability. One definition developed by CIGRE is that at an operating condition and subject to a disturbance the system is voltage stability if voltages at load buses approach their post-disturbance equilibrium points [19].

Real-time monitoring and active control are considerably required to replace conventional excessive infrastructure investments as a solution to improve operational efficiency. Therefore, a new alternative is arising, which is known as the active distribution network in contradiction to the passive distribution network [20].

Voltage stability can be divided into static or dynamic. Dynamic voltage stability is based on differential equations that determine the variation of bus voltages with varying system operating parameters. The methods used in analyzing the dynamic voltage stability include bifurcation analysis, small signal stability analysis, time domain simulations, and the energy function method. Static voltage stability is based on power flow equations and can point out the mechanisms of voltage collapse for different operating conditions. This method takes less computational time and yields most of the required information concerning the voltage stability of the system. Since the system dynamics that influence voltage stability are slow, many aspects can be analyzed by use of static methods which determine the viability of the equilibrium point represented by a given operation of the power system. The methods used in static voltage analysis include; Q-V curves, bus sensitivities, and P-V curves. Voltage stability can be divided into static or dynamic. Dynamic voltage stability is based on differential equations that determine the variation of bus voltages with varying system operating parameters. The methods used in analyzing the dynamic voltage stability include bifurcation analysis, small signal stability analysis, time domain simulations and energy function method [21]. Static voltage stability is based on power flow equations and can point out the mechanisms of voltage collapse for different operating conditions. This method takes less computational time and yields most of the required information concerning the voltage stability of the system [35]. Since the system dynamics that influence voltage stability are slow, many aspects can be analyzed by use of static methods which determine the viability of the equilibrium point represented by a given operation of the power system. The methods used in static voltage analysis include; Q-V curves, bus sensitivities and P-V curves [22]. Range voltage operation is shown in Figure5.

Table 2. Range operation of the voltage in the synchronous area [5]

Voltage limit	Period operation
0.85 pu – 0.90 pu	60 minutes (allowed to operate)
0.90 pu – 1.118 pu	Unlimited
1.118 pu – 1.15 pu3	20 mintes (allowed to operate)

Oral Presentation: Challenges and the Role of the Dispatch Centre in the Management of the Power Transmission System – A Summary Analysis

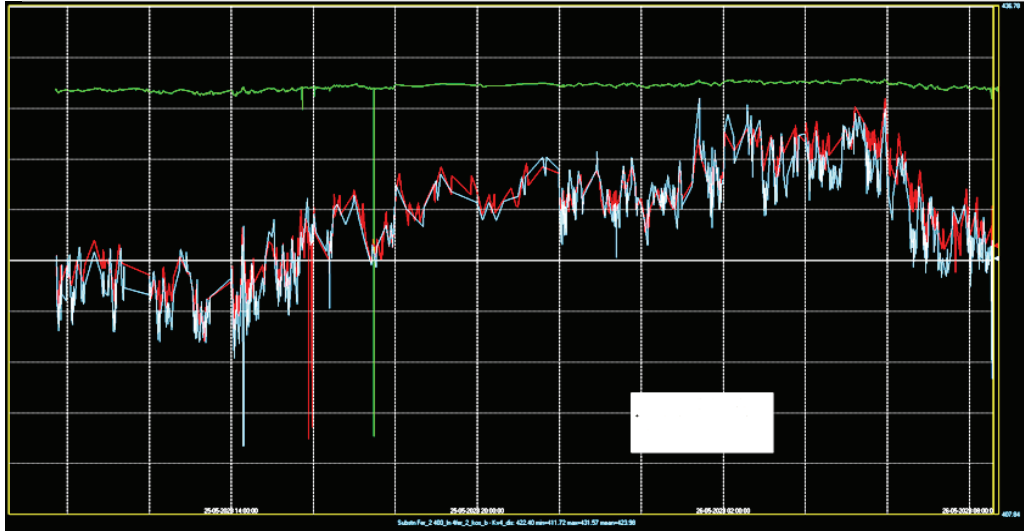


Figure 5. Voltage profile during a day (KOSTT) [18]

The voltage profile is shown in Figure 5 during the day in the Transmission System Operator of Kosovo.

*Outages and management of the unpredicted situation on the power system* – Electric power systems often face unplanned outages of its components such as; lines, and transformers, however, breakdowns or sudden exits of large power plants create large imbalances and at the same time production-consumption mismatch [23]. Figure 6 shows the contingencies calculation platform in the SCADA at Dispatch Center in Kosovo TSO.

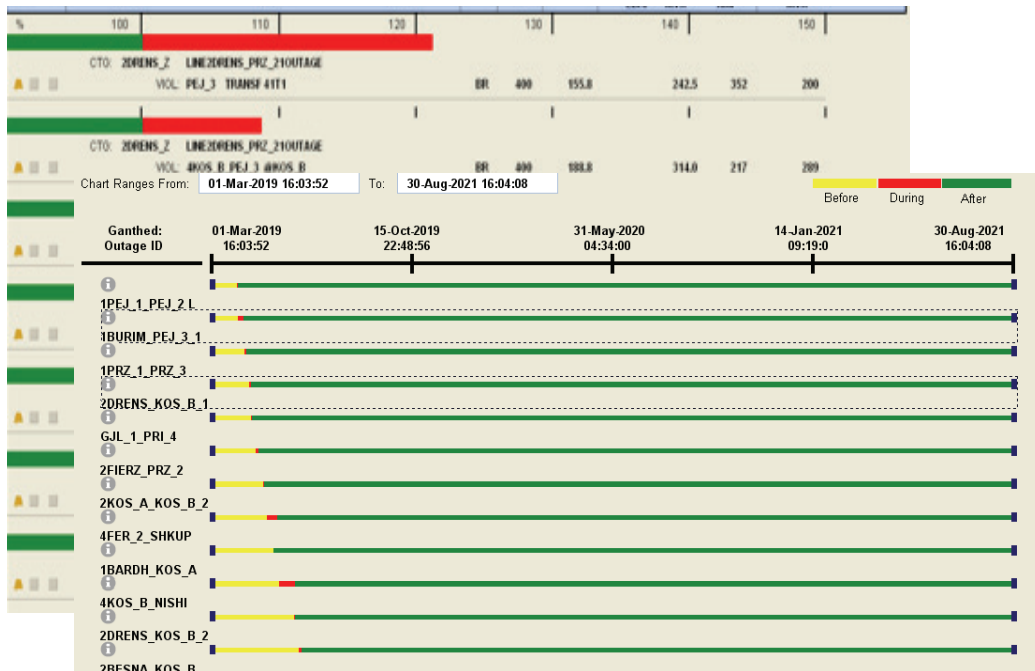


Figure 6. Contingency on the Power System of Kosovo (KOSTT) [18]

The calculation of contingencies and their evaluation for the different levels of these in different branches of the electric power system, or in its entirety, means great challenges for the Dispatch centers. This means that Dispatch Centers play a substantial role in the positive impacts of transmission systems.

Robust operation of a power grid requires anticipation of unplanned component outages that, if not adequately considered, could lead to dramatic and costly blackouts. Planning and operating criteria are designed in order that “the interconnected power system shall be operated at all times so that general system instability, uncontrolled separation, cascading outages, or voltage collapse, will



Oral Presentation: Challenges and the Role of the Dispatch Centre in the Management of the Power Transmission System – A Summary Analysis

not occur as a result of any single contingency or multiple contingencies of sufficiently high likelihood” [1]. Additional more specific criteria help to achieve this famous N – 1 criterion in practice [6]

Energy management systems (EMSs) used for controlling power system operation include numerous functions, one of them being N-1 contingency analysis. In fact, N-1 contingency analysis is a function that analyzes the effects of a single power system component outage on power system operating conditions once the single component (e.g., transmission line, power transformer, generating unit) has been removed from the system. In general, when performing N-1 contingency analysis calculated branch flows are compared with the current carrying capacity of transmission lines and maximum loading of transformer branches, and voltage deviations of network nodes are compared against allowable deviations from nominal values. Contingency analysis is also used in the planning/development stage since most grid codes demand the application of the abovementioned N-1 criterion [24].

### 4. COORDINATION WITH TSO AND BLOCK AREA IN THE SYNCHRONOUS AREA

To enhance stability or to stabilize the system after disturbances, various types of control methods have been developed. Since angle stability is a fast, dynamic phenomenon with a timescale from milliseconds to a few seconds, only limited local fast control actions (e.g., fast valving or the use of braking resistors) have been available to prevent instability. Some more advanced exceptions are excitation control using feedback linearization, preventive control, emergency control, generation shedding, and controlled islanding against cascading events, which are becoming more common in practical power system control. Thus, this section focuses on frequency control and voltage control. Of course, as more fast control devices and methods have been used and developed (e.g., energy storage system and demand response), new control methods to deal with angle instability are expected [25].

### 5. ELECTRICITY MARKET MANAGEMENT AND COORDINATION

The base existing electrical system in most countries was developed when energy production was relatively cheap. As a result, conventional power systems usually have large centrally dispatched power plants, long transmission lines, and unidirectional distributed systems with extra capacity to improve reliability. Although the conventional power system structures had many problems such as a large amount of technical and nontechnical losses (10% up to 52% ) and environmental pollution (40% of CO2 coming from power generation ), it has been used in the same way for the last century. Recently, rapid technological advancement has been changing people’s lifestyles and accordingly, the electricity demand, resulting in about a 2% increase in electrical energy consumption per year, a trend that is predicted will continue. This rising demand, climate change, growing fuel costs, outdated power system infrastructures, and new power generation technologies have motivated changes in the power system architecture. The most important factor is the large number of distributed generations (DGs) being installed on the distribution network [26]. The electricity market platform is predicted in Figure 7 (KOSTT).

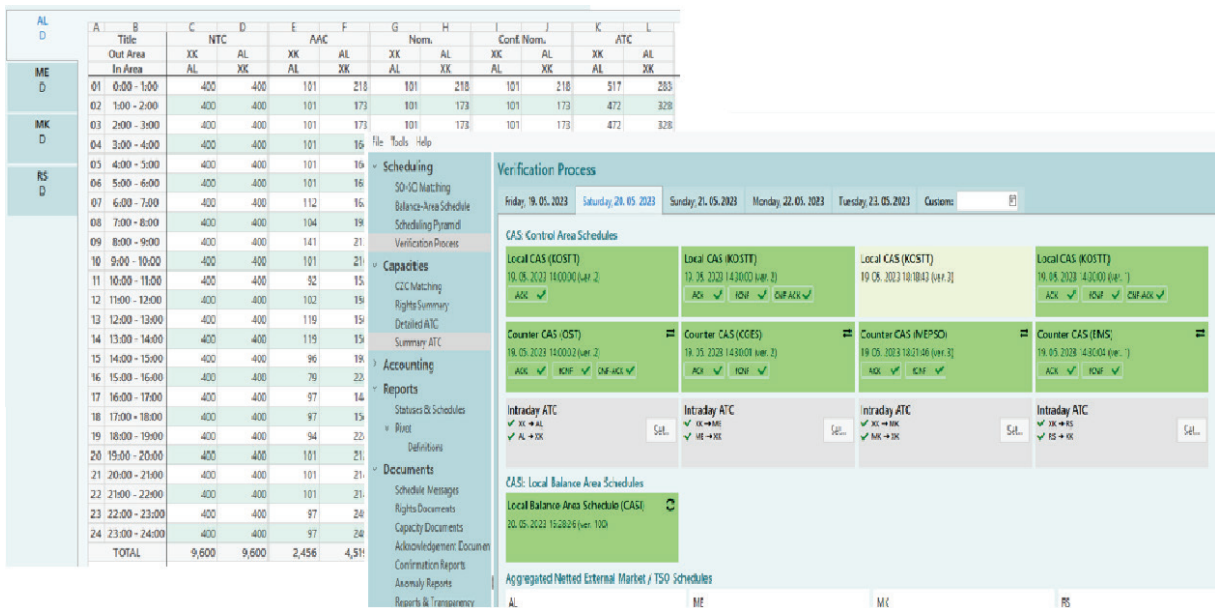


Figure 7. Electricity market processing by Dispatch Center of TSO (18)





Oral Presentation: Challenges and the Role of the Dispatch Centre in the Management of the Power Transmission System – A Summary Analysis

## 6. CONCLUSION

The electrical system, respectively the control dispatch center within the transmission system constitutes an important component within the management and operation of the transmission system. Coordination with the block and neighboring systems has a significant and crucial weight in the functioning of the system as a whole. Maintaining the energy balance, and coordination with the transmission, generation, and distribution systems are some of the most important tasks in the smooth operation of the transmission system. Operation in emergency conditions and contingencies also constitutes a significant factor in the safe and reliable operation of the transmission system. The importance of the control dispatch center also includes the processing and implementation of the energy market, enabling exchanges and transactions between multiple operators within the framework of energy exchanges and balances. Contingency management, system optimization and economic dispatching are also equally important segments that are the task of the dispatch center in monitoring, controlling, and optimizing the transmission system. The integration and synchronization of renewable resources play a role in energy developments and requirements for the energy transition, however, this also constitutes a challenge for the dispatch center in their proper management, always keeping in mind the maintenance of energy parameters and balance. Online monitoring and operation and configuration during faults and problems in cases of energy imbalance, and deviations from the operating band of the electrical parameters of the system components is the responsibility of the control center of the transmission system. The work in question contains an overview of the tasks, challenges, control, and management of the power system from the dispatch center that is in the function of maintaining the networks and the reliability of the power system within the European ENTSO transmission networks of the synchronous zone.

## BIBLIOGRAPHY

- [1] Jun J. J. Zhang et al., "Parallel dispatch: a new paradigm of electrical power system dispatch," in IEEE/CAA Journal of Automatica Sinica, vol. 5, no. 1, pp. 311-319, Jan. 2018, doi: 10.1109/JAS.2017.7510778.
- [2] Rexhepi, V. (2023). The dispatch center's role in the power grid operation and control. *Elektrotehniski Vestnik*, 90(1/2), 51-59.
- [3] Strielkowski W, Civin L, Tarkhanova E, Tvaronavičienė M, Petrenko Y. Renewable Energy in the Sustainable Development of Electrical Power Sector: A Review. *Energies*. 2021; 14(24):8240. <https://doi.org/10.3390/en14248240>
- [4] Shaqiri, R. (2016). Reducing the Losses in the Electrical Power System of Kosovo by Implementation of New Type of Transformers in the Power Distribution System. *Materials Science Forum*, 856, 331-336. <https://doi.org/10.4028/www.scientific.net/msf.856.331>
- [5] Cai Zhi, Xu Dan, Dai Sai, Cui Hui Ding Qiang, "Future Power Grid Dispatch and Control Mode with Large-scale Clean Energy Integration in China:, 4th International Conference on Sustainable Energy and Environmental Engineering (ICSEEE 2015).
- [6] Fotis G, Vita V, Maris TI. Risks in the European Transmission System and a Novel Restoration Strategy for a Power System after a Major Blackout. *Applied Sciences*. 2023; 13(1):83. <https://doi.org/10.3390/app13010083>
- [7] Medjoudj, R., Bediaf, H., & Aissani, D. (2017). Power System Reliability: Mathematical Models and Applications. InTech. doi: 10.5772/intechopen.71926
- [8] Mladenov V, Chobanov V, Georgiev A. Impact of Renewable Energy Sources on Power System Flexibility Requirements. *Energies*. 2021; 14(10):2813. <https://doi.org/10.3390/en14102813>
- [9] Rexhepi, V., & Ymeri, A. (2019). The performance of the renewable energy sources in the power distribution systems—case study.
- [10] A E. Mariani, S.S. Murthy, *Advanced Load Dispatch for Power Systems: Principles, Practices and Economies*, 2012, Springer.
- [11] OBAID, Z.A., CIPCIGAN, L.M., ABRAHIM, L. et al. Frequency control of future power systems: reviewing and evaluating challenges and new control methods. *J. Mod. Power Syst. Clean Energy* 7, 9–25 (2019). <https://doi.org/10.1007/s40565-018-0441-1>
- [12] Shrestha A, Gonzalez-Longatt F. Frequency Stability Issues and Research Opportunities in Converter Dominated Power System. *Energies*. 2021; 14(14):4184. <https://doi.org/10.3390/en14144184>.
- [13] Das, P., Das, S., Biswas, P., Roy, P., Pal, B., Sasmal, M., ... & Paul, D. (2022, July). Review on Power System Reliability Indices and Evaluation Techniques. In *Journal of Physics: Conference Series* (Vol. 2286, No. 1, p. 012023). IOP Publishing.
- [14] E Ela, *Operating Reserves and Variable Generation*, National Renewable Energy Laboratory, 2011
- [15] European Network of Transmission System Operators for Electricity (EENTSOE), *Frequency ranges*, April 2021, StG CNC.
- [16] Nordström, H. (2022). Fast Frequency Reserves to Ensure Frequency Stability Regarding N-1 Criteria: Individual project report in FEG3214 Power System Stability and Control.
- [17] Henrik Nordstrom, *Fast Frequency Reserves to Ensure Frequency Stability Regarding N-1 Criteria*, august 2022
- [18] Transmission System and Market Operator, J.S.C, [www.kost.com](http://www.kost.com), Prishtina, Kosovo, 2023, [www.kost.com](http://www.kost.com).
- [19] Salama, H. S., & Vokony, I. (2022). Voltage stability indices—A comparison and a review. *Computers & Electrical Engineering*, 98, 107743. <https://doi.org/10.1016/j.compeleceng.2022.107743>



### Oral Presentation: Challenges and the Role of the Dispatch Centre in the Management of the Power Transmission System – A Summary Analysis

- [20] Moreno Escobar JJ, Morales Matamoros O, Tejeida Padilla R, Lina Reyes I, Quintana Espinosa H. A Comprehensive Review on Smart Grids: Challenges and Opportunities. *Sensors*. 2021; 21(21):6978. <https://doi.org/10.3390/s21216978>.
- [21] Liang X, Chai H, Ravishankar J. Analytical Methods of Voltage Stability in Renewable Dominated Power Systems: A Review. *Electricity*. 2022; 3(1):75-107. <https://doi.org/10.3390/electricity3010006>
- [22] Devaraj, D., & Preetha Roselyn, J. (2011). On-line voltage stability assessment using radial basis function network model with reduced input features. *International Journal of Electrical Power & Energy Systems*, 33(9), 1550-1555. <https://doi.org/10.1016/j.ijepes.2011.06.008>
- [23] Khalid S, Song J, Raouf I, Kim HS. Advances in Fault Detection and Diagnosis for Thermal Power Plants: A Review of Intelligent Techniques. *Mathematics*. 2023; 11(8):1767. <https://doi.org/10.3390/math11081767>
- [24] Bulat, H.; Frankovi'c, D.; Vlahini'c, S. Enhanced Contingency Analysis—A Power System Operator Tool. *Energies* 2021, 14, 923.
- [25] P. Kundur et al., "Definition and classification of power system stability IEEE/CIGRE joint task force on stability terms and definitions," in *IEEE Transactions on Power Systems*, vol. 19, no. 3, pp. 1387-1401, Aug. 2004, doi: 10.1109/TPWRS.2004.825981.
- [26] Poria Astero and Bong Jun Choi, *Electrical Market Management Considering Power System Constraints in Smart Distribution Grids*, energies, MDPI, may 2016.



# The Relationships Between Concentrations of Particulate Matter (Pm2.5 And Pm10) and Meteorological Parameters in the Sarajevo Canton: Seasonal Variations

[s.dacic@epbih.ba](mailto:s.dacic@epbih.ba)**SABINA DACIC-LEPARA\****EPC Elektroprivreda B&H d.d., Sarajevo, Bosnia and Herzegovina***ADNAN MUJEZINOVIC***Faculty of Electrical Engineering, University of Sarajevo, Bosnia and Herzegovina***ORHAN LEPARA***Faculty of Medicine, University of Sarajevo, Bosnia and Herzegovina***Bosnia and Herzegovina**

## SUMMARY

The term "particulate matter" (PM) refers to airborne solid or liquid particles of various sizes and compositions. According to its size, particles are often divided into the following categories: PM10, or particles with a diameter of less than 10 micrometers; PM2.5, or small particles. The health of people, the environment, local ecosystems, and the economy can all suffer from excessive PM concentrations. It has been demonstrated that atmospheric particulate matter mass concentration was significantly influenced by pollutants sources emission, external transport, meteorological conditions, and secondary formation of air pollution. It has been shown that annual cycle (seasonal fluctuations) typically illustrates the relationship between particular human activities (such as the use of a given kind of resource) and the meteorological parameters (temperature, humidity and wind speed) that follow or influence the type of pollution. Therefore, it will be interesting to examine whether there are differences in PM concentration in relation to the season. In particular, meteorological factors have a significant impact on the diffusion, dilution, and accumulation of air pollutant mass concentration. Secondary generation will increase the mass concentration of air pollutants. The study of air pollution distribution characteristics, the relationship between weather and mass concentration of pollutants, as well as the relationship between various contaminants in the air, can therefore be more useful for developing efficient controls to reduce air pollution. In this paper, the correlation between meteorological parameters and PM concentration in the area of Sarajevo Canton for the period of 2022 will be examined. Data from the Federal Hydro-Meteorological Institute (FHMT) will be used for this research. FHMT has established air quality monitoring stations in many cities to monitor pollutants mass concentration and continuously provides information on air quality, as well as other meteorological and hydrological information through its website.

## KEYWORDS

PM2.5, PM10, seasonal variation, meteorological factors, air pollution, correlation analysis



**Oral Presentation:** The Relationships Between Concentrations of Particulate Matter (Pm<sub>2.5</sub> And Pm<sub>10</sub>) and Meteorological Parameters in the Sarajevo Canton: Seasonal Variations

## 1. INTRODUCTION

The world's air quality has undergone a marked deterioration in recent times, primarily as a consequence of the swift expansion of global industry and economy, coupled with the deleterious effects of human activities such as fuel combustion and vehicular emissions. This has substantially heightened the likelihood of severe meteorological phenomena, including atmospheric hazed [1]. There exists a strong association between atmospheric particulate matter (PM) and numerous adverse health effects, such as elevated risk of cancer over the course of an individual's lifespan, genotoxicity, diminished pulmonary function, as well as afflictions of the cardiovascular and nervous systems [2]. Urban centers are most severely impacted by particulate matter (PM) air pollution, primarily stemming from two key sources: road traffic and domestic heating through wood and coal combustion. Motor vehicles discharge their pollutants via both exhaust and non-exhaust mechanisms, with the former caused by the burning of fossil fuels, and the latter resulting from factors such as road surface and vehicular component deterioration, as well as the resuspension of road dust [3]. Presently, global air quality regulations endeavor to curtail concentrations of PM<sub>2.5</sub> and PM<sub>10</sub>, as well as to mitigate the chemical composition of particulate matter that has been linked to deleterious health outcomes [4]. In accordance with their aerodynamic size, fine and coarse particles that constitute airborne pollution are categorized as PM<sub>2.5</sub> and PM<sub>10</sub> [5]. PM<sub>10</sub> comprises both PM<sub>2.5</sub> and PM<sub>2.5-10</sub>, with the former being classified as fine particles. The majority of 2.5 to 10  $\mu$ m particles originate from natural causes, such as deserts, although they can also be attributed to anthropogenic activities, such as road dust and industrial pollution [6]. Atmospheric particulate matter with aerodynamic diameters of 2.5 and 10 micrometers is referred to as PM<sub>2.5</sub> and PM<sub>10</sub>, respectively. Anthropogenic PM<sub>2.5</sub> contains a diverse range of constituents, including metals, sulfates, nitrates, and carbon-based compounds. The capacity of fine particulate matter (PM<sub>2.5</sub>) to accumulate within the respiratory tract and lungs renders it a lethal component to human health. Excessive concentrations of metallic elements in PM<sub>2.5</sub> can cause extensive damage to proteins, lipids, and cellular DNA [7]. The World Health Organization regulates air contaminants, including particulate matter below 10 micrometers (PM<sub>10</sub>), that can be inhaled by humans [8]. The World Health Organization (WHO) advises that the 24-hour average PM<sub>10</sub> concentration must not surpass 50  $\mu$ g/m<sup>3</sup>, with the Air Pollution Control Regulation stipulating that this limit must not be exceeded on more than 35 occasions per year [5]. Compelling scientific evidence indicates that even at low concentrations, PM<sub>10</sub> can have detrimental effects on human health, with variations in their composition and toxicity being influenced by factors such as season, weather, and primary sources of particulate matter [9]. Empirical evidence suggests that air quality tends to be better in larger cities, particularly during the heating season (autumn, winter, and spring), as compared to smaller towns where poor air quality can be noticeably perceived during this time of the year [10]. The concentration of atmospheric particulate matter (PM) is considerably influenced by local and regional meteorological factors, such as wind speed, wind direction, vertical atmospheric stability, long-range transportation, and pollution dispersion [11]. It is postulated that meteorological conditions play a vital role in the dispersion, alteration, and removal of air pollutants from the environment [9]. Jin et al. demonstrated that there were significant spatiotemporal variations in PM<sub>2.5</sub> concentrations, with these fluctuations being associated with meteorological and socioeconomic factors [12]. Studies have indicated that PM<sub>10</sub> and PM<sub>2.5</sub> concentrations have a strong negative correlation with wind speed and a positive correlation with temperature and relative humidity, respectively. The authors suggest that relative humidity and wind speed are two critical variables that impact the distribution of PM<sub>2.5</sub> and PM<sub>10</sub> concentrations [13]. Yang et al. investigated the seasonal and regional variations in the association between PM<sub>2.5</sub> and meteorological factors. They found that the relationship between relative humidity (RH) and PM<sub>2.5</sub> concentration was positively correlated in north China and Urumqi, but negatively correlated in other regions of China, except for Hainan Island. On the other hand, wind speed (WS) and PM<sub>2.5</sub> showed an inverse association across all regions except for Hainan Island. The correlation between pressure (PS) and PM<sub>2.5</sub> concentration was strongly positive in northeast China and mid-south China, but only moderately positive in other regions. The strongest positive correlation between PM<sub>2.5</sub> concentration and RH was observed in winter and spring, while in autumn, temperature (TEM) and PM<sub>2.5</sub> were negatively correlated. Furthermore, the positive correlation between PS and PM<sub>2.5</sub> concentration was strongest in fall compared to other seasons [14]. Qi et al. have found that distinct meteorological variables have varying effects on PM concentration, and the impact of a single meteorological factor on pollutant concentration is limited. The combinations of temperature and wind speed, temperature and pressure, and humidity and wind speed have also shown strong correlations with PM concentration [15].

## 2. MATERIALS AND METHODS

Sarajevo, a city in Europe, is currently among the most polluted cities in the continent. The city has a moderate continental climate, with an average yearly temperature of 9.5°C. The coldest month is January, with an average temperature of -1.3°C, while the warmest month is July, with an average temperature of 19.1°C. To assess the air quality in Sarajevo Canton, automatic measurement stations are used, and the data used in this study were obtained from the measurement station located on Ilidža. Ilidža is an urban area with an altitude of 499 meters above sea level, a latitude of 43°49'40" N, and a longitude of 18°26'04" E. The region is densely



**Oral Presentation:** The Relationships Between Concentrations of Particulate Matter (Pm<sub>2.5</sub> And Pm<sub>10</sub>) and Meteorological Parameters in the Sarajevo Canton: Seasonal Variations

populated, with a population of 66,730, and is characterized by single-story structures that use central heating, wood, coal, and petroleum products for domestic heating. The study was conducted from January 1 to December 31, 2021. PM<sub>2.5</sub> and PM<sub>10</sub> were analyzed using the HORIBA APDA-372 device. The measurements were taken at exactly 4 p.m. each day to avoid the influence of other circumstances that could affect the results. In addition, meteorological parameters such as relative humidity, temperature, wind speed, and atmospheric pressure were also taken at exactly 4 p.m. each day. The processed data for this study were obtained from the Federal Hydrometeorological Institute of Bosnia and Herzegovina.

### 3. STATISTICAL ANALYSIS

The SPSS program version 19.0 was used to conduct all statistical calculations (SPSS, Inc., Chicago, Illinois). Continuous variables whose distribution was not normal were expressed as median, and continuous variables whose distribution was normal were written as mean standard deviation (interquartile range). Kolmogorov-Smirnov test was used to evaluate the distribution of the variables. Depending on the distribution of variables, a comparison between the groups was performed by the ANOVA test Bonferroni post hoc test and Kruskal-Wallis test followed by Mann-Whitney U-test. Moreover, Spearman's test was used to evaluate correlations because the variables were not normally distributed. P values less than 0,05 were considered statistically significant.

### 4. RESULTS

**Table 1.** Average annual concentrations of particulate matter (PM<sub>2.5</sub> and PM<sub>10</sub>) and values of meteorological parameters

PM <sub>2.5</sub> (µg/m <sup>3</sup> ) – 10,8 (6,1-21,35)
PM <sub>10</sub> (µg/m <sup>3</sup> ) – 16,4 (1,025-31,7)
Temperature (°C)– 16,85 (8,15-23,67)
Relative humidity (%) – 49,0 (32,0-67,0)
Wind speed (m/s) – 1,9 (1,2-2,7)
Atmospheric pressure (hPa) – 943,3 (939,8-946,77)

Data are presented as median and interquartile range

Table 1 presents the mean values of PM<sub>2.5</sub> and PM<sub>10</sub> concentrations, as well as the meteorological parameters' values. The median concentration of PM<sub>2.5</sub> was found to be 10.8 (ranging from 6.1 to 21.35) µg/m<sup>3</sup>, whereas the median concentration of PM<sub>10</sub> was 16.4 (ranging from 1.025 to 31.7) µg/m<sup>3</sup>. The annual average air temperature was 16.85 (ranging from 8.15 to 23.67) °C, relative humidity was 49.0% (ranging from 32.0% to 67.0%), wind speed was 1.9 (ranging from 1.2 to 2.7) m/s, and atmospheric pressure was 943.3 (ranging from 939.8 to 946.77) hPa.

**Table 2.** Monthly average concentrations of particulate matter (PM<sub>2.5</sub> and PM<sub>10</sub>)

Variables	PM <sub>2.5</sub> (µg/m <sup>3</sup> )	PM <sub>10</sub> (µg/m <sup>3</sup> )
January	55,3 (25,2-92,1)	57,1 (28,2-95,8)
February	12,2 (7,73-31,87)	16,9 (9,77-35,22)
March	12,4 (9,4-19,1)	18,4 (13,4-23,0)
April	4,75 (2,5-8,12)	7,7 (5,5-12,35)
May	8,08±2,84	13,9 (8,9-19,8)
June	9,59±3,95	15,55 (10,57-25,85)
July	6,7 (3,9-11,5)	14,3 (8,4-22,1)
August	9,9 (6,3-11,4)	14,9 (10,6-19,9)
September	5,6 (3,9-8,05)	9,25 (6,27-13,75)
October	17,74±9,89	27,14±15,57
November	28,03±17,59	34,0±21,05
December	39,2 (18,8-88,4)	42,3 (28,0-92,0)

Data are presented as median and interquartile range or as mean±SD.

**Oral Presentation:** The Relationships Between Concentrations of Particulate Matter (Pm<sub>2.5</sub> And Pm<sub>10</sub>) and Meteorological Parameters in the Sarajevo Canton: Seasonal Variations

Table 2 displays the mean monthly concentrations of PM<sub>2.5</sub> and PM<sub>10</sub>. The maximum values of PM<sub>2.5</sub> were reported in December and were 39.2 (18.8-88.4) µg/m<sup>3</sup>, whereas the minimum values were observed in April and were 4.75 (2.5-8.12) µg/m<sup>3</sup>. The maximum values of PM<sub>10</sub> were recorded in December and were 42.3 (28.0-92.0) µg/m<sup>3</sup>, while the minimum values were observed in April and were 7.7 (5.5-12.35) µg/m<sup>3</sup>.

**Table 3.** Seasonal variations of meteorological parameters

Variables	Winter	Spring	Summer	Autumn	p
Temperature (°C)	5,35 (1,4-10,22)	15,95 (9,92-21,57)	28,4 (23,5-31,4)	17,7 (11,7-20,5)	<b>&lt;0,001</b>
Relative humidity (%)	66,0 (52,25-84,25)	35,0 (22,25-54,75)	34,0 (26,0-51,0)	55,0 (43,0-75,0)	<b>&lt;0,001</b>
Wind speed (m/s)	1,3 (0,80-2,0)	2,25 (1,7-3,1)	2,6 (2,0-3,1)	1,5 (0,9-2,0)	<b>&lt;0,001</b>
Atmospheric pressure (hPa)	943,31±7,55	942,72±7,21	942,28±3,04	943,10±7,06	0,717

Data are presented as median and interquartile range or as mean±SD.

The average air temperature in winter was 5.35 (1.4-10.22) °C, while in spring, it was 15.95 (9.92-21.57) °C. In summer, the average air temperature was 28.4 (23.5-31.4) °C, and in autumn, it was 17.7 (11.7-20.5) °C. The differences in the average temperatures between seasons were statistically significant (p<0.001). The average relative humidity in winter was 66.0 (52.25-84.25) %, while in spring, it was 35.0 (22.25-54.75) %. In summer, the average relative humidity was 34.0 (26.0-51.0) %, and in autumn, it was 55.0 (43.0-75.0) %. The differences in relative humidity values between seasons were statistically significant (p<0.001). The average wind speed in winter was 1.3 (0.80-2.0) m/s, in spring 2.25 (1.7-3.1) m/s, in summer 2.6 (2.0 -3.1) m/s, and in autumn, it was 1.5 (0.9-2.0) m/s. The differences in wind speed values between seasons were statistically significant (p<0.001). However, the value of atmospheric pressure did not differ significantly between seasons (p=0.717) (table 3).

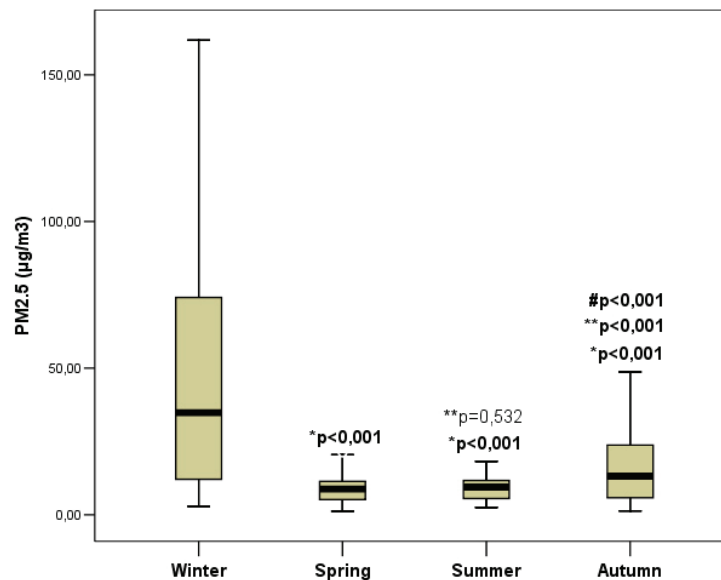


**Figure 1.** PM<sub>2.5</sub> concentration in relation to season

Data are presented as median and interquartile range; \*p – in comparison to Winter; \*\*p – in comparison to Spring; #p – in comparison to Summer

The concentrations of PM<sub>2.5</sub> were found to be the highest during the winter season, with a mean concentration of 34.85 (11.82-74.67) µg/m<sup>3</sup>. These concentrations were significantly higher compared to those recorded during spring 8.80 (5.2-11.5) µg/m<sup>3</sup> (p<0.001), summer 9.4 (5.52-11.75) µg/m<sup>3</sup> (p<0.001), and autumn 13.20 (5.6-23.9) µg/m<sup>3</sup> (p<0.001). Furthermore, significant differences in PM<sub>2.5</sub> concentrations were noted between autumn and spring (p<0.001), as well as between autumn and summer (p<0.001), but no significant difference was found in PM<sub>2.5</sub> concentrations between spring and summer (p=0.532) (figure 1).



**Oral Presentation:** The Relationships Between Concentrations of Particulate Matter (Pm2.5 And Pm10) and Meteorological Parameters in the Sarajevo Canton: Seasonal Variations

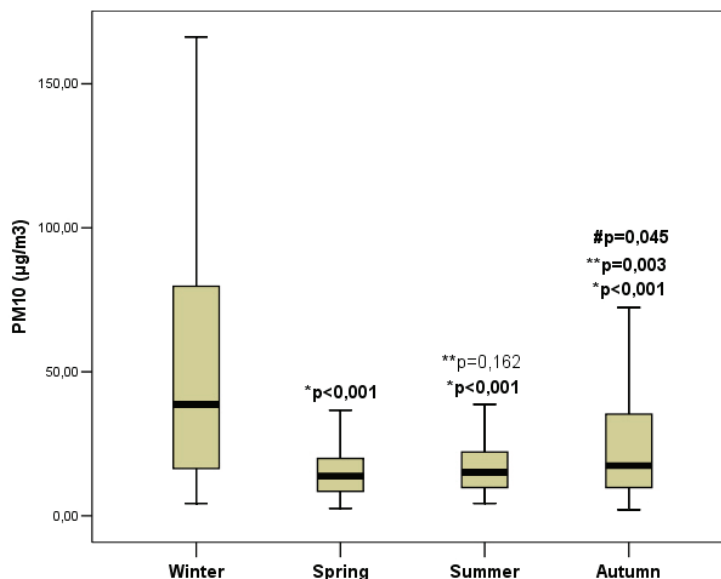


**Figure 2.** PM10 concentration in relation to season

Data are presented as median and interquartile range; \*p – in comparison to Winter; \*\*p – in comparison to Spring; #p – in comparison to Summer

The concentrations of PM10 were highest during winter, with an average of 38.60 (16.40-79.82)  $\mu\text{g}/\text{m}^3$ , and were significantly higher compared to concentrations during spring with an average of 13.70 (8.5-19.95)  $\mu\text{g}/\text{m}^3$  ( $p<0.001$ ), summer with an average of 15.0 (9.75-22.17)  $\mu\text{g}/\text{m}^3$  ( $p<0.001$ ), as well as compared to autumn with an average of 17.40 (9.40-35.60)  $\mu\text{g}/\text{m}^3$  ( $p<0.001$ ). Significant differences in PM10 concentrations were observed between autumn and spring seasons ( $p=0.003$ ), as well as between autumn and summer seasons ( $p=0.045$ ). No significant difference was found in PM10 concentrations between spring and summer ( $p=0.162$ ) (figure 2).

**Table 4:** Spearman's correlation coefficient between PM2.5 and meteorological parameters

Variables	PM2.5 ( $\mu\text{g}/\text{m}^3$ )			
	Winter	Spring	Summer	Autumn
Temperature ( $^{\circ}\text{C}$ )	-0,092	<b>-0,369**</b>	0,168	<b>-0,301**</b>
Relative humidity (%)	<b>0,313**</b>	<b>0,253*</b>	0,189	<b>0,223*</b>
Wind speed (m/s)	<b>-0,695**</b>	-0,143	0,020	<b>-0,618**</b>
Atmospheric pressure (hPa)	0,129	<b>0,238*</b>	<b>-0,281**</b>	<b>0,364**</b>

\*\* $p<0,01$

During the winter period, a statistically significant positive correlation was observed between PM2.5 concentration and relative humidity ( $\text{Rho}= 0.313$ ;  $p<0.01$ ), while a statistically significant negative correlation was observed between PM2.5 concentration and wind speed ( $\text{Rho}= -0.695$ ;  $p<0.01$ ). In the spring season, PM2.5 concentration showed a statistically significant positive correlation with relative humidity ( $\text{Rho}= 0.253$ ;  $p<0.05$ ) and atmospheric pressure ( $\text{Rho}= 0.238$ ;  $p<0.05$ ), while a statistically significant negative correlation was observed between PM2.5 concentration and air temperature ( $\text{Rho}= -0.369$ ;  $p<0.01$ ). In the summer season, only a statistically significant negative correlation was observed between PM2.5 concentration and atmospheric pressure ( $\text{Rho}= -0.281$ ;  $p<0.05$ ). In the autumn season, PM2.5 concentration exhibited a statistically significant positive correlation with relative humidity ( $\text{Rho}= 0.223$ ;  $p<0.05$ ) and atmospheric pressure ( $\text{Rho}= 0.364$ ;  $p<0.01$ ), while a statistically significant negative correlation was observed between PM2.5 concentration and air temperature ( $\text{Rho}= -0.301$ ;  $p<0.01$ ) as well as between PM2.5 concentration and wind speed ( $\text{Rho}= -0.618$ ;  $p<0.01$ ) (table 4).

**Oral Presentation:** The Relationships Between Concentrations of Particulate Matter (Pm2.5 And Pm10) and Meteorological Parameters in the Sarajevo Canton: Seasonal Variations

**Table 5.** Spearman's correlation coefficient between PM10 and meteorological parameters

Variables	PM10 ( $\mu\text{g}/\text{m}^3$ )			
	Winter	Spring	Summer	Autumn
Temperature ( $^{\circ}\text{C}$ )	-0,030	-0,172	<b>0,292**</b>	-0,161
Relative humidity (%)	<b>0,274**</b>	0,185	0,054	0,077
Wind speed (m/s)	<b>-0,663**</b>	-0,062	0,113	<b>-0,583**</b>
Atmospheric pressure (hPa)	0,117	0,175	<b>-0,285**</b>	<b>0,399**</b>

\*\* $p < 0,01$

In the winter season, PM10 concentration showed a significant positive correlation with relative humidity (Rho= 0.274;  $p < 0.01$ ). Conversely, a negative correlation was observed between PM10 concentration and wind speed in the winter season (Rho= -0.663;  $p < 0.01$ ). In summer, a significant positive correlation was recorded between PM10 concentration and air temperature (Rho= 0.292;  $p < 0.01$ ). In the autumn months, PM10 concentration showed a significant positive correlation with atmospheric pressure (Rho = 0.399;  $p < 0.01$ ). However, in the summer months, a significant negative correlation was found between PM10 concentration and atmospheric pressure (Rho= -0.285;  $p < 0.01$ ) (table 5).

## 5. DISCUSSION

Upon analysis of PM2.5 and PM10 values in the year 2022, our findings indicated that the greatest concentrations of these parameters were observed in December, with the lowest concentrations being recorded in April. The highest concentrations of PM2.5 were identified in winter and were significantly greater when compared to concentrations in spring, summer, and autumn. Significant variations in PM2.5 concentrations were noted between autumn and spring, as well as between autumn and summer, whereas no significant differences in PM2.5 concentrations were observed between spring and summer. Similar results were observed in the context of PM10 and its relationship with season. Despite only a slight seasonal variation being observed throughout the study period, the average concentrations of PM10 and PM2.5 were found to be highest in winter and lowest in spring. This can be attributed to the reduced mixing heights during winter due to cold weather, which can cause PM fractions to be trapped closer to the ground. Additionally, the concentrations of PM may increase due to additional sources of PM during this period, including increased traffic, cold engine starts, residential heating, and potentially due to weather conditions [16]. The winter season exhibited the most elevated levels of PM10 contamination, while both winter and summer seasons had the greatest PM2.5 concentrations. Shen et al. discovered significant associations between PM2.5 and PM10, with the mean mass fraction of PM2.5 in PM10 being roughly 72.5%. The PM2.5 fraction varied throughout the sampling periods, with spring having the lowest PM2.5 fraction, and the other three seasons displaying only minor variations [17]. Zhao et al. conducted a study that involved analyzing patterns of PM2.5 concentrations by breaking down each time series into three main elements: trend, seasonality, and holidays. The study found that certain days and months tended to have higher or lower PM2.5 concentrations, consistent with earlier findings. Specifically, the results showed that January and Fridays typically have higher PM2.5 concentrations, whereas Sunday tends to have lower concentrations compared to most other days of the week. Additionally, July was found to be another month with high PM2.5 concentrations. Interestingly, the lowest PM2.5 values were observed on Mondays and Sundays equally, while Saturdays had higher concentrations compared to Fridays in most studies [18]. In their study, Zhang et al. aimed to investigate the impact of newly implemented environmental protection policies and the spatiotemporal variations and contributing factors to PM2.5 concentrations in Beijing during 2013-2018. The study revealed that annual declines in PM2.5 concentrations were observed, which provided evidence of the effectiveness of air pollution control measures. Furthermore, the concentration of PM2.5 was found to be higher in winter, particularly in the southern parts of the region [19]. The concentration of PM2.5 before and after precipitation is influenced by various factors such as the initial concentration of PM2.5, the intensity, and duration of precipitation. The scavenging effect of precipitation on PM10 is related to the initial concentration of PM10. Higher initial PM10 concentration results in greater removal by precipitation. PM2.5 and PM10 are more concentrated when winds come from the west, while the most significant scavenging effect on PM2.5 and PM10 occurs during the north and northwest winds. Increasing wind speed to 2 m/s can lower PM2.5 and PM10 concentrations. However, under south, southeast, and east wind conditions, PM10 concentration increases when the wind speed is above 4 m/s [20]. In this study, the correlation between PM2.5 and meteorological factors was analyzed across different seasons. Results revealed a significant positive correlation between PM2.5 and relative humidity, as well as a significant negative correlation between PM2.5 and wind speed during



**Oral Presentation:** The Relationships Between Concentrations of Particulate Matter (Pm<sub>2.5</sub> And Pm<sub>10</sub>) and Meteorological Parameters in the Sarajevo Canton: Seasonal Variations

winter. Meanwhile, during spring, PM<sub>2.5</sub> concentration was significantly positively correlated with relative humidity and atmospheric pressure, but significantly negatively correlated with air temperature. In summer, only a significant negative correlation was observed between PM<sub>10</sub> concentration and atmospheric pressure. During autumn, PM<sub>2.5</sub> concentration showed a significant positive correlation with relative humidity and atmospheric pressure, but a significant negative correlation with air temperature and wind speed. Additionally, PM<sub>10</sub> concentration significantly positively correlated with relative humidity in winter, air temperature in summer, and atmospheric pressure in autumn, while negatively correlated with wind speed in winter and atmospheric pressure in summer. Numerous studies have indicated that meteorological factors such as temperature, humidity, wind speed, and atmospheric stability can impact the concentration and dispersion of PM<sub>2.5</sub> and PM<sub>10</sub> in the atmosphere [21-23]. Kliengchuay et al. conducted a study which demonstrated that haze events, defined as daily PM<sub>10</sub> concentrations that exceeded the PCD standard, were primarily observed during the dry season, specifically from February to April. March was the month with the highest concentration of PM<sub>10</sub>. The authors found that there was a negative correlation between relative humidity and temperature with PM<sub>10</sub> concentration [24]. Tella et al. conducted a study and found that there is a positive correlation between PM<sub>10</sub> concentration and temperature and wind speed, while humidity exhibited a negative correlation. The highest PM<sub>10</sub> concentration was observed during the warm months from May to September, as indicated by the regression model, which had a strong predictive accuracy with an R<sup>2</sup> value of 0.298, RMSE of 12.737, and MAE of 10.343. Among the meteorological factors studied, temperature, wind speed, and humidity were identified in descending order of significance as the main factors affecting PM<sub>10</sub> concentration in the research area [25]. In alignment with our findings, Zhang's investigation similarly identified a positive correlation between relative humidity (RH) and particulate matter (PM) concentration. The author postulates that the escalation in RH may induce heightened photochemical reactions and resultant secondary aerosol particulate matter generation within the atmosphere [23]. In the study conducted by Bai et al., it was observed that the aerosol scattering coefficient, absorption coefficient, extinction coefficient, and single scattering albedo exhibited elevated values when the relative humidity (RH) level reached the range of 90-100%. These findings provide evidence that high RH levels can potentially facilitate the production of particulate matter (PM) [26]. From 2015 to 2019, significant reductions in PM<sub>2.5</sub> pollution levels were observed in Harbin, with marked seasonal fluctuations in PM<sub>2.5</sub> concentration and its variability. Heating had a significant effect on PM<sub>2.5</sub> concentration in 2019, and in conjunction with changing weather conditions, resulted in significant differences in PM<sub>2.5</sub> concentration during heating and non-heating periods. The findings revealed a negative correlation between mean temperature and mean wind speed with PM<sub>2.5</sub> [27]. During the study period, the most significant meteorological variables affecting PM<sub>2.5</sub> concentration among the 28 cities were the lowest temperature and average relative humidity, accounting for 31.96% of the temporal variation. Regarding the spatial distribution of PM<sub>2.5</sub> concentration, air pressure and maximum temperature played crucial roles in spring and summer, while sunshine hours had a more substantial impact in autumn and winter. These results highlight the importance of developing effective clean air policies for the future and provide theoretical support for accurate prediction and prevention of PM<sub>2.5</sub> pollution [28]. The results of the correlation analysis revealed that PM<sub>2.5</sub> concentrations exhibited positive correlations with air pressure, while displaying negative correlations with temperature, relative humidity, rainfall, and wind speed. The direction of the wind also played a crucial role in determining the direction of PM<sub>2.5</sub> dispersion, which ultimately affected the concentration of PM<sub>2.5</sub>. Specifically, in Hong Kong, PM<sub>2.5</sub> levels were higher during winter months due to the influence of north winds, while south winds during summer months were associated with lower PM<sub>2.5</sub> levels. Therefore, meteorological conditions played a critical role in the aggregation, dispersion, and distribution of PM<sub>2.5</sub>. Household emissions, when held constant, were also found to have a significant impact on PM<sub>2.5</sub> concentrations. These findings have important implications for the development of effective measures to mitigate PM<sub>2.5</sub> pollution [29]. The convergent cross-mapping (CCM) analysis indicates that temperature, relative humidity, and atmospheric pressure are the primary meteorological factors that influence PM<sub>2.5</sub> concentrations, with boundary layer height, wind speed, and wind direction playing a lesser role. Among all combinations of meteorological elements, temperature, temperature-humidity, and temperature-wind speed-wind direction are the most significant single and multiple factors in determining PM<sub>2.5</sub> concentrations. The coherence values for multiple meteorological factors are significantly higher than those for a single meteorological factor, indicating that the combination of multiple meteorological factors contributes to the variation in PM<sub>2.5</sub> concentrations [30].

## 6. CONCLUSION

The study showed that the highest concentrations of PM were observed during winter, while the lowest concentrations occurred in spring. In autumn and spring, temperature was negatively correlated with PM<sub>2.5</sub>, but positively correlated with PM<sub>10</sub> in summer. Relative humidity was positively associated with PM<sub>2.5</sub> in all seasons except summer, and with PM<sub>10</sub> only in winter. Wind speed showed negative correlations with PM<sub>2.5</sub> and PM<sub>10</sub> in winter and autumn only. In summer, atmospheric pressure was negatively associated with PM and PM<sub>2.5</sub> and PM<sub>10</sub>, while a positive correlation was found in autumn. The impact of meteorological factors on the concentration of PM varied according to the season.



Oral Presentation: The Relationships Between Concentrations of Particulate Matter (Pm<sub>2.5</sub> And Pm<sub>10</sub>) and Meteorological Parameters in the Sarajevo Canton: Seasonal Variations

## BIBLIOGRAPHY

- [1] YANG, Hong; LIU, Zehang; LI, Guohui. A new hybrid optimization prediction model for PM<sub>2.5</sub> concentration considering other air pollutants and meteorological conditions. *Chemosphere*, 2022, 307: 135798.
- [2] TIAN, Yingze, et al. Size distribution, meteorological influence and uncertainty for source-specific risks: PM<sub>2.5</sub> and PM<sub>10</sub>-bound PAHs and heavy metals in a Chinese megacity during 2011–2021. *Environmental Pollution*, 2022, 312: 120004.
- [3] JANDACKA, Dusan; DURCANSKA, Daniela. Seasonal variation, chemical composition, and PMF-derived sources identification of traffic-related PM<sub>1</sub>, PM<sub>2.5</sub>, and PM<sub>2.5–10</sub> in the air quality management region of Žilina, Slovakia. *International Journal of Environmental Research and Public Health*, 2021, 18.19: 10191.
- [4] AHMAD, Mushtaq, et al. Chemical Composition, Sources, and Health Risk Assessment of PM<sub>2.5</sub> and PM<sub>10</sub> in Urban Sites of Bangkok, Thailand. *International Journal of Environmental Research and Public Health*, 2022, 19.21: 14281.
- [5] BOZDAĞ, Aslı; DOKUZ, Yeşim; GÖKÇEK, Öznur Begüm. Spatial prediction of PM<sub>10</sub> concentration using machine learning algorithms in Ankara, Türkiye. *Environmental Pollution*, 2020, 263: 114635.
- [6] FAN, Hao, et al. Spatio-temporal variations of the PM<sub>2.5</sub>/PM<sub>10</sub> ratios and its application to air pollution type classification in China. *Frontiers in Environmental Science*, 2021, 9: 692440.
- [7] BERA, Biswajit, et al. Variation and dispersal of PM<sub>10</sub> and PM<sub>2.5</sub> during COVID-19 lockdown over Kolkata metropolitan city, India investigated through HYSPLIT model. *Geoscience Frontiers*, 2022, 13.1: 101291.
- [8] MALLET, Marc Daniel. Meteorological normalisation of PM<sub>10</sub> using machine learning reveals distinct increases of nearby source emissions in the Australian mining town of Moranbah. *Atmospheric pollution research*, 2021, 12.1: 23-35.
- [9] FALLAHIZADEH, Saeid, et al. The effects of meteorological parameters on PM<sub>10</sub>: Health impacts assessment using AirQ+ model and prediction by an artificial neural network (ANN). *Urban Climate*, 2021, 38: 100905.
- [10] KIREŠOVÁ, Simona; GUZAN, Milan. Determining the Correlation between Particulate Matter PM<sub>10</sub> and Meteorological Factors. *Eng*, 2022, 3.3: 343-363.
- [11] FERENCZI, Zita, et al. Long-term characterization of urban PM<sub>10</sub> in Hungary. *Aerosol and Air Quality Research*, 2021, 21.10: 210048.
- [12] JIN, Jie-Qi, et al. Using Bayesian spatio-temporal model to determine the socio-economic and meteorological factors influencing ambient PM<sub>2.5</sub> levels in 109 Chinese cities. *Environmental Pollution*, 2019, 254: 113023.
- [13] ZHAO, Chen-Xi, et al. Temporal and spatial distribution of PM<sub>2.5</sub> and PM<sub>10</sub> pollution status and the correlation of particulate matters and meteorological factors during winter and spring in Beijing. *Huan jing ke xue= Huanjing kexue*, 2014, 35.2: 418-427.
- [14] YANG, Qianqian, et al. The relationships between PM<sub>2.5</sub> and meteorological factors in China: Seasonal and regional variations. *International journal of environmental research and public health*, 2017, 14.12: 1510.
- [15] QI, Xiaoyu, et al. Data analysis and mining of the correlations between meteorological conditions and air quality: A case study in Beijing. *Internet of Things*, 2021, 14: 100127.
- [16] MOHAMMED, Ga; KARANI, George; MITCHELL, Dc. Trace elemental composition in PM<sub>10</sub> and PM<sub>2.5</sub> collected in Cardiff, Wales. *Energy Procedia*, 2017, 111: 540-547.
- [17] Shen GF, Yuan SY, Xie YN, Xia SJ, Li L, Yao YK, Qiao YZ, Zhang J, Zhao QY, Ding AJ, Li B, Wu HS. Ambient levels and temporal variations of PM<sub>2.5</sub> and PM<sub>10</sub> at a residential site in the mega-city, Nanjing, in the western Yangtze River Delta, China. *J Environ Sci Health A Tox Hazard Subst Environ Eng*. 2014;49(2):171-8.
- [18] Zhao, N., Liu, Y., Vanos, J. K., & Cao, G. (2018). Day-of-week and seasonal patterns of PM<sub>2.5</sub> concentrations over the United States: Time-series analyses using the Prophet procedure. *Atmospheric environment*, 192, 116-127.
- [19] Zhang, L., An, J., Liu, M., Li, Z., Liu, Y., Tao, L., ... & Luo, Y. (2020). Spatiotemporal variations and influencing factors of PM<sub>2.5</sub> concentrations in Beijing, China. *Environmental Pollution*, 262, 114276.
- [20] Meng X, Wu Y, Pan Z, Wang H, Yin G, Zhao H. Seasonal Characteristics and Particle-size Distributions of Particulate Air Pollutants in Urumqi. *Int J Environ Res Public Health*. 2019 Jan 31;16(3):396.
- [21] Yang, Z., Yang, J., Li, M., Chen, J., & Ou, C. Q. (2021). Nonlinear and lagged meteorological effects on daily levels of ambient PM<sub>2.5</sub> and O<sub>3</sub>: Evidence from 284 Chinese cities. *Journal of Cleaner Production*, 278, 123931.
- [22] Luo, Y., Liu, S., Che, L., & Yu, Y. (2021). Analysis of temporal spatial distribution characteristics of PM<sub>2.5</sub> pollution and the influential meteorological factors using Big Data in Harbin, China. *Journal of the Air & Waste Management Association*, 71(8), 964-973.
- [23] Zhang, M., Chen, S., Zhang, X., Guo, S., Wang, Y., Zhao, F., ... & Bilal, M. (2023). Characters of Particulate Matter and Their Relationship with Meteorological Factors during Winter Nanyang 2021–2022. *Atmosphere*, 14(1), 137.
- [24] Kliengchuay, W., Worakhunpiset, S., Limpanont, Y., Meeyai, A. C., & Tantrakarnapa, K. (2021). Influence of the meteorological conditions and some pollutants on PM<sub>10</sub> concentrations in Lamphun, Thailand. *Journal of Environmental Health Science and Engineering*, 19, 237-249.
- [25] Tella, A., Balogun, A. L., & Faye, I. (2021). Spatio-temporal modelling of the influence of climatic variables and seasonal variation on PM<sub>10</sub> in Malaysia using multivariate regression (MVR) and GIS. *Geomatics, Natural Hazards and Risk*, 12(1), 443-468.
- [26] Bai, D.; Wang, H.; Tan, Y.; Yin, Y.; Wu, Z.; Guo, S.; Shen, L.; Zhu, B.; Wang, J.; Kong, X. Optical Properties of Aerosols and Chemical Composition Apportionment under Different Pollution Levels in Wuhan during January 2018. *Atmosphere* 2019, 11, 17.



**Oral Presentation:** The Relationships Between Concentrations of Particulate Matter (Pm2.5 And Pm10) and Meteorological Parameters in the Sarajevo Canton: Seasonal Variations

- [27] Gao, X., Ruan, Z., Liu, J., Chen, Q., & Yuan, Y. (2022). Analysis of Atmospheric Pollutants and Meteorological Factors on PM<sub>2.5</sub> Concentration and Temporal Variations in Harbin. *Atmosphere*, 13(9), 1426.
- [28] Wang, S., Gao, J., Guo, L., Nie, X., & Xiao, X. (2022). Meteorological influences on spatiotemporal variation of PM<sub>2.5</sub> concentrations in atmospheric pollution transmission channel cities of the Beijing–Tianjin–Hebei region, China. *International Journal of Environmental Research and Public Health*, 19(3), 1607.
- [29] Li, X., Feng, Y. J., & Liang, H. Y. (2017, July). The impact of meteorological factors on PM<sub>2.5</sub> variations in Hong Kong. In *IOP Conference Series: Earth and Environmental Science* (Vol. 78, No. 1, p. 012003). IOP Publishing.
- [30] Zhang, X., Xu, H., & Liang, D. (2022). Spatiotemporal variations and connections of single and multiple meteorological factors on PM<sub>2.5</sub> concentrations in Xi'an, China. *Atmospheric Environment*, 275, 119015.



# The Impact of Interconnection Line Synchronization on Power System Dynamic Stability

[giorgi.erikashvili@gse.com.ge](mailto:giorgi.erikashvili@gse.com.ge)

GIVI SHOVDADZE, GIORGI VAKHTANGADZE, NINO DOLIDZE, OMARI BURDIASHVILI, GIORGI ERIKASHVILI\*

*Georgian State Electrosystem***Georgia**

## SUMMARY

In most cases, the power systems of neighbouring countries are synchronously connected with one or more cross-border lines. After the tripping of the only OHL that interconnects two power systems, it is essential to reconnect it automatically for proper operation of power systems and re-establish parallel synchronous operation, which is realized by automatic recloser of transmission line. After the mentioned outage, both power systems continue operation separately, therefore, synchronization parameters (Phase angle, Frequency, Voltage magnitude) vary differently. If the difference in these parameters between two terminals is within the permissible range, reconnection of the cross-border line shall be considered successful. For this purpose, both terminals of the line are equipped with Synchronoscopes, which monitor and measure the difference between parameters and if parameters are in permissible ranges, it allows both sides to do the automatic synchronization on their own.

During the system operation, the necessity of changing the synchronization parameters often arises, mainly caused by the unsuccessful attempt of automatic recloser. Synchronization with significant active power disturbance has an effect on grid stability, particularly the power systems with low inertia. Therefore, before changing the ranges of synchronization parameters, they should be verified by assessing the effect on power system stability. Such analysis is performed in power system engineering software. Initially, it is necessary to set up and execute load flow calculations in typical regimes, especially in the minimum consumption mode with low system inertia. In the next step, tripping of the interconnector is done and then the two systems reconnect again by means of automatic recloser. Therefore, it is critical to observe parameters and study what kind of effect could it have on stability.

It is common when mismatches of model performance occur compromise accuracy. Hence, it is essential to analyse parameters periodically. For the purpose of verification, some dynamic simulations are conducted based on real events by the use of SCADA SP7 and WAMS 8.5 systems' data, which reflect the transient processes, occurring during the synchronization. The values of permissible synchronization parameters are determined by use of mentioned verified model. The research analysis, performed by using power system engineering software PSS/E 33.5 and synchronization analysis module, was set up in PYTHON programming language, which ensures the mentioned software to work properly.

The article v recommendations on determining optimal synchronization parameters for low inertia power systems (on the example of the power system of Georgia), which have weak interconnections with neighbouring countries. This paper also provides some suggestions that should be foreseen during synchronization in order to avoid undesirable events.

## KEYWORDS

Synchronization - Low Inertia - WAMS - SCADA - PSS/E - Synchronization Parameters - Automatic Recloser



## 1. INTRODUCTION

Georgian power system is interconnected with the power systems of Türkiye, Azerbaijan, Armenia and Russia through high voltage overhead lines. The system synchronously operates in IPS/UPS synchronous zone through Azerbaijani or Russian power systems. Simultaneous parallel operation with both mentioned systems isn't recommended due to loop flows circulating through the power system of Georgia that cause an overload of the network elements. Georgian power system is quite small and characterized by low inertia ( $\sum H < 100$  sec). Therefore, even a small deficit in power can cause a significant frequency deviation.

It also should be noted that some interconnectors pass through difficult terrain and therefore, the tripping of the lines are common events, particularly in winter periods. After the emergency outage, it is essential to reconnect OHL via Automatic Recloser with proper synchronization parameters (phase angle, frequency, voltage magnitude) in order to re-establish parallel operation and remain the system stability. For this purpose, both terminals of the line are equipped with synchrosopes which monitor and measure the difference between the mentioned parameters and send the signals to circuit breakers. In the best-case scenario, for successful synchronization and to remain the stability of both systems the difference between synchronization parameters should be equal to zero, but in reality, this isn't possible. Therefore, it is crucial to define the permissible difference in phase angle, frequency, and voltage magnitudes to minimize the risk of unsuccessful synchronization and the negative effect on system stability. If the frequency on the side of an open circuit breaker doesn't match prior to the closing circuit breaker, during the synchronization sudden change of active power will affect the systems and create an unstable flow of energy, chiefly caused by the fact that system with high frequency trying to increase the frequency to the lower one. Consequently, reclose may complete either successfully or lead to serious active power oscillations on the interconnector, exceeding the settings of dividing automatic and trip the line respectively. Concerning the difference between voltage magnitudes, it stipulates bulk reactive power flow through the interconnector.

In case of significant difference between phase angles of the systems has a similar effect on the system as in case of above-discussed case. If we try to synchronize two systems when there is a quite high difference between phase angles after closing the circuit breaker the active power (MW) with high peak amplitude will flow through the interconnector immediately, that has a significant negative impact on the power system with low inertia. To see the critical importance of defining the optimal permissible phase angle difference, it would be better to see the power-angle curve on an example of the simple model that shows the relationship between active power and phase angle ( $\delta$ ):

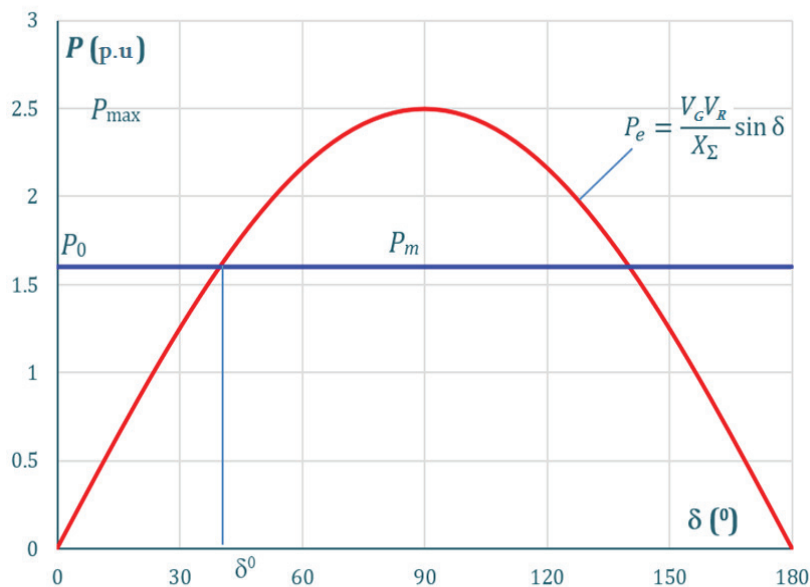


Figure 1. Power-angle curve

The red curve represents the active power transferred from the generator to the receiver and is given by:

$$P_e = \frac{V_G V_R}{X_\Sigma} \sin \delta$$

(1)

Where,

$P_e$ – transmitted electrical power

$W_G$ – generator voltage

$W_R$ – voltage of receiver

$\delta$  – angle between generator and receiver voltages

$X_T$ – total reactance

This equation shows that transferred power depends on the sin of the angles between the voltages of the generator and the receiver. When  $\delta$  equals zero active power isn't transferred. As the angle reaches the 90° power transfer increases to the maximum value and further increase results in a power transfer decrease. [1] The same effect is in case of synchronization of two systems, the closer the difference in the phase angles to 90°, the more active power is transferred from one system to another. If one of these two systems is quite small and is characterized by low inertia, high power oscillation can cause a large rate of change of frequency that might trigger the emergency shut down of generation or demand units by the protection system and endanger power system stability. So, for power systems with low inertia, it has critical importance to define optimal permissible synchronization parameters by using the verified system model to maintain system stability.

## 2. POWER SYSTEM MODEL VALIDATION

Before starting the determination of optimal synchronization parameters it's important to identify the strategy to improve the grid model and ensure accurate information for available models. Therefore, before identifying optimal synchronization parameters, the model is validated by use of the data from SCADA and WAMS systems. This process can be defined as the set of steps and activities intended to verify that models are performing as expected. In the first stage, we are taking information from the SCADA system to restore steady-state regime. Consequently, with all input variables known at all busbars, following can be calculated in power system engineering software PSS/E:

- Active power flow;
- Reactive power flow;
- Active power losses;
- Reactive power losses;
- Line loading;
- Transformer loading;
- Voltage drop.

On Figure 2 500-400 kV grid of Georgia is presented. It shows the simulated and measured values of voltages at all 500 kV substations and active power flows on 500 kV lines after validation the system model in steady-state regime with SCADA measurements.

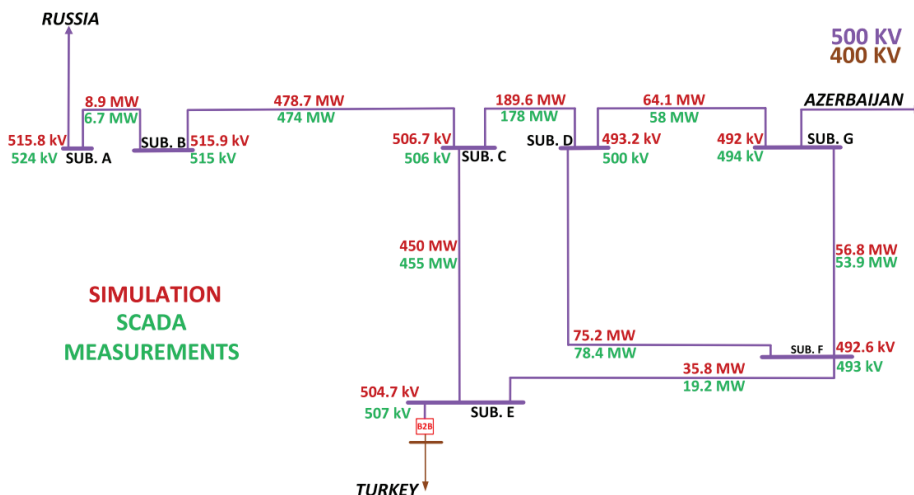


Figure 2. 500-400 kV grid of Georgia



Table 1 and Table 2 illustrate voltage and active power flow differences between simulated and measured data from main substations:

**Table 1.** Simulated and measured voltage values in main substations

Substation	Voltages from simulation in PSS/E, kV	Voltage measurement from SCADA, kV	Simulation error
Substation A	515.8	524	1.56%
Substation B	515.9	515	0.19%
Substation C	506.7	506	0.15%
Substation D	493.2	500	1.37%
Substation E	504.7	507	0.46%
Substation F	492.6	493	0.08%
Substation G	492.0	494	0.41%

**Table 2.** Simulated and measured power flows between main substations

OHL	Active power flow from simulation in PSS/E, MW	Active Power flow from SCADA, MW	Simulation error, MW
Sub. A >> Sub. B	8.9	6.7	2.2
Sub. B >> Sub. C	478.7	474	-4.7
Sub. C >> Sub. D	189.6	178	-11.6
Sub. D >> Sub. G	64.1	58	-6.1
Sub. C >> Sub. E	450	455	5
Sub. G >> Sub. F	56.8	53.9	-2.9
Sub. D >> Sub. F	75.2	78.4	3.2
Sub. F >> Sub. E	35.2	31.2	-4

By the second stage, the goal is the system dynamic model to reasonably predict outcome of network event. System modelling for stability purposes is one of the critical issues in the power system synchronization analysis. In order to achieve this, each dynamic components of the system model (generators, exciters, turbine governor, etc.) must be valid which is hard to fulfil. The system model requires to achieve high level of validity, therefore it's crucial to minimize the mismatches of model performance that compromise accuracy. If some error appears in the output window, it's essential to check the model that could not be initialized and figure it out. It is considered that the average relative simulation error should be less than 10-12%. For this purpose, we have imported the measurements of WAMS system, which reflect the real transient processes occurring in the system during the synchronization. The data shows the exact values of synchronization parameters, according to which the line was automatically reclosed ( $\Delta f=0.08$  Hz,  $\Delta Y=15.31$  kV,  $\Delta \delta=19.1^\circ$ ), where the voltage magnitude of neighbouring system was higher compared to the power system of Georgia, the frequency and phase angle of neighbouring power system were lagging from the respective parameters of Georgian power system. Simultaneously, the simulation of automatic reclosing has been set up, considering all specified synchronization parameters (phase angle, frequency, voltage magnitude), with the validated load flow model in PSS/E, which matches real steady-state conditions. After modelling of automatic reclosing of the line in the software mentioned above by the use of the PYTHON programming language, the simulated sudden change of active power flow at the interconnector was compared to measurement data to see how the simulation outputs corresponded to the actual event, especially during the first period of oscillation.

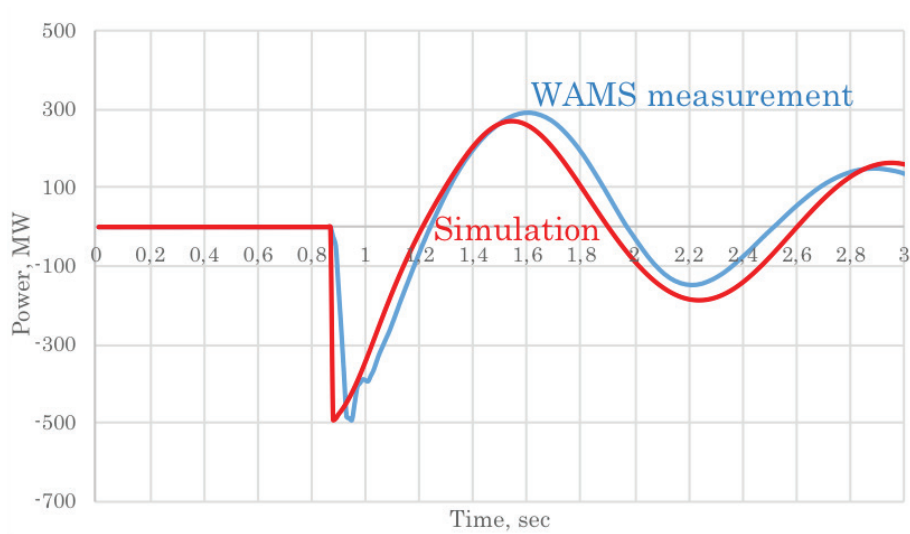


**Figure 3.** Active power flow during synchronization

According to Figure 3, where the red colour represents the simulated event in PSS/E, while the blue curve illustrates the measurements of the WAMS system, they track each other closely. Steady-state condition lasts 0.94 sec. After the automatic reclosure of the interconnector, active power with high peak amplitude flows through the line. The curve shows that active power reaches up to 491 MW in simulation, whereas, according to the real data from WAMS system, active power oscillation reaches to 498 MW directed from Georgian power system to the neighbouring power system. Average amplitude of actual power error obtained less than 1.4%. As the simulation error it is quite low, the power system model is acceptable to perform simulations to determine permissible synchronization parameters.

In order to define the optimal parameters of safe synchronization of Georgian power system with neighbouring big/powerful one, modelling of switching on respective interconnection line with different combination of synchronization parameters has been carried out in verified dynamic model of power system modelling software PSS/E.

### 3. SIMULATION

Simulation has been performed using minimum/maximum winter and summer scenarios. At first, the following preliminary synchronization parameters have been selected: difference between the frequencies of the power systems (Georgia and its neighboring state) to be synchronized  $\Delta f = 0.1$  Hz, difference between the phase angles of mentioned power systems  $\Delta \delta = 40^\circ$  and difference between the voltage levels  $\Delta U \leq 75$  kV. Modeling in each of presented 4 scenarios by the use of mentioned synchronization parameters has been carried out for the following 4 cases (16 simulations in total):

1. Frequency of Georgian power system is higher than the one of neighboring power system (to be synchronized with Georgia), the phase angle of Georgian power system leads the one of neighboring power system;
2. Frequency of Georgian power system is higher than the one of neighboring power system (to be synchronized with Georgia), the phase angle of Georgian power system lags the one of neighboring power system;
3. Frequency of Georgian power system is lower than the one of neighboring power system (to be synchronized with Georgia), the phase angle of Georgian power system leads the one of neighboring power system;
4. Frequency of Georgian power system is lower than the one of neighboring power system (to be synchronized with Georgia), the phase angle of Georgian power system lags the one of neighboring power system.

The differences between the frequencies and phase angles of the power systems to be synchronized in a moment of switching on off interconnection line have impact on the amount of active power swing at that interconnection line which in its turn causes deviation of system frequency and arises frequency derivative. The amount of the latter one is depended on the amplitude of the active power swing at mentioned line and total inertia of the respective system. Therefore, the less the system inertia and bigger the amplitude of power swing is, the bigger the amount of frequency derivative will be. Based on the fact that Georgian power system is characterized with small synchronous inertia, modeling process should define the amount of the frequency derivative.

Nowadays, there is frequency derivative protection arranged at some part of demand and generation facilities in Georgian electricity power system. Besides frequency derivative, it's also noteworthy the amplitude of the active power swing at interconnection line since big amplitude can cause activation of systems dividing automatic arranged on that line and hence its re-outage (after synchronization). Hence, if modeling process show that 1) frequency derivative protection of demand/generation facilities has been activated or conditions being very close to the activation of mentioned protection have been formed or 2) active power swing at respective cross-border line has triggered systems dividing automatic, another modeling process with decreased (stricter) marginal synchronization parameters should be performed.

### 3.1. Difference between frequencies $\Delta f = 0.1$ Hz, difference between the phase angles $\Delta\delta = 40^\circ$

As mentioned before, first modeling has been performed using the following synchronization parameters:  $\Delta f = 0.1$  Hz,  $\Delta\delta = 40^\circ$  in all four characteristic scenarios (winter maximum and minimum demand, summer maximum and minimum demand). Above mentioned four cases (regarding the difference in system frequencies and phase angles of the power systems to be synchronized) described above by bullets have been investigated for all four characteristic scenarios. Figures 4 and 5 show the modeling results, in particular, the active power swing at respective interconnector.



Figure 4. Active power swing at interconnector in case  $\Delta\delta = 40^\circ$ , when phase angle of Georgian power system leads the one of neighboring power system in a moment of synchronization

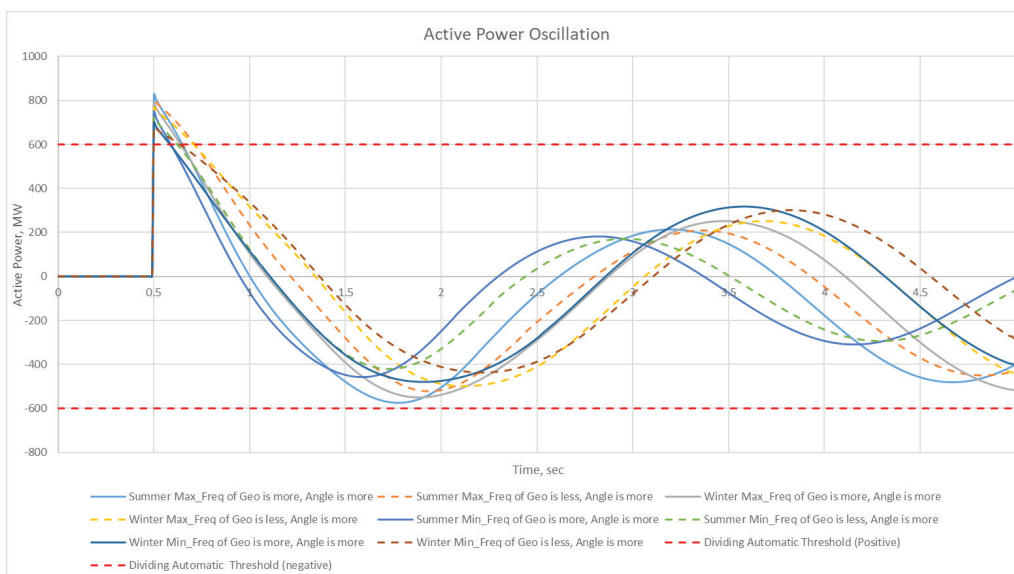


Figure 5. Active power swing at interconnector in case  $\Delta\delta = 40^\circ$ , when phase angle of Georgian power system lags the one of neighboring power system in a moment of synchronization

On figures 4 and 5 as well as on the ones below:

- *Freq of Geo is more/less* means that frequency of Georgian power system is higher/lower than the one of neighboring power system;
- *Angle is more/less* means that the phase angle of Georgian power system leads/lags the one of neighboring power system.

Curves illustrated above show that active power swing at cross-border line do not cause activation of systems dividing automatic (duration of cross of dividing automatic power threshold is less than assumed time delay of respective automatic), represented by red dashed line (600 MW is taken as an example). However, performing synchronization with the parameters of  $\Delta f = 0.1$  Hz and  $\Delta = 40^\circ$  can be risky due to the high amount of frequency derivative. Table 3 below shows frequency derivative values (-0.4 Hz/sec assumed setpoint of frequency derivative automatic for several demand units in Georgian power system).

**Table 3.** Frequency derivative values, when permissible difference between power systems phase angles  $\Delta\delta = 40^\circ$

		Frequency derivative, Hz/sec							
		Winter min		Summer min		Winter max		Summer max	
$\Delta\delta$	Variation	Neg.	Pos.	Neg.	Pos.	Neg.	Pos.	Neg.	Pos.
<b>40°</b>	Freq>, Angle>	-0.772	0.506	-1.107	0.631	-0.862	0.504	-0.963	0.636
	Freq>, Angle<	-0.575	0.614	-0.748	0.886	-0.667	0.717	-0.811	0.827
	Freq<, Angle>	-0.501	0.549	-0.709	0.652	-0.550	0.574	-0.667	0.656
	Freq<, Angle<	-0.545	0.868	-0.736	1.248	-0.608	0.922	-0.779	1.081

Here as well as in the following tables below:

- Fre>, Angle> means that frequency of Georgian power system is higher than the one of neighboring power system and phase angle of Georgian power system leads the one of neighboring power system
- Fre>, Angle< means that frequency of Georgian power system is higher than the one of neighboring power system and phase angle of Georgian power system lags the one of neighboring power system
- Fre<, Angle> means that frequency of Georgian power system is lower than the one of neighboring power system and phase angle of Georgian power system leads the one of neighboring power system
- Fre<, Angle< means that frequency of Georgian power system is lower than the one of neighboring power system and phase angle of Georgian power system lags the one of neighboring power system

As it is seen from table 3, frequency derivative protection of consumers in Georgian power system goes in action in all considered scenario in case of selected synchronization parameters ( $\Delta f = 0.1$  Hz,  $\Delta\delta = 40^\circ$ ), causing tripping of some part of the demand in Georgia. Respectively, it is necessary to perform modeling with decreased (stricter) synchronization parameters.

### 3.2. Difference between frequencies $\Delta\phi = 0.1$ Hz, difference between the phase angles $\Delta\delta = 30^\circ$

Modeling has been performed using the following synchronization parameters:  $\Delta\phi = 0.1$  Hz,  $\Delta\delta = 30^\circ$  in above-mentioned all four characteristic scenarios of winter and summer. Mentioned four cases described above by bullets have been investigated for all four scenarios. Figures 6 and 7 show active power swing at respective interconnector.



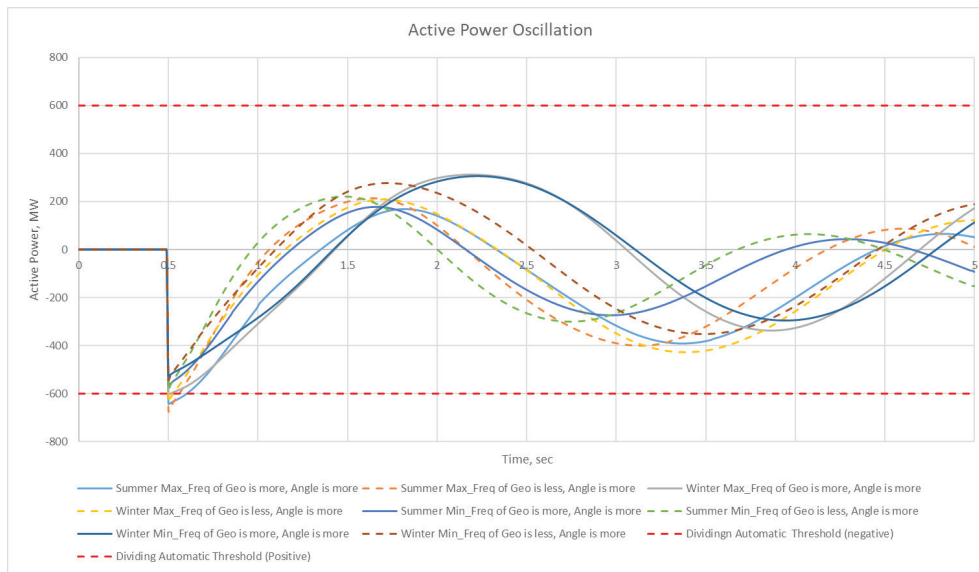


Figure 6. Active power swing at interconnector in case  $\Delta\delta = 30^\circ$ , when phase angle of Georgian power system leads the one of neighboring power system in a moment of synchronization



Figure 7. Active power swing at interconnector in case  $\Delta\delta = 30^\circ$ , when phase angle of Georgian power system lags the one of neighboring power system in a moment of synchronization

Curves above show that active power swing at cross-border line do not cause activation of systems dividing automatic (duration of cross of dividing automatic power threshold is less than assumed time delay of respective automatic), represented by red dashed line (600 MW is taken as an example). Despite of that, performing synchronization with the parameters of  $\Delta f = 0.1$  Hz and  $\Delta\delta = 30^\circ$  can be somewhat risky due to the high amount of frequency derivative, in particular, table 4 below shows frequency derivative values (-0.4 Hz/sec assumed setpoint of frequency derivative automatic for several demand units in Georgian power system).

Table 4. Frequency derivative values, when permissible difference between power systems phase angles  $\Delta\delta = 30^\circ$

		Frequency derivative, Hz/sec							
		Winter min		Summer min		Winter max		Summer max	
$\Delta\delta$	Variation	Neg.	Pos.	Neg.	Pos.	Neg.	Pos.	Neg.	Pos.
30°	Freq>, Angle>	-0.635	0.423	-0.907	0.482	-0.698	0.447	-0.813	0.494
	Freq>, Angle<	-0.461	0.433	-0.581	0.623	-0.538	0.498	-0.625	0.590
	Freq<, Angle>	-0.370	0.439	-0.492	0.495	-0.387	0.450	-0.466	0.496
	Freq<, Angle<	-0.430	0.695	-0.562	0.962	-0.467	0.727	-0.593	0.850

As it is seen from table 4, frequency derivative protection of consumers in Georgian power system goes in action in all considered scenario except two of them in case of selected synchronization parameters ( $\Delta\phi = 0.1$  Hz,  $\Delta\delta = 30^\circ$ ), which initiates tripping of some part of the demand in Georgia. Respectively, it is necessary to perform modeling with decreased (stricter) marginal synchronization parameters.

### 3.3. Difference between frequencies $\Delta f = 0.1$ Hz, difference between the phase angles $\Delta\delta = 20^\circ$

Modeling has been performed using the following synchronization parameters:  $\Delta\phi = 0.1$  Hz,  $\Delta\delta = 20^\circ$  in above-mentioned all four characteristic scenarios of winter and summer. Mentioned four cases described above by bullets have been investigated for all four scenarios. Figures 8 and 9 show active power swing at respective interconnector.

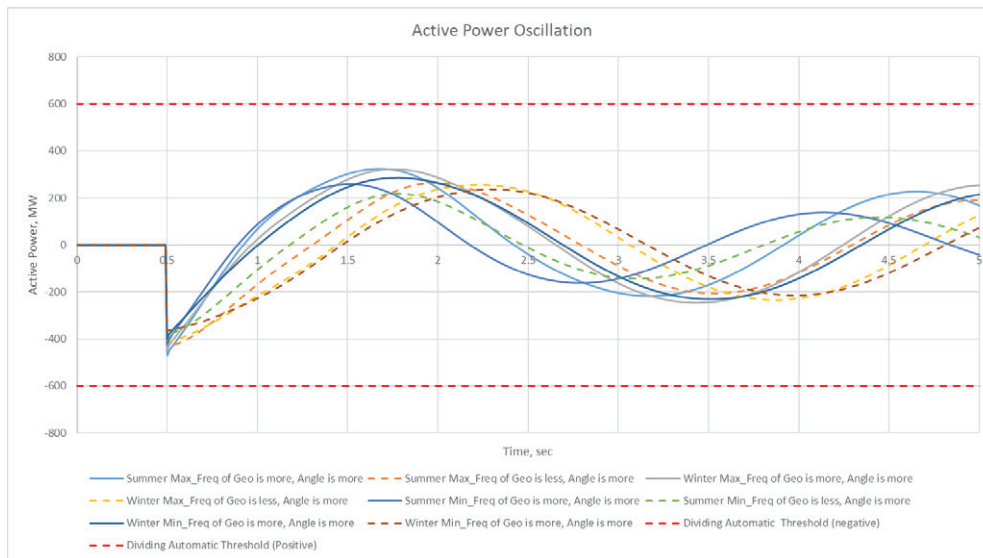


Figure 8. Active power swing at interconnector in case  $\Delta\delta = 20^\circ$ , when phase angle of Georgian power system leads the one of neighboring power system in a moment of synchronization

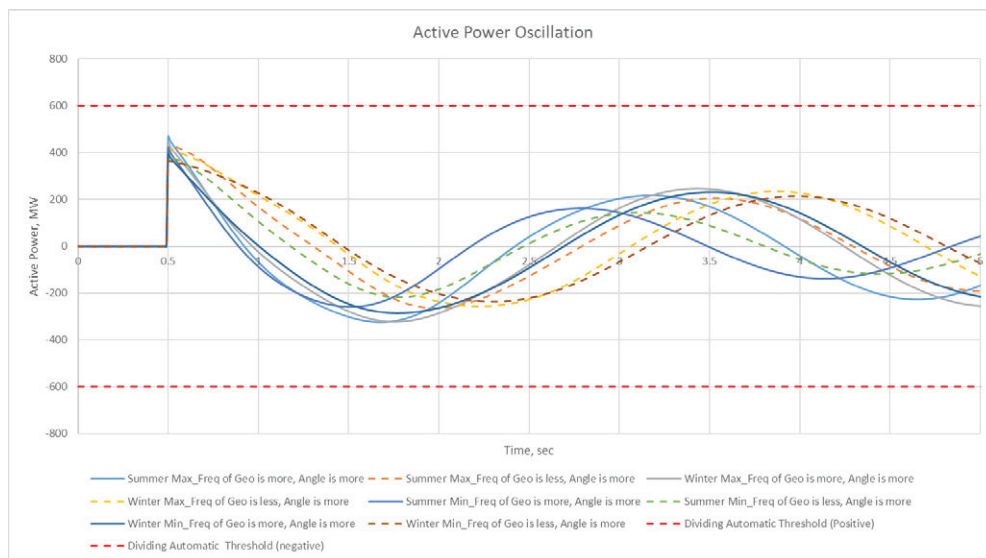


Figure 9. Active power swing at interconnector in case  $\Delta\delta = 20^\circ$ , when phase angle of Georgian power system lags the one of neighboring power system in a moment of synchronization

Results illustrated on above figures show that active power swing at cross-border line do not cause activation of systems dividing automatic, represented by red dashed line (600 MW is taken as an example). Despite of that, performing synchronization with the

parameters of  $\Delta\phi = 0.1$  Hz and  $\Delta\delta = 20^\circ$  can be somewhat risky due to the high amount of frequency derivative, in particular, table 5 below shows and frequency derivative values (-0.4 Hz/sec assumed setpoint of frequency derivative automatic for several demand units in Georgian power system).

**Table 5.** Frequency derivative values, when permissible difference between power systems phase angles  $\Delta\delta = 20^\circ$

		Frequency derivative, Hz/sec							
		Winter min		Summer min		Winter max		Summer max	
$\Delta\delta$	Variation	Neg.	Pos.	Neg.	Pos.	Neg.	Pos.	Neg.	Pos.
<b>20°</b>	Freq>, Angle>	-0.478	0.302	-0.716	0.377	-0.513	0.319	-0.608	0.397
	Freq>, Angle<	-0.345	0.319	-0.407	0.374	-0.394	0.352	-0.444	0.359
	Freq<, Angle>	-0.300	0.351	-0.278	0.339	-0.338	0.385	-0.281	0.338
	Freq<, Angle<	-0.307	0.511	-0.390	0.737	-0.326	0.526	-0.408	0.616

As it is seen from table 5, when synchronization is done with the parameters of  $\Delta\phi = 0.1$  Hz and  $\Delta\delta = 20^\circ$ , frequency derivative protection of consumers in Georgian power system was activated in 7 considered scenarios, causing tripping of some part of the demand in Georgia. The biggest amount of negative frequency derivative -0.716 Hz/sec has been recorded in summer minimum scenario, in case with frequency of Georgian power system being higher than the one of neighboring power system and phase angle of Georgian power system leading the one of neighboring power system. Further decrease of synchronization parameters in order to decrease frequency derivative is not reasonable since it will also vastly decrease the probability of implementation of the successful synchronization. Despite of this, additional modeling with decreased (stricter) synchronization parameters -  $\Delta\phi = 0.1$  Hz,  $\Delta\delta = 10^\circ$  - has been carried out.

### 3.4. Difference between frequencies $\Delta\phi = 0.1$ Hz, difference between the phase angles $\Delta\delta = 10^\circ$

Compared to above-reviewed results, stricter synchronization parameters:  $\Delta\phi = 0.1$  Hz,  $\Delta\delta = 10^\circ$  do not cause activation of systems dividing automatic. Therefore, observation in this case has been only done on frequency derivative levels. Table 6 includes frequency derivative values arisen in Georgian power system.

**Table 6.** Frequency derivative values, when  $\Delta\delta = 10^\circ$

		Frequency derivative, Hz/sec	
		Summer min	
$\Delta\delta$	Variation	Negative	Positive
<b>10°</b>	Freq>, Angle>	-0.458	0.217
	Freq>, Angle<	-0.257	0.206
	Freq<, Angle>	-0.196	0.237
	Freq<, Angle<	-0.221	0.460

As it is seen from table 6, when synchronization is done with the parameters of  $\Delta\phi = 0.1$  Hz and  $\Delta\delta = 10^\circ$ , frequency derivative is higher than its permissible level only in one case. In particular, in summer minimum demand scenario, when frequency of Georgian power system is higher than the one of neighboring power system and phase angle of Georgian power system leads the one of neighboring power system, synchronization with the parameters of  $\Delta\phi = 0.1$  Hz and  $\Delta\delta = 10^\circ$  causes trip of some consumers in Georgia by frequency derivative protection.

Further decrease of marginal synchronization parameters in order to decrease frequency derivative is not reasonable since it will also cause an important decrease of probability of implementation of the successful synchronization.



### 4. CONCLUSION

Synchronization of Georgian power system with comparably bigger one with different marginal parameters has been analyzed in frame of current study. Based on the results, there is no risk of activation of systems dividing automatic existing at respective interconnection line. All the analyzed scenarios are safe in terms of frequency derivative of generation units, as for the same protection of demand units, it is expected to trip of some consumers by mentioned protection is the most part of the considered scenarios.

Based on the received results, in order to avoid consumer tripping by frequency derivative protection in case of synchronization, the following recommendations may be given:

- Proposed synchronization parameters for Georgian power system are as follows:  $\Delta\phi = 0.1$  Hz,  $\Delta\delta = 20^\circ$  and  $\Delta U \leq 75$  kV;
- Frequency derivative setpoint of frequency derivative protection for demand objects should be increased (by 25-30%);
- Implementation of synchronization of Georgian power system with its neighboring and bigger one with the marginal synchronization parameters of  $\Delta\phi = 0.1$  Hz,  $\Delta\delta = 20^\circ$  in all characteristic scenario, when frequency of Georgian power system is higher than the one of neighboring power system and phase angle of Georgian power system leads the one of neighboring power system, arises negative frequency derivative with the amount which is close to the setpoint of frequency derivative protection for demand objects. Therefore, in case of these scenarios, it's advisable that synchronization device do not send command with the above-mentioned marginal synchronization parameters.

The method described in this paper should be used by any system operator to determine the optimal parameters for power systems with low inertia in order to avoid undesirable events during synchronization with more powerful one, that can trigger activation of respective automatics and tripping of the relevant demand/generation units.

### BIBLIOGRAPHY

- [1] P. Kundur, "Power system stability and control" (McGraw-hill; 1994 Jan 1, pages 20-22)



# Investigation of The Effect of Batteries on Frequency Control in Power System

[m\\_furkanyilmaz@hotmail.com](mailto:m_furkanyilmaz@hotmail.com)**MUHAMMET FURKAN YILMAZ\*, ALI ÖZTÜRK***Electrical Electronics Engineering Duzce University***MUSTAFA SAKA***Electrical Electronics Engineering Iskenderun Technical University***CENK ANDIÇ***Electrical Engineering Istanbul Technical University***Türkiye**

## SUMMARY

Power systems are growing day by day. Frequency control has also become critical with the load increase of the system. The sizes of the generation units in the system and the capacities of the connected and planned batteries have also increased. The amplitude of the oscillations that may occur in the system has intensified with the increase in the loads at the consumption points. In this study, the frequency response model of a multi-area power system is investigated. In the multi-area power system created in the Matlab Simulink program, the effect of the battery against the instantaneous load degradation was investigated. The generation units were automatic generation control with the help of the controller. Automatic generation control was performed with the help of PID (ratio-integral-derivative) controllers. The established power system model has been optimized with a heuristic algorithm. The response of the batteries connected to the system to the oscillations that will occur in the system has been investigated. With the addition of the battery system, it has been observed that there is an improvement in the damping of the oscillations in the system. It has been observed that by increasing the number of battery systems connected to the system, even better results are obtained in minimum overshoot and settling time.

## KEYWORDS

Frequency Control, Automatic Generation, Control (AGC), Energy Storage Batteries

## 1. INTRODUCTION

When it comes to electric power, the amount of energy consumed per person and the installed capacity of generation sources are typically presented as variables. However, it is also important to emphasize the improvement of quality in electrical energy. To ensure that all elements in the electrical system operate under optimum conditions, an adequate level of energy quality must be provided. The balance between active power and reactive power is crucial during the operation of the system. This balance can be achieved by maintaining the desired conditions for frequency and voltage.

Instantaneous imbalances at any point in the power system will cause variations in the system frequency. To address this undesirable situation, an effective control mechanism is used [1]. Relays are used to achieve linear load shedding [2] and trip generation [3, 4] units to ensure stability. However, in dynamic systems, some generators connected to the system can compensate for load changes. Under normal operating conditions, all areas are expected to meet their own loads and adhere to the planned transfer schedule [5]. All control areas should agree on mutual benefits in both normal and abnormal situations. Ultimately, being connected to a grid is the sole advantage in such emergency situations [6].

The control loop should possess sufficient stabilizing capability [7]. As soon as load changes occur in the areas, any error in frequency should be eliminated. Transient frequency deviation should be minimized [6, 8].

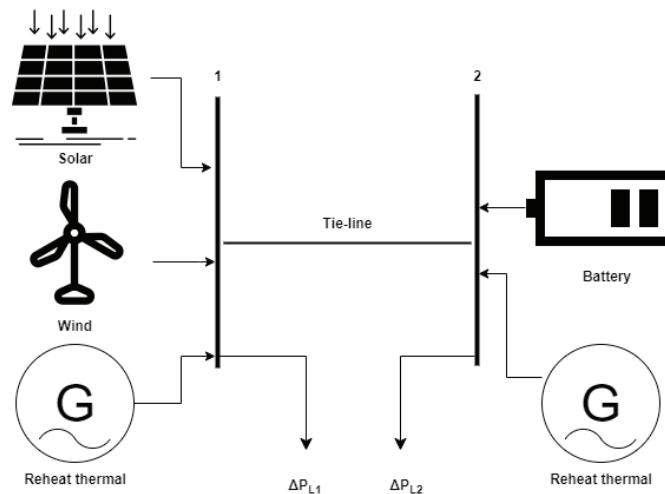


*Figure 1. Interconnected test system*

In the study, a two-area interconnected system model was established to conduct a test study. The created model includes renewable energy sources, reheating thermal units, and a battery unit [9,10] that supports them. The reactions occurring in the system during a disturbance in the load condition were observed.

## 2. MATERIAL AND METHOD

### 2.1. Load Frequency Control

The speed regulator provides the primary speed control function. Additional control provided by a central control unit is distributed to the generation sources. In a multi-area interconnected and controlled system, load frequency control (LFC) refers to the control of both frequency and the planned level of energy flow between the areas [1].

In load frequency control, under normal operating conditions, all areas are expected to meet their own loads and adhere to the planned transfer schedule. All control areas should mutually benefit in both normal and abnormal situations. The sole advantage of being connected to a grid is evident in these emergency situations. Load frequency control mainly consists of a four-step system. The primary frequency control is the control mechanism performed by the governors of the generators. By directly considering the system frequency, the aim is to maintain the balance of active power in the system by contributing to the increase or decrease in production. The secondary frequency control is the control mechanism performed by the interconnected areas through controllers from a central control unit. By evaluating the deviating load flows and frequency deviations in the connection lines of the areas, the central control unit performs the secondary frequency control by sending set points to the generators. Tertiary frequency control is





a manual adjustment of production by increasing or decreasing it. Time control prevents any time deviations between the system frequency and real-time.

### 2.2. PID Controller

There are several control methods available for load frequency control. The Proportional-Integral-Derivative (PID) control method [11] is a successful approach. The proportional component aims to reduce the error by multiplying the incoming error feedback with a coefficient. The integral component is obtained by calculating the area between the error curve and the desired value curve. The derivative component incorporates the slope of the error curve to reduce the error. The effects of these components are summarized in Table 1.

Table 1. Effects of PID elements

Control Response	Rise time	Settling time	Overshoot	Steady state error
Kp	decrease	small change	increase	decrease
Kd	small change	decrease	decrease	no change
Ki	decrease	increase	increase	eliminate

The PID controller operates based on a feedback mechanism. It starts by calculating the error, which is the difference between the desired set point and the actual value of the system at a given time. This error value is then used as input for a new calculation cycle. The objective is to reduce the error value.

The gains of a PID controller are adjusted to minimize control errors in a process. In the literature, various heuristic methods such as artificial intelligence [12], fuzzy logic [13], Artificial Bee Colony [14], and Particle Swarm Optimization (PSO) algorithms have been used for optimizing controller gains. PSO algorithm is observed to be useful due to its simplicity, smaller code size compared to other algorithms, and faster convergence to accurate results [15].

In this study, the gains of a two-zone system PID controller are adjusted using the PSO algorithm. Renewable energy sources and batteries are used in the two-zone system, in line with the development trends of modern grid systems. The increase in renewable energy usage has also led to an increase in battery usage. Future grids are planning to use batteries with large capacities. The research focus of our established test system is how to ensure frequency control in the future grid with a changing structure.

### 2.3. Particle Swarm Optimization Algorithm

Particle Swarm Optimization (PSO) is an iterative method like other heuristic optimizations. It is a population-based optimization algorithm inspired by the behavior of flocks of birds, designed to solve complex multivariate functions that take a long time to solve with derivative-based methods [16]. Each particle in the swarm represents a solution to the problem. These particles use their previous experiences in each iteration to converge to the optimal solution point by making improvements.

The algorithm consists of a swarm and individuals within the swarm. Individuals represent their positions in the solution space and adjust their positions toward the best point in the swarm based on previous experiences. Other individuals adjust their positions accordingly to be closer to the best position. This way, they settle in a point closer to the solution.

The convergence process of the swarm individuals can be summarized as follows:

1. The initial velocity and direction of each individual are randomly determined, and the iteration begins.
2. The fitness (i.e., the quality of the solutions) of individuals is evaluated.
3. The best approach for each individual is determined.
4. The individual located at the best (global) point is selected from the swarm.
5. The velocities and positions of individuals are recalculated, and the position update is repeated.
6. The results are evaluated, and if the solutions are good enough, the search process stops; otherwise, the process continues from step 2.

Having a larger number of individuals in the swarm may increase the optimization time, but it benefits the accuracy of the solution.

Table 2. Values of parameter of PSO

Methods	Problem Dimension
PSO	15 (PID)
c1	c2
1.5	1.5
$\omega$	
0.9	
VL	VH
-1	-1
$\alpha$ max	P
-	
N	Iteration max
30	10

### 3. SOLUTION OF THE PROBLEM

#### 3.1. Testing System

In addition to the growth seen in power systems, technological advancements have made it necessary to use new resources and equipment. This study focuses on the importance of integrating renewable energy sources into the system. The use of renewable energy sources in the system increases the possibility of sudden fluctuations in production. Fluctuations in active power can have negative effects on frequency. To minimize changes in frequency, energy storage systems need to be utilized. In this study, a test system was created to examine the fluctuations in frequency. The test system incorporates renewable energy sources and batteries.

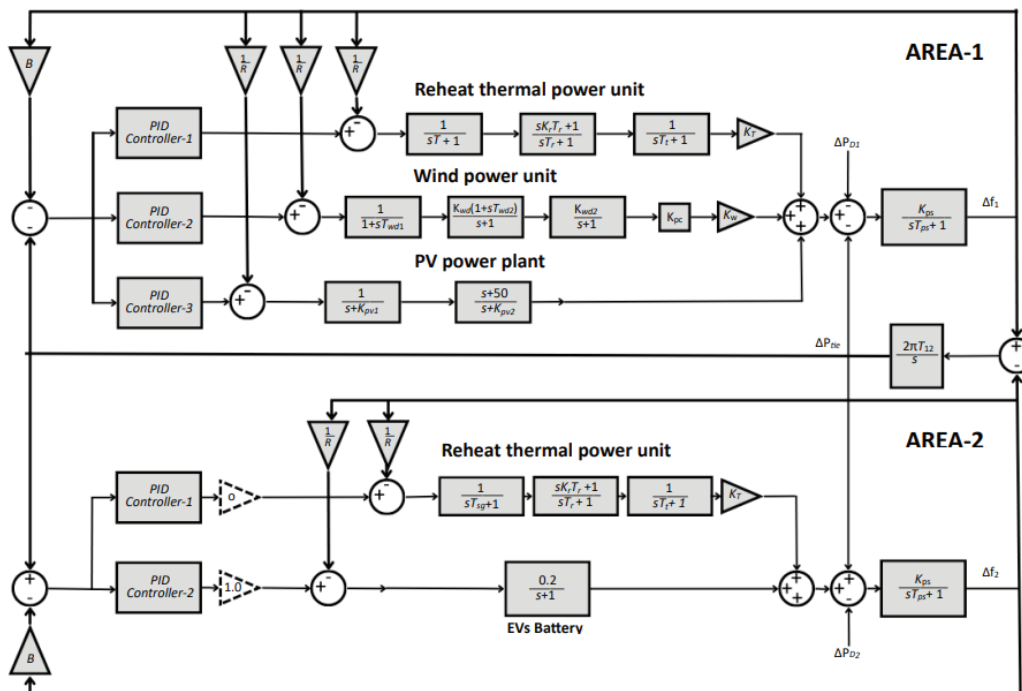


Figure 2. Block diagram of a two-area power system including EV battery [17, 18, 19, 20].

The configuration of the control system is based on a two-area interconnected system, integrated with renewable energy sources and battery models. A disturbance has occurred in Area 1 load, which has caused an undesirable frequency deviation in the system.

The system test is performed by calculating the changes in the Area Control Error (ACE). ACE is the sum of the frequency deviation and the deviation from the planned power flow in the interconnection line. The gains of the PID controllers are updated to minimize the ACE.

**Table 3.** Parameter of two area interconnected system [17, 18, 19, 20].

Parameter	Value	Parameter	Value	Parameter	Value
$f$	60 Hz	$R=R_1=R_2$	2.4 Hz/pu	$T_t$	0.3 s
$P_{r1}=P_{r2}$	1000MW	$B=B_1=B_2$	0.432puMW/Hz	$T_{gh}$	0.2 s
$P_L$	1000 MW	$K_G$	0.130438 pu	$T_{rs}$	5 s
GRC	$\pm 0.05s$	$K_{ps}$	68.95 Hz/pu MW	$T_{rh}$	28.75 s
$b_g$	0.05 s	$K_r$	0.3 s	$T_w$	1 s
$c_g$	1	$K_w$	0.138	$T_{ps}$	11.49
$X_c$	0.6 s	$K_H$	0.326084 pu	$T1_2$	0.0433
$Y_c$	0.6	$K_T$	0.543478	$T_{wd1}$	0.041
$K_v$	-18	$K_{wd1}$	1.25	$T_{wd2}$	0.6
$K_{pv1}$	0.502525	$K_{wd2}$	1.30	$T_{cr}$	0.01 s
$K_{pv2}$	99.4975	$T_{sg}$	0.08 s	$T_f$	0.23 s
$K_{pc}$	0.8	$T_r$	10 s	$T_{cd}$	0.2 s

### 3.2. Case of No Battery

Case 1 represents the scenario where the battery is not present in the system. The test model is set up to examine the situation where renewable energy sources are integrated into the system but the energy storage unit is not connected. In Figure 4, frequency fluctuations in Area 1 are observed. In Figure 5, frequency fluctuations in Area 2 are shown. Figure 6 illustrates the power flow occurring in the interconnection line.

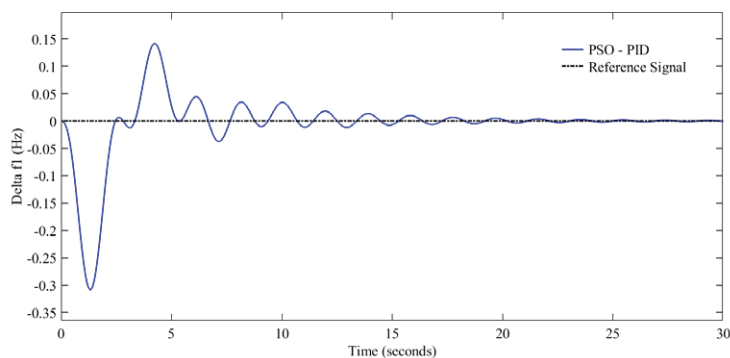


**Figure 4.** Change of Frequency in area-1 with no EV

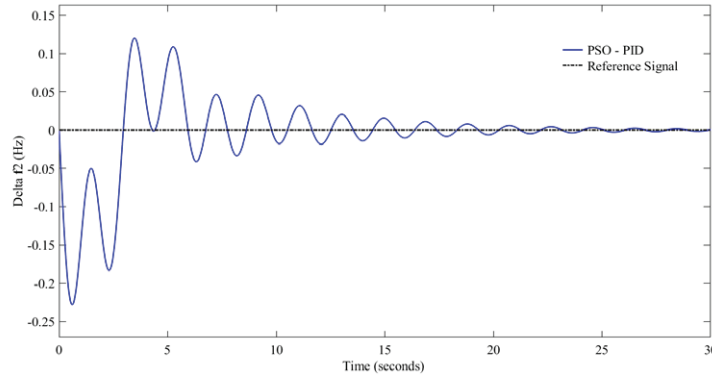


Figure 5. Change of Frequency in area-2 with no EV

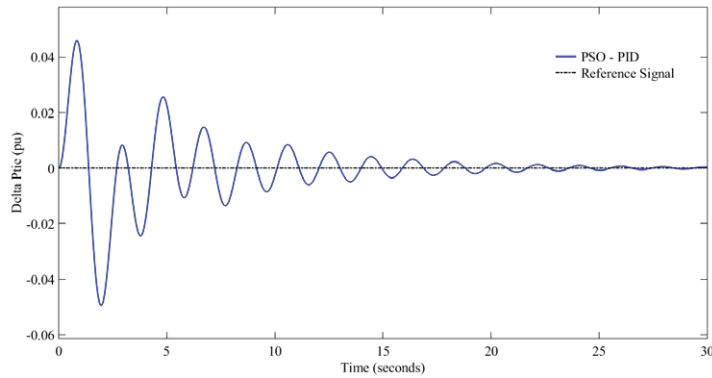


Figure 6. Change of tie-line power with no EV

### 3.3. Cases that the Battery Contributes to the System

In Case 2, the battery is integrated into the system. The connection of the battery to the system is done gradually at different levels: 25%, 50%, 75%, and 100%. The main objective is to examine the contribution of the battery to the system during load changes.

Figure 7 shows the frequency fluctuations in Area 1 for all the scenarios studied. Figure 8 displays the frequency fluctuations in Area 2 for all the scenarios studied. Figure 9 illustrates the power flows occurring in the interconnection line for all the scenarios.

The purpose of these studies is to analyze how the battery's presence and varying levels of integration affects the frequency stability and power flow in the interconnected system.

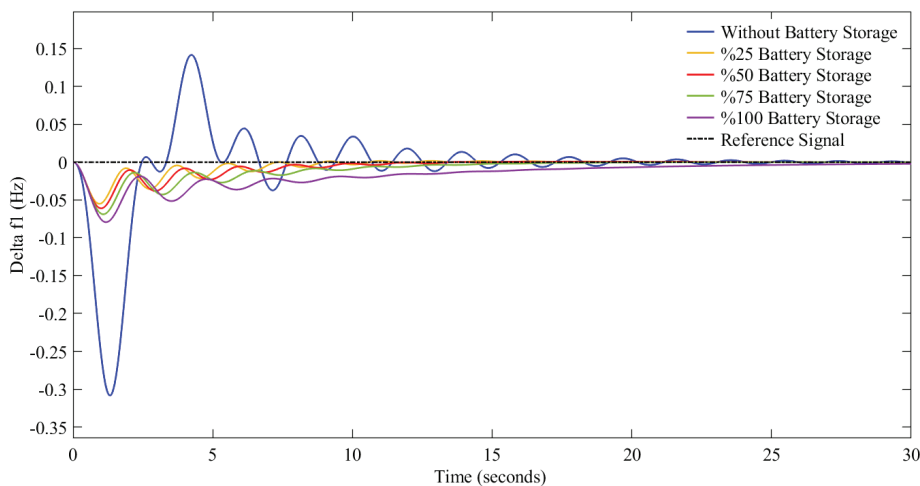


Figure 7. Change of Frequency in area-1 with EV

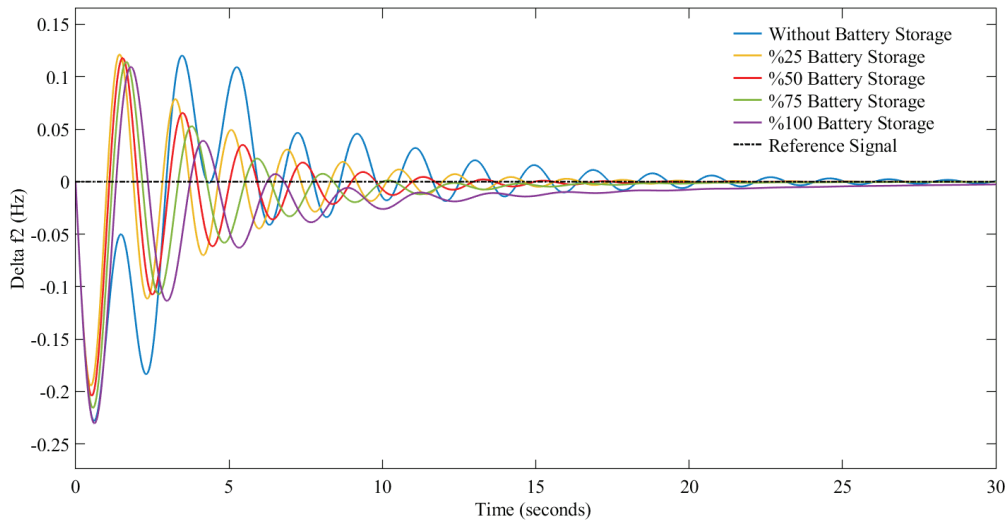


Figure 8. Change of Frequency in area-2 with EV

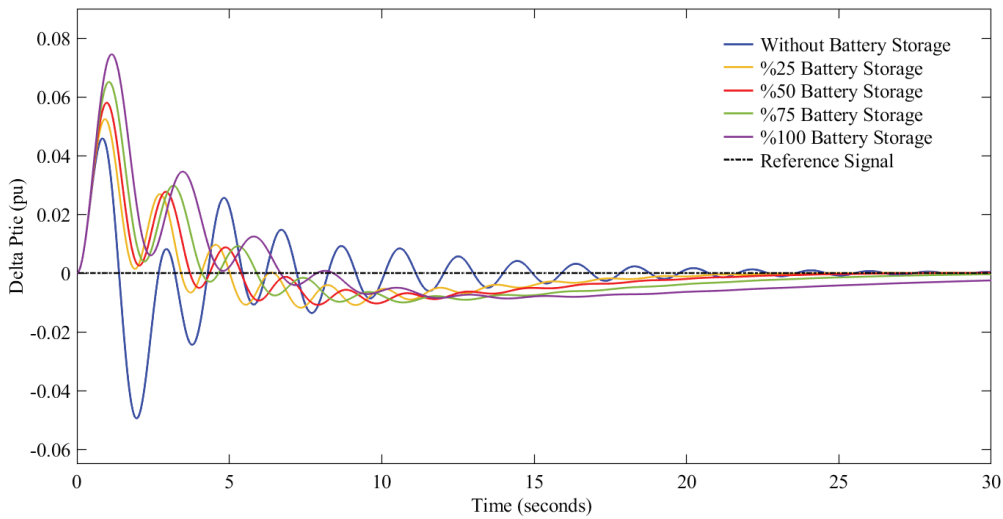


Figure 8. Change of tie-line power with EV

The optimized controller gains obtained in the study are specified in Table 4. The state values are given as 1 when no battery is used, 2 when the battery usage is at 25%, 3 when the battery usage is at 50%, 4 when the battery usage is at 75%, and 5 when the battery usage is at 100%.

Table 4. PID controller optimization parameters

Controller	$K_p$	$K_i$	$K_d$
PID Controller 1	2.57	-0.64	1.09
PID Controller 2	1.45	0.23	2.94
PID Controller 3	-0.33	1.86	-2.21
PID Controller 4	2.19	-2.47	-1.89
PID Controller 5	0.57	2.99	-0.72

Overshoot, undershoot and settling time values were calculated for each of the regions. In addition, the values observed in the interconnection line are given in Table 5.

**Table 5.** Values of overshoot, undershoot settling time

Parameters		PSO -Without Battery Storage	PSO - %25 Battery Storage	PSO - %50 Battery Storage	PSO - %75 Battery Storage	PSO - %100 Battery Storage
$\Delta\phi_1$	Overshoot (M <sup>+</sup> )	0.1413	-	-	-	-
	Undershoot (M <sup>-</sup> )	0.3085	0.05502	0.06105	0.06891	0.07932
	Settling Time (s)	22.63	6.683	7.276	9.88	16.38
$\Delta\phi_2$	Overshoot (M <sup>+</sup> )	0.1203	0.1212	0.1179	0.1143	0.1094
	Undershoot (M <sup>-</sup> )	0.2279	0.1943	0.204	0.2156	0.2305
	Settling Time (s)	25.57	11.64	10.6	11.55	17.51
$\Delta\Pi_{LIC}$	Overshoot (M <sup>+</sup> )	0.04588	0.05249	0.05804	0.06514	0.07452
	Undershoot (M <sup>-</sup> )	0.0495	0.0118	0.01081	0.01	0.008644
	Settling Time (s)	19.17	13.35	15.85	17.97	23.07

## 4. CONCLUSION

The aim of the study was to investigate the effect of battery in a two-area control system with optimized controllers using the PSO (Particle Swarm Optimization) algorithm. The system responses were observed by increasing the level of battery integration into the system. The given figures illustrate the frequency deviations in each area and the power flows in the transmission lines. The fluctuations in frequency and the load flow in the transmission lines varied as the level of battery integration changed.

Upon examining the test result values, it was observed that the battery improved the balanced operation of the frequency. The frequency responses in both areas were analyzed, and it was observed that the presence of batteries in an electrical system is highly effective in enhancing the quality of electrical energy. During disturbances, the instant contribution of batteries to the system helped dampen the fluctuations in active power, resulting in a quicker restoration of frequency balance. The level of battery integration into the system also plays a crucial role. As the battery integration increased, the damping speed in the system increased, leading to more efficient solutions. Moreover, increased battery integration caused changes in the power flow in the transmission lines. The magnitude of changes in power flow increased with higher levels of battery integration. If the planning during battery integration into the system is not done correctly, there is a possibility of increased loading on the transmission lines.

In conclusion, the positioning and quantity of batteries need to be carefully adjusted. Proper planning and coordination are essential during the integration of batteries into the system to ensure optimal performance.

## BIBLIOGRAPHY

- [1] Prabha, Kundur. Power System Stability and Control, 1994, 581-626.
- [2] Paul, Anderson; Mahmood, Mirheydar. An Adaptive Method for Setting Underfrequency Load Shedding Relays (IEEE Transactions on Power Systems, May 1992, 647-655).
- [3] Mania, Pavella; Damien, Ernst; Daniel, Ruiz-Vega. Transient Stability of Power Systems: A Unified Approach to Assessment and Control, 2000.
- [4] G. G., Karady; Jun, Gu. A Hybrid Method for Generator Tripping (IEEE Transactions on Power Systems, 2002, 1102-1107).
- [5] Hassan, Bevrani. Robust Power System Frequency Control, 2014.
- [6] Olle I., Elgerd. Electric Energy Systems Theory, 1971, 310-340.
- [7] Karl J., Astrom; Tore, Hagglund. PID Controllers: Theory, Design, and Tuning, 1995, 64-69.
- [8] Ibraheem, Nasiruddin; Prabhat, Kumar; D.P., Kothari. Recent Philosophies of Automatic Generation Control Strategies in Power Systems (IEEE Transactions on Power Systems, Feb 2005, 346 - 357).
- [9] S. K., Aditya; D., Das. Battery Energy Storage for Load Frequency Control of an Interconnected Power System (Electric Power Systems Research, 2001, 179-185.)
- [10] S., Kalyani; S., Nagalakshmi; R., Marisha. Load Frequency Control Using Battery Energy Storage System in Interconnected Power System (International Conference on Computing, Communication and Networking Technologies / ICCCNT'12, 2012, 1-6).





### Oral Presentation: Investigation of The Effect of Batteries on Frequency Control in Power System

- [11] J., Nanda; B., Kaul. Automatic Generation Control of an Interconnected Power System (Proc. IEE, May 1978, 385-390).
- [12] H.L., Zeynelgil; A., Demiroren; N.S., Sengor. The Application of ANN Technique to Automatic Generation Control for Multi-area Power System (International Journal of Electrical Power & Energy Systems, 2002, 345-354).
- [13] Ertuğrul, Çam; İlhan, Kocaarslan. A Fuzzy Gain Scheduling PI Controller Application for an Interconnected Electrical Power System (Electric Power Systems Research, 2005, 267-274).
- [14] Haluk, Gözde; M. C., Taplamacioglu; İlhan, Kocaarslan. Comparative Performance Analysis of Artificial Bee Colony Algorithm in Automatic Generation Control for Interconnected Reheat Thermal Power System (International Journal of Electrical Power & Energy Systems, 2012, 167-178).
- [15] Haluk, Gözde; M. C., Taplamacioglu; İlhan, Kocaarslan; M.A, Şenol. Article Swarm Optimization Based Pi-Controller Design to Load-Frequency Control of a Two Area Reheat Thermal Power System. (Isı Bilimi ve Teknigi Dergisi / Journal of Thermal Science and Technology, 2010, 13-21).
- [16] J., Kennedy; R., Eberhart. Particles Swarm Optimization (IEEE International Conference on Neural Networks, 1995, 1942-1948).
- [17] Ravi, Shankar; S.R., Pradhan; Kalyan, Chatterjee; Rajasi, Mandal. A Comprehensive State of the Art Literature Survey on LFC Mechanism for Power System (Renewable and Sustainable Energy Reviews, 2017, 1185-1207).
- [18] Yatin, Sharma; Lalit Chandra, Saikia. Automatic Generation Control of a Multi-Area ST – Thermal Power System Using Grey Wolf Optimizer Algorithm Based Classical Controllers (International Journal of Electrical Power & Energy Systems, 2015, 853-862).
- [19] Dipayan, Guha; Provas Kumar, Roy; Subrata, Banerjee. Load Frequency Control of Interconnected Power System Using Grey Wolf Optimization (Swarm and Evolutionary Computation, 2016, 97-115).
- [20] C., Andic; S., Ozumcan; A., Ozturk; B., Turkey. Honey Badger Algorithm Based Tuning of PID Controller for Load Frequency Control in Two-Area Power System Including Electric Vehicle Battery (2022 4th Global Power, Energy and Communication Conference / GPECOM, 2022, 307-310).



# Development of Energy Monitoring System for Sustainable Production in the Textile Industry

?????????

**DUYGU DURDU KOÇ, KÜBRA YILMAZ, ARIF ŞENER, TUĞÇE DEMİRDELEN**

*Ulusoy Tekstil San. ve Tic. A.Ş.*

*Adana Alparslan Türkeş Science and Technology University*

**Türkiye**

## SUMMARY

The textile industry has been a pioneer in both employment- and export-related activities, economically speaking, in our country. Although the production of textile products has a complex process, it involves the intense use of water, energy, chemicals, and dyes. However, the heavy use of resources in the textile industry leads to high amounts of waste water and greenhouse gas emissions. By establishing a traceable system in energy consumption areas, examining the energy consumption of textile production lines and machines will ensure efficient energy usage. Therefore, this study was carried out to implement an energy monitoring system for the machines in the spinning and dyeing section, which is one of the sections where energy is most used in the textile industry. With the regular tracking made possible by the energy monitoring system developed for the examination and tracking of energy consumption lines, the foundations for energy efficiency initiatives were established. With the data provided by the system, it was determined that the compressors were not meeting the requirements of the plant, and with the integration of a new compressor determined according to the plant needs and production parameters, a 25% saving was achieved in energy consumption in the pressurized air systems. As a result, the annual electricity consumption was reduced by 283,760 kWh and the carbon emission of 149,540 kgCO<sub>2</sub>e/kg was prevented, reducing the emissions of 40,415 trees. In this way, not only the detection of inefficient equipment but also the needs analysis was carried out through the online tracking system.

## KEYWORDS

Textile, Energy Monitoring System, Energy Efficiency, Sustainability, Climate Neutral



## 1. INTRODUCTION

Due to the rapidly developing and changing world order, industrial activities and population growth in our country have led to an increasing energy demand. In light of this situation, implementing environmentally friendly policies by promoting the diversification and utilization of energy production, consumption, and renewable energy sources has become of great importance. Preventing a projected 20% increase in energy-related CO<sub>2</sub> emissions by the year 2035, as forecasted by the International Energy Agency, depends on the implementation of these policies [1].

Industrial establishments, both at the national and international levels, aim to use energy, which constitutes the basis of their production activities, in the most efficient manner possible. Depletion of energy reserves and the consequent increase in energy costs raise concerns about energy supply, while climate change and environmental factors make energy efficiency efforts even more crucial. Particularly for energy-intensive facilities like the textile industry, a systematic approach and sustainability have become essential. It is at this stage that energy monitoring systems come into play. In industrial enterprises, with the help of monitoring systems, screen designs and visualization methods allow for the rapid detection of faults and timely intervention in production lines [2].

Monitoring systems can be designed based on process or machine-specific needs. Counters added to designated points and established automation allow for simultaneous monitoring of points or resources where performance needs to be measured. However, to enable more detailed and comprehensive monitoring, especially in energy-intensive areas and process lines, the addition of extra counters is crucial for the integration of efficiency studies into the monitoring system at the right points [3]. The data recorded by the system can be analyzed together with total consumption and production values. Moreover, the amount of energy sources such as electricity, natural gas, as well as steam and water used in processes, can also be measured and monitored through the monitoring system. Additionally, by integrating relevant sensors into the system and supporting them with automation, values such as humidity, pressure, and temperature can be recorded [4].

Continuous recording of energy and other consumption sources used in processes enables the control of efficiency studies and achievement of improvement goals. Furthermore, providing data flow to facility managers in cost studies will also offer additional advantages in terms of management.

## 2. ENERGY MANAGEMENT AND MONITORING SYSTEMS

Systems that provide detailed information about energy for commercial building managers, industrial facility managers, financial managers, and facility managers, and offer the opportunity to collect and analyze data, are referred to as energy monitoring systems. Collecting data from various points within the facility where production takes place, recording this data, and automatically obtaining data from the reading points have made energy monitoring systems appealing by highlighting their usefulness. The collected data is generally stored in a database. This allows the analysis of the business's energy consumption and enables online monitoring of energy consumption and financial reports' documentation.

A decline in energy quality will lead to inefficient operation of machinery and equipment in the facility, resulting in decreased lifespans. However, the inefficiency of the energy used cannot be detected without measuring its consumption and quality. Consequently, proper improvement efforts cannot be implemented. Controlling equipment that consumes high levels of energy, recording their data, and being able to compare this data with historical data are of great importance for implementing appropriate improvement efforts [5]. Therefore, it is essential for the facility to be able to digitally perform the necessary measurements, control measurement values, and have a software program established to enable tracking and reporting for users. Based on the generated reports, facility managers can analyze the data and implement energy efficiency programs more effectively [6].

Energy monitoring systems offer significant advantages for the implemented facilities. With this method:

- Collection, monitoring, and analysis of energy data
- Desktop access for managers
- Access to data over time
- Comparison of energy consumption with historical data+-
- Enabling accurate improvement efforts

can be listed among the benefits.



Oral Presentation: Development of Energy Monitoring System for Sustainable Production in the Textile Industry

Energy monitoring system to be implemented within the enterprise will assist machine operators, unit managers, factory directors, and owners in project investments aimed at achieving efficient energy utilization. Simultaneous monitoring of energy data based on consumption provides significant convenience in tracking energy performance, especially in businesses with multiple independent processes. This also allows for prompt identification of any potential malfunctions and enables quick intervention in case of any issues. On the other hand, businesses without an energy monitoring system can only track their consumption through bills. However, this method does not facilitate the identification of energy-intensive areas or the determination of inefficient energy usage zones [7].

### 2.1. Improving Energy Quality

In businesses, factors such as raw materials, labor, and energy consumption directly impact costs. However, among these factors, the cost of energy is significantly influenced not only by the quantity used but also by the quality of its utilization. Energy monitoring systems come into play here by evaluating the quality of the energy used, enabling the identification of the root cause of any issues that arise, and verifying the accuracy of improvement efforts. They help detect the causes of harmonic distortions that can affect all production processes and ensure their separation from sensitive loads. Moreover, they assist in determining sudden voltage drops and surges, as well as the energy consumption during machine equipment's operation at both load and idle times, which aids in eliminating production losses.

### 2.2. Reducing Energy Costs

The integration of energy monitoring systems into facilities enables the optimization of utility bills and electricity contracts, while also assisting in the reduction of energy consumption and costs. Industrial enterprises, through the implementation of these systems, can determine department-specific energy consumption by monitoring consumption values using both meters and developed software. As a result, reporting on unit-based energy consumption values becomes possible, providing opportunities for improvements in units that exceed the expected consumption levels. Furthermore, for facilities located in organized industrial zones and other areas, managing peak demand and optimizing load profiles for electricity consumption to avoid penalties can also be achieved through this system.

### 2.3. Enhancing Sustainability

Energy monitoring systems have made consumption resources and the associated costs more visible for businesses. As a result, businesses have become more competitive by implementing improvement projects and cost-cutting methods. However, strengthening the competitive aspects of businesses should not be limited to the implementation of improvement projects; continuity must be ensured. In this regard, it is essential for the established system to be properly monitored by business authorities, and analyses must be accurately evaluated to carry out the necessary actions. Consequently, through accurate analyses enabled by the energy monitoring system, any initiatives launched within the facility will be built on sustainable foundations. Among these initiatives, consumption and cost evaluations primarily direct businesses towards renewable energy, a major component of sustainable energy. As part of this approach, facilities often install solar power plants within their premises to meet a significant portion of their energy needs, thus reducing both carbon emissions and costs.

## 3. MATERIALS AND METHODS

The textile industry stands out as one of the sectors where different resource usage and associated consumption are intensive due to its diverse production processes. The first step in textile product manufacturing, which involves yarn production, goes through different stages such as winding, dyeing, drying, and transferring, where various machines and energy sources are utilized [8]. This situation indicates that energy costs constitute approximately 8-14% of the total cost generated by the sector. The decrease in energy resources and the subsequent rise in energy costs direct industrial establishments towards efficient energy use to enhance their competitive aspects [9]. Efficient energy utilization primarily depends on identifying how, in which areas, and to what extent energy is used. The analysis of crucial energy consumers within a facility can be accomplished with an accurate monitoring system.

Within the scope of this study, the dyeing facility belonging to Ulusoy Tekstil, which is located in the Adana Organized Industrial Zone and conducts yarn production with four factories, is considered. This facility performs critical dyeing processes, including package, hank, beam, and gradient dyeing. During these processes, primary and secondary energy sources such as water, electricity, natural gas, and steam are utilized. The diversity of energy sources and the production of different-quality yarns, combined with the number of processing steps and machines used in the dyeing process, make it challenging to identify significant energy users. Consequently, an on-site monitoring system has been established based on the emerging needs for efficient energy use.



Oral Presentation: Development of Energy Monitoring System for Sustainable Production in the Textile Industry

In line with the study objectives, to control water consumption, a system was designed to utilize the high-temperature dyed water, which is discharged as waste after the dyeing process and heated to 130°C, to heat the water in the hot water tanks. For the control of this system, a PLC (Programmable Logic Controller) and Scada (Supervisory Control and Data Acquisition) based software were created with a ladder diagram, as shown in Figure 1. Subsequently, control panels were installed, as depicted in Figure 2, to monitor the system. The control panel was prepared and mounted in a designated area outside the facility.

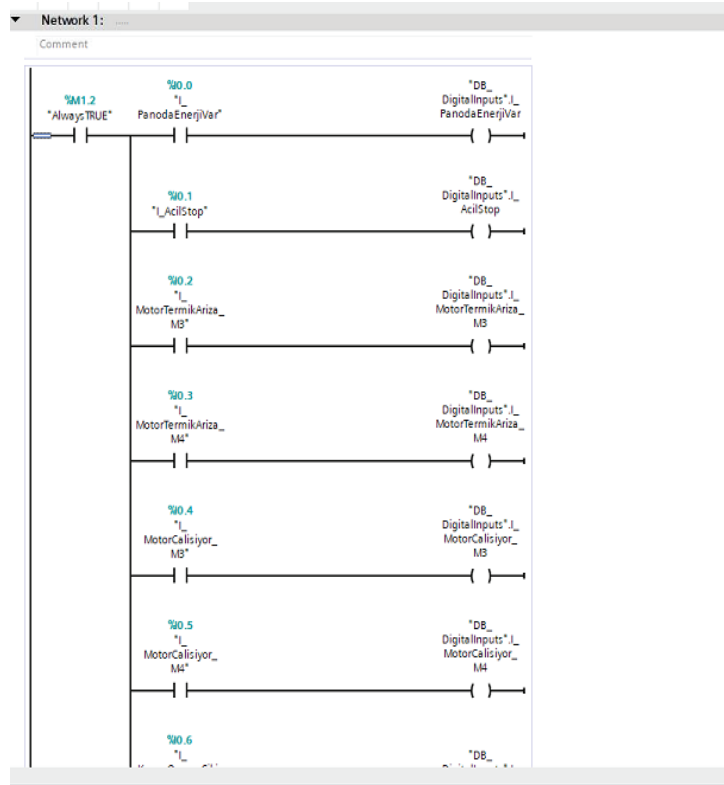


Figure 1. PLC and SCADA system Ladder diagram



Figure 2. PLC and SCADA system control panel

The necessary components for the automation system, including PLC (Programmable Logic Controller), Simplex 540 control device, electrical panel, pneumatic valve, electrical switchgear components (fuses, contactors, thermal relays, terminals, fans, electrical

Oral Presentation: Development of Energy Monitoring System for Sustainable Production in the Textile Industry

cables, etc.), have been prepared. To enable the control of boiler outputs and pools, pumps, valves, and sensors were installed to facilitate monitoring of the system. Through the Scada system, information and controls related to the heat recovery from wastewater systems of dyeing machines, boiler room data, transformer data, generator data, compressor data, and natural gas data were integrated into the system, allowing for monitoring from the screen, as depicted in Figure 3.

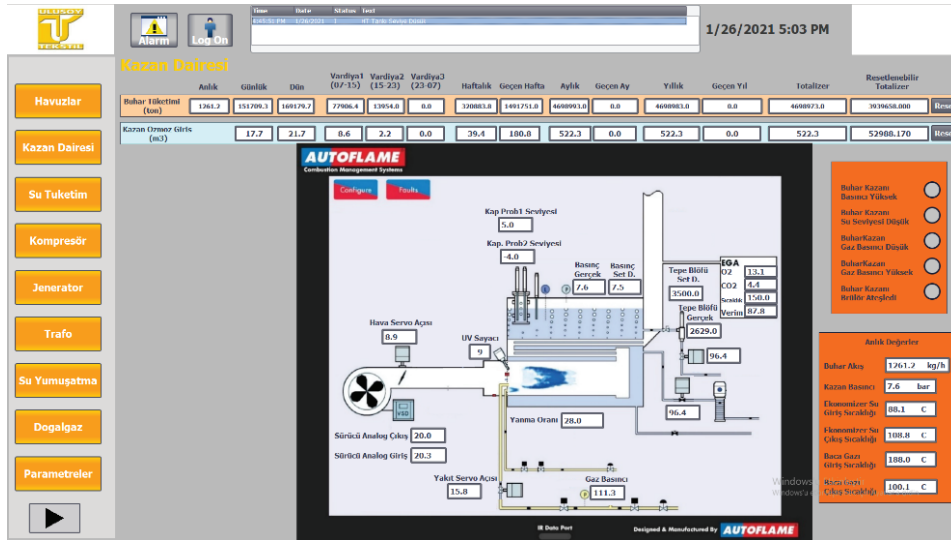


Figure 3(a). Boiler room data display

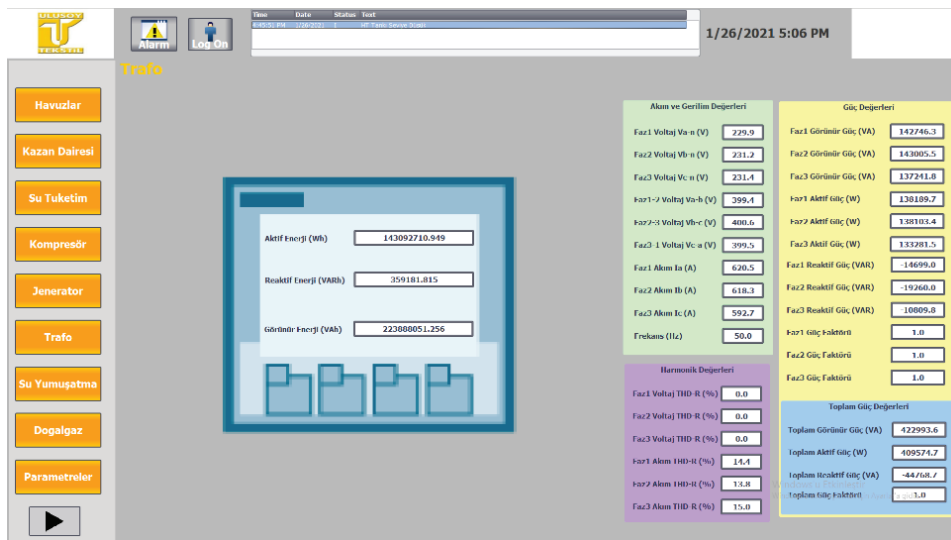


Figure 3(b). Transformer data display



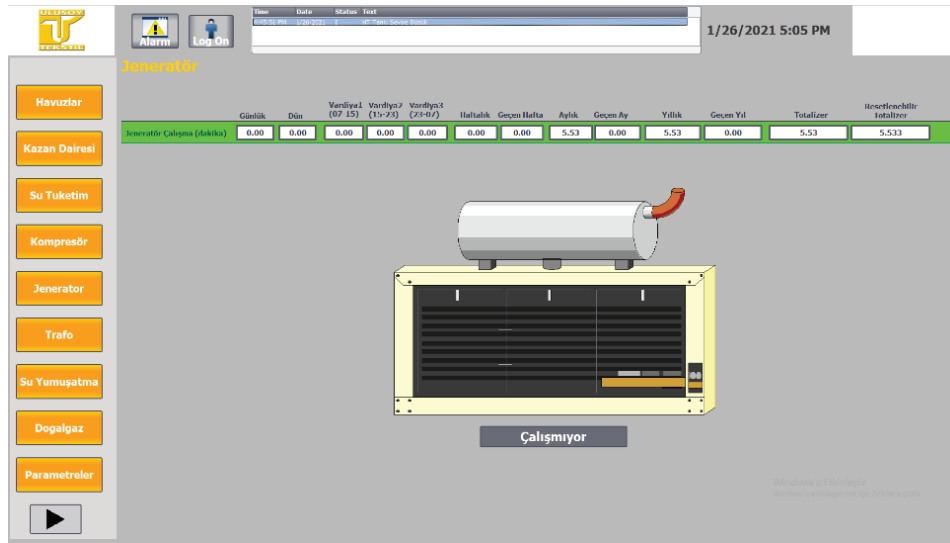


Figure 3(c). Generator data display

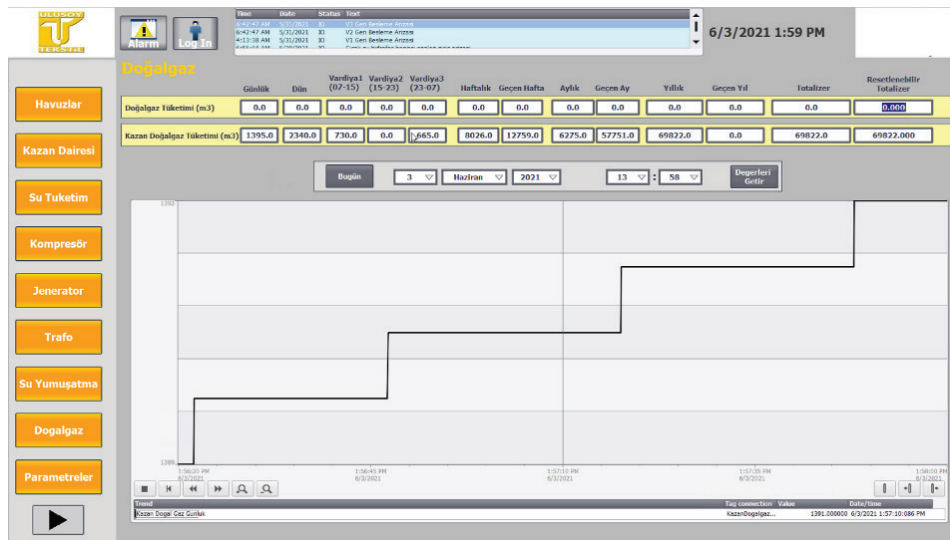


Figure 3(e) Natural gas data display

In the compressor room, the display of air flowmeter outputs related to compressed air usage has also been added to the main computer system. Ensuring the optimal air supply during the combustion process of the boiler is crucial to prevent heat losses and increase combustion efficiency. In industrial boilers, providing sufficient air for a certain amount of fuel is achievable with the help of fans. Dampers, inlet valves, or, with advancing technology, speed control devices are frequently used to control the air. By utilizing combustion control systems to achieve the air-fuel mixture, safe and efficient combustion is ensured.

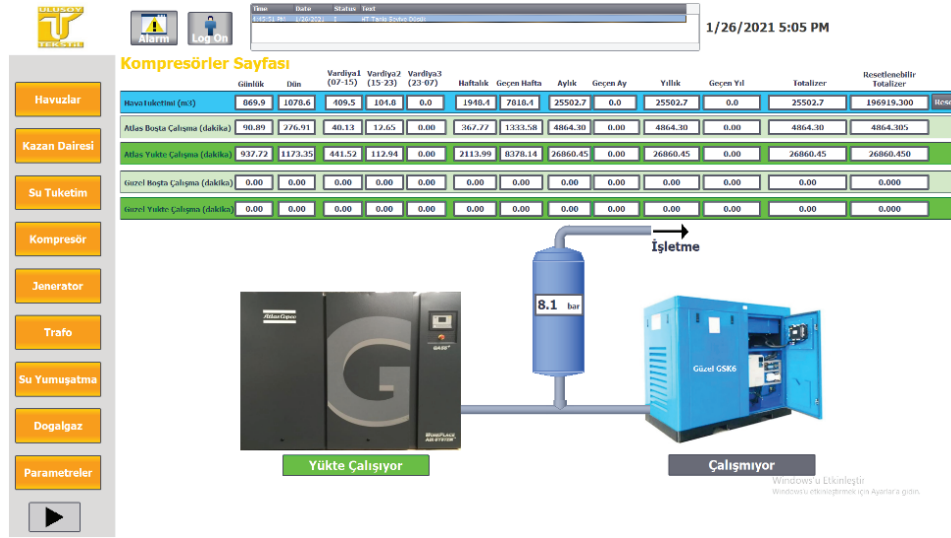


Figure 3(d) Compressor data display

The first data indicating combustion efficiency are the burning temperature and the oxygen (or carbon dioxide) concentration in the flue gas. In practice, combustion conditions are not perfect, and additional air supply is required for fuel combustion. Therefore, examining the density of flue gas and carbon dioxide levels is necessary to find the correct mixture. For this purpose, an AUTOFLAME combustion management system has been added to the boiler room, and all data related to steam/natural gas and flue gas quality has been transferred to the control screen through this system. Additionally, as seen in Figure 5, an energy analyzer has been installed on the electrical transformer, making it possible to monitor current, voltage, harmonics, daily electrical consumption, and values.



Figure 5. Substation Analyzer Data (Current, Voltage, Power Values)

In addition, in the steam boiler, water and steam consumption, as well as natural gas usage, are calculated, and boiler values are monitored simultaneously. Alongside the monitoring system, an archive of consumption and usage, as shown in Figure 6, has been created. Archive information provides the opportunity to observe daily, weekly, monthly, and even yearly consumptions and enables efficiency calculations. Through these efforts, activities such as software development, monitoring, online information control, and sharing over the internet have laid the foundations for the transition to Industry 4.0.

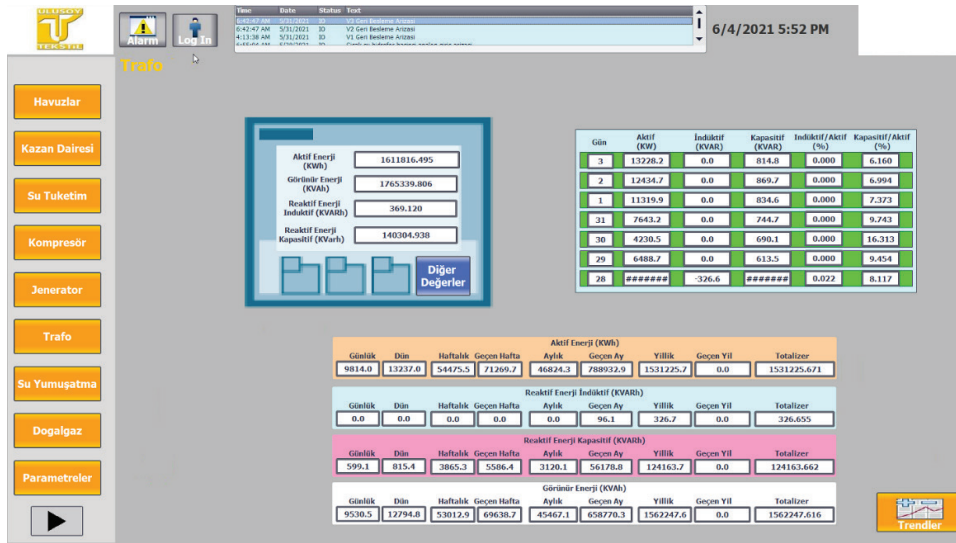


Figure 6. Transformer Room tracking screen (daily, weekly, monthly, yearly)

### 3.1. Energy Efficiency in Compressed Air Systems

Compressed air is obtained by drawing in air from the atmosphere or the environment and compressing it within the compressor. Operating conditions and production methods make compressed air a convenient means of energy transfer. This is due to the advantage that the air taken from the atmosphere can be discharged back into the atmosphere without requiring any return line. Thanks to this advantage, compressed air is widely used at different stages of production in industrial facilities. Particularly in the textile sector, after direct consumption of water, natural gas, and electricity, compressed air systems have the highest consumption value. The high usage rate of compressed air systems indirectly affects electricity consumption as well.

Changes arising from processes in businesses can cause fluctuations in air demand, leading to an increase or decrease in demand. In such cases, integrating a backup compressor or additional air tanks into the system is necessary to balance the increased demand according to the system's needs. For businesses with older system compressors, this situation may lead to higher energy consumption and additional costs beyond normal levels.

### 3.2. Increasing Energy Efficiency in Compressed Air Systems

With the integration of the monitoring system into the facility and the design of the screen based on significant energy users, the monitoring and necessary analysis of energy consumption by responsible operators, maintenance personnel, and facility managers have been made functional within the facility. As a result, the identification of points where energy is heavily used has become easier. From the data obtained through the relevant screens, considering the operational needs of the facility, it was observed that the compressors providing compressed air to the facility do not meet the appropriate values as required by the process. In this regard, to evaluate the existing compressors, namely Atlas Copco GA55(a) and Atlas Copco GA55 Plus(b), measurements were conducted using an analyzer as shown in Figure 7, and the flow rates and power consumption were depicted in Graphic 1 and Graphic 2, respectively.

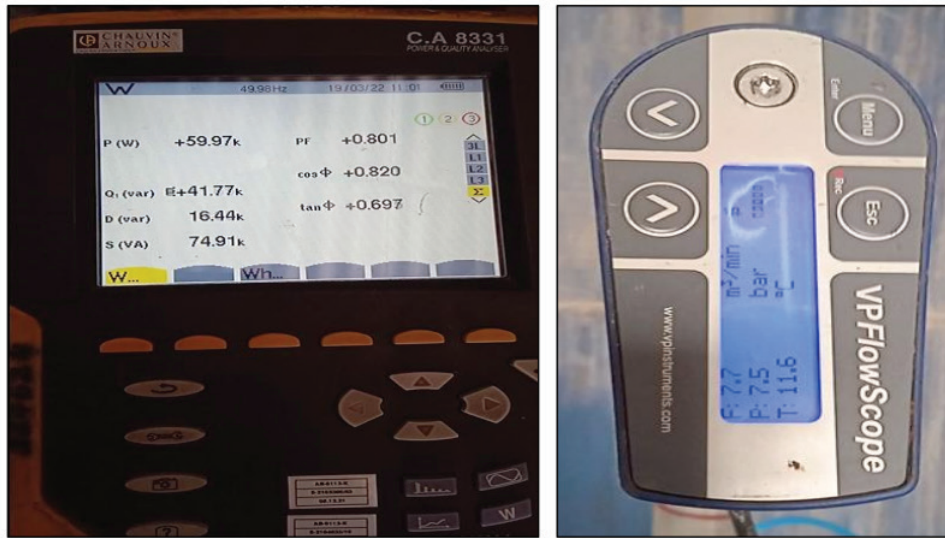
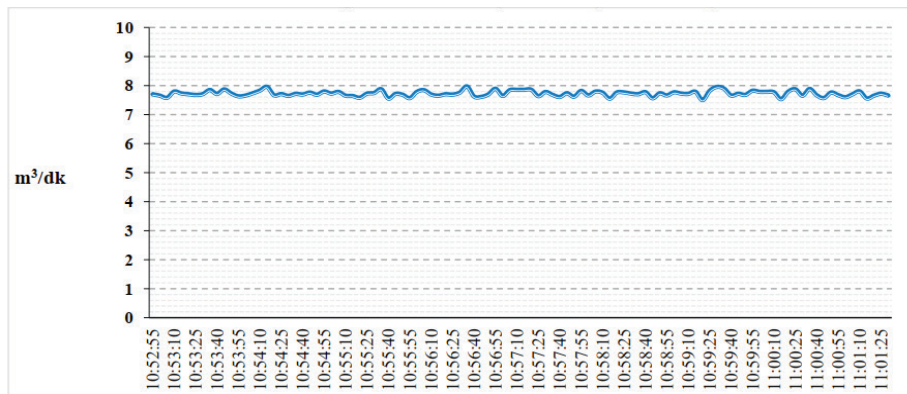
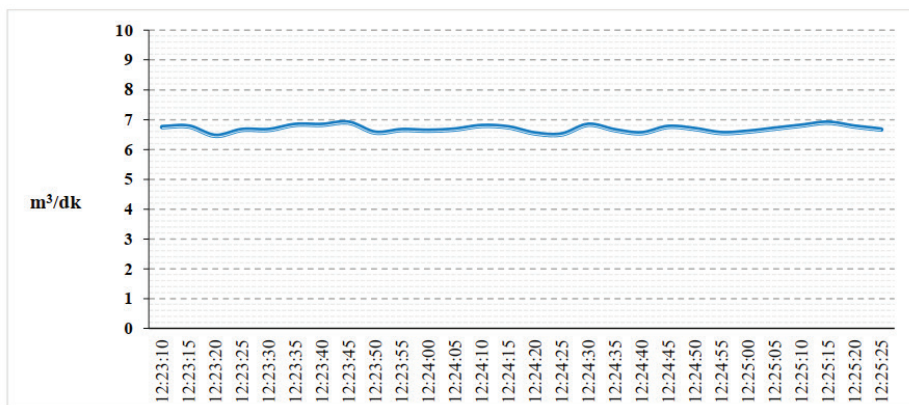


Figure 7. Power and flow measurement of existing compressors

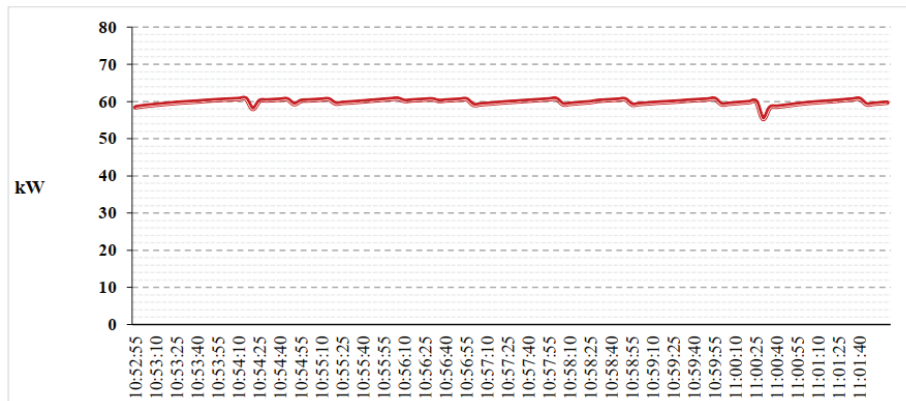


Graphic 1(a). Current compressor flow measurement (m3/min)

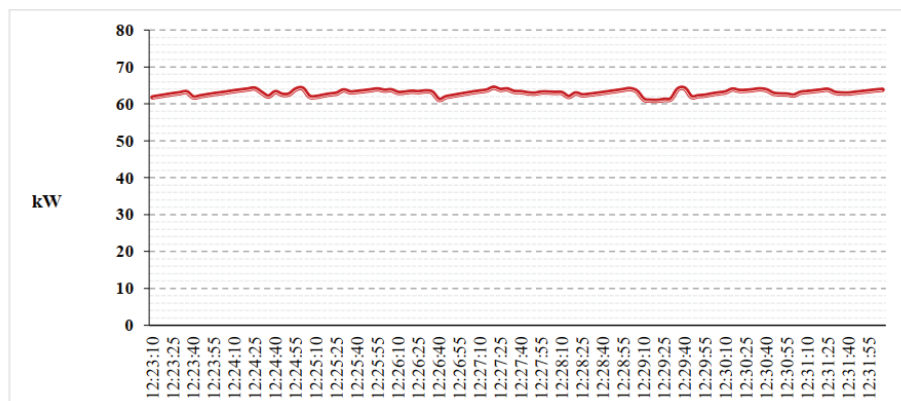


Graphic 1(b). Current compressor flow measurement (m3/min)





Graphic 2(a). Current compressor power consumption (kW)



Graphic 2(b). Current compressor power consumption (kW)

The power measurements conducted with the analyzer and the average values of the flow measurements for these two compressors, which have been redundantly integrated into the system to prevent any potential breakdown, are shown in Table 1.

Table 1. Power (kW) and flow (m3/min) measurement averages of compressors

	Flow (m3/dk)	Pressure (bar)	Power (kW)
Max	7,97	7,54	60,75
Average	7,72	7,49	59.84
Min.	7,5	7,37	55,3

The values obtained from the compressors were analyzed to measure the air demand and the total electrical energy consumed for this air demand. Based on these values, the Specific Energy Consumption (SEC) value, which represents the amount of energy expended to produce a unit of air, was calculated by dividing the average power consumption (kW) by the average compressed air flow rate (m3/min). For the Atlas Copco GA55 compressor, the average power consumption was 58.14 kW, the dryer power consumption was 1.39 kW, the total system power consumption was 59.53 kW, the average flow rate was 7.60 m3/min, and the average pressure was measured at 7.60 bar. The SET value for this compressor was calculated as 7.83 kW/(m3/min). For the Atlas Copco GA55 Plus, the average power consumption was 62.91 kW, the average flow rate was 6.70 m3/min, and the average pressure was measured at 8.1 bar. The SET value for this compressor was calculated as 9.39 kW/(m3/min). These values are summarized in Table 2 below.

**Table 2.** Measurement values for the existing compressors

	Atlas Coppo GA 55	Atlas Coppo GA Plus
Average Power (kW)	59,53	62,91
Average Flow (m3/min)	7,6	6,7
Pressure (bar)	7,6	8,1
SEC (kW/(m3/min))	7,83	9,39
Total Power	<b>122,44</b>	
Total Flow	<b>14,30</b>	
Total SEC Value (kW/(m3/min))	<b>8,56</b>	

Based on the measurement values obtained with the analyzer and flow meter, and the calculated SEC values, criteria have been determined for selecting a compressor suitable for the operational conditions. In this context, it was ensured that the new compressors, like the existing ones, are air-cooled, and additionally, heat recovery will be applied to the new compressors, distinguishing them from the existing ones. Accordingly, values for a compressor that meets the operational requirements have been determined and are presented in Table 3.

**Table 3.** Measurement values for existing compressors

Label Information of New Compressor to be Purchased	
Compressor Power (kW)	55
Compressor Package Power (kW)	67,9
Compressor Flow (m3/min)	11,29
Compressor SEC Value (kW/(m3/min))	6,02
Pressure (bar)	7,0

In addition to the measurement and calculation studies for the existing and new compressors, cost analysis has been conducted, and the results are presented in Table 4.

**Table 4.** Project investment value and savings amount

SAVINGS ACCOUNT		
Current Flow Amonut	14,3	m3/dk
Current Total Compressor Power Consumption	121,05	kW
Current Dryer Power Consumption	1.391	kW
Total Power Consumption	122,44	kW
Flow Requirement After Applicator	14,3	m3/dk
Post Application Power Consumption	88,04	kW
Savings Amount	34,4	kW
Electric Unit Prce	1,52	TL/kWh
Working Process	8.000,00	h/Yil
Annual Energy Saving Amount	275.200,00	kWh/Yil
Annual Financial Savings Amount	418.689,28	TL/Yil
Total Project Cost	1.992.456,00	TL
Payback Period	4,76	Yil





### 4. CONCLUSION

In industrial facilities, the increasing costs have made it imperative to undertake improvement efforts towards efficient energy utilization. To identify energy-intensive areas and inefficient energy utilization, accurate measurements must be conducted regularly and recorded for analysis. This necessitates the implementation of a monitoring system supported by proper data flow through well-designed automations within the facility.

Within the scope of the project at the yarn dyeing plant, the waste heat from the process has been utilized to further heat clean water to reach the optimal temperature for the dyeing process. In addition to automation hardware, various data related to the factory's production processes, including boiler room data, transformer data, generator data, compressor data, natural gas consumption data, water consumption data, and water softening data, have been digitized and integrated into the system for remote access through a user-friendly interface. The project continues to be developed for ongoing improvement and enhanced traceability.

Effective utilization of the monitoring system's provided data is crucial to derive its benefits and ensure its further development. The compressor screen, which is one of the data interfaces, has been utilized to evaluate compressed air system-related data, such as air flow rates, on-load and off-load operating hours, and power consumption measured with the aid of an analyzer. The analysis of numerical data, combined with the consideration of operational conditions, has highlighted the need for replacing existing compressors with more efficient ones. Based on the operational requirements and needs, new compressors have been selected, which provide the required flow rate of 14.30 m<sup>3</sup>/min with an energy consumption of 88.04 kW. This has resulted in an annual saving of 275,000 kWh and a reduction of 144,925 kgCO<sub>2</sub>/kWh of carbon emissions, which is equivalent to eliminating the carbon emission burden of 39,168 trees.

### BIBLIOGRAPHY

- [1] Türkay M., Yılmaz Ş., Şan B. Ş., Aras B., Denk A., Kılavuz M. T., Kublay A. G., Ören Y.C., Yardımcı A., Türkiye'nin Enerji Verimliliği Haritası ve Hedefler, Koç Üniversitesi Tüpraş Enerji Merkezi, 1-35, 2012.
- [2] Kaya, M., 2012. Sanayide Enerji Verimliliği Potansiyeli ve Basınçlı Hava Sistemlerinde Verimlilik. Yüksek Lisans Tezi, Yıldız Teknik Üniversitesi, İstanbul.
- [3] Kıyılmaz B., Sanayide Enerji Yönetimi Esasları ve Enerji Verimliliğinin Araştırılması, Yüksek Lisans Tezi, Muğla Sıtkı Koçman Üniversitesi, Fen Bilimleri Enstitüsü, Muğla, 2019, 558714.
- [4] Uzun A., Değirmen M., Energy Efficiency and Energy Management in Industrial, International Journal of Economic Studies, 2018, 4(2).
- [5] Şahin A., Elektrik Dağıtım Tesislerinde Enerji İzleme Sistemleri, Yüksek Lisans Tezi, İstanbul Teknik Üniversitesi, Fen Bilimleri Enstitüsü, İstanbul, 2010, 384832.
- [6] Motegi N., Piette M., Kinney S., Dewey J., Case Studies of Energy Information Systems and Related Technology: Operational Practices, Costs, and Benefits, International Conference for Enhanced Building Operations, USA, 13-15 October 2003.
- [7] Hepbaşlı A., Enerji Verimliliği ve Yönetimi: Yaklaşımlar ve Uygulamalar, 1.Baskı, Esen Ofset Matbaacılık, İstanbul, 174, 2010.
- [8] Aypak N., Gülbül A., Etemoğlu B., Çakal C., Aydemir E., Gümüş Z., Basınçlı Hava Sistemlerinde Enerji Verimliliği El Kitabı, 1.Baskı, BUSİAD Yayınları, Bursa, 2016.
- [9] Uzun A., Değirmen, M., 2018. Endüstriyel işletmelerde enerji verimliliği ve enerji yönetimi. Uluslararası Ekonomik Araştırmalar Dergisi, 4(2):83-97.



# The First Lessons from Rocket Attacks on the Ukrainian Power System Relatively Power Unit's Automation and Control Systems

[olegagamalov@gmail.com](mailto:olegagamalov@gmail.com)

**OLEG AGAMALOV**

*Tashlyk Pumped Storage Power Plant*

*Ukraine*

## SUMMARY

As known, since February 2022 Ukraine subjected to brutal aggression by Russia and especially its influence on the Ukrainian power system, which undergoes numerous rocket attacks. Analysis of the transients of power units in these conditions allows expanding and redefining requirements to automation and control systems, and namely synchronization and governor, which should ensure the work at large deviations and oscillations in frequency and voltage, and also to the importance of mode of the synchronous condenser. The conclusions of this work may be used for other power systems, which undergo significant disturbances due to military aggression or significant weather disasters.

## KEYWORDS

Frequency transient – Voltage transient – Governor – Automatic voltage regulator – Power system stabilizer – Synchronization system – Synchronous condenser



Oral Presentation: The First Lessons from Rocket Attacks on the Ukrainian Power System Relatively Power Unit's Automation and Control Systems

### 1. INTRODUCTION

Since the beginning of the full-scale invasion, Russia has already launched more 5000 missile, 3500 air and 1100 drone strikes on Ukraine's critical infrastructure, power generation and transmission, and housing and communal services facilities. For many months in a row, Russia purposefully destroyed the Ukrainian energy industry. As a result of the Russian strikes, not a single thermal power plant or hydro power plant was left in Ukraine that was not damaged. In general, during the war, Ukraine lost more than 90% of wind generation, three-quarters of thermal generation, almost half of nuclear generation (at the expense of Zaporizhzhia nuclear power plant, controlled by the Russians), a third of solar generation and block thermal power plants. The shelling on November 23, 2022 year led to a temporary blackout of all nuclear power plants and most thermal and hydroelectric power plants of Ukraine. The country experienced the first blackout. There were interruptions in electricity, water, heating and mobile communications in almost all regions. It seemed that the blackouts would last for a long time. However, already in the middle of February, the constant power supply began to be restored, and the fan outages stopped. In the first days of spring, Minister of Energy Herman Galushchenko even announced about the surplus of power in the Ukrainian power system: "As of today, we have a surplus in the power system. This gives us the feeling that we have really won this energy battle," the government official said. He also asserts that if the Russians do not strike again at the Ukrainian power system, there will be no more emergency shutdowns: "It has already been the third week that electricity production fully covers consumption. We have certain reserves and, in principle, we have plans to continue to support our power system in such a way that people do not experience supply restrictions," the minister said.

So how did Ukrainian energy companies manage to restore the balance in the power system and the supply of electricity to consumers so quickly after the Russian devastation? What is the secret of such a quick recovery? In "Ukrenergo" - the transmission operator of the Ukrainian power system - they say that it happened according to a "temporary scheme". Volodymyr Kudrytskyi, the chairman of the board of Ukrenergo, explained that the repair work on all damaged energy facilities does not stop, but full restoration is still a long way off: "In order to restore the situation that existed before the invasion, it takes many months of hard painstaking work. And quite large capital investments to buy new equipment, install it, and restore the completely reliable power supply schemes that Ukraine had until a year ago." Currently, the Ukrainian energy system is operating in an emergency mode with a minimum safety margin for both power grids and generation. The temporary and uncertain improvement was made possible by the enormous efforts of the military, who tried to prevent critical destruction, energy workers, who began repairs immediately after the shelling, and international partners, who quickly provided funds and equipment for these repairs. Ukrainian partners supplied not only generators, but also transformers, so that both distribution operators and transmission operator (Ukrenergo) had something to replace the damaged ones. All observers emphasize another point that worked for the quick restoration of the power system. Also, during the year of the war, consumption decreased by almost a third. The import of electricity from Europe, which became possible thanks to the fact that Ukrainian power system joined to the European power grid in the first month of the war, helped to maintain the balance in the Ukrainian energy system.

But except for early noted global factors, some technical moments and solutions were defined that allow for operative recovery of the power plants and transmission grid after rocket strikes. Further, we will consider these technical moments and solutions relative power unit's automation and control systems. Also, it may be noted that these solutions can be applied for the safe operation of power systems in significant weather disasters.

### 2. EXAMPLES OF TRANSIENTS AS A RESULT OF ROCKET STRIKES

Below, we consider and analyze two transients that occurred and were registered at the Tashlyk pumped storage power plant (TPSPP) as a result of missile strikes on the Ukraine's power system.

#### 2.1. Missile strike on December 16, 2022 year.

The transient was registered at the Tashlyk pumped storage power plant after a missile attack on the power system of Ukraine on December 16, 2022 shown on Figure 1:

Oral Presentation: The First Lessons from Rocket Attacks on the Ukrainian Power System Relatively Power Unit's Automation and Control Systems

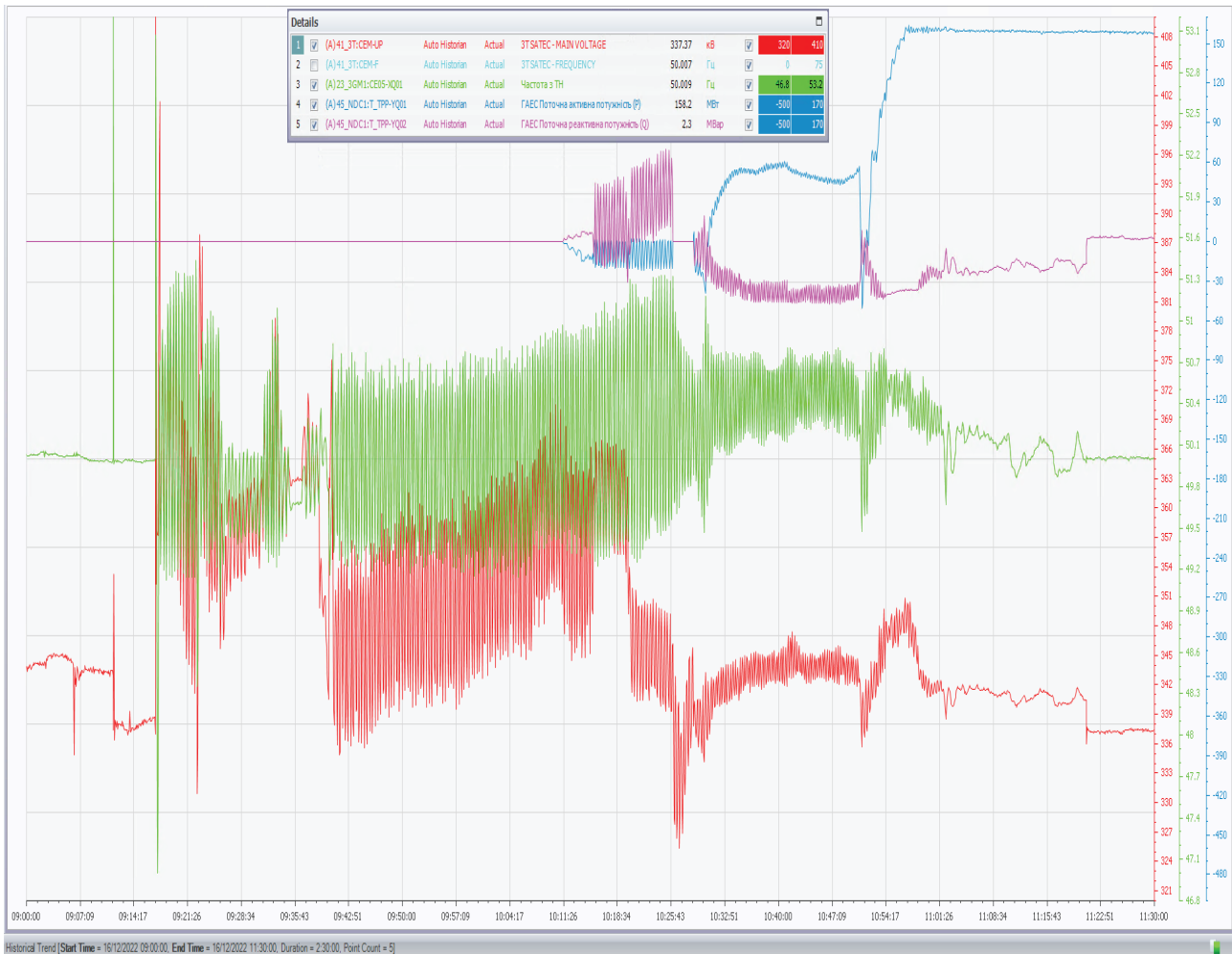


**Figure 1.** The transient was registered at the Tashlyk pumped storage power plant (TPSPP) after a missile attack on the power system of Ukraine on December 16, 2022.

On Fig. 1 have shown: red color – voltage of bus bar 330 kV, green color – frequency of system, blue color – active power of hydro unit 2GM of TPSPP, magenta color - reactive power of hydro unit 1GM of TPSPP.

After a missile attack due to a power imbalance in the power system had observed long oscillations of frequency and voltage for about an hour and a half. Oscillations of frequency were in range [49.4÷51.3] Hz. Oscillations of voltage of bus bar 330 kV had increasing in range [346÷359] kV (mean value) with double amplitude of oscillations  $\approx 17$  kV. For decreasing of these oscillations hydro unit 1GM of TPSPP was turned on in the mode of the synchronous condenser with the pump direction of rotation, and with a mean value of reactive power of about -43 MVar with double amplitude of oscillations  $\approx 20$  MVar due to the voltage oscillations. At the same time, it should be noted that for the possibility of hydro unit synchronization to the grid, a manual device of precise synchronization was used, which has wider permissible limits for the deviation of slip, frequency and voltage. After this, the increase of voltage of bus bar 330 kV was stopped, and the double amplitude of oscillations was decreased to  $\approx 10$  kV. For further stabilization of system's mode the hydro unit 2GM of TPSPP was turned on as a generator. But due to frequency oscillations governor of this unit could not work in automatic frequency/power mode, and was switched to the manual operation mode for the opening of the wicket gate. It allowed further turn on the hydro unit 2GM of TPSPP as a generator with active power 160 MW, decreased the double amplitude of frequency oscillations with 1.9 Hz to 0 Hz, and set the frequency to about 50 Hz.

## 2.2. Missile strike on January 26, 2023 year.

The transient was registered at the TPSPP after a missile attack on the power system of Ukraine on January 26, 2023 shown on Fig. 2:

Oral Presentation: The First Lessons from Rocket Attacks on the Ukrainian Power System Relatively Power Unit's Automation and Control Systems



**Figure 2.** The transient was registered at the Tashlyk pumped storage power plant (TPSPP) after a missile attack on the power system of Ukraine on January 26, 2023.

On Fig. 2 have shown: cyan color – voltage of bus bar 330 kV, red color – frequency of system, green color – active power consumption of hydro unit 1GM of TPSPP in the synchronous condenser mode, magenta color - reactive power of hydro unit 1GM of TPSPP, blue color – active power consumption of hydro unit 3GM of TPSPP in the synchronous condenser mode, orange color - reactive power of hydro unit 3GM of TPSPP.

After a missile attack due to a reactive power imbalance in the power system had observed significant increase in voltage of bus bar 330 kV. To prevent this increase to dangerous values hydro units 1GM and 3GM of TPSPP were turned on in the mode of the synchronous condenser with the pump direction of rotation, and with a mean value of reactive power of about -44 MVar for 1GM and -74 MVar for 3GM. It allowed decreasing the voltage of bus bar 330 kV to acceptable values (349 kV). After this, the increase of voltage of bus bar 330 kV was stopped, and the safe operational mode of TPSPP and of the adjacent grid was provided.

### 3. ANALYSIS OF WORK OF POWER UNIT'S AUTOMATION AND CONTROL SYSTEMS IN OBSERVED TRANSIENTS

Based on early consideration and other observed transients of TPSPP hydro units and of the adjacent grid maybe some propositions and conclusions relative to requirements for power unit's automation and control systems.

#### 3.1. Power unit's synchronization system.

As know, synchronous generators or motors must be connected to the power system only when the slip (speed difference), voltage difference, and angle difference are within acceptable parameters. For example, IEEE Standards C50.12 and C50.13 provide specifications for the construction of cylindrical-rotor and salient-pole synchronous generators, and specify, that "Generators shall be designed to be fit for service without inspection or repair after synchronizing that is within the limits listed..." [1, 2]. The limits for both types of generators are:



**Oral Presentation:** The First Lessons from Rocket Attacks on the Ukrainian Power System Relatively Power Unit's Automation and Control Systems

- Angle  $\pm 10$  degrees.
- Voltage 0 to +5 percent.
- Slip  $\pm 0.067$  Hz.

However, in significant transients, these parameters may vary in a wider range (see Fig. 1), but for stabilization of the power system, a unit must be promptly connected to the grid. So, it is necessary to have in the synchronization system of a power unit a set of settings with wider ranges in deviations of angle, voltage, and slip. Especially it is important if in a power system appearance oscillations of frequency and voltage, and promptly connecting the unit to the grid may mitigate these oscillations.

### 3.2. Power unit's governor.

After synchronization and turning on a power unit in the grid, it is necessary to increase its active power. But if in the grid exist frequency oscillations power unit's governor cannot work in automatic mode (power/frequency drop characteristic) for increasing and achieving a value of active power in accordance with the given setting. So, it needs promptly increasing power in manual mode subject to all the necessary technological limitations, opening the wicket gates of hydro units or control valves for turbo units. This should be provided for when designing the governors of hydro- and steam turbines.

### 3.3. Using the synchronous condenser mode.

It is important to ensure the possibility of operation of power units in the mode of the synchronous condenser (SC), which in emergency modes of power system, in the event of damage to substations and the grid, has the technical capabilities to ensure or recovery power system stability due to:

- maintenance of system inertia and, accordingly, the value of RoCoF (rate of change of frequency) in the event of imbalances of active power;
- maintaining the level of short-circuit currents (SCC), which is important for ensuring the selective operation of protections and emergency automation;
- maintenance of the voltage levels of control points of the grid in transients, which allows for a more predictable assessment of power flows along the main transmission ties, this is especially important in transitional operational modes;
- maintain synchronizing and damping moments at the main transmission ties, connected to the places of installation of SC;
- long-term and continuous control of reactive power levels at the main transmission ties, connected to the places of installation of SC;
- high overload properties and quick response to overload, which can be used (and was used on the TPSPP during the system accident on November 23, 2022) when energizing long overhead lines 330, and 750 kV, and charging them with reactive power when switching on and checking their technical condition (absence of short circuit after the missile attack);
- the ability to counteract grid disturbances;
- low consumption of active power (TPSPP units are up to 10 MW).

Based on the experience of working the Ukrainian power system during massive missile attacks, it is expedient to consider the preventive start-up of hydro units connected to the controlled points of the grid in SC mode (with turbine or pump direction of rotation), which should increase stability in the event of damage to the network.

## 4. CONCLUSION

In this work, we consider some requirements for the automation and control systems of the power unit, based on the experience of the Ukrainian power system after massive missile attacks. The general approach that unites all these requirements is the necessary increase in the robustness of the automation and control systems of the power units to changing parameters of the power system during oscillations to prevent blackouts or recovery after blackouts. Some of these requirements are:

- in synchronization system of power units should be provided for the set of setting with wider ranges in deviations of angle, voltage, and slip. Especially it is important if in a power system appearance oscillations of frequency and voltage, and promptly connecting the unit to the grid may mitigate these oscillations.





**Oral Presentation:** The First Lessons from Rocket Attacks on the Ukrainian Power System Relatively Power Unit's Automation and Control Systems

- in governor of power units should be provided for manual mode subject to all the necessary technological limitations, opening the wicket gates of hydro units or control valves for turbo units for promptly increasing (changing) power, and mitigation of electromechanical oscillations.
- power units should be ready for work in synchronous condenser mode which in emergency modes of power system, in the event of damage to substations and the grid, has the technical capabilities to ensure or recover power system stability by maintaining the system inertia (RoCoF), the level of short-circuit currents (SCC), long-term and continuous control of reactive power levels, high overload properties and quick response to overload, the ability to counteract grid disturbances and low consumption of active power.

Also, the conclusions of this work may be used for power systems, which undergo significant disturbances due to military aggression or significant weather disasters.

### BIBLIOGRAPHY

- [1] IEEE Standard for Salient-Pole 50 Hz and 60 Hz Synchronous Generators and Generator/Motors for Hydraulic Turbine Applications Rated 5 MVA and Above, IEEE Standard C50.12-2005.
- [2] IEEE Standard for Cylindrical-Rotor 50 Hz and 60 Hz Synchronous Generators Rated 10 MVA and Above, IEEE Standard C50.13-2005.
- [3] CIGRE Joint Working Group A1/C4.66 "Guide on the Assessment, Specification and Design of Synchronous Condenser for Power System with Predominance of Low or Zero Inertia Generators", Technical Brochure 885 (November, 2022), p. 120.



# Hypergrid: Coordination and Control of Different HVDC Links

[antonio.zanghi@terna.it](mailto:antonio.zanghi@terna.it)

**ENRICO MARIA CARLINI, TEMISTOCLE BAFFA SCIROCCO, ANDREA URBANELLI,  
DOMENICO IORIO, ANDREA PIGNATA, ANTONIO ZANGHI\***

*Terna Rete Elettrica Nazionale – Via Egidio Galbani 70,  
Rome Grid planning and Permitting Department*

**GABRIELE CALLEGARI, FEDERICO DEL PEDRO, ENRICO PERENZONI**

*CESI S.p.A.*

Italy

## SUMMARY

In the context of the ongoing energy transition, significant infrastructure investments are required in the Italian electrical grid to allow the progressive integration of the massive new RES (Renewable Energy Sources) power plant installations to meet the European and National targets. The energy transition, together with the decommissioning of synchronous generation units, will bring the electrical systems to face many issues related to inertia reduction, lowering of short-circuit levels, reduction of voltage regulation and reactive power system resources. In the Italian framework, a new DC (Direct Current) layer based on different HVDC (High Voltage Direct Current) corridors, so called Hypergrid project, has been planned to guarantee higher system stability and service quality. Hypergrid is composed by new HVDC links which have been studied to maximize the transmission capacity among the Italian bidding zones enabling power flows transport along the south-north direction. Due to geographical and market conditions, south of Italy is the ideal place to maximize RES production thanks to favorable wind and solar irradiation conditions, while consumption is generally located in the central-northern regions. The coordination among new and existing or already planned HVDC links, as in the case of SAPEI and Tyrrhenian Link, will be a fundamental aspect to minimize disturbances and power exchange limitations in case of grid contingencies. The converter stations will constitute the nodes of the grid where AC (Alternate Current) and DC grid will communicate to guarantee the best response in terms of voltage profile control and grid frequency recovery.

The new DC layer (Hypergrid) will be based on VSC technology, and the use of High Voltage DC Circuit Breakers (DCCBs) will enable multiterminal operation with greater flexibility, active-reactive power decoupling and reduced power limitation on different branches in case of failure.

The analyses were focused on the evaluation of coordinated operation to overcome the sudden loss of active or reactive power flow due to grid transients caused by unexpected contingencies or critical grid operational conditions.

Grid conditions with high power flows from South to North of Italy have been simulated and all the main grid variables have been monitored to evaluate the beneficial effects of the new DC layer. The scope of the article is to show the beneficial effects of mutual aid of the new HVDC multiterminal link from Sicily to Lazio and the Tyrrhenian Link, enabling higher exploitation of resources thanks to higher dumping voltage oscillation and reducing power imbalances occurrence in case of grid contingencies.

In case of absence of the Hypergrid project the analysis pointed out the need of RES generation curtailments to guarantee adequacy and security of supply standards. Moreover, without the development of coordination between different HVDC links, grid conditions in case of N-1 would be more severe and it will be more likely to rely on RES curtailments to ensure N-1 security standards and dynamic stability.

## KEYWORDS

Dynamic stability – HVDC – DCCB – RES Curtailment – Inertia

## 1. INTRODUCTION

The most recent national and European target about new RES power plants as “Fit for 55” and “repower EU” require deep transformations in the Italian power generation and electrical system. In a generation mix characterized by high penetration of not-programmable sources (Photovoltaic and Wind Power Plants) it is fundamental to be able to transfer energy from production sites to consumption areas, considering the possibility of sudden generation loss due to weather changes or contingencies of the grid elements. The Italian grid requires additional infrastructural development to adapt the transmission capacity to the generation increase and its location. In addition to projects already foreseen in previous National Electricity Transmission Grid Development Plans [1] (NDPs), new grid reinforcements are required to integrate new RES generation according to Green New Deal EU.

The 2023 National Development Plan (NDP) [2] introduces “Hypergrid” (HG), which will use HVDC adopting AC-DC converters with Voltage Source Converter (VSC) technology. The Hypergrid network has been designed according to a holistic approach, considering the interoperability of the existing AC network and the projects already planned in previous (NDPs) and under construction (including HVDC point-to-point connections). The main drivers on which the Hypergrid project planning is based are:

1. Synergies with existing or underused assets, exploiting the modernization of existing 380 kV and 220 kV AC OHL upgrading up to DC;
2. Potential reuse of areas or sites in disuse functional to the installation of the conversion stations necessary for new backbones development;
3. Increased network security and System Strength by reinforcing interconnections between market areas thanks to DC technology, ensuring greater dynamic stability and reliability in case of grid contingencies [3] [4];
4. Modularity of the several links, intercepting as much as possible in advance the development of new generation sources, through a modular approach the grid becomes able to integrate better the new installed capacity increasing NTC among the different market zones.

## 2. HYPERGRID BACKBONES DESCRIPTION

Hypergrid project is characterized by five main backbones as illustrated in Fig. 1 and described below. This paper gives a focus on the **Ionian-Tyrrhenian project** on which are carried out further insights regarding dynamic grid stability in order to investigate the beneficial contribution introduced by the new HVDC project cooperating with already planned ones as Tyrrhenian link East [1].



Figure 1. Overview of the entire Hypergrid project and associated NTC (Net Transfer Capacity)

### 2.1. HVDC Milan – Montalto

The new HVDC link connects the Central South bidding zone to the North one, directly from Lazio to Lombardy as illustrated in Fig. 1. It will be composed by an undersea cable and an overhead line (OHL), by upgrading the existing 380 kV AC OHL up to 500 kV DC. Two new converter stations of 2 GVA each will be realized in VSC technology using two half-bridge converters of 1000 MVA

each one adopting DCCB in order to manage efficiently the system faults. The new backbone has a total capacity of 2000 MW, and it enables the increase of NTC by +800 MW from Central South and Central North bidding zone and +2000 MW from Central South to the Northern bidding zones.

## 2.2. Central Link

The Central Link, from Umbria to Tuscany, will allow to increase the transfer capacity on the existing 220 kV AC OHL thanks to the use of innovative tower with low electromagnetic impact called "5 F". They avoid overcoming magnetic field limitations by splitting into five bundles the three phases of the conductors [2]. The project, visible in Fig. 1, will contribute to increase by 600 MW the power exchanged between the central-southern and central-northern bidding zones.

## 2.3. Sardinian Backbone: HVDC Fiumesanto – Montalto (Sapei 2) and Sardinian Link

The Sardinian backbone will allow a deep increase of renewable energy integration, facilitating +1000 MW energy flows from Sardinia to the central-southern bidding zone, reducing the overgeneration occurrence and stabilizing the electrical grid. In addition, the presence of a new converter station in the North of Sardinia will further improve the island grid stability dealing with the ongoing reduction of conventional generation, as well as VSC technology contribute to higher quality of service by voltage regulation in the AC node of connection. The project is illustrated in Fig. 1 and it is composed by an undersea 500 kV HVDC cable from Sardinia to Italy and by AC reinforcements on the internal (Sardinian) 220 kV existing lines using the "5 F" tower.

## 2.4 Adriatic Backbone: HVDC Foggia-Villanova-Fano-Forli

With the aim of offering an additional route compared to the Montalto – Milan HVDC and the Central Link and transporting energy flows from the southern to the northern regions in both directions, the Adriatic Backbone will reduce the congestion occurrence in regions characterized by high renewable generation such as Puglia and Basilicata. As shown in Fig. 1, the entire HVDC link starts from the northern part of Puglia to settle in Emilia-Romagna, crossing Abruzzo and Marche. In particular, the planned project involves the development in 2 phases: a first phase consisting in the construction of an HVDC overhead line from Foggia to Villanova and the doubling of the undersea HVDC cable link (already planned HVDC Central-South/Central-North project) between Villanova and Fano, a second phase involving the construction of an HVDC OHL from Fano to Forli. This project involves the synergy with others already planned projects in previous Development Plans exploiting the multi-terminal configuration by using DCCB in the future planned VSC converter stations in Fano and Villanova. The project enables an NTC increase by 600 MW on the South-Central South section, by 1000 MW on the Central-South/Central-North section and by 2000 MW on the North/Northern-Centre section.

## 2.5. Ionian – Tyrrhenian Backbone: HVDC Priolo – Rossano – Montecorvino – Latina

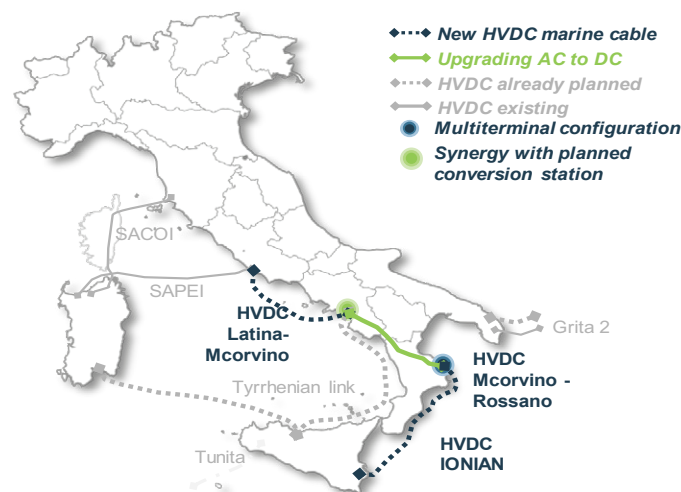


Figure 2. Ionian -Tyrrhenian backbone HVDC project

The Ionian-Tyrrhenian corridor will go from Sicily (Ionian coast) to Lazio as approximately described in Fig. 2 and will have at least two more converter stations in the middle to guarantee operation flexibility, to take advantage of the existing AC and DC infrastructure and maximise economic sustainability. In details, the entire project is illustrated below and divided as follows:

- 500 kV marine HVDC, with 2000 MW VSC technology, in synergy with already planned works such as the Tyrrhenian Link, which will connect the nodes of Montecorvino (Salerno) and Latina, where a new conversion station (2x1000 MVA) will be built.
- Upgrading to 500 kV DC of the existing 380 kV Rossano – Laino power line and the 220 kV Laino – Tusciiano line to create a single HVDC link between Rossano (Cosenza) and Montecorvino. The connection also includes a new conversion station in Rossano (2x500 MVA).
- 500 kV marine HVDC (Ionian HVDC) will be built between the nodes of Priolo (Syracuse) and Rossano. In the first node will be located the conversion station (2x500 MVA).



**Figure 4.** HVDC marine link Montecorvino-Latina (a)



**Figure 5.** HVDC link Rossano-Montecorvino (b)



**Figure 3.** HVDC marine link Priolo-Rossano (c)

The entire Ionian-Tyrrhenian backbone, goes from Sicily to Lazio, passing through Calabria and Campania, it will be characterized by a synergistic coordination with already planned HVDC works such as the Tyrrhenian Link East, at the Montecorvino node (Campania), and existing as the SAPEI, at the Latina node (Lazio). In addition, this project will provide a further connection of Sicily with the Peninsula, in addition to the already planned AC 380 kV Bolano – Annunziata marine cable [1]. With this approach, Sicily's exchange capacity to the continent increases three times, going from the current 1.5 GW to 5 GW.

The planned project enables the exchange capacity increase by 2000 MW in three bidding zones, from Sicily to Central and Southern market areas.

### 3. HYPERGRID FEATURES

#### 3.1. Multi-terminal HVDC grid and DC Circuit Breaker

The past HVDC project has been developed by Terna through a point-to-point configuration, considering two separate converter station connected by an HVDC link. In the last years, multiterminal (MTDC) configuration are being developed at international level



Oral Presentation: Hypergrid: Coordination and Control of Different HVDC Links

such as Zhangbei project in China [5] and Shetland project in Scotland [6]. Multiterminal system involves three or more converter stations connected each other in series or in parallel or in hybrid mode, giving rise to a HVDC grid instead of a point-to-point HVDC infrastructure.

Hypergrid has been developed considering a multiterminal configuration among all the different HVDC corridors, this setting is allowed by means of DCCBs. Their use guarantees high operational flexibility [7] and mutual cooperation among different HVDC links maintaining the overall project economic sustainability.

The development of the so called HVDC Multiterminal grid comes through DCCBs development to allow an optimal integration between existing and new point-to-point HVDC link together with the AC grid. The DCCB technological and commercial development is fundamental to reduce the number of converter stations leading to large investment costs savings and providing, at same time, optimal layout and grid configuration to address safely grid element faults (e.g. converter stations, HVDC OHL and cables, etc.). Multiterminal configuration requires fast, accurate and reliable DCCB and DC busbar also to enable the VSC converter stations to be used as STATCOM during short circuit occurrence, supporting grid voltage stability [8] [9].

In a multiterminal grid each DC terminal could serve multiple purposes:

- providing ancillary services,
- independent full active and reactive power control for voltage/frequency regulation,
- wide-area power oscillations damping,
- improvement of the power flow control to optimize the operation of the AC grid,
- improving stability and flexibility in the overall transmission grid.

In the following paragraphs some of the above-mentioned ancillary services, in particular from the dynamic point of view, will be analysed in order to appreciate the mutual cooperation and positive contribution of a meshed multiterminal grid.

### 3.2. Flows controllability and Capital Light solution

The synergic cooperation among the Italian Hypergrid backbones is allowed thanks to a multiterminal configuration, using DCCB to switch operating currents and interrupt fault currents managing the power flows even during critical conditions.

Multiterminal system, allow to reach a higher energy flows optimization allowing to exploit AC lines with higher power transmission availability. This capability is enhanced if coupled with the so called “capital light” countermeasures, which consist in low intensive capital investments aiming to extract higher value from existing assets by removing grid constraint. The capital light solutions allow to mitigate or remove actual grid limitations leading to higher market efficiency anticipating the beneficial effect introduced by the commissioning of grid development project.

In this context, starting from the last few years, Terna has been developing several capital light projects [2], using innovative solutions both technological and based on operational procedures, as listed below:

- Grid constraint removal, for example adopting higher capacity conductors as thermoresistant ones especially on the limiting backbone for NTC increase;
- New control logic criteria as remote trip power to remodulate the injected power by high rated renewable power plant (e.g., wind farm) allowing to exploit existing asset during normal operational condition and helping in dynamic stability recovery in case of grid contingencies;
- The possibility to allow an overload about 15% of the new HVDC converter stations;
- Sensoring, monitoring and diagnostic technology system: evaluating local weather condition measurement to allow an increase (even in real time) in the transmission power availability of existing infrastructure optimising flow management and power integration (so called Dynamic Thermal Rating – DTR).

Based on the approach described above, in the following paragraphs the methodology adopted to perform the dynamic simulations in presence of the HVDC connections is reported, as well as the results and the conclusions of the performed analyses.



## 4. METHODOLOGY ADOPTED TO PERFORM THE DYNAMIC ANALYSIS

### 4.1. Snapshot of the electrical grid analyzed

The analysed snapshot represents a situation of high-power flows across the Italian sections expected at the horizon year 2030. This situation is representative of hours, in the middle of the day, when a significant amount of RES production is generated by solar photovoltaic, wind on-shore and wind off-shore power plants mainly located in the southern part of Italy, whilst the load centres are mainly concentrated in the Central-North. Consequently, significant power flows across the whole Italian peninsula are expected, as shown in Figure 6, which shows the situation in presence of the Tyrrhenian Link East.



Figure 6. Power flow exchange between Italian market areas

Focusing the attention on Sicily, most of the production is provided by solar photovoltaic and wind power units. Renewable Energy sources provide more than 90% of the generating power, whilst conventional power plants are responsible only for the 7% of the total production in the region.

To deal with the integration of renewable generation limiting the risk of RES curtailment, hydro power plants work in pumping mode, allowing to store a significant amount of energy and helping to increase the system inertia.

Being the production in Sicily significantly greater than the internal demand, even in presence of power exports to Malta and Tunisia, high power flows affect the transmission grid of Calabria, which amounts to about 4000 MW, 1000 MW of which are transmitted using the Ionian HVDC, other 1000 MW through the Tyrrhenian Link East and approximately 2000 MW (that would increase to 3000 MW in absence of the Tyrrhenian Link East) through the AC lines that connect Sicily to the Italian peninsula.

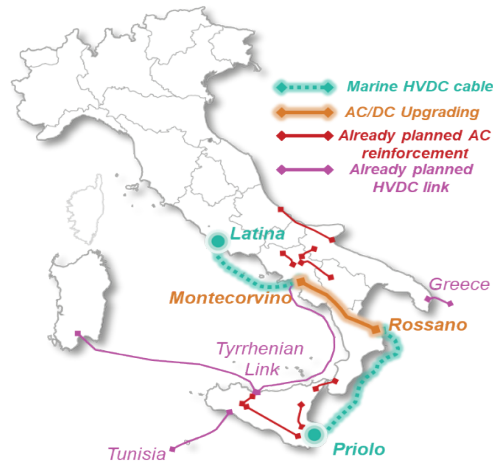


Figure 7. Outcoming flows from Sicily

## 4.2. Area of analysis

The mutual interaction between new and existing or already planned HVDC links is visible in Fig. 8, it is possible to have multi-terminal configuration in the meeting point of Tyrrhenian Link and Ionian-Tyrrhenian project. The cooperation between these two HVDC projects would allow to:

- strengthen the Calabrian network ring (also through capital light actions);
- provide a differentiated way to evacuate power from Sicily, offloading the AC internal high voltage grids of Calabria and Sicily;
- increase the transmission capacity from Sicily to Calabria and vice versa.



**Figure 8.** Mutual interaction between new and existing or already planned HVDC links

Therefore, it was possible to identify areas of analyses in which there is the possibility of critical contingencies, as shown in Fig. 9, for which studies have been carried out and whose results are shown in the following paragraphs.

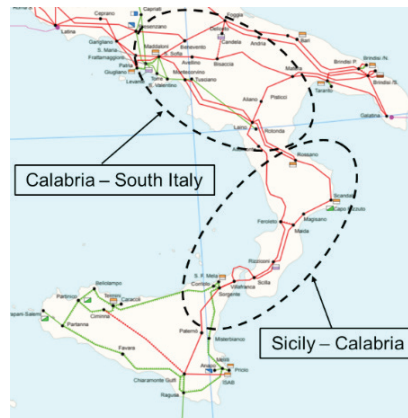


**Figure 9.** Areas interested by dynamic analyses

## 4.3. Dynamic analysis approach

Dynamic analyses, focused on the South Italy areas, show benefits provided by Hypergrid on Italian power system, including increase of the stability margin and reduction of dynamic oscillations. After identifying the areas interested by the analyses, the contingencies to be simulated were identified to manage the interactions between the various HVDC connections which are part of the Hypergrid.

The analyses are characterized as follows:

- $t = 0$  s starts the simulation
- $t = 1$  s a three-phases short circuit is made on one or more lines belonging to the study areas
- $t = 1.1$  s protections and circuit breakers clear the fault and the lines affected by the short circuit are disconnected

Some assumptions were made for these analyses:

- To respect the Italian planning criteria [10], in the event of a contingency involving a double circuit AC line, both circuits are put out of service;
- In the event of a contingency involving a DC overhead line, the converter stations connected to the same DC network are affected by the fault, but just the faulty DC line is disconnected thanks to the intervention of the DC circuit breakers;
- In the event of a DC line failure, even if this line remains out of service as a result of the failure, the HVDC converter stations remain in service in voltage control mode thanks to the adoption of the VSC technology.

The main electrical variables analyzed during the simulations are the following:

- active power flows on the lines connecting the HVDCs under analysis and other significant portions of the grid,
- the voltage of 400 kV nodes to which the analyzed HVDCs are connected and the voltage of the main nodes in the surrounding areas,
- HVDCs active power flows and the reactive power managed by the converter stations,
- the frequency in some network nodes in southern, central and northern Italy, in Sicily and Sardinia to monitor presence of undamped oscillations.

The monitoring of the variables listed above has the following objectives:

- identify the presence of some critical situations for the electrical grid stability,
- identify the improvements introduced by DC connections seen previously with very high-power flows from South to North.

The stability margin is identified by monitoring the variables mentioned above and is representative of a situation having the following characteristics:

- no network instability (voltage or angle),
- adequate voltage profiles following contingencies.

## 5. DYNAMIC ANALYSIS RESULTS

In this chapter the most representative results of dynamic analyses are shown. As previously said, mutual interaction between new HVDC links and existing or already planned HVDC, like Tyrrhenian Link East (TLE), is fundamental to ensure a good system stability in terms of frequency and voltage. If a short circuit is simulated in the Calabria area, with a high-power flow from Sicily to Calabria, there is an instability of electric grid, due to the weakness of the grid in that area. Instead, using at full load the Tyrrhenian Link East, it is possible to offload the internal networks of Calabria and Sicily, providing an alternative transmission way from Sicily to Calabria. In this case, the AC lines between the two regions are offloaded, so the stability margin is increased. Along with this, it is recommended to use Capital Light actions. In Fig. 10 and Fig. 11 the simulated voltages and frequencies in the most representative 400 kV nodes in North, Center and South of Italy are shown in cases with and without the adoption of Capital Light actions.

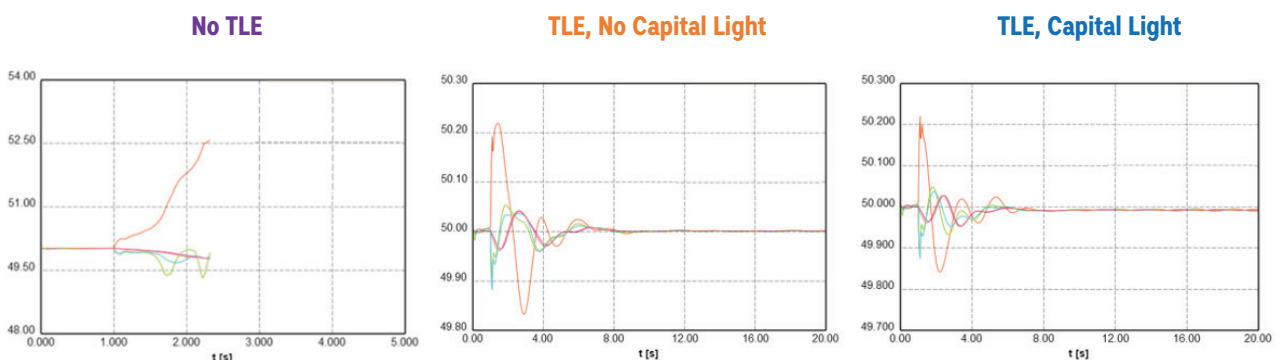
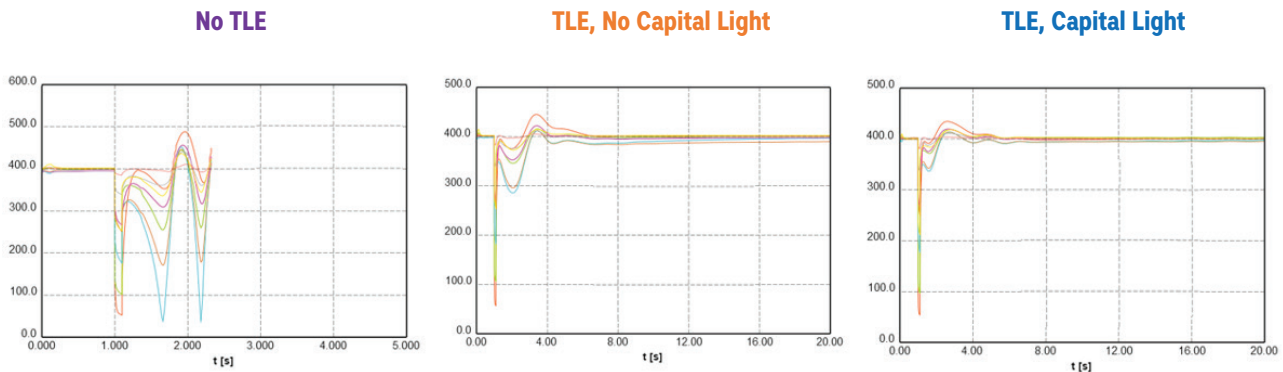


Figure 10. Voltage simulated on 400 kV nodes [kV]



**Figure 11.** Frequencies simulated on some representative S/S of the Italian grid [Hz]

- In the left graphs, without considering the support of the Tyrrhenian Link East, the system is unstable.
- On the contrary, in the central graphs, where the Tyrrhenian Link East is at its full power, it is possible to see that the power system is stable, even in presence of a poor voltage recovery.
- In the right graphs, in presence of the Tyrrhenian Link East at its full power together with some Capital Light actions (specifically consisting in trip of 600 MW of renewable production in Sicily), the oscillations have a limited amplitude and good damping. Voltage recovery is better than in the case without remote disconnection of renewable production in Sicily.

Therefore, the coordination between the power flows on the new HVDC infrastructures with the AC transmission grid is able to increase the stability margin of the system or, in other words, to increase the transmission capacity limits between the Market Areas of the Italian transmission grid allowing the integration of a significant capacity of renewable generation. More specifically, the stability limit identified for the grid in the absence of Hypergrid reinforcements is 2000 MW from Sicily to Calabria. The absence of the Ionian-Tyrrhenian backbone implies a significant reduction in the power flow compared to the Hypergrid grid condition.

On the contrary, the adoption of the HVDC reinforcements associated with Capital Light measures allows to increase the NTC from Sicily to Calabria, thus increasing the space for integrating more renewable generation coming from the southern regions.

## 6. CONCLUSIONS

The EU strategy, to increase more and more the renewable capacity in the electric power systems towards the electricity sector decarbonization, implies to rethink the planning of the future transmission grid with innovative and flexible solutions able to increase the transfer limits between market areas and to assure the system stability also in presence of limited amount of inertia.

To this purpose, the Italian power system represents a significant example to be investigated in detail: the presence of significant amount of renewable generation installed in the South with the main load centers located in the North implies to have significant power flow on the Italian transmission grid in the near future.

To deal with these challenges, TERNA, the Italian Transmission System Operator, is involved in finding innovative solutions for the planning of the transmission grid of the future, ensuring synergic cooperation with already planned electrical infrastructures.

It is needed to development both the “traditional” AC transmission system together with innovative solutions that foresee the adoption of new multi-terminal HVDC transmission links able to significantly increase the power system stability margin. This goal is achievable also thanks to “capital light” actions to allow the integration of more renewable sources without jeopardizing the security of supply and keeping high operational standards in the foreseen transmission grid.

## BIBLIOGRAPHY

- [1] Terna s.p.a., «Avanzamento piani di sviluppo Precedenti - Centro Sud,» Marzo 2023. [https://download.terna.it/terna/Terna\\_PdS\\_2023\\_Avanzamento\\_Piani\\_Sviluppo\\_Precedenti\\_Avanzamento\\_Centro\\_Sud\\_8db254beeb13f67.pdf](https://download.terna.it/terna/Terna_PdS_2023_Avanzamento_Piani_Sviluppo_Precedenti_Avanzamento_Centro_Sud_8db254beeb13f67.pdf).
- [2] Terna s.p.a., «Progetto Hypergrid e necessità di sviluppo,» Marzo 2023. [https://download.terna.it/terna/Terna\\_Piano\\_Sviluppo\\_2023\\_Progetto\\_Hypergrid\\_necessita%C3%A0\\_Sviluppo\\_infrastrutturale\\_8db2549ed056bf0.pdf](https://download.terna.it/terna/Terna_Piano_Sviluppo_2023_Progetto_Hypergrid_necessita%C3%A0_Sviluppo_infrastrutturale_8db2549ed056bf0.pdf).



Oral Presentation: Hypergrid: Coordination and Control of Different HVDC Links

- [3] Aemo, 2020. <https://aemo.com.au/learn/energy-explained/energy-101/energy-explained-system-strength..>
- [4] Aemo, <https://www.aemo.com.au/aemo/apps/visualisations/map.html>.
- [5] H. Pang and X. Wei, «Research on Key Technology and Equipment for Zhangbei 500kV DC Grid,» 2018.
- [6] R. H. C. M. K. LINDEN, «Planning and implementation of an HVDC link embedded in a low fault level AC system,» *Cigre*, 2020.
- [7] M. G. D. V. Hertem, «Multi-terminal VSC HVDC for the European supergrid: obstacles,» 2010.
- [8] «Grid-Forming Control for STATCOMs - a Robust Solution for Networks with a High Share of Converter-Based Resources,» *CIGRÉ*, 2022.
- [9] National Renewable Energy Laboratory., «Research Roadmap on Grid-Forming Inverters,» 2020.
- [10] Terna s.p.a., «Codice di rete - Capitolo II, Sviluppo della rete,» <https://download.terna.it/terna/0000/0105/03.PDF>.



**AUTOMATION AND  
CONTROL**

**POSTER PRESENTATION**



ELECTRIC MACHINES AND  
POWER ELECTRONICS



ELECTRIC  
TRANSMISSION



AUTOMATION AND  
CONTROL

POWER  
GENERATION



ENERGY  
TRANSITION



DISTRIBUTION SYSTEMS  
AND SMART GRIDS



**11-12 OCTOBER 2023**





# Electricity Tampering Detection System Project

**MUNA SALEH AL JABRI\***

*Nama Electricity Distribution*

*Sultanate of Oman*

## SUMMARY

Theft of electricity is one of the challenges facing energy companies. It makes the infrastructure necessary for efficient operations to be unsustainable because electricity companies cannot make enough profits from the electricity they generate and distribute. This work has developed an embedded system that will help prevent the theft of electricity using Internet things technology. The system consists of Arduino Uno mounted for communication and controller functions, while the passive current sensors were used as relay for sensor and operated. Because of this workflow is a functional modem of things based on a system that can detect tampering and separating the consumer.

## 1. INTRODUCTION

Electricity Tampering Detection system is used to detect the electrical theft at the customers' location and saves the current. During last few years, large amount of electrical power was lost by the electrical theft. This type of problem makes the electrical company became very weak. Electricity Tampering Detection system is to reduce the number of electrical thefts.

### Project objectives:

Detect internal and external Electrical energy theft using current sensor.

### Advantage:

- Detect internal and external power theft using sensor current.
- Reduce electrical power losses.
- Solve some meter problem which is any change or illegal communication in this measure by the customer to view the change in the meter.



### 1.1. System Block Diagram

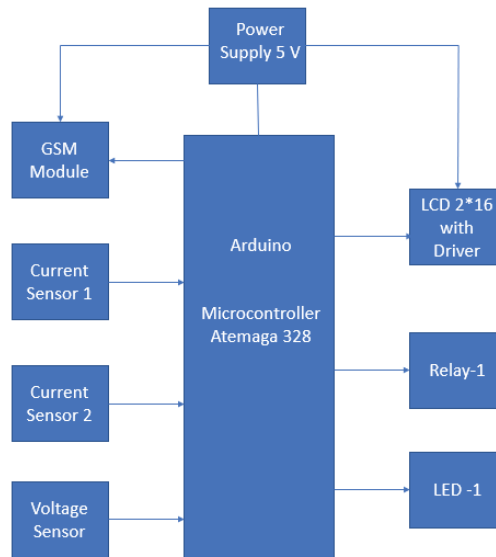


Figure 1. 1 Block Diagram of Electricity Tampering Detection system.

### 2. SYSTEM FLOW CHART

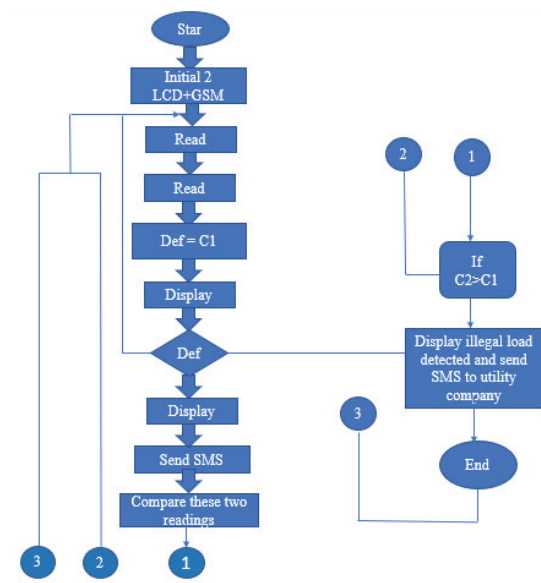


Figure 2. The chart of flow system

### 3. RESULT

Current 1 and Current 2 is equal 0.00 that is there no load like in figure 3.1 indicate to the switch on after meter Current 1 and Current 2 is equal 0.22 as figure 3.2 recall to the readings are same value and the connection working normally. The calculating is no different between its.

Figure 3.3 shown there is different between 2 sensors current1 = 5.1A and Current2 = 5.6A this means is current pass without pass to meter for calculated and send SMS for Electricity Company as in figure 3.4.



Figure 3.1.



Figure 3.2.

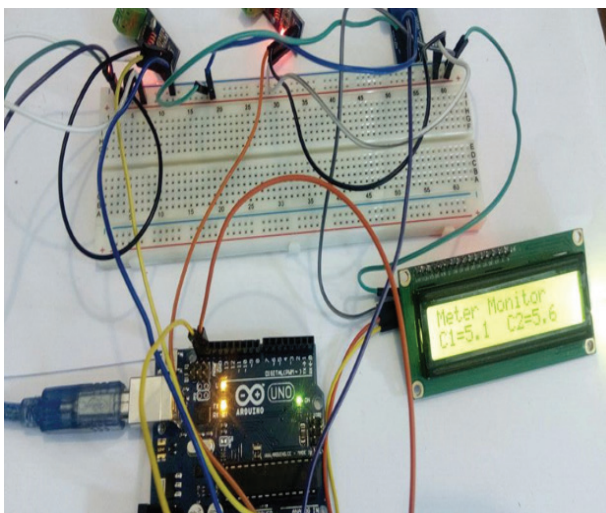


Figure 3.3.



Figure 3.4.

#### 4. CONCLUSION

The project is design for help electricity companies to decrease electrical losses in Oman. The base objective of this project takes from my work environment facing through out of the inspection period, I see many cases have many energy losses. This system is good to decrease losses by check the different between input current and output current flows. This system design to control flow current by microcontroller. That's system has features to help it to be implemented at the real time. For example: for decrease electrical energy losses and decrease amount of manpower for inspection period. Using two current sensors, calculations are calculated to verify the difference between each current. By Arduino used to control all processes of the system and process them and send information using a contact application to verify the processing process of the company's office. The system is useful to reduce the cost involved and power consumption. The system will be easy to use by receiving the system status and message if any error in the system using a GSM modem.

#### 5. RECOMMENDATIONS

The establishment of a good and very useful project that to help electricity companies for checked electrical power and detected it every day is useful work. Also, the system should be used in the fact time because of the creation of the system using fact life is do-nothing work. Stat using this system in all electricity companies soon, with small improvements. A little key for improvements which can do for the future:

- The system should be commercial and available for every electrical company in Oman, the product should be made of an electric industry for production the product has efficient and simple installation when measuring device. Also, good cost.



Poster Presentation: Electricity Tampering Detection System Project

- More realization of the benefits and advantages of the product should be applied to reduce the number of thefts in Oman. In addition, this project will assist Electricity Companies save electricity lines from losses. Also, reduce the cost of oil that is using for generated power.
- Can be using in the future for send the bill by the same that LCD. This application will be good and useful for consumers for test using energy daily or every month with no complaints from the electricity bill.

### BIBLIOGRAPHY

- [1] Farrukh Nagi, J. N. (2008, may 7). 'A MATLAB based Face Recognition System using Image Processing Neural Networks' [online]. Available on <https://www.idsia.ch>. Accessed on 16/10/2016.
- [2] Fernandes, S. (2015). Raspberry Pi Based Human Face Detection [online]. Available on <http://www.ijarcce.com/upload/2015/september-15/IJARCCCE%2042.pdf>. india. Accessed on 16/10/2016.
- [3] Jawad Nagi, S. K. (2008). A MATLAB based Face Recognition System using Image Processing and Neural Networks. [online]. Available on [http://people.idsia.ch/~nagi/conferences/cspa\\_face\\_recognition.pdf](http://people.idsia.ch/~nagi/conferences/cspa_face_recognition.pdf). Accessed on 18/10/2016.
- [4] Miura, K. (2013). Basics of Image Processing and analysis. [online]. Available on [http://www.cnbc.pt/equipment/Basics\\_of\\_image\\_Processing.pdf](http://www.cnbc.pt/equipment/Basics_of_image_Processing.pdf). Accessed on 20/10/2016 .



# ADMS for Planning And Der Control in Distribution Network

[boris.njavro@blueprintenergy.at](mailto:boris.njavro@blueprintenergy.at)

**BORIS NJAVRO<sup>1</sup>, ELENA BOSKOV KOVACS<sup>1</sup>,  
PRIMOŽ SKLEDAR<sup>2</sup>, NEJC PETROVIČ<sup>2</sup>, LUKA MOČNIK<sup>2</sup>, BLAŽ HAFNAR<sup>2</sup>**

<sup>1</sup>*Blueprint Energy Solutions GmBH,*

<sup>2</sup>*Elektro Gorenjska d.d.*

*Austria, Slovenia*

## SUMMARY

By definition, ADMS is a system for managing the electricity distribution network. However, the narrow definition is expanding due to the recent system developments of new functionalities and integration of applications. Modern ADMS is based on the common data model of a distribution network that could be used for many services and supporting new processes, including planning, maintenance and development. The ADMS today assists DSOs to proactively and safely guide outage restoration activities, manage and optimise networks, and effectively manage the integration of distributed energy resources (DERs). At the same time, ADMS is the decision support environment that provides a shared network model spreading deeply into low voltage network (to an extent a digital twin of the electric distribution network) and a common user experience for all roles that are needed to monitor, control and orchestrate assets and DERs across the grid. Elektro Gorenjska (EG) is one of 5 DSOs in Slovenia continuously demonstrating a very good quality of supply ( $\approx 90.000$  customers, SAIFI  $\approx 0,75$  and SAIDI  $\approx 20$  minutes) with a strong strategic focus on innovative projects and solutions. Boosted by its previous performances, EG has embarked on the project of the new ADMS, looking to implement a resilient and future-proof solution and increase its own role and possibilities.

In the beginning of 2023, distributed IT/OT environment in EG was not suitable to support all future roles of modern DSO. The new ADMS planned for implementation in 2025-2026, is considered the core system for the OT, incorporated with the SCADA system, providing support for almost all operational processes in EG. The focus of the ADMS project is to investigate its application and use in the planning of the network and control of an increasing number of DERs. This logic is based on the substantial investment that ADMS already represents, which could be optimised if more DER-related functionalities are added in the same scope to address more business processes with the same implementation.

Major concerns that are addressed in this approach are associated with the analysis of the functionality that ADMS could provide for DER management in comparison with the specialised tools for network planning and DERMS (DER management System), increased demand for data collected and processed by the systems and lack of qualified personnel to fully support this innovative project. EG identified the possibility of extending the ADMS project and building synergies at the level of data management, integration, and digitalisation by coordinating it with the rollout of several internal innovation projects, such as smart metering, data governance and observability of LV network project, that the National recovery and resilience fund finances.

This paper presents how EG approached the implementation of the new ADMS targeting DER functionality and support for the broader scope of DSO operational processes while tackling a range of challenges associated with data governance, human resources and change management. It describes critical challenges and solutions applied resulting in the expanded project roadmap for projects implementation aligned with the DSO strategic goals until 2026.

## KEYWORDS

SCADA, ADMS, DERMS, Network planning, IT/OT Architecture

## 1. INTRODUCTION

Elektro Gorenjska (EG) is one of 5 DSOs in Slovenia continuously demonstrating very good quality of supply (SAIFI  $\approx 0,75$  and SAIDI  $\approx 20$  minutes) with a strong strategic focus on innovative projects and solutions.

The primary activity of the EG is the provision of electricity distribution to end users. It is a regulated activity carried out within the framework of the contract with the company SODO, d. o. o., which has a concession. For many years, EG has also been present in the market of services in energy activities, where it is active mainly in the construction, engineering and provision of other services for the market. It also deals with maintenance, carries out activities in the field of research and development, and design works on projects of efficient use of electricity and energy management.

EG supplies more than 91.000 network users with electricity in the northwest of Slovenia and achieves the highest standards in the field of high-quality and reliable electricity supply (Figure 1).

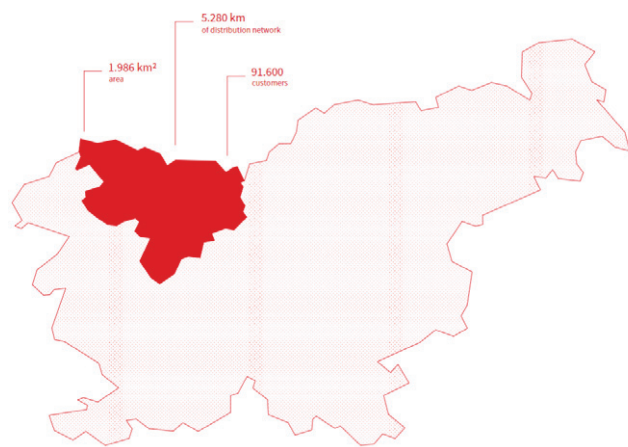


*Figure 1. The geographic area of EG's jurisdiction*

Distributed energy and other relevant technical parameters coming out of EG's business activities are shown in Figure 2.

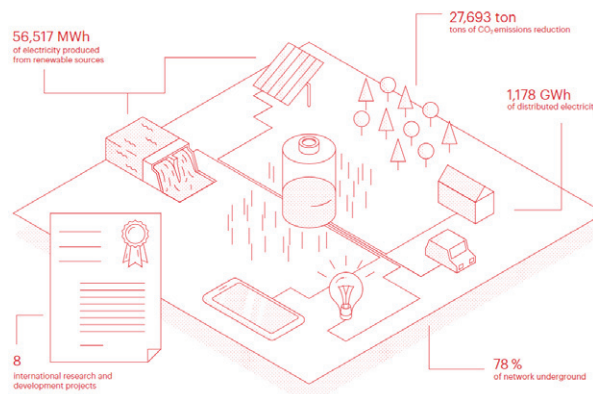


*Figure 2. Overview of the technical performance of EG in 2021*

The energy transition and energy crisis during 2022 and 2023 are the key challenges for DSOs in EU, forcing them to change and upgrade using digitalisation and modern information and operational technologies (IT and OT). Distributed IT/OT environment utilised in EG in 2023 is not suitable to support all future roles of modern DSO. Upgrades have become inevitable in the form of Advanced Distribution Management System (ADMS). New ADMS is considered the core system for the OT, incorporated with the SCADA system, providing support for almost all operational processes in EG.

Based on the situation in EG, in addition to general needs, such as requirements for greater network resilience and requests from regulators to adapt to changes, the need to introduce a new ADMS is primarily based on the following facts:



Poster Presentation: ADMS for Planning And Der Control in Distribution Network

1. To replace the existing system, not supported by the original manufacturer and avoid further custom development and costly maintenance
2. To improve network management in a new business environment: increase of DERs, new flexibility market and services, EVs, microgrids, energy communities...
3. To improve operational efficiency (lower losses, lower customer outages), cyber security, security of supply, and supplement human resources
4. To comply with national and EU directives and regulations.

Therefore, ADMS is considered as a key technological building block in the establishment of a new role for EG, as DSO, as it should enable in the future:

- integration of all information sources for the operational management of the network,
- consolidation of technical, topological and measurement data about the network,
- establishing a platform for advanced data analysis to support decision-making and
- optimisation of the network in terms of load, security, availability, lifetime and planning and development.

The implementation of the new ADMS must also bring certain benefits, both for the EG and for the customers. Some benefits are mainly technical and consequently have a positive effect on business indicators, but the ADMS also brings direct business effects, like:

- Reduction of network operating costs through greater utilisation of equipment, better maintenance and further reduction of losses in the network.
- Reduction or postponement of capital investment costs by optimising the operating conditions of the distribution network.
- Increasing customer satisfaction by reducing downtime and offering new services.
- Better indicators for the regulator by improving the quality of supply and service indicators.

## 2. APPROACH TO MODERN ADMS

ADMS represents a comprehensive solution for monitoring, managing, optimising and planning of the distribution power network, the main backbone of the work of a modern DSO.

The traditional approach to the implementation of ADMS, in the first decade of 21st century, involved upgrading the SCADA system with advanced power calculations and network analyses, which would also include the transfer of technical data and geographic schemes from the GIS system (if the same was implemented for the whole HV and MV network), an option of accessing SCADA/DMS applications for external users via a web browser and a dedicated web server. It was a quite straightforward approach, not considering the majority of challenges (i.e. data quality and quantity) and ended up on the SCADA („That is what we know how works“), with some web-based reports for ambitious engineers working in development. The attempt to implement and use power applications would usually end up in data gaps and gradually be neglected.

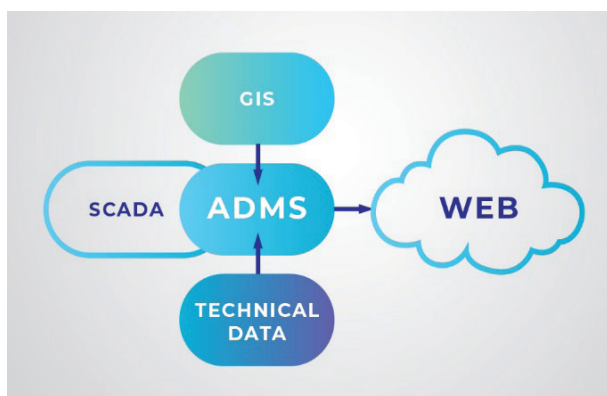


Figure 3. Traditional approach

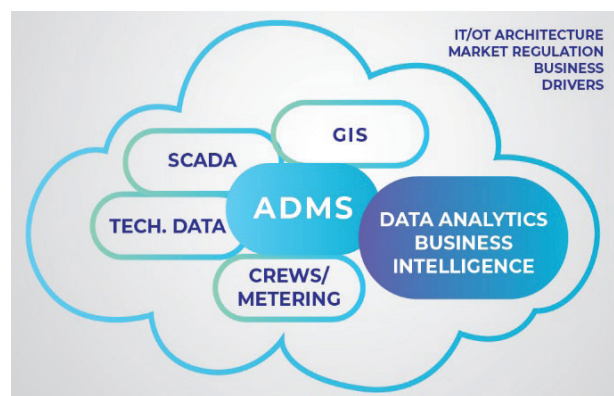


Figure 4. Modern approach



The modern approach (Figure 4) is conditioned primarily by changes in the business environment of DSOs, the market, the appearance of a larger number of DERs, and everything culminated in the new EU energy policy (i.e., Green Deal, Fit for 55, Repower EU). Such approach views ADMS as a key system of all operational technologies in the entire integrated IT/OT architecture of DSO which includes (changes and optimises) almost all business processes: network management, maintenance, development, planning, etc. The modern approach to ADMS implementation takes into account the entire IT/OT environment, requires horizontal and vertical integration with other systems: i.e., GIS, AMI, ERP, CRM, and Asset Management, and upgrades the obtained results with tools for data analysis and business decision-making (i.e., Big Data Analytics, Business Intelligence...).

With the advancement of technology, driven by the commercial strategies of the vendors, ADMS also tends to overlap with the systems it integrates with, taking over their functionality and growing bigger. The same also happens to other systems like GIS. The technical reason is that it uses the same network model and data, and the customer gets an integral and unique interface. Still, the logic of those functionalities and time horizons of different business processes sometimes clashes inside the same environment (i.e., real-time network operation versus system planning for the next 5-10 years). That is something challenging to coexist.

Today, in general, the ADMS project is essentially an IT project with all its features, challenges, and phases. On average, it lasts 2-3 years and includes many employees (50-60 of them in some larger implementations), as well as the Vendor's employees and potential system integrator.

Managing such a complex IT project is extremely important, as is the real support of the company's management, the strategic positioning of the project internally and externally, and effective change management. As stated earlier, the impact of ADMS is not limited only to the operational part of DSO, and it is essential to communicate the impact and changes brought about by ADMS in a timely and effective manner.

Considering the trends in ADMS development, its complexity and impact on the company, the most critical question is how "big" ADMS each DSO needs. Is it better to go with the limited version and fast implementation with the option to upgrade and improve in phases, or to choose the "big bang" approach with full implementation?

EG decided on the first option due to the limits of internal resources but actively investigating the solutions for network planning and management of DERs (energy storages, EV chargers, etc.) and their implementation in the future since the two are considered the biggest challenges for the future.

### 3. NETWORK PLANNING TOOL

The Network Analysis and Planning Tool, often referred to as the Network Planning Tool (NPT), is a set of tools that support the operations of the development and planning department by enabling detailed calculations of the current and future state of the network to plan investments in expansion, renewal, and connections of new customers (loads and power plants). The same tool could also support advanced management functions (which can be part of the ADMS system or separate functions), as well as various network simulation tools. Today, especially, the traditional approach to network planning is challenged by the increased number of DERs, storages, EVs, and other »new« connections, and analyses that have been done for years should be done again.

In general, the functions of the NPT system can be divided into several groups, for example (but not exclusively):

#### 1. Network planning functions:

- Symmetrical and asymmetric calculation of the network static method;
- Probabilistic calculation of power flows
- Calculation of reserve operating states - automatic N-1 analysis;
- Import and work with SCADA and AMI measurements;
- Importing forecasts into the network model and calculation with iterations over time;
- Calculation of Hosting capacity for MV and LV;
- Network versioning
- Economic analysis and comparison of development variants;

#### 2. Operation planning functions:

- Short-term analysis;
- Planning of protective zones of relays;



- SAIFI, SAIDI and other reliability analyses;
- Analysis of voltage profiles.
- Harmonic analysis.

### 3. Analysis of client connections:

- Integration of GIS and reports.
- Network versioning when approvals are issued.
- Nodal Hosting Capacity - Nodal available additional power to connect.

All NPT functions are based on network calculations, mainly power flows, combined for several possible network states or projected loads, thus solving various optimisation functions.

It is challenging to be objective in deciding where to set up the NPT in IT/OT architecture: As a part of the bigger ADMS or a separate module? In general, it depends on the level of development of the network planning and development department – in case the department is on the high level of using IT systems and tools, including data, it is more likely that it will remain a separate module with robust integration interfaces.

Whatever option is used, the effort for data collection for the ADMS should not be multiplied due to different and separate modules. It is advisable to use and collect the data once and improve the quality for more purposes.

The traditional approach to network development is increasingly challenged by the difficulty to predicted consumption and production. Therefore, integration of the historical, current and forecasted data and the use of advanced Data Analytics tools is inevitable. During the preparation of the ADMS project, all functions must be objectively assessed for possible use in network planning and development. All similarities and potential to reuse must be evaluated objectively. Leaving the existing tools for network planning running just because it was implemented recently is not an objective resolution. If it can be replaced by the standard ADMS functions in an integrated environment, it should be discarded. On the other side, the knowledge, experience and data used by the Network planning department must be addressed because it may also speed up the ADMS implementation.

The technology is here to improve all business processes, and ADMS is already supporting most of the processes inside DSO and must not be considered only as a network management tool.

## 4. DERMS

DERMS and ADMS are closely linked in their role in grid management. ADMS is designed to monitor and control the distribution network in real-time, allowing grid operators to manage power flows, voltage levels, and other key parameters, mainly for the HV and MV networks. DERMS, on the other hand, is designed to manage distributed energy resources, including renewables and energy storage systems, and to optimise their use within the LV and MV grid.

One of the key challenges in building a DERMS is ensuring that it can work seamlessly with the ADMS to provide a comprehensive view of the distribution network. This requires close collaboration between DERMS and ADMS developers to ensure the two systems can exchange data and communicate effectively.

Flexibility platforms, in particular, are emerging as a crucial tool for grid operators to manage the integration of renewable energy sources and to balance supply and demand in real-time. These platforms enable grid operators to tap into flexible loads, such as electric vehicles and demand response programs, to help stabilise the grid during periods of high demand or supply fluctuations. However, building flexibility platforms with integrated DERs is a complex task that requires a combination of technical and commercial considerations. Most often, the flexibility platform is linked with the DERMS functionalities. It is also important to ensure that the platform can support the dispatchers along the same path as the ADMS.

To address the above challenges, DERMS Vendors and system integrators must work closely with DSOs and other stakeholders to design platforms that can effectively integrate and manage distributed energy resources while maintaining grid stability and reliability. As the energy industry evolves, DERMS and flexibility platforms will likely become even more important, providing critical support for transitioning to a more sustainable, decentralised energy system.

DERMS is still an emerging new system, but it tends to be tightly integrated with ADMS and could be easily included in the same project (tender documentation). While ADMS vendors exhibited capabilities in certain aspects of a DERMS in the past few years, the fully comprehensive DERMS system is challenging to find.



From the user point of view, the interplay of rules, regulations, and policies also have a profound impact on the definition of DERMS and associated requirements and need to be reviewed as they evolve. During the preparation of the ADMS project, EG analysed the following issues regarding DERMS:

- A DERMS paired with an ADMS can identify and mitigate real-time and forecasted distribution capacity and voltage issues using a combination of DER constraints with active and reactive power dispatches
- Large, highly variable DERs participating in flexibility markets are difficult to forecast and incorporate into distribution calculations.
- The function and role of aggregator in the distribution network is still developing commercially and technically looking for the TSOs as a flexibility market organiser
- Investments in improved data quality, modelling, forecasting, communications, and a DER-aware ADMS are required to achieve any efficient dispatch of DERs in the future. Regardless of future policy or market trends, distribution operations will need these tools to safely and reliably operate the grid as complexity increases with the continued growth of DERs.
- DSOs and industry leaders should continue to be engaged in the various standards, policies, and regulatory bodies that are shaping the industry.
- An ADMS should be the source of power system situational awareness and provide power system calculations, grouping, and other information to an integrated DERMS: the ADMS does not need to communicate with all DERs directly. DERMS is expected to be the platform that reaches out to the majority of DERs either through aggregators or direct connections.
- While tight integration is required, separating these functions reduces the complexity of maintaining redundant models and databases. Additionally, the ADMS is used for the day-to-day operations of the grid; and having a separate DERMS reduces the burden on the ADMS and allows for greater flexibility to evolve as conditions become more defined.

## 5. ADMS FOR PLANNING AND DER CONTROL

In preparations for the new ADMS project, detailed survey, discussions, workshops, and brainstorming sessions has been held in EG for several months, where all aspects of the ADMS scope was assessed. The conclusions and proposal of the working group are now guidelines for the ADMS functionalities. When thinking about functionalities separately for ADMS, DERMS and NPT, the discussion started from the data needed for each system (Figure 5).

For the ADMS, it is a prerequisite to use:

- Real-time data was collected via communication lines and RTUs, substation controllers, etc.
- Technical data on the characteristics of the equipment for calculating their impedances and admittances (transformer's ratios, impedances, line lengths and types...).
- Static and dynamic topological data are used to determine or simulate the connection state of individual components.
- Metering and billing data for better and faster fault's location and improved forecasting
- Other data that may affect energy calculations, e.g., transformer switches, voltage regulators, but also meteorological historical and forecasted data, etc.

NPT uses almost all data intended for the ADMS (listed above) and additionally:

- Time series (profiles) of loads and sources of electricity, which represent network inputs and outputs and may refer to historical data, calculated averages (characteristic profiles) or forecasted data. Time series most often refers to a period of 24 hours.
- Time series of loads for various objects in the network: transformers, lines, etc.
- Spatial data, geopolitical and demographic data, combined with the economic data for the different areas

DERMS requires very similar data as ADMS with additions of technical data for DERs and market data. In addition, we must emphasise that ADMS focuses mainly on HV and MV networks. Still, for the DERMS, the LV network is of much greater importance due to most DERs being connected to the LV network (i.e., solar PVs).

All three systems are basically using the same data and the same network model. It makes the technical, but also financial sense to build all systems on the same data platform but also to share specific functionalities between them. Therefore, the established Data Management or Data Governance processes are the most essential prerequisites for all systems.

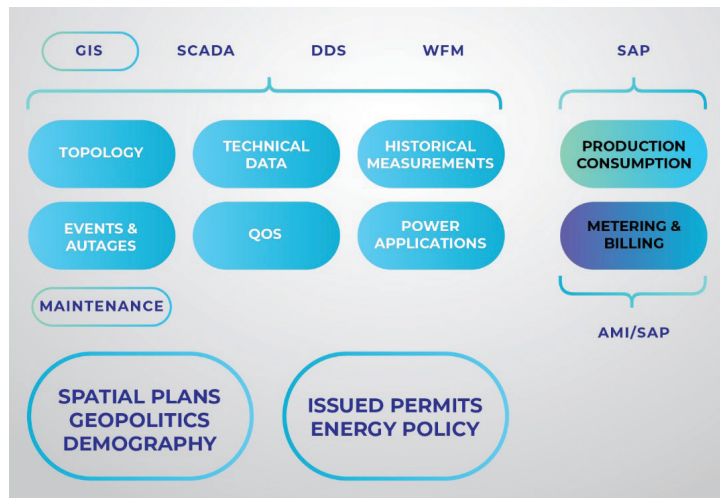


Figure 5. Available data and data sources

The second step in discussion is to check how the systems fit into business processes and the corresponding users. Now we have obvious complementarity of ADMS and DERMS, which are used as part of the same Network management processes, and almost by the same users. The difference is that DERMS is closer to the specific market functions. The NPT, on the other hand, is a mainly part of the Network planning and development process used by the completely separate users.

And the third step is to check the time frames and data horizons needed for the systems. Similarly, ADMS and DERMS need real-time data, while DERMS functions are more focused on the future/forecasted data about energy production, and NPT is using historical data from the years before and is giving results for the future: months and years in front of us. Also, ADMS and DERMS are used continuously, 24/7, with regular operations and incident responses. NPT is used periodically by the network planners focusing on the specific area or part of the network, not needed to be available 24/7.

After analysis of the three steps above and taking into account specifics of the EG and its starting position, it was concluded the following:

- ADMS and DERMS share the same data and network model, users and are based on the same time horizons, therefore makes sense to implement them in the same environment, probably from the same vendor and even to combine the implementation projects.
- NPT’s functions are separately used by different business processes and users, but still shares the same data platform. Therefore, for the implementation of the NPT it makes sense to insist on the using of the same data and network model with independent software. Also, the implementation project is recommended to be separate and run by the separate team.

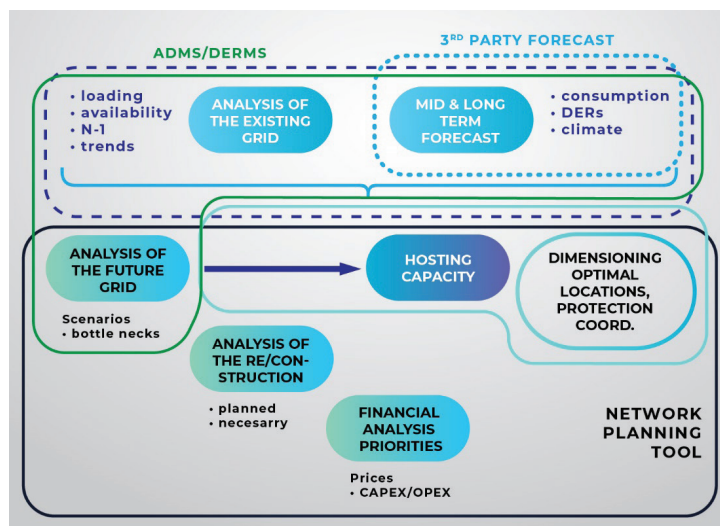


Figure 6. ADMS, DERMS and NPT





## 6. CONCLUSION

EG is poised to revolutionise and re-utilize its operational technologies by implementing the ADMS, a foundational and integrated system coordinated with the SCADA system. As a pivotal aspect of the ADMS project, it is also committed to investigating its practicality and efficiency in network planning and regulating the escalating influx of DERs and flexibility assets in general.

The ADMS stands as an innovative, shared network model that encapsulates the low-voltage network, offering a harmonised user experience for all essential roles involved in the monitoring, controlling, and orchestrating assets and DERs throughout the grid. Notably, DERMS as a specialised module designed to optimise the control of DERs and foster grid stabilisation and resilience — supplements the ADMS harmoniously.

EG's forthcoming ADMS implementation seeks to magnify the return on their considerable system investment by enhancing DERMS and NPT-related functionalities. This strategy promises to encompass more business processes within a single implementation, thereby maximizing the value of the investment.

Potential hurdles encompass the evaluation of the functionality that ADMS could provide for DER management and network planning compared to specialised tools. The mounting demand for data to be gathered and processed by the systems, coupled with the shortage of adequately trained personnel to spearhead this groundbreaking project, also present formidable challenges.

To overcome these obstacles, EG is expanding the scope of the ADMS project and fostering synergies in data management, integration, and digitisation by synchronising it with several ongoing internal innovation projects. These include the implementation of smart metering, data governance, and enhancing low-voltage network observability. Ultimately, the new ADMS is crucial to facilitate the comprehensive implementation of DERMS, seamlessly integrated with ADMS and NPT, all unified within the same data platform.

## BIBLIOGRAPHY

- [1] European Commission: "Assessment and roadmap for the digital transformation of the energy sector towards an innovative internal energy market", October 2019
- [2] ENTSO-E, CEDEC, GEODE, EURELECTRIC and EDSO for Smart Grids: "TSO – DSO DATA MANAGEMENT REPORT", 2016
- [3] ETIP SNET: "VISION 2050 Integrating Smart Networks for the Energy Transition: Serving Society and Protecting the Environment",
- [4] Dr Alan W. McMorran: "An Introduction to IEC 61970-301 & 61968-11: The Common Information Model", University of Strathclyde, Glasgow, UK, January 2007
- [5] Andrej Souvent, Mateja Kavčič: "Using GIS in Smart Grid CIM Data Exchange", public presentation
- [6] "DSO PRIORITIES FOR SMART GRID STANDARDISATION", A EURELECTRIC position paper, Januar 2013
- [7] "AKT o metodologiji za izdelavo razvojnih načrtov elektrooperaterjev", Maribor, 27th January 2022, EVA 2022-2430-0006
- [8] Houda Daki, Asmaa El Hannani, Abdelhak Aqqal, Abdelfattah Haidine, Aziz Dahbi: "Big Data management in smart grid: concepts, requirements and implementation", Journal Big Data, published 28th April 2017.
- [9] Western Power Distribution "Our Business Plan 2023 – 2028 - First Submission", July 2021, Bristol UK.





# Power Quality System within Romanian TSO

[ciprian.diaconu@transelectrica.ro](mailto:ciprian.diaconu@transelectrica.ro)

**CIPRIAN DIACONU\***  
Transelectrica SA

Romania

## SUMMARY

The characteristic features of the Power System these last years, such as higher interconnection, greater share of electricity generated from renewable sources (wind & photovoltaic power plants), wide-scale introduction of power electronics have led to higher importance for power quality monitoring because the efficiency of all activities using electricity (from industry, services and the household sector) depend on its quality. In this context, Transmission System Operator „Transelectrica” will implement a new Power Quality Monitoring System (PQMS). This paper provides a description of the new system PQMS that expand the number of monitoring points at all substations of the national electricity transmission network as well as on the interconnection lines with the neighboring power systems. The new system implements the latest updates of the power quality monitoring legislation (standards SR EN 61000-4-30 and SR EN 50160), ensure the confidentiality, integrity and availability of the measured data and is compliant with cyber security legislation.

## 1. INTRODUCTION

Transelectrica, as Romanian Transmission and System Operator (TSO), manages and operates the electricity transmission system, the transmission network (400 kV, 220 kV and part of the 110 kV), the Romanian electricity market, provides electricity exchanges between the central and Eastern European countries as an ENTSO-E member (European Network of Transmission and System Operators for Electricity). Also Transelectrica is responsible for grid and market infrastructure development ensuring the security of the Romanian power system.

During the years, the Metering Branch OMEPA, part of Romanian TSO, developed the field of Power Quality Monitoring according to Romanian legislation: “The Electricity Transmission power grid - Technical Code” [1], “The Electricity Transmission Power grid – Standard of performance” [2] and international technical standards: IES 61000-4-30 [3] and EN50160 [4], related to power quality.

## 2. HISTORY

In 2004 Electricity Regulatory Authority (ANRE) issued “The Electricity Transmission power grid - Technical Code” [1], with technical quality requirements regarding the frequency, the voltage in HV power grid and the 110 kV grid, and also the quality of voltage and current curves.

## KEYWORDS

Power Quality – Monitoring – System – Analyzer – Standard



Table 1: Power Quality Requirements

<b>Power frequency</b>	Art.101 The frequency rated variation limits are as follows: a) 47.00 – 52.00 Hz for 100% of the year; b) 49.50 – 50.50 Hz for 99,5% of the year; c) 49.75 – 50.25 Hz for 95% of the week; d) 49.90 – 50.10 Hz for 90% of the week.
<b>Voltage</b>	Art.105 Normal voltage values are considered those falling within the admissible voltage ranges as follows: (...) b) in any point of the 400 kV network, the admissible voltage range is between 380 and 420 kV; c) in any point of the 220 kV network, the admissible voltage range is between 198 and 242 kV; d) in any point of the 110 kV network, the admissible voltage range is between 99 and 121 kV.
<b>Voltage curves</b>	Shape of voltage curves: Total harmonic distortion factor: 3% (at $\geq 110$ kV). The ratio between negative and positive sequences: non-symmetry factor of negative sequence: 1% (at $\geq 110$ kV).

OMEPA started the power quality monitoring with portable instruments (2003 and 2008). The goal of the temporary PQ monitoring is to identify sources of disturbances in the power grid, in order to transition to permanent monitoring.

Since 2006 the TSO's specialists attended Power Quality training and certification programs.

Beginning with the year 2006, OMEPA started the process of permanent power quality monitoring, with two pilot systems with stationary analyzers for TSO – DSO interface and the interface with the largest industrial electricity consumers in the country at that time, as presented in Table 2 (23 monitoring points).

Table 2: First steps in permanent PQ monitoring

220/ 110 kV Alba Iulia	110 kV AT1
400/ 110/kV Brasov	110 kV T1
400/ 110 kV Darste	110 kV T2
220/ 110 kV Fantanele	110 kV AT1
220/ 110 kV Gheorgheni	110 kV AT1
400/ 220/ 110 kV Iernut	110 kV AT1
220/ 110 kV Ungheni	110 kV AT1
220 kV Targoviste	220 kV LEA Cuptoare 1 220 kV LEA Cuptoare 2 220 kV LEA Cuptoare 3
220/110 kV Iaz	220 kV AT2
220 kV Otelarie Hunedoara	220 kV T1 220 kV T2
220 kV Campia Turzii	220 kV LEA Cuptoare 1 220 kV LEA Cuptoare 2
400/ 110 kV Tulcea	400 kV T1
220/ 110 kV Resita	LEA 220 kV Otelarie
400/ 110 kV Roman Nord	400 kV T
400/ 220/ 110 kV Slatina	220 kV SRA1 220 kV SRA2 220 kV AT1 220 kV AT2 400 kV AT1

Poster Presentation: Power Quality System within Romanian TSO

The data recorded by the analyzers of pilot systems presented in Table 2, were local read from a laptop/ remote read via serial modem interfaces from a server located at OMEPA Sibiu. The analyzers had no GPS receiver for time synchronization.

In order to fulfil the requirements of “The Electricity Transmission Power grid – Standard of performance” [2] and to meet the requirements of the 2<sup>nd</sup> edition of IEC Standard 61000-4-30 and the first edition of EN Standard 56160, it became necessary to build an PQ monitoring system, with new generation hardware and software, allowing to integrate multiple vendors analyzers and with possibility of expansion.

In 2008 The ISPE Institute designed for Transelectrica the “Feasibility Study and Tender Specification for development a system for integrating the existing PQMS” [5] and in 2011 the system has been put into operation in the OMEPA Data Centre.

The purpose of the system was to permanent monitor the PQ parameters, online data transfer using optical fibre communication for of the data to the central point, data management and storage on dedicated equipment and to offer the possibility of reporting the data via web browser for system’s users.

The PQ Monitoring System integrated multiple types of Class A (as per 61000-4-30) analyzers from different vendors (fixed and portable). The old analyzers were replaced by new generation ones, Class A certificated. In order to meet the 61000-4-30 Standard requirements, they are synchronized by industrial GPS receivers which ensures the uncertainty of time measurement of  $\pm 20$  ms.

At central point, the systems have servers and node storages installed in two fully redundant racks, equipped with UPS in order to ensure continuous operation. On hardware servers it runs virtual servers dedicated to each type of analyzers, and for system management.

Fibre optic communication allows automatic PQ and other electrical parameters transfer from analyzers to the serves, with a good speed, for a large amount of data.

All the system’s users have the possibility of reading the specific data and to report them, according to the rights that have been assigned to them.

Power Quality reports and data are used by TSO for ANRE reporting the PQ in Transelectrica substations and for internal technical use of the Company. Also the PQ monitoring system has the possibility to send energy data to the Metering System for Wholesale Market (backup data).

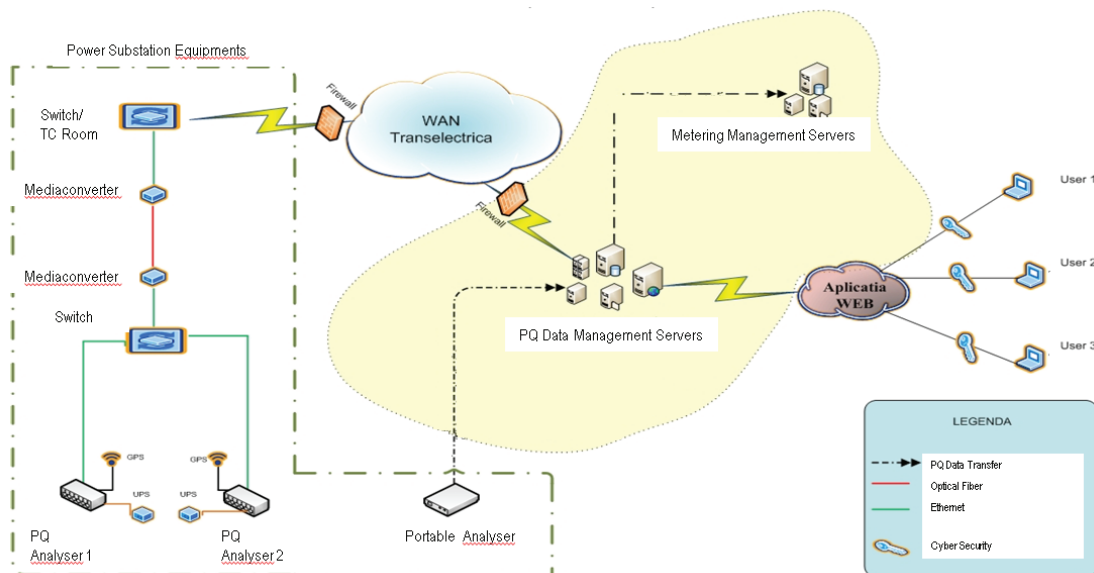


Figure 1. PQ Monitoring System Architecture

Table 3: PQ Monitoring System in 2011

Alba Iulia 110 kV AT1	Slatina 220 kV SRA1	Roman Nord400 kV T
Brasov 110 kV T1	Slatina 220 kV SRA2	Iaz 220 kV AT2
Darste110 kV T2	Slatina 110 kV AT1	Otelarie Hunedoara 220 kV T1
Fantanele110 kV AT1	Slatina 110 kV AT2	Otelarie Hunedoara 220 kV T2
Gheorgheni110 kV AT1	Targoviste 220 kV LEA Cuptoare 1	Pelicanu 400 kV T1
Iernut110 kV AT1	Targoviste 220 kV LEA Cuptoare 2	Pelicanu 110 kV T2
Ungheni110 kV AT1	Targoviste 220 kV LEA Cuptoare 3	Pelicanu 110 kV LEA CSC1
Tulcea 400 kV T1	ResitaLEA 220 kV Otelarie	

In 2011 OMEPA has issued the first edition of Internal Technical Regulation [6], with a chapter dedicated to fixed analyzers and their accessories and started the purchase of new analyzers for the expansion of the PQ monitoring system. In 2012, 15 new analyzers were integrated into the system.

In 2016, a new version of “The Electricity Transmission Power grid – Standard of performance” [2] was released by ANRE. This revision includes new performance indicators for power quality parameter of flicker:

Table 4: New Requirements for PQ monitoring

Short term flicker indicator	0.8 for at least 95% of week, for 110 kV and HV network
Long term flicker indicator	0.6 for at least 95% of week, for 110 kV and HV network

In order to update the technical requirement regarding PQ analyzers and accessories, it was released a new “Internal Technical Regulation regarding the power quality instruments” [7]. Also, in 2019 OMEPA released a technical guide [8] that define technical requirements regarding the design of quality monitoring systems. Both documents take into account the legislative requirements in effect at the time.

### 3. NOWADAYS

As time passed, the system expanded due to integration of new analyzers. They were installed during TSO’s power stations’ refurbishing or modernization and also from renewable energy power plants integration in national power system.

In 2021, the Company purchased four portable analyzers and OMEPA provide temporary PQ monitoring programs for TSO’s use.

Figure 2. PQ Monitoring Map

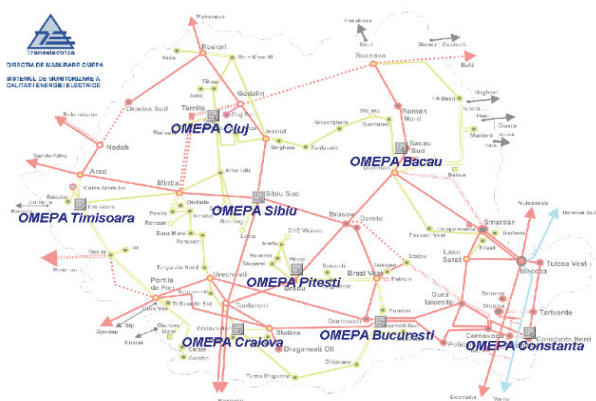


Table 5. 2022 Overview

OMEPA Bacau	17 units
OMEPA Bucuresti	15 units
OMEPA Cluj	4 units
OMEPA Constanta	35 units
OMEPA Craiova	7 units
OMEPA Pitesti	8 units
OMEPA Sibiu	11 units
OMEPA Timisoara	12 units
<b>TOTAL</b>	<b>109 units</b>

Also, as time goes by, the old PQ Monitoring System became outdated due to the rapid technical evolution (hardware and software). Taking this into account, the maintenance for the components of the old system becomes more and more difficult.



### 4. FUTURE

Considering the fact that the future is being built in the present, the Company started the procedures necessary for the purchase a new Power Quality Monitoring System (PQMS). This decision took into account the aging of hardware equipment, the end of life of support for installed software applications, as well as the rapid evolution of technology in IT and PQ monitoring fields.

The process of purchase started with Terms of Reference [9], and during the year 2021 Nova Industrial designed for Transelectrica "Feasibility Study and Tender Specification for Power Quality Monitoring System (PQMS)" [10].

The IT part of the system, located in OMEPA Data Centre, will have the servers and the storages installed in two fully redundant racks, equipped with all accessories necessary to continuous operation. The solution approved by the Company is designed having a modern cyber security solution and the latest requirements for virtualization, which will be installed on hardware servers. The data will be stored on fully redundant storages.

The future system users will have access to data and reports regarding power quality parameters using a web browser interface. The main software application will allow reporting in accordance with the requirements of the Standard of Performance [2] and EN50160 Standard, actual editions.

The goal of the Company is to monitor the power quality in all 80 TSO's power station and all on all interconnection lines with neighboring power systems. The differences between nowadays and future is showed in Figure 3.

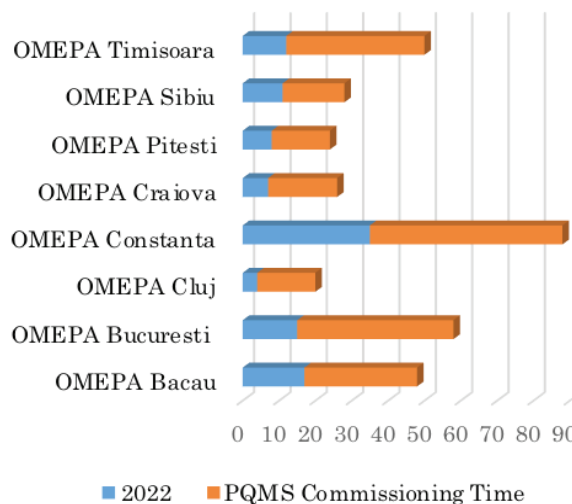
During the new PQMS installation, the obsolete analyzers will be replaced with new ones, equipped with GPS receivers for time synchronization as per IEC 61000-4-30 Standard [3], actual edition. The analyzers that not meet the and of life will be integrated in the new system. At the moment of commissioning, all analyzers will meet the actual requirements of power quality legislation (Table 6).

The future PQMS will allow up to 300 analyzers integration, and also will integrate the old system databases.

Table 6. Commissioning Overview

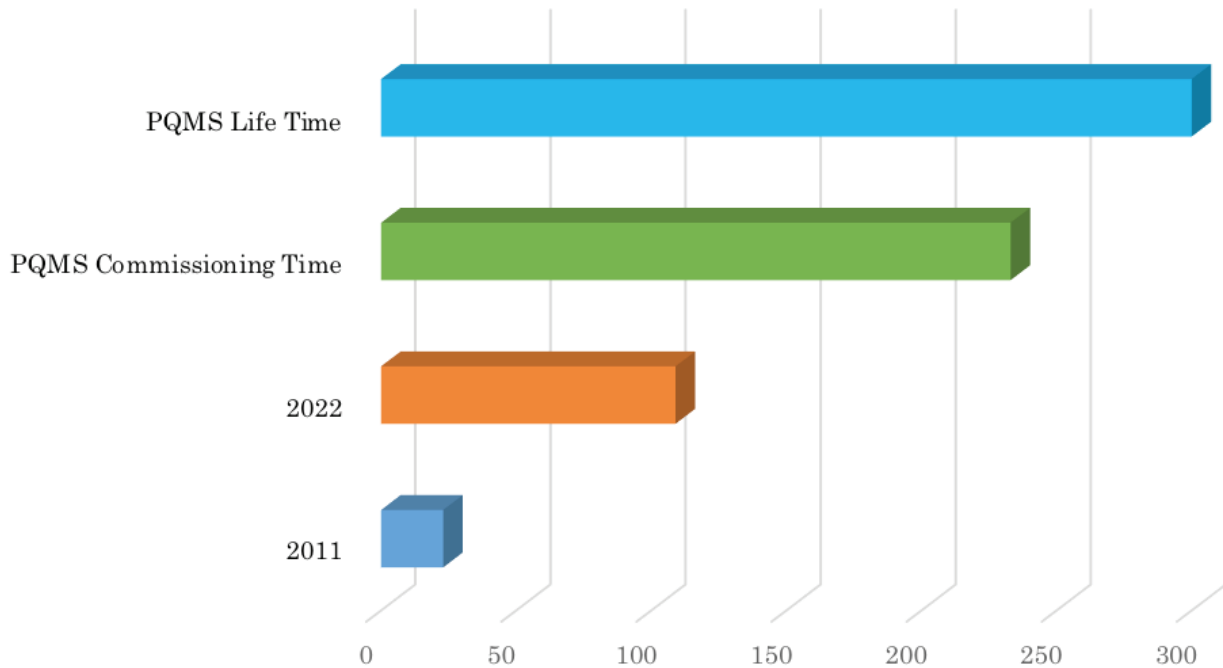
OMEPA Bacau	31 units
OMEPA Bucuresti	43 units
OMEPA Cluj	16 units
OMEPA Constanta	53 units
OMEPA Craiova	19 units
OMEPA Pitesti	16 units
OMEPA Sibiu	17 units
OMEPA Timisoara	38 units
<b>TOTAL</b>	<b>233 units</b>

Figure 3. Benefits of having a new PQMS



### 4. CONCLUSION

Building the new PQMS, Transelectrica will increase the number of monitorization points and will have an overview of power quality in all power stations and on all interconnection lines with neighboring power systems. In 2022 only 46,78% of among the points of interest for the Company are power quality monitored. The evolution in time of PQ monitoring is presented in Figure 4.



*Figure 4. PQ Monitoring Evolution During the Time*

The new system will allow the Romanian TSO to control the voltage curves quality in its own power grid and to report to ANRE the power quality indicators. Also, electrical parameters recorded by analyzers will provide entry data for the reason of internal technical analysis required by the Company. All of the above ensure the confidentiality, integrity and availability of the measured data and is compliant with cyber security legislation.

The development of power quality monitoring of TSO represents an important direction considering the characteristic features of the Power System in the last years, such as higher interconnection, greater share of electricity generated from renewable sources (wind and photovoltaic power plants), wide-scale introduction of power electronics. All of the above led to higher importance for power quality monitoring because of the efficiency of all activities using electricity (from industry, services and the household sector) depend on its quality.

## BIBLIOGRAPHY

- [1] ANRE, Romania, 2004, "The Electricity Transmission power grid - Technical Code", [www.anre.ro](http://www.anre.ro);
- [2] ANRE, Romania, 2016, "The Electricity Transmission Grid – Standard of performance", [www.anre.ro](http://www.anre.ro) (2007 – the first edition);
- [3] IEC 61000-4-30 Standard, International Electrotechnical Commission, 2015, "Electromagnetic compatibility (EMC) - Part 4-30: Testing and measurement techniques - Power quality measurement methods"; (2007 – the 2<sup>nd</sup> edition)
- [4] EN50160 Standard, CENELEC, 2010, Voltage characteristics of electricity supplied by public electricity networks (2007 – the first edition)
- [5] ISPE, Romania, 2008, "Feasibility Study and Tender Specification for development a system for integrating the existing PQMS"
- [6] Transelectrica, Romania, 2011, "Internal Technical Regulation regarding the metering and power quality instruments cod NTI-TEL-M-002-2011-00", [www.transelectrica.ro](http://www.transelectrica.ro);
- [7] Transelectrica, Romania, 2018, "Internal Technical Regulation regarding the power quality instruments cod NTI-TEL-M-005-2018-00", [www.transelectrica.ro](http://www.transelectrica.ro);
- [8] Transelectrica, Romania, 2019, "Implementation guide regarding metering and PQ monitoring systems";
- [9] Transelectrica, Romania, 2019, "Terms of Reference for Power Quality Monitoring System (PQMS)";
- [10] Nova Industrial, Romania, 2021, "Feasibility Study and Tender Specification for Power Quality Monitoring System (PQMS).





# Monitoring and Management of Ambient Conditions of the Electrical Grid with Sensor Network System

[busra.tore@eltemtek.com.tr](mailto:busra.tore@eltemtek.com.tr)

BÜŞRA TÖRE<sup>1</sup>, OZAN AKYOL<sup>2</sup>, SAFFET ERDOĞAN, FERHAT ŞENER  
<sup>1</sup>ELTEKTEK

Türkiye

## SUMMARY

In addition to the increase in energy needs with the proliferation of electric vehicles and technological devices, the limitation problems experienced in energy production make it mandatory to use the efficiency of the existing grid optimally. With the change of global climate, the number of failures experienced due to environmental conditions is increasing day by day and causes long-term interruptions. In today's rapidly changing world, manual operation of the electricity grid is becoming more difficult, and efforts are being made to solve problems related to digitalization.

On the way to smart grids, new sensor designs suitable for the use of the energy sector, communication systems where isolation-reliability is at a high level in addition to accelerating data transmission, information technology systems should be used. As company, a study has been conducted on the roadmap that should be followed in Türkiye on smart grids and PloT.

In this statement, the details of the milestones that will enable digitalization in the energy sector are explained. In the future, it aims to create an energy management system in which predictable maintenance work, risk-based investment planning can be carried out in accordance with the data obtained, which can be monitored and remotely controlled by the electricity grid.

## 1. INTRODUCTION

In Türkiye, various devices such as circuit breakers, disconnectors, transformers, cells, current transformers, and voltage transformers are used in high voltage transmission ( $\geq 36$  kV) and distribution networks ( $\leq 36$  kV). Information regarding voltage, current, frequency, power quality, etc. of these devices can be periodically monitored. However, the environmental conditions in which these devices are installed cannot be monitored. Environmental conditions directly affect the service life and operational investment and costs of these devices. Therefore, due to environmental conditions, these devices age over time and the probability of failure increases.

In the Turkish electricity grid system, there are over 1000 switchgear and transformer centers at high voltage levels, and over 1 million distribution centers and local transformer centers (KÖK) at medium voltage levels. These centers are distributed throughout the geography of Türkiye. Therefore, sensors and software are required to monitor different atmospheric environmental conditions and calculate the operating life of devices in all centers. Recently, sudden temperature changes, storms, floods, and increased numbers of natural disasters caused by global climate change can lead to prolonged power outages in the energy transmission and distribution lines. As a result, unplanned increases in maintenance and repair costs occur.

## KEYWORDS

Predictable maintenance work, Asset management, PloT (Internet of Thing in Power, Industry), 5G, NB-IOT, Energy management system

Poster Presentation: Monitoring and Management of Ambient Conditions of the Electrical Grid with Sensor Network System

In residential and commercial areas, the increase in electric vehicles and technological devices in the coming years will make energy and environmental monitoring and control even more important. For this purpose, it should be possible to measure voltage and current data from low-voltage panels and sockets and perform energy switching operations. The monitorability and controllability of the low-voltage level will also serve as a guide in solving the energy supply-demand problem, determining where energy storage systems should be installed and where grid investments should be made.

In the field of energy, the desired amount of data from the field, the number of devices from which data is to be collected, the evaluation of data, and the number of data points that need to be analysed to prevent interruptions and faults, are doubling every two years. The distributed nature of renewable energy sources also fundamentally changes the traditional communication infrastructure. The necessity of establishing communication whenever needed, during any faults or problems, leads to new search for solutions instead of limited or inadequate communication infrastructures available today.

## 2. SMART GRID MODEL

Currently, new-generation information technologies represented by big data, cloud computing, IoT, AI, and blockchain are advancing. The information network infrastructure in the energy industry is being gradually developed, PloT technology is maturing, and advanced technology is being applied to various aspects of the grid. The development of the information network in the energy industry is shown in Figure 1.

In terms of power infrastructure transformation, blockchain, artificial intelligence, and other advanced technologies are accelerating and gradually elevating the infrastructure transformation. Infrastructure work continues, such as cloud platforms, high-performance data centers, satellite communication networks, business platforms, and data platforms. The integration between intelligent technologies based on image recognition/semantic recognition and traditional automation technology is becoming closer.

Equal importance is given to the integration and operation of advanced technology. The ability to utilize and operate energy production is being improved, the level of operation management is enhanced, smart control and automation technologies are fully implemented, and mobile operations and remote operations are widely applied. There is an urgent need for innovation in the construction of fundamental disciplines. The theoretical foundations supporting the self-consistent completion of advanced technologies such as deduction of the concept of artificial intelligence, quantum computing, independent operator construction, autonomous evolution, and cross-domain distribution are still in urgent need of improvement.

Smart grids and PloT evolve together to create an energy network that integrates energy flow, service flow, and data flow. PloT will create a powerful value creation platform and greatly enhance the operation and service capabilities of the power grid.

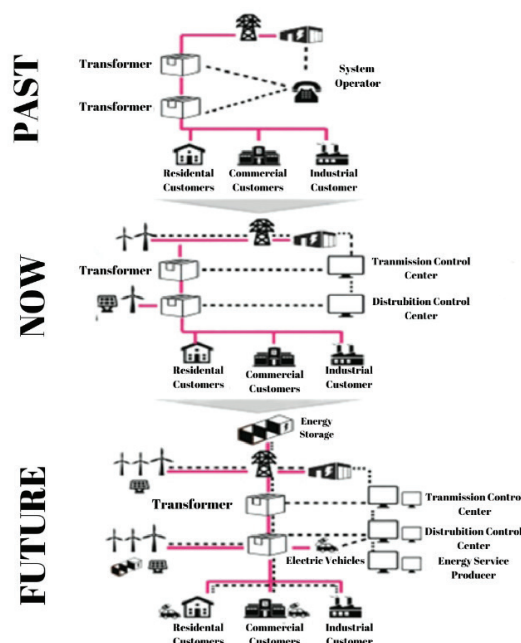


Figure 1: Development of the Electric Grid Structure[1]

Poster Presentation: Monitoring and Management of Ambient Conditions of the Electrical Grid with Sensor Network System

### 2.1. System Architecture

PLoT is an industrial IoT that enables the connection between humans and machines in the energy generation, transmission, and consumption sectors to achieve comprehensive sensing in the electric grid.

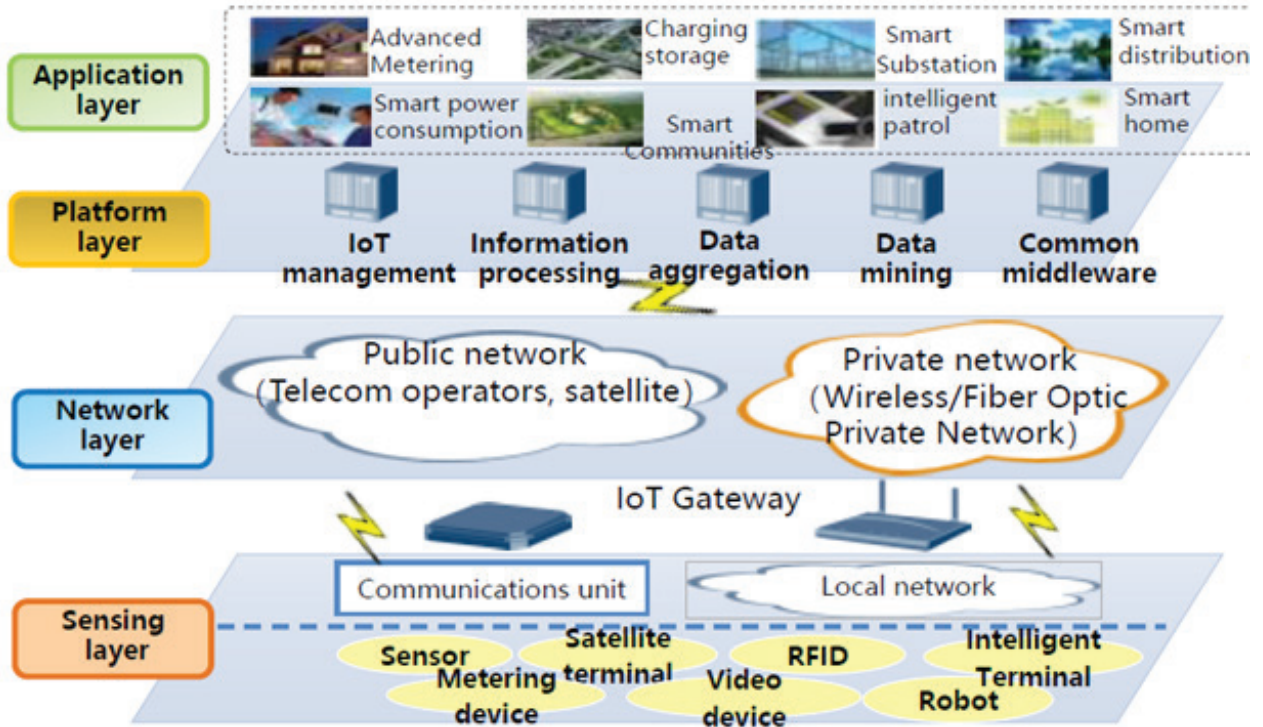


Figure 2: PLoT System Architecture And Layers [2]

The PLoT technical system encompasses five aspects, as illustrated in Figure 3

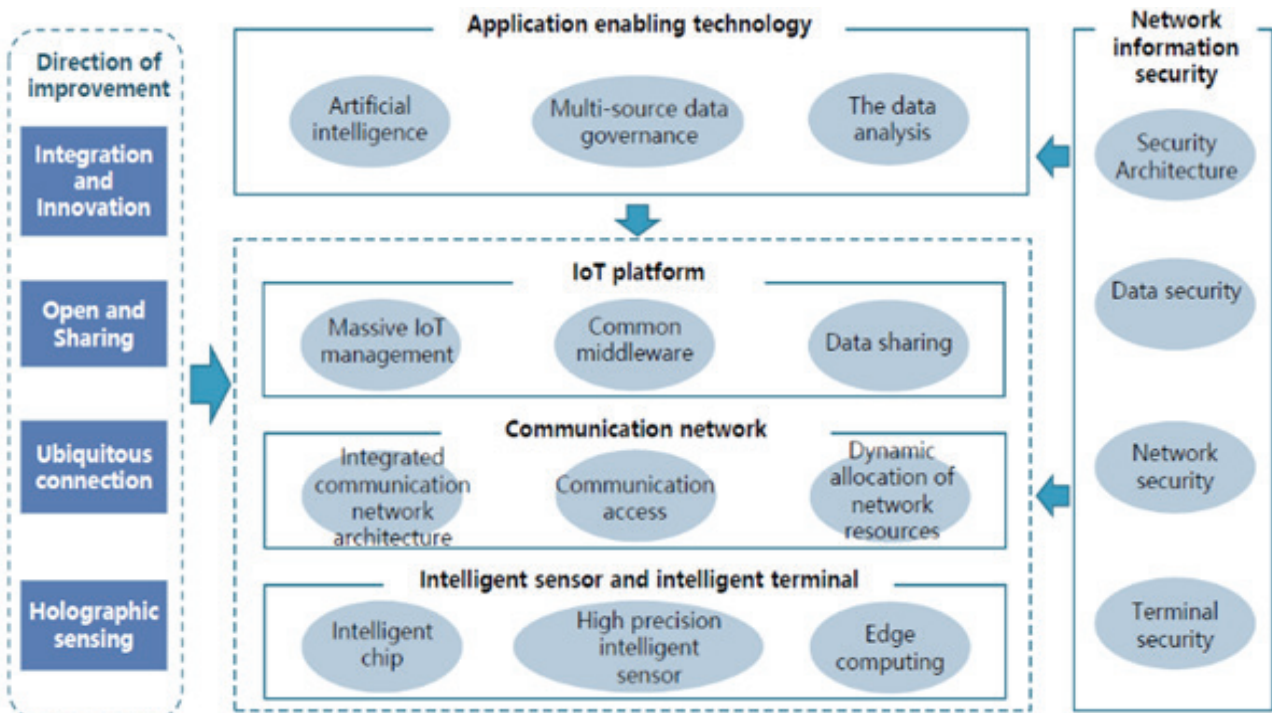


Figure 3: PLoT Technical System [2]

Poster Presentation: Monitoring and Management of Ambient Conditions of the Electrical Grid with Sensor Network System

### 2.2. Application Areas

From the current perspective, the electricity grid consists of four stages: generation, transmission/distribution, conversion, and consumption. PlOT transformation, as shown in Figure 4, will affect all these stages

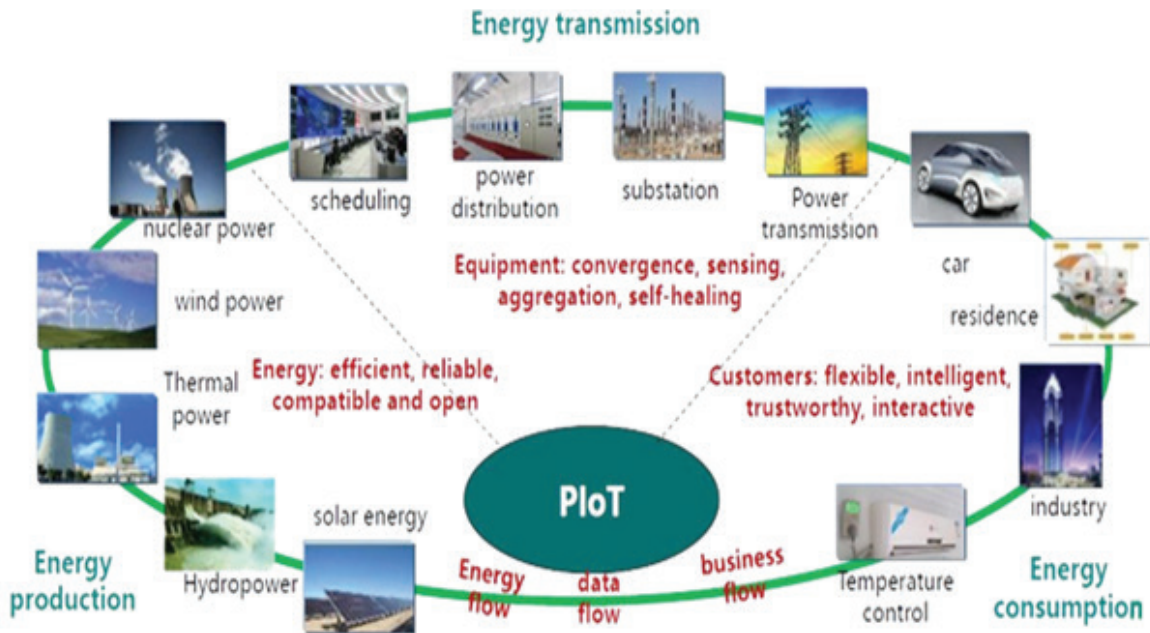


Figure 4: PlOT Applications [2]

It also affects the bandwidth to be transmitted. As devices advance, they provide more information, and operators need to analyse more data. While data transmission becomes crucial in the digitalization of the energy sector, new solutions have been developed to address the communication challenges depicted in Figure 5

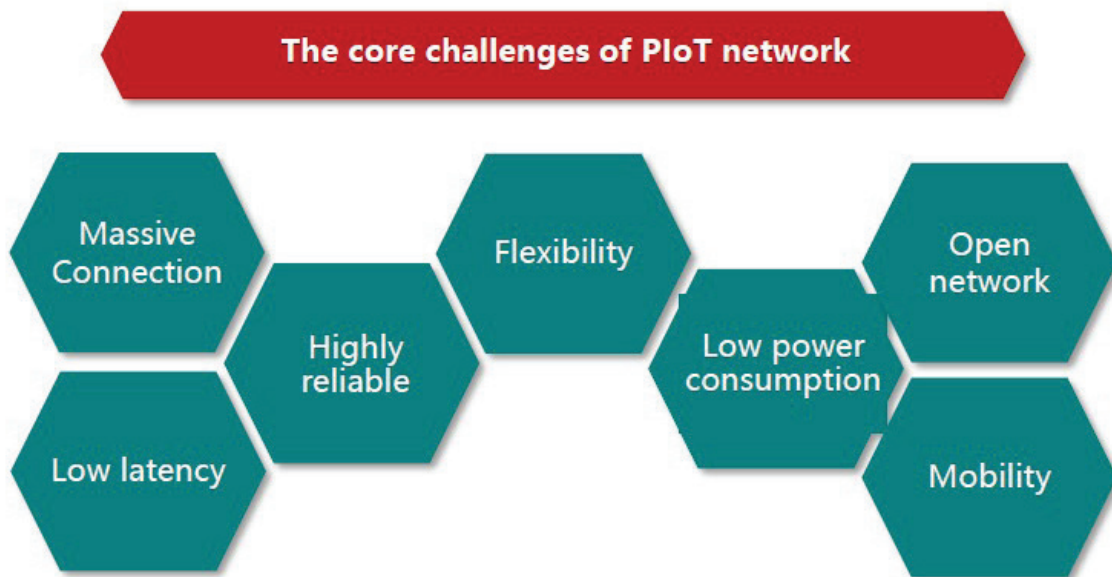


Figure 5: Key Challenges of the PlOT Network [4]

The challenges faced by PlOT technology will vary according to the operational scenarios. The four main scenarios that will occur in smart grids are illustrated in Figure 6

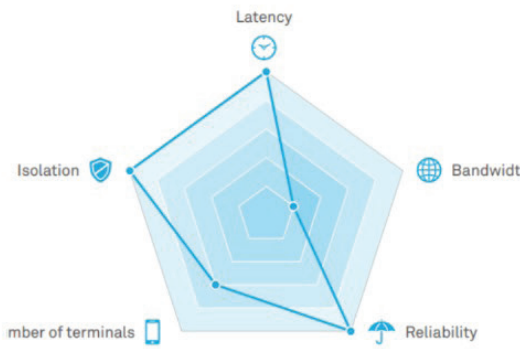




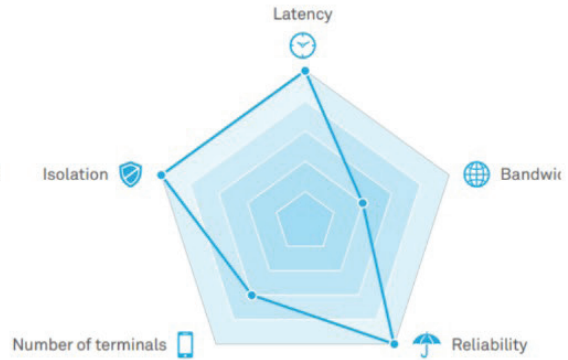
Poster Presentation: Monitoring and Management of Ambient Conditions of the Electrical Grid with Sensor Network System



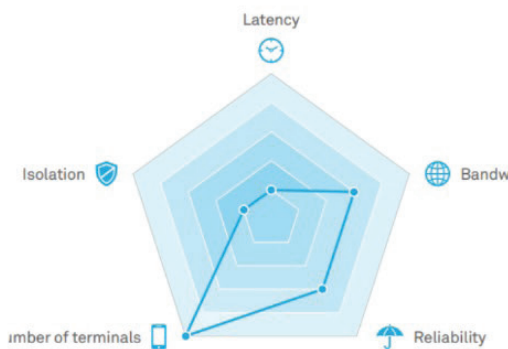
Intelligent distributed feeder automation



Millisecond-level precise load control



Information acquirment of low voltage distribution systems



Distributed power supplies

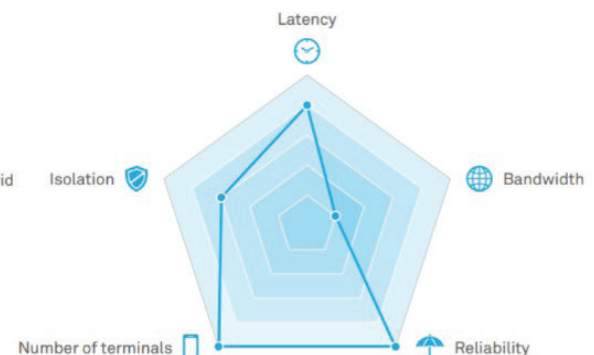


Figure 6: Smart Grid Operation Scenarios [4]

Poster Presentation: Monitoring and Management of Ambient Conditions of the Electrical Grid with Sensor Network System

**2.2.1. Energy Generation**

A power monitoring system can be used to automatically monitor and control the operation of distributed power sources. This system has many functions such as data collection and processing, active power adjustment, voltage/reactive power control, grid islanding detection, timing coordination control, and interconnection with relevant service systems.

**2.2.2. Energy Transmission/Distribution**

By using artificial intelligence algorithms on images obtained from helicopters or drones on energy transmission and distribution lines, faults/deficiencies can be detected, and appropriate adjustments can be made. Real-time images are obtained from devices powered by the electromagnetic field of the energy transmission line, and data on environmental conditions can be obtained through sensors. Predictable faults that can occur with real-time data acquisition can be anticipated, and planned maintenance work can be carried out.

**2.2.3. Energy Conversion**

Most faults that occur during energy transmission and distribution are usually originated from medium-voltage transformers. Since these transformers are mostly manually operated, they pose a danger to operating personnel depending on their location and distance.

In today’s electricity grids, smart grid applications are gaining importance in ensuring operational continuity and reliability. To minimize problems in transformer centers, it is necessary to have a monitoring and controllable structure for environmental conditions. With this structure, the economic lifespans of devices will be determined based on the environment they are in, necessary predictive maintenance work will be carried out, reducing operating costs, and ensuring continuity. Additionally, by obtaining energy and environmental data, the digital twin of the transformer/distribution center can be created, enabling the automated control of feeder outputs.

**2.2.4. Energy Consumption**

The increasing use of electricity, which is a fundamental parameter of daily life, along with the limited availability of energy sources with opposing reactions, has led governments and consumers to seek alternative solutions, direct their existing energy consumption towards efficient usage, and plan for reducing losses. In this context, it has become necessary to monitor and manage energy at the low voltage level.

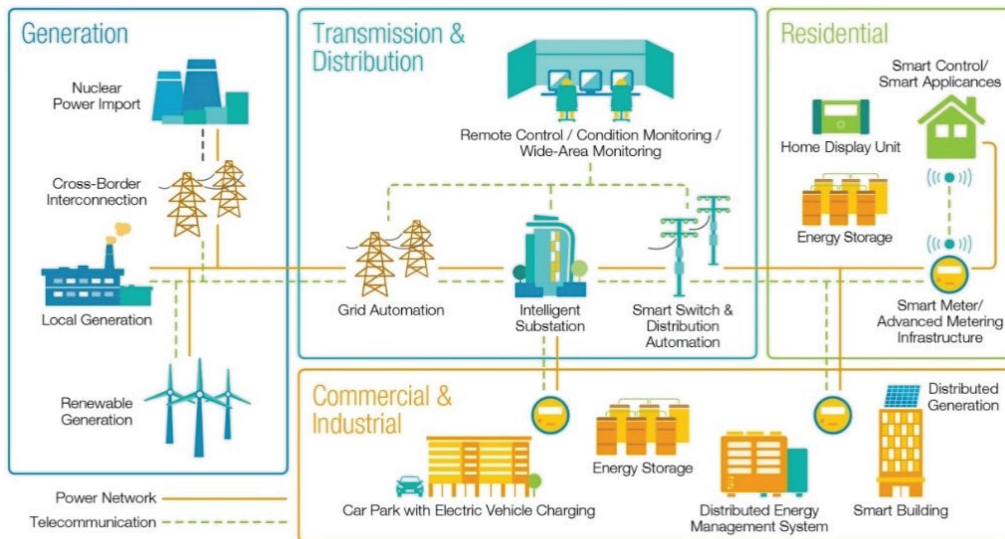


Figure 7: Application Areas

**2.3. IIoT Communication Technologies**

Renewable energy sources, smart devices (meters, sensors, thermostats, etc.), monitoring, and visualization solutions are increasingly digitizing Control Centers. This offers better decision-making capabilities with a wealth of previously unobtainable data,



Poster Presentation: Monitoring and Management of Ambient Conditions of the Electrical Grid with Sensor Network System

enabling faster and more accurate decision-making in the face of events. As a natural outcome of digitization, the capacity to be used in communication stands out in the PloT network considering the challenges faced and the smart grid operation scenarios.

### 2.3.1. 5G

5G is the latest level of cellular technology designed to significantly increase the speed and responsiveness of wireless networks. Data transmitted over wireless broadband connections with 5G can move at multigigabit speeds, potentially reaching up to 20 gigabits per second (Gbps) according to some estimates. This feature enables us to access high-resolution content much faster. Another key feature of 5G technology is the reduction of latency to less than 1 millisecond. In comparison, current 4G technology has an average latency of around 100 milliseconds. 5G is a game-changing technology for real-time applications.

Another benefit is the high number of connections that can be supported. The higher the number of connections, the greater the efficiency. This means that with an increased number of connections, a larger number of IoT applications can be implemented. 5G is described as capable of supporting hundreds of thousands to millions of devices per square kilometer.

With these features, 5G will serve as the foundational communication system for PloT networks.

The architecture of 5G is based on intelligent software and “virtual” hardware. Instead of relying on physical hardware that can be prone to security breaches, data is routed through virtual hubs and switches that can be quickly moved or replaced as needed, ensuring the security of your data.

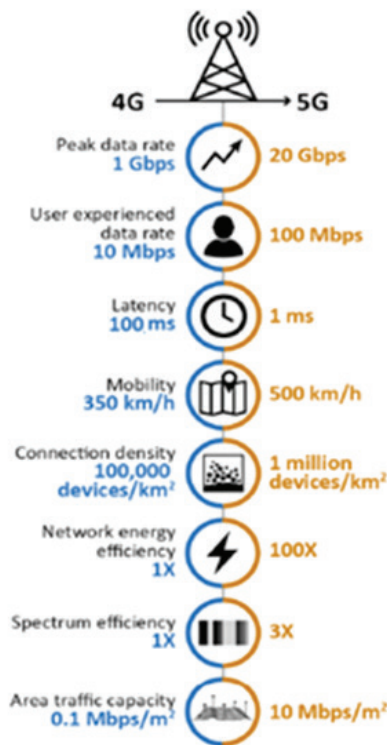


Figure 8: Comparison of 4G and 5G

### 2.3.2. NB – IOT

NB-IoT stands out with its low cost, wide coverage, and large-scale connectivity support, but it also has disadvantages such as low bandwidth, slow data transmission speed, and low operating frequency. It is suitable for remote meter reading and smart management of various meter devices, solving the problem of long-distance transmission of meter data. The NB-IoT cloud management endpoint consists of a network formation method, user device terminal, NB-IoT base station, core network, IoT cloud platform, and industrial application equipment. A notable feature of NB-IoT is the ability to directly upload collected data to the cloud without passing through a gateway, simplifying the distribution process. NB-IoT devices mounted with IoT cards connect to the NB-IoT network. Such devices receive and send information via the base station and connect to the IoT cloud platform through the core network. The IoT cloud platform sends the final data to the user device terminal through information processing and computation.



Poster Presentation: Monitoring and Management of Ambient Conditions of the Electrical Grid with Sensor Network System

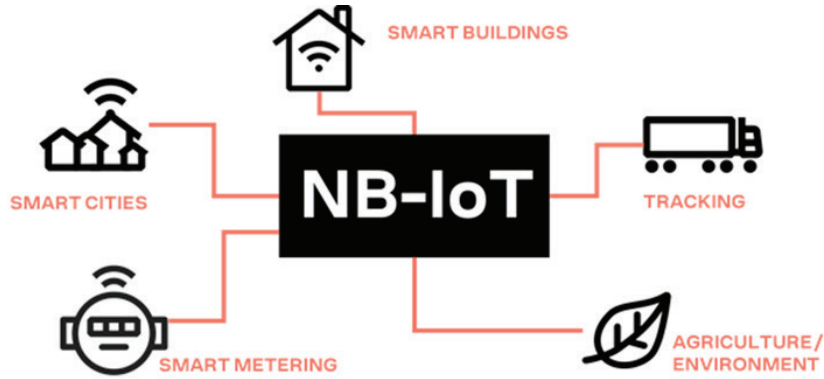


Figure 9: NB-IoT in Energy System

### 2.3.3. Wi-Fi 6

Wi-Fi 6 is a next-generation standard in Wi-Fi technology. Developed in response to the increasing number of devices trying to connect to the internet simultaneously, Wi-Fi 6, also known as “802.11ax,” takes Wi-Fi technology a step further.

Wi-Fi 6 elevates Wi-Fi technology with high speeds approaching the speed of light and significantly extends coverage for home and industrial applications. With its technology, Wi-Fi 6 can overcome connection and speed issues caused by structural factors such as walls and distances, enabling efficient internet usage over long distances.

Wi-Fi 6 strengthens Wi-Fi connectivity within homes, allowing for more efficient and low-latency connections to Wi-Fi networks through an artificial intelligence solution.



Figure 10: Wifi-6

## 3. EXPERIENCES AND OUR VISION

The ideas and projects carried out so far aimed to generate faster and more optimized digital solutions for the energy sector. They involve addressing disruptions caused by climate change, redefining standards, and taking the necessary precautions accordingly. Additionally, depending on the emerging environment, it is envisaged to identify new devices or revise existing ones to meet present-day conditions. In addition to all these, solutions are being developed to address issues brought about by storage systems, Digital Twin solutions, SES (Solar Energy Solutions), WES (Wind Energy Solutions), and electric vehicles.

Poster Presentation: Monitoring and Management of Ambient Conditions of the Electrical Grid with Sensor Network System

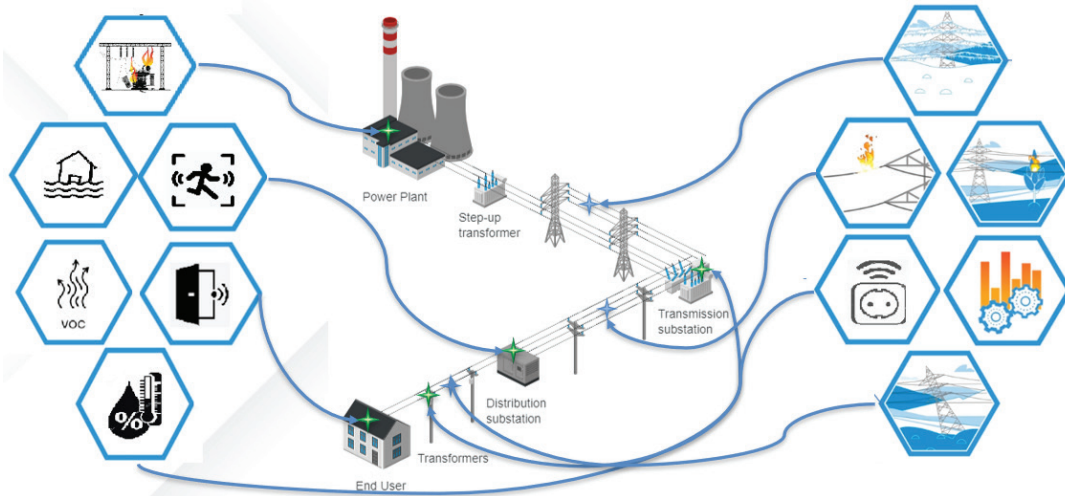


Figure 11: Roadmap in the Turkish power system



Figure 12: Aims as a company

## 4.CONCLUSIONS

Based on the information obtained from the CIGRE WG D2.53 working group and close monitoring of technological developments in countries, we have created a roadmap regarding how digitization should progress in the Turkish power system.

This roadmap aims to enable the acquisition of field data in the Turkish electricity system using IoT technology and in line with Industry 4.0, design devices and software that are compatible with new technologies, enable the monitoring and remote intervention of the energy system up to the edge, predictability of faults and workforce, minimize investments through risk-based assessment, create a national and indigenous system, and prevent cyberattacks and security vulnerabilities.

## BIBLIOGRAPHY

- [1] Baloğlu, Ulaş Baran, « AKILLI ŞEBEKELERDE HESAPSAL YÖNTEM UYGULAMALARI», 2017
- [2] CIGRE D2. Group Discussion 2021.
- [3] 5G PPP, [https://5g-ppp.eu/wp-content/uploads/2014/02/Advanced-5G-NetworkInfrastructure-PPP-in-H2020\\_Final\\_November-2013.pdf](https://5g-ppp.eu/wp-content/uploads/2014/02/Advanced-5G-NetworkInfrastructure-PPP-in-H2020_Final_November-2013.pdf), 2013,
- [4] 5G Network Slicing Enabling the Smart Grid, <https://www-file.huawei.com/-/media/CORPORATE/PDF/News/5g-network-slicing-enabling-the-smart-grid.pdf>
- [5] 5G ve Ötesi / BEYAZ KİTAP <https://www.btk.gov.tr/uploads/announcements/5g-ve-otesi-beyaz-kitap/beyaz-kitap-son.pdf>
- [6] <https://www.superonline.net/tr/wifi>



# Digitization of DSO Business Processes Based on the Agnostic Relational Model of Process Flows on the Example of Public Enterprise Electric Utility of Bosnia and Herzegovina

[j.heljic@epbih.ba](mailto:j.heljic@epbih.ba)**JASMIN HELJIĆ\*, EMINA KREŠTALICA***JP Elektroprivreda BiH d.d. - Sarajevo***Bosnia and Herzegovina**

## SUMMARY

DSO business processes represent a huge area for digitization which is essential for improving efficiency and adding new value. These processes are well-defined and verified in everyday work. Generally, each DSO process consists of a finite number of sequential phases and mandatory activities which has to be done in order to complete one process cycle. For example, the end customer/generator, i.e., the investor, who plans to connect its building to the distribution network shall submit an application for the initial electric power permit to the DSO which will trigger the process cycle for issuing a DSO permit. During this process cycle, many activities need to be done, but those activities are well-known and prescribed by the internal rules of DSO.

This means that the DSO business process structure by its nature can be represented in the relational model. This is very important for creating a stable base of process flows. The structure of process flow can be represented by a combination of three elements: process identification which can be derived from a type of customer request, a role within the company responsible for processing a defined set of activities, and software processing point which is derived from real activities in a specific process phase defined by the DSO.

The process identification defines the type of service the customer wants from DSO. For instance, the end customer who plans to connect its building to the distribution network shall submit an application for the initial electric power permit to the DSO in writing, on a standard form prescribed by the DSO meaning each DSO business process has a unique identification. The software processing point is a software logical unit based on prescribed activities for employees in a specific process phase in some of the distribution processes and the processing role is the software entity that defines the obligations and duties of the employee in the DSO for the specific work segment.

Using hierarchical queries to retrieve process flow structures represented by combinations of the above entities in a software system that automates the DSO business process we can create a stable software infrastructure that eases everyday activities.

## KEYWORDS

DSO Business Processes, Digitalization, BPM, DSO, Automation, Relational Model, Database Modeling, Process Flows



**Poster Presentation:** Digitization of DSO Business Processes Based on the Agnostic Relational Model of Process Flows on the Example of Public Enterprise Electric Utility of Bosnia and Herzegovina

### 1. INTRODUCTION

As a rule, the business processes of DSO are organized business processes, considering the role of DSO as a pillar of the electric power system. What should be kept in mind is that the DSO will become a much more dynamic system in the future, and the boundaries between electricity customers and companies will become more complex. There is a spectrum of potential DSO models ranging from highly centralized to highly distributed. Factors that influence the DSO model are regulators, politics, legislation, network constraints, and other local conditions. [1]

Depending on the model of the DSO, the structure of business processes will also depend. Many business processes are specific to the company because their structure is influenced by internal regulations in addition to external factors.

Automation and digitization of business processes in the form of software solutions that support processes are a great benefit for businesses. In this paper, we will try to present the concept of modeling ODS business processes based on the agnostic relational model of process flows on the example of the Public Enterprise Electric Utility of Bosnia and Herzegovina which can significantly facilitate the development of enterprise information systems.

### 2. IN-HOUSE DEVELOPMENT OF ENTERPRISE INFORMATION SYSTEMS

Electric power companies that have in-house software development can take into account the specifics of the way of work that is inherent to the company, unlike ready-made packages that exist on the market.

Enterprise system development is a specialized area of software engineering focused on creating software solutions that are used by small and large organizations to support their daily business operations. This type of software development is used to develop software with specific and complex tasks and processes and usually requires teams of people to analyze, build, test, integrate, implement, and maintain. The focus of enterprise system development is on the needs of the organization, not the individual user. The development of enterprise software enables organizations to standardize their processes, improve the productivity and efficiency of employees, and have insight into the entire business, as well as constant optimization of costs and risks. [2]

Companies usually use in-house software development in case of trivial or complex and unusual requirements. [3] Complex and unusual requirements are what makes a particular company's business specific. Those specifics are very complex for generalization, which leads us to the conclusion that internal knowledge about processes is a key factor in the process of automation and digitization.

On the other hand, the structure and nature of business processes can significantly affect the efficiency of the development of enterprise solutions. ODS business processes are mostly sequential processes that can be divided into a finite number of discrete phases, which by its nature represents a stable basis for software requirements. The software development of enterprise information systems can be improved by using a defined model for representing business processes on automation and digitization projects in ODS.

### 3. BUSINESS PROCESS MODELING

In principle, each ODS process consists of a finite number of sequential phases and mandatory activities that must be performed in order to complete one process cycle. For example, the end customer/producer, i.e. an investor who plans to connect the facility to the electricity distribution network will submit a request for a preliminary electric power consent to the competent DSO, which will start the process cycle for issuing consent. During the process cycle, many activities are performed that are well-known and prescribed by the internal rules of the DSO. This means that the structure of DSO business processes can by its very nature be presented in a relational model, which is one of the most widespread models for modeling real problems and dynamic data management.

The basic idea is the use of relations, which represent sets of data in a logical form that refers to a specific entity. An entity represents a person, object, event, or concept in the user environment about which data needs to be stored and monitored. Each relation is represented as one table. One column of a relation usually contains the value of one attribute, which has its own name by which we distinguish it from others in the same relation. The values of one attribute are data of the same type. A single relation row typically represents a single instance of an entity or records a relationship between two or more instances.

The combination of several relations opens up many possibilities of representing not only a certain object but also the process flow as a defined structure of events that should result in some value or result.





**Poster Presentation:** Digitization of DSO Business Processes Based on the Agnostic Relational Model of Process Flows on the Example of Public Enterprise Electric Utility of Bosnia and Herzegovina

### 4. ELEMENTS OF A BUSINESS PROCESS

We can present business processes in different ways: descriptively, graphically, mathematically, etc. Developers who develop an information system within ODS use available information about business processes in order to design the system architecture in the best way. Business processes can be logically grouped according to the field of business, for example, business processes from the segment of issuing electricity consents to end customers, processes from the segment of connection to the electricity distribution network, processes from the domain of resolving property-legal relations, etc.

We can mark each of these areas in a certain way, e.g. in capital letters of the alphabet: A - business processes from the segment of connection to the ED network, B - from the domain of resolving property-legal relations, etc. Furthermore, each business process within a certain segment can be labeled according to the principle, A1, A2, A3, etc. With this, we have already made an initial identification of the process.

The second step is to analyze the processes that belong to a certain segment in order to define discrete logical units that include a common set of activities, which can be viewed as separate processing points that represent a sequential step in the unfolding of the process. For example, we can mark processing points with capital letters A, B, C, D, etc. An example of a processing point can be the receipt of a request for a specific service marked with the letter A. The receipt of a request represents the first step in the sequence and belongs to all processes from A1 to An. The second processing point can be, for example, the control of the attached documentation, which we will mark with the letter B, the third assignment of the case to the processor, which we can mark with the letter C, etc.

It is important to identify all processing points, i.e. the longest process sequence that belongs to a certain segment of business processes. With this, we created the prerequisites to present each process from a certain segment as a set of a certain number of processing points, e.g.  $A1=\{A, B, C, D\}$ ,  $A2=\{A, C, D\}$ ...  $An=\{A, C, F, G\}$ . Processes do not necessarily have all processing points. This is conditioned by the nature of the business process.

An example of a hypothetical business process A1 for the preparation of an electric power consent in DSO could look like this:

- A** Receipt of requests
- B** Scheduling requests
- C** Documentation control
- D** Drafting of consents and contracts
- F** Control of consents and contracts
- H** Archiving of consents and contracts
- M** Receipt of the signed contract
- N** Assignment of contracts for implementation
- O** Work order
- P** Deployment of usage contracts
- Q** Creating a usage agreement

On the other hand, the business process for concluding a new contract for the user identified as A2 could look like this:

- A** Receipt of requests
- C** Documentation control
- P** Deployment of usage contracts
- Q** Creating a usage agreement

Note that process A1 and A2 have common points A, C, P, and Q, but process A1 has other points that are not used by process A2: B, D, F, H, M, N, O.

### 5. TRANSLATION OF A BUSINESS PROCESS INTO A RELATIONAL MODEL

In order to create a flexible business process modeling concept in business process support applications, we need to introduce an additional application element. It is a place of data processing, which refers to a role within a business process, and not to a formal





**Poster Presentation:** Digitization of DSO Business Processes Based on the Agnostic Relational Model of Process Flows on the Example of Public Enterprise Electric Utility of Bosnia and Herzegovina

affiliation to one of the organizational parts of the company, which is a variable category. For example, the energy worker represents a role that is constant in ODS. The power engineer is a necessary role in the preparation of power consents, and on the other hand, he can formally belong to different organizational parts, whereby the names and roles of individual organizational parts can change over time. Therefore, roles should be separated from the organizational scheme, so that the business process remains stable during organizational changes. After clearly defining the roles that are part of the business processes, we acquire the conditions to associate the processing points of a certain process with the roles, i.e. places of processing.

In the example of the A1 hypothetical business process, we can do the following translation:

**Role: Counter worker**

- A** Receipt of requests
- B** Scheduling requests
- C** Documentation control

**Role: Energy worker**

- D** Drafting of consents and contracts
- F** Control of consents and contracts
- H** Archiving of consents and contracts

**Role: Counter worker**

- M** Receipt of the signed contract

**Role: Energy worker**

- N** Assignment of contracts for implementation
- O** Work order

**Role: Lawyer**

- P** Deployment of usage contracts
- Q** Creating a usage agreement

If we categorize processing points by roles, we get the following sequences of business process A1, that is, a set of activities for a particular role:

**Role: Counter worker**

- A** Receipt of requests
- B** Scheduling requests
- C** Documentation control
- M** Receipt of the signed contract

**Role: Energy worker**

- D** Drafting of consents and contracts
- F** Control of consents and contracts
- H** Archiving of consents and contracts
- N** Assignment of contracts for implementation
- O** Work order

**Role: Lawyer**

- P** Deployment of usage contracts
- Q** Creating a usage agreement

Each of the above sequences is visible only to the role for which it is intended. The subject moves sequentially from point to point, that is, from role to role, with everyone doing the work for which they are responsible.

Poster Presentation: Digitization of DSO Business Processes Based on the Agnostic Relational Model of Process Flows on the Example of Public Enterprise Electric Utility of Bosnia and Herzegovina

The nature of the business process implies that the data model on which the processing point is based may differ to some extent from process to process. For example, the processing point that implies the control of the attached documentation in the process of drafting the electric power consent is different from the control in the process of concluding a new contract, because the documentation itself is not identical. This is solved in the relational model by observing each point uniquely at the level of the process to which it belongs, although activities such as checking, validation, and data entry are still the same. A processing point represents a container that can have different contents depending on the process.

### 6. AN EXAMPLE OF THE IMPLEMENTATION OF THE MODEL IN ELECTRIC UTILITY OF BOSNIA AND HERZEGOVINA

Distributed Information System For Customer Connections (DISP) is custom-made software constructed to significantly digitize processes managed by the DSO of Electric Utility of Bosnia and Herzegovina (EPBiH), especially the customer/generator connection process. It is based on the General Conditions for Electricity Supply prescribed by the Regulatory Commission for Energy as well as a procedural framework (internal procedures) by the Electric Utility of Bosnia and Herzegovina. [4]

The customer/generator connection process contains many steps which are dispersed across different segments of the company, starting from the request for connection to the distribution network application in one place, going through the department of power engineering which defines the technical conditions of the connection process, to contractors who are responsible for setting up customer connection and finally to financials and bookkeeping and accounting departments.

Using the relational model described above DISP incorporated and unified around 30 different processes related to customer connections.

Point A in the request form for obtaining a power permit for the end customer (labeled Z03 in EPBiH) doesn't have the same scope of activities as the scope in process Z15 (contract assignment). In other words Zxy – A combination uniquely identifies the application segment of activities and works in point A within process Zxy. Combining this relation with the place of data processing produces a unique sequence for any type of work from the procedural framework. These sequences are called branches in DISP terminology. The places are assigned to the users based on the real work of employees. Figures 1 and 2 depict the logical and physical model of the DISP.

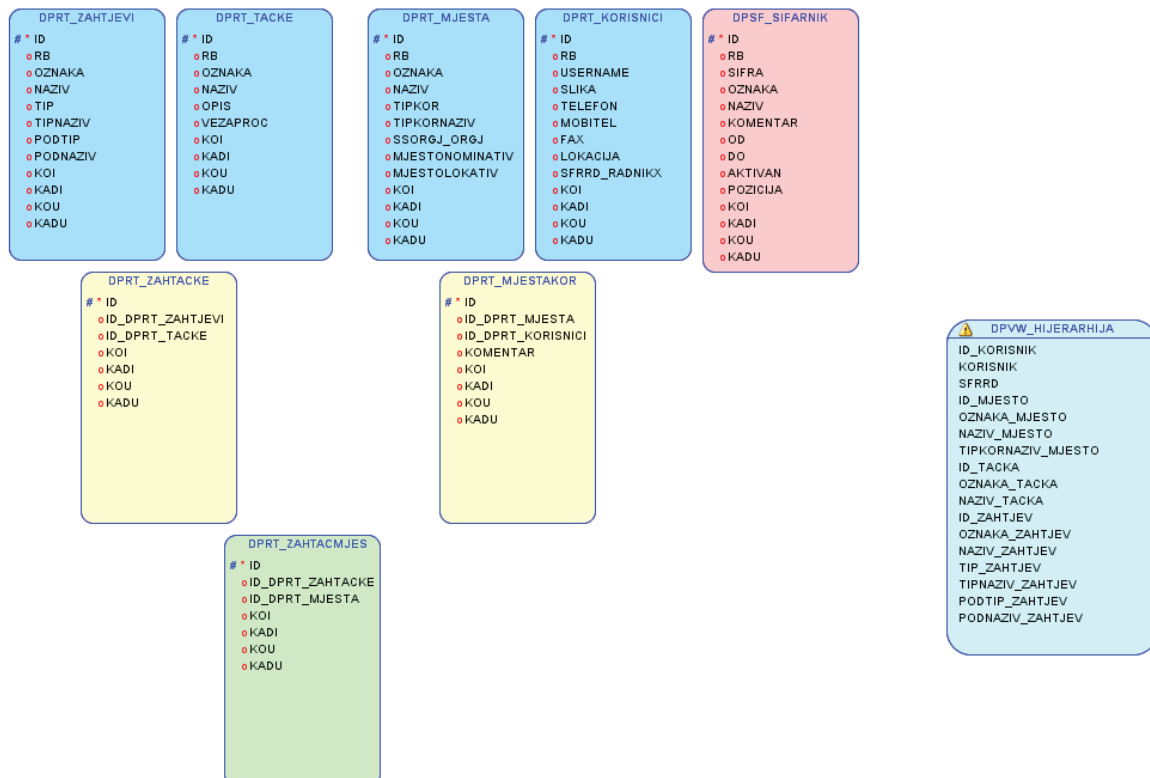


Figure 1. Logical model of DISP presented in Oracle SQL Developer Data Modeler

Poster Presentation: Digitization of DSO Business Processes Based on the Agnostic Relational Model of Process Flows on the Example of Public Enterprise Electric Utility of Bosnia and Herzegovina

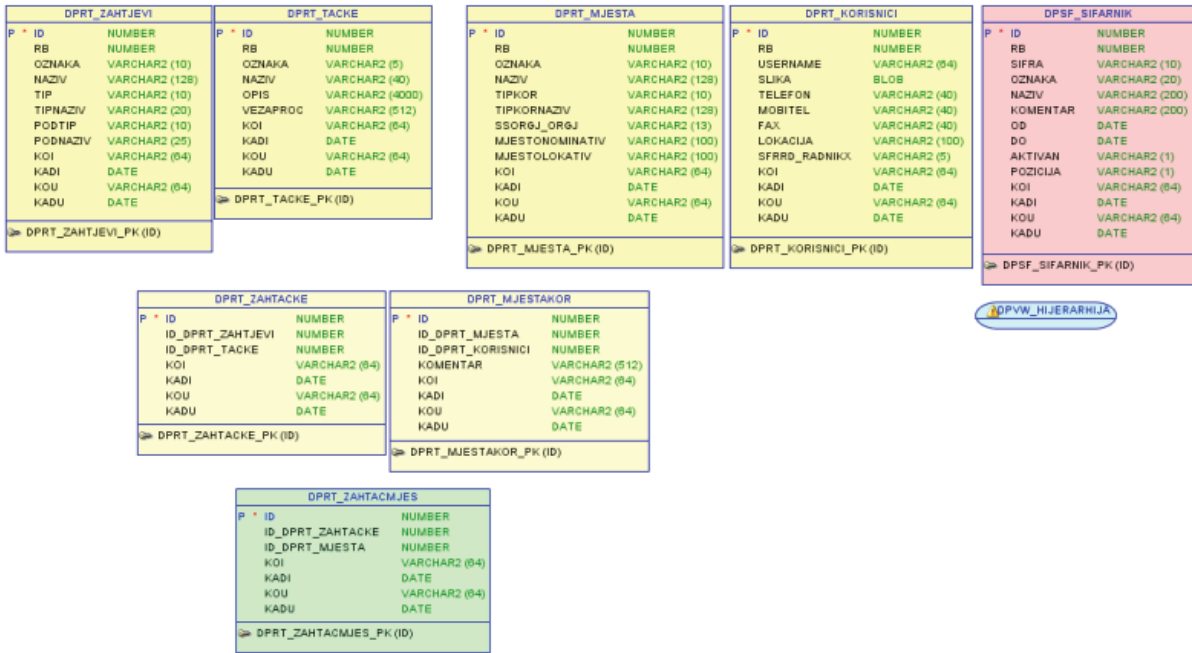


Figure 2. Physical model of DISP presented in Oracle SQL Developer Data Modeler

The data foundation for a processing point is defined by the data model. The logical data model was developed after a detailed analysis of request forms and all other documents which are part of the procedural framework. Besides the official documents, other data were analyzed which are obtained and used from different internal practices of the employees. The processing points are based on the transactional table.

The process flows modeling through the described relational model becomes the basis for creating a simple user interface. Methods that retrieve relational records which represent processes from a database can be translated into a hierarchical tree structure at the application layer as shown in Figure 3.

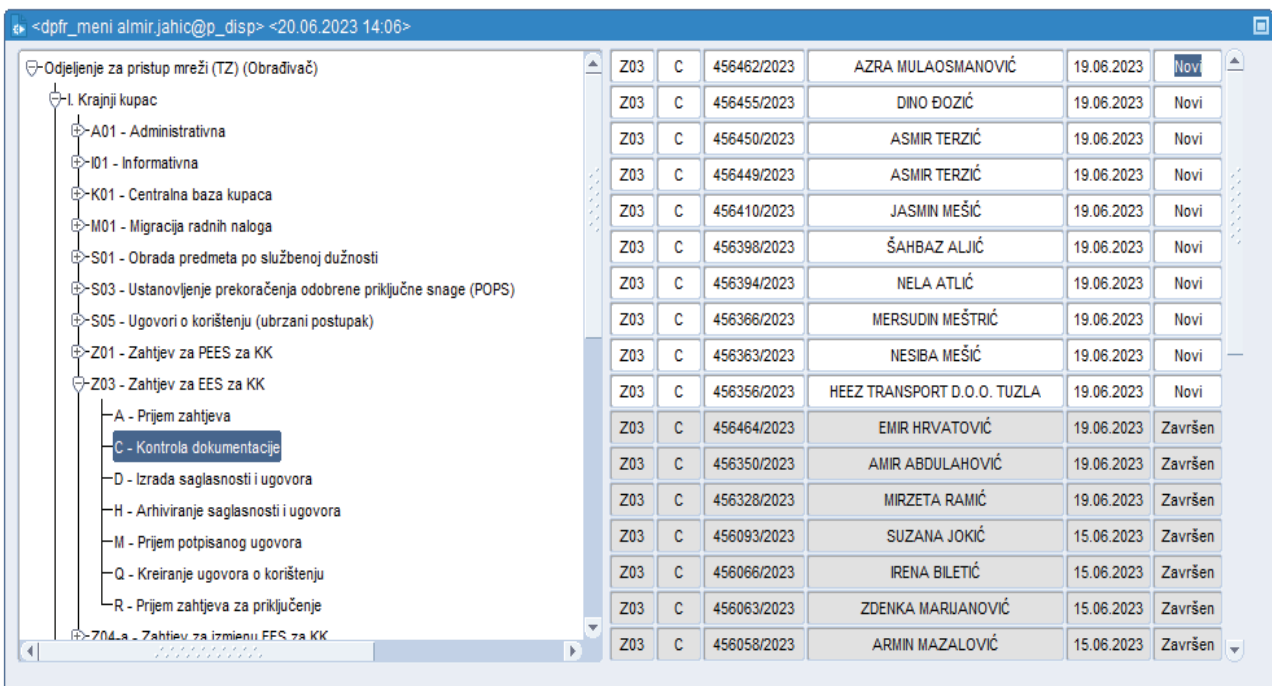


Figure 3. User interface based on hierarchical tree



**Poster Presentation:** Digitization of DSO Business Processes Based on the Agnostic Relational Model of Process Flows on the Example of Public Enterprise Electric Utility of Bosnia and Herzegovina

The application layer is uniform and easy to use. Due to the fact that the system logic is stored within the database, the application layer is quite simple to maintain. Some specific situations related to process flows had to be defined within the application layer instead in the database, but these situations are very rare and don't affect the simplicity of the code. The DISP user interface is the same for every user. It is divided into two areas. The left area contains a hierarchical menu adapted to every place of data processing, and the right area contains the list of customer cases (requests) which can be filtered based on the chosen level of the hierarchical menu from the left area. The root of the hierarchical menu is the place of data processing (ie employee's role within the process). When the hierarchical menu is expanded every user will be able to see just those sequences of processing points which are related to predefined activities within his or her scope. The sequence depends on the request type and place of data processing.

## 7. CONCLUSION

The structure of process flow can be represented by a combination of three elements: process identification, a role within the company responsible for processing, and a software processing point. By using a relational model to describe process flows, most of the business logic can be stored in the database, thus simplifying the maintenance of existing and adding new processes. The application layer, on the other hand, becomes more fluid and intuitive for use by users within DSO.

Due to the fact that DSO will become a much more dynamic system in the future, it is very important to be agile and able to adjust enterprise information systems to new realities. The agnostic relational model of process flows presented in this paper was tested and verified in the Electric Utility of Bosnia and Herzegovina. It has been in use for more than 10 years, and it has proven to be a very efficient and stable foundation for the digitization of business processes in the company.

## BIBLIOGRAPHY

- [1] Distribution System Operator (DSO) Models for Utility Stakeholders Available at: [https://webassets.bv.com/2020-02/20 Distribution System Operator Models for Utility Stakeholders WEB updated 022720.pdf](https://webassets.bv.com/2020-02/20%20Distribution%20System%20Operator%20Models%20for%20Utility%20Stakeholders%20WEB%20updated%20022720.pdf)
- [2] Iryna Kravchenko, "Enterprise software development: Full guide", 20 Apr 2022 Available at: <https://diceus.com/enterprise-software-development-guide/>
- [3] Clydebuilt Business Solutions White Paper: Developing In-House vs. Off the Shelf, 2012
- [4] General Conditions for Electricity Supply. Mostar, FERK, 24 October 2014. Available at: [http://www.ferk.ba/\\_en/images/stories/2017/ferk\\_general\\_conditions\\_electricity\\_%20supply\\_89\\_2014.pdf](http://www.ferk.ba/_en/images/stories/2017/ferk_general_conditions_electricity_%20supply_89_2014.pdf)



**ELECTRIC MACHINES AND  
POWER ELECTRONICS**

**ORAL PRESENTATION**

**ELECTRIC MACHINES AND  
POWER ELECTRONICS**



**ELECTRIC  
TRANSMISSION**



**AUTOMATION AND  
CONTROL**

**POWER  
GENERATION**



**ENERGY  
TRANSITION**



**DISTRIBUTION SYSTEMS  
AND SMART GRIDS**



**11-12 OCTOBER 2023**



# Determination of the Location of Partial Discharges in the Power Transformer Model Using UHF Sensors

djordje.dukanac@ems.rs

**DJORDJE DUKANAC**

Joint Stock Company "Elektromreza Srbije"

Serbia

## SUMMARY

Power transformers are essential components of power generation plants, transmission systems and large industrial plants. Any malfunction of the power transformer would reduce the reliability of the power system. The reliable operation of power transformers is important for the safety of the supply of electricity to consumers and mainly depends on the state of the electrical insulation of the power transformer. Therefore, all types of internal insulation damage in the power transformer should be determined as soon as possible. Partial discharges (PDs) are a reliable indicator of the condition of the electrical insulation. Partial discharges caused by initial weaknesses in the insulation system of the power transformer cannot be completely ignored, because they can warn in advance of possible serious deficiencies, which in the worst cases could cause irreversible failure of the power transformer. In general, partial discharge can occur at voltages higher than 5 kV.

Using simulations in Ansys HFSS (High Frequency Structure Simulator) and three different models of power transformer construction from simple to the most complex one, this paper investigates waveforms and delays of ultra-high frequency (UHF) PD electromagnetic signals at four UHF sensors mounted at different locations of a small power transformer tank of core construction. Then location of PD source was determined. Full-wave electromagnetic simulations are performed on the model of a small power transformer of core construction. Electromagnetic waves are emitted and received by dipole antennas as source of partial discharges in the insulation of the power transformer and UHF sensors.

The active parts of the power transformer can influence the shape and size of the received signals on UHF sensors, the source of which is a partial discharge in the electrical insulation of the power transformer. At the same time, the attenuation and distortion of the signal on the receiving UHF antenna is all the greater if the path of the partial discharge signal is more distorted in relation to the straight line that connects the source of the partial discharges and the corresponding UHF sensor.

All reflections of electromagnetic UHF PD waves from the walls of the tank, three-phase magnetic core and three-phase primary and secondary windings are taken into account. All diffractions of UHF PD waves around active metal parts and through narrow apertures of winding coils and disks of transformer are included. The simulation is based on finite element method. It is a numerical method that is applied to differential equations with limit values in order to obtain an approximate solution. The underlying problem is defined here as high-frequency problem, as opposed to a quasi-static problem or a low-frequency problem. Advantages and disadvantages of this computer simulation will be described.

## KEYWORDS

Partial Discharge (PD) – Power Transformer – Signal propagation – Source location – UHF sensor – Ansys HFSS





**Oral Presentation:** Determination of the Location of Partial Discharges in the Power Transformer Model Using UHF Sensors

## 1. INTRODUCTION

Finding the location of partial discharges (PDs) in a simplified power transformer model using two, three or four ultra-high frequency (UHF) transmitters, using simulations in MATLAB, with some basic assumptions (i.e. suitable delayed limit PD waveforms, appropriate mineral oil dielectric permittivity, and average signal attenuation in the oil) is presented in [1]. In [2], simulations of UHF partial discharge signal propagation using finite-difference time-domain (FDTD) modelling were carried out using the XFDTD 7.0 software, taking into account transformer tank, cylindrical or cuboid obstacle. In [3], a computational model of the power transformer was built in CST Microwave Studio and was used to evaluate attenuations of PD signals and, on the basis of them, find optimal UHF sensors positions. .NET Windows Presentation Foundation (.NET WPF) and Helix 3D were used to model the transformer structure with simplified obstacles in [4]. In [5], results of attenuations of UHF PD signals in 3-D computational model of oil-filled transformer tank with winding and results gained from appropriate experimental setup were compared. In [6], PD Location in Power Transformers was carried out on experimental configuration with two different obstacles, one of the core and the second of the winding. Two sensor diamond-shaped arrays were used with four UHF sensors each. FDTD technique was used to simulate propagation of UHF PD signals in simplified model consisting of conductive transformer tank with mineral oil in [7]. In [8], it was resulted that PD pulses with steeper front time cause to smaller energy and peak values of the acquired UHF signals. In [9], four electric field probes and binary particle swarm optimization method were used in PD source location in a power transformer model using finite integration technique (FIT) in simulation software CST Microwave Studio. In MATLAB, the non-iterative method was executed for PD location using the time difference of arrival of the UHF signals and the coordinates of the UHF sensors in [10]. It had been observed in [11] that the sensor location had no significant effect on the observed UHF PD waveforms on electric field sensors. In [12], the simulation results show that the sensors will receive a stronger signal when the distance to the PD source is reduced and the amplitude of the EM wave is drastically weakened after diffraction on the windings and core.

Using simulations in Ansys HFSS and three different models of power transformer construction from simple to the most complex one, this paper investigates waveforms and delays of UHF PD electromagnetic signals at four UHF sensors mounted at different locations of a small power transformer tank of core construction. Then location of PD source was determined. Full-wave electromagnetic simulations are performed on the model of a small power transformer of core construction. Electromagnetic waves are emitted and received by dipole antennas as source of partial discharges in the insulation of the power transformer and UHF sensors, respectively.

All reflections of electromagnetic UHF PD waves from the walls of the tank, three-phase magnetic core and three-phase primary and secondary windings are taken into account. All diffractions of UHF PD waves around active metal parts and through narrow apertures of winding coils and disks of transformer are included. The simulation is based on finite element method. It is a numerical method that is applied to differential equations with limit values in order to obtain an approximate solution. The underlying problem is defined here as high-frequency problem, as opposed to a quasi-static problem or a low-frequency problem. Other features, i.e., advantages and disadvantages of this computer simulation will be described.

## 2. INFLUENCES ON UHF PD WAVE PROPAGATION IN POWER TRANSFORMER

Power apparatus is generally in the form of metal-shielded equipment. Released energies from partial discharges, such as light, heat and electromagnetic waves, are prevented from passing through the metal case, so they must be detected by a suitable sensor inside the case.

The recorded signal on the UHF sensor is affected by the following [1]:

- Special type, strength and position of the source of partial discharges;
- Frequency response, installation location, sensitivity and UHF sensor radiation emission and reception diagram;
- Appropriate propagation path of UHF waves between the source of partial discharges and the UHF sensor, which is usually determined by the internal structure of the power transformer;
- Sensitivity of the measuring device.

The power transformer is made of different materials that can be:

- 1) dielectric (e.g., mineral oil, oil-paper insulation, pressboard);
- 2) electrically conductive (e.g., copper);
- 3) soft magnetic (e.g., electrical steel).

**Oral Presentation:** Determination of the Location of Partial Discharges in the Power Transformer Model Using UHF Sensors

The active parts of the power transformer can influence the shape and size of the received signals on UHF sensors, the source of which is a partial discharge in the electrical insulation of the power transformer. At the same time, the attenuation and distortion of the signal on the receiving UHF antenna is all the greater if the path of the partial discharge signal is more distorted in relation to the straight line that connects the source of the partial discharges and the corresponding UHF sensor.

Signal attenuation originates from the loss of signal energy when bouncing off the metal tank and metal active parts of the transformer core and the high and low voltage windings. Whenever it encounters any metal obstacle, part of the signal will be reflected and the remaining part will continue to propagate by diffraction (bending) the wave around the obstacle.

If, in the simulation in this work, the oil-paper insulation of the high and low voltage windings and the intermediate insulation from the pressboard were taken into account instead of mineral oil, additional attenuation and refraction would occur at the boundaries: oil-(oil-paper insulation) and (oil-paper insulation)-oil or oil-pressboard and pressboard-oil.

### 3. SIMULATION MODELS

#### 3.1 Transmitting/receiving antenna

The dipole antenna used in the computer simulation for the source of partial discharges and the sensor of UHF signals is shown in Fig. 1. The arms of the antenna measure 60 mm x 5 mm and are made of copper.

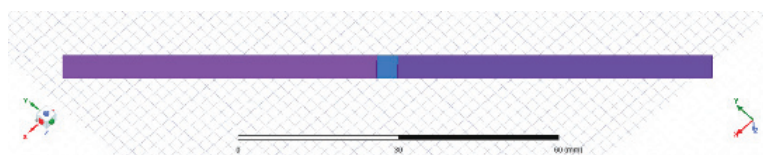


**Figure 1:** Transmitting and receiving antenna model. Dipole antenna measuring 124 mm x 5 mm [13].

Fig. 2(a) shows the considered dipole antenna whose radiation is limited by a cube, side 500 mm, in order to test the overall gain of the antenna. The dipole antenna is with the central point in the position [250; 250; 250] mm. Fig. 2(b) shows the polar diagram of the total gain of a dipole UHF antenna expressed in decibels [dB], at a frequency of 1 GHz, for the position of the antenna in Fig. (2a). It can be seen from Fig. 2(b) that the transmitting dipole antenna does not emit the same radiation power in all directions.

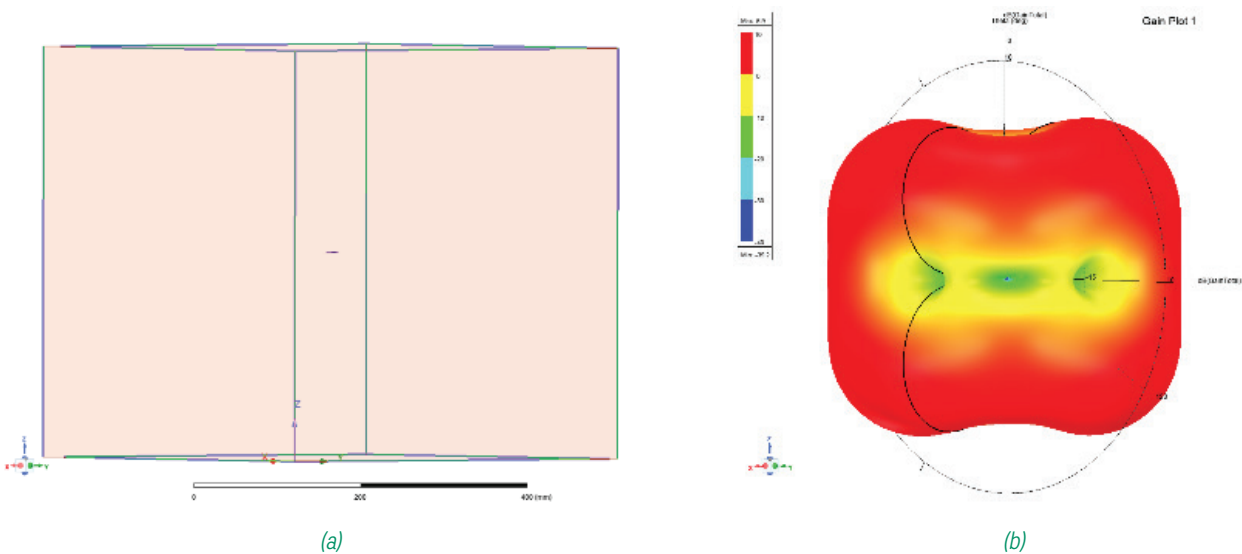


**Figure 2:** (a) Dipole UHF antenna and radiation limiting cube turned approximately 45° around the z-axis in a counter-clockwise direction. (b) Polar diagram of the total gain of the antenna expressed in decibels [dB] for the position of the dipole UHF antenna in Fig. (2a) [13].

In the x-y plane where the UHF antenna is located, along the longitudinal axis of the transmitting antenna, as well as  $\pm 15^\circ$  in relation to the center of the antenna, the radiation intensity is the lowest. Also, the radiation intensity along the vertical z-axis of antenna



**Oral Presentation:** Determination of the Location of Partial Discharges in the Power Transformer Model Using UHF Sensors

symmetry is weaker. The three-dimensional radiation pattern itself is more cubic than spherical. Therefore, even a receiving UHF antenna will not have equally good reception of radiated power in all directions.

### 3.2 Power transformer models (from the simplest to the most complex)

The model of a small three-phase energy transformer with a power of 5 MVA and a transformation ratio of 66/11 kV was considered. The dimensions of the transformer tank are: length 2300 mm, width 880 mm and height 2800 mm.

In order to compare and analyze the influence of the actual construction of the power transformer, examples of UHF signal propagation from the source of partial discharges to the receiving UHF antennas will be considered for the following cases:

- 1) for an empty transformer tank made of stainless steel 304 and filled with transformer mineral oil;
- 2) for the transformer tank made of stainless steel 304 and filled with transformer mineral oil in which the three-limb magnetic core of the transformer is located;
- 3) for a typical construction of a power transformer consisting of:
  - transformer tank made of stainless steel 304;
  - transformer insulating mineral oil;
  - three-limb, four-stage (with 7 stages) magnetic core of the power transformer;
  - three-phase low-voltage copper transformer winding;
  - three-phase high voltage copper transformer winding.

Adopted positions (center points) of receiving UHF antennas are as follows:  $S_1[65; 65; 2750] \text{ mm}$ ,  $S_2[1150; 440; 2758] \text{ mm}$ ,  $S_3[2235; 815; 2755] \text{ mm}$ ,  $S_4[70; 810; 2760] \text{ mm}$ .

Three-phase high-voltage and low-voltage windings, due to the limited capabilities of the Ansys Electronics Desktop HFSS (High-Frequency Structure Simulator) software and the computer (i.e., processor and random-access memory), had to be simplified. The real insulation of the three-phase windings is neglected and is approximately considered to be of the dielectric strength of mineral oil because all the paper insulation of the windings is impregnated with oil, thereby reducing the dielectric strength of the insulation.

The low-voltage (LV) and high-voltage (HV) windings are made of 42 discs of the corresponding sizes. The intermediate insulation between adjacent coils of LV and HV disks in the radial direction, 1.2 mm thick, is not taken into account, it is considered to be copper. Each high-voltage disk is divided into two parts along the vertical axis with a gap of 1.2 mm, although it should be composed of four parts. The reason for this is the limited capabilities, first of all, of the random-access memory (for storing data that is simultaneously processed), and then of the processor (i.e., data processing speed) in the computer and finally the user program itself, because the model of the HV winding is multiply complicated in terms of the number of its parts. By ignoring the two gaps of 1.2 mm each, the signal attenuation is slightly higher. An opening of 1.2 mm is small for an electromagnetic wave whose wavelength in mineral oil (of dielectric constant 2.2) is equal to 20.23 cm at the wave frequency of 1 GHz. Due to wave diffraction at such a small opening, the strength of a signal beam through such an opening is dissipated in various directions relative to the opening itself, i.e., the power of that beam weakens in the direction of the shortest possible distance to the UHF sensor.

The real intermediate insulation between the higher and lower voltage windings is ignored and considered as having the dielectric strength of mineral oil, because the layers of pressboard insulation are also impregnated with oil, thus reducing the dielectric strength of the pressboard.

It was assumed that the source of partial discharges is placed at the point:  $T = [2045; 600; 1250] \text{ mm}$ . It is located on the front left side of the 1st pillar of the core in the upper part of the 1st phase of the winding. It is placed between the LV and HV windings, closer to the LV winding, between the 27th and 28th disks of the low-voltage winding, and behind the lower part of the 26th disk of the high-voltage winding.

The largest possible distance in the tank is 3728.86 mm, which corresponds to an electromagnetic wave delay of 18.644 ns. However, the distances between the partial discharge source and the UHF sensor are usually much shorter. The source of partial discharges is designed as a broadband pulse with a minimum frequency of 0 Hz, a maximum frequency of 1 GHz and an amplitude of 1 V.



Oral Presentation: Determination of the Location of Partial Discharges in the Power Transformer Model Using UHF Sensors

## 4. SIMULATION RESULTS

### 4.1. PD location equations

In order to determine the location of the source of partial discharges [1], it is necessary to use a distributed array of three or more UHF sensors to simultaneously record partial discharge signals and enable triangulation. The received UHF signals can be processed to determine the signal arrival time difference between them. The location of the source of partial discharges can then be determined from the time differences of signal arrival between UHF sensors [10,11].

For four UHF sensors, the following four equations can be written with four unknown variables [1]:

$$v_o(T_1 + T_2) = \sqrt{(x_T - x_1)^2 + (y_T - y_1)^2 + (z_T - z_1)^2} \quad (1)$$

$$v_o(T_1 + T_{21}) = \sqrt{(x_T - x_2)^2 + (y_T - y_2)^2 + (z_T - z_2)^2} \quad (2)$$

$$v_o(T_1 + T_{31}) = \sqrt{(x_T - x_3)^2 + (y_T - y_3)^2 + (z_T - z_3)^2} \quad (3)$$

$$v_o(T_1 + T_{41}) = \sqrt{(x_T - x_4)^2 + (y_T - y_4)^2 + (z_T - z_4)^2} \quad (4)$$

where:

$v_o = 20.23 \frac{cm}{ns}$  – UHF signal speed in mineral oil;

$x_T, y_T, z_T$  – coordinates of the source  $T$  of partial discharges;

$x_k, y_k, z_k$  – coordinates of UHF sensor  $k$  ( $k = 1,2,3,4$ );

$T_1$  – the arrival time of the partial discharge signal from the source  $T$  to the reference transmitter  $S_1$ ;

$t_{21}$  – difference between signal arrival times from source  $T$  to sensor  $S_2$  and reference sensor  $S_1$ ;

$t_{31}$  – difference between signal arrival times from source  $T$  to sensor  $S_3$  and reference sensor  $S_1$ ;

$t_{41}$  – difference between signal arrival times from source  $T$  to sensor  $S_4$  and reference sensor  $S_1$ .

### 4.2. Simulation models and results comparison

In Fig. 3, for the position of the source of partial discharges  $I$ , a simplified model of the power transformer is shown, which consists of a tank made of stainless steel 304 filled with insulating mineral oil. The recorded waveforms of the output signals of the corresponding UHF sensors are shown together in Fig. 4 in different colors.

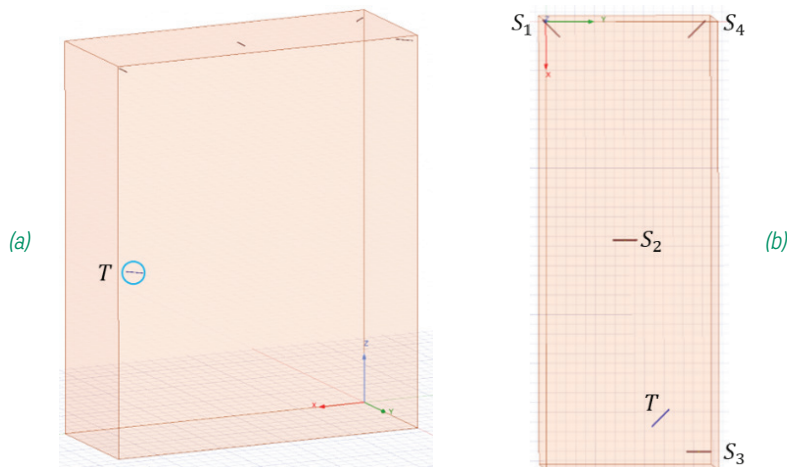


Figure 3: Power transformer tank filled with mineral oil. (a) Front view. (b) Top view.



Oral Presentation: Determination of the Location of Partial Discharges in the Power Transformer Model Using UHF Sensors

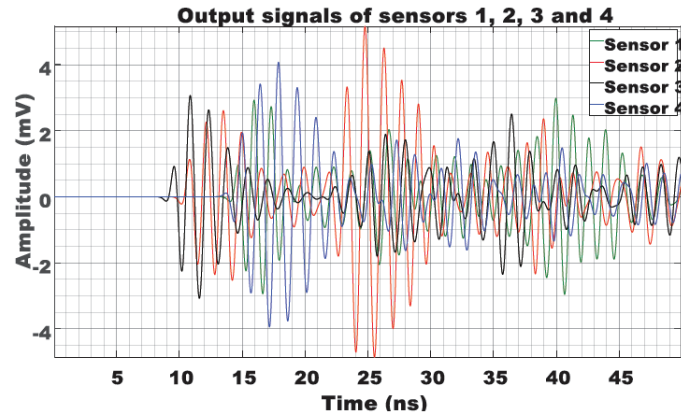


Figure 4 : Displays of output signals of sensors 1-4 from Figure 3 in different colors (with green for  $S_1$ , red for  $S_2$ , black for  $S_3$  and blue for  $S_4$ ).

In Figure 5, for the position of the source of partial discharges  $T$ , a more complex model of the power transformer is shown, which consists of a stainless-steel tank 304 filled with insulating mineral oil and a three-limb core made of electrical steel.

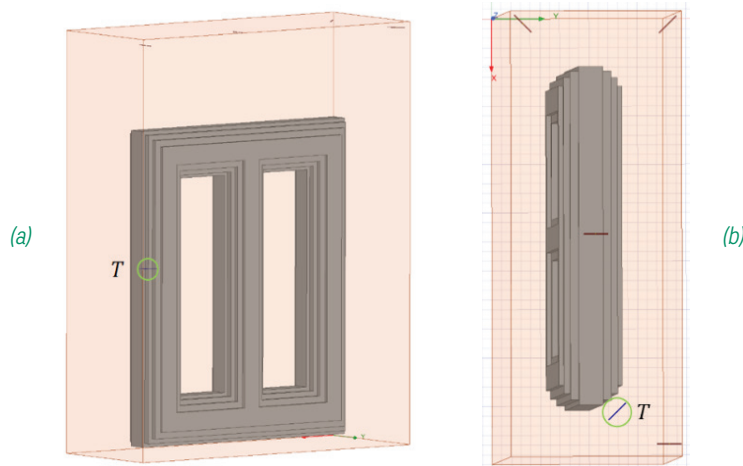


Figure 5: Power transformer tank filled with mineral oil with a three-limb magnetic core. (a) Front view. (b) Top view.

The recorded signal waveforms at the output of appropriately placed UHF sensors are shown together in Figure 6 in different colors.

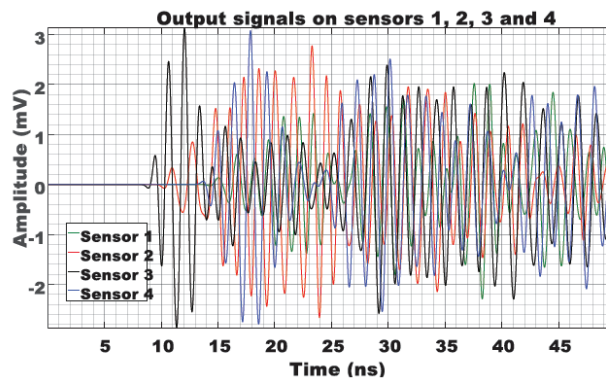


Figure 6: Displays of output signals of sensors 1-4 from Figure 5 in different colors (with green for  $S_1$ , red for  $S_2$ , black for  $S_3$  and blue for  $S_4$ ).

Figure 6 shows in the first wave packet the reduction of the amplitudes (i.e., attenuation) of the recorded signals on UHF sensors 1 and 4 by more than 1.3 times compared to the state of the signal in Figure 5 when there is no influence of the three-limb magnetic



**Oral Presentation:** Determination of the Location of Partial Discharges in the Power Transformer Model Using UHF Sensors

core. The first wave packets of signals 1 and 2 became wider than usual by about 10 ns in Figure 5 due to reflections from the core and tank.

Figure 7, for partial discharge source position  $T$ , shows a common model of a power transformer consisting of a tank of stainless steel 304 filled with insulating mineral oil, a three-limb core of electrical steel, and three-phase low and high voltage windings made of copper. The output signal waveforms of the default UHF sensors are shown together in Fig. 8 in different colors.

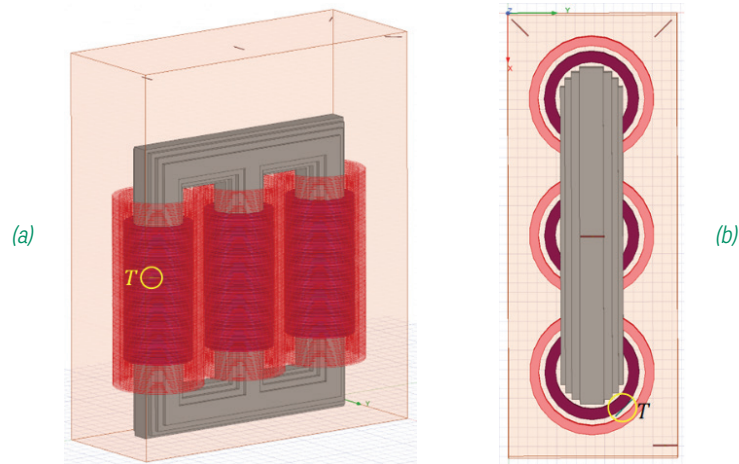


**Figure 7:** The metal tank of a power transformer with a three-limb magnetic core and three-phase copper windings, which is filled with mineral oil. (a) Front view. (b) Top view.

In Figure 8, one can see an additional drop in the amplitudes (i.e. attenuation) of the recorded signals, especially on UHF sensors 2 and 3 (more than 4 times), then on UHF sensor 1 (more than 2.8 times) and a relatively smaller drop on UHF sensor 4 (more than 1.3 times), compared to the signal condition in Figure 6 when there is no influence of the three-phase copper winding. Figures 4, 6 and 8 show how the shapes of the envelopes of the amplitudes of individual signals on UHF sensors are different, due to the effects of diffraction (i.e., deflection) around and reflection from various metal obstacles.

Table I shows the moments of the first peaks of the partial discharge signals on UHF sensors 1–4 for three examples of power transformer construction. From the results in Table I, it can be seen that the metal core almost does not affect the signal paths of partial discharges from the source to the UHF sensors  $D_3$  and  $D_4$ , while the signal paths to the sensors  $D_2$  and  $D_1$  are extended and the signals arrive later in 0.09 ns and 0.28 ns, respectively. The three-phase windings and the three-limb magnetic core affect the signal delay of (0.35–0.98) ns, depending on the position of the UHF sensor in relation to the state when the metal tank of the power transformer is empty. The largest delay is for sensor 1 and the smallest for sensor 3, 0.63 ns for sensor 4 and 0.84 ns for sensor 2.

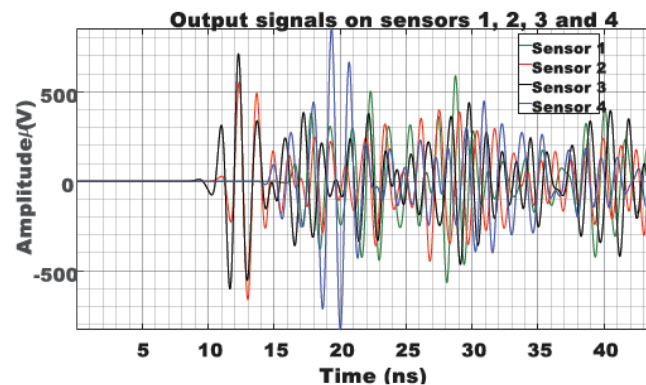


**Figure 8:** Displays of output signals of sensors 1–4 from Figure 7 in different colors (with green for  $S_1$ , red for  $S_2$ , black for  $S_3$  and blue for  $S_4$ ).





Oral Presentation: Determination of the Location of Partial Discharges in the Power Transformer Model Using UHF Sensors

**Table 1:** Moments of the appearance of the first peaks of the partial discharge signals on sensors 1-4 for three examples of power transformer construction.

Construction	$t_1 [ns]$	$t_2 [ns]$	$t_3 [ns]$	$t_4 [ns]$
metal tank ( $\alpha$ )	14.022	10.1623	8.9408	13.7044
+metal core ( $\beta$ )	14.3033	10.2517	8.8602	13.6894
+windings ( $\gamma$ )	14.9995	11.0034	9.2934	14.3304

Table II shows the differences in the arrival times of partial discharge signals at UHF sensors 1–4 for the theoretical case and three examples of power transformer construction.

**Table 2:** Calculated differences in the arrival times of partial discharge signals at sensors 1–4 for the theoretical case and three examples of power transformer construction. The sensor  $D_1$  is taken as the reference sensor.

Construction	$dt_{21} [s]$	$dt_{31} [s]$	$dt_{41} [s]$
ideal case ( $\zeta$ )	-3.856975E-09	-4.988049E-09	-2.275738E-10
metal tank ( $\alpha$ )	-3.859711E-09	-5.081138E-09	-3.175711E-10
+metal core ( $\beta$ )	-4.051567E-09	-5.443014E-09	-6.138738E-10
+ windings ( $\gamma$ )	-3.99616E-09	-5.706145E-09	-6.691245E-10

Table III shows the mutual deviations of the differences in the arrival times of partial discharge signals at UHF sensors 1–4 and the mean value of their absolute values for the three considered simulated cases compared to the theoretical – perfect case. The sensor  $D_1$  is taken as the reference sensor.

**Table 3:** Mutual deviations of the differences in the arrival times of the partial discharge signals to sensors 1–4 and the mean values of their absolute values for the considered three simulated cases compared to the ideal (theoretical) case.

Differences in arrival times	$D_2 - D_1$	$D_3 - D_1$	$D_4 - D_1$
$\Delta(dt_{\alpha\zeta}) [s]$	-2.735678E-12	-9.308934E-11	-8.999738E-11
$\Delta(dt_{\alpha\zeta sr}) [s]$		6.19408E-11	
$\Delta(dt_{\beta\zeta}) [s]$	-1.945919E-10	-4.549654E-10	-3.863E-10
$\Delta(dt_{\beta\zeta sr}) [s]$		3.452858E-10	
$\Delta(dt_{\gamma\zeta}) [s]$	-1.39185E-10	-7.180961E-10	-4.415507E-10
$\Delta(dt_{\gamma\zeta sr}) [s]$		4.329439E-10	

The mean deviation of the absolute values of the differences in the arrival times of the partial discharge signals at UHF sensors 1–4 compared to the ideal case is the largest in the 3rd simulated case, and the least in the 1st simulated case.

Table IV shows the calculated positions of the sources of partial discharges for the theoretical case and three examples of the simulated construction of the power transformer.



Oral Presentation: Determination of the Location of Partial Discharges in the Power Transformer Model Using UHF Sensors

**Table 4:** Calculate the position of the source of partial discharges for the theoretical case and three examples of simulated power transformer construction

Construction	$x [m]$	$y [m]$	$z [m]$
ideal case ( $\zeta$ )	2.045E+00	6E-01	1.25E+00
metal tank ( $\alpha$ )	2.059012E+00	6.654313E-01	1.209642E+00
+ metal core ( $\beta$ )	2.019612E+00	8.568329E-01	1.33064E+00
+ windings ( $\gamma$ )	2.155093E+00	9.387108E-01	1.131878E+00

Table V shows mutual deviations in the calculated positions of the sources of partial discharges and the mean value of their absolute values for the three considered simulated cases in relation to the theoretical – perfect case.

**Table 5:** Mutual deviations in the calculated positions of the sources of partial discharges by axes and the mean value of their absolute values for the considered three simulated cases in relation to the ideal case.

Deviations in calculated positions	$x$ -axis	$y$ -axis	$z$ -axis
$\Delta d_{\alpha\zeta} [cm]$	1.401207E+00	6.543125E+00	-4.035813E+00
$\Delta d_{\alpha\zeta sr} [cm]$		3.993382E+00	
$\Delta d_{\beta\zeta} [cm]$	-2.538764E+00	2.568329E+01	8.063954E+00
$\Delta d_{\beta\zeta sr} [cm]$		1.209534E+01	
$\Delta d_{\gamma\zeta} [cm]$	1.100931E+01	3.387108E+01	-1.181217E+01
$\Delta d_{\gamma\zeta sr} [cm]$		1.889752E+01	

The mean deviation of the absolute values in the calculated positions of the sources of partial discharges in relation to the perfect case is the largest in the 3rd simulated case, and the least in the 1st simulated case.

## 5. DISCUSSION ABOUT ANOTHER CASE OF PD SOURCE LOCATION

In the article [13], the position of the source of partial discharges was considered, as in Fig. 9, which, viewed from the rear, was located on the left side of the middle limb of the electrical steel core under the yoke, in the middle part of the 2nd phase of the three-phase copper windings. It was placed between the low voltage winding and the high voltage winding, closer to the low voltage winding, opposite the 22nd disk of the low voltage winding and against the lower part of the 22nd disk of the high voltage winding. In that case, as well as for the given arrangement of the UHF sensors, the mean value of the absolute values of the deviation of the position of the source of partial discharges in relation to the actual position was the highest when the metal tank and the three-limb core of the power transformer were taken into account and was 11.3 cm. When the three-phase windings were also taken into account, the mean value of the absolute deviation of the position of the source of partial discharges was 8.2 cm. When only the metal tank of the power transformer was considered, the mean value of the absolute deviation of the position of the source of partial discharges was 1.74 cm.



Oral Presentation: Determination of the Location of Partial Discharges in the Power Transformer Model Using UHF Sensors

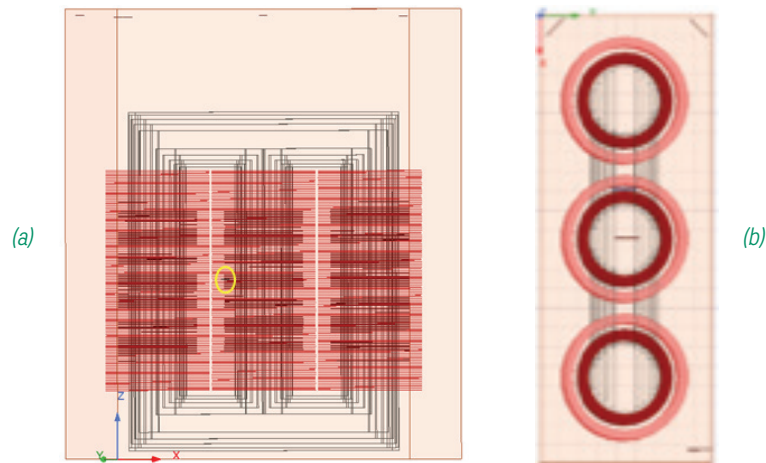


Figure 9: Complex model from article [13]: Power transformer tank filled with mineral oil with three-limb core and three-phase windings. (a) Rear view. (b) Top view [13].

In relation to the example in the article [13], in the example in this paper, the mean deviation of the absolute values of the differences in the arrival times of the partial discharge signals at the UHF sensors 1–4 compared to the ideal case is, respectively, greater by 0.183 ns and 0.357 ns in the case of influences metal core and metal core and windings together on the paths of signal propagation from the source to the UHF sensors.

It can be concluded that in the case described in article [13], the influence of the magnetic core on determining the location of the source of partial discharges was greater than the influence of the magnetic core and windings together, i.e., contrary to the example shown in this paper, although in both cases the three-phase windings additionally affected the UHF signal delays from the source of partial discharges to individual UHF sensors to a correspondingly lesser or greater extent depending on the size and number of metal obstacles. The magnitudes and ratios of the differences in the arrival times of the partial discharge signals to the UHF sensors can unexpectedly affect the magnitudes and ratios of the results obtained for the positions of the partial discharge sources when determining the influence of the magnetic core and the magnetic core and copper windings together.

## 6. CONCLUSION

The aim of this work was to analyze the impact of the actual construction of the power transformer on the propagation of electromagnetic UHF waves from the source of partial discharges in the electrical insulation in the tank of the power transformer from the place of their origin to the receiving UHF antennas.

With the help of simulations in HFSS, pictorial representations of the received signals are made possible, all reflections and diffractions of the signals on the way from the source to the UHF sensor are included. The disadvantage is that the source of partial discharges is not a point source, i.e., it does not radiate with the same power of radiation in all possible directions from the source.

The position of the source of partial discharges, which is seen from the front, is located on the front left side of the 1st pillar of the core in the upper part of the 1st phase of the winding. It is placed between the LV and HV windings, closer to the LV winding, between the 27th and 28th disks of the low-voltage winding, and behind the lower part of the 26th disk of the high-voltage winding.

Given the metal tank and three-limb magnetic core of the power transformer, and for the given UHF sensor arrangement, the mean absolute deviation of the position of the partial discharge source is 12.1 cm from the assumed position, because the signal path is extended, compared to when there is only an empty steel tank. When the three-phase windings are also taken into account, the mean value of the absolute values of the deviation of the position of the source of partial discharges is the highest and is 18.9 cm. When only the steel tank of the power transformer is considered, the mean value of the absolute values of the deviation of the position of the source of partial discharges is the smallest, i.e., 4 cm.



**Oral Presentation:** Determination of the Location of Partial Discharges in the Power Transformer Model Using UHF Sensors

### BIBLIOGRAPHY

- [1] D. Dukanac "Application of UHF method for partial discharge source location in power transformers" (IEEE Transactions on Dielectrics and Electrical Insulation, vol. 25, no. 6, December 2018, pages 2266–2278).
- [2] A. M. Ishak, M. D. Judd, W. H. Siew "A Study of UHF Partial Discharge Signal Propagation in Power Transformers using FDTD Modelling" (45th International Universities Power Engineering Conference UPEC2010, Cardiff, UK, 2010, pages 1–5).
- [3] C. P. Beura, M. Beltle, S. Tenbohlen "Positioning of UHF PD Sensors on Power Transformers Based on the Attenuation of UHF Signals" (IEEE Transactions on Power Delivery, vol. 34, no. 4, August 2019, pages 1520–1529).
- [4] N. Xue, J. Yang, D. Shen, P. Xu, K. Yang, Z. Zhuo, L. Zhang, J. Zhang "The Location of Partial Discharge Sources inside Power Transformers Based on TDOA Database with UHF Sensors" (IEEE Access, vol. 7, October 2019, pages 146732–146744).
- [5] T. Umemoto, S. Tenbohlen "Validation of Simulated UHF Electromagnetic Wave Propagation in Power Transformers by Time and Frequency Domain Measurements" (2018 IEEE International Conference on High Voltage Engineering and Application (ICHVE), Athens, Greece, 2018, pages 1–4).
- [6] Z. Tang, C. Li, X. Cheng, W. Wang, J. Li, J. Li "Partial Discharge Location in Power Transformers Using Wideband RF Detection" (IEEE Transactions on Dielectrics and Electrical Insulation, vol. 13, no. 6, December 2006, pages 1193–1199).
- [7] L. Yang, M.D. Judd, G. Costa "Simulating propagation of UHF signals for PD monitoring in transformers using the finite difference time domain technique" (The 17th Annual Meeting of the IEEE Lasers and Electro-Optics Society, Boulder, CO, USA, 2004, pages 410–413).
- [8] N. Shirdel, A. Akbari, H. R. Mirzaei, M. S. Abrishamian "Three-Dimensional Simulation of UHF Signal Propagation in Transformer using FDTD Method" (Proceedings of the 2011 International Conference on Power Engineering, Energy and Electrical Drives, Torremolinos (Málaga), Spain, 2011, pages 1–6).
- [9] L. A. M. M. Nobrega, E. G. Costa, A. J. R. Serres, G. V. R. Xavier, M. V. D. Aquino "UHF Partial Discharge Location in Power Transformers via Solution of the Maxwell Equations in a Computational Environment" (Sensors 2019, 19(15), 3435, August 2019, pages 1–13).
- [10] D. Antony, P. Mishra, A. Todi, N. A. John, A. M. Patankar, "Partial discharge localisation in transformers using UHF technique: non-iterative method," (International Journal of Information Technology, vol. 13, May 2021, pages 291–297).
- [11] D. L. G. Huertas, J. L. A. Quijano "Full-Wave Simulation of Partial Discharge in Power Transformers" (2018 International Conference on Electromagnetics in Advanced Applications (ICEAA), Cartagena, Colombia, 2018, pages 1–4).
- [12] J. Du, W. Chen, B. Xie "Simulation Analysis on the Propagation Characteristics of Electromagnetic Wave Generated by Partial Discharges in the Power Transformer" (2016 IEEE Conference on Electrical Insulation and Dielectric Phenomena (CEIDP), Toronto, ON, Canada, 2016, pages 1–4).
- [13] Đ. Dukanac "Analysis of the Influence of Active Parts of the Power Transformer on the Propagation of Signals from Source of Partial Discharges to UHF Sensors (in Serbian)" (Energija, Economy, Ecology, vol. XXIV, no. 1, 2022, pages 74–80).



# Pressboard Barriers in Smart Connection Systems for High Voltage Power Transformers

[e.ozturk@enpay.com](mailto:e.ozturk@enpay.com)

**EMRE ÖZTÜRK<sup>1\*</sup>, HAKAN COŞER<sup>2</sup>, UĞUR AYĞÜN<sup>3</sup>**  
*ENPAY Transformer Components*

**Türkiye**

## SUMMARY

In recent years, because of fluctuating demand for electricity, it has become more indispensable to transfer higher and higher MW electric power from the generating stations to the users. Transmission losses are reduced by HVAC or HVDC applications. Thanks to the availability of advanced insulation materials and optimized producing practices, it is now possible to have voltage ratings of transformers up to 1200 kV. This voltage range requires advanced insulation materials, insulation design tools and smart solutions. One of the most important components which is made of Transformerboard are functional smart connection systems. By the help of these smart connection systems, significant amount of savings can be achieved in electricity distribution transmission lines.

In this paper, we experience this insulation technology 'smart connection with pressboard barriers design' for the following two solutions in order to meet the requirements of the transformer manufacturers and therefore the plant operators.

- Dual Switchingboard
- Up-Down Cable Box Connection

The Dual Switchingboard is an insulation component which connects the other components located between the high voltage windings. Dual Switchingboard systems are designed for a safer connection between windings in transformers. It allows the same transformer to be used with different connections in different electrical substations for different voltage ratings. Unlike the standard tap changers for regulating windings, The Dual Switchingboard is designed for switching between the transformers windings when one transformer is turned off and physically opened up.

The Up-Down Cable Box Connection is a special Exit insulation system and connection element between HV winding tail and HV bushing which allows the same transformer to be used with different connections in electrical substations and same voltage ratings. With this special form of connection same transformer can be connected to underground cable ends, overhead lines or test devices at FAT.

Switchingboard and Up-Down Cable Box Connection is an important product considering the time required for switching or assembling. It stays in contact with the open air while switching or rotating turret process. This information should be taken into account during the products design phase.

Barrier transitions, locations, thicknesses, and diameters should be designed by taking all the mentioned parameters into consideration the contacts that will perform the switching function on the main current carrying conductor should be positioned at the places where the electric field is the lowest, and these contacts should be selected with the technical properties that will allow

## KEYWORDS

HVAC, HVDC, Transformerboard, Smart connection systems, Dual Switchingboard, Up-Down Cable Box



switching repeatedly. In terms of preventing gas trapping, the design should be made by considering the continuity of the insulation material. Dual Switchingboard and Up-Down Cable Box Connection system are designed in accordance with this knowledge.

This paper aims to show optimizing process of transformer by means of smart connections with pressboard barrier design. This article examines the Dual Switchingboard and Up-Down Cable Box smart connections.

“Transformers are vital components of electrical system equipment’s for efficient and reliable operation of electric power network. In any Industry, electrical transformers play an important role.” [1]

“The improvement of the characteristics of power transformers is an ongoing duty for manufacturers since this equipment constitutes one of the most expensive and strategic components of electric power transmission and distribution systems. Any failure of such components can result in significant economic losses. Hence, the manufacturers need to improve the reliability of these equipment’s and reduce their costs by; reducing their size, requiring smaller insulating gaps which lead to higher heat densities to cool, and increasing their life cycle.” [2]

With regard to CEA regulations, one no; “For substations/switchyards where single-phase unit banks are installed, a single-phase backup transformer/reactor is required. For reference purposes, connection arrangement for bringing spare unit into the circuit in case of failure of one of the other units is given by field operators. Failure of GT/Power Transformers leads to huge loss in terms of revenue, time, reliability of the system and the requirement of additional transformer leads to additional capital, material for manufacturing/commissioning and time requirement for replacement. Also, due to long repair time of transformers, utilities have to maintain capital spare which is costly and in the absence of required care and maintenance, may fail without ever being utilized, incurring further loss. Standardization will be a big step in reducing these difficulties.” [3] In accordance with the mentioned regulations, it can be suggested that at the time of emergency situations, the use of transformers in different locations where power plant operators can easily switch voltage ratios, reduces electricity generation costs by preventing long interruptions. During the power generation plant design phase, all smart connectivity capabilities in transformers should be taken into consideration by making small optimizations on design of the specific transformer components.

In design of these smart connection systems, transformer insulation design principles come into prominence. The principles regarding transformer insulation design are founded on the use of cellulose for insulations which is basically used in mineral oil and ester oil. HV power transformer design and manufacturing methods are based on this knowledge for more than twelve decades. In insulation design, electrical field stress distribution on oil impregnated solid insulations is taken as the fundamental criteria. This stress is distributed in accordance with the permittivity and conductivity of materials (cellulose-based insulation, transformer liquids etc.), and the geometry of metal parts. Furthermore, the insulation arrangement is constituted according to the design curves and limit values related to materials. They are based on experience and based on manufacturing, process, workmanship, quality of materials “Moisture in cellulose and oil is an ageing indicator and gains importance since utilities should keep transformers in service even if the estimated life cycle is exceeded. Water content receptivity of mineral/ester oil and cellulose changes with temperature. This relation is represented in moisture equilibrium diagrams. The load cycles of power transformers cause a continually exchange of water between paper/pressboard and oil.” [4] Deficiency of materials that are essential for producing liquid-cooled transformers, such as grain oriented silicone steel, copper, mineral oil, ester oil and their increasing and fluctuating prices necessitate to find alternative solutions to reduce the total cost, weight, and dimensions of the transformers. In addition, it has become necessary to make some savings during the usage of the transformer with smart solutions.

In this paper, we experience this insulation technology smart connection with pressboard barriers design for the following two solutions in order to meet the requirements of the transformer manufacturers and therefore the plant operators.

- Dual Switchingboard
- Up-Down Cable Box Connection

The Dual Switchingboard is an insulation component which connects the components located between the high voltage windings. Dual Switchingboard systems are designed for a safer connection between windings in transformers. It allows the same transformer to be used with different connections in different Electrical Substations for different voltage ratings by changing connection type. Unlike the standard tap changers for regulating windings, The Dual Switchingboard is designed for switching between the transformers windings when one transformer is turned off and physically opened up.

High voltage winding end can be positioned at the top or in the middle of the axial height of the coil. Common practice for each Dual Switchingboard system is the phase current through other phase connection.

The Up-Down Cable Box Connection is a special Exit Insulation System and connection element between HV winding tail to HV bushing and allows the same transformer to be used with different connection different in Electrical Substations and same voltage





Oral Presentation: Pressboard Barriers in Smart Connection Systems for High Voltage Power Transformers

ratings. With this special connection same transformer can be connected to underground cable end, overhead line or test devices at FAT.

The distance to grounded parts depends on system voltage and design of the Dual Switchingboard or Up-Down Cable Box Connection. Determining of the current and voltage will certainly affect the contact's quantity of switching board, amount of copper conductor, mineral or ester oil etc. and this is important for both material cost and the weight and dimensions of the transformers. Pressboard barriers allow reducing the clearances and the distance of transformer top tank plate therefore provide saving from materials for power transformer manufacturers. The Up-Down Cable Box Connection and Dual Switchingboard are critical insulated connection components that are used to provide not only safe connection between windings, but they also allow cost optimization of steel, mineral oil, ester oil, transportation by minimizing volume of transformer tank or turret. Switchingboard and Up-Down Cable Box Connection is an important product considering the switching or assembling time it stays in contact with the open air while switching or rotating turret process. This information should be taken into account during the Products Design phase.

## 1. DESIGN PROCESS

### 1.1. Dual Switchingboard

Dual switchingboard is a component similarly designed with LEADS which can be examined as; "The insulation in transformers can be classified as major and minor insulation. The major insulation involves insulation between the windings, the windings and the core, high voltage LEADS (Exit insulation systems) and ground while minor insulation is the insulation within the windings, for instance: interturn and interdisc insulation." [5]

Position of Dual Switchingboard as leads, can be in a separated tank or in a transformer tank with active part. Connection to winding can be at the top or in the middle of winding for each position. (Figure 1)

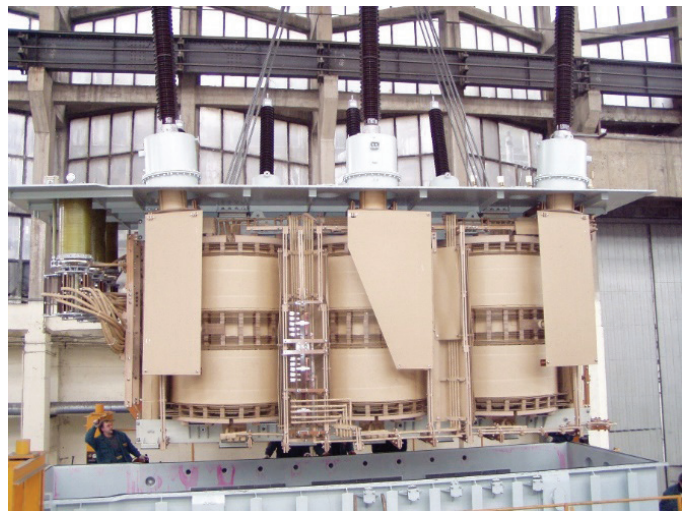
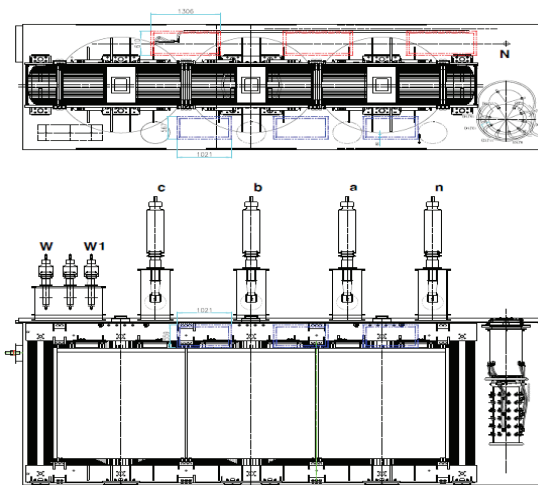


Figure 1

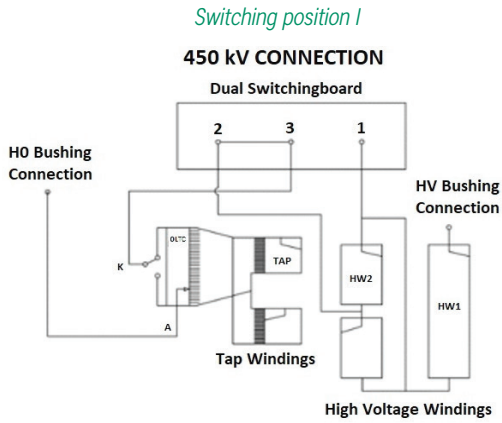
Dual Switchingboard and Up-Down Cable Box Connection insulation design should be investigated with FEM analyze program. Carefully engineered insulation structures based on electrical field calculation leads to compact designs, so far realized up to all voltage ratios. (In this process analyses, the ElecNet software and software package Maxwell by ANSYS is used). 450 kV connection and 300 kV connection parts can be analyzed with a 2D, and 3D model. (Figure 4-6) Insulation barriers and oil boundary layers run parallel to the surrounding equipotential surfaces; Insulation barriers can be used such a manner that creep stress practically precluded on high stressed area. Main current value was determinate conductor shape and "whilst decide the oil-ducts and insulation requirements, highest stress part of the lead exit should be deeply analyzed." [6] The highest stress value should be restricted under a definite value for preventing PD (partial discharge) and oil-breakdown from this part. The safe maximum permissible stress depends upon the thickness of oil ducts. The studies are made with the curves of partial discharge inception voltage versus width of oil duct for degassed oil.



Oral Presentation: Pressboard Barriers in Smart Connection Systems for High Voltage Power Transformers

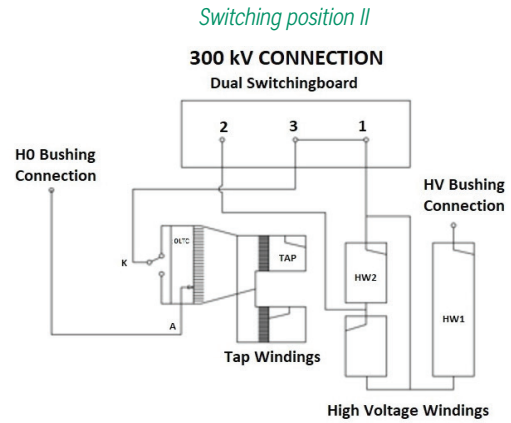
Briefly 400 kV Dual Switchingboard design input data;

BIL: 1200 kV SIL: 1050 kV



	BIL	SIL	Max. Current
1 - Gnd	1000 kV	505 kV	410 A
2,3 - Gnd	581 kV	248 kV	410 A
1 - 3	934 kV	446 kV	410 A

Figure 2



	BIL	SIL	Max. Current
1,3 - Gnd	506 kV	318 kV	620 A
2 - Gnd	1200 kV	888 kV	620 A
3 - 2	944 kV	571 kV	620 A

Figure 3

For Dual Switchingboard additional strong insulation barriers secure the connecting tube bends against short circuit forces. Barriers and supports designed according to short circuit forces and clamps fixed all system strongly. The geometry of the plugs and sockets is chosen in such a way to avoid any confusion when positioning the contacts. Dimensions of main conductor was determined due to current value then iterate the calculation to increasing diameter for electrostatic shield diameter to decrease electric field on critical surfaces. (Figure 2-3) Repeatedly removable special contacts are located inside the electrostatic shield where the electrical field is low or zero.

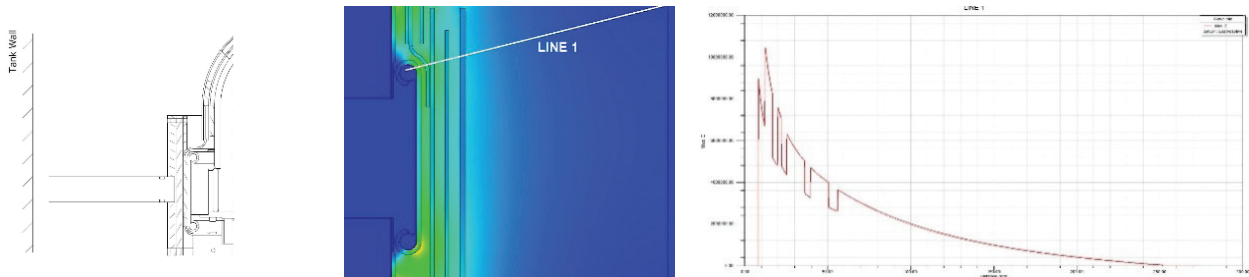


Figure 4: Curve that belongs to line 1 (V/m)

Above illustrations show field distribution and an example of field distribution curve, belong to line. All oil ducts were investigated and shaped continuous channel for best cooling.

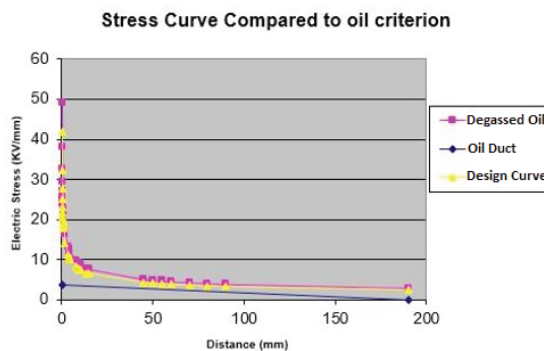


Figure 5: Electrostatic Field Distribution Between Barrier and Ground



The field stress distribution of such a Dual Switchingboard is highly non-uniform, as will be seen in above curves. (Figure 5) The geometries of the structures should be arranged to optimize the field stress distribution. For this optimization, it is necessary to comprehend and compare the geometries.

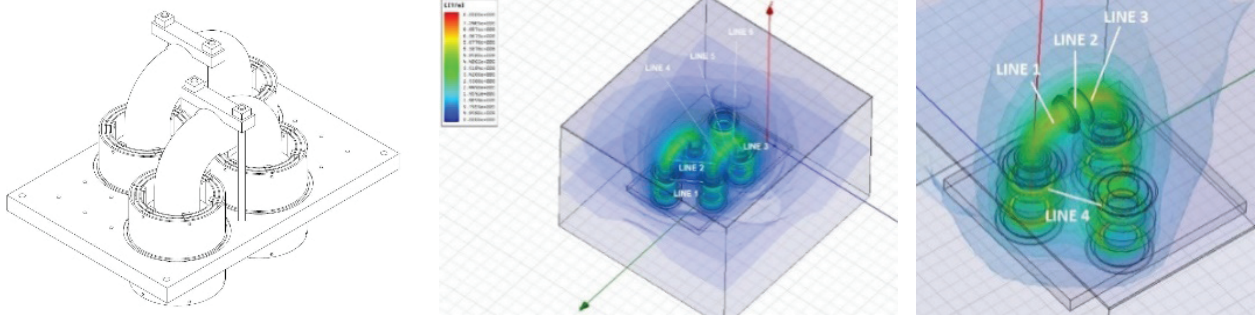
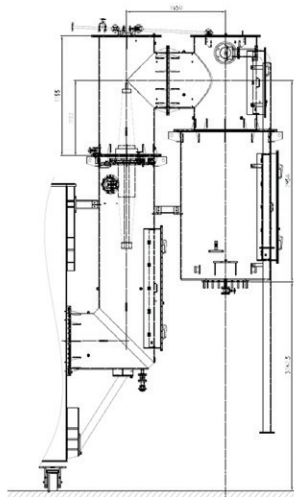


Figure 6: 3D field calculation results

### 1.2. Up-Down Cable Box Connection

A special shield within the up-down connection creates the functionality of the design. Special types of smart electrostatic shield geometries include not only the minimization of the electric field, but also mechanical connections that can be easily assembled and disassembled. This connection system has been designed in such a way that it allows the self-assembly of the system as well as the turret assembly in considerably shorter time. The disassembled turret allows transportation in two parts, the total mass height is reduced, minimizing the transportation cost and time.

BRIEFLY 500 kV Up-Down Cable Box Connection Design input data (Figure 7);



Nominal Voltage	kV	400
BIL	kV	1425
Max. Current	A	410

Figure 7

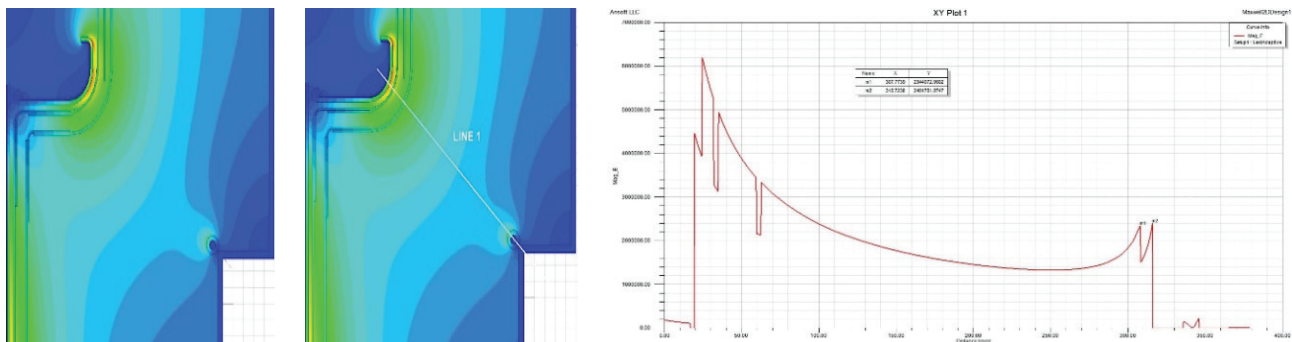


Figure 8: 2D field calculation results



Oral Presentation: Pressboard Barriers in Smart Connection Systems for High Voltage Power Transformers

Above illustrations show field distribution and an example of field distribution for critical direction. All oil ducts were investigated in detail and shaped continuous channel for best cooling.

“Insulation barriers, made from Transformerboard, are used for subdividing large oil gaps into smaller oil gaps.” [7] Transformerboard has pure cellulose fibres that increase the oil strength and provide a higher safety margin. While designing conductor’s barriers the important point is to obtain the ‘field conform’ structure, i.e., electrical field patterns are perpendicular to barriers and equal potential field patterns are parallel with barriers as will be seen from the above FEM analyze illustrations. (Figure 8)

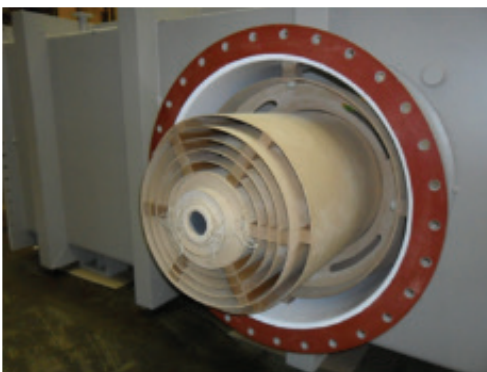
Barriers and supports for both smart connection systems are designed according to short circuit forces and Vibration forces (transportation) and clamps fixed all system strongly.

We can see the advantages of using smart connection with barrier instead of traditional thick paper insulation systems in simulation tests.

## 2. SIMULATION

### 2.1. Drying Process Advantages of Smart Connections with Barriers

Through testing, the advantages of barrier systems will be evaluated.



Barrier system



Paper insulation

Figure 9: Demonstration figures with barrier system and traditional paper insulation

Water content tests were conducted on equal two models dried for 1 week at 105°C under 0,01 mbar in same oven. (1 week, 168 h, under 0,01 mbar, at 105°C- two systems were equalized by keeping the same safety factor in electric fields studies at similar voltage levels.)

Pressboard barriers reached to required values, but it was concluded that the water content of paper insulation was not at acceptable level. A water content 1-2 % was measured on paper insulation. (Figure 10)

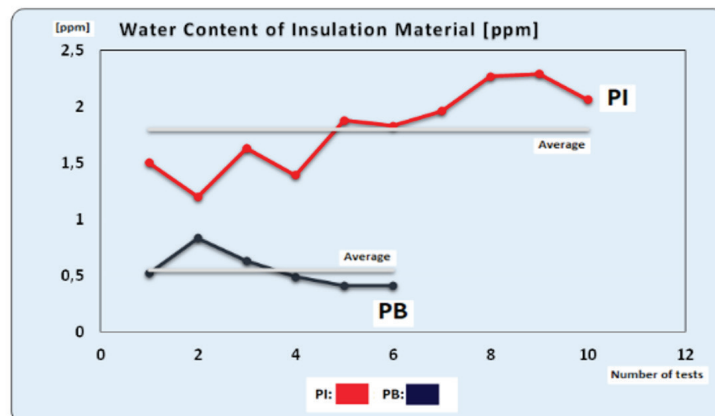


Figure 10: Water Content of Insulation Materials (Paper insulation, pressboard barriers.)





Due to thickness of the thick paper insulation, the drying is not practical. The Initial moisture (water content) remained has a significant effect on ageing of material.

“The main factors in the aging of paper insulation and pressboard insulation in a transformer are the presence of oxygen, temperature, and humidity. (Figure 11)

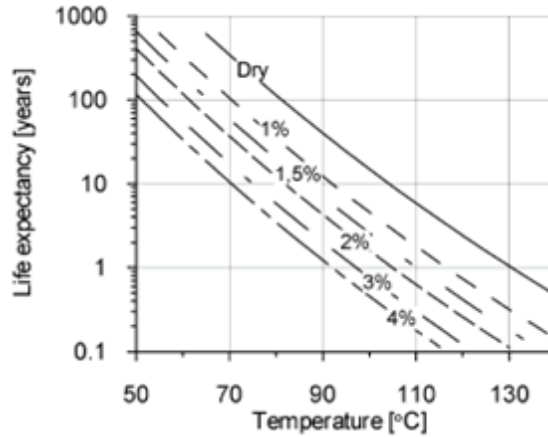


Figure 11: Expected life for solid insulation and its dependence upon moisture and temperature.

Ageing of cellulosic insulation in transformers is caused by oxidation, carboxylic acids, and water, which enhance the catalytic efficiency of the acids by promoting their dissociation.” [9]

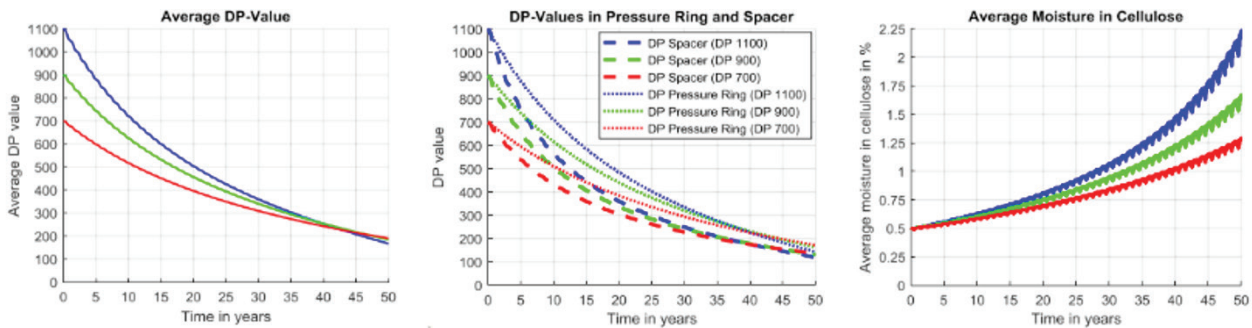


Figure 12: Aging with different initial DP values (blue lines:  $DP_{init} = 1100$ , green lines:  $DP_{init} = 900$ , red lines:  $DP_{init} = 700$ )

“It is the initial moisture content in the solid insulation material, which is important to extend the lifetime of a transformer. A realistic simulation shows that the time to reach an average DP value of 200 is with 0.5% initial moisture about 11 years longer than with 0.8 % initial moisture.” (Figure 12) [8]

Barrier transitions, locations, thicknesses, and diameters should be designed by taking this into consideration The contacts that will perform the switching function on the main current carrying conductor should be positioned at the places where the electric field is the lowest, and these contacts should be selected with the technical properties that will allow switching repeatedly. In the design against gas trapping, the design should be made by considering the continuity of the insulation material. Dual Switchingboard and Up-Down Connection System are designed in accordance with this knowledge.

Barriers with duct’s more stable as good as increasing the efficiency of the pre-conditioning process as VP drying and mineral oil or ester oil impregnation. Thanks to oil ducts, the heat and liquid is transferred effectively in all cellulose barriers.



Oral Presentation: Pressboard Barriers in Smart Connection Systems for High Voltage Power Transformers

### 3. ASSEMBLE OF SMART CONNECTIONS

Dual Switchingboard:

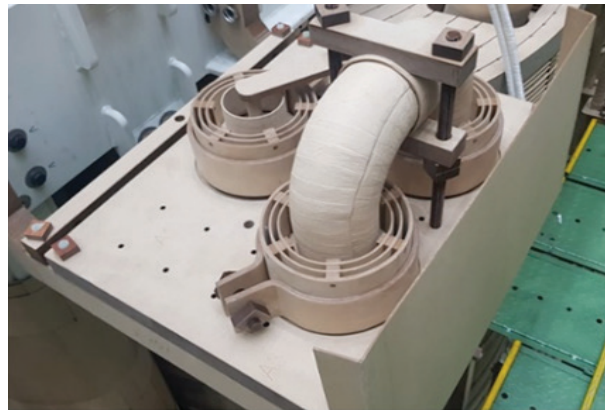
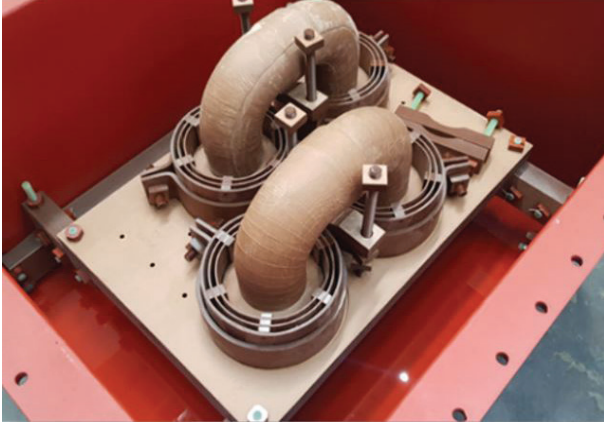
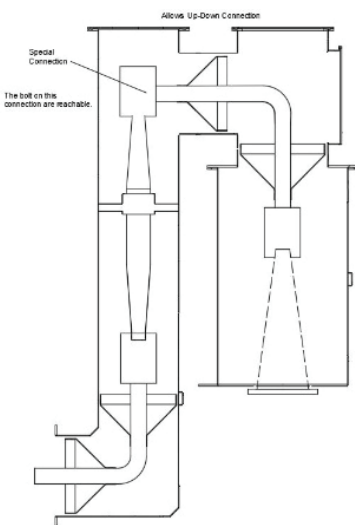
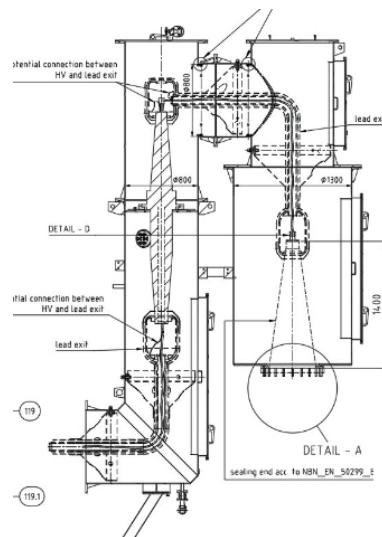


Figure 13

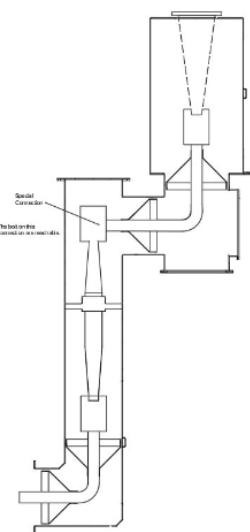
Up-Down Cable Box Connection:



Down position



Detailed Drawing



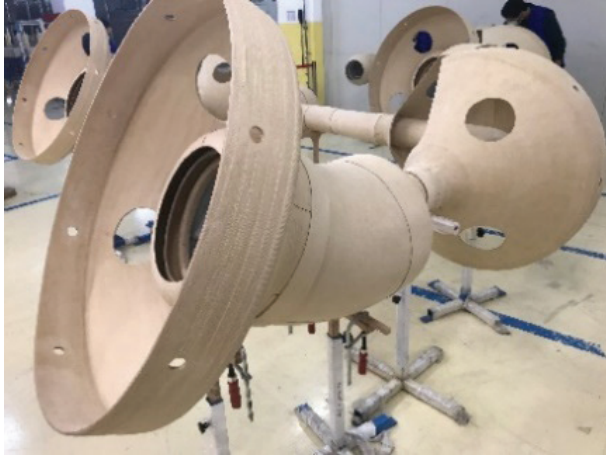
Up position

Figure 14





With the use of a barrier system during the design phase, these two positions can be changed easily and quickly in the site. Therefore, the moisture absorption of the insulation materials and the exposure time to atmospheric conditions are limited. (Figure 14)



*Up-Down Cable Box Connection*



*Assembled in Transformer*

Figure 15

Service advantages:

- 1- Easier assembly process in a shorter time
- 2- Less handling work on site
- 3- Using the Dual Switchingboard for parallel connections significantly shortens the transformer cover open time, thus minimizing air, moisture exposure time to the transformer.
- 4- These connections switch the transformer to another ratio or connection direction without the need to add or wrap another insulating material such as paper. After the system connections are made, it is ready to energize in a short time.
- 5- Minimize transportation costs by allowing separated turret transportation.

## 4. CONCLUSION

Dual Switchingboard and Up-Down Cable Box Connection systems (Figure 13-15) are designed with thin oil ducts which allows lower electrical fields so that the complete system becomes more stable and reliable. In comparison to thick paper insulation, pressboard barrier systems increase the efficiency of the pre-conditioning process prior to FAT. Drying and oil impregnation processes are easier on pressboard barriers thanks to thin layers.

Therefore, distribution of heat in barrier systems is more effective. Ageing dependent on temperature is decelerated due to the fact that barrier systems allow the balanced heat distribution at pre-conditioning process. Vaporization of the water in barrier systems with pressboard is easier. Shorter durations and lower temperatures of drying are needed for barrier systems in smart connection due to the fact that the water content must be lower than 0.5% before FAT. This causes the DP value of the material to be higher. In addition, during operation, heat is effectively removed from the oil channels as the barrier systems contain thin pressboard insulation and oil channels. This ensures slower ageing of the insulation material covering the current carrying conductor.

Increase in DP value and effective remove of heat means longer duration of transformers which include smart connection systems such as Dual Switchingboard and Up-Down Cable Box Connection.

## BIBLIOGRAPHY

- [1] B. Koti Reddy Design Changes to Improve Transformers Performance
- [2] C. Perrier, A. Beroual, J-L. Bessede, Improvement of Power Transformers by using Mixtures of Mineral Oil with Synthetic Esters



Oral Presentation: Pressboard Barriers in Smart Connection Systems for High Voltage Power Transformers

- [3] Central Electricity Authority Regulations »STANDARD SPECIFICATIONS FOR TRANSFORMERS AND Reactors (66 kv & ABOVE VOLTAGE CLASS)«
- [4] Maik Koch, Improved Determination of Moisture in Oil-Paper-Insulations by Specialised Moisture Equilibrium Charts, Beijing, China ,2005
- [5] J. Dai, Z. D. Wang, P. Jarman, 13 - Moisture and Aging Effect on the Creepage Discharge Characteristics at the Oil/Transformerboard Interface under Divergent Field, 2008 Annual Report Conference on Electrical Insulation Dielectric Phenomena
- [6] E.Öztürk , Exit Insulation Systems (EIS)&Middle Exit Systems, 12. International Conference on Transformer Trafosome 2013, Innovative Quest for transformer Technology for Efficient and reliable Power, Bengaluru 15 Nov 2013
- [7] H.P.Moser Transformerboard, 1987
- [8] J. Raith, Ch. Bonini, M. Scala Siemens AG Oesterreich, Transformers Weiz, Global Technology Centre , ' Simulation of long-term transformer operation with a dynamic thermal, moisture and aging model ' 5th International Colloquium on Transformer Research and Asset Management ,17 July 2020.
- [9] Selim YUREKTEN, Faruk ERENLER, Emre ÖZTÜRK Comparison between Pressboard Barrier System and Wrapped Crepe Paper Method in the design of 800 kV Winding Link Connection Insulation System



# Istanbul: City Centre Infeed with Voltage Source Converter-Based HVDC

[arman.derviskadic@hitachienergy.com](mailto:arman.derviskadic@hitachienergy.com) / [behbahani22@itu.edu.tr](mailto:behbahani22@itu.edu.tr) / [tourandazkenari@itu.edu.tr](mailto:tourandazkenari@itu.edu.tr) / [ozdemiraydo@itu.edu.tr](mailto:ozdemiraydo@itu.edu.tr)

**ARMAN DERVISKADIC, MAURO MONGE, PETER LUNDBERG**

*Hitachi Energy*

*Italy, Sweden*

**FATEMEH MOHAMMADI BEHBAHANI, DR. MEGHDAD TOURANDAZ KENARI, PROF. AYDOGAN OZDEMIR**

*ITU - Istanbul Technical University*

*Türkiye*

## SUMMARY

By 2025 Istanbul is expected to become Europe's largest urban area. The fast-growing population trends suggest that it very likely will be the only European urban area to reach a population of 20 million inhabitants. Furthermore, the rise of EU industrial reshoring opportunities will most probably lead to subsequent extensions of organized industrial zones (in Turkish "Organize Sanayi Bölgesi"). Urban electrical power systems with steep demand increases need innovative technical solutions that can address several challenges simultaneously. As power loads in Istanbul are increasing, the metropolitan power network will continuously be upgraded in order to meet the demand for huge amount of power. In most crowded areas land space is becoming scarce and expensive, and therefore, substantial difficulties arise whenever new right-of-way must be secured to carry additional power over traditional transmission lines. As power transmission levels increase, the risk of exceeding the short-circuit capability of existing switchgear equipment, as well as other network components, becomes another real threat to the further expansion of power networks. Strategies to develop urban power networks must also address issues like power congestion, pollution, acoustic and electrical noise, electromagnetic fields, power quality and control, and permits, among others.

With HVDC technology all the above issues can be overcome. The HVDC converter stations based on Voltage Source Converters with small footprint are ideal for infeed to city centres. To reduce the visual impact and to increase resilience to different environmental conditions, the converter station may be built as an enclosed building containing all equipment. To minimize the footprint and the total volume, the converter station may be built on two or more floors. This design principle gives a station design suitable for high power handling on a compact site that would be useful where land area is at a premium.

In addition, several system benefits can be achieved by Voltage Source Converter (VSC) technology which makes it easy to apply in heavily loaded grids, such as independent full active and reactive power control, no added contribution to the short-circuit levels, the balance of power flows on multiple urban infeeds, enhanced grid stability, etc.

Finally, the use of VSC-HVDC enables long underground transmission distances and high transmission capacity through XLPE DC cables as compared to equivalent AC cables. The DC cables can easily be installed using existing right-of-ways and the capacity can thus be significantly increased on existing power corridors. In addition to the mentioned benefits, an advantage would be the possibility of removing obsolete and polluting generating plants from the city centre, improving the air quality and allowing for a clean-air breath-taking view of Sultanahmet across the Bosphorus.

A number of different topologies are possible for single or multi-infeed, giving large freedom of design to adapt to the specific network situation. Design and technical analysis of an HVDC transmission system, capable to feed more than 1'000 MW to Istanbul city is presented in this paper.

## KEYWORDS

HVDC, Voltage Source Converters, City Center Infeed, Grid Stability, Converter Station, Right of Way



### 1. INTRODUCTION

Population growth and global warming are among the most pressing challenges that humanity faces nowadays. Increasing population and ongoing urbanization lead to larger and denser cities, carrying along an important side effect of urban life: air pollution. Air pollution in Türkiye is the most lethal of the nation's environmental issues, with almost everyone across the country exposed to more than World Health Organization guidelines. Road transport and coal-fired power stations in Türkiye are major polluters with severe impacts on public health: cardiovascular diseases, strokes, chronic obstructive pulmonary diseases, lung cancers, acute respiratory infections.

The European public opinion increasingly puts climate and environmental action at the top of its policy priorities and strongly support the transition to a low-carbon economy (and in some countries, i.e. Germany, nuclear-free economy). By following similar trends in Türkiye, as presented in the Turkish National Energy Plan 2022 [1], the share of fossil resources based electric power generation, which was 83.3% in 2020, will decline to 70.4% by 2035 and will reach 20.8% by 2053. The share of coal will decrease to 21.4%, by 2035 (3.6%, by 2053) and the shares of oil and natural gas will fall to 26.5% (5.6%) and 22.5% (11.7%) by 2035 (2053), respectively. At the same time, to match the growth in the future forecasted electricity demand, the share of renewable energy sources in the installed capacity, which was 42.4% in 2020, will reach 69.1% by 2053, of which the intermittent renewable energy sources in electricity generation, will rise from 11.7% in 2020 to 61.4% by 2053. More details about the renewables sector in Türkiye will be given in section II.

Istanbul, besides being the magical place where East meets West, will become a very interesting playground for electrical engineers as it will be the place where steep electricity demand increase meets large shares of intermittent power generation. Projections towards the future suggest that:

- Power loads will be increasing as the city continues its urbanization and industrialization
- Traditional power generation will slowly shut down following the decarbonization trends up to the 2050s
- Intermittent renewable generation will grow in the neighbouring regions up to the 2050s

The metropolitan power networks will be continuously upgrading in order to meet the future demand for power, but will be limited by some social-economical and technical constraints, i.e.: land space being scarce and expensive, difficulties to obtain new right-of-ways and authorizations to build new transmission infrastructure, power congestions, acoustical and electromagnetic noise, short-circuit power restrictions, power quality and control, among others.

The choice between investing in AC grid reinforcements or HVDC transmission depends on technical, economical and environmental factors. When more AC-circuits are added to a city center network, the short circuit power increases, especially if AC-cables are added, due to their low reactance per meter. In extreme cases, this may lead to an upgrading need on several substations to cope with the new network kA situation. The HVDC technology based on VSC converters, which will be presented in section III, can solve all the above mentioned issues. VSC converter stations can be designed to be very compact and reduce the overall footprint, ideal for infeed to city centers. HVDC cables, which allow higher transmission capacity compared to equivalent AC-cables, can be installed underground boosting the capacity of existing power corridors, within the limits of existing right-of-ways. The footprint of converter stations and cables will be described in section IV.

System benefits from the VSC technology, such as independent full active and reactive power control, no added short circuit power, the possibility to balance power flows on multiple urban infeeds make it easy to apply in heavily loaded grids. Finally, from an environmental point of view, the HVDC technology gives virtually no alternating magnetic field as will be described in section VI.

With the integration of intermittent renewable energy sources, the need for flexibility in the system is growing. One of the ways to improve the flexibility is to increase the interconnection capacity with neighbouring countries or to increase the power transmission capacity between high density renewable generation areas and load consumption areas. HVDC transmission can add significant system benefits in both cases. The case study presented in this paper in section V will closely look to opportunities to boost the transmission infrastructure in the Istanbul metropolitan area by including an HVDC transmission corridor across the Bosphorus.

### 2. RENEWABLES ENERGY PENETRATION IN TÜRKIYE

Türkiye's location as a bridge between Europe and Asia transforms the country into a regional energy hub. Besides this geographical location, natural resources have made Türkiye a suitable area for generating and transmitting renewable energies. Regarding Türkiye's potential for renewable energy, current flexibility opportunities, and potential in the future, it is intended to increase the share of intermittent renewable energy sources like wind and solar in overall electricity generation.



Oral Presentation: Istanbul: City Centre Infeed with Voltage Source Converter-Based HVDC

For other renewable energy sources, the installed capacity will increase to 35.1 GW in hydroelectric power plants and 5.1 GW in geothermal and biomass power plants. The share of renewable energy sources in installed capacity will reach 64.7% by 2035. The average yearly additional capacity needs for solar and wind energy are 3.1 and 1.4 GW, respectively.

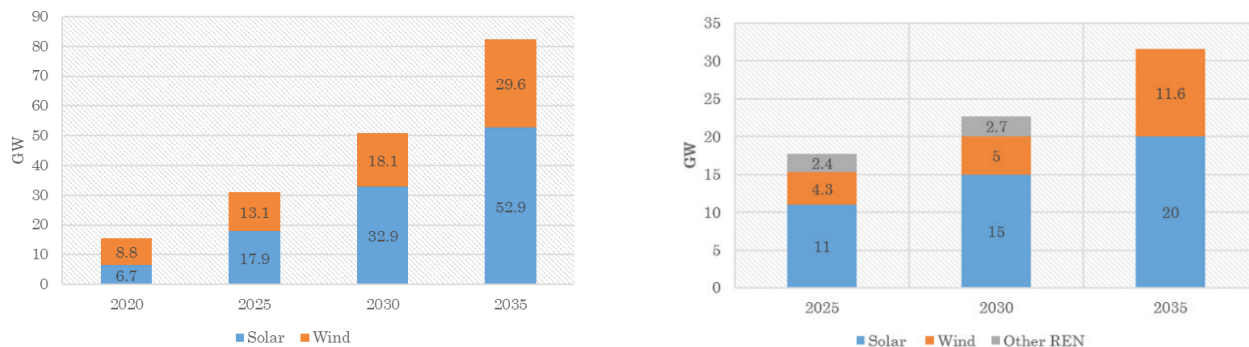


Figure 1: Installed capacity by source and New Installed Capacity Commissioned in Five-Year Periods [1]

The proportion of intermittent renewable energy sources in the production of power will gradually rise to 34.3% by 2035. In the same way, by 2035, 54.8% of power will be generated using renewable energy sources. They are getting close to their maximum installed capacity and generation potential.

The amount of electricity consumed, which increased from 128 TWh to 306.1 TWh between 2000 and 2020 at an average annual growth rate of 4.4%, will rise to 510.5 TWh by 2035 at an average annual growth rate of 3.5%. Average annual electricity consumption is anticipated to rise by 3.7% in the industrial sector, 2.3% in the residential sector, and 2.2% in the services sector throughout the estimation period.

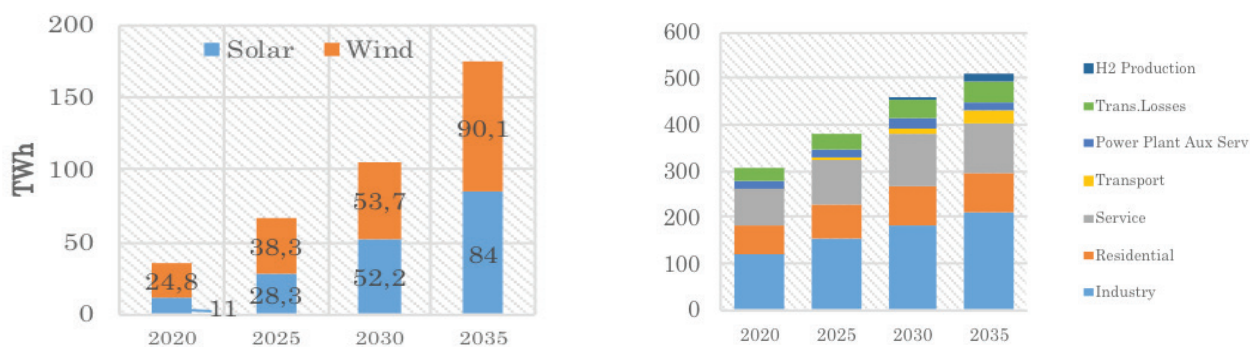


Figure 2: Electricity Generation by Source [1] and Electricity consumption by sector [1]

### 3. HVDC TECHNOLOGY BASED ON VSC CONVERTERS

Operational challenges with high share of wind and solar photovoltaic generating plants are linked to short circuit capacity, system inertia, grid voltage stability, grid congestions, supply-demand balance. HVDC transmission has proven to be a cost-effective solution and its integration within the current AC system can contribute in several ways to achieve a timely energy transition. HVDC based on VSC technology, which is celebrating 25 years since the first HVDC link [2], [3] based on VSC converters was commissioned, contributes by adding several system benefits, such as: flexibility in active and reactive power control for voltage/frequency regulation, higher reliability and security of power supply, provision of ancillary services, wide-area power oscillations damping, black start capability and restoration of the AC grid, improvement of the power flow control to optimize the operation of the AC grid closer to its thermal limits, improvement in stability and flexibility in the overall transmission grid.



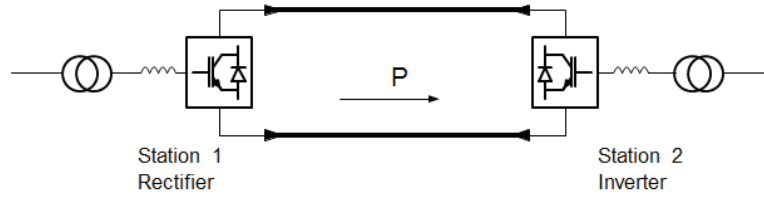


Figure 3: A schematic diagram of a point-to-point VSC-HVDC system based on MMC.

An HVDC system can be summarized as in Figure 3. In this example the “Station 1” operates in DC-Voltage Control Mode while the “Station 2” operates in Active Power Control Mode and adjusts its DC voltage until the AC power matches the power order received by the TSO. The VSC converter, as hinted by the name, behaves as a voltage source behind an impedance, with high controllability of the waveform, both in amplitude and in frequency. Figure 4 shows a schematic diagram for an HVDC converter based VSC technology; the latest generation of voltage source converters is the Modular Multilevel Converter (MMC) with Half Bridge cells. In general, the use of VSC type converters guarantees high standards in terms of flexible operation thanks to the capability to fully control independently both the active and the reactive power flow within the operating range of the HVDC system.

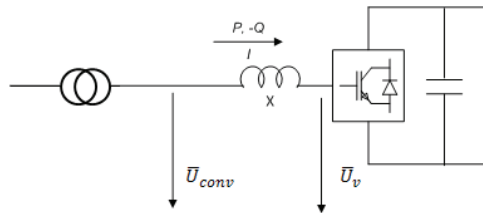


Figure 4: A schematic diagram of a point-to-point VSC-HVDC system based on MMC.

The grid voltage could also be defined as point of common coupling voltage ( $U_{PCC}$ ). By controlling the converter valve voltage ( $U_v$ ) several operation modes can be achieved. The active and reactive power at the point of common coupling can be expressed as:

$$P = U_{Conv} I \cos \varphi \approx \frac{U_v U_{Conv}}{X} \sin \delta \tag{i}$$

$$Q = U_{Conv} I \sin \varphi \approx \frac{U_{Conv}(U_v \cos \delta - U_{Conv})}{X} \tag{ii}$$

As described in Figure 5, and by virtue of equation (i), by controlling the voltage angle difference between converter valve voltage ( $U_v$ ) and grid voltage ( $U_{PCC}$ ), the active power can be controlled. Active power should be controlled in a coordinated way: the converter station 1 controls the active power (P-control) while the converter station 2 controls the DC voltage (UDC-control) so that the active power on the DC side is balanced. By virtue of equation (ii), by controlling the voltage amplitude difference between converter valve voltage ( $U_v$ ) and grid voltage ( $U_{PCC}$ ), the reactive power can be independently modified. The overall control is achieved with local measurement of voltage and currents, both AC and DC, and does not require extensive coordination with other converter stations beside the definition of the respective control modes.

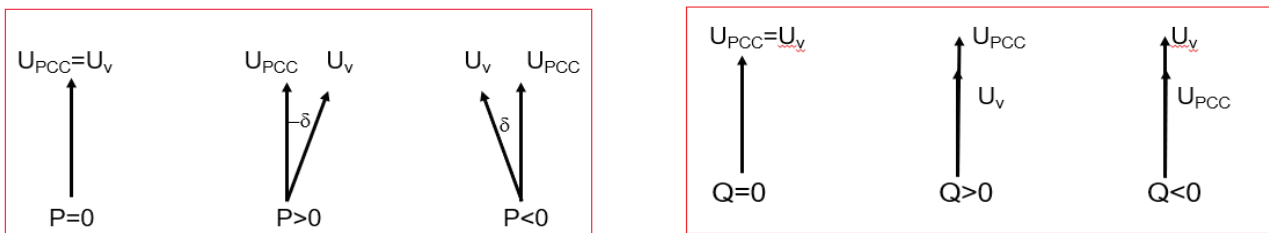


Figure 5: simplified active and reactive power control principle of Voltage Source Converter technology

The consumption of reactive power at densely populated metropolitan areas varies during the day. The resulting voltage fluctuations may be counteracted by using switched capacitor banks and shunt reactors. Such switched passive components cannot handle





dynamic phenomena like faults and transients in the transmission system. HVDC with VSC converters have the dual function of controllable active and reactive power injection or consumption as needed; The rapid and accurate voltage control capability of the HVDC based on VSC converters makes it possible to operate the grid closer to its upper limits since rapid reactive power compensation maintains the voltage levels to optimal and stable levels. The resulting higher voltage level allows more power to be transferred through adjacent AC lines operating closer to the thermal current limits and improving the overall system's efficiency. Furthermore, the system can be regulated quickly and respond to transients and other sudden changes in the network conditions. Finally, the current out of the VSC-based HVDC station is controllable also during large events such as short-circuits at the connected AC network. In this way also the current contribution to the fault is controllable and predictable. This feature becomes very important in case of increasing multi-infeed into an existing AC network since the increased power supply does not necessarily imply a much higher level of short circuit current contribution, allowing the existing protective devices (eg. AC power breakers) to still work in the new scenario.

A number of different topologies and system configurations are possible for point-to-point HVDC transmission, giving large freedom of design to adapt to each specific network situation. The two most suitable topologies for the scope presented in this paper are:

- **Symmetric monopole**,  $\pm 320$  kV – 1.400 MW (the limiting factor of the rated power is the ampacity of the HVDC cable system), shown in Figure 6. The advantages of this topology are the low costs and the low transmission losses. The disadvantage of this topology is the loss of 100% of the transmission capacity at power at trip
- **Bipole**,  $\pm 525$  kV – 2.000 MW with HVDC Cables and 3.000 MW with HVDC overhead lines, shown in Figure 7. The advantage of this topology is the higher availability, a converter outage or transmission line outage results in a loss of 50% of the installed capacity. For this reason, systems with high rating are typically built in bipolar configuration, also since N-1 criteria have to be considered. The disadvantage of this topology is the temporary ground current which could be avoided at the expense of a metallic return conductor.

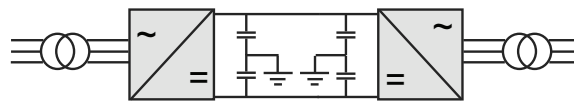


Figure 6: System configuration: symmetric monopole

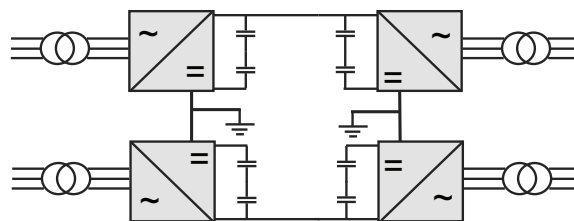


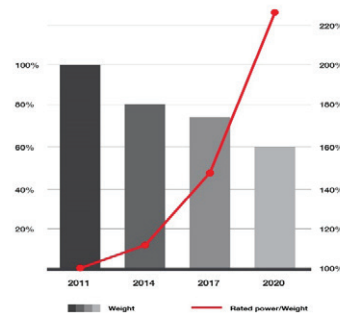
Figure 7: System Configuration: bipole

## 4. FOOTPRINT OF CONVERTER STATION AND CABLES

When designing converter stations in areas where space requirements are not strict, the conventional design is normally used as proven to be more efficient. However, situations where land space being scarce and expensive, to minimize the foot-print and the total volume, the converter may be built in two or more floors as an enclosed building containing all equipment.

This design principle gives a new HVDC converter station design suitable for high power handling on a very compact site that would be useful where land area is at a premium. In the last decade the main driver for compact design was driven by offshore wind applications. In the offshore wind sector the industry has experienced continuous improvement of HVDC modularized design and interface management which led to optimization of AC and DC equipment and enabled offshore platforms with 40% reduction in weight/volume. This challenge has been addressed by compact main circuit equipment, optimized redundancy with maintained availability and layout optimization. In Figure 8, it is shown the progress in layout optimization over the last decade, where is emphasized the rated capacity of the HVDC converter stations versus the platform size.

Platform weight/Capacity development


**Figure 8:** Platform weight-capacity optimization at Hitachi Energy

The following offshore HVDC converter station dimensions can be used as reference, derived from recent HVDC offshore installations:

**Table 1:** Ratings and offshore station dimensions for different topologies

Topology	Symmetrical Monopolar	Bipolar
Rated Power	1320 MW	2000 MW
Rated Voltage	$\pm 320$ kV	$\pm 525$ kV
N. Cables	2 x HVDC	2 x HVDC 1 x neutral
Onshore station dimensions	160 x 80 m	180 x 160 m
Offshore station dimensions	70 x 40 x 40 m	100 x 50 x 40 m

Such compact HVDC converter stations are ideal for feeding electricity with low losses into densely populated urban centres, introducing several operational advantages as power control capabilities which are used to control the power flow in the AC network, to optimize the load flow through the existing AC lines, to support reduction of the overall losses in the existing AC grid, to increase capacity of transmission and to improve the stability of the power transmission system. Detailed studies are shown in [4] and [5].

Innovative urban planning methods will be needed to benefit from optimal utilization of energy resources and efficient measures shall be taken to solve the challenges of energy planning in large cities, with the goal of providing stable and secure electricity supply. In the future, compact HVDC converter stations will be a strong tool in urban planning in densely populated metropolitan areas. A conceptual drawing of a multiple-layers HVDC converter stations is shown in Figure 9. By this approach is possible to grant integration of HVDC transmission assets in normal urban environments along with residential, commercial and industrial areas.

From sustainability perspective, future opportunities in utilizing each converter station to its fullest potential has been explored and possible solutions include:

- Installation of solar power capacity of 150 up to 500 kW on the rooftops, with energy outputs depending on location, size of the installation area, orientation and inclination angle of the solar panels, etc.
- Installation of green rooftops, which could lead to thermal improvements due to lower energy utilization for cooling and heating, and support on CO2 reduction, improving air quality, support biodiversity and wildlife
- Utilize waste heat from converter station, like it has been done in the converter station Ertsmyra (Nordlink) in Norway which utilizes 50-60% of the waste heat for heating up facilities located nearby

Based on the above considerations several renders have been produced where HVDC converter stations are fully integrated in urban environments and in countryside environments, as shown in Figure 10.

Another issue is that entering an urban area with new high-voltage overhead lines is very difficult or even impossible due to scarcity of available land. In such cases, the alternatives may be increased generation capacity in the city, installation of new transmission



Oral Presentation: Istanbul: City Centre Infeed with Voltage Source Converter-Based HVDC

lines by AC-cables or installation of new HVDC transmission systems based on HVDC cables. Both the alternatives with AC and DC cables can be motivated and are technically feasible.

In the case that the HVDC alternative is chosen several system benefits could be achieved:

- HVDC system transmit more electrical power over longer distances which means fewer transmission lines are needed, saving both money and land
- The power handling of a given cable dimension is higher for DC than for AC due to better utilization of the insulation and lower losses in conductor and shield
- AC-cables may be difficult to implement due to reactive power balancing problems, added short circuit power and in some cases limited transmission distance. An AC-cable network has a large generation of reactive power during low-load, forcing measures such as shunt reactors to be implemented. The DC cable alternative gives no technical limit to the transmission distance, adds no short circuit power and enables improved reactive power balance due to the properties of the HVDC converters based on VSC technology.
- HVDC transmission lines have negligible electromagnetic fields. The magnitude of the magnetic field generated by a pair of HVDC cables in typical installation conditions is far lower than the earth magnetic field we all are exposed to.
- HVDC cable technology can save significantly the land usage as shown in the graphic in Figure 11.

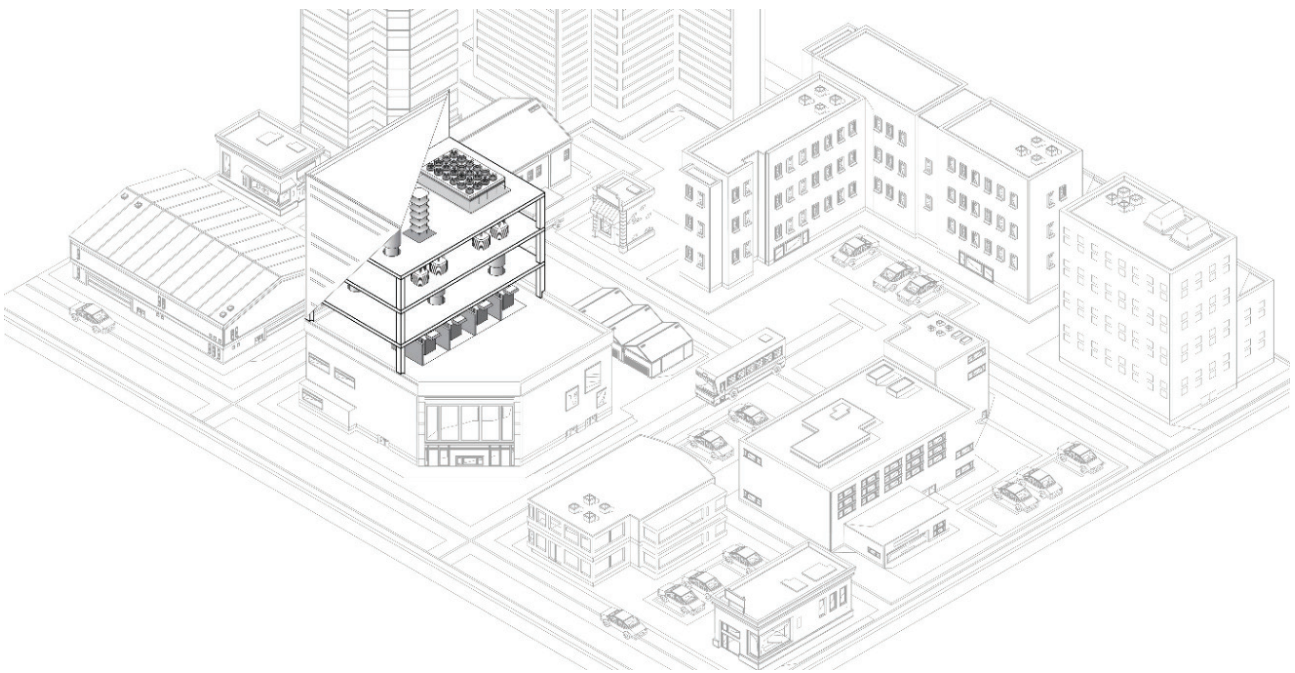


Figure 9: Render – Integration of a multiple-floors HVDC Converter station in a metropolitan environment



Figure 10: Renders of HVDC converter stations integrated in urban, countryside and mountain environments



## More power, less space

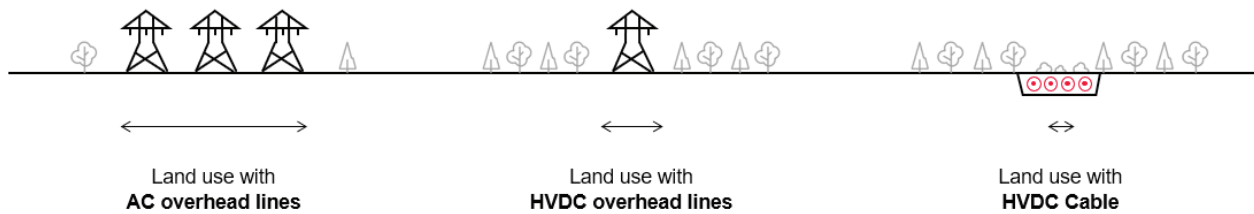


Figure 11: Typical 3 GW transmission line

## 5. CASE STUDY – ISTANBUL CITY CENTER INFEED

Several alternatives for a possible HVDC transmission application in Türkiye are analysed in [6]. The locations of converter stations and power rating of the transmission system were selected according to power generation and consumptions density of Türkiye. Traditionally, HVDC systems were installed when there was need to transmit bulk power over very long distances to connect consumption industrial and urban areas with far-away generating plants, with high efficiency and low electrical losses.

This paper focuses on a different application, which is to collect intermittent renewable generation at a region where there is an overgeneration of renewables and to enable grid operators to integrate efficiently higher share of green power and to transmit it to the city centre of Istanbul, to increase stability, to foster flexibility and at the same time to achieve several system benefits for the urban transmission grid and reduce CO<sub>2</sub> emissions. It is very difficult and sometimes is impossible to increase the transmission capacity by conventional HVAC technology due to mainly space and right-of-way constraints, statutory clearance delays etc. To overcome such issues and efficiently integrate increasing amount of green power into urban centers, innovative HVDC technology solutions are very useful.

Energy demand in Istanbul is increasing rapidly due to:

- Population increases over 20 million inhabitants (and increase of per capita power consumption)
- Industry expansion: the extensions of “Organize Sanayi Bölgesi” (organized industrial zones) supported by the global trends and fostered by the EU industrial reshoring challenges.
- Investments in data centers to meet digitalization trends with consequent increase in power consumption
- New requirements for mobility: fast-trains, metro and e-mobility

The combined effect of decarbonization trends and increase of electricity consumption could lead power shortages in the coming future. Therefore, power will be supplied by generating plants located in other provinces where the electricity consumption is noticeably less than their production. Like all European main cities that are investing to become more environmentally sustainable, Istanbul is targeting to reduce its carbon footprint by integrating more and more renewable energy in the energy mix.

Its location on the Bosphorus, makes Istanbul easily accessible by submarine HVDC cables. This advantage drives the choice of the provinces which are most suitable to feed renewable power to Istanbul. Table shows the production of renewable energy sources in some Turkish provinces in February 2023 [7]. Izmir with 1798.15 MW up to 2022 is the capital of wind energy, followed by Balıkesir and Çanakkale in the Marmara region, which are the cases in this study with the last update 1251 MW and 990.42 MW of wind energy, respectively. The fourth largest wind province is the Aegean province of Manisa with 736.5 MW of installed capacity by 2022, and Hatay in the South is the fifth largest wind province with 414.65 MW in this period.



Table 2: Distribution of electricity energy production by province and source (MWh) [7]

Province	Solar energy	Wind energy
ADANA	-	17.548,28
AFYONKARAHİSAR	32.729,77	-
ANKARA	36.444,23	-
ANTALYA	21.464,11	-
BALIKESİR	9.534,67	3.093,43
ÇANAKKALE	1.619,46	3.440,77
DENİZLİ	21.700,13	-
ERZURUM	9.982,80	-
ISTANBUL	188,81	907,70
IZMIR	32.665,34	691,09
KAYSERİ	36.601,93	-
KONYA	68.987,75	0.13
MANİSA	29.563,30	-
MARSIN	21.383,23	-
ŞANLIURFA	49.816,34	-

When combining renewable generation capacity and submarine cables accessibility, the provinces of Balıkesir and Çanakkale have been selected for this case study to transmit their surplus power to Istanbul. In Çanakkale and Balıkesir are installed respectively 6% and 20% of the total Turkish wind power installed capacity. Both provinces are among the top seven provinces with the highest number of wind power plants in operation. The total amount of available generation capacity divided by source is shown in Figure 12.

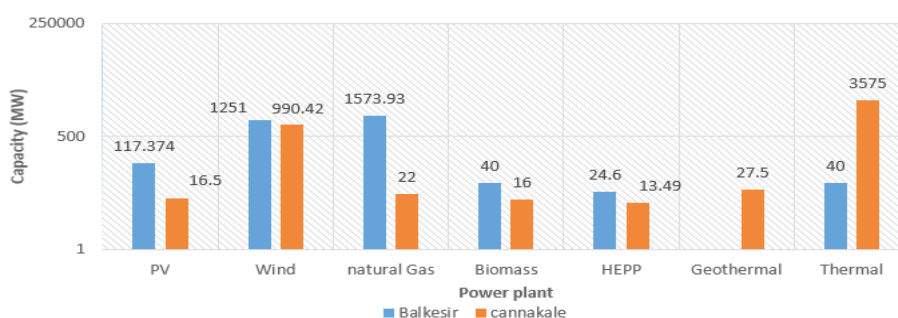


Figure 12: Balıkesir and Çanakkale installed power capacity

Table 3 shows the ratio between production and consumption in those provinces, showing that there is a significant surplus in power production and making them eligible to supply power to Istanbul city center in this case study.

Table 3: Power production potential and consumption [8]

Province	Production (MWh)	Consumption (MWh)	Production/Consumption Ratio (%)
Çanakkale	28,091,330	3,907,000	719
Balıkesir	13336050	4,885,000	273
Istanbul	13,752,440	52,894,000	26



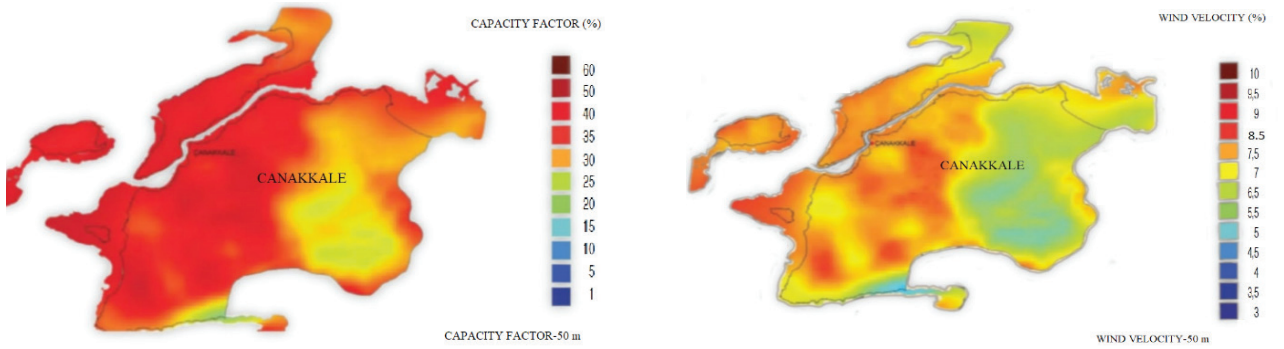


Figure 13: Çanakkale WEPA map [9]

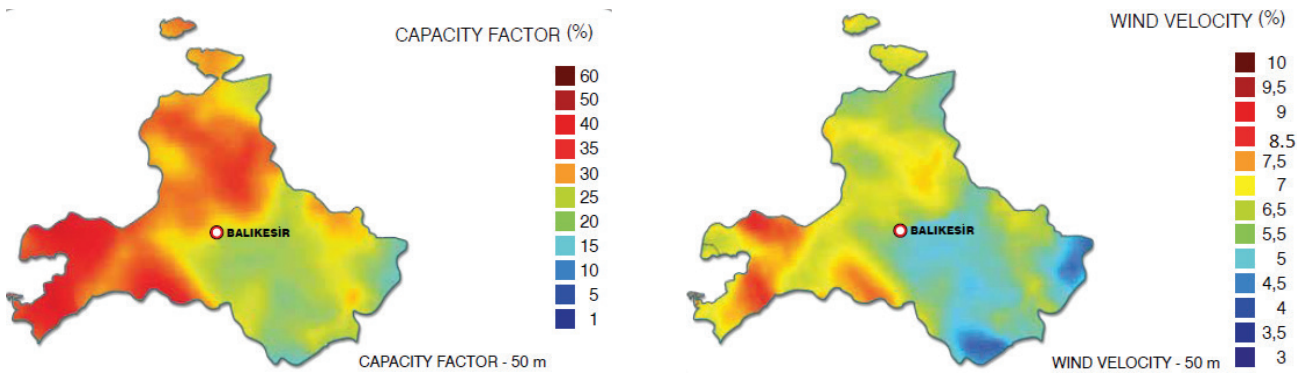


Figure 14: Balıkesir WEPA map [9]

Figures 13 and 14 show the Balıkesir and Çanakkale WEPA maps which prove the high wind potential in those provinces. Balıkesir has 3,000 km<sup>2</sup> of available land to install wind farms, and the maximum installable wind power capacity is 14,000 MW [10] while Çanakkale has 2,602.51 km<sup>2</sup> and the maximum installable wind power capacity is 13,012.56 MW [10]. Besides huge potential, the planned capacity increases up to 2025 is still limited and will reach respectively 1294 and 1170.42 when adding wind farms under-construction.

As shown in Figure 3, the point-to-point HVDC Transmission system needs two converter stations. The sending converter station for this case study has been selected in Çanakkale, four options have been evaluated: BEKIRLIT-1, BEKIRLIT-2, İÇDAS, and CENAL T. Concerning Balıkesir, at present there are no substations with desirable capacities facing the Bosphorus and therefore evaluations could be continued under the assumption that a new substation could be built to meet future needs.

The receiving station alternatives in Istanbul which have been selected in this case study are IST.DG.A, YENİBOSNA, ALİBEYKOY and İKİTELLİ.

Table 4 shows the distances between the above-mentioned substations.

Table 4: Distances between substations

Arrival Substation	Departure Substation	Distance (km)
BEKIRLIT-1	AliBeykoy	188
BEKIRLIT-2	AliBeykoy	176
İÇDAS	AliBeykoy	160
CENAL T	AliBeykoy	153
BEKIRLIT-1	IST.DG.A	178
BEKIRLIT-2	IST.DG.A	170





Arrival Substation	Departure Substation	Distance (km)
IÇDAS	IST.DG.A	162
CENAL T	IST.DG.A	130
BEKIRLIT-1	Yeni BOSNA	187
BEKIRLIT-2	Yeni BOSNA	178
IÇDAS	Yeni BOSNA	163
CENAL T	Yeni BOSNA	141
BEKIRLIT-1	IKITELLI	187
BEKIRLIT-2	IKITELLI	177
IÇDAS	IKITELLI	158
CENAL T	IKITELLI	143

After cadastral analysis, it is found that IST.DG.A. is the most suitable location in Istanbul since all other substations are surrounded by densely built areas. IST.DG.A has similar issues, being surrounded by a 2.7 km<sup>2</sup> industrial zone, however it has been identified a suitable area close to IST.DG.A. where a new transmission substation could be built: the old ATATURK airport under dismission.

Based on the above considerations, two alternative scenarios are investigated in details.

**SCENARIO 1:**

- At present the wind farms connected to BEKIRLIT-2 with 1200 MW installed capacity.
- Forecasted expansion to 3000 MW up to 2035.
- Mean distance between BEKIRLIT-2 and wind power plants is 52 km on average (AC cables)
- Length of HVDC submarine cables: 176 km from IST.DG.A substation in Istanbul

**SCENARIO 2:**

- New substation to be built near Bandirma, which is 107 km away from IST.DG.A substation in Istanbul.
- Forecasted expansion to 3000 MW up to 2035.
- Mean distance between the new substation and wind power plants is 79 km on average (AC cables).
- Length of HVDC submarine cables: 107 km from IST.DG.A substation in Istanbul

In both scenarios could be planned 2 alternative solutions, based on the forecasted expansion of renewable energy sources in the region. In case of a conservative scenario, it could be planned an HVDC symmetrical monopolar system, rated 1320 MW ±320 kV. In case of an optimistic scenario, it could be planned and HVDC bipolar system rated 2000 MW ±525 kV.

**6. EMC CONSIDERATIONS**

Municipality authorities normally include stringent limits on allowable EMI levels and not complying with these limits can have significant economic impact in terms of delays and penalty fees. High frequency modeling of HVDC converter stations is of high relevance for such systems. Various aspects, such as electromagnetic modeling of high voltage multi-level converter substations [11], of HVDC converter transformers [12], and air core reactors [13] have been investigated in recent work. A complete system modelling, aiming at quantitative prediction of near and far field EM field disturbance levels has been developed. The simulation methodologies and workflows allow to predict radiated EM field levels at an early design stage and with an accuracy comparable to field measurements. This is especially critical for large components such as the transformers and phase reactors: early EMC simulations therefore influence the choice of converter transformer or reactor design variants

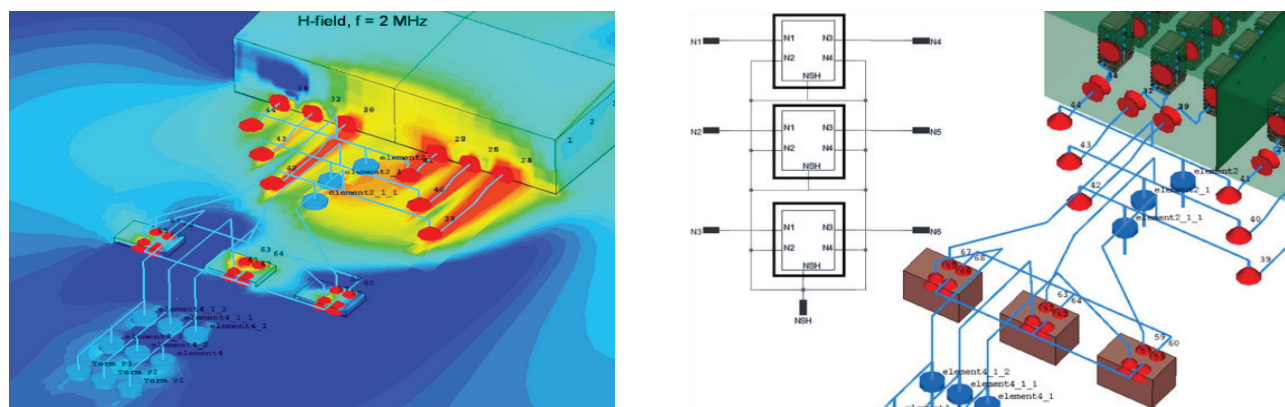


**Figure 15:** Schematic, 3D and H-field (near field) simulations of an HVDC converter station with three 1-ph transformers

In Figure 15 the impact of a traditional HVDC converter station is investigated and modelled. The frequency range of interest is between 10 kHz and 10 MHz. The numerical simulation methodology for modelling and predicting the radiated EM field disturbance is based on co-simulations of coupled 3D and circuit models, performed in CST Studio Suite using the transmission line matrix (TLM) time domain solver.

With such plots the electromagnetic coupling and radiation mechanisms in a substation can be visualized and used to optimize the station layout in terms of component placement and bus bar routing for minimal resonances and radiation, and therefore to avoid radiated disturbances instead of being constrained to introduce measures such as filtering and shielding. Also, the critical radiation frequency ranges and levels can be determined and compared to the specified EM field disturbance limits. As a consequence, high frequency filters can be optimized and installed for the critical frequency ranges only. Furthermore, expensive shielding enclosures can be reduced to a minimum and installed only where necessary.

In case of city-center infeed, with reference to Figure 9, the critical equipment (converter transformers and reactors) could be installed inside a shielded hall, making the simulations easier. In many cases however, the reactors are installed outdoors, where electromagnetic coupling and radiation cannot be neglected anymore, and dedicated EM studies must be performed to comply with EMI regulations.

## 7. CONCLUSION

The EU long term strategy aims to reach climate neutrality by 2050, requiring transmission grid developments. In order to address so ambitious targets, high cooperation level and knowledge sharing between TSOs, technology providers and academic institutions will be fundamental, with the aim to optimize technical and economic resources and to identify cost competitive solutions for allowing the energy transition to happen at the pace we need. In this paper the technology outlook has been developed by the technology provider while the country specific considerations about renewables future scenarios and grid integration have been developed by the university with the goal to share knowledge about HVDC systems with the new Turkish electrical engineers. This first analysis could be expanded in the future by joint simulations and dynamic studies how and HVDC system for city center infeed could boost grid stability in future scenarios.

Globally, power loads in cities are increasing, especially in densely populated areas where land is already scarce, and difficulties can arise whenever new right-of-way must be secured for traditional transmission lines. HVDC Converter Stations based on VSC technology with small footprint are ideal for power infeed to city centres. HVDC technology enables large amounts of power to be delivered in heavily loaded networks by adding several system benefits such as independent full active and reactive power control and no added short circuit power.

Hitachi Energy is continuously working on solutions for such applications adapting innovative and compact HVDC technology solutions for the most efficient integration of green power into city centres by reducing footprint and energy losses and enabling the meeting of carbon emission targets.

Istanbul is experiencing a rapid increase in electricity consumption, seeing peak demand increasing at unprecedented speed. A new HVDC transmission system could supply between 1320 MW and 3000 MW increasing the share of renewable power fed to the city from Balıkesir and Çanakkale provinces. Such link would improve flexibility and strengthen the existing transmission infrastructure to ensure a reliable power supply in the metropolitan area of Istanbul.



Oral Presentation: Istanbul: City Centre Infeed with Voltage Source Converter-Based HVDC

### BIBLIOGRAPHY

- [1] Türkiye National Energy Plan, Republic of Türkiye, Ministry of Energy and Natural Resources, 2022
- [2] Gotland HVDC Light - the world's first commercial extruded HVDC cable system. CIGRÉ 2000, 14-205
- [3] The Gotland HVDC Light project-experiences from trial and commercial operation. 16th Cired, 2001
- [4] Bjorn Jacobson et al. "City Infeed with HVDC Light® and Extruded Cables", 16th Conference of the Electric Power Supply Industry, Mumbai, India, 2006
- [5] Bjorn Jacobson et al. "500 MW City Center Infeed with Voltage Source Converter based HVDC", 40th Meeting of Study Committee B4 and Colloquium on Role of HVDC, FACTS and Emerging Technologies in Evolving Power Systems, Bangalore, India., 2005
- [6] Aydogan Ozdemir et al. "Design and technical analysis of 500-600 kV HVDC transmission system for Türkiye", 10th International Conference on Electrical and Electronics Engineering (ELECO), 2017
- [7] T.R. ENERGY MARKET REGULATORY AUTHORITY Strategy Development Department, "ELECTRICITY MARKET SECTOR REPORT", 2023.
- [8] [www.enerjiatlasi.com](http://www.enerjiatlasi.com)
- [9] Mehmet Kabak1, Sinem Akalin, "A model proposal for selecting the installation location of offshore wind energy turbines", International Journal of Energy and Environmental Engineering (2022) 13:121-134.
- [10] <https://www.gmka.gov.tr/dokumanlar/yayinlar/Balikesir-Enerji-Yatirim-Rehberi.pdf>
- [11] Didier Cottet et al. "Electromagnetic Modeling of High Voltage Multi-Level Converter Substations", APEMC, 2019
- [12] Bernhard Wunsch et al. "Broadband Models of High Voltage Power Transformers and Their Use in EMC System Simulations of High Voltage Substations", APEMC, 2018
- [13] Didier Cottet et al. "Hybrid Model for Air Core Reactors in EMC Simulations of High Voltage Converter Stations", APEMC, 2019



# Coupled Numerical Electromagnetic-Structural Simulation For Transformer Winding

[mattia.medini@hitachienergy.com](mailto:mattia.medini@hitachienergy.com)**MATTIA MEDINI\*, LUIGI DE MERCATO***Hitachi Energy***Switzerland**

## SUMMARY

Short-circuit phenomenon on transformer windings is one of the most critical conditions at which this component could be subjected. This is an abnormal condition in an electrical circuit where the current travels along an unintended path with very low electrical impedance. This results in an excessive current flowing through the circuit, leading to the generation of extremely high Lorentz forces on the transformer windings. These forces have to be properly calculated since the windings must be designed for withstanding these loads. In particular, this calculation involves a multi-physic coupling between the electromagnetic solution and a structural analysis for properly simulating the nature of the loads by means of finite element simulation. In fact, the details that must be followed by an analyst for performing both electromagnetic and structural simulations with the Ansys Workbench software package are here reported. A Maxwell simulation (Eddy current or transient, 2.5D or 3D) is performed for predicting the distribution of the Lorentz forces on transformer windings and busbars. The computed forces are volumetric nature, i.e. distributed as force densities, as those really induced during the short-circuit test on the conductive components. Consequently, they are mapped on the structural mesh as an input to the structural simulation (static structural or transient, 3D geometry). Sensitivity studies for understanding the best mesh set-up were performed and guidelines have been identified. In fact, it is important to set-up them in such a way that the results from Maxwell simulation are correctly interpolated onto the structural mesh. As outcome of the above-mentioned methodology, all the steps, set-up, checks and verifications that must be followed for correctly performing this type of multi-physic simulation were defined and reported in this work.

## KEYWORDS

Transformer, Winding, Short-Circuit, Finite Element Simulation, Electromagnetic-Structural



## 1. INTRODUCTION

Transformer coils are usually subject to various electrical, mechanical and thermal stresses during their lifetime. The external short-circuit event can be considered as one of the most demanding load conditions, where high current levels and forces are generated in the transformer windings. A reliable prediction method is hence necessary in order to avoid any damage that would compromise the functionality of the entire electrical machine. A one-directional multi-physic approach is here proposed where a transient load condition is first calculated using the MAXWELL code on an axisymmetric geometry and Lorentz forces are then transferred to a 3D ANSYS structural model for a time domain transient analysis. This procedure takes the advantages of a relatively simple 2.5D finite element model for an efficient prediction of the electromagnetic field and forces on cylindrical geometries, together with the possibility of including all the pure structural features, such as radial and axial spacers, contacts and supports, in the mechanical model. The short-circuit test as described in the IEC 60076-5 standard [1] has been numerically simulated on a 2000 kVA transformer. The electromagnetic fields and the structural stresses computed on the low voltage winding have then been compared to corresponding results extracted from traditional approaches based on analytical simplified methods.

## 2. METHODOLOGY

The magnetic field  $B$  induced by the total currents (Ampere-turns) of primary and secondary windings is described by Maxwell's equations. The choice of the governing equations to solve is based on the phenomena that should be captured in the EM computation. These can be:

- Steady-state (magnetostatic): sufficient to calculate the forces applied to an entire volume, but cannot predict neither a non-uniform current density distribution in LV foil winding, nor the non-uniform force density field
- Time-harmonic (eddy current) and transient: capable to catch a non-uniform current density distribution and the consequent Lorentz force density field.

Several investigations have been performed to show the impact of different formulations, when evaluating the Lorentz force distribution in the windings, under short circuit conditions. A transient type of analysis is run using the axisymmetric 2.5D module of the Maxwell® code. This formulation gives the most precise results with short circuit computations, being short circuit a physically transient phenomenon where the time constants depend, as a first approximation, to the ratio between the equivalent short circuit inductance and the short circuit resistance of the coil. Applying the vector potential formulation, the governing equations for the magnetic field is given by the relationship:

$$\nabla \times (1/\mu \nabla \times \vec{A}) + \sigma \frac{\partial \vec{A}}{\partial t} = \vec{J} \quad (1)$$

$$\vec{B} = \nabla \times \vec{A} \quad (2)$$

from which the resulting Lorentz force density can be calculated as:

$$\vec{f} = \vec{J} \times \vec{B} \quad (3)$$

This formula is used in Maxwell® 3D computations to compute Lorentz force in conductive domain. Another method to compute magnetic force densities is integrating the Maxwell's stress tensor flux over each infinitesimal volume. The formula in Eq. (4) is used in all the other cases.

$$\vec{f} = \bar{\nabla} \cdot \bar{T} \, d\Omega = \bar{T} \cdot \bar{n} \, d\Gamma \quad (4)$$

where:

- $A$  = magnetic potential vector [V s/m]
- $B$  = magnetic flux density [T]
- $J$  = current density [A/m<sup>2</sup>]
- $\mu$  = magnetic permeability [H/m]
- $\sigma$  = electric conductivity [S/m]



- $f$  = force density [N/m<sup>3</sup>]
- $\bar{T}$  = Maxwell's stress tensor
- $d\Omega$  = infinitesimal volume where  $\bar{\nabla} \cdot \bar{T}$  is integrated
- $d\Gamma$  = boundary surface

A uni-directional type field coupling is here adopted. This approach assumes that structural deformations due to electromagnetic forces do not affect the electrical parameters of the coil and no feedback is required. The mapping on the 3D structural mesh of the Lorentz forces, calculated on the Maxwell 2D axi-symmetric model, is made sweeping the force densities on each coil section around the symmetry axis. A transient structural analysis is then performed. This type of analysis is used to determine the dynamic response of a structure under the action of any general time-dependent loads. The time scale of the loading is such that the inertia effect is included in the simulation.

The governing equations of motion can be written in the matrix form as:

$$M\ddot{u}(t) + C\dot{u}(t) + Ku(t) = f(t) \tag{5}$$

where M, C, and K are the mass, damping (neglected here) and stiffness matrices of the dynamic system, u(t) represents the displacements of the nodal points of the system, f(t) are the volume equivalent forces, and dots indicate differentiation with respect to time. The material is assumed to be linear-elastic, therefore the relationship between the stress tensor  $\sigma$  and the strain tensor  $\epsilon$  is given by the Hooke's law:

$$\sigma_{ij} = d_{ijkl}\epsilon_{kl} \tag{6}$$

where dijk is the stiffness tensor, and the stiffness tensor is calculated from the displacement vector according to the following formula:

$$\epsilon = \frac{1}{2} [\nabla u + (\nabla u)^T] \tag{7}$$

This procedure takes the advantages of a simple electromagnetic computation on a 2.5D finite element model for an efficient prediction of the field and forces on cylindrical geometries, together with the possibility of including all 3D structural features, such as radial and axial spacers, contacts and supports, into the mechanical model.

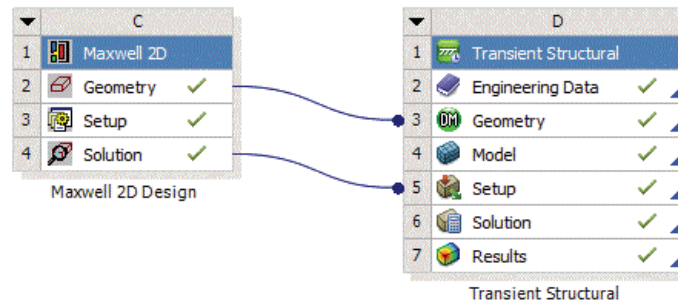


Figure 1: Ansys project page

The necessary steps for a calculation of the stress status on the windings and busbars in according with the proposed methodology are briefly listed below:

- 1- Construction of the 2D or 3D winding geometry in ANSYS®-DesignModeler for the electromagnetic simulation
- 2- Definition of material electrical properties
- 3- Definition of electromagnetic boundary conditions and excitations
- 4- Set-up of finite element mesh for electromagnetic simulation
- 5- Execute the electromagnetic simulation
- 6- Construction of the 3D full geometry (conductor + non electrical parts) in ANSYS®-DesignModeler for the structural simulation
- 7- Definition of material mechanical properties



- 8- Definition of contact parameters between parts in the structural model
- 9- Set-up of finite element mesh for structural simulation
- 10- Definition of boundary conditions for structural simulation
- 11- Interpolation of Lorentz forces from electromagnetic analysis onto the structural model
- 12- Structural analysis
- 13- Results post processing.

### 3. ELECTROMAGNETIC MODEL

This study has been focused on a three-phase transformer having the following features:

- Rating power ( $S_n$ ) = 2000 kVA
- Frequency ( $f$ ) = 50 Hz
- Short-circuit voltage ( $V_{sc}$ ) = 6.64%
- Connection group = Dyn11
- Low voltage winding parameters:  $V_{LV} = 400$  V,  $I_{LV} = 2886.4$  A
- High voltage winding parameters:  $V_{HV} = 16000 \pm 2 \times 2.5\%$  V,  $I_{HV} = 72.2$  [A]

The EM analysis is computed over a 2D geometry of a single phase of the transformer. An example of such geometry is shown in the following figure, where the coil consists of 3 radially stacked Low Voltage (LV) foil segments 1330 mm and 11 axially stacked High Voltage (HV) disks.

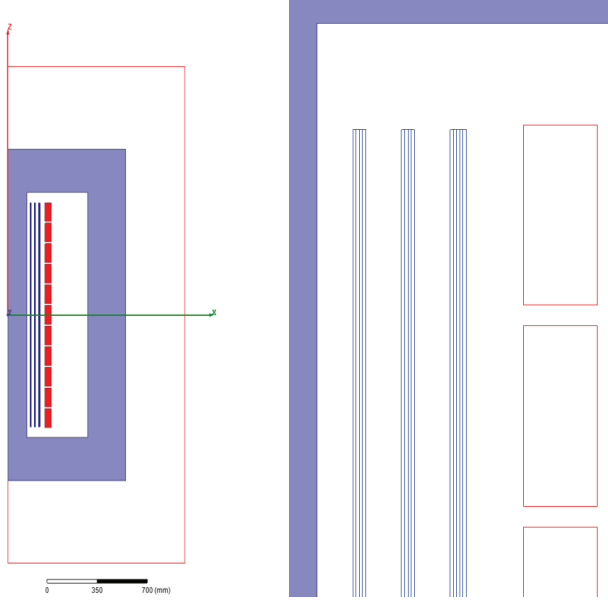


**Figure 2:** Magnetic F.E. domain with detail of the coil end

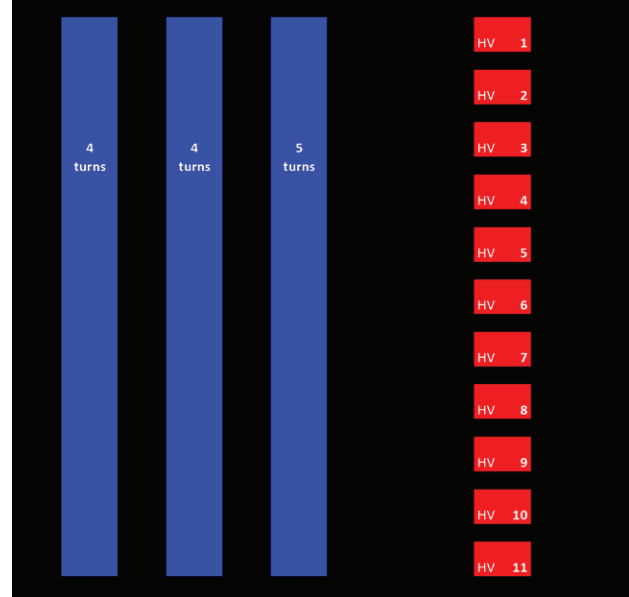


**Figure 3:** Coil configuration

The short-circuit currents are calculated as follow.

$$i_{LV}(t) = \sqrt{2} \frac{\hat{I}_{LV}}{k} \left[ \sin \left( 2\pi f t - \frac{\pi}{2} \right) + e^{-\frac{t}{\tau}} \right] \quad (8)$$

$$\hat{I}_{LV} = \frac{U}{\sqrt{3} Z_{SC}} \quad (9)$$

$$\tau = \frac{Z_{SC}}{2\pi f} = \frac{L_{SC}}{R_{SC}} \quad (10)$$

$$i_{HV}(t) = i_{LV}(t) \frac{N_{LV}}{N_{HV}} \quad (11)$$



Where:

- $\hat{I}_{LV}$  = LV short circuit peak current
- $\tau$  = short circuit time constant
- $Z_{SC}$  = short circuit impedance
- $U$  = rated voltage of the transformer, LV side
- $L_{SC}$  = short circuit inductance
- $R_{SC}$  = short circuit resistance
- $N_{LV}$  = LV number of turns
- $N_{HV}$  = HV number of turns

Values for  $k$  coefficient can be taken from [1]:

Table 1: Values for factor  $k \times \sqrt{2}$

X/R	1	1,5	2	3	4	5	6	8	10	14
$k \times \sqrt{2}$	1,51	1,64	1,76	1,95	2,09	2,19	2,27	2,38	2,46	2,55

Note: For other values of X/R between 1 and 14, the factor  $k \times \sqrt{2}$  may be determined by linear interpolation.

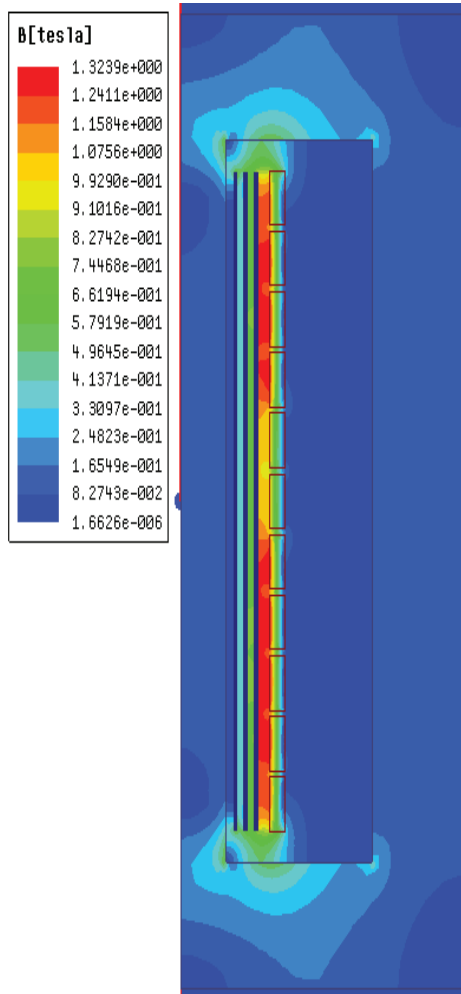


Figure 4: Magnetic field densities at current peak

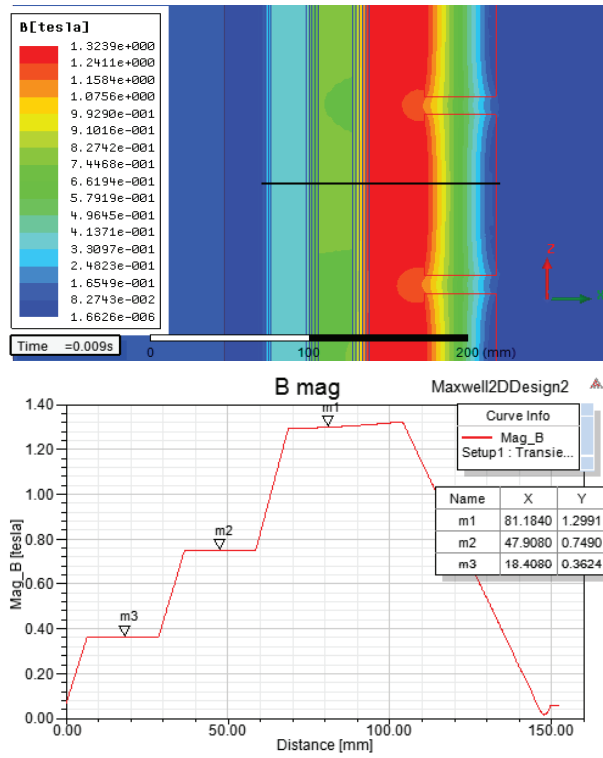


Figure 5: Leakage flux values

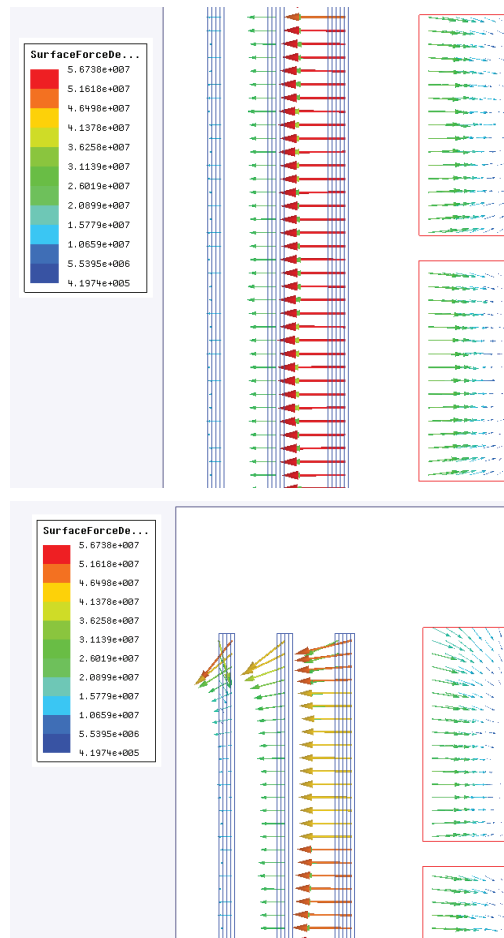


Figure 6: Specific Lorentz forces at the middle and the top end of the coil



### 4. STRUCTURAL MODEL

#### 4.1. Geometry

This study has been focused only on the low voltage winding, which is considered as the most vulnerable part of the transformer for the given load condition, but the same approach can be applied also for the HV winding and other components involved on the structure. Thanks to the cyclic symmetry, just one octave of the geometry could be studied once appropriate frictionless boundary conditions have been applied on the symmetry cuts. The structure could be sub-divided in the following components according with their functionality (colors refer to Figure 7):

- Axial spacers (green)
- Radial spacers (red)
- Coils (inner and outer sections) (gray)

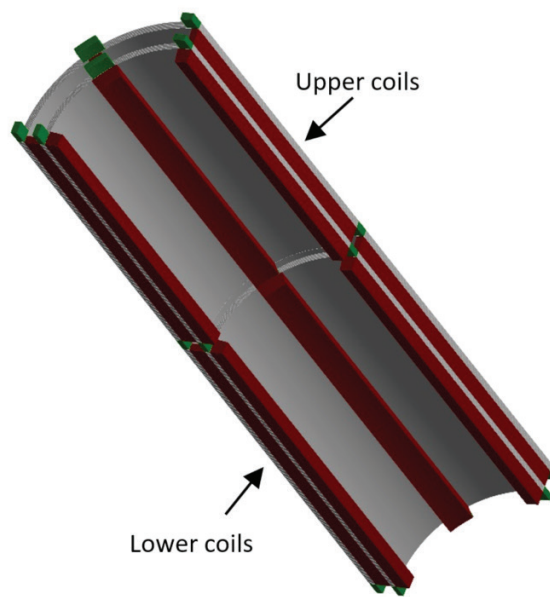


Figure 7: Generic low voltage winding geometry for structural F.E. analysis

#### 4.2. Materials

Laminated foils used for the conductive material have orthotropic mechanical properties due to the lamination process followed for production. Mechanical properties of the adopted materials are listed on the following table.

Table 2: Material properties

Component	Material	$E_x$ [N/mm <sup>2</sup> ]	$E_y$ [N/mm <sup>2</sup> ]	$E_z$ [N/mm <sup>2</sup> ]	$\nu$	$\rho$ [Kg/m <sup>3</sup> ]	$Rp_{0.2\ min}$ [MPa]	$Rm_{\ min}$ [MPa]
Axial and radial spacers	Triglass™ glass reinforced polyester		20000		0.42	1900	n.a.	200
Coils	Aluminium alloy	69080	69080	86560	0.34	2770	33	73

#### 4.3. Mechanical mesh

For the finite element mesh only Hexa 20 quadratic elements have been used. The following mesh controls have been applied in order to guarantee a good quality of the computational grid:

- Azimuthal sweep with at least 35 divisions along a 90° sector on each layer



Oral Presentation: Coupled Numerical Electromagnetic-Structural Simulation For Transformer Winding

- A minimum of 1 element per each coil along the radial direction
- Hex dominant method with an All Quad free face mesh type on axial and radial spacers
- An overall body sizing of about 2% of the inner diameter of the innermost layer
- A mapped face meshing on top and bottom faces of radial spacers
- Edge sizing of about 6% of the inner diameter of the innermost layer along the vertical edge of layers
- Vertical sweep with at least 6 divisions on axial spacers
- An automatic sweep on radial spacers

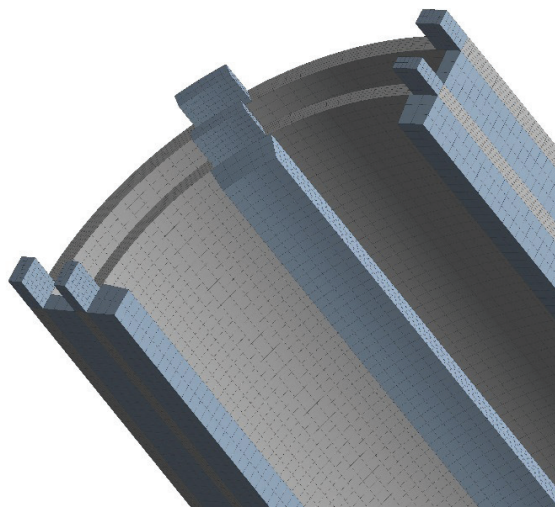


Figure 8: Example of finite element mesh

#### 4.4. Load and boundary conditions

According to EN-60076-5 standard, the winding must sustain without damage the effects of over-currents originated by external short circuits. For this reason, the peak of the Lorentz forces density have been interpolated on the structural mesh as shown on the figure below.

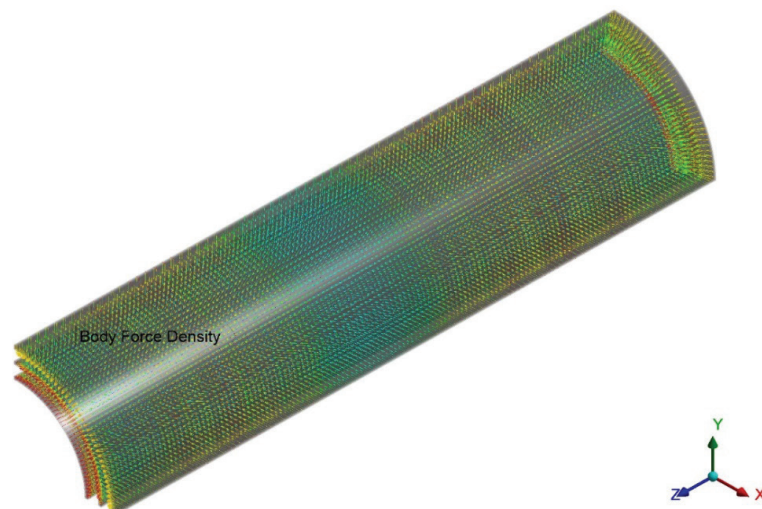


Figure 9: Example of Lorentz forces interpolation onto the structural mesh

### 5. NUMERICAL RESULTS

The structural analysis on the low voltage windings showed that no damage occurs on the coils when subjected to a short-circuit loads as described above. In fact, the von Mises stress peak calculated by FEM simulation is around 20.6 MPa (please refer to following figure), whereas the admissible limit for the adopted material is 33 MPa.

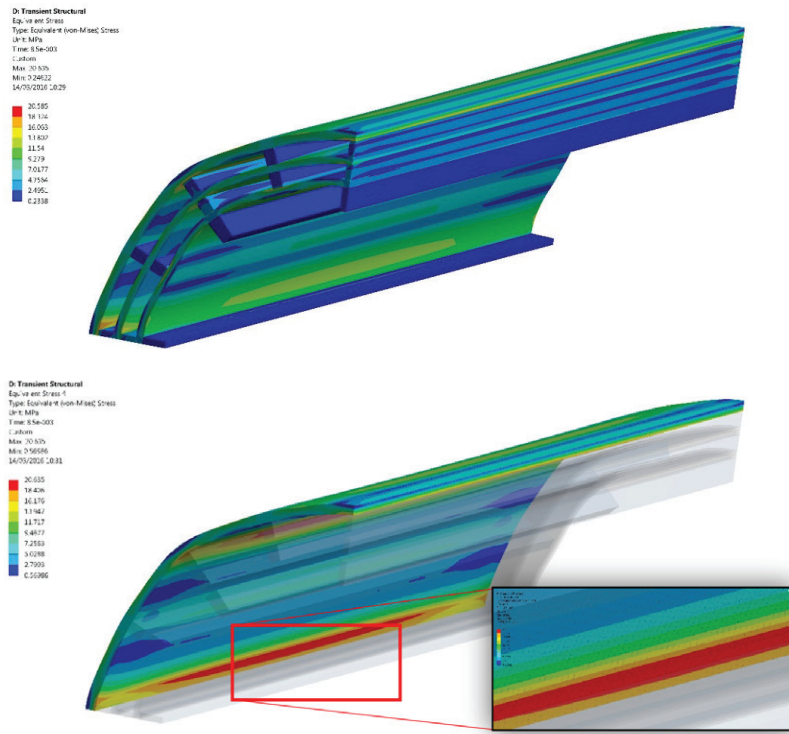


Figure 10: Example of von Mises contour plot (deformation magnification factor = 200)

An analytical calculation with the Mariotte’s formula has been performed on the same design for comparing the obtained results with the numerical ones. In fact, the mean hoop stress [MPa] can be calculated by means of the following equation:

$$\sigma_{mean} = P * D / 2 * t \tag{12}$$

Where:

- $\sigma_{mean}$  : mean hoop stress that acts in the azimuthal direction of the winding
- P: pressure that acts on the section under investigation
- D: internal diameter of the section under investigation
- t: thickness of the section under investigation

The stress status calculated with the above equation is 10 MPa, 52% lower than the one calculated with FEM simulations. This discrepancy is mainly given by the limitation of the analytical equations that cannot properly predict the stress variation in the azimuthal direction of the winding. In fact, due to the presence of the duct sticks in the cooling channel, bending moments are induced on the windings conductors that generates localized stress peaks (please refer to Figure 10).

### 6. CONCLUSION

A procedure has been proposed for the structural assessment of transformer windings subject to short circuit load condition, by means of multi-physic coupling between the electromagnetic solution and a structural analysis. The numerical results show how the non-axisymmetric features of the geometry, such as radial and axial spacers, are responsible for a non-uniform stress distribution across the winding. This shows the limits of the analytic method based on the Mariotte’s model where only hoop and compressive





stresses are considered, whereas the effect of the bending moment induced by the duck sticks is completely ignored. For this reason, it is possible to affirm that this procedure is a significant breakthrough in the prediction of a realistic stress distribution in transformer windings subject to any kind of electromagnetic induced forces.

### BIBLIOGRAPHY

- [1] IEC 60076 Part 5 Third edition 2006. "Power transformers -Ability to withstand short circuit"
- [2] Mechanical stresses in transformers windings, Billing, 1944
- [3] Kulkarni S.V., Khaparde S. A., "Transformer engineering – Design and practice" Marec Dekker, New York 2004
- [4] Determination of short-circuit forces in transformer windings, Ignacz, P. institute of Electrical Power Research



# Current Transformers Dimensioning in the Context of Digital Substations

[anamaria.iamandi@transelectrica.ro](mailto:anamaria.iamandi@transelectrica.ro)**ANAMARIA IAMANDI**  
*CNTEE Transelectrica SA***Romania**

## SUMMARY

To ensure the power system performance indicators in accordance with European Commission regulations, power utilities must pay a special attention to substation design and configuration, protection system architecture, primary and secondary equipment technology, as well as the introduction of IEC 61850 standard.

Protection equipment are strongly dependent by the measurements received from current transformers (CTs) as their operating decision depends both on the rated ratio between the primary and secondary current, the accuracy of the current measurement transformers (CTs) and the saturation degree of the current transformers.

Utilities, along with main vendors in power system field, are developing different study to improve CT operation in different system condition. There are two main solutions: to improve the saturation coefficient and to connect low loads in CTs secondary winding. Digital substations, along with IEC 61850 process bus introduce the advantage of using digital equipment characterised by secondary loads.

The current study evaluates the CT behaviour in different system conditions (short circuit level, system reactance and primary time constant) and the improvements of digital technologies on CT dimensioning. The case study is realized on a 220 kV transmission substation from Romanian Power System (RPS) which is currently under rehabilitation works in digital configuration.

## KEYWORDS

CT dimensioning, digital substations, digital equipment, IEC 61850 process bus



## 1. INTRODUCTION

Modern society is strongly dependent by the power energy consumption in all activity sectors. Faults can cause severe damages, leading to blackouts across extended area, even synchronous interconnected area (as the separation of the Continental Europe power system on 8 January 2021 [1]), having a crucial economic and social impact. Therefore, it's mandatory to high-speed fault detection in order to maintain the power system stability.

Protection equipment are evaluated in terms of "speed, selectivity, reliability and cost" [2]. The main purpose of enlarging protection equipment' performances are to improve fault clearance time while increasing both reliability and security criteria.

Protection system operating decision depends both on the rated ratio between the primary and secondary current, the accuracy of the current measurement transformers (CTs) and on the saturation degree of the current transformers. Therefore, the correct operation of the protection system is closely related to the capability of the measurement transformers.

CT's saturation may lead to both impossibility to operate or to unwanted trip decisions of the protection equipment, affecting both security and reliability protection equipment principles.

Digital substations, along with digital technology facilitate the introduction of digital protection equipment together with IEC 61850-9-2/2LE process bus.

The benefits introduced by digital protection equipment allowed the protection engineers to develop new protection schemes with a high degree of reliability and security. Digital protection equipment comprises the experience and techniques of previous protection equipment technologies into more compact and low-power consumption. They are equipped with communication function, facilitating tripping operation in the remote end. Data measurements from different substation are synchronized to a common time stamp by using Global Positioning System receivers.

Regarding CT saturation study, the main advantage resulted by using digital protection equipment is represented by their low secondary load. Supplementary, digital protection engineers have developed different protection function to detect CT saturation core and to reconstruct the secondary current curve.

This paper is divided into 4 sections: Section 2 presents the protection system philosophy according to European Network of Transmission System Operators (ENTSO-E), Section 3 studied the CT behaviour during magnetization while Section 4 is dedicated for case study: framing the studied area, CT dimensioning and result discussions.

## 2. PROTECTION SYSTEM DESIGN

The European Network of Transmission System Operators, ENTSO-E, recommends for European TSO's HV and EHV substation to be equipped with a redundant protection scheme, which is formed by a main protection equipment and a backup protection equipment, or with a fully redundant protection scheme, formed by two main protections equipment. The two protection scheme must act independent and simultaneous by each other.

Figure 1 shows a simplified diagram of a redundant protection system [2].

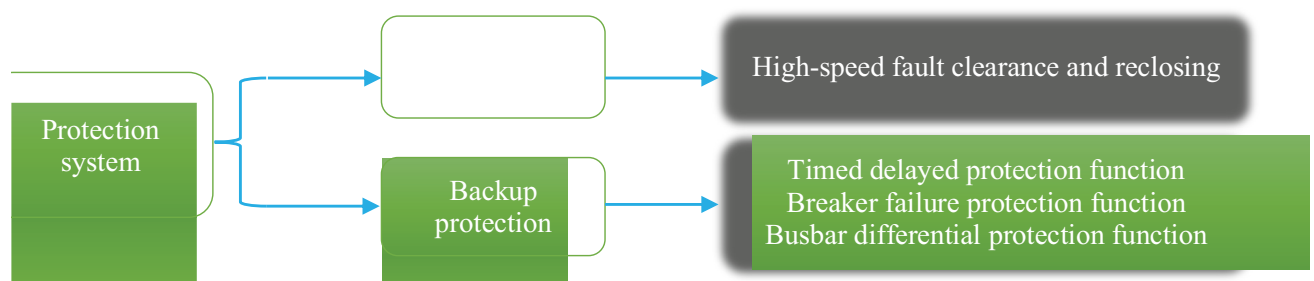


Figure 1. The principal diagram of a protection system

There are different redundancy approaches regarding protection system design in digital substation, depending on the TSO's philosophy.

In [3], there are given some guidelines for overhead transmission lines (OHLs), power transformers and busbars. OHLs are protected by distance protection with/without teleprotection system and differential protection. Power transformers are protected

by differential protection and, as backup protection, by distance protection and overcurrent protection. Busbars are protected by differential protection. These protection functions are not restrictive, the TSOs can complete the protection scheme in accordance with their experience and their national grid codes.

### 3. CURRENT TRANSFORMER DIMENSIONING

Real CTs have copper losses, core losses and leakage flux and require a certain current to magnetize the core. As a result, the secondary current of a CT is not perfectly proportional to the primary current. For most operating conditions, CTs reproduce the primary currents well. However, under certain conditions, the CT core saturates and the CT fails to correctly reproduce the primary current [4].

Figure 3 shows the typical CT magnetization curve (B-H curve) showing the hysteresis loop for a CT exposed to a high-current fault, which produces core saturation in both half cycles of the magnetic flux waveform. Fault clearance reduces the primary current to zero. Remanence is the magnetic flux that remains in the magnetic circuit after the removal of the primary current [4].

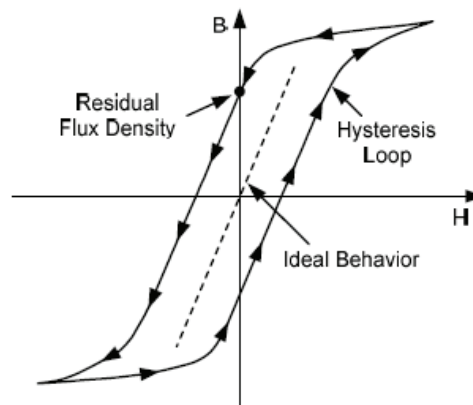


Figure 3. CT hysteresis loop

The CT saturation equation is determined starting with the equation of CT's magnetomotive forces:

$$i_1 * N_1 = i_0 * N_1 + i_2 * N_2 \quad (1)$$

$$N = \frac{N_1}{N_2} \quad (2)$$

$$i_1' = \frac{i_1}{N} \quad (3)$$

$$i_2 = i_1' - i_0 \quad (4)$$

Where:

$i_1$  – the instantaneous value of the primary short-circuit current [Aprim];

$i_2$  – the instantaneous value of the secondary short-circuit current [Asec];

$i_0$  – the instantaneous value of the secondary magnetizing current [A];

$i_1'$  – the instantaneous value of the primary short-circuit current related to secondary winding [Asec];

$N_1$  – primary winding ratio [-];

$N_2$  – secondary winding ratio [-];

$N$  – rated ratio [-].

Figure 2 depicts the equivalent circuit of a CT, referred to the transformer secondary side.

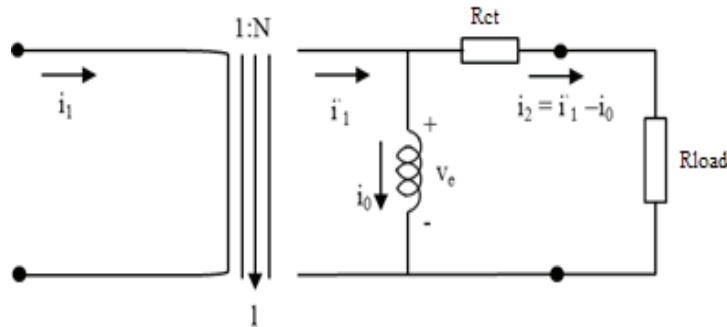


**Figure 2.** The equivalent scheme of a conventional current transformer

Following, in Figure 2 is applied the law of electromagnetic induction and the definition relation of electromotive voltage. Furthermore, are considered the succeeding simplifying hypotheses:

- the fault occurs during harmful electrical transients phenomenon;
- the remanent flux is neglected.

The CT saturation coefficient is notated with  $K_T$  (in the specialized literature it can be found also under the name “correction coefficient for the aperiodic component”). The equation (5) represent the relation used to evaluate the CT core in order to avoid saturation.

$$K_T = 1 + \omega * \tau_P * \left( 1 - e^{-\frac{t_{op}}{\tau_P}} \right) \quad (5)$$

$$\tau_P = \frac{1}{\omega} * \frac{X}{R} \quad (6)$$

Where:

$\tau_P$  – primary time constant [s];

$t_{op}$  – the operating time of a protection equipment [A] (must be smaller than time needed to reach saturation);

$X/R$  – system ratio.

The saturation coefficient is influenced by: primary time constant, system ratio, protection equipment operating time, CT internal resistance and the load connected in CT secondary winding.

In Section 3 is evaluated the influence of above mentioned parameters on saturation coefficient considering both electromechanical protection relay and digital protection relay.

## 4. CASE STUDY

### 4.1. Framing the studied area

The aim of the case study is to observe the behaviour of CT during saturation in different power system conditions: different short-circuit level, system reactance and primary system time constant.

In this paper is studied the CT behavior installed on 220 kV Overhead Transmission Line (OHL) A- B from 220 kV substation A. The studied substation is a 220/110 kV substation from Romanian Power System (RPS) located in the middle of the country.

The existing substation configuration is double busbar scheme with transfer busbar. Both primary and secondary equipment are in conventional technology.

The OHL protection system is redundant, equipped with main protection equipment and backup protection equipment, both in electromechanical technology.



Figure 4. Framing the studied network area

Following, there are determined the power system condition (system ratio - X/R [-] and primary system time constant - τ [s]) and the protection equipment operating time.

4.2 Power system data

The power system condition was determined by performing fault simulation in different location, as it follows: (1) close to CT and protection equipment, (2) on adjacent transmission substation busbar, (3) at 2nd transmission substation busbar, (4) on 220 kV side of autotransformer from substation B, (5) on 400 kV substation B busbar and (6), (7) in close proximity of hydroelectric power plant.

In Figure 5 is shown the single line diagram of the studied area together with fault locations.

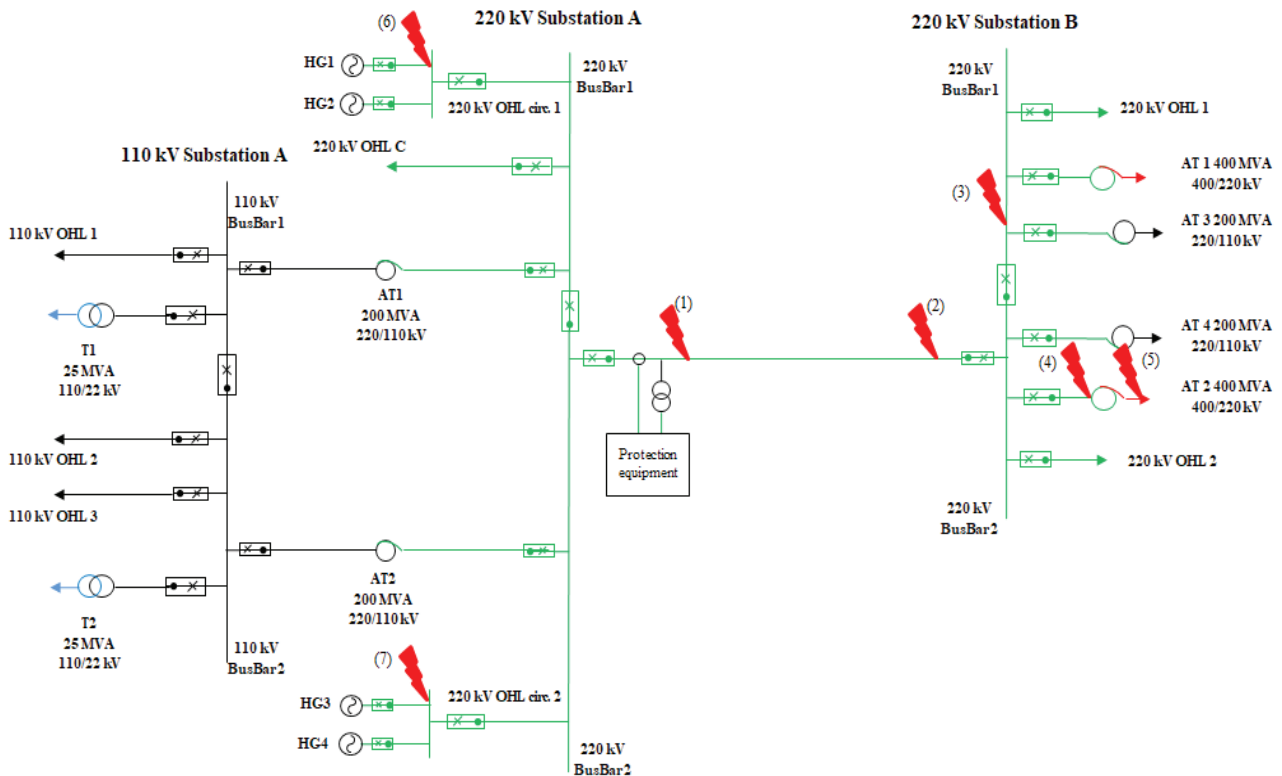


Figure 5. Single line diagram of the studied network area





In Table I are presented the computation results of primary system data for the studied fault locations.

Table 1. Power system data

Studied substation	Fault location	X/R [-]	$\tau$ [s]
220 kV substation A	(1)	8.25	0.0263
	(2)	9.38	0.0299
	(3)	9.52	0.0303
	(4)	11	0.035
	(5)	11	0.035
	(6)	8.14	0.0259
	(7)	8.14	0.0259

### 4.3 Protection equipment operating time

Protection equipment operating time represent the time needed to determine and to transmit the operating decision. It is not considered the trip relay execution time and the circuit breaker operating time.

#### ➤ Operating time of the electromechanical protection equipment

In Table II are presented the operating time for a electromechanical protection equipment according to technical specifications guaranteed by manufacturer [5].

Table 2. Electromechanical protection equipment' operating time [5]

Relay	Operating time [ms]
Starting element	35
Trip element	
- Un→0V; I0→3In	40
- Un→0V; I0→3In	25
- Un→0V; I0→3In	20

According to Table II, the electromechanical protection equipment' operating time varies between 55 ÷ 75 ms, depending on fault location.

Following, it is presented a post – event analysis to validate the technical specifications.

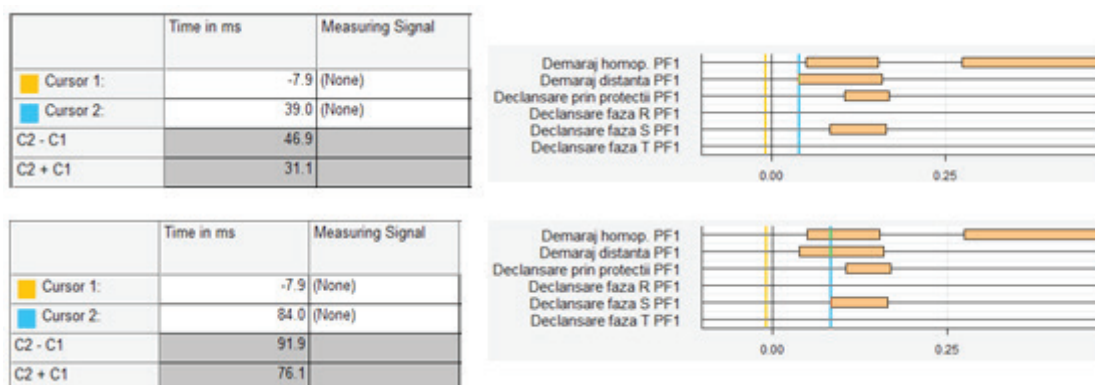


Figure 6. The electromechanical protection equipment' oscilopertubography record from o fault located on 220 kV OHL A - B



In Figure 5, the pick-up time is 46,9 ms and the operating time for R3Z24a + R3Z3u protection system is 91,9 ms.

To have a better perspective of the R3Z24a + R3Z3u protection system influence on CT saturation, in case study's simulation will be considered the following values corresponding to R3Z24a + R3Z3u operating time: 55 ms, 75 ms, 92 ms.

➤ **Operating time of the digital protection equipment**

In the second part of the case study it will be considered the studied substation in digital configuration, equipped with digital protection equipment. The main protection equipment vendors guarantee a minimum operating time of 1,5 periods (30 ms).

To validate, there are analyzed two oscilopertubography records extracted from two different digital protections.

In Figure 6 the fault is located on close proximity of protection equipment location, eliminated within Z1 distance time and the protection equipment operating time is 14,8 ms.

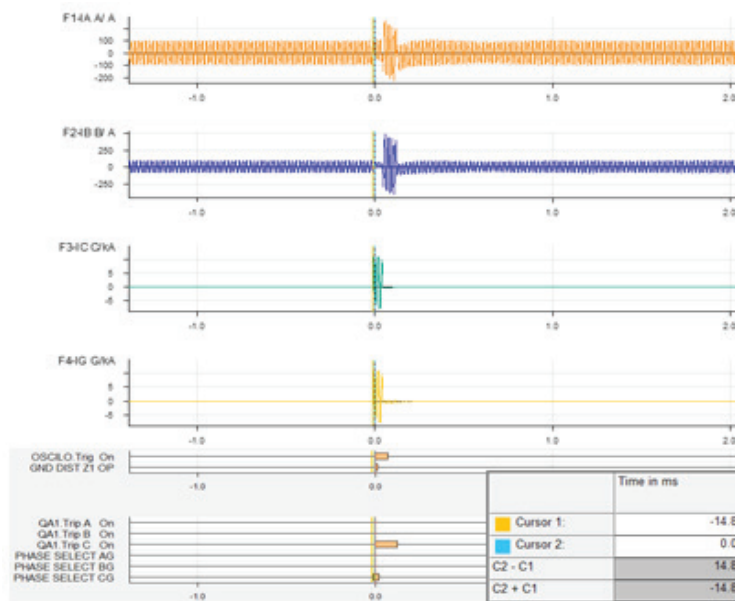


Figure 7. Digital protection oscilopertubography record to a fault located in close proximity of protection equipment

In Figure 7 the fault is located on the remote line length, eliminated within Z1 distance time and the protection equipment operating time is 25.3 ms.

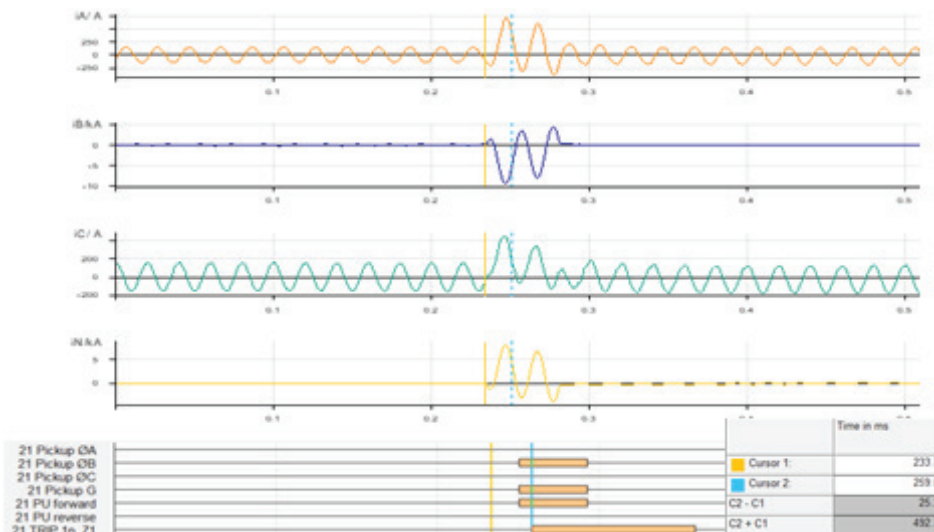


Figure 8. Digital protection oscilopertubography record to a fault located on the remote line length



The second part of the case study's simulations are performed considering the 15 ms, 25 ms, 30 ms values for protection system in digital configuration.

### 4.4 Simulation Results

CT dimensioning mainly depends on CT saturation coefficient  $K_T$ . The present case study evaluates the influence of protection equipment operating time in electromechanical and digital technologies on  $K_T$  using the equation (5) presented in Section II.

Figure 8 shows the influence of protection equipment in electromechanical technology on  $K_T$ . For primary time constant of  $\tau_p = 0,026$  s,  $K_T$  slowly varies with the increasing of operating time. In case of  $\tau_p \geq 0,030$  s, the operating time strongly influence CT saturation coefficient.

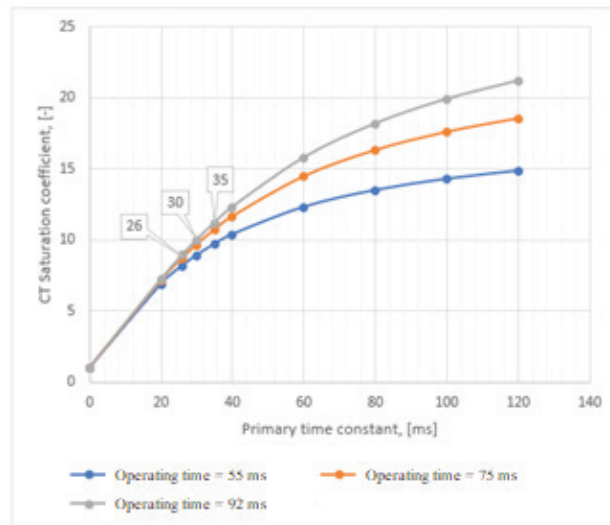


Figure 9. The influence of electromechanical protection equipment operating time on CT saturation coefficient

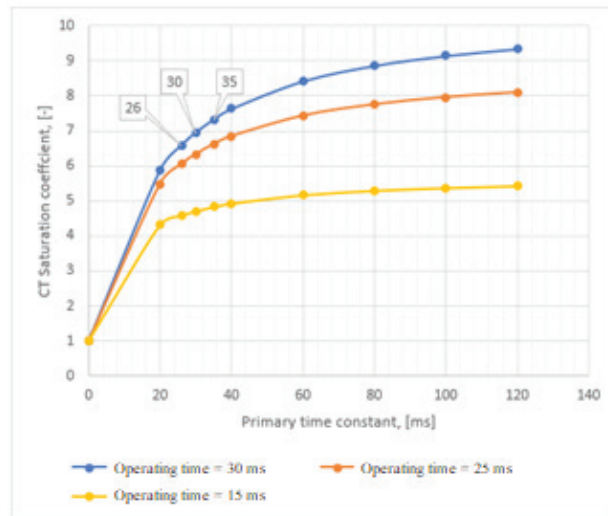
In Table III are presented the  $K_T$  and  $\tau_p$  values for each operating time top [ms]. It was considered  $\tau_p \approx 26$  ms for (1), (6) and (7) fault locations,  $\tau_p \approx 30$  ms for (2) and (3) fault locations, while for fault locations (4) and (5) it was considered  $\tau_p \approx 35$  ms.

Table 3. CT saturation coefficient considering electromechanical protection equipment

$\tau_p$ [ms]	$t_{op}$ [ms]	$k_T$ [-]
26	55	8,18
	75	8,71
	92	8,93
30	55	8,92
	75	9,65
	92	9,99
35	55	9,71
	75	10,7
	92	11,2

Figure 9 shows the influence of protection equipment in digital technology on  $K_T$ .

In Table IV are presented the  $K_T$  and  $\tau_p$  values for each operating time top [ms]. It was considered  $\tau_p \approx 26$  ms for (1), (6) and (7) fault locations,  $\tau_p \approx 30$  ms for (2) and (3) fault locations, while for fault locations (4) and (5) it was considered  $\tau_p \approx 35$  ms.



**Figure 9.** The influence of digital protection equipment operating time on CT saturation coefficient

**Table 4.** CT saturation coefficient considering digital protection equipment

$\tau_p$ [ms]	$t_{op}$ [ms]	$k_T$ [-]
26	15	4,58
	25	6,05
	30	6,59
30	15	4,71
	25	6,33
	30	6,96
35	15	4,83
	25	6,12
	30	7,33

From both Figure 9 and Table IV, it can be observed that regardless of the fault location, the CT saturation coefficient has small values and is slightly influenced by protection equipment operating time.

Comparing the values from Table III with the values from Table IV, it is observed that for the same primary time constant, the CT saturation coefficient has smaller values in case of digital protection operating time.

## 6. CONCLUSION

The proper operation of protection equipment is strongly influenced by the secondary values previously transformed by current measurement transformers. The secondary values accuracy are mainly influenced by CT saturation.

The current paper studies the influence of protection equipment operating time in digital and electromechanical technology on CT dimensioning, as well as its behavior in different system condition: primary time constant, short circuit level, system ratio.

Comparing the simulation results of the two types of protection equipment connected in CT winding secondary, electromechanical and digital equipment, it is observed that CT saturation coefficient has smaller values in the case of a digital protection equipment.

In order to avoid CT saturation regardless system condition and secondary load connected in its winding secondary, the CT should be re-dimensioned considering the saturation coefficient. This solution involves high acquisition and maintenance costs and large CT dimensions. Another solution, facilitated by the digital technology progress, is to introduce digital equipment together with IEC 61805-9-2/2LE process bus, as digital equipment has low secondary leads compared to electromechanical protection equipment.



### BIBLIOGRAPHY

- [1] \*\*\*, "ENTSO-E Final Report on system separation in the Continental Europe Synchronous Area on 8 January 2021", ENTSO-E, 2021, available at: <https://www.entsoe.eu/news/2021/07/15/final-report-on-the-separation-of-the-continental-europe-power-system-on-8-january-2021/>;
- [2] Working Group B5.19 CIGRE. "Protection Relay Coordination", 432, ISBN: 978-2-85873-120-6, October, 2010; (Public Utilities Fortnightly, December 2003, pages 39-41);
- [3] \*\*\*, "Best protection practices for HV and EHV AC-Transmission Systems of ENTSO-E Electrical Grids", ENTSO-E CE Subgroup System Protection and Dynamics, ENTSO-E StO Protection Equipment Subgroup, June 2018;
- [4] H. J. Altuve, N. Fischer, G. Benmouyal, D. Finney, "Sizing Current Transformers for Line Protection Applications", 66th Annual Conference for Protective Relay Engineers, April 2013, pp. 1-18,
- [5] A. Emanoil, "Îndreptar. Protecția prin relee, Volumul II" Editura Tehnică, București, 1984.



# Impact of Renewable Generation on Distance Protection and Adaptive Algorithms to Optimise Performance

[venkatesh.c@ge.com](mailto:venkatesh.c@ge.com) / [ilia.voloh@ge.com](mailto:ilia.voloh@ge.com) / [rajesh.ananth@ge.com](mailto:rajesh.ananth@ge.com)**VENKATESH CHAKRAPANI\****GE Grid Solutions***United Kingdom****ILIA VOLOH***GE Grid Solutions***Canada****RAJESH ANANTH***GE Grid Solutions***United Arab Emirates**

## SUMMARY

Distance relays remain primary transmission line protection for more than a century and they have significantly evolved to handle issues due to changes in transmission network to meet ever-growing demand e.g., protection of series compensated lines, single-pole tripping, and others. This along with the use of local information only to make a trip decision and the backup zones feature makes distance protection an unavoidable choice to protect transmission lines. Additionally, the evolution of relay technology helped distance relays to realize complex characteristics such as polygons, however, MHO characteristic is still in use due to its ease of setting the characteristic and especially when top reactance line is not reliable.

In the recent years, rapidly increasing amount of the renewable generation, including inverter-based resource contribution to grid is presenting challenges to the line protection. These new resources are behaving quite differently compared with conventional synchronous generation with each country following its own grid code, i.e. different inverter-based resource (IBR) response for the same fault type and system conditions which is not the case for conventional synchronous generation. The proprietary nature of controller design and the flexibility of operating the inverter in different operating scenarios as listed below,

- Positive sequence injection (negative sequence suppression)
- Negative sequence injection
- Mixed sequence injection
- Reactive current priority
- Equal current priority

makes it difficult to evaluate the actual performance of distance and its supervising elements.

The MHO characteristic which is constructed using operating and polarizing quantities is directly impacted by the choice of polarizing quantity i.e., the characteristic is dynamic. This dynamic characteristic results in large expansion for forward faults and when the source is weak.

## KEYWORDS

Renewable Energy, Inverter Based Resource, Power System Protection, Distance Protection





**Oral Presentation:** Impact of Renewable Generation on Distance Protection and Adaptive Algorithms to Optimise Performance

The growing presence of inverter-based resource contribution to grid further aggravates the issue by resulting in uncontrolled (MHO swings due to varying source impedance – magnitude and angle) dynamic characteristic.

In this paper, we discuss the impact of ‘real-controller’ models and different operating modes on the following,

- Fault type supervision (both ground and phase),
- Directional element,
- Distance characteristics (Quadrilateral, MHO)

The ‘real-controller’ models are from a collaborative study led by SANDIA national laboratories and North American Reliability Corporation (NERC) and funded by US Department of Energy. This includes the real models from four different original equipment manufacturers with a mix of Type 3, Type 4 and PV solar, integrated into an electromagnetic transient program as a black-box model along with the conventional system model. Multiple test scenarios were considered like fault type, fault resistance, fault location and it also includes the response to different original equipment manufacturers for each considered test scenario.

We then provide solutions to the problems and introduce the concept of controlled dynamic MHO – an innovative solution for distance protection to prevent incorrect operation in the presence of IBR where the source impedance varies drastically and weak sources in general. This new feature controls the dynamic MHO behaviour and brings in the flexibility of having both uncontrolled (when MHO swings are not encountered) and controlled dynamic MHO characteristic (when MHO swings are encountered). This overcomes the issue with existing approach where the uncontrolled MHO expansion can result in overreaching issue causing zone 1 mis-operation.

## 1. INTRODUCTION

The global commitment to move towards ‘Net-Zero’ carbon emissions to tackle climate change is the key driver to phase out existing generation based on fossil fuels and move towards renewable energy in energy sector, with wind and solar being predicted as the major contributors. As these renewable energy sources are intermittent i.e., unlike synchronous generation where the speed is constant, windturbine speed varies with time and it demands for power electronic device to act as an interface.

The global commitment towards climate change and with a new technology (voltage source converter) paving its way, is driving fast and wide-spread deployment of the renewable generation in recent years. These new technologies, wind (Type-3 and Type-4) and solar with the presence of the power electronic interface is presenting new challenges to the line protection which is the focus of this paper. This is further complicated by the following factors,

- The proprietary nature of power electronic interface controller design,
- Lack of availability of the validated models in simulation packages,
- The absence of the global standard causing each country following its own standard resulting in different fault quantities behaviour for the same system and fault scenario i.e., fault behaviour is not deterministic which is not the case in the conventional synchronous generation.
- Flexibility of operating the power electronic interface in different operating modes, especially Type-4 with VSC which is gaining widespread deployment

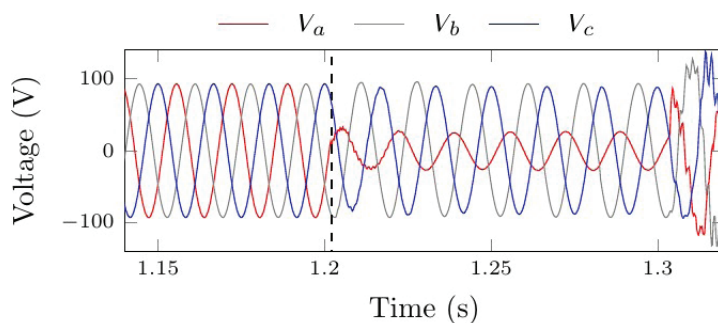
All these factors make it even more difficult to evaluate the performance of distance relays. This paper discusses the impact of this new renewable generation technology,

including inverter-based resources (IBR) on the following, Quadrilateral and MHO characteristics, Fault type supervision (FTS) and Directional elements using COMTRADES obtained from the real world and simulation model, which incorporates ‘real-controller’ design as a black-box.

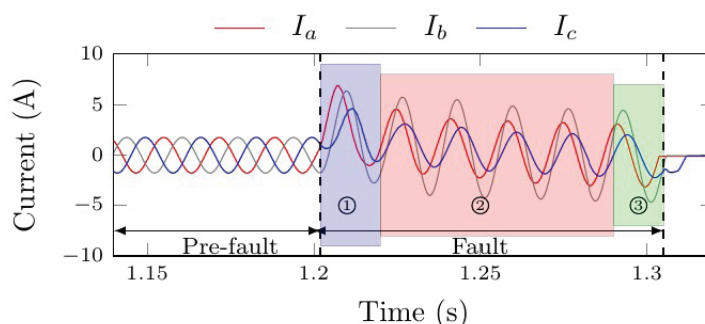
## 2. OVERVIEW OF THE PROBLEM

In the presence of the IBR, power electronics interfaces the renewable energy source and the grid. This power electronic interface is capable of fast fault current injection, which not only limits the fault current, but also impacts the fault current signatures (what we refer as low- inertia generation source).

Oral Presentation: Impact of Renewable Generation on Distance Protection and Adaptive Algorithms to Optimise Performance



(a) Secondary voltage signals



(b) Secondary current signals

**Figure 1:** IBR response for AG fault. Stage 1 – disturbance detection, Stage 2 – Controller transients, Stage 3 – Steady state fault

Figure 1 shows one such IBR response for a Type 4 wind generator feeding single phase to ground fault AG. We can observe the current traces (Figure 1 (b)) do not correlate to the typical fault current unbalance. This is because IBR controller is expected to enter a new operating mode once the disturbance is detected in the stage 1 (Figure 1 (b)). This transition involves controller transients in the stage 2 (Figure 1 (b)) before it settles down (stage 3) into the target value set by the chosen operating mode during fault. Table 1 shows the voltage ride-through performance requirements for the IBR during both balanced and unbalanced faults [1].

**Table 1:** Performance Requirements

	Wind – Type III	All other IBR units
Step Response Time	NA	≤2.5 cycles
Settling Time	≤ 6 cycles	≤ 4 cycles

As a result, the impact on the phase currents produced by the IBR's is observed in the sequence-components domain. In case of conventional generation, the negative and zero- sequence current quantities are considered as preferred candidates to detect faults, involving ground. More specifically, negative sequence current, because zero sequence quantity may be influenced by the mutual coupling in the presence of parallel lines. However, in the case of IBR's, the negative-sequence current is not reliable, when compared to the zero-sequence current, because of the presence of the solidly grounded star-delta interface transformer of the IBR is expected to provide reliable zero-sequence current to make a correct decision.

This impacts all the elements which rely on the negative-sequence current to make a secure and dependable decision, such as, Quad reactance line polarization, Ground Directional element, and others. This also impacts the behaviour of dynamic MHO characteristics as the dynamic behaviour of MHO characteristic is governed by the chosen polarizing value.

With positive-sequence memory voltage as polarization, the dynamic behaviour of ground elements is a function of loop currents. In contrast to the conventional case, the MHO expands to the first and fourth quadrants and the source oscillations during the controller transient period directly translates to swings in MHO characteristic with reach as a hinge point, resulting in uncontrolled dynamic MHO.



Oral Presentation: Impact of Renewable Generation on Distance Protection and Adaptive Algorithms to Optimise Performance

Different grid codes impose different performance requirements and operating priority. As a result, the fault current values depend on the control modes and the design parameters of the controller which can vary to meet different grid code requirements. This impacts the conventional current-based relaying algorithms, including Distance, Directional and FTS which were designed based on the traditional voltage and current relationship.

### 3. POWER SYSTEM MODEL

In the case of renewable energy sources, the availability of analytical model to mimic the fluctuating nature of the renewable source pattern helps to analyse interaction between renewable energy source and the grid. However modelling IBR's power electronic interface poses a significant challenge due to the proprietary nature of IBR controller design and lack of availability of validated models. Although many literatures have tried to model the IBR controller behaviour to evaluate the performance of distance relays, the current values obtained from the simulation models is questionable due to the factors discussed above.

In this paper, COMTRADES obtained from the simulation model [2] which incorporates 'real-controller' as a black box model in electromagnetic transient program were used.

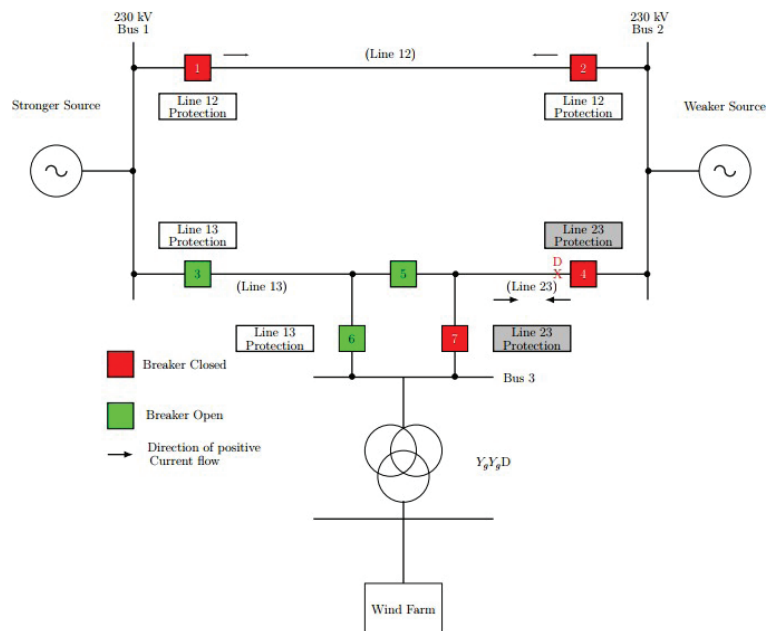


Figure 2: Power System Model

Figure 2 shows the single line diagram of the power system model considered for evaluating the performance of the distance relay. The power electronic interface of IBR consists of 'real-controller' models i.e., actual firmware from four different original equipment manufacturers (OEM) as a black box,

- a) OEM 1: Type 4 wind
- b) OEM 2: Type 4 wind
- c) OEM 3: Type 3 wind
- d) OEM 4: PV Solar

This is then connected to the delta-star step-up transformer which is then connected to the collector bus. The output of the collector bus is then connected to the 3-winding step-up transformer which is connected to Bus 3 forming point of interconnection to the grid. Transmission line 23 is the line of interest, where different fault types are considered at fault location D with each OEM's and the performance of relay controlling breaker 7 is analysed.



Oral Presentation: Impact of Renewable Generation on Distance Protection and Adaptive Algorithms to Optimise Performance

## 4. QUADRILATERAL CHARACTERISTIC

In the presence of IBR, the use of negative sequence polarization is not recommended, specifically when IBR is operated in negative sequence suppression mode. Although the recent German grid code and the draft IEEE P2800 mandate a certain amount of negative sequence injection, the angle of  $I_2$  may vary with respect to  $V_2$  for Type III wind turbines for a few cycles after fault initiation, as a result zero sequence current information shall be used to polarize the top reactance line provided zero sequence information is reliable. This is obtained using the following checks on  $I_0$  magnitude and angle,

- $|I_0| > 0.1 \text{ pu}$
- $|\angle I_0 - \angle I_{ph}| < 50$

However, when zero-sequence information is not reliable, Quadrilateral characteristic can be automatically switched to MHO characteristic for reliable operation. For a conventional generation, for such scenario, polarization will be switched to negative sequence provided negative sequence polarizing quantity checks are satisfied. After switching, if negative sequence polarizing quantity checks are not satisfied Quad characteristic will be switching to MHO, instead of further switching to phase current as polarizing quantity with fixed tilt. This is because the inherent tilting of MHO during power export or import is expected to provide reliable operation when Quad characteristics is no longer reliable.

Adaptive Quad top reactance line polarization can be achieved as follows,

- **Conventional generation**
  - best polarization based on system conditions is selected ( $I_0$  or  $I_2$ ). If both are not reliable then Controlled or Uncontrolled MHO is used. The concept of controlled MHO is introduced in the next section.
- **Renewable generation**
  - Quad is automatically switched to controlled or uncontrolled dynamic MHO when zero sequence current polarization is no longer reliable.

## 5. MHO CHARACTERISTIC

The dynamic characteristics provides better resistive reach especially for faults close to the local end and the dynamic behaviour depends upon the chosen polarizing method. Although, many options were available, polarization based on memorized information was quite popular, because it provides reliable polarizing information in case of three phase close- in fault. Electro-mechanical designs were having limitations in utilizing the memorized voltage, as it decays with time, resulting in new characteristics as time evolves, where the characteristics slowly shrinks as time evolves for forward fault making it difficult to detect close- in high resistance faults.

With the evolution of technology i.e., the introduction of digital relays helps to retain the memory voltage for a selected duration resulting in a characteristic which does not change as time evolves. Additionally, it also provides the flexibility to mimic the electro-mechanical relay behaviour in digital relays.

With a phase, cross and positive sequence voltage as a choice for the polarization, memorized positive sequence voltage polarization is a preferred choice, as it can provide maximum resistive reach coverage. However, this becomes an issue for weak systems (like IBR), where the expansion can be huge.

### 5.1. Real world wind farm case:

Figure 3 shows a real- world wind farm case where zone 1 overreached and caused mis- operation. It also shows the estimated expansion vector for the forward fault. It can be observed that the angle of  $E_{est}$  constantly drifts as time evolves. The estimated angle (Figure 3 (b)) was in the third quadrant at time  $t_1$  and it moved to fourth quadrant at  $t_2$  causing the MHO to slowly drift from third to fourth quadrant.



Oral Presentation: Impact of Renewable Generation on Distance Protection and Adaptive Algorithms to Optimise Performance

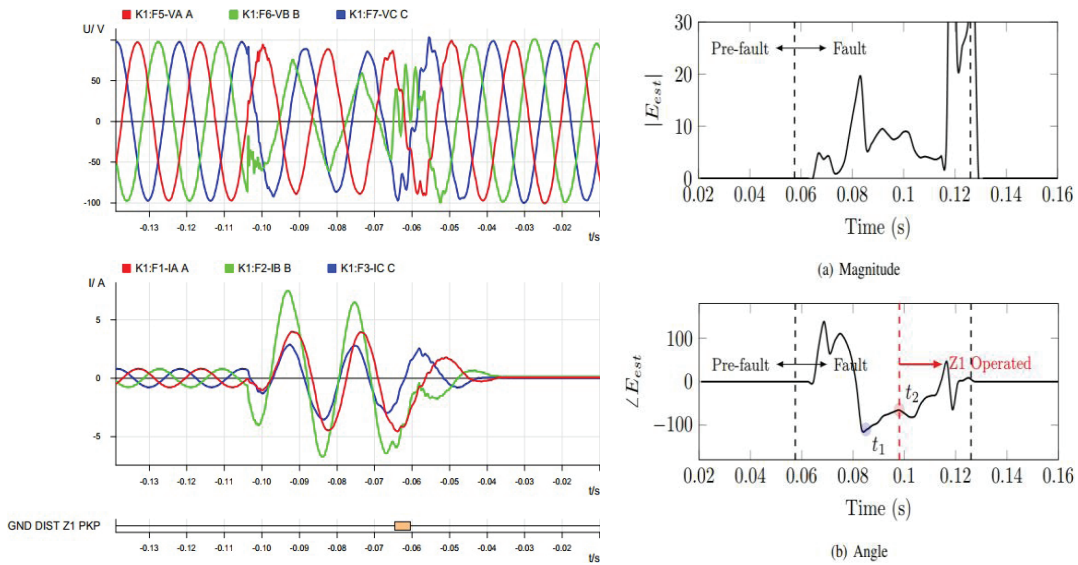


Figure 3: Zone 1 Ground element overreach

The MHO drift is shown in Figure 4, where during the time  $t_1$  the huge expansion was occurring in the third quadrant and the comparator was not satisfied, which explains why the zone1 initially did not operate. At the time of zone 1 operation i.e. at  $t_2$  MHO drifted to fourth quadrant causing mis-operation.

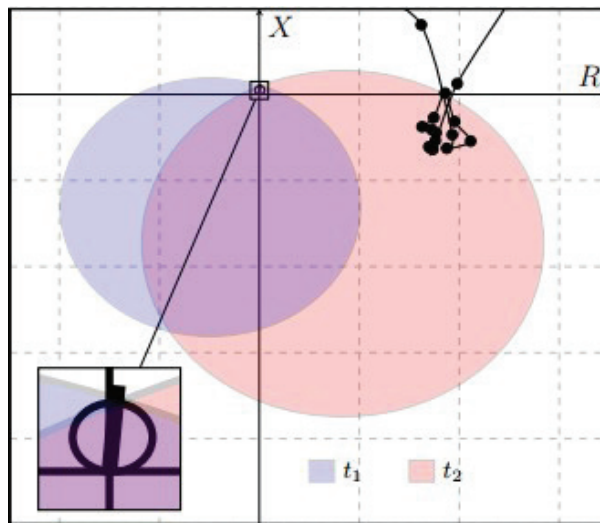


Figure 4: Uncontrolled MHO causing ground Z1 to mis-operate

### 5.2. Controlled Dynamic MHO (Patent Pending):

The uncontrolled dynamic behaviour which is observed in the previous sub-section was mainly due to the selection of polarizing voltage, which was used to overcome the limitations of static characteristics. The polarizing voltage plays a crucial role in shaping the dynamic MHO characteristic. The obvious solution to avoid MHO swings is to use offset operating characteristic, but the offset characteristic provides limited fault resistance coverage for faults close to the relay and fails to provide an extra layer of directional security.

The concept of dual polarization was first introduced by [3] where different signals can be mixed to create a polarizing signal. This brings in the flexibility of controlling the MHO using settings by properly selecting and scaling the inputs to the dual polarization scheme. However, the control based on settings provides only fixed control, and the resulting dynamic characteristic cannot handle the issues due to drifting MHO which is observed in the presence of IBR's

Oral Presentation: Impact of Renewable Generation on Distance Protection and Adaptive Algorithms to Optimise Performance

To overcome this limitation, the concept of controlled dynamic MHO was introduced using the dual polarizing scheme as shown in equation 1, where X and Y are the input voltage polarizing quantities, G and P are the scaling factors. Additionally, making one of the scaling factors to zero helps to switch from dual to single, thereby, bringing in the full flexibility in the polarization to control the dynamic MHO.

$$V_{pol} = G \cdot X + P \cdot Y \tag{1}$$

For a given choice of dual mix, the G and P values are estimated and used in equation 1 which is then applied to one of the comparator input to achieve control on the dynamic characteristic.

In-order to estimate the G and P scalars, first  $E_{est}$  Figure 5(b) is calculated for the considered polarization. Equation 2 and 3 shows the  $E_{est}$ , which is estimated by the relay for ground and phase elements with positive sequence memory voltage polarization i.e. single polarization and this principle can be extended to any considered polarization.

$$E_{est,ground} = \frac{V_2 + V_0 - I_1 Z_{s1}}{I_{Loop}} \tag{2}$$

$$E_{est,phase} = -Z_{s1} \tag{3}$$

where,  $V_2$  and  $V_0$  are negative and zero sequence relay voltage respectively.  $I_1$  is the positive sequence relay current,  $Z_{s1}$  is the positive sequence source impedance and  $I_{Loop}$  is the relay loop current. This information is then used along with the user defined deterministic characteristic as shown in Figure 5 to estimate the values of G and P

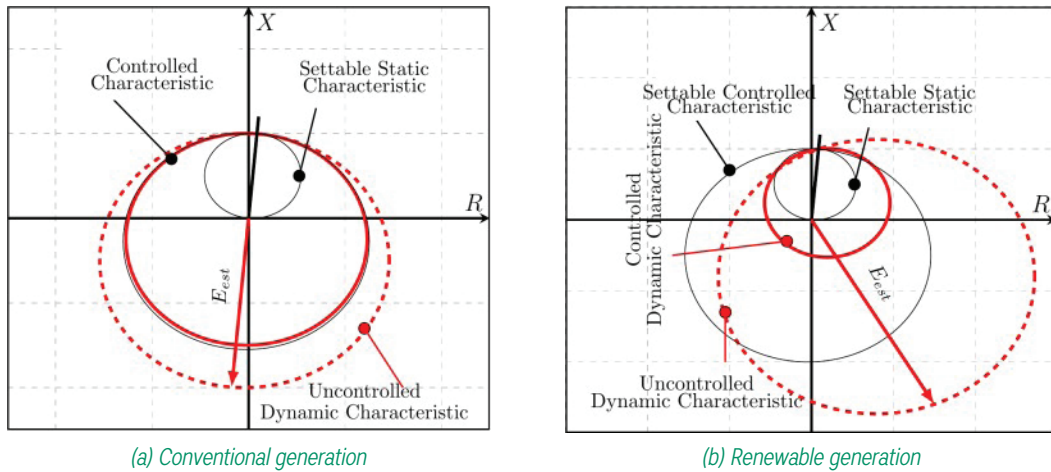


Figure 5: Dynamic MHO

If the dynamic MHO characteristic is inside the user defined deterministic characteristic, the values of G and P are driven in such a fashion that the characteristics is not controlled i.e. single polarization based on  $V_{1M}$  is used so that it provides the best maximum expansion as possible (Figure 6 a,b – pre-fault and immediately after fault). When the dynamic characteristics lies outside the defined deterministic characteristic as shown in Figure 5 (a),(b), polarization is switched to dual and controlled action is achieved by using  $V_{pol}$  based on the weighted  $V_{1M}$  (memory) and phase voltage, where G and P define weights based on the estimated expansion, and the resultant characteristic based on the new dual polarized  $V_{pol}$  lies within the defined area at every instant of time (Figure 5(a),(b) and Figure 6 (a),(b)). As soon as the actual characteristics is deviating from the defined characteristic, polarization is switched to dual and controlled MHO tries to control the dynamic MHO with estimated G and P values. The corresponding controlled MHO plot at the time of mis-operation ( $t_2$ ) is shown in Figure 6c. The controlled dynamic MHO tries to shrink and adjust based on the settable characteristics, thereby ensuring security.



Oral Presentation: Impact of Renewable Generation on Distance Protection and Adaptive Algorithms to Optimise Performance

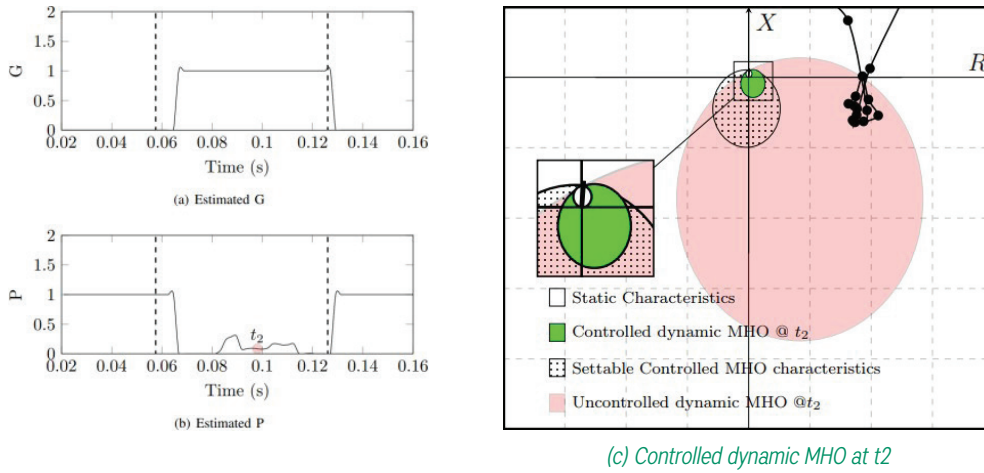


Figure 6: Performance of controlled dynamic MHO

## 6. FAULT TYPE SUPERVISION

Different types of FTS exist [4] which are mature and have proven track record in the field for many decades. However, the possibility of having different fault current signature for the same fault type and system conditions e.g., different IBR owner can have different slope setting or different priority mode making it difficult to come up with a new current based FTS to cover all possible fault signatures. In-order to overcome this, voltage-based FTS is proposed as this is not new to distance relays where voltage-based FTS will be used when current signals are not reliable [5]. Changes in slope setting and with certain priority modes may improve the voltage profile, but still the desired quantity is embedded in the voltage signal.

## 7. DIRECTIONAL ELEMENT

To ensure secure operation, Distance characteristics is supervised by Directional elements. In addition to supervision, these Directional elements can be used to form a closed boundary for Quad characteristics.

### 7.1. Issues with negative sequence current as operating quantity:

To determine the fault direction, negative sequence current quantity is typically preferred for ground elements mainly because it is insensitive to zero-sequence mutual coupling [5]. However, we have already observed that negative sequence current information may be suppressed by IBR depending upon the mode of operation and even if negative sequence current is present, the information may not be reliable. As a result, for IBR based generation, only Directional element based on zero sequence information is used to supervise the distance and negative sequence information is bypassed.

### 7.2. Issues in setting phase Directional element:

The different reactive power requirements mandated by grid codes and the flexibility of operating the IBR in different modes (Table 1) during the disturbance may result in leading fault currents. This may impact the Directional element performance if it is not properly set to handle leading power factor.

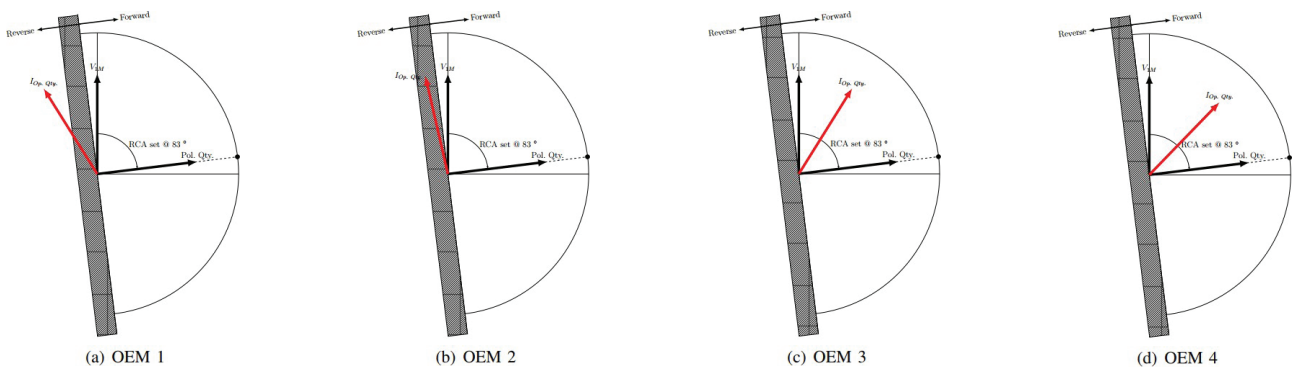


Figure 7: Reverse phase Directional element performance for forward fault AB with different OEM (black – polarizing quantity, dashed red - operating quantity, red-operating quantity after directional RCA adjustment)



Oral Presentation: Impact of Renewable Generation on Distance Protection and Adaptive Algorithms to Optimise Performance

Figure 7 shows the behaviour of different OEM for the same fault type (i.e. phase to phase fault involving phases A and B) at location D in Figure 2. In all the four cases, the phase directional was set to handle 7 degree leading to 173 degree lagging loads/fault currents. It can be observed from Figure 7(a) and Figure 7(b) where the reverse phase Directional element declared the fault as reverse, whereas the actual fault was in forward direction. This is because the fault current was leading around 32 degree and 13 degree in OEM 1 and OEM 2 respectively. The phase directional was set to handle only 7-degree leading fault/load currents. This resulted in reverse zone (Zone 3) getting picked up for a remote-end forward fault in the case of OEM 1 and OEM 2. Whereas, in OEM 3 and OEM 4 the direction was properly declared leading to correct operation of the forward zones. This is mitigated by properly setting the Directional element to handle leading fault currents.

## 8. FREQUENCY

Frequency tracking plays a crucial role and impacts the decision of any protection element which is based on phasor information. The impact on phasor estimation due to off-nominal frequencies are minimized by either resampling or tuning the filter coefficients based on the tracked system frequency. In conventional generation i.e., synchronous machines, the inertia of the rotating shaft restricts abrupt change in frequency during any disturbance. However, in case of renewable generation, more specifically with grid forming IBR's which can decide the frequency, it may vary drastically.

Under such scenarios, the problem of under-reaching zone 1 mis-operation can be mitigated by the following options:

- using controlled dynamic MHO which is biased towards security. It overcomes the issues due to frequency excursions for e.g., reverse zone pickup for the forward fault
- adaptively delaying the zone decision when frequency excursions are detected in either voltage or current or in-between voltage and current signals.

## 9. CONCLUSIONS

This paper has demonstrated the importance of re-looking at the distance protection for protecting lines fed by renewable generation. The major issue is due to the change and variations in fault current signature for faults fed by IBR's. This is mainly due to the flexibility and the choice of operating mode i.e., priority for which the IBR is programmed to operate. Additionally, controller design parameters also have an impact on fault current signature during the transition. Impact of the above mentioned on the phase currents during fault is directly seen in the sequence components with negative sequence getting impacted more in a specific operating mode. Although standards and grid codes have recently mandated the negative sequence current injection, the quantity may not be reliable during the initial few cycles, especially with Type III wind turbines. This paper discussed how this impacts the FTS and Ground Distance Directional elements which rely on the negative sequence quantity to make a decision and solutions were provided to overcome this problem by using sequence voltage- based information for FTS and bypassing the negative sequence Directional elements for Ground Distance.

It is also not recommended to use negative sequence current to polarize the top reactance line for Quad characteristics. In-order to overcome the limitations with zero sequence current polarization, this paper has discussed the advantage of using the Quad with best polarization selection, which automatically selects the best polarization at a particular point in time, thereby retaining the adaptive tilting feature and automatically switching to MHO to ensure reliable operation when zero sequence quantity is no longer reliable.

This paper also discussed the impact of IBR's on the century old MHO behaviour and provides interesting insights into unexpected MHO behaviour. The reason behind such behaviour i.e., uncontrolled dynamic MHO was explained analytically, and it introduced an innovative solution "Controlled Dynamic MHO" to overcome the uncontrolled dynamic MHO behaviour.

## BIBLIOGRAPHY

- [1] "IEEE Draft Standard for Interconnection and Interoperability of Inverter-Based Resources (IBR) Interconnecting with Associated Transmission Electric Power Systems.," *IEEE Standard P2800*.
- [2] Sandia National Lab., "Impact of inverter based resource negative sequence current injection on transmission system protection.," [Online]. Available: <https://www.osti.gov/servlets/purl/1595917/>.
- [3] S. Wilkinson, "Static distance relays with improved polarizing signal". Patent 4342064, 1982.
- [4] C. Venkatesh and I. Voloh, "Cross country faults - protection challenges and improvements," in *74th Conference for Protective Relay Engineers*, Texas A & M, USA, 2021.
- [5] GE Publication -1601-0089-AK1, "D60 Line Distance Protection System," 2020. [Online]. Available: <https://www.gegridsolutions.com/app/viewfiles.aspx?prod=d60&type=3>.



# Prevention of High Voltage Network Disturbance Propagation by On-Line Monitoring and Diagnostic of Relay Protection

[Alexey.nebera@kontron.sl](mailto:Alexey.nebera@kontron.sl)**ALEXEY NEBERA\****Kontron Smart Energy***JANEZ ZAKONJSJEK***Kontron Smart Energy***PROF. BOŠTJAN POLAJŽER***University of Maribor, FERl***GORAZD HROVAT***ELES***Slovenia**

## SUMMARY

Proper operation of relay protection is a necessary precondition for Power system reliability. Malfunction of relay protection is one of the main contributors to extended network outages. Protection engineers make a lot of effort to establish and maintain sensitivity, selectivity and reliability of protection systems, but due to the big number of substations and protection devices each of them can be checked and serviced only once in a few years. Until then almost any failure in a protection device and its external circuits usually remains hidden and pose a risk of malfunction and bigger network disturbance. Meanwhile modern numerical relays provide variety of communication possibilities and monitoring information, but most of this data, are still not regularly collected and analyzed in the Power systems.

Authors are describing a new on-line protection monitoring and diagnostic system, a real time simulation-based testbed for its testing in high voltage networks and the results of the testing.

## KEYWORDS

Power system – Relay protection – Mis operation – Malfunction – Monitoring – Diagnostics



Oral Presentation: Prevention of High Voltage Network Disturbance Propagation by On-Line Monitoring and Diagnostic of Relay Protection

### 1. INTRODUCTION

After a whole lot of scientific, engineering and organization efforts to develop, design, install and maintain relay protection in power systems, it is very important to get an objective measure of its actual performance in real-life conditions. This measure can be derived from accurate statistics about its proper operations and malfunctions. One of the best sources about relay protection performance in large interconnected power systems can be found in NERC "State of reliability" reports, published each year. As stated in 2022 report [1]: "When designed and implemented properly, automated tools can enhance the reliable and secure use of new technologies and concepts that become available. On the other hand, maintaining, prudently replacing, and upgrading bulk power system control system assets can lead to protection and control system Misoperation. Misoperation can initiate more frequent and/or more widespread outages."

As can be seen on the Figure 1 below, an average rate of protection misoperations for major US power system lies mostly in the range of 6-8% and in some cases can reach 11% of total amount of operations. This is quite a substantial amount of protection malfunctioning which requires further analysis. Main causes of protection misoperation in 2021 with corresponding percentage are shown on the Figure 2. As stated in the report, the top causes of misoperations over the past five years have consistently been Incorrect Settings and Relay Failures/Malfunctions which reflects both the growing complexity of modern power systems and microprocessor based protection IEDs.

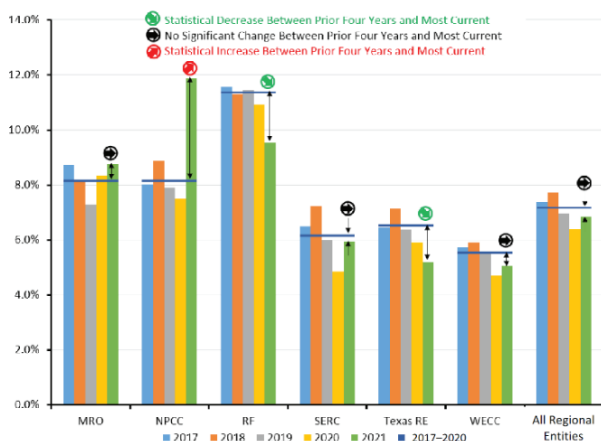


Figure 1: Changes and trends in annual Misoperation rate cause code

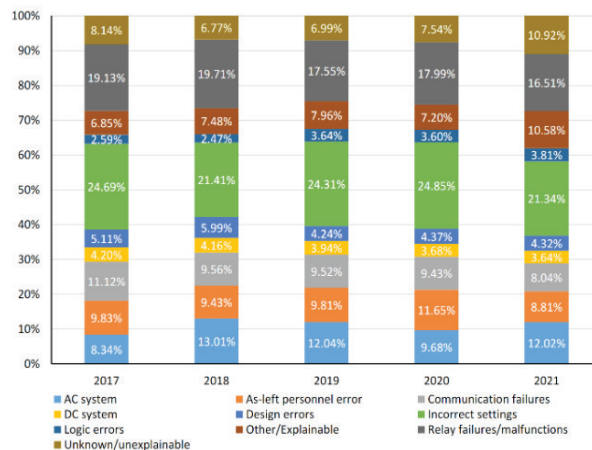


Figure 2: Misoperation by cause code

During misoperation analysis it can be also noted that Human error is one of potential causes for misoperations. Human error is involved in about 40% of all misoperations and manifests itself in:

- As-left personnel error – test switches left open, wiring errors not associated with incorrect drawings, carrier grounds left in place, settings placed in the wrong relay, or settings left in the relay that do not match engineering intended and approved settings
- Design errors – incorrect schematics or equipment application
- Incorrect settings – inaccurate or insufficient modeling, calculation errors
- Logic errors – programming errors in custom user logic, wrong assignment or mapping of signals.

Thus, it can be seen that growing complexity of power systems and their protection requires more efforts to improve reliability and avoid extended outages due to protection malfunctioning. On the other hand, power system personnel in real life are always limited in time and can itself be a source of potential reliability threats. In the meantime, modern protection IEDs are able to provide a lot of measurement and diagnostic information which is not used to a full extent nowadays since it's just impossible to do manually without automated monitoring and analysis systems.

### 2. AUTOMATED PROTECTION MONITORING AND DIAGNOSTICS

A distinctive aspect of relay protection is a big average time between operations – from none too few operations a year depending on equipment type and voltage level. This gives us enough time to discover potential failure and act upon it, if there is a regular information exchange between protection devices and protection engineers' office.



**Oral Presentation:** Prevention of High Voltage Network Disturbance Propagation by On-Line Monitoring and Diagnostic of Relay Protection

Let's consider the protection misoperation causes shown above, along with data allowing to identify the problem.

**Table 1:** Information available to identify protection problems

Misoperation cause	Available information	Ways of retrieval
AC system	Analog measurements of voltage and current sensed by protection IEDs. Measurements from more than one IED located on the same bay or busbar can be compared to identify significant mismatch.	<ol style="list-style-type: none"> <li>1) Live RMS values via IEC 60870-5-103, 104 or IEC 61850-8-1 MMS messages</li> <li>1) Live sampled values via IEC 61850-9-2 or 61869-9 streams</li> <li>2) Sampled values in disturbance record files</li> </ol>
As-left personnel error	Protection IED configuration info: <ul style="list-style-type: none"> <li>• Protection functions state (on/off)</li> <li>• Operational switching key position on the protection cubicle or panel</li> </ul> Analog measurements of voltage and current Approved settings vs actual protection configuration files comparison	Discrete signals via IEC protocols or relay contacts As for AC system above <ol style="list-style-type: none"> <li>1) File retrieval by IEC 61850-8-1 MMS messages</li> <li>2) File retrieval by a protection IED manufacturer engineering software</li> </ol>
Communication failures	Communication channels state	Discrete signals via IEC protocols
DC System	Availability of DC supply	Discrete signals via IEC protocols or relay contacts
Design errors	Disturbance record files including analog as well as protection start and trip signals	File retrieval by IEC 61850-8-1 MMS messages
Incorrect settings	Approved settings vs actual protection configuration files comparison Disturbance record files including analog as well as protection start and trip signals	<ol style="list-style-type: none"> <li>1) File retrieval by IEC 61850-8-1 MMS messages</li> <li>2) File retrieval by a protection IED manufacturer engineering software</li> </ol>
Logic errors	Disturbance record files including analog as well as protection start and trip signals	File retrieval by IEC 61850-8-1 MMS messages
Relay failures/malfunctions	Self-diagnostic signals	Discrete signals via IEC protocols
Other/Explainable		
Unknown/Unexplainable		

As can be seen from the table above, most of device and its circuits failures can be explicitly detected based on information available in modern protection IEDs. It should be noted that partially monitoring functions can be implemented even for electromechanical devices as long as disturbance records in a digital form are regularly available from standalone fault recorders.

Other problem types require additional consideration:

- Design errors, Incorrect settings and Logic errors are usually hardly identifiable in a normal state of a power system just by looking on any information provided by a protection IED. However, they can be detected by studying protection start signals during disturbances. As there are more protection starting events than actual tripping, start signals rarely got carefully studied by protection engineers<sup>1</sup> and often not configured in disturbance records. More dangerous errors will manifest themselves in starting faults or excessive starts, thus providing a valuable insight and possibility to prevent protection misoperation<sup>2</sup>.
- Unknown/Unexplainable causes – the very existence of this group reflects a lack of information, as well as inevitable time and resource limitations of protection departments with low automated ways of disturbance information gathering and analysis. Authors believe that properly implemented protection monitoring and diagnostic system will allow to significantly decrease amount of unknown causes of protection malfunctions.

*1 It is interesting to note that the definition of protection malfunction or misoperation is only related to protection tripping events, thus protection start signals not followed by a trip are much less investigated and reported.*

*2 Evaluation of start signals for a protection with many stages require accurate modelling of a power system disturbances as well as protection functional and logical blocks*



**Oral Presentation:** Prevention of High Voltage Network Disturbance Propagation by On-Line Monitoring and Diagnostic of Relay Protection

Besides the task of information extraction from remote protection devices and other potential data sources like standalone fault recorders, protection manufacturers engineering software and SCADA systems are additional important aspects to be considered.

To extract the full potential of protection monitoring and diagnostic system (PMD), maximum of usual routine analysis operations should be done automatically, including:

- synchronization and stitching of disturbance records from various devices and/or periods of the disturbance (fault and auto-reclosing)
- fault location and fault type determination
- evaluation of actual protection operation based on network topology and event tree analysis
- analysis of self-diagnostic signals and evaluation of hardware and software IED state and conditions of power supply, secondary circuits and communication networks
- protection configuration checking by automatic comparison of actual settings (a file received from an IED directly or via a manufacturers engineering software workstation) with a reference settings file initially prepared for configuration

Ability of consistent automated analysis provision for different types of protection device manufacturers, versions etc. relies upon a careful information model of underlying power system and protection devices with all their circuits, functions and signals. To minimize initial configuration efforts as well as subsequent updates of PMD information model it is worth to implement an integration functions with Network Model Management or SCADA/EMS/DMS systems. This exchange needs to support IEC Common Information Model (CIM) standards to allow automated import of power system topology and parameters to PMD. On the other hand, protection IED data retrieval should support IEC 61850 standard series as the most widely used now and in the observable future. Since neither CIM nor 61850 fully cover all the details of protection information modelling, PMD needs to map both standard worlds and maintain additional information extensions to implement its functions.

An automated protection monitoring and diagnostics system implementing the features described above has been developed by Kontron Smart Energy and tested together with Slovenian TSO ELES and Maribor University.

### 3. TESTING OF PMD

The PMD system was tested during March 2023 at the Faculty of Electrical Engineering and Computer Science (FERI) of Maribor University on the RTDS (Real Time Digital Simulator) testbed. A 220-kV power line between substations Podlog (Slovenia) and Obersielach (Austria) was simulated together with corresponding equivalent impedances and generating facilities on both line ends. The whole testbed as shown on Figure 3, included two main parts:

- 1) Substation level, located in Maribor university (FERI) where part of ELES high voltage network is represented by the RTDS simulator.
- 2) Control center level represented by Kontron Smart Energy infrastructure in Kranj.

Two monitored protection devices IED 1 and IED 2 on Figure 5 represented by Siemens 7SD522 line current differential and distance protection were connected over current and voltage amplifiers as well as binary signals (tripping and breaker closing commands) transducers to the RTDS.

Protection IEDs are controlling circuit breakers on both ends of the simulated power line and have two communication channels:

- to a local computer with Siemens DIGSI engineering software used to configure and control these IEDs
- to a PMD server in Kontron's Smart Energy cloud infrastructure located on the control center level.

A number of different system operating conditions together with different fault types and impedances within and outside of protected power line has been simulated in real time, which caused corresponding operation of protection IEDs.

During the testing an automated PMD data retrieval via IEC 61850-8-1 as well as analysis functions listed above were confirmed to be successfully working.





Oral Presentation: Prevention of High Voltage Network Disturbance Propagation by On-Line Monitoring and Diagnostic of Relay Protection

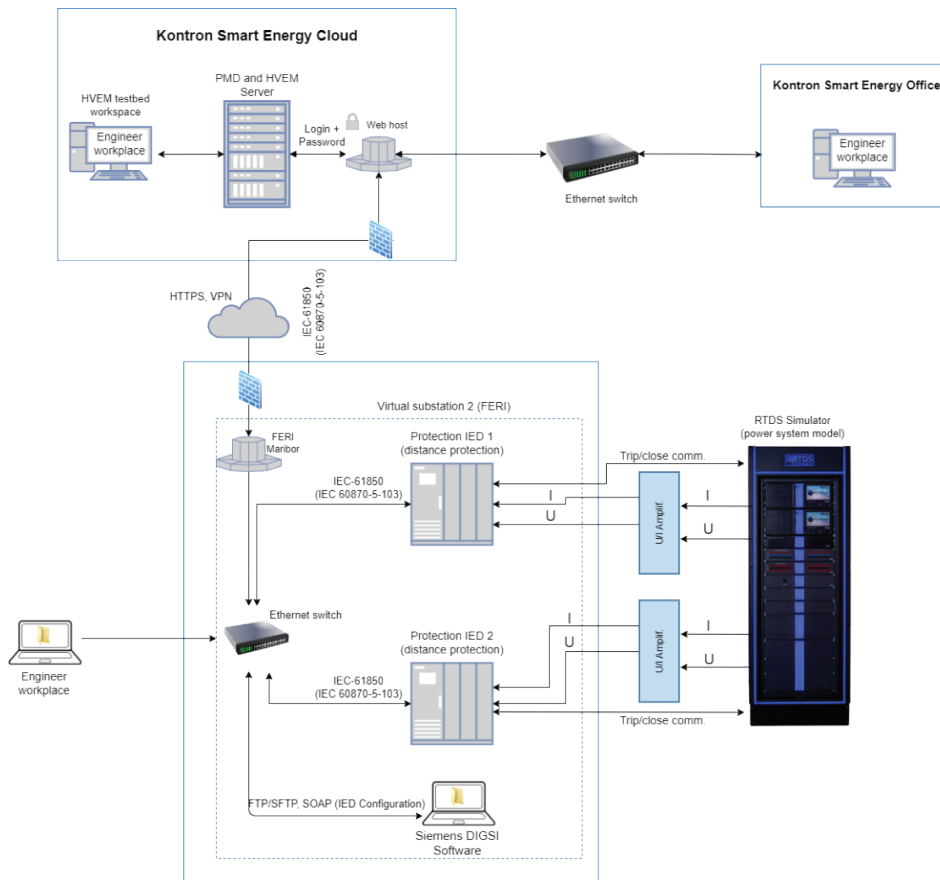


Figure 3: PMD testbed architecture

It is worth to note that successful operation of relay protection in isolating a fault in power system is only possible in conjunction with associated high voltage equipment, namely instrument transformers and circuit breakers. Problems in instrument transformers and their secondary circuits may cause inaccuracies or inability of relay protection to sense a fault, while failures of circuit breakers lead to the fault extension in time and geography.

That is why a follow-up testing was implemented, based on disturbance records gathered on the Maribor FERI testbed and devoted to a possibility of circuit breaker (CB) monitoring.

As shown on Figure 4, various parts of a fault clearing time during a CB opening can be estimated based on a disturbance record analog and discrete signals if they are properly configured. The most important ones are 1) the arcing time directly influencing the CB commutation life and 2) the inherent opening time reflecting the state of CB drive.

### 4. CONCLUSION AND FUTURE WORK

After detailed analysis of all available results is possible to conclude, that application of automated protection monitoring and diagnostics system along with high voltage equipment monitoring functions would contribute to more efficient work of TSO/DSO specialists. Some of the findings are listed below:

- 1) Automatic collection of disturbance records within a very short time after a certain event (fault) occurred in the observed power system. It is possible to automatically receive disturbance information in matter of minutes, when all disturbance records, related to the same event, can be collected from different substations within the PMD system and prepared for further automatic analysis. Manual activities as used today may require for this work many hours or even days.
- 2) Initial analysis of disturbance records from several involved substations and preparation of basic report may take by PMD system between 10 minutes up to a couple of hours, when a big number of power facilities is included. Manual work, as performed today, takes usually at least few hours for simple events and up to couple of days for more complex faults.



**Oral Presentation:** Prevention of High Voltage Network Disturbance Propagation by On-Line Monitoring and Diagnostic of Relay Protection

- 3) ETA (Event Tree Analysis) within PMD system may take in most cases half an hour for rather complex event but may need much shorter time for single fault in power system. Such analysis may take even a couple of days when competent specialist needs to make it manually.
- 4) Automatic collection of binary signals, related to self-supervision of protection IEDs contributes definitely to higher availability of complete secondary system as well to its more reliable operation.
- 5) General practice in current situation is to manually download and analyse only disturbance records from IEDs which reacted to certain events by a tripping command. This is related to very high work load in protection departments which makes it practically impossible to study not only tripped IEDs, but also IEDs which have started but not tripped due to their time parameters. Implementation of the PMD system makes it possible to download disturbance records and study also the responses of IEDs which initiated only starting signals.
- 6) Estimation of circuit breaker time components during the opening (and closing if possible) operation, including arcing time or phase-to-phase time difference, allows evaluate the impact of operations on the circuit breaker lifetime.
- 7) Both protection monitoring and CB as well as instrument transformer monitoring functions develop a solid base for the potential change towards Condition Based Maintenance with corresponding economic benefits for power system companies.

Future development of the presented system can be considered in the next directions:

- Pilot project implementation on the high voltage substations to:
  - estimate the real-life system performance
  - gather detailed statistics of protection operations and technical state changes
  - develop and test an optimal system architecture reflecting cybersecurity needs.
- Functional extension including more detailed:
  - protection starting signal analysis with corresponding modelling
  - monitoring of circuit breakers and instrument transformers based on real time measurements in addition to disturbance records
  - secondary equipment monitoring, including the collection of self-diagnostic signals from communication equipment involved in protection operations in addition to the signals from protection IEDs.

## BIBLIOGRAPHY

- [1] NERC: State of Reliability, August 2022. Assessment of 2021 Bulk Power System Performance. July 2022
- [2] The Risk of Hidden Failures to the United States Electrical Grid and Potential for Mitigation. Arthur K. Barnes, Adam Mate, and Jose E. Tabarez. IEEE/PES 53RD North American Power Symposium, November 2021.
- [3] Fukui C., Kawakami J. An expert system for fault section estimation using information from protective relaying and circuit breakers // IEEE Trans. on Power Delivery. Vol. 1. Oct. 1986. P. 83-90.
- [4] Kezunovic M., Spasojevic P., Fromen C.W., Sevcik D. An expert system for substation event analysis // IEEE Trans. on Power Delivery. Vol. 8. Oct. 1993. P. 1942-1949.
- [5] D. C. Elizondo et al. Hidden Failures in Protection Systems and their Impact on Wide-Area Disturbances. In Proc. of the 2001 IEEE Power Engineering Society Winter Meeting, Feb. 2001.
- [6] Informational analysis of processes in electrical power systems / Y. Liamets, Y. Romanov, D. Zinoviev, J. Zakonjšek, G. Nudelman // Proc. 15th Int. Conf. Power System Protection. – Bled, Slovenia, 2006. – P. 87-96.
- [7] IEEE Power System Relaying Committee WGK15, Centralized Substation Protection and Control, December 2015.
- [8] Lyamets Yu.Ya., Efimov E.B., Nudelman G.S., Zakonshek Ya. / Principle of information perfection of a relay protection // Elektrotehnika (Russian Electrical Engineering). 2001. # 2. P. 12-17.
- [9] Standard PRC-004-6 — Protection System Misoperation Identification and Correction. NERC
- [10] BH K/O CIGRE u elektronskoj formi na e-mail adresu (office@bhkcigre.ba). Referat se dostavlja u MS Word (.doc) formatu.
- [11] Zhang N., Kezunovic M. / Verifying the Protection System Operation Using an Advanced Fault Analysis Tool Combined with the Event Tree Analysis // Northern American Symposium (NAPS), 2004.
- [12] S. H. Horowitz et al. Boosting Immunity to Blackouts. IEEE Power Energy Mag., 1(5):47–53, Sep. 2003 pages after title page must start from this line, i.e. 1" (2.5 cm) margin from the top (Times or Helvetica, size 11 or 12). Pages will be automatically numbered.

**ELECTRIC MACHINES AND  
POWER ELECTRONICS**

**POSTER PRESENTATION**

**ELECTRIC MACHINES AND  
POWER ELECTRONICS**



**ELECTRIC  
TRANSMISSION**



**AUTOMATION AND  
CONTROL**

**POWER  
GENERATION**



**ENERGY  
TRANSITION**



**DISTRIBUTION SYSTEMS  
AND SMART GRIDS**



**11-12 OCTOBER 2023**



# Short Circuit Analytical Prediction for Transformer Winding

[mattia.medini@hitachienergy.com](mailto:mattia.medini@hitachienergy.com)**MATTIA MEDINI\*, LUIGI DE MERCATO***Hitachi Energy***Switzerland**

## SUMMARY

A transformer is one of the most expensive components in the electric power distribution systems. The financial losses due to its inefficiency make it one of the most important components of any production systems. For this reason, any kind of possible failure should be avoided, and one of the most common is due to the inability to withstand the short circuit phenomenon. This is an abnormal condition in an electrical circuit where the current travels along an unintended path with very low electrical impedance leading to an extremely high Lorentz forces on the transformer windings. These forces must be properly calculated since the windings must be designed for withstanding these loads. In fact, the short-circuit forces could induce a structural instability on the windings or generate a stress status higher than the admissible one. With the final purpose of dimensioning the transformer winding to the short-circuit load, the SCAP excel tool (Short Circuit Analytical Prediction) was developed. The scope of this work is to provide a summary of the state of the art of the existing methods for the short-circuit stress analysis on transformers windings, analyzing and comparing them in order to understand their limits and their strengths. Furthermore, due to the winding type variability, it is not possible to choose a best method for all of them. For this reason, different analytical equations have been implemented for considering various winding shapes. In addition to this, a parametric study by means of finite element simulations was performed for extending the range of validity of the analytical equations to more complex geometries (like oval shaped windings). In this way, tendency lines, based on geometrical variables of the winding, have been identified and used as corrective factors. The same workflow was followed for understanding how other aspects affect the structural instability and stress status of the windings, in particular, it was identified that the quality of the adhesion among the conductive foils strongly affects the structural strength of the entire winding. This behavior was studied by means of finite element simulations, since no analytical equations were retrieved for addressing this condition. Furthermore, another aspect studied by means of finite element simulations is the retaining effect provided by the outer sections to the innermost ones. In fact, the transmission of the forces among sections (stack effect) cannot be calculated by simple analytical formulas but only by simulations. This paper shows a reliable and quick tool developed for the prediction of the capability of a winding to withstand the short-circuit forces, and its validation against experimental data.

## KEYWORDS

Transformer, Winding, Short-Circuit, Electromagnetic-Structural

### 1. INTRODUCTION

Transformer coils are usually subject to various electrical, mechanical and thermal stresses during their lifetime. The external short-circuit event can be considered as one of the most demanding load conditions, where high current levels and forces are generated in the transformer windings. A reliable and quick tool for predicting the stress status on the winding is necessary especially at bidding stage when finite element investigations are not required.

### 2. DETERMINATION OF THE FORCES

During the short-circuit event the main mechanical excitation is due to the Lorentz force. Consider a region  $\Omega$  having  $J$  current density and immersed in a  $B$  magnetic field, the resulting Lorentz force is:

$$\vec{F} = \int_{\Omega} \vec{J} \times \vec{B} d\Omega \tag{1}$$

This force is perpendicular to the plane formed by the magnetic density field and elemental conductor. Figure 1 shows the direction of the force with respect to the magnetic field and current directions.

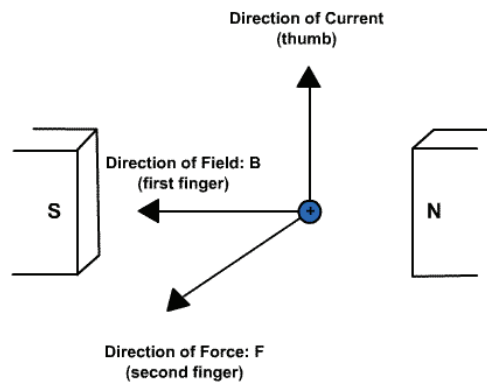


Figure 1: Right hand rule for determination of Lorentz force

Being the force dependent on both the current and on the magnetic density field, it is important to have a complete understanding of them. As shown on Figure 2, the curvature of the magnetic field near the ends of the windings causes a deviation in the force’s direction. For this reason, the magnetic field can be divided in the radial and axial component, responsible respectively of the axial and radial component of the forces.

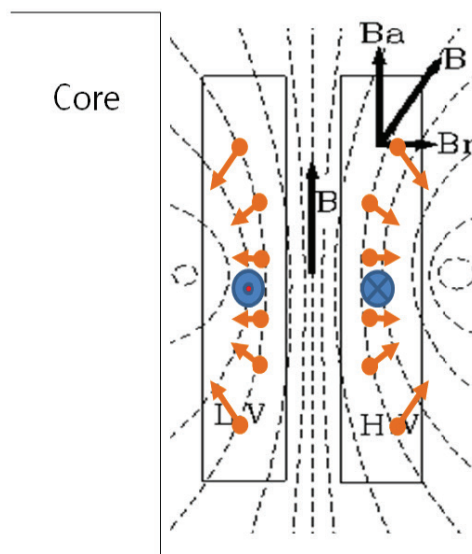


Figure 2: Variation of the forces (orange), magnetic field (- - -) and current (blue).



The following methods can be used for the calculation of loads on windings:

### 2.1. Radial forces methods

The three following methods were developed by Borsani [1], Valdes [2] and Degli Esposti [3] [4]. The assumptions behind these methods are:

- Pure axial magnetic flux
- Maximum and constant value of the magnetic field along the vertical cooling duct between primary and secondary winding, corresponding to  $B_m = \mu_0 \frac{NI}{h_w}$
- Linear distribution of the magnetic field along the windings  $B(x) = B_m \frac{x}{a}$

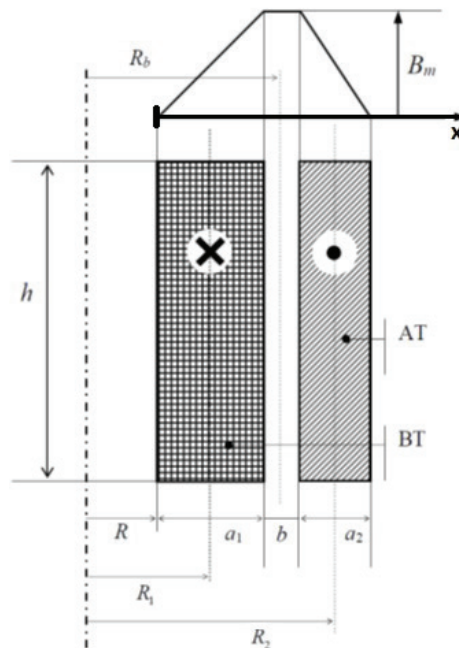


**Figure 3:** Distribution of magnetic field and geometry description

Where:

- $B_m$ : maximum value of the leakage magnetic flux
- $\mu_0$ : Permeability of free space
- $N$ : Number of turns of the winding
- $I$ : Current
- $h_w$ : Electrical height of the winding under investigation
- $x$ : Coordinate system
- $a$ : Radial thickness of winding

### 2.2. Axial forces methods

The axial component of the forces in a transformer with conventional concentric windings cannot be calculated with high accuracy by elementary methods, mainly because the curvature of the magnetic field cannot be considered without using complex solutions, which require the use of a computer. Furthermore, being the magnitude of the axial forces very low and less critical compared to the radial one, the decision is to ignore these forces in the analytical calculation.





## 2.3. Total forces methods

These methods can be adopted in order to directly obtain both axial and radial forces. For the sake of completeness, below are listed the available methods even if they have not been implemented into the tool:

- Billing two dimensional methods [5]
  - Line conductor parallel to current sheet
  - Two parallel current sheets
- Ignacz' two-dimensional method
- Fourier series
  - Roth's method
  - Rabins' method

## 3. DETERMINATION OF THE STRESS

Once the radial pressure acting on the windings is calculated, it is possible to calculate the induced stresses. Their calculation vary depending on the mechanical model chosen. In bibliography, the following methods have been adopted:

- Pressure vessel model: the assumptions behind this method are
  - Axial symmetry of geometry and loads
  - Constant thickness
  - Ratio between diameter and thickness must be  $> 20$
  - Absence of abrupt variation of diameter.
- Thin beam model: the assumptions behind this method are
  - The material follows the Hooke's law
  - One dimension much greater than the other two
  - Z number of spacers evenly distributed along the azimuthal direction
  - Curvature of the winding is not considered
  - Supports modelled as a fixed connection.
- Thin curved beam model: the assumptions behind this method are
  - The material follows the Hooke's law
  - One dimension greater than the other two
  - Z number of spacers evenly distributed along the azimuthal direction
  - Supports modelled as a fixed constraint
  - The conductor of the section forms a closed ring of radial length  $h$ , axial height  $t$ , and mean radius  $R$ .

Based on the winding geometry, the user can select the most suitable methods among the one reported above. In fact, all the above methods have been implemented into the analytical tool.

## 4. STABILITY PROBLEM

The inner winding (LV shown on Figure 2) is subjected to an inwards force, this means that instability could be triggered. For this reason, a second investigation on the possible instability issue must be performed after the stress verification. For this calculation, three different models are available based on the assumptions on the duct sticks positioned on the cooling channel:

- Free buckling: the winding could deform without any constrain (please refer to following figure)

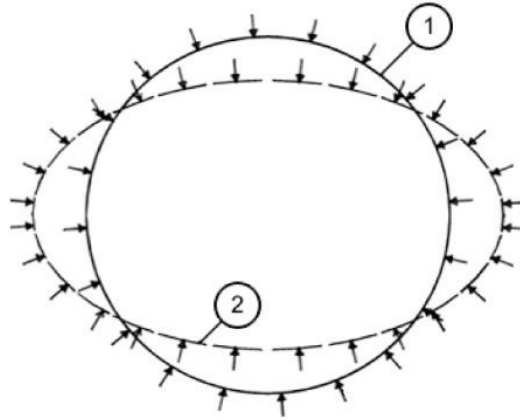


Figure 4: Free buckling phenomenon

- Forced buckling: the winding is constrained by the duct sticks positioned on the cooling channel. They can be modeled as hinges or fixed constrains based on the real contact garanted during the manufacturing.

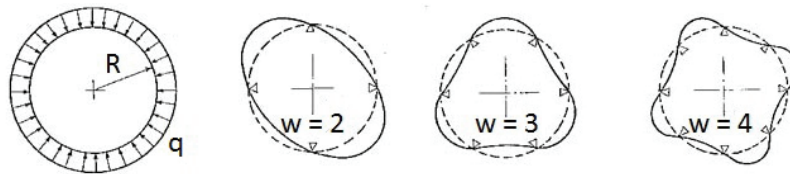


Figure 5: Sticks modelled as hinge

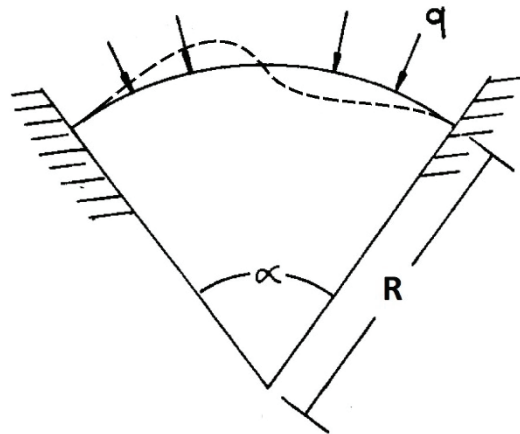


Figure 6: Sticks modelled as fixed constrain

## 5. ASSUMPTIONS OF ANALYTICAL EQUATIONS

All the above-mentioned analytical methods have some intrinsic assumptions:

- Circular and oval shaped winding
- Coaxial windings
- Pure axial magnetic leakage flux
- Maximum and constant value of the magnetic leakage flux across cooling ducts
- Linear distribution of the magnetic leakage flux across conductors



Poster Presentation: Short Circuit Analytical Prediction for Transformer Winding

- The magnetic leakage flux does not vary along the non-conductive materials
- The sections of the same plane share:
  - Axial height
  - Axial number of turns
  - Current density
  - Phase of the current
- Spacers evenly distributed
- Sections considered as a single resistant element (e.g. n turns bonded together having thickness t are equivalent to 1 turn having n-t thickness)
- Each circular section of the inner winding is modelled as structurally independent from the others:
  - No load transmission between sections
  - Spacers are rigidly fixed to ground

Among all these assumptions, the two that are most limiting the range of validity of these equations are the ones underlined. For this reason, a series of numerical parametric study (coupling Maxwell 3D software embedded into ANSYS with a structural simulation) have been performed for extending the range of validity of this analytical tool (please refer to the following chapter).

## 6. FEM PARAMETRIC STUDY

FEM parametric studies have been performed for addressing the following topics:

- Oval winding: with the analytical formulas available in literature, it is possible to study only sections with circular shape
- Relative motion within each section: with the analytical formulas available in literature, it is possible to study only sections modeled as monolithic blocks. However, it is important to study the behavior of the winding when a good adhesion among the conductor foils cannot be guaranteed
- Containing effect of the outer sections: with the analytical formulas available in literature, it is possible to study only sections modeled individually without any transmission of the load between different sections
- Elasto-plastic model: Neuber's correction have been added to the tool for calculating the equivalent plastic strain induced on the winding during short circuit.

### 6.1. Oval winding

A series of numerical simulation have been performed for understanding how the stress status and the buckling instability is influenced by moving from a perfectly circular geometry to an oval winding. This study have been performed for different ovality factors defined as follow:

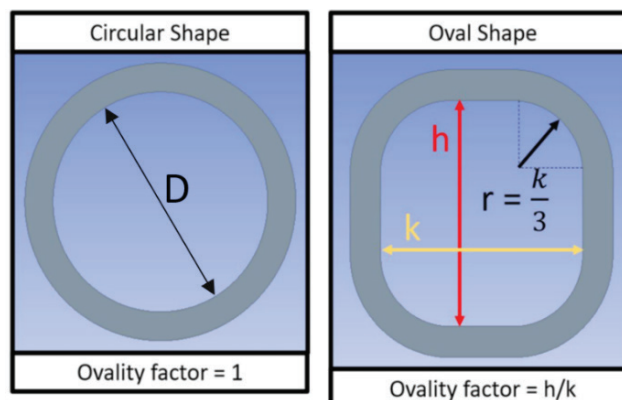


Figure 7: Ovality factor



For each ovality factor, from 1 to 1.8 that are considered the lower and upper limits during the manufacturing process, a FEM simulation has been performed. The other parameters that affect the geometries (D, h, k and r shown on Figure 7) are defined for ensuring the following equation:

$$Perimeter_{circular} = Perimeter_{oval} \tag{2}$$

This aspect in fact is crucial for having a proper comparison between two different shapes, since having the same perimeter means comparing two windings with the same electrical dimensions. This means that the obtained results (stress status and instability) are strictly related to the ovality factor, since it is the only parameter that changes among the different geometries. The obtained results function of the ovality factor are shown on the following figure.

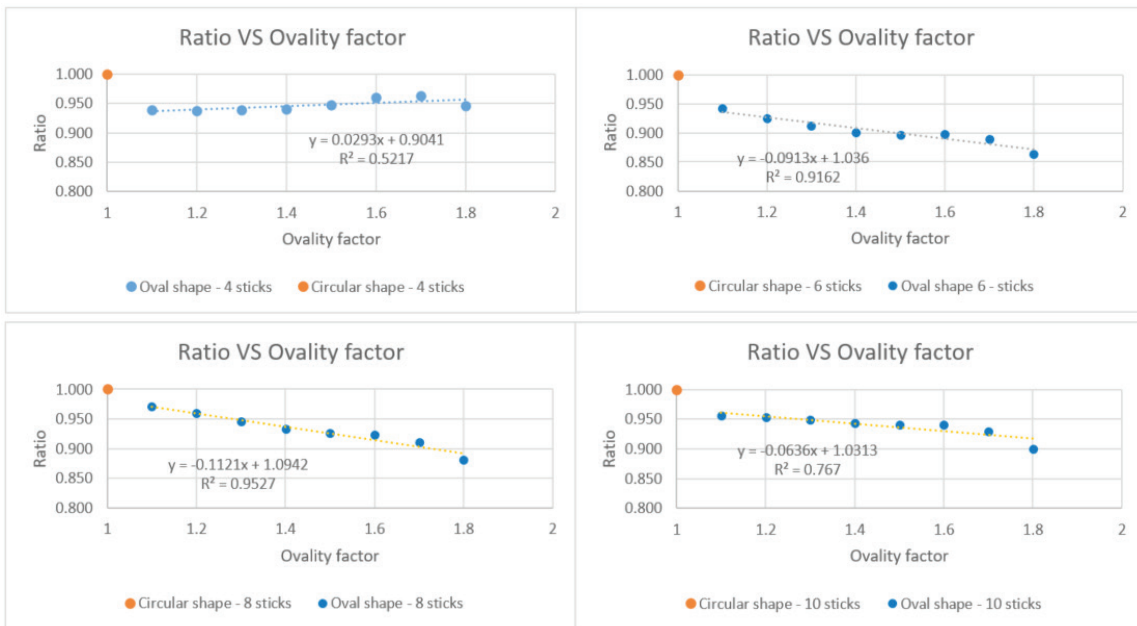


Figure 8: Ratio VS ovality factor for different number of duct sticks (Buckling analysis)



Figure 9: Ratio VS ovality factor for different number of duct sticks (Stress analysis)



The ratio shown on the y-axis of the above figures are defined as follow:

- For the buckling analysis:

$$Ratio_n = \text{Load multiplier ovality } n / \text{Load multiplier circular winding} \quad (3)$$

- For the stress analysis:

$$Ratio_n = \text{Stress peak ovality } n / \text{Stress peak circular winding} \quad (4)$$

As one can see on Figure 8, the ratios obtained for the different ovality factors are lower than 1. This means that the oval windings are more vulnerable to instability compared to circular ones. Furthermore, the ratios are following a linear path function of the ovality. For this reason, tendency lines have been extracted from the parametric studies and introduced on the excel tool as “corrective factor” for adjusting the analytical results, obtained for a circular shape, to oval configurations. Same approach have been followed for understanding how the stress status is influenced by the ovality factor. As one can see on Figure 9, also for the stress analysis it is possible to extract tendency lines for understanding the stress status on oval winding.

### 6.2. Relative motion between foils

The second study that has been performed is related to the possibility of selecting the quality of the adhesion between the conductive foils. This in fact is a fundamental aspect that has to be considered for understanding the capability of a transformer to withstand a short-circuit event. However, the analytical formulations available in literature don't provide the possibility of making this investigation, since they are applicable only to a monolithic section or to a section made by multiple foils perfectly bonded each other. For this reason, a numerical simulation campaign has been performed. Its aim is the definition of how the moment of inertia of the section changes based on the adhesion between the modeled foils. For this reason, the two following conditions have been addressed:

- Bonded: this configuration represents the condition in which the conductive foils inside a section are perfectly bonded each other
- Poor adhesion: this condition represents the case in which the foils can slide one on top of each other and the only prevention to this movement is the friction between them. For simulating this condition, frictional contacts with friction coefficient equal to 0,2 have been adopted.

This investigation was performed using ANSYS mechanical with a series of non-linear buckling simulations changing the nature of the contact between the modeled foils. The obtained results shown the importance of ensuring a good adhesion among the conductive foils during the manufacturing process. For this reason, they were introduced into the tool for considering how the results are influenced by this fundamental aspect.

### 6.3. Containing effect of the outer sections

The analytical formulations available in literature can be adopted only for calculating the stress status generated on a section considered independently. In fact, both the analytical formulations for the obround geometry and Mariotte theory, for the circular shape winding, don't consider cross influence between sections. Considering now how a real winding is manufactured, it is possible to understand that the stress status present into each specific section is influenced not only by the Lorentz forces generated on it. In fact, there is a transmission of loads from the different sections, and this can be explained with reference to the magnetic field shown on the following figure.

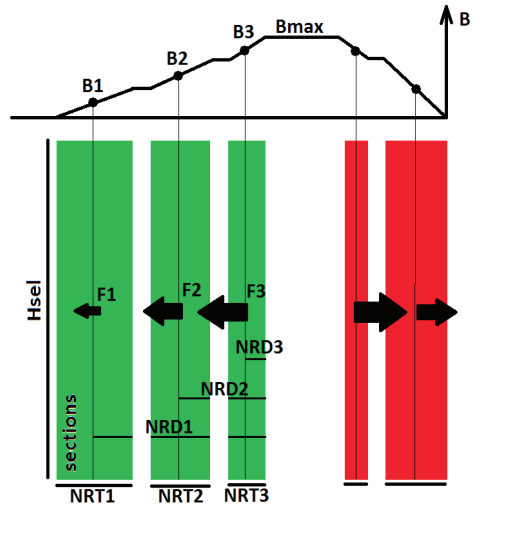


Figure 10: Magnetic field distribution

For this reason, a series of numerical simulations have been performed for understanding how the stress on the sections are influenced by the transmission of the loads from other sections. Tendency lines have been extracted and added to the equations implemented for the HV winding for considering this phenomenon on the calculation.

### 6.4. Neuber's correction

The original tool was implemented for considering only the linear behavior of the adopted material. However, during a short-circuit experimental campaign, it was understood the importance of also considering the plasticity of the material for assessing the capability of a winding to withstand a short-circuit event. In fact, strain gauges were applied on the HV winding and a plastic deformation was measured after the test (please refer to the following figure). However, the magnitude of this deformation was small enough for passing the short-circuit test and, for this reason, the calculation on the residual strain using the Neuber's correction has been implemented into the tool.

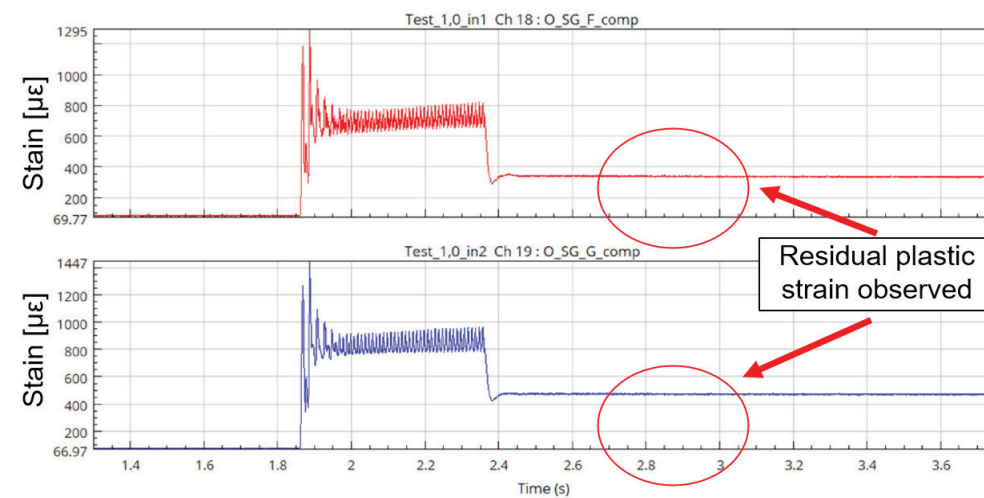


Figure 11: Residual plastic strain measured on the winding

## 7. VALIDATION

A comparison between analytical calculation and experimental results has been performed for validating the SCAP tool. The obtained results are summarized on the following table.





Table 1: Comparison between analytical and experimental results

Design Name	SC Test Result	SCAP 2.1			Comparison SCAP - TEST	
		Yield Safety factor	Plastic strain [%]	Overall SCAP result	LV	HV
1	FAIL	0.13	1.61	FAIL	OK	OK
		Yield	Plastic strain [%]			
2	PASS	0.82	0.01	PASS	OK	OK
		Yield	Plastic strain [%]			
3	PASS	3.59	-	PASS	OK	OK
		Yield	Plastic strain [%]			
4	PASS	0.33	0.41	FAIL	OK	NO
		Yield	Plastic strain [%]			
5	FAIL	0.20	1.10	FAIL	OK	OK
		Yield	Plastic strain [%]			
6	PASS	1.01	-	PASS	OK	OK
		Yield	Plastic strain [%]			
7	PASS	0.69	0.06	PASS	OK	OK
		Yield	Plastic strain [%]			
8	PASS	0.96	0.02	PASS	OK	OK
		Yield	Plastic strain [%]			
9	PASS	0.73	0.04	PASS	OK	OK
		Yield	Plastic strain [%]			
10	PASS	0.48	0.16	PASS	OK	OK
		Yield	Plastic strain [%]			
11	PASS	2.3	-	PASS	OK	OK
		Yield	Plastic strain [%]			
12	PASS	0.96	0.02	PASS	OK	OK
		Yield	Plastic strain [%]			
13	PASS	1.45	-	PASS	OK	OK
		Yield	Plastic strain [%]			
14	PASS	0.72	0.08	PASS	OK	OK
		Yield	Plastic strain [%]			
15	PASS	0.41	0.23	FAIL	OK	NO
		Yield	Plastic strain [%]			
16	PASS	0.39	0.26	FAIL	OK	NO
		Yield	Plastic strain [%]			
17	PASS	0.39	0.26	FAIL	OK	NO
		Yield	Plastic strain [%]			
18	PASS	0.41	0.24	FAIL	OK	NO
		Yield	Plastic strain [%]			
19	PASS	1.17	-	PASS	OK	OK
		Yield	Plastic strain [%]			
20	PASS	0.56	0.11	PASS	OK	OK
		Yield	Plastic strain [%]			
21	PASS	0.65	0.06	PASS	OK	OK
		Yield	Plastic strain [%]			
22	PASS	0.67	0.08	PASS	OK	OK
		Yield	Plastic strain [%]			
23	PASS	1.37	-	PASS	OK	OK
		Yield	Plastic strain [%]			
24	PASS	0.50	0.15	PASS	OK	OK
		Yield	Plastic strain [%]			

As one can see on the above table, the SCAP tool agrees with the experimental results for 19 designs over the 24 tested. For the 5 designs not aligned, the predicted plastic strain is close to the admissible limit of 0.2% and, for these designs, the recommendation is to perform a more accurate and detailed finite element simulation on the real manufactured geometry. In fact, it is worth to remember that the proposed tool is fundamental at bidding stage, but if the obtained results are close to the admissible limit, some further FEM investigations must be performed.

### CONCLUSION

This paper shown a reliable and quick tool developed for the prediction of the capability of transformers windings to withstand the short-circuit forces. In fact, specially at bidding stage when more detailed FEM simulations are not required, having a quick calculation performed with a reliable tool is of fundamental importance. The final tool is based on analytical equations and parametric FEM simulations for enlarging their range of validity. As a conclusion, it has been shown the validation of the tool with a certain amount of short-circuit campaigns performed in the past and the obtained results demonstrate the reliability of this analytical tool for a very complex multi-physics phenomenon.



### BIBLIOGRAPHY

- [1] Calcolo e progetto dei trasformatori industriali, Borsani, Delfino, 1974.
- [2] Sforzi elettrodinamici sugli avvolgimenti di un trasformatore, Giorgio Valdes.
- [3] Lezione: Reattanze degli avvolgimenti - Degli Esposti, G., Università degli studi di pavia, facoltà di ingegneria elettrica
- [4] Lezione: Sforzi elettrodinamici - Degli Esposti, G., Università degli studi di pavia, facoltà di ingegneria elettrica Università di Pavia.
- [5] Mechanical stresses in transformers windings, Billing, 1944
- [6] Waters, M. The measurement and calculation of axial electromagnetic forces in concentric transformer windings, 1953.



# Optical Current Transformers

[tiago.guimaraes@siemens-energy.com](mailto:tiago.guimaraes@siemens-energy.com)**TIAGO SANTOS GUIMARAES***Siemens Energy***THOMAS JUDENDORFER***Trench Germany***Germany**

## SUMMARY

This work intends to present optical current transformers as the new interface paradigm between high voltage systems and protection, control, supervision, and measurement equipment for modern substations. Also, it is intended to address the reason for the late adoption of this technology that has already been mature for years, as well as the actions to resolve such obstacles. Finally, it is intended to postulate that optical current transformers – or even, more generally, low-power instrument transformers – represent, in the context of digital substations, the new paradigm, a one-way technological leap in the electrical sector. Optical current sensors appeared in the 1970s and 1980s. Since then, the scientific community and high-voltage equipment manufacturers have improved these technologies so that they could be applied to replace current transformers with a ferromagnetic core. Currently, the technology is mature enough to allow the complete replacement of ferromagnetic equipment by optical equipment at the interface of high voltage circuits with protection, control, supervision, and measurement equipment. However, it should be noted that the availability of a mature technology was not sufficient for large-scale adoption. Regulatory barriers, absence of specific standards, little economic advantage and even a conservative culture in relation to the adoption of new technologies by agents in the electricity sector were factors that admitted to the delay in adherence.

Manufacturers in partnership with the scientific community and technical committees worked assiduously to resolve these obstacles. But, above all, the communication paradigm based on analogue signals between primary equipment and relays made optical current transformers too modern and disruptive a solution to be adopted.

However, with the recent advent of the digital substation, optical current transformers were finally able to enjoy more compatible adjacent systems. Thus, it is natural to state that the optical current transformer is for the digital substation as well as the ferromagnetic current transformer for the analogic substation.

Therefore, postulating that the digital substation is, without doubt or return, the new paradigm for modern substations, optical current transformers also follow this technological leap.

Optical current transformers had their technological maturation before the associated systems and even the market was mature enough to adopt them. This resulted in the fact that ferromagnetic current transformers persisted as the preferred solution even if a more modern solution was available. However, the advent of the digital substation brought the perfect condition for the adoption of optical current transformers. It is expected that optical current transformers, in the context of the digital substation, represent a technological leap with no return and are the technology of choice for modern substations.

## KEYWORDS

Optical current transformer, digital substation, high voltage



## 1. INTRODUCTION

High voltage Current transformers (CTs) are used to convert the primary current of the system to standardized low and easy measurable values, which will be used for metering, protection, and control of high voltage systems. The technology used today is based on magnetic induction, called inductive current transformers, (ICT). This have been used for decades and we can say that it is a consolidated technology. But this technology has its limitations like saturation of cores, limitation on measurement on a bigger frequency range.

In recent years, the high voltage electrical system has undergone significant changes driven by advancements in technology and the increasing demand for reliable and efficient power transmission. These changes have necessitated the development and implementation of new technologies to accurately measure voltage and current on these systems.

One major change in the high voltage electrical system is the integration of renewable energy sources, such as solar and wind power. As we transition towards a more sustainable future, these renewable sources are being connected to the grid at higher voltage levels, resulting in complex power flow patterns and increased voltage variations. Traditional measurement techniques are often inadequate to capture the dynamic behavior of these systems, making it crucial to employ new technologies that can provide precise measurements. In summary, the high voltage electrical system has undergone significant changes due to the integration of renewable energy sources and the emergence of smart grids. These changes necessitate the adoption of new measurement technologies to accurately monitor voltage and current. The advancements in measurement technologies not only improve the efficiency and reliability of power transmission but also enable better fault detection and maintenance, ultimately ensuring the smooth operation of high voltage electrical systems in a rapidly evolving energy landscape.

## 2. CURRENT TRANSFORMERS

### 2.1. Inductive current transformers construction

Inductive Current Transformers (ICTs) are based on the Faradays law of induction, where we have the primary current passing by the primary winding, normally some thousands of Amperes, that will be transformed to a lower value, normally 1 or 5 Amperes and also guaranteeing the isolation between the high voltage of the primary and the secondary. The ratio between the primary and secondary currents are fixed by the numbers of turns used. The core is made of ferro magnetic material, normally in a toroidal format. This core is then wrapped with the secondary winding. The primary winding is passing thought the core. The core and the secondary winding are located inside a shell made of aluminium. This shell is grounded, and we have many layers of paper that will be also impregnated with the insulation fluid to promote the galvanic insulation between the primary and the secondary. An aluminon tube is connecting the shell and the base of the CT, in addition this is also grounding the shell. The secondary cables are coming through this tube to be connected to the secondary box where we have the secondary terminals. The tube is insulated with paper and have also aluminium foil layers for a better distribution of the electric field. The set composed of the core, secondary winding, shell, insulation paper and aluminium foils is called the active part. Housing and supporting the active part, there is a head, usually made of aluminium, an insulator, made of porcelain or polymeric, and a base, made of aluminium or steel. Attached to the base is a secondary box where we have the secondary terminals.

At the top of the head there is a bellow to compensate for the variation in the volume of the insulating fluid with temperature. On figure 1 we can see the main parts of a Current Transformer.

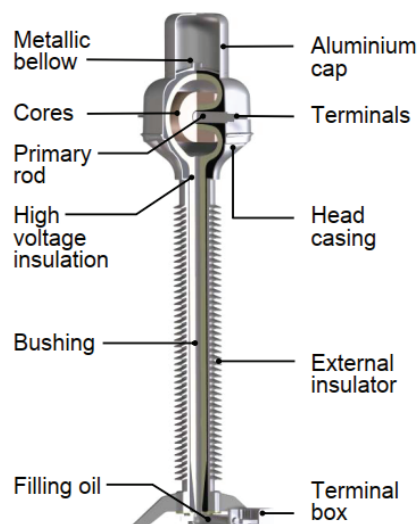


Figure 1: Main parts of a Current transformer

## 2.2. Optical current transformers construction

Optical current transformers (OCT) use of the ability of electric current to interact with light, modulating one of its characteristics, be it intensity, phase, polarization, or spectrum [1]. One can therefore infer the magnitude of a current by comparing a beam of light before and after interfering with it. This work focuses on OCT based on the Faraday effect, although other operating principles are possible.

OCTs are composed of a primary loop surrounded by a passive magneto-optical sensor. An electronic sensing module generates a beam of light that, conducted by optical fibers, travels through the sensor and returns to it. From the difference between the polarization angle of the emitted light and the captured light, it is possible, by Faraday effect, to infer the instantaneous value of the current. Note that the magnitude of the Faraday effect is temperature dependent. Therefore, in addition to the emission and return optical fibers, a third temperature sensor fiber is required to correct the measurement.

The sensing module is coupled to a unit called Merging Unit (MU), which, in turn, provides measured values in a digital output based on the 61850 protocol. It should be noted that all electronic components are installed in a grounded cabinet and located at from the ground in the substation, thus providing electromagnetic immunity.

The magneto-optical sensor is supported by an insulator, usually polymeric, inside which the optical fibers that connect the sensor to the electronic module pass. The remaining space inside the insulator is filled with an inert gas such as clean, dry air.

Fig. 2 illustrates the main building blocks of a OCT.

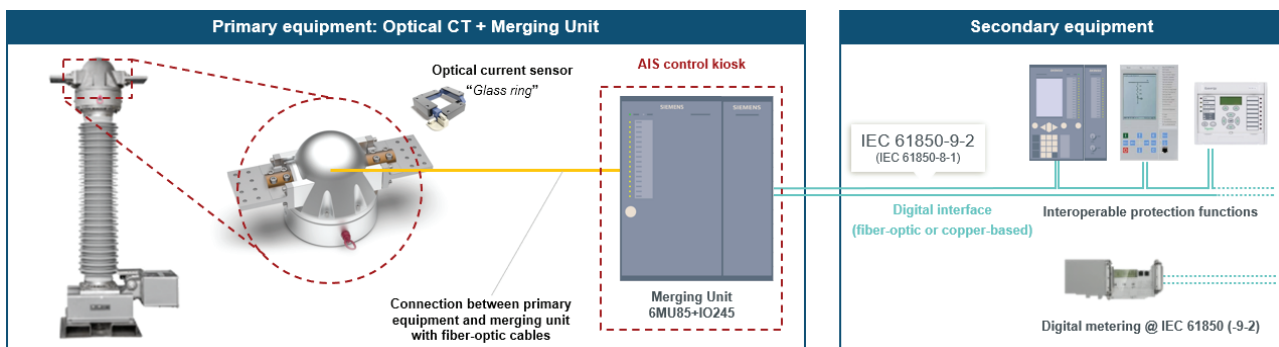


**Figure 2.** Optical CT and the main components

The list below summarizes the main components of an optical CT as well as its main function(s).

- Primary circuit: Conduct primary current.
- Optical sensor: Enable the interference of the primary current with the light signal.
- Insulator: Provide mechanical support and provide electrical isolation by galvanic separation.
- Head: Encapsulate the optical sensor
- Base: Support the entire weight of the equipment, promote vertical stability, and allow attachment to the support structure
- Connection box: House to the terminals for connection with the merging unit.
- Merging Unit (sensing module included): Send and capture the light signal to/from the sensor, calculate the primary current, convert and make available the secondary values in a digital output according to the IEC 61850 protocol.

## 2.3. Comparison of the constructive aspects of an inductive CT with an optical CT

In the inductive current transformers, one might be surprised that the voltage level to which a transformer is energized is irrelevant to the ferromagnetic core. The shell works as a Faraday cage, making the electric potential due to external electric fields at any point on its surface or internal to it to be zero.

On the other hand, attention is drawn to the fact that energized parts of the order of hundreds of kilovolts are physically very close to grounded parts. The primary turns (operating at phase voltage) are separated from the shell (operating at grounded potential) by mere centimetres of layers of paper impregnated with an insulating fluid.



It is, therefore, natural to conclude on the importance and complexity of the equipment's internal insulation. In fact, even though the ferromagnetic core(s) is(are) the component(s) that perform(s) the function for which the equipment is intended, it is noted that the greatest technological challenge – and therefore where the greatest know-how of manufacturers lies – is internal insulation.

Despite having different operating principles, we can try to establish an analogy between the components of an OCT with those of an ICT. The primary circuit, the head, the insulator, the base and the secondary box, although with different constructions, remain with the same functions. The sensor would be equivalent to the ferromagnetic core(s). The optical fibers, to the secondary circuit. The insulating fluid, to the inert gas. The downpipe, the paper, the aluminium sheets, the bellows, the shell are eliminated, as the functions to which these components were intended simply no longer exist. Merging unit is added, a new component with new functions.

It is evident, therefore, that the OCT acquires a much simpler construction than the ICT by eliminating several components, especially those related to the equipment's internal insulation. Furthermore, even components that are maintained or replaced by another of similar function are now much lighter. On the other hand, a new electronic component is added, the merging unit, which brings with it its own complexities.

As a result of its simplified construction, the mass of an OCT is significantly less than that of an ICT of the same voltage class. As an example, a 550 kV ICT insulated with fluid-impregnated paper traditionally used in the electrical system has a mass of approximately 1300 kg, while an equivalent OCT has a mass of approximately 350 kg, excluding the merging unit.

### 2.4. Comparison on the performance of an inductive CT and an optical CT

By eliminating the ferromagnetic core, the main drawbacks of the ICT in relation to its function are solved, most notably: saturation at high currents, loss of accuracy at low currents and the remanent flux after short circuit.

Over the years, several strategies have been developed to overcome these ICT problems: separation of cores intended for different purposes (cores intended for measurement and cores intended for protection, separately), ferromagnetic materials with lower losses (meaning more accuracy for measurement cores), application of air-gaps in protection cores (to limit the remanent flux and enable fast reclosing), etc.

In contrast, the magneto-optical operating principle eliminates ferromagnetic saturation and the need for excitation current, enabling transduction in an extremely wide primary current range. In practice, this means that the same sensor can simultaneously meet the strictest measurement and protection accuracy classes established in IEC 61869-2.

In addition to the best performance for measurement and protection services at nominal frequency, OCTs are simultaneously able to provide readings over a wide frequency spectrum, whereas the reading of an ICT is only meaningful at its nominal frequency. With the increasing number of applications based on power electronics such as, for example, renewable energy and static compensators, the monitoring of harmonic currents becomes more relevant, allowing OCTs to explore new functionality purposes.

## 3. THE TECHNOLOGY TRANSITION

### 3.1. Defining the technological transition.

KALBACH [4] proposes a systematic classification for technological innovations into four categories so that an adequate transition plan can be defined. This proposal classifies innovations according to technological progress and impact on the market. In this proposal, the technological transition from ICT to OCT is classified as a breakthrough, which, by definition, presents great technical progress, with low impact on the market. This is an improved operating principle for the same product. The technical advantage is clearly superior, while the function, application, target audience and business model remain unchanged. In short, it is a substitute product that is considerably superior to the existing one.

### 3.2 Barriers to technological transition

Once the clear technical advantage has been demonstrated, it is time to discuss the difficulties encountered in the transition from inductive technology to electro-optics, as well as alternatives to overcome them. The work [1] presents an extensive discussion on the subject, listing such barriers and grouping them into three categories: (1) commercial barriers, (2) financial barriers and (3) organizational barriers. This work proposes the necessary and other desirable conditions (catalysts) for the breakthrough.





### 3.3. Necessary conditions for technological transition

#### 3.3.1 Technological advantage

Breakthrough necessarily assumes that the new technology is superior to the existing one. As already discussed in the previous sections of this article, in this aspect the OCT deserves great attention, presenting a clear technological advantage over the ICT.

#### 3.3.2 Technological maturity

This requirement is particular to critical systems, which are those whose failure implies immense – or even inestimable losses. As an example, power transmission systems, aircraft, life support medical equipment, among others, can be mentioned. The need for resilience to failures demands the simultaneous use of redundancy and high reliability components. It is natural, therefore, to conclude that these systems only allow the use of components based on sufficiently mature and proven technologies.

#### 3.3.3 Economic viability

The scale adoption of any technology depends on its economic viability. Buyers will only choose a product whose value proposition exceeds its price. It is important to point out that the chosen product will not necessarily be the one with the lowest price, but the one with the most attractive cost/benefit ratio.

In this context, the commercial success of the OCT depends on its cost/benefit ratio being more attractive than that of the product it intends to replace, the ICT. It is natural, at first, to directly compare the cost of acquiring equipment, but this metric does not reveal the complete picture. An alternative, more complete metric is Total Cost of Ownership. Therefore, in the transduction technology decision stage, buyers should consider not only the acquisition cost, but also the operating cost, the disposal cost. Additionally, it will be necessary to deduct the savings due to the optimization of the adjacent material, such as, for example, savings due to the replacement of secondary copper cables with optical fiber, lighter support structure, less robust civil base, etc.

#### 3.3.4 Regulatory aspects

The business environment for electricity transmission concessions is strictly regulated. This brings security, stability, and predictability to the actors; factors that are fundamental for a business that involves critical infrastructure and that has concession cycles in the range of decades. It is natural that in this environment the predictability of a consolidated technology is sometimes preferred to the innovations of a new technology. Therefore, the technological transition in the context of critical systems necessarily depends on new technical proposals being explicitly regulated in norms and procedures.

In the case of the OCT, emphasis is placed on the need for an international technical standard and an explicit provision for this equipment in the Grid Procedures. Many efforts have been made in this regard by technical committees made up of representatives of the various actors in the electricity sector. Currently, OCT are already fully covered by the IEC 61869 family of standards, although revisions of this standard are expected soon. On the other hand, the inclusion of OCT in Grid Procedures remains pending in some cases.

#### 3.3.5 Suitable adjacent systems

Every product exists in a “technological ecosystem” with which it interacts and therefore needs to be compatible. In the case of substantially different new technological concepts, a recursive compatibility problem is created. As an example, we might think that the adoption of electric cars is restricted by the limited availability of charging stations. On the other hand, there is little incentive to install more charging stations because there are not so many electric cars. This problem greater when more complex the necessary adaptations in adjacent systems are needed, consequently, the greater the inertia of the technological transition.

The compatibility problem seems to be overcome in the case of OCT. Standard IEC61869 decided to define as OCT not only the set consisting of the electro-optical sensor, insulator and secondary box, but also to include the merging unit. It is enough, therefore, to select a merging unit that has the capacity to provide an output compatible with the input expected by the IED.

Even if the point-to-point connection between merging unit and IED is possible, the work [1] sustains that the peak of financial optimization – and this work conjectures: also the peak of technical optimization – will be OCT applied in a fully digital substation, with communication via process bus based on protocol IEC61850.



### 3.4 Methods of technological transition

#### 3.4.1 Convincing top management

The adoption of a new technological paradigm exceeds the limits of the technical departments of companies, as it is not enough for the new solution to be excellent from a technical point of view; its impact on the business must be positive. The company's strategy – in the short and long term – is a point not to be neglected. This assessment can only be done outside of each department, as it needs to consider the company as a whole. Evidently, the integration between the teams and the direction of the path to follow is a task of the leadership.

Therefore, the topic of innovation in the electricity sector – not only about OCT and digital substations, but all innovation – should not be restricted to technical forums, but also permeate the management level.

#### 3.4.2 Qualification of human resources

The adoption of a new technology demands technical qualification of human resources in all spheres of the business: manufacturers, utilities, regulators, operators, designers, builders, maintainers, laboratories, educational institutions, among others. Entities involved in research and development are the originators of technology and, therefore, are responsible for the primary dissemination of knowledge. Technology user entities must be open to constructive interaction of knowledge. It should be noted that it is not just a matter of theoretical qualification - which is certainly indispensable - but also support, mainly from manufacturers, in solving practical problems, whether foreseen or untimely.

#### 3.4.3 References and pilot projects

The players in the electricity sector – in particular the utilities – are traditionally conservative entities in relation to new technologies. Note that technological transitions take years. As examples, we can mention the migration of old electromechanical relays to modern LEDs, the migration of lightning arresters with porcelain insulators to polymeric ones, among many other possibilities. This high inertia is not due to a supposed aversion to innovation, but to the concession contracting model. Since the utilities are remunerated based on the availability of the transmission asset, new technologies will only be adopted when their technical maturity, especially in terms of reliability, is solidly demonstrated.

From this fact arises the need for as many more pilot projects as possible. These projects, in general, start operating in redundancy with existing equipment and without interfering with measurement, protection and control systems. Once technological solidity is demonstrated, the new equipment goes from redundant to main.

The work [1] raised 20 applications worldwide, but it is known that currently this number is significantly higher. In the Ibero-American region, the Chinú 245 kV substation in Colombia, owned by the ISA concessionaire, stands out, which has three OCT operating correctly without operational problems since the end of 2017.

## 4. CONCLUSIONS

Optical current transformers had their technological maturation before the associated systems and even the market was mature enough to adopt them. This resulted in the fact that inductive current transformers persisted as the preferred solution even if a more modern solution was available. However, the advent of the digital substation brought the perfect condition for the adoption of optical current transformers. It is expected that optical current transformers, in the context of the digital substation, represent a technological leap with no return and are the technology of choice for modern substations.

## BIBLIOGRAPHY

- [1] J.B. Rosolem et al., "Estudo e Disseminação das Tecnologias de Transformadores de Instrumentos de Baixa Potência (LPIT)", CIGRE Brasil, Grupo de Trabalho GT A3.01
- [2] D.K. Lima, J.C. Santos, "Transformadores para Instrumentos Óticos: Sua Viabilidade no Setor Elétrico Brasileiro", *Revista O Setor Elétrico*, Edição 54, Jul 2010.
- [3] V.C. Oliveira, P.M. Da Silveira, and J.M.C. Filho, "Transformadores de instrumentos óticos como alternativa aos convencionais", in *XXV Seminário Nacional de Produção e Transmissão de Energia Elétrica*, Belo Horizonte, Nov. 2019.
- [4] J. Kalbach, "Clarifying Innovation: Four Zones of Innovation", <https://experiencinginformation.com/2012/06/03/clarifying-innovation-four-zones-of-innovation/>, Jun. 2012.



# Instrument Transformers Using Alternative and Eco-Friendly High Voltage Insulation Systems

[tiago.guimaraes@siemens-energy.com](mailto:tiago.guimaraes@siemens-energy.com)**TIAGO SANTOS GUIMARAES***Siemens Energy***Germany****LORENZO GIOVANELLI, DANIELE BUSCEMI***Trench Italia***Germany**

## SUMMARY

Demand of energy is increasing, and it's expected to be more and more growing due the installation of new users' electrical assets and the electrification completion of all areas not yet served. Besides this increasing demand, the market trend also shows a growing attention to assets optimization and a preference for environmental low-impact solutions and equipment. Customers are looking and giving more and more value to solutions and equipment that have a reduced environment impact during the complete supply chain including Manufacturing, Service, End of life. A failure on an Instrument Transformer (IT) has a big impact in terms of continuity of electrical power supply then one of the main challenges of equipment manufacturers is to develop products that use eco-friendly solutions but keeping at the maximum level the product reliability and performances. Historically two of the main high voltage insulation systems of ITs use Paper/Mineral Oil or SF6 gas. These technologies are well known and reliable. Trench Group is working since some years to develop solutions matching this market trend, without any kind of compromise in terms of product reliability and performances. After deep investigation about different solutions, Trench has developed new products portfolio that use a fully eco-friendly high voltage insulation systems instead of the existing mineral oils and SF6 gas; Trench eco-friendly new products portfolio includes Instrument Transformers Ester/Paper Insulated.

Ester/Paper HV insulation is not a new technology itself because it has been applied to power transformers (PT) since decades, starting from distribution ones and more recently to big power transformers. However, the use of well-known ester is a good base but not enough for the application on ITs design. This because if we compare an IT and a PT there're some important differences in the high voltage insulation design and production steps.

Designers were able to develop ITs using an ester fluid and keeping the product dimensions and performances as mineral oil insulated one. This means that the Customer has the opportunity to install an eco-friendly IT in the same space and with the same performances as the mineral oil insulated one and then they can also replace existing installed fleet with reduced cost impacts for upgrade; furthermore, thanks to an optimised design, the reliability of ester ITs is the same or even better than the equivalent mineral oil insulated ones. Investigation activities have been conducted testing natural and synthetic esters, on CTs and VTs for different voltage levels up to 420kV and specific electrical tests were performed according IEC 61869. On the top of features ensured by an IT mineral oil insulated, the use of ester adds follow main advantages:

- 1 – Using ester there's no risk of any dangerous pollution during the life cycle of the product.
- 2 – In case of failure, the self-extinguishing behavior of ester ensure a rapid fire termination and then increase the safety level of equipment.

## KEYWORDS

High Voltage, Instrument Transformer, Natural-Ester, Synthetic-Ester

## 1. INSTRUMENT TRANSFORMERS ESTER INSULATED (ITS)

Since the beginning of instrument transformers development (IT), paper and mineral oil were used as main high voltage insulation system. During the years their design has been improved and optimized step by step up to now when this kind of insulation is worldwide used with fully satisfaction of users.

Modern ITs are sealed products and then, in standard conditions, no contact between mineral oil and environment is possible. However, considering the transformer has a lifetime of more than 30 years, in very few cases an oil leakage can happen, and this brings to a potential oil development in the environment. Considering the small oil quantity contained in ITs compared to power transformers and their high reliability, paper/mineral oil was and is the most common technology accepted worldwide.

In the last 30 years the technology of power transformers is moving gradually to ester insulation systems (fig.1) together with the growing sensitivity of the users to environment topics and then also the ITs are and will be in the focus of this change. Mineral oil is not a biodegradable fluid, then alternative as ester fluids were investigated to replace the mineral oil applications. General information about synthetic esters can be found already in the paragraph 1 of this paper. In this paragraph we focus on ITs showing the investigation findings and giving some guidelines about the application of this insulation technology.

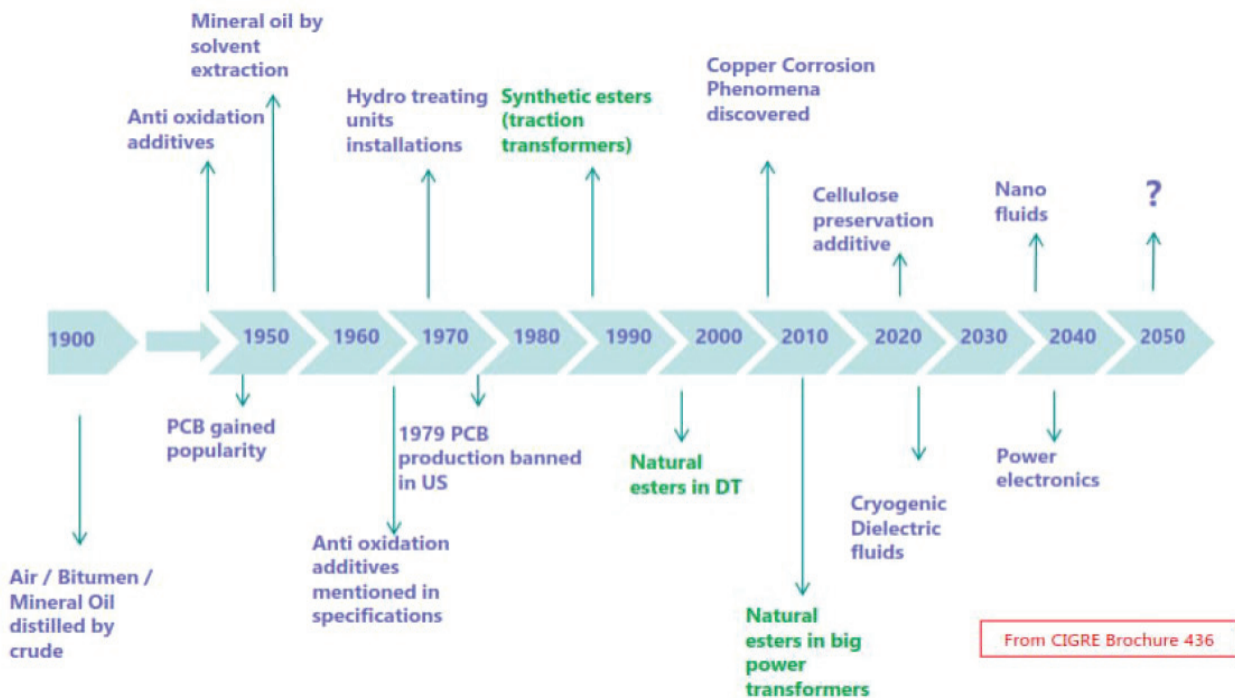


Figure 1: Reference CIGRE Brochure 436

### 1.1. High Voltage Insulation - Design and Production Process

A typical sectional view of high voltage oil insulated IT (current transformer top core design) is shown in figure 2. The high voltage insulation is made by high quality insulating paper and mineral oil impregnated. The bushing part uses a design similar to bushing for power transformers while the top part is made applying paper's layers using semiautomatic special machines. The paper compactness is a key factor to ensure the high dielectric strength keeping the dielectric stresses inside the design limits for the whole service lifetime and in all service conditions. During manufacturing process, ITs are dried applying high vacuum and high temperature and then filled with degassed and filtered mineral oil (ref. IEC 60296). Sealings between the different assemblies are ensured by rubber gaskets and the oil volume variations due the temperature change is compensated by an inox steel bellows.



Figure 2: High Voltage oil Current Transformer installed and sectional view (top cores design)

The high compactness of the insulating paper ensures the best electrical performances but also became a critical point during manufacturing oil filling step because paper impregnation become difficult, and tens of hours are necessary to be completed in proper way. Low-viscosity fluids are used to allow better paper impregnation and, additionally, to reduce the viscosity of mineral oil the transformer is usually filled with a temperature of 50/60°C on vacuum conditions. Ester fluids have naturally a higher viscosity compared to mineral oils (table V) and then the paper impregnation became a more critical item to be considered during manufacturing. Investigation trials and electrical tests have been performed checking the possibility to use the same main insulation design (paper type and thickness, manufacturing process) and to adapt carefully the drying and impregnation process to the different ester fluids.

Synthetic and natural esters were investigated and a solution to apply them has been found optimising the whole production process including also the ester filling temperature (increased up to 80-90°C) and the impregnation time (increased at least two times respect mineral oil one). Partial discharges electrical tests were performed at the end of each process trial and finally it was possible find values as mineral oil insulated ITs confirming that the manufacturing process was completed in proper way.

Table 1: Typical viscosity values

	Mineral Oil	Synthetic ester	Natural Ester
Viscosity at 40°C (cSt)	9.5	29	35

### 1.2. Electrical Tests

Dielectric type tests according IEC61869 Standard have been performed in high voltage laboratories with positive results. Different types of ITs have been tested (current and voltage ITs) as well different voltage levels up to Um 420kV confirming that the ITs ester filled have the same performances as mineral oil insulated ones.

### 1.3. Internal arc fault protection

IEC61869 Standard defines a specific special test referred to the behavior of an IT during an internal arc fault. Tests on ITs using mineral oil have been performed with positive results fulfilling the level "Protection class I and Protection stage 2". Using the same proven design and replacing the mineral oil with ester the behavior of the IT will be the same with the benefit that the fire generated by the arc will be lower and damped quickly due esters' higher flash point and self-extinguishing characteristics, increasing then the product safety level.

### 1.4. Service installation and maintenance

Overall an ester IT needs the same activities usually indicated for mineral oil insulated one. IT is filled with ester, sealed and tested in the manufacturer's factory then no specific or additional activities have to be planned by the user during the installation due the



presence of ester instead of mineral oil. About maintenance ITs are hermetically sealed and usually the only regular maintenance is the external visual check to detect eventual damages or oil leakages and this's valid for mineral as well ester insulated ITs. Oil DGA (Dissolved Gas Analysis) can be performed also on ester ITs but, due the actual limited experience on ester ITs installed fleet, the involvement of IT's manufacturer is recommended to have a specific evaluation of the results and a correct judgement of IT's status.

### 1.5. Additional Items to be considered

To guarantee the best reliability ITs are sealed and, additionally, it's very important ensure that all the materials in contact with the insulation liquid will not release any pollution in the fluid because this will reduce the dielectric strength of the main insulation. Compared with mineral oil ester fluids are surely better about environment aspects but this does not mean that all materials suitable to be used in contact with mineral oil are also suitable to be applied with esters (synthetic or natural). Specific and deep compatibility tests investigation, also using existing experience from power transformer and bushing manufacturers (see item 1.2.2), have been performed to check if the materials tested with mineral oil an be used as well with synthetic and natural esters. For these reasons it's not recommended to fill/refill with ester (synthetic or natural) an IT that was originally designed to be used with mineral oil without the full knowledge about internal design and materials used to prior check their suitability with ester.

### 1.6. Oxidation stability

The modern high voltage ITs are fully sealed type, a metallic bellows compensates the oil volume due the temperatures changes and keep the inner pressure as the ambient one (fig.11). This design prevents any kind of oxidation phenomenon during service conditions also in case of ester insulation.

### 1.7. Very low ambient temperature

Usually the "pour point" of the filling insulation fluid defines the minimum temperature at which the IT can be installed and used. The standard mineral oil for ITs is usually suitable up to -35/-40°C and there're some kinds able to reach lower temperature (up to -50°C or even lower). Synthetic ester can be used in whole set of ambient conditions as mineral oil while natural ester only up to -25°C (table 2).

Table 2: Typical pour point values

	Mineral Oil	Synthetic ester	Natural Ester
Pour Point (°C)	-50	-56	-25

## 2. RISK ASSOCIATE TO MINERAL OIL

Despite HV equipment is manufactured according to the state of the art, there is still a non-negligible fire and explosion (F&E) failure probability. We have information about the failure rate on the figure 3

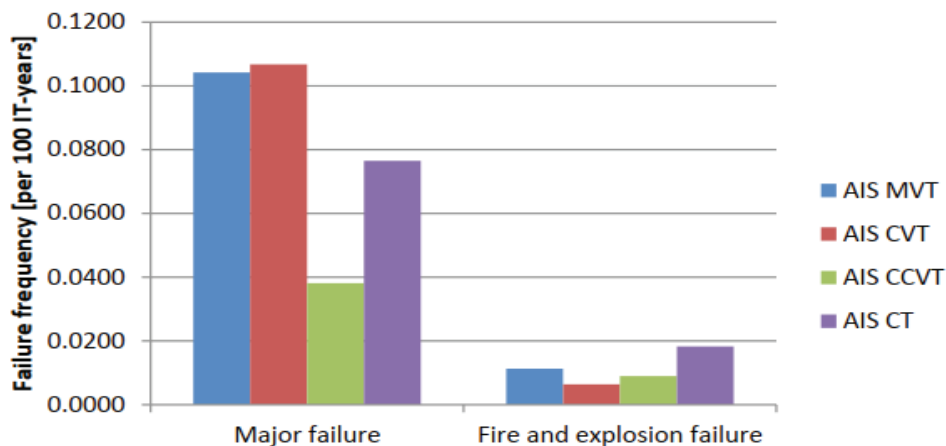


Figure 3: Failure class





Data from Cigrè WG A3.06 «Final Report of the 2004-2007 International Enquiry on Reliability of High voltage Equipment, Part 4: Instrument transformers»

In case of fire and explosion the end user is incurring in:

- a) Penalties;
- b) Investment and revenue losses;
- c) Environmental pollution, due to the nature of insulating liquid;
- d) Impact on communities, in case evacuation is needed
- e) On site workers: injury, hospitalization, death
- f) Image damage

Esters (natural and synthetic), as mineral oil replacement, might mitigate the effects of F&E failures as:

- 1) They are non-toxic and biodegradable, thus limiting the polluting effect in case of leaks and burns
- 2) They have an intrinsic flame self-extinguish behavior;
- 3) Far more energy is needed to trigger the fire point;

On figure 4 we can have information about the biodegradability of different insulation fluids

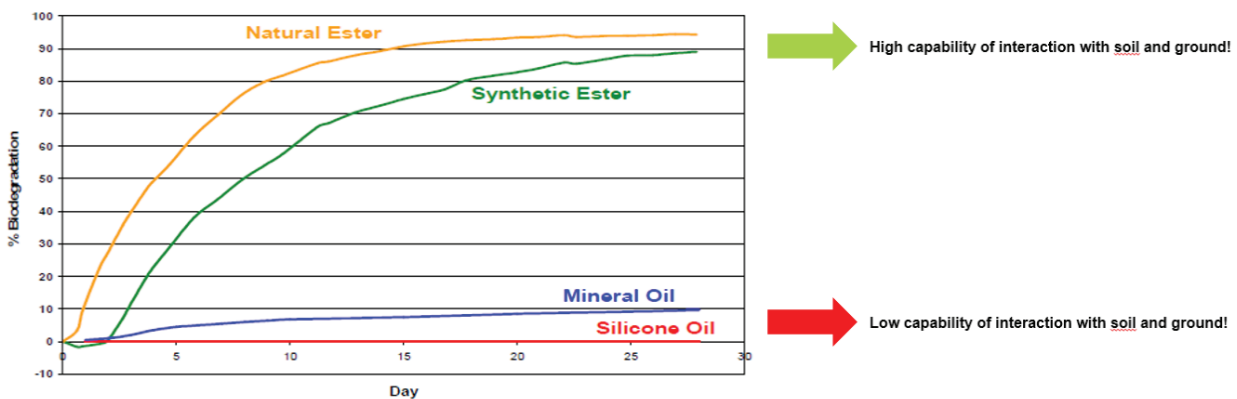


Figure 4: Biodegradability levels (OECD testing)

Esters (natural and synthetic), as mineral oil replacement, might mitigate the effects of F&E failures as:

- 1) They are non-toxic and biodegradable, thus limiting the polluting effect in case of leaks and burns
- 2) They have an intrinsic flame self-extinguish behavior;
- 3) Far more energy is needed to trigger the fire point;

### 3 CONCLUSIONS

The experiences done and the tests performed show that it is possible design and produce a high voltage IT ester filled keeping the same dimensions and performances as mineral oil insulated one. From user's perspective an ester IT ensure same or even better technical performances and it needs the same maintenance activities as mineral oil insulated one with the additional benefit to be filled with a biodegradable fluid.

Ester ITs match users' needs that want to keep the high voltage liquid insulation system but at the same time they're looking for an environment friendly solution to replace mineral oil.



### BIBLIOGRAPHY

- [1] IEEE Power and Energy Society, "C57.154.2012 IEEE Standard for the Design, Testing, and Application of Liquid-Immersed Distribution, Power, and Regulating Transformers Using High-Temperature Insulation Systems and Operating at Elevated Temperatures," IEEE, no. October, 2012.
- [2] I. Fofana, "50 Years in the Development of Insulating Liquids," IEEE Electrical Insulation Magazine, vol. 29, no. 5, pp. 13-25, 2013, doi: 10.1109/MEI.2013.6585853.
- [3] G. Myhre et. al, "Climate Change 2013: The Physical Science Basis, Fifth Assessment Report", Intergovernmental Panel on Climate Change. 30. September 2013.
- [4] Safety data sheet acc. RL 1907/2006/ EG (Reach) Alphagas 1 Luft 203001\_01.
- [5] F. Negri and A. Cavallini, "Comparison of the charge trapping tendency between ester impregnated cellulose sheets and mineral oil ones," 2019 IEEE 20th International Conference on Dielectric Liquids (ICDL), 2019, pp. 1-4, doi: 10.1109/ICDL.2019.8796632.
- [6] F. Negri, "Fundamental study on the application of natural esters on instrument transformers," 2019 IEEE 20th International Conference on Dielectric Liquids (ICDL), 2019, pp.1-4, doi: 10.1109/ICDL.2019.8796527.
- [7] F. Negri, L. Giovanelli, M. Yazdani and K. Kaineder, "Green Substation: Dream or Reality?," 2021 IEEE Electrical Insulation Conference (EIC), 2021, pp. 568-571, doi: 10.1109/EIC49891.2021.9612316.



# Reliability Analysis and Condition Monitoring of Power Transformers from the Romanian Power Grid

[bogdan.leu@transelectrica.ro](mailto:bogdan.leu@transelectrica.ro)

**BOGDAN LEU\*, MIHAI MARCOLȚ**  
*Transelectrica*

**Romania**

## SUMMARY

In this paper, the reliability of the power transformers from the Romanian Electric Transport Network is studied by analyzing the incidents that occurred over a 5-year period, between 2017-2021, where the system's reliability indices are calculated: SAIFI, SAIDI, CAIDI, ASAI.

Also, the analysis of the reliability of the transformers affected by the incidents during this period will be carried out in relation to the use of the technical condition monitoring systems. Reporting on the use of technical condition monitoring systems is carried out to identify the technical contribution brought by them on the power transformers or on the network area where they were installed and what contribution they could have brought if they had been installed on all the analyzed transformers.

And at the same time, the energy not delivered to consumers, the hours of unavailability, the components that failed most or the variation in the reliability of the transformers involved in the incidents during the studied period will be analyzed depending on the region, the year of their appearance or the power level of the transformers.

## KEYWORDS

Power Transformer, Condition Monitoring, Reliability, Asset Management.



Poster Presentation: Reliability Analysis and Condition Monitoring of Power Transformers from the Romanian Power Grid

### 1. ANALYSIS OF POWER TRANSFORMERS INCIDENTS OVER A 5-YEAR PERIOD

In the Romanian transmission grid, there were 201 incidents that occurred on transformer units in the period 2017-2021, distributed according to figure 1 depending on the age, power level or geographical area where the transformer is operated.

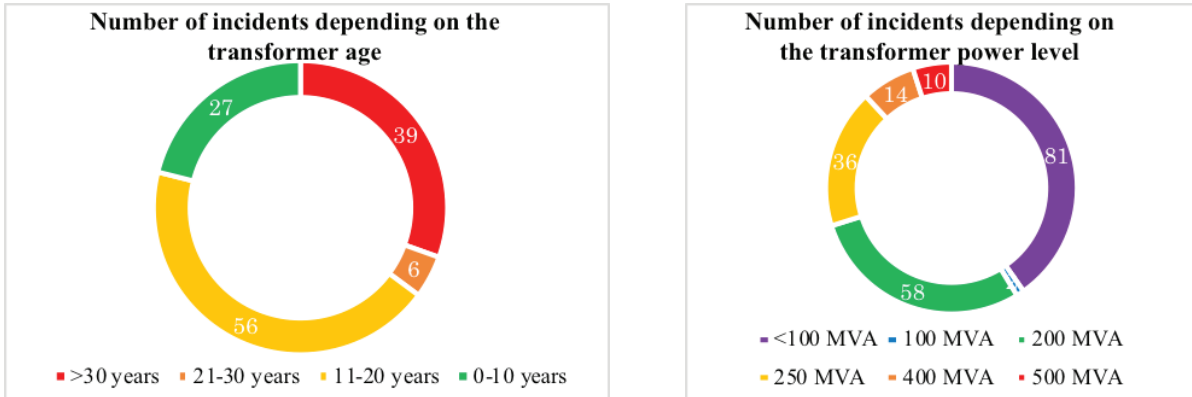


Figure 1: The number of incidents according to the age and power level of the transformer

According to figure 1, it can be seen that the age segments of power transformers where the failures are highest, corresponds to the 11-20 years category, and that of the oldest transformers, more than 30 years after being commissioned is on the second place. An aspect that greatly influences these weights is given by the fact that in most of the substations in the national transmission grid, the power transformers have been replaced in the last 20 years and they are the majority taking into consideration all substations, right for which the incidence of failures in this category of transformers is higher.

Regarding the power level of the transformers, the category most exposed to incidents turns out to be that of low power units, under 100 MVA that serve either the supply of the medium voltage part of the transmission substations, or those of the distribution operators' substations, or they are internal service transformers that feed the transmission substations' own consumption. One reason is primarily the very large number of them compared to the higher power level transformers, but also the degree of loading and the greater number of incidents in the distribution network that lead to their tripping.

The fewest faults occur in the 500 MVA, 400 MVA transformers because on the one hand they are fewer in number in the transmission grid, but at the same time the scheduled interruptions of the power lines they connect to are fewer and more carefully supervised, because they energize important grid nodes and regions that serve many residential consumers, or large industrial consumers. [1] [2]

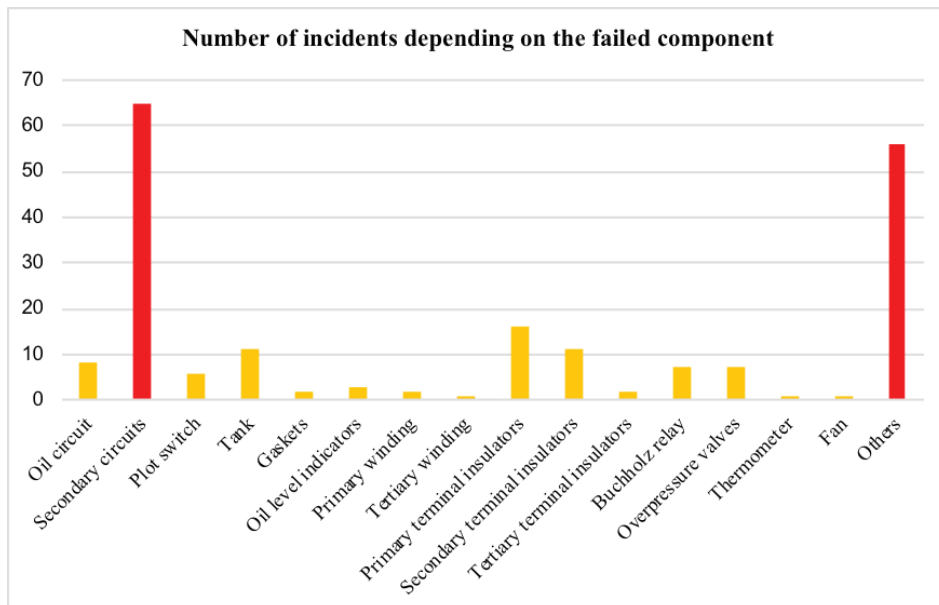


Figure 2: The number of incidents depending on the component that failed



Poster Presentation: Reliability Analysis and Condition Monitoring of Power Transformers from the Romanian Power Grid

Regarding the number of incidents that occurred as a result of the failure of one of the components of the transformers, this type of distribution can be observed in figure 2, where the failures that occurred as a result of relay protection trips are in first place. These trips of the secondary circuits can have various causes, which are most often influenced by current circulations, voltage fluctuations or faults coming from the busbars where the transformer cell is connected or on its connection with a power line circuit. Also, a high percentage in the distribution in figure 2 is represented by other causes, which mean defects that are independent of the operation of the transformer and its components, such as a defect that appeared in the electrical distribution network that propagated further to the substation where the transformer is installed, including triggering it. [1][2]

## 2. ANALYSIS OF THE RELIABILITY OF POWER TRANSFORMERS AFFECTED BY INCIDENTS OVER A PERIOD OF 5 YEARS

To analyze the reliability of the power transformers affected by the incidents in this case study, for the period 2017-2021, the main reliability indices were calculated: SAIFI, SAIDI, CAIDI, ASAI to determine the level of interruptions according to each transformation unit.

Within this chapter we have 119 cases, corresponding to the 119 transformation units that were involved in the 201 incidents during the analyzed period.

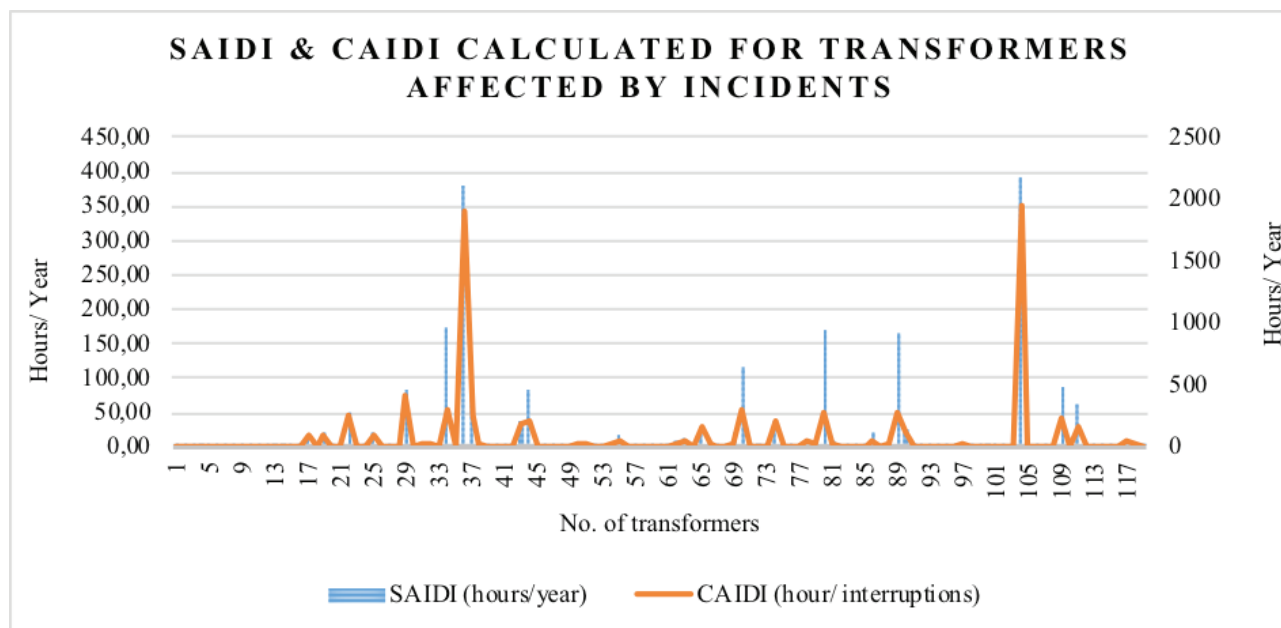


Figure 3: Representation of SAIDI and CAIDI reliability indices for the power transformers affected by incidents

Thus, in figure 3 it can be seen the representation of the SAIDI indices, which show the situation of the interruption hours/year corresponding to each transformer involved in the 201 incidents, respectively the representation of the CAIDI indices, which show the situation of the average interruption hours resulting from the incidents corresponding to each transformer.

What is important to note in the graph above are transformers 36 and 106, where both the SAIDI and CAIDI indices had the highest values, because they correspond to incidents 103 and 130 that produced the highest unavailability during the period analyzed, of 1894 hours, respectively 1958 hours. It follows from this that a single major incident at the level of unavailability for each of the transformers, significantly influenced the values of these reliability indices, which also predominate in this graph.

And on a general level, from figure 3 we can still observe a fairly flat evolution among the transformers involved in incidents, which means that, apart from a few exceptions, the vast majority of incidents resulted in fairly small interruptions during the 5 years, so the reliability was quite high.

If we extract the SAIDI values that exceed 150 hours/year, they are represented by 1 autotransformer of 220/110kV 200MVA, respectively 2 transformers of 110/20kV 40MVA and 16MVA. So again, it is the low power level transformers that have the lowest reliability. [3][4]



Poster Presentation: Reliability Analysis and Condition Monitoring of Power Transformers from the Romanian Power Grid

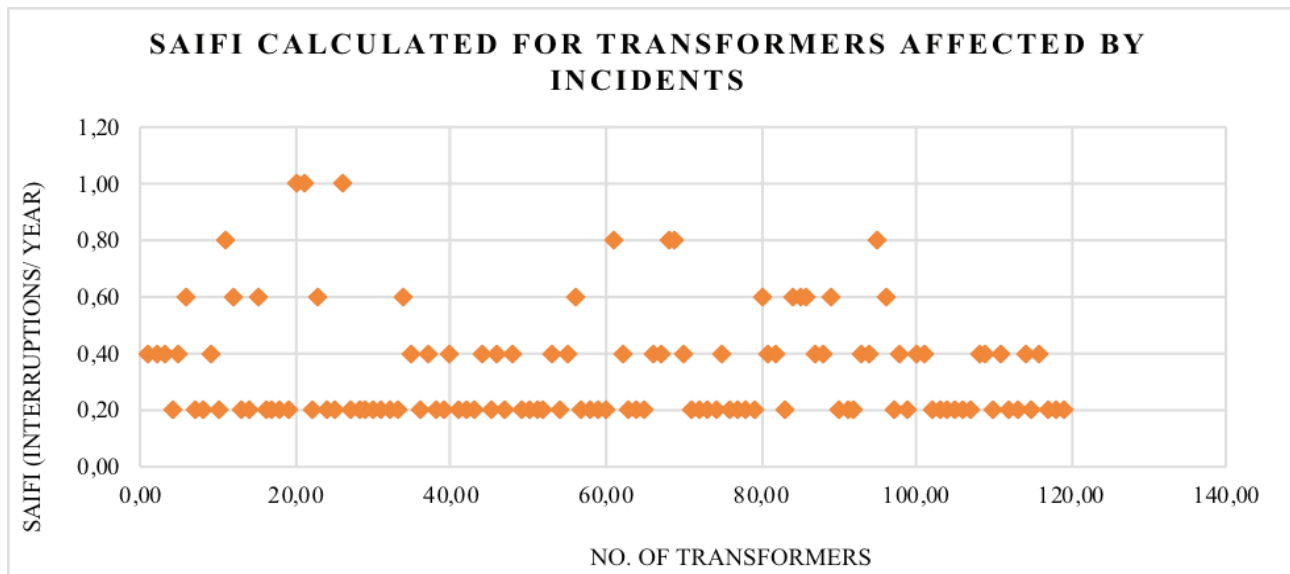


Figure 4: Representation of SAIFI reliability indices for the power transformers affected by incidents

Regarding the representation of the SAIFI index that shows the distribution of the number of outages per year for each of the 119 transformation units, it can be seen in figure 4 how the values are between 0.2 and 1, which means there are between 1 and 5 outages in period 2017-2021 for each unit. The vast majority of cases are in the area with values of 0.2 and 0.4, which indicates a good global level of reliability from the perspective of the SAIFI index. And in the upper area with values of 1 and 0.8, a very poor level of reliability, there are only 8 transformers, 3 of which are under 100MVA, 2 of 200MVA, 1 of 250MVA and 2 of 500MVA. Among these, the ones that attract particular attention are the 500MVA ones, which transit important power flows at the power grid level and on which a more thorough diagnosis is required to identify the elements that led to these incidents for the emergency of future potentials unavailability limitation. [3][4]

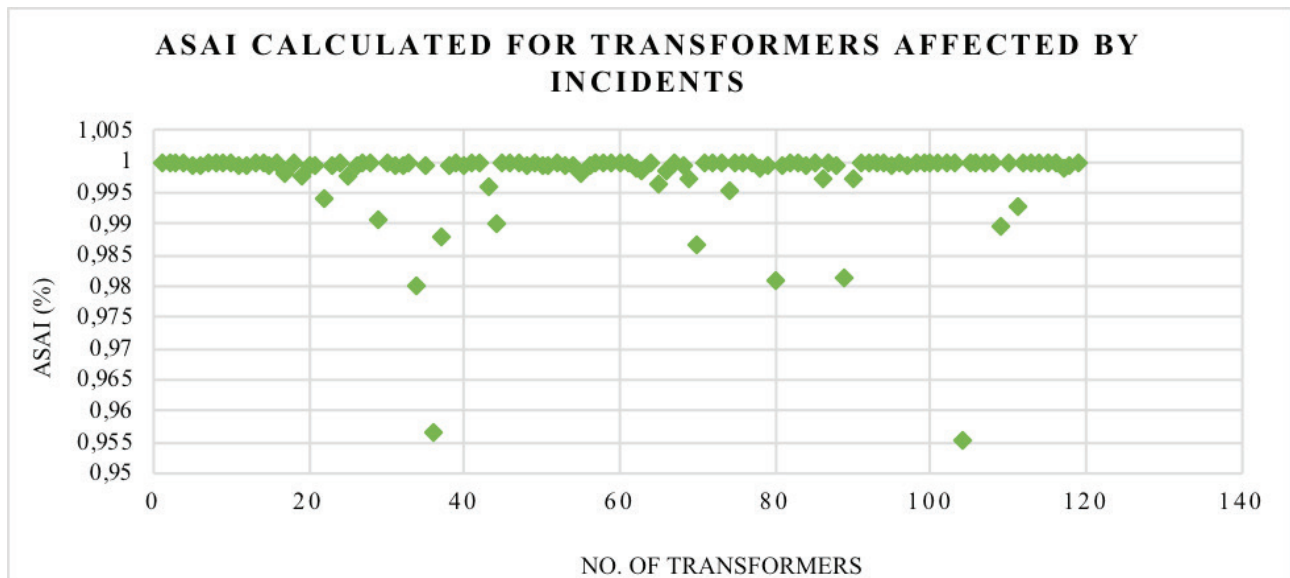


Figure 5: Representation of ASAI reliability indices for the power transformers affected by incidents

Figure 5 shows the distribution of the ASAI index, which indicates the average operating availability of the transformers involved in incidents at power grid level during this period. Most cases fall within very good reliability margins with values above 99% and 98% respectively. Among them, there are only 2 cases that are below the 98% margin, namely the transformers involved in incidents 103 and 130 described previously, where the long unavailability of 1895 and 1958 total outage hours impacts the very low ASAI index values of 95.7% and respectively 95.5%. [3][4]





Poster Presentation: Reliability Analysis and Condition Monitoring of Power Transformers from the Romanian Power Grid

### 3. ANALYSIS OF THE INFLUENCE OF CONDITION MONITORING SYSTEMS ON THE RELIABILITY OF THE POWER TRANSFORMERS AFFECTED BY INCIDENTS OVER A PERIOD OF 5 YEARS

Next, in order to determine the influence that the technical condition monitoring systems had or could have had in the equation of this case study, for the transformers in the 201 incidents that took place in the period 2017-2021, the statistical graphs below were made.

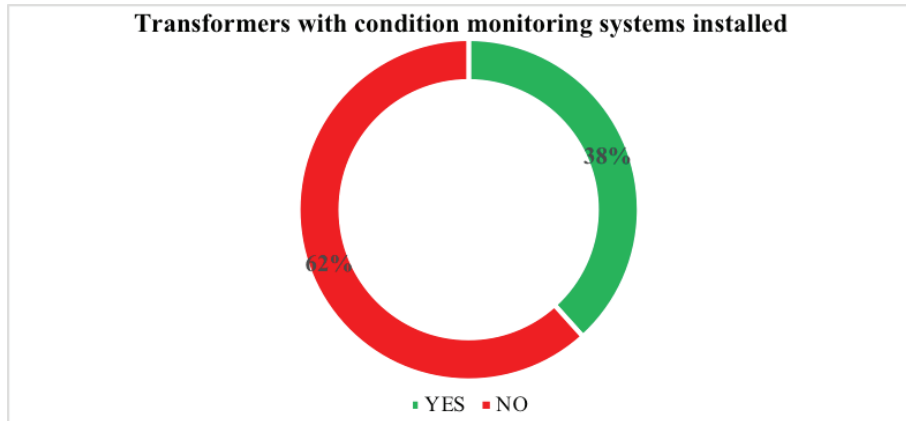


Figure 6: Percentage of transformers that had condition monitoring systems installed at the time of the incident

As can be seen in figure 6, a percentage of 38% of the transformation units involved in the 201 incidents in this case study had condition monitoring systems installed, while 62% of them did not. And further, both segments of transformers will be addressed in order to identify the contribution they could bring in limiting the number of incidents.

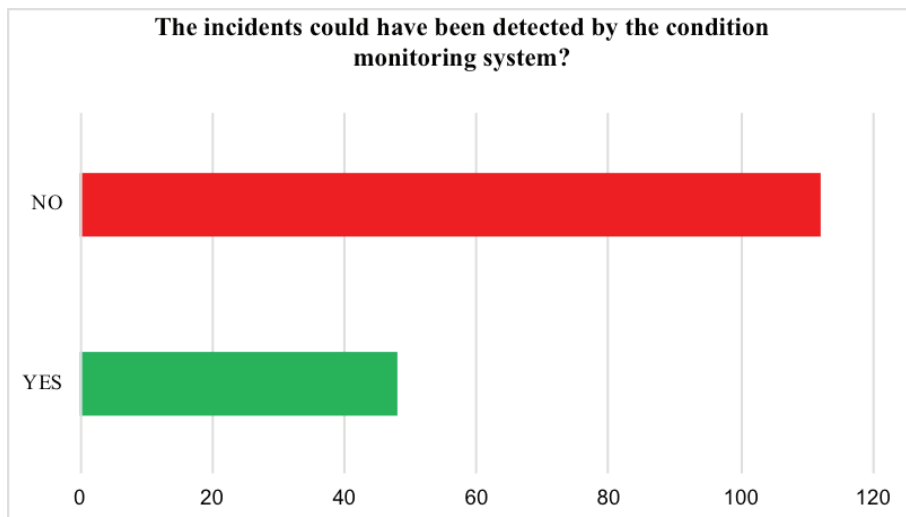


Figure 7: Proportion of incidents occurring at transformer components that can normally be monitored using condition monitoring systems

In order to better understand whether the monitoring systems could have led to the avoidance of the incidents on the transformers on which they are installed, the graph in figure 7 was made, where the incidents were divided into two categories as follows:

- Incidents detectable by the condition monitoring systems: that is, the incidents where the affected component that produced the unavailability of the entire transformer could be monitored through the sensors of the condition monitoring system. For example, in the case of a defect in the insulators of the primary terminals, by performing preventive maintenance following the analysis of the results of the electrical and thermal parameters measured by the system, there was a good chance that the incident could be avoided;

Poster Presentation: Reliability Analysis and Condition Monitoring of Power Transformers from the Romanian Power Grid

- Incidents undetectable by monitoring systems: that is, incidents that occurred as a result of causes independent of the systems' monitoring capabilities. For example, an incident in the distribution network that also led to the tripping of the transformer. [2]

**Could the incidents have been avoided if condition monitoring systems were installed?**

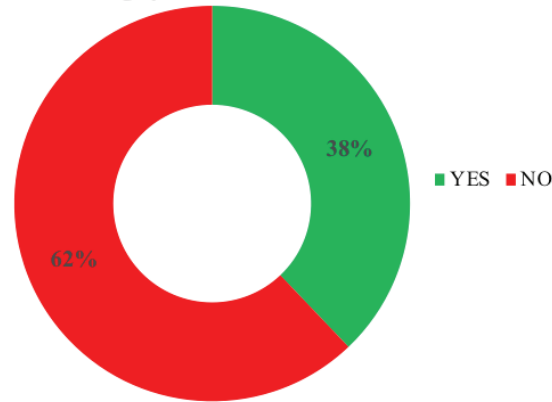


*Figure 8: The percentage of incidents that could theoretically have been avoided if condition monitoring systems had been installed*

Figure 8 has the role of representing the incidents that theoretically could have been avoided out of the total of 201 if the transformers that do not have monitoring systems installed, would have these systems so the technical condition parameters could be monitored and preventive maintenance carried out in order to avoiding failure of different components. And from the total number of incidents, a percentage of 38% of incidents resulted from the failure of some components that can usually be monitored with the help of the condition monitoring systems. And in the case of the 38% of transformers involved in these incidents, on a theoretical level, if the components that failed were monitored, the incidents could be avoided by correlating with preventive and predictive maintenance activities. An example of such an incident that could be avoided by using the condition monitoring systems is an internal fault with arcing on the transformer windings, which by monitoring oil dissolved gas levels and internal temperatures could be seen as a fault developing in time. [2]

## CONCLUSIONS

In conclusion, in this work it was possible to observe the state of the power transformers within the Romanian transmission grid, analyzing the incidents that took place at their level, from two different perspectives:

- From the reliability point of view of. It could be seen how they had very good reliability, with a few exceptions, here including the 500MVA power transformers, on which a more thorough diagnosis is required regarding the cause of their disconnection. However, if we look at the incidents from a quantitative point of view, it has been proven that the transformers with high power levels (over 250MVA) have the lowest number of incidents, while the low power level transformers (under 100MVA) are the most exposed to the occurrence of incidents;
- From the point of view of their behavior in the presence of technical condition monitoring systems. It could be observed that in most of the cases where incidents occur on the transformation units, they are independent of the monitoring of the operating parameters and a majority percentage of 62% indicates that they could not have been avoided. Instead, what is important is that almost half of these incidents could be detected by monitoring systems, and their installation brings benefits in terms of predictive maintenance, and it is necessary to install condition monitoring systems on all power transformers at transmission grid level.

## BIBLIOGRAPHY

- [1] Working Group SC A2.37, "Transformer Reliability Survey", Technical Brochure, CIGRE, 2015.
- [2] CNTEE Transelectrica SA, 2023 (<https://www.transelectrica.ro/>).
- [3] V. Lackovic, "Basic Reliability Analysis of Electrical Power Systems - Course No: E03-020," Continuing Education and Development, Inc., New Jersey, USA.
- [4] N. A. S. Dr. J. Abdul Jaleel, "Evaluation of Reliability Indices of a Power System Based on Reactive Power Injection," International Journal of Engineering Research and Technology, Vols. ISSN 0974-3154 Volume 6, 2013.



# Reliability of Transformers

[shkola50@gmail.com](mailto:shkola50@gmail.com)

**ANATOLY SHKOLNIK**

*Engineering Consulting & Supervision*

**Israel**

## SUMMARY

The article discusses the reliability of transformers, types of damage and their causes. Despite many years of experience in the design and manufacture of transformers, omissions can lead to serious damage during operation. A transformer is a multi-component device and its reliability depends on the reliability of its constituent parts and materials. The most important parts of a transformer are the windings, the core, the switching device and the bushings. The most important materials are solid insulation elements (usually cellulose materials) and insulating oil. Initially, it is assumed that the transformer as a whole, all its parts and materials comply with the recommendations of the standards and factory instructions in terms of design, manufacture, testing and operation. However, the damage of transformers is relatively high. In this case, damage to windings (34%), switching devices (31%) and HV bushings (14%) prevails [1].

## KEYWORDS

Transformer – Reliability – Damages



## 1. WINDINGS

### 1.1. Design

Modern methods of calculation and design of windings practically exclude errors. In addition, if there are errors, as a rule, they are detected during acceptance tests at the factory and corrected.

Resistance to external short-circuit currents is confirmed either by type tests or by a calculation simulating various types of short circuits in the network. But at the same time there are no restrictions on the permissible number of short circuits that the transformer must withstand. Windings have a certain resource of resistance to electromechanical influences. In addition, there is also a maximum allowable short circuit temperature, and if there are frequent short circuits, this can lead to damage. Overload resistance is determined by the class of insulation used in the windings.

If do not observe the permissible thermal conditions, use non-calibrated temperature meters or allow malfunctions in the operation of the cooling system, this will lead to degradation of the insulation and subsequent damage to the winding.

The design of the transformer assumes its tightness and protection from moisture and air. However, leakage can lead to the penetration of moisture into the transformer and, if water gets on the winding, to a short circuit between the turns of the winding, between the windings, discharges and breakdowns of the barrier insulation.

The combined effect of elevated temperature, oxygen and water accelerates the degradation of solid insulation and oil. It is important to decide when assessing the reliability with taps: connections between phase windings; between windings and bushings, between windings and tap changer. The poor connections of taps/leads may lead to local overheating and, as a result, to damage of the oil, insulation and conductor parts. The short circuits between the taps/leads may lead to deformation/displacement of the windings.

### 1.2. Technology

The manufacturing technology has also been tested for a long time, but sometimes deviations from the instructions occur during the production process. A complete check on the quality of workmanship is not always feasible and this can lead to "self-activity" which can lead to damage. The worst case scenario is when this violation in production was not detected during testing, but manifested itself during acceptance tests on site or during operation. An important point is the correct storage of insulating materials and especially pressed laminates. Highly moistened materials do not have time to dry during the standard heat treatment of the active part.

Standard methods and schemes for measuring the insulation characteristics of an assembled transformer are not always able to detect wetted insulating parts. The absence of the necessary length of wire during the winding need to the creation of an additional connection that is not provided by the design. This leads to a decrease in the resistance of the winding to short-circuit currents.

The absence of design details during the assembly of the active part leads to their replacement with improvised parts and materials. This leads to a decrease in the insulating properties and the possible formation of partial discharges and breakdown in them.

### 1.3. External factors of influence

In the process of transportation, installation and operation, mistakes are also made that lead to damage to the transformer. There are frequent cases of violation of the rules for the transportation of transformers, leading to their damage. The installation of a device that fixes accelerations during transportation suggests possible damage. There are many external factors that need to be taken into account and measures taken to prevent negative consequences. When transporting a transformer, a number of conditions must be taken into account: - completeness of the transformer, including filling with oil or dry gas; - means of transportation, unloading and loading; - delivery route and road conditions, taking into account weather and soil conditions, permissible speeds and height restrictions, etc. Restoring a transformer after a failure does not guarantee that the original reliability will be achieved.

## 2. BUSHINGS

Bushings are part of the transformer components and are highly reliable. If we do not consider the old designs of bushings, of which there are few left in operation, then the bushings can be divided into two most common type: OIP and RIP. Both of these types are made in two versions: through passage (draw lead) and with bottom connection. Because bushings are structurally autonomous, then the negative processes (PD) occurring in them are not reflected in the oil indicators in the transformer tank.



To assess their condition, it is necessary to measure their insulation parameters on a disconnected transformer or monitoring control during operation. The most dangerous are bushing explosions with severe consequences for both the transformer and equipment and personnel in the damaged area. In terms of the development of a fire and the creation of the greatest damage, OIP bushings are the most dangerous. The oil-impregnated insulation of the bushing, after the destruction of the outer insulator, supports combustion, unlike bushings with RIP.

Draw lead bushings reduce the reliability of the transformer compared to bottom connected bushings, because violation hermetic of the tap in the head of the bushing leads to the penetration of water to inside of the transformer.

It is important that during the manufacturing process a reliable connection of the measuring tap to the internal shield electrode is made. A bad contact connection can lead to partial discharges and breakdown in insulation.

### 3. TAP CHANGER

TC devices are part of the transformer and are highly reliable. Structurally, TC are divided into two types: NLTC and OLTC. The NLTC is located in the transformer tank and is designed to switch in several positions when the transformer is off. In station transformers, switching is extremely rare and this can lead to local overheating of the contacts. In addition, corrosive oil can corrode these joints. The on-load tap-changer consists of two parts: selector switch and diverter switch. Selective contacts are less problematic, while contactor contacts are subject to sparking and wear, which requires periodic preventive measurements and work, including their replacement and oil changes. Vacuum interrupter significantly increase the reliability of the diverter switch.

### 4. HISTORY OF DAMAGE IN TRANSFORMERS.

#### 4.1. Design errors

Story #1. Structural design errors. Transformer 20 MVA 161/4.1/1.8 kV YNyd. A two-phase earth fault in the 161 kV line resulted in a high current in the tertiary winding due to the low impedance between the 161 kV winding and the tertiary winding. The connecting conductors between the LV windings and the neutral, between the phases of the tertiary winding are made of copper rods without insulation. As a result of the occurrence of strong electro-mechanical forces, there was a displacement and contact between the conductors of the tertiary winding (short circuit). A change in the direction of the current in the contiguous conductors led to an instantaneous repulsion of these conductors and the short circuit was eliminated. After the removal of the active part from the tank, deformation of the conductor rods and arc traces from a short circuit were found on the conductor rods of the tertiary winding (Fig. 1a).

Story #2. Transformer 30 MVA 138 /35 kV Dyn (Fig.1b) was taken out of service due to the formation of combustible gases in the oil. After removing the active part from the tank, a burnt lower threaded contact was found between the bushing conductor rod and the intermediate shoe with internal thread. Taps of the HB winding are connected to this shoe. Threaded connections are used to press the contact surfaces of conductors, and the use of a threaded surface for current conduction is undesirable, since they do not provide reliable contact in the thermodynamic mode.



Figure 1a



Figure 1b





## 4.2. Technological errors in manufacturing.

Story #3. The transformer 20 MVA 161/36 kV Dyn (Fig. 2a) of the mobile substation was repeatedly switched on for a relatively short time on the 36 kV line with a single-phase earth fault in order to eliminate it. As a result of the occurrence of strong electro-mechanical forces on the turns of the LV winding, a wire break occurred, which was accompanied by an arc. An electric arc burned between the turns of the insulation, which led to a short circuit between the turns. The reason for the breakage of the conductor in the winding is due to the fact that during the manufacture of the winding, a shortage of wire was detected on the drum and an additional wire was connected. This connection did not provide the necessary resistance to external short circuits. The method used to eliminate the short circuit on the line is a bad option.

Story #4. Autotransformer 167 MVA 420/161/36 (Fig.2b) was taken out of service as a result of an internal short circuit. After removing the active part, a breakdown was detected between two taps connecting the control winding to the switching device. The breakdown occurred between two connecting compression sleeves, which connect a bundle of parallel wires from the winding to a stranded flexible wire. Due to overheating of the contact connections and their contact, the paper insulation was degraded and its breakdown occurred. This led to a short circuit in two stages of the control winding.

Story #4. The 126 MVA 400/11.5 kV transformer (Fig. 2c) was taken out of service due to the formation of combustible gases in the oil. After opening the windows in the area where the taps of the HV winding were connected to the conductor board of the HV bushing, a poor contact connection of the tap tip was found. Due to significant overheating in this zone, oil degradation and the formation of gases occurred.

Story #5. Transformer 45 MVA 161/36 kV (Fig. 2d) was taken out of service due to the formation of combustible gases in the oil. After removing the active part, a bad contact was found on the tank of the diverter switch.

Story #6. The 20 MVA 161/36 kV Dyn transformer (Fig. 2e) was taken out of service due to the formation of combustible gases in the oil. After removing the active part, the core ground wire without insulation was found, which touched the core sheets and this led to the formation of discharges.

Story #7. Transformer 30 MVA 161/22 kV (Fig.2f) was taken out of service due to the formation of combustible gases in the oil. After removing the active part, a break was found between the ground wire of the beam and its tip.

Story #8. Autotransformers 167 MVA 420/161/36 (Fig.2g) was taken out of service due to the formation of combustible gases in the oil. After removing the active part, a loose bolt was found between the beam and the shoe for attaching the core.



Figure 2a



Figure 2b



Figure 2c



Figure 2d



Figure 2e



Figure 2f

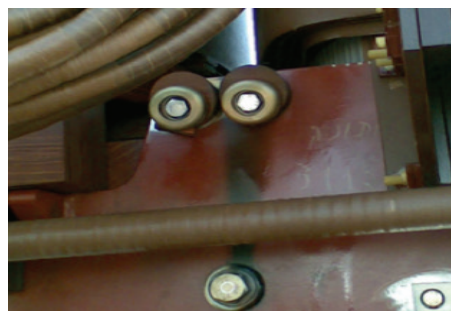


Figure 2g





### 4.3. Errors when mounting / dismantling the transformer.

Story #9. Violation of tightness in the upper part of the 161 kV bushings. Transformers 45 MVA 161/36 kV Dyn (Fig. 3a), 45 MVA 161/22 kV YNd (Fig. 3 b), 167 MVA 420/161/30 single-phase autotransformer (Fig. 3c) were decommissioned as a result of internal short circuit in the HV winding. After removing the active part from the tank in the bushing through passage, a leak was found in the upper part of his head. Rain water or condensate water penetrates past or through the rubber seal as drops into the transformer tank. Drops fall on the winding and flow down between the turns, which leads to a short circuit between them or to a breakdown between the winding and grounded metal parts.

Story #10. The ingress of foreign bodies in the process of assembly / disassembly work on the active part leads to short circuits. In the transformer 45 161/22 (Fig. 3d), the wire hitting the winding outlet led to a short circuit to the tank.

Story #11. In the transformer 75 161/22 (Fig. 3e), the conductor entering the taps of the LV winding led to a short circuit between them and, as a result, to a complete short circuit of one phase coil. The combustion products of the insulation (soot) spread and settled on the insulating barriers of the windings.



Figure 3a



Figure 3b



Figure 3c



Figure 3d

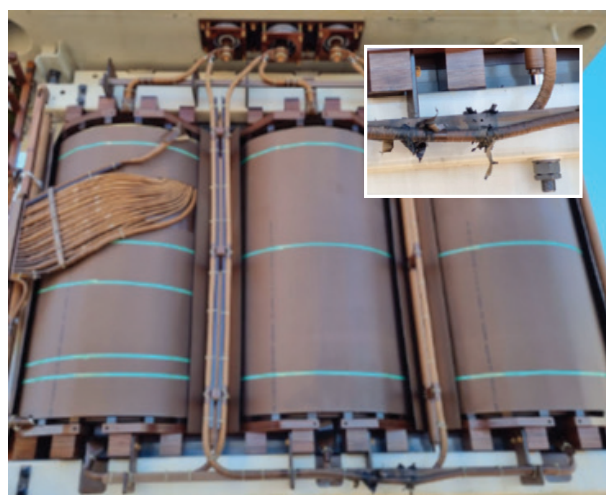


Figure 3e

### 4.4. Problems with switching devices.

Damage to voters is extremely rare. In contactors, as a rule, contact wear is detected. If timely maintenance / replacement of contacts and oil changes are carried out, then serious damage does not occur.

### 4.5. Bushing problems

Story # 12. Transformer 45 MVA 161/36 kV Dyn (Fig. 4 a) are decommissioned as a result of explosions of 170 kV bushings of the RIP type. The suspected cause of the breakdown is caused by partial discharges between the upper inner contact of the short tube and the first shield electrode in the insulating core. The bearing inner tube is not metal, but made of insulating material (fiber glass).



Story # 13. Transformers 50 MVA 161 / 13.8x2 kV (Fig.4 b) were decommissioned as a result of explosions of 170 kV bushings of the OIP type. The supposed cause of the breakdown is caused by partial discharges between the internal shielding electrodes.



Figure 4

## 5. CONCLUSION

The presented transformer damage histories testify to extremely small cases of winding damage caused by design and technological errors of transformer manufacturers. In many cases, winding failures are related to external problems, which should be given more attention, since there are no insignificant details in the design of the transformer. Each opening of the transformer due to the identified “minor” problems can lead to a decrease in reliability and to a disruption in the supply of electricity. Switching devices in vacuum interrupters significantly increase their reliability and reduce their maintenance costs.

To ensure the reliability of bushings, regular checks (tg/C) are required, and after 10 years of operation, it is desirable to use monitoring of tg/C and PD.

## BIBLIOGRAPHY

- [1] CIGRE brochure 642, Transformer Reliability Survey, CIGRE WG A2.37, 2015.
- [2] CIGRE brochure 735, Transformer Post-Mortem Analysis, CIGRE WG A2.45, 2018.



# Analysing Electromagnetic and Thermal Effects of Using Aluminium Shield and Magnetic Shunt Combinations at High-Voltage Level Autotransformers

[mert.kocanali@besttransformer.com](mailto:mert.kocanali@besttransformer.com)

NECMETTİN MERT KOÇANALI, İREM HAZAR, RAMAZAN ALTAY, MAHMUT AKSOY, EMRE KERVAN, OZAN ALİ MUTLU  
*Balkesir Elektromekanik Sanayi Tesisleri A.Ş.*

Türkiye

## SUMMARY

Due to increasing need of energy, capacity of grids is increasing simultaneously. The need for high-voltage autotransformers which are particularly used for connecting grids at different voltages increased as well. Facing with high stray losses and high hot-spot temperatures is very common at this high-voltage levels. We performed electromagnetic and thermal coupled analyses by using a FEM software, ANSYS.

In this study, our aim is to demonstrate effect of various shield&shunt applications at high-voltage level autotransformers. We modelled and simulated different combinations of aluminium shield and magnetic shunt applications. These models included tank, steel parts, core, and windings. Thanks to the results of these simulations, obtained hot-spots could be evaluated if they were above the flash point of transformer oil or maximum temperature rating class of transformer insulation paper. We determined and applied the best shield&shunt combination on a real transformer which has given the least stray losses and hot-spot temperatures observed on steel parts and tank. The results of FEM simulations were validated by thermal camera images and temperature sensor measurements.

## KEYWORDS

Emag-thermal analysis, stray losses, tank shielding





Poster Presentation: Analysing Electromagnetic and Thermal Effects of Using Aluminium Shield and Magnetic Shunt Combinations at High-Voltage Level Autotransformers

### 1. INTRODUCTION

Power transformer is one of the most important and expensive member of energy transmission and energy conversion business in a grid. Thus, it must be reliable and safe. Power transformer rated power and accordingly its size is getting larger with the increasing power transmission capacity. This increasing power levels leads to possible overheating problems due to high losses [1].

In general, a transformer is a highly efficient device with an efficiency of 90% and more [2]. Therefore, there is not enough space to increase efficiency. However, considering the number of transformers installed worldwide, a small efficiency increase can bring a huge power-economic benefit. Therefore, research is needed to reduce losses in transformers [3,4].

Losses of transformers can be divided into two types: no-load and on-load losses [5,6]. No-load loss caused by core. On the other hand, on-load losses caused by omic, eddy and stray losses. For high voltage autotransformers, stray loss can be too high due to high leakage flux. The higher rated power the higher stray loss as well. These stray losses may result as temperature rise on magnetic parts of transformer like tank wall, clamps, flitch plates etc. Hot spots may be observed as over the limit. These limit values are usually determined according to the insulation class, IEEE standards and specifications given by customer. When these limits are exceeded, dimension, location and material of shunts and shields are changed with the help of FEM analyses.

In this study, ANSYS@Maxwell and ANSYS@Mechanical modules are used to determine which application of shield and shunts are the most appropriate to get less temperature rise on magnetic parts of the transformer [7].

In the literature, there are studies to determine and reduce the hot spot on tank wall and other structural components of the transformer. To determine the hot spot, transformer stray losses should be examined.

Calculation of stray losses is not a simple task as the transformer has nonuniform structure. The calculation is complex for the following reasons:

- magnetic nonlinearity,
- difficulty in calculating the stray area and its effects quickly and accurately,
- inability to isolate certain stray loss components from the load under test
- lost values,
- limitations of experimental verification methods for large power transformers.

Stray losses in the tank due to the leakage field from the various clamping structures (frames, flitch plates, etc.) and the windings and the area of the high-current-carrying terminals are discussed [8,9,10].

For this purpose, the use of the finite element method provides advantages in the design and improvement phase. Due to the geometric designs of the transformer's hot spot point as well as other components, losses on these elements can be calculated with high accuracy, especially with three-dimensional analysis. In addition, the finite element method provides convenience because the electromagnetic parameters such as electrical conductivity and magnetic permeability of the metal material from which the structural components are produced significantly affect the losses on these components.

In the study of Moghaddami, usage of horizontal shunts on a power transformer are examined by FEA. Using horizontal shunts instead of vertical shunts has similar effect on reducing stray losses. Plus, horizontal shunts weight 25% less than vertical shunts. Thus, it is very cost effective [11].

In the study of Xiao, usage of lung magnetic shielding, tank magnetic, and tank coper shielding applications are examined by using FEM tools. Usage of lung magnetic shielding makes very positive effect on tank losses by collecting leakage flux on itself. But overheating of the lung magnetic shield should also be considered. By adding appropriate size of magnetic or copper tank shield, leakage flux orientation can be controlled, and overheating can be avoided [12].

In this study, more than one study was carried out to achieve the best case by reducing transformer losses. A thermal model is proposed to obtain the temperature distribution in the transformer created as a result of the final study. The proposed model is formulated with ANSYS@Maxwell and ANSYS@Mechanical software, which performs field analysis and solves energy equations based on the FEM. These values are calculated using the characteristics and dimensions of the transformer. These losses are characterized as heat generated in the thermal analysis procedure. The expected result from using the proposed model is to find the hottest region in the transformer by determining the temperature distribution of the basic components of the transformer. Finally, the thermal field of the 502 MVA oil-immersed power transformer was modelled in 3D and analysed by FEM. The obtained results were compared with the test results performed in power transformer laboratory in the factory.



Poster Presentation: Analysing Electromagnetic and Thermal Effects of Using Aluminium Shield and Magnetic Shunt Combinations at High-Voltage Level Autotransformers

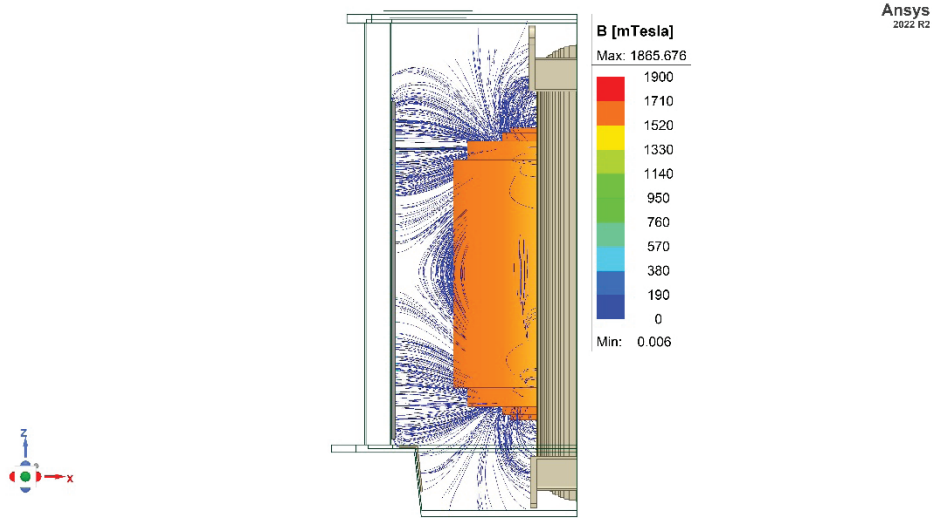


Figure 1: Magnetic field distribution

## 2. DESIGN PARAMETERS

Table 1: Design parameters of the autotransformer

Rated power	502MVA		
Connection type	YNa0d1		
Cooling system	ONAN / ONAF I / ONAF II		
Core leg type	3 / 2		
Core material	M4-30 PH 110		
	HV winding	LV winding	TV winding
Rated voltage (kV)	380	110	13,8
Number of turns	522	221	48

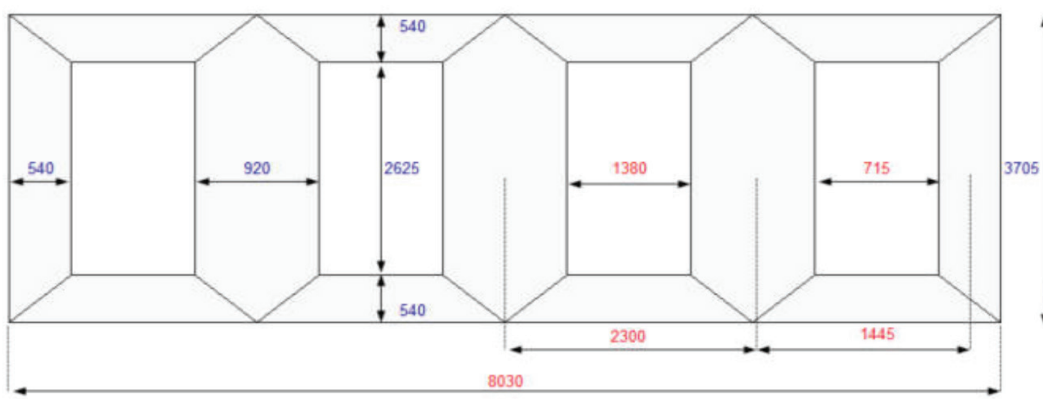


Figure 2: Core dimensions

Table 1 gives some idea about the transformer design parameters. The voltage and number of turns used in the analysis are also given in the table. It has three different cooling stages depending on its rated power. Its core structure consists of 3 main legs and 2 return legs as seen at Figure 2.



Poster Presentation: Analysing Electromagnetic and Thermal Effects of Using Aluminium Shield and Magnetic Shunt Combinations at High-Voltage Level Autotransformers

### 3. ANALYSIS

#### 3.1. Electromagnetic Analysis

The transformers have an active part and a whole tank with a base geometry for modelling. The core, core clamping structure (frames and flitch plates), windings, transformer tank and wall shunts are constructed as base components in electromagnetic model. Additionally, the transformer tank is modelled with tank wall. Due to symmetry property of used software, models for electromagnetic solutions are half geometry of active part. Symmetry axis of model is core axis of active part.

Magnetic properties of used materials in model are shown in Figure-xx. Relative permeability of materials is defined as “B-H Curves” for obtaining truer results. The material type for tank walls and core frames (St-37-2) is steel plate and defined as “mild steel”. The type of used CRGO electrical steel in core is “M4-30 PH 110”. However, the type of used CRGO electrical steel for wall shunts is M5 with 0.50 mm width. Stacking factors for “M4-30 PH 110” and “M5” electrical steel are defined according to stacking directions (X, Y, Z)

In following Figure 3; peak ampere values, number of turns and phase angles are used as input data respectively for all of 3 wounded legs of phases in electromagnetic models. The reason of using ampere value as peak value is due to the calculation method of used software. Phase angles are provided with different values in for each phase. Because phases and related windings have electrical difference with 120 degrees according to other phases’ windings.

Name	Type	Description
LV_A_output	Current	Type = Current, Current = 1941.44*221*sqrt(2) A, IsSolid = Stranded, Phase = 0deg, Direction = Point out of terminal
LV_A_input	Current	Type = Current, Current = 1941.44*221*sqrt(2) A, IsSolid = Stranded, Phase = 0deg, Direction = Point into terminal
LV_B_output	Current	Type = Current, Current = 1941.44*221*sqrt(2) A, IsSolid = Stranded, Phase = 120deg, Direction = Point out of terminal
LV_B_input	Current	Type = Current, Current = 1941.44*221*sqrt(2) A, IsSolid = Stranded, Phase = 120deg, Direction = Point into terminal
LV_C_output	Current	Type = Current, Current = 1941.44*221*sqrt(2) A, IsSolid = Stranded, Phase = 240deg, Direction = Point out of terminal
LV_C_input	Current	Type = Current, Current = 1941.44*221*sqrt(2) A, IsSolid = Stranded, Phase = 240deg, Direction = Point into terminal
ADU_A_input	Current	Type = Current, Current = 693.4*95*sqrt(2) A, IsSolid = Stranded, Phase = 0deg, Direction = Point into terminal
ADU_A_output	Current	Type = Current, Current = 693.4*95*sqrt(2) A, IsSolid = Stranded, Phase = 0deg, Direction = Point out of terminal
ADU_B_input	Current	Type = Current, Current = 693.4*95*sqrt(2) A, IsSolid = Stranded, Phase = 120deg, Direction = Point into terminal
ADU_B_output	Current	Type = Current, Current = 693.4*95*sqrt(2) A, IsSolid = Stranded, Phase = 120deg, Direction = Point out of terminal
ADU_C_input	Current	Type = Current, Current = 693.4*95*sqrt(2) A, IsSolid = Stranded, Phase = 240deg, Direction = Point into terminal
ADU_C_output	Current	Type = Current, Current = 693.4*95*sqrt(2) A, IsSolid = Stranded, Phase = 240deg, Direction = Point out of terminal
YG_A_input	Current	Type = Current, Current = 693.4*522*sqrt(2) A, IsSolid = Stranded, Phase = 0deg, Direction = Point into terminal
YG_A_output	Current	Type = Current, Current = 693.4*522*sqrt(2) A, IsSolid = Stranded, Phase = 0deg, Direction = Point out of terminal
YG_B_input	Current	Type = Current, Current = 693.4*522*sqrt(2) A, IsSolid = Stranded, Phase = 120deg, Direction = Point into terminal
YG_B_output	Current	Type = Current, Current = 693.4*522*sqrt(2) A, IsSolid = Stranded, Phase = 120deg, Direction = Point out of terminal
YG_C_input	Current	Type = Current, Current = 693.4*522*sqrt(2) A, IsSolid = Stranded, Phase = 240deg, Direction = Point into terminal
YG_C_output	Current	Type = Current, Current = 693.4*522*sqrt(2) A, IsSolid = Stranded, Phase = 240deg, Direction = Point out of terminal
Tertiary_A_input	Current	Type = Current, Current = 48.31*48*sqrt(2) A, IsSolid = Stranded, Phase = 0deg, Direction = Point into terminal
Tertiary_A_output	Current	Type = Current, Current = 48.31*48*sqrt(2) A, IsSolid = Stranded, Phase = 0deg, Direction = Point out of terminal
Tertiary_B_input	Current	Type = Current, Current = 48.31*48*sqrt(2) A, IsSolid = Stranded, Phase = 120deg, Direction = Point into terminal
Tertiary_B_output	Current	Type = Current, Current = 48.31*48*sqrt(2) A, IsSolid = Stranded, Phase = 120deg, Direction = Point out of terminal
Tertiary_C_input	Current	Type = Current, Current = 48.31*48*sqrt(2) A, IsSolid = Stranded, Phase = 240deg, Direction = Point into terminal
Tertiary_C_output	Current	Type = Current, Current = 48.31*48*sqrt(2) A, IsSolid = Stranded, Phase = 240deg, Direction = Point out of terminal

Figure 3: Excitations

#### 3.2. Thermal Analysis

Temperature rise on the tank and steel parts of transformer is calculated by using obtained losses from e-mag analysis. Ambient temperature is defined to the outer surfaces of the transformer tank. Oil temperatures are defined to inner surfaces of the tank and the other metallic clamping parts surfaces. Oil temperature is defined as a gradient from bottom to top. The ambient and the top and bottom oil temperatures are determined by formulas at IEC 60076 standard and the design tools created by BEST transformer company.

In the thermal analysis setup, radiation is defined to the outer surface of the tank to see the effect of cooling by radiation from the tank. The emissivity value is taken by the RAL paint tables. Convection from tank to the air is defined to the outer surface of the tank as well. Convection coefficient of air is directly taken from the ANSYS Mechanical library. On the other hand, convection boundary conditions for oil is defined to inner surface of the tank and the other metallic parts surface. These convection coefficients are obtained and validated by some internal studies and test performed in BEST transformer. Approximate chart of convection coefficients can be found at Figure 4.

Used heat transfer coefficient depending on oil temperature and temperature differences between oil and the tank wall.





Poster Presentation: Analysing Electromagnetic and Thermal Effects of Using Aluminium Shield and Magnetic Shunt Combinations at High-Voltage Level Autotransformers

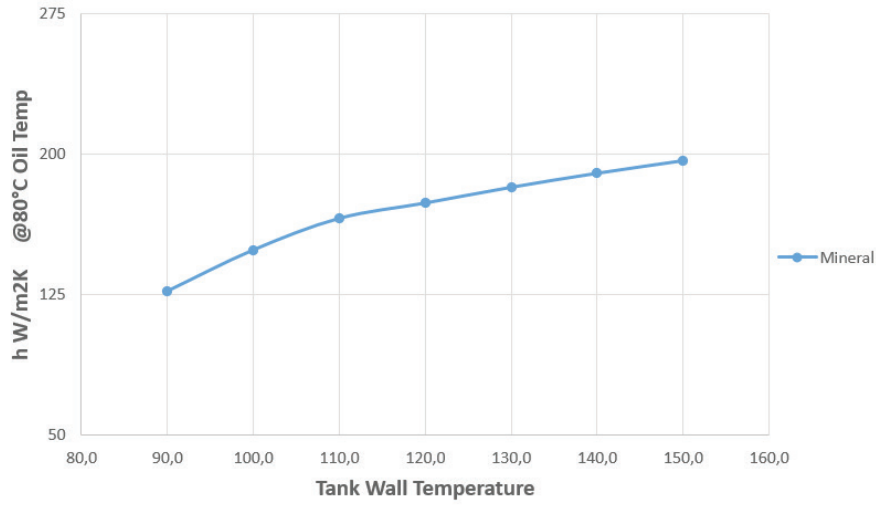


Figure 4: Convection coefficient / temperature chart

### 4. ANALYSES AND TEST RESULTS

Table 2: Results of analyses

Combination		Hot spot (°C)		
		Tank	Top Clamp	Bottom Clamp
1	No shunt or Al shield	117,9	134,0	112,8
2	20mm vertical shunt and Al shield	117,6	127,3	109,2
3	30mm vertical shunt and Al shield	114,4	126,8	107,5
4	30mm horizontal shunt and Al shield	119,1	127,8	109,3

By considering the FEM analyses, it is seen on Table 2 the most desirable result is obtained by the combination 3 which has thicker shunt compared to the combination 2 and vertical shunt unlike the combination 4.

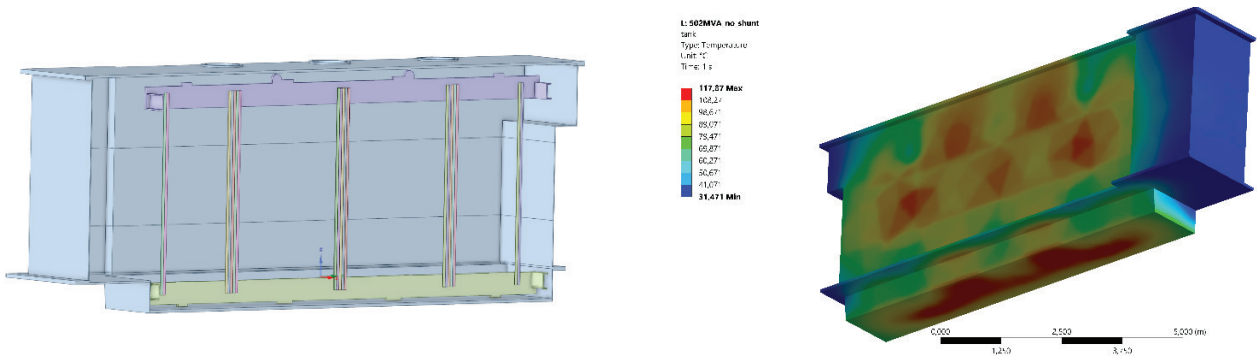


Figure 5: Combination 1 geometry and thermal results

For the combination 1, hot spot is not that high as expected. But the hot area is very large and visible compared to the other combinations.



Poster Presentation: Analysing Electromagnetic and Thermal Effects of Using Aluminium Shield and Magnetic Shunt Combinations at High-Voltage Level Autotransformers

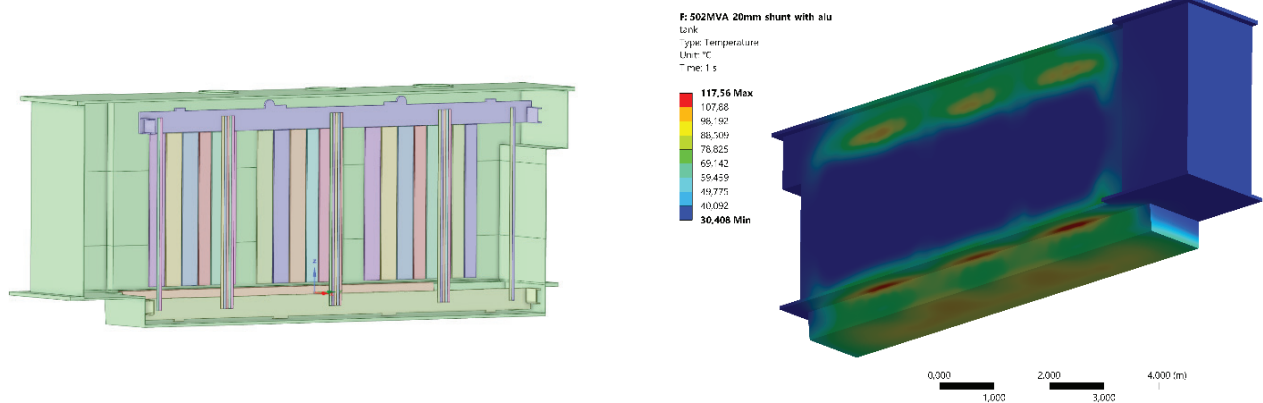


Figure 6: Combination 2 geometry and thermal results

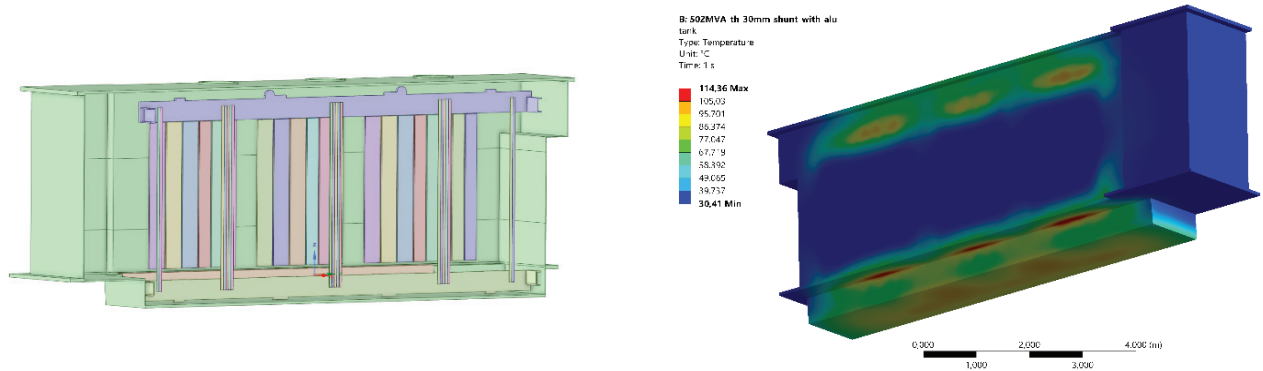


Figure 7: Combination 3 geometry and thermal results

For combination 2, shunts are saturated due to insufficient thickness and this result in higher hot spots compared to the combination 3.

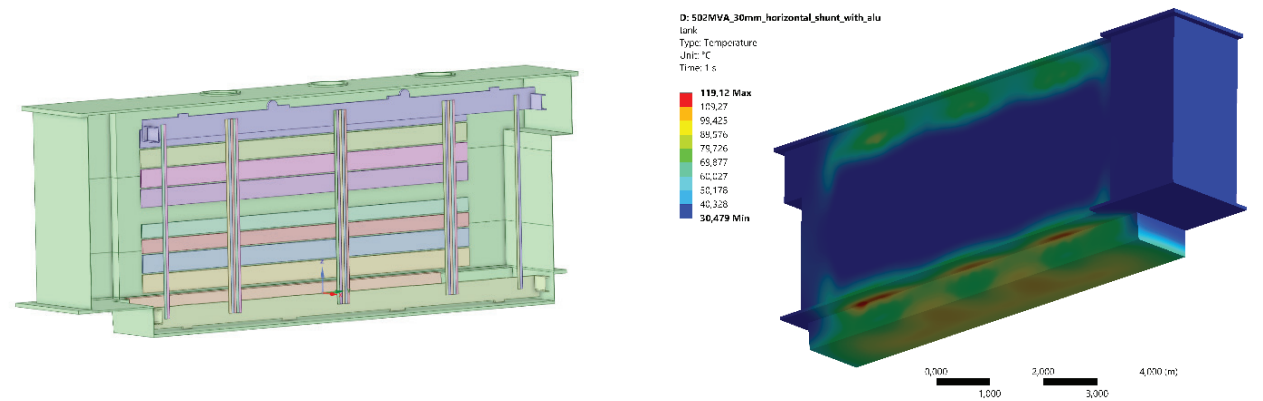


Figure 8: Combination 4 geometry and thermal results

For combination 4, horizontal shunts are also very effective in various applications. But for our case, according to the analyses it is not effective as vertical shunt.



Poster Presentation: Analysing Electromagnetic and Thermal Effects of Using Aluminium Shield and Magnetic Shunt Combinations at High-Voltage Level Autotransformers

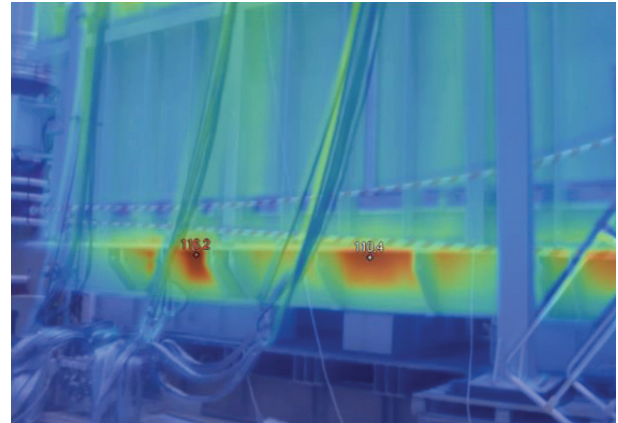
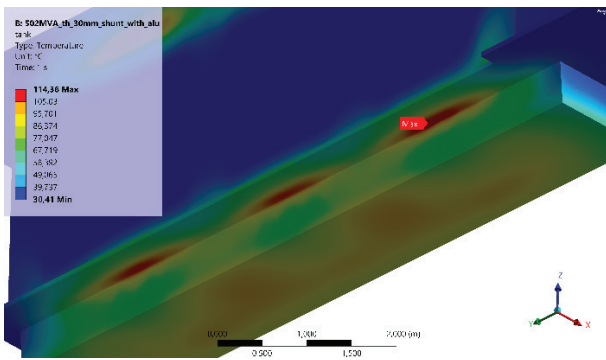


Figure 9: Analysis result and test result

Test result shows that the analysis result is quite consistent with only about 1% error.

## CONCLUSION

In this study, it is seen that on high rated autotransformer different combinations of magnetic shunt and Al shield applications result with different magnetic and thermal behaviour. Thanks this paper some basic knowledge about; autotransformer design parameters, stray losses, magnetic flux and field behaviour, thermal equivalent of losses on metallic parts are gained. Also, some basic knowledge is gained about prediction of hot spot of a transformer by using FEM analysis software. In further studies it is aimed that more variety of shunt and shield combinations can be tried with the help of this paper.



**Poster Presentation:** Analysing Electromagnetic and Thermal Effects of Using Aluminium Shield and Magnetic Shunt Combinations at High-Voltage Level Autotransformers

### BIBLIOGRAPHY

- [1] Li, Y., Li, L., Jing, Y., Li, S., & Zhang, F. (2013, October). Calculation and analysis of hot-spot temperature-rise of transformer structure parts based on magnetic-thermal coupling method. In 2013 International Conference on Electrical Machines and Systems (ICEMS) (pp. 2259-2262). IEEE.
- [2] New EU Requirements for Transformers—Ecodesign Directive From the European Commission, SIEMENS, Munich, Germany, 2015
- [3] Li, L., Fu, W. N., Ho, S. L., Niu, S., & Li, Y. (2014). Numerical analysis and optimization of lobe-type magnetic shielding in a 334 MVA single-phase auto-transformer. *IEEE Transactions on Magnetics*, 50(11), 1-4.
- [4] Del Vecchio, R. M., Poulin, B., Feghali, P. T., Shah, D. M., & Ahuja, R. (2017). *Transformer design principles: with applications to core-form power transformers*. CRC press.
- [5] Park, K. H., Lee, H. J., & Hahn, S. C. (2019). Finite-element modeling and experimental verification of stray-loss reduction in power transformer tank with wall shunt. *IEEE Transactions on Magnetics*, 55(12), 1-4.
- [6] Najafi, A., Ozgonenel, O., & Kurt, U. (2017, November). Reduction stray loss on transformer tank wall with optimized widthwise electromagnetic shunts. In 2017 10th International Conference on Electrical and Electronics Engineering (ELECO) (pp. 6-10). IEEE.
- [7] ANSYS Inc., C.P.U., Available at: [www.ansys.com](http://www.ansys.com) [Accessed 1 June 2022].
- [8] Kulkarni, S. V., & Khaparde, S. A. (2017). *Transformer engineering: design, technology, and diagnostics*. CRC press.
- [9] Karsai, K., vd. *Studies in Electrical and Electronic Engineering*, 25. Cilt., 1987.
- [10] Del Vecchio, R., Del Vecchio, R. M., Poulin, B., Feghali, P. T., Shah, D. M., & Ahuja, R. (2017). *Transformer design principles*. CRC press.
- [11] Moghaddami, M., Sarwat, A Moghaddami, M., Sarwat, A. I., & De Leon, F. (2016). Reduction of stray loss in power transformers using horizontal magnetic wall shunts. *IEEE Transactions on magnetics*, 53(2), 1-7. I., & De Leon, F. (2016). Reduction of stray loss in power transformers using horizontal magnetic wall shunts. *IEEE Transactions on magnetics*, 53(2), 1-7.
- [12] Xiao, C., Dezhi, C., & Baodong, B. (2021, April). Study of loss and temperature considering different shielding structure in power transformer. In 2021 IEEE International Magnetic Conference (INTERMAG) (pp. 1-5). IEEE.

**ELECTRIC  
TRANSMISSION**  
**ORAL PRESENTATION**



ELECTRIC MACHINES AND  
POWER ELECTRONICS



**ELECTRIC  
TRANSMISSION**



**AUTOMATION AND  
CONTROL**

**POWER  
GENERATION**



**ENERGY  
TRANSITION**



**DISTRIBUTION SYSTEMS  
AND SMART GRIDS**



**11-12 OCTOBER 2023**





# Transmission Capacity Maximization Using Dynamic Thermal Rating in Croatian Power System

[tomislav.plavsic@hops.hr](mailto:tomislav.plavsic@hops.hr)**TOMISLAV PLAVŠIĆ\*, ZORAN BUNČEĆ, ANA KEKELJ, JADRANKO KUČICA, KREŠIMIR MESIĆ**  
*Croatian Transmission System Operator HOPS***Croatia**

## SUMMARY

Present demands for increasing the transmission network capacity, emerging from the huge grid connection demands from renewable energy sources and high expectations for the increase of cross-zonal electricity trade in European Union, are more and more challenging for transmission system operators. Croatian Transmission System Operator is on the one hand facing these pressures from the renewable energy sources investors and from the electricity market, and on the other hand significant obstacles in realization of the transmission network extension plans, mostly due to the environmental and spatial issues. Dynamic line rating has in recent years been recognized as the transitional technology that can enable optimal utilization of the existing assets, and therefore a solution to the challenges that arise from the lack of transmission network capacity. The paper provides an overview of dynamic line rating technology and presents experiences and conclusions drawn from already implemented dynamic line rating technology in Croatian transmission system. An integration of dynamic line rating limits in power system applications is described and future plans for usage of dynamic line rating technology in Croatian transmission system are presented.

## KEYWORDS

Transmission System Operator, transmission network capacity, renewable energy sources, dynamic line rating





### 1. INTRODUCTION

Demands for enabling the transmission of increased amounts of electricity, coming from the various electricity sector stakeholders, is growing in recent years, facing transmission system operators with significant challenges in providing the required transmission capacity. In European Union, those demands have been transformed into legal requirements, resulting in Regulation 2019/943 which requires from all EU transmission system operators to make available 70% of their transmission capacity for cross-zonal trade.

Standard practice to increase the capacity of the transmission network is to expand it by building new lines (overhead or cable), or to increase the transmission capacity of the existing lines. Transmission system operators have been challenged in past decades with difficult possibilities to develop and expand the transmission network, due to the long period of issuing all the necessary building permits. In average, process of building new 400 kV tie line in Croatia usually lasts 10 years and that is a too long period for the present requirements and demands. In order to respond to the mentioned challenges in a timely manner, transmission system operators are rapidly optimizing use of the existing transmission network.

Dynamic line rating (DLR) of the overhead transmission lines (OHL) is one of the “smart” ways and solutions how the existing transmission network capacities can be maximized, while respecting the prescribed criteria for safe and reliable network operation. DLR of OHL uses the fact that the ampacity of OHL depends on ambient conditions and the OHL is designed for high summer weather conditions. As less severe weather conditions exist for most of the year, the ampacity of the existing lines can be significantly increased (up to 200%). The major task thereby is to derive the present and forecast the future ambient conditions, calculate the current carrying capacity, and integrate these results to dispatch centre processes, considering adequate security margins. This technology allows to load an individual transmission line under favorable environmental conditions, without the risk of permanent damage of conductors or the risk of violating the safety distance of conductors to the ground. The application of DLR requires knowledge about the maximal allowable temperature of OHL conductor, which is also proportional to sag. Upon working with the key future operational conditions, DLR requires weather forecasts in order to allocate the possible additional capacity to the market in system operator processes (IDCF intra-day congestion forecast, DACF day ahead congestion forecast, D2CF two-days ahead congestion forecast).

As the Croatian Transmission System Operator (HOPS) is having a significant demands to increase the transmission network capacity, while keeping pace with advanced technologies, the need to determine an efficient way to implement DLR technology has emerged. This means determining the type of DLR technology to be installed, determining the technical and organizational prerequisites for installation and determining the order of installation priorities.

In the second chapter the DLR technology is described, while third chapter presents experiences with DLR technology in HOPS as well as reasons for DLR implementation. In fourth chapter an integration of dynamic line rating limits in power system applications is described, while fifth chapter presents future plans for DLR implementation in Croatian transmission network.

### 2. DLR TECHNOLOGY IN GENERAL

All components of the ETDS (Electricity Transmission and Distribution System) are influenced by various meteorological factors and their variability in time and space. For example, the cooling of conductors is not the same when there is wind, rain, strong sunlight, or high air temperature along the transmission line. Of significant interest are the direction and speed of the wind, temperature, pressure, relative humidity of the air, as well as the amount of precipitation and solar radiation (Figure 1).

Considering that the current transmission capacity limit of the transmission line is determined according to a standard that takes into account the safety clearance from the ground during summer weather conditions with an air temperature of 40°C, wind speed of 0.6m/s at a 90° angle of incidence, solar radiation of 1200W/m<sup>2</sup>, and conductor temperature up to a maximum of 80°C, it is evident that there is room for improvement by implementing continuous monitoring of the transmission line and meteorological conditions.

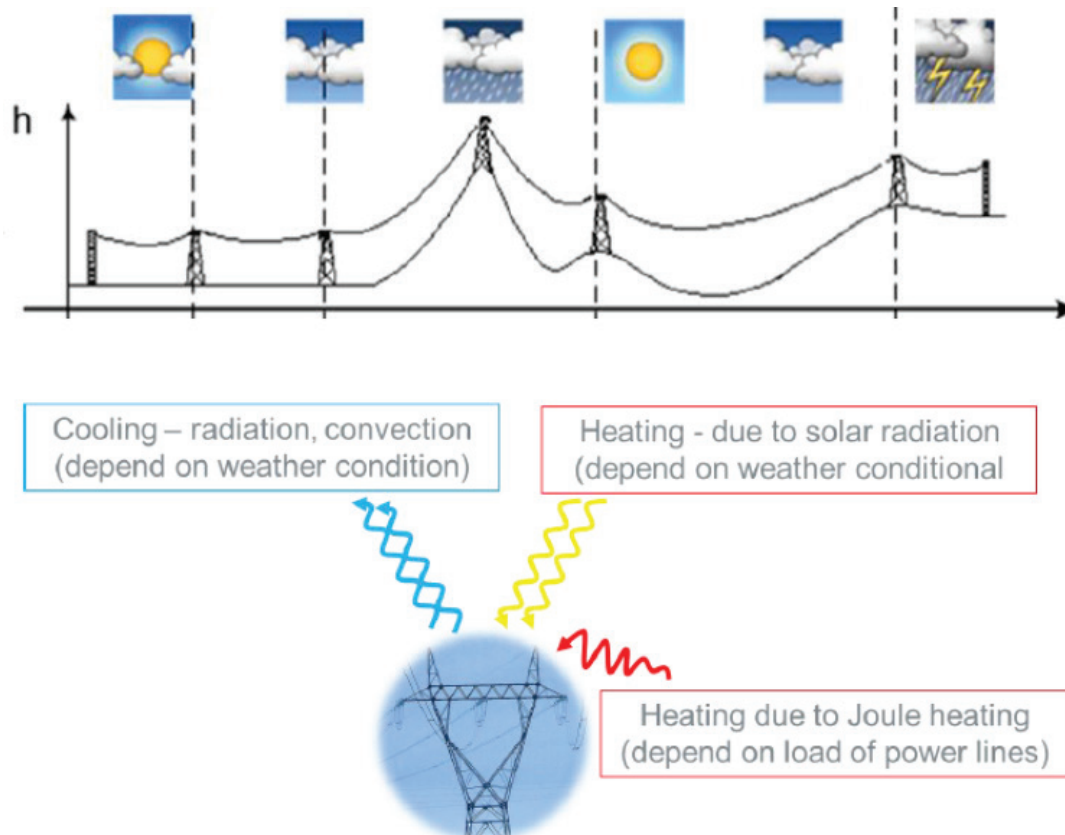


Figure 1. Different weather conditions along the line used in DLR algorithm

Generally, technologies for determining the DLR limit can be divided into two types:

- Direct method for determining the DLR limit: As the name suggests, the DLR limit is determined directly by measuring the conductor temperature or sag angle. Direct methods have the advantage of providing more accurate measurements of the sag angle or conductor temperature at the installation site. However, they require the installation of measurement equipment on the conductor (requiring disconnection of the conductor for installation or maintenance). Depending on the terrain relief that the transmission line passes through, a larger number of measurement sensors may need to be installed. Additionally, direct methods generally do not provide DLR limit predictions for several hours in advance.
- Indirect method for determining the DLR limit: This method is based on a spatial model of the transmission line, meteorological forecasts, and measured meteorological data. Indirect methods have the advantage of easier integration of a transmission line into the DLR system (no need to disconnect the transmission line for equipment installation). They provide DLR limit predictions for the future and enable monitoring of the “critical sag” over time. However, the drawback of the indirect method is its dependence on the availability and accuracy of meteorological forecasts, introducing a certain level of uncertainty in the system’s results.

After the decision was made to install the DLR system in HOPS, an analysis of available technologies that can be used to determine the DLR limit was conducted.

### 3. HOPS EXPERIENCES WITH DLR TECHNOLOGY WITHIN SINCROGRID PROJECT

In order to better utilize the potential of the existing transmission network, HOPS has decided to install a DLR system as part of the SINCROGRID project on the systematic 220 kV power lines from north to south of Croatia. SINCROGRID was a PCI project in which have jointly participated transmission system operator from Slovenia (ELES) and Croatia (HOPS). The project includes the deployment of compensation devices, an advanced dynamic thermal rating system, a battery electricity storage system, as well as a virtual cross-border control centre. This system was partially funded by the European Union (EU). As part of the Sincro.Grid project, the SUMO DLR system has been procured and implemented on the following 220 kV power line in HOPS grid (Figure 2):



a) Senj - Melina

b) Krš Pađene - Brinje

c) Konjsko – Krš Pađene

d) Zakučac - Konjsko

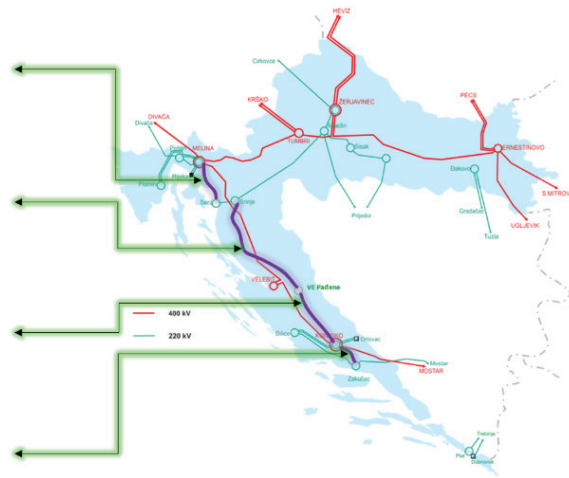


Figure 2. Power lines with implemented DLR technology in SINCROGRID project

Several leading manufacturers in the EU have been considered, and it was decided to install the SUMO system, developed by the Slovenian manufacturer SolveraLynx, as part of the SINCROGRID project. The SUMO system is based on indirect methods for determining the DIR limit. It was installed in 2020 and has been operational in the National Control Center (NCC) since the autumn of 2020.

The results of the SUMO system are utilized in the SCADA (Supervisory Control and Data Acquisition) ABB Network Manager and NetVision DAM systems for EMS (Energy Management System) calculations. These systems use the DLR calculation results to generate forecast files, such as the Intraday Congestion Forecast (IDCF), and for N-1 calculations. The DLR limit is primarily influenced by factors such as wind speed, wind angle, and air temperature. During periods of strong vertical winds and low air temperature, the calculated DLR limit from the system often reaches up to 2000A. Considering that the observed power lines are over 50 years old and have limitations in the installed current measuring transformers (CMT), a calculation was performed in the SCADA system to restrict the DLR limit to a value within the measurement range of the CMT. For the SINCROGRID power lines, this value is set at 1200A, representing approximately a 150% increase compared to the static limit defined by the standards, which is 780A for the observed DLR power lines. Since the DLR system was commissioned, no significant unavailability of the system has been recorded.

Given that the mentioned power lines are situated in coastal areas and often in valleys where high air temperatures occur without wind, there may be situations where the calculated DLR limit is lower than the technical limit of the power lines. Empirically, these situations occur during the summer months, and their frequency ranges from 5% to 10% of the total time annually (Figure 4). As overload protection is disabled on these power lines, it is crucial for the dispatcher to respond promptly if the current load on the power lines exceeds the current DLR limit. Since the installation on the mentioned 4 power lines, there have been no instances where the current load exceeded the utilized limit. In the event of such a situation, the dispatcher at the NCC would receive an alarm through the SCADA system.

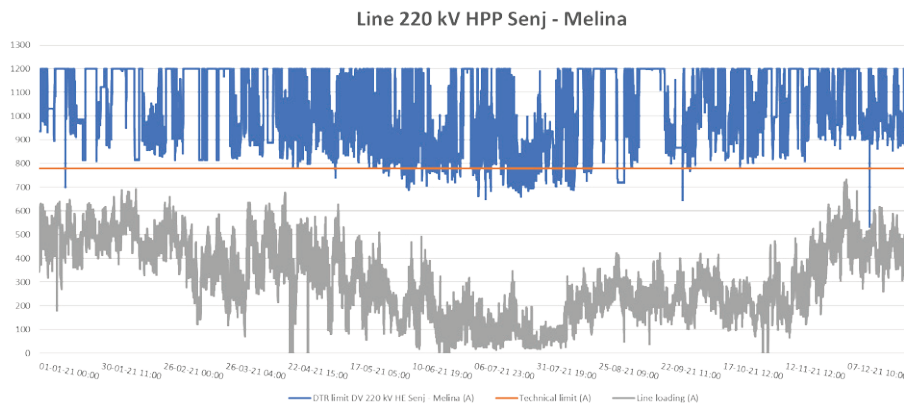


Figure 3. Comparioson of line loading, DLR limit and static limit during 2021. on line HE Senj - Melina

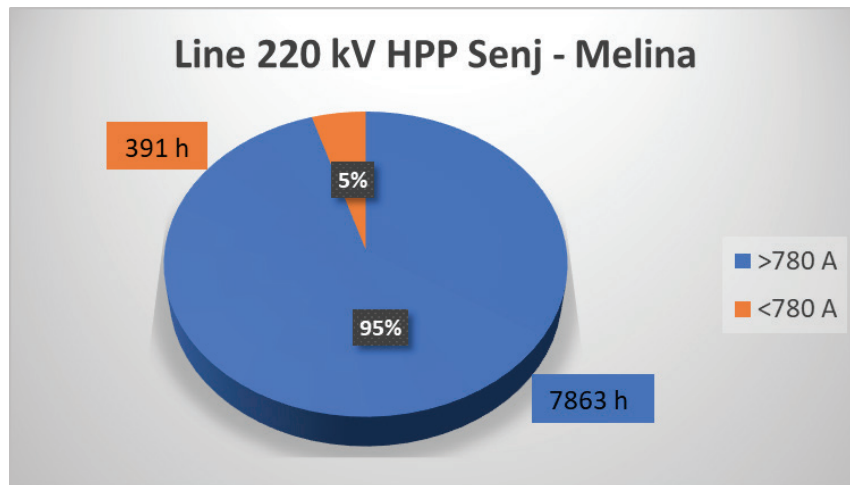


Figure 4. Number of hours when DLR limit is higher than static one

In recent years, there has been a significant trend of increasing electricity production from renewable sources and electricity consumption due to investments in electromobility, air conditioning, and space heating. This trend is even more pronounced among the leading operators within the ENTSO-E region, which poses a challenge for power system operators in terms of network congestion or lack of cross-border capacities. This can be addressed through measures such as redispatching generation, building new transmission lines, or implementing DLR systems. However, redispatching entails significant costs, potential energy losses, and constructing new power lines is a slow and financially demanding process for power system operators. Therefore, operators often opt for the installation of DLR systems where a slight increase in transmission capacity is necessary.

Given that DLR technology is quite advanced, and various solutions employing direct or indirect methods are available, leading operators such as RTE, TENNET, SWISSGRID, ELIA, and REE utilize predominantly hybrid-based systems. This choice is made because operators not only require the current limit but also need DLR limit forecasts (up to 48 hours in advance) for market mechanisms and forecast file preparation. To determine or control the current DLR limit, conductor sag angle, or temperature, operators employ sensors and meteorological stations installed along the transmission line route. Additionally, for DLR limit forecasting, systems based on meteorological predictions are utilized.

The application of DLR limits by operators significantly varies and depends on the type of problem they aim to address through DLR systems. Some operators use the DLR limit only in situations where it positively impacts congestion, i.e., when it is beneficial for congestion management. In cases where the calculated DLR limit is lower than the technical limit, they use the technical limit. Other operators employ the DLR limit even when it is lower than the static limit, reducing the transmission capacity of the power line. When applying DLR calculations to cross-border lines, operators exchange values through data exchange systems, and the resulting limit is the lower calculated value.

Considering all the aforementioned factors, it is evident that power system operators extensively utilize DLR technologies and strive to optimize the existing power system infrastructure. The experiences of leading operators are positive, and given the current situation, an increased implementation of DLR technologies in power system operations can be expected.

## 4. INTEGRATION OF LIMITS IN POWER SYSTEM APPLICATIONS

### 4.1. Overload limits in power system applications

Overload limits of network elements (transformers, transmission lines and busbars) in real time power system applications and operation planning are basis for:

- real time monitoring of N-0 violations,
- contingency analysis for N-1 violations,
- congestion forecast for operational planning,
- security constrained optimal power flow for optimization of redispatch actions and minimization of losses .

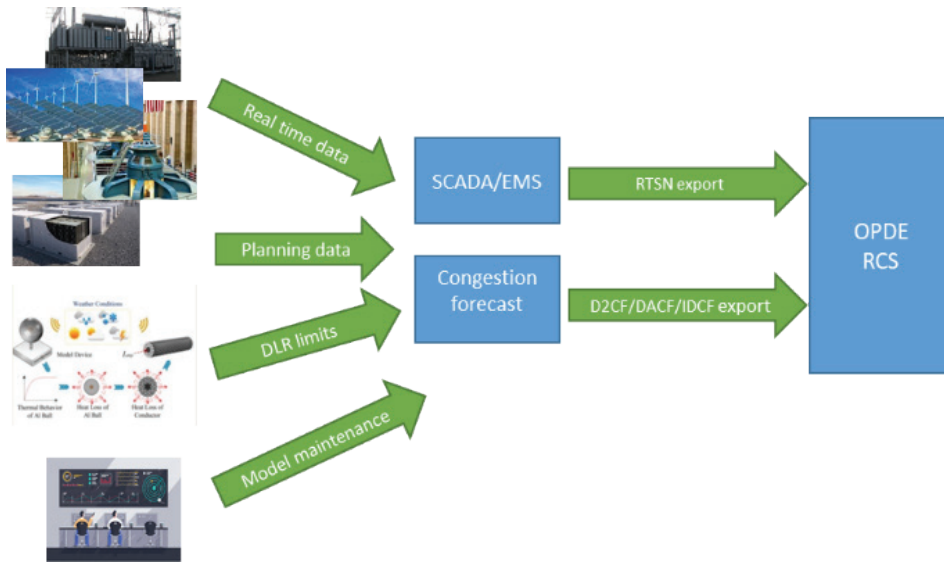


Figure 5. Power system operation and planning applications data exchange

Static thermal limits in power system applications are defined for current measurements and are calculated based on smaller limit of network equipment and limit of current transformer (120% of nominal primary current). Static limits of transmission lines in Croatia are based on thermal limits declared by manufactures for different types and construction design of conductors for selected set of operating conditions based on experience (temperature, wind speed, ... ). Summer and winter limits are used only on lines that are estimated to have large influence on power system operation.

Static limit in power system applications are declared for SCADA measurements and EMS values as presented in Figure 6:

- 80 % of limit generates SCADA warning visualized on power system diagrams and in alarm lists in yellow color
- 100 % limit generates SCADA alarm visualized on power system diagrams and in alarm lists in red color
- 100 % limit generates contingency in N-1 contingencies list and is used as limit in SCOPF application in both real-time and system planning.
- Overload protection trip is activate when 100% limit is violated more than 30 minutes.
- Limits in Internal grid models from HOPS used for D-2, D-1 and intra-day operational planning processes within Regional Security Coordinators (RSCs) are exchanged via Operational Planning Data Environment (OPDE) in Common Grid Model Exchange Standard (CGMES) and UCTE DEF formats are also exported from static limits in SCADA.

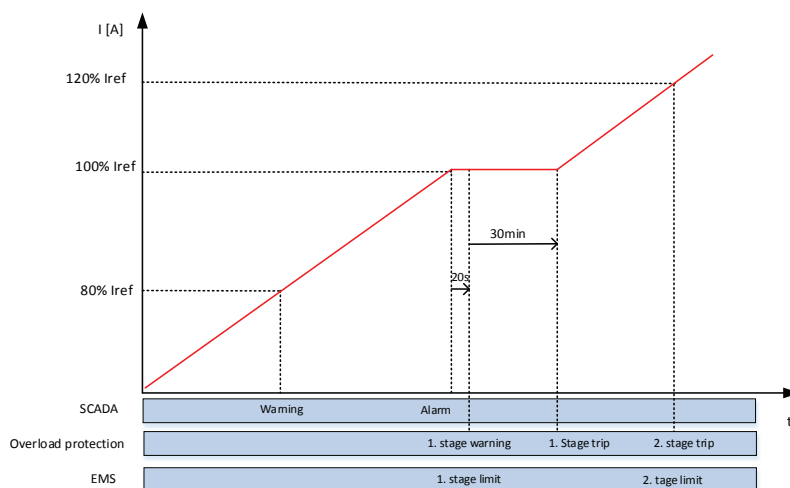


Figure 6. Configuration of SCADA/EMS and limits overload protection configuration



### 4.2. DLR limits in power system applications

DLR limits in power system applications can be activated or deactivated manually by the dispatcher (Figure 7). In case DLR limits are activated and they pass all validation checks, new limit is continuously calculated based on DLR current value and CMT nomina value as described in chapter 3. Selection is done once in SCADA/EMS system and transferred automatically to other systems. In case there is DLR activated on the power line overload protection is permanently deactivated.

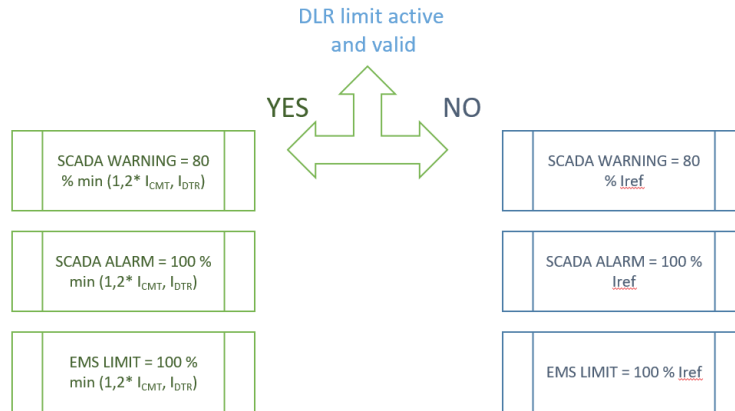


Figure 7. Block diagram on configuration of limits based on DLR availability

When DLR limit is activated, the new measurement is created in SCADA/EMS system and the value is telemetered from DLR system via IEC 60870-5-104 protocol. The special function in SCADA/EMS system is used to use that measurement as an input to limits in the database both for measurements and EMS variables. The SCADA warning and alarm are calculated as 80% and 100% of DLR value. The example on activation of limits on real time current measurement is presented in Figure 8.



Figure 8. Example of activation of limits on real time data with static limits and DLR limits active

In operational planning processes prognostic DLR limits are used in IDCF for three hours ahead the real-time in UCTE DEF and CGMES files. The limits in the current version of CGMES 2.4.5. are exported in Equipment Display (EQ) files and are degrading the performance of overall file exchange. In CGMES v 3.0. it is foreseen to export the limits in Steady State Hypothesis (SSH) files.

## 5. FUTURE PLANS WITH DLR IN HOPS

### 5.1. Determination of installation of the DLR system

When determining the location, for the future installation of DLR system, according to the internal methodology in HOPS several key items were taken into account, on the basis of which a list of proposed locations with installation priorities was created:

- Meeting the criteria of 70% according to Regulation (EU) 2019/943
- Statistical yearly analysis of N-1 violations
- Goals and national assessment of the recovery and resilience plan for Croatia





- Condition of primary equipment
- Planned reconstructions
- Various

During 2019, the remaining regulations from the Clean Energy Package for all Europeans entered into force, of which the most important for this topic is Regulation (EU) 2019/943 (hereinafter: Regulation). Specifically, according to Article 16(8) of Regulation, transmission system operators shall not limit the volume of interconnection capacity to be made available to market participants as a means of solving congestion inside their own bidding zone or as a means of managing flows resulting from transactions internal to bidding zones. This paragraph shall be considered to be complied with where the following minimum levels of available capacity for cross-zonal trade are reached:

- for borders using a coordinated net transmission capacity approach, the minimum capacity shall be 70% of the transmission capacity respecting operational security limits after deduction of contingencies, as determined in accordance with the capacity allocation and congestion management guideline adopted on the basis of Article 18(5) of the Regulation (EC) No 714/2009;
- for borders using a flow-based approach, the minimum capacity shall be a margin set in the capacity calculation process as available for flows induced by cross-zonal exchange. The margin shall be 70% of the capacity respecting operational security limits of internal and cross-zonal critical network elements, taking into account contingencies, as determined in accordance with the capacity allocation and congestion management guideline adopted on the basis of Article 18(5) of the Regulation (EC) No 714/2009

## 5.2. Future goals

By monitoring the share of capacity available for cross-zonal trading, HOPS recognizes the need for optimizing and strengthening the network in order to ensure the requirement of Article 18(8) of the Regulation. Respecting the above mentioned, HOPS proposed the following lines for the implementation of DLR: TL 220 kV Pehlin - Divača, TL 400 kV Melina - Divača, TL 220 kV Zakučac - Mostar, TL 400kV Konjsko - Mostar, OHL 400 kV Melina - Velebit, OHL 400 kV Velebit-Konjsko, OHL 220 kV Senj-Brinje, TL 400 kV Tumbri-Krško 1&2, OHL 110 kV Crikvenica-Vrataruša, OHL 110 kV Senj-Vrataruša, TL 110 kV Buje-Koper, TL 110 kV Matulji- Il.Bistrica, TL 400 kV Žerjavinec - Cirkovce, TL 220kV Žerjavinec - Podlog.

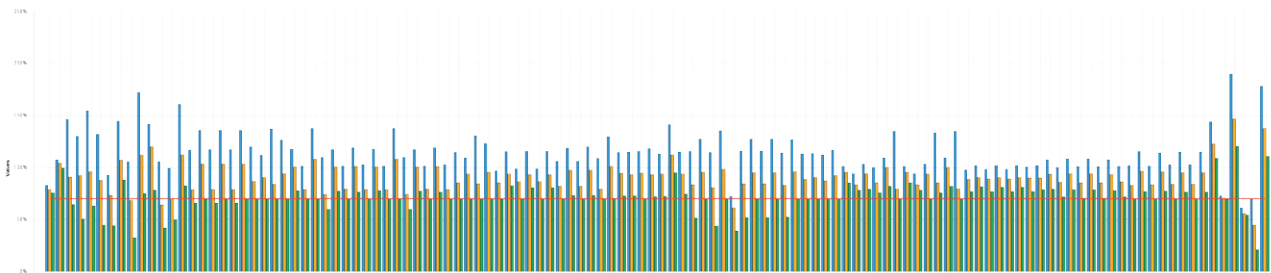


Figure 9. MACZT during year 2023.

## 5.3. Application of DLR system in individual grid models

Individual grid models contain information on the maximum allowed current of the element ( $I_{max}$ ), and the same information is used for different timeframes (D-2, D-1, D) of common grid models for calculation of N-1 grid security conditions and capacity. Individual grid models are created by usage of NetVision DAM, and data is loaded from the local system. Individual grid models can use seasonal (fixed during seasonal periods), dynamic and fixed values of the maximum allowed transmission current during the whole year. TSOs use the same operational security limits for capacity calculation that are used during N-1 security analysis conducted in accordance with Article 72 of SOGL, and with defined operating parameters in accordance with Article 25 of SOGL. The  $I_{max}$  values are temporary limits in accordance with Article 25 of SOGL, which means that overloading is allowed only for a certain limited time. Such values represent real technical properties and will not be reduced by any additional safety limits (uncertainties in capacity calculation are covered by FRM or TRM limits).

The results of the power flows and operational security analysis are taken into account during the coordinated security analysis within the common tools for data exchange and security assessment of regional coordinated centers (AMICA, Advanced Multisite Integral Congestion Assessment), as well as in local tools for these purposes as described in Figure 5 (ABB NetworkManager SCADA/



EMS, NetVision DAM). It is certainly expected that the use of dynamic values for I<sub>max</sub> will contribute most of the time to improved operating security conditions and higher remaining capacities. Between 15th of May and 15th of August during the year, dynamic limit values can be lower than the static ones, and in that period of time more attention must be taken during analysis.

When calculating cross-border capacities, the dynamic values of I<sub>max</sub> are taken from the common grid model and defined parameters (I<sub>max</sub>Factor, I<sub>max</sub>A) within the CNEC list (list of elements important for cross-border trade), and the maximum admissible power flow of the grid elements is calculated for further calculations of cross-border capacities. For NTC based calculation approach, the limiting elements important for cross-border trading when using the DLR system will have a higher admissible maximum power flow, and accordingly more opportunities for cross-border trading (calculation is done by internal tools). For the Flow Based calculation approach, the results of Flow Based parameters are available daily on JAO website and remaining available capacities (RAM) have been provided for each CNEC, which form the Flow Based domain of available capacity trading (Figure 10).

TSOs aim to gradually exclude seasonal and fixed physical (thermal) limits of the network element, and replace them with dynamic line rating in case the benefits are greater than investment costs. The expected increase in the economic surplus is usually considered within the period of the next 10 years during cost benefit analysis. The network element data and the application of the DLR system with DLR<sub>min</sub> [A] and DLR<sub>max</sub> [A] values are available on the JAO website.

By considering the results of the CCRs, it is possible to notice interdependence in CCR, and therefore it is important to take into account that the dynamic limits of other trading zones can be limiting for the Croatian trading zone during summer months, when dynamic limit values are lower. The aforementioned impacts can be observed by monitoring the first limiting element of the region in the domain of capacity trading.

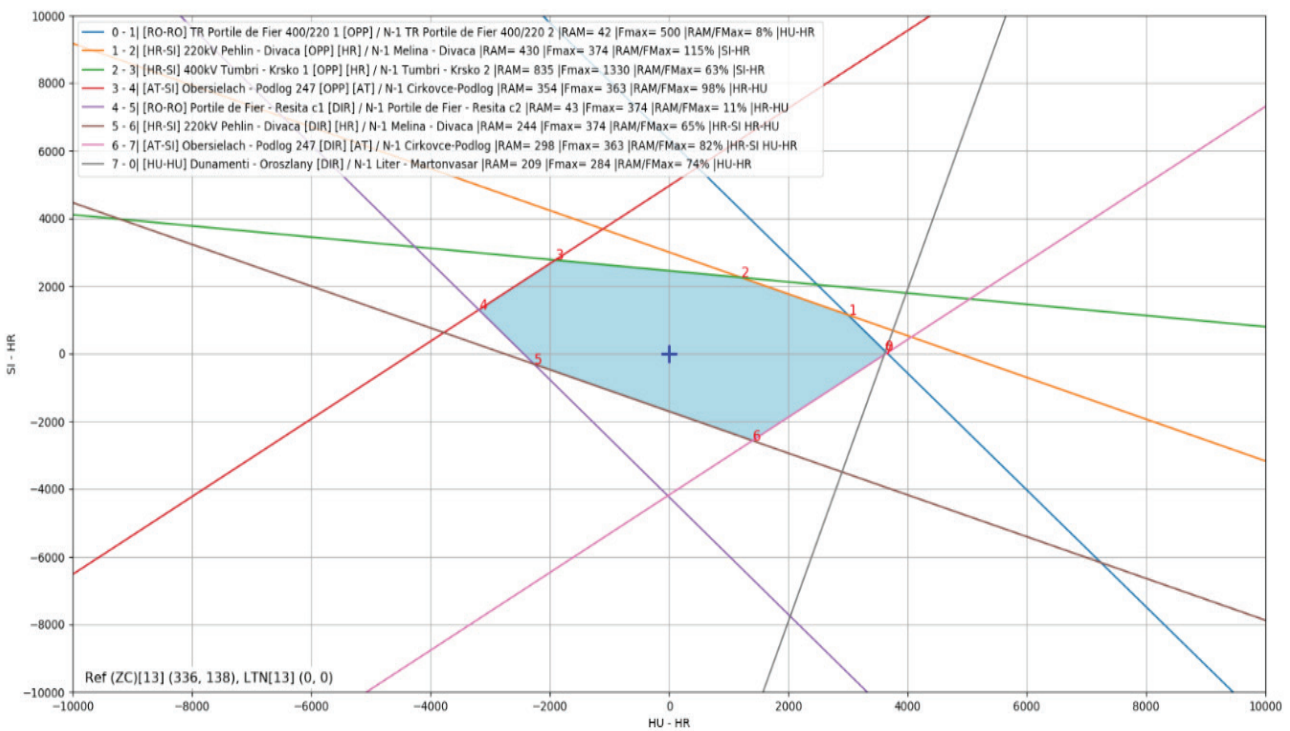


Figure 10. Flow based domain for HR Core borders on BD20230510

In addition to the application of the DLR system during system operations, it's necessary to establish DLR systems and integrate the system in the planning phase for very short-term forecasts of DLR values (1-6h) and short-term forecasts of DLR values (24-48h). Very short-term forecast of DLR values is mostly for consideration of the N-1 security criteria. The main advantage of this principle is the adequate preparation of system operations in order to solve possible overloads in a timely manner. Furthermore, electricity markets need transmission capacity forecasts one or two days in advance. The short-term forecasts of DLR values with the help of real and (weather) forecast data, it is possible to optimize and maximize usage of the transmission network and offer to market the maximum while respecting the operational security of the system. The market direction analysis aims to increase utility of available transmission capacities by application of an algorithm that includes the common capacity allocation for amounts of energy and power reserves.



### 6. CONCLUSION

The connection of renewable energy sources to the Croatian transmission network increasingly affects system security and creates problems in the daily power system operation. The dynamics of the revitalization of existing transmission lines and the construction of new ones is not able to follow the dynamics of the renewable sources connection to the transmission network. The transmission system operator is challenged with operational situations where the N-1 criterion is more often violated, and forced to find a solution to prevent the electricity supply from being threatened at any time. Corrective measures to eliminate congestions such as power plants redispatch create additional costs for the transmission system operator. Following the examples and experiences of many European transmission system operators and the experiences drawn from the SINCROGRID project, the paper proposes the implementation of a “smart” technology solution in the form of DTR technology in Croatian transmission network. The goal of the introduction of DTR technology is to increase the capacity of transmission lines for most of the time and thus follow the connection of renewable energy sources in the period until the necessary revitalization of existing transmission lines and the construction of new ones has been realized. This “smart” solution brings other benefits to HOPS and helps to fulfill the objectives of the EU Regulation.

### BIBLIOGRAPHY

- [1] A Review of Dynamic Thermal Line Rating Methods With Forecasting, IEEE TRANSACTIONS ON POWER DELIVERY, VOL. 34, NO. 6, DECEMBER 2019; Dale A. Douglas, Huu-Minh Nguyen, Ian Grant
- [2] “Dynamic line rating implementation as an approach to handle wind power integration”, Degree project, Saifal Talpur, Sweden 2013.
- [3] “Analysis of Dynamic Thermal Rating System of Transmission Lines”, Jiashen Teh, 2016.
- [4] “Comprehensive review of the dynamic thermal rating system for sustainable electrical power systems”, Ching-Ming Lai, Jiashen Teh, Energy Reports, Volume 8, November 2022
- [5] “Comparative analysis of dynamic line rating models and feasibility to minimise energy losses in wind rich power networks”, Mathew Simms, Lasantha Meegahapola, Energy Conversion and Management, Volume 75, November 2013
- [6] “Dynamic thermal rating of transmission lines: A review”, Soheila Karimia , Petr Musilekb, Andrew M. Knight, Renewable and Sustainable Energy Reviews, Volume 91, August 2018



# Classification of Power Quality Events in the Transmission Grid: Comparative Evaluation of Different Machine Learning Models

[umut.guvengir@tubitak.gov.tr](mailto:umut.guvengir@tubitak.gov.tr)**UMUT GÜVENGİR\*, DILEK KÜÇÜK, SERKAN BUHAN,**  
*TÜBİTAK Marmara Research Center***CUMA ALİ MANTAŞ, MURATHAN YENİCELİ**  
*Turkish Electricity Transmission Corp. (TEİAŞ)***Türkiye**

## SUMMARY

Automatic classification of electric power quality events with respect to their root causes is critical for electrical grid management. In this paper, we present comparative evaluation results of an extensive set of machine learning models for the classification of power quality events, based on their root causes. After extensive experiments using different machine learning libraries, it is observed that the best performing learning models turn out to be Cubic SVM and XGBoost. During error analysis, it is observed that the main source of performance degradation for both models is the classification of ABC faults as ABCG faults, or vice versa. Ultimately, the models achieving the best results will be integrated into the event classification module of a large-scale power quality and grid monitoring system for the Turkish electricity transmission system.

## 1. INTRODUCTION

Automatic detection, monitoring, analysis, and classification of power quality events are crucial for effective management of the electricity transmission grid. Classification of power quality events has been extensively studied in the literature, especially in the last two decades. In the context of designing the event classification module, relevant articles in the literature have been systematically reviewed and categorized in terms of the methods and algorithms used in these studies. Although obtaining raw data, dividing the data into parts, and processing the data using signal processing methods are common and standard stages in event classification studies, extracting the necessary features of the data to be used in classification algorithms, selecting the best features among these extracted features, and classifying these selected features using different methods and algorithms can increase the accuracy of classification. Various signal transformations are used in the feature extraction stage while metaheuristic optimization algorithms are preferred in the feature selection stage. Finally, machine learning algorithms, including deep learning-based algorithms, are used in the classification stage.

In this work, we present the evaluation results of different machine learning models for the classification of power quality events with respect to their root causes. At the end of our tests, the classification of possible root causes of events is achieved with high accuracy by using different machine learning algorithms. The best performing models will be integrated into the event classification module of a large-scale AI-based power quality and grid monitoring system designed and implemented for the Turkish electrical grid. Further comparative tests will also be conducted using deep learning models, as part of future work. In the rest of the paper, first a survey of relevant studies is presented, next, evaluation results of the machine learning-based event classification are provided, after a discussion of these significant results, the paper is concluded with a summary of points.

## KEYWORDS

Power quality event, fault classification, machine learning, artificial intelligence



**Oral Presentation:** Classification of Power Quality Events in the Transmission Grid: Comparative Evaluation of Different Machine Learning Models

## 2. LITERATURE SURVEY

Articles published on event classification in the literature generally focus on the classification of event types itself, and there are relatively fewer studies on the classification of possible root causes of events. Since the methods and algorithms used in feature extraction, feature selection, and classification stages in event classification can also be used in the classification of event causes, articles that do not focus on event causes have also been examined.

In the process of classifying the causes of an event, it is crucial to extract the necessary features from the signal by processing the raw data correctly. Classification algorithms only work efficiently when the relevant features of the signals are extracted. For this stage, many different signal processing methods have been proposed and employed in the literature. Wavelet Transform (WT) based methods have gained more popularity recently with the utilization of Continuous Wavelet Transform (CWT), and more frequently Discrete Wavelet Transform (DWT). Although the selection of the mother wavelet function is crucial for this method, the Daubechies-4 (db4) mother wavelet is mostly used in the literature as it detects fast transient signals with higher accuracy in power quality studies [1-3]. The DWT method is preferred more due to its minimum processing time and high accuracy compared to other signal processing methods which include Stockwell Transform (S-Transform), Hilbert Huang Transform (HHT), and Curvelet Transform (CT) [4-6]. After applying the selected signal processing method to the raw event data, statistical features such as mean value, maximum value, variance, standard deviation, RMS, kurtosis, skewness, and entropy are calculated to generate the scalar features of the signals to be utilized during the classification stage [3]. It is also commonly observed in the literature that metaheuristic optimization algorithms, clustering, and dimension reduction methods are utilized for selecting the optimal subset of the feature set to prevent high variance and overfitting problems in the classification stage [3, 7, 8].

Rule-based algorithms and expert systems were mainly used for classification purposes in the studies conducted in the last decade; however, machine learning algorithms, including deep learning-based algorithms, are applied more frequently in the current studies in parallel with the recent developments in the field of artificial intelligence [9]. Furthermore, it has been observed that classification of the root causes of events is performed with combined (ensemble) algorithms which involves application of multiple algorithms together [1].

Some notable machine learning algorithms include Artificial Neural Network (ANN), which has an adaptive structure and improve its performance by adjusting its parameters during the training process, Support Vector Machine (SVM), which is a vector space-based classification algorithm that finds a linear or nonlinear multidimensional decision boundary that separates a dataset into two distinct parts, K-Means Clustering and K-Nearest Neighbor (KNN) algorithms, which are methods to reveal hidden patterns in data by dividing it into groups containing similar objects [10-13]. Other machine learning algorithms include Logistic Regression (LR), Decision Tree (DT), Extreme Learning Machine (ELM), and XGBoost [1, 4, 14]. Although deep learning is often referred to as a separate category of artificial intelligence, it is often considered as a subcategory of machine learning, as well. Convolutional Neural Networks (CNN) are particularly used in the field of image processing whereas Recurrent Neural Networks (RNN) are mainly utilized for time-series data [15, 16]. Autoencoders are also found to be effective in detecting the relationships in the input data [17]. Some notable studies about the classification of root causes of events can be found in [3, 4, 9, 10, 18-23].

## 3. EVALUATION OF EVENT CLASSIFICATION MODELS

### 3.1. Power Quality Events

The purpose of the event classification is primarily to identify a wide range of root causes of faults and events by recognizing waveforms on the power quality and grid monitoring system. In this study, there are 13 event classes considered, the first 11 of which correspond to transmission system faults: AG, BG, CG, ABG, ACG, BCG, ABCG, AB, AC, BC, ABC faults, line energizing, and line de-energizing. There will also be more additions of root causes of events to be classified by the module in the future such as induction motor starting, transformer energizing, capacitor and reactor switching.

### 3.2 Classification Models and Features

In the feature extraction stage, DWT method has been used. With the DWT method, the three-phase voltage and current signals in each data have been transformed into 5 detailed and 1 approximate coefficient signals using the 5-level db4 mother wavelet. To convert these coefficient signals into scalar magnitudes, statistical features such as mean, standard deviation (SD), root-mean-square (RMS), energy, skewness, kurtosis, Shannon entropy, and maximum bandwidth have been used. These calculated scalar magnitudes are used later as extracted features specific to the signal in the classification stage.



**Oral Presentation:** Classification of Power Quality Events in the Transmission Grid: Comparative Evaluation of Different Machine Learning Models

Machine learning algorithms (without deep learning algorithms) have been currently used during the classification stage, yet, as part of future work, deep learning based machine learning algorithms will be employed for classification, as well. The feature set obtained by processing the event data are used during the classification phase, both using the algorithms in the "Classification Learner" module of the MATLAB platform and various machine learning algorithms implemented in the scikit-learn open-source machine learning library<sup>1</sup> implemented with the Python programming language. These algorithms generally include statistical algorithms such as ANN, SVM, DT, and clustering methods. There are 30 different classifiers (including various derivatives of these models) in the "Classification Learner" module of the MATLAB platform, and 8 different classifiers are applied in the Python environment.

### 3.3 Training and Test Datasets

Training and test datasets are created using PSCAD simulation software; however, real events collected from the Turkish electricity transmission grid will be classified in the aforementioned grid monitoring system. The datasets comprise 150 training and 150 testing samples for each class where these samples are produced with the sampling frequency of 4 kHz and each sample includes 3-phase voltage and current data for 0.25 seconds. To ensure data diversity, the time of the fault occurrence, the fault resistance, the location where the fault occurred on the transmission line, the operation time of the circuit breaker, the resistance, inductance and capacitance values of the load were changed as parameters in a wide range.

### 3.4. Evaluation Results

Firstly, 30 machine learning models in MATLAB software are trained and tested on the datasets. The evaluation results are presented in Table 1 where the best and worst performing models and their accuracies are shown in boldface.

*Table 1. Evaluation Results of Machine Learning Models in MATLAB*

Model	Accuracy	Model	Accuracy
<b>Cubic SVM</b>	<b>97.5%</b>	Wide Neural Network (NN)	92.3%
Linear SVM	97.0%	Trilayered NN	92.1%
Linear Discriminant	96.7%	Cosine KNN	92.0%
Medium NN	96.1%	SVM Kernel	91.0%
Medium Gaussian SVM	96.1%	Gaussian Naive Bayes	89.8%
Coarse Gaussian SVM	96.0%	Bagged Trees	92.5%
Quadratic SVM	95.3%	Logistic Regression Kernel	89.8%
Fine KNN	94.8%	Cubic KNN	88.5%
Narrow NN	93.9%	Kernel Naive Bayes	88.2%
Boosted Trees	93.7%	Medium Tree	87.1%
Subspace Discriminant	93.5%	RUSBoosted Trees	87.1%
Weighted KNN	93.4%	Fine Tree	87.0%
Bilayered NN	93.2%	Coarse KNN	77.1%
Subspace KNN	92.8%	Fine Gaussian SVM	36.6%
Medium KNN	92.5%	<b>Coarse Tree</b>	<b>29.3%</b>

Next, similar tests are performed using the open-source scikit-learn machine learning library written in Python and evaluation results of 8 machine learning models are shown in Table 2.

<sup>1</sup> <https://scikit-learn.org/>





Oral Presentation: Classification of Power Quality Events in the Transmission Grid: Comparative Evaluation of Different Machine Learning Models

Table 2. Evaluation Results of Machine Learning Models in scikit-learn Library

Model	Accuracy	Model	Accuracy
XGBoost	97.0%	RBF SVC	92.7%
Linear SVC	96.6%	Decision Tree	91.9%
Logistic Regression	94.1%	Random Forest	90.7%
KNN	93.3%	Gaussian Naive Bayes	90.2%

As the best performing algorithm, the confusion matrix of the Cubic SVM algorithm is presented in Figure 1.

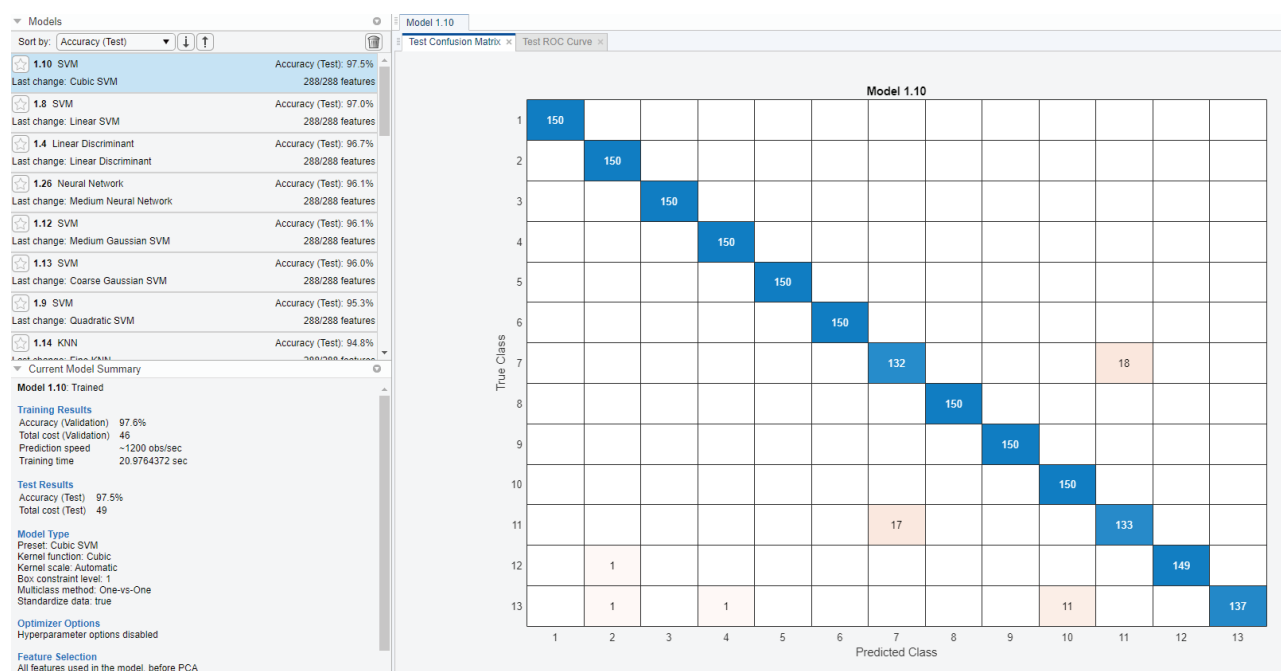


Figure 1. Confusion Matrix for the Cubic SVM Algorithm

### 4. DISCUSSION OF THE RESULTS

It can be seen from Table 1 and 2 that the Cubic SVM algorithm, which is a variation of the SVM algorithm, succeeded the classification of 13 different event cause types with a high accuracy of 97.5% in MATLAB whereas the XGBoost algorithm, which is a DT algorithm, achieved this classification with a high accuracy of 97% in the scikit-learn library of Python. As can be observed from the confusion matrix in Figure 1, the algorithm classifies almost all event cause types with high accuracy, but makes a few mistakes when distinguishing between actual ABC and ABCG faults, which stands as the main source of performance degradation for both models.

As part of future work based on the current study:

- Similar experiments will be performed after fine-tuning model parameters.
- Deep learning models will be tested and compared with machine learning models.
- A wider range of (finer granularity) event classes will be considered during classification.
- Other statistical features and feature extraction methods will be applied to the current problem settings.
- The best performing machine learning models will be integrated into the large-scale electric power quality and grid monitoring system (called TEKIS), a preliminary version of which was presented in [24].



**Oral Presentation:** Classification of Power Quality Events in the Transmission Grid: Comparative Evaluation of Different Machine Learning Models

## 5. CONCLUSION

In this study, we present the evaluation results of an extensive set of machine learning models for the classification of power quality events with respect to their root causes. The corresponding tests are performed in two distinct platforms: MATLAB tool and scikit-learn open-source machine learning platform. It is observed that the highest performing model in the MATLAB platform is Cubic SVM and the best performing model in scikit-learn library is XGBoost. The best performing models will be integrated into the event classification module of a large-scale nationwide grid monitoring system. Deep learning models and finer granularity event classes will be employed as part of future studies.

## 6. ACKNOWLEDGMENT

This research and technology development work is carried out within the scope of TEİAŞ Electric Power Quality and Grid Monitoring System (TEKİS) Project (with project number 5212802) developed for TEİAŞ by TÜBİTAK Marmara Research Center.

## BIBLIOGRAPHY

- [1] P. Radhakrishnan, K. Ramaiyan, A. Vinayagam, & V. Veerasamy "A stacking ensemble classification model for detection and classification of power quality disturbances in PV integrated power network" (Measurement, 2021, 175)
- [2] Z. Dawood, C. K. Babulal "Power quality disturbance classification based on efficient adaptive Arrhenius artificial bee colony feature selection" (Int Trans Electr Energ Syst., 31, 2021)
- [3] H. Erişti, Ö. Yıldırım, B. Erişti, & Y. Demir "Optimal feature selection for classification of the power quality events using wavelet transform and least squares support vector machines" (International Journal of Electrical Power & Energy Systems, 49, 2013, pages 95-103)
- [4] H. Erişti, Ö. Yıldırım, B. Erişti, & Y. Demir "Automatic recognition system of underlying causes of power quality disturbances based on S-Transform and Extreme Learning Machine" (International Journal of Electrical Power & Energy Systems, 61, 2014, pages 553-562)
- [5] M. Sahani, & P. K. Dash "Automatic power quality events recognition based on Hilbert Huang Transform and weighted bidirectional Extreme Learning Machine" (IEEE Transactions on Industrial Informatics, 14(9), 2018, pages 3849-3858)
- [6] I. S. Samanta, P. K. Rout, & S. Mishra "Feature extraction and power quality event classification using Curvelet transform and optimized Extreme Learning Machine" (Electrical Engineering, 103, 2021, pages 2431-2446)
- [7] O. A. Alimi, K. Ouahada, A. M. Abu-Mahfouz, & S. Rimer "Power system events classification using genetic algorithm based feature weighting technique for support vector machine" (Heliyon, 7(1), 2021)
- [8] R. Hooshmand, & A. Enshae "Detection and classification of single and combined power quality disturbances using fuzzy systems oriented by particle swarm optimization algorithm" (Electric Power Systems Research, 80(12), 2010, pages 1552-1561)
- [9] S. Xie, F. Xiao, Q. Ai, & G. Zhou "Classification of underlying causes of power quality disturbances using data fusion" (2018 International Conference on Power System Technology (POWERCON), 2018, pages 4118-4123)
- [10] R. J. Haddad, B. Guha, Y. Kalaani, & A. El-Shahat "Smart distributed generation systems using artificial neural network-based event classification" (IEEE Power and Energy Technology Systems Journal, 5(2), 2018, pages 18-26)
- [11] M. Shafiullah, M. J. Rana, M. E. Haque, A. Islam, S. M. Rahman, M. S. Alam, & A. Ali "An intelligent approach for power quality events detection and classification" (2021 1st International Conference on Artificial Intelligence and Data Analytics (CAIDA), 2021, pages 194-199)
- [12] Rahul & B. Choudhary "An advanced genetic algorithm with improved support vector machine for multi-class classification of real power quality events" (Electric Power Systems Research, 191, 2021)
- [13] Y. Liu, T. Jin, M. A. Mohamed, & Q. Wang "A novel three-step classification approach based on time-dependent spectral features for complex power quality disturbances" (IEEE Transactions on Instrumentation and Measurement, 70, 2021, pages 1-14)
- [14] L. Yang, Y. Li, & C. Di "Application of XGBoost in identification of power quality disturbance source of steady-state disturbance events" (2019 IEEE 9th International Conference on Electronics Information and Emergency Communication (ICEIEC), 2019, pages 1-6)
- [15] C. I. Garcia, F. Grasso, A. Luchetta, M. C. Piccirilli, L. Paolucci, & G. Talluri "A comparison of power quality disturbance detection and classification methods using CNN, LSTM and CNN-LSTM" (Applied Sciences, 10(19), 2020, page 6755)
- [16] R. Machlev, A. Chachkes, J. Belikov, Y. Beck, & Y. Levron "Open source dataset generator for power quality disturbances with deep-learning reference classifiers" (Electric Power Systems Research, 195, 2021)
- [17] C. O'Donovan, C. Giannetti, & G. Todeschini "A novel deep learning power quality disturbance classification method using autoencoders" (Proceedings of the 13th International Conference on Agents and Artificial Intelligence (ICAART 2021), 2, 2021, pages 373-380)
- [18] E. Styvaktakis, M. H. J. Bollen, & I. Y. H. Gu "Automatic classification of power system events using RMS voltage measurements" (IEEE Power Engineering Society Summer Meeting, 2, 2002, pages 824-829)
- [19] M. H. J. Bollen, I. Y. H. Gu, P. G. V. Axelberg, & E. Styvaktakis "Classification of underlying causes of power quality disturbances: Deterministic versus statistical methods" (EURASIP J. Adv. Signal Process, 2007)



**Oral Presentation:** Classification of Power Quality Events in the Transmission Grid: Comparative Evaluation of Different Machine Learning Models

- [20] R. Sinvula, K. M. Abo-Al-Ez, & M. T. Kahn "Harmonic source detection methods: A systematic literature review" (IEEE Access, 7, 2019, pages 74283-74299)
- [21] W. Wang, H. Yin, C. Chen, A. Till, W. Yao, X. Deng, & Y. Liu "Frequency disturbance event detection based on synchrophasors and deep learning" (IEEE Transactions on Smart Grid, 11(4), 2020, pages 3593-3605)
- [22] Y. Ma, X. Xiao, & Y. Wang "Identifying the root cause of power system disturbances based on waveform templates" (Electric Power Systems Research, 180, 2020)
- [23] X. Jiang, B. Stephen, & S. McArthur "Automated distribution network fault cause identification with advanced similarity metrics" (IEEE Transactions on Power Delivery, 36(2), 2021, pages 785-793)
- [23] X. Jiang, B. Stephen, & S. McArthur "Automated distribution network fault cause identification with advanced similarity metrics" (IEEE Transactions on Power Delivery, 36(2), 2021, pages 785-793)
- [24] D. Küçük, S. Buhan, T. Demirci, M. B. Özkan, M. S. Çınar, E. Altıntaş, U. Güvengir, S. B. Çelik, S. Uçar, C. A. Mantaş, M. Yeniceli, N. Noyan, M. Yeşil, Ş. N. Güler, İ. E. Kayaoğlu, U. Yener & K. Ç. Bayındır "TEKİS: TEİAŞ Electric Power Quality and Grid Monitoring System" (Power Systems Conference, 10, 2022)



# Impact of the Hydrological Risk on the Power Grid: A Case Study on a Portion of the Italian Transmission Power System Exposed to the Hazard of Flooding

[silverio.casulli@terna.it](mailto:silverio.casulli@terna.it) / [emanuele.ciapessoni@rse-web.it](mailto:emanuele.ciapessoni@rse-web.it)**ENRICO MARIA CARLINI, FRANCESCO MARZULLO (1), SILVERIO CASULLI\*, FRANCESCA SCAVO, GRETA MAGNOLIA, FEDERICO FALORNI, ALESSANDRO LAZZARINI***Terna S.p.A.***EMANUELE CIAPESSONI, DIEGO CIRIO, ANDREA PITTO, LEONARDO MANCUSI,***Ricerca sul Sistema Energetico – RSE S.p.A.***Italy**

## SUMMARY

The increasing frequency and severity of extreme events in the last few years poses new challenges for the planning of more resilient power grids. This calls for new tools and methodologies to perform a resilience informed planning of modern grids. To this purpose, the Italian TSO Terna and Ricerca sul Sistema Energetico – RSE S.p.A have developed a risk-based methodology with the aim to assess the resilience of the electricity system to prioritize the interventions for resilience enhancement in the context of long-term grid planning.

Due to its geomorphologic configuration and geological characteristics, more than one third of the Italian Peninsula territory is “exposed” to hydrogeological hazards (mainly landslides and floods), which represent the third cause of failures in the Italian electric system, after wind and wet snow events.

In this work the authors propose probabilistic models for floods and for the grid asset vulnerability to the same hydrological hazard and integrate them in the resilience risk-based assessment methodology, thus extending its application domain to flooding events, with the goal to evaluate the failure return periods of the grid assets due to floods, a first step to quantify the risk associated to such threat. The case study related to some sample areas of the grid particularly exposed to floods demonstrates the possibility of application of the methodology to hydrological threats.

## KEYWORDS

Hydrological risk; flooding; hazard map; vulnerability model; failure probability; power system resilience; transmission power grid.



Oral Presentation: Impact of the Hydrological Risk on the Power Grid: A Case Study on a Portion of the Italian Transmission Power System Exposed to the Hazard of Flooding

### 1. INTRODUCTION

Hydrogeological phenomena represent a serious and impacting threat to critical infrastructures (roads, energy systems, water, and gas pipelines, etc.) [1]. In the Italian electric system, hydrogeological extreme events are quite rare: a total number of 50 events were recorded on the Italian transmission grid in the period 2010-2021: they led to component outages, not necessarily connected to load disruptions. Only 9 major events with significant load disruptions were counted between 2013 and 2020, against over 1000 events due to snow and wind, but they were responsible for 2800 MWh of Energy Not Supplied (ENS) equal to about 10% of the total ENS due to extreme events in the same period, representing the third cause of utility outages, after wind and wet snow. In general, they are a major cause of energy supply disruptions worldwide and both the number of extreme hydrogeological events and the amount of relevant economic losses significantly increased in the period 1960-2014 [2].

The pie chart in Figure 1 reports some statistics about the types of hydrogeological threats which have been recorded in the Italian transmission system. The most common events are shallow landslides and debris flows, classified as landslide hazardous events, and river overflows and floods due to heavy rainfalls, classified as hydrological hazardous events. In general, substation equipment is more affected by floods while line towers are more affected by landslides. However, a strict classification is not simple because hydrogeological phenomena are very complex and linked to each other: e.g. a flood can evidently also cause debris flows, strong rainfalls can cause substation floodings but they can also provoke river overflows with consequent erosive phenomena which can lead to river bank failures and mechanical instability of the tower foundations close to the riverbanks. Debris flow can also bring trees in touch with overhead line conductors, causing faults to ground or mechanical damages.

What is clear is the wide variety of modes how hydrogeological threats can affect the transmission grid, with both tower and substation failures, as evidenced by historical failure events recorded in the Italian power system.

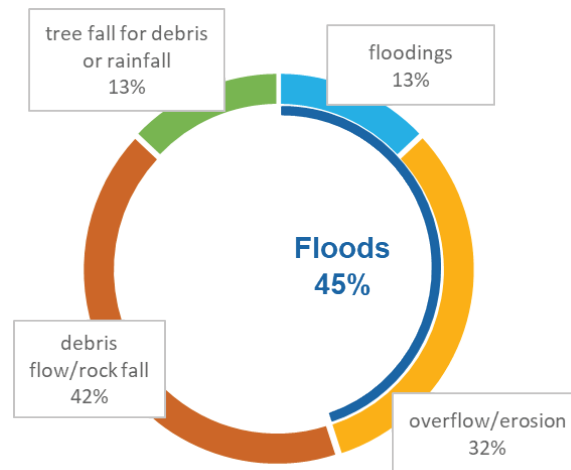


Figure 1. Statistics about the types of hydrogeological threats.

Figure 2 shows examples of damage to the electricity grid infrastructure due to foundation instability due to riverbank failure and flooding.



(a)



(b)

Figure 2. Examples of hydrogeological events impacting the electrical infrastructure (a) failure of a river bank, (b) flooding of a substation. Source: TERNA.



Oral Presentation: Impact of the Hydrological Risk on the Power Grid: A Case Study on a Portion of the Italian Transmission Power System Exposed to the Hazard of Flooding

In the sequel, the focus is on the flooding events, because more refined modelling of threats is available at the present research knowledge.

## 2. RECALL OF THE RISK BASED RESILIENCE ASSESSMENT METHODOLOGY

Figure 1 recalls the architecture of the methodology for resilience assessment jointly developed by Terna and RSE [3].

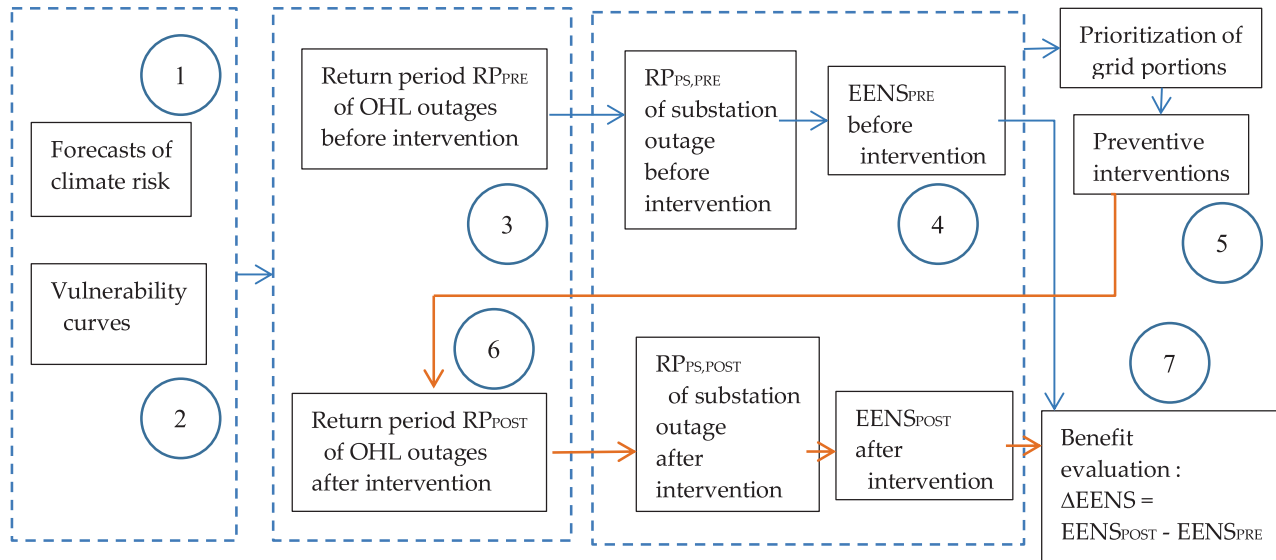


Figure 3. Architecture of the resilience assessment methodology [3]: the circles include the number of each step of the methodology.

The methodology consists of the following 7 main steps:

1. Calculating the probability of occurrence of meteorological phenomena in the future as a function of predefined intensity thresholds using a climatological model.
2. Quantifying the vulnerability of the grid components as a function of the intensity of the meteorological event considered, through the development of vulnerability curves applied to a georeferenced grid model.
3. Combining the probabilistic model of the weather event (derived in step 1) with the vulnerability curve (from step 2) of the grid components, specifically lines, which leads to the Return Period of outages of the components in “pre-intervention phase” ( $RP_{PRE}$ ) i.e. in the initial conditions.
4. Determining the Return Period ( $RP_{PS,PRE}$ ) of the substations and the corresponding value of expected energy not served by applying a cascading outage simulator.
5. Identifying possible interventions aimed at increasing resilience based on the analysed meteorological events and the characteristics of the reference area and its relevant lines with reference to the critical substations in terms of return period and damage extent.
6. Evaluating the impact of the interventions identified in step 5, for instance measured in terms of increase of the Return Period of the line ( $RP_{POST}$ ). This is achieved by running the cascading outage simulator, assuming that the interventions have been implemented, and determining the new return period of the substations.
7. Calculating the resilience benefit associated with each identified intervention in terms of reduction of the Expected Energy Not Served (EENS).

The methodology is general and can be applied to any kind of threat. Moreover, it can potentially consider preventive, mitigation, and restoration measures. However, the present paper focuses on preventive solutions and on the events caused by floods in the transmission grid, because it represents one of the main threats affecting the Italian transmission grid. Accordingly, this work presents the vulnerability model of the components which are most exposed to this threat, i.e., the overhead lines (OHL) and substation equipment.





Oral Presentation: Impact of the Hydrological Risk on the Power Grid: A Case Study on a Portion of the Italian Transmission Power System Exposed to the Hazard of Flooding

## 3. VULNERABILITY MODEL FOR GRID ASSETS TO FLOODS

This section focuses on the analytical model for the vulnerability of grid assets (both line towers and substation equipment) to floods.

### 3.1. The proposed analytical model to assess grid asset vulnerability to floods

The proposed model considers the displacement  $u$  (in m) of the power system component, produced by a flow of water as the stress variable acting on the components. This displacement can be due to two elements:

- Hydrostatic pressure of the height of the water flow,
- Dynamic pressure caused by the impacting speed of the water flow on the infrastructure.

This model currently neglects the dynamic force due to the impacts of water borne objects (e.g. tree logs), due to the high uncertainty affecting the data concerning vegetation (e.g. actual forecast standing density, mechanical and geometrical properties of the tree logs).

The vulnerability model accounts for two main phenomena:

- excessive reduction of the clearance between energized parts (e.g. conductors of OHLs) and the ground,
- mechanical damage due to water flow height and speed.

Sophisticated models based on FEM [4] can model in detail the interaction between individual structures (e.g. a line tower) and the environment, but their application is difficult to extend to large power systems. Thus, tools to support resilience informed decision making in the long-term planning call for an analytical model which can be a trade-off between accuracy and applicability.

The proposed physically inspired model accounts for the two aforementioned phenomena. It is obvious that the vulnerability of power system components to floods depends on the features of the specific component, e.g. underground cables are not vulnerable to floods.

### 3.2. Flashover model

The phenomenon of electric flashover to ground occurs when the distance in the air between the energized part of the component and the ground is less than a certain minimum distance (dielectric distance). This is the major cause of failure of substation equipment which are characterised by smaller dielectric distances with respect to line towers.

In order to model the conditional probability of failure due to flashover, a normal distribution of the flood height is used centred on a value equal to the difference between the lowest height  $h_{\text{MIN}}$  of energized parts of the component with respect to the ground decreased by the dielectric distance which in turn is a function of the voltage level of the component [5].

The methodology specifies parameter  $h_{\text{MIN}}$  for each substation piece of equipment (two- and three-winding transformers, circuit breaker, measurement transformers), based on standard parameters available from Terna for the modelling of the Italian Transmission System.

### 3.3. Mechanical damage model

Displacement  $u$  - that is the stress variable of the model - is caused by the action of the environmental variables  $h$  and  $v$  (respectively the height and speed of the flood) on the structures. The vulnerability curve takes the lognormal form in (1), derived from [6][7].

$$PV = \Phi \left[ \frac{1}{\beta_s} \ln \left( \frac{u_x}{S_s} \right) \right] \quad (1)$$

where  $F$  is the cumulative normal distribution function. Parameters  $b_s$  and  $S_s$  depend on the level of damage of the structure. In this paper, parameters corresponding to complete disruption are assumed because resilience analyses are focused on severe damages on the grid infrastructures and service, with long recovery time.

Displacement  $u_x$  undergone by the component in (2) and caused by a flood is given by the sum of two contributions  $u_x = u_{st} + u_{dyn}$  caused by two distinct actions:  $u_{st}$  due to the hydrostatic pressure of the waterflow at height  $h$ ,  $u_{dyn}$  due to the dynamic pressure of the waterflow with speed  $v$ .



**Oral Presentation:** Impact of the Hydrological Risk on the Power Grid: A Case Study on a Portion of the Italian Transmission Power System Exposed to the Hazard of Flooding

Displacement  $u_{st}$  due to hydrostatic pressure is in (2), derived from [7].

$$u_{st} = g \cdot h^2 \cdot b \cdot \frac{\rho}{2k} \quad (2)$$

where  $r$  is the density of the waterflow,  $b$  is the width of the structure,  $k = 4pm^2/T_n^2$  is the stiffness of the structure where  $m$  and  $T_n$  are the mass and the natural period of the structure:  $T_n$  in turn depends on the height of the same object based on (3) from [6].

$$T_n = 0.0625 \cdot H^{3/4} \quad (3)$$

Displacement  $u_{dyn}$  due to the dynamic pressure is instead linked to the speed of the flow. On the basis of the composition of the flow (in terms of solid and liquid phases), the model can account for these two types of contribution linked to the flow speed:

1) impact of the flood which determines an impulsive force on the structure given in (4), from [7].

$$F_{dyn1} = \rho \cdot A \cdot v^2 \quad (4)$$

where  $A$  is the effective area of the object impacted by the flood (also considering the solidity factor in the case of lattice structures)

2) impact of solid objects borne by the flow on the structure. In case of round boulders, the impulsive force due to the shock is estimated by Hertz equation [8] in (5).

$$F_{dyn2} = 4 \cdot 10^6 \cdot K_c \cdot \sqrt{v} \cdot R^2 \text{ in N} \quad (5)$$

where  $R$  is the radius of the boulder,  $v$  is the speed in m/s,  $K_c$  is the load reduction factor [8].

In the present paper the focus is on the floods, i.e., the dominant phase in the flows is the liquid phase while the solid phase (composed by mud, stones, water borne objects) is neglected even though solid objects can contribute to the displacement of the structure due to the impulsive forces they apply to the infrastructure.

### 3.4. Integration of an example of flood protection system: the plinth

Grid operators have developed many solutions to protect their substations from flooding events, such as barriers to substations, drainage pumps, etc. the present paper integrates an example of these measures, specifically the application of a plinth to increase the elevation of the substation equipment, in the vulnerability model proposed above.

Specifically, height  $h_{MIN}$  described in subsection 3.2 is given by  $h_{MIN} = h_c + h_{bs}$  where  $h_{bs}$  is the height of the plinth and  $h_c$  is the lowest height of energised parts from the plinth (also accounting for possible by-pass insulators).

As far as the mechanical damage model proposed in subsection 3.3 is concerned, the presence of a plinth height decreases the water height "seen" by the impacted grid structure (assuming the plinth completely resilient to the flood). This implies that the flow height considered in subsection 3.3 is given by the actual water height at plinth level i.e. the water height at ground minus the plinth level.

## 4. INTEGRATION OF THE VULNERABILITY MODEL IN THE METHODOLOGY

This section presents the probabilistic model adopted for flood events and the integration of this model with the aforementioned vulnerability model inside the Terna-RSE methodology for the prioritization of the intervention for resilience enhancement in the national Italian transmission system.

### 4.1. Probabilistic modelling of floods

The main database used for the flood hazard assessment are the results of the Italy application of the EU Directive 2007/60/EC [9]. This Directive established a framework on the assessment and management of flood risk in Europe: in Italy the Legislative decree



**Oral Presentation:** Impact of the Hydrological Risk on the Power Grid: A Case Study on a Portion of the Italian Transmission Power System Exposed to the Hazard of Flooding

49/2010 transposed Directive 2007/60/EC, taking into account the national legislation.

The Directive required each member state to prepare Flood Risk Management Plans (FRMPs) covering every aspect of flood risk. FRMPs should be periodically reviewed and if necessary updated through new information about changes occurred, also taking into account how climate change will affect flooding.

The Italian FRMPs are developed by the Prime Competent Authorities, constituted by the 5 River Basin District (Po River, Eastern Alps, Northern Apennines, Central Apennines and Southern Apennines) and the 2 Regional Authorities (Sicily and Sardinia).

Prime Competent Authorities have prepared Flood Hazard maps according to the following scenarios:

1. low probability (extreme events),
2. medium probability (likely return period  $\geq 100$  years)
3. high probability

The Ministry for Environment, Land and Sea Protection publishes the information regarding Flood Hazard maps through the website "National Geoportal" [10], according to the indications of INSPIRE Directive 2007/2/EC [11] on the infrastructure for spatial information sharing.

The latest Flood Hazard maps are from the December 2021 update and show, for each scenario, the flood extents. In the current release, only in some areas they also show water depth and, in a few cases, flow velocities.

Since, in addition of flood extent, also the inundation depth and flow velocity are key factors for estimation of direct flood damage, we have developed a tool, using a Python script, to estimate these values in areas of interest where these data are not available.

For a fast application, our tool calculates water depths based only on an inundation map with an associated Digital Elevation Model (DEM). To identify flooded domain boundary locations (grid-cells), flood inundation polygons from "National Geoportal" are used. The tool calculates water depth by deducting local floodwater elevation (above mean sea level) from the topographic elevation at each grid-cell within the flooded domain. Elevation of each grid-cell at the boundary locations of flooded domain (red line in Figure 4) is derived from a Digital Elevation Model (DEM). While any DEM can be used, its horizontal and vertical resolutions can have a major impact on the tool's accuracy: in our elaborations we use the 5-m DEM of the Italian Regions which, from the tests carried out, was found to be able to provide good performance.

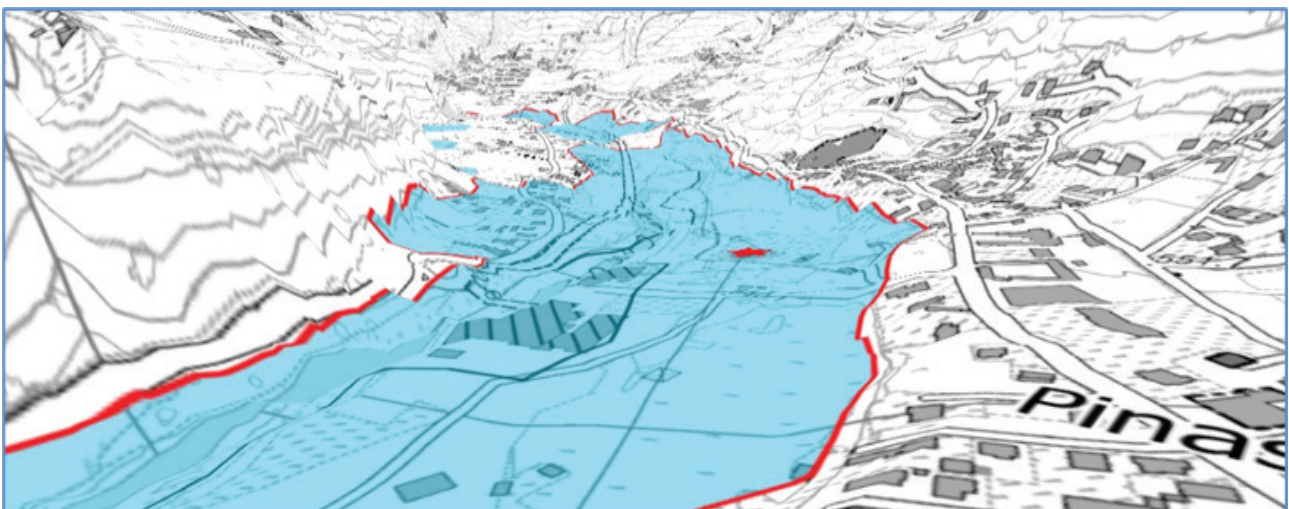


**Figure 4.** A 3D view of an inundation map with an associated Digital Elevation Model.

The core of the tool algorithm is the identification of local floodwater elevation. The water depth calculation follows this following procedure similar to those in Figure 5: (1) conversion of the inundation polygon to a line layer, (2) creation of a raster layer from the line layer that has the same grid-cell size and alignment as the DEM, (3) extraction of the DEM value (elevation) for these grid-cells (referred to as boundary grid-cells), (4) allocation of the local floodwater elevation for each grid-cell within the flooded domain using a two-dimensional interpolation from the nearest boundary grid-cell end (5) calculation of water depth at any point using the difference in surface floodwater elevation and inundated land elevation from topographic elevation at each grid-cell within the flooded domain.



Oral Presentation: Impact of the Hydrological Risk on the Power Grid: A Case Study on a Portion of the Italian Transmission Power System Exposed to the Hazard of Flooding

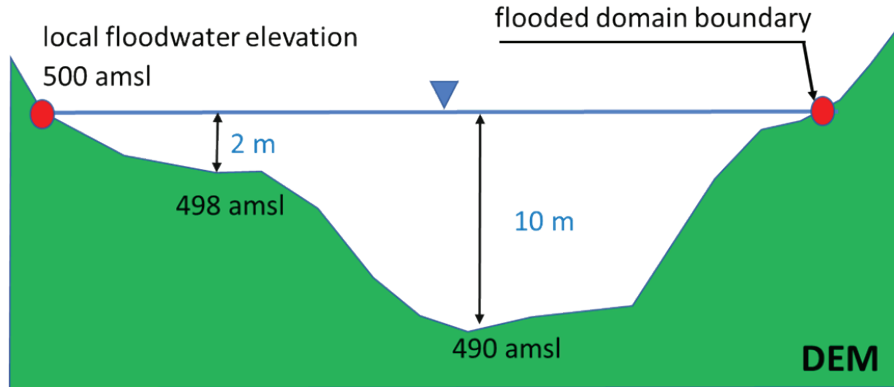


Figure 5. Theoretical floodplain cross section illustrating the floodwater depth estimation.

To carry out the interpolation referred to in point 4, we used the interpolation method available for *scipy.interpolate.griddata* that is a module included in *Scipy*: a Python library useful for scientific computing.

Once the local floodwater elevation along a stretch of the stream is obtained, the script also calculates the local slope of this 3D surface using the *gdal.DEMProcessing* that is a module included in *GDAL*: an open source MIT licensed translator library for raster and vector geospatial data formats.

Local slope and water depth are two essential variables to evaluate an estimate of the flow velocity.

In fact, to estimate the flow velocity we adopt Manning’s equation that is an empirical formula estimating the average velocity of a liquid flowing in an open channel.

$$v = \frac{1}{n} \cdot R^{1/6} \cdot \sqrt{R \cdot i} \cong \frac{1}{n} \cdot h^{2/3} \cdot \sqrt{i} \tag{6}$$

where  $v$  is flow velocity (m/s),  $n$  the Manning roughness coefficient ( $s \cdot m^{-1/3}$ ),  $h$  the water depth (m),  $R$  the hydraulic radius (m) which can be approximated to  $h$  in case of large cross sections and  $i$  is the stream slope or hydraulic gradient which we assimilate to the local slope of the water surface.

### 4.2. Calculation of the failure return periods for the grid assets

The vulnerability model shown in section 3 is combined with the GEV (Generalized Extreme Value) distribution density of the stress variables elaborated in subsection 4.1 in order to evaluate the failure probability of components to floods, as already reported in the TERNA-RSE methodology for other threats and briefly recalled below for flood threat.

In particular, the uncertainty in the flood threat intensity is modelled considering the extreme value distributions modeling the maximum annual values for the flood heights, while flood speed does not contribute to uncertainty because it’s deterministically determined as a function of the height based on uniform flow equation. Equation (7) provides the annual failure probability of component  $j$  located at  $x_j$  given density function  $p_{Thr}^{(yr)}$  and a component vulnerability model  $P_{V,j}$ .

$$P_{F,j}(x_j) = \int_S P_{V,j}(x_j) \cdot p_{Thr}^{(yr)}(x_j) ds \tag{7}$$

where  $x_j$  is the location of component  $j$ .

## 5. CASE STUDY

This section presents the results of the application of TERNA-RSE methodology extended to flooding events. It’s worth noting that the dimensions of the substation equipment do not reflect the actual layout of each substation, but they are chosen in ranges of typical values to demonstrate the effectiveness of the approach in assessing the failure return periods of the grid asset and the benefits brought by the analysed countermeasures.



Oral Presentation: Impact of the Hydrological Risk on the Power Grid: A Case Study on a Portion of the Italian Transmission Power System Exposed to the Hazard of Flooding

## 5.1. Test areas and summary of the simulations

The case study consists in the analysis of six primary substations in the North and the North-West of Italy in areas exposed to floods due to the morphological configuration of the terrain. In particular, three of them belong to the Milan Department, while the other three to the Turin department of the grid. The inundation maps with flood return periods of 500 200 and 50 years from the Basin authority are adopted for the threat modelling. For the present test case, standard data are assumed for the geometric data of the components.

As far as the parameters of the fragility curves are concerned, the study case adopts the following value  $S_s = 0.096$  for the median displacement in the vulnerability models related to the substation equipment, while the model uses the following formula  $S_s = 0.0134 * H$  adapted from [7] for the towers of the lines. The same standard deviation  $b_s = 1.18$  is adopted for all the components.

Two aspects are studied in the present case study:

1. The effect of the application of plinths as flood defence systems in substation equipment,
2. The effect of climate changes.

Conventionally, during substation design, engineers assume the application of plinths with a height corresponding to the flood height corresponding to a specific return period (say, 100 years) increased by a margin [12]. On the other side, substation design must consider more and more the potential effects of climate changes which can determine increasingly severe and frequent events in the next decades. Recent efforts are spent in climatology to evaluate plausible scenarios of future trends for precipitations [13][14].

To this purpose the paper presents the simulations summarized in Table 1.

Table 1. Summary of the simulations.

	Stationary climate	Non stationary climate
Absence of plinths	Sim 1 (base case)	Sim 3
Application of plinths	Sim 2	Sim 4

This paper does not intend to address these complex tasks to evaluate plausible scenarios of climate evolution with reference to floods. The scope is only to demonstrate the ability of the proposed methodology also to compute failure return periods over future periods, starting from a given assumption about climate changes over these periods. In the present case study, only for demonstrative purposes, the non-stationarity of climate is simulated by assuming a multiplication factor  $k_{cc}$  on the historical flood heights for the return periods of 50, 200 and 500 years.

Simulations are performed on the main equipment (circuit breakers, relays, measurement transformers, power transformers, generators, and busbar systems) for all the primary substations involved in the case studies, which include both the six substations potentially exposed to flood events (substations with ID's 1, 2, 3, 4, 10 and 12 in the sequel of the paper) and further nine substations which are connected to the six substations through branches.

For the sake of clearness, Table 2 reports the correspondence between the line code and the codes of the two substations at the line terminals.

Table 2. List of components in the grid portion analysed.

Lines	From	To
Line 1	Substation 2	Substation 4
Line 2	Substation 5	Substation 6
Line 3	Substation 7	Substation 8
Line 4	Substation 9	Substation 1
Line 5	Substation 10	Substation 11
Line 6	Substation 15	Substation 2
Line 7	Substation 13	Substation 14
Line 8	Substation 2	Substation 6
Line 9	Substation 12	Substation 3





Oral Presentation: Impact of the Hydrological Risk on the Power Grid: A Case Study on a Portion of the Italian Transmission Power System Exposed to the Hazard of Flooding

5.2. Base case Sim 1: stationary climate and absence of plinths

This simulation assumes the stationarity of climate and no plinths applied to substation equipment. Figure 6 reports an example of the water depth and speed maps with a return period of 500 years for substation 1.

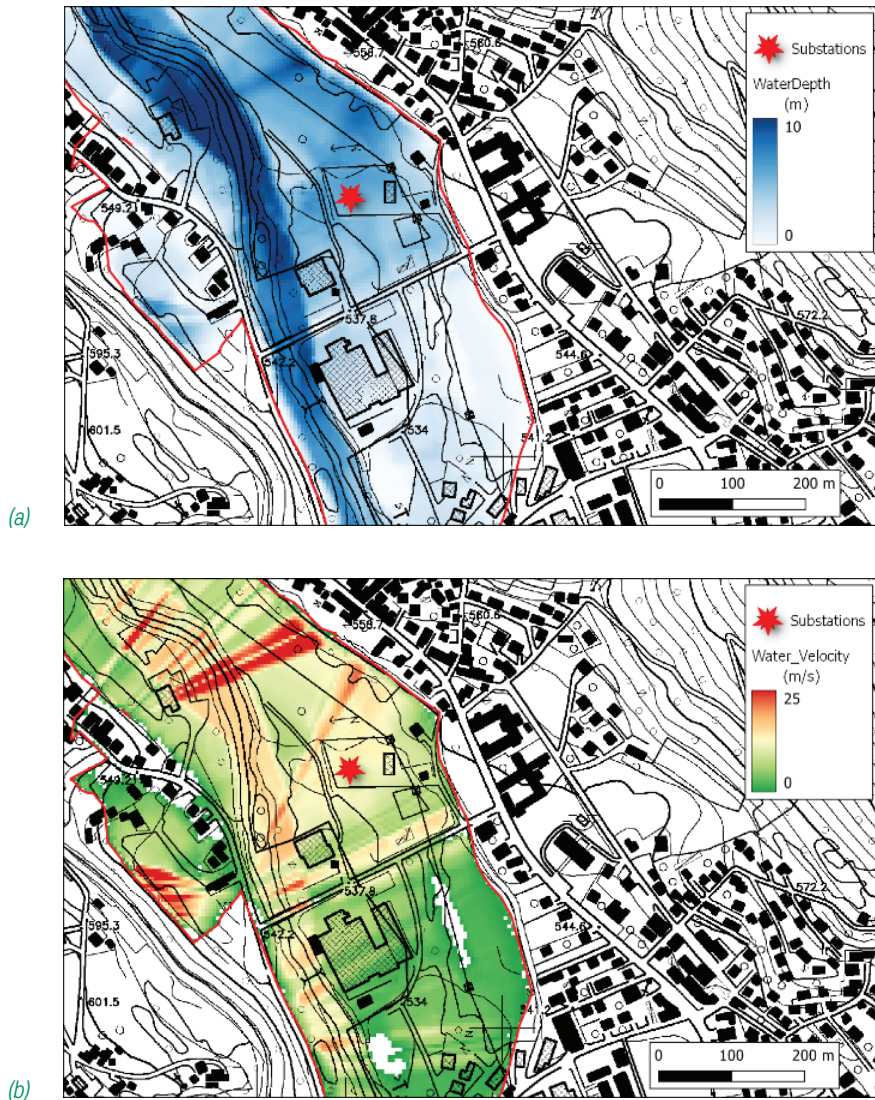


Figure 6. Map of the water depth (a) and speed (b) with return period of 500 years for SUBSTATION 1.

The «water depth» map shows how the maximum values are within the «channel» while they are lower in the « inundated land » area. This is similar also for the «water velocities» map except for limited zones, or strips with higher velocity estimates also in the «inundated land», where the evaluation of the «hydraulic gradient» is less accurate. Current developments are aimed to improve the accuracy of this estimation also in the abovementioned strips.

Table 3 reports the list of both concentrated and distributed components ranked in increasing RPs up to 500 years. It's worth noting that the components with the lowest RPs are located in the Piedmont Region, in the North of Italy, where some several faults on grid components have been recorded by Terna in the last two decades. The top-ranking components are substation equipment, in particular relays and circuit breaker due to their limited clearance distances. Line 1 has a failure RP lower than 50 years which is due to the significant flood heights and speeds which characterise the area and which can determine a mechanical damage on the towers of the line. Substation equipment failures may cause the disconnection of the entire substation which may have more severe impacts on the system with respects a single failure of a line. A risk-based approach is useful to assess the contribution of such different contingencies to the overall risk of energy not served to the customers.





**Oral Presentation:** Impact of the Hydrological Risk on the Power Grid: A Case Study on a Portion of the Italian Transmission Power System Exposed to the Hazard of Flooding

**Table 3.** List of components with increasing failure RPs (« L » stands for line, «CB» stands for circuit breaker, « Trmeas » for « measurement transformer »)

Type	Comp ID	Failure RP (years)
Relay	RELAY_SUBSTATION 1	3
Relay	RELAY_SUBSTATION 1	3
Relay	RELAY_SUBSTATION 2	15
Relay	RELAY_SUBSTATION 2	15
Relay	RELAY_SUBSTATION 2	15
Relay	RELAY_SUBSTATION 2	15
CB	CB_SUBSTATION 1	20
CB	CB_SUBSTATION 1	20
Line	LINE 1	26
Bus	BUS_SUBSTATION 1	41
Relay	RELAY_SUBSTATION 3	42
Relay	RELAY_SUBSTATION 3	42
Trmeas	Tmeas_SUBSTATION 1	65
CB	CB_SUBSTATION 2	114
CB	CB_SUBSTATION 2	114
CB	CB_SUBSTATION 2	114
CB	CB_SUBSTATION 2	114
Line	LINE 2	121
Line	LINE 3	149
Bus	BUS_SUBSTATION 2	186
Line	LINE 4	209
Trmeas	Tmeas_SUBSTATION 2	261
CB	CB_SUBSTATION 3	329
CB	CB_SUBSTATION 3	329
Line	LINE 5	374

### 5.3. Sim 2: application of plinths

This simulation assumes stationary values for the flood heights over the decades (i.e. stationarity of climate), but, unlike sim 1, plinths to increase the elevation of the substation equipment are applied. The comparison of the RP's of the substation equipment between sim 1 and sim 2 highlights that, as expected, the application of plinths cause a significant increase of the return periods of substation equipment. Specifically, all the substation equipment has a failure RP higher than 500 years. Thus, they be considered « resilient » in the future application of the Cost Benefit Analysis (CBA) for the prioritization of the interventions.

### 5.4. Sim 3: sensitivity to possible climate changes

This simulation is aimed at demonstrating the ability of the tool to quantify the effects of a possible climate evolution scenario on the failure return periods of grid asset in future periods. For didactic purposes, the simulation assumes an increase of the severity of the floods in all the areas under study, considering a factor  $k_{cc}$  equal to 1.5, and it assumes no interventions have been done (absence of plinths to raise substation equipment position). For the sake of simplicity, in the present paper the esondation areas used for the



**Oral Presentation:** Impact of the Hydrological Risk on the Power Grid: A Case Study on a Portion of the Italian Transmission Power System Exposed to the Hazard of Flooding

stationary case (sim 1) are kept the same, even though it's worth noting that an evolution of the climate towards more severe flood heights would also imply a modification of the esondation areas (in terms of shape and extension) related to 50, 200 and 500 years.

Table 4 compares the failure RPs for simulations 1 (stationarity of climate) and 3 (presence of climate changes).

**Table 4.** Comparison of failure return periods for grid components in the areas under study under the assumption of stationary climate in sim 1 (a) and of climate changes in sim 3 (b)

(a)	Type	Comp ID	Failure RP (years)	Type	Comp ID	Failure RP (years)	(b)
	Relay	RELAY_SUBSTATION1	3	Relay	RELAY-SUBSTATION1	2	
	Relay	RELAY_SUBSTATION1	3	Relay	RELAY-SUBSTATION1	2	
	Relay	RELAY_SUBSTATION2	15	Relay	RELAY-SUBSTATION2	3	
	Relay	RELAY_SUBSTATION2	15	Relay	RELAY-SUBSTATION2	3	
	Relay	RELAY_SUBSTATION2	15	Relay	RELAY-SUBSTATION2	3	
	Relay	RELAY_SUBSTATION2	15	Relay	RELAY-SUBSTATION2	3	
	CB	CB_SUBSTATION1	20	Relay	RELAY-SUBSTATION12	3	
	CB	CB_SUBSTATION1	20	Relay	RELAY-SUBSTATION12	3	
	Line	LINE 1	26	Line	LINE 3	4	
	Bus	BUS_SUBSTATION1	41	Line	LINE 1	6	
	Relay	RELAY_SUBSTATION3	42	CB	CB-SUBSTATION1	11	
	Relay	RELAY_SUBSTATION3	42	CB	CB-SUBSTATION1	11	
	Trmeas	Tmeas_SUBSTATION1	65	Line	LINE 2	16	
	CB	CB_SUBSTATION2	114	Bus	BUS-SUBSTATION1	21	
	CB	CB_SUBSTATION2	114	CB	CB-SUBSTATION2	24	
	CB	CB_SUBSTATION2	114	CB	CB-SUBSTATION2	24	
	CB	CB_SUBSTATION2	114	CB	CB-SUBSTATION2	24	
	Line	LINE 2	121	CB	CB-SUBSTATION2	24	
	Line	LINE 3	149	CB	CB-SUBSTATION12	28	
	Bus	BUS_SUBSTATION2	186	CB	CB-SUBSTATION12	28	
	Line	LINE 4	209	Relay	RELAY-SUBSTATION3	28	
	Trmeas	Tmeas_SUBSTATION2	261	Relay	RELAY-SUBSTATION3	28	
	CB	CB_SUBSTATION3	329	Trmeas	Tmeas-SUBSTATION1	33	
	CB	CB_SUBSTATION3	329	Line	LINE 4	36	
	Line	LINE 5	374	Bus	BUS-SUBSTATION2	49	
				Bus	BUS-SUBSTATION12	56	
				Trmeas	Tmeas-SUBSTATION2	81	
				Trmeas	Tmeas-SUBSTATION12	87	
				Line	LINE 6	102	
				Line	LINE 5	144	
				Line	LINE 7	210	
				CB	CB-SUBSTATION3	220	
				CB	CB-SUBSTATION3	220	
				Bus	BUS-SUBSTATION3	358	
				Line	LINE 8	422	
				Line	LINE 9	423	



Oral Presentation: Impact of the Hydrological Risk on the Power Grid: A Case Study on a Portion of the Italian Transmission Power System Exposed to the Hazard of Flooding

A widespread decrease of failure RP is highlighted in the results: 25 components in sim 3 have a RP lower than 50 years (against 12 components with RPs < 50 years in the base case). In particular, the comparison of the two lists highlights some criticalities at substation 12 where relays and circuit breakers show RPs lower than 30 years: the same components are considered « resilient » in the base case under climate stationarity assumption.

Figure 7 compares the RPs for the components with RPs < 500 years in sim 3: this allows to easily detect the criticality of components at substation 12 under the specific assumption of the climate evolution.

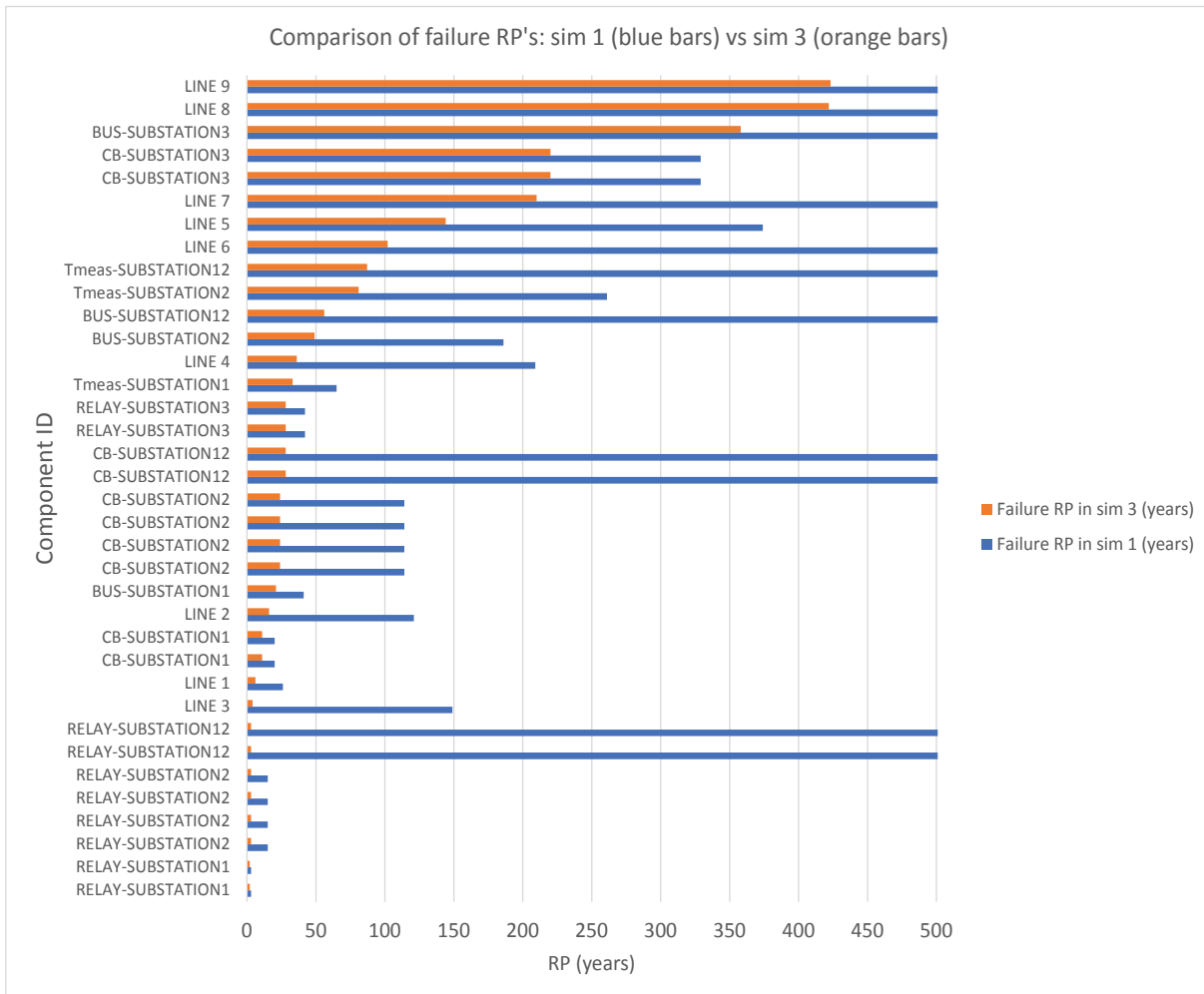


Figure 7. Comparing sim 1 and sim 3 results for the components with RPs < 500 years in sim 3. Resilient components are indicated with a conventional value of 500 years.

### 5.5. Sim 4: application of plinths under climate changes

This simulation assumes that plinths are applied to substation equipment in presence of climate changes which cause more severe flood heights in the future (still considering a factor  $k_{cc} = 1.5$ ). Figure 8 compares the failure RPs of the substation equipment before (sim3) and after (sim 4) the application of the plinths: in fact, the countermeasure does not affect lines. The countermeasure causes a drastic increase of failure RPs for substation equipment, especially at substations 1, 2 and 12, as shown in Figure 8. After such measure, all the substation equipment can be considered « resilient » (because their RPs are all higher than 500 years) in view of the future application of the CBA for intervention prioritization.



Oral Presentation: Impact of the Hydrological Risk on the Power Grid: A Case Study on a Portion of the Italian Transmission Power System Exposed to the Hazard of Flooding

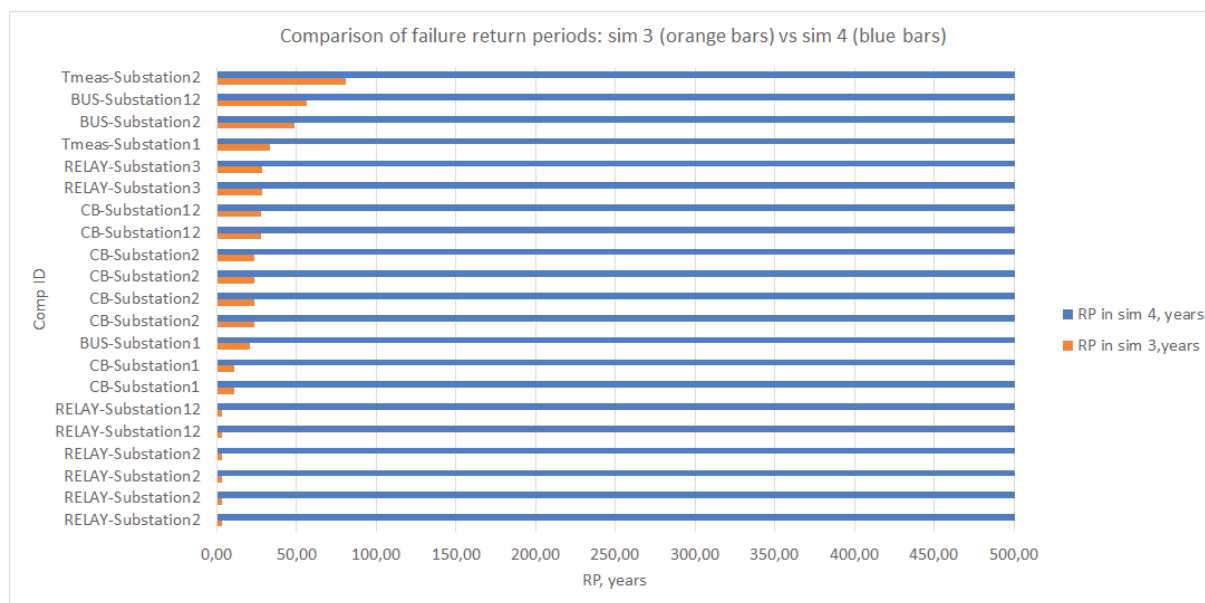


Figure 8. Comparison of failure return periods of substation equipment: sim 3 (dashed line) vs sim 4 (solid line).

## 6. CONCLUSIONS

This paper has presented the first steps for the extension of the methodology jointly developed by the Italian TSO Terna and RSE to quantify the effects of hydrological risk on the Italian transmission system, and to plan adequate interventions to harden the system in case of hydrological threats. In particular, the part of the methodology aimed to model the flood threat, the vulnerability of grid asset to floods, as well as the failure return periods of grid asset, has been presented and applied to a portion of the Italian peninsula. The preliminary simulations performed assuming typical ranges for the dimensions of substation equipment show that the failure return periods of concentrated components, in particular relays and circuit breakers, are the lowest ones. It's also worth reminding that the consequences of the disconnection of a substation (following a substation equipment failure) are generally more severe than the ones provoked by the loss of a single OHL due to tower damages for floods. Simulations also highlight the importance to account for climate changes: in fact, a 50% increase of the flood heights at different RPs can determine a drastic reduction of the failure return periods of grid asset (also substation equipment), which calls for the application of flood protection systems such as plinths. The analytical vulnerability models can integrate the application of plinths, assessing the effectiveness of this countermeasure in increasing the failure RPs, which makes these models suitable for a CBA aimed at the prioritization of interventions for resilience enhancement.

Future works will consist in extending the modeling framework to include other hydrogeological threats and the relevant grid asset vulnerability, such as the instability of transmission line tower foundations due to scouring and riverbank erosion.

## BIBLIOGRAPHY

- [1] G. M. Karagiannis, Z. I. Turksezer, L. Alfieri, L. Feyen, E. Krausmann, "Climate change and critical infrastructure – floods", EUR 28855 EN, Publications Office of the European Union, Luxembourg, 2019.
- [2] L. Gao, B. Tao, Y. Miao, L. Zhang, X. Song e W. Ren, «A globaldata set for economic losses of extremehydrological events during 1960-2014,» Water Resources Research, vol. 55, p. 5165-5175.
- [3] E. Ciapessoni, D. Cirio, A. Pitto, M. Lacavalla, P. Marcacci, G. Pirovano, F. Marzullo, F. Scavo, F. Falorni, A. Lazzarini, "A methodology to compute resilience indicators for the Italian Transmission System", Proc. of CIGRE 2021 Centennial Session, Aug 2021.
- [4] A. Amicarelli et al., "SPHERA v.9.0.0: A Computational Fluid Dynamics research code, based on the Smoothed Particle Hydrodynamics mesh-less method", Computer Physics Communications. Vol. 250, pp. 1-52, 2020.
- [5] E. Ciapessoni, D. Cirio, A. Pitto, L. Mancusi and A. Abbate, "Modeling the vulnerability of power system components to debris flows for power systems resilience analyses," Proc. of 2022 17th International Conference on Probabilistic Methods Applied to Power Systems (PMAPS), Manchester, United Kingdom, 2022.
- [6] E. Haugen, A. Kaynia. "Vulnerability of structures impacted by debris flow", in Proc. of 10<sup>th</sup> Int. Symposium on Landslides and Engineered Slopes, Taylor & Francis, London, 2008.



**Oral Presentation:** Impact of the Hydrological Risk on the Power Grid: A Case Study on a Portion of the Italian Transmission Power System Exposed to the Hazard of Flooding

- [7] FEMA, "What is Hazus: An Introduction to FEMA's Hazus Program", HAZUS factsheet, March 2021.
- [8] J.S.H. Kwan, Supplementary Technical Guidance on Design of Rigid Debris-resisting Barriers. Geo report no. 270, July 2012.
- [9] European Commission (EC), "Directive 2007/60/EC of the European Parliament and of the Council of 23 October, 2007 on the Assessment and Management of Flood Risks", Official Journal of the European Union, L288, pp. 27-34, 2007.
- [10] National Geoportal website at: <http://www.pcn.minambiente.it/mattm/en/>
- [11] European Commission (EC), "Directive 2007/2/EC of the European Parliament and of the Council of 14 March 2007 establishing an Infrastructure for Spatial Information in the European Community (INSPIRE)", Official Journal of the European Union, L108, pp. 1-14, 2007.
- [12] Electricity NorthWest, "Substation Flood Protection", Electricity Policy Document 355, Dec 2017.
- [13] D. Jacob, J. Petersen, P. Yiou e al., "EURO-CORDEX: new high-resolution climate change projections for European impact research", Regional Environmental Change, vol. 14, p. 563-578, 2014.
- [14] M. García-Valdecasas Ojeda, F. Di Sante, E. Coppola, A. Fantini, R. Nogherotto, F. Raffaele, F. Giorgi, "Climate change impact on flood hazard over Italy", Journal of Hydrology, Volume 615, Part A, 128628, Dec 2022, pp 1-18.



# Fault Detection in Power Transmission Lines with Artificial Intelligence

[busra.tore@eltemtek.com.tr](mailto:busra.tore@eltemtek.com.tr) / [ali.efe@teias.gov.tr](mailto:ali.efe@teias.gov.tr)

**BÜŞRA TÖRE, EMRE KILCI, OZAN AKYOL, FERHAT ŞENER**  
ELTEMTEK

**METE UZAR, ALİ EFE, İBRAHİM BAHCIVAN**  
Türkiye Elektrik İletim A.Ş. (TEİAŞ)

Türkiye

## SUMMARY

Ensuring Sustainability in Energy Transmission through Early Detection of Potential Faults caused by Power Outages is of great importance. For this reason, periodic preventive maintenance and inspection activities are carried out on energy transmission lines. The activity of aerial inspection of energy transmission lines conducted involves the use of aerial vehicles integrated with electro-optical systems to perform flights along the routes of overhead lines with operating voltage levels of 170 kV and 400 kV. High-resolution photographs and video data obtained because of these flights are analysed and reported by personnel using the software developed within the company. The detected faults are then integrated into the existing OMS (Operation Management System)

To minimize human error and increase the workload efficiency in the process of detecting and reporting faults performed by the analysis and reporting teams, a project has been developed to utilize artificial intelligence and image processing methods to detect the most encountered physical faults in transmission lines. The project includes the stages of problem identification, data collection, data preparation, modelling, evaluation, model improvement, distribution, and integration.

## KEYWORDS

Energy transmission line, artificial intelligence, image processing, object detection.





### 1. INTRODUCTION

Faults occurring in energy transmission lines can lead to power outages. To ensure uninterrupted transmission, it is necessary to regularly inspect the energy transmission lines at specified intervals, detect potential faults that may occur in the lines, and rectify them before they occur. High-resolution images and videos obtained from flights performed by aerial vehicles integrated with electro-optical systems are examined for transmission lines and transformer centres in the interconnected network. The detected potential fault situations are then communicated to their respective areas of responsibility. In order to increase the workload efficiency and minimize human error in the process of detecting and reporting faults, artificial intelligence models that operate with alternative scenarios are being developed and implemented.



*Figure 1: Pole image obtained from the flight.*

There are over 60 types of faults controlled in transmission lines. In this study, priority has been given to the most frequently encountered faults that can be detected using object detection algorithms. These faults include bird nests on poles, broken or missing insulators, and arc marks on insulators.

This study aims to develop deep learning models for the detection of bird nest faults, identification of insulator types (glass, silicone, porcelain), detection of insulator fractures and deficiencies, and detection of arc marks on insulators. These models will be integrated with the system to perform inference on a live system and open a record of the detected faults in OYS system.

### 2. OBJECT DETECTION ALGORITHMS

Deep learning algorithms are utilized in solving problems such as computer vision, natural language processing, speech technologies, and time series analysis. Within computer vision algorithms, there are subcategories such as object detection, object tracking, image classification, and image segmentation. In this study, the faults to be detected are considered as objects, and the goal is to detect them using object detection methods from these subcategories.

Object recognition models can be categorized as single-stage and two-stage models. In two-stage object detection models, region proposals are generated before the extracted features are used for object classification. (See Figure 2) Potential areas where objects might be present are determined and individually passed through convolutional layers. In single-stage object detection models, on the other hand, bounding boxes are directly predicted on the image without the region proposal step used in two-stage models. This process takes less time compared to two-stage models, making it particularly preferable for real-time applications.

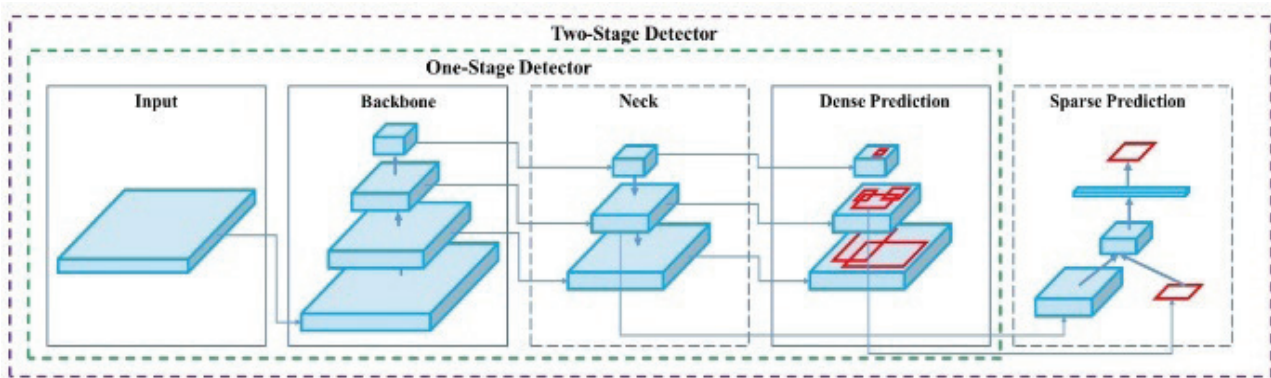


Figure 2: Single-stage and two-stage network architectures [3]

Among the most important two-stage object detection models are RCNN, Fast RCNN, Faster RCNN, Pyramid Networks, while single-stage models include YOLO, SSD, RetinaNet.

### 2.1. YOLO Algorithm

The YOLO (You Only Look Once) algorithm is a single-stage, real-time object detection algorithm that divides images into a grid system. Each grid cell is responsible for detecting objects within itself. It treats object detection as a single regression problem. Due to its fast performance and high accuracy rate, YOLO is one of the most widely used object detection algorithms in the world. Over time, different versions of YOLO have been developed. In this study, YOLOv5, developed by Ultralytics, is considered as it offers high success rates, faster performance compared to two-stage networks, and ease of use.

#### 2.1.1. YOLOv5

Like other single-stage object detection algorithms, YOLOv5 consists of three components: backbone, neck, and head. The backbone extracts important features from the image. In YOLOv5, the CSP (Cross Stage Partial Networks) is used as the backbone. The model neck is responsible for creating feature pyramids. A feature pyramid is a feature extractor that takes a randomly sized single-scale image as input and produces feature maps at multiple levels in a convolutional structure, scaled proportionally. (See Figure 3) Feature pyramids enable models to generalize object scaling. They assist in detecting the same object at different sizes and scales, and they are particularly useful for models to perform well on unseen data. YOLOv5 uses PANet to extract feature pyramids. The head is the final part of the model and is used for detection. In this part, an output vector is generated containing bounding boxes, class probabilities, and objectness scores. YOLOv5 uses a similar structure for the head as in YOLOv3 and YOLOv4.

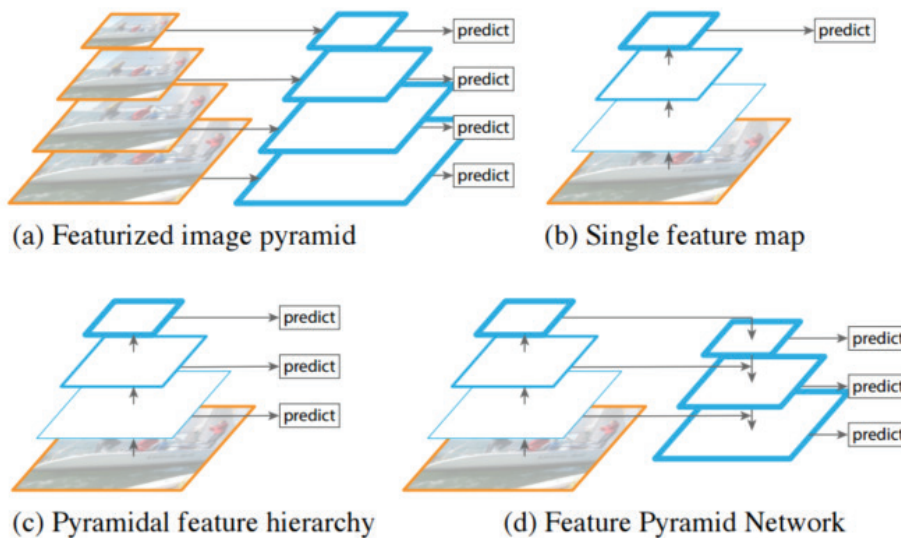


Figure 3 Feature pyramid network [2]

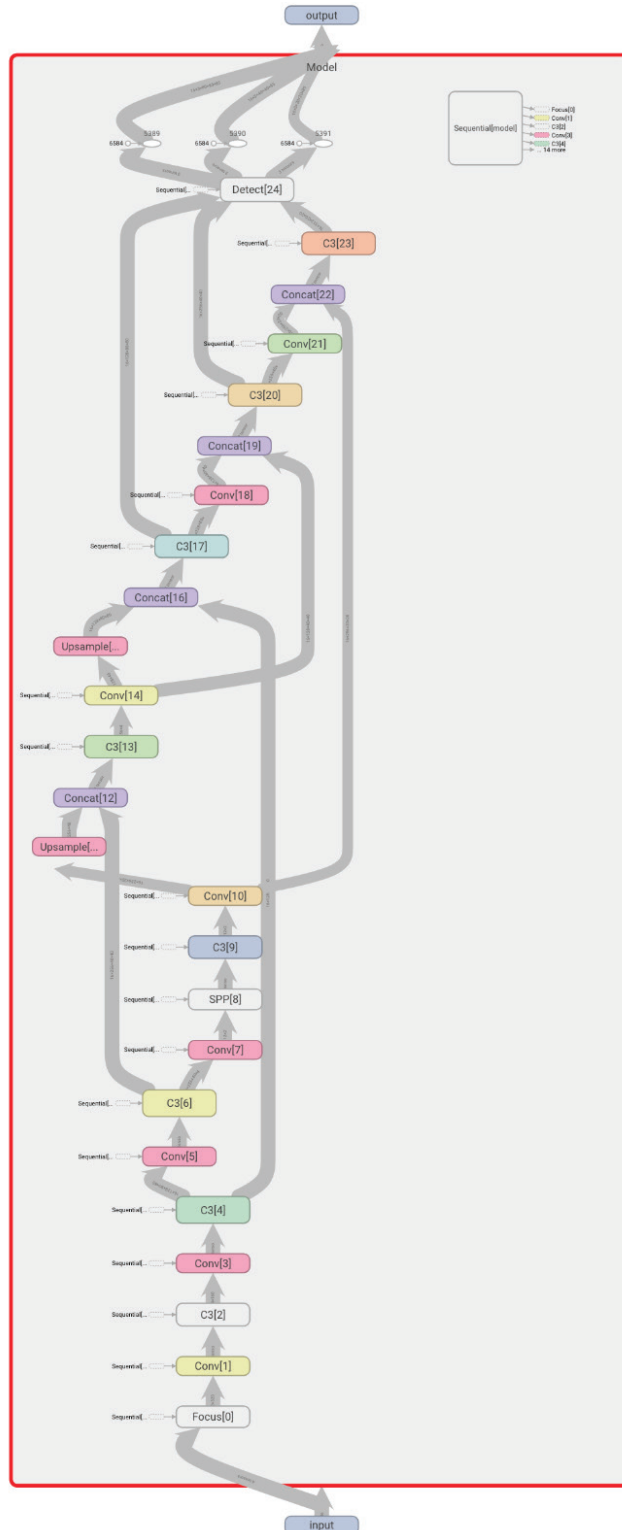


Figure 4: YOLOv5 Architecture

The Leaky ReLU activation function is used in the hidden layers, while the Sigmoid activation function is used in the final detection layer. The optimization function can be either SGD or Adam.

YOLOv5 is built on the PyTorch framework. In this study, the adapted version of the original YOLOv5 code, specifically tailored for AI servers, was utilized.





### 3. MODEL DEVELOPMENT

In the initial stage, the types of faults to be detected were determined as bird nests, insulator fractures, and arc marks on insulators. In this regard, the images collected during the flight and containing detected faults were used to create the dataset for developing the models. The detected faults in the images were labelled within bounding boxes. An average of 1000 to 5000 labels were assigned per class. In classes with insufficient data, data augmentation techniques were used to synthetically increase the number of samples.

For the detection of bird nest faults, processing is directly performed on the original photographs obtained during the flight. The detection of insulators also takes place on the original-sized image. Insulators are detected in different classes based on their types (porcelain, glass, composite). In the stage of detecting faults on insulators, the outputs of the cropped insulator detection model, which are resized to smaller dimensions, are used as input to improve accuracy and performance instead of the original-sized photograph.



Figure 5: Detection of different types of insulators



Figure 6: Detection of bird nest fault

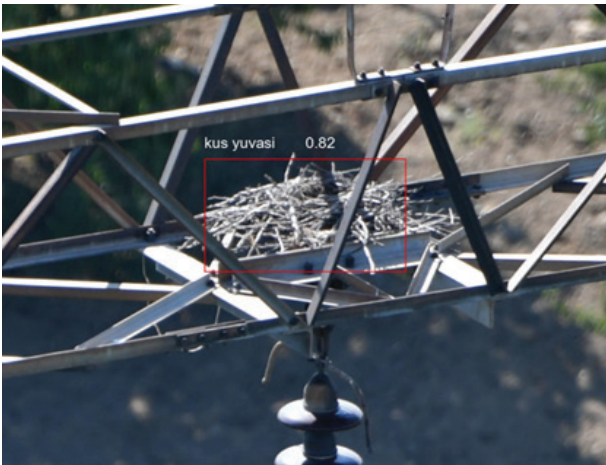


Figure 7: Detection of missing part fault



Figure 8: Detection of broken part fault on insulator

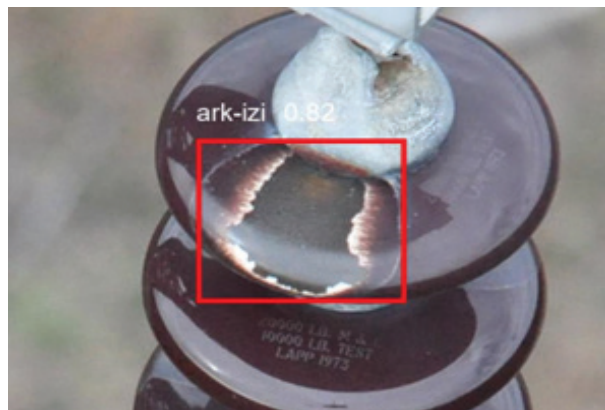


Figure 9: Detection of arc mark fault on insulator



All model development activities were conducted on the Training server, while inference and integration processes were performed on Inference server. The model training process utilized Neural Processing Unit (NPU) cards.

The pretrained YOLOv5x model was used as the base model, trained on the MS COCO dataset. Since the training process started with pretrained models, training was conducted for around 20-50 iterations (epochs). Data was trained in batches of 32-64 on single and multiple (distributed) NPUs.

### 4. INTEGRATION PROCESS

The software developed for fault detection in electricity transmission lines and transmission of detected faults over the Internet is used. The integration process involves transferring the data to be scanned for fault detection from the server where this application runs to the Inference server where the inference process takes place. Furthermore, the integration process involves transferring the detected faults back to this server for opening a fault record on the web application. Data transfer is facilitated through queue management conducted via RabbitMQ on a separate server.

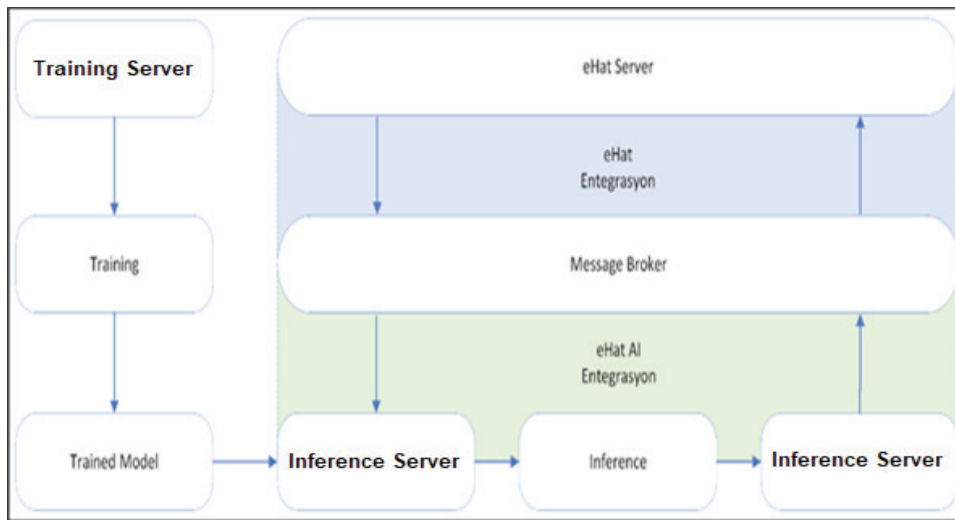


Figure 10: System Overview

### 5. INFERENCE

The created models were evaluated based on several performance metrics. The confusion matrix, as presented in Table 1, was utilized to calculate these performance metrics.

Table 1. Confusion Matrix

Prediction/Actual	Positive	Negative
Positive	TP	FP
Negative	FN	TN

**Accuracy:** It is the ratio of correctly predicted instances to the total instances of a class.

$$Accuracy = (TP + TN) / (TN + FP + TP + FN) \text{ (1)}$$

**Precision:** It shows the proportion of truly positive instances among the instances predicted as positive.

$$Precision = (TP) / (FP + TP) \text{ (2)}$$

**Recall:** It indicates the proportion of truly positive instances that were predicted as positive.

$$Recall = (TP) / (TP + FN) \text{ (3)}$$



Table 2. Accuracy Ratio

Metric/Fault Type	Bird Nest	Broken Insulator	Arc Mark on Insulator
Accuracy	%75	%100	%60
Precision	%73	%35	%30

To develop successful deep learning models, it is recommended to have a minimum of 5000-10000 labeled data per class. However, some types of faults, such as arc marks, may have limited data, or in the case of broken insulators, there may be instances in the image that closely resemble a fault, leading the model to incorrectly identify them as actual faults. These factors can negatively impact the success rate of the models.

One challenge in bird nest fault detection is the significant variations in the characteristics of bird nests. The diverse range of sizes and materials of bird nests makes it difficult to create a generalized model. In the case of fractures on insulators, especially in low-resolution images, glare caused by sunlight and stains on the insulator can be mistakenly detected as a fracture fault. Gaps at the connection points of insulators can sometimes be perceived as missing parts. Additionally, sunlight glare, stains, and writings on the insulator can cause the image to be detected as an arc mark fault.

Adjustments to the threshold values in class probabilities can be made to change the TP and FP rates, which would also affect accuracy and precision values.

The flights are conducted on a project basis, resulting in images with different characteristics from different regions. Therefore, when the dataset is expanded with data from different regions, more generalized models can be obtained with higher success rates.

## 6. RESULTS

Artificial intelligence, like in other fields, is finding increasing application in the energy sector. In this study, an application was developed to enhance the success rate of fault detection in power transmission lines using artificial intelligence and to reduce the time spent on fault detection, thus making the process more efficient. It was observed that some of the most encountered faults on transmission lines were detected using the developed artificial intelligence models. In the next phase, with more data obtained, the goal is to establish more successful and faster models to detect a wider range of fault types.

## BIBLIOGRAPHY

[1] Joseph Redmon, Ali Farhadi, "YOLOv3: An Incremental Improvement"

[2] Tsung-Yi Lin, Piotr Dollár, Ross Girshick, Kaiming He, Bharath Hariharan, Serge Belongie, "Feature Pyramid Networks for Object Detection"

[3] Alexey Bochkovskiy, Chien-Yao Wang, Hong-Yuan Mark Liao, "YOLOv4: Optimal Speed and Accuracy of Object Detection"

[4] Syed Sahil Abbas Zaidi, Mohammad Samar Ansari, Asra Aslam, Nadia Kanwal, Mamoona Asghar, Brian Lee, "A Survey of Modern Deep Learning based Object Detection Models"

[5] <https://docs.ultralytics.com/>

[6] <https://github.com/ultralytics/yolov5>





# FACTS for Improved Controllability of High Voltage Power Transmission Network in Georgia

[giorgi.arziani@parvusgroup.ge](mailto:giorgi.arziani@parvusgroup.ge)

**GIORGI ARZIANI\*, TEONA ELIZARASHVILI, BAIA KVATADZE, LUKA BARAMIDZE**  
*Parvus Consulting, Georgian Technical University*

**Georgia**

**METE UZAR, ALİ EFE, İBRAHİM BAHCIVAN**  
*Türkiye Elektrik İletim A.Ş. (TEİAŞ)*

**Türkiye**

## SUMMARY

Georgia's electrical power system is relatively small. The system's total installed capacity does not exceed 4 GW. Generation mix is dominated by hydropower plants, with a share of 74 %. The rest of the energy comes from thermal, wind, and small-scale (micro) solar power plants. Generation sources are not evenly distributed throughout the country. Most and the largest hydropower plants are located in the western part of the country, while consumption centers are developed in the east. Consequently, high voltage transmission network is predominantly oriented from west to east. The imbalance between power flows from the east and west is particularly noticeable in spring and summer when the abundance of water in rivers leads to the non-operation of eastern thermal power plants. As a result, power flows from west to east. It is important to note that the inclusion of potential power plants outlined in Georgia's Ten-Year Network Development Plan will worsen the current operational scenario.

The fundamental problem lies in the transmission infrastructure itself. The West-East corridor mainly consists of 500 kV and 220 kV high voltage lines (HVL) and substations. The route is not redundant as the 220 kV network has less transmission capacity compared to the 500 kV one. The network doesn't match the N-1, minimum reliability criterion. Consequently, tripping the 500 kV Imereti HVL often leads to severe system disturbances. To prevent blackouts and maintain the new equilibrium in the power system, emergency automatics are activated, which then sheds the predefined load and generation in the system.

On the other hand, according to Kirchhoff's current law, the current flows through the lower impedance path; thus 500 kV line with naturally lower impedance is always carrying more power than the 220 kV (higher impedance) route. Due to the varying impedances of the routes, the power flow is unevenly distributed between the two HVLs. This leads to more severe transient processes when disconnecting a 500 kV line, compared to parallel networks with equal load distribution.

One possible solution to address the problem is to artificially equalize the series impedances of the 500 kV and 220 kV networks. One of the technological options to accomplish this is by utilizing FACTS (Flexible AC transmission system) devices. For that purpose, the authors investigated different scenarios through the modeling and simulation of a high-voltage network with integrated series and shunt FACTS devices. Instead of modelling the whole high voltage network of the country, the authors used a prototype network that mimics the main characteristics of electrical processes in Georgia power system. The paper examined the potential impact of the Unified Power Flow Controller (UPFC) on the power transfer capability of the 500 / 220 kV west-east corridor of the Georgian power system. The analyses of electrical regimes with and without FACTS devices showed that an optimal combination of FACTS devices effectively resolved both power flow asymmetry and reactive power deficits in the system. This resulted in reduced transmission losses, maintained operational voltage limits, and enhanced the transfer capacity of the corridor.

## KEYWORDS

FACTS, UPFC, power flow control, voltage control, STATCOM, SSSC, transmission network.



### Prototype network

To assess the potential impact of FACTS devices on the electrical grid, the authors developed a prototype model (Figure 1) that mimics the characteristics of the Georgia power system. While not an exact replica, this model captures the grid’s essential features and incorporates the electromagnetic processes found in the Georgian transmission network.

The prototype includes two 500 kV terminals, referred to as Terminal 1 and Terminal 2. Additionally, the model incorporates a parallel transmission network operating at 220kV, consisting of four terminals—Terminal 3, Terminal 4, Terminal 5, and Terminal 6. Terminal 1 and Terminal 3 represent the primary generation centers within the network and are interconnected by a 500/220 kV transformer. Terminal 2 and Terminal 6, on the other hand, serve as significant consumption centers within the system and are also connected by a 500/200 kV transformer.

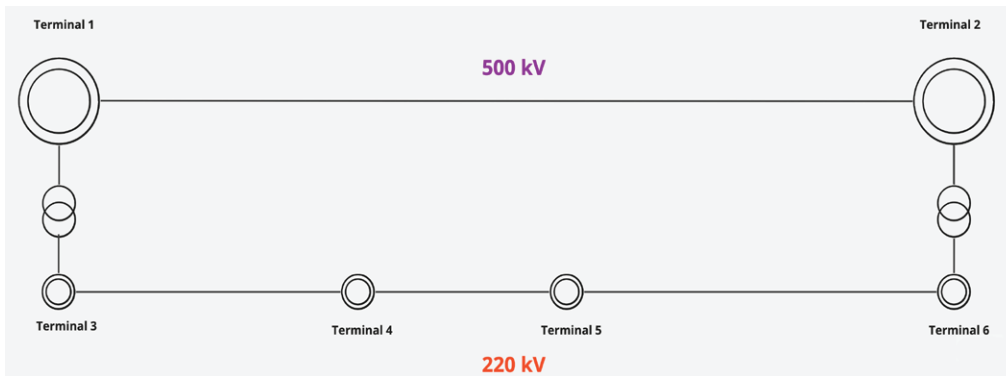


Figure 1: Prototype Transmission Network Diagram

### Unified Power Flow Controller (UPFC)

The FACTS technology offers several advantages over conventional power flow and stability control measures, including fast response, absence of mechanical moving parts, and flexible functionality [1]. Consequently, it represents a significantly superior solution for power system applications. By leveraging FACTS technology, power grids can maximize resource and energy utilization while enabling continuous control adjustments of critical parameters such as power system voltage, line impedance, phase angle, and power flow. This optimization enhances the transmission capacity of existing lines, thereby deferring the need for new transmission infrastructure. By using this method, it is possible to reduce transmission costs, save space, and minimize the environmental impact of constructing new infrastructure.

A Unified Power Flow Controller (UPFC) is a combination of series and shunt FACTS technology, specifically the Static Synchronous Compensator (STATCOM) and the Static Synchronous Series Compensator (SSSC) [2]. The UPFC diagram is given in Figure 2.

The shunt compensator within the UPFC can generate reactive current and compensate for reactive power in the power system, thus keeps the node voltage within acceptable operational limits. Its ability to compensate for line voltage, however, is limited.

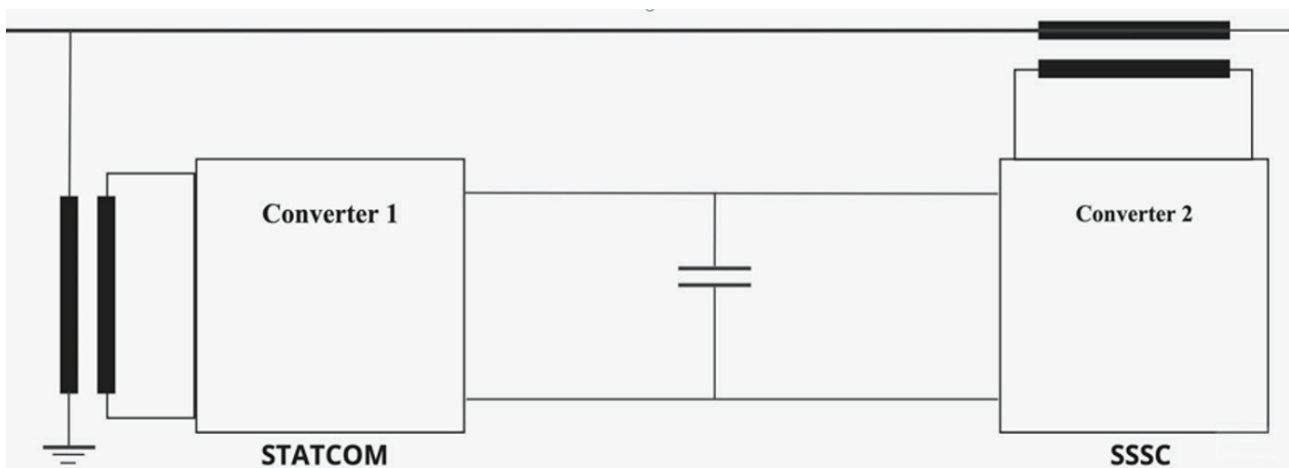


Figure 2: Unified Power Flow Controller Diagram



On the other hand, the series compensator in the UPFC is highly capable in controlling power flow, but it lacks effectiveness as a reactive current compensator. By combining series and shunt devices, the UPFC emerges as the most comprehensive technology in this field. A proposed integration in the system is given in Figure 3. The primary functionality of the UPFC can be categorized into two main control modes: voltage control mode and power flow control mode. In the voltage control mode, the device regulates the voltage magnitude and phase angle to minimize voltage fluctuations due to load variations or other types of disturbances. In the power flow control mode, the UPFC actively controls the power flow on the transmission line – changing line characteristics by adjusting the series converter impedance – thereby diverting or redistributing power flow.

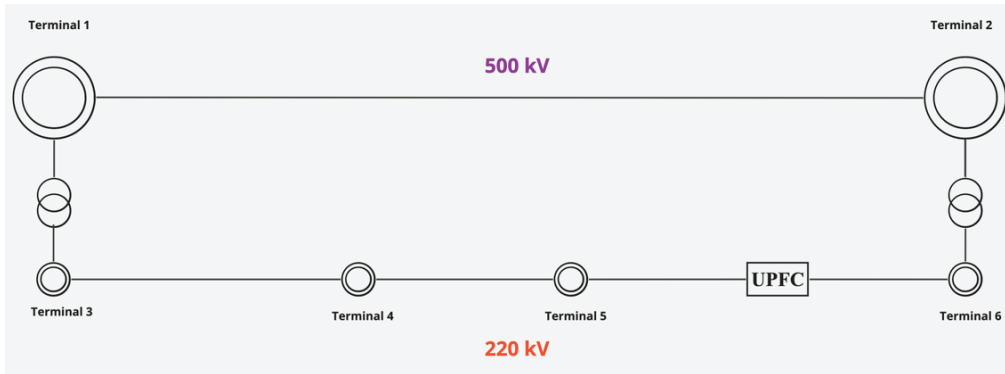


Figure 3: Prototype Transmission Network Diagram with UPFC

Modelled scenarios

To assess the potential impact of FACTS devices, the authors analyzed three different steady state electrical regimes with and without FACTS and examined power flow and voltage profiles in the parallel transmission lines.

Due to the inherent nature of high voltage transmission lines, a significant asymmetry in power flow is to be expected in this system due to the lower impedance of the 500kV line. Furthermore, as the generation is concentrated at Terminal 1 and the consumption is concentrated at Terminal 2, with limited reactive power, the overall voltage profile of the network is significantly affected. The challenge in the system of this nature is, therefore, two-fold – power flow asymmetry and poor voltage profile [3]. Moreover, transient processes are amplified in this scenario. Remedial Action Scheme (RAS) implemented in the Georgia power system, proportionally disconnects generation and consumption centers in the system to achieve a new system equilibrium. In the case of asymmetric power flow distribution, if a fault occurs, the total operational capacity of generation and load to be disconnected is greater compared to the symmetric case. Hence, there is a need to integrate FACTS devices into the transmission system to balance power flow.

Scenario 1

Figure 4 shows the base scenario for the system without FACTS. The power transferred through the 500kV HVL measured at Terminal 2 is 322.5MW. On the other hand, the power flow at 220kV line measured at Terminal 6 is 74MW.

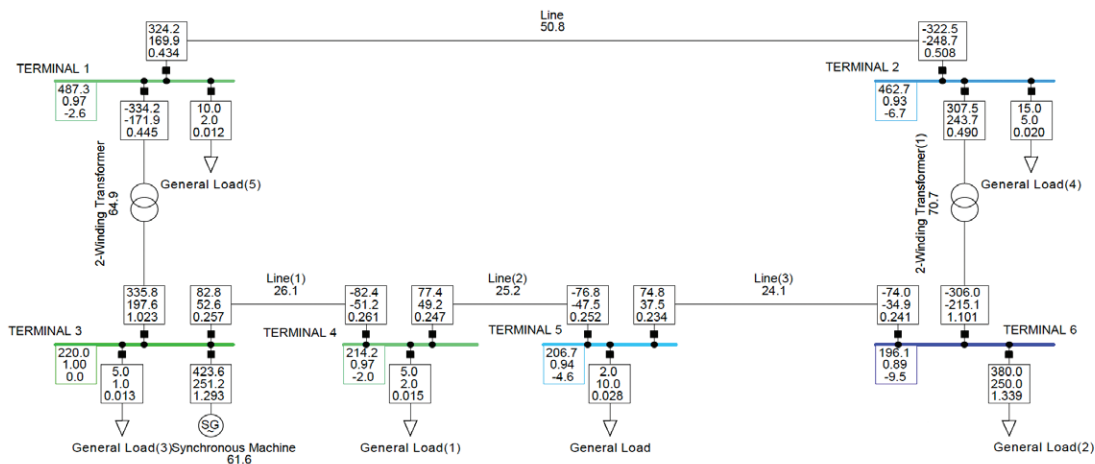


Figure 4: Scenario 1 – 500/220 kV Parallel Transmission Model



This shows a ratio of approximately 1 to 4 in terms of power flow distribution between the parallel lines. The transmission losses as a percentage of generation are ~1.56% in this scenario (Figure 5). The 500kV HVL is loaded by 50.8% of its ampacity; the 220kV HVL corridor from Terminal 3 to Terminal 6 is loaded on average by 25.13%.

Load Flow Calculation				Grid Summary	
AC Load Flow, balanced, positive sequence		Automatic Model Adaptation for Convergence	No		
Automatic Tap Adjust of Transformers	No	Max. Acceptable Load Flow Error for			
Consider Reactive Power Limits	No	Nodes		1.00 kVA	
		Model Equations		0.10 %	
Grid: Grid	System Stage: Grid	Study Case: Study Case	Annex:	/ 1	
Grid: Grid Summary					
No. of Substations	0	No. of Busbars	6	No. of Terminals	0
No. of 2-w Trfs.	2	No. of 3-w Trfs.	0	No. of syn. Machines	1
No. of Loads	6	No. of Shunts	0	No. of SVS	0
Generation	= 423.63 MW	251.22 Mvar	492.52 MVA		
External Infeed	= 0.00 MW	0.00 Mvar	0.00 MVA		
Inter Grid Flow	= 0.00 MW	0.00 Mvar			
Load P(U)	= 417.00 MW	270.00 Mvar	496.78 MVA		
Load P(Un)	= 417.00 MW	270.00 Mvar	496.78 MVA		
Load P(Un-U)	= 0.00 MW	0.00 Mvar			
Motor Load	= 0.00 MW	0.00 Mvar	0.00 MVA		
Grid Losses	= 6.63 MW	-18.78 Mvar			
Line Charging	=	-114.31 Mvar			
Compensation ind.	=	0.00 Mvar			
Compensation cap.	=	0.00 Mvar			
Installed Capacity	= 640.00 MW				
Spinning Reserve	= 216.37 MW				
Total Power Factor:					
Generation	= 0.86 [-]				
Load/Motor	= 0.84 / 0.00 [-]				

Figure 5: Scenario 1 – Grid Summary

The voltage deviations are presented in Figure 6. As seen from the voltage violation summary table, the maximum voltage deviation occurs at Terminal 6 which represents the receiving end of 500 kV corridor which itself limited the power transfer capability of the 500 kV HVL and reduces supply quality of the load connected to the electrically nearby areas.

Load Flow Calculation				Complete System Report: Voltage Profiles, Grid Interchange					
AC Load Flow, balanced, positive sequence		Automatic Model Adaptation for Convergence	No						
Automatic Tap Adjust of Transformers	No	Max. Acceptable Load Flow Error for							
Consider Reactive Power Limits	No	Nodes				1.00 kVA			
		Model Equations				0.10 %			
Grid: Grid	System Stage: Grid	Study Case: Study Case	Annex:	/ 1					
	rtd.V [kV]	Bus - voltage [p.u.] [kV] [deg]		-10	-5	Voltage - Deviation [%]			
						0	+5	+10	
TERMINAL 1	500.00	0.975 487.29 -2.61							
TERMINAL 2	500.00	0.925 462.67 -6.68							
TERMINAL 3	220.00	1.000 220.00 0.00							
TERMINAL 6	220.00	0.891 196.07 -9.51							
TERMINAL 4	220.00	0.974 214.18 -1.98							
TERMINAL 5	220.00	0.940 206.71 -4.60							

Figure 6: Scenario 1 – Voltage Violation

Scenario 2

In Scenario 2, a reactive power source was incorporated in the network model to offset the voltage deviation in the system. The VSC- (Voltage Source Converter) based shunt reactive power source improved the overall voltage profile and also reduced the transmission losses in the system. The power flow on the 500 kV HVL measured at Terminal 2 is 325.3MW while the power measured at 200kV Terminal 6 is 71.3 MW (based on Figure 7).

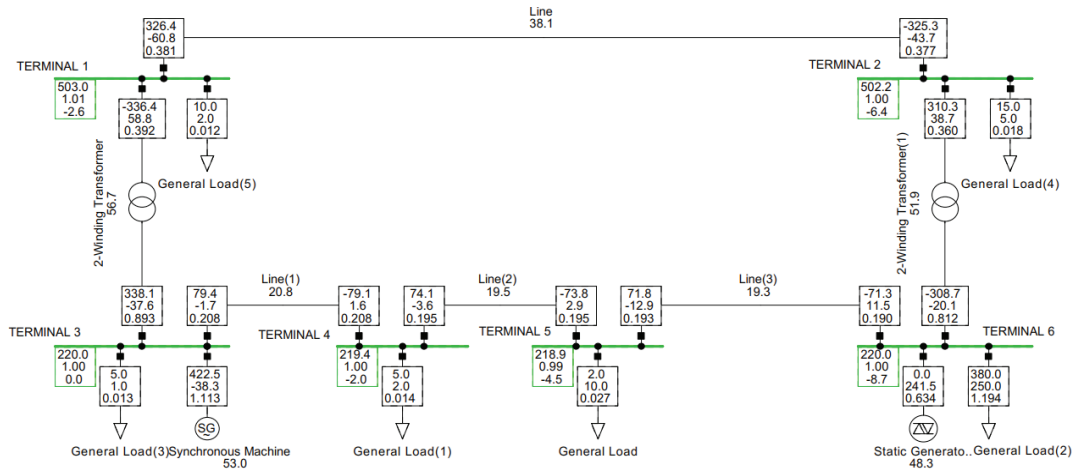


Figure 7: Scenario 2 – 500/220kV Parallel Transmission Model with Reactive Power Compensation

The system loss as a percentage of total generation is ~1.3% which is a slight improvement over Scenario 1 (based on Figure 8). Since shunt compensation had no effect on the asymmetry in power flow, further FACTS integration was necessary to address the issue.

Load Flow Calculation				Grid Summary	
AC Load Flow, balanced, positive sequence		Automatic Model Adaptation for Convergence		No	
Automatic Tap Adjust of Transformers	No	Max. Acceptable Load Flow Error for		1.00 kVA	
Consider Reactive Power Limits	No	Model Equations		0.10 %	
-----					
Grid: Grid	System Stage: Grid	Study Case: Study Case	Annex:	/ 1	
-----					
Grid: Grid Summary					
No. of Substations	0	No. of Busbars	6	No. of Terminals	0
No. of 2-w Trfs.	2	No. of 3-w Trfs.	0	No. of syn. Machines	1
No. of Loads	6	No. of Shunts	0	No. of asyn. Machines	0
No. of SVS	0				
Generation	= 422.52 MW	203.22 Mvar	468.85 MVA		
External Infeed	= 0.00 MW	0.00 Mvar	0.00 MVA		
Inter Grid Flow	= 0.00 MW	0.00 Mvar			
Load P(U)	= 417.00 MW	270.00 Mvar	496.78 MVA		
Load P(Un)	= 417.00 MW	270.00 Mvar	496.78 MVA		
Load P(Un-U)	= 0.00 MW	0.00 Mvar			
Motor Load	= 0.00 MW	0.00 Mvar	0.00 MVA		
Grid Losses	= 5.52 MW	-66.78 Mvar			
Line Charging	=	-127.90 Mvar			
Compensation ind.	=	0.00 Mvar			
Compensation cap.	=	0.00 Mvar			
Installed Capacity	= 1040.00 MW				
Spinning Reserve	= 217.48 MW				
-----					
Total Power Factor:					
Generation	= 0.90 [-]				
Load/Motor	= 0.84 / 0.00 [-]				

Figure 8: Scenario 2 – Grid Summary

The voltage profile is presented in Figure 9. The voltage deviation is significantly improved compared to Scenario 1; however, the power flow asymmetry is still present with a ratio of approximately 1 to 4. The the 500kV HVTL line is loaded by 38.1% compared to its ampacity; the average line load for the 220kV corridor from Terminal 3 to Terminal 6 is ~19.86%.



Load Flow Calculation				Complete System Report: Voltage Profiles, Grid Interchange			
AC Load Flow, balanced, positive sequence				Automatic Model Adaptation for Convergence	No		
Automatic Tap Adjust of Transformers	No			Max. Acceptable Load Flow Error for			
Consider Reactive Power Limits	No			Nodes		1.00 kVA	
				Model Equations		0.10 %	
Grid: Grid	System Stage: Grid	Study Case: Study Case	Annex: / 1				
	rtd.V [kV]	Bus - voltage [p.u.]	Bus - voltage [kV] [deg]	-10	-5	Voltage - Deviation [%]	
						0	+5 +10
TERMINAL 1	500.00	1.006	502.97 -2.57				
TERMINAL 2	500.00	1.004	502.17 -6.36				
TERMINAL 3	220.00	1.000	220.00 0.00				
TERMINAL 6	220.00	1.000	220.00 -8.71				
TERMINAL 4	220.00	0.997	219.40 -1.98				
TERMINAL 5	220.00	0.995	218.86 -4.46				

Figure 9: Scenario 2 – Voltage Violation

### Scenario 3

Based on scenario 2, the authors determined that shunt compensation relieved the significant voltage deviation in the system. To address the power flow asymmetry, series compensation was implemented in the system through the addition of the UPFC. Based on the results of the simulation, the authors found that the implementation of the UPFC solved both the voltage deviation and power flow asymmetry issues. The power measured at the 500kV Terminal 2 is 264.2MW while the power measurement is 132.3MW at the 220kV Terminal 6 as shown in Figure 10.

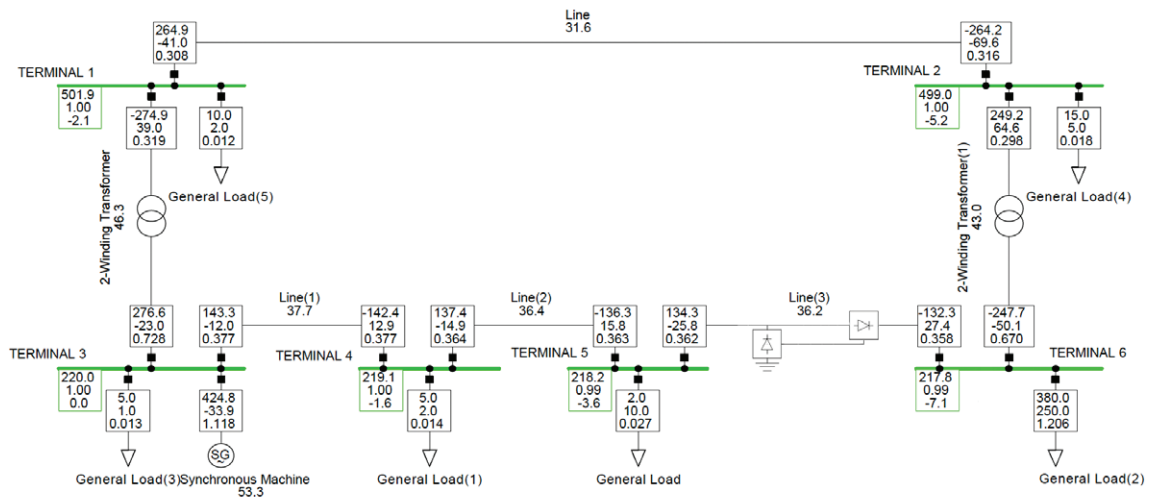


Figure 10: Scenario 3 – 500/220kV Parallel Transmission Model with UPFC

The transmission loss as a percentage of total generation is ~1.83% according to Figure 11. The grid losses are slightly increased compared to Scenarios 1 and 2; this increase is due to the fact that the UPFC forces a portion of the power to flow through a higher impedance path. However, this distribution of power flow prevents transmission line overloading caused by asymmetry. Thus, increasing overall system stability.





Load Flow Calculation				Grid Summary	
AC Load Flow, balanced, positive sequence				Automatic Model Adaptation for Convergence	No
Automatic Tap Adjust of Transformers	No			Max. Acceptable Load Flow Error for Nodes	1.00 kVA
Consider Reactive Power Limits	No			Model Equations	0.10 %
Grid: Grid	System Stage: Grid	Study Case: Study Case	Annex:	/ 1	
Grid: Grid Summary					
No. of Substations	0	No. of Busbars	6	No. of Terminals	0
No. of 2-w Trfs.	2	No. of 3-w Trfs.	0	No. of syn. Machines	1
No. of Loads	6	No. of Shunts	0	No. of asyn. Machines	0
Generation	= 424.81 MW	193.31 Mvar		466.73 MVA	
External Infeed	= 0.00 MW	0.00 Mvar		0.00 MVA	
Inter Grid Flow	= 0.00 MW	0.00 Mvar			
Load P(U)	= 417.00 MW	270.00 Mvar		496.78 MVA	
Load P(Un)	= 417.00 MW	270.00 Mvar		496.78 MVA	
Load P(Un-U)	= 0.00 MW	0.00 Mvar			
Motor Load	= 0.00 MW	0.00 Mvar		0.00 MVA	
Grid Losses	= 7.81 MW	-76.69 Mvar			
Line Charging	=	-126.83 Mvar			
Compensation ind.	=	0.00 Mvar			
Compensation cap.	=	0.00 Mvar			
Installed Capacity	= 1040.00 MW				
Spinning Reserve	= 215.19 MW				
Total Power Factor:					
Generation	= 0.91 [-]				
Load/Motor	= 0.84 / 0.00 [-]				

Figure 11: Scenario 3 – Grid Summary

The voltage deviation is provided in Figure 12. Similar to Scenario 2, the UPFC integration shows a voltage profile improvement over Scenario 1. The line load as a percentage of maximum line capacity for the 500kV line is 31.6%. The average line load for the 220kV corridor from Terminal 3 to Terminal 6 is ~36.76%. This is a significant improvement over Scenarios 1 and 2 in terms of power flow redistribution; The UPFC integration had a positive impact on improving power flow asymmetry in the transmission network.

Load Flow Calculation				Complete System Report: Voltage Profiles, Grid Interchange					
AC Load Flow, balanced, positive sequence				Automatic Model Adaptation for Convergence	No				
Automatic Tap Adjust of Transformers	No			Max. Acceptable Load Flow Error for Nodes	1.00 kVA				
Consider Reactive Power Limits	No			Model Equations	0.10 %				
Grid: Grid	System Stage: Grid	Study Case: Study Case	Annex:	/ 1					
	rtd.V [kV]	Bus - voltage [p.u.]	[kV] [deg]	-10	-5	Voltage - Deviation [%]			+10
				0	+5				
TERMINAL 1	500.00	1.004	501.87 -2.10			■			
TERMINAL 2	500.00	0.998	499.02 -5.19			■			
TERMINAL 3	220.00	1.000	220.00 0.00						
TERMINAL 6	220.00	0.990	217.80 -7.11			■			
TERMINAL 4	220.00	0.996	219.14 -1.56			■			
TERMINAL 5	220.00	0.992	218.23 -3.58			■			

Figure 12: Scenario 4 – Voltage Violation

## CONCLUSION

The simulation conducted in this study demonstrates that an optimal combination of FACTS devices effectively resolves both power flow asymmetry and reactive power deficits in the transmission corridors. Specifically, the series FACTS component addresses the asymmetry in parallel transmission lines, while the FACTS shunt component rectifies the reactive power imbalance at the receiving terminals of the network. These improvements mitigate the risks associated with power flow asymmetry and inadequate voltage profiles.



Oral Presentation: FACTS for Improved Controllability of High Voltage Power Transmission Network in Georgia

In the event of a transmission fault scenario, the total operational capacity of disconnected generation and consumption centers is significantly reduced compared to the base case. To further enhance the understanding of these findings, the authors plan to continue their research by analyzing additional electrical regimes including transients and taking into account the construction of 500 KV parallel network of west-east corridor. Future work will involve conducting simulation analyses in dynamic scenarios to gain deeper insights into the performance and effectiveness of the proposed FACTS devices.

### BIBLIOGRAPHY

- [1]. T. Elizarashvili, G. Arziani (2022). FACTS with energy storage for renewable integration in Georgia power system. Cigre 2022 Kyoto Symposium, Japan
- [2]. Yin, J., & Yin, J. (2017). Unified power flow controller technology and application. Elsevier Science & Technology. (Pages 19-39)
- [3]. Georgian State Electrosystem (2023). Ten-Year Network Development Plan of Georgia.



# Challenges and Opportunities for Multi-Purpose Interconnectors and Wind Offshore Generation

[arman.derviskadic@hitachienergy.com](mailto:arman.derviskadic@hitachienergy.com) / [michela.migliori@terna.it](mailto:michela.migliori@terna.it)**ARMAN DERVISKADIC, ELIN RAHMQVIST, ALBERTO PERSICO***Hitachi Energy***Sweden****ENRICO MARIA CARLINI, CORRADO GADALETA, MICHELA MIGLIORI, MATTEO TULLI, FRANCESCA LONGOBARDI***Terna***Italy**

## SUMMARY

The new ambitious climate and energy targets set at European level in the “Green Deal” package (“Fit-for-55”) [1], faces important challenges to network planners. In the Italian context, the new policy scenario defined by the Transmission System Operator (TSO) (Terna) and the Gas Operator (Snam) [2] foresees the installation of +70 GW of new renewable generation capacity by 2030, to reach the 65% share of renewables on the total electricity demand objective. Of this relevant increase in Renewable Energy Sources (RES) capacity, about 9 GW are related to new offshore wind power plants (OWPPs).

In fact, the recent advancements in floating technologies and dynamic cables have determined a huge increase of OWPPs connection requests also in the Mediterranean Sea, where the deep seabed has so far been an important limitation in this regard. In Italy, about 100 GW of offshore wind connection applications have been registered by Terna at the end of the 2022, mostly concentrated in the South of the Country and in the main Islands, due to the major availability of the primary source. The most rational connection schemes adopted by Terna on the basis of the actual state of the art, the rated powers, the water depth localization and the distance from the nearest coast have been presented in [3]. Nowadays, all the provided connection solutions for OWPPs includes the direct interconnection of the wind farm to a robust Extra-High Voltage (EHV) onshore node.

In a future decarbonized context, the grid development for interconnection levels increase within and between Member States is a key pillar of the energy transition to realize a flexible and secure European interconnected power system. In this perspective, the “multi-purpose” interconnectors (MPIs) are of great interest to the TSO, as they could represent a new coordinated, synergistic and efficient solution to increase the cross-border transfer capacity while fulfilling the integration of large cluster of OWPPs, becoming an off-shore connection hub for green energy. Furthermore, they could provide significant advantages in terms of redundancy, balancing services exchange and authorization issues.

In this paper, the perspectives of multi-purpose interconnectors within the Italian power system are addressed focusing on the HVDC technology enabling to transfer relevant power over very long distances in the submarine configuration, considering real clusters of OWPPs.

## KEYWORDS

Interconnection, Wind Offshore, Renewable energy, HVDC, Fit For 55, Multipurpose Interconnector



### 1. INTRODUCTION

The Paris Agreement [4], the “Clean Energy for all Europeans Package” [5] adopted in 2019 to decarbonize EU’s energy system and the “European green Deal” [1] for turning the EU into the first climate neutral continent by 2050, reducing the emissions by at least 55% by 2030 with respect to 1990 levels, are the most important policy references within a profound transformation of the European energy landscape.

In this context, the off-shore wind technology is rapidly expanding, assuming a central role in achieving the challenging goal of 65% of load covered from green sources at 2030. The inherent advantages consist of the reduced environmental footprint, the better exploitation of the wind source over the sea, the greater wind turbines size and power capacity leading to improved performances [3].

All over the world the offshore wind capacity at the end of 2022 has reached around 64 GW, +8,8 GW compared with the 2021 [6]. At European level, 2,5 GW of new wind capacity has been connected to power grids in 2022, and the European offshore wind capacity achieved 30 GW (46% in UK). Other important goals regarded Italy and France commissioning their first offshore projects and Norway commissioning 60 MW of new floating offshore wind generation.

The relevant technological progress achieved in floating solutions speeded up the investors interest in this renewable energy source also in deep seabed (i.e. the Mediterranean Sea), historically out of the wind market due to sea bathymetry constraint. In Italy, an exponential growth of OWPPs initiatives is occurring in the last 3 years: the capacity has increased from around 4,5 GW at the end of 2020 to around 110 GW at the first half of 2023. The Figure 1 shows the connections applications to the National Transmission Grid (NTG) evolution in each market zone of the Italian power system [7], [8]: over the 80% of the new initiatives is located in the South of the Country and in the main Islands because of the greater load factors related to higher wind source availability. This distribution adds further complexities to the planning problem since these areas are characterized from not densely meshed transmission infrastructure and low load [9]: the expected relevant renewable power injections need to be routed to the Centre and the North, exacerbating grid congestion over the continental primary backbones.

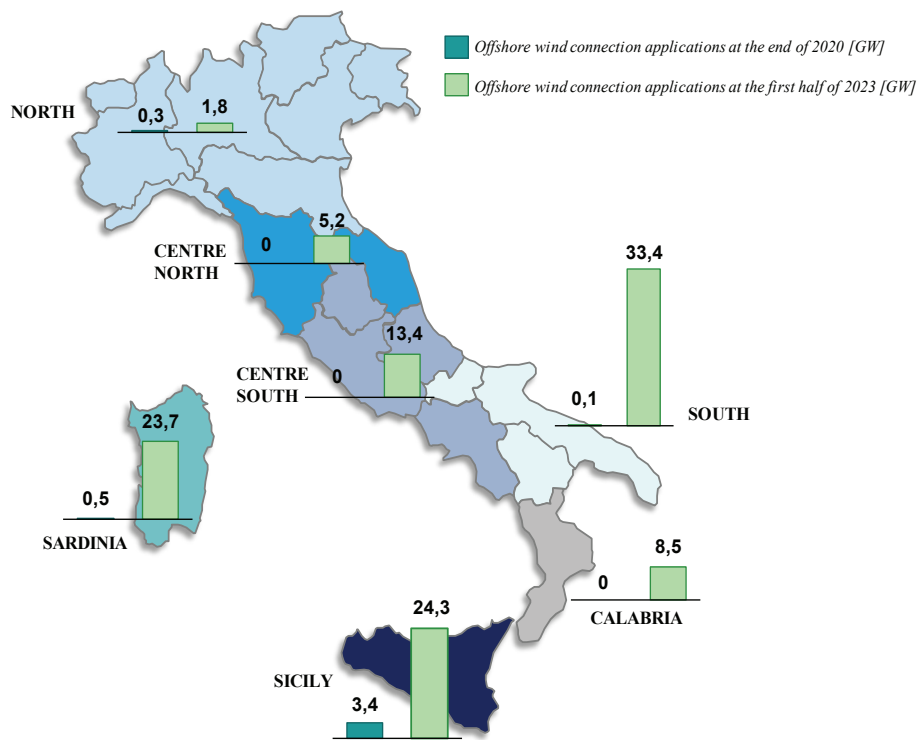


Figure 1. Evolution of OWPPs connection applications in Italy per market zone.

Since the lack of experience and the initiatives rate of concretization unpredictability, the Italian TSO carried out a wider technical survey, as presented in [3] and [10], aimed at defining the standard connection schemes for OWPPs: nowadays, all provided connection solutions involve HVAC radial links from the off-shore wind farm to a robust Extra High Voltage (EHV) on-shore node of the NTG (400 kV or 230 kV voltage level). Given the water Mediterranean Sea depth, the HVAC connection has been adopted as the most suitable solution up to 100÷120 km of distance from shore and for rated power up to 1 GW: the AC dynamic cables (66/150 kV



already available on the market) and floating offshore sub-stations show higher technological maturity if compared with the HVDC ones. Therefore, the requirements already included in the Italian Grid Code [11] and in the EU Network Code [12] are still applicable.

However, in relation to the potential technological advancements, new connection options could be developed in the view of an increasing integration of the offshore wind generation adopting an holistic approach in planning phase, able to realize synergies between transmission infrastructures. In this paper, the MPI solution perspectives for a test system in a future energy scenario in the very long term, considering huge RES penetration will be assessed by the means of the official Day Ahead zonal market (DAM) simulator [13] adopted by the Italian TSO for the Cost-Benefit Analysis (CBA).

In particular, different configuration of multi-purpose interconnectors will be simulated creating new off-shore bidding zones, evaluating yearly energy exchanges, RES integration variation and benefits for the entire system under study.

## 2. MULTI-PURPOSE INTERCONNECTORS: TECHNICAL REVIEW

The MPIs can represent a coordination solution to combine offshore wind integration and cross-border/internal market sections interconnection in a unique project [14], mainly in HVDC technology. In fact, OWPPs are in general radially connected to power grids and HVDC project are, mostly, point-to-point interconnection between different bidding zones. An illustrative outline of single-purpose and multi-purpose interconnector is depicted in Figure 2.

The technical survey performed among of the main suppliers proving most relevant references in the European framework in the North Sea pointed out that all the analyzed projects are located in depth seabed less than 100 meters and the 70% of offshore wind farms have been connected in HVDC technology. However, for distances less than 100-150 km from shore and for rated power up to 1 GW, the HVAC solution has been preferred.

The Mediterranean Sea has major differences from the North Sea: the depth of the seabed reaches thousands of meters already a few kilometers from the coast, making the floating solutions necessary to avoid huge investments in bottom fixed configurations typically adopted in the oil & gas industry.

In the view of overcoming technical limitations, the combined solution could ensure a better utilization of the overall transmission capacity for electricity market when not fully employed from wind energy.

For this purpose, many technical and regulatory concerns have to be addressed:

- the multi-terminal HVDC system, since the conventional 2-terminal interconnector should include at least another (3-terminal or more) to connect the OWPPs without the need of off-shore wind specific connection assets;
- the offshore wind farms access to different electricity market, since the MPIs collect clusters of OWPPs and interconnect them with different European countries;
- the coordination of transmission assets sharing, since the MPIs could replace multiple radial connection schemes and potentially enable new standards and scale of development, while reducing publica opposition;
- the coordination of connections and interconnections autorizhations, with potential marine and terrestrial activities optimisation.

In Europe, the Kriegers Flack Combined Grid Solution (KG CGS) [15] is the first example of combination of existing and expected OWPPs connection to power grids with an interconnection project between Germany (state of Mecklenburg-Western Pomerania) and Denmark (region of Zealand). The KF CGS includes the three different wind farms: Kriegers Flak (rated power 600 MW, Denmark), Baltic 1 (rated power 48 MW, Germany) and Baltic 2 (rated power 288 MW, Germany), for a total capacity of 966 MW. A back-to-back VSC AC/DC converter station in Germany, near Rostock, is used to adapt the AC to the synchronous area of continental Europe. The KG CGS is illustrated in Figure 3 and since 2020 is completely in operation.

The 410 MW back-to-back HVDC converter station located in Bentwisch Germany enables interconnection of the two asynchronous AC power systems of Denmark and Germany with three offshore wind farms connected to shore with HVAC.

The development of the Master Controller for Interconnected Operation (MIO) controls the entire system by adjusting power flows in real-time to ensure reliable energy flow and trading between the regions. The MIO optimizes and controls various control modes such as different wind production level, bidirectional power flow for energy trading and operation under contingencies and can be seen in Figure 4. For normal operations the MIO will look at wind forecast to plan and optimize the power flows of the system taking into account the market and grid contingencies at that point in time. The MIO is also an expert system supporting the dispatch centers with how to handle different modes of operations depending on the network configurations, sending out control set-points,



advice functions etc. to enhance the grid performance. The back-to-back HVDC converter station can also support the voltage stability of the overall system with production or consumption of reactive power utilizing the HVDC Light technology.

In the long-term horizon, so called "Hybrid Projects" in HVDC technology could allow increased rated power over long distances, combining the renewable energy integration with different EU Countries interconnection, allowing a more sustainable sea use and an optimization of investments and system benefits.

Other MPIs planned in Europe from National Grid are the Nautilus Interconnector [17] (1,4 GW in HVDC between Great Britain and Belgium which could connect up to 2,8 GW of off-shore wind) and the EuroLink Interconnector [18] (1,8 GW in HVDC connecting Great Britain and Netherlands to Dutch offshore wind by the means of an off-shore converter platform).

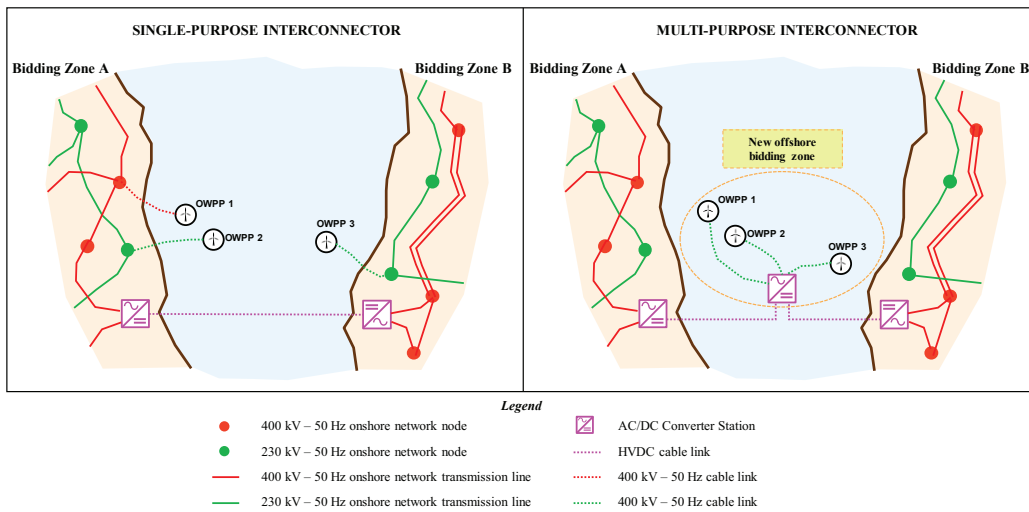


Figure 2. Single-purpose and multi-purpose interconnector.

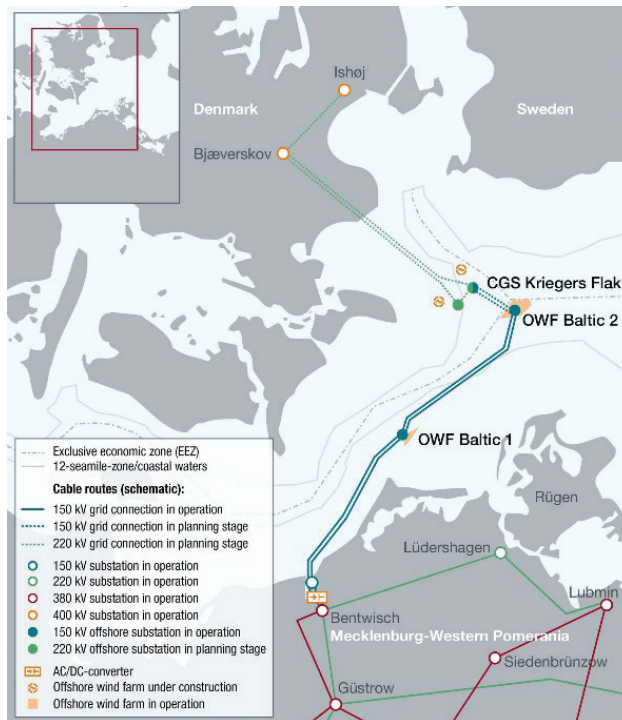


Figure 3. Kriegers Flak Combined Grid Solution, from [16]. Since 2020 the KF CGS is completely in operation.



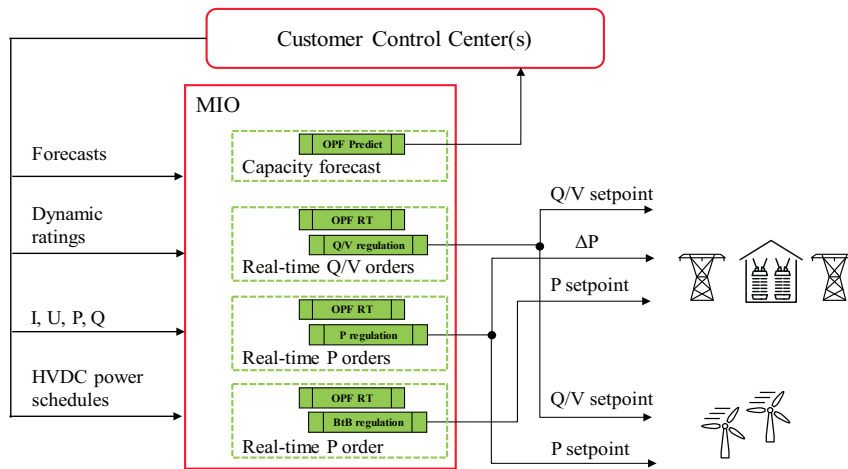


Figure 4. Master Controller for Interconnected Operation (MIO).

### 3. FLOATING WIND: TECHNICAL REVIEW

There are no existing floating HVDC converter stations today, but much can be learned both from floating HVAC substations and also oil & gas industries. The main difference between the floating HVAC and HVDC stations are the different type of equipment (including converter valves) and consequent additional space requirements and thus, heavier platforms required for HVDC offshore platforms. The first floating offshore wind demonstrator project was installed in 2009 in Norway, Hywind I. It consisted of one wind turbine of 2,3 MW [19]. The early projects of floating wind did not have any floating substations due to the small capacities, the first floating HVAC substation was installed in Japan, near Fukushima with an installed capacity of 25 MVA. It was located on depths between 100-120 m, 20 km from the coast and was installed in 2013 and decommissioned in 2021 [20]. Today, many companies are focusing on developing floating substations and in 2022 a project to update the standard DNVGL-ST-0145 that addresses the design and safety for bottom fixed substations has been started to also include floating substations and cover technology gaps for HV equipment and dynamic cables [21]. The green platform project "Ocean Grid" in Norway is a research project to develop new technology and standards for the offshore wind market in Norway both for bottom fixed and floating solutions. Aibel together with Hitachi Energy, DNV and SINTEF Ocean will look at floating HVDC converter stations for 1,5 GW, 320 kV DC and 3 GW, 525 kV DC in the Ocean Grid research project. The goal is to develop a floating converter station to a level ready for sale with a target of availability of 99% [22].

There are different concepts for floating offshore wind stations seen in Figure 5, all inspired by designs from floating wind turbines. The 66 kV floating substation in Fukushima used an advance spar design. However, there are different constraints for a floating substation compared to floating wind turbines that need to be considered for the platform designs. First of all, a substation is significantly heavier than a floating wind turbine and even heavier for a HVDC converter station as mentioned earlier. Additionally, the weight distribution is different which will have an impact on the overall design of the floating platform. There are also multiple cables connected to the floating substation, both array cables from the wind farm and the HV cables for transmission to shore that needs to be considered in the overall design [23].

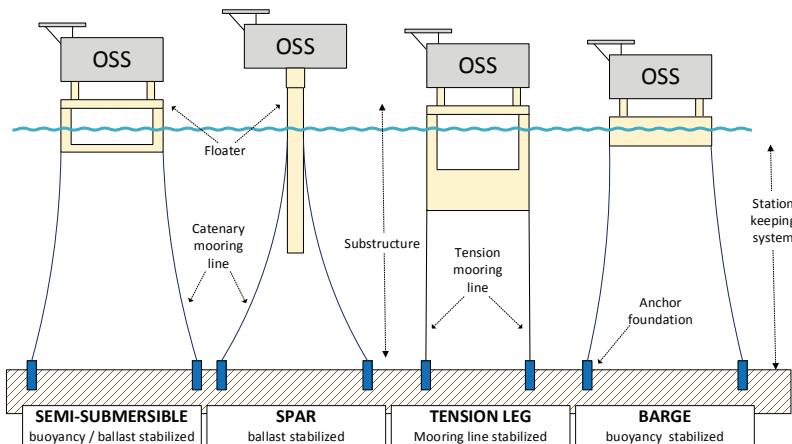


Figure 5. Concepts for floating substations [23].



The dynamic HV cables needed for floating wind farms are a key element that requires development. The existing dry type design for submarine cables, utilizes extruded lead sheaths surrounding the cable core to ensure that the insulator system is kept dry. However, lead sheaths have poor fatigue endurance and thus, not suitable for floating that will require dynamic cables that can handle extreme accelerations during storms and cycling movements for the whole lifetime of the cable. An alternative is wet type design for submarine cables where water will go into the polymer sheaths and saturates the insulation system over time. There are both cost, technical and environmental benefits with wet type design [24]. Today, this kind of cables exists for voltage up to 66 kV AC voltage but more development is required for higher voltages and HVDC dynamic cables [23].

Commercial installations of floating HVDC converter stations are expected to come later to the market than floating HVAC substations, as deep-water areas close to shore will be exploited first before going for longer transmission links where HVDC is the technology of choice due to low transmission losses. Depending on local seabed conditions the breakeven distance between HVAC and HVDC is approximately 80-120 km for offshore installation. However, looking at options for MPIs and other benefits with HVDC such as system support to AC grids the market for floating HVDC converter stations might come earlier. While there are no installed floating HVDC converter stations today there are experiences with long-haul sea transports of HVDC equipment that can give some indications on long-term performance of the equipment in a floating environment. The main technical challenges are due to the dynamic motion and acceleration mainly for the stress on the main circuit equipment such as converter valves, GIS and transformers. For AC equipment and auxiliary systems much can be learned from HVAC installations and also floating oil and gas platforms. Bottom-fixed HVDC stations can be economically competitive up to around 100 m depending on the seabed and as an intermediate step towards floating that can limit risks and costs is a combination of floating wind turbines with bottom-fixed HVDC stations on depths around 100 m.

#### 4. METHODOLOGY AND CASE STUDY

In this paper, zonal market simulations have been performed in order to assess the benefits related to different configuration of the MPIs in a very long-term energy scenario characterized by a relevant RES capacity installed. In particular, the variation in terms of Socio-Economic Welfare (SEW indicator) and “overgeneration” (i.e. renewable energy not integrated) have been evaluated in different cases.

The zonal market model, adopted in the ENTSO-E “Ten Year Network Development Plan” (TYNDP), represents the European network by the means of bidding zones interconnected by a single branch whose transmission capacity is equivalent to the sum of existing and planned transmission capacity (so called “bus-bar” model).

The official Italian TSO DAM simulator “Promed Grid” allows to execute with an hourly detail over the entire target year, an optimal unit commitment of power plants and the coordinated hydro-thermal dispatching while fulfilling all system constraints. In output, SEW indicator, power flows on the equivalent branches, average zonal price, RES generation curtailment and several others significant indicators are obtained.

In this study, a test market model in the very long-term 2040 target year has been considered with a focus on a limited number of interconnected bidding zones. In particular, starting from a “base case” including 7 bidding zones (A, B, C, D, E, F, G), different configurations of MPIs have been simulated implementing 2 new offshore bidding zones (named OBZ1 and OBZ2) interconnected with already existing bidding zones and between them, based on different configuration evaluated. In order to evaluate the benefits for the system under the “same conditions”, no additional transmission capacity or off-shore generation capacity has been implemented in the analyzed cases with respect to the initial ones.

The Table 1 describes the five cases analyzed and the Table 2 reports the details of MPIs. The Figure 6 represents the simulated market configuration in each different case: the filling of the cells stands for the interconnection between bidding zones while the variation of the transmission capacity across the border compared to the base case is made explicit in proper cells. It is important to note that each MPIs implemented corresponds to a reduction of the transmission capacity between affected bidding zones. In particular, the 1.200 MW MPI between B and F market zones replace all the original transfer capacity (i.e. B and F are connected only by the means of the new offshore bidding zone and no more directly).



Table 1. Summary of analyzed cases.

CASE	Bidding Zones		MPIs		Offshore Generation Capacity [GW]	
	Onshore	Offshore	N°	MW	Onshore Bidding Zones	Offshore Bidding Zones
Base Case	7	0	0	0	16,2	0
Case 1	7	1	1	1.000	14,9	1,3
Case 2	7	2	2	2.200	13,9	2,3
Case 3	7	2	3	3.200	13,9	2,3
Case 4	7	2	4	4.200	13,9	2,3

Table 2. MPIs characteristics.

Zone FROM	Zone TO	MPI Rated Power [MW]
C	G	1.000
B	F	1.200
OBZ1	OBZ2	1.000
OBZ2	A	1.000

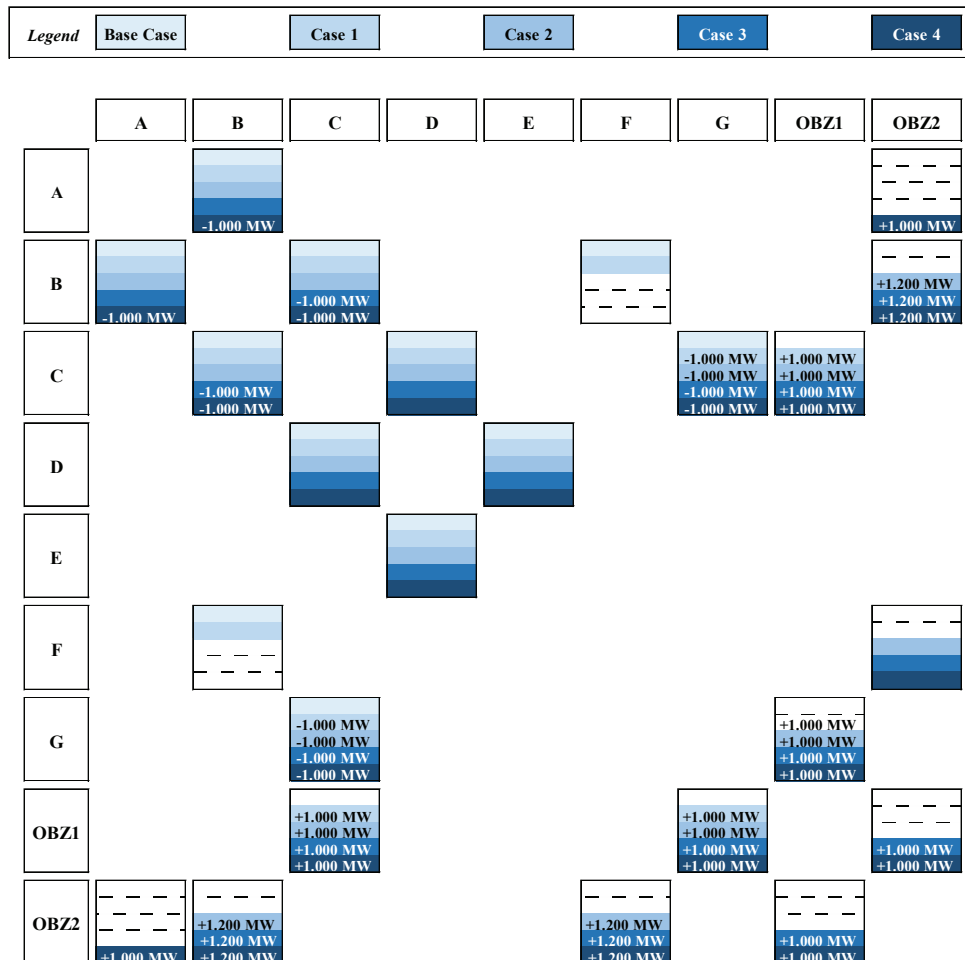


Figure 6. Summary of simulated market configuration in each case analyzed with transmission capacity variation respect to the base case details.

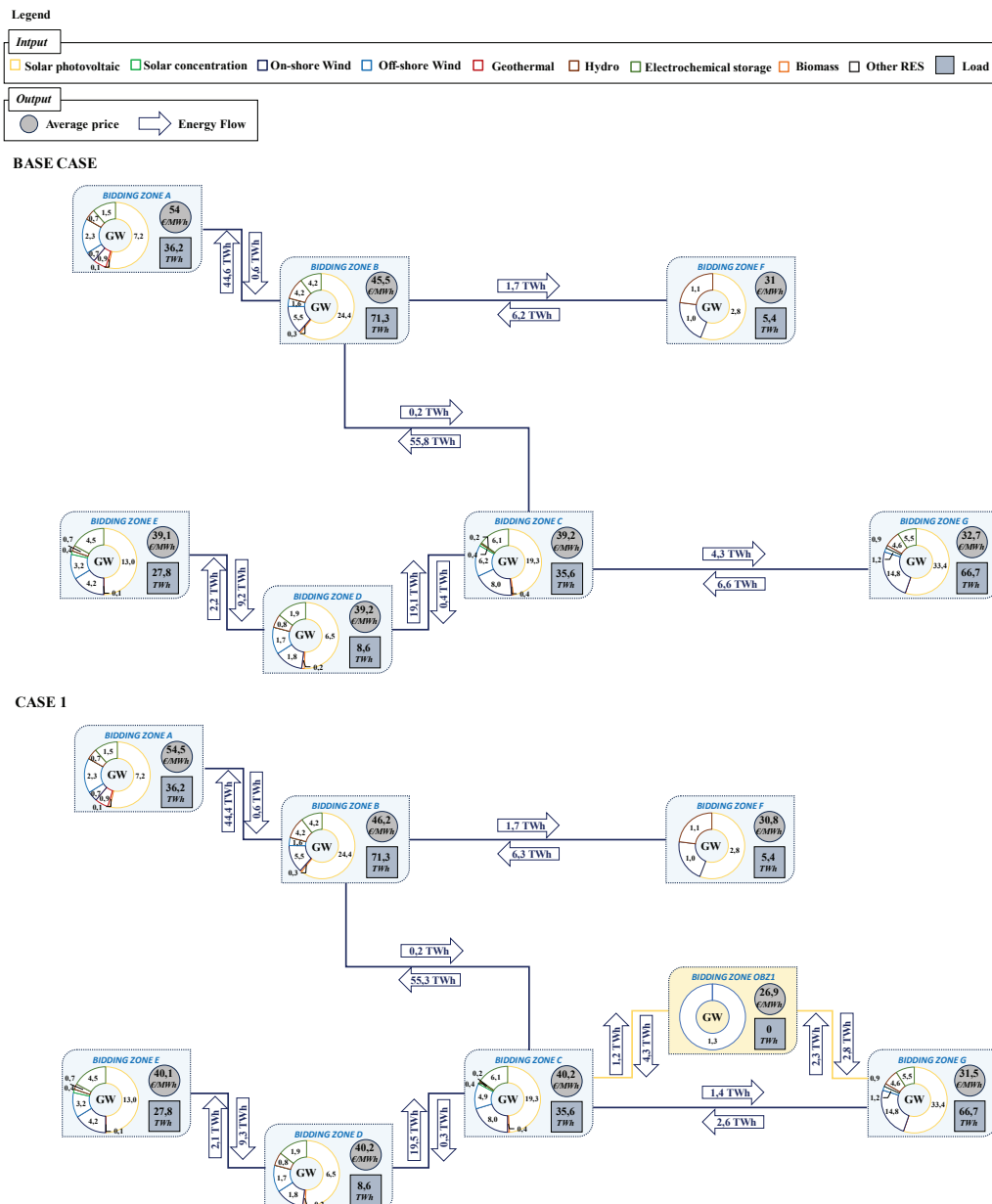


### 5. RESULTS

In this section, the results obtained from market simulations in each analyzed case are presented. In particular: Figure 7 illustrates the input (RES capacity installed and load consumption) and the output (energy flows and yearly average energy price), Figure 8 summarizes the yearly Load Factors (LF) of each equivalent branch between bidding zones under study, Figure 9 depicts the overgeneration evolution per bidding zone and, lastly, Figure 10 reports the global SEW indicator (sum of each zones under study single contributions) variation in each simulated configuration.

Main outcomes can be synthesized as follows:

- the implementation of new offshore bidding zones connected by MPIs collecting future OWPPs allows a better usage of the transmission capacity between bidding zones (higher interconnections load factors) in comparison with the base case, considering all the offshore generation capacity within onshore bidding zones;
- the MPIs allow to reduce the system overgeneration (around -5%) in comparison with the base case, ensuring a greater integration of RES sources;
- the implementation of MPIs in the market model leads to higher SEW indicators in comparison with the base case. In particular, the case 4 (considering the offshore bidding zones fully interconnected between them and with adjacent ones) shows the better performance among all investigated configurations.



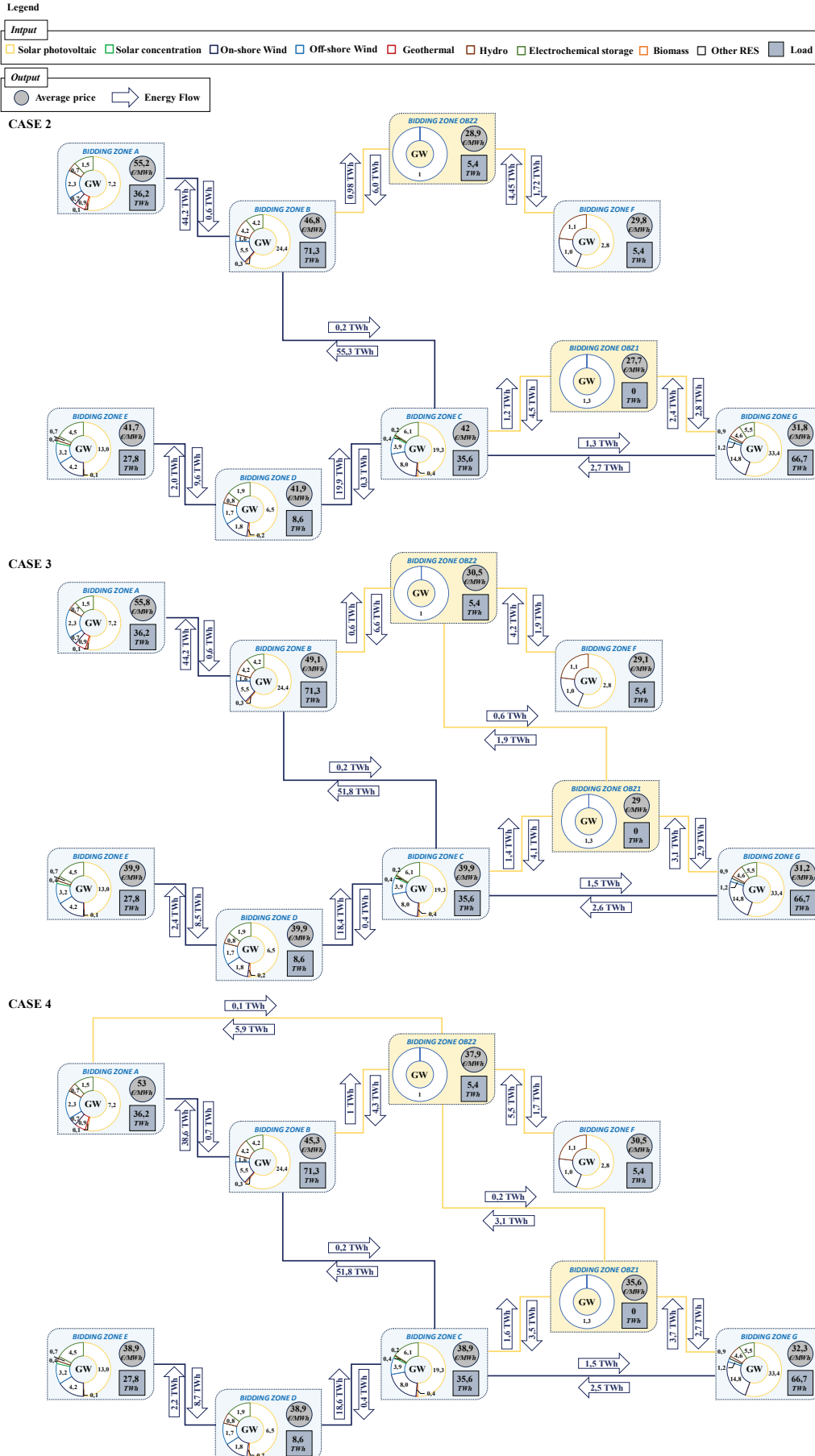


Figure 7. Market simulation results for each studied case.



Border	BASE CASE	CASE 1		CASE 2		CASE 3		CASE 4	
	LF	LF	Δ TC	LF	Δ TC	LF	Δ TC	LF	Δ TC
A - B	84,8%	84,5%		84,2%		84,0%		87,7%	-1.000
B - C	78,0%	77,3%		76,4%		82,4%	-1.000	81,2%	-1.000
C - D	44,6%	45,5%		46,5%		43,1%		43,5%	
D - E	33,9%	34,0%		34,6%		32,5%		32,6%	
C - G	85,5%	94,7%	-1.000	95,4%	-1.000	95,4%	-1.000	94,7%	-1.000
C - OBZ1		64,6%	+1.000	66,7%	+1.000	65,3%	+1.000	60,7%	+1.000
OBZ1 - G		61,5%	+1.000	61,9%	+1.000	71,1%	+1.000	75,0%	+1.000
B - F	80,3%	81,3%			-1.200		-1.200		-1.200
B - OBZ2				70,8%	+1.200	72,5%	+1.200	52,9%	+1.200
OBZ2 - F				62,3%	+1.200	61,5%	+1.200	73,1%	+1.200
OBZ2 - OBZ2						28,1%	+1.000	39,4%	+1.000
OBZ2 - A								71,7%	+1.000

Figure 8. Yearly Load Factors (LF) [%] of each equivalent branch between bidding zones under study in each case analyzed with the detail of variation in Transmission Capacity (ΔTC) [MW].

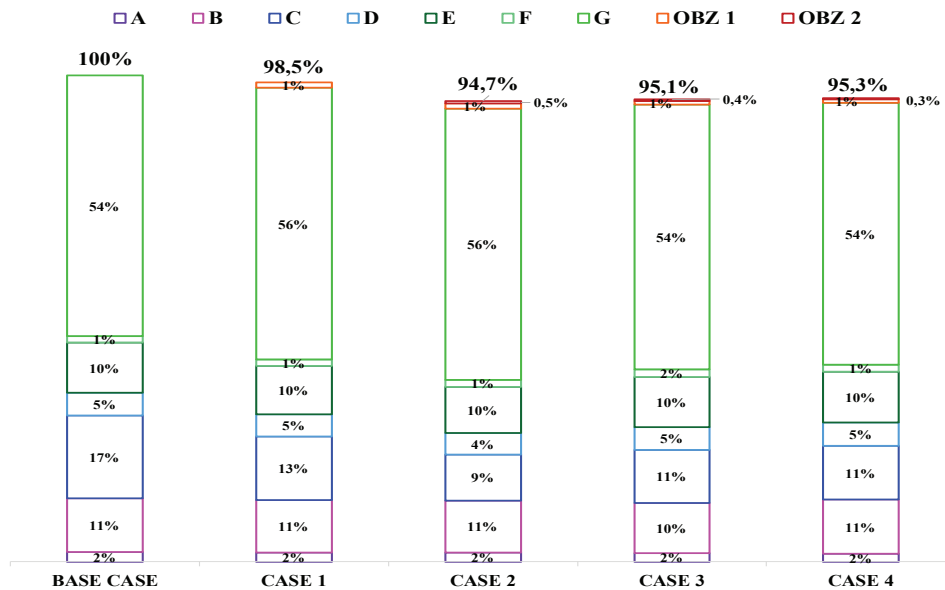


Figure 9. Overgeneration [%] in each bidding zone under study in each case analyzed.



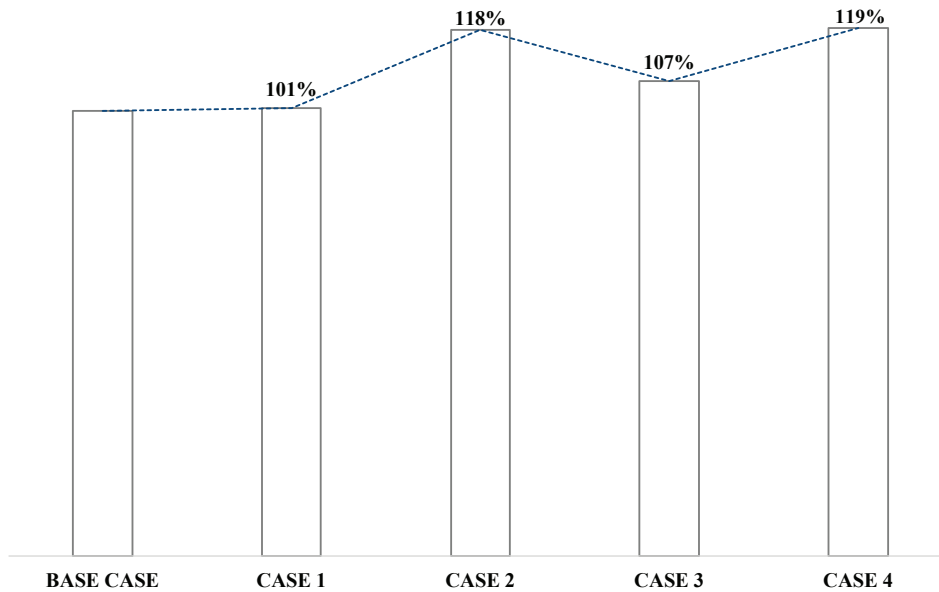


Figure 10. Global SEW indicator [%] in each case analyzed.

## 6. CONCLUSIONS

In this paper, the multi-purpose interconnectors perspectives have been investigated with the aim of assessing potential benefits in combining the offshore wind collection and the transmission infrastructure development in a unique project, in the view of a more sustainable, flexible and efficient usage of the transmission capacity and of the maritime spaces in the future decarbonized system.

A technical review of MPIs in the European context has been provided together with main challenges for offshore floating HVDC equipment.

Market simulations on a test system in the very long-term horizon have been performed in different cases, in order to assess system benefits (SEW and overgeneration reduction indicators) and transmission capacity usage: the implementation of new offshore bidding zones interconnected with the onshore ones and between them lead to best performances in terms of overgeneration reduction (around -5% in comparison with the base case), SEW (+20% maximum in comparison with the base case) and transfer capacity utilization (higher load factors of equivalent links) .

Future works will focus on market and network studies concerning large interconnected power systems.

## BIBLIOGRAPHY

- [1]. European Commission, 'Fit for 55': delivering the EU's 2030 Climate Target on the way to climate neutrality, 2021, <https://eur-lex.europa.eu/legal-content/EN/TXT/PDF/?uri=CELEX:52021DC0550>.
- [2]. Terna S.p.A., Snam S.p.A., "Documento di descrizione degli scenari 2022". In Italian. Available online: [https://download.terna.it/terna/Documento\\_Descrizione\\_Scenari\\_2022\\_8da74044f6ee28d.pdf](https://download.terna.it/terna/Documento_Descrizione_Scenari_2022_8da74044f6ee28d.pdf).
- [3]. E. M. Carlini, C. Gadaleta, M. Migliori, A. Conserva, D. Monno and S. Moroni, "Integration of Wind Offshore Generation into the Italian Transmission Network: connection solutions and case study," 2022 AEIT International Annual Conference (AEIT), 2022, pp. 1-6.
- [4]. United Nations Framework Convention on Climate Change, "Paris Agreement". Available online: [https://unfccc.int/sites/default/files/english\\_paris\\_agreement.pdf](https://unfccc.int/sites/default/files/english_paris_agreement.pdf).
- [5]. European Commission, Directorate-General for Energy, Clean energy for all Europeans, Publications Office, 2019, <https://data.europa.eu/doi/10.2833/9937>.
- [6]. Global Wind Report 2023. Available online: [https://gwec.net/wp-content/uploads/2023/03/GWR-2023\\_interactive.pdf](https://gwec.net/wp-content/uploads/2023/03/GWR-2023_interactive.pdf)
- [7]. Terna, S.p.A. Allegato A.24 al Codice di Rete, "Individuazione Zonale Della Rete Rilevante" ; Terna Group: Rome, Italy, 2021.
- [8]. Italian Regulatory Authority for Energy, Networks and Environment. Decision 19 March 2019. /2019/R/EEL. In Italian. Available online: <https://www.arera.it/allegati/docs/19/103-19.pdf>.
- [9]. L. Michi, E. M. Carlini, M. Migliori, F. Palone, S. Lauria, "Uprating studies for a 230 kV-50 Hz Overhead Line", presented at the 13th Int. IEEE PES PowerTech Conf., Milan, Italy, June 2019.



- [10]. E. M. Carlini, S. Moroni, A. Zagnoni, C. Gadaleta, A. De Cesare, C. Giordano, M. Migliori, "Linee guida per la connessione e l'integrazione dell'eolico offshore nella RTN", *L'Energia Elettrica*, vol. 2, 2023.
- [11]. Terna S.p.A.; Italian Network Code, Annex A.17, "Wind farms: General connection rules to HV networks – Protection, regulation and control system". In Italian. Available online: [https://download.terna.it/terna/Allegato%20A.17\\_8d787c9c8a17ba6.pdf](https://download.terna.it/terna/Allegato%20A.17_8d787c9c8a17ba6.pdf).
- [12]. Normativa tecnica di recepimento del RfG Regolamento (UE) 2016/631. In Italian. Available online: <https://download.terna.it/terna/0000/1151/51.pdf>.
- [13]. P. Capurso; B. Cova; E. Elia; P. Portoghese; M. Stabile; F. Vedovelli; A. Venturini, »Market integration in Europe: a market simulator taking into account different market zones and the increasing penetration of RES generation«. Cigre General Session. 2008. Paris, August 2008, paper C1-104.
- [14]. D. Devoy, E. Wells, R. Lodhia, M. Moran, M. Bray and C. A. Smith, »The use of Multi-Purpose Interconnectors to meet net zero by 2050«, The 17th International Conference on AC and DC Power Transmission (ACDC 2021), Online Conference, 2021, pp. 150-154, doi: 10.1049/icp.2021.2460.
- [15]. A. - Marten, V. Akhmatov and R. Stornowski, "Kriegers Flak combined grid solution — novel double use of offshore equipment", 15th IET International Conference on AC and DC Power Transmission (ACDC 2019), Coventry, UK, 2019, pp. 1-8, doi: 10.1049/cp.2019.0002.
- [16]. 50hertz, Elia Group, "Krieger Flack – Combined Grid Solution", Available online: <https://www.50hertz.com/en/Grid/Griddevelopment/Concludedprojects/CombinedGridSolution>.
- [17]. National Grid, "Nautilus Interconnector", 2021. Available online: <https://www.nationalgrid.com/document/143431/download>.
- [18]. National Grid, "EuroLink Interconnector", 2022. Available online: <https://www.nationalgrid.com/document/148471/download>.
- [19]. Equinor, "StatiolHydro inaugurates floating wind turbine", 9 September 2009. <https://www.equinor.com/news/archive/2009/09/08/InnovativePowerPlantOpened>.
- [20]. Fukushima FORWARD, "Fukushima Floating Offshore Wind Farm Demonstration Project", <http://www.fukushima-forward.jp/english/reference/index.html>.
- [21]. 30 partners join DNV to start Joint Industry Project for floating offshore wind substations, <https://www.dnv.com/news/30-partners-join-dnv-to-start-joint-industry-project-for-floating-offshore-wind-substations-222575>.
- [22]. Ocean Grid, "Floating HVDC platform", <https://oceangridproject.no/research/floating-hvdc-platform>
- [23]. N. Rouxel, "Floating Substations: the next challenge on the path to commercial scale floating windfarms", <https://www.dnv.com/article/floating-substations-the-next-challenge-on-the-path-to-commercial-scale-floating-windfarms-199213>.
- [24]. Ocean Grid, "Progress updates – Wet design cables", <https://oceangridproject.no/sp2-updates>



# Comparative Performance Analysis of Network Reduction on the Transmission Expansion Planning

[ahmet.ova@teias.gov.tr](mailto:ahmet.ova@teias.gov.tr)**AHMET OVA, ERDİ DOĞAN***Turkish Electricity Transmission Corporation***ŞEVKİ DEMİRBAŞ***Gazi University, Electrical Electronics Engineering)***Türkiye**

## SUMMARY

Transmission Expansion Planning (TEP) is an optimization study that aims to determine new transmission lines to be added to the grid within the scope of different purpose functions in order to meet the increasing electrical energy demand economically and reliably by maintaining the stability of the transmission grid in future planning periods. It is difficult to model the large and complex structure of transmission grids for static and dynamic analyzes to be made on transmission grids. Rather than modeling the grid exactly, it is easier to construct an equivalent model in terms of representing the full grid. In this study, a TEP problem has been studied in which the investment costs of the lines and the cost of energy not supplied are minimized. While the Modified Ward method has been used to create the equivalent model, a novel meta-heuristic optimization approach, Forensic Based Investigation Optimization (FBIO), has been implemented so as to solve the TEP problem. FBIO has been applied on the original and equivalent IEEE 24-bus test system. TEP problem is modelled by using Python Programming Language and power flows are calculated with DC power flow equations. Experimental analyses have shown that there is not a significant difference in the obtained solutions between the original case and the equivalent case of the IEEE 24-bus test system.

## KEYWORDS

Transmission expansion planning, FBIO, DC model, Equivalent model, Modified Ward.



### 1. INTRODUCTION

Modern transmission networks are planned and operated in an interconnected structure in order to meet the electricity demand in an uninterrupted, high quality and reliable manner. It is necessary to add new transmission lines to the transmission networks in order to both meet the increasing demand and maintain the system balance. In recent years, the increase in the interest in renewable energy sources, the increase in the integration of renewable energy sources into the network, the changes in the generation and load profile have affected the structure of the transmission networks. This situation has caused the large and complex structure of transmission networks to be even more complex.

It is necessary to strengthen and expand the transmission network in order to meet the increasing transmission capacity need in parallel with the increase in generation capacity and load demand and to protect system security. Transmission Expansion Planning (TEP) is an optimization study that aims to determine new transmission lines to be added to the network within the scope of different purpose functions in order to meet the increasing electrical energy demand economically and reliably by maintaining the stability of the transmission network in future planning periods [1]. TEP emerges as an optimization problem that aims to find the most appropriate solution to problems such as when, where and with what characteristic a new transmission line will be established.

It is very difficult to model the large and complex structure of transmission networks for static and dynamic analyzes to be made on transmission networks. Rather than modeling the network exactly, it is easier to construct an equivalent model in terms of representing the full network. It is important to create an equivalent network in order to better understand the behavior of the network. There are some advantages to using the equivalent network. If a region of the network is to be dealt with, it will be sufficient to analyze only the equivalent model of that region. If fault analysis is to be carried out in a region again, it will be sufficient to create a regionally equivalent network. In general, when the behaviour of a certain region of the network is concerned, this region is expressed as the internal network and the remaining part of the network is expressed as the external network.

Equivalent networks are classified as static and dynamic according to their application areas. Dynamic equivalent network is used to analyze the dynamic behaviour of the network for steady and transient states. Among the dynamic equivalent network generation methods that are widely used in the literature, there are methods such as coherency [2], modal analysis [3], optimal model coherent aggregation [4], inertial and slow coherency aggregation [5]. Static equivalent network is used in static analysis such as power flow calculations, operation and planning studies in the system. It is also used in transmission expansion planning [6], generation planning [7], unit commitment [8] and creation of flow-based market coupling algorithms [9]. Among the static equivalent network generation methods commonly used in the literature are Ward [10], REI [11], Kron [12] and Zhukov [13] methods.

In this study, firstly, the creation of the static equivalent network model, which is aimed to be used in optimization-based transmission system planning studies, is examined and the reduced model of the IEEE 24-bus test system has been obtained. The Modified Ward method has been used to create the static equivalent model. In order to make performance evaluations by using the equivalent model in transmission system planning studies, a TEP problem, in which the investment costs of the transmission lines and the cost of energy not supplied are minimized in determining the new transmission lines to be added to the network, has been addressed. Forensic Based Investigation Optimization (FBIO) method which is a meta-heuristic optimization method with a human-based search procedure, has been proposed in order to solve the problem [14]. The software developed in order to create the optimization model and solve TEP problem was designed utilizing Python Programming Language.. The Panda Power has been used in modeling the IEEE 24-bus test system and in carrying out power flows with the DC model. The optimization method has been applied both on the original and equivalent IEEE 24-bus test system to solve the static TEP problem and the obtained solutions have been evaluated and compared in this study. Simulation results have validated that the equivalent model of the network reducing complexity in real-life grids can be used in order to solve the TEP problem.

### 2. TECHNICAL BACKGROUND AND PROPOSED METHOD

In order to create a static equivalent model of the transmission grid, the full grid is divided into 3 subgrids, internal, boundary and external. The internal grid is actually the grid where the analysis will be made, the behavior of the grid will be observed and the equivalent model will be created. Boundary grid is the grid that includes the busbars and lines where the internal grid and the external grid are connected. The external grid, on the other hand, is excluded and it does not need to be modeled in detail. Figure 1 shows the division of the full grid into 3 subgrids for the static equivalent model.

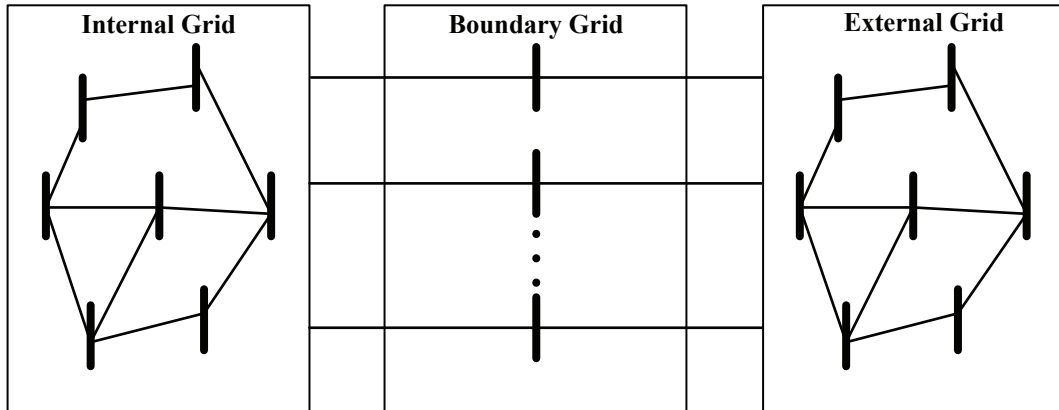


Figure 1. Subdivision of the full grid

Among the static equivalent network modeling methods, Ward [15]–[17] and REI [17]–[19] methods are widely used. Especially the Ward method is used in many studies. Although the Ward method is a proven method under different load and topology conditions in transmission grids, the solution process is long. On the basis of the classical Ward method, in the internal grid where the equivalent network will be formed, the load and generation are converted into fixed shunt admittance and connected to the external network through the busbars in the boundary network.

As a result, an equivalent model of the internal grid is created [10]. In the REI method, the busbars in the external grid can be converted to a single REI busbar or to 2 REI busbars, 1 load busbar and 1 generation busbar [11]. In this study, the Modified Ward method has been used. While the classical Ward method uses the method of creating a new current vector by adding the currents in the erased busbars to the neighboring busbars and converting this current vector to apparent power, in the Modified Ward method, the method of transferring the active and reactive powers of the erased busbars to the neighboring busbars according to the impedance ratio of the lines with the neighbouring busbars is used [20].

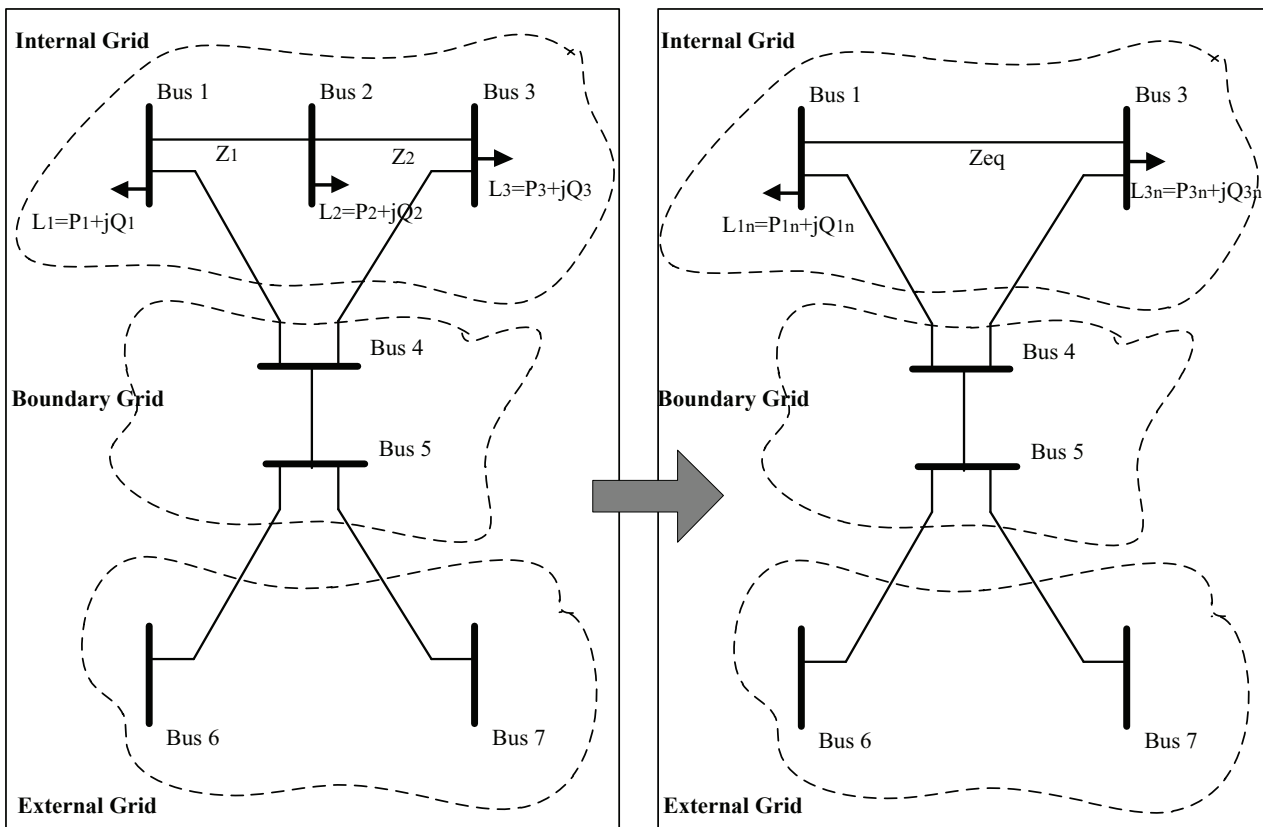


Figure 2. Example grid using the Modified Ward method



Figure 2 shows the single line diagrams of the new and original of the example grid with 7 busbars. First of all, the full grid is divided into 3 subgrids. The grid with Bus 1, Bus 2 and Bus 3 is the internal grid, and the reduction work has been done in this area. The grid with Bus 4 and Bus 5 is a boundary network and is kept constant. The grid with Bus 6 and Bus 7 is the external grid. Bus 2 is eliminated when the Modified Ward method is applied to the internal network consisting of 3 busbars and 2 lines. Active and reactive powers in Bus 2 are transferred to Bus 1 and Bus 3. After the application of the Modified Ward method, the equivalent loads in Bus 1 and Bus 3 are calculated with the equations given in Eq. 1 and Eq. 2, while the equivalent impedance of the line between Bus 1 and Bus 2 is calculated with the equation given in Eq. 3 [21].

$$L_{1n}: P_{1n} + jQ_{1n} = P_1 + jQ_1 + \frac{Z_2}{Z_{eq}} (P_2 + jQ_2) \tag{1}$$

$$L_{3n}: P_{3n} + jQ_{3n} = P_3 + jQ_3 + \frac{Z_1}{Z_{eq}} (P_2 + jQ_2) \tag{2}$$

$$Z_{eq} = Z_1 + Z_2 \tag{3}$$

### 3. CASE STUDY OF NETWORK REDUCTION ON THE IEEE 24-BUS TEST SYSTEM

This section includes obtaining static equivalent models of the IEEE 24-bus test system using the PSS/E program [22]. The efficiency of the equivalent model has been examined in terms of total active and reactive power changes and error rates in active and reactive power flows over transmission lines. Before performing the equivalent grid creation, the number of generation busbars in the internal grid can be reduced if desired. By converting the active and reactive power generation in the generation busbars as negative load, respectively, the generation busbars are converted into load busbars.

The original topology of the IEEE 24-bus test system used in this study consists of total 24 busbars, 33 transmission lines and 5 transformers at 138 kV and 230 kV voltage levels. A total of 7 busbars and 12 lines located at 138 kV voltage level have been determined as external network. Internal grid is 230 kV grid and the grid consists of 11 busbars and 21 lines. The boundary grid consists of 6 busbars and 5 transformers. The internal grid where the static equivalent network will be formed consists of 11 busbars and 21 transmission lines. As a result of the application, a reduced grid consisting of 7 busbars and 16 transmission lines is obtained. Compared to the original grid, a reduction ratio of 36% is calculated at the bus scale. Figure 3 shows the original IEEE 24-bus test system and the resulting equivalent network.

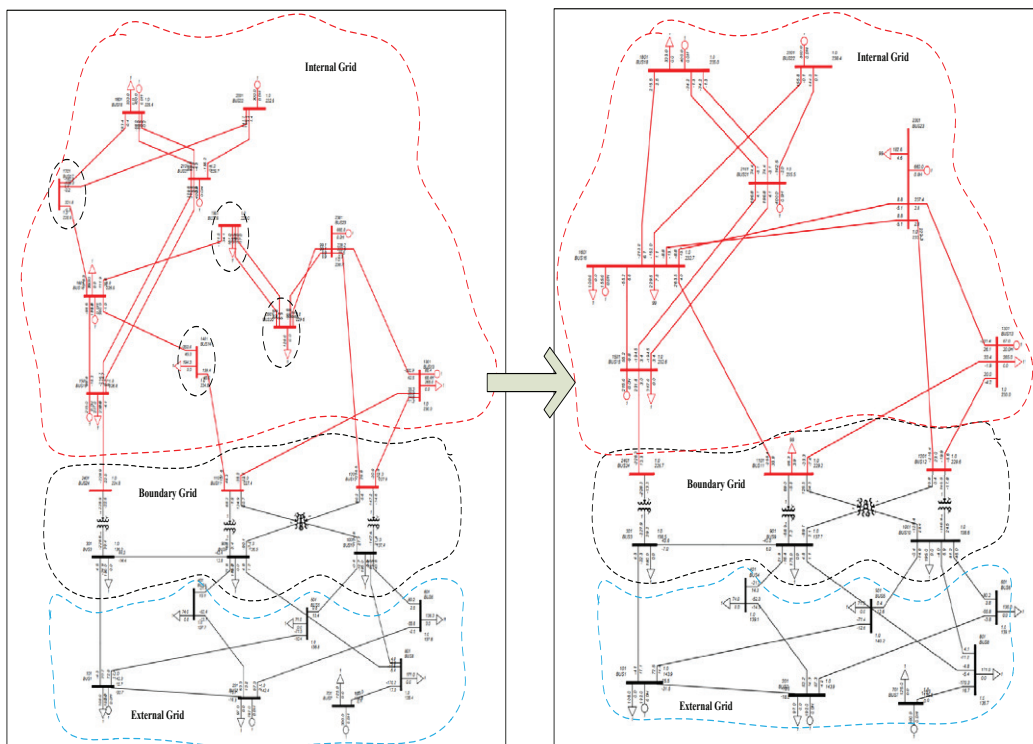


Figure 3. The original IEEE 24-bus test system and the resulting equivalent grid





In Table 1, the active values flowing from the 5 transformers in the boundary grid in the original and equivalent model of the test system and their change rates are given. When the table is examined, it is seen that the maximum change in transformers in the boundary network is 1.17%. It can be inferred that the deviation in active power flows is insignificant compared to the gain from a 36% reduced rate in the network.

Table 1. Load flow results for Original and Equivalent model

Transformers	Original Model P(MW)	Equivalent Model P(MW)	Change P(MW)	Rate of Change (%)
T1	228.9	228.3	0.6	0.26
T2	68.2	69	0.8	1.17
T3	124.9	125.5	0.6	0.48
T4	147.2	146.5	0.7	0.47
T5	90.2	89.8	0.4	0.44

## 4. STUDY OF TEP ON THE ORIGINAL AND EQUIVALENT IEEE 24-BUS TEST SYSTEM

In this study, a TEP problem in which the investment cost of the transmission lines and the loss of load cost are minimized in determining the new transmission lines to be added to the network for a period of time during the planning period is discussed. The FBIO method, which is a novel meta-heuristic optimization method with a swarm-based search procedure, is used to solve the problem. The proposed method is applied for 2 different cases on the original and equivalent IEEE 24-bus test system using the DC model to solve the static TEP problem.

### 4.1. Mathematical model of tep problem

The objectives of the multi-purpose TEP problem include minimizing the investment costs of new transmission lines to be added to the network for the planning period and the loss of load in this study.

Notations used in the mathematical model:	
$TC$	total cost
$IC$	investment cost
$LC$	loss of load cost
$C_{ij}$	cost of line added from bus $i$ to bus $j$
$a_i$	penalty cost at bus $i$
$r_i$	dummy generation at bus $i$
$f$	active power flows through the lines
$g$	active power generations
$\bar{g}$	maximum generation capacity
$r$	loss of load
$d$	loads
$\bar{d}$	maximum loads
$f_{ij}$	active power flow between buses $i$ and $j$
$f_{ij}^c$	active power flow between buses $i$ and $j$ in the single outage of line $c$
$\bar{f}_{ij}$	maximum active power flow between buses $i$ and $j$
$B_{ij}$	line susceptance $ij$
$n_{ij}^0$	initial number of lines from bus $i$ to bus $j$
$n_{ij}$	number of new lines added from bus $i$ to bus $j$
$\bar{n}_{ij}$	maximum number of new lines which can be added from $i$ to $j$
$\theta_{ij}$	voltage phase angle difference between bus $i$ and bus $j$
$\Omega$	set of all candidate lines
$\Omega_{ctl}$	set of congested lines



The mathematical model of the objective function in the TEP problem can be formulated as follows:

$$TC = IC + LC \quad (1)$$

$$Min. TC = \sum_{ij} C_{ij} n_{ij} + \sum_i a_i r_i \quad (2)$$

Here, TC is the total cost and includes the line costs (IC) to be added to the grid and the loss of load cost (LC).

**Constraints:**

In order to find the most suitable solution within the framework of the objective function determined in the TEP problem, the constraints related to the power system requirement should be taken into account.

$$f + g + r = d \quad (3)$$

$$f_{ij} - B_{ij}(n_{ij}^0 + n_{ij})\theta_{ij} = 0 \quad (4)$$

$$0 \leq g \leq \bar{g} \quad (5)$$

$$0 \leq r \leq \bar{d} \quad (6)$$

$$0 \leq n_{ij} \leq \bar{n}_{ij} \quad \forall (i, j) \in \Omega \quad (7)$$

$$|f_{ij}| \leq (n_{ij}^0 + n_{ij})\bar{f}_{ij} \quad (8)$$

While the constraint in Equation (3) expresses the active power balance in the busbars, the constraint in Equation (4) expresses the active power flow in the lines. The maximum and minimum limits of generation in power plants are given by Equation (5), and the maximum and minimum limits of loss of load occurring in busbars are presented by Equation (6). The maximum number of new transmission lines to be added to a corridor in the network is ensured by using Equation (7) while the thermal limits of the lines are considered with Equation (8). In the TEP problem, Equation (3) and (4) are modeled as equality constraints, while Equation (4), (5), (6), (7) and (8) are modeled as inequality constraints.

**4.2. Forensic Based Investigation Optimization (FBIO)**

FBIO, a human-based meta-heuristic method developed by Chou and Nguyen in 2020, has been used to solve the identified TEP problem [14]. FBI optimization is inspired by the forensic investigation process in order to find of the locating and tracking of the suspects in criminal cases. There are two main mechanisms for inquiring about the suspects: investigation and pursuit. Investigation team performs exploration phase and pursuit team performs exploitation phase.

**4.3. Case studies**

In this section, the transmission system planning study has been carried out on the original and equivalent IEEE 24-bus test system [23]. Optimum transmission lines have been obtained on the basis of the objective function determined for both cases. In the system, it is assumed that the generation and load increased by 3 times compared to the current situation for the planning period and this generation and load is dispatched as deterministic approach. For the new lines to be added to the system due to increased load and generation, a total of 45 new candidate corridors(right of way), 38 of which are corridors of existing lines and 7 of which are new corridors, have been determined. It is assumed that a maximum of 3 lines can be built for each corridor. In addition, the results have been obtained by taking into account the N-1 security criterion for both cases. The best solutions obtained for the cases(Case 1A: on the original IEEE 24-bus test system, Case 1B: N-1 constraint condition for Case 1A, Case 2A: on the equivalent IEEE 24-bus test system, Case 2B: N-1 constraint condition for Case 2A) have been compared in Table 2.



**Table 2.** Solutions of the cases

Corridor	Case 1A	Case 1B	Case 2A	Case 2B
	<b>Number of lines built</b>			
1-5	1	-	1	2
2-4		1		
2-6		1		
4-9		-		1
5-10		1		1
6-10	1	3	1	2
7-8	2	3	2	3
11-13				2
11-14		2		
11-16				2
12-13		1		1
14-16	1	2		
15-16		2		
15-21	-	2		2
15-24	1	2	1	1
15-23				2
16-17	2	3		
16-18	-	-	2	
16-19	1	2		
16-22				1
17-18	1	2		
17-22		2		
18-21		2		
19-20		1		
10-11		2		2
9-11				1
10-12		1		
3-24	1	2	1	2
1-8		2		
<b>Total added lines</b>	<b>11</b>	<b>39</b>	<b>8</b>	<b>25</b>
<b>Total cost (M\$)</b>	<b>370</b>	<b>1771</b>	<b>212</b>	<b>892</b>

When the results in Table 2 are evaluated, it is seen that the results obtained with the case studies using the equivalent model are lower cost than the results obtained with the original model in terms of the number of lines added to the system and the total cost. As 14, 17, 19 and 20 busbars have been reduced while creating the equivalent model, partial changes have been observed in the results obtained in Case 2A and Case 2B. Depending on the Reduced 4 busbars, the line needs in the corridors have also partially changed. For example whereas in Case 1A new lines have been added for corridors 14-16,16-17,17-18 and 16-19, there have been obtained no new line solutions for these corridors in Case 2A. The reason for this is that 16-18 corridor has been formed in the equivalent model created with reduction, so the need for new lines connected to this corridor have not been risen. In the Figure 4, it can be seen comparison of the results between Case 1A and Case 2A.

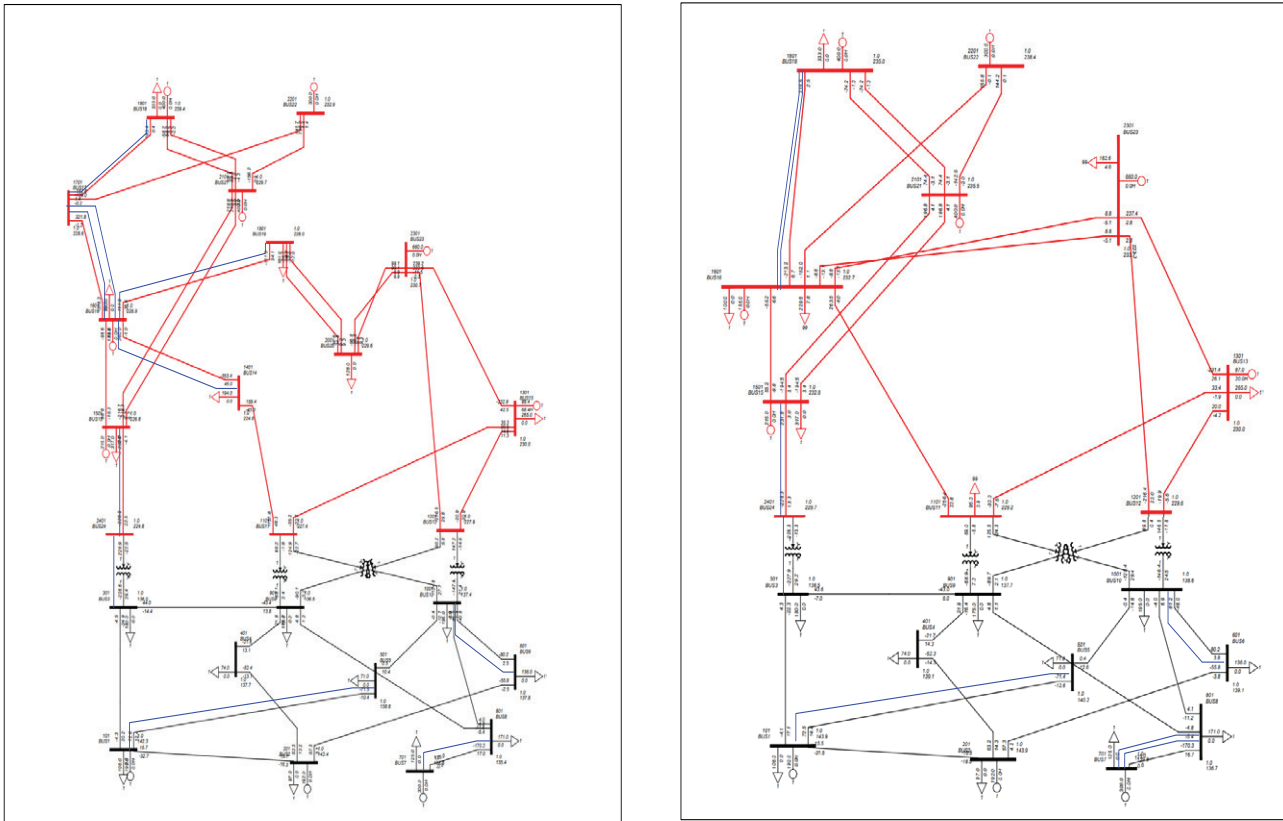


Figure 5. New topology for Case 1A and Case 2A after TEP

## 5. CONCLUSION

In this study, TEP and grid reduction studies have been carried out in order to determine the location and number of new transmission lines to be added to the system in order to meet the increasing load demand in long term planning periods uninterruptedly and economically. The TEP study has been performed on the original IEEE 24-bus test system and the equivalent model obtained using PSS/E in order to validate the result of created reduced network. While the equivalent model has been created by utilizing the Modified Ward method, the FBIO method has been used to solve the TEP problem. It has been observed that the obtained equivalent grid reflects the original grid with its static aspect. In addition, it has been seen that the results obtained with FBIO give the best results, similar to the results obtained using different optimization methods in the literature. It should be noted that although the benefits of using equivalent model are endorsed, some candidate transmission lines which need to be invested in the internal network might be disregarded due to the omission some busbars. Future studies include the implementation of TEP for 5 and 10 year planning horizons based on different generation and load scenarios on the Turkish transmission grid.

## BIBLIOGRAPHY

- [1] M. Mahdavi, C. Sabillon Antunez, M. Ajalli, and R. Romero, "Transmission Expansion Planning: Literature Review and Classification," *IEEE Syst. J.*, vol. 13, no. 3, pp. 3129–3140, 2019, doi: 10.1109/JSYST.2018.2871793.
- [2] H. Kim, G. Jang, and K. Song, "Dynamic reduction of the large-scale power systems using relation factor," *IEEE Trans. Power Syst.*, vol. 19, no. 3, pp. 1696–1699, 2004, doi: 10.1109/TPWRS.2004.831697.
- [3] S. Member, R. De Janeiro, S. Mendxr, and R. De Janeiro, "MODAL DYNAMIC EQUIVALENT FOR ELECIRIC POWER SYSTEMS," vol. 3, no. 4, pp. 1723–1730, 1988.
- [4] R. A. Schlueter, "Optimal Model Coherent Aggregation of Dynamic Equivalents for Transient Stability Studies," *IEEE Power Eng. Rev.*, vol. PER-4, no. 7, p. 38, 1984, doi: 10.1109/MPER.1984.5525879.
- [5] J. H. Chow, R. Galarza, P. Accari, and W. W. Price, "Inertial and Slow Coherency Aggregation Algorithms for Power System Dynamic Model Reduction," *IEEE Trans. Power Syst.*, vol. 10, no. 2, pp. 680–685, 1995, doi: 10.1109/59.387903.
- [6] S. de la Torre, A. J. Conejo, and J. Contreras, "Transmission expansion planning in electricity markets," *IEEE Trans. Power Syst.*, vol. 23, no. 1, pp. 238–248, Feb. 2008, doi: 10.1109/TPWRS.2007.913717.



- [7] J. H. Roh, M. Shahidehpour, and Y. Fu, "Market-based coordination of transmission and generation capacity planning," *IEEE Trans. Power Syst.*, vol. 22, no. 4, pp. 1406–1419, Nov. 2007, doi: 10.1109/TPWRS.2007.907894.
- [8] C. E. Murillo-Sánchez, R. D. Zimmerman, C. Lindsay Anderson, and R. J. Thomas, "Secure planning and operations of systems with stochastic sources, energy storage, and active demand," *IEEE Trans. Smart Grid*, vol. 4, no. 4, pp. 2220–2229, 2013, doi: 10.1109/TSG.2013.2281001.
- [9] K. Van den Bergh, J. Boury, and E. Delarue, "The Flow-Based Market Coupling in Central Western Europe: Concepts and definitions," *Electr. J.*, vol. 29, no. 1, pp. 24–29, 2016, doi: 10.1016/j.tej.2015.12.004.
- [10] J. B. Ward, "Equivalent Circuits for Power-Flow Studies," *Trans. Am. Inst. Electr. Eng.*, vol. 68, pp. 373–382, 1949, doi: 10.1109/T-AIEE.1949.5059947.
- [11] P. Dimo, "Nodal Analysis of Power Systems." p. 290, 1975.
- [12] S. Y. Caliskan and P. Tabuada, "Towards Kron reduction of generalized electrical networks," *Automatica*, vol. 50, no. 10, pp. 2586–2590, 2014, doi: 10.1016/j.automatica.2014.08.017.
- [13] S. M. Ashraf, B. Rathore, and S. Chakrabarti, "Performance analysis of static network reduction methods commonly used in power systems," *2014 18th Natl. Power Syst. Conf. NPSC 2014*, May 2015, doi: 10.1109/NPSC.2014.7103837.
- [14] J. S. Chou and N. M. Nguyen, "FBI inspired meta-optimization," *Appl. Soft Comput. J.*, vol. 93, p. 106339, 2020, doi: 10.1016/j.asoc.2020.106339.
- [15] J. Srivani and K. S. Swarup, "Power system static security assessment and evaluation using external system equivalents," *Int. J. Electr. Power Energy Syst.*, vol. 30, no. 2, pp. 83–92, 2008, doi: 10.1016/j.ijepes.2007.06.008.
- [16] S. Deckmann, A. Pizzolante, A. Monticelli, B. Stott, and O. Alsac, "Numerical Testing of Power System Load Flow Equivalents," *Proc. Annu. Reliab. Maintainab. Symp.*, no. 6, pp. 2292–2300, 1980.
- [17] S. M. Ashraf, B. Rathore, and S. Chakrabarti, "Performance analysis of static network reduction methods commonly used in power systems," *2014 18th Natl. Power Syst. Conf. NPSC 2014*, no. 1, 2015, doi: 10.1109/NPSC.2014.7103837.
- [18] S. C. Savulescu, "Equivalents for Security Analysis of Power Systems.," *Radiophys. Quantum Electron. (English Transl. Izv. Vyss. Uchebnykh Zaved. Radiofiz.*, no. 5, pp. 2672–2682, 1980, doi: 10.1109/mper.1981.5511545.
- [19] M. Yesil and E. Irmak, "A New Bus Reduction Approach based on Extended REI Model," *Proc. - 2022 IEEE 4th Glob. Power, Energy Commun. Conf. GPECOM 2022*, no. June, pp. 400–405, 2022, doi: 10.1109/GPECOM55404.2022.9815757.
- [20] Y. Jiang, N. Acharya, and Y. Pan, "Model reduction for fast assessment of grid impact of high penetration PV," *2017 19th Int. Conf. Intell. Syst. Appl. to Power Syst. ISAP 2017*, 2017, doi: 10.1109/ISAP.2017.8071384.
- [21] M. J. Reno, R. J. Broderick, and S. Grijalva, "Formulating a simplified equivalent representation of distribution circuits for PV impact studies," *Sandia Natl. Lab. ...*, no. April, 2013, [Online]. Available: [https://www.researchgate.net/profile/Matthew\\_Reno/publication/264458156\\_Formulating\\_a\\_Simplified\\_Equivalent\\_Representation\\_of\\_Distribution\\_Circuits\\_for\\_PV\\_Impact\\_Studies/links/53e0294b0cf2a768e49f5bec.pdf](https://www.researchgate.net/profile/Matthew_Reno/publication/264458156_Formulating_a_Simplified_Equivalent_Representation_of_Distribution_Circuits_for_PV_Impact_Studies/links/53e0294b0cf2a768e49f5bec.pdf).
- [22] M. Zahid Hasan, N. Al Masood, A. Hasib Chowdhury, and A. Haque, "Coherency based Reduction of a Large Power System using PSS/E," *2019 IEEE Int. Conf. Power, Electr. Electron. Ind. Appl. PEEIACON 2019*, no. 1, pp. 83–86, 2019, doi: 10.1109/PEEIACON48840.2019.9071957.
- [23] A. Ova, E. Dogan, and S. Demirbas, "Transmission Expansion Planning Using A Noval Meta-Heuristic Method," *Int. J. Renew. Energy Res.*, vol. 12, no. 4, pp. 1988–2001, 2022, doi: 10.20508/ijrer.v12i4.13495.g8567.



# Strategic Positioning of Transmission System Operators to Achieve Long-Term Goals and Sustainability of the Green Transition - Analysis and Case Study

[dsabolic@hops.hr](mailto:dsabolic@hops.hr)

**IGOR IVANKOVIĆ, DUBRAVKO SABOLIĆ\*, IRA ŽUPIĆ, ANTUN ANDRIĆ**  
*Croatian Transmission System Operator, Ltd.*

**Croatia**

## SUMMARY

This paper analyzes the impact of the two dominant business processes of the last several years on transmission system operators' short-term and long-term sustainability. The two processes are the green transition and the disturbance in energy markets that began in 2021. We will examine the case of the Republic of Croatia, but we will provide more general conclusions and policy recommendations. Methodologically, we will put these topics into Porter's five forces framework and study the strategic industry environment in which the electricity grid operators work. In many previous strategic analyses of a grid operator as an economic agent within an industrial context, some relevant values produced by or around the power grid were overlooked because they did not belong to the "classical", more tangible, and obvious category of values worth competing for. When the borders of the industry are reinterpreted through the lens of all relevant stakeholders, the agents with some interests vested in the business but are not traditionally perceived as members of the industry, the strategic outlook of grid operation could become more in line with perceived reality. Finally, we will consider the space for the company's strategic decisions to ensure the fulfillment of its elementary functions and the strategic social goals of the green transition. We also analyze the strategic risks associated with such disruptive events in the electrical and energy industries.

## KEYWORDS

Electricity transmission – business strategy – business sustainability – green transition.





**Oral Presentation:** Strategic Positioning of Transmission System Operators to Achieve Long-Term Goals and Sustainability of the Green Transition - Analysis and Case Study

### 1. INTRODUCTION

In the general literature in the field of business strategy, the competitive pressures the company is exposed to are usually considered. Because of them, it is forced to deal with the analysis of the strategic moves of the competition and the adoption of its own strategic responses. For example, the well-known Porter's five competitive forces model [1] talks about pressures from industry competitors, suppliers, customers, potential competitors, and substitutes. However, when it comes to transmission companies, at first glance, they are not exposed to any competitive pressures because, as natural monopolists: (i) they have no competitors; (ii) they have significant bargaining power vis-à-vis suppliers and customers; (iii) they have no threat of potential competition, (iv) there are no likely substitutes. Moreover, the fact that their revenues are regulated creates even more of the impression that such companies are isolated from all the influences of the competitive environment.

Perhaps the best time to analyze business sustainability is the time of a grave crisis, such as the one that occurred in European electricity markets months before the onset of the Ukrainian war. Naturally, the war did not help, either. However, it did not start the market disturbance that began in 2021. Hugely inflated energy prices affected the TSO operating costs primarily through energy costs for coverage of grid losses. Immediately, the prices for energy and capacities used in ancillary services started to follow. Evidently, such developments would put TSO operations under considerable, short-term stress. Ideally, the EU legal framework should allow tariff adjustments for eligible costs that need some time to be carried out, but after a while, everything should be all right for TSOs. Yet, at least in some examples, the sectoral policy, which could not be isolated from the general situation in the society, could not follow because it wanted to amortize the inflation of costs hitting the citizens and businesses.

In the case of Croatian TSO, this price shock coincided with some other policy developments already going on, putting the company under considerable new financial risks. The decarbonization process is the main driving force in the contemporary energy sector. The EU institutions promote fast green switch with very ambitious goals. As a result, the grid infrastructure, by far not entirely prepared, has to undergo significant changes in many aspects.

The main goal to be achieved through the EU's "Clean Energy for All Europeans" legislative package of 2019 is the "green transition" of the entire economy, with a big emphasis on the protection of consumers, given the expected immense scale of the economic endeavor to achieve that, and the risks associated thereof. A good place to start browsing the relevant EU legislative acts and related policies is here: [https://ec.europa.eu/energy/topics/energy-strategy/clean-energy-all-europeans\\_en](https://ec.europa.eu/energy/topics/energy-strategy/clean-energy-all-europeans_en). The most critical piece of legislation from that package for our current topic in this paper is [2]. The Republic of Croatia has joined the energy transition to the use of renewable energy sources by adopting the Energy Development Strategy until 2030 with a view to 2050 [3] and the Integrated National Energy and Climate Plan for the Republic of Croatia for the period from 2021 to 2030 [4].

By 2020, with 28% of production and consumption from renewable energy sources, the goal has already been exceeded. With the subsidy systems in place, 1030 MW of new production plants for renewable energy sources and high-efficiency cogeneration have been constructed. The goal of at least a 36.6% share of renewable energy sources in total electricity consumption to be achieved by 2030 is one of the reasons for further amendments to legislation. It pertains primarily to the Electricity Market Act [5], which has already entered into force, and the new Act on Renewable Energy Sources and High-Efficiency Cogeneration that is still being prepared (at the time of writing of this paper).

On the principal level, Croatian national legislation copied the EU's in every respect, including many areas that are not mentioned in this paper. Fostering rapid decarbonization is seen as one of the future pillars of the national economy and its long-term reform [4]. On that path, many individual policy steps that make up the overall national policy need to be envisaged and implemented with mutual coordination to not create non-necessary legal, economic, or other obstacles.

### 2. THE TSO, THE PORTER'S FIVE-FORCE MODEL, AND THE RES CONNECTION

As it is well known, the essential functions that TSOs provide are the following:

- A. *Transmission of electricity.*
- B. *Provision of system services.*
  - voltage and frequency maintenance,
  - system restoration after disturbances.

To accomplish that, TSOs purchase the so-called "ancillary services" from external vendors. The ancillary services are:

- *frequency control*



**Oral Presentation:** Strategic Positioning of Transmission System Operators to Achieve Long-Term Goals and Sustainability of the Green Transition - Analysis and Case Study

- *voltage and reactive power control*
- *black start service*
- *island operation service.*

C. *Organizing the real-time market or another efficient market-balancing mechanism.*<sup>1</sup>

D. *Connection of new network users to the transmission grid.*

Looking at items A to D, one can immediately see that TSOs produce several products which are not substitutes for each other. Some of these products can be considered as having a character of public good – A and B.<sup>2</sup>

At first, building new electricity generation facilities may seem capially intensive, so economic entry/exit barriers could be high. However, from the standpoint of a TSO, the new power-plant investors or operators *are not necessarily those who seek grid connection*. Instead, the connection seekers are so-called *project developers*<sup>3</sup> – often small entrepreneurs who spot opportunities, take care of the initial development of project documentation, and then sell the projects to “more serious” investors or industry insiders. Project development itself is not capially intensive. The entry/exit barriers are very low.

However, the etiquette of “public good” is not really essential here. The important thing is that the TSOs produce different products that are not mutual substitutes but complements and address various types of “buyers” who need them. Besides obvious tangible products and services listed above, some other values may not be that evident at first. Hence the value.

We shall now discuss the values created around TSO’s activities in provisioning one of the essential services – the grid connection. The entities that affect the TSO’s strategy are to be found among those who want or would want to exploit any of the marketable values that emerge around the TSO business, many of them as (sometimes unintentionally produced) side effects.

For the reader’s convenience, we shall briefly recall the basic Porter’s “Five-force model”, which was extensively described in [1]. Fig. 1 gives the essence of that model. Within that framework, let us systematically analyze the entities that can exert strategic impact on TSO business when it comes to the network connection of new power-producing or power-consuming facilities. By doing that, we shall refer to the example of Croatian TSO, bearing in mind that there may be notable differences in other geographical contexts. However, the other EU and out-of-EU countries have similar regulatory settings.

Table 1 presents the classification of players with strategic impact on the TSO in the case of the connection of a new facility to the transmission network.

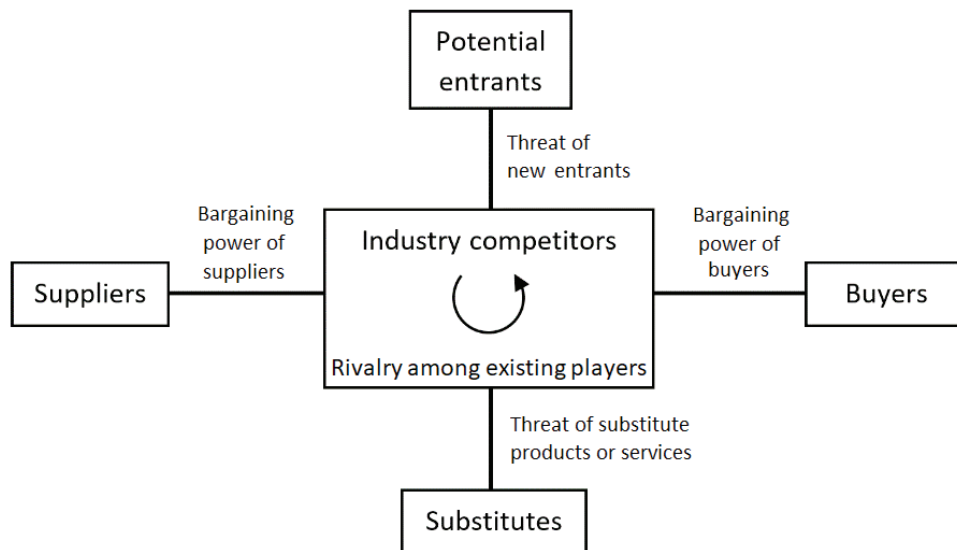


**Figure 1.** Porter’s model of the forces driving industry competition. Source: [1].

<sup>1</sup> It is not always (or not solely) performed by TSOs; however, the TSO’s role in it is always indispensable.

<sup>2</sup> For the definition and interesting discussions on public goods, see [6].

<sup>3</sup> Hereinafter, we will use the term “project developers” for those who develop projects of any new facilities that require a network connection but do not necessarily provide capital nor engage in plant operation at a later stage.



Oral Presentation: Strategic Positioning of Transmission System Operators to Achieve Long-Term Goals and Sustainability of the Green Transition - Analysis and Case Study

**Table 1.** A brief review of marketable values produced by a TSO as the grid connection provider. Source: the authors.

Product				
Connection of new large power generation/consumption facilities to the transmission grid.				
<b>Marketable values</b>				
1. The tradable contract for connecting a new facility to the high-voltage transmission grid. (This is, in fact, the guarantee for the future physical capability of either delivering the energy produced or drawing the energy needed for consumption. It is the necessary condition for the facility's operation.) 2. The physical connection infrastructure (both the direct part and the DLNU'). 3. Tariff for the TSO to cover the costs and provide regulated profits for its' owner(s). 4. The incompleteness of the contracts(s) for connection. 5. Added social welfare (new production of energy or products/services; new working places; better supply of goods; contribution to a cleaner environment, etc.). 6. Political gains/losses (for example, new RES are politically desirable; new polluting facilities are not; there may be NIMBY problems, etc.). 7. Local community gains/losses (e.g., collection of municipality fees; side-projects of local importance; loss of physical space; interference with the urban or natural environment, etc.).				
Strategic forces and players around the TSO – Value # 1				
Tradable contract for connection to the TSO's network				
Competitors	Potential entrants	Substitutes	Suppliers	Buyers
Other TSOs (e.g., in the neighbor-ring countries).	None. (TSO is a natural monopolist.)	Contracts with other TSOs (e.g., in the neighbor-ring countries).	<ul style="list-style-type: none"> <li>- Consultants (legal, technical).</li> <li>- Attorneys (external).</li> <li>- Government (supplying relevant regulation and/or various permits, if applicable, land ownership/usage).</li> <li>- Local government (local regulation, land ownership/usage, urbanistic rules, communalities, various permits if applicable).</li> <li>- Individual persons (physical and/or legal – land ownership/usage, etc.)</li> <li>- TSO itself.</li> </ul> Suppliers' bargaining power: Consultants, attorneys, individuals: low. Government (central and local): high.	<ul style="list-style-type: none"> <li>- Project developers.</li> <li>- Investors.</li> </ul> Buyers' bargaining power: low.
Strategic forces and players around the TSO – Value # 2				
Physical connection infrastructure				
Competitors	Potential entrants	Substitutes	Suppliers	Buyers
Other TSOs (e.g., in the neighboring countries).	None. (TSO is a natural monopolist.)	Contracts with other TSOs (e.g., in the neighbor-ring countries).	<ul style="list-style-type: none"> <li>- Consultants (technical, legal, commercial).</li> <li>- Technical designers.</li> <li>- Construction companies.</li> <li>- Construction quality controllers.</li> <li>- Equipment suppliers.</li> <li>- Equipment installers.</li> <li>- Project integrators.</li> <li>- Project management teams.</li> <li>- Government (supplying general construction law, performing inspections, etc.)</li> <li>- TSO itself</li> </ul> Suppliers' bargaining power: Government: high. Others: medium, sometimes high, depending on the general market situation for products/services.	<ul style="list-style-type: none"> <li>- Project developers.</li> <li>- Investors.</li> </ul> Buyers' bargaining power: low.



**Oral Presentation:** Strategic Positioning of Transmission System Operators to Achieve Long-Term Goals and Sustainability of the Green Transition - Analysis and Case Study

Strategic forces and players around the TSO – Value # 3				
Tariff for the TSO				
Competitors	Potential entrants	Substitutes	Suppliers	Buyers
<ul style="list-style-type: none"> <li>- Project developers.</li> <li>- Investors.</li> <li>- DSO(s).</li> <li>- Public (whoever pays for transmission services).</li> <li>- Suppliers of goods and works in TSO investment projects.</li> <li>- Internal competitors within TSO.</li> </ul>	<ul style="list-style-type: none"> <li>- Project developers.</li> <li>- Investors.</li> </ul>	<p>None. (TSO is a natural monopolist.)</p>	<ul style="list-style-type: none"> <li>- Regulatory agency.</li> <li>- TSO itself (by supplying info for tariff calculation).</li> <li>- Government (by passing relevant regulation).</li> </ul> <p>Suppliers' bargaining power (other than TSO's): high.</p>	N/A
Strategic forces and players around the TSO – Value # 4				
Incomplete contracts with the TSO				
Competitors	Potential entrants	Substitutes	Suppliers	Buyers
None.	None.	None.	<ul style="list-style-type: none"> <li>- TSO itself.</li> <li>- Legal consultants/attorneys.</li> <li>- Regulatory agency (if it approves the conditions or acts as a dispute resolution body).</li> <li>- Project developers/investors.</li> <li>- Courts.</li> </ul> <p>Suppliers' bargaining power: Courts and regulators: high. Others: anywhere between low and high, depending on the supplier's ability to spot and exploit inadequacies in the contract.</p>	<ul style="list-style-type: none"> <li>-Project developers.</li> <li>-Investors.</li> <li>-TSO itself.</li> </ul> <p>Buyers' bargaining power: anywhere between low and high, depending on the buyer's ability to spot and exploit inadequacies in the contract.</p>
Strategic forces and players around the TSO – Value # 5				
Social welfare				
Competitors	Potential entrants	Substitutes	Suppliers	Buyers
Everyone.	Everyone else.	None.	<ul style="list-style-type: none"> <li>- TSO itself.</li> <li>- Project developers/investors.</li> </ul>	Everyone.
Strategic forces and players around the TSO – Value # 6				
Political gains and losses				
Competitors	Potential entrants	Substitutes	Suppliers	Buyers
N/A	N/A	N/A	<ul style="list-style-type: none"> <li>- TSO itself.</li> <li>- Project developers/investors.</li> </ul>	<ul style="list-style-type: none"> <li>- Government.</li> <li>- Local government.</li> </ul>
Strategic forces and players around the TSO – Value # 7				
Local community gains and losses				
Competitors	Potential entrants	Substitutes	Suppliers	Buyers
N/A	N/A	N/A	<ul style="list-style-type: none"> <li>- TSO itself.</li> <li>- Project developers/investors.</li> </ul>	Local community.

For clarity, we shall now provide more thorough explanations of the table entries, where needed.

**Vales # 1 and 2** – Competitors are neighboring TSOs because the project developers or investors can seek opportunities in other countries if they cannot get the connection contract with the local TSO. For the same reason, other TSOs' contracts can be considered substitute products.



**Oral Presentation:** Strategic Positioning of Transmission System Operators to Achieve Long-Term Goals and Sustainability of the Green Transition - Analysis and Case Study

**Value # 3** – Although the transmission tariff is directed to the TSO only, some competitors are interested in shifting their own costs to the TSO, hoping it would cover them from its tariff. For example, project developers may expect the TSO to cover the costs of technical, legal, and economic analyses. Investors may *hope* TSO would pay for at least a good part of DLNU *and* the investment into connecting infrastructure. Both developers and investors can achieve it in the longer run by organizing political pressure to direct the development of the regulatory framework in the desired direction. With a political relevance *sui generis*, the public can also ask for the tariff decrease (or prevent the increase). It is the same as consuming a part of the now-existing tariff. Next, there is an entire ecosystem of companies (construction, equipment suppliers, etc.) that serve the long-term needs of a TSO to refurbish the legacy network and invest in new parts of it. They all compete to be awarded procurement contracts from the TSO. In the long run, the TSO’s tariff covers all the costs related to those contracts. Finally, there is a moment of *internal competition* inside the TSO. Internal departments can compete for their respective shares in tariff revenues, which they see as the right to spend a certain amount of money each year. The authors believe internal competition must not be neglected as it can profoundly affect the firm’s strategy. For example, if the departments not engaged in the new grid connection business prevail in terms of internal political power within the organization and attract more money, the investment plans to accompany the connection of new facilities may be put at risk.

**Value # 4** – By “suppliers,” we understand everyone who puts up inputs to be combined to produce the output value, that is, the incomplete contracts with the TSO. Obviously, TSO is one of those providers. Then, internal and external legal counsels help compile the legal acts. The regulatory agency usually has to analyze and approve the contract conditions from the standpoint of non-discrimination. Project developers and investors have a legitimate interest and the right to propose agreement conditions. Finally, the courts give the final verdict and thus influence the business.

**Table 2.** Croatian power system – fundamental indicators of the size, 2018-2021. Source: [7], p. 101.

Year <sup>&amp;</sup>		2021	2020	2019	2018	
Total final electricity consumption	GWh	16837	15857*	16821	17298	
Peak hourly load	MWh/h	3072	2872*	3038	3168	
Generation, Hydro	GWh	6568	5134	5606	6691	
Generation, Thermal <sup>§</sup>	GWh	4020	4073	3709	3206	
Generation, Wind <sup>#</sup>	GWh	1904	1594	1343	1240	
Total domestic generation	GWh	12492	10801	10658	11137	
Gross cross-border exchange, inflow	GWh	11504	10490	11399	12892	
Gross cross-border exchange, outflow	GWh	7159	5434	5236	6532	
Net gross cross-border exchange	GWh	4345	5056	6163	6160	
Total installed generation capacity	MW	5031	4875	4817	4619	
Wind generation capacity <sup>#</sup>	MW	981	729	671	529	
Share of wind in total installed capacity <sup>#</sup>	%	17.59	14.95	13.93	11.45	
Coverage of total domestic consumption	Wind	%	11.31	10.05	7.98	7.17
	Hydro + Wind	%	50.32	42.43	41.30	45.86
	Net gross exchange	%	25.81	31.88	36.64	35.61
	Total domestic gen.	%	74.19	68.12	63.36	64.38

Notes:

& The year 2020 was the “Covid-year”, so the notably decreased consumption should be viewed with that in mind.

\* The two figures differ from the source because they were erroneously stated there. Corrected by the authors.

§ Only the industrial plants connected to the transmission grid are included.

# The figures pertain to the wind plants connected to the transmission grid by the end of the year. The total RES capacity is considerably larger because there are small facilities connected to the distribution grid.



Oral Presentation: Strategic Positioning of Transmission System Operators to Achieve Long-Term Goals and Sustainability of the Green Transition - Analysis and Case Study

Table 3. Evolution of the cumulative wind plant capacity connected to the Croatian transmission grid by the year. Source: HOPS, info available in the Croatian language at: http://www.hops.hr/popis-objekata-oie-koji-imaju-sklopljen-ugovor-o-koristenju-mreze. Accessed: 31 May 2023

Year	2021	2020	2019	2018	2017	2016	2015	2014	2013	2012	2011	2010	2009
Installed wind capacity, MW	981	729	671	529	529	427	366	287	245	162	98	42	42
Share in total capacity, %	19.5	14.95	13.9	11.3	11.4	9.44	8.04	6.80	5.95	3.99	2.42	1.05	1.06

Note: From Nov. 2021 until the completion of this paper (Jun. 2023), there have not been new connections, so the 2021 figures still stand.

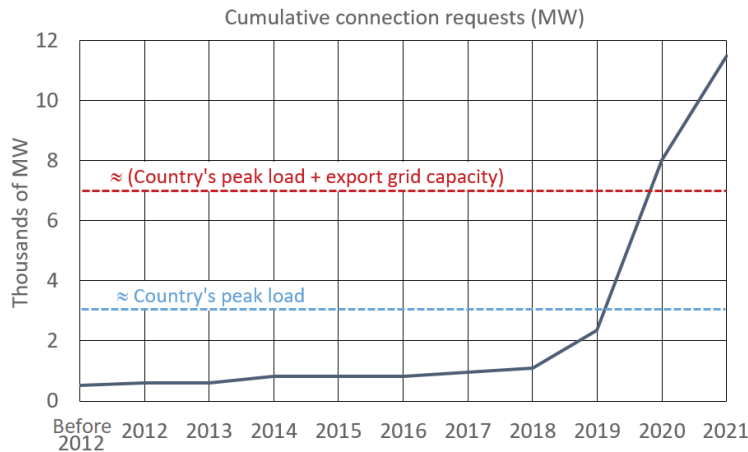


Figure 2. Development of cumulative demand for new RES connections to the transmission grid, received by Croatian TSO. Source: HOPS and authors' calculations.<sup>4</sup>

### 3. CONNECTION OF NEW RES TO THE CROATIAN TRANSMISSION NETWORK<sup>5</sup>

The new RES connection to the Croatian high voltage grid poses some interesting economic challenges before the TSO and other stakeholders in the system. In this section, our focus will remain on TSO, yet not underestimate the interests and concerns of other players.

Table 2 shows some fundamental indicators of the Croatian electricity system size from 2018-2020. Table 3 displays the dynamics of grid connection of the already operating RES. Fig. 2 gives the requests for new RES grid connections submitted by the investors to the Croatian TSO through the years, until the end of 2021. The curve shows a tremendous increase in new requests that started to happen during 2018, but it gradually subsided by the end of 2021.

Although a total of 885 megawatts of RES capacity currently works on the transmission network (now all wind farms), there are many new requirements that, if eventually realized, would amount to almost 11.5 thousand megawatts connected to the transmission network. There is still no mention here at all of distributed generation, which will inevitably appear in large numbers in the distribution network.

An excellent starting point is to note that the country's peak load is about 3 thousand megawatts, which is almost four times less than the total RES connection requirements. Further, the total available output cross-border net transmission capacities (NTCs) are in a similar range of values (although they can vary significantly over time, so we can use the figure of around 3 thousand megawatts to indicate the average expected value). Today, the NTC concept is gradually being abandoned, and cross-border capacities will be determined by the so-called flow-based methods.

Bearing all this in mind, the question of overall economic feasibility of such an investment program immediately arises. Quadruple production capacities in relation to peak load would imply a frequent need to export excess energy, or finding new ways of spending it (e.g. power storage, hydrogen production, electric vehicles). However, the sum of the country's peak load and the expected maximum export capacity is still far below the already expressed interest in building new RES capacities.

<sup>4</sup> It is based on the informative table published and updated on the HOPS's website until Q3 2021 but was later removed as the FIFO list-keeping was abandoned. The authors had stored the document when it was still actual.

<sup>5</sup> This section benefited from [8], yet the data presented here were updated.





**Oral Presentation:** Strategic Positioning of Transmission System Operators to Achieve Long-Term Goals and Sustainability of the Green Transition - Analysis and Case Study

Another unrealistic underlying assumption is that someone outside the country would buy the excess energy from RES. This could only stand if no one else would invest in RES or any other type of generator.

Even after such a simple and superficial economic analysis, TSOs can be sure that, for example, in the context of Croatia, some 10 candidate-gigawatts of new RES capacity will most likely not come.<sup>6</sup>

However, strong contemporary political tendencies toward comprehensive decarbonization should be considered. For example, one of the main challenges is to replace fossil fuels in transport and other industries with hydrogen [9], which is obtained by electrolysis of water using electricity produced from RES. This would probably contribute to a significant increase in electricity consumption for the operation of a large number of new electrolysis plants. For now, estimating how significant that increase would be and at what speed is difficult. For example, according to IRENA ([10], p. 32), using hydrogen in transport, power generation, storage, building, and other industries may increase electricity consumption twofold or more by 2050, as many water electrolysis plants would have to be driven. However, it would be too presumptuous for now to attach any concrete figure to it.

The problem with managing a large and sudden surge of new potential renewable energy projects is that neither the TSO nor anyone else can know which of the many will eventually be successfully implemented early enough. This creates unprecedented financial risks for TSOs. This is the case, at least in Croatia, where access to the “market” for new RES projects is completely liberal in the current regulatory regime. Therefore, the very initiation of the project (including grid connection requests from TSOs at a very early stage) became essentially costless.

The earliest parts of operational legislation (by-laws) regulating the connection of renewable sources appeared in Croatia in 2006. Since then, the main rules of the game related to connection to the transmission (or distribution) network are as follows (with some less important details left out):

- The investor must pay for the connection the actual cost. This refers to the direct cost of laying the cable to the network access point, and the construction of the substation, a necessary part of the infrastructure for the RES plant.
- Suppose the newly planned RES plant would cause the need for DLNU investments in upgrades at “deeper levels” of the network. In that case, the investor is obliged to pay the actual cost of the upgrade multiplied by the usage-sharing factor. It is a technically calculated number between 0 and 1 – the share of new grid capacity that will be used by the respective new RES plant.

The rule described above in the second point refers to the notorious fact that networks cannot be upgraded in arbitrarily small increments. For example, suppose that the TSO has calculated that the network should be upgraded due to the new RES plant by further increasing the “total capacity” assets of 100 units in the deeper network. Let’s say it’s impossible (or infeasible) to do a smaller upgrade than that. If the technical calculation showed that the RES plant only used about 20 units, the investor would have to pay 20 percent of the actual investment price. The rest would go to the expense of TSO, but this 80% of new assets could not be used effectively.

In a better situation, if there were five similar candidate projects for the same network region, each would ideally cover 20% of the total costs so that the TSO would recover everything. However, each unsuccessful project would burden TSO with 20% of the upgrade costs. Therefore, the risks of the RES project directly increase the risks of the TSO.

With an increasing number of candidate projects, in 2018 the TSO formed a “FIFO list” (First-In-First-Out) to maintain order in managing connection requests non-discriminately. However, the FIFO list was abandoned quite quickly due to significant differences in project sizes, spanning from 20 MW to 950 MW, and other potential legal and operational complications.

Namely, a wide range of legal problems can arise from the seemingly fair FIFO model. For example, what if two very different projects entered the FIFO list so that the much larger one (say, 200 MW) arrived earlier and the smaller one (say, 20 MW) came a little later?

Assume (reasonably) that it is easier and less time-consuming to obtain initial permits and other necessary documentation for a smaller project. Let us even assume that it does not require DLNU. The owner of this project can then rightly question the principle of FIFO priority and demand the TSO to sign the connection contract as soon as it obtains the necessary documentation, i.e., before the big project. Finally, assume that the TSO still insists on the priority of the FIFO list. In that case, one can sue the TSO to the commercial court, the competition authorities, and/or the energy regulator for discrimination – all of which carry potentially high financial and reputational risks with a long-term outlook. A solitary case would not matter; however, as mentioned, the number of cases exploded.

Moreover, all projects of the past, which did not then immediately require DLNUs, were connected to the network without contributing to the network conditioning. This could now be interpreted as a kind of “free-riding” on infrastructure that was already sufficiently developed and whose costs were already implicitly covered by the tariff. Let us note that in the old days, until a few decades ago, when the construction of new small production facilities did not happen so often, this was not a problem. At the time, large new

<sup>6</sup> We still do not mention the variability of RES production, another major technical and economic problem.



**Oral Presentation:** Strategic Positioning of Transmission System Operators to Achieve Long-Term Goals and Sustainability of the Green Transition - Analysis and Case Study

generators bore all the necessary grid upgrade costs as part of the overall investment simply because they were vertically integrated with grid operators within the same company. Today, on the contrary, many relatively small individual RES power plants are seeking connection to the grid simultaneously as many significant, and sometimes very large, RES projects, which causes a considerable change in the grid connection paradigm.

The data from Fig. 2 correspond to 121 projects that aspire to be connected to the high-voltage network. This was the figure when the writing of this paper began in early September 2021. By mid-October, the list had grown to 159 projects. However, new additions to that list subsided, probably because of the regulatory uncertainties still in place.

In some cases, several projects tend to access the same “special zone”, a narrow area where all projects should be connected to a single network node or perhaps to several nearby ones. Together, they cause the need for joint investment in deep network upgrades. The regulatory rules of the game (see [11], Art. 17) are now as follows:

- The entity requesting the connection is called the “special zone organizer”. The organizational form of the zone organizer is not essential here. It can be, for example, a dedicated company founded for this purpose only by one or more investors whose projects aspire to that special zone. However, it must bear the entire previous investment of DLNU, which applies to all candidate projects that aspire to a special zone.<sup>7</sup>
- As mentioned, direct connection funds’ costs go entirely to the RES project.
- When individual projects are included, they should pay the special zone organizer their relevant shares of the DLNU cost. Each project would have to have a contract with the zone organizer. Note that, for any of these projects, the moment of joining can come at any time, if ever.

In such a regulatory setting, the zone organizer is put in a challenging situation, having to bear the risk of failure of these projects and the cost of capital for an undefined period of waiting for them to actually join in. Sometimes one-time DLNU investments can be very high. In the Croatian case, preliminary TSO analyses showed that (in one specific case of special zones) they could amount to around 135 million euros. Hardly any zone organizer (presumably, a small business entity with limited liability) can handle this order of magnitude, and hardly anyone can bear the associated financial risks of the same magnitude for an unfathomable duration.

Realizing that probably no one would be willing to enter into such a risky arrangement, additionally burdened by obvious non-bankability, TSO began to think about and discuss with the regulator and state authorities a system of determining a fixed rate per MW to reimburse DLNU costs. This naturally leads to the concept of LRAIC (Long-Run Average Incremental Cost). LRAIC, as a regulatory standard for cost accounting, is intensively and successfully used in the telecom industry, for example, in regulating prices for access to a separate local loop and other parts of the network under a natural monopoly. A comprehensive overview of this can be found in [12]. However, the same principles can be applied in any industrial context, including that of the power system.

Although eventually the idea was accepted as such, and although the TSO submitted its tariff proposal (as well as the DSO did) more than a year ago, the legislative process has not been completed yet, presumably because of the level of costs that accompanies the ambitious plans for new RES installations was deemed too high by some stakeholders. Note that this leads us again to the problem of competition for marketable values created around the TSO business, specified under #3 (but also related to #5 and #6) in Table 1.

To sum up this complicated chapter, the strategic challenges that a TSO faces nowadays all result from the (legitimate) interests various stakeholders around it have, coming down to the following tendencies:

- It is expected that the transmission network maintains the usual standard of security of operation and, at the same time, grows at an increasing pace to accommodate the expected and desired fast growth of the RES portfolio.
- However, the costs of that endeavor, which should be recovered through increased tariff revenues or directly from RES investors, are politically less acceptable because they either burden the final electricity bills or raise the economic barriers to entry. (Note that in the end, the electricity consumers pay all the increased costs, no matter the channel through which they propagate. The difference is only in how soon it becomes apparent to the consumers and/or the wider public.)
- The network upgrades for new RES projects are, by necessity, lumpy. In other words, significant incremental investments are needed, and sometimes they can be triggered even by small new projects. Therefore, an entire spectrum of grave risks arises from the necessity of complex coordination of the financing of the infrastructure part of the investments (more narrowly, the DLNU).
- The constantly evolving regulatory rules and policy measures can complicate the situation even more if not well thought out in advance.

<sup>7</sup> According to the current new law, there is one more detail: it is actually 80% of the total DLNU cost. The rest should be borne by the TSO; however, in reality, the regulator did not formally recognize this new extra cost.



### 4. MORE COMPLICATIONS: THE ENERGY CRISIS

Fig. 3 [13] shows the electricity price indexes at several power markets from 2019 to 2022 and the indexed futures prices from Q1 2023 to the end of 2024. After a decade of relative stability around the average of some 50 euros per MWh (please also refer to price information in [14]), the prices surged from Q3 2021 to enormous levels that occasionally, during 2022, rose to a thousand euros per MWh. Unsurprisingly, the new market circumstances affected the TSO business greatly, especially the financial liquidity, given that the tariffs cannot be adjusted momentarily. In "normal times", the eligible costs, especially those caused externally, out of the TSO's possibility to counter fight, should be recognized by the regulatory authority and embedded into the transmission tariff.

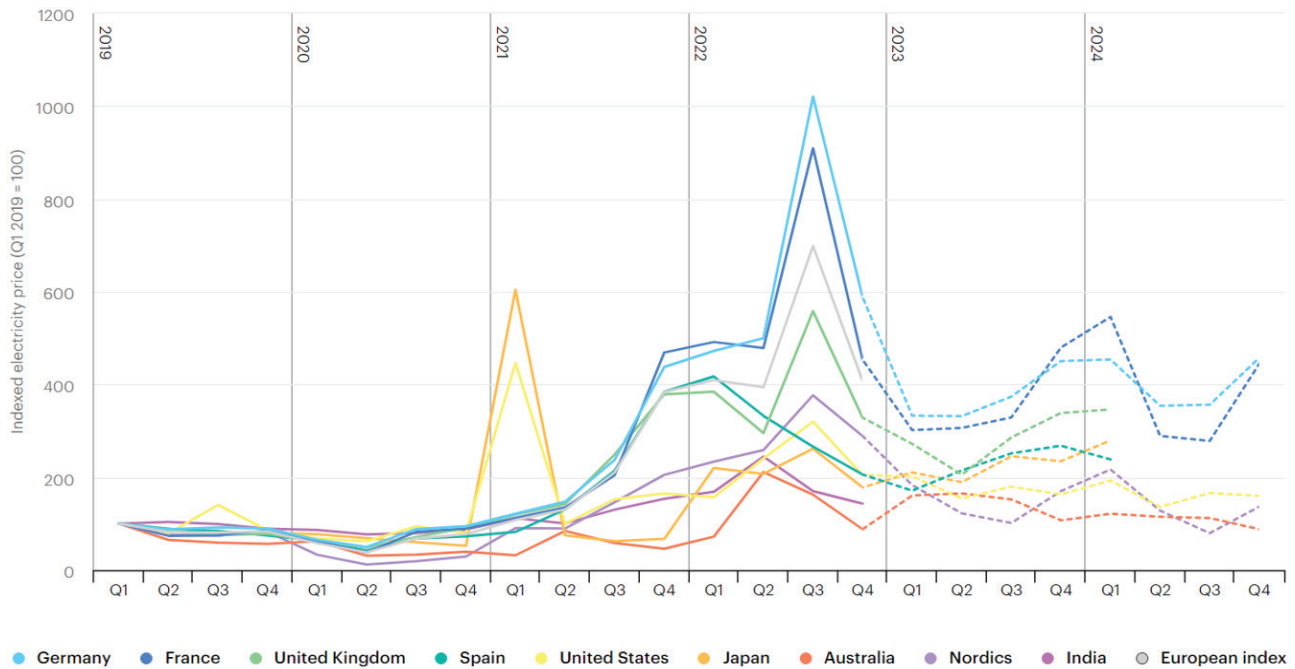


Figure 3: Electricity price indexes at several power markets and the IEA index from Q1 2019 to Q4 2022, with future price indexes, extended to the end of 2024. The indexes are computed from demand-weighted averages of prices. Source: [13].

Yet, on this occasion, the price surge was so dramatic that it was hard for the public policymakers to react in the usual way. The magnitude of the shock was so great that it called for a broader policy action, whereby TSOs, as just a tiny part of the economy, however important, could be expected to step aside for a while and leave the government space to act in this unprecedented emergency situation. While the EU institutions quickly responded with general political guidance, the national measures presumably differed across the EU space.

#### 4.1. Policy response to the crisis in Croatia

The primary political instruments to tackle the crisis were two consecutive Government regulations with the legal force of law<sup>8</sup> [15,16]. Accordingly, the two cited regulations were adopted one after another in six months, effectively covering approximately Q4 2022 to Q3 2023.

The essential feature of both regulations is to keep the retail prices of electricity, gas, and heating at the pre-crisis levels or only slightly higher. Differently than the first Regulation, the second one provided that the price of energy for coverage of grid losses in Q2 and Q3 of 2023 is to be fixed at the level of €70.28 per MWh, while the rest part up to the market price is to be paid to the providers from the state budget. However, the process was not understood by all the industry players in the same way, resulting in a *de facto* inability of the TSO (and DSO) to enjoy this favorable temporary provision. The wholesale prices for electricity in June 2023 ranged close to € 120 per MWh, and at the moment of completion of this article, the TSO was still paying the full market price for energy.

<sup>8</sup> This form of a legislative act in Croatia is an extraordinary measure, allowing the Government, in cases of urgency, to circumvent lengthy procedures in the Parliament and adopt a piece of special legislation equally potent as if it were adopted by the Parliament. However, such regulations must be upheld by the Parliament in no more than six months, or they automatically cease to exist.



Oral Presentation: Strategic Positioning of Transmission System Operators to Achieve Long-Term Goals and Sustainability of the Green Transition - Analysis and Case Study

Regarding the income side, both Regulations stipulated that the TSO not be allowed to propose tariff changes to the regulator while they are applied (from Q4 2022 to the end of Q3 2023). Therefore, the TSO instantly found itself in a financial gap that, near the end of 2022, with market prices hitting up occasionally to almost a thousand euros per megawatt hour, looked quite catastrophic. Fig. 4 briefly reviews some fundamental TSO business indicators during the last several years to illustrate the gradient of deterioration even though TSOs are considered "safe" for their comfortable regulated monopoly position<sup>9</sup>.

In such circumstances, the only possible immediate reaction of the TSO was to reduce the investment plans and push the investments to the indefinite future. In that way, what started as a short-term liquidity problem transgressed swiftly to the long-term horizon and to the strategic domain. Some could use this example to challenge policy-making in the first place. However, what really happened was an unprecedented market shock bolstered by the full-scale war in Ukraine that significantly contributed to the energy crisis in Europe. The policy first dealt with essential questions of energy supply and affordability, which was no surprise. Yet, the example shows how vulnerable the entire green transition agenda really is. However, the really relevant question is what happens after Q3, 2023.

The European Commission recently issued a Recommendation [17], stating: "The Commission invited Member States to phase out national fiscal measures introduced to protect households and firms from the energy price shock, starting with the least targeted ones. It indicated that, if support measures needed to be extended because of renewed energy price pressures, Member States should target such measures much better than in the past towards vulnerable households and firms." The phasing out should be completed by the end of 2023. However, from the standpoint of the TSO and other firms with revenues subject to regulatory approval, it cannot be assessed what kind of rules will continue to exist after the second existing Regulation expires. Hence the short-term risk.

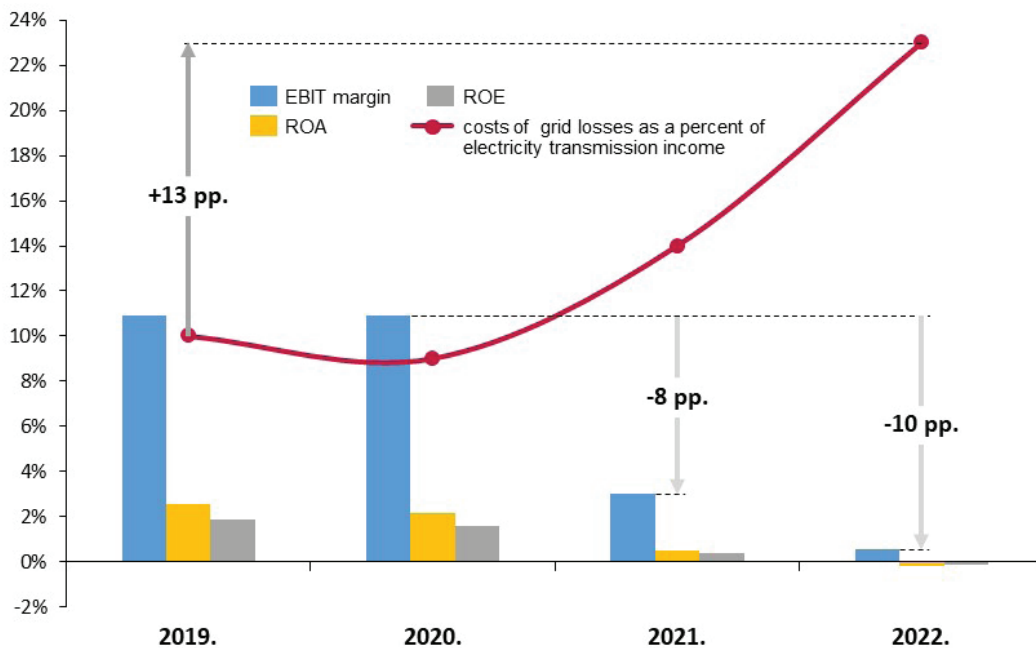


Figure 4. Basic business indicators of Croatian TSO. Source: HOPS, and authors' calculation.

### 5. CONCLUSION

Based on the above-described case study from Croatia, we have incorporated the strategic analysis of TSO business into the mainframe of Porter's five forces model, whereby we broadened the definitions of industry boundaries and the values created within that industry to reflect the competitive pressures the TSOs face in carrying out their job.

Although the TSO business is a natural monopoly, its strategy cannot be studied without paying attention to other marketable values a TSO is involved with. Other stakeholders may have more or less legitimate interests vested in TSO-created values. Contrary to

<sup>9</sup> As much as being a regulated monopolist can be risk-free when everything is normal, an exposition to politically driven regulation can pose ultimate risks to a company. This is one of the motivations for our strategic re-consideration of the TSO business.



**Oral Presentation:** Strategic Positioning of Transmission System Operators to Achieve Long-Term Goals and Sustainability of the Green Transition - Analysis and Case Study

the traditional belief that TSO managers can lay in peace and enjoy a monopoly position, they must engage with strategic decision-making regularly because the regulated tariff is not the only thing such companies deal with. Numerous entities may want to extract benefits for themselves at the expense of publicly financed grid operators. The psychological rationale for such behavior probably comes from the fact that pushing own costs to a publicly funded entity (or extracting own benefits from it) cannot be easily identified.

Nevertheless, as TSOs have to worry about the integrity of system operation on all time horizons, they have to think through and apply tactical and strategic measures to avoid risks coming from the environment. As the green transition is a process with a forceful political backup, dealing with numerous actors from that industry proves incredibly challenging. Given the scope of the whole endeavor, the fact that the legacy networks have to be significantly upgraded, and the lack of investment coordination in the liberalized market, the financial and operational risks in front of TSOs grow very fast. It may be that the policy is not aware of it nor prepared to provide better regulatory solutions that would make TSO business less prone to endangering risks. The current energy market crisis showed how fragile the system is. Now that everyone could see why it is necessary to replace fossil fuels and embrace renewables, if not for other reasons than for the sake of own energy adequacy, the Croatian example showed how a market disturbance, otherwise belonging to short-term liquidity problems, could very quickly endanger the long-term ability to provide new infrastructure for the very green transition.

## BIBLIOGRAPHY

- [1] Porter, M. (1985), *Competitive Advantage*. The Free Press, New York, 1985.
- [2] EU (2019), Directive (EU) 2019/944 of the European Parliament and of the Council of 5 June 2019 on common rules for the internal market for electricity and amending Directive 2012/27/EU, OJ L 158/125, 14.6.2019. <https://eur-lex.europa.eu/legal-content/EN/TXT/PDF/?uri=CELEX:32019L0944&from=EN> (Accessed: 21 Nov. 2021)
- [3] Croatian Parliament (2020), Energy Development Strategy of the Republic of Croatia until 2030 with an outlook to 2050 (in the Croatian language), OG 25/2020. [https://narodne-novine.nn.hr/clanci/sluzbeni/2020\\_03\\_25\\_602.html](https://narodne-novine.nn.hr/clanci/sluzbeni/2020_03_25_602.html) (Accessed: 21 Nov. 2021).
- [4] Croatian Government (2019), Integrated National Energy and Climate Plan for the Republic of Croatia for the Period 2021-2030. [https://mingor.gov.hr/UserDocImages/UPRAVA%20ZA%20ENERGETIKU/Strategije,%20planovi%20i%20programi/hr%20necp/Integrated%20Nacional%20Energy%20and%20Climate%20Plan%20for%20the%20Republic%20of\\_Croatia.pdf](https://mingor.gov.hr/UserDocImages/UPRAVA%20ZA%20ENERGETIKU/Strategije,%20planovi%20i%20programi/hr%20necp/Integrated%20Nacional%20Energy%20and%20Climate%20Plan%20for%20the%20Republic%20of_Croatia.pdf) (Accessed: 21 Nov. 2021).
- [5] Croatian Parliament (2021), Electricity Market Act (in the Croatian language), OG 111/2021. [https://narodne-novine.nn.hr/clanci/sluzbeni/2013\\_02\\_22\\_358.html](https://narodne-novine.nn.hr/clanci/sluzbeni/2013_02_22_358.html) (Accessed: 21 Nov. 2021)
- [6] Anomaly, J. (2015), Public goods and government action, *Politics, Philosophy & Economics*, 14(2), p. 109-128, doi: 10.1177/1470594X13505414.
- [7] HOPS (2021a), Annual Report 2020 (in the Croatian language), p. 101. <http://www.hops.hr/page-file/WAVZXYJGgaU0agr0C3XF0/godisnji-izvjestaji/HOPS%20GI%202020%20-%2029-7-2020.pdf> (Accessed: 21 Nov. 2021).
- [8] Sabolić, D. and Išić, L. (2022), Practical Issues in Public Policy Management for Electricity Production Decarbonization – Case Study: Integration of New Renewable Plants into Croatian Grid, *Proceedings of the Twenty-Ninth World Business Congress, International Management Development Association (IMDA)*, pp. 8-15. Jyväskylä, Finland, Jun. 2022.
- [9] EC (2020), Communication from the Commission to the European Parliament, the Council, the European Economic and Social Committee and the Committee of the Regions. A hydrogen strategy for a climate-neutral Europe. [https://ec.europa.eu/energy/sites/ener/files/hydrogen\\_strategy.pdf](https://ec.europa.eu/energy/sites/ener/files/hydrogen_strategy.pdf) (Accessed: 21 Nov. 2021).
- [10] IRENA (2018), *Hydrogen From Renewable Power Technology, Outlook for the Energy Transition*, p. 32. [https://www.irena.org/-/media/files/irena/agency/publication/2018/sep/irena\\_hydrogen\\_from\\_renewable\\_power\\_2018.pdf](https://www.irena.org/-/media/files/irena/agency/publication/2018/sep/irena_hydrogen_from_renewable_power_2018.pdf) (Accessed: 21 Nov. 2021).
- [11] Croatian Government (2018), Regulation on Issuance of Energy Approvals and Determination of Conditions and Deadlines for Connection to the Electricity Network (in the Croatian language), OG 7/2018. [https://narodne-novine.nn.hr/clanci/sluzbeni/2018\\_01\\_7\\_180.html](https://narodne-novine.nn.hr/clanci/sluzbeni/2018_01_7_180.html) (Accessed: 21 Nov. 2021)
- [12] ITU (2009), *Regulatory Accounting Guide*. [https://www.itu.int/ITU-D/finance/Studies/Regulatory\\_accounting\\_guide-final1.1.pdf](https://www.itu.int/ITU-D/finance/Studies/Regulatory_accounting_guide-final1.1.pdf) (Accessed: 21 Nov. 2021)
- [13] IEA (2023), *Electricity Market Report 2023*, p. 36. <https://iea.blob.core.windows.net/assets/255e9cba-da84-4681-8c1f-458ca1a3d9ca/ElectricityMarketReport2023.pdf> (Accessed: 30 May 2023).
- [14] ACER (2021). ACER's Preliminary Assessment of Europe's high energy prices and the current wholesale electricity market design. [https://extranet.acer.europa.eu/Official\\_documents/Acts\\_of\\_the\\_Agency/Publication/ACER's%20Preliminary%20Assessment%20of%20Europe's%20high%20energy%20prices%20and%20the%20current%20wholesale%20electricity%20market%20design.pdf](https://extranet.acer.europa.eu/Official_documents/Acts_of_the_Agency/Publication/ACER's%20Preliminary%20Assessment%20of%20Europe's%20high%20energy%20prices%20and%20the%20current%20wholesale%20electricity%20market%20design.pdf) (Accessed: 30 May 2023).
- [15] Croatian Government (2022), Regulation on elimination of disturbances on the domestic energy market (in the Croatian language), OG 104/2022, 106/2022, 121/2022, 156/2022. <https://narodne-novine.nn.hr/search.aspx?upit=Uredba+o+otklanjanju+poreme%c4%87aja+na+doma%c4%87em+tr%c5%bei%c5%a1tu+energije&naslovi=da&sortiraj=1&kategorija=1&pp=10&qtype=3&pretraga=da> (Accessed: 30 May 2023)
- [16] Croatian Government (2023), Regulation on elimination of disturbances on the domestic energy market (in the Croatian language), OG 31/2023. [https://narodne-novine.nn.hr/clanci/sluzbeni/2023\\_03\\_31\\_531.html](https://narodne-novine.nn.hr/clanci/sluzbeni/2023_03_31_531.html) (Accessed: 30 May 2023)
- [17] EC (2023), Recommendation for a COUNCIL RECOMMENDATION on the 2023 National Reform Programme of Malta and delivering a Council opinion on the 2023 Stability Programme of Malta, COM(2023) 618 final, p. 3 (§7), Brussels, 24 May 2023. [https://commission.europa.eu/system/files/2023-05/COM\\_2023\\_618\\_1\\_EN.pdf](https://commission.europa.eu/system/files/2023-05/COM_2023_618_1_EN.pdf) (Accessed: 31 May 2023).





# An Innovative Solution for Reducing Emfs: The “5-Phases” Pylons.

[francesco.palone@terna.it](mailto:francesco.palone@terna.it)**MARIA ROSARIA GUARNIERE, ROBERTO SPEZIE, FRANCESCO PALONE\*, GABRIELE TRESSO***Terna, Sapienza University of Rome***Italy**

## SUMMARY

The development and refurbishment of high-voltage Overhead Power Lines (OHLs) are frequently impeded by concerns related to electromagnetic fields and environmental impact.

This issue is particularly significant in Italy due to the presence of challenging legislation concerning Extra Low Frequency electromagnetic fields (ELFs), which also applies on existing OHLs.

As a result, there is a tendency to resort to underground cables more frequently, even when not technically required. However, this approach leads to increased costs for electricity system users, heightened risk of extended outages, and significant technical challenges, especially for higher voltage levels (reactive power management).

To overcome this issue, Terna has developed an innovative design for high-voltage and extra-high-voltage overhead lines. This design enables a significant reduction in electric and magnetic fields, audible noise, and radio interference when compared to conventional solutions.

The new OHL towers have been defined as “5-phases” pylons. They adopt 5 different conductors (or conductors bundles, according to the voltage levels) having a mutual voltage displacement of 0°, 120° and 240°, as in conventional 3-phases transmission systems. This design feature eliminates the need for special transformers or static converters to connect the existing infrastructure to the new “5-phases” OHLs.

To cope with the foreseen development of renewable power plants, Terna has designed the new “5-phases” OHLs to accommodate a significant loadability increase if compared to conventional OHLs of the same voltage levels: The expected thermal loading capacity reaches 500 MW, 1000 MW, and 3400 MW for 155 kV, 230 kV, and 400 kV OHLs, respectively. This enhanced loadability enables efficient integration of renewable power generation into the electricity grid.

The visual impact of the new “5-phases” pylons has been significantly reduced through a design that incorporates a reduced height and footprint compared to conventional OHL designs. This reduction in visual impact helps mitigate the aesthetic concerns associated with overhead lines.

Furthermore, the “5-phases” pylons have excellent performance in terms of electromagnetic fields (EMFs) and audible noise. This makes them a versatile and powerful solution both for constructing new OHLs and refurbishing existing ones, even in urbanized areas (as often happens for old and ageing Italian 150 and 230 kV OHLs, dating back from the first half of the past century).

The paper introduces the innovative design of the new “5-phases” pylons, with specific focus on the electromagnetic field (EMF) performances.

Section 1 and 2 provides an overview of the fundamental principle behind EMF mitigation for these pylons. Sections 3 and 4 discuss the EMF and audible noise performance of the “5-phases” OHLs for voltage levels 230 kV. Conclusions are reported in section 6.

## KEYWORDS

Overhead High Voltage Line, Pylons, EMFs





Oral Presentation: An Innovative Solution for Reducing Emfs: The “5-Phases” Pylons.

## 1. INTRODUCTION

Electromagnetic fields are necessary for power to be transmitted through an overhead power line (OHL). According to the Poynting theorem, the amount of active power carried by a power line can be expressed as:

Where:

$$P = Re \left[ \iint_{St} (E \times H^*) dS \right] \quad (1)$$

- P represents the transferred active power;
- E is the electric field vector;
- H is the magnetic field vector;
- dA represents the differential area element;
- St the plane transverse to the axis of the power line.

This expression describes the power transfer resulting from the interaction between the electric and magnetic fields along the power line.

Equation (1) shows that only with the simultaneous presence of an electric field and magnetic field is possible to transport active power. Without an electric field and magnetic field, the transmission of power would not be possible.

Regarding the effects of electric and, most significantly, magnetic fields at extremely low frequencies (ELF) on human health, there has been a longstanding debate in the scientific community.

Numerous studies have been conducted to investigate the potential health effects of ELF magnetic fields; however, a definitive causal relationship has never been established.

On the basis of these studies, reference levels have been identified for public exposure to electric and magnetic fields: for the 50 Hz power frequency, in Europe, these levels are 5 kV/m for the electric field and 200  $\mu$ T for magnetic induction [3].

Italian regulation has adopted even stricter limits for the magnetic field even in the absence of a scientifically proven causal relationship between electric and magnetic field at 50 Hz and damage to health: The DPCM 08/07/2003 [2] sets a maximum acceptable value of 10  $\mu$ T, to be fulfilled both in new and existing lines, and a quality target of 3  $\mu$ T, to be fulfilled for new OHLs.

These exposure limits and values reflect the precautionary approach taken by Italian regulation to minimize potential risks associated with electric and magnetic fields.

In addition to Italy, there are other countries that have implemented strict limits:

- in Slovenia there is a limit of 10  $\mu$ T for the new construction and 100  $\mu$ T for the existing ones; the same limit is often assumed also in other countries such as Slovenia, Belgium (Flanders region) and in Russia for residential areas.
- a 20  $\mu$ T limit is prescribed in New York [11] and Florida, as well as in Russia [12] in uninhabited areas)
- in Croatia there is a limit of 40  $\mu$ T for house, school, retirement homes, etc..
- Bulgaria has minimum distance requirements for new constructions, but there are no specific exposure limit values for magnetic induction.
- in Belgium there are regional limits varying between 100  $\mu$ T and lower values,
- in Poland there is a limit of 75  $\mu$ T.

The international comparison highlights how Italian legislation is among the most precautionary. It is also the only one to establish significantly lower limits compared to EU recommendations for public exposure to magnetic induction from existing power lines.

Complying with these limits results in greater constraints on the routing of power lines, requiring increased overhead ground clearance, higher structural costs, and potential environmental and landscape impacts. It also leads to higher costs associated with the frequent use of underground power lines, even in cases where they may not be technically necessary.

To improve the efficiency and competitiveness of the national electricity system, Terna has developed the new “5-Phases” transmission tower. This innovation is the result of an extensive process of study and technological research, representing the latest and most efficient evolution [8].



Oral Presentation: An Innovative Solution for Reducing Emfs: The "5-Phases" Pylons.

### 2. INNOVATIVE DESIGN OF THE Pylon CALLED "5-PHASES" FOR REDUCTION EMF

Until now, the most effective solution for reducing the magnetic induction generated by an overhead line has been the transition from a single circuit to a double optimized circuit.

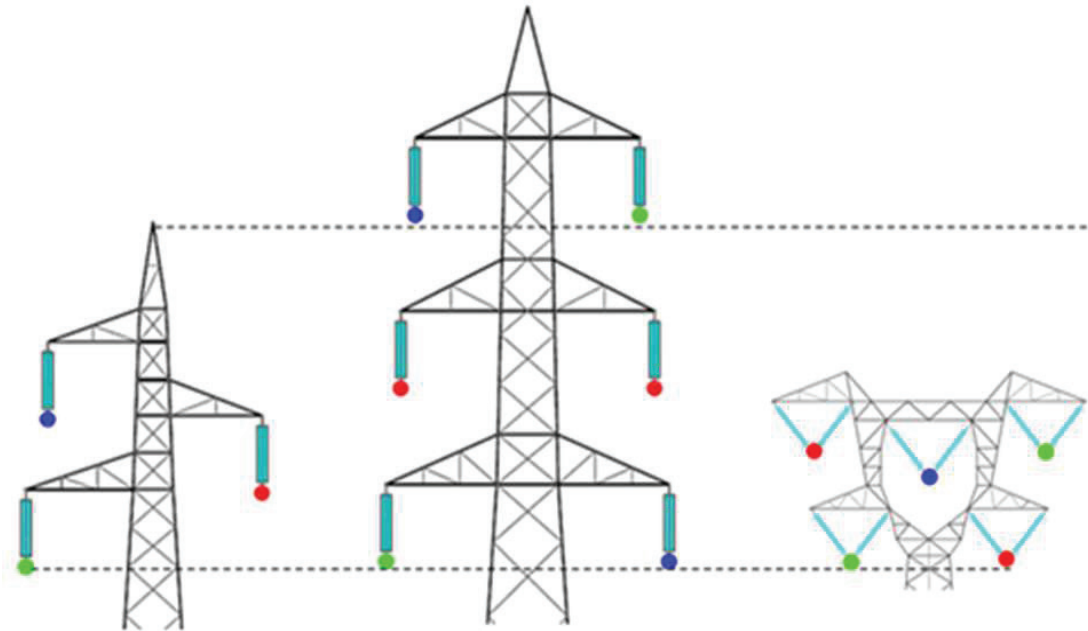


Figure 1. Conventional single (left) and double circuit (centre) 230kV OHL and "5-phases"(right) pylons arrangement

As show in Figure 2, the partition of the total current of each phase (Figure 2), between two opposite conductors (or bundles of conductors for higher voltage levels), and the anti-symmetrical arrangement of the phases, enable a significant reduction in the resulting magnetic field produced by the infrastructure. Figure 3 show that, this reduction can be estimated to be around 50% of the maximum magnetic induction value at the centerline.

Additionally, increasing the conductor cross-section allows for a reduction in losses while maintaining the same current flow.

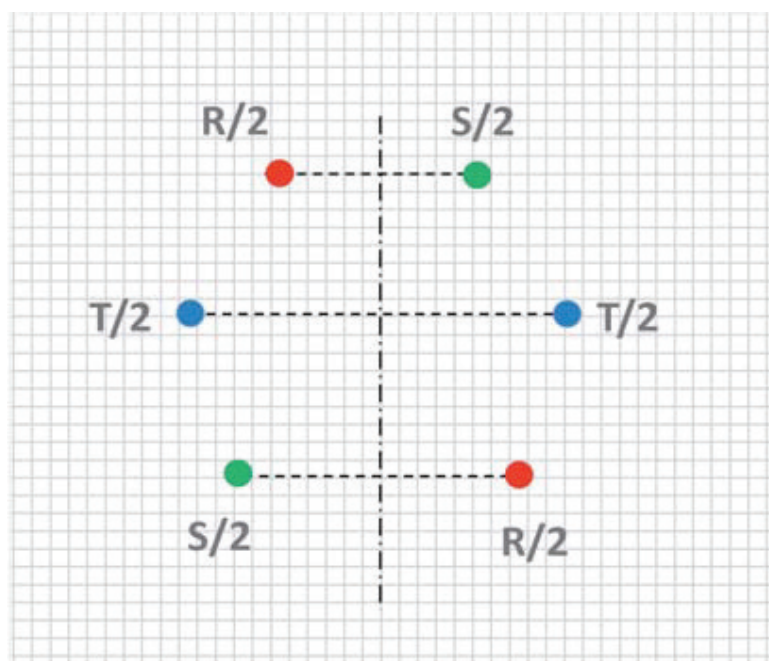


Figure 2. Anti-symmetrical phases arrangement and phase -splitting



Oral Presentation: An Innovative Solution for Reducing Emfs: The "5-Phases" Pylons.

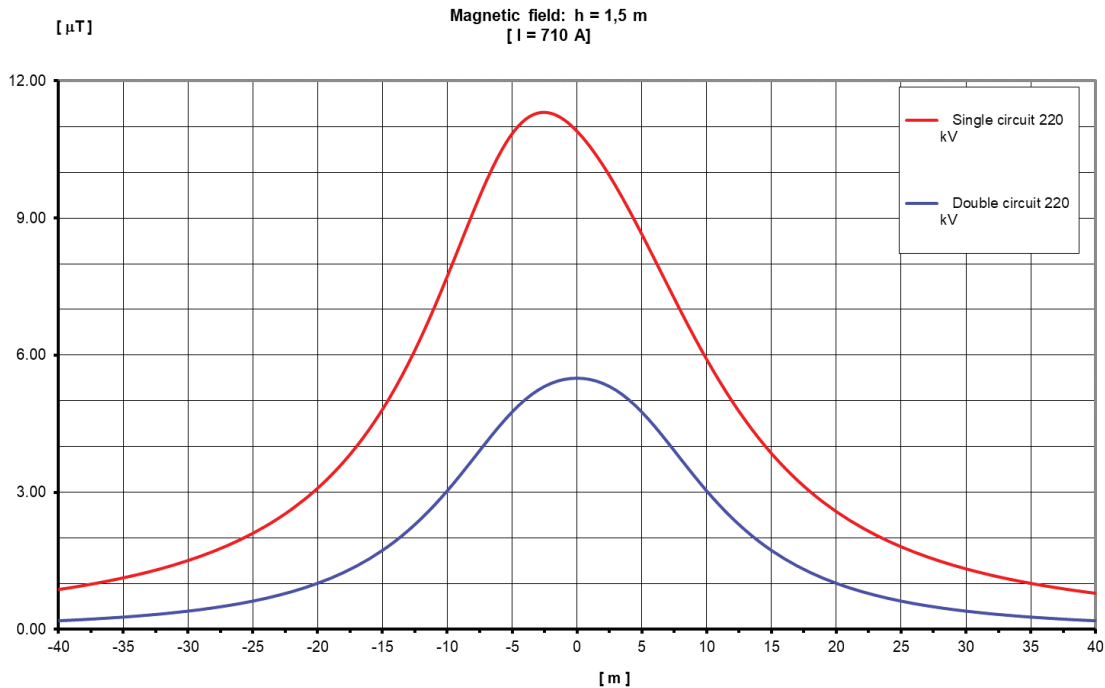


Figure 3. Magnetic field distribution of an Single circuit and Double circuit at 220 kV, at the same height.

However, an important drawback is the increase in the overall height of the transmission tower, which has a significant impact on the environment, landscape, and the authorization process.

### 3. ELECTRIC AND MAGNETIC FIELD OF THE 5-PHASES PYLONS

The "5-phases" overhead pylons (OHLs), utilize an optimized 5-bundle geometry. This involves splitting the current of two phases into four different conductor bundles, while using a single conductor bundle for the remaining phase, as shown in Figure 4.

The most effective arrangement for reducing magnetic induction involves dividing the current of two phases into four separate bundles of conductors positioned at the corners of a rectangle, while the remaining phase is placed at the center (Figure 4). This novel solution is scalable using conventional methods and maintains cost-effectiveness by minimizing material quantity and cost. Implementing this optimal arrangement, has been the focus of the authors' work for several years, culminating in the development of the "5-Phases" solution.

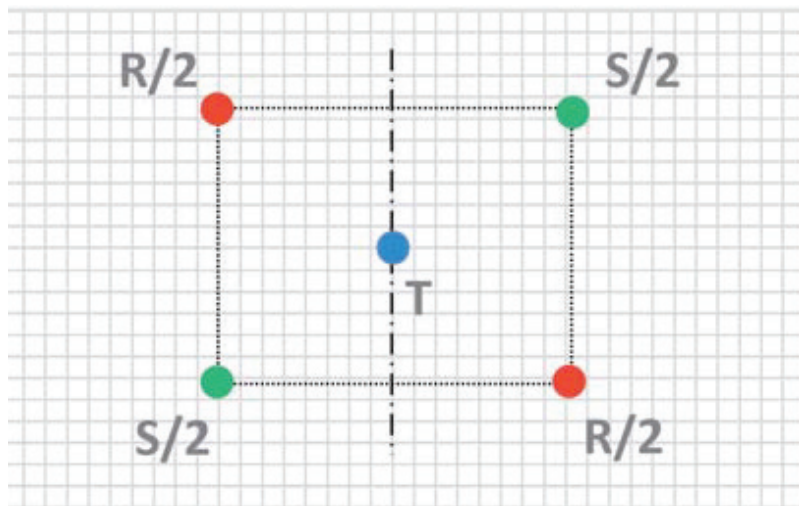


Figure 4. Optimal phase arrangement in "5-Phases" towers



Oral Presentation: An Innovative Solution for Reducing Emfs: The "5-Phases" Pylons.

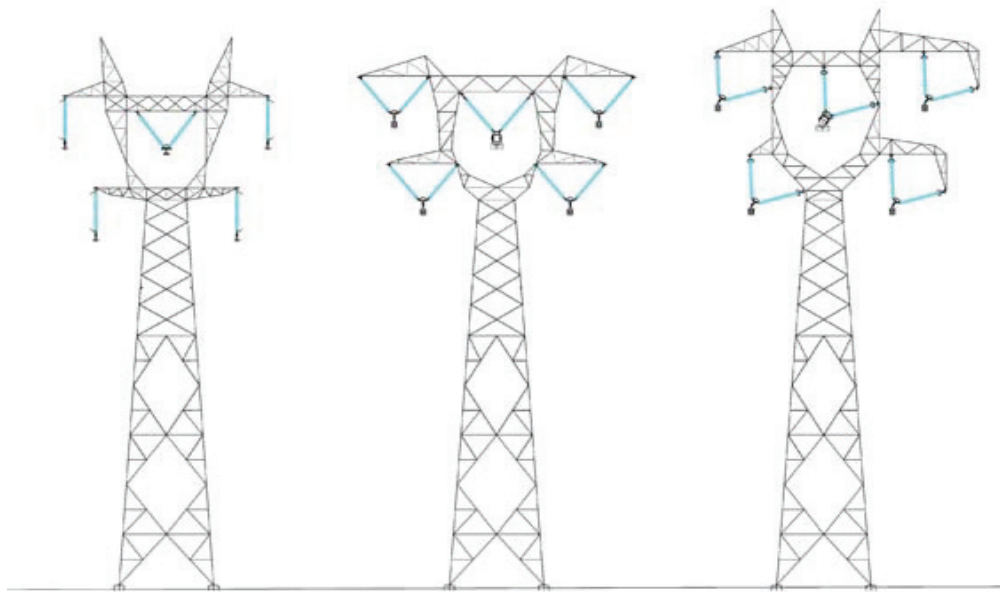


Figure 5. Typical "5-Phases" 230 kV pylons: tension tower (left), straight suspension tower (centre) and suspension angle lattice tower (right)

The "5-Phases" tower has achieved a significant reduction in magnetic induction. Underneath the overhead line, the magnetic induction value decreases by over 80% compared to a traditional single circuit line, and by over 60% when compared to a double circuit line (Figure 6). What's even more noteworthy is that the maximum value measured under the line is lower than the targeted quality objective of 3  $\mu\text{T}$  and is comparable to the magnetic induction generated by an underground cable in a high-voltage power line.

The above reported figure (Figure 7) clearly shows that using 5-phases pylons it is possible to increase the ampacity from 1000 to 2500 A while reducing the width of the 10  $\mu\text{T}$  contour line, i.e., the line ROW (Right Of Way). This can be an interesting solution for the complete refurbishment of existing 230 kV backbones, increasing the power transmission while keeping the same ROW.

On the other hand, "5-phases" pylons can be used on specific sections of the OHL, to cope with local infringements of the EMF thresholds (for example, where housing have been built inside the ROW of OHLs dating back from 1940÷1970), without limiting the current loading of existing backbones.

Moreover, the new tower's geometry enables a significant reduction in the overall height of the tower (for the same height above ground) compared to a conventional single and double circuit overhead line (Figure 8).

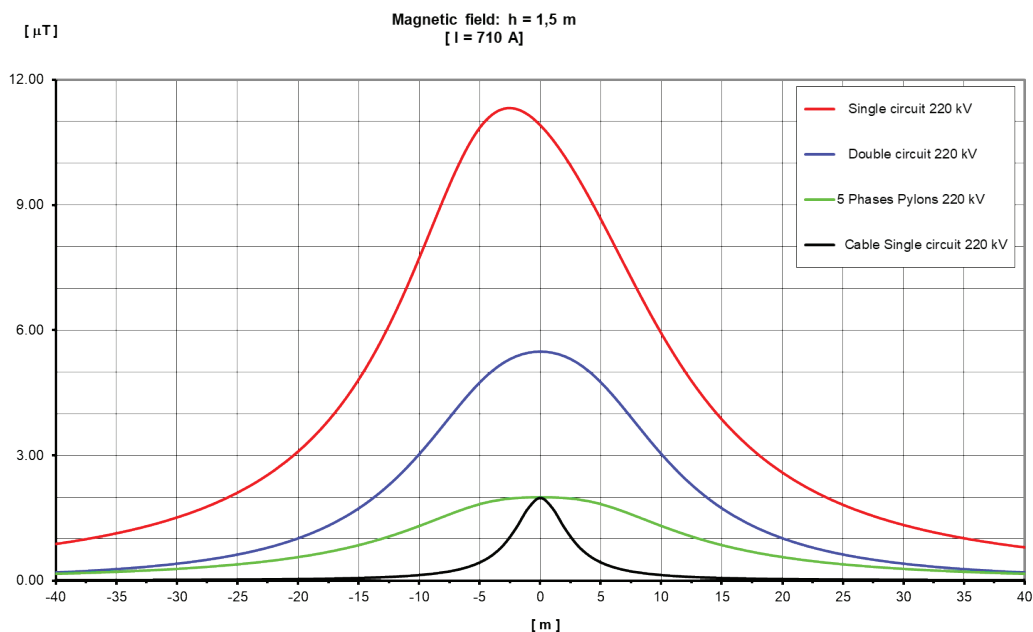


Figure 6. The comparison of magnetic induction distributions among different technological solutions for 220 kV lines: conventional Single Circuit Overhead Lines, Double Circuit, "5 Phase" lines (at the same usable height), and underground cables.



Oral Presentation: An Innovative Solution for Reducing Emfs: The "5-Phases" Pylons.

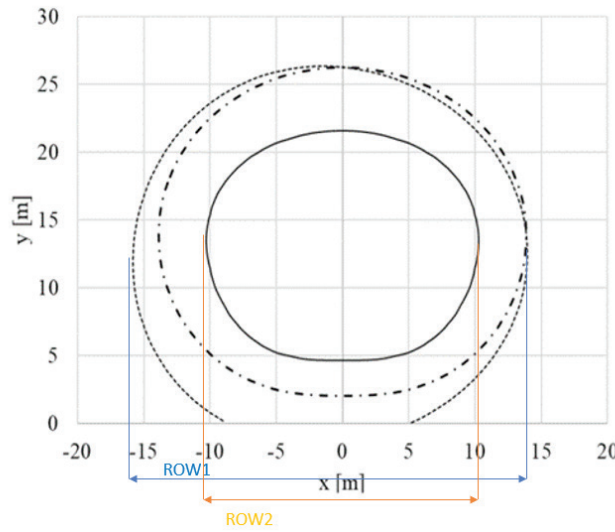


Figure 7. 10 μT contour lines for different 230 kV line configurations. Dashed line: typical single circuit line, as in Figure 1 (1000 A ampacity); solid line: use of 5F pylons for mitigating EMF on critical parts of the existing line route keeping the same ampacity (1000 A loading); dashdot line: use of 5F pylons for refurbishment the whole backbone, increasing the ampacity to 2510 As

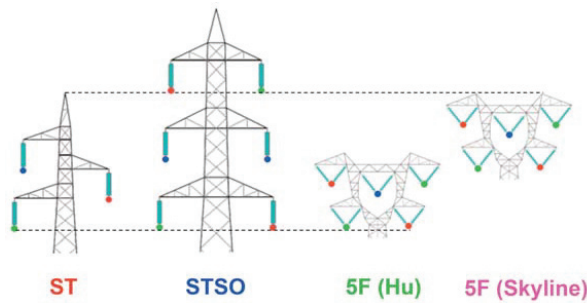


Figure 8. A schematic comparison of the different support geometries for magnetic field mitigation in 220 kV lines is shown. The "5-Phases" support is highlighted, showcasing its equivalent usable height and total height compared to the original line.

Compared to a traditional solution, the new tower presents a good reduction in the maximum electric field. In case of "Skyline" solution, a significantly lowered maximum electric field limit is observed Figure 9.

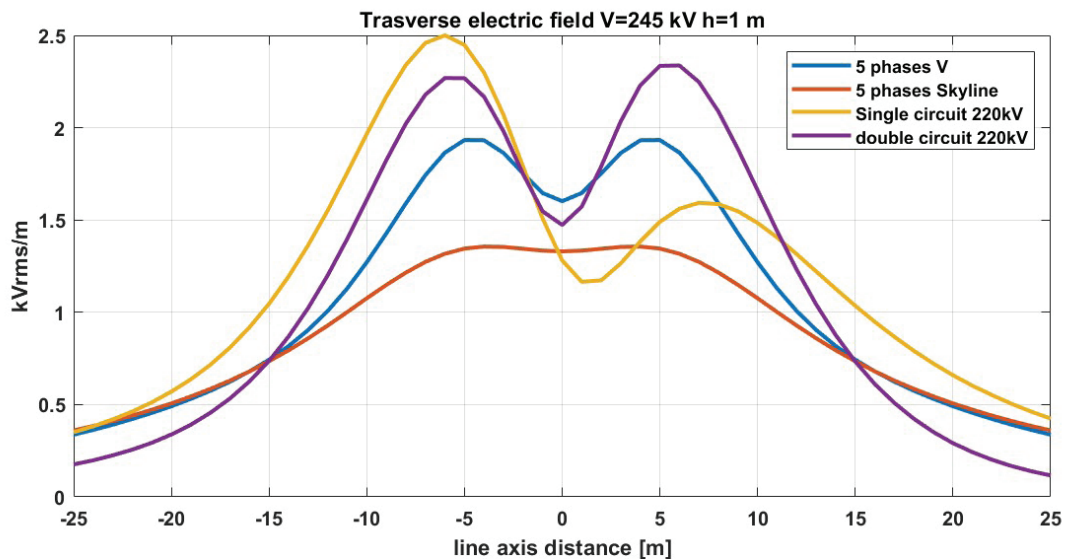


Figure 9. Comparison of electric fields among different tower geometries, according to the EPRI methodology.





Oral Presentation: An Innovative Solution for Reducing Emfs: The “5-Phases” Pylons.

#### 4. CORONA EFFECT AND NOISE AND RADIO INTERFERENCE

It is known that the corona effect is caused by the ionization of the air in the region of high electric potential gradient on the surface of conductors. As the electric field on the conductor’s surface increases, it accelerates the charged particles, leading to an avalanche discharge process and eventually generating localized discharges. This phenomenon, far from being linear, has directly and indirectly observable consequences:

- Acoustic noise, with tonal components (in the case of AC overhead lines) or a relatively flat spectrum at high frequencies (in the case of DC lines).
- Radio interference, with emission spectrum concentrated on frequencies ranging from a few hundred kHz to several MHz.
- Active power losses, which can become significant for extremely high-voltage lines under disturbed weather conditions.
- Ozone (O<sub>3</sub>) production. Ion production, in the case of DC overhead lines.

Acoustic noise and radio interference represent a significant challenge when designing “5-Phases” overhead lines. This challenge is particularly noticeable in Italian [13] contexts due to stringent regulations regarding environmental acoustics and the prevalence of urbanization in areas impacted by electrical infrastructure.

The estimated value of the sound pressure level for a 220 kV overhead power line in a “5-Phases” configuration is compared with a traditional transmission tower Figure 10.

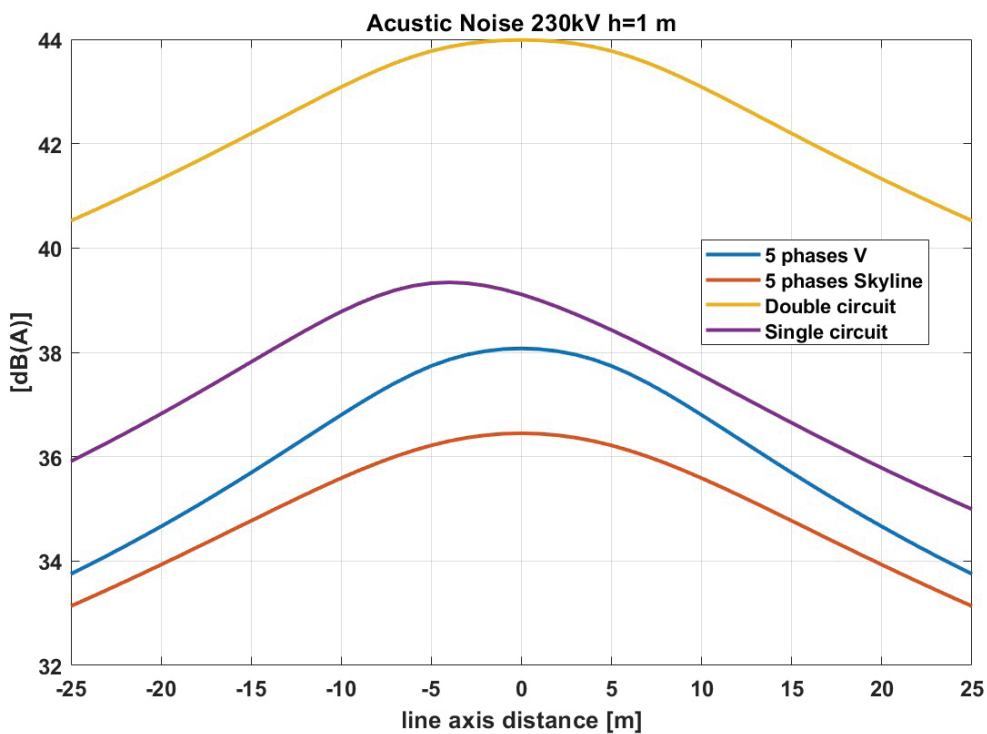


Figure 10. Profile of the acoustic noise generated by 220 kV power lines under wet conductor conditions (with the same total height as the Single circuit), according to the EPRI methodology.

When comparing the noise levels of a “5-Phases” line to traditional single circuit and double circuit lines, with the same height above ground and ground clearance of the conductors, the noise generated by the “5-Phases” line is either lower or equal to that of a traditional single circuit line and significantly lower than that of a double circuit line.

The increase in the electric potential gradient on the conductors, resulting from the higher compactness of the “5-Phases” line, is effectively counterbalanced by the larger conductor diameters (40.5 mm instead of 31.5 mm). In the Skyline option, the advantage in terms of audible noise is even more significant. In fact, it can be observed that the acoustic pressure level is significantly lower, by approximately 3 dBA, compared to the traditional option.

“5-Phases” pylons have radio interference levels that are comparable to those of traditional single and double pylons.



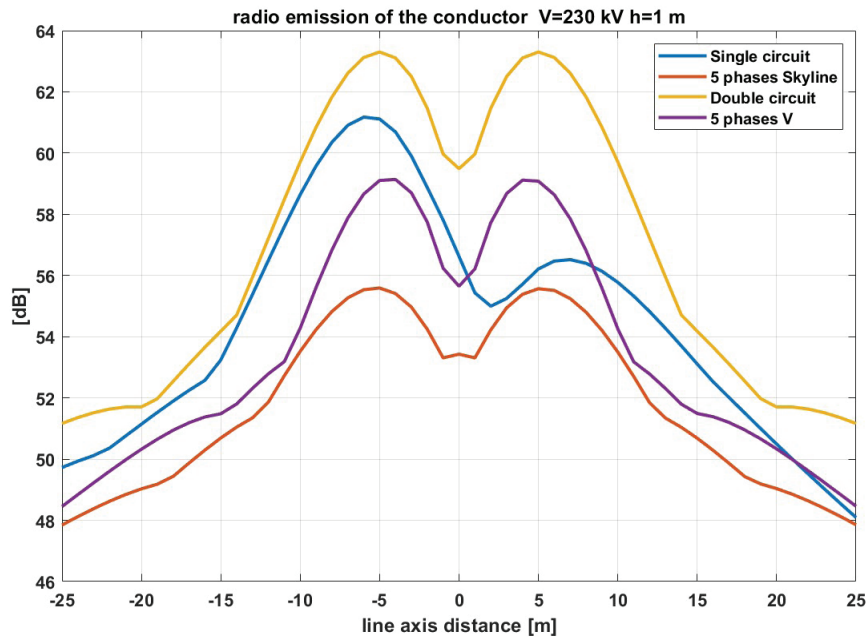


Figure 11. Radio interference generated by 220 kV power lines under conditions of wet conductor, according to the EPRI methodology.

## 5. CONCLUSION

Considering the ever-increasing attention to environmental and social sustainability of electricity infrastructures, Terna developed an innovative transmission tower solution: the "5-Phases" pylons, capable of significantly reducing EMFs, while increasing line ampacity and loadability.

Typical application examples at 230 kV allow to keep the magnetic field below the 10  $\mu$ T threshold, often applied in different countries for new and existing OHLs.

The refurbishment of existing, ageing, OHLs using "5-phases" pylons, will allow for significantly greater ampacities than those of conventional overhead lines: representing an effective and efficient tool for enabling the energy transition, without further land consumption.

Most significantly, the components and technologies to be used in the "5-Phases" line will be the same as those normally adopted in ac OHLs, therefore eliminating technological risks often associated with innovative design and solutions.

## BIBLIOGRAPHY

- [1] M.R. Guarniere, R. F. Palone, R. Spezie, L.Zuccolo, "Linee aeree adette a "5 fasi" per la riduzione dei campi elettrici e magnetici" (in Italian) in L'Energia Elettrica, n°1, vol. 100, Jan 2023.
- [2] A. M. Lopez Diaz, M. .R. Guarniere, F. Palone, R. Spezie "Soluzioni progettuali per la miglior interazione visiva dei nuovelettrodotti aerei" (in Italian).L'Energia Elettrica, settembre/ottobre2022 n°5.
- [3] Landini, M., Mazzanti, G., & Mandrioli, R.. Procedure for Verifying Population Exposure Limits to the Magnetic Field from Double-Circuit Overhead Power Lines. Electricity, 2(3), 2021, pp 342-358.
- [4] Resolución sobre las Modificaciones a la Metodología para la Determinación de los Cargos por Servicio de Transmisión de Energía Eléctrica. (Diario Oficial de la Federación. Jueves 23 de Diciembre de 1999).
- [5] M.R. Guarniere, R. F. Palone, R. Spezie, L. Buono, L. Papi, G. Tresso "Loadability curves for the new Terna's "5F" highcapacity overhead lines", EEEIC 2023 Madrid.
- [6] State of New York Public Service Commission, "Statement of Interim Policy on Magnetic Fields of Major Electric Transmission Facilities", Cases 26529 and 26559, Issued and Effective September 11, 1990.
- [7] GN 2.1.8/2.2.4.2262-07 "Limits of magnetic fields at 50 Hz in residential and public buildings and residential areas."
- [8] Italian decree July, 8th 2003 "Establishment of exposure limits, warning values and quality objectives for the protection of the public from exposure to electric and magnetic fields at mains frequency (50Hz) generated by power lines", available online <https://www.gazzettaufficiale.it/eli/id/2003/08/29/03A09749/sg>.



Oral Presentation: An Innovative Solution for Reducing Emfs: The "5-Phases" Pylons.

- [9] European Environment Agency - report 21/2019: Healthenvironment, healthy lives: how theenvironment influences healthand well-being in Europe, Publications Office of the European Union, 2020.
- [10] E. Stracqualursi; R. Araneo; S. Celozzi: The Corona Phenomenonin Overhead Lines: CriticalOverview of Most Commonand Reliable Available Models. Energies, 14, 6612, 2021.
- [11] State of New York Public Service Commission, "Statement of InterimPolicy on Magnetic Fields of Major Electric Transmission Facilities",Cases 26529 and 26559, Issued and Effective September 11, 1990
- [12] GN 2.1.8/2.2.4.2262-07 "Limits of magnetic fields at 50 Hz inresidential and public buildings and residential areas."
- [13] Decreto del Presidente del Consiglio dei Ministri 14 novembre 1997 - Determinazione dei valori limite delle sorgenti sonore.



# An Innovative OHL Design for Renewable Energy Harvesting and Transmission: The “5-Phases” Pylons

[francesco.palone@terna.it](mailto:francesco.palone@terna.it)

**MARIA ROSARIA GUARNIERE, ROBERTO SPEZIE, FRANCESCO PALONE\*, LUCA BUONO, LORENZO PAPI, PIERLUIGI VACANTE, STEFANO LAURIA, MARCO MACCIONI**

*Terna, Sapienza University of Rome*

*Italy*

## SUMMARY

Due to the local availability of renewable energy sources, the decarbonization process will increase the need for new transmission lines, to harvest the renewable energy plants production and connect them to the load centres.

This is also the case of Italy, where most of the new renewable energy resources (wind and photovoltaic) are foreseen in the south, whereas most of the load is in the North.

Due to the relatively long distances, the challenging environmental and electromagnetic Field (EMF) constraints, Terna developed an innovative solution for high-voltage and extra-high-voltage overhead lines, which allows for a substantial increase of Surge Impedance Loading (SIL) and thermal loading, as well as lower losses and EMF, if compared to typical solutions. These new OHL towers have been defined as “5-phases” or “5F” pylons, as they adopt 5 different conductors (or conductor bundles, according to the voltage levels).

At present time, Terna designed “5-phases” pylons for 150, 230 and 400 kV line, for the Italian National Transmission grid. Furthermore, Terna also developed a preliminary design for 735 kV “5-phases”, for installations abroad.

The paper deals with the performances of the “5-phases” OHLs in terms of active power loadability, with a specific focus on renewable energy sources harvesting and transmission from the power plants to the load centres. Aside from the conventional constraints (conductors thermal current limit, voltage limits, steady-state stability margin), reactive power capability of the renewable generation has been also considered for evaluating the line loadability. Series compensation using conventional capacitor banks has also been taken into account, enhancing the already excellent performances of the new lines.

Results show that a 230 kV “5-phases” OHL can evacuate 1000 MW of renewable generation to a distance of 200 km; a 400 kV “5-phases” OHL can easily evacuate 3400 MW of renewable generation at a distance of 400 km, suggesting that the “5-phases” OHLs can be an effective and efficient solution for the integration and transport of renewable energy into existing transmission grids.

Section II deals with the main characteristics of “5-phases” OHLs in terms of loadability; section III deals with the adopted methodology for evaluating the loadability curves. Section IV to VII reports the loadability curves for 150 kV, 230 kV, 400 kV and 735 kV.

## KEYWORDS

High Voltage Overhead Line, Surge Impedance Loading, Pylons.



Oral Presentation: An Innovative OHL Design for Renewable Energy Harvesting and Transmission: The “5-Phases” Pylons

## 1. INTRODUCTION

Terna, the Italian Transmission System Operator, has recently introduced a new generation of HV and EHV lines, known as “5-phases” or “5F”, which offer a significant reduction in EMF exposure for the population and an increase in power transfer capacity compared to conventional overhead lines. The 5F lines provide an effective and efficient solution for refurbishing existing AC transmission backbones due to their reduced visual impact, lower EMF emissions and high loadability [1],[2],[3].

This paper presents a loadability study of the 5F configuration for various standard voltages in Europe, including 150 kV, 230 kV, and 400 kV, as well as higher voltages typically used for long-distance transmission, such as 735 kV. The results demonstrate that the novel 5F line configuration, when applied to the 400 kV and 735 kV levels, can achieve power transfer capacities of up to 3200 MW over a distance of 400 km at 400 kV, and up to 6000 MW over a distance of 1000 km at 735 kV, while adhering to conservative angle displacement and voltage drop limits.

## 2. MAIN CHARACTERISTIC OF “5-PHASES”

The term “5-phases” refers to the use of 5 different conductors or conductor bundles in the design of overhead power lines. Each conductor or conductor bundle represents one “phase” of the line, according to the terminology used by the International Electrotechnical Commission (IEC). These conductors or bundles are arranged with axial symmetry, which optimizes the electromagnetic field (EMF) at ground level. Electromagnetic fields (EMFs) pose significant environmental authorization challenges, which are pertinent not only in Italy but also in various countries worldwide. The presence and impact of EMFs necessitate careful consideration and adherence to regulatory frameworks to ensure the protection of the environment and public health [4],[5],[6],[7],[8].

Figure 1 provides an example of typical 5-phases pylons for a 230 kV line. In Figure 2, the circuit arrangement of the “5-phases” lines is compared to conventional single-circuit and double-circuit lines, highlighting their compactness, reduced height, and visual impact. Functionally, they behave as single-circuit lines. However, due to the close spacing of the unique conductor arrangement, the electrical properties of the 5-phase lines closely resemble those of a conventional double-circuit line operated with both circuits in parallel. Notably, the outer phases of the “5-phases” lines carry half the current compared to the central phase.



Figure 1. Suspension (left) and anchor (right) towers for “5-phases”



Oral Presentation: An Innovative OHL Design for Renewable Energy Harvesting and Transmission:  
The "5-Phases" Pylons

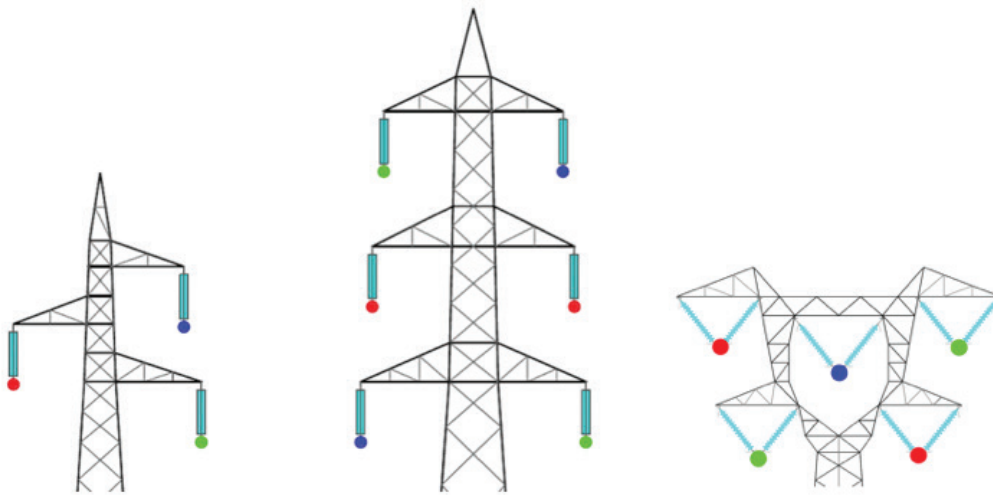


Figure 2. Circuit arrangement and visual impact comparison for single circuit, double circuit and 5F 230 kV line. Each individual phase of the 3-phase system is represented by a different color.

Consequently, the surge impedance and propagation constants of the "5F" lines are slightly below 50% of those of a conventional single-circuit line. Even when standard conductor bundles are used for the outer phases, the "5-phases" line delivers the same performance as a conventional double-circuit line, while occupying a single-circuit right-of-way and avoiding the visual impact associated with double-circuit lines. This comparison becomes even more favorable when larger conductor bundles are considered, as they lead to a reduction in impedance and propagation constant values ( $Z_c$  and  $K_s$ ). Table I summarizes the electrical properties and parameters of the proposed configurations.

Table 1. Electric parameters of "5F" OHLs.

Rated Voltage	$Z_c$ [ $\Omega$ ]		SIL [MW]		$S_z$ [MVA]
	$K_s=0$	$K_s=67\%$	$K_s=0$	$K_s=67\%$	
150 kV	182	104	124	216	483
230 kV	179	103	296	514	1000
400 kV	129	75	1240	2133	3464
735 kV	122	70	4428	7718	6365

### 3. CONSTRUCTION OF LOADABILITY CURVES

The loadability curve of a transmission line represents the maximum active power that can be transmitted as a function of its length. This curve is determined while considering various constraints, including maximum current, voltage drop, and phase angle separation between terminal voltages.

The curves presented in this paper were obtained by maintaining a constant sending voltage ( $U_s$ ) at 1 per unit (pu) and applying the following constraints:

1. Maximum current ( $I_z$ ): the magnitude of the current at both line terminals is set equal to the line ampacity,  $I_z$ .
2. Voltage drop and maximum current ( $\Delta U, I_z$ ): the voltage difference between terminal magnitudes is set at  $\epsilon$  pu (i.e.,  $U_r = (1 - \epsilon) * U_s$ ), while one terminal current is kept at  $I_z$ .
3. Phase angle separation plus terminal voltage drop ( $\Delta\theta, \Delta U$ ): both the phase angle and magnitude differences between terminal voltages are imposed.

The loadability curve represents the lower envelope of the three power versus length curves obtained based on the aforementioned criteria.





Oral Presentation: An Innovative OHL Design for Renewable Energy Harvesting and Transmission: The "5-Phases" Pylons

In cases where the line loading at the thermal limit exceeds the SIL (Surge Impedance Load), which is common for overhead power lines (OHLs), the constraint based on maximum current (Iz) can result in current magnitudes along the line exceeding the ampacity (maximum current rating). To simplify the analysis, the criterion ensures that the maximum current does not exceed 102% of Iz in all the considered cases.

Furthermore, it is important to note that the thermal limit for Extra High Voltage (EHV) "5F" lines is primarily determined by the rating of the substation equipment, which is currently limited to 5 kA. As a result, the verification of the thermal limit is only necessary at the line terminals.

According to existing literature [9], the maximum transmittable power of an AC power line is influenced by two key parameters: the electrical length and the characteristic power of the line. It is commonly assumed that a 50 Hz AC power line can transmit its Surge Impedance Load (SIL) over an "electrical" length of approximately 500 km [10].

By knowing the length of the line, it becomes possible to estimate the transmittable power as a ratio of its SIL using St. Clair curves (Figure 3). These curves provide a graphical representation of the relationship between the electrical length of the line and the corresponding transmittable power.

Gutman, Dunlop and Marchenko [11] studied the loadability of an ac line under the following operating constraints:

- thermal rating;
- maximum voltage drop;
- angular stability margin.

For high-voltage lines that are sufficiently long, it is often acceptable to neglect the line attenuation constant and focus solely on the voltage phase displacement. In this case, the maximum transmittable power for a given phase displacement can be expressed, as described in reference [12], by the following equation:

$$P_{max} = P_0 \cdot \frac{\sin(\delta_{limit})}{\sin(\beta \cdot L)} \tag{1}$$

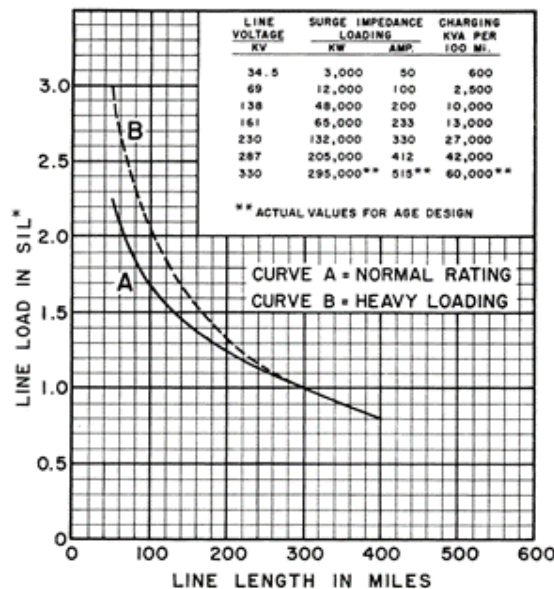


Figure 3. Original St. Clair curves (at 60 Hz).

with:

- $P_0$  : the line SIL;
- $\delta_{limit}$  : the maximum permissible phase difference;
- $\beta$  : the propagation constant;
- $L$  : the length of the power line.





**Oral Presentation:** An Innovative OHL Design for Renewable Energy Harvesting and Transmission: The "5-Phases" Pylons

In case of lossless lines, the propagation constant is:

$$\beta = \frac{2\pi \cdot f}{c} \sim 1.05 \cdot 10^{-3} km^{-1} \quad (2)$$

In the case of an uncompensated line, it can transmit its surge impedance loading for approximately 500 km. This assumption is made under the conservative assumption of a maximum phase difference equal to 30°, which corresponds to a static safety margin of 50%:

$$\frac{\delta_{limit}}{\beta} \sim 500 km \quad (3)$$

To increase the transmissible power of a line, capacitive series compensation can be employed, which effectively reduces the phase displacement of the line. This reduction in phase displacement allows for higher power transmission capacity.

The resulting maximum transmittable power can be evaluated using the following equation:

$$P_{max} = \frac{P_0}{\sqrt{(1 - k_s)}} \cdot \frac{\sin(\delta_{limit})}{\sin(\beta \cdot L \cdot \sqrt{(1 - k_s)})} \quad (4)$$

with  $k_s$  being the degree of series compensation (usually  $\alpha \leq 0.7$ ).

To maintain a reasonable level of accuracy while simplifying the previous equation, it can be approximated as follows:

$$P_{max} \sim \frac{P_0}{(1 - k_s)} \cdot \frac{\delta_{limit}}{\beta \cdot L \cdot (1 - k_s)} \quad (4)$$

The high Surge Impedance Load (SIL) of "5F" lines, combined with their high ampacity, enables bulk power transmission over longer distances compared to conventional overhead power lines (OHLs). This characteristic makes 5F lines advantageous for transmitting large amounts of power over extended distances.

Additionally, the low electromagnetic field (EMF) emissions and reduced visual impact of "5F" overhead power lines allow for the refurbishment of existing AC backbones with a substantial increase in transmittable power. This means that existing power line infrastructure can be upgraded to accommodate higher power transmission without significant visual or environmental impact.

Calculations have been conducted to quantify the performance of "5F" power lines at standard voltage levels commonly used in Italy (150 kV, 230 kV, 400 kV), as well as higher voltages typically utilized for long-distance transmission (e.g., 735 kV). These calculations aim to evaluate the capabilities and benefits of "5F" power lines across various voltage levels.

## 4. LOADABILITY CURVES FOR 150 KV "5-PHASES" POWER LINES

With the growing development of renewable energy sources, the sub-transmission network operating at 150 kV in southern Italy has evolved into a collection grid for wind farms and photovoltaic power plants. Currently, it serves two primary purposes: connecting renewable power plants to the National Transmission Grid and facilitating power transmission between adjacent market zones over short to medium distances.

Terna, the Italian transmission system operator, has been studying various solutions to improve the reliability of 150 kV overhead power lines. However, due to the increasing size of renewable energy plants and the challenges posed by environmental and electromagnetic field (EMF) constraints, traditional single circuit and double circuit lines have become less suitable for these tasks. In some cases, energy-intensive battery storage systems have been employed to avoid curtailing wind farm production on heavily loaded 150 kV lines [13].

The higher power transfer requirements in this context pose significant challenges in terms of loadability constraints. While the adoption of High Temperature-Low-Sag conductors (HTLS) partially addresses the thermal loading issue, it worsens static stability and voltage drop, especially for line lengths exceeding a few kilometers.

On the other hand, the 150 kV "5-Phases" pylons offer excellent performance in terms of transmissible power, even over considerable distances. These pylons have a high thermal rating (1860 A) and a low surge impedance (182 Ω). Figure 4 demonstrates their



Oral Presentation: An Innovative OHL Design for Renewable Energy Harvesting and Transmission:  
The "5-Phases" Pylons

capability to transmit power over typical distances of less than 50 km, with transmissible power for collecting renewable energy exceeding 450 MW. For longer distances, such as transits between adjacent market areas in Italy (approximately 250 km), the adoption of series capacitors allows for the transmission of over 400 MW while respecting conservative constraints on voltage drop (2.5%) and angular stability (50% static stability margin).

The loadability performance of "5F" 150 kV lines surpasses that of single circuit lines, offering significant increases in transmissible power. This feature is particularly valuable for harvesting renewable energy. As wind power plants and photovoltaic installations continue to grow in size, there is a need for more powerful transmission lines. The "5F" solution can effectively be employed to connect large arrays of wind farms to the Extra High Voltage (EHV) or High Voltage (HV) interconnecting substations.

Moreover, the 150 kV "5F" pylons exhibit excellent EMF performance, with magnetic fields remaining below the stringent threshold of 10  $\mu$ T, even at full power. This makes them suitable for deployment in urbanized and industrial areas where strict EMF regulations are in place.

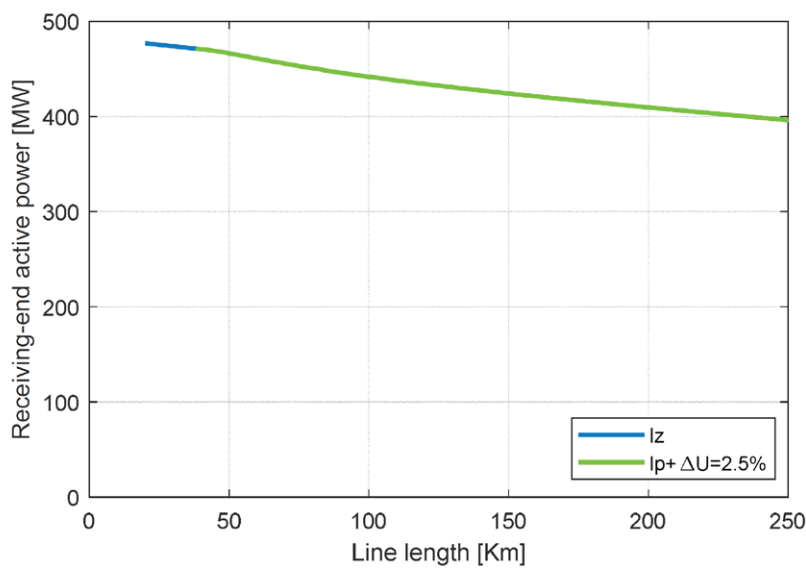


Figure 4. Loadability curves for 150 kV lines. Blue curves: thermal limit ( $I_z$ ); green line: voltage drop limit ( $\Delta U + I_z$ ).

## 5. LOADABILITY CURVES FOR 230 KV "5-PHASES" POWER LINES

In the 1940s and for approximately 30 years thereafter, the 230 kV power lines served as the main backbone of the Italian national transmission grid. However, with the subsequent development of the 400 kV grid, the role of the 230 kV lines shifted to subtransmission or bulk distribution, particularly in densely populated urban areas such as Milan, Turin, Rome, and Naples.

Factors such as progressive urbanization and the implementation of electromagnetic field (EMF) limits further reduced the actual utilization of the 230 kV lines. Additionally, most of these lines were constructed between 1928 and 1960, making them close to the end of their service life and necessitating refurbishment and upgrading solutions [9].

To address these challenges, the concept of "5-Phases" pylons emerged as an interesting option for refurbishing the 230 kV lines. These pylons allow for the reuse of the lines as transmission backbones for bulk power transfer between different market zones while complying with stringent EMF limits.

The "5-Phases" pylons offer several advantages. They can accommodate high thermal ratings, with 40.5 mm conductors capable of carrying a substantial amount of power. Additionally, these pylons have a low surge impedance of 180  $\Omega$ , further enhancing their power transfer capabilities.

Figure 9 illustrates the maximum active power at the receiving end as a function of line length. Notably, the high ampacity of the line can be effectively utilized throughout the considered length range while maintaining a voltage drop of 2.5%. For example, at a line length of 400 km, the loadability is 840 MW, which is a significant fraction of the thermal limit.

The conservative limit of a 30° phase angle separation between terminal voltages only becomes relevant towards the end of the considered length range, specifically for line lengths of 396 km or greater.



**Oral Presentation:** An Innovative OHL Design for Renewable Energy Harvesting and Transmission:  
The “5-Phases” Pylons

Operating with both terminal currents equal to the ampacity (the “Iz” constraint) is only feasible up to a line length of 66 km due to the voltage drop reaching 2.5%. For lengths greater than 66 km, loadability is determined by the “ $\Delta U + I_p$ ” constraint. In practice, the difference between these two curves is minimal. Reactive power support at the receiving end of the line is required to achieve these loadability performances.

The loadability capabilities of “5F” 230 kV lines enable a substantial increase in transmittable power. By utilizing “5F” pylons, aging backbones can be refurbished, achieving a twofold increase compared to typical single-circuit lines without requiring additional right-of-way (ROW).

Moreover, “5F” 230 kV lines comply with the stringent 10  $\mu\text{T}$  EMF limit even within the ROW, even at the maximum transmittable power (i.e., the thermal rating of the considered 40.5 mm ACSR conductors). This makes them suitable for urban environments and for resolving existing bottlenecks caused by EMF limit violations in residential areas close to existing lines. Additionally, “5F” 230 kV lines can be a cost-effective solution for transporting renewable energy over medium distances.

## 6. LOADABILITY CURVES FOR 400 KV “5-PHASES” POWER LINES

With the increasing adoption of renewable energy sources, there is a significant need for higher transmissible power. Conventional 400 kV single circuit lines may not always be sufficient, and double circuit overhead lines (OHLs) face challenges due to their increased visual impact caused by their height.

The use of High Temperature-Low-Sag (HTLS) conductors to increase active power transmission on existing 400 kV backbones is often limited by constraints related to electromagnetic fields and loadability, in addition to thermal loading considerations such as voltage drop and static stability margin. Therefore, the advantages offered by the “5-Phases” pylons are particularly significant for refurbishing existing 400 kV backbones and developing new lines.

The 400 kV “5-Phases” pylons provide a substantial gain in terms of transmissible power due to their high thermal rating ( $I_z=5000$  A) and low characteristic impedance (129  $\Omega$ ). The loadability curve for the 400 kV “5F” line with 67% compensation is depicted in Figure 6. The line can be operated near or at its thermal limit throughout the entire length range and can transfer up to 3270 MW over a distance of 400 km while keeping the voltage drop and phase angle difference within 2.5% and 30 degrees, respectively. For the maximum power and distance combination mentioned, the phase displacement between terminal voltages does not exceed 25°, which is below the static stability criterion for “normal loading”.

Loadability is primarily governed by the “Iz” constraint up to a length of 186 km. Beyond that length, the voltage drop must be maintained at 2.5%, so the “ $\Delta U + I_p$ ” constraint applies. Similar to the 230 kV case, operation based on the latter constraint necessitates reactive power support at the receiving end of the line. The power factor at maximum power reaches 0.977 for a length of 400 km.

Thanks to the large conductor bundles utilized in the 400 kV “5F” line, transmission losses at maximum loading are kept slightly below 1.4% per 100 km, amounting to 5.5% for the 400 km line.

Similarly, to the 230 kV line, adopting a lower series compensation degree would significantly reduce loadability towards the end of the studied length range. However, it’s worth noting that even without series compensation, it is possible to transmit over 3400 MW for distances up to 100 km.

Considering that the 400 kV “5F” OHL, despite enabling a twofold increase in active power transmission, generates a lower or equal magnetic field compared to traditional single circuit lines, “5F” pylons provide an effective and efficient solution for refurbishing existing backbones in urban or industrial areas without requiring an increase in the right-of-way (ROW).

Furthermore, 400 kV “5F” pylons can address local bottlenecks on existing lines caused by EMF limits near residential buildings. When operated at the same rated current as typical single circuit lines (2500 A), “5F” pylons meet the stringent requirement of 10  $\mu\text{T}$  even within the ROW, enabling the full utilization of challenging backbones passing through residential areas. It’s worth mentioning that 400 kV OHLs serve as transmission system backbones in Europe, and the refurbishment using “5F” pylons could offer substantial advantages for the integration of renewable energy sources.



Oral Presentation: An Innovative OHL Design for Renewable Energy Harvesting and Transmission: The "5-Phases" Pylons

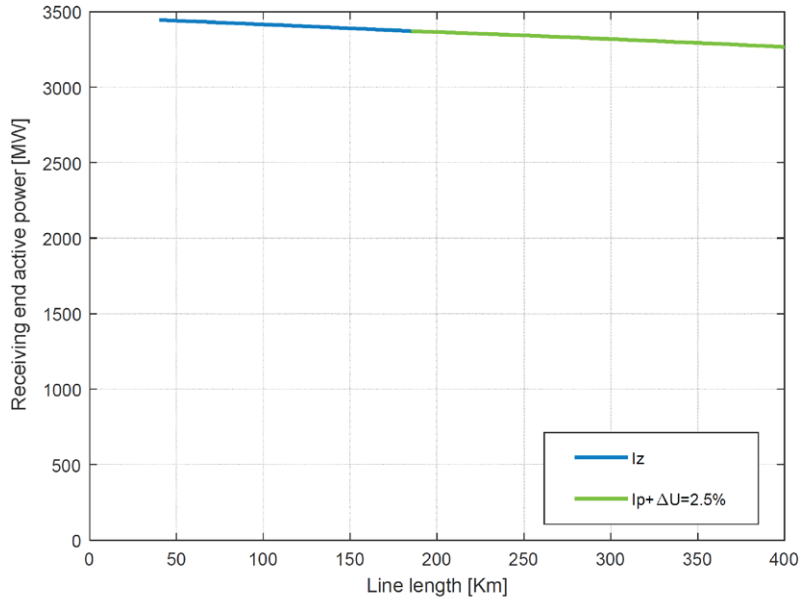


Figure 5. Loadability curves for 400 kV lines. Blue curves: thermal limit (Iz); green line: voltage drop (ΔU, Iz).

### 7. LOADABILITY CURVES FOR 735 KV "5-PHASES" POWER LINES

The "5-phases" solution can be extended to the highest voltage levels, such as 735 kV, for the purpose of bulk power transmission over very long distances. When implemented at the 735 kV level, the "5F" solution demonstrates the capability to transfer up to 6000 MW over a distance of 1000 km, while adhering to conservative limits on angle displacement and voltage drop. Figure 7 illustrates that the thermal current limit, "Iz," remains valid up to approximately 300 km distance, while the 2.5% voltage drop constraint, "Ip+ΔU," applies up to a length of 1000 km. Notably, due to series compensation, the static stability limit of θ = 30° is never reached.

It is important to mention that the ampacity limit of Iz = 5 kA, imposed by commercially available substation equipment, necessitates operation below the Surge Impedance Load (SIL). However, this constraint enables extremely low losses, approximately 0.5% per 100 km at full power. This remarkable result not only surpasses the performance of standard single circuit 735 kV AC lines but also compares favorably to Extra High Voltage (EHV) DC lines. Considering the excellent magnetic field exposure results for the general public, the 735 kV "5F" lines represent an appealing solution for bulk power transfer, even in industrialized and populated areas.

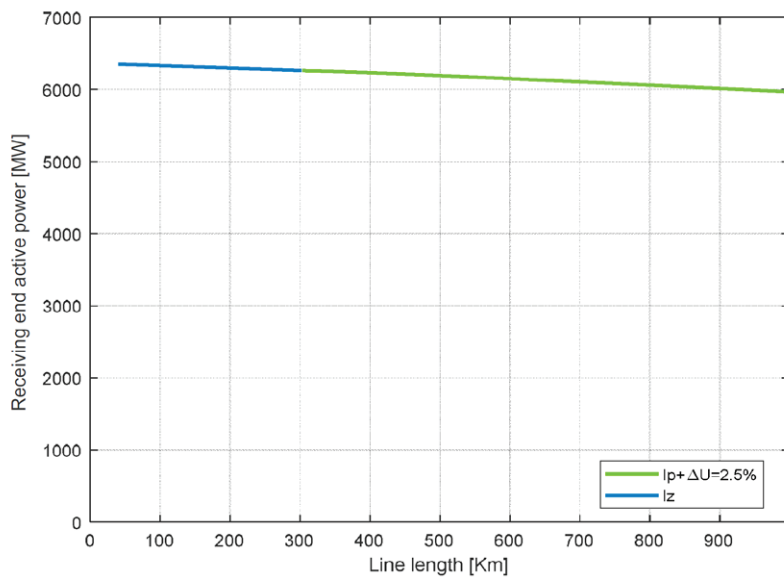


Figure 6. Loadability curves for 735 kV lines. Blue curves: thermal limit (Iz); green line: voltage drop (ΔU, Iz).



Oral Presentation: An Innovative OHL Design for Renewable Energy Harvesting and Transmission:  
The “5-Phases” Pylons

### 7. CONCLUSION

The “5-phases” lines offer an effective solution for the refurbishment of aging overhead power lines (OHLs), particularly in urbanized areas. They provide both low electromagnetic field (EMF) levels and increased loadability compared to conventional single-circuit lines. Even when considering conservative limits on voltage drop ( $\Delta V = 2.5\%$ ) and phase displacement ( $\theta = 30^\circ$ ) between the sending and receiving ends of the line, the “5F” configuration can deliver significantly higher active power.

For 150 kV OHLs, which are commonly used for harvesting renewable energy from wind farms and solar power plants, the “5F” solution enables the transmission of up to 400 MW over a distance of 250 km. When applied to the typical transmission grids in Europe, “5F” lines can deliver 850 MW and 3200 MW (at 230 kV and 400 kV, respectively) over a distance of 400 km. At the highest voltage level of 735 kV, the “5F” solution demonstrates the ability to transfer up to 6,000 MW over a distance of 1000 km, while adhering to conservative limits on angle displacement and voltage drop. These results highlight the advantages of “5-phases” OHLs for bulk power transmission, even in the presence of stringent EMF regulations.

### BIBLIOGRAPHY

- [1] M.R. Guarniere, F. Palone, R. Spezie, L.Zuccolo, “Linee aeree dette a “5 fasi” per la riduzione dei campi elettrici e magnetici” (in Italian) in *L’Energia Elettrica*, n°1, vol. 100, Jan 2023.
- [2] A. M. Lopez Diaz, M. .R. Guarniere, F. Palone, R. Spezie “Soluzioni progettuali per la miglior interazione visiva dei nuovi elettrodotti aerei”(in Italian).*L’Energia Elettrica*, settembre/ottobre 2022 n°5.
- [3] M.R. Guarniere, F. Palone, R. Spezie, L. Buono, L. Papi, G. Tresso, S. Lauria, M. Maccioni “Loadability curver for the new Terna’s “5F” high capacity overhead lines”, *EEEIC 2023 Madrid*.
- [4] Italian decree July, 8th 2003 “Establishment of exposure limits, warning values and quality objectives for the protection of the public from exposure to electric and magnetic fields at mains frequency (50 Hz) generated by power lines”, available online <https://www.gazzettaufficiale.it/eli/id/2003/08/29/03A09749/sg>.
- [5] Landini, M., Mazzanti, G., & Mandrioli, R.. Procedure for Verifying Population Exposure Limits to the Magnetic Field from Double-Circuit Overhead Power Lines. *Electricity*, 2(3), 2021, pp 342-358.
- [6] Jiménez, V. J. H., Castronuovo, E. D., & Rodríguez-Morcillo, I. S..Optimal statistical calculation of underground cable bundles positions for time-varying currents. *International Journal of Electrical Power &Energy Systems*, 95, 201), 26-35.
- [7] GN 2.1.8/2.2.4.2262-07 “Limits of magnetic fields at 50 Hz in residential and public buildings and residential areas.”
- [8] State of New York Public Service Commission, “Statement of Interim Policy on Magnetic Fields of Major Electric Transmission Facilities”,Cases 26529 and 26559, Issued and Effective September 11, 1990
- [9] Lauria, S., & Palone, F. (2012, September). Operating envelopes of the Malta-Sicily 245 KV-50 HZ cable. In 2012 IEEE International Energy Conference and Exhibition (ENERGYCON) (pp. 287-292). IEEE.
- [10] Clair, H. S. (1953). Practical concepts in capability and performance of transmission line. *Power Apparatus and Systems*, 72(6), 1152-1157.
- [11] Gutman, R., Marchenko, P. P., & Dunlop, R. D.. “Analytical development of loadability characteristics for EHV and UHVtransmission lines”. *IEEE Transactions on Power Apparatus and Systems*, (2), 606-617, 1979.
- [12] Kundur, P. S., & Malik, O. P. (2022). *Power system stability and control*. McGraw-Hill Education.
- [13] Benato, R., Bruno, G., Palone, F., Polito, R. M., & Rebolini, M.(2017). Large-scale electrochemical energy storage in high voltage grids: Overview of the Italian experience. *Energies*, 10(1), 108.
- [14] L. Michi, E. Carlini, M. Migliori, F. Palone “Uprating studies for a 230 kV-50 Hz Overhead Line”, *IEEE Powertech conference*, Milano, Agosto 2019



# A Compact 24-Pulses Converter for Overhead Lines De-Icing and Reactive Power Compensation

[lorenzo.papi@terna.it](mailto:lorenzo.papi@terna.it)

LUCA BUONO, GAIA LEONE, FRANCESCO PALONE, LORENZO PAPI, ROBERTO SPEZIE,  
GABRIELE TRESSO, PIERLUIGI VACANTE

Terna S.p.A.

Italy

## SUMMARY

Ice and snow accumulation on conductors can hinder the safe operations of high voltage overhead lines (HV OHLs). In Italy, this topic is of concern for the HV OHLs crossing the mountainous areas in the Alps and Apennines; the same issue has been faced by many utilities, prompting the need for prevention and mitigation solutions. Different configurations have been proposed and implemented, mainly focusing on extra high voltage (EHV) lines with large conductor cross-sections and significant length; in some cases, static converters have been used both to act as a HVDC current source for de-icing and as Static Var Compensator (SVC) during normal system operation. The innovative solution proposed by Terna is instead focused on de-icing the relatively short (20-40 km) 132 and 150 kV backbones of the Italian sub-transmission grid in the Alps and Apennines, which are generally equipped with small (14.75 -22.8 mm diameter) conductors.

To cope with the stringent footprint constraints and harmonic distortion limits in the installation sites, Terna developed a 24-pulses thyristor AC/DC converter able to deliver up to 20 MW at MVDC (about 15 kVdc) during de-icing operation and up to about 20 Mvar when operating as SVC. The use of a 24-pulse transformers removes the need for harmonic filtering, minimizing the overall footprint of the solution. The paper deals with the design and performance evaluation of the thyristor based 24-pulse converter in the Italian 132 kV sub-transmission network in the Alps. A detailed ATP-EMTP model of the thyristor converter and the attendant transformer has been developed, in order to evaluate its behaviour both in de-icing and SVC operation.

The paper is divided as follows: section I reports the introduction to the work, section II summarizes the main characteristics of the proposed 24-pulse de-icing converter and its attendant transformer; Section III deals with the converter performances during de-icing operation in the 132 kV network, whereas section IV deals with the converter performances during SVC operation. The foreseen footprint and installation layout is reported in Section V; conclusions are summarized in section VI, evidencing that the proposed solution can effectively perform de-icing of a 22.8 mm conductor for a 100 mm snow cladding diameter in 80 minutes. At the same time, harmonic emissions are significantly below the limit values foreseen in the relevant standards. Results also show that, when not employed for de-icing, the proposed converter can provide reactive power for voltage regulation.

## KEYWORDS

De-icing, Overhead Lines, Reactive power, SVC.





### 1. INTRODUCTION

In harsh weather conditions, ice sleeves can form around conductors and shield wires. Due to the presence of the ice sleeves, the weight on the span significantly increases and can potentially damage the support structures. Therefore, it is necessary to implement de-icing systems in order to prevent damage to the power line and reduce service disruptions. Several configurations and technical solutions are reported in literature [1], also considering HVDC installation [2].

Due to the morphological structure of the Italian mainland, there are many mountainous power lines where the problem of ice sleeves persists. Wet snow accumulation around the conductor, if combined with low temperatures and low line ampacity, contributes to the formation of the sleeves. This problem is a significant concern in Italy due to the potential harm that may cause to the conductors, shield wires, and in certain instances, even the supporting structure.

Terna is currently evaluating the possible installation of an innovative de-icing system to take corrective actions to melt the sleeve as soon as it starts to form [7][8]. The underlying physical principle behind the melting of the ice sleeve is Joule Effect. By allowing a current to flow through the conductors, the dissipated heat will contribute to melting the ice sleeve. The heat generated due to the Joule effect needs to be sufficient to raise the temperature of the icy portion of the sleeve in contact with the conductor to its melting point. Once this temperature is reached, the heat will primarily transfer to the icy layer in contact with the conductor, causing it to melt. As a result, once the upper external surface of the sleeve is reached, it will fall off due to gravity.

Currently, Terna only has preventive solutions for ice sleeve melting and lacks corrective actions. The presence of a deicing system allows for avoiding interventions along the power lines in extreme conditions. It is therefore an important innovation for the safety of the operational personnel, as it helps to prevent interventions in severe conditions. Additionally, it represents a useful tool that allows for better management of the electrical system in case of adverse weather conditions.

An example of a delicate intervention was the repair of the support of the Dobbiaco-Somprade power line, located 2,200 meters above sea level, which posed a significant technical challenge. The critical position required access to remote and hard-to-reach areas, increasing the complexity of the repairing operations. To address this situation, careful planning of the intervention and the adoption of special activities were necessary. The use of helicopters was required to reach the affected area. Operators needed to be properly trained to work in extreme conditions and ensure their safety during the intervention. Furthermore, climate and weather conditions could present additional challenges. Low temperatures, strong winds, or the presence of snow could make the operations even more complex and require additional precautions. The repairing of the power line support at that altitude required a specialized approach, with a particular focus on operator safety and detailed operational planning, considering the challenging environmental conditions. By using the de-icing system, a remote approach can be employed, which is faster, more efficient and safer. It is also worth considering that the de-icing system will prevent damage to the infrastructure, avoiding long service disruptions of the power lines and bringing significant economic benefits.

### 2. MAIN CHARACTERISTICS

The system consists of three main parts: the HV/MV transformer, the AC/DC converter and the DC side disconnectors, as shown in Figure 1. The transformer is arranged with one primary star connected winding and four extended delta secondary winding. The converter is a 24-pulse thyristor-bridge.

The five disconnectors (D1,...,D5) on the DC-side are necessary for the permutation of the phases of the overhead line. The system must be designed to be remotely controlled.

The system must have a rated power of 20 MW, in order to enable the circulation of sufficient current to melt the ice sleeves on conductors typically used in overhead power lines of the RTN located in the Alpine and Appennine areas (maximum resistances in the range of 5 to 6  $\Omega$ ). Following the occurrence of an ice sleeve formation event, the operational procedure unfolds as follows:

- Put the high-voltage line affected by the ice sleeve temporary out of service;
- Short-circuit the phases at the far end of the line;
- The 24-pulse converter, fed by the HV/MV transformer, provides the DC current output for the de-icing actions.

The de-icing procedure can be divided in three intervals, considering a total time interval of 15 minutes:

1. For the first 5 minutes, the positive pole of the converter feeds the phase #A of the OHL by switching the disconnector D1 and the negative pole feeds phase #B and #C by closing disconnectors D3 and D5. The schematic layout of the procedure is shown in Figure 2.a;



Oral Presentation: A Compact 24-Pulses Converter for Overhead Lines De-Icing and Reactive Power Compensation

2. Suddenly, for other 5 minutes, D1 and D5 are opened and the positive pole of the converter feeds the phase #B of the OHL through the disconnector D2 and the negative pole feeds phase #A and #C through the disconnectors D3 and D4. The schematic layout of the procedure is shown in Figure 2.b;
3. Finally, during the last 5 minutes, D4 and D5 are opened and the positive pole of the converter feeds the phase #A and #B of the OHL through the disconnectors D1 and D2 and the negative pole feeds phase #C by closing the disconnector D3. The schematic layout of the procedure is shown in Figure 2.c.

Due to the logic adopted, each phase of the OVHL is fed by half of the DC-side current for 10 minutes and the full current for the remaining 5.

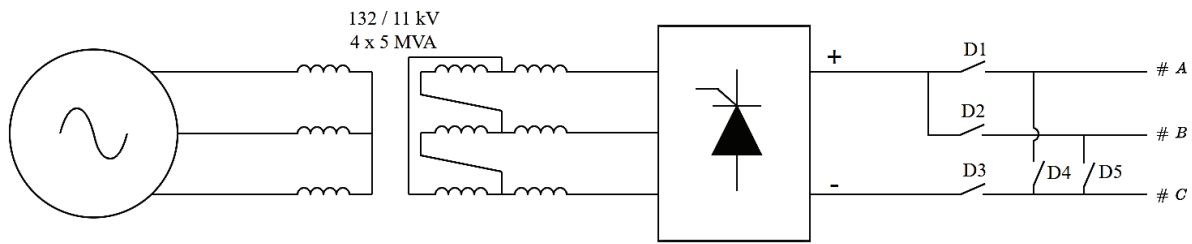


Figure 1. De-icing system equivalent circuit.

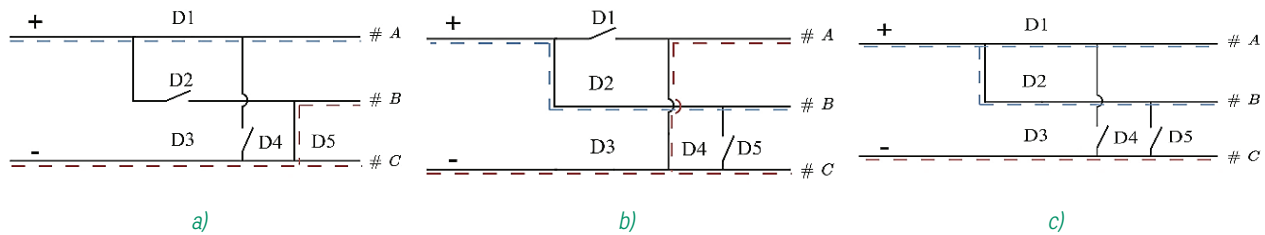


Figure 2. Schematic layout of the de-icing procedures: a) time interval from  $t=0$  to  $t=5$  min; b) time interval from  $t=5$  min to  $t=10$  min; c) time interval from  $t=10$  min to  $t=15$  min.

### 3. ELECTRICAL AND THERMAL PERFORMANCES

The selection of a 24-pulse system is motivated by the requirement to adhere to the limitations regarding the harmonic injection into the power grid. This constraint consists of a maximum value of the allowable *Total Harmonic Distortion* (THD) on the AC side [3]. To evaluate the harmonic distortion, a simulation was carried out using ATP-EMTP software. As predicted, the AC-side phase currents (Figure 3), show a significant reduction in AC-side harmonics.

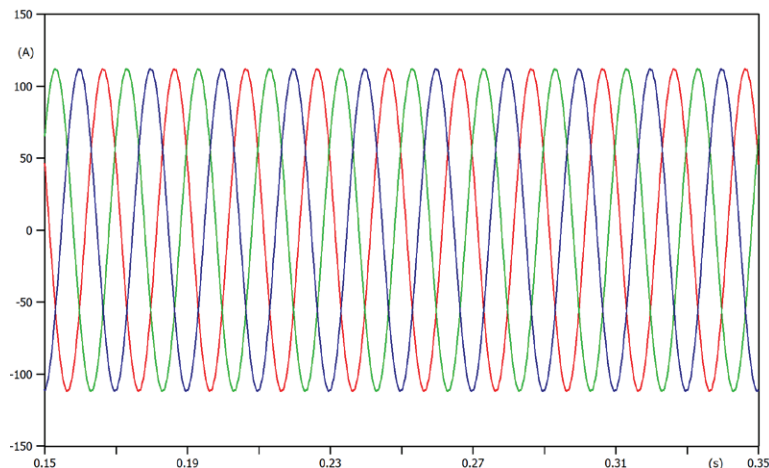


Figure 3. AC-side phase currents.



The Fourier analysis on the AC-side currents was also conducted using ATP-EMTP software. The simulation results confirm that the harmonic content is negligible. Indeed, as shown in Figure 4, the maximum rms value, reached by the 23rd harmonic and expressed as a percentage of the fundamental, is around 0.63%. This is further proven by the low THD value that is around 0.89% when considering up to the 500th harmonic.

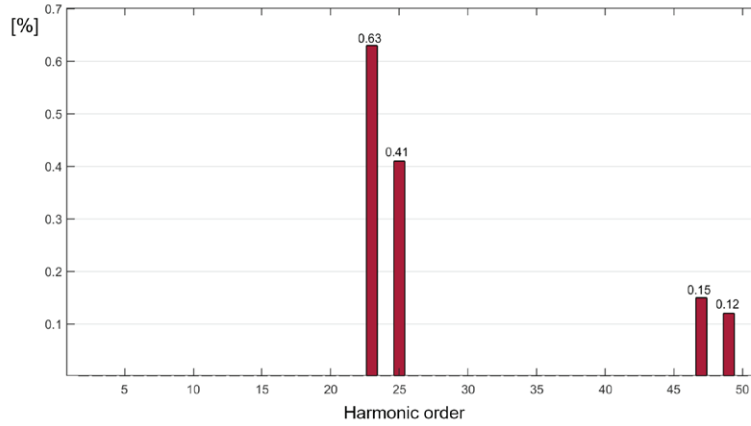


Figure 4. Fourier analysis of AC-side phase currents.

The five disconnectors shown in Figure 1 are essential for the operation of the system given the need for phase permutation between the two DC poles. In addition, an adequate choice of the opening/closing times allows the optimization of the conductors' thermal behavior and therefore avoid an excessive overheating. This is an important aspect to consider because the proposed de-icing system intervenes along the entire length of the line even though the ice sleeves may not necessarily be present. It is possible that only the spans at higher altitudes will be affected by this phenomenon. Therefore, injecting high currents could lead to excessive overheating of the conductor in the unaffected spans.

To verify the effectiveness of this logic, a thermal analysis was carried out. The aim of the following analysis is to determine whether the conductors in the unaffected spans remain within their operating limits, temperature-wise, for the entirety of the time that it's required for the sleeve to melt. Therefore, in addition to the thermal analysis, it is important to determine how long it takes for the sleeve to melt. This aspect will be further discussed later in this section. The study of thermal transients and the development of a simulation model for these transients were derived from the analysis of technical brochures by CIGRE [1][5]:

- CIGRE brochure 207.
- CIGRE brochure 601.

Both brochures provide the closed-form solution of the thermal balance equation for the conductor during the transient:

$$mc \frac{dT_{av}}{dt} = P_J(T_{av}) + P_S - P_C(T_{av}) - P_r(T_{av}) \quad (1)$$

Where:

- $P_J$ : Power absorbed due to Joule effect, [W/m];
- $P_M$ : Power absorbed associated with hysteresis and eddy current losses, [W/m];
- $P_S$ : Power absorbed due to radiation, [W/m];
- $P_r$ : Power emitted through radiation, [W/m];
- $P_C$ : Power emitted through convection, [W/m];
- $T_{av}$ : Average temperature of the conductor, [K];
- $m$ : Mass per unit length of the conductor, [kg/m];
- $c$ : Specific heat of the conductor [J/kgK].



Oral Presentation: A Compact 24-Pulses Converter for Overhead Lines De-Icing and Reactive Power Compensation

The CIGRE 207 brochure introduces the thermal time constant of the conductor, which is defined, in the case of heating, as “the time interval required for the conductor to reach 63.2% of its asymptotic temperature.” This constant is expressed as follows:

$$\tau_h = \frac{mc\theta_m}{I^2R_{ac} + P_S} \quad (2)$$

In the specific case of aluminum conductors with a steel core, the thermal time constant becomes:

$$\tau_h = \frac{(m_a c_a + m_s c_s)\theta_m}{I^2 R_{ac} + P_S} + \frac{m_s c_s \ln\left(\frac{D}{D_2}\right)}{2\pi\lambda_a} \quad (3)$$

Where:

- $\theta_m$ : Difference between the conductor’s asymptotic temperature and ambient temperature, [°C];
- $D$ : Conductor diameter, [m];
- $D_2$ : Steel core diameter, [m];
- $\lambda_a$ : Radial thermal conductivity of aluminum, [W/mK];
- $m_a$ : Mass per unit length of the aluminum section of the conductor, [kg/m];
- $m_s$ : Mass per unit length of the steel section of the conductor, [kg/m];
- $c_a$ : Specific heat of aluminum at ambient temperature, [J/kgK];
- $c_s$ : Specific heat of steel at ambient temperature, [J/kgK];
- $R_{ac}$ : AC resistance of the conductor calculated at ambient temperature, [ $\Omega$ /m].

For completeness, Figure 5 in the brochure illustrates an example of a generic conductor’s heating following an instantaneous current increase.

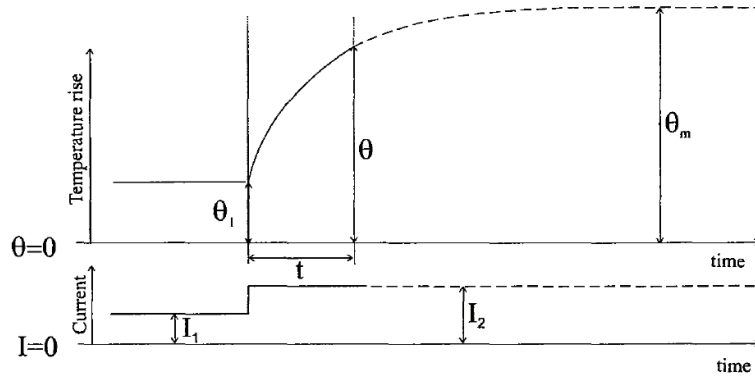


Figure 5. Generic conductor’s heating.

The CIGRE 601 brochure, similarly to the CIGRE 207 brochure, introduces a thermal time constant. The thermal time constant is then expressed as:

$$\tau_h = \frac{mc\theta_m}{P_T} \quad (4)$$

In the specific case of aluminum conductors with a steel core, the thermal time constant becomes:

$$\tau_h = \frac{(m_a c_a + m_s c_s)(\theta_m - \theta_1)}{P_T} + \frac{m_s c_s \ln\left(\frac{D}{D_2}\right)}{2\pi\lambda_a} \quad (5)$$

$$P_T \approx \Delta(P_J + P_M) \quad (6)$$



The introduction of a thermal time constant is equivalent to approximating the temperature behavior of the conductor over time with an exponential function. However, with the availability of software that allows for the rapid solution of differential equations, the introduction of an approximation and the resulting errors are no longer advantageous.

The use of numerical methods allows for obtaining the temperature profile of the conductor during the transient that occurs following an increase in current without resorting to any approximation. Two different approaches have been used:

1. Numerical methods known as Runge-Kutta methods, which are a set of iterative methods used for solving differential equations. Specifically, the implementation of Verner's seventh-order method has been considered.
2. Trapezoidal integration: starting from the discretized equation of the thermal balance, as given below, and with a specified temperature increment  $\Delta\theta$ , the time interval in which this increment is observed is calculated.

$$\Delta t_i = \frac{mc(\theta_i)\Delta\theta}{P_j(\theta_i) + P_s - P_c(\theta_i) - P_r(\theta_i)} \quad (7)$$

The simulation results show the temperature profile of the conductor unaffected by sleeve considering the logic described earlier. Considering a conductor with a diameter of 22.8 mm, a 25 km long overhead line and a DC-side current of 1070 A, the obtained temperature rise remains within the operating limits of the conductor (Figure 6). It is possible to increase the current up to 1200 A, however it results in conductor overheating up to 100°C (Figure 7).

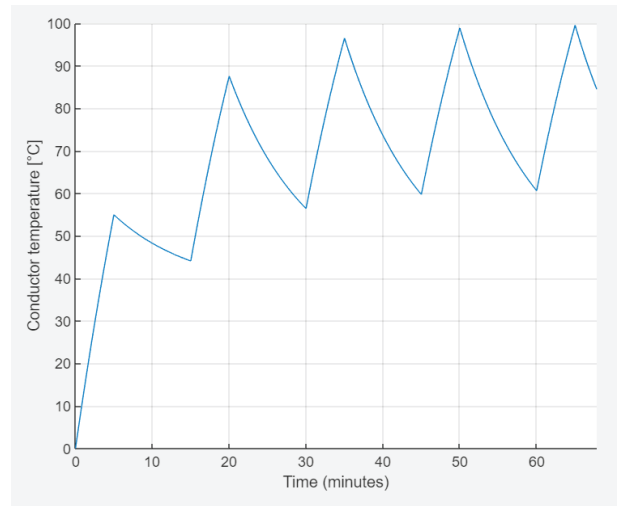
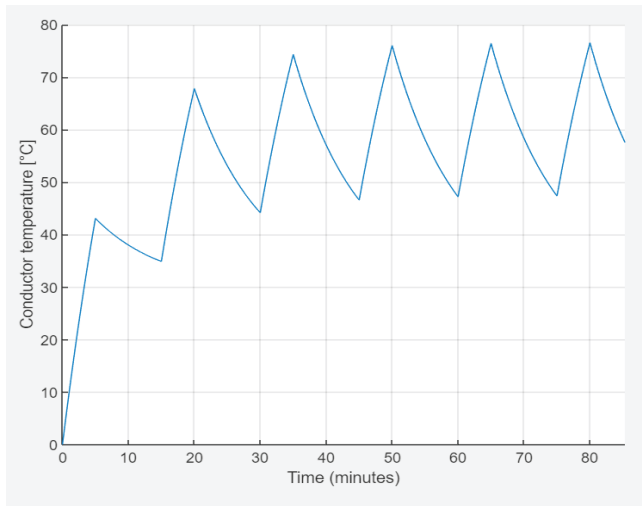


Figure 6. Conductor's thermal transient with a DC-side current of 1070 A. Figure 7. Conductor's thermal transient with a DC-side current of 1200 A.

The reasoning behind increasing the current up to 1200 A is that the time needed to melt the sleeve significantly decreases, going from 80 minutes to around 60.

The time required for the melting of the sleeve was calculated as follows [6]:

$$\Delta t = \frac{\rho_{ice} \cdot [L_f + c_{p_{ice}}(T_f - T_a)] \cdot V_{ice}}{P_j + P_s - P_c - P_r} \quad (8)$$

being

- $\rho_{ice}$  : Ice density, [kg/m<sup>3</sup>];
- $L_f$  : Ice latent heat of fusion, [J/kg];
- $c_{p_{ice}}$  : Specific heat of ice, [J/kg°C];
- $T_f$  : Ice melting point, [°C];
- $T_a$  : Ambient temperature, [°C];
- $V_{ice}$  : Ice sleeve volume, [m<sup>3</sup>].



The current that was used to determine  $P_j$  is the mean value, over 15 minutes, of the current that is injected in each phase. In our specific case where each phase is injected with the full DC-side current for 5 minutes and with its half for the following 10, each 15 minutes, said current is then equal to  $2/3$  of the DC-side current.

## 4. STATIC VAR COMPENSATOR PERFORMANCES

*Static Var Compensators (SVCs)* are devices that can vary their absorption of reactive power within a specific range of values. They are referred to as static because the lack of rotating parts, contrary to synchronous compensator.

The devices that are considered as SVCs are:

- Saturated Reactors (SRs);
- Thyristor-Controlled-Reactors (TCRs);
- Thyristor-Switched-Reactors (TSRs);
- Thyristor-Switched-Capacitors (TSCs);
- Mechanical-Switched-Capacitors (MSCs).

The system analysed in this paper falls under TCRs. This type of systems allows a continuous reactive power regulation that can be achieved by simply changing the value of the firing angle of the thyristor valves.

All SVCs can be used not only for voltage regulation and for reactive power balance, but also to control voltage's amplitude and phase angle and therefore manage the negative sequence voltage with a consequent improvement of the system symmetry. Therefore, the possibility to use the converter presented in this paper as SVC, in addition to its role as HVDC current source for de-icing, was considered and an analysis of its performances has been carried out using the software ATP-ETMP.

This system is able to deliver up to about 20 Mvar when operating as SVC as shown in Figure 8. The regulation of the absorbed reactive power, as said before, was achieved by changing the value of the firing angle in the model of the 24-pulse converter.

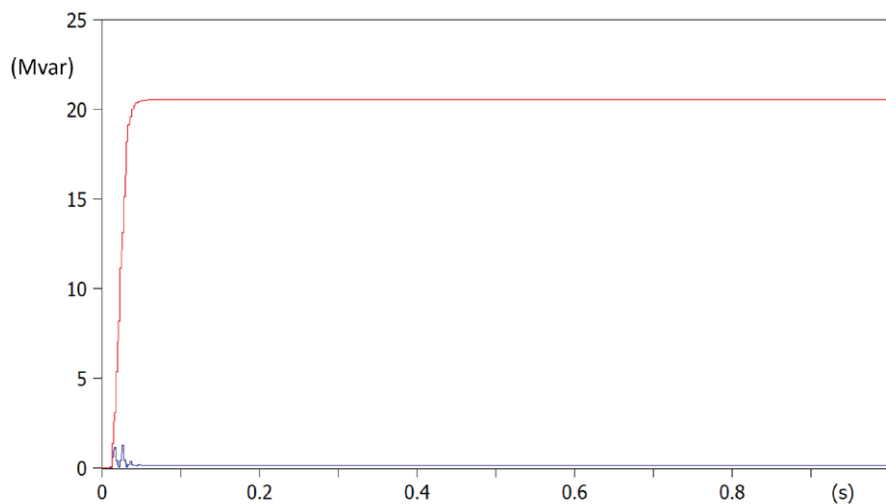


Figure 8. Reactive (red) and active (blue) power.

## 5. FOOTPRINT AND INSTALLATION LAYOUT

The installation of the deicing system has been planned inside a 40-foot container (Figure 9), allowing for easy transportation and placement within the electrical substations. Consequently, the footprint on the ground will be greatly reduced.

Being a containerized solution, it will be easy to transport the de-icing system across different substations according to the meteorological forecast, however, it is necessary to consider the presence of an HV/MV transformer that will need to be connected to the high-voltage busbars and power the deicing system in each of the designated substations.



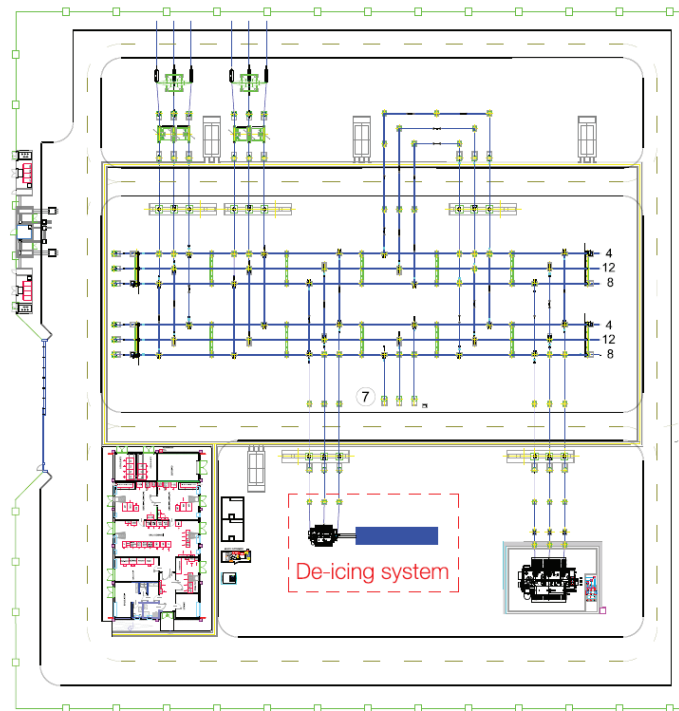


Figure 9. Layout of the substation in presence of the de-icing system.

## 6. CONCLUSIONS

The proposed system can be an efficient solution to prevent damages, reduce service disruptions and the associated costs. The coupling with a 24-pulse converter reduces significantly the harmonics fed into the grid and therefore allow to meet the standards imposed by the constraints on the THD. A model of this system has been implemented in software ATP-EMTP and shows how the THD is below 1%.

The permutation of the phases between the two DC poles is achieved using disconnectors. Those same disconnectors solve another important issue. Indeed, injecting current in a line where not all spans are necessarily affected by ice sleeves could potentially lead to the excessive overheating of the conductors in the unaffected spans. A specific choice of the opening/closing times of the disconnectors allow the melting of the ice sleeve without an excessive overheating of the conductors. A thermal analysis has been carried out, evidencing the effectiveness of the disconnectors.

The use of a 24-pulse converter allows the de-icing system to operate also as a SVC. The software ATP-EMTP has been used to investigate the performances of the system during this operating condition: results show that up to 20 Mvar can be delivered under this configuration. Finally, considerations on the system footprint and layout have been made, highlighting the convenience of this de-icing system. Indeed, the system presented in this paper is significantly more compact compared to other existing de-icing systems and, being containerized, can be transported and easily positioned in the designated stations.

## BIBLIOGRAPHY

- [1]. Zhang, Z., Zhang, H., Yue, S., and Zeng, W., "A Review of Icing and Anti-Icing Technology for Transmission Lines", *Energies*, 16(2), 601 (2023).
- [2]. Horwill, C., Davidson, C. C., Granger, M., and Dery, A. "An application of HVDC to the de-icing of transmission lines", in *2005/2006 IEEE/PES Transmission and Distribution Conference and Exhibition*, pp. 529-534, May 2006.
- [3]. IEEE 519-2022, "Standard for Harmonic Control in Electric Power Systems", 08/05/2022.
- [4]. Working Group SC 22-12 CIGRE. "Thermal behaviour of overhead conductors" (TB 207 August 2002).
- [5]. Working Group B2-43 CIGRE. "Guide for thermal rating calculations of overhead lines" (TB 601 December 2014).
- [6]. M. Huneault, C. Langheit and J. Caron, "Combined models for glaze ice accretion and de-icing of current-carrying electrical conductors," in *IEEE Transactions on Power Delivery*, vol. 20, no. 2, pp. 1611-1616, April 2005, doi: 10.1109/TPWRD.2004.838466.
- [7]. Working Group SC B2.29 CIGRE. "Systems for Prediction and Monitoring of Ice Shedding, Anti-Icing and De-Icing for Overhead Power Line Conductors and Ground Wires" (TB 438 August 2002).
- [8]. SC B2 CIGRE. "Techniques for Protecting Overhead Lines in Winter Conditions". (Green Books 2022).



# A Modular Design for OHL Grounding Systems Based on Deep Electrodes

francesco.palone@terna.it

MARIA ROSARIA GUARNIERE, ROBERTO SPEZIE, FRANCESCO PALONE, LUCA BUONO,  
LORENZO PAPI, GABRIELE TRESSO, PIERLUIGI VACANTE

Terna

Italy

## SUMMARY

Due to the decarbonization process, in terms of short circuit power, the network strength is significantly decreasing, consequently to the replacement of conventional (synchronous) generation with inverter-based renewable energy sources, according to both National Energy Strategy (SEN) [1] and the “Comprehensive National Energy and Climate Plan” (PNIEC in Italian), these issues are expected to be exacerbated due to the complete phase out of coal-fired power plants in 2025 [2]. With a lower short circuit power, single phase to ground faults caused by Back Flashover (BFO) cause higher voltage dips, involving a larger network area and causing higher economic losses to more and more users. This trend has been already evidenced in the Italian Transmission Network, prompting the need for countermeasures and remedial solutions [3],[4],[5],[6].

Several parameters influence the Back Flash Over Rate (BFOR) of an Overhead line (OHL): site characteristics (ground flash density, soil resistivity), geometrical characteristics of the overhead lines (towers height, number of shielding wires, shielding angle, clearance distance etc.) and grounding system performances [7],[8],[9]. Unfortunately, the global warming process and the expected frequent and severe droughts will increase the average annual soil resistivity [10]; at the same time, the tropicalization of the European (Mediterranean) climate will increase the ground flash density per km<sup>2</sup> [11]. All these circumstances will lead to an increase in the number of faults and in the voltage dips severity.

Terna developed a new grounding system arrangement, for increasing the performances of OHLs in terms of BFOR; due to environmental and authorization constraints, the new design does not include long counterpoises, which are not feasible in the Italian context (authorization and land use constraints)[12],[13]; instead recourse was made to grounding rings and, most significantly, deep electrodes, which allows for excellent performances both in terms of safety (touch and step voltages) and at high frequency behaviour (i.e. for lightning current).

To evaluate the performances of the proposed grounding systems, a detailed EMT study using PEEC method has been developed; results have also been validated against a more traditional circuital approach, evidencing the excellent performances of the proposed grounding arrangement: the proposed solution can reduce by up to 50% the expected BFR and attain a significant reduction of the life-cycle cost, if compared to the previous conventional design.

The paper deals with the new standard design for Terna’s OHL grounding system and with the attendant procedure for selecting the most efficient grounding system topology. The design of the new deep electrodes grounding system is reported in Section II; power quality target values and voltage dip costs for users are reported in section III. Section IV deals with the new procedure for selecting the optimal topology for each tower; conclusions are eventually reported in section V.

## KEYWORDS

OHL, grounding system, step voltage, voltage dip,



### 1. INTRODUCTION

Climate change is expected to bring about various consequences, including an increase in lightning strikes (keraunic level) and prolonged drought periods. Simultaneously, the integration of renewable energy sources into the power grid amplifies the impact of ground faults caused by back-flashover, leading to power quality issues like voltage dips.

In response to these challenges, Terna, the Italian Transmission System Operator, has devised an inventive grounding system design for high-voltage (HV) and extra-high-voltage (EHV) overhead lines. This ground-breaking design aims to enhance performance while minimizing environmental harm. Terna has also developed a unique methodology for selecting the most suitable design for each tower, considering factors such as construction expenses, voltage dip costs, site conditions (such as keraunic level and soil resistivity), and pylon characteristics (e.g., height, number of shield wires). By taking these aspects into account, Terna seeks to identify the most cost-effective configuration for each tower, ensuring optimal outcomes.

The new modular grounding system design offers significant benefits, including reduced failure rates and minimized land usage. This article introduces Terna’s standardized design for grounding systems in overhead lines and elaborates on the development of the optimization procedure to determine the most financially efficient topology for each tower.

### 2. DESIGN OF THE NEW DEEP ELECTRODES GROUNDING SYSTEM

In 1990, ENEL (the former vertically integrated Italian system operator) developed a standard grounding system design known as LF91 [14]. This design consisted of six different topologies (Table 1), incorporating up to six counterpoises of varying lengths, with a maximum length of approximately 30 meters. The selection of the grounding system was based solely on soil resistivity, regardless of the rated voltage of the overhead power lines, tower height, or keraunic level. The 50-Hz resistance for each topology could be determined using the formula:

$$R = K_g \cdot \rho_E \tag{1}$$

Where R is the resistance,  $K_g$  is a geometry coefficient specific to the grounding system topology,  $\rho_E$  is the soil resistivity, and L is the length of the counterpoise. This straightforward method was also adopted by Terna, the company that took over ENEL’s assets in 2003.

Table 1. Tower grounding system according to the old ENEL/TERNA LF91 standard.

Soil resistivity [Ωm]	Grounding system topology	
	Topology	$K^{(a)}$ [m <sup>-1</sup> ]
$\rho_E \leq 50$	MT1	0.0385
$50 < \rho_E \leq 150$	MT2	0.0369
$150 < \rho_E \leq 300$	MT3	0.0304
$300 < \rho_E \leq 600$	MT4	0.0251
$600 < \rho_E \leq 1300$	MT5	0.0183
$1300 < \rho_E \leq 2000$	MT6	0.0152

<sup>a</sup> K represents the grounding system resistance at power frequency for a soil resistivity of site equal to 1 Ωm.

In the 1990s, ENEL’s grounding system design (LF91) was developed based on power system scenarios characterized by strong centralized power generation from large thermoelectric or nuclear power stations, with limited distributed renewable energy sources. The impact of overhead line (OHL) faults on such scenarios was less significant compared to the future decarbonized electric system, which would rely more on renewable energy sources. Consequently, the LF91 design, which is now 30 years old, is no longer suitable for new OHLs or for refurbishing older aging towers.



Oral Presentation: A Modular Design for OHL Grounding Systems Based on Deep Electrodes

Moreover, the future regulatory framework for power quality is expected to increase the operating costs for Transmission System Operators (TSOs) due to voltage dips. These voltage dips can cause losses for industrial users, necessitating compensation measures.

Considering these challenges, Terna, the successor of ENEL, has taken the following steps:

- Developed a new standard modular design for OHL grounding systems that are more resilient to climate change effects and environmentally friendly.
- Developed a new methodology for selecting the optimal grounding system topology, taking into account environmental factors such as ground flash density and soil resistivity, as well as geometrical characteristics of the overhead lines (tower heights, conductor coordinates and diameters, number of shielding wires). The aim is to reduce the cost for users caused by voltage dips resulting from OHL back-flashover events.

The document mentions two examples of the new modular design, which can be seen in Figure 1 and Figure 2.

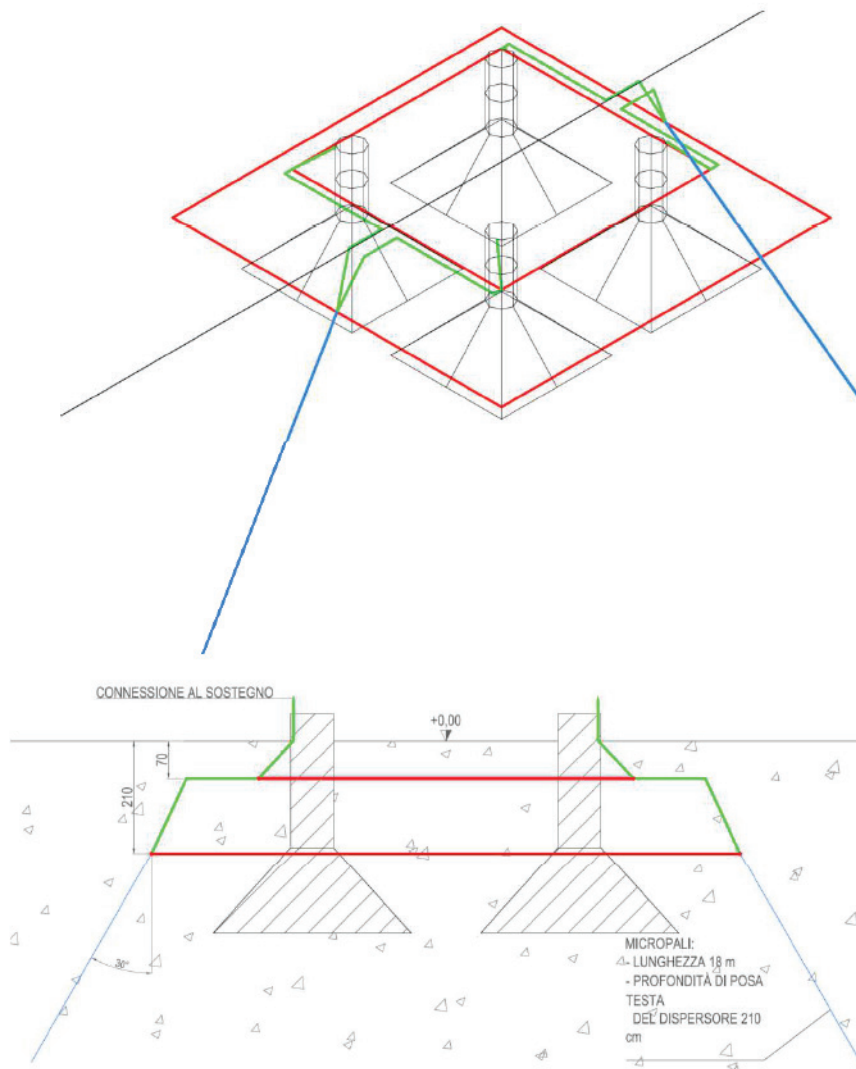


Figure 1. New Terna modular design DDP2, for average OHL lighting performances

The modular design of Terna's new grounding system incorporates both superficial and deep electrodes, offering seven different topologies with increasing lightning performance (DDP0 to DDP6). All topologies feature two rings to mitigate step and touch voltages. The first ring, installed at a depth of around 0.7 meters next to the pylon main legs, reduces touch voltages. The second ring, located around 3 meters from the tower at a depth of 2.1 meters, is designed to mitigate step voltages and protect against damage caused by ploughing. These rings, along with the connection leads to the pylon, are made of a zinc-coated steel bar measuring 40 x 4 mm, chosen to deter theft (copper theft being a major issue in Italy).

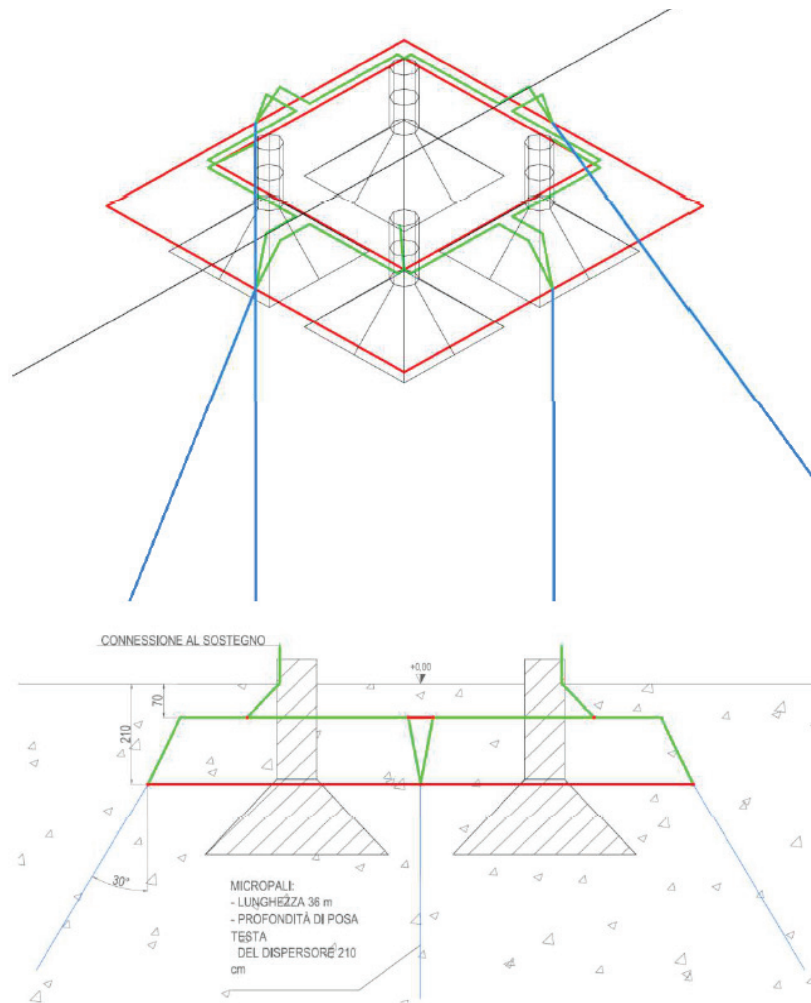


Figure 2 New Terna modular design DDP5, for average OHL lighting performances

As the required lightning performance increases, deep electrodes are incorporated into the design. Instead of using regular rods, Terna utilizes micropiles with a diameter of 10 cm and varying lengths from 18 to 36 meters. Micropiles offer several advantages, including easy and fast installation using dedicated equipment (including transportation via Terna’s helicopters when necessary) (see Figure 3). They can be installed in challenging soils, in any direction, with good accuracy, allowing for more efficient topologies without exceeding the OHL right-of-way. Micropiles reach deeper soil layers which are less affected by prolonged droughts.



Figure 3. Installation of micropiles for the new grounding systems in the alps.





An important advantage of Terna’s deep grounding systems (DGS) using micropiles is their more consistent performance compared to superficial grounding systems, which exhibit significant resistance variations throughout the seasons [16],[17]. Moreover, micropiles enable the use of high conductivity concrete, which is injected under high pressure into the micropiles, forming a conductive covering ( $\rho_c < 5 \Omega\text{m}$ ). This reduces the overall grounding resistance and protects the steel tube from corrosion.

The new solution requires significantly less land use compared to the previous LF91 standard design. Figure 4 provides an example for a typical 150 kV OHL in a high resistivity soil, comparing the old LF91 design (MT5 or MT6) with the new DDP 5 design. Despite a 90% reduction in land use, the performance of the new grounding systems is improved over the old design (see also table 2).

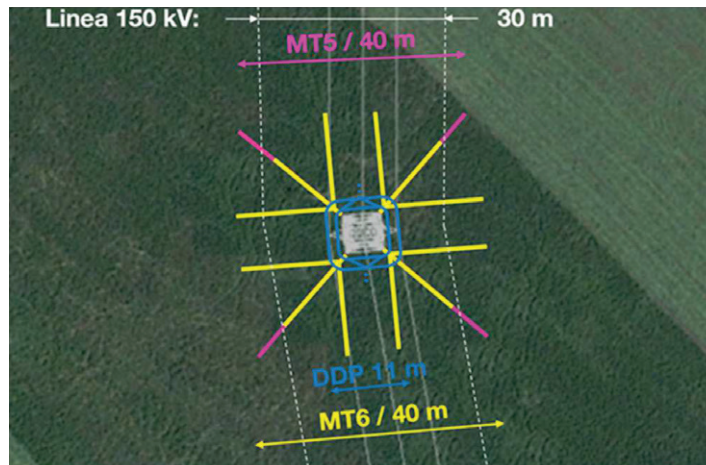


Figure 4. Land use comparison between typical previous (magenta and yellow lines) and the novel (blu line) design, for 150 kV Terna tower in a high resistivity soil.

Table 2. Comparison between old (LF91) and new design, for a 1300  $\Omega\text{m}$  soil resistivity.

Grounding system	Grounding resistance 50 Hz	Grounding impedance 100 kHz
MT5 (OLD)	23.8 $\Omega$	22.9 $\Omega$
MT6 (OLD)	19.8 $\Omega$	19.3 $\Omega$
DDP5 (NEW)	15.0 $\Omega$	13.9 $\Omega$
DDP6 (NEW)	12.6 $\Omega$	11.4 $\Omega$

The new design also enhances safety by incorporating superficial rings, which improve step and touch voltages compared to the old design based solely on counterpoises. The installation of a superficial layer with high resistivity above the pylon foundation (shown in Figure 5) ensures compliance with the stringent requirements for touch voltages ( $U_t < 204 \text{ V}$  for a 0.5 s fault duration) specified in EN 50341-1 [18] when necessary.

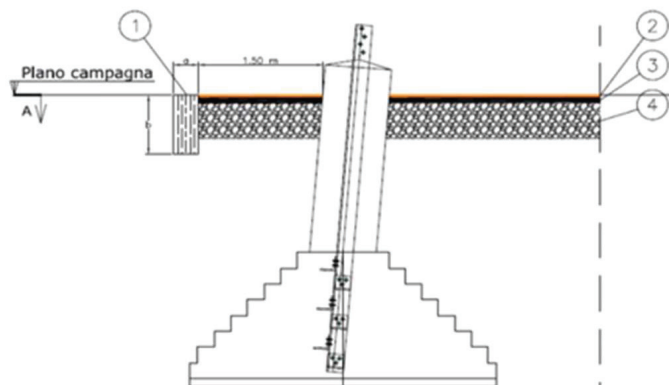


Figure 5 High resistivity layer, for further mitigation of touch and step voltages (to be installed if the pylon is located nearby urbanized areas); (1): wood or concrete curb, for mechanical protection; (2) 2 cm external coating for chromatic camouflage; (3) 5 cm asphalt layer; (4) 30 cm crushed rock layer.





## 3. POWER QUALITY IN POWER TRANSMISSION SYSTEMS

### A. Economic consequences of voltage dips

Power quality is a key concern for both Transmission System Operators (TSOs) and Distributor System Operators (DSOs) [19], particularly due to the increasing sensitivity of end-user equipment [20]. The proliferation of electronic devices used by industrial and residential users has amplified the economic impact of power quality issues. The primary parameters of voltage quality include frequency, voltage magnitude, voltage variations, voltage dips, transient overvoltages, and harmonic distortion [21].

In the past decade, the University of Milan conducted research on behalf of the Italian regulatory authority (ARERA) to assess the economic damages caused by voltage dips for industrial users, which were found to average €2.5 per kilowatt (kW) [22]. Recently, ARERA initiated a test project involving users connected to EHV/HV grids in collaboration with Terna [15]. Power monitoring systems will be installed at EHV/HV user substations to verify target voltage dip values. The compensation provided to users will be calculated as follows:

$$I = K \cdot \sum_{i=1}^n (C_p \cdot P_{Li}) \quad (2)$$

with:

- K: multiplication factor depending on the number of measured voltage dips;
- PL: loads influenced by voltage dips, [kW];
- C<sub>p</sub>: penalty costs, [€/kW].

### B. Expected load influenced by single phase to ground fault

Terna conducted a sensitivity analysis to estimate the impact of a single phase-to-ground fault on the total and industrial load, based on the following assumptions:

- A typical network scenario was considered.
- A 90% residual voltage threshold was used.
- Industrial loads were assumed to account for 40% of the total load [23].
- Line-to-ground faults were simulated at a distance of 10 km from the 132, 150, and 230 kV substations, and 15 km from the 400 kV substations (approximately one-fourth of the average length of overhead lines).

For each high-voltage (HV) and extra-high-voltage (EHV) overhead line (OHL) in the Italian transmission and sub-transmission system (132, 150, 230, and 400 kV), a single phase-to-ground fault was simulated to determine the total load affected by a voltage dip exceeding 10%. The simulation results indicate the following average industrial load levels experiencing a voltage dip with a residual voltage below 90% due to a back-flashover:

- 850 MW for faults on 400 kV OHLs;
- 300 MW for faults on 230 kV OHLs;
- 100 MW for faults on 150 kV OHLs;
- 75 MW for faults on 132 kV OHLs.

## 4. TECHNICAL AND ECONOMIC EVALUATION OF THE OPTIMAL GROUNDING TOPOLOGY

To optimize the allocation of economic resources, it is possible to select the grounding system topology for each tower in a way that minimizes both construction and operation costs. The operation costs are primarily associated with the losses resulting from voltage dips over the lifetime of the overhead line (OHL). The total cost (C) attributed to voltage dips caused by back-flashover (BFOR) on a single OHL tower can be evaluated using the following formula:



Oral Presentation: A Modular Design for OHL Grounding Systems Based on Deep Electrodes

$$C_{BFOR} = \frac{L_u \cdot P_L \cdot C_u}{N_T} \cdot BFOR = K_{TOT} \cdot BFOR \tag{2}$$

with:

- $L_u$ : useful life of OHL, [years], assumed to be 40 years;
- $P_L$ : average power influenced by a voltage dip higher than 10% of rated voltage [kW];
- $C_u$ : average economic damages of user for a single voltage dip, [€/kW];
- $N_T$ : number of towers per 100 km [pu/100 km].

According to the equation presented before, an optimization algorithm has been developed:

$$\min_{n=1 \rightarrow N_{TGS}} (C_{TGS}(n) + K_{TOT} \cdot BFOR(n)) \tag{2}$$

being  $C_{TGS}$  the expected costs of tower grounding system and  $N_{TGS}$  the number of tower grounding system topologies ( $N_{TGS}=7$  for the new grounding system design).

The simplified flowchart of the proposed algorithm for optimal choice is presented in Figure 6. The algorithm begins by evaluating the expected back-flashover (BFOR) using the IEEE Flash software. Parameters for the BFOR analysis are prepared using Matlab software, which generates an input file in ASCII format. The IEEE Flash software [24] is then invoked to calculate the expected total cost for each topology.

The algorithm proceeds by comparing the total costs obtained for each topology and selecting the topology that results in the minimum total cost. This optimal topology choice allows for better allocation of economic resources in terms of construction and operation costs associated with voltage dips caused by back-flashover events on the overhead line.

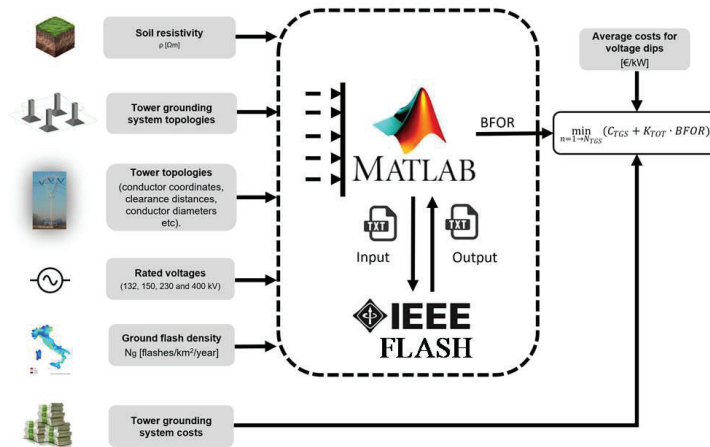


Figure 6. Simplified flow chart of the proposed optimal choice procedure

The described procedure is conducted for all voltage levels, considering different keraunic levels [25], soil resistivity, and tower heights. Terna’s standard design ensures that overhead lines with the same voltage levels share the same tower design. To facilitate the selection of the appropriate grounding system topology, the optimization results are presented in abacus form for each voltage level.

Figure 7 illustrates the abacus specifically designed for overhead lines with a rated voltage of 400 kV or higher. These abaci provide valuable information to Terna’s designers, enabling them to identify the most suitable grounding system topology based on the specific parameters and requirements of each voltage level.

In Figure 7, the upper part of the abacus provides information on the expected number of flashes to the line (NL) in flashes per 100 km per year. This information is obtained based on the tower height and ground flash density (Ng). The lower part of the abacus allows for the selection of the optimal grounding system topology based on NL and soil resistivity ( $\rho E$ ).



To utilize the abacus, the designer follows the design procedure indicated by the black arrows in Figure 7. For each OHL tower, the designer inputs the tower height and ground flash density into the abacus to determine the expected flashes affecting the line (NL). Using this value and the local soil resistivity, the designer can then select the most suitable grounding topology from the available options within the new modular design, ranging from the less performant (DDP0) to the most performant (DDP6) topologies.

This approach ensures that economic resources are allocated optimally, minimizing the impact of voltage dips on customers across all sub-transmission and transmission voltage levels. It allows for efficient decision-making in selecting the appropriate grounding system topology based on the specific conditions of each OHL tower.

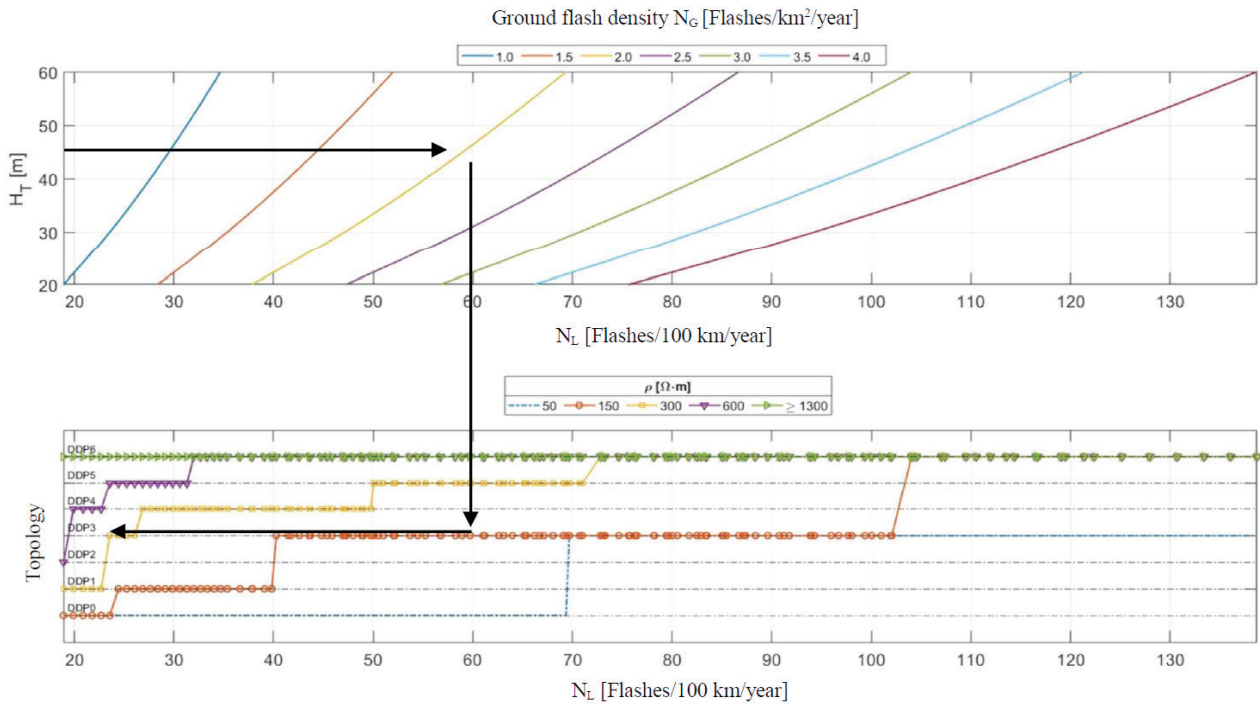


Figure 7. Abacus for grounding system topology selection for OHLs having a rated voltage  $U_r \geq 400kV$ .

## 5. CONCLUSION

The increasing integration of renewable energy sources and the phasing out of conventional power plants are leading to a decrease in system strength within the European grid. This trend, despite the efforts of transmission system operators (TSOs), is expected to result in significant voltage dips caused by single-phase to ground faults, particularly those related to back-flashovers. TSOs are facing a major challenge in addressing these voltage dip issues in the near future.

In response to these challenges, Terna has developed a new standard design for overhead line (OHL) grounding systems, incorporating both shallow and deep electrodes, the grounding system has now been patented by Terna. The use of superficial rings helps to reduce step and touch voltages, ensuring compliance with safety requirements outlined in the EN 50341-1 standard. Deep electrodes, implemented in the form of micropiles, are used to lower grounding resistance and minimize failure rates. The length of the micropiles varies between 18 to 36 meters, providing enhanced performance and resilience.

Furthermore, the new standard design significantly reduces land consumption by approximately 90% compared to the previous design. This reduction has a positive impact on the environmental and social aspects associated with the installation of pylons.

The selection of the optimal grounding system topology from the modular design is facilitated through the use of simple abaci. These abaci, developed through an optimization process, take into account site-specific factors such as flash density and soil resistivity, as well as line characteristics such as tower height and voltage level. The objective is to minimize overall costs, including construction costs and economic losses incurred by users due to voltage dips caused by back-flashovers.

Overall, the new standard design, which incorporates deep micropiles, offers increased resilience to the anticipated effects of climate change on soil resistivity. This is in contrast to the more common design approach that relies predominantly on superficial counterpoises.



## BIBLIOGRAPHY

- [1] "Italian Ministry of Economic Development," Italy's National Energy Strategy, 2017, [online] Available: [https://www.sviluppoeconomico.gov.it/images/stories/documenti/BROCHURE\\_ENG\\_SEN.PDF](https://www.sviluppoeconomico.gov.it/images/stories/documenti/BROCHURE_ENG_SEN.PDF).
- [2] "Comprehensive National Energy and Climate Plan" Italy's National Energy Strategy, [online] Available: [https://www.mise.gov.it/images/stories/documenti/PNIEC\\_finale\\_17012020.pdf](https://www.mise.gov.it/images/stories/documenti/PNIEC_finale_17012020.pdf).
- [3] F. Palone, F. M. Gatta, A. Geri, S. Lauria and M. Maccioni, "New Synchronous Condenser – Flywheel Systems for a Decarbonized Sardinian Power System," 2019 IEEE Milan PowerTech, Milan, Italy, 2019, pp. 1-6, doi: 10.1109/PTC.2019.8810780.
- [4] L. Michi, E.M. Carlini; L. Caciolli; D. Polinelli; P. Capurso; A. Proietti; A. Berizzi; C. Bovo, "The effects of new 2030 scenario: reduction of short-circuit power and widening of voltage dips," 2018 AEIT International Annual Conference, Bari, 2018, pp. 1-6, doi: 10.23919/AEIT.2018.8577274.
- [5] E. M. Carlini, S. Neri, A. Marietti, A. Borriello, L. Barison and L. Campisano, "Integration of synchronous compensator in Terna's remote control and remote operation system," 2019 AEIT International Annual Conference (AEIT), Florence, Italy, 2019, pp. 1-4, doi: 10.23919/AEIT.2019.8893418.
- [6] L. Caciolli, "The impact of renewable energy sources on Italian Power System" (in Italian language), AEIT Trento 2012 available at <http://www.aeit-taa.org/Documenti/AEIT-TAA-2012-12-21-Terna-Caciolli-Impatto-FER-su-Sist-Elet.pdf>.
- [7] CIGRE WG 33.01, "Technical Brochure TB 63 - Guide to procedures for estimating the lightning performance of transmission lines," CIGRE, 1991.
- [8] H. Linck, M.A. Sargent, "Lightning Performance of Modern Transmission Lines," in proc. CIGRE 1974 session, paper 33-09, Paris, August 21st – 29th 1974.
- [9] H. Zhang, Q. Wang, F. M. Faria da Silva, C. L. Bak, K. Yin and H. Skouboe, "Backflashover Performance Evaluation of the Partially Grounded Scheme of Overhead Lines with fully Composite Pylons," in IEEE Transactions on Power Delivery, doi: 10.1109/TPWRD.2021.3071926.
- [10] Cammalleri C., Naumann G., Mentaschi L., Formetta G., Forzieri G., Gosling S., Bisselink B., De Roo A., and Feyen L., "Global warming and drought impacts in the EU", JRC Technical report 2020, DOI 10.2760/597045 available online at <https://publications.jrc.ec.europa.eu/repository/handle/JRC118585>.
- [11] Rädler, A.T., Groenemeijer, P.H., Faust, E. et al. Frequency of severe thunderstorms across Europe expected to increase in the 21st century due to rising instability. *npj Clim Atmos Sci* 2, 30 (2019). <https://doi.org/10.1038/s41612-019-0083-7>.
- [12] F. M. Gatta, A. Geri, S. Lauria, M. Maccioni and F. Palone, "Tower Grounding Improvement Versus Line Surge Arresters: Comparison of Remedial Measures for High-BFOR Subtransmission Lines," in IEEE Transactions on Industry Applications, vol. 51, no. 6, pp. 4952-4960, Nov.-Dec. 2015, doi: 10.1109/TIA.2015.2448613.
- [13] F. M. Gatta, A. Geri, M. Maccioni, S. Lauria, F. Palone and G. Pelliccione, "Design approaches for EHV OHL 'compact' tower grounding systems," 2017 IEEE International Conference on Environment and Electrical Engineering and 2017 IEEE Industrial and Commercial Power Systems Europe (EEEIC / I&CPS Europe), Milan, 2017, pp. 1-6, doi: 10.1109/EEEIC.2017.7977754.
- [14] F.M. Gatta, A. Geri, S. Lauria, M. Maccioni and F. Palone "Lightning Performance Evaluation of Italian 150 kV Sub-Transmission Lines," *Energies* 2020, 13(9), 2142; <https://doi.org/10.3390/en13092142>.
- [15] ARERA 524/2020/R/eel, "Regolazione individuale delle microinterruzioni per i clienti finali in alta e altissima tensione," 2020 available at <https://www.arera.it/it/docs/20/524-20.htm>.
- [16] N. Bhardwaj, O. P. Rahi and M. G. Sharma, "Seasonal influence on the substation grounding grid performance and its optimal design to neutralize the influence," 2016 IEEE 1st International Conference on Power Electronics, Intelligent Control and Energy Systems (ICPEICES), 2016, pp. 1-5, doi: 10.1109/ICPEICES.2016.7853431.
- [17] Papadopoulos, T.A.; Ceylan, O.; Papagiannis, G.K. Two-layer earth structure parameter estimation and seasonal analysis. In Proceedings of the 53rd International Universities Power Engineering Conference (UPEC 2018), Glasgow, Scotland, UK, 4–7 September 2018.
- [18] EN 50341-1 "Overhead electrical lines exceeding AC 45 kV - Part 1: General requirements - Common specifications," CENELEC, 12/2012.
- [19] S. Küfeoglu, M. Lehtonen "Macroeconomic Assessment of Voltage Sags," *Sustainability* 2016, 8, 1304; doi:10.3390/su8121304.
- [20] Council of European Energy Regulators - Working Group on Quality of Electricity Supply. "Quality of electricity supply: initial benchmarking on actual levels, standards and regulatory strategies." April 2001. Available at: link.
- [21] CEI EN 50160. "Voltage characteristics of electricity supplied by public electricity networks."
- [22] M. Delfanti, E. Fumagalli, P. Garrone, L. Grilli, and L. Lo Schiavo. "Toward Voltage-Quality Regulation in Italy." In IEEE Transactions on Power Delivery, vol. 25, no. 2, pp. 1124-1132, April 2010. DOI: 10.1109/TPWRD.2009.2035918.
- [23] Terna S.p.A. "Dati Statistici sull'Energia Elettrica in Italia."
- [24] T. E. McDermott. "A New version of the IEEE Flash program." IEEE PES T&D 2010, New Orleans, LA, USA, 2010, pp. 1-4. DOI: 10.1109/TDC.2010.5484339.
- [25] M. Bernardi and R. Tommasini. "Number of lightning to earth in Italy." In 2012 International Conference on Lightning Protection (ICLP), Vienna, Austria, 2012, pp. 1-5. DOI: 10.1109/ICLP.2012.6344368.
- [26] R. Spezie, F. Palone, L. Buono TERN A S.p.a "Grounding System for Towers of Overhead Power Lines" International Publication Number WO 2022/208422A1



# Adriatic Corridor: A Step Towards Deployment of Italian Multiterminal HVDC Systems

[andrea.urbanelli@terna.it](mailto:andrea.urbanelli@terna.it)**ENRICO MARIA CARLINI, TEMISTOCLE BAFFA SCIROCCO, LUCA BELMONTE, DAVIDE DI PASQUALE, ANDREA URBANELLI\****Terna Rete Elettrica Nazionale***STEFANO MALGAROTTI, CORRADO MUSSI***CESI - Energy & Automation Competence Center***Italy**

## SUMMARY

The energy transition will be achieved mainly through the massive installation, in the near future, of new renewable source power plants. In Italy, they will be installed mainly in the South, consistent with the greater presence of the primary sources (wind, sun), while the large load centers are placed in the North. New HVDC corridors integrated into the existing HVAC Transmission network need to be planned to transport this energy over long distances in an efficient, controllable, reliable, and safe manner, becoming, in expectation, a true “hybrid” transmission system. In this paper a detailed focus on the forecasted Italian HVDC “Hypergrid” project is presented: this project involves new submarine HVDC links and retrofit of existing HVAC lines into HVDC corridors allowing to build an authentic “DC layer” over the transmission system.

An HVDC overlay in the national electricity system can be an effective and cost-competitive solution for a complete decarbonization, a better renewables and territory exploitation and a greater electrification of the Country. One of the key elements for forward-looking holistic planning are the synergies with existing and under-exploited assets such as, for example, the upgrading of existing power lines, with the conversion or reconstruction on the same route to allow the retrofit into DC, leading to an improvement in overall operating performance and overcoming the difficulties in building new power lines due to legal, regulatory, environmental and local constraints. Moreover, the choice of VSC technology coupled with the potential reuse of part of the spaces of existing or planned converter stations for installing essential components such as High Voltage DC Circuit Breakers (DCCBs) enables multiterminal operation (Hypergrid) with greater flexibility, active-reactive power decoupling, black start capability, lower short circuit power requirements, and a smaller converter station footprint compared to LCC. In fact, it is recognized in the technical literature that a transition from point-to-point HVDC links to multiterminal systems can save much investment costs, since the number of converter stations can be reduced.

In this framework, starting from the new innovative drivers envisaged within Terna’s National Development Plan, a case study related to the analysis of the new HVDC Adriatic Corridor is presented, with examples of failures that may occur in such network, with a special focus on the importance of DCCBs in the optimal operation of planned HVDC layer.

This type of analysis, carried out in EMT (PSCAD) environment, represent a first step in the planning of the future DC multiterminal grids that will be the key enablers for the Italian energy transition.

## KEYWORDS

HVDC Layer, VSC, Hybrid transmission system, Retrofit into DC, High Voltage DC Circuit Breakers (DCCBs), Decarbonization



### 1. FUTURE ENERGY FRAMEWORK

The energy transition requires close cooperation among key players in the energy sector to achieve the target of reducing climate-changing emissions and ensuring diversification of supply sources. The 2023 Terna’s National Development Plan (NDP 23) [1] aims to promote the future penetration of renewable generation by ensuring the quality and stability of the electric transmission grid. The main system benefits expected from the new electricity infrastructure planned in DP 23 are the increasing of transmission capacity between market areas, integration of RES plants, reduced CO2 emissions, and improvement of system robustness.

The scenarios developed by Terna-Snam [2] shown in Figure 1, which form the basis of the NDP 23, envisage a coherent vision of the possible future evolutions of the Italian energy system in the medium and long term, also due to the strategic choices of Italy and European countries.

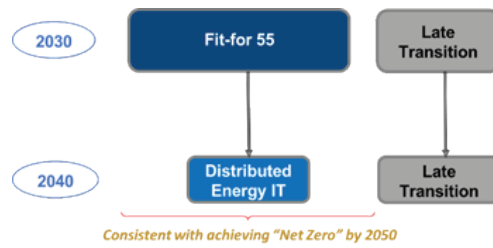


Figure 1. Future energy scenarios

These scenarios are consistent with the European Ten Year Network Development Plan 2022 (TYNDP 2022) developed by the electricity and gas grid operators’ associations ENTSO-E and ENTSOg. Terna has adopted the Fit for 55 (FF55) and Late Transition (LT 2030) scenarios for the 2030 horizon year: the former is consistent with the policy targets of the homonymous EU climate package, and the latter is in line with the National Trend (NT) Italy scenario published in February 2021 based on the December 2019 National Energy and Climate Plan targets.

The Distributed Energy Italy (DE-IT), aligned with the ENTSOs scenario and consistent with the Net Zero target to 2050, and the Late Transition scenario (LT 2040) were adopted for the 2040 time horizon.

The FF55 and DE-IT are the developed scenarios that allow reaching the relevant EU target goals, while the LT 2030 and LT 2040 are defined as “contrasting” scenarios of their respective policy scenarios to catch the uncertainties associated with planning over long time horizons, assuming much-delayed achieving of emission reduction targets due to no binding policy targets.

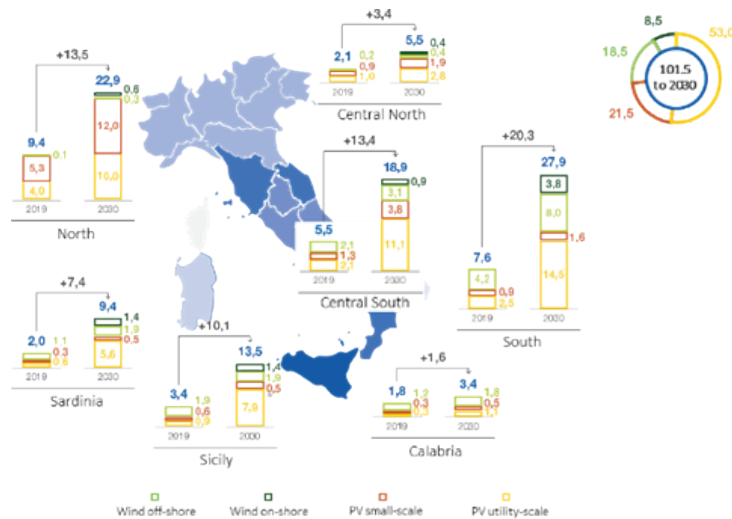


Figure 2. FF55 RES targets scenario

In FF55 scenario, the renewable capacity expected increases by 70 GW for installed wind and photovoltaic power compared to the current values, as shown in Figure 2. The total renewable generation (hydro, wind, PV, bioenergy, and geothermal) is 239 TWh by 2030, with a RES penetration of the total electricity demand of about 65 %. The FF55 scenario also forecasts a moderate increase in net import, from 38 TWh in 2019 to 52 TWh in 2030, mainly due to Terna’s planned investments to increase the transmission capacity





of cross-border interconnections and ensure greater RES integration at the European level. Natural gas-fired electricity generation (including from cogeneration plants) is reduced to about 46%, while coal-fired generation is totally absent. The integration of new RES will also be ensured by the development of about 95 GWh of new storage systems.

The definition of the energy scenarios is crucial for estimating the impacts of the infrastructure interventions envisaged in the NDP 23 and the main expected benefits at the system level. The scenarios are characterized by an important growth in renewable capacity, which has been distributed on the grid according to the connection requests received by Terna to ensure planning consistent with the geographical location of new RES plants. Grid development projects are essential to enable increasing electrification of consumption, as well as to ensure the integration of energy produced by RES and, thus, achieve decarbonization targets. The FF55 scenario for the analysis developed in the next paragraphs is considered.

### 2. ADRIATIC BACKBONE: HVDC FOGGIA-VILLANOVA-FANO-FORLÌ

With the aim of offering an additional route compared to the other HVDC links proposed in the NDP 23 and transporting energy flows from the southern to the northern regions in both directions, the Adriatic Backbone will reduce the congestion occurrence in regions characterized by high renewable generation such as Puglia and Basilicata. As shown in Figure 3, the entire HVDC link starts from the northern part of Puglia to settle in Emilia-Romagna, crossing Abruzzo and Marche. In particular, the planned project involves the development in 2 phases: a first phase consisting in the construction of an HVDC overhead line from Foggia to Villanova and the doubling of the undersea HVDC cable link (already planned HVDC Central-South/Central-North project) between Villanova and Fano, a second phase involving the construction of an HVDC OHL from Fano to Forlì. This project involves the synergy with others already planned projects in previous Development Plans exploiting the multi-terminal configuration by using Direct Current Circuit Breakers (DCCB) in the future planned VSC converter stations in Fano and Villanova. The project enables an NTC increase by 600 MW on the South-Central South section, by 1000 MW on the Central-South/Central-North section and by 2000 MW on the North/Northern-Centre section.

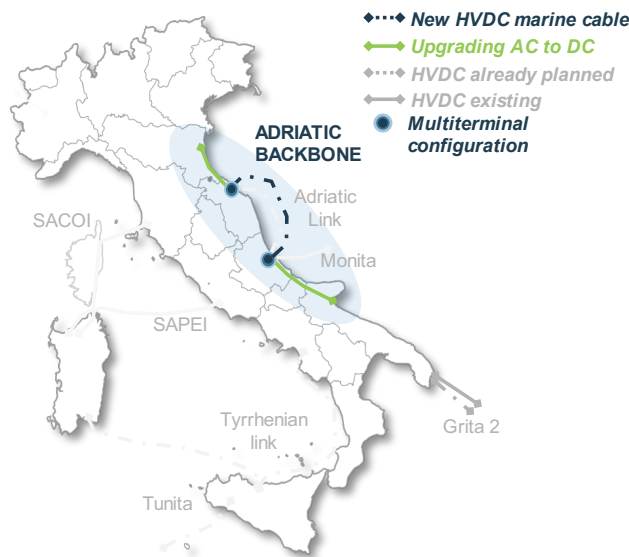


Figure 3. Adriatic backbone HVDC project

### 3. DESCRIPTION OF PSCAD MODEL USED FOR THE SIMULATIONS

PSCAD model [3] used for the study is strongly focused on a detailed representation of the HVDC portions of the Corridor, while a simple equivalent Thevenin representation is adopted for AC networks.

The HVDC-VSC converter stations are modelled through a “type 4” model as per CIGRE TB 604 prescriptions( [4]), i.e. through a so-called “Detailed Equivalent Circuit Model”. Both outer (d and q axis) and inner (capacitor voltage balancing algorithm and circulating current suppression control) control loops have been modelled; the parameters (gains, time constraints etc.) of such control loops are taken from CIGRE benchmark models for DC networks (CIGRE TB 804, [5]), while the main characteristics of the converter stations have been assumed as follows:



Table 1. Main characteristics of the converter stations implemented in the system

Case id.	Description
Nominal DC power	1000 MW (1000 A / ±500 kV)
Rated power of converter transformer	1250 MVA
Transformer ratio	400 / 275 kV
Transformer short-circuit impedance	0.18 pu
Valve arm reactor	50 mH
Smoothing reactor	25 mH
DC control mode:	
- Forli 1 station	DC voltage
- all other stations	DC power
AC control mode	Q control
AC filter	None

So as to get realistic voltage waveshapes, surge arresters have been connected to the DC busbars of each converter station, as per standard HVDC practice ([6]).

HVDC breakers have been assumed to be of the so called “hybrid type”, in accordance with the conceptual scheme here below.

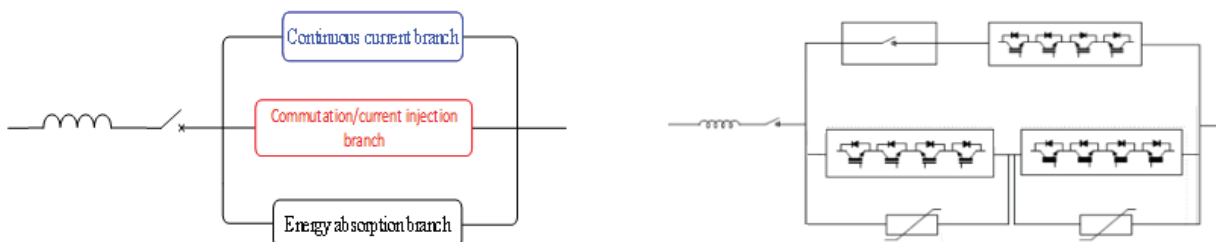


Figure 4. Hybrid HVDC circuit breaker: conceptual scheme

PSCAD representation of such breakers is reported here below, together with main parameters.

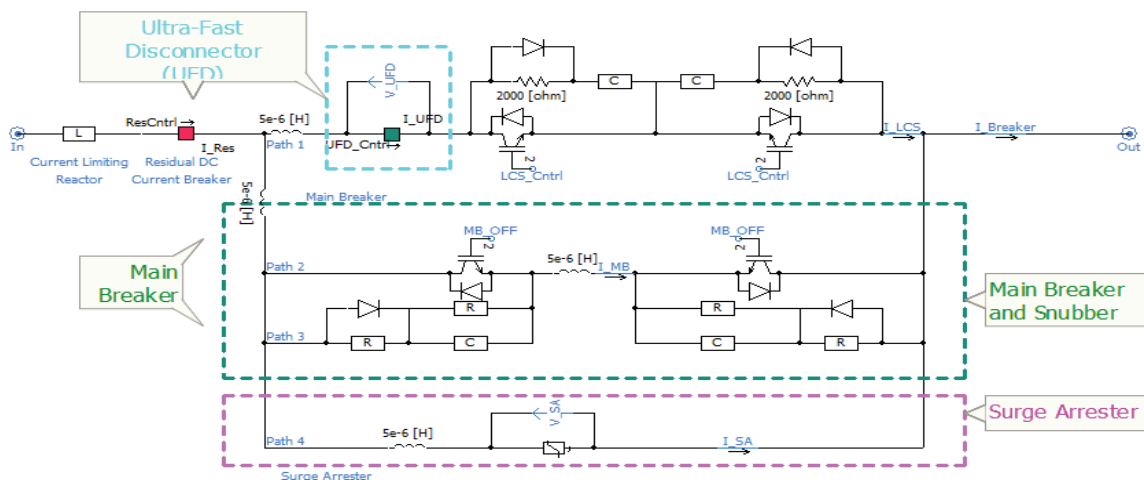
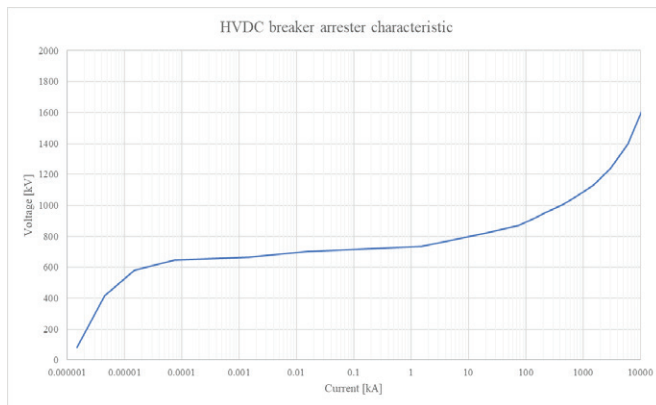


Figure 5. PSCAD model of hybrid circuit breaker



Parameter	Value
Current limiting reactor	100 mH
Overcurrent for CB intervention	10 kA
Commutation time	3 ms
Reclosing time	300 ms

Figure 6. PSCAD model of hybrid circuit breaker: main parameters

For what concerns selected HVDC breaker parameters it is underlined that ([7], [8], [9]):

- Surge arrester characteristics are practically identical to the ones of Zhangbei project HVDC breakers (see Table 6-11 of [7] - 800 kV TIV @ 25 kA)
- Commutation and reclosing time are the same specified for Zhangbei project HVDC breakers (see Table 6-11 of [7])
- For what concerns current limiting reactor, a rather low value has been assumed so as to stress current interruption capability of the breakers (for reference, in Zhangbei project values of 150 – 300 mH are adopted [7]).

All values above are tentative values: fine tuning of such parameters should be performed in a further development stage of the project, accounting also for equipment insulation and other requirements.

The overhead lines and submarine cables are modelled through a frequency dependent model based on the expected geometry of the conductors; sea electrodes are represented as lumped resistances.

AC network to which HVDC converter stations are connected have been represented as Thevenin equivalents with X/R ratio equal to 10 so as to provide short-circuit power as resulting from Terna planning studies.

### 4. PROTECTION STRATEGY

#### Without HVDC breakers

In case HVDC breakers are not installed, it has been assumed the protection strategy summarized here below<sup>1</sup>:

1. after a fault, when the valve current goes above the overcurrent protection (2.5 ÷ 3 pu approximately), the converter pole is blocked and a tripping signal is sent to the correspondent AC breaker;
2. 40 ms after receiving tripping signal, AC breaker opens;
3. 100 ms after converter block, Neutral Bus Switch is opened to speed up the current decay ([10])
4. 500 ms after AC breakers close, poles are de-blocked, the link is re-energized and power ramps up.

#### With HVDC breakers

Fault isolation and clearing is ensured by HVDC circuit breakers intervention, on the basis of current threshold and timing as reported above. It is underlined that no selectivity logic (e.g. interlocking) is considered, nevertheless the speed of response of such equipment seems enough to properly isolate only the portion of the grid affected by the fault, without opening sound lines.

<sup>1</sup> It is underlined that “aggressive” timings and use of NBS has been considered ([10]) so as not to overestimate the positive impact of HVDC breakers when compared to this scenario



## 5. SIMULATION RESULTS

Several transient cases have been simulated so as to verify, at a high-level<sup>2</sup>, the performances of the Adriatic Corridor. The following kind of transient events have been simulated, in different portions of the Corridor to assess the performance of the proposed Interconnection with and without HVDC breakers: power reversal, AC faults, permanent DC faults and temporary DC faults.

As a reference, in the present section results relevant to the following cases are shown:

*Table 2. Simulated test cases*

Case id.	Description
C1	Permanent fault, half length of Adriatic Link cables (pole +)
C2	Temporary pole to ground fault on overhead line (Forli-Fano)
C3	Temporary pole to pole fault on overhead line (Forli-Fano)

For all graphs, the following legenda applies:

*Table 3. Legenda for converter stations in the system*

Legenda	Description
IDCP	DC current, positive pole (flowing from the converter station to the DC line)
PDC	DC power
EDCP	DC busbar voltage (positive pole to ground)
EDCN	DC busbar voltage (negative pole to ground)
FOR	Station "Forli 1"
FOR2	Station "Forli 2"
FAN	Station "Fano"
VIL	Station "Villanova"
FOG	Station "Foggia 1"
FOG2	Station "Foggia 2"

---

<sup>2</sup> i.e. with the purpose of investigating the overall performances of the Corridor under fault conditions but without the aim, for example, of:

- specifying insulation characteristics of the components
- optimize the HVDC circuit breakers parameters (current limiting reactor vs surge arrester vs current threshold for intervention)
- perform a fine tuning of control functions and control parameters



Case id C1 – Permanent fault, half length of Adriatic Link (pole +)

WITHOUT HVDC CIRCUIT BREAKERS

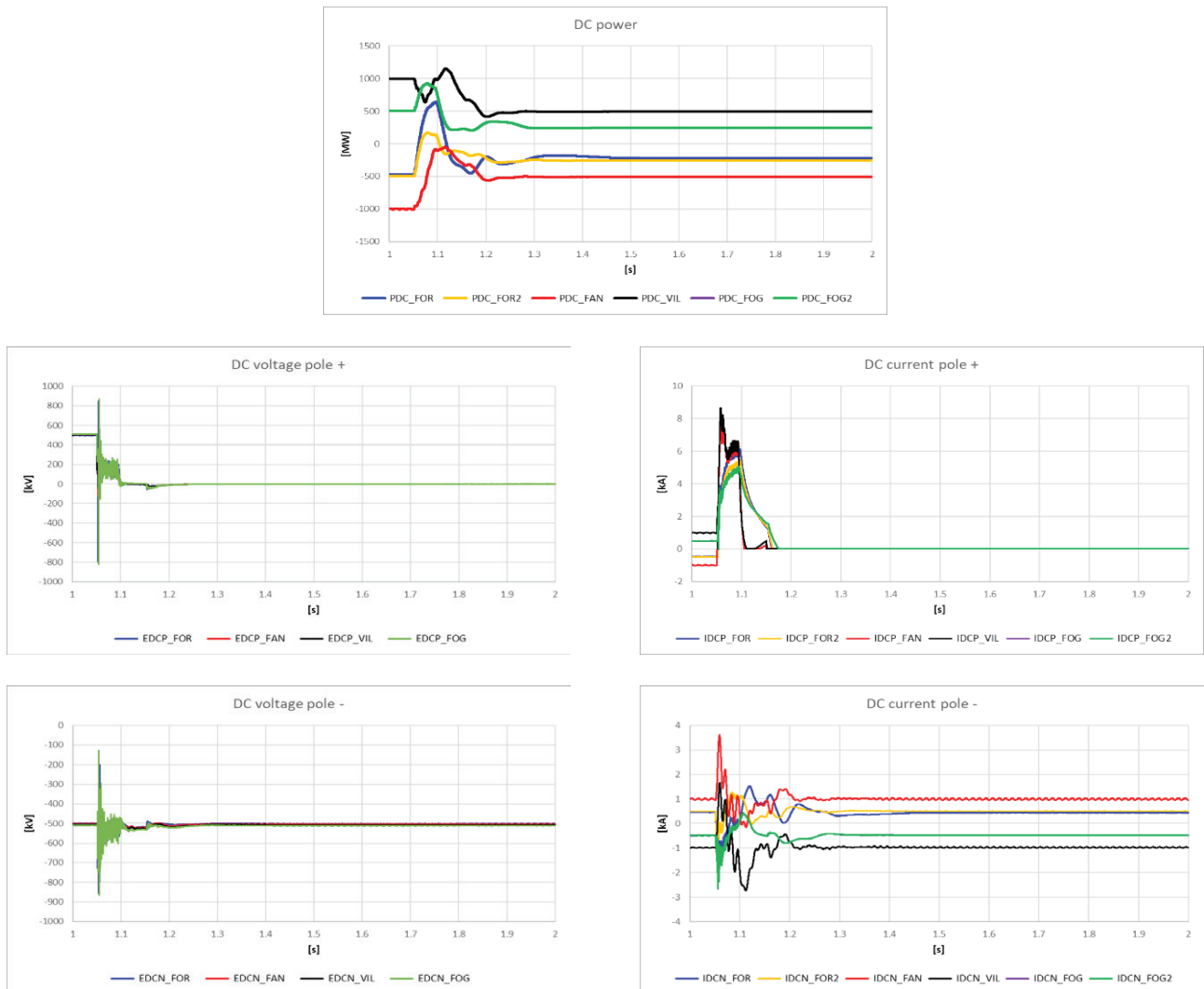


Figure 7. Case id.C1 without HVDC breakers. DC power (top), voltage (middle) and current (bottom)



WITH HVDC CIRCUIT BREAKERS

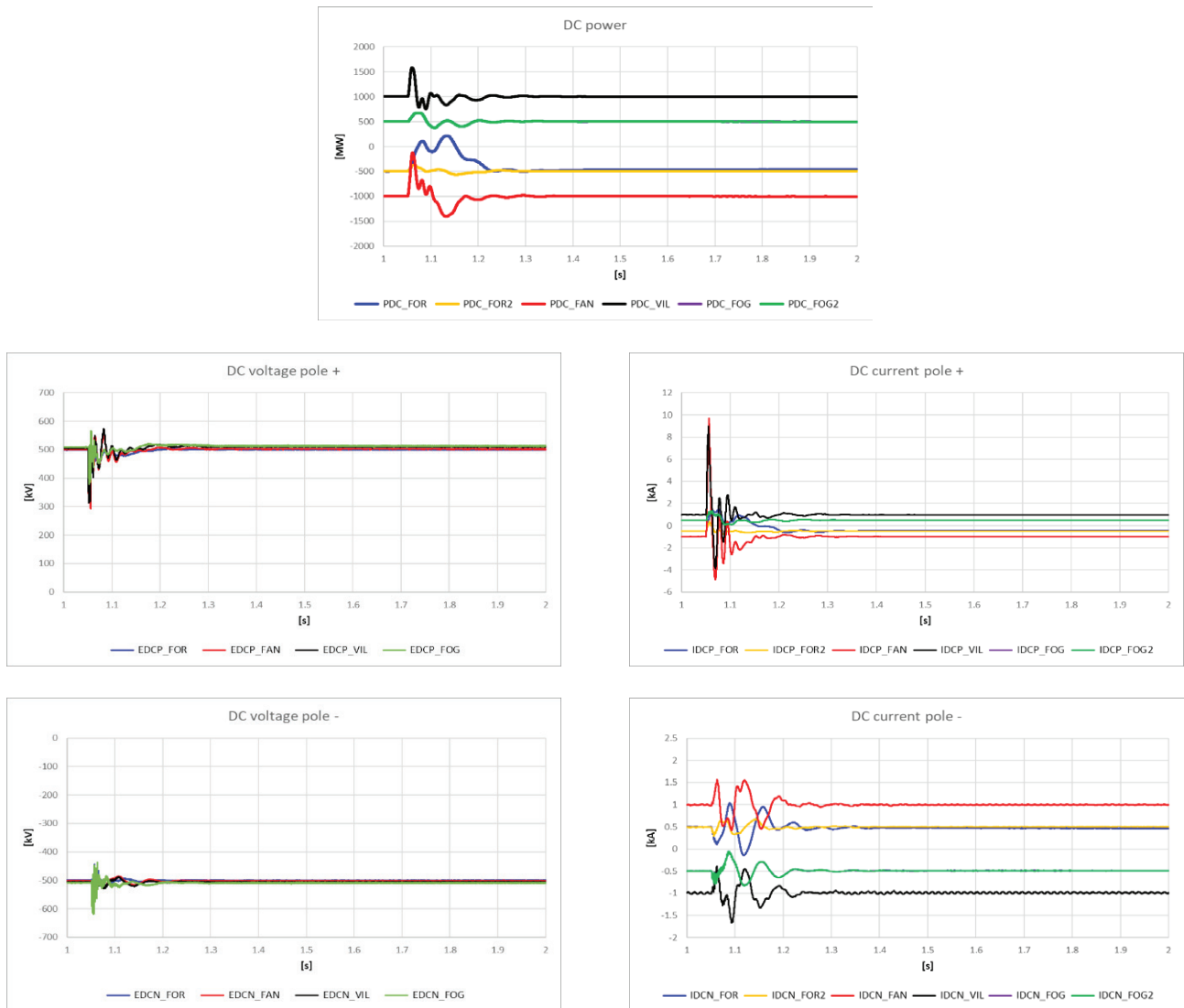


Figure 8. Case id.C1 with HVDC breakers. DC power (top), voltage (middle) and current (bottom)

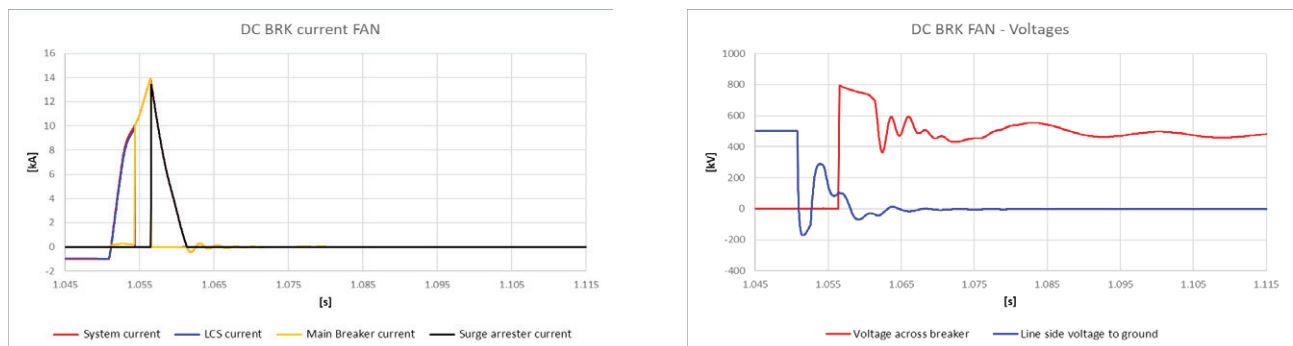


Figure 9. Case id.C1. Fano HVDC breaker. LEFT: Current in the various branches of the HVDC Circuit Breaker (Overall current: RED trace; load commutating switch: BLUE trace; main breaker: YELLOW trace; surge arrester: BLACK trace). RIGHT: Voltage across HVDC circuit breaker (red trace) and voltage-to-ground downstream the breaker (blue trace).

Without DCCBs, positive poles of all converter stations have to be blocked, until faulted cable is isolated by means of disconnectors. Only after having isolated the faulted cable, the sound portions of pole + can be re-energized. Before faulted cable isolation takes





place, only 50% of power transmission capability is available on the whole corridor (through negative pole and return line/electrodes) as shown in the relevant graphs above.

Thanks to the HVDC breakers, the DC fault can be isolated by opening the two breakers installed at the end of the faulted cable without blocking any of the converters.

The HVDC breakers shall open a current of approx. 14 kA which is compatible with the state-of-the-art for such technology (25 kA in Zhangbei Project, as per Table 4-4 of CIGRE TB 873, [7]); the dissipated energy is around 20 MJ, much lower than the capabilities of the Zhangbei arresters (125 MJ for hybrid breakers, [7]).

### Case id C2 – Temporary pole + to ground fault on overhead line, 5 km from Forli

#### WITHOUT HVDC CIRCUIT BREAKERS

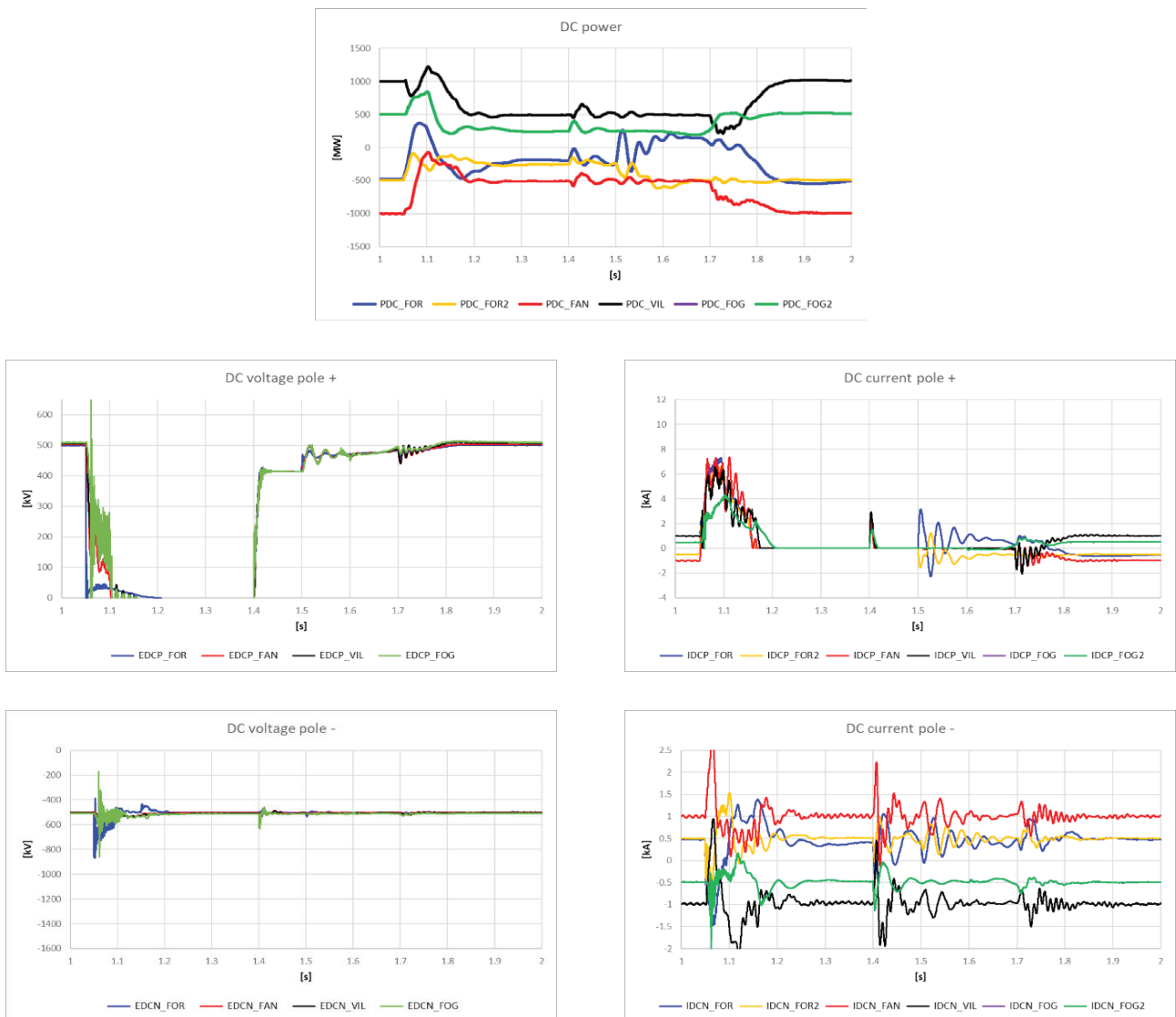


Figure 10. Case id.C2 without HVDC breakers. DC power (top), voltage (middle) and current (bottom)



WITH HVDC CIRCUIT BREAKERS



Figure 11. Case id.C2 with HVDC breakers. DC power (top), voltage (middle) and current (bottom)

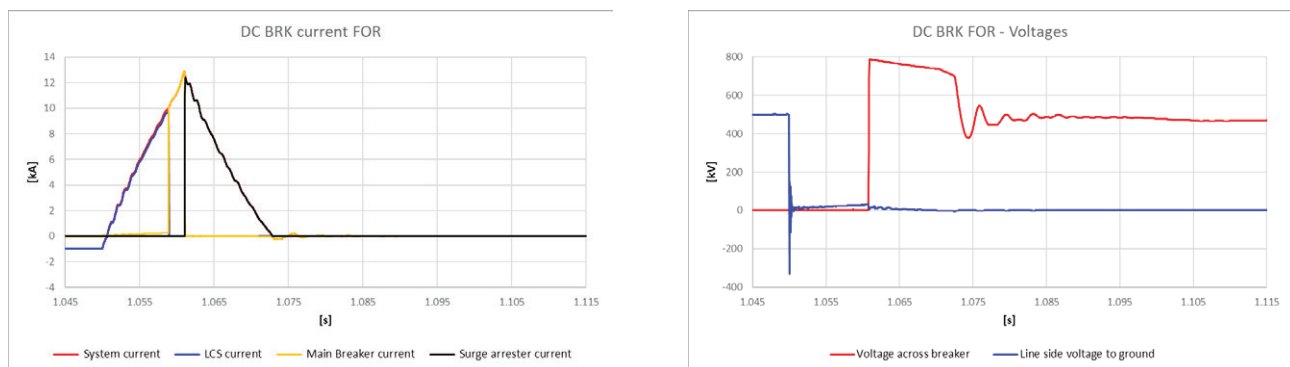


Figure 12. Case id.C2. Forli HVDC breaker. LEFT: Current in the various branches of the HVDC Circuit Breaker (Overall current: RED trace; load commutating switch: BLUE trace; main breaker: YELLOW trace; surge arrester: BLACK trace). RIGHT: Voltage across HVDC circuit breaker (red trace) and voltage-to-ground downstream the breaker (blue trace).

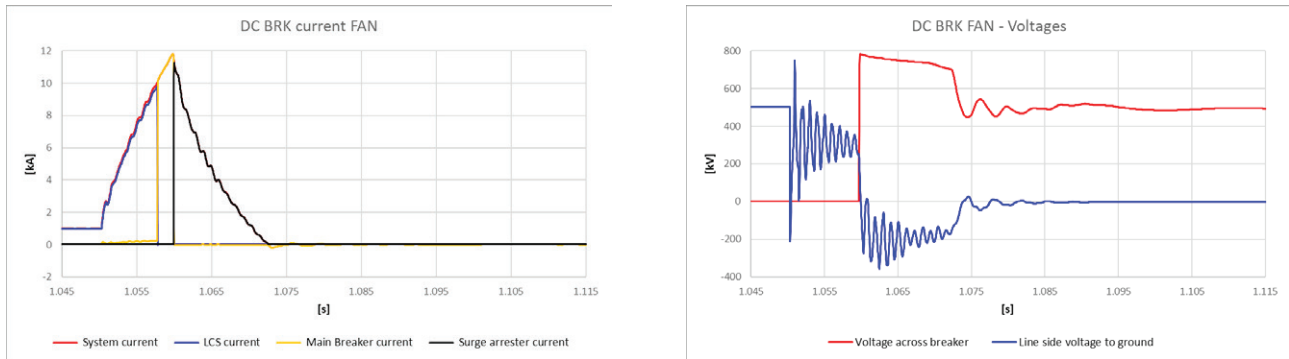


Figure 13. Case id.C2. Fano HVDC breaker. LEFT: Current in the various branches of the HVDC Circuit Breaker (Overall current: RED trace; load commutating switch: BLUE trace; main breaker: YELLOW trace; surge arrester: BLACK trace). RIGHT: Voltage across HVDC circuit breaker (red trace) and voltage-to-ground downstream the breaker (blue trace).

Without HVDC breakers, 50% power transfer capability is temporarily lost after fault due to blocking of all positive pole converters.<sup>3</sup> Thanks to the HVDC breakers, full selectivity is obtained and power is lost only on positive pole of Forli-Fano portion of the Adriatic Corridor. The sound stations in power control mode (Fano, Villanova and Foggia 2) are able to keep their pre-fault power set point, minimizing the impact on the AC nodes. In order to avoid divergence of DC voltage, 100 ms after Forli 1 station is isolated from the rest of the multiterminal system (i.e. at time 1.2 s in the graphs) Foggia 1 changes its control mode from DC Power to DC voltage. After that, it behaves as a power slack and its power is controlled so as to compensate the variation of power due to the fault (i.e. to keep voltage at the nominal value).

The HVDC breakers shall open a current of approx. 13 kA; the dissipated energy is around 50 MJ.

### Case id C3 – Temporary pole to pole fault on overhead line, 5 km from Forli

#### WITHOUT HVDC CIRCUIT BREAKERS

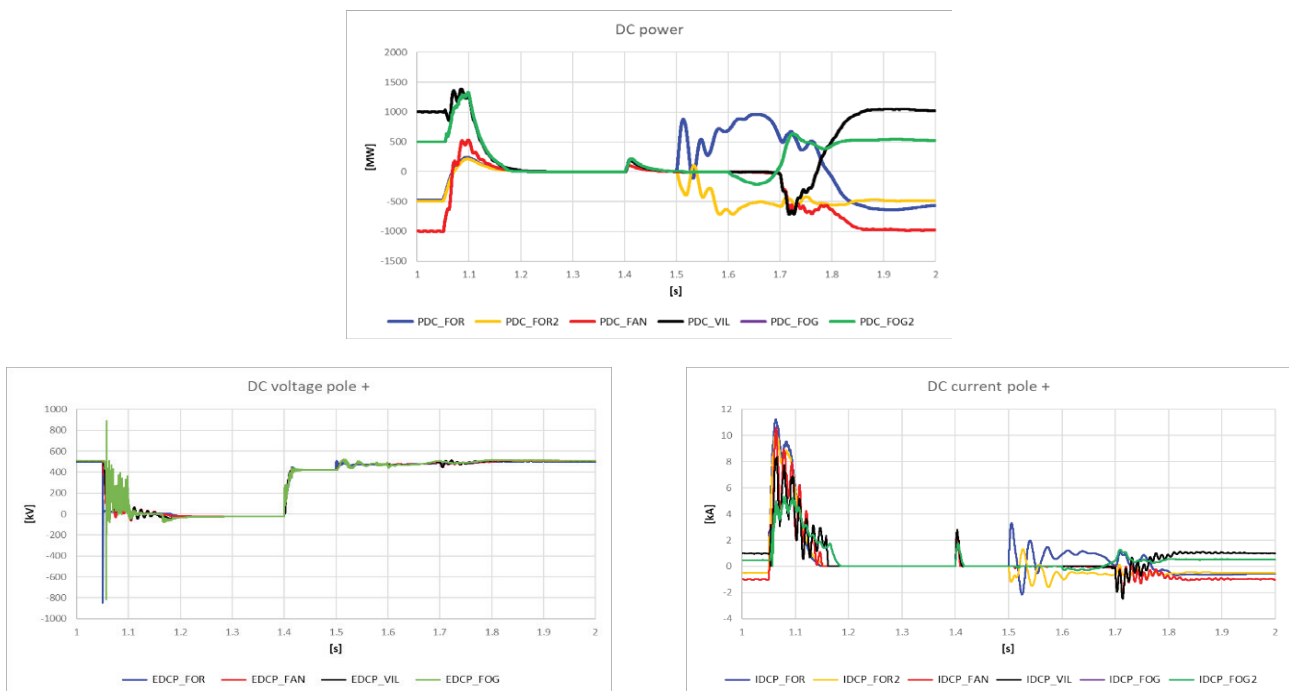


Figure 14. Case id.C3 without HVDC breakers. DC power, voltage and current (pole + and pole - are identical in this case, therefore only positive pole is shown)

<sup>3</sup> It is underlined that the optimization of the DC line re-energization process (which starts at time t=1.4 s in the graphs) is not one of the goals of the present simulations; pole + current spikes and oscillations observed between t=1.4s and t=1.7 s are due to this re-energization and may be smoothed with a better refinement of the DC line re-energization sequence.



WITH HVDC CIRCUIT BREAKERS

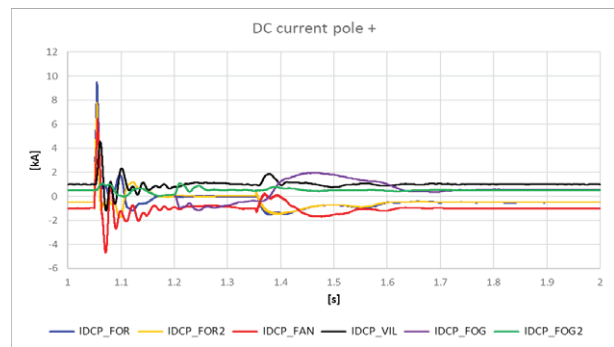
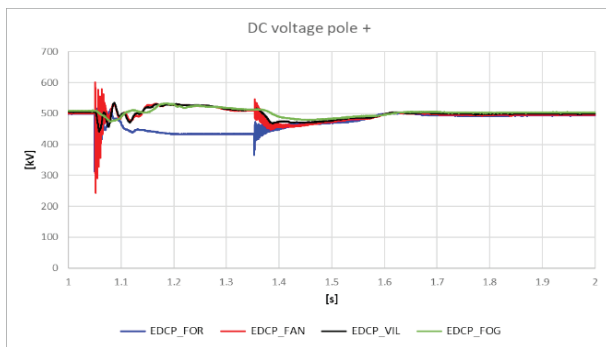
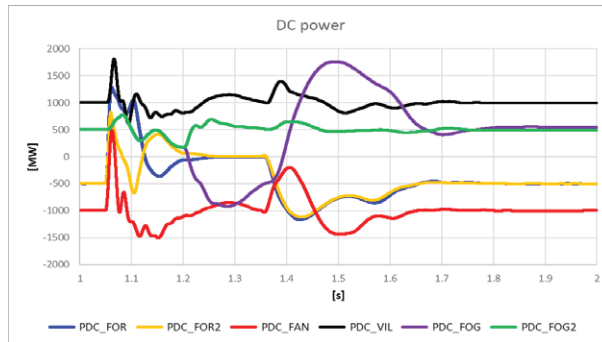


Figure 15. Case id.C3 with HVDC breakers. DC power, voltage and current (pole + and pole - are identical in this case, therefore only positive pole is shown)

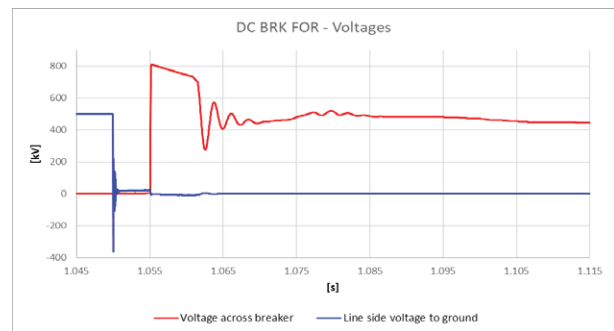
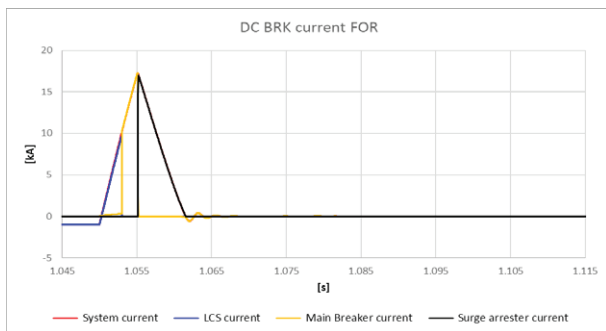


Figure 16. Case id.C3. Forli HVDC breaker. LEFT: Current in the various branches of the HVDC Circuit Breaker (Overall current: RED trace; load commutating switch: BLUE trace; main breaker: YELLOW trace; surge arrester: BLACK trace). RIGHT: Voltage across HVDC circuit breaker (red trace) and voltage-to-ground downstream the breaker (blue trace).

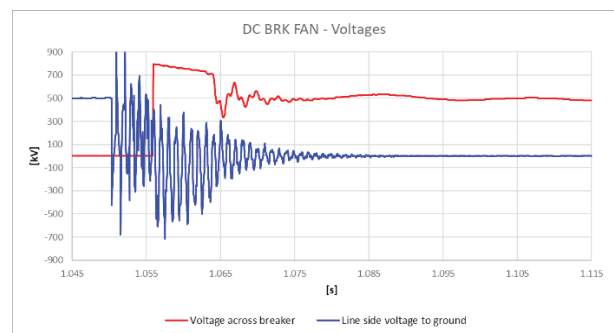
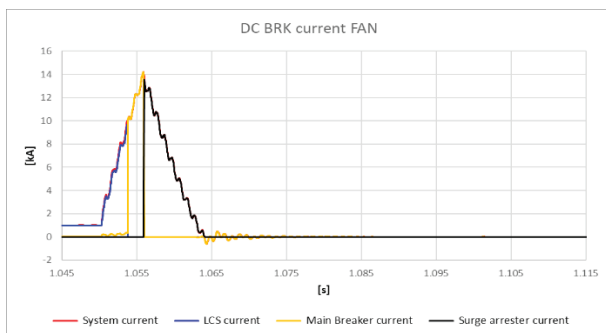


Figure 17. Case id.C3. Fano HVDC breaker. LEFT: Current in the various branches of the HVDC Circuit Breaker (Overall current: RED trace; load commutating switch: BLUE trace; main breaker: YELLOW trace; surge arrester: BLACK trace). RIGHT: Voltage across HVDC circuit breaker (red trace) and voltage-to-ground downstream the breaker (blue trace).



Pole-to-pole faults are the most critical in terms of interruption capability for HVDC breakers: simulated breaking current is around 17.5 kA with 40 MJ to be dissipated. General behaviour of the corridor is similar to the one resulting from a temporary pole to ground fault in the same point (Case id C5), but affecting in the same way both positive and negative poles.

## 6. CONCLUSION

The Adriatic Corridor part of the Hypergrid project represents a change of mindset to address future challenges of the merging energy scenario. From one side, the new RES energy trend cannot be supported by the grid without adequate DC and AC reinforcements because traditional instruments and planning standards are not able to withstand the timing of new RES projects. The new DC layer will enable to have an increase of NTC between bidding zones and more controlled flows, but also a greater flexibility if compared to an AC grid especially during faults. In this paper the operation feasibility of DCCBs applied in the Adriatic Corridor project is presented. Thanks to the HVDC breakers, full selectivity is obtained and the results show how, in all the DC fault cases proposed, full power can be transferred by the other sound equipment, without blocking the relative converters with fast response. The maximum DC current interrupted in the studied scenarios is approx. around 17.5 kA, obtained in a pole-to-pole fault, while the maximum dissipated energy is about 50 MJ, which is compatible with the state-of-the-art for such technology. Moreover, VSC technology, coupled with DCCBs, enables multiterminal operation with greater flexibility along with adaptive control modes, to be properly designed, that lead stability to the system in all the contingencies proposed.

## BIBLIOGRAPHY

- [1] Terna, Marzo 2023. [Online]. Available: <https://www.terna.it/it/media/comunicati-stampa/dettaglio/piano-sviluppo-2023>.
- [2] Terna, «Documento di Descrizione degli Scenari 2022,» 2022. [Online]. Available: [https://download.terna.it/terna/Documento\\_Descrizione\\_Scenari\\_2022\\_8da74044f6ee28d.pdf](https://download.terna.it/terna/Documento_Descrizione_Scenari_2022_8da74044f6ee28d.pdf).
- [3] J. C. Garcia e F. Mosallat, «“MMC- Technologies”, Manitoba HVDC Research Centre,» 26 February 2015. [Online].
- [4] CIGRE TB 604, “Guide for the Development of Models for HVDC Converters in a HVDC Grid”, Working Group B4.57, December 2014.
- [5] CIGRE TB 804, “DC grid benchmark models for system studies”, Working Group B4.72, June 2020.
- [6] IEC 60071-11, “Insulation co-ordination - Part 11:Definitions, principles and rules for HVDC system”, December 2022.
- [7] CIGRE TB 873, “Design, test and application of HVDC circuit breakers”, Joint Working Group B4/A3.80, July 2022.
- [8] G. Tang, «Research on Key Technology and Equipment for Zhangbei 500 kV DC Grid,» *High Voltage Engineering*, vol. 44, n. 7, pp. 2097-2106, July 2018.
- [9] X. Zhang, Z. Yu, R. Zeng e e. al., «State-of-the-art 500 kV Hybrid Circuit Breaker for DC Grid: Design, Development, and Experiment — The World’s Largest Capacity HVDC Circuit Breaker,» *IEEE Industrial Electronics Magazine*, 2020.
- [10] A. Hassanpoor, Y.-j. Häfner, A. Nami e V. K, «Cost-Effective Solutions for Handling Dc Faults in VSC HVDC Transmission,» *EPE2016*.



# Hybrid High Voltage AC and DC System Strength Evaluation With Large Penetration of Renewable Energy Sources

[luca.belmonte@terna.it](mailto:luca.belmonte@terna.it)

ENRICO MARIA CARLINI, TEMISTOCLE BAFFA SCIROCCO, ANGELO CALDARULO BUGLIARI,  
FRANCESCO PISANESCHI, LUCA BELMONTE\*

*Terna Rete Elettrica Nazionale*

STEFANO BARSALI

*University of Pisa*

Italy

## SUMMARY

The Italian electricity system is undergoing significant evolutions as part of the energy transition in the country. The European targets of the Fit-for-55 package include a 55% reduction of CO<sub>2</sub> emissions by 2030 (compared to 1990 levels). This means that energy produced from Renewable Energy Sources (RES) in Italy must cover at least 65% of final consumption in the electricity sector by 2030 (compared to 55% previously envisaged by the National Integrated Energy and Climate Plan (PNIEC)). This will require an additional 70 GW (mainly new photovoltaic and wind power) by 2030, compared to the additional 40 GW envisaged in the PNIEC. Direct current (DC) technology, with its many advantages over alternating current (AC) transmission, is the most suitable means of transporting this large amount of renewable generation to the grid in a safe and stable manner. High Voltage Direct Current (HVDC) systems will allow full control of energy flows in the DC grid, which is not possible in conventional AC grids. In this way, it will be possible to better manage the energy flows generated by the increasing number of RES power plants, which by their nature are not predictable, over long distances thereby reducing losses for the same transmitted power. The increasing penetration of RES can challenge Transmission System Operators (TSOs) to maintain the security of supply and system reliability. Potential power system stability issues may arise when a large number of RES are connected to a weak power system. In this scenario the concept of *System Strength* should be properly investigated taking into account the interaction of multiple Inverter-Based Resources (IBRs) in the system. When several IBRs are connected to the same portion of the network, they can interact each other even dynamically through control loops actions, causing the system to become unstable. From a static point of view the existing Short Circuit Ratio (SCR)-based methods may be not effective in reflecting the interaction effects among multiple RES power plants. Indeed, the static indicators found in the literature tend to underestimate or overestimate the system strength. They show critical issues related to their formulation based on short-circuit power, which in case of large penetration of RES power plants does not longer represent an appropriate indicator of system stability. In this paper, in order to assess system strength, dynamic simulations are carried out in MATLAB/Simulink environment. High Voltage Direct Current (HVDC) Voltage Source Converters (VSC) and IBR with different control logics are implemented. The aim is to investigate their dynamic response analyzing various control logics configurations applied on power sources. HVDC links using VSC technology will be able to improve the AC system stability, containing power fluctuations and ensuring a better control of the voltage profiles. In addition, appropriate control strategies for VSC converters of the IBRs generation are investigated.

## KEYWORDS

System Strength, HVDC VSC, RES, SCR, Power System Stability





Oral Presentation: Hybrid High Voltage AC and DC System Strength Evaluation With Large Penetration of Renewable Energy Sources

## 1. INTRODUCTION

The ongoing energy transition, accelerated by the latest decarbonisation targets (REPowerEU [1]), foresees a further increase in new RES capacity compared to the targets mentioned in the “Fit-for-55” package and PNIEC, also to ensure greater diversification of energy supply and accelerate the transition towards a zero-emission system.

The spatial RES distribution and the new generation mix will require significant topological changes in the power system. It will be essential to speed up permitting procedures, optimising synergies among existing and planned infrastructures and taking into account technical and economic aspects of long-distance direct current transmission.

Terna, in the National Development Plan 2023 [2], has planned new infrastructure investments to meet the national and European targets. Among all the alternatives considered, the development of a DC layer using HVDC Voltage Source Converter (VSC) technology was considered the most competitive solution in terms of environmental and economic sustainability for the Italian electricity system. This solution will ensure greater use of renewable energy, thanks to increased transmission capacity along with a better power flows balance and control.

The ongoing energy transition implies the progressive penetration of renewable energy power plants in the power system connected to the grid through static converters (inverters) along with decommissioning of conventional generation. Synchronous generators effectively regulate the voltage at their terminals responding promptly to frequency variations by modulating the power exchanged with the grid. They also contribute to short-circuit current and rapid voltage recovery. In this emerging context, it is therefore necessary to investigate the *System Strength*, seen as the ability of the electrical system to maintain and control the voltage waveform at any node of the grid in case of faults or disturbances [3]. In other words, the more a system is robust, the faster it can restore the voltage profile at the nodes.

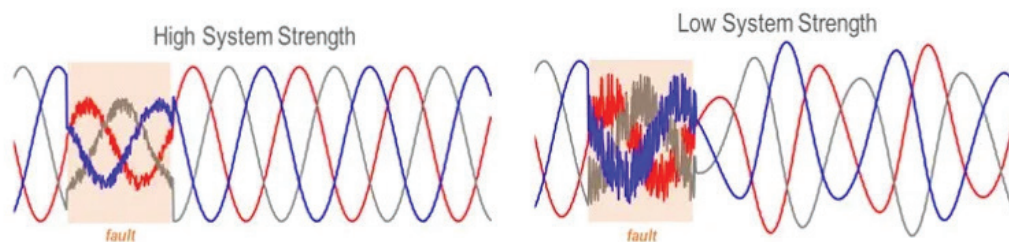


Figure 1. Dynamic voltage response after a fault in case of high (left) and low (right) System Strength level [4]

System strength of a node is proportional to the availability of short circuit power [5] and reactive power. On the other hand, it decreases as the penetration of IBR generation increases. The contribution of IBRs to short-circuit power is limited compared to the synchronous generators one, which can provide a maximum short-circuit current ( $I_{cc}$ ) up to 5÷6 times the rated current, contrary the  $I_{cc}$  of inverters in case of photovoltaic systems is around 1÷2 times the rated current. It follows that the short-circuit power of High Voltage Alternate Current (HVAC) networks will be progressively reduced as synchronous generators are replaced by the new IBRs and at the same time, the area of voltage disturbance due to a fault increase [6]. The inverters of the current IBRs generators implemented in the system are almost exclusively controlled in grid following mode (GFL); their operation is therefore closely linked to the voltage waveform at the point of interconnection (POI). The GFL control logic, controlled by the phase locked loop (PLL), determines the offset angle of the voltage vector at the inverter terminals with respect to the grid voltage vector. A weak grid leads to several problems for inverters interfacing renewable generation units. Compared to synchronous machines, IBRs requires stable voltages at the grid nodes to which they are connected. Any disturbances could lead to control system instability of the inverters. Voltage stability is closely related to reactive power generation and the dynamics of the voltage regulation control loops. Under steady-state conditions, the inverter control systems do not amplify or modify disturbances in response to small voltage signals. Instead, in case of large disturbance, the control systems could remain synchronised with the grid and amplify the disturbance itself. Therefore, to investigate the system strength level, it will be necessary to assess not only the amount of IBRs that can be accommodated in each grid section but also the optimal design and configuration of their control system.

## 2. SYSTEM STRENGTH ASSESSMENT WITHIN THE ITALIAN TRANSMISSION GRID

In order to assess the system strength level of the grid, qualitative analyses are carried out on the National Transmission Grid (NTG) using a large penetration of renewable power plants scenario. The analysis reproduces a snapshot in which the electrical load is



Oral Presentation: Hybrid High Voltage AC and DC System Strength Evaluation With Large Penetration of Renewable Energy Sources

largely covered by RES generation, while conventional generation is reduced to the minimum necessary to maintain system stability. Power flows among market zones are close to the limits. System strength is typically measured in terms of Short Circuit Ratio (SCR). In literature, this index is given by the ratio of the short-circuit power at the node and the total power of the IBRs. In a network characterised by large penetration of IBRs, the SCR index could overestimate the network system strength level. It does not consider the electrical distance among IBRs that are located on the same network section and that dynamically influence each other, mostly in case of rapid changes in renewable power injection. The classical definition of the SCR index assumes that the IBRs belonging to a given portion of the network are electrically independent [7]. Under real operating conditions, the IBRs can influence each other, and the resulting electromagnetic oscillations generate instability phenomena that can reduce the system strength of the grid [8] [9]. In order to better assess the stability of AC/DC systems in case of large IBRs penetration, the International Council for Large Electrical Systems (CIGRE) has proposed the Multi-Infeed Short Circuit Ratio (MISCR) indicator [10]. The MISCR assesses the interaction among the different IBRs through an interaction factor, called Multi-Infeed Interaction Factor (MIIF), which is given by the ratio of the voltage variation at the reference node and the voltage variation at the node where the short circuit occurs:

$$MIIF_{ji} = \frac{\Delta U_j}{\Delta U_i}$$

To calculate the MISCR indicator, the nodes close to the one where the short-circuit is simulated have been considered. The MIIF coefficient weights properly the active power injected by the IBRs adjacent to the node where the indicator is evaluated. Formally, the MISCR indicator can be expressed as:

$$MISCR_i = \frac{S_{cci}}{P_i + \sum_{j \neq i=1}^N MIIF_{ji} * P_j}$$

where  $S_{cci}$  is the short-circuit power at the node  $i$ ,  $P_j$  is the active power injected by the inverter-based resource at the node  $j$  that affects the voltage stability at the node  $i$  and where the indicator is evaluated (and to which the IBR  $P_i$  is connected). Based on the defined generation scenario, short-circuit power values are calculated at all 380 kV and 220 kV nodes of the NTG. Starting from short-circuit power values at each node and the installed renewable capacity at the afferent or electrically adjacent nodes, the MISCR indicator is calculated through an iterative process. Figure 2 shows the maps with the values of the average short-circuit power and the installed RES capacity at all nodes of the NTG, represented with provincial granularity. The network System Strength is expressed by the average value of the MISCR in the nodes of the province and is graphically depicted in the map in Figure 3. In line with the available literature, a conservative MISCR threshold of 3 was considered. Below this value, the system strength level of the network is considered to be insufficient [10]. Additional renewable power plant installations could lead to a risk of instability in the area.

The most critical areas identified by this analysis will be further investigated using tools capable of simulating dynamic phenomena. The static indicator summarised and presented above provide an initial qualitative assessment of the level of system strength of a given portion of the grid. A new approach is required to be adopted that allow to properly detects and quantify electrical interactions among all the IBRs connected to the system.

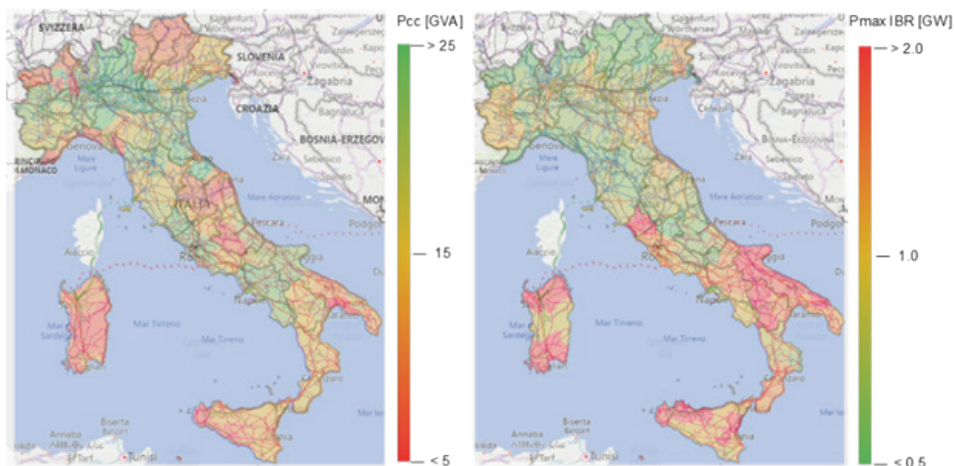


Figure 2. Average short-circuit levels (left) and total RES installed capacity (right) per province in the Italian forecast Transmission Grid



Oral Presentation: Hybrid High Voltage AC and DC System Strength Evaluation With Large Penetration of Renewable Energy Sources

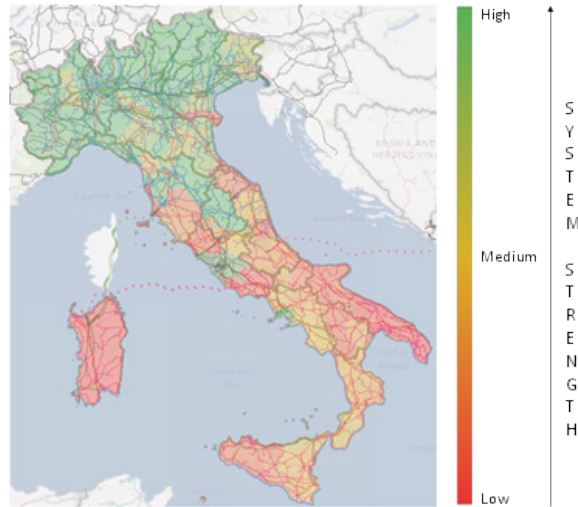


Figure 3. System Strength levels in the Italian forecast Transmission System per province

In this way, next session will consider a hypothetic electrical power system where the amount of IBRs is close to 100%. The performed analysis shows how the stability of the system depends by several factors such as spatial dislocation, capability, and control loop topology of each inverter-based resource. Stability issues phenomena could occur in the system if these parameters are not properly considered in the planning process of the new electrical power system able to handle this energy transition.

### 3. DYNAMIC ASSESSMENT OF SYSTEM STABILITY

Several scholars have shown that indexes referring to different ways of calculating short circuit ratio are not able to give a complete evaluation of the actual stability of a system with a large share of inverter-based resources connected [11] [12]. The reason why of the inadequacy of these methods resides in that the concept of system strength is less and less related to Scc which is mainly provided by synchronous generators [12].

Therefore, despite preliminary assessments can be done by using static stability indexes, a test system has been prepared for dynamically checking the stability of systems with different share of inverter interfaced resources, also including the possible contribution from VSC-HVDC systems, basic control loops of converters (PLL, power control, etc.), reactive power compensation and transmission lines.

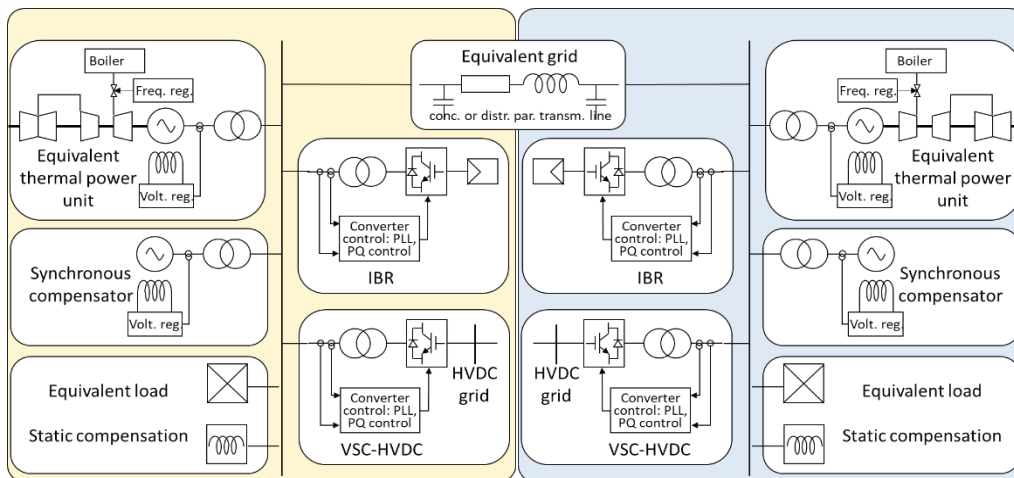


Figure 4. Reference system for stability assessment.

The test system is inspired by a two-area network where the two areas are connected to each other through a line or an equivalent grid. The two systems are conceived to include conventional generation which can be either thermal generation (steam plants in figure, or CCGT) or hydroelectric generation, with rotating machines and the relevant frequency and voltage regulation systems.



Oral Presentation: Hybrid High Voltage AC and DC System Strength Evaluation With Large Penetration of Renewable Energy Sources

To help the grid accept high share of renewables, static and rotating compensation systems are considered, as well as the possible use of HVDC systems for delivering energy elsewhere. By using different values for the rated power of the conventional generators, for the relevant inertia and for the equivalent transformer parameters, different grid scenarios can be represented.

For instance, while referring to the Italian scenario, we can represent a weak part of the south grid using a generator with electrical parameters and rated power chosen to match the short circuit level at the point of interconnection but with a large enough inertia to account for the behavior of the entire interconnected European system.

The same model can also be used to represent an islanded part of the grid, as the Sardinian network, using the real values of the running rotating generators and existing transformers. Both inertia and electrical parameters to be used are the actual machine parameters.

Several parameters are likely to affect the stability of the system: the rated power of the conventional rotating machines, the length of the interconnecting line, the level of local compensation but also the path followed by the power produced by the renewable sources and the control loops of the converters either referring to HVDC systems or IBRs.

At the present level of the research, the aim of this paper is to highlight the effect of these parameters during the normal operation of the grid. To cope with transients following faults, a more detailed knowledge of the converter control system must be ensured. While a synchronous generator response to a grid fault can be assessed, at least for preliminary studies, by simply knowing the machine parameters, the response of a converter strongly depends on how its control loops have been designed to protect the converter valves from overload and for ensuring or not the so-called Fault Ride Through Capability.

### 4. RESULTS ON A SIMPLIFIED TEST SYSTEM

To show the model behavior and some preliminary results a test system derived from the general scheme of Figure 4 is used.

The test system represents an area where 1GW of IBR is to be installed and where the possibility of transmitting up to 1GW of power through VSC based HVDC links is given. The area is connected with a 200km 400kV line to a part of the grid where a second 1GW HVDC terminal exists together with some residual rotating generation.

It's worth remarking that, at a first level of analysis, VSC based HVDC systems and IBR converters have a similar impact on the grid stability when both types of converters are controlled in terms of real and reactive power to be exchanged with the grid. This means that the converters are synchronized with the grid using a Phase Locked Loop system. As already mentioned in [13], the transfer function of the PLL system is likely to affect the overall system stability. Any converter using a PLL system for synchronization and controlling real and reactive power exchange shows a similar behavior whatever its specific function is (IBR, VSC-HVDC). Solutions using different control methods such as Grid Forming, Grid Supporting or droop control in voltage regulation mode can help increasing the stability of the system.

The scenario used in this study is shown in Figure 5. It represents a small system interconnected with the rest of the system by two HVDC links and hosts a large amount of generation from renewable sources connected with a static converter.

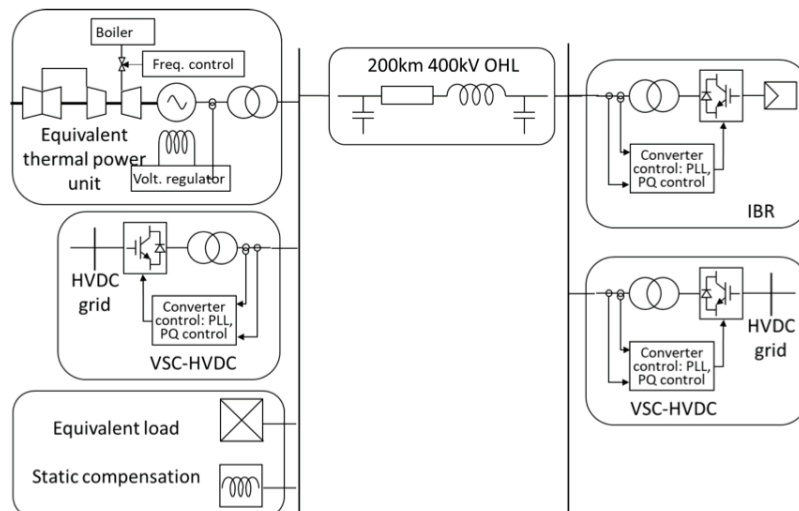


Figure 5. Simple test system



Oral Presentation: Hybrid High Voltage AC and DC System Strength Evaluation With Large Penetration of Renewable Energy Sources

The converter connected generation and the conventional generation are in different areas 200km far from each other and connected with a 400kV overhead line. The rated power of the VSC-HVDC converter is 1000MW each and the converter-based generation is 1000MW as well.

Supposing the renewable generation to replace the conventional one, the size of the rotating generator is reduced until some kind of unstable behavior is detected.

Converters with PQ control and PLL

The first test is made by supplying the local load (50MW) with the synchronous generator while the three converters (two VSC HVDC terminals and one representing an equivalent converter for a total of 1GW of IBR) in power control mode are simply running in parallel with zero power setpoint (both real and reactive power).

This situation is analyzed for three different generator and unit transformer size: 250MVA, 200MVA and 150MVA.

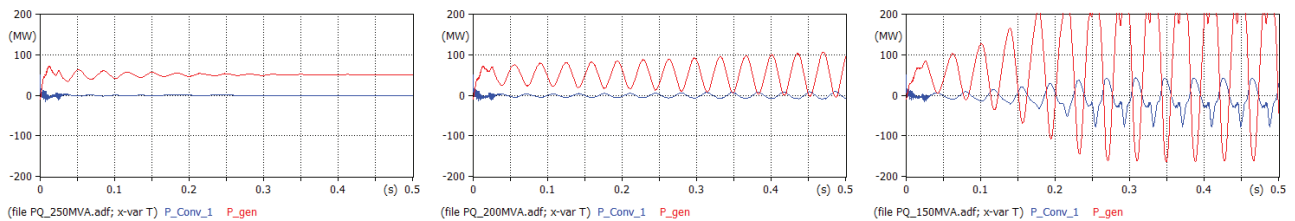


Figure 6. Real power supplied by the synchronous generator (red) and by one HVDC terminal (blue). Generator rated power: 250MVA, 200MVA and 150MVA from left to right

Figure above shows the system behavior using real power exchanged by the synchronous generator and by one of the HVDC converter. The other HVDC and the IBR converters are not represented here but show a similar trend. When the generator power is large enough (say 250MVA) the system is stable and the initial transient, due to the not perfectly balanced initial state, quickly settles. Otherwise, the system becomes unstable, and the oscillations grow.

When the system is stable, with a 250MVA generator, it is possible to increase the power generated by the IBR which is then transmitted away from the system through the two HVDC links. As an example, we here supposed that the IBR ramps up to 1GW in 1s, while the two HVDC links takes 500MW each still in 1s. Although the transient is very quick compared to the usual ramping of the resources, the system is clearly stable as shown in figure below.

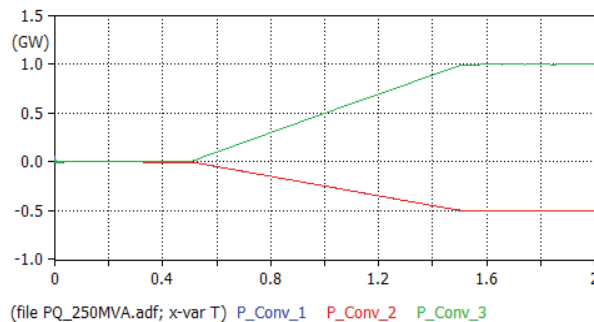


Figure 7. Real power supplied by the IBR (green) and by the HVDC terminals (red and blue). Positive values mean power flowing from the converter to the AC grid.

The next picture represents the system frequency as measured by the PLL of one of the converters. It suggests that the unstable behaviour, which jeopardizes the system operation with small generators, is excited by the PLL controller.





Oral Presentation: Hybrid High Voltage AC and DC System Strength Evaluation With Large Penetration of Renewable Energy Sources

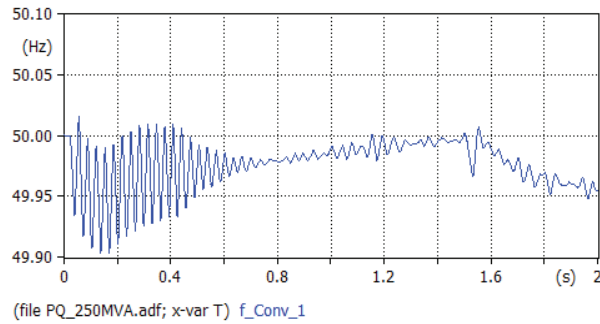


Figure 8. Frequency measured by the PLL of one of the HVDC converter controllers.

It's worth remarking that, in this preliminary study, standard parameters have been used for controller loops and that the reference schemes for the controllers are taken from [14]. In real case analyses, it is indeed very difficult getting actual control schemes and parameters from manufacturers, so, in most cases, reference shall be done to literature data.

To confirm PLL, and therefore, PQ control, is the responsible of the unstable trend, we modified the case with the 200MVA generator by first setting the generator inertia to a practically infinite value so its speed will never change, and then by replacing the PLL measure with a constant frequency signal generator since the system frequency cannot move from 50Hz.

Results in term of generator and HVDC converter power output are represented in Figure 9 below.

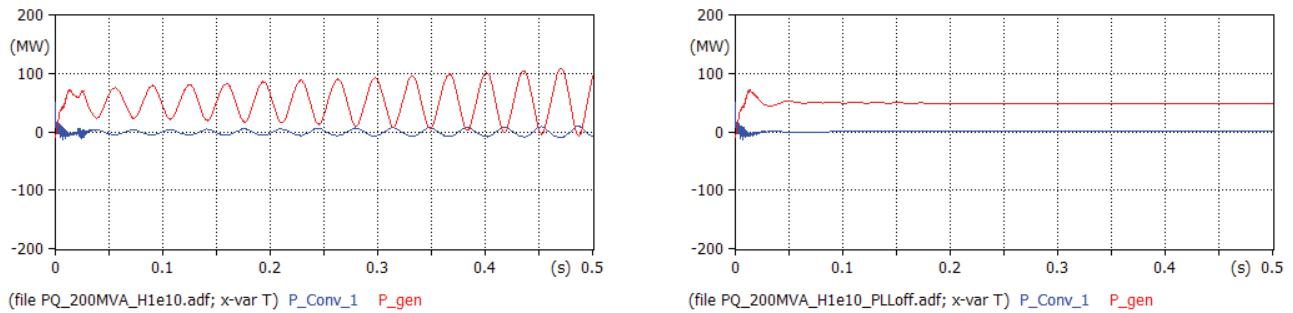


Figure 9. Real power supplied by the 200MVA synchronous generator (red) and by one HVDC terminal (blue). Left: generator with infinite inertia and PLL in operation. Right: generator with infinite inertia and PLL replaced by a constant frequency signal generator

It's clear that, even if the system frequency is fixed, the synchronization loop still results in a not stable operation. If the constant frequency signal generator is activated indeed, the system is able to operate and deliver the power generated by the IBR similarly to the previous 250MVA generator case.

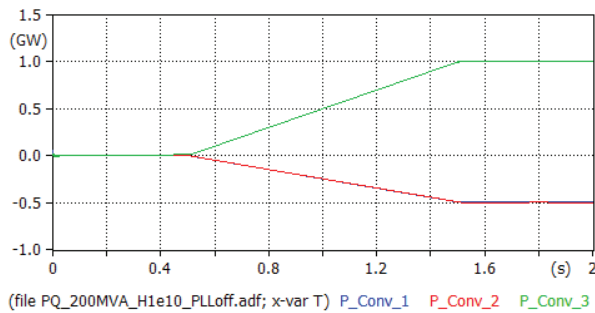


Figure 10. Real power supplied by the IBR (green) and by the HVDC terminals (red and blue). Positive values mean power flowing from the converter to the AC grid.

Obviously, this kind of operation is not practically feasible as the system frequency will be continuously changing and the converters need to be synchronized to make their control loops correctly operate.





Oral Presentation: Hybrid High Voltage AC and DC System Strength Evaluation With Large Penetration of Renewable Energy Sources

HVDC converters in grid forming mode with frequency and voltage droop

In the near future, we can expect that, in some areas, the amount of conventional (hydro or thermal) generation in some hours approaches to zero. Solutions should be found to face this condition. Synchronous compensators can be used. They give the system a voltage reference and provide it with short-circuit power but have not negligible costs, introduce power losses and need a place where to be installed.

When VSC-HVDC terminals are available, the chance to operate them in the so called Grid Forming (GFM) mode can be investigated.

There are different ways of conceiving the GFM mode. We will here consider to make the converter operate as a voltage source of controlled amplitude and frequency where amplitude depends on the reactive power exchanged and frequency on the real power according to droop characteristics according to the following equations:

f(t) = f\_0 - k\_p(p(t) - p\_0)
v(t) = v\_0 - k\_v(q(t) - q\_0)

The values of the parameters f\_0, p\_0, v\_0, q\_0 define the operating point at rated frequency and voltage, while k\_p and k\_v are the droop values usually expressed in terms of percentage when using per unit values.

In we consider the voltage equation written in terms of per unit values, the converter controller outputs a demand for the modulation indexes on the three axes of the Park reference frame as:

m\_d = v
m\_q = 0
m\_0 = 0

These three modulation indexes are then transformed into the phase indexes through the reverse Park transformation matrix using the angle calculated starting from the frequency value given by the frequency equation above as:

vartheta(t) = 2pi integral\_0^t f(tau) dtau

It is a very simple concept, and no inertia simulation is included as the real power to frequency (ore reactive power to amplitude) links are algebraic. It is indeed possible to include also some dynamic transfer function to improve the performance, but it is outside the scope of this preliminary analysis wishing to simply point out some basic concepts.

The system operation is checked with two different sizes for the synchronous generator (250MVA and 100MVA) and even without any synchronous generator in service. Except the first case, the second and third case are not stable with HVDC converters operating in PQ control mode with PLL synchronization system.

The figures below show the stable operation of the system by drawing the power exchanged by the generator (when running) and by one of the HVDC converters.

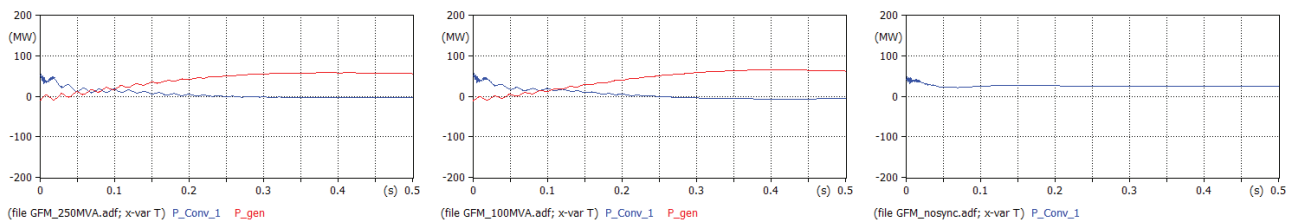


Figure 11. Real power supplied by the synchronous generator (red) and by one HVDC terminal (blue). From left to right: with 250MVA generator, 100MVA generator, without synchronous generator

After the initial transient, as in the simulations before, the IBR converter ramps up to 1GW and the two HVDC converters automatically deliver half the available power each. There is no need of setting any power reference ramp to the HVDC controller as the droop controller is able to balance the system. Frequency will increase according to the droop value set. In these tests, frequency droop is set to 5% and the final value correctly approaches 51.2Hz. The different trend in the three cases depends on the contribution of the synchronous generator governor.



Oral Presentation: Hybrid High Voltage AC and DC System Strength Evaluation With Large Penetration of Renewable Energy Sources

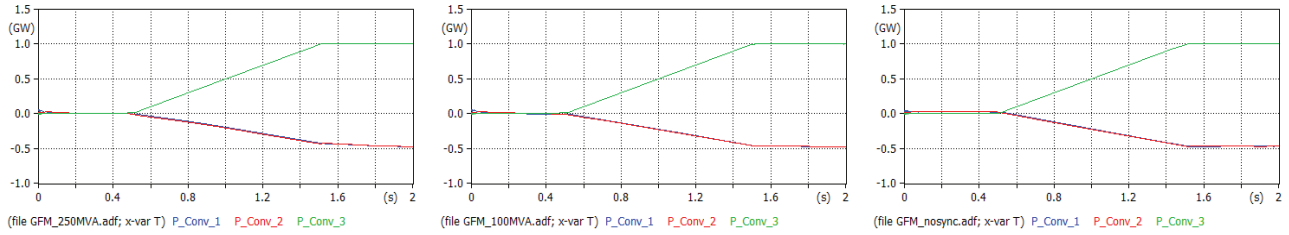


Figure 12. Real power supplied by the IBR (green) and by the HVDC terminals (red and blue). Positive values mean power flowing from the converter to the AC grid. From left to right: with 250MVA generator, 100MVA generator, without synchronous generator.

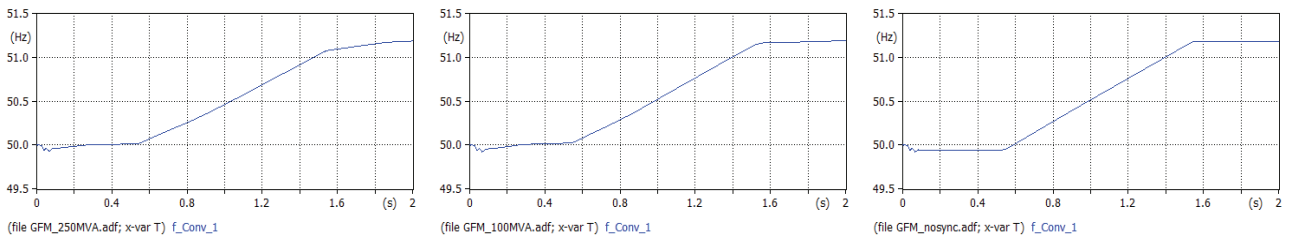


Figure 13. Frequency measured at the terminals of one of the HVDC converter controllers. From left to right: with 250MVA generator, 100MVA generator, without synchronous generator.

To reduce the frequency change, a lower droop can be adopted as shown in the result of the figure below where a 2.5% droop is used.

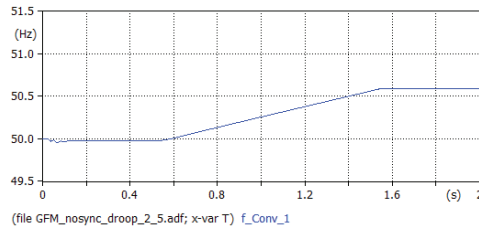


Figure 14. Frequency measured at the terminals of one of the HVDC converter controllers with a 2.5% frequency droop and without synchronous generator.

Finally, the next figures show the behaviour of the voltage amplitude regulators as they result in the amount of reactive power exchanged by each converter in the test case without synchronous generator. The IBR is assumed not to exchange reactive power, while the transmission line initially outputs about 140Mvar and, while loaded with 500MW of power finally outputs about 50Mvar. This transient and the relevant changes in voltage amplitude and reactive power flows are managed by the converter voltage droop controllers.

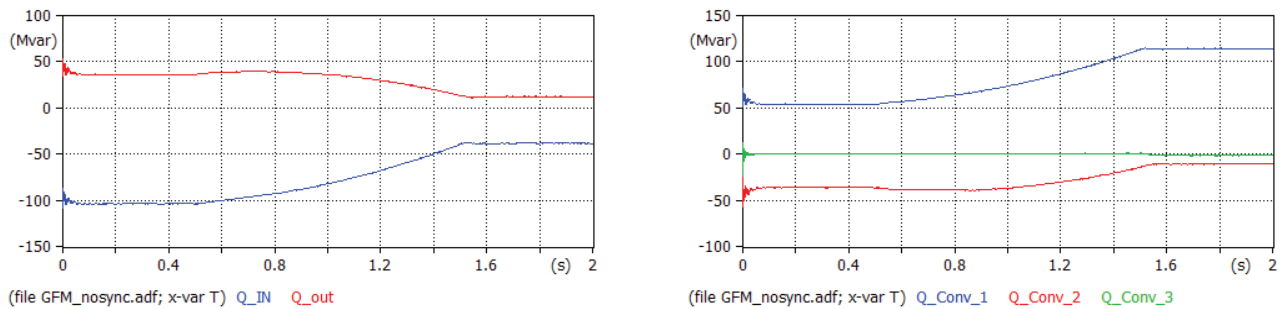


Figure 15. Left: Reactive power exchanged by the transmission line at its terminals (left terminal: blue, right terminal: red) with positive sign from left to right – Right: Reactive power supplied by the IBR (green) and by the HVDC terminals (red and blue). Positive values mean power flowing from the converter to the AC grid.



Oral Presentation: Hybrid High Voltage AC and DC System Strength Evaluation With Large Penetration of Renewable Energy Sources

### 5. CONCLUSION

Increased RES integration through inverter-based systems raises issues on System Strength. Static indicators such as SCR and its derivatives are no longer a suitable tool to measure the System Strength of an inverter-based network. The reason for the inadequacy of these methods is that the concept of system strength is strictly related to  $S_{cc}$ , which is mainly provided by synchronous generators. An initial qualitative analysis with more complex static indices such as MISCR is necessary to capture the potentially most critical areas, for which detailed analyses with dynamic tools are required. The results of the simulations show that the control systems of the IBR units in the system play a fundamental role in terms of system stability. In this respect, the use of HVDC VSC technology plays a key role increasing system strength through effective node voltage control and oscillation damping in a scenario where large amount of renewables generation needs to be delivered over long distances. By implementing droop control Grid Forming mode in HVDC VSC converter substations, the system is able to exchange power over the AC grid while maintaining stability also reducing conventional synchronous generation availability to zero. It's worth remarking that in case of transients following faults, a more detailed knowledge of the converter control system must be ensured, and further studies will be conducted on this in continuation of this activity.

### BIBLIOGRAPHY

- [1] E. Commission, July 2022. [Online]. Available: [https://commission.europa.eu/strategy-and-policy/priorities-2019-2024/european-green-deal/repowereu-affordable-secure-and-sustainable-energy-europe\\_it..](https://commission.europa.eu/strategy-and-policy/priorities-2019-2024/european-green-deal/repowereu-affordable-secure-and-sustainable-energy-europe_it..)
- [2] Terna SpA, «Progetto Hypergrid e Necessità di Sviluppo,» March 2023. [Online]. Available: <https://www.terna.it/it/sistema-elettrico/rete/piano-sviluppo-rete>.
- [3] AEMO, «System Strength Explained,» 2020. [Online].
- [4] AEMO, [Online]. Available: <https://aemo.com.au/learn/energy-explained/energy-101/energy-explained-system-strength..>
- [5] Terna, «Codice di trasmissione, dispacciamento, sviluppo e sicurezza della rete: Allegato A.8,» [Online]. [Consultato il giorno 2012].
- [6] E. Carlini, L. Cacioli, D. Polinelli, P. Capurso, A. Proietti, A. Berizzi e C. Bovo, «The effects of new 2030 scenario: reduction of short-circuit power and widening of voltage dips,» *IEEE*, 2018.
- [7] D. Wu, G. Li, M. Javadi, A. M. Malyscheff, M. Hong e J. N. Jiang, «Assessing Impact of Renewable Energy Integration on System Strength using Site-Dependent Short Circuit Ratio,» *IEEE Transaction on Sustainable Energy*, vol. 9, n. 3, 2018.
- [8] NERC, «Essential Reliability Services Task Force Measures Framework Report,» November 2015. [Online].
- [9] S. Shah, «G-PST/ESIG Webinar Series: Impedance Scan Tools for Stability Analysis of IBR Grids,» 30 June 2022. [Online]. Available: <https://www.esig.energy/event/webinar-impedance-scan-tools-for-stability-analysis-of-ibr-grids/>.
- [10] «CIGRE' Working Group B4.41, "Systems with Multiple DC Infeed",» December 2008. [Online].
- [11] O. Damanik, O. C. Sakinci, G. Grdenic e J. Beerten, «Evaluation of the use of short-circuit ratio as a system strength indicator in converter-dominated power systems,» *IEEE PES Innovative Smart Grid Technologies Conference Europe (ISGT-Europe)*, OCTOBER 10-12, 2022, Novi Sad, Serbia, 2022.
- [12] A. Boricic, J. L. R. Torres e M. Popov, «System Strength: Classification, Evaluation Methods, and Emerging Challenges in IBR-dominated Grids,» *2022 IEEE PES Innovative Smart Grid Technologies - Asia (ISGT Asia)*, November 1-5, 2022, Singapore, 2022.
- [13] L. Harnefors, M. Bongiorno e S. Lundberg, «Input-Admittance Calculation and Shaping for Controlled Voltage-Source Converters,» *IEEE Transactions on Industrial Electronics*, vol. 54, n. 6, 2007.
- [14] A. Yazdani e R. Iravani, *Voltage-sourced converters in power system*, Wiley, 2010.

## *ELECTRIC TRANSMISSION POSTER PRESENTATION*



ELECTRIC MACHINES AND  
POWER ELECTRONICS



**ELECTRIC  
TRANSMISSION**



**AUTOMATION AND  
CONTROL**

**POWER  
GENERATION**



**ENERGY  
TRANSITION**



**DISTRIBUTION SYSTEMS  
AND SMART GRIDS**



**11-12 OCTOBER 2023**





# Protection and Metering Solutions for Transmission Tie Lines in the Romanian Power Systems

[iulia.constantin@transelectrica.ro](mailto:iulia.constantin@transelectrica.ro)

**IULIA CRISTINA CONSTANTIN\*, CIPRIAN GHEORGHE DIACONU**  
CNTEE Transelectrica SA

Romania

## SUMMARY

A secure and continuous supply of electricity is achieved with the help of protection and control systems, which ensure the reliable operation of the power system. The secondary system is completed by the metering and monitoring systems, which are an essential part of good facility management. These systems provide valuable insight into facility and equipment performance and support better management of energy use and costs, improved system feedback and optimisation.

As the complexity and ratings of electrical power systems increase, the demands on the protective and metering devices are also increased. 400 kV and 220 kV electrical substations belonging to the Transmission and System Operator of Romania are provided with an integrated control, protection and automation system made in numerical technology, hierarchical, decentralized and redundant. The integrated control, protection and automation system of a 400 kV and 220 kV cell (electric line) will be composed of a control subsystem and a protection and automation subsystem (including teleprotection system).

In the Romanian transmission power system, the secondary circuit schemes for metering and power quality monitoring are organized into three functionally independent systems, being structured as follows:

- the local metering system for the balance;
- the local metering subsystem for settlement;
- the local power quality monitoring subsystem.

Additional to the systems mentioned before, on the transmission tie line from Romanian are implemented phasor measurement units (PMUs) which determinate important operational and functional improvements as: real - time visualization, design of an advanced early warning system, analysis of the causes of system perturbances, enhancement in state estimation, real - time congestion management, real - time angular, voltage and frequency stability, improved damping of inter-area oscillations, design of adaptive protection and control systems.

The paper aims to describe the approach used for protection, control and metering of the electrical tie lines (OHLs) in the Romanian Power System at the 400 kV and 220 kV.

## KEYWORDS

Protection, control, metering.



## 1. THE ARCHITECTURE OF THE PROTECTION AND CONTROL SYSTEM OF AN INTERCONNECTION SUBSTATION

The 400 kV and 220 kV substations of the Romanian transmission network are provided with a control, protection and automation system, made with numerical technology equipment, hierarchical, decentralized and redundant.

At the substation level, the communication between the system components will use the IEC 61850 protocol.

The control subsystem assembly (command, supervision, remote control) of the substation is composed of the following equipment:

- 2 process computer (located in the control room) for storing and processing data specific to the station management process - UCCP 1/2
- two operator workstations (HMI) of the substation management subsystem, (located in the control room), with general substation management functions - UCCS 1/2
- interface equipment for data processing and transmission to the remote control centers to which the substation is subordinated (gateway), having as basic functions: commands transmission, information processing, data exchange with the remote control centers.
- redundant optic fiber network for the management of control and protection system, including switches with switching functions and priority management, "as a rule" ring type Fiber Optic ETHERNET 100 MBps IEC 61850-8-1, capable of transmitting a data flow having the speed of 10/100Mbps;
- 2 bay control units (BCU) in each bay
- 1 BCU for cooling adjustment and monitoring on each transformer unit;
- 1 BCU for general station signals (BCU Auxiliares Bay Computers) (telecommunications, Slc.c. and c.a., anti-burglary);
- 1 unit for protection parametrization - UPP (for evaluation, registration, management of data from the digital relays, located at National Dispatching center and SSCPA, connected to the UPP in the station;
- UPP located in the station, intended for adjustment and analysis activities of the control-protection system, which can access the BCUs and the protection systems
- 4 communication interfaces, on 2 communication flows to ensure redundancy, necessary for communication with the communication equipment from remote.
- two GPS synchronization modules for the entire system;

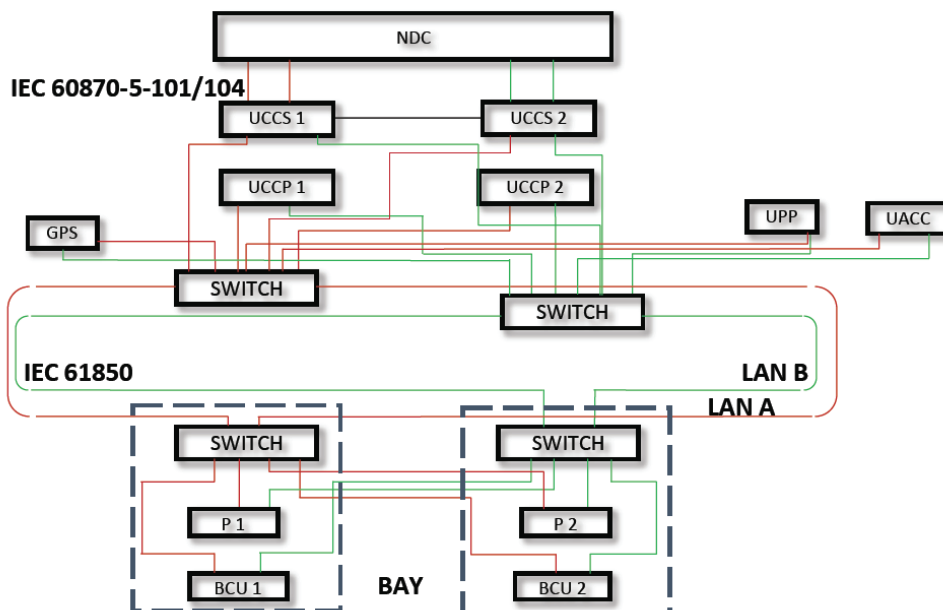


Figure 1. The simplified architecture of the control and protection system of a Romanian transmission substation





## 2. PROTECTION AND CONTROL FUNCTIONS OF A TRANSMISSION TIE LINE

The purpose of this paragraph is to describe the protection and control functions, implemented in the corresponding protection and control systems used for protecting and monitoring electrical overhead lines (OHLs) in the Romanian Power System at the 400 kV, 220 kV and 110 kV voltage levels. These modern techniques also apply to the tie lines of the electrical transmission network (400 kV OHLs).

400 kV, 220 kV and 110 kV electrical substations belonging to Transelectrica SA (Transmission and System Operator of Romania) are provided with an integrated command, control, protection and automation system made in numerical technology, hierarchical, decentralized, redundant and open. The integrated command, control, protection and automation system of a 400 kV, 220 kV and 110 kV cell (line/coupling) will be composed of a command and control subsystem and a protection and automation subsystem (including teleprotection system).

Command and control subsystem performs all the typical functions of supervisory control and data acquisition for the primary equipment in 400 kV, 220 kV and 110 kV line cells. The system will be open both hardware and software. For the voltage level of 400 kV, 220 kV and 110 kV, control and data acquisition related to the cell are included in control numerical terminals [4].

Numerical protection terminals include all or a big part of the following protection functions:

- distance protection function [21]
- non-directional phase and ground overcurrent protection function [50/50N, 51/51N]
- temporized directional ground overcurrent protection function [67N]
- differential protection [87L]
- under frequency protection function [81U]
- temporized over voltage protection function [59]
- power swing blocking protection function [68]
- out of step protection function [78]
- switch on to fault protection function [50HS]
- autoreclose protection function [79]
- synchronism control function [25]
- data recording: recording events, faults records, oscillograms, fault locator.

The numbers in the parenthesis in the list above represent American National Standards Institute (ANSI) device function numbers.

A one-line diagram showing typical protection functions included in a 400 kV tie line protection system is shown in Fig. 1.

In the integrated command, control, protection and automation system of the station, communication between system components is using IEC 61850 protocol. Remote control from dispatcher steps territorial/ Central is using IEC 60870-5-101 and IEC 60870-5-104 protocols.

In Romanian Electrical Power System (EPS) distance protections are widely used as main protection for long transmission power lines. A typical characteristic of a distance protection is shown in Fig.3. Line differential protections are used for protecting short transmission power lines.

Modern numerical protection systems have numerous integrated protection functions, including also power-swing blocking and out of step. These functions are very important for 400 kV OHLs, even more so for the tie lines.

The main purpose of the power-swing blocking function is to differentiate faults (1) from power swings (4) and block the distance protection from operating during stable or unstable power swings.

Most power-swing blocking elements are based on traditional methods that monitor the rate of change of the positive-sequence impedance [6].

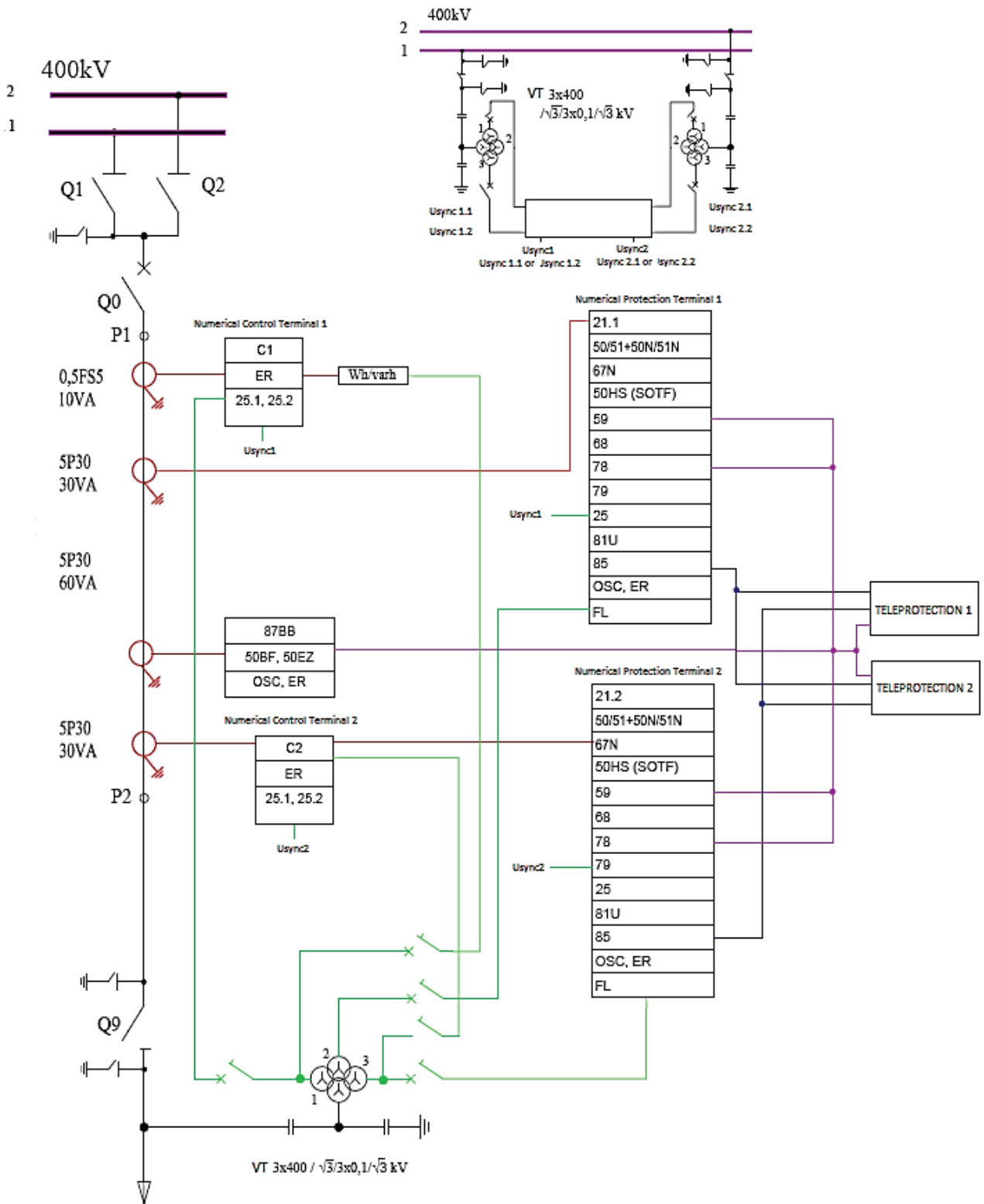


Figure 2. The Block diagram of a typical 400 kV tie line numerical protection terminal [5].

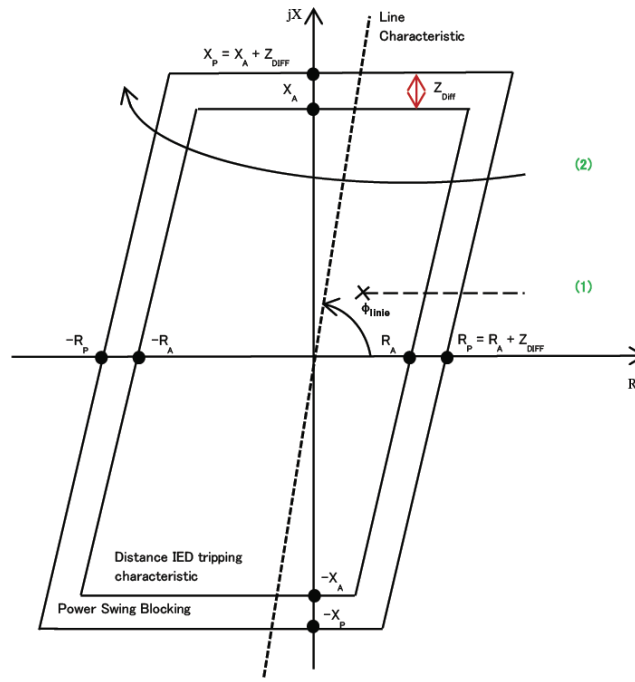


Figure 3. Polygonal impedance characteristic

### 3. TELEPROTECTION SYSTEMS

A distance protection can usually provide rapid tripping only for faults that are localized on about 80% of the transmission line, with faults beyond the reach point only being cleared after a time delay. Increasing the proportion of the line for which fast tripping is assured, can only be achieved at the cost of a loss of selectivity, therefore unwanted tripping for faults on adjacent circuits [7].

Communication links are generally provided to allow distance protection at the line ends to communicate with each other in order to determine the presence of an internal fault.

Alternatively, analog comparison protection systems cannot function at all without the aid of end-to-end communications.

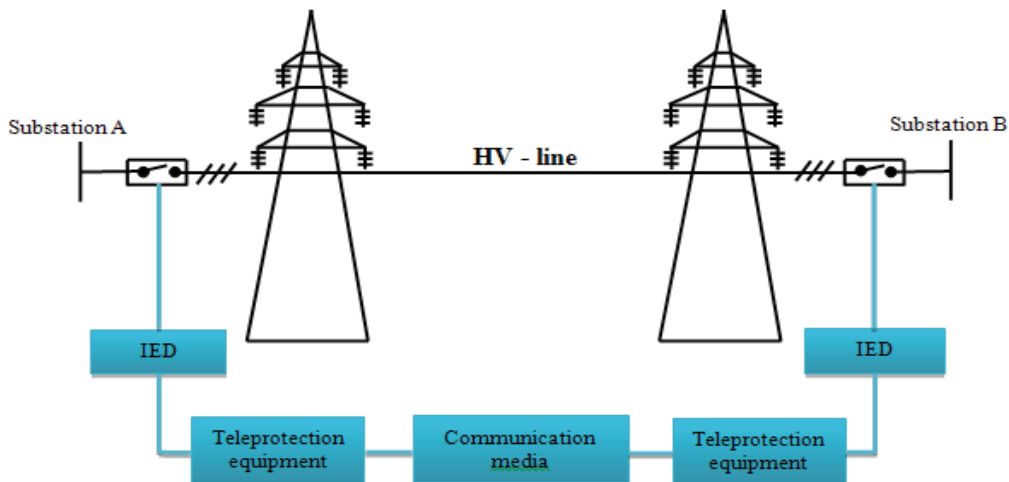


Figure 4. Teleprotection system architecture [8]

Teleprotection equipment use communication links to provide trip information to the remote IED. There are two main categories of teleprotection schemes used for transmission tie lines are "Direct" and "Permissive" [8].



### 3.1. Direct transfer tripping

This scheme does not need local information for a trip decision, therefore intertrip signals are sent directly to the master trip relay. The reliability of the communications circuit is directly related to the systems reliability [9].

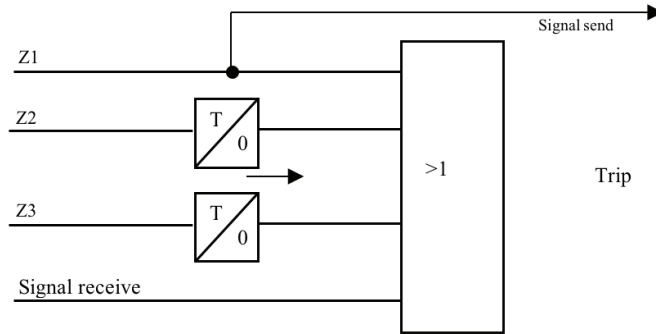


Figure 5. Direct Transfer Tripping [8].

It is used to send the tripping command to the remote end when one of the following protection function has elaborated a trip command: busbar differential, breaker failure, end zone.

### 3.2. Permissive teleprotection

Permissive schemes are more secure than direct transfer tripping schemes by supervising the received signal from the opposite line end which confirms that the fault is internal to the line, “permitting” accelerated tripping. Permissive schemes are characterised by both an initial send criterion and an additional tripping release criterion at the receiving end before accelerated tripping is permitted. The principal permissive schemes are permissive underreach transfer tripping (PUTT) and permissive overreach transfer tripping (POTT) [1].

#### 3.2.1. Permissive underreaching transfer tripping

A fault detected within a non-delayed underreaching distance protection zone set “forward” into the line, is definitively internal to the line. Under-reaching elements are used to key permissive trip to the remote terminal. The remote terminal is allowed to trip if it sees the fault as forward with its overreaching element and the remote end sees it with its under-reaching element [8].

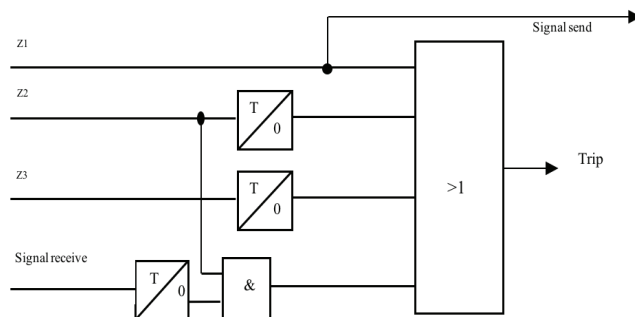


Figure 6. Permissive under-reaching transfer tripping [8]

## 4. SYNCHROPHASORS MEASUREMENT SYSTEM

Synchrophasor measurements and Wide Area Monitoring (WAM) systems are now widely deployed in power systems worldwide, and have proven to be a very valuable resource to observe and understand the dynamics of power systems. As power systems worldwide experience a transition to low carbon resources, the lower inertia and greater variability influence the dynamic characteristics of the power system, and the task of supervising dynamic characteristics of the power system is increasingly important.



According to the resources available, existing WAM system applications in current installations can be divided into off-line and real-time applications and more specifically into applications for monitoring, control, protection, model validation and post-mortem analysis [9].

## 5. METERING DEVICES FOR ACCOUNTING

Metering systems (meters and measuring transformers) owned by responsible TSO used for accounting of electricity must be certified by authorized organizations according to the requirements in force on the territory of the respective Party and properly sealed/marked.

Metering devices for accounting of electricity must be safeguarded by seals, keys, passwords etc. in order to avoid illegal access.

- Each Party will provide to the other (when replacement of any appliance is planned/performed):
- Metrological Test Certificate for meters and measuring transformers from the commissioning,
- Test reports of metering systems including information about type and their main characteristics and the results of the testing performed.

The Parties will perform bilateral or unilateral test (according to the mutual agreement for the respective test and both parties' availabilities for attendance the test) of metering systems in accordance with Annex 26 and the plan mutually agreed upon three months prior the test day. Changing of the scheduled test time must be agreed between the Parties at least 15 days prior to the test day. The results of the tests will be recorded in a Test Report.

Each Party is responsible for the protection of its own metering systems against:

- Changing of connection scheme,
- Unauthorized changing of the parameterization of its parts,
- Unauthorized access and the changing of data.

When a Party finds out an accidental deficiency of an element of a metering system it shall notify in written form the other Party about the deficiencies and the measures for their elimination in due time. The other Party shall answer immediately (not later than 24 h before) if its representatives will witness the check, which followed the repair/replacement the fault element. The responsible party is entitled to take an urgent repair of the fault element and to perform test settings. Afterword the check of the metering system shall be performed together with representatives of the other Party or without participation of the other Party in case when the other Party is not able to participate or in case of no written answer. After repair the responsible Party will send Test Report to the other Party, describing the encountered deficiencies and the measures undertaken.

When one of the Parties is going to perform maintenance works, the changing of metering system and/or changing of parameters, which may modify the accuracy and/or operation of the metering system, the Party responsible of the equipment will invite the representatives of the other Party, following the same procedure as per previous provision.

**Table 1.** Energy meters for accounting

	Type	Accuracy classes		Other nominal parameters	Accounting constant	
		Active energy	Reactive energy		Active energy	Reactive energy
<b>Main accounting energy meter</b>	three-phase meter for active and reactive energy, electronic, bi-directional	<b>0.2</b>	<b>2</b>	<b>3X58/100 V; 1(2) A</b>	kWh x 4000000	kvarh x 4000000
<b>Secondary accounting energy meter</b>	three-phase meter for active and reactive energy, electronic, bi-directional	<b>0.2</b>	<b>2</b>	<b>3X58/100 V; 1(2) A</b>	kWh x 4000000	kvarh x 4000000



### 6. CONCLUSION

Modern tie lines protection IEDs include a large number of additional protection elements, control and monitoring functions, which provide the user with almost unlimited flexibility to design secure and dependable protection and control schemes.

Modern applications for the protection of transmission lines are of big interest to users as almost all numerical protective relays now give the user the ability to either modify the existing protection and control logic inside the relay or add specific logic tailored to the user's requirements. This advancement has enabled the user to implement a whole host of tripping, transfer, monitoring and control schemes as part of a custom made logic inside the main protective relay thus allowing the elimination of external relays, auxiliary relays, timers, and wiring. Whether they are installed in new substations or as retrofits in old substations, transmission line multifunctional relays can be successfully applied to satisfy the protection, control and monitoring requirements and the choice of implementing those modern features depends largely on the power system operating requirements, and the user comfort level with modern relays.

### BIBLIOGRAPHY

- [1] I. C. Constantin, I. M. Dragomir, "Transmission Power Line protection using numerical terminals", CNEE 2015.
- [2] M. S. Sachdev, S. R. Aggarwal, C. Diaconu, H.-J. Hermann, S.-H. Kang, N.N. Misra, W. Offhaus, R. Simon, S. Troedsson, Corresponding Members: R. Chano, R. Cormack, S. Kim, P. Mysore, B. Sparling, P. Stewart, M. Yalla, "Modern Techniques for Protecting, controlling and monitoring power transformers", Cigré Study Committee B5 Working Group B5.05 Report, CIGRE June 2011.
- [3] I.C. Constantin, S. St. Iliescu, "Automatic Voltage Regulation of the Transformer Units Implemented in Digital Multifunction Protection Systems", OPTIM 2012.
- [4] Transelectrica SA - Internal Technical Standard of CN Transelectrica SA, "Details and specifications of equipment for the command, control, protection and automation system for the 400 kV, 220 kV and 110 kV voltage levels for OHL / UEL / couple on upgraded electric substations, according to primary schemes", 2014.
- [5] Florin Balasiu, "Numerical Protection and Control Systems in Transmission Substations", 2009
- [6] Working Group B5.15 CIGRE. "Modern Distance Protection Functions and Applications" (359, October 2008).
- [7] "Network Protection & Automation Guide: Protective Relays, Measurement & Control", ISBN: 978-0-9568678-0-3, May 2011.
- [8] A. Iamandi, I.C. Constantin, "Communications schemes used for transmission power lines", CIGRE September 2017.
- [9] CIGRE, Wide Area monitoring systems - support for control room applications, Reference: 750, 2018.





# Algorithm for Calculation of Line Distance Protection Settings

[vladimer.popkhadze@gse.com.ge](mailto:vladimer.popkhadze@gse.com.ge)

**VLADIMER POPKHADZE**  
*Georgian State Electrosystem*

**Georgia**

## SUMMARY

The problem of fast fault clearance and selective tripping terms are the most important challenge for all grid. To fulfil relay protection requirements, grid challenge may divide into couple of different issue, reliable protection settings and fast and accurate devices, that provide fast and selective tripping of a fault. This paper provides an algorithm for calculation of line distance protection settings, three forward zones, that perfectly fit the grid, with selective time delay.

The basic principle of distance protection involves the division of the voltage by the measured current at the relaying point. The result implies, that the relay measures ohmic value of fault, instead of physical impedances of elements.

To understand working principle of the algorithm, by default, calculation includes three forward zone settings. Settings calculation takes place in max\_situation\_for\_the\_line, but sensitivity checks in min situation for the Line, which in result take account contribution factors of currents.

An important feature of Calculation second and third zone settings are their matching with adjacent elements' (such as Line, AT, TR ...) distance protection settings, on a step-by-step basis.

Setting matching implies to use already calculated adjacent element settings in corresponding formula.

Using protection settings instead of physical impedances of elements, gives us an opportunity to always meet the selectivity step.

## KEYWORDS

Max situation for the line; Min situation for the line; Contribution factors of currents; Settings Matching; Adjacent Element; Selectivity Step; Step-by-step basis.



## 1. ZONE SETTINGS

Zone 1 has standard frame (75÷85)-% of the protected line.

For Zone 2, In order to find optimal values for both impedance and time, matching starts from the setting which has lowest impedance and process continue on a step-by-step basis, until the sensitivity requirement not met.

The calculation of Zone 3 requires complex approach; It has also back up protection function for adjacent elements, but in order to avoid miscoordination it should not exceed the Load impedance. Each point of the Grid includes different settings and contribution factors of currents, thus in some case zone 3 may not be back up protection for some adjacent element, in another case may exceed Load impedance altogether.

### Zone 1

Zone 1 has no time delay, so it should not operate beyond the remote bus.

$$\begin{aligned} R_{1S} &= K1 * R_{Line} \text{ (Ohm)} \\ X_{1S} &= K1 * X_{Line} \text{ (Ohm)} \\ Z_{1S} &= \sqrt{R_{1S}^2 + X_{1S}^2} \text{ (Ohm)} \\ T_{1S} &= 0 \text{ (Sec)} \\ \varphi &= \arctg \frac{X_{Line}}{R_{Line}} \text{ (Deg)} \end{aligned}$$

$K1$  – Reliability factor; Range (0,75-0,85) in order to limit zone 1 operate distance due to no time delay;

$R_{1S}$ ;  $X_{1S}$ ;  $Z_{1S}$  – Protected line zone 1 settings; Respectively resistance, reactance and impedance;

$R_{Line}$ ;  $X_{Line}$  – Protected line parameters; Respectively resistance and reactance;

$T_{1S}$  – Zone 1 timer;

$\varphi$  – Protected line angle.

### Zone 2

In general case, distance protection is a function that is used in 110 kV voltage lines and above. So that we can easily find ending points for this protection function. For example: last point for distance protection could be a step-down transformer (from the grid side), in case of single ended point there is no need to have a direction, in another case direction is required.

On the first step, we should find distance protection settings matching by transformer impedance. Impedance is used in case of transformer does not have distance protection function, in another case we use distance protection settings of TR, rather than impedance.

Protection settings for matching process, in case there are missing second and third zone for adjacent elements.

Zone 2

$$\begin{aligned} R_{2S} &= R_{1S} + \frac{K1 * R_{TR}}{K_{cont}} \text{ (Ohm)} \\ X_{2S} &= X_{1S} + \frac{K1 * X_{TR}}{K_{cont}} \text{ (Ohm)} \end{aligned}$$

Zone 3

$$\begin{aligned} R_{3S} &= R_{1S} + \frac{1,2 * R_{TR}}{K_{cont}} \text{ (Ohm)} \\ X_{3S} &= X_{1S} + \frac{1,2 * X_{TR}}{K_{cont}} \text{ (Ohm)} \end{aligned}$$



### Step 1:

There is need to be checked zone 2 result by matching to all adjacent elements' zone 1 settings (from lowest to highest, on a step-by-step basis).

$$R_{2S} = R_{1S} + \frac{K2 * R1_{i Adj.Elem.Set}}{K_{cont}} \text{ (Ohm)}$$

$$X_{2S} = X_{1S} + \frac{K2 * X1_{i Adj.Elem.Set}}{K_{cont}} \text{ (Ohm)}$$

$$Z_{2S} = \sqrt{R_{2S}^2 + X_{2S}^2} \text{ (Ohm)}$$

$$T_{2S} = T_{Adj.Elem.set} + \Delta t \text{ (Sec)}$$

$K2$  – Reliability factor; range - (0,75-0,85);

$K_{cont}$  – Contribution factor of currents;

$R_{2S}$ ;  $X_{2S}$ ;  $Z_{2S}$  : Protected line zone 2 settings; respectively resistance, reactance and impedance;  $R1_{i Adj.Elem.Set}$ ;  $X1_{i Adj.Elem.Set}$  – Adjacent elements' Zone 1 settings; respectively resistance and reactance;

$T_{Adj.Elem.set}$  – The highest timer value of the adjacent elements' those settings, where protected line Zone 2 is sensitive.

$\Delta t$  – Time interval.

Zone 2 has to be sensitive, when short circuit take place at the end of the protected line.

$$Z_{2S(sens)} = \frac{Z_{2S}}{Z_{Line}}$$

$Z_{2S(sens)}$  – Zone 2 sensitivity factor;

### Step 2:

After tested all elements, if the sensitivity requirement not met,  $Z_{2S(sens)} < K_{sens(Z_2)}$ , Setting has to be calculated by adjacent element lowest Zone 2 setting.

$$R_{2S} = R_{1S} + \frac{K2 * R2_{1 Adj.Elem.Set}}{K_{cont}} \text{ (Ohm)}$$

$$X_{2S} = X_{1S} + \frac{K2 * X2_{1 Adj.Elem.Set}}{K_{cont}} \text{ (Ohm)}$$

$$Z_{2S} = \sqrt{R_{2S}^2 + X_{2S}^2} \text{ (Ohm)}$$

$$T_{2S} = T_{Adj.Elem.set} + \Delta t \text{ (Sec)}$$

$R2_{1 Adj.Elem.Set}$ ;  $X2_{1 Adj.Elem.Set}$  – lowest impedance from all adjacent elements' zone 2 settings.

### Step 3:

After matching with lowest impedance from all adjacent elements' zone 2 settings, if sensitivity requirement not met,  $Z_{2S(sens)} < K_{sens(Z_2)}$ , then setting must be calculated by sensitivity requirement.

$$R_{2S} = K_{sens(Z_2)} * R_{Line} \text{ (Ohm)}$$

$$X_{2S} = K_{sens(Z_2)} * X_{Line} \text{ (Ohm)}$$

$$Z_{2S} = \sqrt{R_{2S}^2 + X_{2S}^2} \text{ (Ohm)}$$

$$T_{2S} = T_{Adj.Elem.set} + \Delta t \text{ (sec)}$$



$K_{sens(Z_2)}$  – Sensitivity factor for Zone 2;

$R_{Line}; X_{Line}$  – Protected line parameters; respectively resistance and reactance;

In case of calculation Zone 2 time delay, we have to take account all adjacent element settings (all three zones, with contribution factors of currents) and find minimum best time setting, which operates the relay, according to selectivity requirement.

### Zone 3

There is no specific requirement for zone 3.

Initially, zone 3 must be calculate by matching of the highest zone 2 impedance from all adjacent element.

$$R_{3S} = R_{1S} + \frac{K3 * R2_{max Adj.Elem.Set}}{K_{cont}} \text{ (Ohm)}$$

$$X_{3S} = X_{1S} + \frac{K3 * X2_{max Adj.Elem.Set}}{K_{cont}} \text{ (Ohm)}$$

$$Z_{3S} = \sqrt{R_{3S}^2 + X_{3S}^2} \text{ (Ohm)}$$

$$T_{3S} = T_{Adj.Elem.set} + \Delta t \text{ (sec)}$$

K3 – Reliability factor; range - (0,75-0,85);

$R2_{max Adj.Elem.Set}; X2_{max (Adj.Elem.Set)}$  – Active and Reactive impedances, from all adjacent elements', which has highest impedance of zone 2 settings.

In case of calculation Zone 3 time delay, we have to take account all adjacent element settings (all three zones, with contribution factors of currents) and find minimum best time setting witch operate relay according to selectivity requirement.

To find best value for protected line zone 3, impedance have to be changed between upper and lower ranges.

1. Upper range: from lowest zone 3 impedance of adjacent element to highest zone 3 impedance of adjacent element, and if the protected line zone 3 impedance does not exceed load impedance, then by load impedance.

$$R_{3S} = R_{1S} + \frac{K3 * R3_i Adj.Elem.Set}{K_{cont}} \text{ (Ohm)}$$

$$X_{3S} = X_{1S} + \frac{K3 * X3_i Adj.Elem.Set}{K_{cont}} \text{ (Ohm)}$$

$$Z_{3S} = \sqrt{R_{3S}^2 + X_{3S}^2} \text{ (Ohm)}$$

$$T_{3S} = T_{Adj.Elem.set} + \Delta t \text{ (Sec)}$$

2. Lower range: from highest zone 2 impedance of adjacent element, to lowest zone 2 impedance of adjacent element.

$$R_{3S} = R_{1S} + \frac{K3 * R2_i Adj.Elem.Set}{K_{cont}} \text{ (Ohm)}$$

$$X_{3S} = X_{1S} + \frac{K3 * X2_i Adj.Elem.Set}{K_{cont}} \text{ (Ohm)}$$

$$Z_{3S} = \sqrt{R_{3S}^2 + X_{3S}^2} \text{ (Ohm)}$$

$$T_{3S} = T_{Adj.Elem.set} + \Delta t \text{ (Sec)}$$

Change Setting between upper and lower ranges gives us all available matching results, that gives us opportunity to observe each setting and appropriate time delay. This investigation leads us to easily find acceptable settings.



### Method of calculation Time Settings

Example:

Calculation principle of time setting for "Line 1".

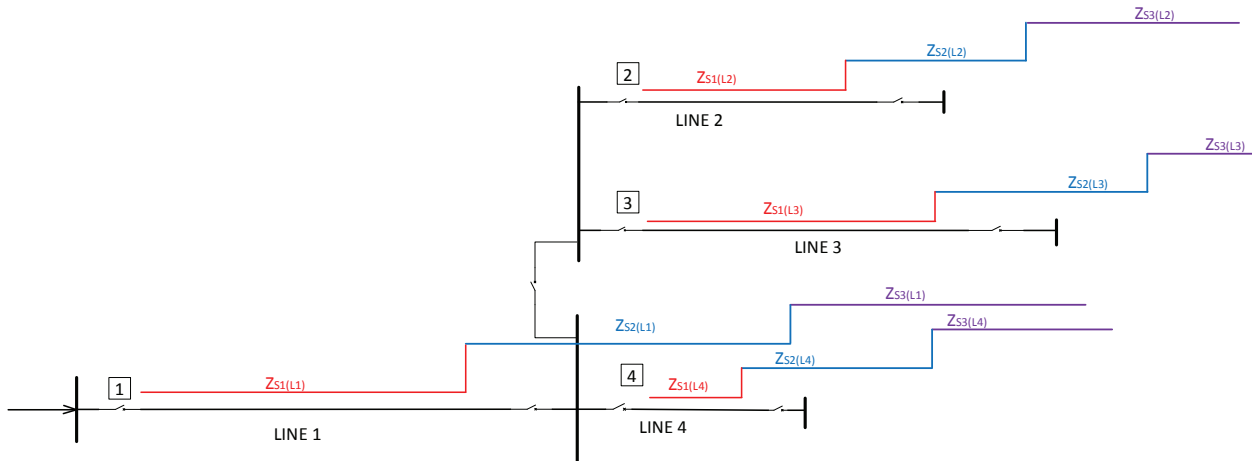


Figure 1. Calculation of Time delay setting

Generally, Zone 1 reach setting is up to 80% of the protected line impedance, thus zone 1 time setting is 0-sec.

Zone 2 timer.

Let's say, Zone 2 impedance setting matches to "Line 2" zone 1 setting.

As shown in the capture 1, Zone 2 impedance is sensitive into "Line 2" Zone 1, into "Line 3" Zone 1 and into "Line 4" Zone 2, thus "Line 1" Zone 2-time delay setting have to be calculated using maximum time setting from "Line 2" Zone 1, "Line 3" Zone 1, "Line 4" Zone 2 and time selectivity step.

Zone 3 timer.

Zone 3 impedance setting calculated by "Line 3" zone 2 setting.

As shown in the capture 1, zone 3 impedance is sensitive into "Line 2" zone 3, into "Line 3" zone 2 and into "Line 4" zone 3, thus "Line 1" zone -time delay setting has to be calculated using maximum time setting from "Line 2" Zone 3, "Line 3" Zone 2, "Line 4" Zone 3 time selectivity step.

### Load impedance

Load Factor equation:

$$Z_{Load} = \frac{U_{min}\%/100 * U_n}{1,73 * I * K_{Load}}$$

$U_{min}\%/100$  – Min voltage value in percent divided by 100;

$U_n$  – Nominal voltage value;

$I$  – Load Current value;

$K_{Load}$  – Load Factor;

### Contribution factors of currents

Contribution factors of currents are division of the currents of protected line and adjacent element, when three phase short circuit take place at the end of the adjacent element.

$$K_{cont} = \frac{I_{Prot.Line}}{I_{Adj.Elem.}}$$



$I_{Prot.Line}$  – protected line current;

$I_{Adj.Elem.}$  – adjacent element current;

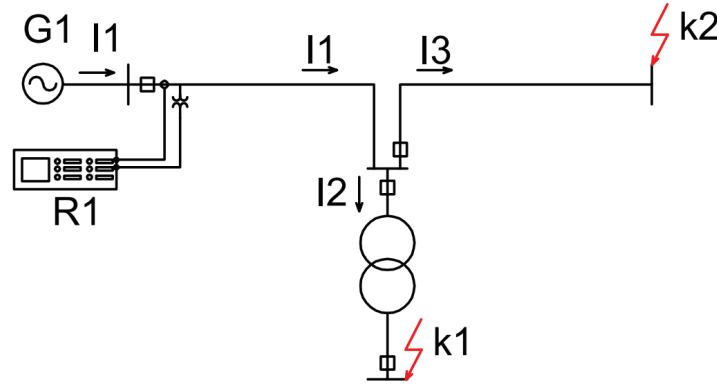


Figure 2. Single Ended Equivalent circuit for calculation of contribution factors of currents

Example: On Capture 2, in equivalent scheme

$$K_{cont1} = \frac{I_{Prot.Line}}{I_{Adj.Elem.}} = \frac{I_1}{I_2} = 1$$

$$K_{cont2} = \frac{I_{Prot.Line}}{I_{Adj.Elem.}} = \frac{I_1}{I_3} = 1$$

In both cases, contribution factor is equal to 1, because single ended shceme.

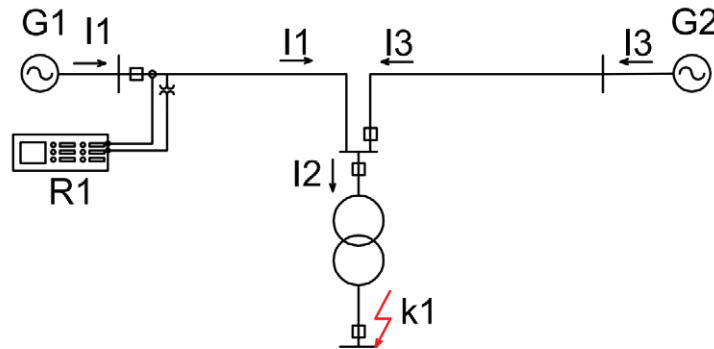


Figure 3. Double Ended Equivalent circuit for calculation of contribution factors of currents

$$K_{cont1} = \frac{I_{Prot.Line}}{I_{Adj.Elem.}} = \frac{I_1}{I_1 + I_3} \neq 1$$

Contribution factors of currents must be calculated individually for all adjacent elements, by manually. Take account different situations of the grid.



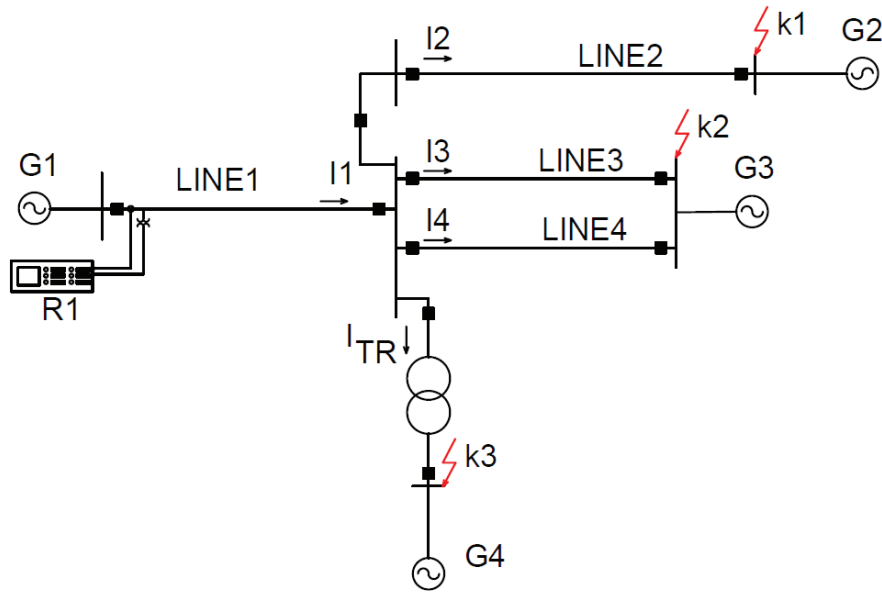


Figure 4. Scheme to define currents' contribution factors

Contribution factors of currents:

$$K_{contL2} = \frac{I_1}{I_2} - \text{when three phase short circuit take place at K1;}$$

$$K_{contL3} = \frac{I_1}{I_3} - \text{when three phase short circuit take place at K2;}$$

$$K_{contL4} = \frac{I_1}{I_4} - \text{when three phase short circuit take place at K2;}$$

$$K_{contTR} = \frac{I_1}{I_{TR}} - \text{when three phase short circuit take place at K3;}$$

Currents are taken account at the same voltage.

Max situation for the line implies the grid conditions, when maximum short circuit current path through the protected line, but Min situation for the line implies the grid conditions, when minimum short circuit current path through the protected line.

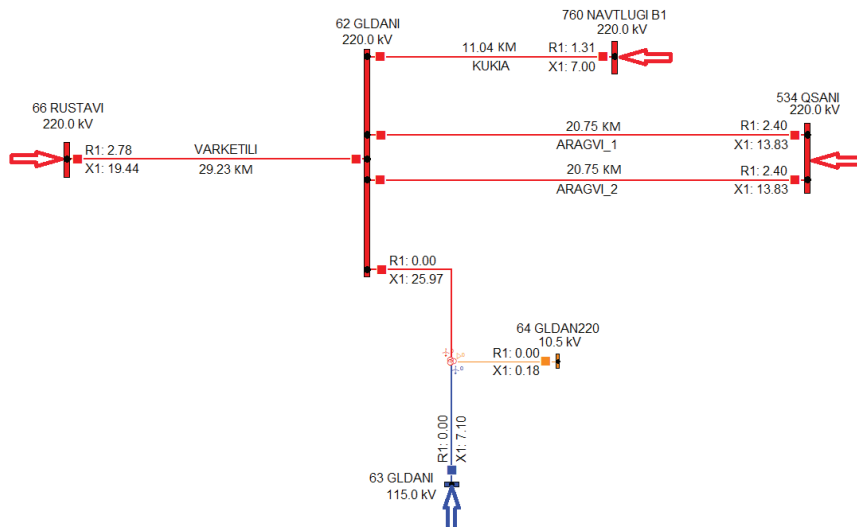


Figure 5. Network diagram for Example 1



### Example 1:

L1 – “VARKETILI”

L2 – “KUKIA”

L3 and L4 – “ARAGVI 1” and “ARAGVI 2”

Example 1 describes distance protection settings for line “VARKETILI” 220 kV. (Figure 5)

Example describes real case for 220 kV line which is situated in the east of Georgia.

Protected line “VARKETILI” electrical parameters:

$$L = 47 \text{ km AC} - 500/64 \text{ mm}^2 \quad r_1 = 0,059 \text{ Ohm/Km} \quad x_1 = 0,413 \text{ Ohm/Km}$$

$$R1 = 2,78 \text{ Ohm}$$

$$X1 = 19,48 \text{ Ohm}$$

$$Z1 = 19,6 \text{ Ohm}$$

To simplify our calculation lets take account only impedances. It will be less accurate, but in comparison, it gives us nice image.

Adjacent element distance protection settings and contribution currents in max and min situations.

Line “KUKIA”

$R1 = 1,05 \text{ Ohm}$	$R2 = 2,5 \text{ Ohm}$	$R3 = 6 \text{ Ohm}$
$X1 = 5,05 \text{ Ohm}$	$X2 = 15 \text{ Ohm}$	$X3 = 60 \text{ Ohm}$
$Z1 = 5,16 \text{ Ohm}$	$Z2 = 15,2 \text{ Ohm}$	$Z3 = 60,3 \text{ Ohm}$
$T1 = 0 \text{ Sec}$	$T2 = 0,3 \text{ Sec}$	$T3 = 2 \text{ Sec}$

$$K_{cont.L2.max} = \frac{2693}{6253} = 0,431$$

$$K_{cont.L2.min} = \frac{1864}{6318} = 0,295$$

Double circuit lines “ARAGVI 1” and “ARAGVI 2”

$R1 = 2 \text{ Ohm}$	$R2 = 4,1 \text{ Ohm}$	$R3 = 8 \text{ Ohm}$
$X1 = 11,5 \text{ Ohm}$	$X2 = 23 \text{ Ohm}$	$X3 = 50 \text{ Ohm}$
$Z1 = 11,67 \text{ Ohm}$	$Z2 = 23,36 \text{ Ohm}$	$Z3 = 50,63 \text{ Ohm}$
$T1 = 0 \text{ Sec}$	$T2 = 0,3 \text{ Sec}$	$T3 = 2,5 \text{ Sec}$

$$K_{cont.L3,4.max} = \frac{2671}{1443} = 1,851$$

$$K_{cont.L3,4.min} = \frac{1339}{3347} = 0,4$$

AT 1

$R1 = 0,5 \text{ Ohm}$	$R2 = 1,5 \text{ Ohm}$	$R3 = 2,5 \text{ Ohm}$
$X1 = 21 \text{ Ohm}$	$X2 = 28 \text{ Ohm}$	$X3 = 50 \text{ Ohm}$
$Z1 = 21 \text{ Ohm}$	$Z2 = 28 \text{ Ohm}$	$Z3 = 50 \text{ Ohm}$
$T1 = 0 \text{ Sec}$	$T2 = 0,3 \text{ Sec}$	$T3 = 3 \text{ Sec}$

$$K_{cont.AT1.max} = \frac{2166}{2544} = 0,851$$

$$K_{cont.AT1.min} = \frac{1406}{3143} = 0,447$$



Poster Presentation: Algorithm for Calculation of Line Distance Protection Settings

In widespread quick calculation method, there are 0,8; 1,2 and 2 factors to find first, second and third zones. Results could be:

$$\begin{aligned} Z1 &= 0,8 * 19,6 = 15,68 \text{ Ohm} & T1 &= 0 \text{ Sec} \\ Z2 &= 1,2 * 19,6 = 23,52 \text{ Ohm} & T2 &= 0,3 \text{ Sec} \\ Z3 &= 0,8 * 19,6 = 39,2 \text{ Ohm} & T3 &= 0,6 \text{ Sec} \end{aligned}$$

In algorithm

$$Z1 = 0,8 * 19,6 = 15,68 \text{ Ohm} \quad T1 = 0 \text{ Sec}$$

According to currents' contribution factors, shortest element for distance relay is Line 3 and Line 4

$$Z2 = 15,68 + \frac{0,8 * 11,67}{1,851} = 20,72 \text{ Ohm}$$

Sensitivity:

$$Z2_{Sens} = \frac{Z2}{Z_{prot.Line}} = \frac{20,72}{19,6} = 1,06$$

Required sensitivity is 1,2 so another step is match to the Line 2's Zone 1.

$$Z2 = 15,68 + \frac{0,8 * 5,16}{0,431} = 25,259 \text{ Ohm}$$

Sensitivity:

$$Z2_{Sens} = \frac{Z2}{Z_{prot.Line}} = \frac{25,259}{19,6} = 1,288$$

Due to, zone 2 overreach in Line 3 and Line 4 zone 1 setting, time delay has to be accepted with Line 3 and Line 4 Zone 2 time delay. If we considered selectivity step 0,3 then

$$T2 = 0,3 + 0,3 = 0,6 \text{ Sec}, \text{ different from previous example } T2 = 0,3 \text{ Sec}$$

For zone 3 there, first step could be matching to the longest zone 2 setting, out of adjacent elements.

According to currents' contribution factors, the longest Zone 2 for distance relay has Line 2.

$$Z3 = 15,68 + \frac{0,8 * 15,2}{0,431} = 43,89 \text{ Ohm}$$

Sensitivity:

$$Z3_{Sens} = \frac{Z3}{Z_{prot.Line} + \frac{Z_{adjacent.Line}}{K1 * K_{cont.Elem.min}}} = \frac{43,89}{19,6 + \frac{5,16}{0,8 * 0,295}} = 1,06$$

Due to, zone 3 overreach in Line 3 and Line 4 zone 1 setting, time delay has to be accepted with Line 3 and Line 4 Zone 2 time delay. If we considered selectivity step 0,3 then

$$T3 = 2,5 + 0,3 = 2,8 \text{ Sec}, \text{ different from previous example } T3 = 0,6 \text{ Sec}$$

Below there are results from macro "CoLDPS2020" that take account principle of algorithm.

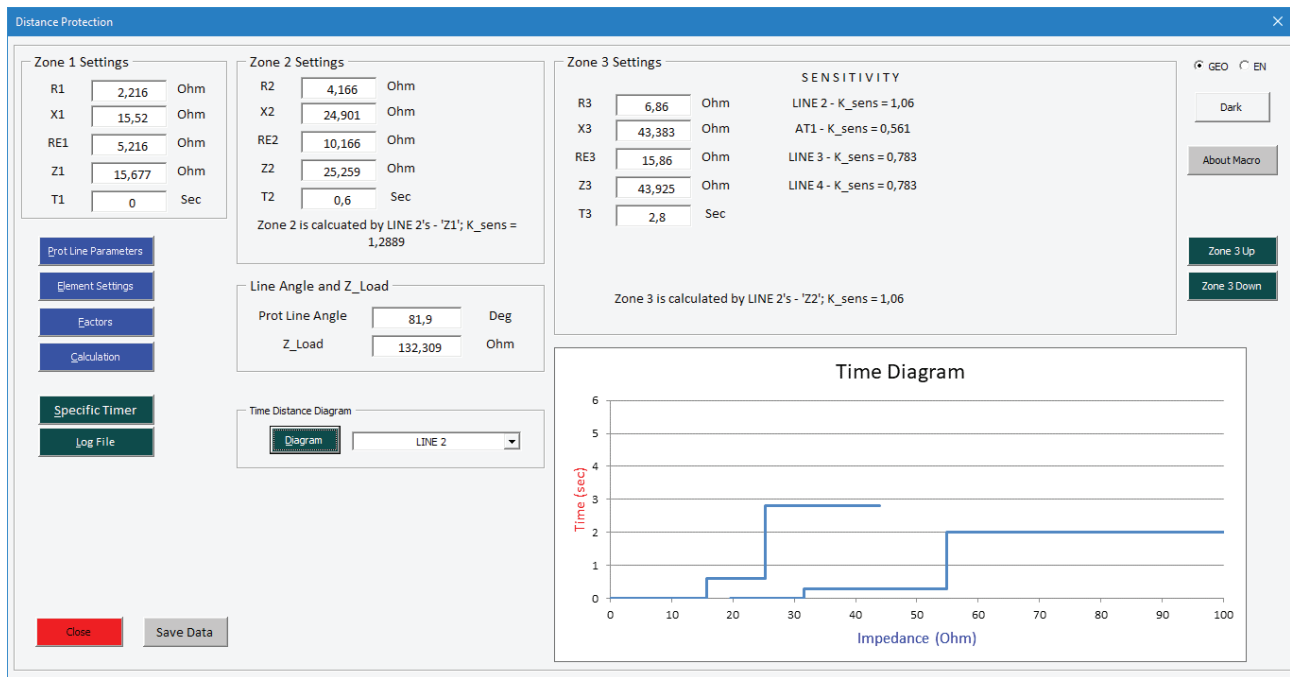


Figure 6. Distance Time diagram in case of Line 3,4

Figure 5 shows that zone 2 is calculated by matching with Line 2's Z1, due to meet the sensitivity requirement; Zone 3 is calculated by adjacent element highest zone 2 setting. In case of Zone 3 there are sensitivities, adjacent elements are considered.

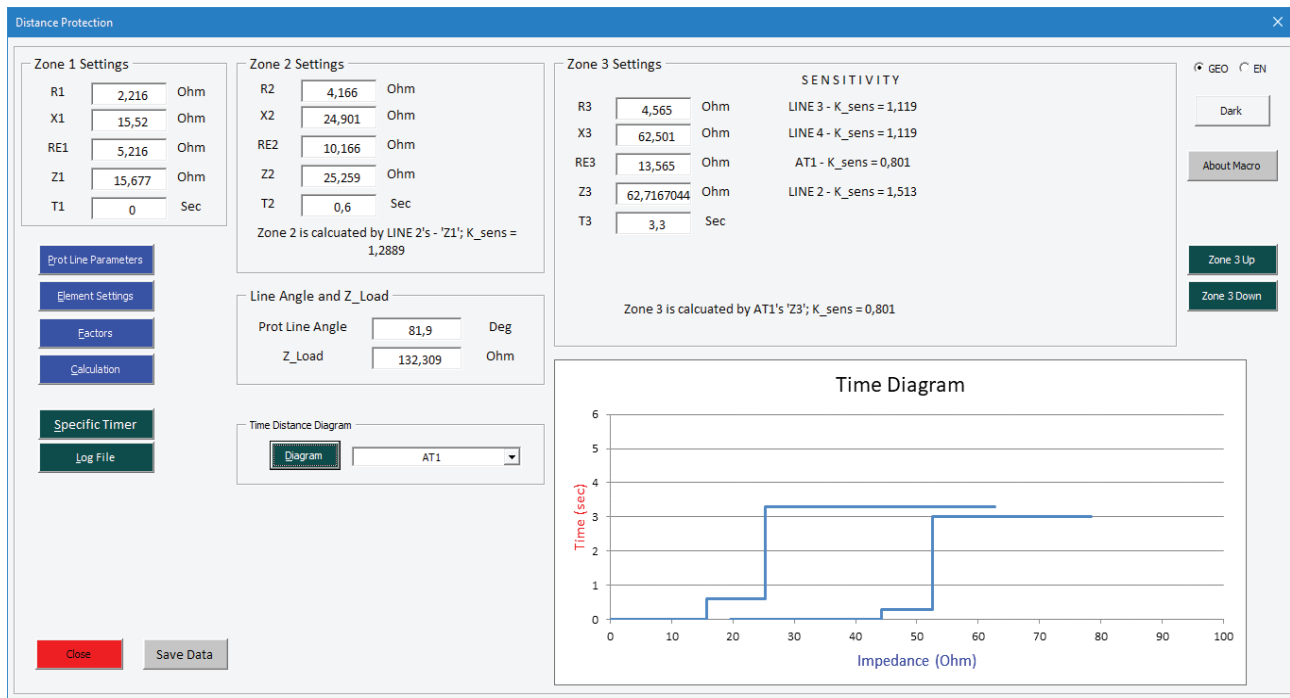


Figure 7. Zone 3 Up

Figure 6 shows how change third zone time delay T3 by increasing impedance "Upper Case".

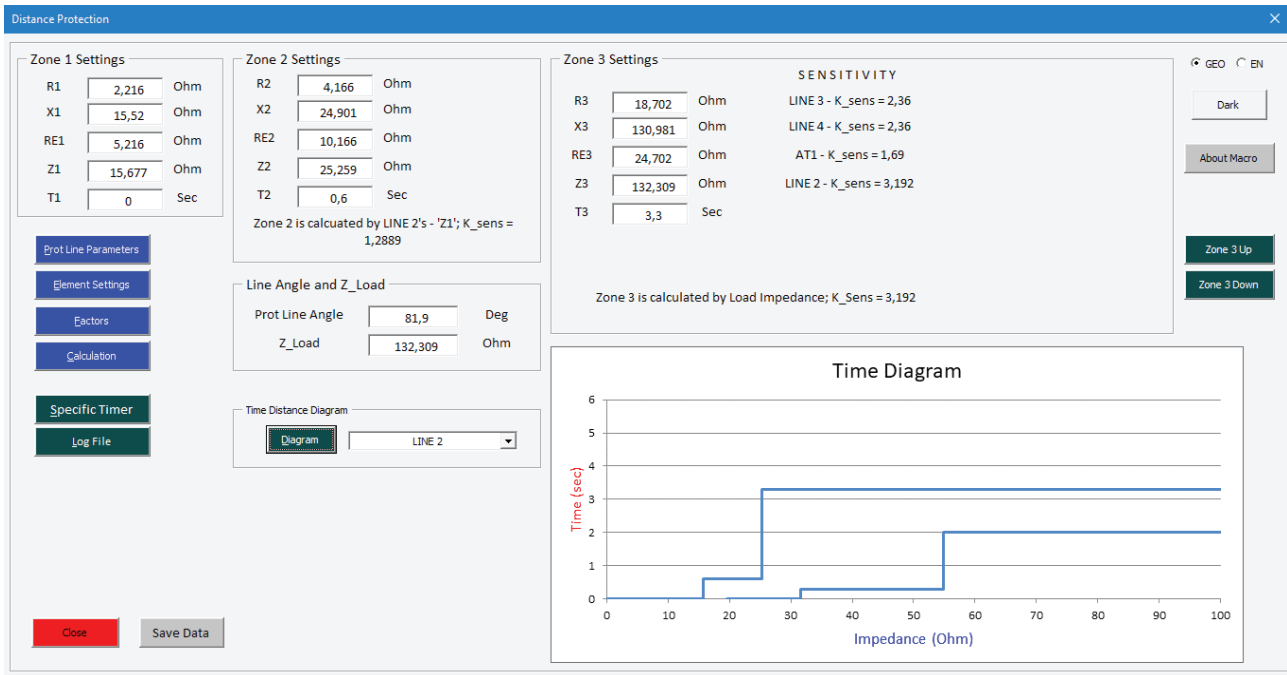


Figure 8. Zone 3 calculated by load impedance

Figure 7 shows upper limit of distance protection zone settings, that could be calculated by load impedance.

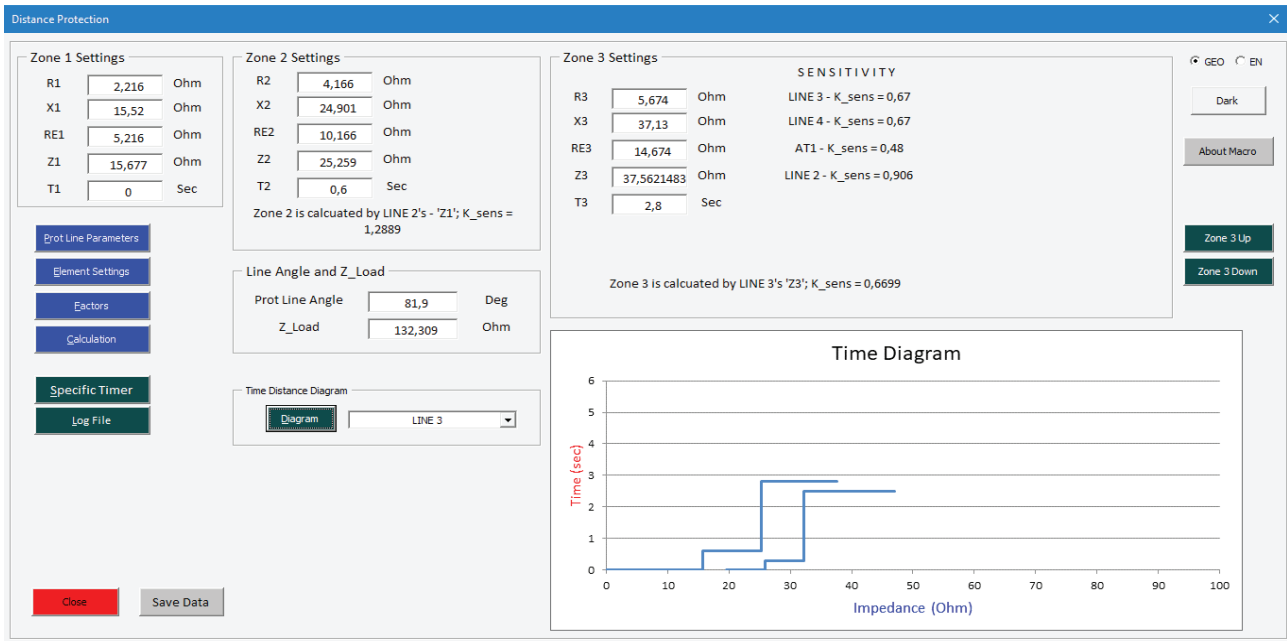


Figure 9. Zone 3 Down

Figure 8 shows how change third zone time delay T3 by decreasing impedance "Lower Case".



### CONCLUSION

Calculation of protection settings are quite complicated and requires routine calculation for different cases, that include a lot of factors and numbers. Thus, there is risk to make a mistake.

An algorithm for protection settings gives us an opportunity to check routine cases for any number of adjacent element and find sensitive and selective zone settings and their selective time delays.

Instead of using pure impedances of elements, algorithm include contribution factors of currents, that enable calculation process to adjust zone settings to the grid conditions.

CoLDPS (Calculation of Line Distance Protection Settings) algorithm enable user added to any relay protection software and then use relay protection settings to reduce calculation routine practice and time. Also, it has a function to save adjacent element and factors data for future reasons, that also reduce time of full calculation process.

### BIBLIOGRAPHY

- [1] PROTECTION GUIDELINES, ISSUE 7, REMOTE PROTECTION LINES 35-330 kV; 1996 (РУКОВОДЯЩИЕ УКАЗАНИЯ ПО РЕЛЕЙНОЙ ЗАЩИТЕ, ВЫПУСК 7, ДИСТАНЦИОННАЯ ЗАЩИТА ЛИНИЙ 35-330 КВ; 1996)
- [2] Network Protection & Automation Guide; 1987



**ENERGY  
TRANSITION**

**ORAL PRESENTATION**



ELECTRIC MACHINES AND  
POWER ELECTRONICS



ELECTRIC  
TRANSMISSION



AUTOMATION AND  
CONTROL

POWER  
GENERATION



ENERGY  
TRANSITION



DISTRIBUTION SYSTEMS  
AND SMART GRIDS



**11-12 OCTOBER 2023**



# Geopolitics Impact on Electrical Grids during Energy Transition

[rebolinimassimo@gmail.com](mailto:rebolinimassimo@gmail.com)**MASSIMO REBOLINI***Fellow Honorary Member CIGRE***Italy**

## SUMMARY

The development of renewable energies and the ecological transition towards a reduction of greenhouse gases in the atmosphere, with the aim of limiting the increase in global temperature of the planet to a value of 1.5 degrees Celsius, have given rise to a large amount of studies and essays on the topic of geopolitics and its importance in achieving the set goals. Geopolitical risk and its management has even entered the assessments of global industrial companies [1] while in the WEC's World Energy Issue Monitor 2022 Report, over 2,200 leaders of 100 countries globally reported that geopolitics is the key factor in the energy transition which creates more impact on the objectives and with a high degree of uncertainty [2].

Geopolitics is not an exact science but involves a complex of disciplines: polemology, history of political systems and their institutions, physical and political geography, demography, climate, energy technologies and their development, religion and even literature.

The article is divided into three parts: the first deals with the Geopolitics of Electricity, the second with the Geopolitics of Renewables and Energy Transition, and the third gives examples of geopolitical impacts on Transitions in the Italian Electricity System, also highlighting its role in the development of the Grid and its importance in predicting future dynamics. For Italy, we will consider four phases: the first from 1913 to 1948, the second from 1948 to 1988 characterised by the First Energy Transition: from Renewables (hydroelectric and geothermal) to Fossil (Oil); the third from 1988 to 2010 dealing with the Second Energy Transition: from Oil to Gas and finally from 2011 onwards the third Energy Transition awaiting us: from Fossil to Renewable.

The strongest impact of geopolitics is on the Scenarios and related models that all International Organisations (IEA, WEC) and Network Operators design for Network Planning. The events of recent years are a significant example of this: Pandemic in 2020-2021 and Russian-Ukrainian War (2014-2022). Figure 1 (taken from IEA GER2020) shows the percentage change in electricity demand from 1900 to 2020 and, as can be seen, is strongly characterised by geopolitical events or serious health events or economic crises worldwide.

## KEYWORDS

Geopolitics of Renewables, Energy Transition, Electricity Generation Sources.

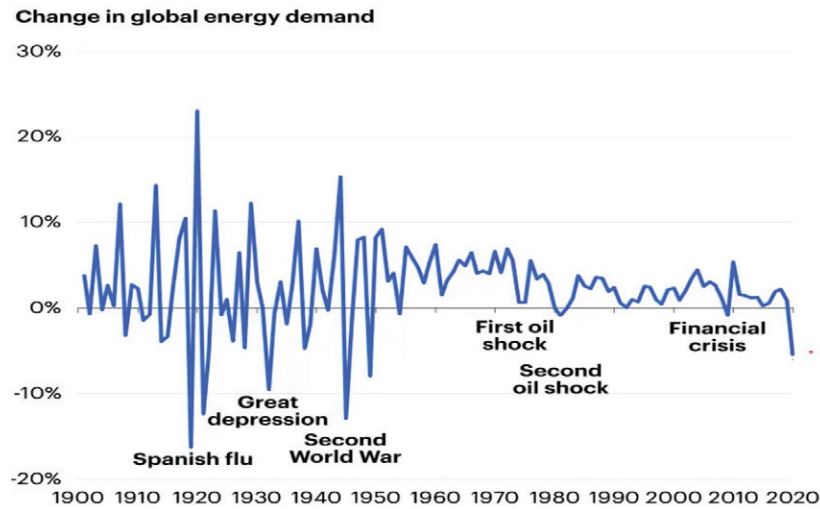


Figure 1. Change in Global Energy demand 1900-2020

## 1. GEOPOLITICS OF ELECTRICITY

Many articles, as is well known, deal with the Geopolitics of Energy Resources while recent studies deal precisely with the Geopolitics of Electricity and in particular Electricity Networks. Among all of them is reference [3] that emphasises interdependence, control of electricity flows and interconnections between countries as keys to interpretation to be analysed.

Although the shape of Electricity Networks defines both political and economic spaces, the geopolitical significance of electricity remains underestimated. The main driver for the considerations we will make are network interconnections that with cross-border links define new spaces and synchronous systems that form 'network communities' with a shared destiny not only in terms of electricity supply but also in terms of security and welfare. Worldwide, there are areas that are more interconnected and others less so. The latter regions will then become the site of geopolitical competitions and generate techno-economic spheres of influence. A corollary of this is that the vulnerability of states also depends on how robust and resilient the Electricity Grid is. The dynamics of interconnection development in the history of grids emerges primarily from political decisions related to the geographical location of sources for electricity generation: fossil fuels (coal, gas, oil) and water up to the current dynamics of capturing electricity from sun and wind. From a geopolitical point of view, the drivers for the development of interconnections can be summarised as follows:

1. technical and operational: interconnections improve the security and flexibility of the Grid by increasing its resilience to old and new risks whose triggers include cyberattacks, extreme weather events, earthquakes, technical failures, overloads and conflicts;
2. socio-economic: important factors linked to the Net are telecommunication and internet systems, logistics to provide drinking water, medical care; this gives insight into the fact that synchronous power networks create a community of common destiny by promoting a political and welfare order;
3. climatic and environmental: the expansion of generation from renewable sources which by their nature are intermittent and non-programmable creates changes in the topography and control of the grid not only in terms of space but also in the demand for electricity and in electricity markets, with consequent checks on the adequacy of the grid itself
4. geopolitical which are a key driver for the development of interconnections as they create a demarcation between the grid community and the outside world. The case of the connection of the Ukrainian network to the European network is a classic example. Another aspect to consider is, in contrast to this, the interest in developing connections that reinforce the influence and strength of states.

## 2. GEOPOLITICS OF RENEWABLES AND ENERGY TRANSITION

The diagram in Figure 2, taken from [4], summarises the complexity seen from a geopolitical perspective of useful resources for power generation. The scheme is applicable to all resources, including renewables, which must also consider Electricity System Technologies that are not immune from being impacted by their development and control in terms of security, reliability and resilience





to external events, not least those related to terrorist acts or armed conflicts. In the transition of the Italian Electricity System, the topic that in the outline is reported under the heading of Interstate Relations, which concerns geopolitical issues related to the Mediterranean and the impact on the implementation of interconnections between Italy and North Africa.

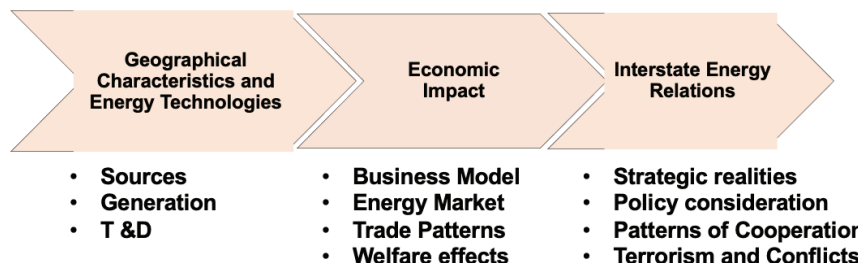


Figure 2. Geopolitics of Renewables (taken from D. Sholten Geopolitics of Renewables and revised by the author)

We highlight, by way of example, some critical geopolitical issues for which please refer to the report in ref.[5].

For RES technologies, Table 1 was drawn up, based on the IRENA platform available in [6], in which the number and percentages of patents registered by individual countries were highlighted for some applications. It was divided according to the percentages as of 2005 and the percentages assigned to 2021, where the total number of patents cumulated over the period 2000-2021 was also included. It can be clearly seen that in the economic phase dominated by globalisation, China is the country with the greatest dynamism in R&D, in all 4 technologies examined and enabling the new Energy Transition: Wind Power, Photovoltaics, Fuel Cells, Batteries. Research is an essential driver to implement new solutions without forgetting that it is only the first step of the so-called Technology Readiness Level.

Table 1- Number and percentages Patents assigned for Nations for FER Technologies											
Wind (175.686 patents at 2021)			Solar-FV (379.181 patents at 2021)			Fuel Cells (188.837 patents at 2021)			Batteries (508.310 patents at 2021)		
Nations	2005	2021	Nations	2005	2021	Nations	2005	2021	Nations	2005	2021
Germany	24%	5,3%	Japan	50%	14%	Japan	60%	32,2%	Japan	43%	21%
Japan	23%	6,2%	Corea Sud	11,5 %	10,8%	USA	14%	18,6%	SouthKorea	11,4%	10,2%
USA	10%	13,4%	USA	11%	15,7%	Germany	7%	6,6%	USA	15,6%	13,8%
China	5%	39%	Cina	7%	44,7%	SouthKorea	7%	9,5%	China	11%	44%
Russia	5%	2%	Germania	6,5%	3%	China	3%	20,1%	Taiwan	3,3%	1,9%
SouthKorea	5%	7,2%	Russia	1,5%	<1%	Canada	3%	3,2%	Australia	2,6%	<1%
Danmark	4,5%	3%	Olanda	1,5%	<1%	UK	2%	<1%			
UK	3%	1,4%	UK	1%	<1%	France	1%	<1%			
Spain	3%	3%	Australia	1%	1,3%	Taiwan	<1%	1,7%			
France	2%	<1%	Taiwan	<1%	3,6%						
Taiwan	<1%	1,4%									

Other critical issues on metals and materials that may affect and limit the transition have already been addressed in the article ref [7] and concern the materials needed to build generation plants, but also innovation on systems, components and equipment of electricity grids.

Finally, a recent IEA study [8] confirms China’s strong production capacity (among other things, dragged down by coal-fired generation) compared to European countries and North America in solar PV on every segment of the supply chain: Modules, Cells, Wafers and Polysilicon (Fig. 3). This, as the study points out, will require heavy investments to develop ‘in house’ or diversify ‘supply chains’ in this key technology for the energy transition.

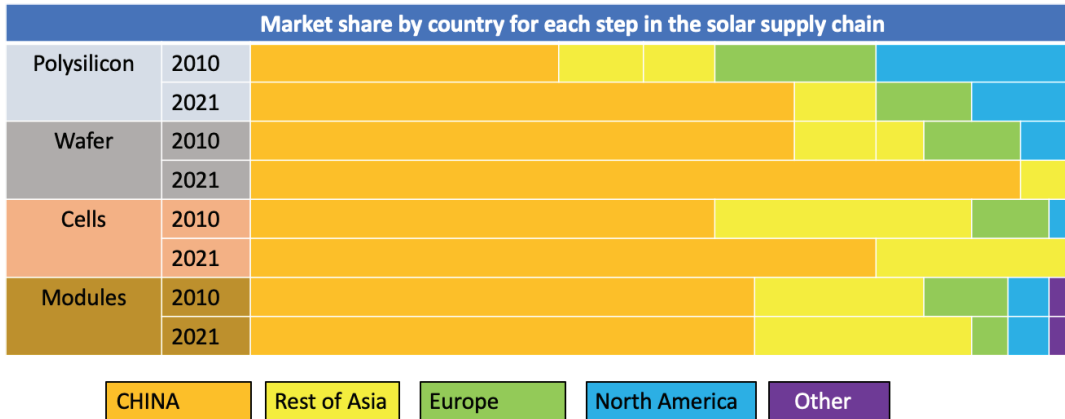


Figure 3. Market Share from 2010 to 2021 for Solar Plants in the World

Moreover, in order to achieve the reduction of CO2 emissions, it is necessary to have effective and efficient governance not only at the European but also at the global level. The institutional landscape has historically consisted of a multiplicity of multilateral or plurilateral or corporate bodies, in some cases reflecting inconsistent objectives. For instance, plurilateral organisations (a small circle of members) such as OPEC, GEFC have specific focus on energy resources, oil and gas respectively, while multilaterals such as IAEA and IRENA have specific focus on nuclear and renewables respectively. IRENA then intentionally uses the term Energy Transformation instead of Transition to emphasise the broader implications of the transition to a low-carbon energy phase.

IEA, which was founded in 1974 in the wake of the oil crisis, includes the OECD countries (in 2020 it comprised 30 member states and 8 associations) and finds criticism from non-members such as China and India. Political bodies are also differentiated into plurilateral (e.g. G7, G20) or multilateral such as UN Energy and UN SE4All (Sustainable Energy For All).

Moreover, the transition is declined differently in the various countries or regions (understood as vast geographical areas e.g. Europe, North America, etc.) having an overall impact at all levels: global, regional, national or local. The only mechanism that in the first place can create new connectivity and wider energy spaces is the development of new interconnection infrastructures between various states and their management in the planning of electricity grids so as to create new markets, institutional regulatory structures and promote the spread of new technologies.

### 2.1. Geopolitics and the Italian Electricity Grid 1913- 1948

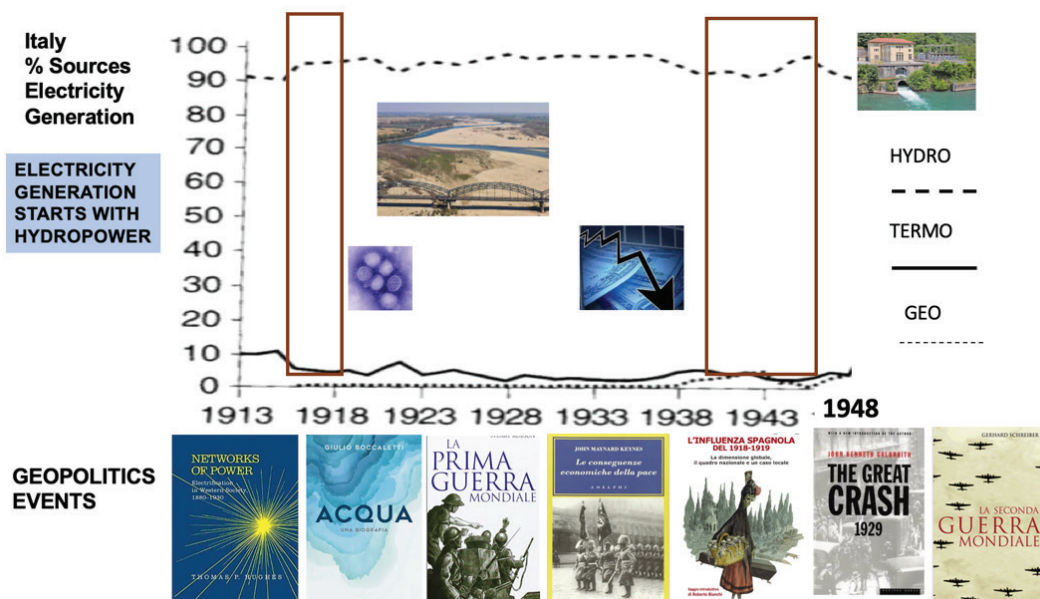


Figure 4. Geopolitics and Italian Electrical Grid



Figure 4 shows the percentage of electrical energy produced by source in our country from 1913 to 1948, while the horizontal axis shows the years with an indication of the major geopolitical events represented by books describing them.

After an initial period characterised by the war between Alternating Current and Direct Current, which is well described by T. Hughes in his book "Networks of Power", and which we can well say was also influenced by geopolitics, the first electricity grids became established. From a geopolitical point of view, this took place in a dramatic historical period characterised primarily by the First World War and the Spanish flu pandemic. Just as in the USA and Japan, in Italy too water management was at the centre of the first industrialisation that provided electricity for the construction of intermediate goods and machinery. It is worth remembering that in Italy, it was Edison that focused on the hydroelectric potential of the Adda River to power Milan's public transport system by electrifying it. The largest power station in Europe for the time was then built, capable of producing 10 MW, which went into service in 1898, and as early as 1900 hundreds of manufacturing companies, which still used steam engines, converted to using electric motors. In 1918, hydroelectric generation was 4100 GWh. In 1922, 1200 MW of power was hydroelectric versus 395 MW thermal. Two decades later in 1938, the installed power in Italy reached over 4000 MW, with a hydroelectric generation of 14580 GWh [9]. A more detailed technological description can be found in [10] where the electrification history of many countries in south-eastern Europe is also given. It should be noted that in Germany in 1932, generation exceeded 22129 GWh with a clear predominance of lignite power plants in which the country was rich and which led to a parallel technological development of machinery and thermoelectric plants; the first 20 MW thermoelectric power plant was the Elverlingen power plant which went into operation in 1914.

It should also be remembered that on the eve of the First World War, Great Britain had world dominance in coal production, the country supplied half of all internationally traded coal and held a virtual monopoly on the quality of hard, smokeless coal that is the fuel of choice for shipping. Britain was also the first country to grasp the link between oil, source control and power politics. As early as 1911 Winston Churchill, Lord of the Admiralty, lobbied hard to convert the navy's propulsion system from coal to oil. Also during this period, the rise of Tsarist Russia on world markets is worth mentioning. Concentrated in the Baku area of Azerbaijan, oil production took off under Ludwig Nobel, brother of Alfred Nobel (inventor of dynamite and the prize named after him). Under his leadership Russia became the world's second largest producer of crude oil, attracting new investors and operators to what became a Caucasian version of western Pennsylvania. This development in Russia will suffer a backlash following the events of the war and the subsequent period of civil war at home.

Germany's dependence on coal and iron was the reason at the 1919 peace conference to hit it with the cession of the Saar to France and other clauses penalising fossil resources with important geopolitical repercussions, which were amply highlighted by J. Maynard Keynes [11], whose rereading also opens up profound reflections on the current conflict between Russia and Ukraine, and which were among the causes of the Second World War. Boccaletti's [12] book on the dynamics and interactions between climatic catastrophes and the attempt that state authorities made to govern the landscape and water security in the post-World War I period is shown in Figure 4. The development also took strength from extreme climatic events and environmental catastrophes. Just think of the flooding of the Tennessee, Cumberland and Mississippi rivers in 1927, the worst in American history, which eventually inundated over 7 million hectares under 7 metres of water, causing 500 deaths and 7000 homeless, causing damage equivalent to a third of the US federal budget and which, as a result of hydroelectric laws, involved the government and federal authorities in the design of new infrastructure, including the most famous Hoover Dam. frastrutture, tra le quali la più famosa Hoover Dam. A historical description of the development of the European network can be found in [13], which highlights the factors that led to the implementation of interconnections between European states even in the presence of nationalisms and regimes characterised by different institutional forms.

Interconnections that in our country were also developed by climatic events that today we would define as due to climate change but that also occurred in the past, albeit less frequently. For example, the winter of 1921/22, which followed a hot and dry summer during which it did not rain for more than 100 consecutive days, led to a shortage of water that resulted in a serious decrease in hydroelectric generation. The regions of Piedmont, Lombardy and Veneto, already the epicentre of industrial activities at the time, appointed commissioners to ration the supply of electricity. The critical situation was overcome thanks to the existing interconnection lines with Switzerland and the interconnection of this with France, which also allowed electricity to be received from the coal-fired power stations in Nancy and Vincey via Zurich (Figure 5). For the Italian network in the period 1914-1925, please refer to reference [14] for details, while a summary of the development of electricity transmission and connections to 1928 can be found in ref. [15].



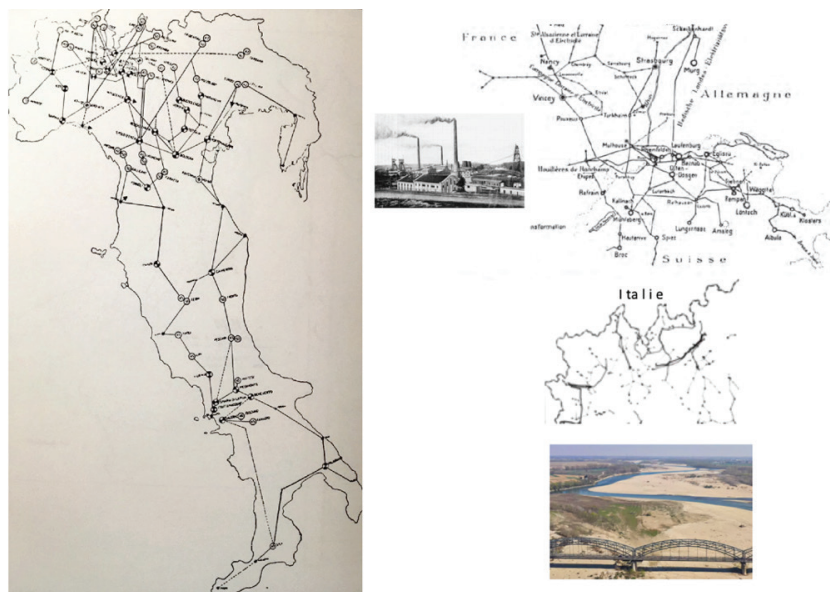


Figure 5: Italian Grid and import electricity from Switzerland and France during drought in 1921

The author, engineer A. Tacconi, refers to the initiative of private individuals in the realisation of the network, in particular, he writes: "This development required an enormous use of capital and led to the concentration of companies, small companies that served one or a few load centres disappeared, and as they grew stronger, they expanded into industrial groups to which national and international finance provided ample support. Thus the electricity industry conceived and perfected and carried out its programmes in complete freedom and with absolute spontaneity facilitated by the legislation on water and power lines that has never hindered the development of any private initiative'. The cited article does not consider interconnections with neighbouring countries, but gives emphasis to the electrical connection between the 8 systems of continental Italy: Sistema Piemontese, Sistema Lombardo, Sistema Adamello, Sistema della Venezia Tridentina, Sistema Adriatico, Sistema Italia Centrale and Sistema Meridionale. On the whole, hydroelectric generation exploits water from the rivers of the Alps and the Apennine region with different flow diagrams and with compensation through mountain reservoirs, especially in the Alps. The connection of the various systems brought benefits in allowing energy exchanges at times of the year when there was an abundance or deficit compared to local needs. Compared to hydroelectric production, the thermal power stations, usually one for each system, served a safety and integration purpose by being located close to load centres, allowing them to produce for any eventuality that would limit the availability of hydraulic energy. The six thermal power stations at the time (Genoa, Piacenza, Turbigo, Livorno, Naples and Marghera) had a total capacity of 550 MW. In the same article, the author concludes by writing: 'In this way, if and when it is necessary to supplement the white coal of our mountains with the black coal that nature, our stepmother, has denied us the availability of, except through gold exchanges, this can be done with the minimum expenditure and maximum yield. The entire phase after the First World War was devoted to the development of internal interconnections aimed at exploiting endogenous resources (hydroelectric or thermoelectric). However, in the period between 1921 and 1934, initiatives to plan a European grid became established thanks to political bodies such as the League of Nations, but even more thanks to technical bodies such as the IEC, CIGRE, and UNIPEDE where the presence of distinguished engineers meant that the idea of a European grid essentially became a technological project. Figure 6, taken from [13], shows two hypotheses of a European Network, the first by the French engineer Viel and the second by the German engineer O. Oliven.



Figure 6: European Networks assumptions 400 kVAc by G. Viel and O. Oliven (taken from rif[13] V.Lagendijk The power of Europe in the construction of electricity Networks)



The Great Economic Depression of 1929 with global consequences had a catastrophic geopolitical impact. In the USA, it was tackled by F.D. Roosevelt in a timely manner, launching a series of programmes in his first 100 days, including electrification, which was accompanied by the construction of dams and the implementation of the Tennessee Valley Authority, a grandiose project based on development but also on the preservation of the landscape, with a strategic role for the state in society and consequently involving the political structure.

In Europe the planning of a European Network suffered a fatal setback despite the measures promoted to increase public works; in 1933 Hitler's National Socialist Party won the elections and the construction of infrastructures such as motorways, railway lines and air transport were not conceived to facilitate the integration of resources between European states, but to create self-sufficient and autarkic regimes. Italy decided to invade Ethiopia in 1935, suffering severe diplomatic consequences from the League of Nations, which imposed economic sanctions that initiated the 'autarkic' period in our country as well. The adventure also put an end to Agip's participation in the BOD (British Oil Development) which, in competition with the IPC (made up of the large French and Anglo-American groups) had been granted the concession to develop the fields on the left bank of the Euphrates, in the Mossul area in Kurdistan. Agip acquired 52% of the share package, after promising surveys that estimated 2.5 million tonnes per day of crude oil, it was decided to transport it not by pipeline but by rail. A description of this can be found in [16]. For Italy, a detailed description of the Electricity Grid is described by M. Silvestri on technological developments in Italy from 1929 to the eve of the Second World War and in particular in the paragraph on technology and political power [17], highlighting the fact that 'Military and political Italy ignored what technical and scientific Italy did and knew'.

We enter the worst geopolitical event of the last century: the Second World War. A useful research in addition to reference [18] is the one elaborated by J. Cohn, M. Evenden and M. Landry entitled "Water Powers: the Second World War and the mobilisation of hydroelectricity in Canada, the United States and Germany" Journal of Global History - Cambridge University Press [19] and by D. Edgerton in [20] more focused the latter on the control of resources: coal, iron and oil during the conflict. Article ref. [19] elaborates on the impact on hydropower generation and transmission networks. It only mentions a few geopolitical aspects that seem significant to take as examples. Hydroelectric generation was used by many countries to support war production, but in quite different forms. The USA and Canada developed hydroelectric plants even more in the pre-war period so that they did not have critical wartime constraints, while Germany had a transmission network with fossil fuel (coal) generation and during the war showed all its dependence on the use of this essential source for steel production and other uses and was subject to transport bottlenecks along river axes.

Hydroelectric generation was only partly solved by the annexation of territories, Anschluss of Austria in 1936 allowed Germany to acquire Alpine hydroelectric plants. In all countries, during the conflict, there was a move towards centralisation of the authority to govern hydroelectric resources, while in the USA this occurred, as already mentioned, from 1932 when Roosevelt called for centralised and coordinated planning of the Transmission Networks. There had been debate in Germany since the First World War as to whether the electricity system should be centralised (with high-powered power stations at the mouth of a mine and with long interconnecting lines) or rather distributed in analogy to the German Middle Ages, in which each German town had its own mill. It was Hitler who decided by law in 1935 to favour a centralised and interconnected electricity system and after the currency crisis of 1936 to turn the German economy to rearmament. In the preparation of the Plan in 4 years, Germany, in order to conserve coal for industrial processes, launched the construction of 7 dams and hydroelectric plants, including Kaprun in the Salzburg Alps, the construction of which began in 1938, but only made a modest contribution to the electricity system at the end of 1944. The plant was only completed after the war thanks to contributions from the Marshall Plan. With the invasion of Norway in the spring of 1940, the German utility leaders began to consider how to interconnect the Norwegian electricity system (characterised by large hydroelectric generation) with that of Germany.

Interesting is the reference mentioned in [19] on the subject of the network encompassing the whole of Europe and the confrontation that took place in 1942 between the advocates of a 400 kVdc overhead line connection, preferred by RWE, and those including F. Todt (Inspector General for Water and Power), who saw a preference for 400 kVdc cable connections as they were more protected from the weather and, more importantly, remained "invisible" to air attacks (Figure 7 taken from [19]). The interconnection was not pursued and it was preferred, for reasons of time, to import the aluminium produced in Norway, although in reality, the lack of bauxite from countries under German control (France, Yugoslavia) proved to be a major bottleneck and ended up reducing aluminium production to below pre-war levels, while the interconnection with Switzerland ended up supplying only 1.5% of German consumption in the war years. In its aggression against Russia, Germany managed to capture the source of electricity generation on the Dnieper River in Ukraine, but the plant was destroyed by the retreating Soviets, damaging industries and coal mines in the region. The development of the war forced A. Von Speer to find more suitable solutions to deal with the conflict: construction of modular thermal power plants, measures to improve consumption efficiency in the production processes of the war industry and designing armaments by reducing the use of strategic materials.



Figure 7: European Electrical Networks in cable lines 400 kVdc – taken from rif.[19]

One consideration is that the German Transmission Network remained surprisingly operational even in the final stages of the conflict, for despite German fears of attacks on power stations and transmission lines, the Allied bombing campaign focused on other targets: ball-bearing industries, refineries, steel plants, with indirect damage to the distribution network, while the Allies' Operation Chastise in 1943, which targeted dams, ended up costing a high price in terms of aircraft shot down while the dams affected were promptly repaired. In the post-war assessment by the United States Strategic Bombing Survey, the lack of Electric Transmission Network targets was identified as a serious strategic omission that prolonged the war. In Italy, measures were taken to make the dams less visible by means of 'camouflage' techniques, frequencies were standardised and internal interconnections were increased; a sort of T-network was constructed with a line from Turin to Venice along the axis of the Po River and a line from north to south from Verona to Terni, in 1941 a line from Florence to Verona was also planned and completed during the war. The Italian Transmission Network, against all odds, remained relatively unscathed by military action.

### 2.2. Geopolitics and First Italian Electric Grid Transition 1948-1988

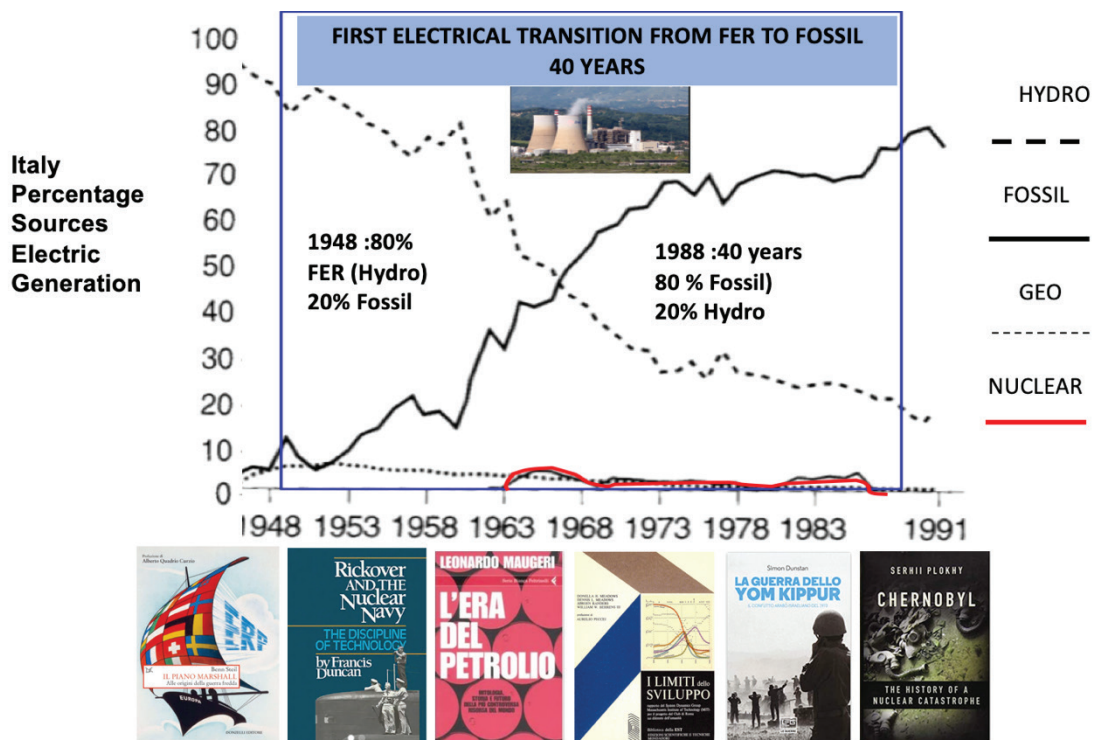


Figure 8: First Italian Electrical Transition





This period saw the first Energy transition from Renewable Sources (Hydroelectric and Geothermal) to the Fossil Source (Oil) that took place within 40 years (Fig. 8). The development of the Italian electricity grid took place, as in Europe, thanks to the ERP funding of the so-called Marshall Plan [21] which was drawn up at the origins of the ‘cold war’ and which, thanks to Truman, who broke the isolationist tendency (between 1945 and 1949 international organisations such as the United Nations, the International Monetary Fund and the World Bank were set up), enabled European reconstruction with a four-year economic aid plan (1948-1952). It was preceded by Truman’s decision to write off the German public debt, which was about 4 times the GDP in 1938. The success of the Plan enabled the economic miracle that was the basis of European recovery and belied all the detractors who were not lacking even at the time. One can also speak of a miracle in view of the geopolitical situation in Europe, which remained catastrophic well after the end of the war in 1945 and lasted until 1952. In fact, World War II was never just a territorial conflict but also a war of race and belonging. The Jewish holocaust (which had dramatic consequences as we know from 1948 to the present day in the Near and Middle East), the ethnic cleansing of Poland, western Ukraine and Polish-Ukrainian ethnic violence, the genocide of Serbs in Croatia, the displacement and expulsion of Germans from occupied territories and the more than 11 million refugees, the Yalta decision, (agreeing with Stalin in February 1945 to move the borders of the USSR westwards and consequently the forced displacement of entire populations in Eastern Europe), created from multicultural states a series of monocultural and ethnic nation-states that had serious geopolitical consequences to this day. The history of these events is encapsulated in the book in ref. [22].

The largest beneficiary of the Marshall Plan was the United Kingdom with \$3,175.9 million out of a total of \$13,211.2 million for the different European states. Italy was the second largest beneficiary with \$1,474.4 million and West Germany the third with \$1,389.0 million. In Italy, thanks to the Plan, 14 new lignite- and oil-fired thermoelectric units for almost 900 MW were built. From that time on, the oil era began and thermoelectric units with greater power were implemented technologically. From 1960 to 1988, the development of fossil-fuel power stations continued in Italy with a gradual increase in power sizes. At the beginning of the 1970s, the maximum power output of air-cooled turbogenerators was around 100 MW, in the late 1980s it increased to 600 MW, and in the 1980s, thanks to the use of hydrogen as a cooling medium, the nominal output of turbogenerators reached 600 MVA and more. These increases in the power sizes of thermal power plants allowed for better efficiencies and lower investment and operating costs per MW installed. In 1951 with the establishment of the UPCTE, the network, as can be seen in Figure 9, consisted of the systems of the member nations (France, Austria, Belgium, Holland, FRG, Italy and Luxembourg), while in 1955 the exchanges between the constituent states of the UCPTC network were still limited and there were no other connections with other synchronous areas.

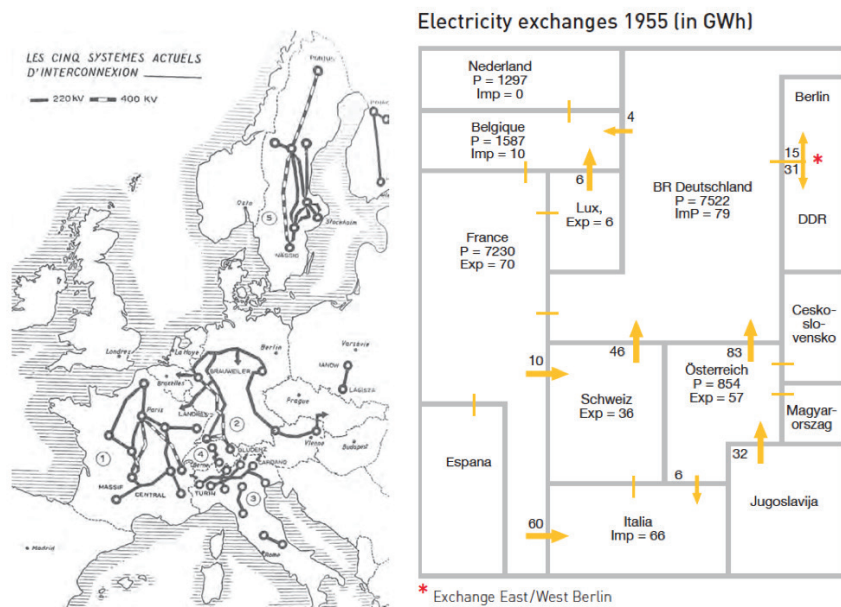


Figure 9: Rete Elettrica Europea nel 1955 e Scambi transfrontalieri tra Stati (elaborata dall'autore e tratta da rif [13] e da UCPTC The 50 Year Success Story)

Certain geopolitical events such as the 1967 war and even more so the 1973 war between Israel and the Arab states in the region (Syria, Egypt and Jordan), had a strong impact on the world due to the rising cost of oil, which had become the fuel par excellence of the Electricity Generation. An in-depth review of the geopolitics related to oil is given by Maugeri in his volume in ref. [23]; this led to a greater use of coal (especially for states with important lignite resources). Italy then proposed the nuclear solution. It should be remembered that the use of nuclear power also came from a geopolitical event, with the two US atomic explosions that led Japan to unconditional surrender and the devastating effects on the two cities affected. It was the brainchild of Admiral H. Rickover who directed



the development of naval nuclear propulsion and who promoted nuclear fuel as a source for generating electricity. In 1953, Eisenhower, in a famous speech to the United Nations, launched the 'Atoms for Peace' conference for international cooperation in the peaceful exploitation of nuclear energy. Rickover followed up with Westinghouse on the construction of the first 60 MWe PWR-type Shippingport nuclear power plant (originally planned for an aircraft carrier), which became operational in December 1957 (and ended its service life in 1982). Ref. [24] shows the vision and contribution that this engineer made to the technology for the use of nuclear energy. The success of the first prototype realisations (including Calder Hall in the UK and Obnisk in the USSR) led to the construction of the first commercial power plant without public funding (General Electric's 630 MW Oyster Creek BWR). In Italy, it was private companies that promoted nuclear power, putting Italy in third place after the USA and the UK in the sector (with the Latina, Garigliano and Trino Vercellese power stations later passed to ENEL with nationalisation). This was the period when nuclear generation took over. With the recession due to the oil crisis and overcapacity in the USA, orders for new plants began to fall. The TMI accident of 1979, although limited in its consequences, ended up dealing a blow to private financing. At that point, a fact also ascribable to geopolitical factors and not just technology intervened: on 26 April 1986, the serious Chernobyl disaster occurred, involving an RBMK 1000-type reactor whose design was far removed from western ones in terms of both management and technology, as highlighted by M. Sivestri in ref. In 1987, the referendum in Italy triggered a series of political discussions that in the space of three years led to the closure of the Latina power station (1987), the Caorso power station, which had been in operation for just eight years, the closure of Trino Vercellese (26 July 1990, a week after Saddam Hussein invaded Kuwait, beginning a chain of geopolitical events that have disrupted the entire Near and Middle East to this day), although it was subject to interventions to increase its reliability and safety, and the reconversion of the Montalto power plant (in 1988), which led to the construction of Italy's largest thermal power plant (3200 MWe), a polycombustible fossil fuel (oil, gas) plant that emitted tonnes of CO<sub>2</sub> into the atmosphere from its construction in 1992 until its decommissioning in 2016, while the nuclear power plant (1220 MWe-BWR) located in Leibstadt (with the same BWR General Electric technology) on the Rhine River in Switzerland, has generated electricity since 1984, exporting it to Italy thanks to the interconnections of the transmission grid between the two countries. For a history of nuclear power, see refs. [26] and [27] full of analysis and geopolitical impacts on the scenarios of the 1980s. In 1972, the International Conference on the Human Environment was held, which coincided with the publication by a team led by D.L. Meadows at MIT of the First Report on the Limits of Development. The study was commissioned by the Club of Rome and financed by the Volkswagen Foundation on the initiative of Aurelio Peccei, who in 1968 at the Accademia dei lincei referred to the 'difficult present and future situation of mankind'. From this study began the discussions on models and scenarios for political action to be taken for the environment and available resources, economic development, energy and international relations that led to the vision "Beyond the Limits of Development" in which, twenty years after the alarm sounded by the Club of Rome, the same scientists indicated the conditions for a possible future [28]. In 1979, with the USSR's invasion of Afghanistan, the Komeinist revolution in Iran and the subsequent war between Iran and IRAQ, geopolitical events took place that would have dramatic consequences in the Middle Eastern theatre, an area rich in energy resources, first and foremost oil. From 1980 onwards, interchange between states began to develop in the Italian network and in the European network, with the construction of new interconnections, in particular with the development of 380 kVAc overhead lines (Fig For the period under discussion, a detailed history of the development of the electricity grid and interconnections, both domestic and foreign, can be found in [29]. Conceptually, in the text, interconnections are understood to be those lines that allow new production centres to be connected to the electricity grid in order to transfer it to the centres with the greatest load, but precisely with the increase in interconnections with foreign countries, the grid "becomes more and more a transmission system that with the development of the market allows electricity to be transferred from the least expensive foreign producer to the large domestic industrial user interested in purchasing energy at lower generation costs".Figure 10).

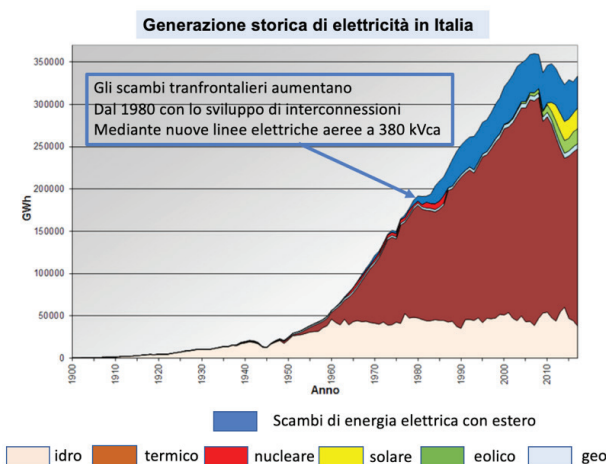
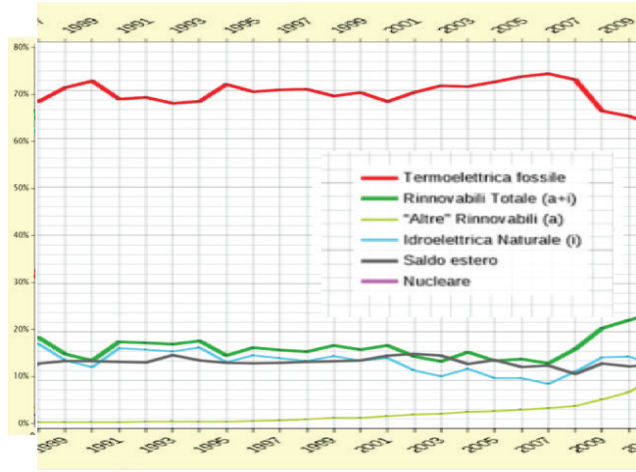


Figure 10: Source Generation Electricity and cross border exchanges 1900-2015



Geopolitics and Second Transition 1989-2010

Second Transition From Oil to Gas :1988-2009



Gross Generation	1988 (TWh)	2009 (TWh)
Solids	30,8	39,8
Gas Naturale	32,4	147,4
Gas Derivati	3	3,8
Oil	88,9	15,8
Other Fossil	1,8	19,8
Hydro	43,5	53,4
Geothermal	3,1	5,3
Renewables (Wind & Solar)	0	7,1
Aux services and Pumping	-14,2	-17,3
TOTAL	189,1	275,3
Import-Export	31,3	47-2,1
TOTAL Demand	220,4	320,3

OIL FROM 44% TO 5,3% GAS FROM 17% TO 51,8% Italian Gross Electricity Generation

Geopolitics Events

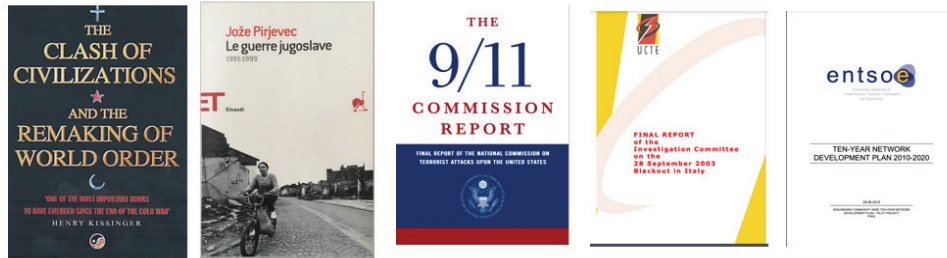


Figure 11: Geopolitics Event and Second Transition from Oil to Gas

At the end of the 1980s, following the effects of the Yom Kippur War and the ensuing oil crisis, the Second Energy Transition began in our country with the switch from oil to gas as the main source of Fossil Fuel Thermoelectric, which in the period continued to prevail over other sources for electricity generation (with a percentage of over 70% of the total). While in 1988, gas-fired fossil thermoelectric power accounted for 15% of total electricity generation, by 2007 it had already reached 50%, with fuel oil now reduced to 6% and destined to be almost completely replaced by gas and coal (the latter around 17% of the total fossil fuels used and around 12% of total electricity generation (Figure 11). In Europe, the end of the USSR in 1989 created the need to connect and synchronise the two networks of the now reunified Germany with an extension to the CENTREL (Centre Eastern European Countries) network consisting of the Czech Republic, Hungary, Poland and Slovakia. This took place in the first phase with 3 connections in HVDC BtB, while later, in October 1995, full synchronisation was achieved with the UCPTe network, which had also included Spain, Portugal and Greece in 1987. A major impact on the Italian network occurred in 1981 with the declaration of independence of Slovenia and Croatia with which the dissolution of Yugoslavia and the conflict in the Balkans began and lasted until 1999 (Figure 12).

1989 – 2001 Dissolution of Yugoslavia



Figure 12: Dissolution of Yugoslavia 1989-2001





With the destruction of the two 400 kV Stations in Ernestinovo and Konjosko and the associated transmission lines in Croatia and Bosnia-Herzegovina, the electricity system became fragmented, and as the conflict continued, Greece found itself isolated from the UCPTA grid. The long process leading to the planning and realisation of the HVDC connection between Italy and Greece (GRITA - Fig. 13) began in 1991. The geopolitical event gave impetus to research and innovation, first with the resolution of the problems the cable had to face due to the depth of the connection (a record for the time: 1000 metres deep), through the Otranto Channel, but even more so with the financing of the work. For the technical problems, please refer to the extensive bibliography in the AEIT journals, while for the economic burdens for the construction of the work, it should be remembered that it was thanks to the EU that funding equal to 75% of the cost was granted free of charge.

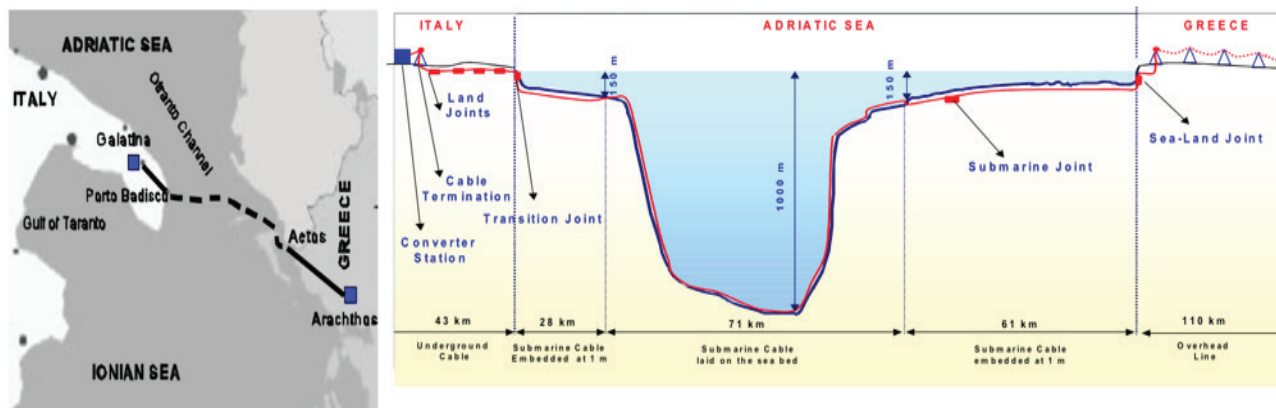


Figure 13: HVDC Link Italy-Greece

Still in relation to the geopolitical event of the Balkan Wars and again with reference to the impact these events had on the networks, page 441 of Ref. [30] reads:

*“In the diplomatic action of the USA, the German government was also involved, as is evident from the decision to ensure through Siemens to the city of Sarajevo under siege, an independent source of electricity from the power station controlled by the Serbs. To this end, a memorandum of understanding was signed that provided for the laying of a 110 kV underground cable across the slopes of Mount Ingman, which was successfully completed in the following months despite the raging fighting in the area”.*

On 9 June 1999, the agreement that later became UN Resolution 1244 was signed, providing for the withdrawal of Serbs from Kosovo and their replacement by NATO troops.

In 2001, the terrorist attack on the Twin Towers of the World Trade Center and the Pentagon provoked a reaction that first led the US to intervene in October 2001 in Afghanistan and, in 2003, to the invasion of Iraq. With these events, energy security issues and the resilience of power grids in various respects, including terrorist acts, become more acute. The transition towards greater use of gas in Italy came about after the reform of the electricity sector that led to the privatisation of ENEL and the separation of grid management (entrusted to GRTN) from grid ownership (entrusted to private operators, first and foremost Enel-Terna). Since 2002, the Grid Manager has been sounding various alarms about the security and adequacy of the grid to meet consumption [31]. Critical situation due to the generation power deficit that had accumulated over the years, which was due to both the uncertainties of the electricity market and the remuneration to be assigned to operators, but also to the lack of authorisations from the regions and municipalities for the construction of new power stations (as of 12 September 2002, 49 preliminary inquiries had been initiated for new power stations totalling 2,620 MW, but the first authorisation decree was still awaited) and new power lines. S.Fiorano-Robbia OHL at 380 kV, started by ENEL in 1991, was continued by GRTN, authorised in April 2004 and completed in just 9 months on 20 January 2005 [32].

To increase interconnection capacity instead, Decree 151/2002 was passed to incentivise private interconnectors (merchant lines). These latter initiatives did not make it possible to avoid the Italian blackout of September 2003, for which see ref. [33]. It should be added that of the 42 merchant lines that presented a declaration of interest for a total power of 13,858 MVA and a total investment of over 3 billion euros, only three were actually built. In the meantime, in the list of new thermoelectric power stations to be built, operators presented new projects for combined-cycle turbogas power stations, which, thanks to advances in technology in terms of both cost and construction time, but even more so in terms of the yields achieved, operational flexibility and environmental aspects, were emerging as the preferred solution. Figure 14 taken from [34] shows the evolution of GTCC (Gas Turbine Combined Cycle) efficiencies from 1985 to 2018, which increased from 45% to over 60%.

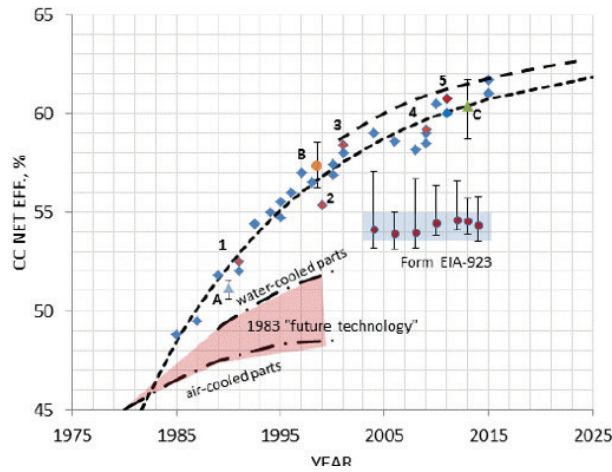


Figure 14: Evoluzione dei rendimenti dei Cicli Combinati (GTCC) tratta da rif. [34]

An evolution of the Italian thermolectric park with the development of ‘Greenfields’ CCTG power plants in the period 2003-2008 is reported in Ref. [35]. This increase in CCTG plants was also linked to the forecast increase in renewable sources (solar and wind), which are intermittent and non-programmable by nature. It should be added that in the winter of 2006-2007, there was already a strong criticality in the supply of gas for electricity generation, both in the presence of a colder and drier climate than typical winter values (with temperatures colder than the average of winters in the last 44 years) and with problems on the Italian electricity market with the markets of neighbouring countries due to low hydroelectric production, and also due to the first crisis between Ukraine and Russia. An analysis can be found in Ref. [36] where structural causes are indicated that are worth mentioning for their topicality:

- continuous increase in gas demand from the thermolectric sector as a result of an increase in GTCC power plants;
- insufficient expansion of gas network interconnection capacities with foreign countries;
- delays in the construction of regasification terminals to expand the supply flow;
- storage capacity that has become inadequate for a continuously growing market’.

On 13 September 2008 with the bankruptcy of Lehman Brothers the most serious financial crisis since 1929 began. Between 2008 and 2013 begins a period of depression with high commodity prices (oil among them). This also affects the electricity markets and the investment activities of private and public operators in electricity networks including electricity generation. Many European countries are affected: Greece, Spain, Portugal, Ireland, Iceland and finally Italy. For economic analysis see ref. [37]. In 2009, ENTSO-E is established to replace the existing international associations of network operators, comprising 42 European TSOs with the aim of promoting the electricity market and cross-border trade by guaranteeing the security and reliability of the Grid, data exchange and interoperability of Networks, and emergency operating procedures. In 2010, the Turkish Grid was synchronised.

Figure 15 shows the European grid as of 2011 and the total exchanges between the various countries, which in 2011 reached a value of about 412 TWh, of which 371 TWh in Entso-e.

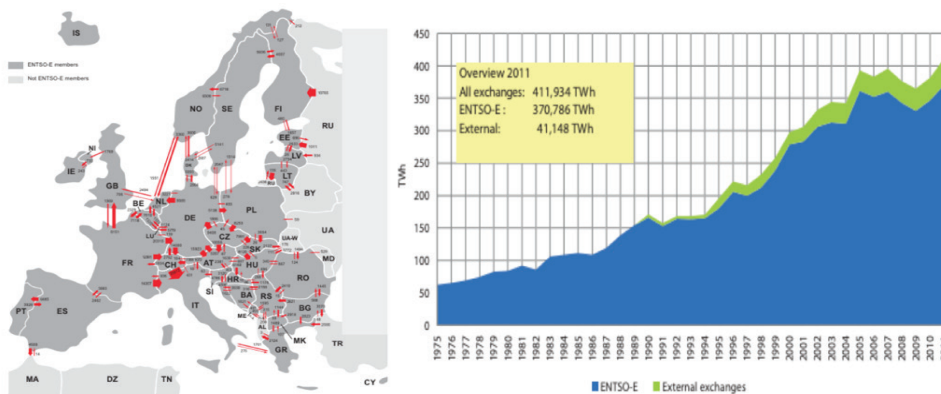


Figure 15: ENTSO-E GRID and total amount in TWh and cross border exchanges ( Entso-e Statistical Yearbook 2011)



We will now briefly highlight what happened in the Mediterranean due to geopolitical events and their impact on the interconnections between the Italian Network and those of North African countries. Also from 2001, a series of agreements began, thanks also to organisations such as the OME, between Italy and the countries of North Africa to create new connections between the Italian grid and the Maghreb grids (Algeria, Tunisia, and Libya), the vision being that of making Italy a hub for an interchange of electricity that would create synergies between the various possible sources of generation (not only gas but also renewable energies such as wind and especially solar). In addition to connections between southern Europe and North Africa, studies and tests were also developed at that time for a synchronous connection between the states of North Africa, from Morocco to Egypt, called Medring (which dates back to a concept born in 1990 and which the first sea cable connection between Spain and Morocco activated in 1997) in which Italy actively participated. In 2005, an initial attempt to synchronise the Libyan network with the Tunisian one failed. In 2007, a BtB connection was hypothesised, but geopolitical events soon made the attempts unfeasible. A brief history of the Mediterranean network can be found in Ref. [38]. Table 2 shows the studies and projects of HVDC links in the Mediterranean and lists those between Italy and North African countries. As can be seen, the geopolitical events affecting North Africa deal a first blow to all initiatives. After the uprisings in Kabylia that created difficulties in Algeria at least until 2005 see [39], in December 2010 the uprising in Tunisia broke out, which in 2011 spread to all countries in the area and went by the name of the Arab Spring with the flight, arrest or killing of the heads of state of Tunisia, Egypt and Libya respectively. With the intervention of France, the US and the UK, the Libyan conflict begins, opening up a new geopolitical front and, as we shall see, affecting the next energy transition.

**TABELLA 2 STUDI COLLEGAMENTI HVDC MEDITERRANEO**

Studio di Fattibilità	anno	Operatori	Scopo	Anno completamento Fattibilità / Preliminare	Realizzazione e date Principali	Impatto Eventi Geopolitici
Italia-Grecia	1991	ENEL-PPC	Collegamento per connettere Grecia alla rete UE	1994	Finanziato da UE per il 75%-Gara Europea 1994 / Costruzione 1995-2001	1990-1999 Dissoluzione Jugoslavia e Conflitto nei Balcani
Italia-Tunisia	1991	STEG-ENEL	Costruzione a Tunisi Centrale Termica da 1400 MW (3x450)	1992	Non proseguito	Riforma settore elettrico in Italia
Italia-Tunisia	2003	GRTN/TERNA - STEG	Scambio energia 500/1000 MW tra le Reti	2004/2008	29/6/2007 Firmato accordo tra Governo Italiano e Tunisino MoU Terna-STEG	Primavere Arabe 2010-2011 cade Ben Ali
Italia-Algeria	2002	TERNA-SONELGAZ	Scambio energia 500/1000 MW tra le Reti	2003 / 2005	Accordi 31/10/2001 Due alternative fattibili	Primavere Arabe 2010-2011
Italia-Libia	2003	TERNA-GECOL	Scambio energia 500/1000 MW tra le Reti	2006	Trattato di Bengasi del 2008 tra Italia e Libia Accordo Mise/Terna 2007 Completato Studio 2009	Primavere arabe 2010-2011; Guerra in Libia
Italia-Croazia	2006	TERNA-HEP	Scambio energia 500/1000 MW tra le Reti per generazione Croazia Kosovo, Bosnia	2009	Completato studio fattibilità Non proseguito	Kosovo

### 2.3. Geopolitics Event and Third Energy Transition 2011 - 2030

The Third Energy Transition that is expected to increase the percentage of generation from renewable sources to over 40% in 2025 and to 55% is shown in Figure 16.

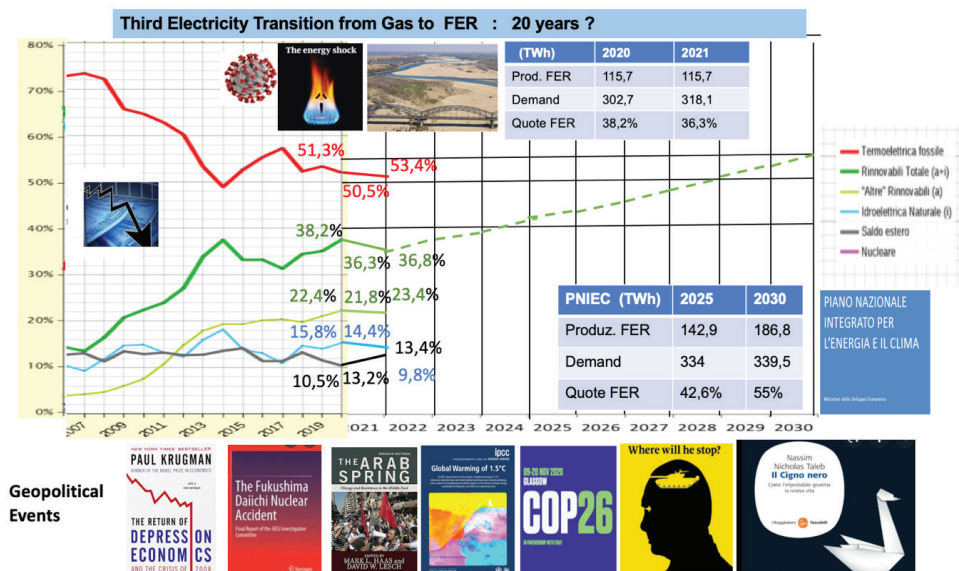


Figure 16: Geopolitics Events and Third Transition from Gas to FER



It can be considered to have started in 2006 with the Conto Energia Decree, which, following a European Directive, provided incentives for the installation of photovoltaic conversion plants, not to support the costs of construction, but to encourage the increase in the production and sale of electricity from this source. Subsequently, further energy account incentives were enacted: the second between 2007 and 2010, the third 2010-2011, the fourth 2011-2012, the fifth 2012-13, and continuing again with the RES 1 Decree of 2018-2020.

This was during a period characterised by other serious geopolitical events. We have already mentioned the severe financial crisis of 2008-2012.

The Fukushima accident in 2011 dealt a further fatal blow to nuclear power in Italy with the 2011 referendum. Certain geopolitical factors determined the subsequent scenarios in Italy on the dynamics of the Energy Transition, the development of interconnections and the control of the Electricity System. Since 2012, cooperation in the Mediterranean has resumed thanks to the establishment of MedTSO and MedRe, a cooperation that will also have to deal with the critical issues arising from the geopolitics of the Mediterranean which, although technologically surpassing, with Prysmian’s new cable-laying ship Leonardo da Vinci, the limits of sea cable laying that reach 3,000 metres, will have to deal with the sea boundaries dictated by the Exclusive Economic Zones and the initiatives underway to dictate constraints on the exploitation of resources and new gas and oil deposits that have in the meantime emerged from new explorations (Fig. 17).

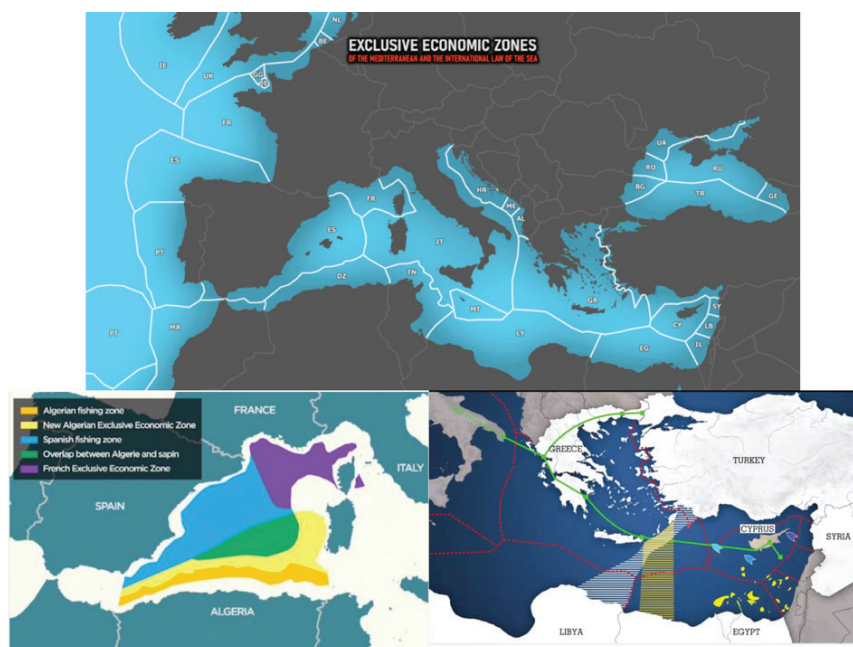


Figure 17: Mediterranean Crisis Area

For a more detailed description of the crisis areas and geopolitical developments in the Mediterranean, see ref. [40].

-In 2013, the South East European Regional Council CIGRE was established in Montenegro, reaffirming the spirit of cooperation and interchange between the Electricity Networks of all Balkan states, Austria, Czech Republic, Ukraine, Romania, Greece, Türkiye, Israel and Georgia.

-In 2015, the IPCC Report provides the models that give the targets to be achieved for CO2 emissions to limit the global temperature increase to 1.5 C and that are taken up by subsequent climate policy agreements and serve as a reference for the definition of the European Grid Development Plans.

-In 2015, the Chinese Plan called BRI (Belt Road Initiative) is presented, a synthesis of two components: the Silk Road Economic Belt and the 21st Century maritime Silk Road that President Xi Jinping presented in 2013. The Belt component refers to a land belt encompassing the countries along the Silk Road from Central and Western Asia to the Middle East to Europe, while the Road component refers to the oceanic routes connecting China to Southeast Asia, Oceania, Africa, through the maritime basins of the South China Sea, South Pacific and Indian Oceans, and the Mediterranean Sea. At the same time, the book by Zhenya Liu cf.[41] is published, which sets out a vision of a global power grid uniting areas of the world based on available renewable resources. Figure 18 shows both the BRI economic corridors and the global power grid.



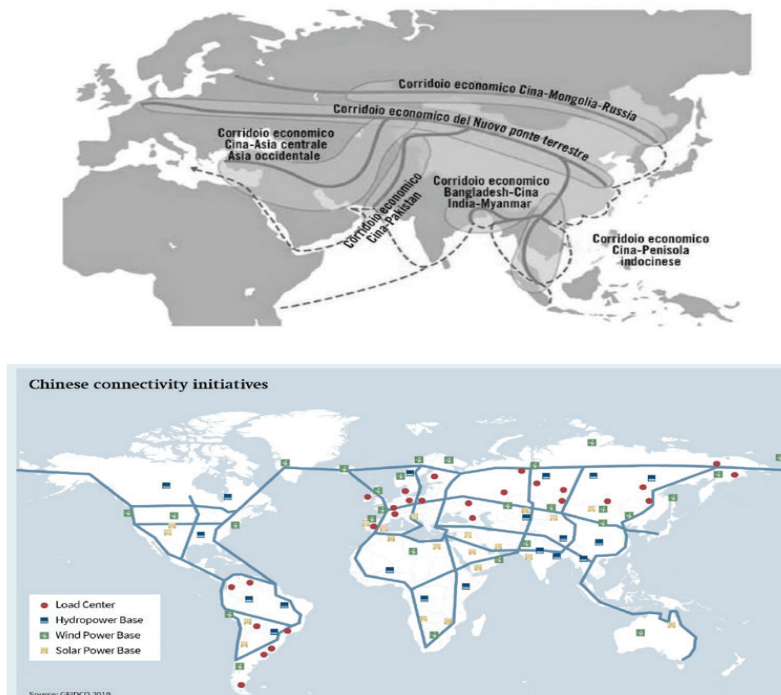


Figure 18: China BRI and Connectivity Initiatives (from Powering the Globe di E.Downe-Columbia University/SIPA)

- In 2016, ENEL closed 26 thermoelectric power plants deemed obsolete and launched the Futur-e project to redevelop the sites. The impact of the development and control of the electricity grid due to the development of non-programmable Renewable Energies, in particular wind power, was reported as early as 2010 crf. [42] and stemmed from the location of generation from RES in central-southern Italy, which highlighted the need, in order to overcome grid congestion, for new development interventions both with the upgrading of existing power lines and with a new transversal between the Adriatic and Tyrrhenian ridges, already with the hypothesis of a DC link between Calabria and Campania.

But geopolitics doesn't stop: with the Trump presidency, the US begins a policy of duties towards China and the EU that undermines the momentum of global cooperation to achieve the CO2 reduction targets needed to limit the rise in global temperature. In turn, the Chinese BRI also starts to pose geopolitical criticalities in the Mediterranean. A compilation of the critical issues is published in 2018 in Ref. [43].

- In 2017, the SEN introduced the possibility of a phase-out of Italy's existing coal-fired power plants in 2025 or 2030. A series of studies are carried out to verify this possibility as early as 2025.
- In November 2019, the sea cable connection (423 km in the Adriatic Sea with cable laying up to 1215 m) and land cable connection (22 km) in HVDC 500 kVdc bipolar 2x600 MW between Italy and Montenegro will be inaugurated and which, in the light of the critical issues that followed, will enable the implementation of those security and energy exchange considerations with the ENTSO-E countries of South-Eastern Europe. -In the PNIEC of December 2019, based on a policy framework also defined in the EU, the values shown in Figure 16 are given as targets for renewables.

But three new critical issues are added at this point (the first is not foreseeable, the second concerns climate change in the Mediterranean, which RSE studies already indicated as a hot spot, with an increase in drought phenomena occurring punctually in 2021/2022, while the third is part of geostrategic assessments that are not entirely unpredictable)

either a global pandemic due to Covid-19 spreads from January 2020. The repercussions have the effect of quickly rendering the scenarios adopted by all international bodies (IEA, WEC etc.) unreliable;

- in winter 2021 and spring/summer 2022 there is a severe drought period, which creates criticality in hydropower generation;
- in February 2022, Russia's invasion of Ukraine completely changes the scenarios assessed, causing a major impact on the gas resource in particular (an impact that also affects all EU countries). On 16 March 2022, the Ukrainian Electricity Grid is emergency synchronised with the ENTSO-E System, concluding what was started in 2017 with the signing of an agreement



between the operator Ukrenerg and ENTSO-E. Figure 16 shows the percentage values of generation sources in 2020 and 2021 compared to the electricity demand on the Italian grid, while for 2022 I have reported the percentages as of August.

Figure 16 shows how, while on the one hand the RES (wind, solar, geothermal, biomass thermal) increase, the hydroelectric source strongly decreases, and with 2021 and 2022 the contribution of the foreign balance increases. The total energy interchange in Europe in 2021 is also reported to be 902,628 GWh, of which 48,012 GWh for the Italian grid.

The value to be obtained for Generation from RES by 2030 of 55% is, considering the geopolitical situation, ambitious, but the current criticalities could also play a role as an impulse to reduce the time needed for authorisations and for the realisation of new interconnections, both internal and for those envisaged in the European Fourth List of Projects of Community Interest, which affect Italy as in ref. [44], recalling that a true energy transformation can only be achieved by further integrating the Electricity Networks with each other.

### 3. CONCLUSION

There is an international scientific consensus on the technological path to follow for decarbonisation, which is based on six technological pillars: a) Generation of electricity with zero greenhouse gas emissions; b) Electrification of end uses; c) Use of green synthetic fuels: hydrogen, synthetic hydrocarbons; d) Smart Power Grids; e) Improving efficiency and consumption of critical materials with reuse and recycling; f) Sustainable land use.

The critical aspect to achieve these goals remains the geopolitical factor and Governance for infrastructure development: electricity grids, road networks, railways, telecommunications, sea and air navigation routes. The article dwells on the electricity grid and the 'key driver' that determines the positive evolution towards the goals set: the electricity interconnections between states.

The Italian electricity system is an integral part of the European electricity system that has grown with a historical dynamic that has increased its control and operation to the point of being able to determine a vast area for the definition of an electricity market and its regulation.

European electricity grids integrated to form a Synchronous System have defined communities that not only share electricity supplies, but a common destiny in terms of security and welfare.

An attempt has been made to highlight the historical evolution of the Italian grid, which has been heavily impacted by geopolitical events over time.

### BIBLIOGRAPHY

- [1] A.Grant,Z.Haider,A.Levy "How global companies can manage geopolitical risk" McKinsey & Company -July 2021.
- [2] WEC "World Energy Issues Monitor 2022" January 2022;
- [3] K.Westphal,M.Pastukhova,J.Maria Pepe " Geopolitics of electricity:Grids,Space and (political) Power" SWP Research Paper – German institute for International and security Affairs March 2022,Berlino
- [4] D.Sholten (Editor ) "The Geopolitics of Renewables " Ed.Springer , 2018
- [5] C.Bonnet,S.Carcanague,E.Hache,G.Seck,M.Simoen " Vers une Geopolitique de l'Energie plus complexe? " Policy Research Working Paper,Janvier 2019.
- [6] w.irena .org/ Inspire 2021
- [7] M.Rebolini "Risorse e tecnologie per la Nuova Transizione Energetica:criticità e soluzioni" Rivista Energia Elettrica N.3 vol. 97 maggio/giugno 2020
- [8] IEA " Special Report on Solar PV Global Supply Chains " July 2022
- [9] TERNA "Dati statistici sull'Energia Elettrica in Italia ";
- [10] SEERC CIGRE HISTORY "Early electrification and empowerment of region where current electricity was born " ed.2020
- [11] John Maynard Keynes " Le conseguenze economiche della pace " prima edizione 1919 ; ed.2007 Adelphi Editore
- [12] Giulio Boccaletti " Acqua,una biografia" Ed.Le Scie ,Mondadori 2022
- [13] Vincent Lagendijk "The Power of Europe in the construction of electricity networks" Ed.2008 Aksant editoreny "
- [14] Storia dell'industria elettrica in Italia Vol.2 Il potenziamento tecnico e finanziario 1914-1925 a cura di L.De Rosa Editori Laterza 1993
- [15] A.Taccani "Sviluppo delle trasmissioni e connessioni elettriche in Italia " Elettrotecnica XV 1928 n.21
- [16] M.Canali "Mussolini e il petrolio iracheno" Ed.Einaudi 2007
- [17] M.Silvestri " Storia dell'Industria Elettrica in Italia -Gli sviluppi tecnologici " dal Volume 3 Espansione e Oligopolio 1926-1945 Editori Laterza 1993





### Oral Presentation: Geopolitics Impact on Electrical Grids during Energy Transition

- [18] Storia dell'industria elettrica in Italia 1926-1945 a cura di G.Galasso Ed.Laterza 1993
- [19] J.Cohn,M.Evenden,M.Landry " *Water Powers:the Second World War and the mobilization of hydroelectricity in Canada,the United States and Germany* " Journal of Global History 2020 pag.123-147 Cambridge University Press.
- [20] D.Edgerton " *Controlling resources :coal, iron and oil in Second World War (SWW)* " Cambridge history of SWW vol.3 Ed.Cambridge University Press ,2015
- [21] Benn Steil " *Il Piano Marshall* ";Donzelli Editore 2017
- [22] K.Lowe " *Il Continente selvaggio;L'Europa alla fine della Seconda Guerra Mondiale* " Viking Ed.2012; edizione italiana Ed.Laterza 2013
- [23] Leonardo Maugeri " *L'Era del petrolio* " Ed.Feltrinelli 2006
- [24] Admiral H.Rickover " *The Never-Ending Challenge of Engineering* " compilato a cura P.Cantonwine , Illinois nel Luglio 2013 -Library of Congress-USA
- [25] M.Silvestri " *Il futuro dell'Energia* ",Torino 1988
- [26] P.Fornaciari " *Il Petrolio,l'Atomo e il Metano* " Italia Nucleare 1946-1997 Ed21Secolo,1997
- [27] A.Candela " *Storia ambientale dell'Energia Nucleare* " Ed.Mimesis (Milano-Udine) 2017
- [28] Donella H.Meadows,Dennis H.Meadows,J.randers " *Oltre i Limiti dello Sviluppo* " Ed.Il saggiatore1992
- [29] A.Ninni " *Interconnessione e standardizzazione* " in Storia dell'industria elettrica vol.5 1963-1990 Edizioni Laterza 1994.
- [30] Joze Pirjevec " *Le guerre jugoslave* " 1991-1999 ; Ed.Einaudi 2002
- [31] S.Machi( Presidente GRTN) " *Il Sistema Elettrico italiano:situazione attuale e prospettive* ";secondo Italian Energy Summit-Milano,18 settembre 2002
- [32] M.Rebolini,G.Bruno,C.Maffei(GRTN),D.DeMarco,R.Rendina,A.Salvador(TERNA) " *Elettrodottoia 380 kV S.Fiorano-Robbia* " Riv.Energia Elettrica GenFeb2005
- [33] F.Iliceto " *Piani di Difesa contro i disservizi nei Grandi Sistemi Elettrici Interconnessi* " Rivista Energia Elettrica n.1 Vol.81 Gen/feb 2004.
- [34] S.Can Gulen ( Bechtel Corp USA) " *Etude on Gas Turbine Combined Cycle Power Plant -Next 20 Years* " Proceedings Of ASME Expo 2015, Montreal,Canada
- [35] L.Michi,A.Camponeschi (Enel produzione) " *Evoluzione del parco termoelettrico italiano nel periodo 2003-2008: valutazione delle principali criticità ed esperienze di esercizio* " Rivista Energia Elettrica n.1 vol.84 gen-feb2007
- [36] M.Gallanti,M.Borgarello,A.Gelmini (CESI Ricerca) " *Le criticità del sistema gas per l'inverno 2006-2007* " Rivista Energia Elettrica n.4 vol.83 lug/ago 2006.
- [37] Paul Krugman " *Return Depression economics and the Crisis of 2008* " Ediz.Norton and C. 2008
- [38] M.Celozzi et alii ,MEDGRID " *Co-development of the Mediterranean Transmission Grids* " paper C1-207 CIGRE Session 2012 Parigi
- [39] Dossier n.41 XV Legislatura Italiana - Senato " *Algeria:sviluppi di situazione* " Aprile 2006
- [40] AA.VV. " *Mediterraneo Allargato* " Osservatorio di politica Internazionale -Senato della repubblica,Camera Deputati,Ministero Affari Esteri,Settembre 2021 ;Ediz. a cura ISPI
- [41] Zhenya Liu " *Global Energy Interconnection* "Ed.Chine Electric Power Press pubblicato da Academic Press -Elsevier ,2015.
- [42] C.Genesi e altri (UNI Pisa) e E.M.Carlini e altri ( Terna) " *Impatto dello sviluppo della rete elettrica sulla dispacciabilità eolica* Rivista Energia Elettrica n.4 vol.87 lug/ago 2010.
- [43] Aspenia n.82- 2018 *La terza rivoluzione cinese-La battaglia per l'Eurasia e la geoeconomia del mare.*
- [44] Piano di Sviluppo Terna 2021 page 38



# Short-Term Solar Radiation Prediction Based on Long Short-Term Memory for Çukurova Region

[besenboga@atu.edu.tr](mailto:besenboga@atu.edu.tr)

**İNAYET ÖZGE AKSU<sup>1</sup>, BURAK ESENBOĞA<sup>2\*</sup>, ABDURRAHMAN YAVUZDEĞER<sup>3</sup>, KÜBRA YILMAZ<sup>4</sup>, DUYGU DURDU KOÇ<sup>4</sup>, ARİF ŞENER<sup>4</sup>, TUĞÇE DEMİRDELEN<sup>2</sup>**

<sup>1</sup>*Artificial Intelligence Engineering Department, Adana Alparslan Türkeş Science and Technology University*

<sup>2</sup>*Electrical and Electronics Engineering Department, Adana Alparslan Türkeş Science and Technology University*

<sup>3</sup>*Energy Systems Engineering Department, Adana Alparslan Türkeş Science and Technology University*

<sup>4</sup>*Ulusoy Textile Industry and Commerce Incorporated Company*

**Türkiye**

## SUMMARY

Due to its high solar energy potential, solar PV power plants have recently been used all over the world. Although PV power plants are strongly preferred, the system's fundamental drawback is unstable output power characteristics. The instability and intermittent nature of the power produced from solar PV panels make its integration into the grid difficult. To overcome this problem and to make optimum economic planning, solar radiation estimation studies carried out in solar power plants have become very important. Solar radiation estimation helps grid operators and power system designers to create an optimal solar power plant. In this paper, time series prediction using Long Short-Term Memory (LSTM) Network method is used for short-term solar radiation estimation. Short-term radiation estimation is realized by using real-time data for the solar power plant installed in the Çukurova region of Adana. Different error criteria are calculated to show the superiority of the prediction model. The accuracy and reliability of the proposed method are presented by comparing the estimated radiation values with real-time data. Therefore, this study presents an LSTM based estimation method to assist researchers in solar power plant installation.

## KEYWORDS

Neural networks, Optimization methods, Short-term, Power estimation, Photovoltaic plants



### 1. INTRODUCTION

In recent years, there is a growing desire to shift towards renewable energies, leading to what is known as energy transition. This transition involves moving away from our current energy system, which heavily relies on non-renewable resources, and instead embracing a diverse energy mix primarily based on renewable sources. One of the key challenges in this transition is integrating renewable energies into the existing electricity grid while maintaining a balanced network, where electricity production matches consumption. However, renewable sources such as solar and wind energy are characterized as intermittent because their generation fluctuates depending on weather conditions. This intermittency poses a challenge to effectively harnessing these renewable energies. To overcome this challenge, it is crucial to develop solutions that enable intermittent energy sources to be utilized effectively. These solutions encompass the advancement of storage technologies, implementation of consumption control measures, and expansion of the electricity grid infrastructure. Moreover, accurate forecasting of photovoltaic production will play a vital role in the future. By predicting the amount of electricity that can be generated from solar panels, it becomes possible to better plan and manage the integration of renewable energy into the grid. This forecasting helps grid operators and energy planners make informed decisions about the optimal utilization of renewable energy resources.

The production of solar energy through photovoltaic (PV) systems relies on the amount of sunlight received by the solar panels. However, this process is influenced by various uncontrollable factors such as weather conditions, wind, clouds, temperature, and the intensity and duration of sunlight. These factors introduce fluctuations in energy generation, leading to intermittent power output from PV systems. These intermittencies can cause voltage and frequency variations in the transmission system, resulting in operational challenges. To address the issues caused by these intermittent solar power generation processes, researchers have been investigating the topic of predicting solar photovoltaic power generation. The aim is to develop methods and models that can forecast the amount of power that will be generated by PV systems. By accurately predicting the energy output, it becomes possible to anticipate and mitigate the impact of intermittencies on the power grid, ensuring a more stable and reliable electricity supply. This research topic has gained significant attention in recent years, as it plays a crucial role in optimizing the integration of solar energy into the overall energy system.

In a study [1], the focus is on solar irradiance prediction models, as this parameter is crucial due to its correlation with climate conditions and its ability to capture important weather-related frequencies. Another research paper [2] introduces a data-driven approach that utilizes a wavelet recurrent neural network (RNN) to forecast solar irradiance for a two-day period. The wavelet transform plays a key role in extracting relevant environmental features like wind speed, humidity, and temperature. The model's performance is evaluated using meteorological data from the University of Catania in Italy, showing promising results. In [3], a probabilistic model is proposed for solar irradiance prediction, employing a joint probability distribution function. It is presented an estimation method for evaluating photovoltaic (PV) output power by leveraging solar radiation data. The model is trained using practical data gathered from diverse weather conditions, including cloudy and rainy days, with the aim of creating an economically viable system that generates reliable power output [4]. It is offered a model for predicting PV output power based on weather forecasts provided by the European Centre for Medium-Range Weather Forecasts, covering a three-day period [5].

In [6], a combined physical model is proposed to forecast solar irradiance specifically for inclined surfaces. This method integrates three decomposition models and four transposition models to enhance the accuracy of the predictions. It is presented an effective approach to address the limitations of long short-term memory (LSTM) models in time-series encoding for irradiance prediction. Their model incorporates convolution operators to enrich the prediction capabilities, particularly when dealing with limited datasets [7]. A framework is developed to predict day-ahead photovoltaic (PV) power using a long-short-term memory recurrent neural network (LSTM-RNN). This framework aims to provide accurate daily pattern predictions for specific days [8]. Husein and Chung employ a similar approach, utilizing LSTM-RNN based deep learning models to accurately predict day-ahead solar irradiance. Their study includes case studies from Germany, the USA, Switzerland, and South Korea [9]. In another study [10], an efficient forecasting method is proposed for solar irradiance, focusing on time horizons ranging from 1 minute to 10 minutes ahead. This method utilizes a modified surface irradiance forecasting approach, incorporating derived data from actual sky images. The aim is to achieve precise short-term predictions of solar irradiance. Additionally, it is introduced a computational mapping framework based on deep learning techniques for solar PV power prediction. This framework enables real-time interaction between sky images and surface irradiance. In this approach, the sky image datasets are pre-processed and clustered using a convolutional autoencoder (AE) for feature extraction and the K-means clustering method [11].

Based on the literature mentioned earlier, it is observed that forecast accuracy tends to be lower on cloudy days, while it improves with more reliable weather forecasts. To address this, the study adopts an approach based on long short-term memory (LSTM), a type of artificial neural network (ANN), for short-term predictions. The LSTM-based method is specifically chosen because it has shown promise in improving the accuracy of forecasts, particularly in situations where weather conditions are less predictable, such

as during cloudy periods. By leveraging the capabilities of LSTM, the study aims to enhance the precision of short-term predictions for solar power or irradiance, considering the specific challenges posed by variable weather patterns.

## 2. MATERIALS AND METHODS

Long Short-Term Memory (LSTM) is a type of recurrent neural network (RNN) architecture that is designed to address the limitations of traditional RNNs when it comes to capturing and learning long-term dependencies in sequential data. It was introduced by Hochreiter and Schmidhuber in 1997 [12]. LSTMs are particularly useful in tasks involving sequential data, such as speech recognition, natural language processing, time series analysis, and machine translation, among others. They are well-suited for these tasks because they can effectively model and process sequences of variable length while maintaining memory over long time periods. The key innovation of LSTMs lies in their ability to capture and store information over extended sequences. They achieve this by incorporating memory cells, which are responsible for retaining information over time. LSTMs consist of multiple memory cells that interact with each other through various gating mechanisms. The core components of an LSTM cell are cell state, input gate, forget gate, output gate and candidate activation as shown in Figure 1.

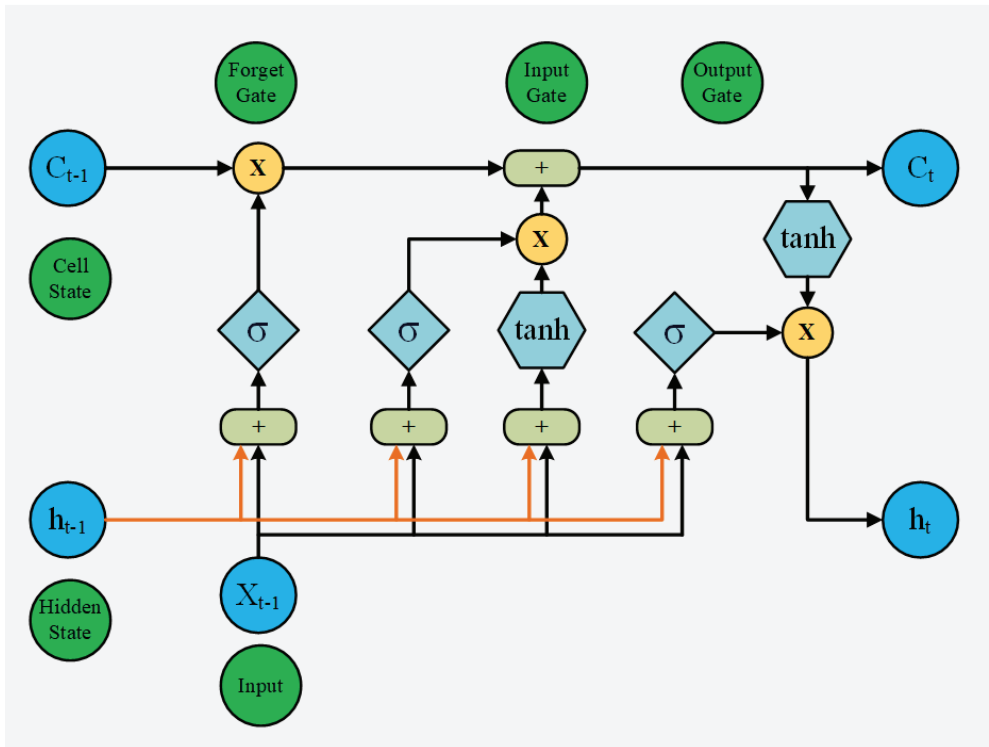


Figure 1: The structure of the Long Short-Term Memory

Cell state represents the memory of the LSTM cell and carries information from one time step to another. The cell state can selectively retain or discard information through the use of gates. Input gate determines the degree to which the current input should be used to update the cell state. Forget gate controls the extent to which the previous cell state should be forgotten or discarded. Output gate regulates the amount of information that is exposed from the current cell state. Candidate activation represents the new information that could potentially be added to the cell state. By modulating the input, forget, and output gates, LSTMs can effectively manage the flow of information through time and selectively retain or discard information based on its relevance. This ability to retain long-term dependencies makes LSTMs powerful in modeling complex sequential patterns. To ensure the proper functioning of the LSTM architecture, specific values need to be computed for various variables. These variables include the forget gate ( $f_t$ ), the candidate internal state ( $S$ ), the input gate ( $i_t$ ), the memory cell state ( $h_t$ ), the output gate ( $o_t$ ), and the internal memory of the unit ( $C_t$ ).

$$f_t = \sigma(W_f X_t + U_f h_{t-1} + b_f) \quad (1)$$

$$i_t = \sigma(W_i X_t + U_i h_{t-1} + b_i) \quad (2)$$

$$S = \tanh(W_c X_t + U_c h_{t-1} + b_c) \quad (3)$$



$$C_t = i_t S_t + f_t S_{t-1} \tag{4}$$

$$o_t = \sigma(W_o X_t + U_o h_{t-1} + V_o C_t + b_o) \tag{5}$$

$$h_t = o_t \tanh(C_t) \tag{6}$$

Where  $\tanh$  and  $\sigma$  are the activation functions,  $X$  is the memory cell's input vector at time  $t$ .  $b_f, b_c, b_i$  and  $b_o$  are biases.  $W_f, W_c, W_i, W_o, U_c, U_i, U_f, U_o$  and  $V_o$  are weights of the neural network.

### 3. RESULTS AND DISCUSSIONS

In this study, real-time data obtained from the PV plant established in the Çukurova region have been used to perform solar radiation prediction. The training has been carried out with the 10-day solar radiation data obtained from the Çukurova region. Solar radiation estimation has been performed based on LSTM with 2-day data. Real solar radiation against predicted solar radiation values by LSTM is shown in Figure 2. The results obtained from data set highlight the effectiveness of the LSTM neural network architecture for short-term solar radiation prediction in the Çukurova region. The LSTM model accurately captures the underlying patterns and fluctuations in solar radiation. These results show that the proposed LSTM can be a valuable tool for forecasting solar radiation, which is essential for various applications such as solar energy generation and grid integration.

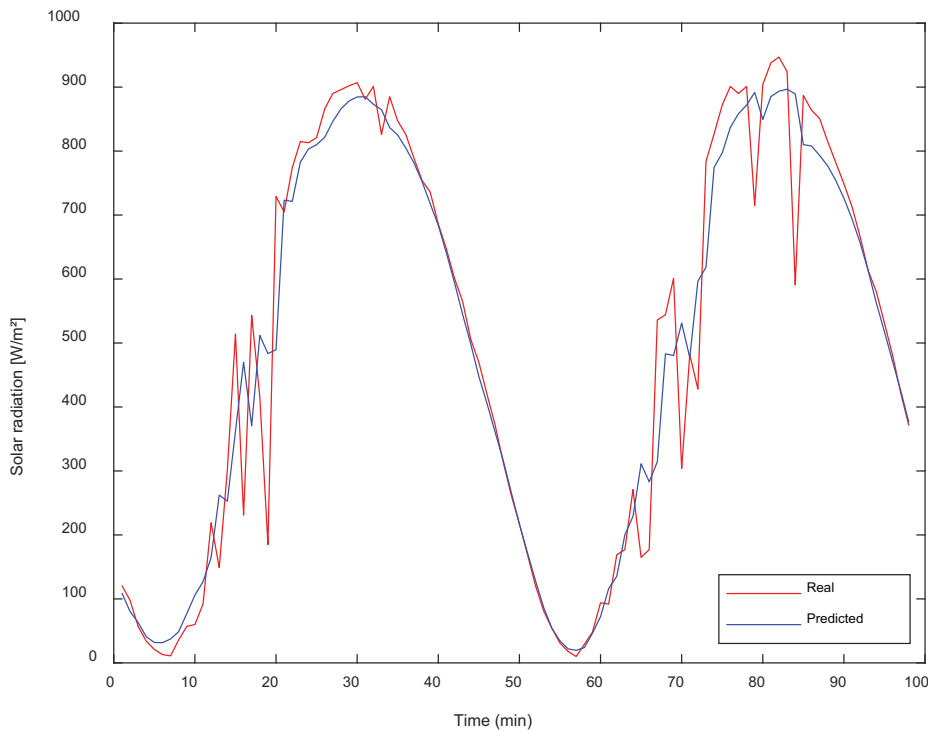


Figure 2: Real solar radiation against predicted solar radiation values by LSTM

The LSTM neural network architecture utilizes its recurrent neural network architecture to effectively capture the sequential nature of the solar radiation time series data. LSTM units enable the model to learn and remember important patterns and dependencies over time, resulting in more accurate predictions. The success of the LSTM model can be attributed to its ability to capture both short-term and long-term dependencies in the data. Solar radiation is influenced by various factors such as time of day, seasonality, weather conditions, and cloud cover. The LSTM model effectively learns the complex relationships between these factors and the solar radiation values, allowing it to make accurate predictions even in the presence of changing environmental conditions. Regression graph based on LSTM neural network architecture is shown in Figure 3.

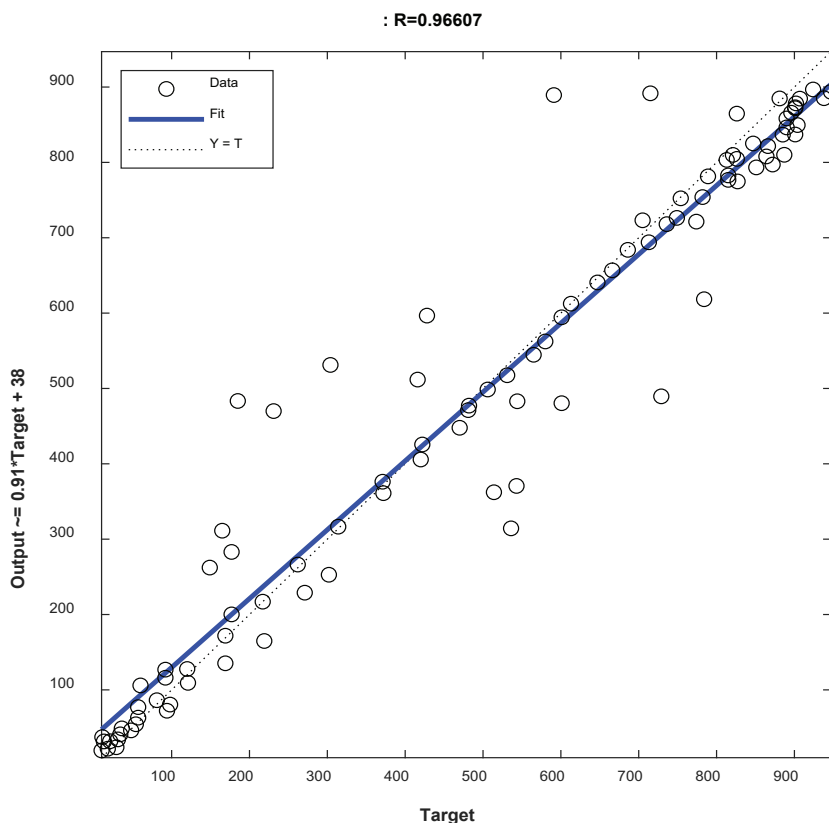


Figure 3: Regression graph based on LSTM neural network architecture

The performance of the LSTM neural network architecture may vary across different regions and time periods. Factors such as geographical location, local weather patterns, and data quality can affect the model’s predictive capability. Therefore, it is important to train and evaluate the model using region-specific data to ensure reliable and accurate predictions.

In conclusion, our study demonstrates the effectiveness of the LSTM neural network architecture for short-term solar radiation prediction in the Çukurova region. The model’s ability to capture temporal dependencies and accurately forecast solar radiation values holds great potential for applications in solar energy generation, energy management, and other related fields. Additionally, incorporating additional meteorological and environmental variables could potentially improve the accuracy of solar radiation predictions.

#### 4. CONCLUSION

Due to the rapid growth in global energy demand, the existing energy resources are projected to be inadequate. To tackle this challenge, there is a growing demand for renewable energy sources as a potential solution. Among these alternatives, solar energy is the most commonly adopted due to its perception as an abundant and sustainable resource. This study focuses on estimating the levels of solar irradiation acquired from PV panels. Real-time data is utilized to estimate short-term radiation for a solar power plant located in the Çukurova region of Adana. To achieve this objective, the LSTM Network method, which has gained recent popularity in the literature, is utilized as the preferred approach for the estimation process. In this study highlights the effectiveness of LSTM networks in solar radiation estimation, demonstrating their ability to leverage temporal dependencies and accurately predict solar radiation values. The adoption of LSTM-based models holds great promise for advancing solar energy applications, contributing to the transition towards sustainable and efficient renewable energy systems.

#### 5. ACKNOWLEDGMENT

This research was funded by the ULUSOY textile R&D Center under the project number 2023/001.





### BIBLIOGRAPHY

- [1] E. D. Obando, S. X. Carvajal and J. P. Agudelo, «Solar radiation prediction using machine learning techniques: A review», IEEE Latin Amer. Trans., vol. 17, no. 4, pp. 684-697, Apr. 2019.
- [2] G. Capizzi, C. Napoli and F. Bonanno, "Innovative second-generation wavelets construction with recurrent neural networks for solar radiation forecasting", IEEE Trans. Neural Netw. Learn. Syst., vol. 23, no. 11, pp. 1805-1815, Nov. 2012.
- [3] M. Kakimoto, Y. Endoh, H. Shin, R. Ikeda and H. Kusaka, "Probabilistic solar irradiance forecasting by conditioning joint probability method and its application to electric power trading", IEEE Trans. Sustain. Energy, vol. 10, no. 2, pp. 983-993, Apr. 2019.
- [4] M. H. Rahman and S. Yamashiro, "Novel distributed power generating system of PV-ECaSS using solar energy estimation", IEEE Trans. Energy Convers., vol. 22, no. 2, pp. 358-367, Jun. 2007.
- [5] E. Lorenz, J. Hurka, D. Heinemann and H. G. Beyer, "Irradiance forecasting for the power prediction of grid-connected photovoltaic systems", IEEE J. Sel. Topics Appl. Earth Observ. Remote Sens., vol. 2, no. 1, pp. 2-10, Mar. 2009.
- [6] C. Cui, Y. Zou, L. Wei and Y. Wang, "Evaluating combination models of solar irradiance on inclined surfaces and forecasting photovoltaic power generation", IET Smart Grid, vol. 2, no. 1, pp. 123-130, 2019.
- [7] Y.-Y. Hong, J. J. F. Martinez and A. C. Fajardo, "Day-ahead solar irradiance forecasting utilizing Gramian angular field and convolutional long short-term memory", IEEE Access, vol. 8, pp. 18741-18753, 2020.
- [8] F. Wang, Z. Xuan, Z. Zhen, K. Li, T. Wang and M. Shi, "A day-ahead PV power forecasting method based on LSTM-RNN model and time correlation modification under partial daily pattern prediction framework", Energy Convers. Manage., vol. 212, May 2020.
- [9] M. Husein and I.-Y. Chung, "Day-ahead solar irradiance forecasting for microgrids using a long short-term memory recurrent neural network: A deep learning approach", Energies, vol. 12, no. 10, pp. 1856, 2019.
- [10] F. Wang et al., "A minutely solar irradiance forecasting method based on real-time sky image-irradiance mapping model", Energy Convers. Manage., vol. 220, Sep. 2020.
- [11] Z. Zhen et al., "Deep learning based surface irradiance mapping model for solar PV power forecasting using sky image", IEEE Trans. Ind. Appl., vol. 56, no. 4, pp. 3385-3396, Jul./Aug. 2020.
- [12] S. Hochreiter and J. Schmidhuber, "Long Short-Term Memory", Neural Computation, vol. 9, no. 8, pp. 1735-1780, 1997.

## ENERGY TRANSITION

### POSTER PRESENTATION



ELECTRIC MACHINES AND  
POWER ELECTRONICS



ELECTRIC  
TRANSMISSION



AUTOMATION AND  
CONTROL

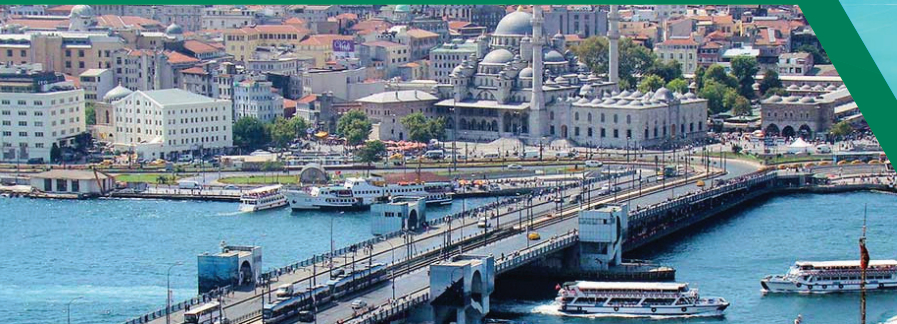
POWER  
GENERATION



ENERGY  
TRANSITION



DISTRIBUTION SYSTEMS  
AND SMART GRIDS



11-12 OCTOBER 2023



# Optimization Module and Auction Mechanism for the Trading of Guarantees of Origin

[milan.josifovic@pupin.rs](mailto:milan.josifovic@pupin.rs)

**MILAN JOSIFOVIC\*, GORAN JAKUPOVIC, TATJANA PETROVIC KONECNI**

*Institute "Mihajlo Pupin", University of Belgrade*

**DEJAN STOJCEVSKI, VLADIMIR STANOJEVIC**

*SEEPEX a.d. Beograd (SEEPEX)*

**Serbia**

## SUMMARY

This paper presents the work of the optimization module of the application for trading guarantees of origin, as well as the auction mechanism itself. First, a brief overview of the entire application, its business process, and the software architecture is given. Then a description of the algorithms, i.e. a mathematical model of the optimization process, is given. The following is a functional description of the software, as well as a description of the software technologies used. In the end, a brief overview of user interface is given with focus on results.

The optimization module was developed using the C++ programming language on the Linux platform (specifically Oracle Linux 7.9). The basic optimization problem is reduced to a linear programming problem, and open source libraries, specifically GLPK (Gnu Linear Programming Toolkit), are used to solve that problem. The interface is made in Java. Data about auctions, participants, bids and other data are stored in a relational MySQL database.

The described module was developed as part of the HORIZON 2020 TRINITY project (H2020-863874 TRANSMISSION SYSTEM ENHANCEMENT OF REGIONAL BORDERS BY MEANS OF INTELLIGENT MARKET TECHNOLOGY).

## KEYWORDS

Guarantees of origin-Optimization-GLPK-Linear programming



### 1. INTRODUCTION

TRINITY (TRansmission system enhancement of regioNal borders by means of IntelligenT market technology) project deals with topics from the research program of the European Union called Research Horizon Framework 2020 Program, within the field of "Building a low-carbon future resistant to climate change: safe, clean and efficient energy" [1].

The primary objective of the Trinity project is to enhance coordination and foster stronger collaboration among transmission system operators (TSOs) in South Eastern Europe (SEE), market operators, electricity producers, and market participants. This endeavour aims to facilitate the integration of the electricity market in the region while maximizing the utilization of renewable energy sources. Additionally, the project seeks to promote the harmonization of cross-border services between the European Union (EU) and non-EU countries.

The three main pillars on which the above project goals are based are Market Unification, Coordination of Transmission System Operators and Integration of Renewable Energy Sources (RES). They are directly covered by the three TRINITY products, which are interconnected thanks to the fourth product, the T-coordination platform. This project is realized in cooperation with 19 companies from 11 European countries.

One of the products being developed as part of this project is the Market Connection Platform, which consists of four independent modules that will enable cross-border trade in electricity and the integration of national markets into the regional market as the first step in creating a single European electricity market. The modules that make up this product are intended for:

- Intraday merging of markets through the auction mechanism
- Trade in capacity reserves for system balancing purposes
- Bilateral trade
- Trade in Guarantees of Origin

The demonstration of these modules is scheduled for 2022 and 2023.

The module for trade in guarantees of origin, jointly developed by IMP (Mihajlo Pupin Institute), EKC (Electricity Coordination Center) and SEEPEX (Electricity Market Operator), will improve the trade in guarantees of origin in the region of Southeast Europe by developing a module for auction and continuous trade.

The guarantee of origin is an electronic document that offers proof of the source of energy used by the end consumer. This type of document was introduced to create greater environmental awareness by allowing end consumers to express their demand for green energy and thus stimulate the production of energy that does not harm the environment. There is no fixed price for guarantees of origin, and their value depends on market demand. The system of guarantees of origin uses certificates that guarantee the attributes of the produced MWh of electricity. The guarantee of origin is issued to the producer for a unit net amount of 1MWh of energy produced from renewable sources in accordance with the national legislation (law on energy, regulation on guarantees of origin and rules on issuing guarantees of origin). The electricity generation period for which the guarantee of origin is issued is a calendar month. The guarantee of origin automatically expires after 12 months from the end of the production period. Also, it may become invalid if it has already been used or withdrawn by the issuing authority.

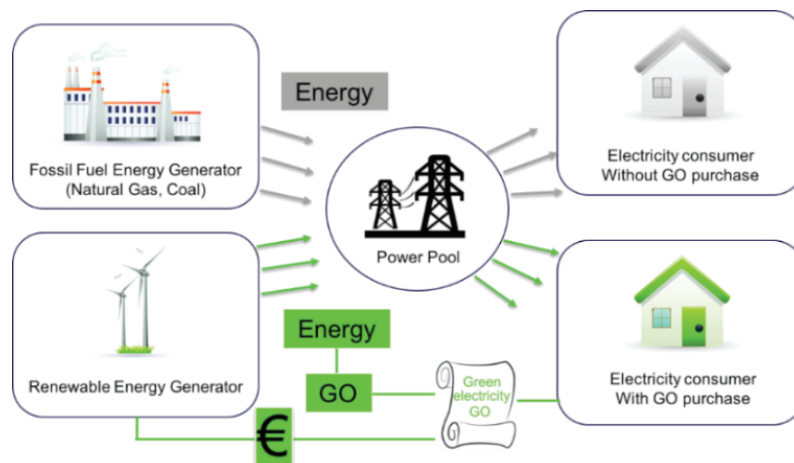


Figure 1: GoO Trading





Figure 2 shows the simplified business process of the guarantee of origin trading module.

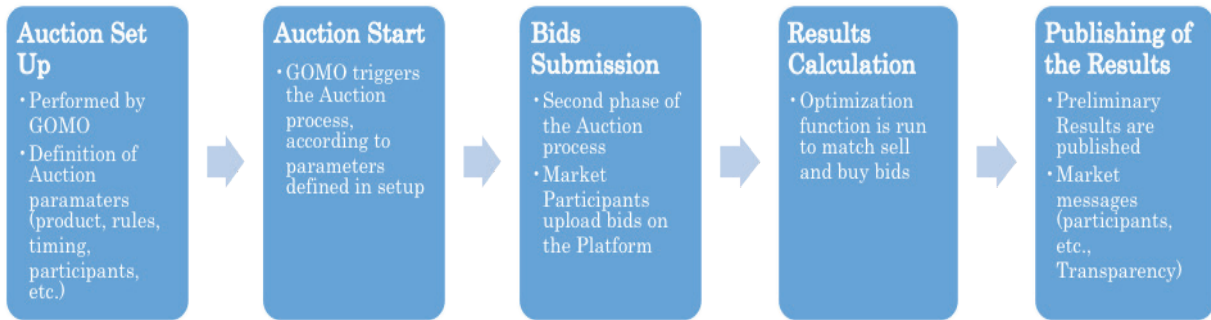


Figure 2: Business process

### 2. GENERAL OVERVIEW OF ARCHITECTURE

The guarantee of origin trade application consists of two units that use a common database

- “Back-end” part, i.e. the optimizer, which consists of a scheduler and an auction optimizer. Its primary function is to facilitate the optimal matching of offers for sale and purchase, ensuring efficient and effective transactions.
- “Front-end” part consisting of WEB interface, REST API and GLASFISH application server. This user-facing part of the application allows market participants to interact with the system, access relevant information, submit offers, and conduct trade activities.

The topic of this paper is the auction process itself and the work of the optimizer itself.

The optimizer aims to find the optimal solution using linear programming for a defined objective function with constraints.

Each product is optimized separately, that is, the auction for one technology represents one optimization problem that needs to be solved. A different set of technologies can appear within one auction:

- Hydro
- Wind
- Solar
- Biomass

A simplified structure of the system is given in Figure 3.

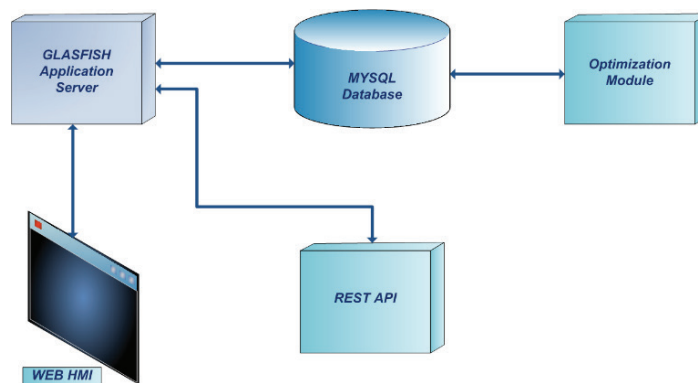


Figure 3: Simplified diagram of a system

### 3. OPTIMIZATION ALGORITHM

For each of the defined technologies (Hydro, Wind, Solar ...) a separate optimization is performed, using the optimization algorithm described in the following text. During one auction, the user is allowed to place bids for different technologies, the optimizer will set and solve an independent optimization problem for each of the mentioned technologies.



### 3.1. Objective function

The objective function of the optimization algorithm is represented by total welfare, which needs to be maximized in the considered time interval. Welfare is defined as the difference between the cumulative amount of money that buyers are willing to pay and the cumulative amount of money for which sellers are willing to sell a given quantity of a product (which for each market participant lies in the interval between zero and the maximum offered quantity for buying/selling) [2].

The objective function is:

$$\max \sum_{i=1}^n q_i^B \cdot (p_i^B + \varepsilon) - \sum_{j=1}^m q_j^S \cdot (p_j^S - \varepsilon) \quad (1)$$

where  $n$  is the total number of purchase offers,  $m$  is the total number of sales offers for the observed auction with a predefined product.

$p_i^B$  - the price at which the  $i$ -th buyer is ready to buy the requested quantity

$p_j^S$  - the price at which the  $j$ -th seller is willing to sell the offered quantity

$q_i^B$  - accepted quantity of  $i$ -th customer (variable)

$q_j^S$  - accepted quantity of  $j$ -th seller (variable)

It should be noted here that in the objective function, the additional term  $\varepsilon$  is introduced in order to maximize traded quantity, in case of quantity (volume) indeterminacy. The value of the parameter  $\varepsilon$  in the objective function can be arbitrarily small, depending on the price resolution applied in the observed market. If the offered prices are given with precision to two decimal places, the following parameter value can be adopted in the objective function:  $\varepsilon = 10^{-3}$ .

### 3.2. Limitations of the optimization problem

Within the optimization problem, which represents the maximization of the previously defined objective function, it is necessary to respect the following linear constraints, which can be divided into two categories [2].

C1: As offers (bids) can be accepted in whole or partially (minimum amount is 1MWh), accepted quantities of offers for purchase/sale must satisfy the following linear constraints:

$$\begin{aligned} 0 &\leq q_i^B \leq Q_i^B \\ 0 &\leq q_j^S \leq Q_j^S \end{aligned} \quad (2)$$

$Q_i^B$  - submitted quantity of the  $i$ -th customer

$Q_j^S$  - submitted quantity of the  $j$ -th seller

The previous two sizes are entered by the participant in the stage of loading bids.

C2: The total traded quantity should be equal to the total amount of accepted buy and sell bids [2]:

$$\sum_{j=1}^m q_j^S - \sum_{i=1}^n q_i^B = 0 \quad (3)$$

## 3. OPTIMIZATION MODULE DESCRIPTION

The optimization module functions as an independent component, and its operational process is illustrated in Figure 3. The process scheduler, known as the *Scheduler*, waits for data of a particular auction. Once the auction concludes (after the data entry phase has ended and the calculation phase begins), the Scheduler forwards the data to the optimizer for subsequent processing.



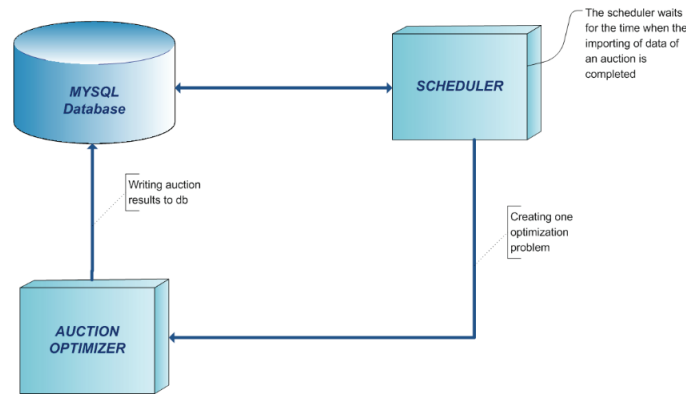


Figure 4: Process of optimization

After the accepted auction, the optimizer creates the structure of a linear problem in CPLEX format and solves it using the GLPK (GNU Linear Programming Toolkit) library for linear programming [3].

In the end, the solutions are entered into the database so that they are ready for further processing, i.e. display via the WEB interface. The obtained solutions represent the optimal values of offers (buying and selling) and their initial prices.

### 4. CALCULATION OF PRICES

The optimization problem is easy to solve since there is only an equilibrium equality constraint. In other words, it can be solved in an iterative procedure by accepting buy and sell offers until the highest sell offer meets the lower buy offer. The traded volume should then be equal to the minimum between the sum of all accepted buy bid quantities and the sum of all accepted sell bid quantities. The main reason why the linear programming formulation is introduced is to find the market clearing price, as a solution to the dual:

$$\min_{\pi} \sum_{i=1}^n Q_i^B (p_i^B - \pi + \varepsilon)_+ + \sum_{j=1}^m Q_j^S (\pi - p_j^S + \varepsilon)_+ \tag{4}$$

where  $(\cdot)_+$  denotes  $\max\{\cdot, 0\}$ , and  $\pi$  is the optimal dual solution corresponding to the price that clears the market, i.e. The Lagrange product related to the constraint C2 that balances demand and supply.

A special case is a case in which there is no limit offer, that is, there are no partially accepted offers. Multiple solutions are then possible for the cost of cleaning. Then the price is calculated as follows:

$$\pi = \frac{1}{2} \times (\min\{P_1, P_2\} + \max\{P_3, P_4\}) \tag{5}$$

where :

$P_1$ =min(completely accepted purchase offers)

$P_2$ =min(unaccepted sales offers)

$P_3$ =max(unaccepted purchase offers)

$P_4$ =max (completely accepted sales offers)

This approach sets the market price at a value that maximizes the total welfare of all buyers and sellers separately, as well as the total social welfare of all participants.

### 5. APPLICATION AND TEST RESULTS

There is 3 software platforms in the GoO (Guarantees of origin)[4] :

- The GO Platform for Issuing Body, to storage and



validate operations.

- The RES Manager platform , to request GoOs for generated energy
- The trading platform (It is the focus of this paper, auction mechanism part)

### 5.1. Interface

Depending on the type of user, the main functions of the interface are:

- Creation of auction scenarios
- Creation and launch of the auction
- Placing bids
- Monitoring of auction trading
- Overview of results
- Access to process records

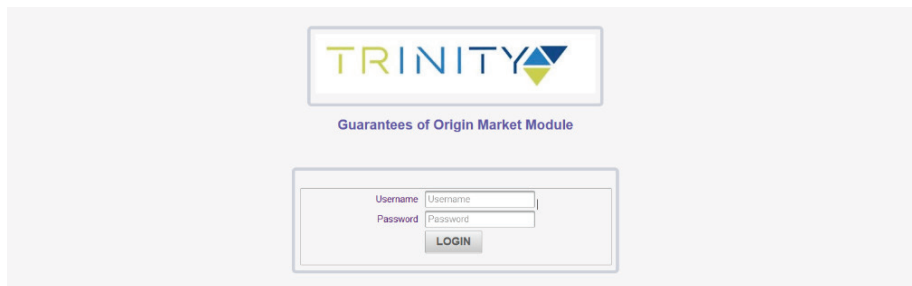


Figure 5: Login page

### 5.2. REST API Web Service

Allows third-party applications to read auction data, place bids and retrieve results. The sequence diagram is given in the following figure.

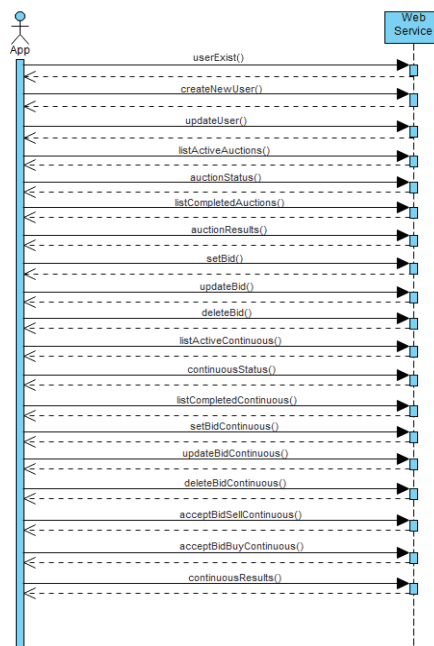


Figure 6: Sequence diagram



5.3. Results overview

The results of the auction are divided into two views. On the first display (Figure 7) you can see: the period for which the guarantee was issued, technology, name of the power plant, quantity (MWh), price for the power plant (€/MWh), name of the seller, domain in which the seller is registered, name of the buyer, the domain in which the customer is registered.

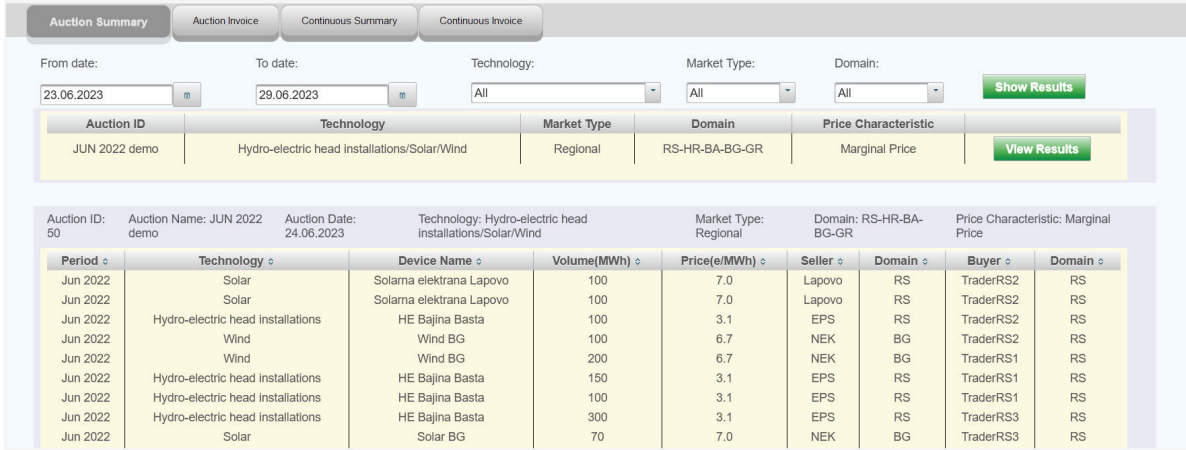


Figure 7: Results of one auction

The second display (Figure 8) provides a detailed overview of the auction results, i.e.: bid identification number, technology type, power plant name, user name, sales/purchase bid status, offered quantity, received quantity, initial price, final price, bid status (rejected - red, partially accepted - orange and fully accepted - green).

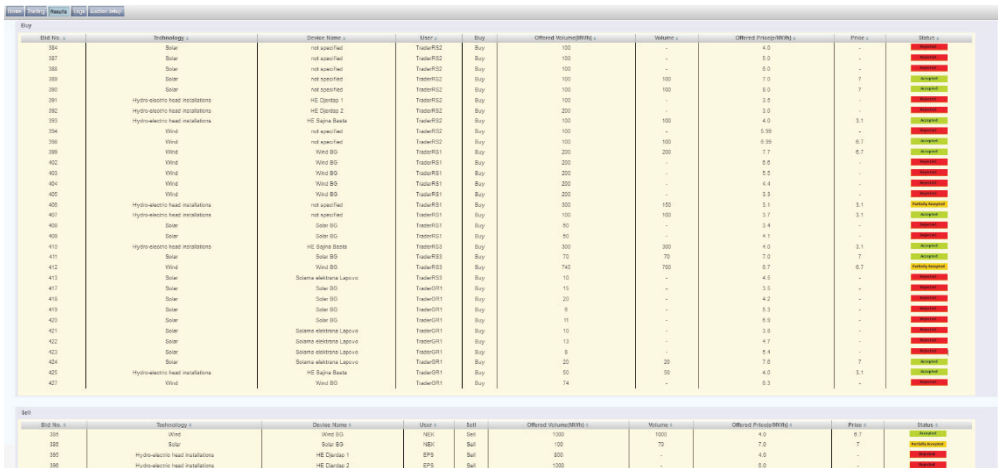


Figure 8: Detailed results of one auction

The above views are available to the GOMO user, i.e. the administrator, while for auction participants these views are limited to their bids.

6. CONCLUSION

Increasing trends in Europe, and throughout the world, give great importance to the implementation of renewable sources of electricity through the application of market mechanisms of the organization of the electricity market. There is a need for tools that will encourage greater production of electricity, and among them is trade in guarantees of origin. Guarantees of origin have the exclusive function of proving to the end customer that a certain share or amount of energy has been produced from renewable sources. Guarantees of origin offer electricity consumers the opportunity to express a voluntary demand for green energy and stimulate electricity production that contributes to a more environmentally friendly energy system. This module enables trading on



the local and regional market, taking into account the needs and role of issuing authorities and market participants. The platform brings several innovations: it establishes a direct link between the Issuing Body and the Guarantees of Origin Market Operator, enables cross-border trade in guarantees of origin between different domains and connects the auction and continuous trade, which is a prerequisite for trade in guarantees of origin throughout the year. This tool will improve the trade of guarantees of origin in the Southeast European region in an organized way, by developing modules for auction and continuous trade and will be adaptable to the specific needs of the market. The work itself is focused on the auction part of the application, while the entire idea of the application also includes continuous trade, so as such a whole it has a wide application on the market.

## 7. ACKNOWLEDGEMENTS

The work described in this paper has been conducted within the HORIZON 2020 TRINITY project (H2020-863874 Transmission system enhancement of regional borders by means of Intelligent market technology). The research and development described in this paper have been produced with the financial assistance of the European Union. The contents of this document are the sole responsibility of the authors and can under no circumstances be regarded as reflecting the position of the European Union. Additionally, the research described in this paper was funded by the Ministry of Education, Science, and Technological Development of Serbia.

## BIBLIOGRAPHY

- [1] T-MARKET COUPLING FRAMEWORK, <http://trinityh2020.eu/>
- [2] TRINITY Project, «D3.2 IMC, CRA, GO and OTCM design and development of business processes».
- [3] Andrew Makhorin, "GNU Linear Programming Kit – Reference Manual for GLPK Version 4.58", Free Software Foundation, Inc., February 2016
- [4] Á. Nofuentes, J. J. Hernández and L. Pons, "Blockchain-based Guarantees of Origin issuing platform," 2022 18th International Conference on the European Energy Market (EEM), Ljubljana, Slovenia, 2022, pp. 1-4, doi: 10.1109/EEM54602.2022.9920988.



# Insuring Power System Reliability Under High Renewables Penetration with Energy Storages - A Case for Ukraine

[mail2ua@gmail.com](mailto:mail2ua@gmail.com)

**SERGII SHULZHENKO**

*General Energy Institute, National Academy of Sciences of Ukraine*

**Ukraine**

## SUMMARY

The recent adoption of the changes to the Ukrainian Law on Electricity Market regarding energy storage implementation and operation in the Power System and general European trend on development of electric vehicles which will replace internal-combustion engine land transportation potentially create conditions for further development of clean generation, e.g., renewables. The high renewable (i.e., wind and solar generation) penetration into the Ukrainian power system was modelled with the use of the unit commitment optimization technique. The influence of the electric vehicle's development on the electricity demand and load shapes was assessed in general. The main objective of the study was to ensure power system reliability using wind and solar generation curtailment or implementation of energy storage for the shifting of wind and solar generation excess to the load-peaking hours. The amount of generation by fossil fuel power plants and base-load nuclear also were in the focus of the study. The integral approximate assessments of the power system's electricity production cost are also presented for these alternatives. The results show that the implementation of energy storage positively affected power system reliability with high penetration of wind and solar generation allowing to decrease the hazard emissions and greenhouse gases.

## KEYWORDS

Energy transition, power system, renewables, power system reliability, greenhouse gases, hazard emissions, unit commitment optimization technique



Poster Presentation: Insuring Power System Reliability Under High Renewables Penetration with Energy Storages - A Case for Ukraine

### 1. INTRODUCTION

The main principles of the EU could be expressed as security of supply, market competitiveness and sustainability [1]. The security of supply in general means acceptable levels of adequacy of resources available for the Power System which are under control of operator(s). Market competitiveness require equal, not-discriminative “rights” for each market participant, and ideally absence of State’s interventions. Sustainability is a complex concept but using simple words – it’s a minimal (ideally absence) negative impact on the nature and humanity from the technical equipment and the systems. This concept is consistent with Sustainable Development Goal 7 “Affordable and Clean Energy”, namely target 7.1 “By 2030, ensure universal access to affordable, reliable and modern energy services” [2]. One of these “modern energy services” is electric power (in terms of Watt), which ideally should be available for consumers 24/7 and appropriate quality. Hence the main task of electricity service providers (in general words), or Transmission System Operators (TSO) is to predict the future needs and ensure possibilities to securely supply of required amount of electric power, which is exactly unknown. Even more, TSO should follow the political tends or goals, which in present time require year-to-year higher penetration of intermittent renewables (wind and solar) into Power Systems. In those conditions as formulated in a number of, e.g., EU Regulations TSO should find the solution(s) to ensure security of electric power supply with minimal environmental impact and under electricity market.

This study is dedicated to assessing the influence on operation of the national Power System from such main factors:

- the increase of the installed capacity of renewables (wind and solar);
- the increase of the national electric vehicle fleet;
- implementation of the industrial size battery energy storages in the Power System, which are used daily to exclude imbalances during each day in the system, hence they are dispatched with centralized commands.

The calculations were made using unit commitment optimisation mathematical model [3,4] and appropriate software tool. The mathematical model is considered specific generation units’ operation modes which are traditional for the Ukrainian Integrated Power System, notably, hydro units of Hydroelectric Pumped Stations, Combined Heat and Power’ units, Thermal Power Plants’ units. The calculations were made for whole projected year, for each day (24 hours) separately, hence 365 calculations for the year were made. The main constraint of the model is the strict balance between electric power generation and consumption for each modelled hour. The power output from Nuclear Power Plants and Combined Heat and Power was modelled as a flat generation. The generation of wind farms and solar stations were set exogenously as the predetermined profiles, which are corresponding to the actual profiles but scaled according to the forecasted installed capacity of wind and solar generation.

The calculations were made for the two scenarios: “Baseline” and “Electric Vehicles”. The basic assumption for the “Baseline” scenario are:

- electricity consumption in the System – 190 TWh per year, which is projected for the period 2035 – 2040;
- absolute maximum of the load - 30.5 GW;
- absolute minimum of the load - 15.2 GW;
- wind generation installed capacity - 7GW, starting from 6.3 GW at the beginning of the year and gradually reach 7 GW at the last quarter of the year;
- PV generation installed capacity - 11 GW, starting from 9.5 GW at the beginning of the year and gradually increases and reaching 11 GW at the last quarter of the year;
- installed capacity of the Nuclear Power Plants - not less then 15 GW, the refuelling periods are considered, so available capacity always lower then installed, the exact installed capacity is a result of optimization;
- thermal power units - installed capacity is a result of optimization according to the required amount of secondary reserves should be always available in the system, considering secondary reserves allocated at hydroelectric power stations;
- installed capacity of Combined Heat and Power connected to the Power System - 3 GW, available capacity is changing during a year according to the heat demand, hence maximum capacity is during a winter period;
- aoutoproducers, small hydro and other renewables is set as a flat generation for each day according to the statistical data;
- generation by hydroelectric power stations with reservoirs is calculated considering the statistical data regarding changes in available hydro resources during a year;





Poster Presentation: Insuring Power System Reliability Under High Renewables Penetration with Energy Storages - A Case for Ukraine

- generation of hydroelectric pumped station is optimizing according to the system' load needs, installed capacity - 1.8 GW; installed capacity of industrial size battery energy storages which are dispatched according to the system' load needs - 2 GW.

The "Electric Vehicles" scenario assumed that in the forecasted period (between 2035 and 2040) more than 1.5 million of electric vehicles will be used in Ukraine:

- 24 thousand of passenger busses (it is 10% compared to the number of busses in 2020 - 237 thousand);
- 183 thousand of heavy tracks (10% compared to the 1834 thousand in 2020);
- 1497 thousand of passenger cars (15% compared to the 9982 thousand in 2020).

The use of such electric vehicles fleet will affect the demand for electricity and will change the system' daily load shapes. To take this into consideration the assumptions regarding charging modes for each considered type of electric vehicles were made:

- one bus is charging for 12 hours, continuously consuming 20 kW of electric power;
- one heavy truck - the charging mode is the same as for a bus;
- one car is charging for 5 hours, continuously consuming 5 kW.

The EV2Grid option for electric vehicles was not considered, and this is conservative assumption based on Ukrainian specifics, hence all these vehicles are treated as the pure consumers. Also assumed that one charging profile for electric vehicles' type is used for every day of the year (fig. 1).

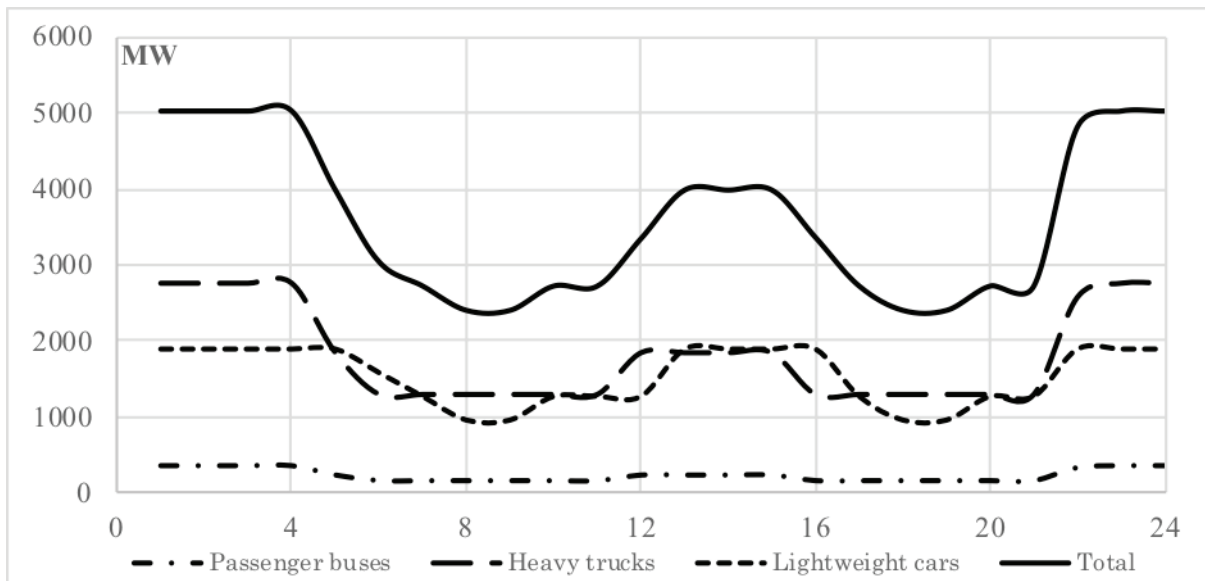


Figure 1: Charging profiles by electric vehicle types

Due to the influence of electric vehicles' charging profile the overall consumption of electricity in the system increasing up to 222 TWh per year, absolute maximum of the load is increasing up to 34 GW (compared to 30.5 GW according to the "Baseline" scenario), absolute minimum jumped up to 18.3 GW (15.2 GW for the "Baseline" scenario).

The results of calculations are presented in the tables below (tab. 1 corresponding to the "Baseline" scenario, and tab.2 for "Electric Vehicles" scenario).



Poster Presentation: Insuring Power System Reliability Under High Renewables Penetration with Energy Storages - A Case for Ukraine

Table 1: The result of calculation for "Baseline" scenario

	Yearly		Monthly electricity production (TWh), fuel consumption and emissions											
	Generation mix, GW / %	Electricity production, TWh / %	1	2	3	4	5	6	7	8	9	10	11	12
	TPP (coal fired)	25.0 / 33.3%	45.5 / 23.5%	6.45	4.97	3.50	2.80	1.98	2.55	2.44	3.14	3.73	4.99	4.12
TPP (nat. gas fired)	2.3 / 3.0%	4.3 / 2.2%	0.20	0.17	0.21	0.33	0.26	0.37	0.39	0.38	0.45	0.51	0.53	0.54
NPP	15.0 / 20.0%	97.8 / 50.5%	9.48	8.56	9.40	8.18	8.70	8.01	8.46	7.57	6.52	7.25	7.38	8.28
CHP, auto producers, other renewables	6.0 / 8.0%	10.3 / 5.3%	1.40	1.25	1.35	0.72	0.60	0.46	0.43	0.38	0.40	0.68	1.18	1.44
Hydro (reservoir)	5.0 / 6.7%	6.1 / 3.2%	0.70	0.62	0.83	0.90	0.73	0.38	0.37	0.39	0.26	0.29	0.35	0.31
Hydro Pumped	1.8 / 2.4%	1.7 / 0.9%	0.07	0.09	0.14	0.15	0.16	0.15	0.16	0.16	0.15	0.16	0.15	0.16
Wind	7.0 / 9.3%	15.2 / 7.9%	1.05	0.94	1.12	1.12	1.02	1.14	0.75	1.11	1.43	0.87	2.55	2.11
PV	11.0 / 14.7%	12.3 / 6.3%	0.16	0.35	0.86	1.15	1.21	1.53	1.66	1.67	1.43	1.17	0.64	0.43
Battery Energy Storages	2.0 / 2.7%	0.4 / 0.2%	0.00	0.00	0.00	0.03	0.02	0.03	0.03	0.05	0.10	0.09	0.04	0.03
<b>Total</b>	<b>75</b>	<b>193.6</b>												
Coal consumption, mln ton	—	25.0	3.5	2.7	1.9	1.5	1.1	1.4	1.3	1.7	2.0	2.7	2.3	2.7
Nat. gas consumption, bill cub. meters	—	4.6	0.5	0.5	0.5	0.3	0.3	0.2	0.2	0.2	0.2	0.4	0.5	0.6
CO <sub>2</sub> emission, mln ton	—	60.9	8.4	6.6	5.1	3.9	2.8	3.4	3.3	4.0	4.7	6.4	5.8	6.8
Sulphur to air, th ton	—	5.9	0.8	0.7	0.8	0.4	0.3	0.3	0.2	0.2	0.2	0.4	0.7	0.8
Nitrogen to air, th ton	—	6.1	0.8	0.7	0.8	0.4	0.4	0.3	0.3	0.2	0.2	0.4	0.7	0.9
Ash to air, th ton	—	6.2	0.9	0.7	0.5	0.4	0.3	0.3	0.3	0.4	0.5	0.7	0.6	0.7
Estimated prod cost, USD/MWh	—	59.9	55.1	56.5	55.3	58.8	57.7	61.0	59.0	62.2	66.5	62.1	64.3	60.8



Poster Presentation: Insuring Power System Reliability Under High Renewables Penetration with Energy Storages - A Case for Ukraine

Table 2: The result of calculation for "Electric Vehicles" scenario

	Yearly		Monthly electricity production (TWh), fuel consumption and emissions											
	Generation mix, GW / %	Electricity production, TWh / %	1	2	3	4	5	6	7	8	9	10	11	12
TPP (coal fired)	25.0 / 31.8%	48.7 / 21.7%	6.92	5.43	4.01	3.24	2.25	3.09	3.03	3.50	4.36	5.01	3.37	4.52
TPP (nat. gas fired)	2.3 / 2.9%	4.0 / 1.8%	0.22	0.14	0.18	0.31	0.29	0.36	0.40	0.41	0.44	0.40	0.40	0.40
NPP	18.5 / 23.5%	126.3 / 56.2%	11.67	10.54	11.59	10.32	11.09	10.07	10.56	9.84	8.44	9.98	10.84	11.36
CHP, auto producers, other renewables	6.0 / 7.6%	10.3 / 4.6%	1.40	1.25	1.35	0.72	0.60	0.46	0.43	0.38	0.40	0.68	1.18	1.44
Hydro (reservoir)	5.0 / 6.4%	6.1 / 2.7%	0.70	0.62	0.84	0.91	0.73	0.38	0.37	0.39	0.26	0.29	0.35	0.31
Hydro Pumped	1.8 / 2.3%	1.6 / 0.7%	0.07	0.07	0.10	0.14	0.15	0.15	0.16	0.16	0.15	0.15	0.15	0.15
Wind	7.0 / 8.9%	15.2 / 6.8%	1.05	0.94	1.12	1.12	1.02	1.14	0.75	1.11	1.43	0.87	2.55	2.11
PV	11.0 / 14.0%	12.3 / 5.5%	0.16	0.35	0.86	1.15	1.21	1.53	1.66	1.67	1.43	1.17	0.64	0.43
Battery Energy Storages	2.0 / 2.5%	0.3 / 0.1%	0.00	0.00	0.00	0.02	0.03	0.04	0.04	0.04	0.06	0.05	0.03	0.01
<b>Total</b>	<b>78.5</b>	<b>224.8</b>												
Coal consumption, mln ton	—	26.7	3.8	3.0	2.2	1.8	1.2	1.7	1.7	1.9	2.4	2.7	1.9	2.5
Nat. gas consumption, bill cub. meters	—	4.5	0.5	0.5	0.5	0.3	0.3	0.2	0.2	0.2	0.2	0.3	0.5	0.6
CO <sub>2</sub> emission, mln ton	—	64.3	8.9	7.1	5.6	4.3	3.1	4.0	3.9	4.4	5.4	6.3	4.9	6.4
Sulphur to air, th ton	—	5.9	0.8	0.7	0.8	0.4	0.3	0.3	0.2	0.2	0.2	0.4	0.7	0.8
Nitrogen to air, th ton	—	6.1	0.8	0.7	0.8	0.4	0.4	0.3	0.3	0.2	0.2	0.4	0.7	0.9
Ash to air, th ton	—	6.7	0.9	0.8	0.5	0.5	0.4	0.4	0.4	0.4	0.5	0.7	0.6	0.7
Estimated prod cost, USD/MWh	—	56.2	53.0	54.2	52.8	55.5	54.2	57.6	55.9	58.2	62.0	57.1	58.1	56.0



Poster Presentation: Insuring Power System Reliability Under High Renewables Penetration with Energy Storages - A Case for Ukraine

The comparison of the results (tab. 3) show:

- due to increase of the electricity consumption caused by the use of electric vehicles, which are pure consumers the larger installed capacity of Nuclear Power Plants could be operated in the Power System. According to the “Baseline” scenario - 15 GW with yearly production of 98 TWh, and 18.5 GW with production of 126 TWh for “Electric Vehicles” scenario;
- the system’s load shapes become more flat due to the influence of the charging profiles of electric vehicles, and this is positively affects the overall system flexibility - less generation from flexible natural gas fired thermal plants, less generation from Hydro Pumping, and less utilization of battery energy storages;
- the estimated system’s production cost of electricity is somewhat lower for “Electric Vehicles” scenario, but of course these estimations are extremely approximate, and under market conditions the prices could be essentially different;
- the flatter system’s load shapes allow to increase usage of inflexible coal fired thermal power plants, which are oldies but produce cheap electricity, and this is leading to bigger volumes of greenhouse gases emissions and hazardous pollutants, but the increase of emissions is not considered as dramatically large.

**Table 3:** The calculation results comparison

	«Baseline» scenario		«Electric Vehicles» scenario	
	Generation mix, GW / %	Electricity production, TWh / %	Generation mix, GW / %	Electricity production, TWh / %
TPP (coal fired)	25.0 / 33.3%	45.5 / 23.5%	25.0 / 31.8%	48.7 / 21.7%
TPP (nat. gas fired)	2.3 / 3.0%	4.3 / 2.2%	2.3 / 2.9%	4.0 / 1.8%
NPP	15.0 / 20.0%	97.8 / 50.5%	18.5 / 23.5%	126.3 / 56.2%
CHP, auto producers, other renewables	6.0 / 8.0%	10.3 / 5.3%	6.0 / 7.6%	10.3 / 4.6%
Hydro (reservoir)	5.0 / 6.7%	6.1 / 3.2%	5.0 / 6.4%	6.1 / 2.7%
Hydro Pumped	1.8 / 2.4%	1.7 / 0.9%	1.8 / 2.3%	1.6 / 0.7%
Wind	7.0 / 9.3%	15.2 / 7.9%	7.0 / 8.9%	15.2 / 6.8%
PV	11.0 / 14.7%	12.3 / 6.3%	11.0 / 14.0%	12.3 / 5.5%
Battery Energy Storages	2.0 / 2.7%	0.4 / 0.2%	2.0 / 2.5%	0.3 / 0.1%
<b>Total</b>	<b>75</b>	<b>193.6</b>	<b>78.5</b>	<b>224.8</b>
Coal consumption, mln ton	—	25.0	—	26.7
Nat. gas consumption, bill cub. meters	—	4.6	—	4.5
CO <sub>2</sub> emission, mln ton	—	60.9	—	64.3
Sulphur to air, th ton	—	5.9	—	5.9
Nitrogen to air, th ton	—	6.1	—	6.1
Ash to air, th ton	—	6.2	—	6.7
Estimated prod cost, USD/MWh	—	59.9	—	56.2

## 2. CONCLUSION

1. The recent adoption of the changes to the Ukrainian Law on Electricity Market regarding energy storage implementation and operation in the Power System and general European trend on development of electric vehicles objectively create strong basis for



**Poster Presentation:** Insuring Power System Reliability Under High Renewables Penetration with Energy Storages - A Case for Ukraine

further development of clean generation, e.g., renewables in consistence with UN Sustainable Development Goal 7 “Affordable and Clean Energy”.

2. Even modest (less than 15% from existing internal-combustion engine transportation fleet) number of electric vehicle usage, and even without the EV2Grid option for electric vehicles, when the electric vehicles are using as the pure consumers, the overall system flexibility is increasing, nevertheless of essential installed capacity of renewables and large share of baseload nuclear power plants and inflexible old thermal power plants.

3. The effect of electric vehicle usage also positively influences the operation mode of the industrial size battery energy storages, i.e., they generate less electric power, and hence they are operating in more smooth modes.

4. Nevertheless of the increase of electricity consumption (which requires more electricity to be produced) due to the usage of electric vehicles the increase of the volume of greenhouse gases emission and hazardous pollutants is not considered as dramatically large, even with the operation of the old coal fired thermal power plants.

5. The general result - without measures allowing make daily system load shapes flatter and without centrally dispatched industry size energy storages the further essential penetration of intermittent renewables into the Power System is hard to ensure.

## BIBLIOGRAPHY

- [1] The main principles of European Community’s energy strategies and projects dedicated to the energy policy and energy markets development (Ministry of Energy and Coal Industry of Ukraine, National Power Company “UKRENERGO”, 2017, link: <https://ua.energy/wp-content/uploads/2017/05/2.-Energetychni-Strategiyi-YES.pdf>)
- [2] UN Sustainable Development Goals. Goal 7 “Affordable and Clean Energy” (link: <https://www.un.org/sustainabledevelopment/energy/>)
- [3] Sergii Shulzhenko “Generation Unit Commitment Mixed Integer Linear Model for Simultaneous Heat and Electric Daily Load Covering” (System Research in Energy, Iss. 1(72), March 2023, pages 25-34, doi.org/10.15407/srenergy2023.01.025)
- [4] S. Shulzhenko, O. Turutiukov, M. Bilenko “Mixed Integer Linear Programming Dispatch Model for Power System of Ukraine with Large Share of Baseload Nuclear and Variable Renewables” (2020 IEEE 7<sup>th</sup> International Conference on Energy Smart Systems (ESS). Kyiv, Ukraine, 2020, pp. 363-368, doi: 10.1109/ESS50319.2020.9160222).



# The Concept of Ukraine's Power System Development Taking into Account the Impact of the Pumped-Storage Power Plant in Modern Conditions

[oariabenko@nuwm.edu.ua](mailto:oariabenko@nuwm.edu.ua)**OLEKSANDR RYABENKO\****National University of Water and Nature Management, Ukraine***SERHII TSURYK***STC «ENPASELECTRO» Ltd., NC CIGRE- UKRAINE***Ukraine**

## SUMMARY

An analysis of the current state of the power system of Ukraine in the conditions of active hostilities on the territory of the state and the presence of significant damage to the objects of the energy structure is given. The list of emergency measures which is necessary for the restoration of electricity supply is defined. Such measures include the repair and restoration of damaged elements of the energy infrastructure, the use of existing and the creation of new bypass power supply grid, the transfer of energy from neighboring regions to emergency areas, the use of diesel power generators, etc. It is emphasized that the restoration of the energy structure is carried out on the basis of using best world experience, modern technologies, European standards, taking into account the synchronization of the energy system of Ukraine with the European energy grid ENTSO-E.

The transformation of the structure of energy capacities of Ukraine for the period of 2019-2022 is described, with the allocation of electricity production by nuclear, thermal power plants and stations based on renewable energy sources. The role of the PSPP in the management of the power system is highlighted. Special attention is paid to expanding the functions of hydro-accumulating power plants. To the traditional function of PSPP - regulating the operation of the power system, working in a complex with nuclear power plants and thermal power plants, the function of meeting the needs of the energy market by regulating the characteristics of the electric current in the system (power, frequency,  $\cos \varphi$ ) was added, as well as the function of accumulating «surplus» energy generated by wind and solar power plants.

The concept of the development of the energy system of Ukraine is highlighted, taking into account the impact of hydro-accumulating power plants at the current stage in the conditions of active hostilities and significant damage to energy infrastructure facilities. This concept is aimed at the implementation of the current energy strategy of Ukraine for the period until 2035.

## KEYWORDS

Power system, Pumped-storage power plant (PSPP), hydro power plant (HPP), nuclear power plant (NPP), thermal power plant (TPP), renewable energy sources (RES), regulation, accumulation





**Poster Presentation:** The Concept of Ukraine's Power System Development Taking into Account the Impact of the Pumped-Storage Power Plant in Modern Conditions

### 1. THE EXISTING POSITION OF UKRAINIAN POWER SYSTEM

In the conditions of active hostilities, which have been ongoing on the territory of Ukraine for the second year, the existing position of the country's power system can be characterized as follows: Russia, as an aggressor country, is trying to completely destroy the energy infrastructure of our country, using both large-scale missile attacks and systematic shelling of energy facilities. Such attacks are carried out on operating power stations and the distribution grid. Almost all thermal and hydraulic stations were subjected to massive attacks. Ukraine lost almost 90% of wind generation and a third of solar generation. At the same time, the production of «green» energy in our country was reduced by half [1]. Transformer substations, distribution devices, electrical equipment, overhead lines were heavily attacked.

The largest destruction of the national power system occurred on November 23, 2022, when a missile attack caused a temporary blackout in Ukraine, due to which most of the country's territory was disconnected from the supply of electricity. As a result of damage to the infrastructure and a decrease in frequency in the power system, the emergency protection at the Rivne, South Ukrainian and Khmelnytsky NPPs was activated, and the temporarily occupied Zaporizhzhya NPP was completely shut down. At the same time, for the first time in the 40-year history of Ukrainian nuclear energy, all NPP power units were shut down [1]. From the point of view of nuclear safety, such a situation could lead to unforeseen consequences. It should be emphasized that Ukrainian engineers mastered the situation and within two days connected all nuclear power units to the national grid (except Zaporizhzhia NPP). The honour of the Ukrainian engineers! The given information shows that the Ukrainian power system withstood difficult war conditions, has high stability and continues to perform its functions, providing the state with electrical energy.

### 2. ENSURING THE OPERATION OF THE UKRAINIAN POWER SYSTEM IN THE CONDITIONS OF HOSTILITIES

Large-scale destruction and damage to elements of Ukraine's energy infrastructure, caused by Russian large-scale missile attacks and systematic shelling, require a quick response and the adoption of appropriate measures to restore electricity supply. The following should be included among such emergency measures.

1. Repair and restoration of damaged power plants and elements of the energy infrastructure - transformers, switchgears, overhead lines, switches, disconnectors and other equipment.
2. Use of existing and creation of new additional (bypass) power supply grids.
3. Transmission of electric energy from neighboring regions, including from foreign sources to emergency areas.
4. Use of industrial and household gasoline and diesel electric generators in emergency situations. Currently, more than half a million such generators have already been imported in Ukraine.

The complexity of the problem lies in the fact that a significant amount of the specified work has to be performed under enemy fire and in the presence of mines. According to preliminary estimates, the damage caused by the destruction of the energy structure of Ukraine by the Russian invaders already amounts to about one hundred billion hryvnias. It should be emphasized that the manufacture of new powerful transformers and unique electrical equipment requires a suitable time. Such a situation requires the searching for alternative options for a quick solution to the problem using temporary solutions. Despite the complexity of the military situation, the reconstruction of important energy facilities is implemented on the basis of the use of best practices, modern technologies and European standards. At the same time, the using constructions and materials are accepted taking into account possible future military risks.

The synchronization of the Ukrainian power system with the European energy network ENTSO-E, which took place on February 23, 2022, gave us the opportunity to carry out export-import transactions with electric energy, cooperating with the European Union. During the period of February-September 2022, Ukraine increased its income from electricity exports to Europe by two and a half times compared to the same period of the previous year, earning almost 430 million dollars. Most of the electricity was supplied to Poland, Slovakia and Romania [1]. Purchases of electrical energy became especially important at the end of 2022 - at the beginning of 2023 during periods of significant damage to the country's energy infrastructure. In April 2023, the export of electricity from Ukraine to Europe partially resumed.

As a result of hostilities on the territory of Ukraine, the enemy managed to destroy a large number of settlements, destroy many industrial and agricultural enterprises. At the same time, thousands of Ukrainians died, millions of citizens were forced to leave their country. Under such conditions, the demand for electrical energy in Ukraine decreased by a third [1]. Typically, that the structure of electricity consumption in the country has changed dramatically - if the volume of its use by household consumers has increased slightly, then by enterprises - it has significantly decreased.



Poster Presentation: The Concept of Ukraine’s Power System Development Taking into Account the Impact of the Pumped-Storage Power Plant in Modern Conditions

The generating capacity of the power system of Ukraine in 2021 was 51.7 GW. Currently, as a result of Russian invaders capturing the Zaporizhzhya NPP and Kakhovskaya HPP, damage to a part of thermal and hydraulic power plants, destruction of a large part of solar and wind power plants, these capacities have halved.

In the table 1. The structure of generating capacities of Ukraine in dynamics for the period from the beginning of active hostilities to the present period is reflected [1, 2]. For comparison, this table also includes relevant information on the capacities of power plants in the EU, France and Germany [3–5].

Table 1: The structure of generating capacities of Ukraine, the EU, France and Germany

No.	Types power plants Countries	Production of electrical energy in percent		
		NPP	TPP	Power plants based on renewable sources
1	Ukraine, 2019	53.9	37.4	8.7
2	Ukraine, 2022	62	30	8
3	EU, 2019	25	37	38
4	France, 2019	70	9	21
5	Germany, 2019	12	46	42

Analyzing the changes in the structure of generating capacities of Ukraine, which occurred as a result of Russian aggression, it is necessary to highlight the significant increasing role of nuclear power plants. Such an increase occurred even without the participation of the occupied Zaporizhzhya NPP (6 units x 1000 MW = 6000 MW), which before the start of active hostilities produced almost a quarter of the country’s electricity. A comparison of the volumes of electricity generated at NPPs and TPPs of Ukraine with the corresponding volumes of France (NPP 70%) and Germany (TPP 46%) shows that our state also uses available sources to ensure its energy and political independence.

### 3. THE ROLE OF PSPP IN MANAGING OF THE POWER SYSTEM

Management of the energy system is based on establishing the needs of consumers in the amount of electrical energy and the corresponding modes of its generation. This process is carried out by building power system load schedules, which express the dependence of the total system power on time and are built in daily, weekly, monthly, seasonal and annual sections (Table 1).

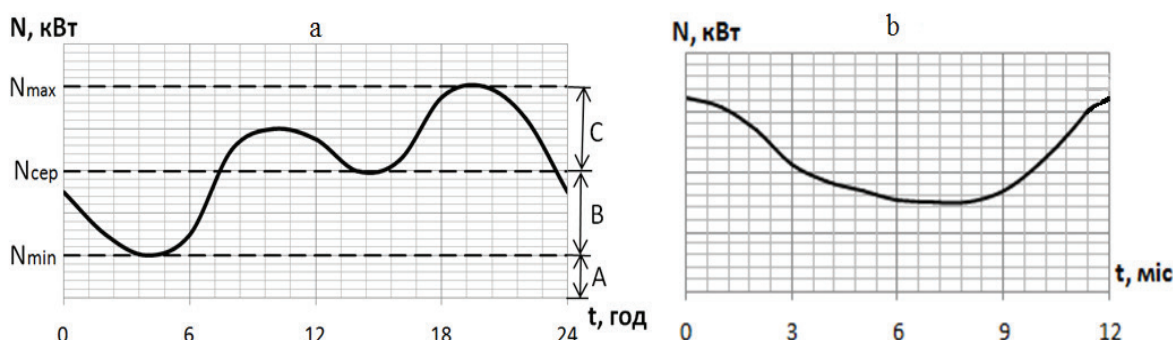


Figure 1: Typical electricity system load schedules: a – daily, b – annual; A – basic, B – semi-peak, C – peak parts

The coverage of the basic part of the daily load schedule is usually provided by thermal and nuclear power plants, and to regulate the semi-peak and peak parts -HPP and PSPP and also 200-300 MW thermal power plant units are used. Such regulation by TPP units is carried out by starting and stopping them in the appropriate periods of the day. Under the operating conditions of the Ukrainian power system, 7-10 TPP units have to be stopped during periods of dips in the system’s daily load schedule and include them during



**Poster Presentation:** The Concept of Ukraine's Power System Development Taking into Account the Impact of the Pumped-Storage Power Plant in Modern Conditions

peak periods. For example, the number of start-stops of Ukrainian TPP units in 2019 was 2,478 [2]. The described mode of operation of TPP units negatively affects the condition of station equipment, requires an increase in fuel consumption, and leads to an increase in emissions of pollutants into the environment.

Under such conditions, the use of PSPP to regulate the operation of the energy system is extremely effective. The specificity of hydroaccumulating power plants is that they have an extremely flexible nature of their work. At the same time, PSPP operate for a certain part of the day in turbine mode, producing electrical energy and supplying it to the energy system, and for part of the day - in pumping mode, consuming «excess» energy from the system. The already mentioned flexible nature of operation, high maneuverability, independence from climatic factors (presence of sunny weather, wind, etc.), short duration of time for unit start-up, independence from non-renewable energy sources and others should be included among the positive features of PSPP [6]. It should be emphasized that in recent decades, USA, China and a number of other countries, in addition to the mentioned methods, also use highly maneuverable gas turbine and steam-gas plants to regulate the operation of energy systems.

#### 4. EXPANDING THE FUNCTIONS OF PSPP

The above-described function of hydroaccumulative power plants, based on their joint work with nuclear power plants and thermal power plants, is traditional and widely used by many countries to manage the operation of energy systems. At the same time, in recent decades, there has been a tendency to significantly expand the functions of PSPP in the power system. In addition to the traditional types of their activities - the production of acutely scarce peak electric energy and the covering of dips in the daily schedule of loads, it was possible to meet the growing needs of the energy market [7]. The following should be included among such additional functions of the PSPP:

- regulation of the main operating parameters of the power system - power, frequency,  $\cos \phi$ , etc.;
- improvement of the quality of electric energy, which is supplied to consumers;
- creation of support reserve and frequency recovery.

The implementation of these additional functions also makes it possible to increase the stability of the energy systems and increase the reliability of the technological equipment of the blocks of nuclear and thermal power plants, which, thanks to the inclusion of the PSPP, get the opportunity to work in optimal modes. The operation of PSPP in the new conditions leads to a significant increase in the number of start-ups and stops of plant units. At the same time, the number of changes in operating modes of hydro-accumulating power plants is expected to be up to 4,000-8,000 per year. For example, the planned indicators are: Drakensberg HPP (South Africa) – 8,000, Gilboa (USA) – 6,000, Dinorwig (England) – 5,000 [8].

Recently, another important function of hydroaccumulating power plants has been revealed, related to the possibility of using them to accumulate «excess» energy produced by wind and solar plants. Such accumulation can be carried out by pumping water into the upper reservoir by the PSPP units when they are operating in pumping mode. The essence of the problem is that the operation of wind and solar power plants is spontaneous, depends significantly on weather conditions (presence or absence of wind and thermal solar radiation) and is largely unpredictable. As a result, situations arise when the amount of energy produced by such powerful stations significantly exceeds the needs of consumers, which leads to a corresponding imbalance [3]. Under such conditions, the use of PSPP for the accumulation of «surplus» energy.

The problem of more complete use of the hydropower potential of rivers by reducing the volume of empty discharges of water through river hydroelectric nodes in periods of spring floods and rain floods by accumulating water in the upper reservoirs of the PSPP is also relevant.

It should be noted that there are many ways of accumulating relatively large amounts of electrical energy - the above-described hydroaccumulation with the help of PSPP, pneumatic storage with the help of pneumatic storage electric plants, the use of lithium-ion, lead-acid, nickel-cadmium, sulfur-sodium, vanadium-redox batteries, etc. [2, 9]. When choosing the type of electric energy storage, it is necessary to take into account all the characteristics of the compared options, including such important factors as the duration of object operation and the corresponding equipment, as well as the cost of further disposal of this equipment. Comparative calculations showed that the cost of hydro-accumulating power plants, taking into account the term of their operation (which is usually assumed to be 80 years for PSPP) and the capacity of the storage pool, is significantly lower, than the cost of lithium-ion and other types of battery systems [2].



Poster Presentation: The Concept of Ukraine’s Power System Development Taking into Account the Impact of the Pumped-Storage Power Plant in Modern Conditions

### 5. WORK OF UKRAINIAN PSPP

There are currently three PSPP operating in Ukraine - Kyivska, Tashlytska, and Dnistrovka, the characteristics of which are given in the table. 2

Table 2: Characteristics of hydraulic power plants of Ukraine

№	The name of PSPP	Existing data		Year of construction	Design data		Annual electricity generation million kWh	Maximum pressure m	Useful volume of the upper reservoir million m3
		Capacity (generator mode) MW	Number of units		Capacity (generator mode) MW	Number of aggregates			
1	2	3	4	5	6	7	8	9	10
1	Kyivska	235.5	6	1972	235	6	200	74.0	3.79
2	Tashlytska	302	2	2007 (2nd a.)	906	6	873	88.5	14.40
3	Dnistrovka	1296	4	2021 (4th a.)	2268	7	2720	154.9	32.70
4	Kanivska	-	-	project	1000	4	1025	108.4	1700

Among the named stations, it is especially necessary to single out the Dnistrovka PSPP (Table. 2). This is a unique object. After the commissioning of all seven units, the total capacity of the station will reach 2,268 MW in generator mode and 2,947 MW in pumping mode. According to these indicators, Dnistrovka PSPP will take first place in Europe and sixth in the world after Fengning HPP (3,600 MW, China), Bath County (3,003 MW, USA), Kanagawa (2,820 MW, Japan), Huizhou (2,448 MW, China), Guangdong (2400 MW, China). The units of the Dnistrovka station are the largest in the world, reversible and have a capacity of 324 MW in generator mode and 421 MW in pump mode.



Figure 2: Dnistrovka PSPP

Within the framework of international cooperation, at the Dnistrovka PSPP and other stations of the PJSC «Ukrhydroenergo» system, block and generator elegas circuit breakers, electromechanical systems and equipment of well-known companies «ALSTOM», «ABB», «Andritz Hydro» and others were installed. Ukraine actively cooperates with such international organizations as International Hydropower Association, International Commission on Large Dams, International Council on Large Electric Systems, International Renewable Energy Agency.

During the period of hostilities on the territory of Ukraine, in conditions of significant damage to the energy structure, the role of hydro-accumulating power plants as a regulator of the energy system significantly increased. In order to prevent unbalancing of the system and the occurrence of emergency situations, it is necessary to increase the number of start-stops of the units of the PSPP. At the same time, the conditions of the passage of flood waters through the Dnieper and Dniester hydroelectric nodes also have a great influence on the operation of the power system.



**Poster Presentation:** The Concept of Ukraine's Power System Development Taking into Account the Impact of the Pumped-Storage Power Plant in Modern Conditions

## 6. THE CONCEPT OF THE DEVELOPMENT UKRAINIAN POWER SYSTEM AT THE CURRENT STAGE

The program for the development of the country's energy sector in peacetime was developed in the Energy Strategy of Ukraine for the period until 2035 [10]. However, the real state of the power system in the conditions of hostilities on the country's territory and significant damage to the objects of the energy structure requires making appropriate corrections in the developed plans. At the same time, the updated concept of the development of Ukraine's power system should take into account the lessons learned from the Russian-Ukrainian war, the revealed trends of more complete use of PSPP, and the existing modern trends in the development of world energy. The list of emergency actions to restore the operation of the energy system in the conditions of hostilities is given in paragraph 2.

The main provisions of the updated concept of the development of Ukrainian power system, which were developed taking into account the above-mentioned factors, can be summarized as follows.

1. Diversification of used energy sources and distribution of power plants of various types throughout the country.
2. Expansion of the network existing power transmission lines, construction and use of backup (bypass) such lines.
3. More complete use of the capabilities of existing nuclear, thermal, HPP, PSPP, wind, solar and other types of power plants.
4. Active use of renewable energy sources through the construction of new large, medium and small HPP and PSPP, wind and solar power stations, waste and biofuel stations.
5. Completion of the construction of the Dnistrovska and Tashlytska PSPPs, as well as the construction of the Kaniv HPP (see Table 2) [11] in accordance with the current Energy Strategy of Ukraine for the period until 2035.
6. Continuation of cooperation between Ukraine and the European Union in terms of synchronizing the work of the Ukrainian power system with the European energy network ENTSO-E using the possibilities of export and import of electric energy.
7. Development of the possibility of «decarbonization» of energy based on the «green hydrogen» program by electrolysis of hydrogen production for energy needs.

## 7. CONCLUSIONS

1. The experience of Ukraine's power system in the conditions of hostilities territory with the use of intensive missile attacks and constant shelling of energy infrastructure facilities showed that the energy system survived these conditions and continues to perform the important state function of providing the country with electrical energy.
2. The operation of Ukraine's power system in recent years has demonstrated that the established principles of the construction of this system, the types of energy objects, which were used, constituent elements and technological equipment are perspective and capable of ensuring the stability of the energy system even in the conditions of hostilities.
3. World and domestic experience of using PSPP has shown that over the last decade, the scope of their functions has significantly expanded, and the role of these stations in regulating the parameters of energy systems has significantly increased. The mentioned circumstances give reason to predict a wider use of PSPPs in the future.
4. The presented concept of the development of the energy system of the country is based on the provisions of the current Energy Strategy of Ukraine for the period until 2035, takes into account the real state of the system which has developed as a result of hostilities on the territory of the state. The concept is oriented on using of world energy industry achievements and defines perspective directions for the restoration and development of Ukraine's power system.

## BIBLIOGRAPHY

- [1] Results of the year: how Ukraine's energy system united with the EU and survived the attacks of Russian terrorists. 2022. <https://www.unian.ua/economics/energetics/pidsumki-roku-yak-energosistema-ukrajini-ob-yednalas-z-yes-ta-vstoyala-pid-obstrilami-rosiyskih-terroristiv-12093249.html>
- [2] Landau Y.O., Bondarenko Y.M., Tsuryk S.A. The importance of PSPP in the development of the power system of Ukraine. Industrial power engineering and electrical engineering, No. 3 (123) 2020. – P.38-45. <http://promelektro.com.ua/archive.html>
- [3] S. Prokopchuk. Small hydropower is a powerful potential of Ukraine. Newspaper of the Cabinet of Ministers of Ukraine «Government Courier». No. 120 (7241). 31.05.2022 <https://ukurier.gov.ua/uk/articles/mala-gidroenergetika-potuzhniy-potential-ukrajini/>



**Poster Presentation:** The Concept of Ukraine's Power System Development Taking into Account the Impact of the Pumped-Storage Power Plant in Modern Conditions

- [4] Nuclear Power in France. 2022. <https://world-nuclear.org/information-library/country-profiles/countries-af/france.aspx>
- [5] Nuclear Power in Germany. 2022. <https://world-nuclear.org/information-library/country-profiles/countries-gn/germany.aspx>
- [6] Riabenko O., Kliukha O., Yakovleva-Havryliuk O., Osadchyi S., Sunichuk S. Increasing the Role of Hydro and Pumped Storage Power Plants in Energy Systems Operation Management. IEEE, 7th International Conference on Energy Smart Systems, ESS Proceedings, 9160299, 2020. P. 424-428.
- [7] Sirota I.G., Sukhetsky B.L., Nikitin O.O., Olefir D.O. Problems and prospects of HPP and PSPP operation in the new electricity market. *Hydropower of Ukraine*, No. 3-4, 2019. P. 15-19. <https://uhe.gov.ua/sites/default/files/2019-12/6.pdf>
- [8] Landau Y.A. Development of atomic energy and PSPP. *Hydropower of Ukraine*, No. 4, 2006. - P. 18-22.
- [9] Vasko P.F., Verbovyi A.P., Ibrahimova M.R., Pazich S.T. Hydro-storage power plants are the technological basis for integrating powerful wind and solar power plants into the power system of Ukraine. *Hydropower of Ukraine*, No. 1-2, 2017. - P. 20-25. <http://dspace.nbu.gov.ua/handle/123456789/141711>
- [10] On the approval of the Energy Strategy of Ukraine for the period until 2035 «Safety, energy efficiency, competitiveness». Cabinet of Ministers of Ukraine. Order No. 605 of August 18, 2017. Kyiv. 2017. <https://www.kmu.gov.ua/news/250302738>
- [11] Galat V., Ryzhyi V., Riabenko A. Challenges in the design of the upper reservoir for the Kaniv pumped-storage scheme, Ukraine. *Hydropower and Dams*. Vol. 25 - Issue 3, 2018. P. 80-83. <https://www.hydropower-dams.com/articles/challenges-in-the-design-of-the-upper-reservoir-for-the-kaniv-pumped-storage-scheme-ukraine/>





**YURIY LANDAU**

*Doctor of Technical Sciences, Chief Advisor of PJSC "UKRHYDROPROEKT"*

**YURIY BONDARENKO**

*Vice President, Head of the Technical Committee of NC CIGRE-UKRAINE, Director General of STC ENPASELECTRO Ltd.*

**SERGIY OSADCHUY**

*Chairman of the Board of PJSC "UKRHYDROPROEKT"*

**Ukraine**

**SUMMARY**

In the countries of South-Eastern Europe, based on the development strategy of the EU «European Green Deal» - the EU Green Deal, the main directions of the development of the electric power industry are decarbonization, energy efficiency, energy security and the accelerated development of renewable energy sources (RES).

The global energy crisis caused by russia's war against Ukraine led to significant changes in the development of electricity in the EU with a significant acceleration of the transition to environmentally clean energy and the input of RES capacities, which will displace the use of fossil fuels, which will ensure energy independence, lead to a change in the configuration of the unified energy system, which will also become more resistant to conflicts. Based on the major changes taking place, a new paradigm of energy security is needed, ensuring a reliable and affordable electricity supply while simultaneously reducing emissions and decarbonizing.

**1. THE INFLUENCE OF PSPP ON THE CURRENT STATE OF THE UNIFIED ENERGY SYSTEM**

The war in Ukraine marked the end of critical dependence on russian fossil fuel exports.

The large-scale EU plan for energy independence was presented in May 2022. The war showed that in the modern world, energy sector is much more than an economy sector. At the same time, ensuring energy security has become a strong additional motivation for accelerating the development of RES.

Thus, the EU plans to increase the supply of RES electricity to 45% by 2030. According to the principled position of the EU, a unified energy system with a large share of photovoltaic power station (PPS) and wind power plants (WPP) in the balance of electricity production will become more stable and secure and will have a different architecture based on decentralization, respectively global trend, with the creation of "producer-consumer" clusters in which electricity is self-balancing, while they remain in parallel operation with the power system. In these conditions, priority development will be given to distribution generation using hybrid power plants, which technologically combine wind turbines, WPPs, PPSs, HPPs, PSPPs, industrial batteries and hydrogen production in various combinations, having significant technological and financial advantages.

Such distributed generation, which works for local grid and individual large consumers of electricity, combined and, if necessary, working for the power system, will provide significant advantages in its work with the improvement of controllability, reduction of flows, consumption of electricity, increase of its survivability and overall energy security of countries EU.

**KEYWORDS**

Pumped-storage power plant (PSPP), hydro power plant (HPP), nuclear power plant (NPP), thermal power plant (TPP), renewable energy sources (RES), photovoltaic power station (PPS), wind power plant (WPP), regulation, unified energy system.



**Poster Presentation:** The Role of PSPP in the Implementation of Strategy of Accelerated Development of RES in the Countries of South-Eastern Europe

In the new conditions of the further development of the EU electric power industry with a change in the structure of generating capacities, with the preservation of nuclear generation, further decentralization, with a gradual reduction of TPP capacities and a rapid growth of RES, the problem of regulation of energy systems becomes key.

Based on world experience, in order to meet the needs for highly maneuverable regulating and accumulative capacities, advantages should definitely be given to the development of PSPP. Of the modern electricity balancing technologies in unified energy system, PSPP are the most efficient and widespread in the world, accounting for about 94% of all regulating capacities, because they are a multifunctional, highly efficient source of power system balancing, frequency and power regulation.

They have significant advantages over industrial batteries in terms of cost, much larger capacity, number of starts per day, year, general period of operation, etc.

In addition, PSPPs produce electricity using massive engine generators that rotate synchronously with the frequency in the grid, and their moment of inertia helps to compensate for fluctuations in the power balance in the system and at the same time stabilizes the frequency, which is very important, considering that asynchronous wind and solar generation they do not have such an inertial reserve on the shaft. With their large capacities, this creates problems with frequency regulation in the grid.

Therefore, where there are favorable natural conditions, first of all, PSPPs are built. Such construction is being carried out in Europe, the USA, China, etc.

Of the total capacity of PSPPs in the world of approximately 170 million kW, their capacity in Europe is more than 53 million kW.

## 2. PECULIARITIES OF THE RAPID DEVELOPMENT OF RES IN THE POWER SYSTEM

With the rapid input of large capacities of wind power plants, PPSs and, accordingly, the growth of needs for balancing capacities in Europe, the construction and input of capacities of PSPPs and industrial battery systems will proceed in parallel.

In the conditions of the open energy market of EU, with the further accelerated input of large capacities of unpredicted generation of PPS and wind turbines, the rapid development of the market of balancing capacities becomes a sustainable market trend, and in the conditions of the development of distributed generation, this will lead to the provision of self-balancing of PPS and wind turbines in a complex with balancing capacities (PSPP, industrial batteries, etc.) as part of generation system.

The countries of South-Eastern Europe have their own peculiarities in the operation of energy systems. Indicators of the structure of electricity generation and production in these countries at the end of 2020 are given in Table 1.

The analysis of the working conditions, the structure of power system generation and electricity production in the countries of South-Eastern Europe shows that in the current conditions, the power systems of these countries technologically remain purely centralized systems, despite the significant volume of renewable energy production up to 37%, including HPP - 22.6 %, PPS, WPP, etc. - 14.4%. It should be noted that the volume of RES electricity production in different countries varies significantly. So, if in Albania, practically all electricity production is provided by RES, namely hydroelectric power plants, in Croatia with RES - 67%, in Greece, Romania - from 40 to 44%, then in Bulgaria - about 16%. At the same time, the capacity of operating PSPP is extremely small, about 2 million kW.

In general, the irrational structure of generating capacities in most countries with a large production of about 48% of electricity at TPPs using fossil fuels leads to large emissions of CO<sub>2</sub> and other pollutants into the environment. Practically, there is no use of distributed generation (except for household PPSs), there are significant intersystem flows of electricity, which leads to additional costs and complicates the operating conditions of power systems.

In order to solve the existing problems in the electricity sector in the countries of South-Eastern Europe in the conditions of the energy transition, with the provision of effective development on a new basis, significant changes are necessary, based on the adopted EU development strategy of the «European Green Deal».

With the further rapid development of RES, as planned by all countries primarily at the expense of PPSs and WPPs, priority development is given to distributed generation with the creation of hybrid generation system with work on individual large electricity consumers and local grids.

In these countries, where a large part of the territory is located in a mountainous area, natural conditions are favorable for the development of WPPs, PPSs and HPPs, taking into account the significant unused cost-effective hydropower potential, as well as high-pressure hydropower plants. The rapid development of PPSs and WPPs in the countries of South-Eastern Europe will supplant TPPs, but requires the parallel introduction of significant balancing capacities.



Poster Presentation: The Role of PSPP in the Implementation of Strategy of Accelerated Development of RES in the Countries of South-Eastern Europe

Table 1: Indicators of the structure of generation and production of electricity in the countries of South-Eastern Europe

No	Name	Albania	Bosnia-Herzegovina	Bulgaria	Croatia	Greece	North Macedonia	Romania	Serbia	Slovenia	In total
1	The total capacity million kW	2.5 (100%)	4.53 (100%)	12.84 (100%)	5.31 (100%)	21.9 (100%)	2.1 (100%)	20.58 (100%)	8.27 (100%)	4.02 (100%)	82.2 (100%)
1.1	Including: TPP	-	2.16 (48%)	5.72 (44.6%)	2.04 (38.5%)	10.86 (50%)	1.3 (62%)	8 (38.8%)	4.43 (54%)	1.54 (38%)	36.4 (44%)
1.2	Nuclear power plant	-	-	2.0 (15.6%)	-	-	-	1.41 (6.8%)	-	0.7 (17%)	4.1 (5%)
1.3	RES In total	2.4	1.95 (43%)	5.11 (39.8%)	3.26 (61.5%)	10.17 (47%)	0.81 (38%)	11.17 (54.3%)	3.2 (39%)	1.77 (44%)	39.8 (48%)
1.3.1	HPP	2.3 (95%)	1.83 (40%)	3.21 (25%)	2.2 (41.5%)	2.47 (12%)	0.71 (34%)	6.64 (32.3%)	2.44 (30%)	1.34 (33%)	23.2 (28%)
1.3.2	WPP, PPS, others	0.02 (1%)	0.12 (3%)	1.9 (14.8%)	1.06 (20%)	7.7 (35%)	0.1 (4%)	4.53 (22%)	0.76 (9%)	0.43 (11%)	16.6 (20%)
1.4	PSPP	-	0.42 (9%)	-	-	0.70 (3%)	-	0.1 (0.1%)	0.61 (7%)	0.3 (7%)	2.1 (3%)
2	Total production billion kW per hour	5.3 (100%)	15.39 (100%)	40.88 (100%)	12.22 (100%)	46.06 (100%)	5.1 (100%)	56.13 (100%)	35.54 (100%)	16.3 (100%)	233 (100%)
2.1	TPP	-	10.44 (68%)	17.56 (43.1%)	4.08 (33.4%)	27.35 (59.4%)	3.6 (70%)	19.85 (35.4%)	24.33 (68.5%)	4.19 (26.6%)	112.1 (48%)
2.2	Nuclear power plant	-	-	16.63 (40.7%)	-	-	-	11.47 (20.5%)	-	6.41 (38.4%)	34.5 (15%)
2.3	RES In total	5.3 (100%)	4.94 (32%)	6.34 (15.5%)	8.13 (66.6%)	18.69 (40.6%)	1.5 (30%)	24.82 (44.1%)	11.0 (30.9%)	5.52 (35%)	86.2 (37%)
2.3.1	HPP	52.8 (99.4%)	4.28 (27.8%)	3.39 (8.3%)	5.36 (43.9%)	2.9 (6.3%)	1.3 (25%)	15.7 (28%)	9.7 (27.3%)	4.82 (30%)	52.7 (22.6%)
2.3.2	WPP, PPS, others	-	0.66 (4.3%)	2.95 (7.2%)	2.77 (22.7%)	15.79 (34.3%)	0.2 (5%)	9.12 (16.1%)	1.3 (3.6%)	0.7 (5%)	33.5 (14.4%)
2.4	PSPP	-	0.2	-	-	0.4 (1%)	-	-	0.3 (0.6%)	0.21 (1%)	-



**Poster Presentation:** The Role of PSPP in the Implementation of Strategy of Accelerated Development of RES in the Countries of South-Eastern Europe

### 3. CONCLUSIONS

At the same time, thanks to the natural conditions of the mountainous terrain, the countries have significant opportunities for the construction of PSPPs for providing regulation capacities, emergency and frequency reserve not only in the countries of South-Eastern Europe, but also in other EU countries. Thus, as research has shown, only in North Macedonia there are sites of promising efficient PSPP with a total capacity of about 12 million kW.

In conditions where the EU plans to increase the production of RES to 45% of the total production by 2030, mainly at the expense of PPSs and WPPs, and RES will become the largest source of electricity, and by 2050 it plans to reach 80%, the process of decentralization will proceed rapidly and growing needs for regulatory capacities.

At the same time, in the future, the countries of South-Eastern Europe can become a European hub of regulatory capacities and auxiliary services in the creation of large capacities of PSPPs, for which there are attractive natural conditions.

It is necessary to develop schemes for the placement of PSPPs, to identify the sites of PSPP, taking into account the conditions of power output, the development of high-voltage power lines, including for the export of balancing electricity and auxiliary services.

### BIBLIOGRAPHY

- [1] Landau Y.O., Bondarenko Y.M., Tsuruk S.A. The importance of PSPP in the development of the power system of Ukraine. Industrial power engineering and electrical engineering, No. 3 (123) 2020. – P.38-45.<http://promelektro.com.ua/archive.html>
- [2] Riabenko O., Kliukha O., Yakovleva-Havryliuk O., Osadchyi S., Sunichuk S. Increasing the Role of Hydsro and Pumped Storage Power Plants in Energy Systems Operation Management. IEEE, 7th International Conference on Energy Smart Systems, ESS Proceedings, 9160299, 2020. P. 424-428.
- [3] Landau Y.A. Development of atomic energy and PSPP. Hydropower of Ukraine, No. 4, 2006. - P. 18-22.
- [4] Galat V., Ryzhyi V., Riabenko A.Challenges in the design of the upper reservoir for the Kaniv pumped-storage scheme, Ukraine. Hydropower and Dams. Vol. 25 - Issue 3, 2018. P. 80-83.<https://www.hydropower-dams.com/articles/challenges-in-the-design-of-the-upper-reservoir-for-the-kaniv-pumped-storage-scheme-ukraine/>



# The Implementation of Intraday Auctions and its Impact on the Croatian Electricity Market

[martina.vajdic@cropex.hr](mailto:martina.vajdic@cropex.hr)

MARTINA VAJDIĆ\*, ANA RAGUŽ, LUKA ŠEŠO, MARKO KELAVA

*Croatian Power Exchange Ltd.*

*Croatia Energy Transition*

Croatia

## SUMMARY

Intraday auctions (abbr. IDA) refer to implicit intraday auctions that are conducted on a pan- European level for the purpose of allocating available intraday transmission capacity using the market coupling mechanism between different bidding zones.

The development of the project was initiated in accordance with Article 55 of the Commission Regulation (EU) 2015/1222 establishing a guideline on capacity allocation and congestion management (abbr. CACM Regulation) which determines the establishment of a single methodology for pricing intraday cross-zonal capacity (abbr. IDCZCP). A single methodology for IDCZCP was approved by the decision of the Agency for the cooperation of energy regulators (abbr. ACER) on 24th January 2019, and was additionally corrected on 10th August 2021.

The IDA will be implemented across Europe to enable pricing of cross-zonal capacity on an intraday time frame, as well as to accommodate a new market coupling that allows variable renewable energy producers to offer their energy based on more reliable production forecasts, thereby reducing imbalances caused by intermittency of their availability.

For each delivery day, three auctions will be organized in the following chronological order:

- IDA 1: D-1 15:00 for all hours of delivery day D
- IDA 2: D-1 22:00 for all hours of delivery day D
- IDA 3: D 10:00 for hours 13-24 of delivery day D

The member states involved in the development of the project are Austria, Belgium, Bulgaria, Croatia, Czech Republic, Denmark, Estonia, Finland, France, Germany, Greece, Hungary, Italy, Latvia, Lithuania, Luxemburg, Netherlands, Norway, Poland, Portugal, Romania, Slovakia, Slovenia, Spain, and Sweden. Project participants are currently working on the procedures and system testing, while the completion of the implementation and launch of the IDA is scheduled for the second quarter of 2024.

The paper will provide an overview of the implementation of the IDA project both at the local and regional level, through the cooperation and joint work of all project parties, including Croatian

Transmission System Operator Plc. (abbr. HOPS) and CROATIAN POWER EXCHANGE Ltd. (abbr. CROPEX). Given that the project is ongoing, and its realization is expected after the submission of this paper, it will not be possible to present the actual results of the implementation of the IDA, but an overview will be given of the expectations from the moment of the project go-live.

## KEYWORDS

Intraday auction – Cross-zonal capacity – Market coupling – Croatian electricity market



Poster Presentation: The Role of PSPP in the Implementation of Strategy of Accelerated Development of RES in the Countries of South-Eastern Europe

### 1. INTRODUCTION TO INTRADAY AUCTIONS PROJECT

Intraday Auctions (abbr. IDAs) shall be implemented across Europe to allow for the pricing of cross-border capacity in the intraday timeframe as well as to accommodate a new market coupling that enables Variable Renewable Energy (abbr. VRE) producers in Europe to offer their energy based on more reliable generation forecasts and thereby reducing the overall imbalances caused by the VRE intermittency. It is therefore of importance that the IDA accommodates a reliable and robust market coupling, that is able to attract the necessary liquidity. As stipulated in the ACER Decision 01/2019, three distinct IDAs shall initially be held for each delivery day. [1]

According to Terms of Reference for IDAs, following assumptions were made:

- The IDAs shall be implemented according to the Algorithm methodology as well as other relevant legislation.
- The same version of the PCR assets (EUPHEMIA and PMB) shall be used for both day-ahead operation and the IDAs operation. A short time gap between the releases is acceptable when following the appropriate Release Deployment process. The SW version would remain the same for these multiple releases. According to further technical requirements, using the same version can be re-evaluated in the future by NEMOs and TSOs.
- Only PCR NEMOs as owners of PCR assets shall be entitled to operate IDAs, while other NEMOs shall be able to procure the services from PCR NEMOs.
- PCR assets will be used for IDAs under similar service requirements as for the day-ahead auctions (SDAC), apart from those incident management services that are incompatible with the tighter operational timings and more frequent usage of the IDAs during the delivery day.
- Mandatory and optional products for IDAs are currently assumed to be a subset of the mandatory and optional products supported by SDAC.
- PCR assets will be adapted to include a cross-matching functionality to match 60 minute MTUs, half-hourly MTUs and 15 minute MTUs products as required for both DAM and IDAs.
- Additional changes for the IDAs will be managed by the change control process that shall align changes between both SDAC and IDAs.
- The invoicing process for reimbursement of the costs related to PCR assets adaptation and operation categorized as joint NEMO and TSO common costs for establishing and amending or categorized as joint NEMO or NEMO and TSO common costs for operating will follow the SIDC principles.
- Given that Euphemia and PMB will serve both SDAC and IDAs, a joint governance model and related cost sharing mechanism must be agreed between SDAC and SIDC. Therefore, a regular dialogue concerning the PCR assets needs to be established between NEMO DA SC and NEMO ID SC as well as between SDAC JSC and SIDC JSC.

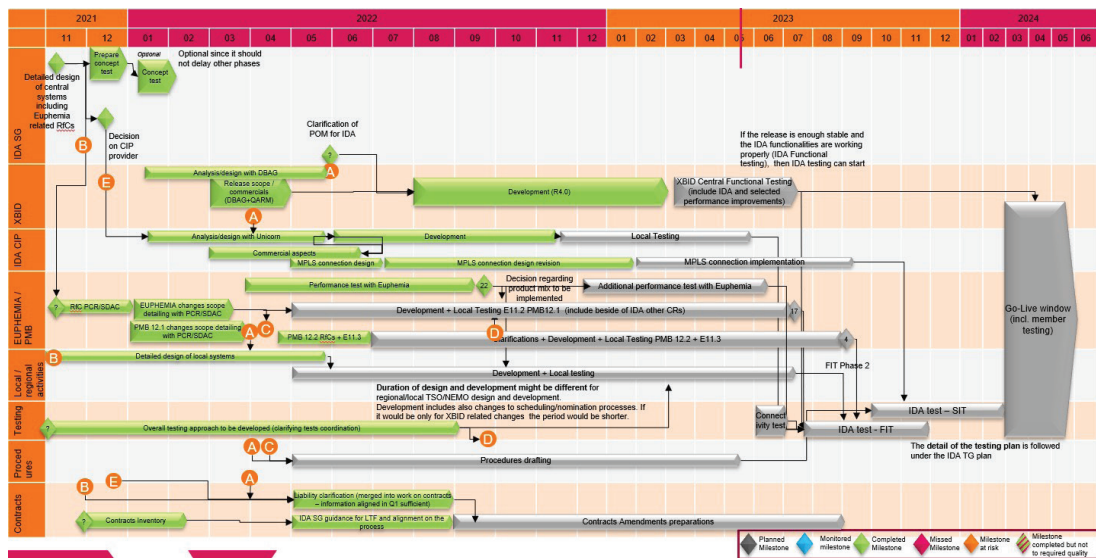


Figure 1. IDA Implementation timeline





Poster Presentation: The Role of PSPP in the Implementation of Strategy of Accelerated Development of RES in the Countries of South-Eastern Europe

Figure 1 shows the timeline for the implementation of IDAs prepared by NEMOs and TSOs. The go-live is planned for Q2 of 2024 one year beyond the legal deadline. IDAs are currently in the testing phase with all involved parties. This phase can be divided in the several stages which are thoroughly described in Chapter 4 of this paper.

### 2. IDA PROCESS

NEMOs and TSOs are jointly preparing the implementation of IDAs. It is envisioned that NEMOs will run the IDAs in the same way as they run the Single Day-Ahead market Coupling(SDAC) and using the same local NEMO systems. The IDAs will be planned to start at:

- D-1 15:00 CET covering for the entire upcoming delivery day;
- D-1 22:00 CET covering for the entire upcoming delivery day;
- D 10:00 CET covering the period from 12:00 CET of the current delivery day until the end of the delivery day.

Figure 2. shows all the systems involved in IDA process whose function is thoroughly described in Figure 3.

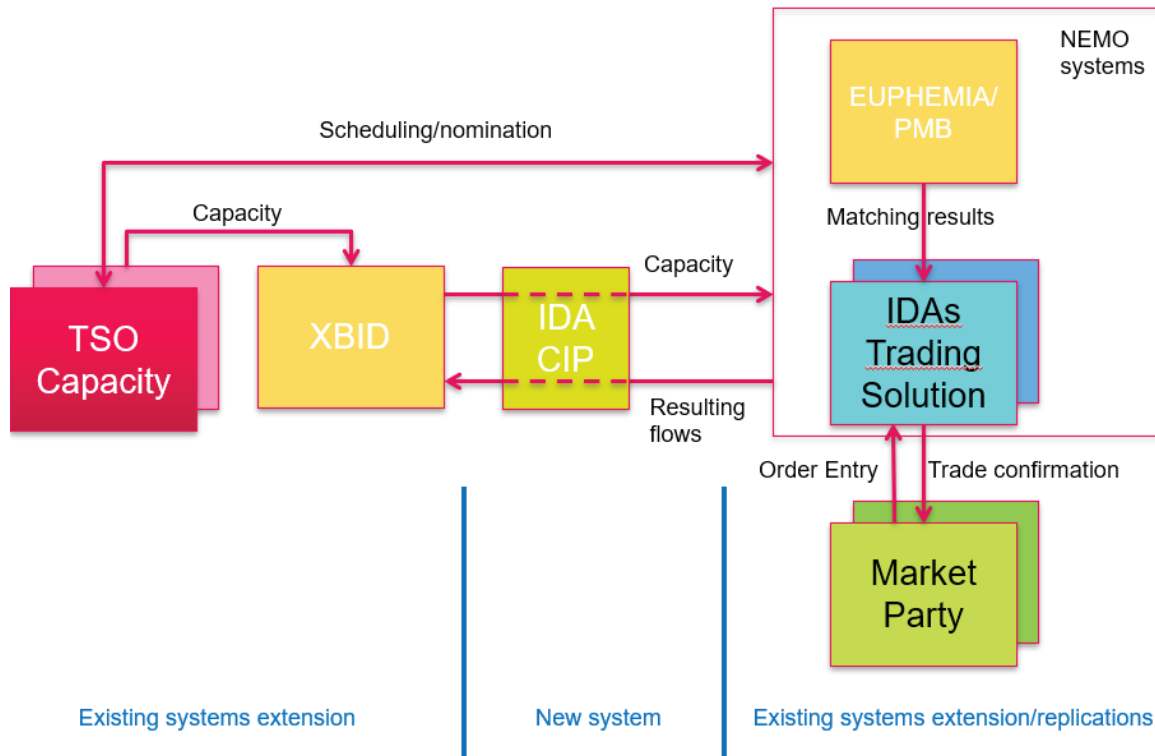


Figure 2. IDA Process

We split the IDAs up into three phases:

- Pre-IDA phase (I, where necessary represented as Ia and Ib – see below) – this is where input for the IDA is collected and submitted (also called “pre-coupling”);
- IDA phase (II) – this is where the IDA is run, and the results are validated (“coupling”);
- Post-IDA phase (III) – this is where firm output of the IDA is submitted and processed. (“post-coupling”).

There is a difference between the sequence for the first IDA and that for the other two IDAs. Flows and Steps that only exist for the first IDA are numbered starting with Ia. Flows and Steps that only exist for the second and third IDA are numbered starting with Ib. Some steps are not performed in all regions. These steps get the letter c appended. Flows and Steps that only exist in case XBID positively validated IDA results, but IDA is finally cancelled are numbered starting with IId.



Poster Presentation: The Role of PSPP in the Implementation of Strategy of Accelerated Development of RES in the Countries of South-Eastern Europe

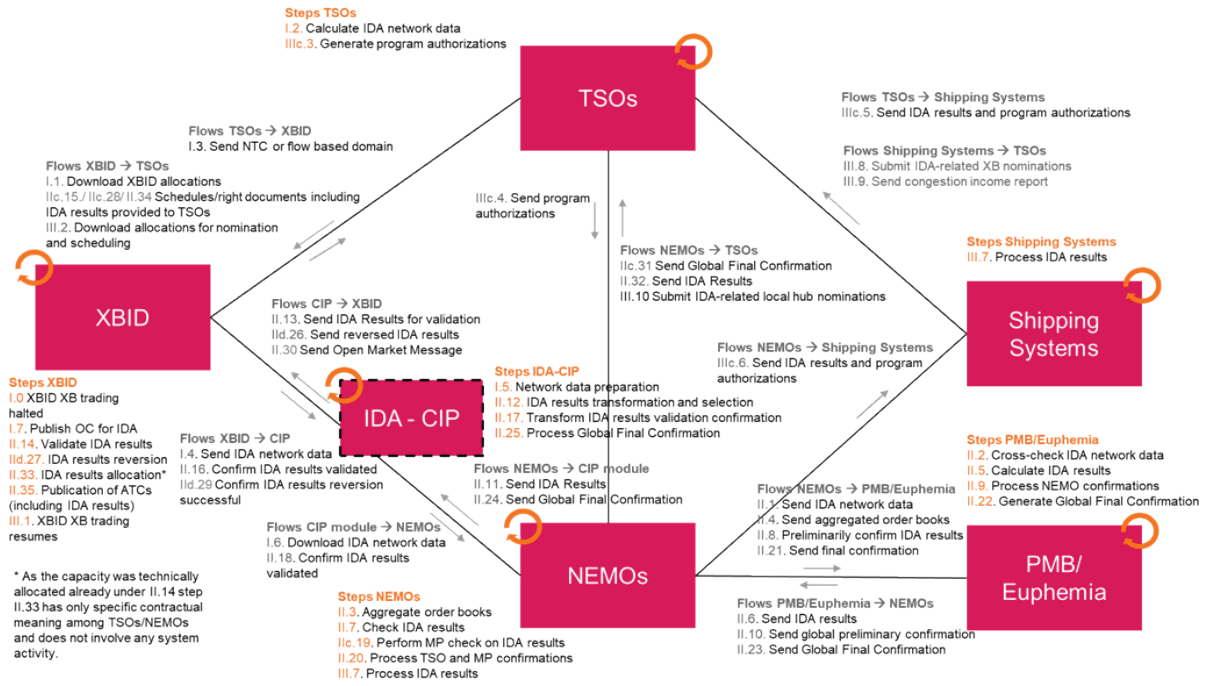


Figure 3. IDA High Level Architecture Diagram [2]

Under normal operation, Cross Border Continuous Trading in XBID will be suspended for a period of maximum 40 minutes (20 minutes prior the above mentioned planned start of each IDA until 20 minutes after the planned start of each IDA) in order:

- to make the Cross Zonal Capacities from XBID available to the IDA;
- to run the IDA taking into account Already Allocated Capacities and Ramping Restrictions;
- to validate the results of the IDA by means of successfully reserving the capacity in XBID which is allocated by the IDA;
- in the event of rejection of the IDA results by any of the other validators revert the reservation of the capacity in XBID, otherwise allocate the reserved capacity.

IDA	Cross-border IDC halt	IDA GCT	Cross-border IDC resume	IDA will open following contracts for trading	All MTU CZ-trading for contracts halted in IDC(CMM) during IDA /ramping disabled/	15MTU CZ-trading for contracts halted in IDC(CMM) during IDA /ramping enabled/	30MTU CZ-trading for contracts halted in IDC(CMM) during IDA /ramping enabled/	60MTU CZ-trading for contracts halted in IDC(CMM) during IDA /ramping enabled/
IDA1	D-1 14:40	D-1 15:00	D-1 15:20	D (all)	D (all)	D-1 23:45-00:00 D (all)	D-1 23:30-00:00 D (all)	D-1 23:00-00:00 D (all)
IDA2	D-1 21:40	D-1 22:00	D-1 22:20	D (all)	D (all)	D-1 23:45-00:00 D (all)	D-1 23:30-00:00 D (all)	D-1 23:00-00:00 D (all)
IDA3	D 09:40	D 10:00	D 10:20	D (12:00-00:00)	D (12:00-00:00)	D 11:45-00:00	D 11:30-00:00	D 11:00-00:00

Figure 4. IDA parametrization in CMM

After completion of the IDA the Cross Border Continuous Trading in XBID will resume until the suspension for the next IDA or the normal gate closure.

### 3. IDA PROCESS TIMING

IDA process normal timing is shown in the Figure 5.



Poster Presentation: The Role of PSPP in the Implementation of Strategy of Accelerated Development of RES in the Countries of South-Eastern Europe

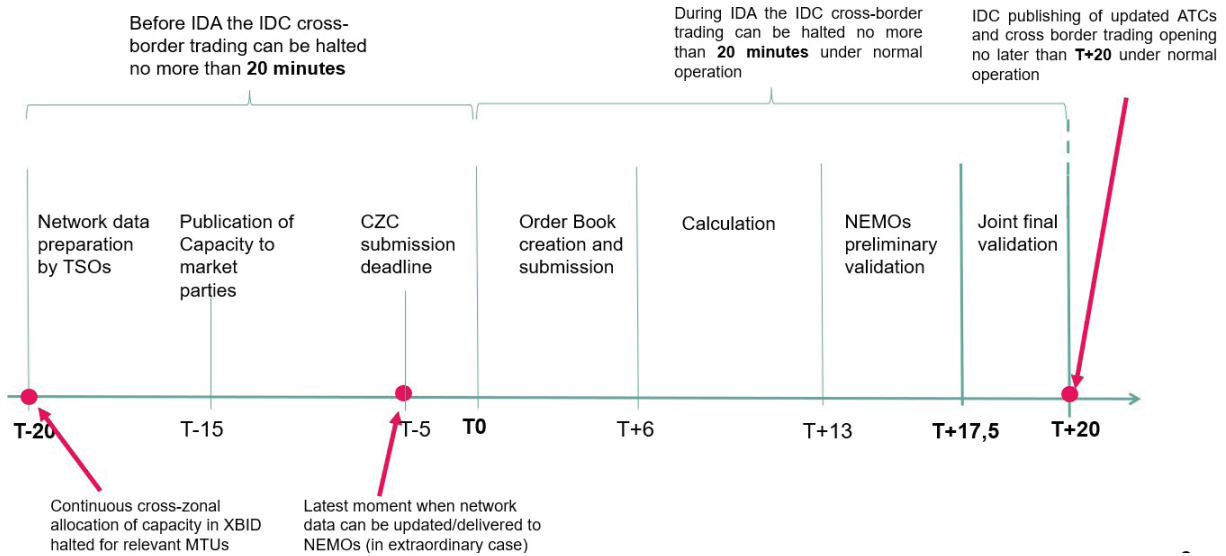


Figure 5. IDA normal process timing

Overview of foreseen times reserved for specific information flow/step are shown in Figures 6to 11. [2]

Pre-coupling + start of coupling phase  
Case where NTC re-calculation by TSOs from FB Domain is based on final AAC (Ex: Target expectation for Core CCR)

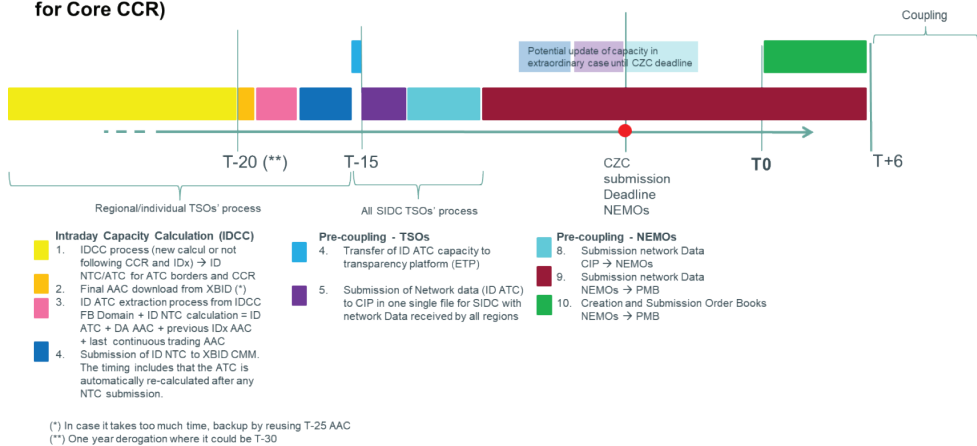


Figure 6. NTC re-calculation by TSOs from FB Domain is based on final AAC

Pre-coupling + start of coupling phase  
The Nordic Model (no MCP is used in CCC ATC-extraction) – Case where NTC are calculated before the T-20 deadline (without the need of Final AAC result)

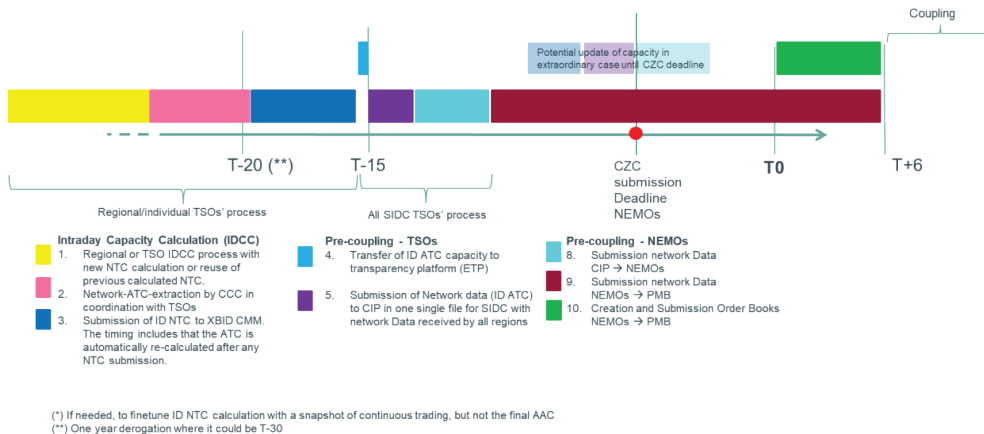


Figure 7. NTC re-calculated before the T-20 deadline



Poster Presentation: The Role of PSPP in the Implementation of Strategy of Accelerated Development of RES in the Countries of South-Eastern Europe

Pre-coupling + start of coupling phase
Case where NTC are re-calculated before the T-20 deadline (without the need of Final AAC result)

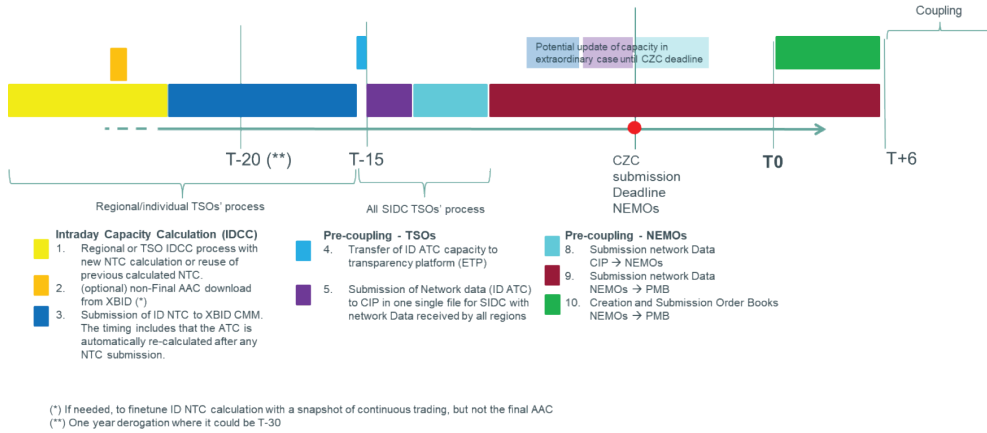
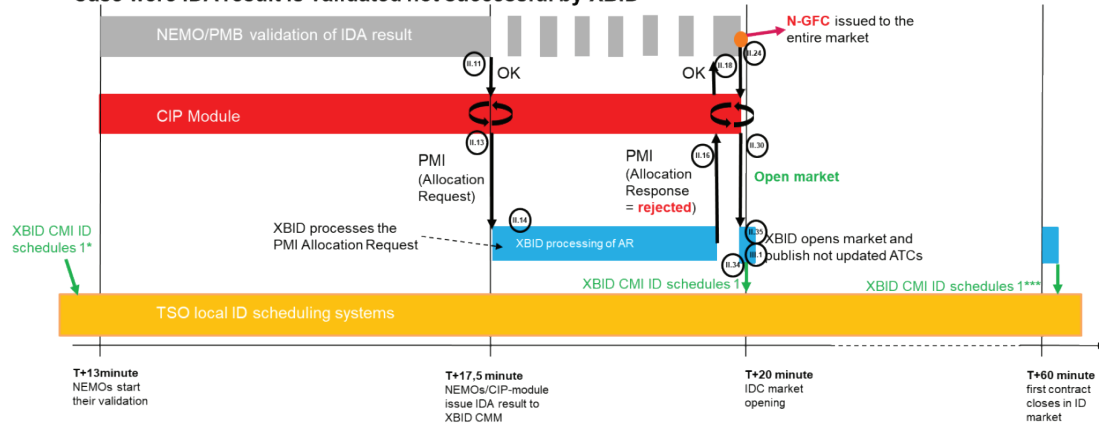


Figure 8. The Nordic Model

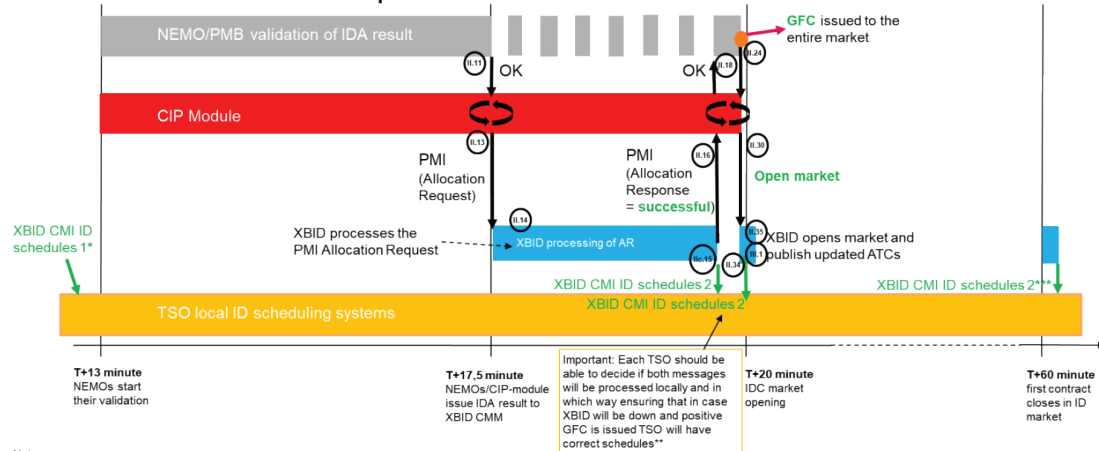
Coupling + Post-coupling phase
Case where IDA result is validated not successful by XBID



Notes:
\*At the time of contract closing XBID CMM shall issue the ID schedules (without IDA) to TSO local ID Scheduling systems
\*\*\* In this example no changes in ID schedules due to continuous trading are assumed.

Figure 9. All validations are positive

Coupling + Post-coupling phase
Case where all validations are positive



Notes:
\*At the time of contract closing XBID CMM shall issue the ID schedules (without IDA) to TSO local ID Scheduling systems
\*\* The reason the schedules are required to be send at the time of a positive Allocation Response is to make certain that if XBID goes down right after successful Allocation Response is issued to CIP, but before market opens as a result of positive GFC, TSOs would still have the schedules in their scheduling systems.
\*\*\* In this example no changes in ID schedules due to continuous trading are assumed.

Figure 10. IDA result validated not successful by XBID



Poster Presentation: The Role of PSPP in the Implementation of Strategy of Accelerated Development of RES in the Countries of South-Eastern Europe

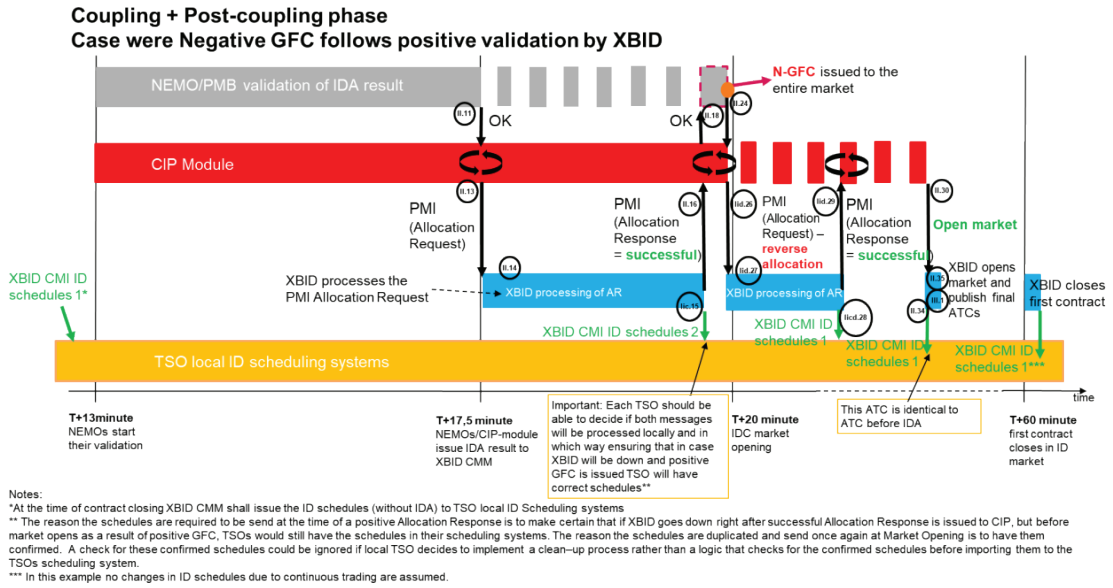


Figure 11. Negative GFC follows positive validation by XBID

### 4. IDA TESTING APPROACH

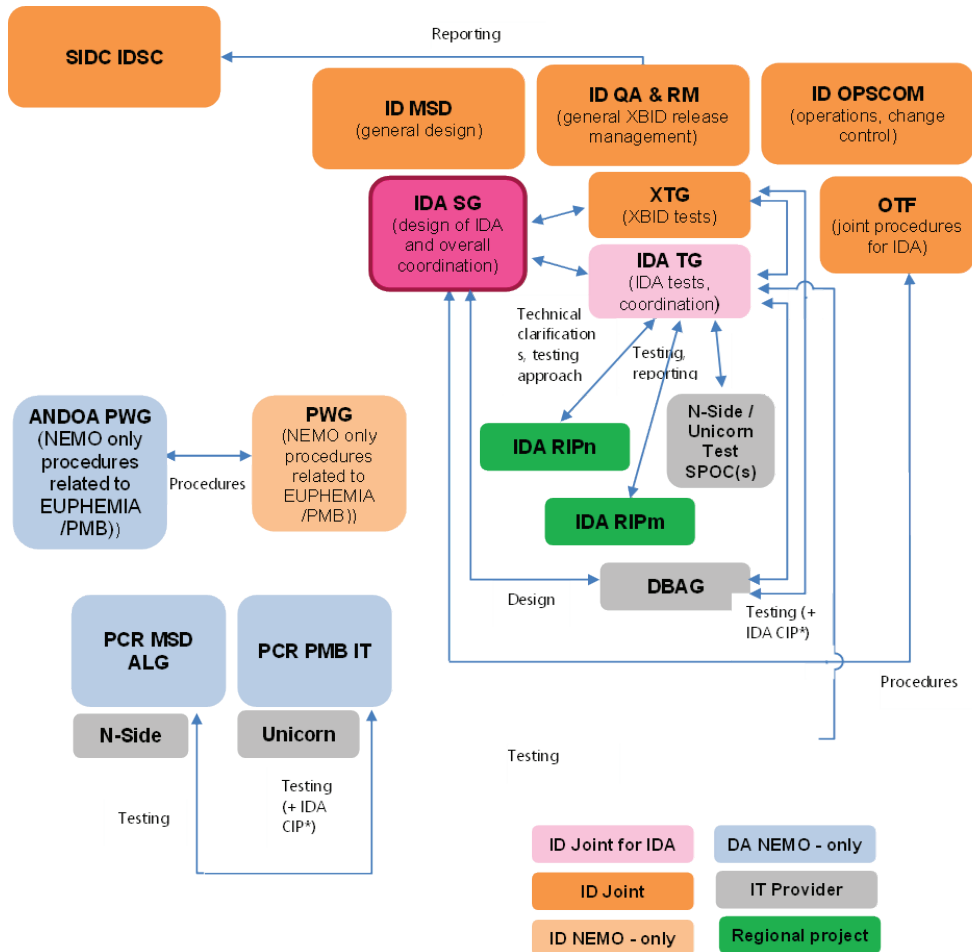


Figure 12. IDA testing organization



Poster Presentation: The Concept of Ukraine’s Power System Development Taking into Account the Impact of the Pumped-Storage Power Plant in Modern Conditions

The objectives assigned to specific test phase are to [3]:

- validate that EUPHEMIA/PMB is amended in line with SIDC IDA SG functional requirements and configurations match the IDA needs;
- validate that XBID system is amended in line with SIDC IDA SG functional requirements and configurations match the IDA needs;
- validate that the local solutions and procedures are matching with the functional requirements and with XBID system/EUPHEMIA/ PMB design and configurations and to prove the usability in such a way that selected parties are prepared to declare they are ready to Go-Live consider the aspects of local systems and procedures and XBID system design and configuration.

The critical Business Processes that need to be tested from individual entity and with all entities together are [3]:

- Pre-coupling
  - o Exchange of Network Data file (includes ATCs, AACs, Net Position Constraints and other network related data)
  - o include NTC recalculation on TSOs side where applicable
  - o include sending the orderbooks for various products
- IDA results calculation in EUPHEMIA
- IDA results validation by TSOs and NEMOs
- Post coupling
  - o TSO matching
  - o NEMO/Shipper nomination
- Backup processes
  - o Manual processes used as the backup for the automated processes. It shall be noted that due to limited time frame for IDAs there should be very limited number/level of the manual processes.
  - o Fallback processes.
- IDA Cancellation (MCS Full-Decoupling situation)

IDA – Testing timeline – Detailed plan (v0.7)

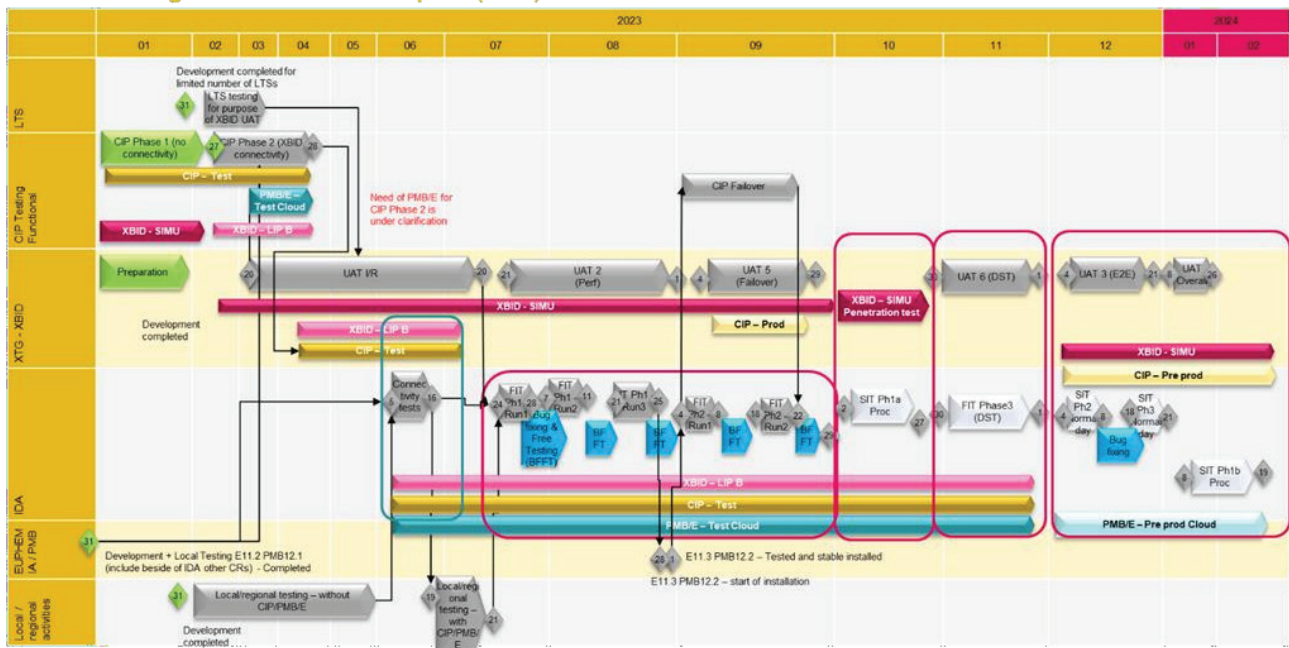


Figure 13. IDA testing timeline





**Poster Presentation:** The Concept of Ukraine's Power System Development Taking into Account the Impact of the Pumped-Storage Power Plant in Modern Conditions

The implementation phase of the IDA project comprises a testing period with all involved parties which can be divided in the several phases [3]:

### 4.1. EUPHEMIA/PMB Functional Integration Test

Aim of the EUPHEMIA/PMB FIT is to validate that new functions and configuration introduced based on RfCs raised by SIDC/IDA towards SDAC OPSCOM are working as specified and that all data between individual NEMO local trading system and EUPHEMIA/PMB test environment dedicated for IDA tests can be exchanged successfully. This phase is fully under PCR parties' responsibility.

### 4.2. Individual/bilateral/regional tests

Where the pre- and post-coupling part of the local/regional systems have been modified, parties have to test this in individual, bilateral or regional testing – testing between systems without the XBID, CIP and EUPHEMIA/PMB. Aim is to ensure all data between parties for a specific border or area (TSOs / NEMOs) can be exchanged and the business processes can be processed successfully (focus to format and content).

### 4.3. XBID Functional Integration Test

Aim of the XBID FIT is to validate that new functions and configuration introduced based on RfCs raised by SIDC/IDA towards DBAG are working as specified and that data between a regional TSO system and XBID test environment dedicated for IDA tests can be exchanged successfully. This phase is fully performed by XTG, and status/outcome is shared by XTG and monitored in SIDC.

- IAT: Integration acceptance test
- UAT I: Functional + Regression
- UAT II: Performance – dedicated performance test for IDA shall be assessed later on
- UAT III: Integration (E2E) – for IDA itself covered by Simulation Integration Test (IDA SIT Phase 2/3)
- UAT VI: DST – this phase is intended to be used also to validate IDA functionalities (IDA FIT Phase 3)
- UAT V: Failover
- UAT IV: Procedures – it is not needed for IDAs as it is addressed under IDA SIT (IDA SIT Phase 1)

### 4.4. IDA CIP Functional Integration Test

Aim of the IDA CIP is to validate that functions and configuration introduced in IDA CIP and interface with the NEMOs and XBID are working as specified. This phase is performed by IDATG using the XTG way of process organization. This test phase is mandatory for all SIDC NEMOs and at least for subgroup of TSOs which may be alternatively replaced by their testing services provider SYSQA.

### 4.5. IDA Connectivity Test

Aim of the IDA connectivity test is to validate that XBID, IDA CIP, EUPHEMIA/PMB and parties local/regional systems can properly communicate. This phase allows the parties also to confirm individually their connection with the central testing infrastructure and helps to

mitigate the risk of a malfunction in the interfaces prior to IDA FIT. This test phase is mandatory for all SIDC NEMOs and TSOs.

### 4.6. Additional individual/bilateral/regional tests with XBID/CIP/PMB

After the connectivity test, and before IDA Functional Integration Test (FIT), a period will be available allowing parties to continue RIP testing, but this time with possibility to use XBID, IDA CIP and EUPHEMIA/PMB. This test phase is optional for SIDC NEMOs and TSOs.

### 4.7. IDA Functional Integration Test (FIT)

Focus of the Functional Integration Test (FIT) is to ensure all data between parties (TSOs / NEMOs) for a specific border delivery area/ RIP, TSOs/CCC and the XBID System, NEMOs and the EUPHEMIA-PMB, XBID and IDA CIP, and IDA CIP and NEMOs can be exchanged,



Poster Presentation: Insuring Power System Reliability Under High Renewables Penetration with Energy Storages - A Case for Ukraine

and the business processes can be processed successfully (focus to format and content) end-to-end. The FIT execution is organized by the IDA Testing Group. FIT is suggested to be organized in 3 phases and runs where fixing period will be introduced between these runs also enabling ad-hoc tests to be performed by each party/RIP to retest specific fixes. Phase 3 shall include DST testing which requires harmonization across all systems. Testing phases are facilitated by IDA TG including daily calls, to enable verification of the process in situation when across more systems impacts will be enforced. This test phase is mandatory for all SIDCNEMOs and TSOs.

4.8. Simulation Integration Test (SIT)

Purpose of the Simulation Integration Test (SIT) is to demonstrate that all IDA business processes for a specific border/interconnector and in conjunction with other borders are processed correctly. This shall also include continues trading and in selected days day ahead trading to cover overall process and all respective assets. This especially means that while in FIT a test case can be seen as isolated situation or isolated interface which functioning is checked in SIT overall picture and overall consistency of the data shall be checked. Business procedures of and between parties and all the systems as defined in the HLA – systems of TSOs, NEMOs, Shipping Agents, CCPs and the central XBID System. The SIT is suggested to be organized in 3 phases where fixing period will be introduced between these runs enabling ad- hoc tests to be performed by each party/RIP to retest specific fixes. It is not foreseen to have multiple test runs within one test phase.

- Phase1 will be focused to procedures testing and be organized by OTF
• Phase2 will be focused to full Normal Day simulation with realistic trading pattern
• Phase3 will repeat Phase2 scope (retesting)

4.9. Member Test

Member testing is an important test stage which needs to be executed at the end of the test campaign and before the go-live.

4.10. Acceptance Test

For overall IDA testing acceptance, a criterion is 5 number of days in a row with normal days running without any issue, is foreseen to be applied on top of other criteria.

5. IMPACT ON CROATIAN ELECTRICITY MARKET

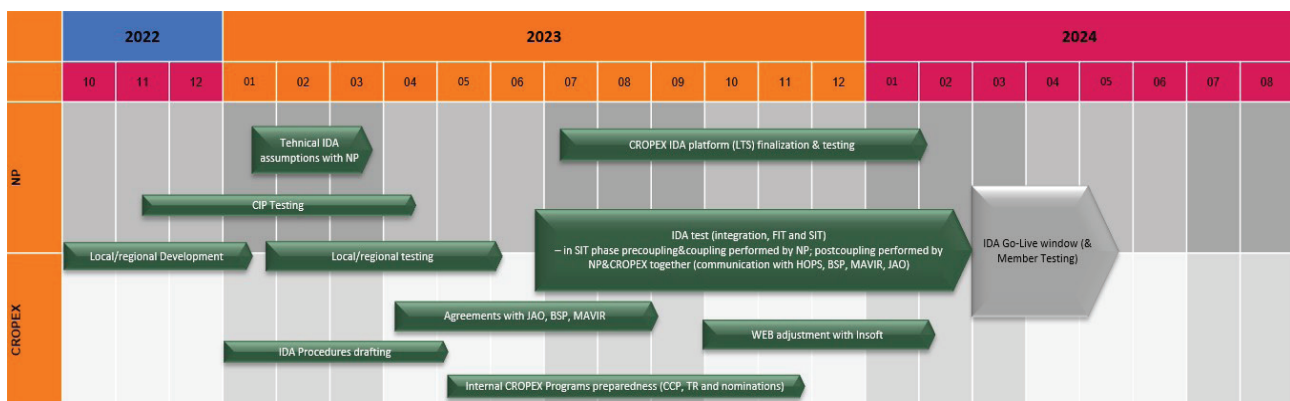


Figure 14. CROPEX IDAs implementation timeline

Figure 14. describes CROPEX IDAs implementation timeline which has started in 2022 with local and regional development and continued with local and regional testing in 2023. Currently, IDA is in integration of functional and simulation testing which, from Croatian part, will be performed in cooperation with Nord Pool, CROPEX IT service provider, and HOPS, Croatian Transmission System Operator.

The introduction of IDAs will have several impacts on the Croatian electricity market as well as for the whole of Europe in general:



Poster Presentation: Insuring Power System Reliability Under High Renewables Penetration with Energy Storages - A Case for Ukraine

- IDAs allow market participants to trade electricity closer to real-time, providing greater market flexibility in adjusting supply and demand. This can help balance the grid more efficiently and reduce imbalances bearing in mind the increasing share of renewable energy sources.
- IDAs provide an additional trading platform for market participants to buy and sell electricity. This can lead to increased liquidity in the spot market, as more participants are able to engage in short-term trading activities.
- With the introduction of IDAs, the prices in the intraday market may converge with the day-ahead market prices more closely. This can result in more accurate price signals and reduce potential price discrepancies between different trading timeframes.
- IDAs promote competition by allowing market participants to adjust their positions in real-time. This increased competition can lead to more efficient price discovery and potentially lower electricity prices for consumers.
- The availability of IDAs can help market participants manage their imbalances more effectively, reducing the need for expensive balancing services. This can lead to cost savings for market participants and potentially lower overall system costs.
- IDAs can facilitate better integration between the Croatian electricity market and neighboring markets. Cross-border trading can be more easily coordinated, allowing for efficient utilization of interconnectors and enhanced regional market coupling.
- Introducing IDAs may also bring operational challenges for market participants, NEMOs and TSOs. Market participants need to adjust their trading strategies to account

for the new trading opportunities and TSOs must ensure the stability and reliability of the grid during increased real-time trading activities.

## 6. CONCLUSION

The first local intraday auction was introduced in Germany in 2014. Since then, it was launched as well in other market areas such as Austria, Belgium, Baltic, France, Great Britain, Netherlands, Nordic, Slovenia, Switzerland. These auctions play a key role in providing further contracts granularity and balancing opportunities. In order to further develop this idea, the IDA project was launched across Europe to enable pricing of cross-zonal capacity on an intraday time frame using the market coupling mechanism between different bidding zones.

The IDAs will be a new market for trading physical power, providing a clear intraday price signal, new trading opportunities and increasing transparency in the market. Prices in the intraday market are different from the day ahead auction because forecasts are updated with new information about weather and availability of assets or transmission lines. If prices are higher in the intraday market, you may want to decrease your consumption, and sell back to the market. If prices are lower, you may want to increase consumption at a lower price than at the day ahead auction. If your consumption forecast has changed, you may want to trade yourself into balance and save costs. With the increasing number of renewable assets, these products are key in reinforcing the intraday reference price, optimizing the short-term market, and facilitating the energy transition.

CROPEX is together with other parties, part of IDAs project from the beginning. It will provide our members with the new trading possibilities in order for them to additionally balance and optimize their positions in the market.

## BIBLIOGRAPHY

- [1] Terms of Reference for SIDC IDAs (15<sup>th</sup> June 2021)
- [2] Intraday Auctions - Detailed design (13<sup>th</sup> September 2021)
- [3] IDA Testing Approach (17<sup>th</sup> January 2023)



**DISTRIBUTION SYSTEMS  
AND SMART GRIDS**  
**ORAL PRESENTATION**



ELECTRIC MACHINES AND  
POWER ELECTRONICS



ELECTRIC  
TRANSMISSION



AUTOMATION AND  
CONTROL

POWER  
GENERATION



ENERGY  
TRANSITION



DISTRIBUTION SYSTEMS  
AND SMART GRIDS



**11-12 OCTOBER 2023**





# Effective Lightning Mitigation Method on Unshielded Distribution Line by Using High Charge Ratings Externally Gapped Line Arresters

[ertugrul.partal@admelektrik.com.tr](mailto:ertugrul.partal@admelektrik.com.tr)

**ERTUGRUL PARTAL\*, MURAT SERKAN SERT, MERİÇ GER**

*ADM Electricity Distribution Corporation, Denizli*

*Türkiye*

## SUMMARY

In this paper, the procedures for evaluating the MV overhead line lightning performance in operation of one of the distribution system operators in Turkey called ADM Electricity Distribution Corporation will be discussed. The historical tripping data and the power outages cost will be analysed, the lightning mitigation measures will be compared and a methodology will be proposed. System operators are often reluctant to apply LSA (Line Surge Arresters) on unshielded since the LSA will be seen as the primary shield against lightning strokes. Tools as Sigma SLP simulation software can be used to determine the optimum LSA configuration but also to determine the min. charge transfer ratings to achieve low failure rates and get the confidence for long-term performance. High charge ratings EGLA (Externally Gapped Line Arresters) will be considered according to the latest standards, practices and developments for such applications. Technical specifications and required testing protocols are mainly in accordance with IEC 60099-8 (Edition 2.0) for EGLA. After installation and completion, this pilot project will be monitored by the distribution system operator (ADM) over 12 months.

## KEYWORDS

Continuity of Supply, Insulation Co-ordination, System Performance against Lightning, Sigma SLP, EGLA type Surge Arresters, IEC 60099-8(2017)





Oral Presentation: Effective Lightning Mitigation Method on Unshielded Distribution Line by Using High Charge Ratings Externally Gapped Line Arresters

## 1. INTRODUCTION

### 1.1. Lightning-induced outages for distribution overhead lines

Lightning is a natural phenomenon that occurs during rainstorms, snowstorms, and other weather conditions. However, in most areas, rainstorms are the primary source of lightning. Lightning can cause power interruptions and affect the reliability of a distribution line. To determine the exposure of a distribution line to lightning, the designer needs to know the Ground Flash Density (GFD), defined as the number of flashes per unit area per unit time. The preferred measure of GFD is the number of cloud-to-ground flashes per square km per year (flashes/km<sup>2</sup>/year). GFD can be estimated using statistical considerations, lightning detection network data, or lightning flash counters. The number of years of data needed to accurately estimate the GFD varies depending on the level of lightning activity in the area and the size of the region under consideration. The Figure 1 shows a visual representation in the EMEA region.

The technology now allows us to analyze larger data sets to define more accurate models and thus be able to respond to a concrete problem in a well-defined geographical area. For this pilot project, we will use LLS (Lightning Location System) data from 2015 to 2022 for the concerned region of South West Turkey.

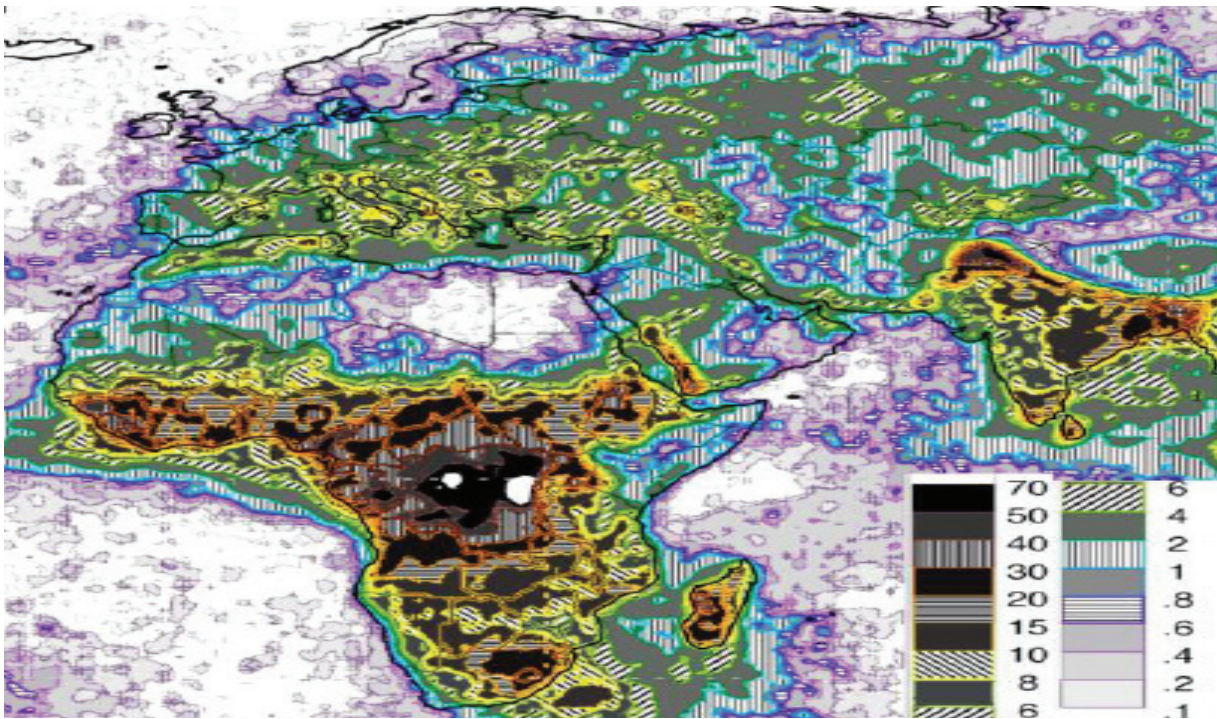


Figure 1. IEEE 1410-2010 - Total (cloud + ground) lightning activity for Africa and Eurasia

### 1.2. Importance of Lightning Location Systems (LLS)

Lightning Location Systems (LLS) are advanced systems that use a network of sensors to detect and locate lightning strikes in a specific area. These systems use different techniques such as time-of-arrival, triangulation, or a combination of both to determine the location of a lightning strike. The information obtained from LLS can be used for various purposes such as weather forecasting, lightning safety, and lightning research. In recent years, LLS has transformed the industry by providing accurate and real-time information about lightning strikes. This has allowed utilities and other organizations to take proactive measures to reduce the impact of lightning on overhead lines and other critical infrastructure.

### 1.3. Lightning Data Consolidation and I3CM LLS solution

The integration of Lightning Data Management in the software I3CM LLS is a key feature that helps to improve the accuracy and efficiency of lightning data analysis. The I3CM LLS, as shown in the Figure 2, helps to define basic parameters such as ground flash density (GFD) and cumulative stroke distributions, which are crucial to define customized lightning parameters along the distribution lines of interests and address lightning performance more effectively. The system allows the importation of existing data and/or the recording of real-time data through the I3CM 5G Devices. This enables the use of real-world data instead of relying on conservative





Oral Presentation: Effective Lightning Mitigation Method on Unshielded Distribution Line by Using High Charge Ratings Externally Gapped Line Arresters

CIGRE models (Two Line Stroke Distribution) for the definition of GFD and cumulative stroke distributions. Additionally, the I3CM LLS provides map visualization of lightning data, which allows for a better understanding of the spatial distribution of lightning strikes and can help to identify areas with high lightning activity.

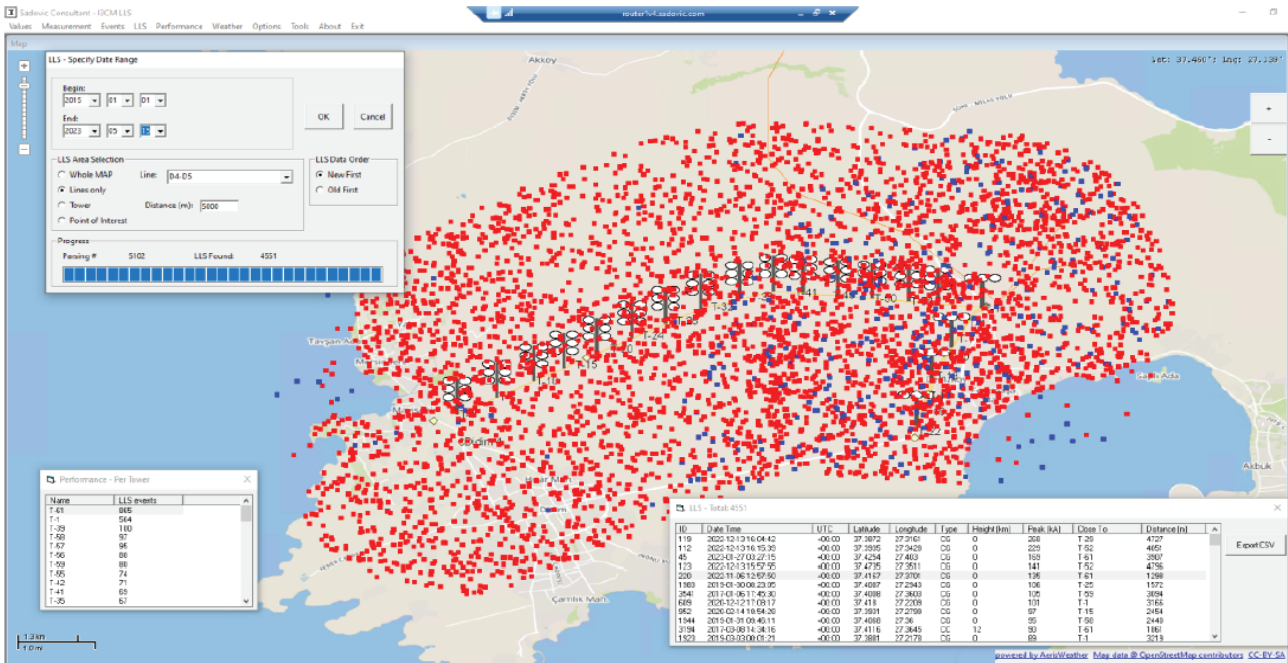


Figure 2. Screenshot of I3CM LLS – All CG lightning strokes between 2015 – 2022 along the line with 5km buffer

## 2. DUE DILIGENCE AND PROCESS REVIEW

As the distribution system operator in Turkey, ADM Electricity Distribution Corporation is committed to ensuring the reliability and safety of their overhead distribution lines. One of the main challenges ADM faces is the impact of lightning on their lines.

To evaluate the performance of our MV overhead lines due to lightning, ADM has selected a specific line in operation for analysis and utilized historical tripping data.

Table 1. Analysis of historical tripping data of the line average number of outages per year over 5 years = 25, Total length of single and double circuits OHL (km) = 20

Year	Total Transient Faults (for both circuits)
2018	14
2019	19
2020	41
2021	12
2022	41

Please note that there are no recorded outages within last 6 months since correct relay coordination and its settings implemented as well as increased repair & maintenance work for this line.

### 2.1. Calculation of Power Outage Costs

A study was carried out to determine the power outage costs, known as Value of Lost Load (VoLL), by considering regional factors and customer categories. The study examines the relationship between grid reliability and outage costs. ADM used survey methods



Oral Presentation: Effective Lightning Mitigation Method on Unshielded Distribution Line by Using High Charge Ratings Externally Gapped Line Arresters

to gather data on the financial and social losses experienced by individuals or companies due to power outages. The data is then used to estimate the balance point between grid investment costs and supply reliability. Different methods such as Ordinary Least Squares (OLS) and Two-Stage Regression were studied to estimate the consumer cost function. The results of the study can be used for various purposes such as determining incentives for distribution companies, compensation for damages caused by outages, and in grid planning and investment analysis.

The study of VOLL was conducted in three regions in Turkey: the South Aegean, North Aegean, and Thrace regions. **The analysis revealed that the optimal annual outage time for the ADM operating area is 4 hours and 53 minutes for households, 4 hours and 59 minutes for small and medium-sized businesses, and 5 hours and 36 minutes for large businesses.** The results also showed that the willingness to pay for electricity interruption is highest in the Thrace region, compared to the other two regions. This aligns with studies in other regions, such as the EU, that have found that willingness to pay values tend to be higher in northern regions.

Additionally, the willingness to accept values were also found to be higher in the Thrace region. These findings have important implications for the investment planning of electricity distribution companies in Turkey.

## 2.2. Review of existing lightning mitigation methods for distribution lines

The CIGRE Working Group C4.57 (Guidelines for the Estimation of Overhead Distribution Line Lightning Performance and its Application to Lightning Protection Design) addresses lightning performance by involving different experts worldwide.

The working group aims to advance the current understanding of how to effectively design lightning protection for overhead distribution lines (OHDLs) in terms of balancing the reliability of power supply with the cost of mitigation methods. Lightning damage is a major problem in OHDL and countermeasures such as shielding wire, surge arresters and reducing grounding resistance are commonly used. However, due to the wide use of OHDL it is not practical to apply countermeasures to every pole, and the design of OHDL is dependent on the country and population density. Additionally, the insulation level of OHDL is relatively low compared to overhead transmission lines, making it impossible to protect against all lightning strikes. Therefore, a more balanced lightning protection design that considers the reliability of power supply and the cost of mitigation methods is needed.

There are several countermeasures that can be used to improve the lightning performance of OHDL. Some of the most common methods include:

Table 2: Overview and analysis of the different mitigation methods for lightning performance improvement

Method of lightning protection	Feasibility check & Economic viability
Add or extend shielding wire(s) / OHGW (OverHead Ground Wires)	<ul style="list-style-type: none"> <li>- OHDLs are generally unshielded due to specific reasons. Strongly depends on tower design. TEDAŞ system owner does not allow OHGW installation.</li> <li>- Not effective for high footing resistance &amp; high soil resistivity</li> <li>- High material &amp; labor costs, <b>Non-economical solution</b></li> </ul>
Increase BIL (Basic Insulation Level) / insulator replacement or extension	<ul style="list-style-type: none"> <li>- Strongly depends on tower design and system clearances</li> <li>- Not effective on unshielded lines.</li> <li>- Does not eliminate the travelling/propagating waves which can endanger grounding points such as transformers and substation surge arresters.</li> <li>- High material &amp; labor costs, <b>Non-economical solution</b></li> </ul>
Improved tower footing resistances	<ul style="list-style-type: none"> <li>- Earth Enhancement Compound, Grounding Electrodes or/and Counterpoises might be completely inefficient, complex and costly.</li> <li>- Only efficient for shielded lines. Eliminates only backflashovers and doesn't influence shielding failures.</li> <li>- High material &amp; labor costs, <b>Improvement is not guaranteed since the OHDL is unshielded</b></li> </ul>
Install Line Surge Arresters	<ul style="list-style-type: none"> <li>- Versatile &amp; Large feasibility</li> <li>- Highest protective effectiveness even for high footing resistances in all terrains</li> <li>- Eliminate all types of lightning failures.</li> <li>- Low material &amp; labor costs, <b>Cost-efficient solutions.</b></li> </ul>



**Oral Presentation:** Effective Lightning Mitigation Method on Unshielded Distribution Line by Using High Charge Ratings Externally Gapped Line Arresters

All these methods have their own advantages and disadvantages, and depending on the specific line characteristics and the lightning environment, a decision must be made for the project implementation.

By comparing the budget and the complexity of the different mitigations measures, ADM can make informed decisions on how to effectively improve the performance of our lines and ensure a reliable power supply for their customers.

Considering the recent experience of TEİAŞ (Transmission Operator in Turkey) with 170kV EGLA Pilot Project implementation, ADM has also been fortunate to be able to demonstrate ease of implementation when the project is done right.

### 3. REVIEW OF LINE SURGE ARRESTERS

#### 3.1. MO LSA as an effective solution

Contrary to popular belief, the use of Metal-Oxide Line Surge Arresters (MO LSA) on distribution lines has always received moderate acceptance due to several challenges. Above all, it should be mentioned that the costs of LSAs have often been a brake on the financial damage resulting from lightning-related outages. One of the main challenges is that OHDL are often unshielded, which leads to a higher charge transfer than the standard Qrs ratings of typically distribution class arresters. Some OHDLs are even unshielded and ungrounded because the soil resistivity is very high and it's difficult to find a good grounding point. In such cases, LSA application is very challenging due to the high charge transfer ratings from direct strokes and the absence of grounding system. Additionally, isolated or impedance neutral systems can lead to high TOV (Temporary Over Voltage) stress and might exceed standard voltage ratings of NGLA (Non-Gapped Line Arresters). The cost of MO LSA is a significant factor, and the solutions and experience of manufacturers are often not convincing for system operators. Furthermore, failures on MO LSA have been reported due to sealing system issues (mainly moisture ingress on NGLA) resulting from flaws during the manufacturing process or aging in operation. This point can of course be discussed because not all designs and qualities of NGLA are equal. The technical specifications can be compromised in these cases.

#### 3.2. EGLA as a solution

A distinction should be made between EGLA and NGLA. The history, the adoption and the development of EGLA in several countries were mainly driven by a technical superiority. Experience feedback has provided high satisfaction and massive usage thanks to its reliability. There is no country that has changed its strategy by going back to NGLA technology while we regularly see countries that used NGLA now switching to EGLA technology. The technical debate and argumentation are often biased for commercial reasons as not all surge arrester manufacturers have a complete EGLA portfolio. Both technologies are often put on an equal level in order not to be penalized, which is also understandable. Today, NGLAs still suffer from a relatively bad reputation because of mechanical failures involving lead cables, disconnectors, or some of the accessories required for their installation.

Although the new IEC 60099-11 standard will address these problems, the failure rates of NGLAs are still much higher than those of EGLAs. It is therefore an obstacle to LSA's widespread adoption.

The EGLA design is much more suitable for use on overhead lines that are constantly solicited by vibration and difficult climatic conditions. An EGLA will eliminate the lightning fault but will remain insensitive to TOV and switching surges thanks to its air gap. Also, the air gap isolation ensures a successful re-closing operation even if the arrester body has failed. The air gap is a simple and robust feature that provides essential properties to the operation of the EGLA for long term reliability. The ZnO blocks are only used when necessary, the rest of the time the SVU (Series Varistors Unit) is not subjected to any electrical stress.

It should also be noted that the current IEC 60099-8 standard for EGLA already covers testing for artificial pollution (follow-current interruption test) and vibration fatigue resistance while NGLA has not evolved yet. The EGLA design provides an attractive advantage of no deterioration on arrester housing and ZnO blocks due to continuous energization, which enables the establishment of compact light-weight designs. In simple words, it means that TOV handling would require more ZnO blocks and switching handling would require larger ZnO blocks. Silicone rubber material can also be reduced due to the absence of tracking and erosion process (lower creepage distance).

Thus, its isolation from the system also gives it the possibility to reduce the active part to its bare minimum. This allows different options to integrate the EGLA in a harmonious way onto the transmission line.

The ultimate argument also remains its cost. Although some users may have seen higher prices than NGLA for market reasons, EGLA requires less material to be produced. Thus, these manufacturing costs remain more attractive than NGLA.



**Oral Presentation:** Effective Lightning Mitigation Method on Unshielded Distribution Line by Using High Charge Ratings Externally Gapped Line Arresters

### 3.3. CONCEPT OF HIGH CHARGE RATINGS EGLA

To tackle the challenges previously described, we propose to use high charge ratings EGLA on the selected distribution line. A superior reliability and a high capability to withstand lightning discharge current would be the key for a successful implementation and long-term performance.

Since the OHDL is not protected by shield wires (OHGW), direct flashovers (shielding failure) are more likely to occur on the line. Back-Flashovers have less probability to occur, only when lightning strikes hit the tower top.

The upper phase conductors will play a very specific role as they will be considered as primary shield that will protect the system and the lower phases. Therefore, the dimensioning of the charge transfer capability of the EGLA on the upper phases becomes a very sensitive criterion that must be verified. Figure 3. shows a theoretical representation of the concept. It should be noted that not all phases must be protected.

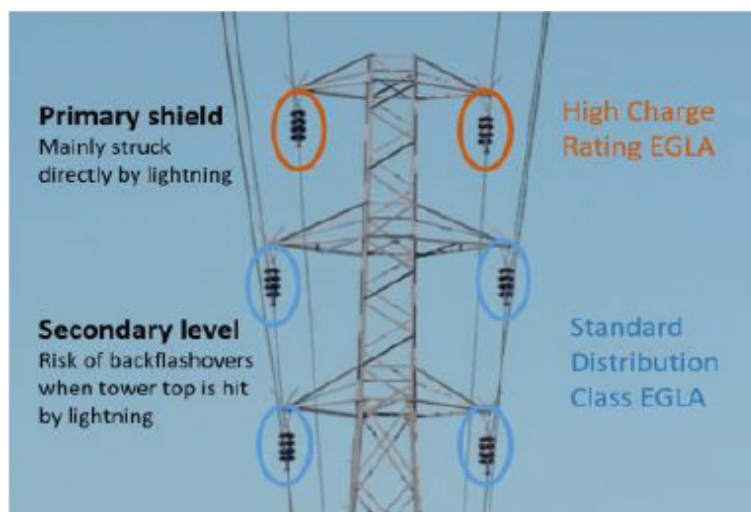


**Figure 3.** General concept for high charge rating EGLA

The EGLA must, with an acceptable low failure rate, be able to withstand possible current and charge stresses imposed by direct strokes to the overhead line. Therefore, it is expected that top phases shall be protected with conventional Station Class types while middle and bottom phases shall be protected with conventional Distribution Class types. The failure rate must be calculated and demonstrated taking into account the stroke distribution along the line.

## 4. METHODOLOGY

### 4.1. Sigma SLP system studies

Sigma SLP is the dedicated simulation software for the computation of lightning performance with a focus on Line Surge Arrester application.

SIGMA SLP is an object-oriented software package for computation of transmission and distribution line lightning performance. In short, it calculates the number of outages to expect based on configurable system parameters and lightning activities. It allows simple application of LSA to define optimum quantities and LSA placement.

The software provides a statistical representation of LSA discharge currents, thermal energy and charge transfers to be compared with LSA ratings. It helps to define maximum expected charge/energy and therefore analysis the failure rate of your installation. A standard stroke distribution can be used for the simulation of lightning activities (Two lines CIGRE stroke distribution from CIGRE TB 63 / 1991) or a customized stroke distribution can be defined by the users to reflect better its own situation.



Oral Presentation: Effective Lightning Mitigation Method on Unshielded Distribution Line by Using High Charge Ratings Externally Gapped Line Arresters



Figure 4. View of Sigma SLP simulation software showing input data and Statistical Study section

## 4.2. Preliminary Results

Since the OHDL is not shielded, most of the lightning induced outages are defined as direct lightning strokes (shielding failure). The statistical approach shows us that some high amplitude lightning strikes between 100kA and 230kA can generate an excessive charge transfer that can damage the EGLA. However, these high amplitudes have a very low probability to occur and therefore the failure rate is very low (<0.1%). This rate is quite acceptable. It should be noted that if we want to increase the charge transfer of the EGLAs to a higher level, the impact on the costs would be significant and not justified from the user's point of view. Our aim is to improve the lightning performance with a defined optimum number of LSA (ie. to improve the outage rate by the 75% while installing only 25% of LSA - 100% being LSA on each phase & tower).

Due to the early phase and the delay of the project execution, some simulation data/study results cannot be disclosed at this stage. For unshielded lines, we expect to have a majority of EGLA on the top phases. About 12 EGLA per mile on a double circuit line are expected. The system studies will help us to significantly reduced the lightning outages by protection the top phases with high charge ratings EGLA (shielding failure/direct flashovers) but also to have a fine tuning using standard EGLA on selected towers with higher footing resistances where lightning strokes can hit the tower top (backflashovers).

## 4.3. Testing of active part (SVU) and EGLA assembly

Besides the recent release (December 2021) of the CIGRE Technical Brochure 855 about LSA's application providing a global and complete picture in 170 pages, the project team TC 37/PT 60099-11 is currently preparing the future standard for LSA's covering both EGLA and NGLA application.

This is a standardization that will be stamped with the dual IEC/IEEE logo, so we are getting closer to full harmonization. EGLA applications have their own standard with IEC 60099-8 which is satisfactory until today but still insufficient. The subject of LSA's must be treated as a whole and therefore requires a merge with the NGLA. Vibration tests already exist for EGLA but the "mechanical tests" section will be expanded to cover LSA specific failure modes. The testing protocols for this project will include the latest updates and considerations such as:

- 2/20μs waveshape for protection level and classification in opposition to conservative 8/20μs waveshape
- High Current Impulse with 2/20μs waveshape represents the maximum allowable lightning peak current magnitude through LSA in service. It refers to a discharge current magnitude due to a direct stroke on power conductors.
- Repetitive charge transfer rating (Qrs) with a 200μs impulse as per IEC 60099-8 to strictly refer to overhead lines application.





Oral Presentation: Effective Lightning Mitigation Method on Unshielded Distribution Line by Using High Charge Ratings Externally Gapped Line Arresters

### 4.4. Integration on existing strings

Line Designers and Surge Arresters specialists must continue to work together in order to facilitate the integration of LSA into overhead line shown in Figure 5 as an example. A proper review and adaptation are necessary for a smart integration together with the insulator string which is the key for a proper gap stability and life expectancy.

The pilot project will allow to standardize the types of EGLA assemblies and its accessories for each type of isolator strings and to allow the system operator to simplify the acquisition and installation procedures.

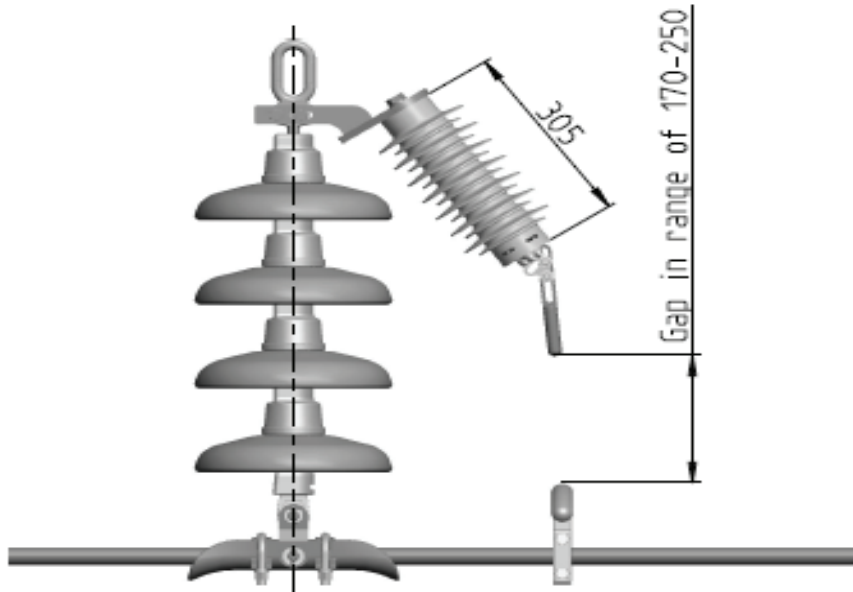


Figure 5. Example of integration for single suspension strings

## 5. NEXT STEPS & CONCLUSION

Due to the early phase and the delay of the project execution, some simulation data/study results cannot be disclosed at this stage. For unshielded lines, we expect to have a majority of EGLA on the top phases and about 12 EGLA per 1.5 km on a double circuit line are expected.

The system studies will help us to significantly reduced the lightning outages by protection the top phases with high charge ratings EGLA (shielding failure/direct flashovers) but also to have a fine tuning using standard EGLA on selected towers with higher footing resistances where lightning strokes can hit the tower top (backflashovers).

The project's success will not just be about proving LSAs' effectiveness, but about establishing a methodological approach for similar issues; the project's effectiveness in reducing outages and improving overall line performance will be evaluated over a 12-month monitoring period after installation.

## BIBLIOGRAPHY

- [1] IEEE 1410-2010 - Guide for Improving the Lightning Performance of Electric Power Overhead Distribution Lines
- [2] Calculation of Power Outage Costs (VOLL) by Regional Factors and Customer Categories and Examining its Relation with Grid Reliability. CIGRE Turkey 2022
- [3] CIGRE TB 855 - Effectiveness of line surge arresters for lightning protection of overhead transmission lines
- [4] EGLA Technology: Background, Development & Future Directions, INMR Berlin 2022





# An Ai-Based Scalable and Integrated Monitoring System for the Electrical Grid

cumaali.mantas@teias.gov.tr

**DİLEK KÜÇÜK<sup>1</sup>, SERKAN BUHAN<sup>1</sup>, TURAN DEMİRCİ<sup>1</sup>, MEHMET BARIŞ ÖZKAN<sup>1</sup>, MUHAMMET SERKAN ÇINAR<sup>1</sup>, ERİNÇ ALTINTAŞ<sup>1</sup>,  
UMUT GÜVENGİR<sup>1</sup>, SEYİT BİLAL ÇELİK<sup>2</sup>, CUMA ALİ MANTAŞ<sup>2</sup>, MURATHAN YENİCELİ<sup>2</sup>, NUMAN NOYAN<sup>2</sup>, MERDEN YEŞİL<sup>2</sup>,  
ŞEHRİ NUR GÜLER<sup>2</sup>, Umut YENER<sup>2</sup>, KAMİL ÇAĞATAY BAYINDIR<sup>3</sup>**

<sup>1</sup>*TÜBİTAK Marmara Research Center, Ankara*

<sup>2</sup>*Turkish Electricity Transmission Corp. (TEİAŞ), Ankara*

<sup>3</sup>*Ankara Yıldırım Beyazıt University, Ankara*

**Türkiye**

## SUMMARY

Monitoring systems for the electrical grid have diverse benefits from the aspects of system management, planning, and prevention of faults, particularly for national transmission system operators. In this paper, we present a scalable and integrated monitoring system (TEKİS) for Turkish electricity transmission grid, where the system is equipped with AI-based capabilities for event and fault classification. The presented monitoring system encompasses tailor-made modules for real-time and retrospective data monitoring, data analysis, detection, and classification tasks. The system also possesses the capability to act as phasor measurement unit as it calculates and transmits phasor data, complying with the related international standards. As part of future work, the system will be automatically integrated with renewable data forecast systems and will utilize and present renewable forecasts conveniently.

## KEYWORDS

Power quality, grid monitoring, smart grid, artificial intelligence, wide area monitoring, phasor measurement unit



### 1. INTRODUCTION

Effective monitoring of electrical power and power quality (PQ) parameters of the electrical grid is known to be useful for early identification of important problems, planning and preventive maintenance purposes as well as for retrospective analysis of significant incidents in the grid. Therefore, several power quality monitoring systems or wide area monitoring systems have been presented in the related literature [1-6], with different capabilities and using different software/hardware technologies. Some of these systems have been implemented for a subset of power and PQ parameters while some other systems have been applied on electricity distribution systems only.

In this study, we present an integrated large-scale monitoring system that facilitates measurement, storage, online monitoring, retrospective analysis, and automatic reporting of the power and PQ parameters, and PQ events and faults in Turkish electricity transmission grid. This current system is the successor of the nationwide power and PQ monitoring system presented in [2] and includes new modules such as its sag directivity detection and load dispatch modules, and Artificial Intelligence (AI)-based ones such as its event/fault classification module. The current system also encompasses integrated user interface modules implemented using modern Web technologies.

The rest of the paper is organized as follows: a general description of the proposed system is given in the upcoming section, then the modules of the TEKİS system are presented in the following section, next, important future research directions are listed, and finally, the paper is concluded by summarizing the main points.

### 2. SYSTEM DESCRIPTION

The proposed system is abbreviated as TEKİS from its open form in Turkish which can be translated as TEİAŞ Electric Power Quality and Grid Monitoring System, where TEİAŞ is Turkish Transmission System Operator (TSO). A preliminary description of TEKİS has been previously presented in [7].

TEKİS is a scalable and integrated system that has a modular structure and hence comprises different software modules performing the following system capabilities in an automated manner:

- Online measurement of PQ parameters and detection of PQ events (in compliance with IEC 61000-4-30:2015+A1:2021 PQ standard)
- Online phasor data measurement (in compliance with IEEE/IEC 60255-118-1:2018 phasor data measurement (PMU) standard)
- Classification of the PQ events with respect to their causes using AI-based learning algorithms with high performance rates
- Online detection and presentation of non-standard user-defined power and PQ events
- Collection and storage of the all measurements together with analysis and classification results in centralized databases
- Real-time graph-based and tabular monitoring of continuously-measured PQ parameters, phasors, and raw voltage and current waveforms corresponding to PQ events
- Map-based visualization of phase angles, PQ events, and user-defined alarms detected on the transmission grid
- Retrospective analysis of the collected PQ parameters and PQ events
- Calculation and presentation of PQ event indices (including voltage sag indices in IEEE Std. 1564-2014)
- Detection of sag directivity using different algorithms and settings (including the methods given in [8])
- Detection of the locations of events in the electricity transmission grid
- Automatic generation of PQ reports according to related standards including EN 50160:2010+A3:2019 and EN 61000-2-4:2002
- Visualization of summary PQ information in the form of convenient dashboards
- Data integration facilities from different devices using various related standards and protocols such as Modbus
- Data exporting facilities in various formats such as CSV, PDF, etc., through its user interfaces
- Data integration facilities to import data from and export data to other energy information/management systems through Web services.



With its capabilities listed above, the proposed TEKİS system can be considered as a significant wide-area monitoring system and as a large-scale smart grid application. Besides, this AI-based modular power quality and grid monitoring system is highly scalable since it can be enriched with new capabilities that can be conveniently implemented and integrated into the system.

### 3. SYSTEM MODULES

The modules of the system can be grouped the following three categories based on their characteristics:

1. Device and communication modules
2. Data storage, processing, and integration modules
3. User interface modules

The modules are hence briefly described in the following subsections corresponding to their category names.

#### 3.1. Device and Communication Modules

First of the modules under this category is an analysis software that performs the actual power, PQ, and phasor measurements, complying with the related standards including IEC 61000-4-30:2015+A1:2021 and IEEE/IEC 60255-118-1:2018, with time synchronization. This module also detects PQ events and saves the raw voltage and current waveforms during these events as COMTRADE files, complying with the related IEEE/IEC Std. C37.111-2013 standard. The analysis software continuously runs on the system's PQ analysis devices installed at the transformer substations of the Turkish electricity transmission grid.

Secondly, communication modules (under this category) continuously run on the PQ devices and the system server in order to transmit the measurements and detected events to the system center. Upon receiving the measurement and event data from the communication module running on the device, the communication module running on the server stores the measurement data on the system's database server and the event files on the system's file server.

#### 3.2. Data Storage, Processing, and Integration Modules

TEKİS has a centralized database (at the system center) that is used to store all of the related measurements including the data from its PQ analysis devices, the data obtained from other PQ devices, and from other energy systems through the data integration modules of the system.

The sag directivity detection module aims to identify the sources of voltage sag events detected and sent to the system servers by the device and communication modules presented in the previous subsection. The module utilizes state-of-the-art techniques and its operation is triggered by the system users through one of the user interface modules, namely, fault analysis and reporting module to be introduced in the next subsection.

Event/fault classification module makes use of different machine learning and deep learning models to identify the root causes of these events/faults. Various machine learning models including SVM, decision trees, random forest, k-nearest neighbors, logistic regression and other modified versions of these models have been tested so far. Hence, this module is based on AI techniques and best performing models after initial experiments will be integrated into this module.

TEKİS also receives relevant information and data from the other energy information and management systems in addition to other PQ devices through its data integration modules. The means of data transfer from these systems and devices are mainly Web services and protocols such as Modbus.

#### 3.3. User Interface Modules

TEKİS has an integrated user interface system that is based on modern Web technologies. The main user interface modules are summarized below and they are made available to the system users based on the user privileges.

1. Real-time trend monitoring module presents power and PQ measurements in addition to the phasor data to the system users as convenient dynamic and synchronized graphs. All of the graphs and tables in this module (and their corresponding data) and those in other modules can be exported in different formats.
2. PQ analysis and reporting module facilitates retrospective analysis of the measurements through its querying interfaces and also encompasses automatic reporting interfaces that produce reports according to related standards such as EN



50160:2010+A3:2019 and EN 61000-2-4:2002. A snapshot of the querying interface of the module is presented in Figure 1. Similarly, a snapshot of the reporting interface of this module is displayed in Figure 2 where an EN 50160-compliant report has been generated.

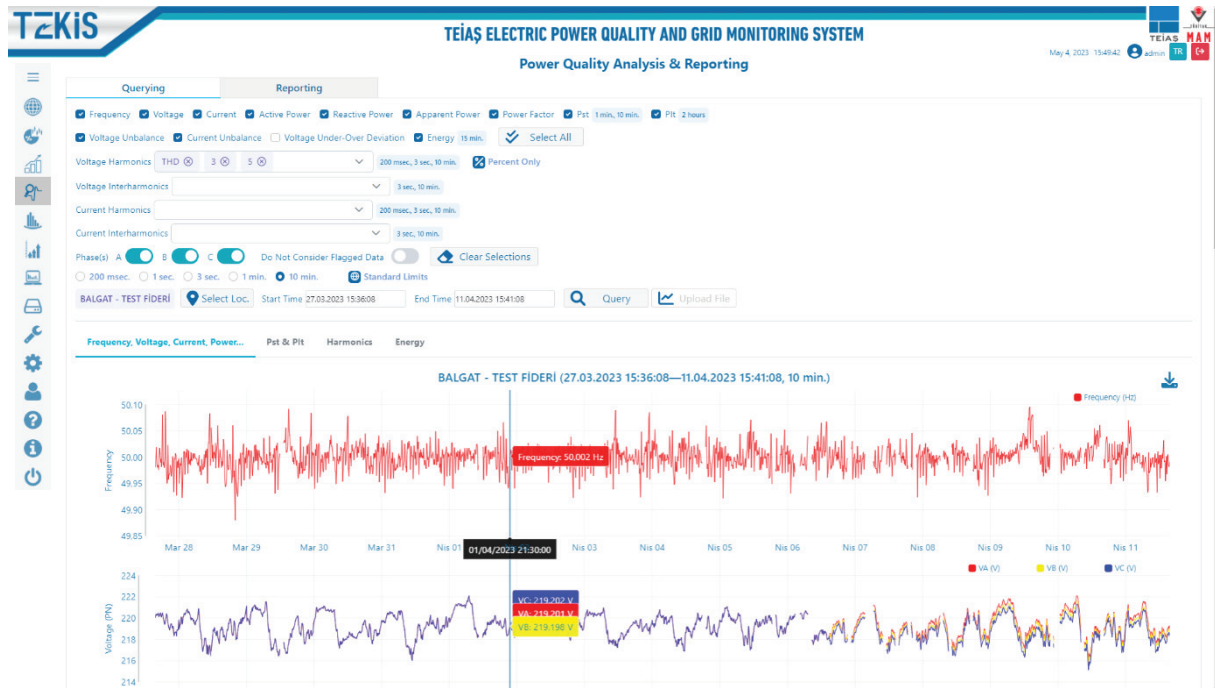


Figure 1. TEKİS Power Quality Analysis and Reporting Module (Querying Interface)

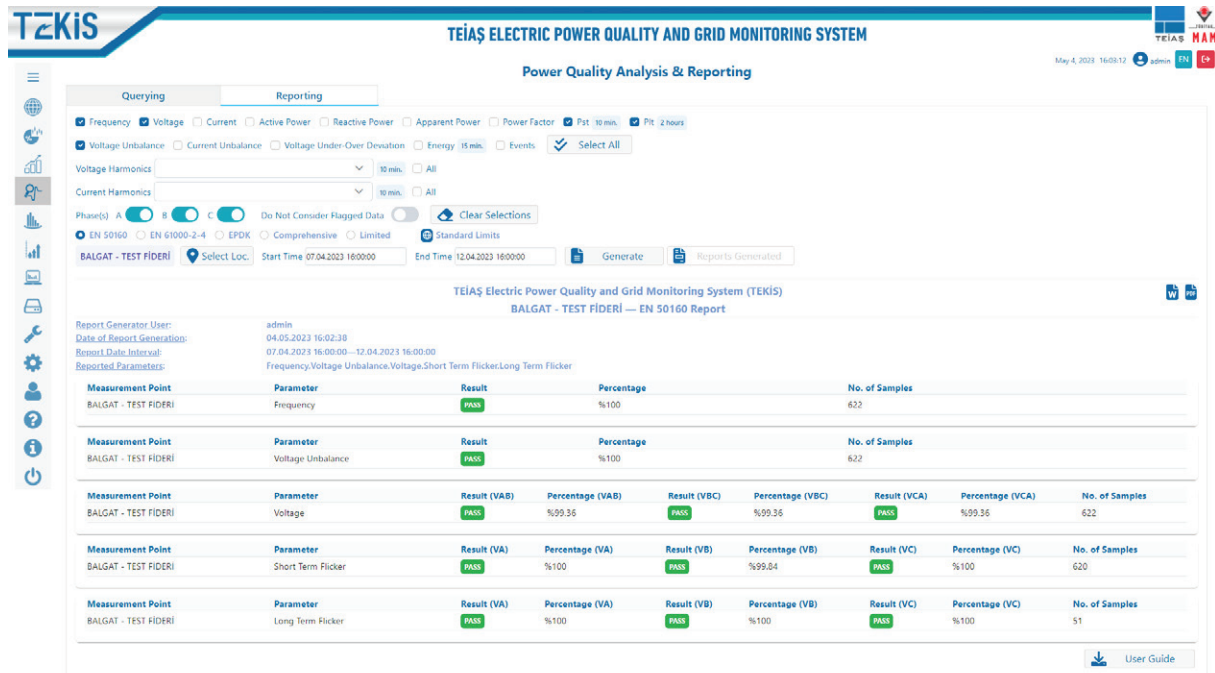


Figure 2. TEKİS Power Quality Analysis and Reporting Module (Reporting Interface)

3. Fault analysis and reporting module is used to inspect various PQ events/faults and generate reports based on the event data. The outputs of the aforementioned sag directivity detection and event/fault classification modules are also presented through this user interface module.



Oral Presentation: An Ai-Based Scalable and Integrated Monitoring System for the Electrical Grid

- Map-based monitoring module aims to visualize the collected PQ measurements and events on the map of the Turkish electricity transmission grid.
- Load dispatcher monitoring module is implemented to present the collected high-resolution phasor data in various convenient forms, to be utilized by the load dispatcher users. A snapshot of this module is given in Figure 3.

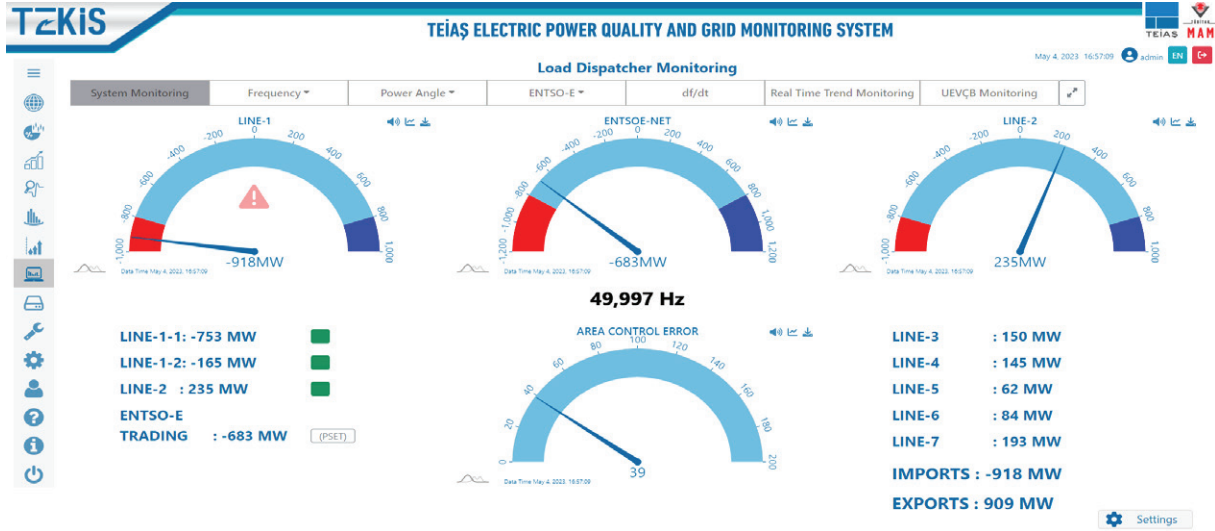


Figure 3. TEKIS Load Dispatcher Monitoring Module

- Device status tracking module aims to present the connection and other related status data of the PQ devices to the system administrators. A snapshot corresponding to this module is shown in Figure 4.

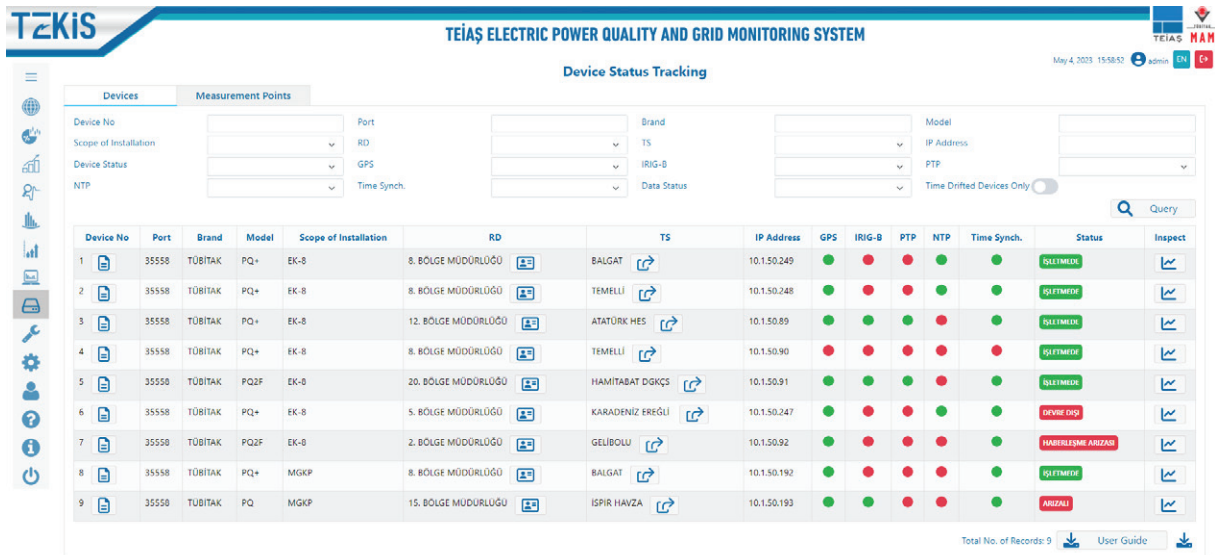


Figure 4. TEKIS Device Status Tracking Module

- Device configuration and calibration module is built in order to carry out the configuration and calibration processes of the PQ devices.

## 4. FUTURE WORK

As part of future work, new features that can be integrated into the TEKIS system (as new system modules) include the following:

- Detection and storage of inter-area power oscillations together with online monitoring and retrospective analysis interfaces for these oscillations





Oral Presentation: An Ai-Based Scalable and Integrated Monitoring System for the Electrical Grid

- Online monitoring of renewable energy forecasts and corresponding generations for different renewable power plants including wind, solar, and hydropower plants.

Particularly considering the second item above, RİTM is a national wind power monitoring and forecast system for wind power plants [9], similarly ATHOM is a national river flow forecast and optimization system for hydropower plants [10], and these two systems can be integrated with TEKİS so that renewable energy forecasts generated by the former two systems can be served to the Turkish TSO through TEKİS system.

## 5. CONCLUSION

In this paper, TEİAŞ Electric Power Quality and Grid Monitoring System (TEKİS) is presented. TEKİS is scalable and integrated system covering a diverse set of modules and including modules based on artificial intelligence techniques. We present the significant capabilities of the system in addition to the descriptions of its individual modules seamlessly integrated into the system. TEKİS is built in order to monitor Turkish electricity transmission system to be used by TEİAŞ (Turkish transmission system operator). The system has various facilities for real-time and map-based monitoring, retrospective analysis, and automatic reporting of power and PQ parameters of the transmission grid, in addition to modules for sag directivity detection and event/fault classification. An important future work based on the current study is the integration of TEKİS with existing national renewable energy monitoring and forecast systems.

## 6. ACKNOWLEDGMENT

This research and technology development work is carried out within the scope of TEİAŞ Electric Power Quality and Grid Monitoring System (TEKİS) Project (with project number 5212802) developed for TEİAŞ by TÜBİTAK Marmara Research Center. The project website is available at <https://tekis.teias.gov.tr/>.

## BIBLIOGRAPHY

- [1] Lim, Y., Kim, H. M., & Kang, S. (2010). A design of wireless sensor networks for a power quality monitoring system. *Sensors*, 10(11), 9712-9725.
- [2] Demirci, T., Kalaycıoğlu, A., Küçük, D., Salor, Ö., Güder, M., Pakhuylu, S., ... & Ermiş, M. (2011). Nationwide real-time monitoring system for electrical quantities and power quality of the electricity transmission system. *IET Generation, Transmission & Distribution*, 5(5), 540-550.
- [3] Palacios-Garcia, E. J., Rodriguez-Diaz, E., Anvari-Moghaddam, A., Savaghebi, M., Vasquez, J. C., Guerrero, J. M., & Moreno-Munoz, A. (2017, June). Using smart meters data for energy management operations and power quality monitoring in a microgrid. In *IEEE 26th International Symposium on Industrial Electronics (ISIE)* (pp. 1725-1731).
- [4] Di Pasquale, S., Giarnetti, S., Leccese, F., Trinca, D., Cagnetti, M., & Caciotta, M. (2015). A distributed web-based system for temporal and spatial power quality analysis. *Power Quality Issues in Distributed Generation*.
- [5] Liu, Y., You, S., Yao, W., Cui, Y., Wu, L., Zhou, D., ... & Liu, Y. (2017). A distribution level wide area monitoring system for the electric power grid-FNET/GridEye. *IEEE Access*, 5, 2329-2338.
- [6] Sinvula, R., Abo-Al-Ez, K. M., & Kahn, M. T. (2020). A proposed harmonic monitoring system for large power users considering harmonic limits. *Energies*, 13(17), 4507.
- [7] Küçük, D., Buhan, S., Demirci, T., Özkan, M. B., Çınar, M. S., Altıntaş, E., Güvengir, U., Çelik, S. B., Uçar, S., Mantaş, C. A., Yeniceli, M. Noyan, N., Yeşil, M., Güler, Ş. N., Kayaoğlu, İ. E., Yener, U. & Bayındır, K. Ç. (2022). TEKİS: TEİAŞ Electric Power Quality and Grid Monitoring System. *Power Systems Conference*.
- [8] Mohammadi, Y., Moradi, M. H., & Chouhy Leborgne, R. (2017). Locating the source of voltage sags: Full review, introduction of generalized methods and numerical simulations. *Renewable and Sustainable Energy Reviews*, 77(May), 821-844.
- [9] Terciyanlı, E., Demirci, T., Küçük, D., Sarac, M., Çadircı, I., & Ermiş, M. (2013). Enhanced nationwide wind-electric power monitoring and forecast system. *IEEE Transactions on Industrial Informatics*, 10(2), 1171-1184.
- [10] Buhan, S., Küçük, D., Cinar, M. S., Güvengir, U., Demirci, T., Yılmaz, Y., ... & Yildirim, M. U. (2019). A scalable river flow forecast and basin optimization system for hydropower plants. *IEEE Transactions on Sustainable Energy*, 11(4), 2220-2229.





# Implementation of Artificial Neural Networks in Conductor Tension Calculations

[obyuce@mitasus.com](mailto:obyuce@mitasus.com)

**ÖMER BURAK YÜCEL\*, BERKAN DEMİR, OSMAN FAKIOGLU, ALTAN ZERVENT**

*Mitas Industry*

*Türkiye*

## SUMMARY

Sag-tension calculations are an integral part of the line design as the outputs of the calculations affect the clearance checks, tower geometry, load calculations, stringing tables, etc. Sag-tension calculations depend on the conductor state change equation, which is highly non-linear with a bunch of parameters and requires an iterative approach to solve. The mathematical burden of solving such a non-linear equation can be overcome by means of some commercial software or spreadsheet programs. At this point, artificial neural networks (ANN) can be introduced as an alternative solution technique. ANNs are the sub-component of artificial intelligence, and they establish the relationship between the selected input and output parameters for a predefined dataset. Since ANNs bring fast and accurate solutions for empirical problems and allow approximate solutions for any kind of mathematical problem, they have become widely popular in all engineering fields. In this study, an ANN architecture is proposed to relate the variables of the state change equation (i.e., mechanical and physical properties of the conductor, atmospheric conditions, etc.) to the tension values that emerge on the conductor. In this way, conductor tension values for any specific condition can be found within seconds with an acceptable level of error. The study focuses on the five main conductor types used in the distribution lines in Türkiye.

## KEYWORDS

Artificial Neural Networks – Tension – Conductor – Distribution - Line



## 1 INTRODUCTION

Sag-tension calculations can be described as the backbone of a line design as it directly affects a line’s mechanical, electrical, geometrical, and structural properties. Sag-tension calculations are based on the conductor state change equation which is derived from the parabolic conductor sagging curves. The theoretical background of the derivations can be found in Kiessling et al. [1]. The conductor state change equation takes into account several parameters. These include the modulus of elasticity of the conductor material, the coefficient of linear expansion, the sag or tension, the temperature, and the unit weight of the conductor. The equation is typically used to determine the change in the sag or tension of the conductor due to changes in temperature or other environmental factors. Some commercial software or spreadsheet programs are utilized in industry practice to solve the equation.

Obviously, the mathematical equations that govern sag-tension calculations are highly non-linear and require an iterative approach to solve, which can be computationally burdensome. To address this challenge, ANNs can be introduced as a promising solution technique. The use of ANNs in the engineering discipline is already common. The capableness of ANNs in the engineering field was firstly by Adeli and Yeh in 1989 [2]. ANNs have been used to simplify civil engineering problems for various purposes [3], such as classification, capacity prediction, and optimization.

This study intends to obtain an ANN structure in order to predict the tension values that emerge on the conductors within the predetermined ranges of the mechanical, geometrical, and environmental variables. To this end, variables are determined on the basis of the conductor state change equation. Afterwards, a neural network architecture was formed, trained, and tested successfully.

## 2. PROBLEM DEFINITION

The conductor state change equation is defined in Eq.1, as follows:

$$\frac{a^2 E \rho_n^2 S}{24 T_n^2} - T_n = \frac{a^2 E \rho_1^2 S}{24 T_1^2} - T_1 (t_n - t_1) \beta E S \tag{Eq.1}$$

Where;

T: Horizontal component of the conductor tensile force

E: Modulus of elasticity

S: Cross-sectional area

ρ: Conductor weight per unit length

a: Span length

β: Coefficient of thermal expansion

t: Conductor temperature

The subscripts of 1 and n represent the first (initial) and the n<sup>th</sup> states. Constituting the first state, the maximum working tension (MWT) on the conductor occurs under either maximum wind, maximum ice, wind+ice, or minimum temperature conditions. The variables of the first state, MWT, are known as well as the weather-related variables of the n<sup>th</sup> state, i.e., temperature and weight per unit length. The conductor tension value associated with the n<sup>th</sup> state ( $T_n$ ) is the parameter to be determined in this respect.

This study focuses on only five main conductor types used in Türkiye’s distribution lines, namely, 3 AWG, 1/0 AWG, 3/0 AWG, 266 MCM, and 477 MCM. These conductors are aluminum conductor steel reinforced (ACSR) type which consists of one or more layers of aluminum wires stranded over a high-strength steel core. They are commonly used in transmission lines as they combine the strength and durability of steel with the lightweight of aluminum. The properties of the selected conductors are tabulated in Table 1.

Table 1. Mechanical and geometrical properties of the selected conductors

Property	Unit	3 AWG	1/0 AWG	3/0 AWG	266 MCM	477 MCM
Initial Mod. of elasticity	kg/mm <sup>2</sup>	6500	6500	6500	6200	6200
Final Mod. of elasticity	kg/mm <sup>2</sup>	8000	8000	8000	8000	8000
Ultimate tensile stress (UTS)	kg	1023	1940	3030	5100	8820
Unit weight	kg/m	0.108	0.2159	0.3429	0.545	0.9749
Diameter	mm	7.14	10.11	12.75	16.28	21.8
Coeff. of thermal expansion	1/°C	1.92E-05	1.91E-05	1.91E-05	1.89E-05	1.89E-05
Cross-sectional area	mm <sup>2</sup>	31.14	62.44	99.23	157.2	281.1



In Turkiye’s distribution line design specification EKAT [4], the coefficient of ice, k, and temperature ranges are categorized into five zones, as presented in Table 2. It is worth underlining that ice accumulation on the conductors either does not or negligibly occur in freezing temperatures due to low humidity. EKAT assumes a fixed value of -5°C for the temperature in ice conditions. It should be noted that this study followed the industry practice, which shows that icing occurs at the temperature range of -8°C and 2°C.

Table 2. Climatic conditions

Zone	k	Atmospheric temperature, °C	
		Min.	Max.
1	0	-10	50
2	0.2	-15	45
3	0.3	-25	40
4	0.5	-30	40
5	1.2	-30	40

These k values yield different ice thickness values for each conductor type in each zone. The formula relating the ice weight per unit length (kg/m) with the parameter “k” and the conductor diameter (mm) is defined in Eq.2, as follows:

$$P_b = k * \sqrt{d} \tag{Eq.2}$$

By taking the unit weight of ice as 600 kg/m<sup>3</sup> as per EKAT and making reverse calculations, it is possible to determine the ice thickness values accumulated around the conductors as presented in matrix form in Table 3.

Table 3. Ice thickness values

Zone	0/0 AWS	1/0 AWS	3/0 AWS	266 MCM	477 MCM
1	0.0	0.0	0.0	0.0	0.0
2	13.6	14.0	14.1	14.1	13.9
3	17.4	18.0	18.3	18.5	18.5
4	23.3	24.4	25.1	25.6	25.9
5	37.8	40.2	41.7	43.3	44.7

As for the wind load, EKAT adopts Eq.3 and Eq.4 to consider wind effects on the conductors:

$$P_w = c * q * d * a_w * 10^{-3} \text{ (kgf) when } a_w \leq 200 \text{ m} \tag{Eq.3}$$

$$P_w = c * q * d * (80 + 0.6 * a_w) * 10^{-3} \text{ (kgf) when } a_w > 200 \text{ m} \tag{Eq.4}$$

Where;

$P_w$ : Wind force acting on the conductor

c: Drag coefficient

q: Dynamic wind pressure, kg/m<sup>2</sup>

d: Conductor diameter

$a_w$ : Wind span



Dynamic wind pressure,  $q$ , varies with the conductor height above the ground as shown in Table 4.

Table 4. Dynamic wind pressure values

Height above the ground (m)	$q$ (kg/m <sup>2</sup> )
0-15	44 (95,51 km/h)
15-40	53 (104,83 km/h)
40-100	68 (118,74 km/h)
100-150	86 (133,54 km/h)
150-200	95 (140,35 km/h)

The drag coefficient,  $c$ , depends on the conductor diameter. The coefficient is taken as 1.2 if the diameter is less than 12.5 mm. It is taken as 1.0 if the diameter is bigger than 15.8 mm and 1.1 otherwise.

The limits of the MWT for the conductors vary from 25% to 36% of the UTS, depending on the conductor type and zone. According to EKAT, MWT occurs under one of the following conditions: maximum ice at -5°C or maximum wind at +5°C. It should be noted that in reality, minimum temperature or wind and ice combined cases at different temperatures may become the dominant conditions. In this study, this possibility was taken into account in the preparation of the ANN training database, and MWT conditions were not limited to those specified in EKAT for the sake of proper training.

The variables and their constraints of the problem are depicted in the above paragraphs. This study aims to predict the conductor tension occurring under specific conditions. In this respect, conductor tension constitutes the only output variable, whereas the input variables are threefold, as follows:

- Wind pressure, ice thickness, temperature, and zone as the climatic variables,
- Span length as the line-related variable,
- Modulus of elasticity, unit weight, diameter, and coefficient of thermal expansion as the conductor-related variables.

It is apparent from Eq.1 that the conductor tension is directly proportional to the modulus of elasticity, diameter, the coefficient of thermal expansion and inversely proportional to the unit weight of the conductor. In this regard, the latter item can be confined into a single term derived in this study and called "conductor coefficient" (CC), containing properties of the conductors as defined in Eq.5.

$$CC = \frac{E \cdot \beta \cdot d}{w}$$

Eq.5

The reason behind the derivation of this term was to reduce the number of input variables and to make the proposed ANN more compact. In consequence, less computational demand and less training time were achieved.

### 3. IMPLEMENTATION OF ANN

As a general definition, neural networks are the subcomponent of artificial intelligence and imitate the learning way of the human brain. ANNs consist of layers and neurons which are connected to each other through weights. Training data, which simply is a set of known input-output pairs, is fed into the network so that it can learn the relationship between the input and output variables by changing its weights. This weight adjustment is completed by way of standard error minimization algorithms. Further explanation of the basics of ANNs can be found in Rafiq et al. [5] and Nielsen [6]. Amongst numerous sub-types of ANNs, the feedforward backpropagation type of neural networks (i.e., hereinafter referred to as multilayer perceptron, MLP) was proven to perform well in function approximation, which constitutes a major portion of civil engineering problems.

There are three main processes for the MLP type of networks: training, cross-validation (C-V), and testing. Briefly, training is the weight adjustment process, C-V can be defined as the observation of the network's performance for unseen data during training to avoid overtraining, and testing is the evaluation of the post-training performance of the network.



In this study, an MLP with a single hidden layer was chosen. The sigmoid function was selected as the activation function of the neurons in hidden and output layers. As the error minimization algorithm, Levenberg-Marquardt was selected due to its superiority over others [7,8]. One hidden layer was used in the network as it has been shown that a single hidden layer is adequate as long as a sufficient number of neurons is assigned [5,9]. The architecture of the proposed network is shown in Figure 1.

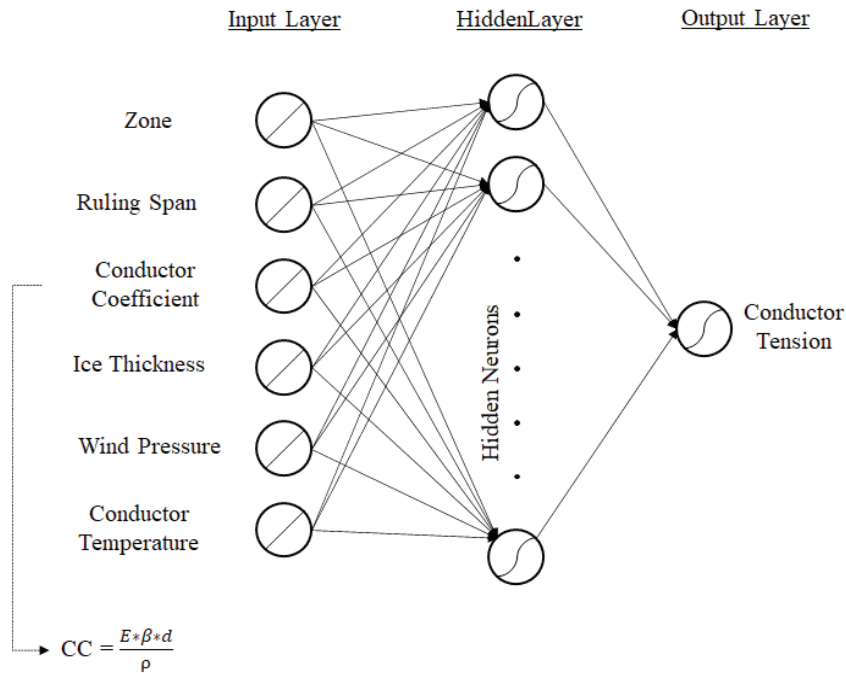


Figure 1. The architecture of the proposed network

Prior to training, the data should be normalized within the sensitive range of the activation function. This is done because networks may suffer from numerical difficulties and slow learning if normalized values are too close to the asymptotes of the sigmoid function [5,10,11]. In this regard, input and output pairs were normalized between 0.2 and 0.8.

The complexity of the network mainly depends on the neuron quantity of the hidden layer, and the best way to determine the optimum number of neurons used in the hidden layer is trial and error [5]. To this end, neural networks with varying hidden neuron quantities (from 5 to 13 in step of 2) were trained in this study.

The sufficiency and distribution of network data are critical for proper learning. According to Carpenter and Hoffman’s [12] rule-of-thumb, which is derived based on a system of equations analogy, the minimum required quantity of training data should be at least 105, considering the network with the highest possible number of hidden neurons used in the proposed architecture. In this study, 5000 uniform-randomly distributed training data were generated, 500 of them reserved for testing, 750 of them for C-V, and 3750 of them for training, fulfilling the minimum required quantity of training data criteria exceedingly.

For statistical and mathematical evaluation of the performance of ANN, mean squared error (MSE) and coefficient of determination (R<sup>2</sup>) values are utilized throughout the study. NeuroSolutions software [13] is used as the neural network software. The number of epochs was set to 1000. Each network with a different number of hidden neurons was executed three times.

#### 4. RESULTS

The proposed ANN architecture was successfully trained, cross-validated, and tested. As shown in Figure 2, the optimum number of hidden neurons was found as 13, for which the minimum MSE values were achieved as 8.71x10<sup>-6</sup> at the 873rd epoch and 9.45x10<sup>-6</sup> at the 773rd epoch for training and C-V sets, respectively, as presented in Table 5. Such low level of error values clearly shows the accuracy of the proposed network.



Table 5. Summary of Best Networks

Best Networks	Training	C-V
Hidden Neurons	13	13
Run #	2	2
Epoch #	873	773
Minimum MSE	8.71052E-06	9.45445E-06
Final MSE	8.71052E-06	9.68942E-06

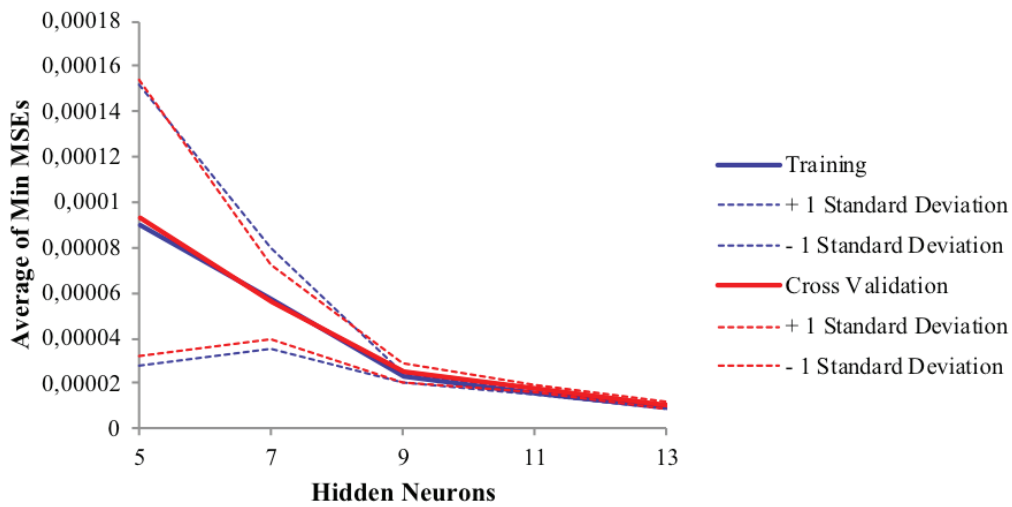


Figure 2. Average of Minimum MSEs with Standard Deviation Boundaries

The testing performance of the network was highly satisfactory since a high correlation was observed between predicted and desired values of the tension values, as shown in Figure 3. The coefficient of determination value was calculated as 0.9972. The test results indicate that the proposed ANN architecture performs well for unseen data as it showed an almost perfect match with the theoretical results.

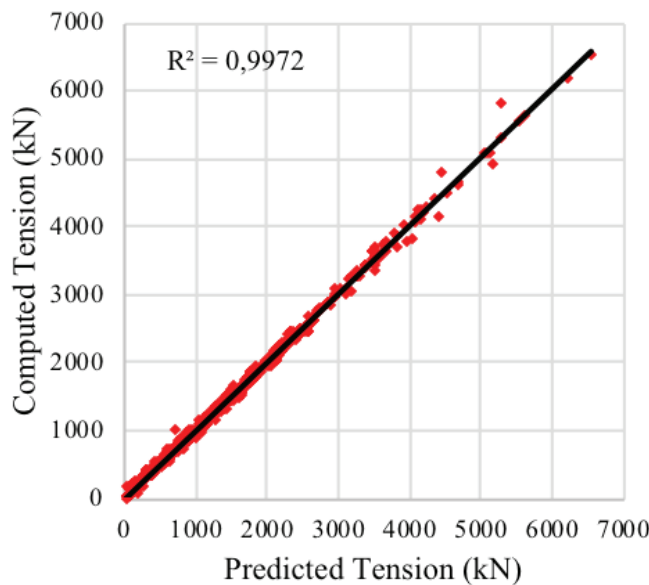


Figure 3. Comparison of predicted tension (ANN) with computed tension for the test data



As shown in Figure 4, a user interface was developed in spreadsheet format so that the engineers can easily use the proposed and successfully trained ANN architecture in conductor tension calculations for the considered conductor types.

### Maksimum İletken Gerilme Yüğü Tahmini

Bu Yapay sinir ağı (YSA) deęitim direklerindeki maksimum iletken gerilme yükünü hesaplar

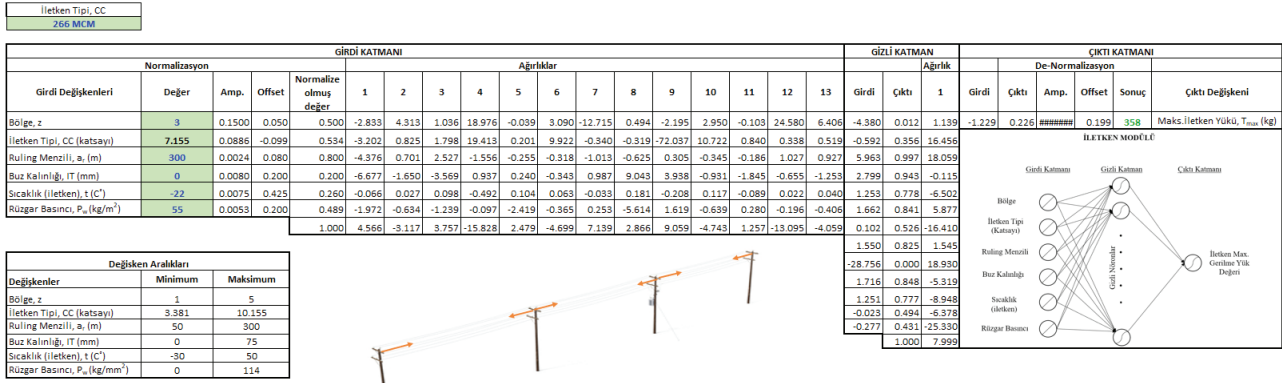


Figure 4. The user interface of the "Conductor Tension Predictor" spreadsheet

## 5. CONCLUSION

Although ANNs have been extensively utilized in the civil engineering field, they have a limited amount of implementations in transmission & distribution line engineering. The authors believe that the industry can benefit from the versatility of ANNs. To this end, this study has been prepared, and it is intended to show that conductor tension calculations can be executed by means of ANNs. The results explicitly demonstrate that the proposed network was able to predict the conductor tensions that emerge on a selected conductor type under a selected climatic condition. As a future improvement, the library of the proposed network can be expanded by introducing more extreme weather conditions and more variety of conductors.

## BIBLIOGRAPHY

- [1] E. Kiessling- P. Nefzger- J.E. Nolasco- U. Kaintzyk, Overhead Power Lines - Planning, Design, Construction, ISBN-13: 978-3-642-05556-0, DOI: 10.1007/978-3-642-97879-1, 539-570.
- [2] Adeli, H. (2001). "Neural Networks in Civil Engineering: 1989-2000." Computer-Aided Civil and Infrastructure Engineering, 16(2), 126-142.
- [3] Flood, I. and Kartam, N. (1994). "Neural Networks in Civil Engineering: Principles and Understanding." Journal of Computing in Civil Engineering (ASCE), 8(2), 131-148.
- [4] Elektrik Kuvvetli Akım Tesisleri Yönetmelięi – EKAT (2010), TY/2010/2, TMMOB Chamber of Electrical Engineers, Türkiye.
- [5] Rafiq, M.Y., Bugmann, G., and Easterbrook, D.J. (2001). "Neural Network Design for Engineering Applications." Computers and Structures, 79(17), 1541- 1552.
- [6] Nielsen, R. H. (1989). "Theory of the Backpropagation Neural Network." Proceedings of the International Joint Conference on Neural Networks- IJCNN, Vol. 1, Washington D.C., 1989, 593 - 605.
- [7] Hagan M.T., and Menhaj, M.B. (1994). "Training Feedforward Networks with the Marquardt Algorithm." IEEE Trans Neural Networks, 5(6), 989-993.
- [8] Yetilmezsoy, K. and Demirel, S. (2008). "Artificial Neural Network (ANN) Approach for Modeling of Pb (II) Adsorption from Aqueous Solution by Antep Pistachio (Pistacia Vera L.) Shells." Journal of Hazardous Materials, 153(3), 1288-1300.
- [9] Hadi, M.N.S. (2003). "Neural Networks Applications in Concrete Structures", Computers and Structures, 81(6), 373-381.
- [10] Chang, C.C., Chang, P.T.Y. and Xu, Y.G. (2000). "Adaptive Neural Networks for Model Updating of Structures." Smart Materials and Structures, 9(1), 59-68.
- [11] Papadrakakis, M., Lagaros, N. D. and Tsompanakis, Y. (1998). "Structural Optimization Using Evolution Strategies and Neural Networks." Computer Methods in Applied Mechanics and Engineering, 156(1), 309-333.
- [12] Carpenter, W.C. and Hoffman, M.E. (1995). "Training backprop neural networks." AI Expert 10(3), March, 30-33.
- [13] NeuroSolutions. NeuroDimension, Inc., Gainesville, Florida, USA.



# Short Circuit Studies with the Presence of Fault Current Limiter Reactor Installed at the Transmission Line Terminals or at the Neutral Point of the Transformer

[Vasheghani.hamed@monencogroup.com](mailto:Vasheghani.hamed@monencogroup.com)

HAMED V. FARAHANI\*, HAMID JAVADI, MASOUD ABDOLHOSSEINPOUR, MAJID ROUSTAEI, FARAMARZ GHELICHI

Monenco

Iran

## SUMMARY

With the rapid increase in the electric energy consumptions along with the design and installation of new power plants, it's needed to develop the capacity of power transmission and distribution network. By adding the new transmission lines and as well as the power plant installation, the equivalent impedance seen from each electrical node or power buses (substation) decrease and its consequent the power capacity and amplitude of Short Circuit Current will be increased considerably, so the electric utility companies should change and upgrade their circuit breakers and as well as the protection system and its required devices. In this situation, also for preserving power network from voltage sag and decreasing torques peak in generators and as well as to increase the network stability, recently the Fault Current Limiter (FCL) can be used. Between the different kind of FCLs, the air core reactors are very common ones which can be simply applied in power networks to hold the short circuit current amplitude in appropriate range. These reactors can be used in two structures that the 1st one installed series with the power transmission lines, and the 2nd one which will be implemented between neutral point of power transformers and ground system. In this paper the short circuit and as well as the power flow studies of two mentioned structures of FCL reactor are presented and the obtained results have been shown and their key parameters are compared too.

## KEYWORDS

Short-Circuit Studies, Power flow, FCL Reactor, Transmission Line, Power Transformer



**Oral Presentation:** Short Circuit Studies with the Presence of Fault Current Limiter Reactor Installed at the Transmission Line Terminals or at the Neutral Point of the Transformer

## 1. INTRODUCTION

Due to the increasing consumption of electric energy, the construction of different power generation resources and consequently the growth and development of existing power transmission lines and distribution grid will be needed. In this regards, the different faults occurrence in power transmission and distribution networks can cause very large short-circuit currents flowing in the power network. In some cases, the short circuit current can increase above the maximum short circuit withstand level of the existing circuit breakers. These circuit breakers may not successfully operate that their mal function cause a great damage to the electrical equipment too. The problems of inadequate CB short-circuit ratings have become more serious than before, because in many substations design, the highest rating of the CB which was available in the market has been selected that can be less than the required value. To face this problem, and also to prevent power system from voltage sag, decreasing torques peak in generators, and increase in network stability, one of the best possible solutions is to use a Fault Current Limiter [1-2].

There are several ways such as static reactors, nonlinear reactors and solid-state limiters for holding short circuit current in appropriate level. In this regard, the implementation of the static reactors are feasible and economic methods and can be used 3 reactors in series with power transmission lines or connecting a reactor between the neutral point of power transformer and the ground system. Applying FCL reactor in series with power transmission lines can cause voltage drop and power loss in normal operation of power system. Since the occurrence of single-phase short-circuit current has the highest probability compared to three-phase short-circuit fault, so the application of FCL reactor used at neutral point of power transformer will be very efficient and economical compared to instead of installing three reactors series with transmission line. In this paper the load flow and short circuit studies of two mentioned FCL structures is presented and the obtained results have been shown and the electric behavior of their key parameters have been compared too.

## 2. PRINCIPLE, REQUIREMENT, AND DIFFERENT KINDS OF FCLS

Considering a single line diagram of a typical electric network shown in Fig.1. If a fault happens at bus 5, the amount of fault current will be restricted by the internal impedance of the network ( $Z_{th}$ ) seen from this bus (Thevenin's Theorem).

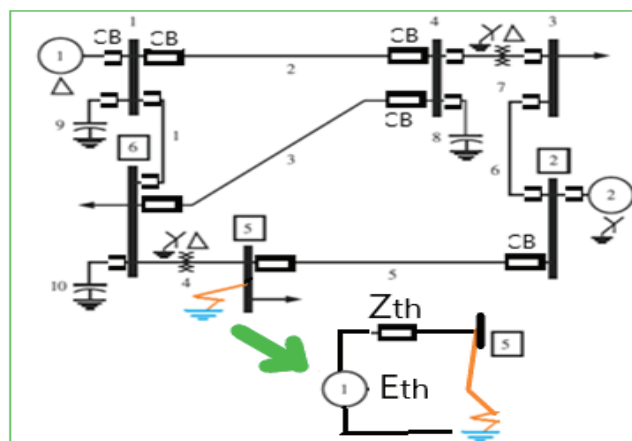


**Figure 1:** Single diagram of a Six buses power network and its Thevenin's equivalent

Depending to the power network, this internal impedance is usually very low, so the magnitude of the fault current will become very high in comparing to its nominal value. During fault condition, the high fault current will affect the protection system, then following it, the operation of the circuit breaker initiates (CB) and the CBs will open the circuit to isolate the fault point. If the fault current amplitude exceeds the breaking capacity of the CB, that CB will not be able to isolate the fault point and the fault condition will be remained in power system and following it, the black-out may be occur. So the application of FCL can be a useful method to decrease the maximum fault current and also to keep the electric power network in safe operation.

Generally, in a power network, the location of FCL must be carefully selected so that the fault current can be restricted within an optimum value. The FCL will limit the fault current and it allows the lower rating CBs be used in the power system. Although, the most kind of FCLs are always connected to power network, but under its normal condition operation the presence of the FCL should not be observed and only at the fault condition, the FCL should response very quickly to limit fault current. So the devices or system which can limit the fault current in the power system are recommended to have the following functional requirements [3],



Oral Presentation: Short Circuit Studies with the Presence of Fault Current Limiter Reactor Installed at the Transmission Line Terminals or at the Neutral Point of the Transformer

- 1) Decreasing the first peak of the fault current as possible,
- 2) Having a low impedance and low energy losses in the normal state,
- 3) No generating harmonics in the normal power system operation,
- 4) Presenting a smooth and gradual change of impedance from the normal mode to fault ones and vice-versa,
- 5) Eliminating sensors and control devices as possible,

Of course, in practice, it's difficult to achieve all the mentioned requirements. The actual characteristics of the FCL should be as close as possible to the ideal requirement. In the recent decades, many approaches for limiting fault currents (FCL) have been introduced as shown in Fig.2, and their brief description can be stated as follows [4-7].

- Usually circuit breakers are expensive and cannot interrupt fault currents until their 1<sup>st</sup> zero current come which will cause the life time limitation too.
- The high impedance transformer with their high losses makes the system inefficient. The fuses have a very low withstand able fault current and it has to be replaced manually.
- The FCL reactor can be classified into two groups (air core and iron core). Air core reactor does not suffer from magnetic saturation and therefore their reactance is independent of current and also they are subjected to voltage drops, power loss during normal operation and minimum installation space.
- The system reconfiguration; using bus-splitting besides adding cost, reduces the system reliability and its operational flexibility.
- Novel concepts based on superconductors (SCFCLs), all kinds of SFCLs, saturated iron-core FCL or SICFCL are noticeable one because of its desirable characteristics such as spontaneous reaction to faults, no need to trigger and no sensitivity to number of faults.

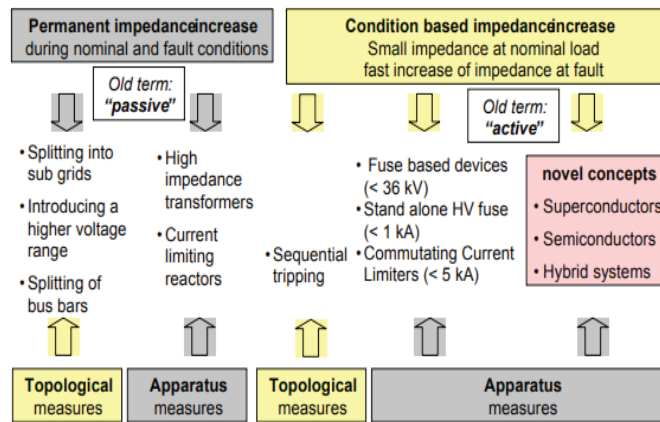


Figure 2: Different kind of Fault Current Limiter Systems

### 3. AIR CORE REACTORS FAULT CURRENT LIMITER

Different kind of short circuit faults in three phases power system can be classified by symmetrical and non-symmetrical faults. Three phases short circuit fault is only the symmetrical fault and the other short circuits (faults) such as single phase to earth, two phases short circuit without or to earth connection and etc. are the non-symmetrical faults. The relative probability of occurrence of various kinds of short circuit faults in overhead and cable power transmission circuits will be respectively 5-8% as the symmetrical fault and 92-95% as non-symmetrical faults which more than 70% of those will be the phase to ground faults [8-10].

Since the occurrence probability of single-phase fault is much more than three-phase fault, and if the responsibility of electrical company has been focused on developing transmission and distribution grid and simultaneously reducing the short circuit current, the use of fault current limiter reactor connected between the neutral point of the power transformers and ground can be a feasible method in comparing to install the FCL reactor in series with three phases of transmission lines [11].

The use of a fault current limiting (or grounding) reactor that connected between the neutral and ground system can proportionally reduce the short circuit current for 95% of the different kind of faults except the three-phases short circuit faults. This Reactor is also



**Oral Presentation:** Short Circuit Studies with the Presence of Fault Current Limiter Reactor Installed at the Transmission Line Terminals or at the Neutral Point of the Transformer

used in order to limit line-to-ground fault current to a value which will not damage the equipment in the power system, yet allow to flow the sufficient fault current to operate protective relays. In normal operation, if the circuit is balanced, current flow through the FCL reactor will be zero, thus, there will be no losses. Additionally, this kind of FCL can reduce single phase short circuit stresses on power transformers which are one of the most widespread type of fault impact in the electrical system. Also a loaded generator may develop a third-harmonic voltage but applying this FCL provides an impedance in the grounding path and can limit the third-harmonic current component [12-13].

## 4. TYPICAL POWER CIRCUIT AND ITS LOAD FLOW STUDY

Suppose an electrical network after several years of its operation and development has a structure in the form of the power network shown in Fig.3.

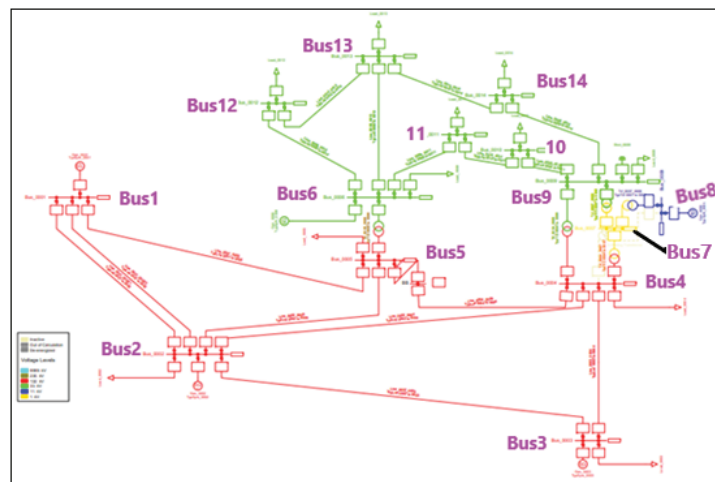


*Figure 3: A typical electric power network for case study*

This network contains 14-buses with 3 voltages level as 132, 33, and 1kV. Data of the transmission lines for this typical power network is given in Table1. In this network at both buses 4 and 5 (high voltage substations), transmission lines and power transformer are connected, so the Bus5 has been chosen to observe the short circuit studies after implementing an equipment to reduce its fault current.

*Table 1: Transmission Line Data of the 14 buses power network*

Line No.	From	To	R(ohm)	X(ohm)	B(mS)
1	Bus 1	Bus 2	6.75	20.62	151.52
2	Bus 1	Bus 2	6.75	20.62	151.52
3	Bus 1	Bus 5	9.41	38.86	286.37
4	Bus 2	Bus 3	8.19	34.5	251.37
5	Bus 2	Bus 4	10.13	30.72	214.65
6	Bus 2	Bus 5	9.92	30.3	195.13
7	Bus 3	Bus 4	11.68	29.8	198.58
8	Bus 4	Bus 5	2.33	7.34	73.46
9	Bus 11	Bus 6	1.034	2.17	0
10	Bus 6	Bus 12	1.34	2.79	0
11	Bus 13	Bus 6	0.72	1.42	0
12	Bus 9	Bus 10	0.35	0.92	0
13	Bus 14	Bus 9	1.38	2.94	0
14	Bus 10	Bus 11	0.89	2.09	0
15	Bus 12	Bus 13	2.41	2.18	0
16	Bus 13	Bus 14	1.86	3.79	0



**Oral Presentation:** Short Circuit Studies with the Presence of Fault Current Limiter Reactor Installed at the Transmission Line Terminals or at the Neutral Point of the Transformer

For this typical power network, to have the optimum size of FCL reactor for achieving the required reduction in short circuit current, this study can be considered as the zero phase of FCLs sizing. In this regard, the application of FCL reactor equal to 0-75% impedance of line No.8 have been considered as the following cases:

**Case1:** Only one reactor connected at neutral point of power transformer,

**Case2:** Three reactors have been applied at the beginning of each phases of the line No.8.

It should be mentioned that in normal network operation of power network, the Case1 has the same electrical behavior in comparing to the original one. For these Cases the load flow calculation has been done by Digsilent Software. The obtained results have been presented in Table 2. In Case2 and due to connected FCL reactor in series with line No.8, the power transfer in 132kV transmission lines will change in comparing to Case1, but the most power transfer changing have been done at the lines No.3, No.6, and No.8 as shown in Table3.

**Table 2:** Load flow results for two structures of FCL reactor

Bus No.	Rated Voltage [kV]	Bus Voltage			
		Basic/ FCL Case1		FCL Case2 at Line No.8	
		Amp [PU]	Deg.[deg]	Amp[PU]	Deg[deg]
1	132	1.06	0	1.06	0.0
2	132	1.04	-4.81	1.04	-5.1
3	132	1.01	-12.45	1.01	-12.84
4	132	1.02	-9.99	1.02	-10.51
5	132	1.02	-8.41	1.02	-8.68
6	33	1.07	-13.85	1.07	-14.21
8	11	1.09	-13.03	1.09	-13.51
9	33	1.06	-14.6	1.06	-15.06
10	33	1.05	-14.75	1.05	-15.20
11	33	1.06	-14.43	1.06	-14.84
12	33	1.06	-14.70	1.06	-15.08
13	33	1.05	-14.79	1.05	-15.17
14	33	1.04	-15.68	1.04	-16.11

**Table 3:** Variation of Power Flow transfer of two FCL structures for Tls connected to bus5

Line No.	Case1: FCL reactor (Neutral)		Case2: FCL reactor (Phases)		DP%
	P[MW]	Q[MVAR]	P[MW]	Q[MVAR]	
3	-69.86	2.20	-71.98	2.24	3%
6	-38.43	-1.45	-39.30	2.17	2.26%
8	64.14	-14.46	58.86	-14.46	-8.3%

It can be noted that the load flow study in Case1 is the same as the basic network and the installing FCL reactor has not any effect on its electrical permanent behavior, but in Case2, the maximum decreasing of power transfer is occurred at transmission line No.8 that can mutually limit the amplitude of FCL reactor impedance. Also, for two mentioned cases the total power losses are calculated by Eq.1.





Oral Presentation: Short Circuit Studies with the Presence of Fault Current Limiter Reactor Installed at the Transmission Line Terminals or at the Neutral Point of the Transformer

$$P_{Losses} = \sum P_{Gens} - \sum P_{Loads} \tag{1}$$

where  $P_{Gens}$ ,  $P_{Loads}$ ,  $P_{Losses}$  are respectively generated power, load power, and power losses

It can be seen that for Case1 the power losses of network don't change but at Case2, the total power losses are gradually increased in comparing to power losses at normal state of network as shown in Fig4.

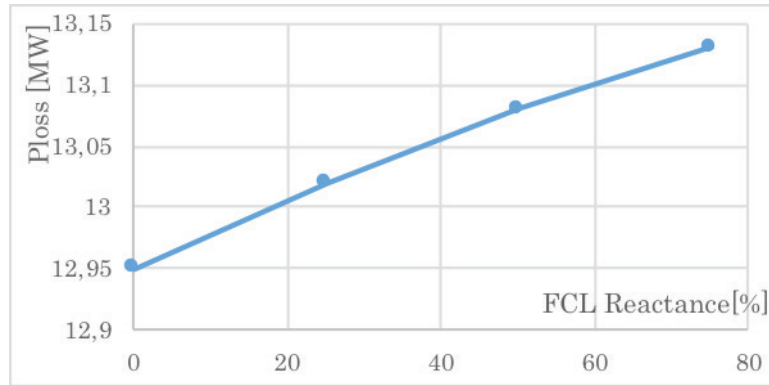


Figure 4: Network power losses as a function of reactance of FCL reactor in Case2

## 5. SHORT CIRCUIT STUDIES

### 5.1. Short circuit results of typical network without FCLs

The single and three phases short circuit fault calculation have been done by Digsilent software and its obtain results are presented in Table4.

Table 4: Short circuit results of the Basic power network

Bus No.	Rated Voltage [kV]	I <sub>sc</sub> -3ph [kA]	I <sub>sc</sub> -1ph [kA]	Bus No.	Rated Voltage [kV]	I <sub>sc</sub> -3ph [kA]	I <sub>sc</sub> -1ph [kA]
1	132	12.78	15.25	8	11	44.29	66.43
2	132	9.19	10.78	9	33	12.29	18.43
3	132	5.22	6.01	10	33	9.57	11.97
4	132	6.25	9.37	11	33	8.80	9.71
5	132	6.30	9.44	12	33	7.10	7.37
6	33	17.51	19.29	13	33	9.87	10.5
7	1	485.49	728.23	14	33	6.59	7.28

As mentioned above, the Bus No.5 of this typical network is the selected bus to study its short circuit current reduction. For this purpose, the application of the air core reactor has been recommended as the fault current limiter. As mentioned, two structures were introduced to limit the fault current. The first structure will only influence on the single phase fault, but the second one will influence on both the single and three phases short circuit faults.

### 5.2. Short circuit results of typical network with FCL reactor

In this regards, an air core reactor will be used to limit the fault current in bus5 of this typical power network. It is evident the size of reactor is very important factor in decreasing of the fault current, so the impedance of the series reactor can be selected as a certain part of transmission line impedance which has most contribution on fault current at Bus5. From short circuit results it is significant that the line connected between buses Bus5 and Bus4 has the maximum sharing current on the different faults at Bus5.



**Oral Presentation:** Short Circuit Studies with the Presence of Fault Current Limiter Reactor Installed at the Transmission Line Terminals or at the Neutral Point of the Transformer

In this study the impedance of series reactor (FCL) is considered as 0 to 50% of transmission line impedance (Bus4-Bus5) to do sensitivity analysis. Tables5 presents only the single phase fault current during implementation of the fault current limiter reactor (FCLR) at neutral point of power transformer. This FCL structure can efficiently decrease the 1ph short circuit current at bus 5. In maximum value of FCL reactor, 14.72% reduction of fault current is achieved as shown in Fig.5.

**Table 5:** Short circuit results of typical power network using FCL reactor at neutral point

1ph to ground fault at Bus 5		
ZFCL	Isc-Total (at Bus5)	
%	kA	Dec. [%]
0	9.44	0.000
2.5	9.25	2.013
5	9.09	3.708
7.5	8.96	5.085
10	8.86	6.144
12.5	8.77	7.097
15	8.69	7.945
17.5	8.62	8.686
20	8.57	9.216
22.5	8.51	9.852
25	8.47	10.275
50	8.05	14.72

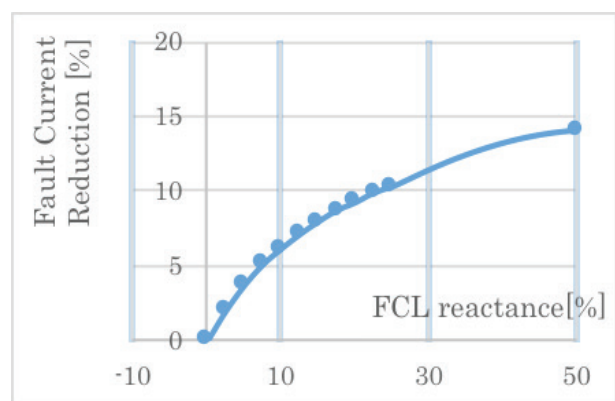
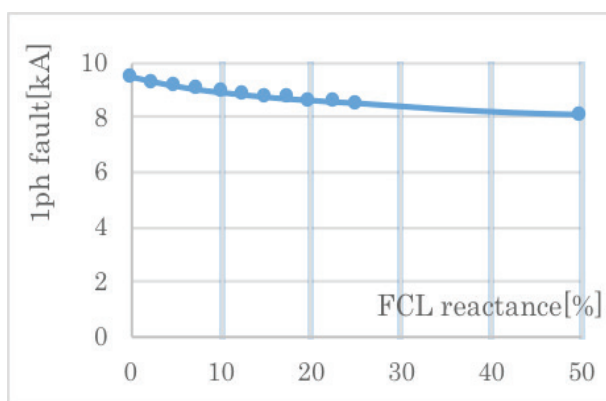


**Figure 5:** Influence of FCL reactor (Case1) on single phase short circuit current

But, when the FCL reactor connected series with power transmission line, it can also influence on 1ph and also 3ph short circuit faults. So for this FCL structure the fault results are presented in Table6. It can be seen for the same value of FCL reactor, the reduction of fault current for 3ph and 1ph fault current are very close and those are respectively 5.7% and 5.6% for maximum ZFCL reactance equal to 50%. As it can be seen from Table6, the FCL reactor installed series with transmission line has also lower reduction effect on single phase fault current in spite of this type of fault has a very high probability occurrence in comparing to 3phs faults.



Oral Presentation: Short Circuit Studies with the Presence of Fault Current Limiter Reactor Installed at the Transmission Line Terminals or at the Neutral Point of the Transformer

Table 6: Short circuit results of typical power network using reactor series with transmission line No.8

ZFCL	3phs Fault at Bus 5		1ph Fault at Bus 5	
	Isc-Total		Isc-Total	
	%	kA	Dec. %	kA
0	6.3	0.000	9.44	0
2.5	6.28	0.317	9.42	0.21
5	6.27	0.476	9.4	0.42
7.5	6.25	0.794	9.38	0.64
10	6.24	0.952	9.36	0.85
12.5	6.23	1.111	9.34	1.06
15	6.21	1.429	9.32	1.27
17.5	6.2	1.587	9.3	1.48
20	6.19	1.746	9.28	1.69
22.5	6.17	2.063	9.26	1.91
25	6.16	2.222	9.24	2.12
50	5.94	5.7	8.91	5.6

On the other hand, Fig.6 shows the comparison of fault current reduction as a function of FCL reactor impedance for two FCL reactor structures (Case1 and Case2). As we can see for the case of using of FCL reactor connected at neutral point of power transformer, the reduction rate of fault current is higher than the using of FCL reactor in series with power transmission lines. In point of view of the 1ph fault current limiting, the effect of the Case1 will be triple.

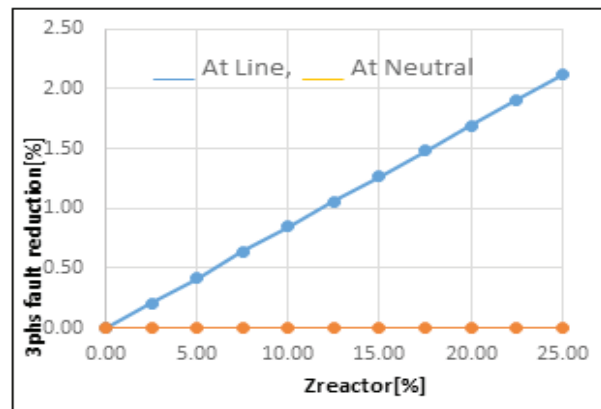
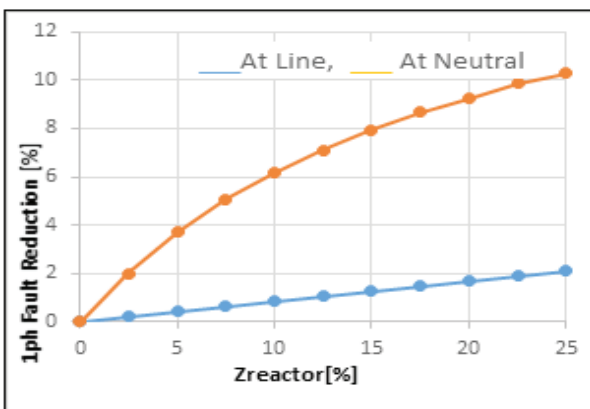


Figure 6: 1ph and 3phs Faults Current Reduction as a function of FCL impedance

In this typical network with the given structure and rating power, if the fault current limiting reactor is selected with an impedance of 25% of line No.8, the fault current reduction in Case1 will be 4.5 times of Case2. It can be the optimum value of the reactance of FCL reactor. However, as mentioned above, the using of the neutral FCL reactor has more effect on single phase fault current but it has not any effect on 3phs fault one and it may often be ignored due to the rare occurrence of three phases fault in power system. A general comparison of these FCL structures is presented in Table7.



Oral Presentation: Short Circuit Studies with the Presence of Fault Current Limiter Reactor Installed at the Transmission Line Terminals or at the Neutral Point of the Transformer

Table 7: Comparison of two applied structures of the air core reactor FCL

Item	Connected at neutral point of Power transformer	Connected at the terminals of Transmission Lines
Weight	Less weight	Heavy weight
Size and space	Less	High
Cost	Less cost due to use only one FCL reactor	As the three FCL reactors are required, it has high cost
Loss	During normal operation has not loss	Since, these FCLs are connected series with phases, they have losses
Topology	Simple	Complex
Implementation status	In recent decade, FCL based on Reactor is significantly installed	

### 5.3. Influence of the FCL Reactor on fault current of the neighbor buses

For this typical network, when the Bus5 is selected as the bus installation of two structures of FCL reactor, the Bus1, Bus2, Bus4, and Bus6 will be the neighbor buses of Bus5. The Influence of using the FCL reactor connected between the neutral point of power transformer and the ground on their single phase fault current is presented in Table8. It shows that this influence is very low and by increasing FCL reactance the decreasing of fault current will gradually increase. It has no effect on 1ph fault of bus 6 due to delta-star power transformer connected between the bus6 and the bus5.

Table 8: Reduction of single phase fault current due to FCL Reactor connected to neutral point

Reactor Size	Isc-(1ph fault at Bus1)		Isc-1ph fault at Bus4		Isc-1ph fault at Bus6	
	Total (at Bus)		Total (at Bus)		Total (at Bus)	
%	kA	Dec. %	kA	Dec. %	kA	Dec. %
0	15.250	0.000	9.370	0.000	19.290	0.000
2.5	15.240	0.066	9.370	0.000	19.290	0.000
5	15.240	0.066	9.364	0.064	19.290	0.000
7.5	15.240	0.066	9.361	0.109	19.290	0.000
10	15.210	0.262	9.350	0.213	19.290	0.000
50	15.19	0.395	8.96	4.37	19.26	0.15

The influence of the FCL reactor connected in series with power transmission line (Bus5-Bus4) on three and single phase fault currents are presented respectively in Table9 and Table10. It can be seen that, the fault current limiting at bus4 has very low influence on its neighbor buses and this weak influence is depended on the sharing current infeed to fault point and its reduction for maximum sharing current which incoming from Bus4, will be noticeable.



Oral Presentation: Short Circuit Studies with the Presence of Fault Current Limiter Reactor Installed at the Transmission Line Terminals or at the Neutral Point of the Transformer

Table 9: Reduction of 3phs fault current due to FCL reactors connected series with line (B5-B4)

Reactor Size	Isc-3ph fault at Bus1		Isc-3ph fault at Bus4		Isc-3ph fault at Bus6	
	Total (at Bus)		Total (at Bus)		Total (at Bus)	
	%	kA	Dec. %	kA	Dec. %	kA
0	12.780	0.000	6.250	0.000	17.510	0.000
2.5	12.780	0.000	6.230	0.320	17.510	0.000
5	12.770	0.078	6.220	0.480	17.505	0.045
7.5	12.770	0.078	6.200	0.800	17.495	0.080
10	12.770	0.078	6.110	2.240	17.490	0.114
50	12.76	0.156	5.87	6.08	17.45	0.342

Table 10: Reduction of 1ph fault current due to FCL reactors connected series with line (B5-B4)

Reactor Size	1ph fault at Bus1		1ph fault at Bus4		1ph fault at Bus6	
	Total (at Bus)		Total (at Bus)		Total (at Bus)	
	%	kA	Dec. %	kA	Dec. %	kA
0	15.250	0.000	9.350	0.000	19.290	0.000
2.5	15.245	0.033	9.350	0.000	19.290	0.000
5	15.240	0.065	9.330	0.214	19.288	0.017
7.5	15.23	0.130	9.310	0.428	19.285	0.031
10	15.225	0.164	9.160	2.032	19.280	0.052
50	15.214	0.675	8.80	5.883	19.25	0.430

## 6. CONCLUSION

In this paper, the fault current limiters used in power network are investigated and concentrated on the air core reactor which could be implemented as two following structures:

- 1- Connected between the neutral point of power transformer and the ground (Case1)
- 2- Connected on series with the power transmission line close to H.V. substation (Case2)

The load flow and short circuit studies of two different FCL structures have been simulated by Digsilent software and the obtained results have been compared. In this regard, the following items have been concluded:

- In steady state condition of power system operation, using the Case2 causes more power losses of grid and will need to achieve the new operation mode of power network.
- The Case2 (with three FCL reactors) needs higher space installation and it will be more expensive in comparing to the Case1
- One FCL reactor connected between the ground and the neutral point of star connection of power transformer reduces fault current three times more in comparing of using the same reactor at each transmission line phases.
- For this typical network, the optimum impedance of FCL reactor is equal to 25% impedance of line No.8 has respectively given the 10.3% and 2.5% reduction of 1ph fault current amplitude for Case1 and Case2 structures and the rate of current reduction of the Case1 is more than 3 times of Case2.



**Oral Presentation:** Short Circuit Studies with the Presence of Fault Current Limiter Reactor Installed at the Transmission Line Terminals or at the Neutral Point of the Transformer

- Reactor connected between the neutral point and the ground has no effect on three phase fault current as well as on electrical parameters at normal operation of power network.
- Reactor connected series with transmission lines can decrease single and three phases fault current but the rate of currents reduction is soft, so for having the same reduction as the single phase fault current, the size and number of FCL reactors should be tripled at least.
- The Case2 has more influence on the decreasing of the sharing current infeed to the faulted bus.

## 7. BIBLIOGRAPHY

- [1] CIGRE, "Fault current limiters – application, principles and experience", WG A3.16, 2005
- [2] S. Eckroad, EPRI Project Manager "Survey of Fault Current Limiter (FCL) Technologies–Update" August 2008
- [3] S. C. Mukhopadhyay, "A Lecture on Current Limiter", Massey University, Palmerston North, New Zealand, 2014
- [4] Mohamadreza Arab Baferani, et al. "Method to Design Saturated Iron-core Fault Current Limiters", IET Generation, Transmission & Distribution, 2019, Vol. 13
- [5] Min Jee Kim, Gyeong-Ho Lee, Seung-Hyun Bang, Hae Yong Park, "The Application of Fault Current Limiter at Icheon Substation in Korea", 1st International Conference on Electric Power Equipment - Switching Technology (ICEPE-ST), 2011.
- [6] Md Shafiqul Alam, Mohammad Ali Yousef Abido, and Ibrahim El-Amin, "Fault Current Limiters in Power Systems: A Comprehensive Review", energies, 2018
- [7] Kadir Ahmed Dafedar et al. "A Novel 110kV Fault Current Limiter for Improving the Reliability of a Substation", IJSRST, Volume 1, Issue 4, 2015
- [8] WAI-KAI CHEN, "The Electrical Engineering Handbook", Elsevier Academic Press, 2004
- [9] Nirupama s. "Faults in Power System: Statistics and Kinds | Electrical Engineering"
- [10] H. JAVADI, "Fault Current Limiter Using a Series Impedance Combined with Bus Sectionalizing Circuit Breaker", Electrical Power and Energy Systems, Elsevier, 2011
- [11] P. Montaser, et al. "Interim Studies Report (Conceptual Study for Adding Fault Current Limiter (FCL) in the 132kV System)", Monenco Consulting Engineers, October, 2022
- [12] Science Direct Topics, "Current Limiting Reactors - an overview", 2022
- [13] Hillkar, "Air Core Neutral Grounding Reactors", 2022





# Impacts of Variable Renewable Energy on new Wholesale Market in Georgia

[giorgi.khorbaladze@gse.com.ge](mailto:giorgi.khorbaladze@gse.com.ge) / [zviad.gachechiladze@gse.com.ge](mailto:zviad.gachechiladze@gse.com.ge)

**GIORGI KHORBALADZE, ZVIAD GACHECHILADZE**

*Georgian State Electrosystem*

**Georgia**

## SUMMARY

The Government of Georgia has been reforming the country's electricity market since 2019, after new law on energy and water supply came into force. The law sets a general legal framework for implementation of the European union directives and regulations. Currently, the market operates in simulation mode, but in 2023, three market segment will become operational:

- ✓ Bilateral contract market;
- ✓ Day ahead/Intraday market;
- ✓ Balancing and ancillary services market;

Variable renewable energy (VRE) has been growing in the past years around the world. Many countries included VRE in their national energy plan to meet the environmental and economic challenges of the future. In this regard, Georgia is not an exception, in recent years, interest in the construction of wind and solar power plants has increased. In 2025-year, ten-year network development plan (TYNDP) of Georgia gives us information about the plans to build the power plants (PPs), according to which in 2025-year, 394 MW wind and 91 MW solar capacity will be added to power system. Apart from, Georgian transmission system operator (GSE) and European consultant's consortium DlgSILENT-DMCC-R2B, examined the possibilities of integration of VREs into the power system. The results of the study are the following:

- ✓ By 2025, it is possible to integrate 500 MW wind and 250 MW solar power plants in the power system;
- ✓ By 2030, above-mentioned values for wind and solar energy reaches respectively - 1330 MW and 520 MW (100% potential utilization);

While renewables offer significant benefits in many respects, there are also growing concerns about their direct and indirect negative effects on market. Solar generation may be correlated with country's consumption and used to smoothen daytime peak hours. But, during the days of cloud movement, generation will change immoderately, that will create necessity for additional fast reserves in the system.

Unlike solar power plants, wind energy is not usually correlated with power consumption. During peak consumption, wind may stop and/or commence during off-peak. However, effective factor for wind generation is that generation occurs generally during periods when hydro generation deficit occurs and that the generation is well distributed over the year. Therefore, in case wind energy volatility is balanced on an hourly and shorter timeframe, wind energy generation might have positive effect on generation adequacy and annual energy balance of Georgia.

## KEYWORDS

Georgian power system, Balancing service provider (BSP), Balancing market, Market modelling, Electricity market reform.



Oral Presentation: Impacts of Variable Renewable Energy on new Wholesale Market in Georgia

This paper mainly focuses on the balancing market, which is used to activate balancing energy. Specifically, it uses PLEXOS models to analyse the effects of VREs on the Georgian Balancing Market. Moreover, Georgia relies on domestic resources to deal with volatilities in the system. In this respect, Georgian experience can provide insights for policymakers and regulators in other developing economies to understand the impact of VREs on electricity markets.

A review of studies assessing future impacts of VRE on Georgian electricity markets demonstrate that higher penetrations of VRE will tend to:

- ✓ Flexibility, and reserves;
- ✓ Reduce wholesale electricity prices and potentially increase balancing service prices;
- ✓ Reduce average capacity factors of dispatchable thermal generating units;
- ✓ Decrease the revenue and operating profits of less-flexible thermal power plants; and
- ✓ Reward flexible (both existing and new generating units) power plants over less-flexible and high-capital cost units.

## 1. INTRODUCTION

Renewable energy sources, have become popular in recent years due to their lower environmental impact and decreasing costs. As the world continues to shift towards more sustainable energy options, the integration of renewable energy into the electricity market has significant results. Developing renewable energy sector have important role in Georgia's commitments against climate changes. With the high penetration of renewable energy, the cost of renewable energy has dropped. In the electricity market condition, generators with low marginal cost are dominant during the bidding process.

Renewable energy integration can also have an impact on the reliability of the grid. Unlike fossil fuel-based energy production, renewables are dependent on weather, which can be unforeseeable. To ensure the reliability of the grid, energy storage technologies can be used to store excess energy when it is generated and release it when it is needed.

In order to maintain system stability transmission system operator (TSO) is obliged to maintain the balance between demand and supply. TSO procures balancing services. This paper assesses the integration of VRE in the Georgian electricity market. The purpose of market implementation is to improve reliability. The balancing & ancillary services market is a guarantee of an efficient performance of the power system, as well as an opportunity of network development and integration of VRE.

This paper mainly uses PLEXOS models to analyse the effects of VREs on the Georgian market in 2025 year. Moreover, Georgia relies on domestic resources to deal with volatilities in the system. In this respect, Georgian experience can provide insights for policymakers and regulators in other developing economies to understand the impact of VREs on electricity markets.

## 2. MODELLING TOOL - PLEXOS

The impact of renewables integration to the Georgian power system is analysed based on a PLEXOS model. This software is used for market modelling worldwide. It can optimize the power system from long-term (1-40 years) to medium-term (1-5 years) to short-term (less than 1 year). Modelling is performed using deterministic linear programming techniques. Software algorithm aims to minimize an objective function subject to the expected cost of electricity dispatch subject to a number of constraints including availability and operational characteristics of power plants (PPs), fuel costs and transmission constraints. The advantage of linear programming is its ability to efficiently determine the optimal solution to a problem that might have a large number of decision variables.

In this analysis we are primarily concerned with short-term modelling (2025 year is modelling year). PLEXOS models every trading period and maintains chronological consistency across the full optimization horizon.

This is crucial to accurately model technical/economical parameters for generators. The involvement of these constraints introduces integer decision variables. In the software, wind and solar PPs are created as „free“ generation, because they have no marginal costs. These resources are considered non-dispatchable and cause challenges for the Georgian power system operation and modelling.

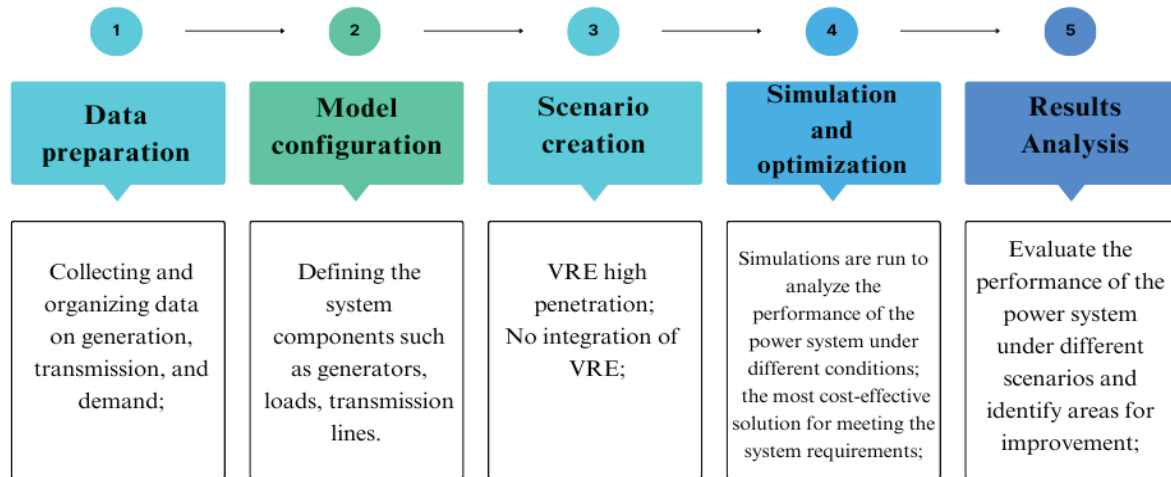


### 3. METHODOLOGY

#### 3.1. Modeling Approach

To make this analysis the Georgian power system is modelled in PLEXOS. The TYNDP includes a list of PPs that will be integrated into the power system in 2025. Among them, a large integration of VRE is being implemented. So, in the software, the current and the candidate PPs are created take into consideration their technical and economical parameters.

Modelling consists of several stages, shown in picture 1:



Picture 1: Modelling stages

#### 3.2. Data Preparation

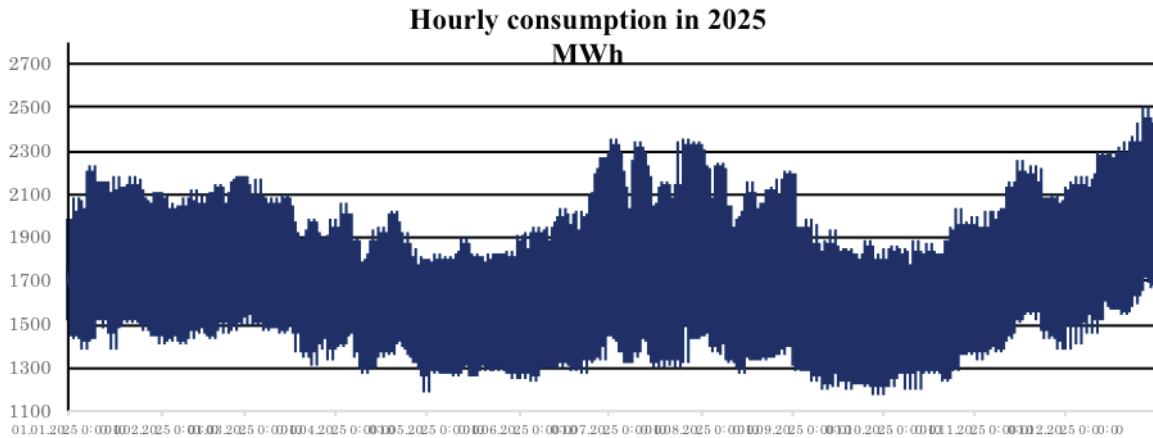
##### 3.2.1. Electricity Consumption

There are several methods used for electricity forecasting, including statistical models, machine learning techniques, and time series analysis. Recently, machine learning techniques are increasingly being used for electricity forecasting due to their ability to handle complex data sets and nonlinear relationships between variables. These techniques include artificial neural networks, support vector machines, decision trees, and random forests.

For the PLEXOS modelling purposes, there is created a neural network model for predicting Georgian power system monthly electricity load consumption using Python, following these steps:

1. Collect and pre-process the data: Collect the historical data of hourly electricity load consumption for 15 years. Pre-process the data by cleaning, normalizing, and splitting it into training sets.
2. Neural network model creation: You can use Python’s deep learning framework to build the neural network model. The model should have an input layer and an output layer.
3. Train the model: Train the neural network model using the training set. You can use various optimization algorithms, such as Adam or stochastic gradient descent, to minimize the loss function and improve the accuracy of the model.
4. Evaluate the model: Evaluate the model’s performance using the testing set. You can use metrics such as mean absolute error (MAE), mean squared error (MSE), and root mean squared error (RMSE) to evaluate the model’s accuracy.
5. Make predictions: Once the model is trained and evaluated, you can use it to make predictions on new data.

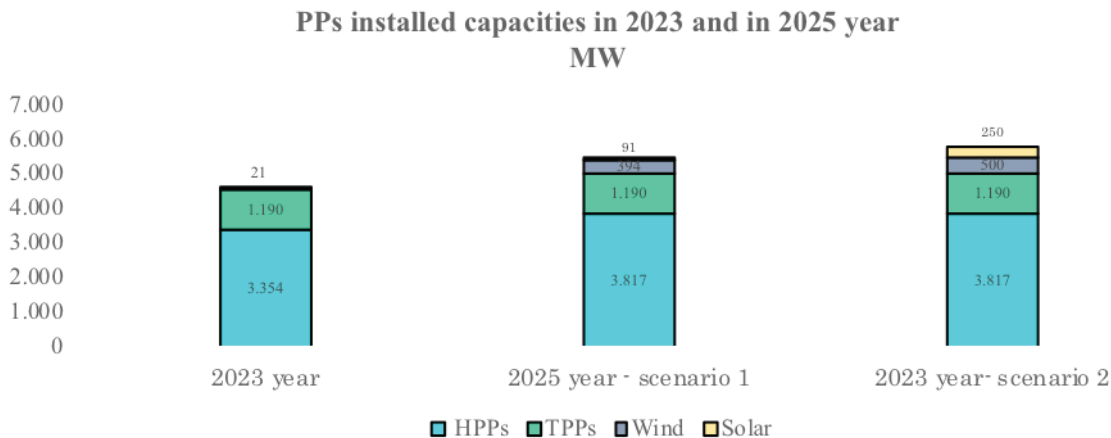
Taking into account the mentioned 5 steps, based on the monthly consumption, hourly consumption pattern of 2025 was created (take into consideration typical hourly shape of daily consumption), which looks as follows:



Picture 2: Predicted hourly consumption of 2025

### 3.2.2. Current and Candidate Power Plants & Their Technical/Economical Parameters

At present, total installed capacity of PPs operated in Georgia is up to 4 564 MW. From this, 2 381 MW is generated by the so called “regulated” HPPs (with water storage), 973 MW by run-of-river HPPs, 110 MW by Gas Turbines, 21 MW Wind farms and 1 079 MW by thermal power plants and combined-cycle gas turbines.



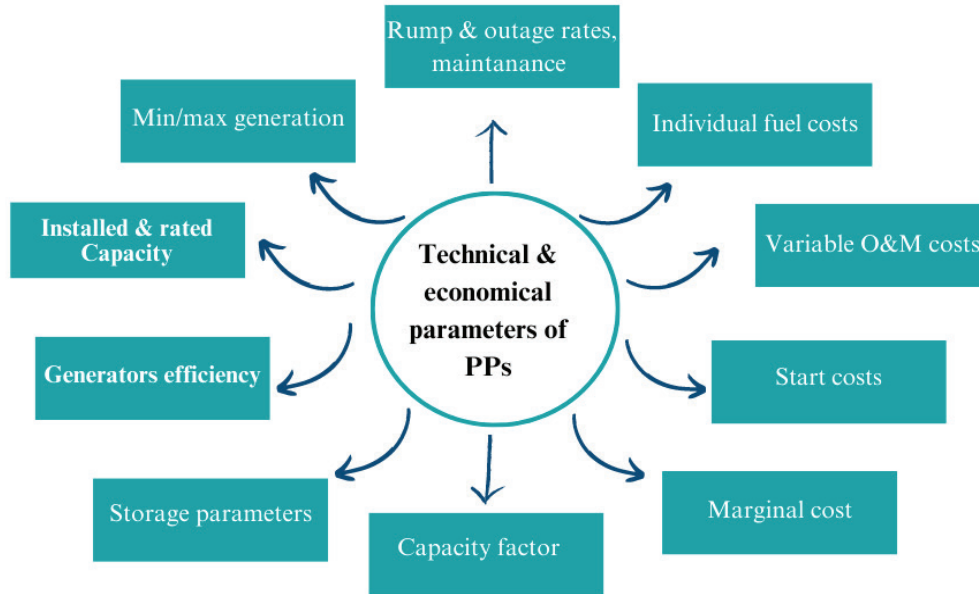
Picture 3: PPs installed capacities in 2023 and in 2025 year

In the 10 years network development plan, for the year 2025 following things are considered:

- ✓ total hydro capacity is 3 817 MW;
- ✓ thermal stays the same as it is now;
- ✓ As for the wind and solar capacity, it increases to 395 and 91 MW respectively (see scenario 1 in picture 3).

Apart from, GSE, with the support of European consultant’s consortium DlgSILENT-DMCC-R2B, examined the possibilities of integration of VREs into the power system. The results of the study are the following: by 2025, it is possible to integrate 500 MW wind and 250 MW solar power plants in the power system, Hence, for 2025-year, 500 MW and 250 MW is added in the PLEXOS model (see scenario 2 in picture 3).

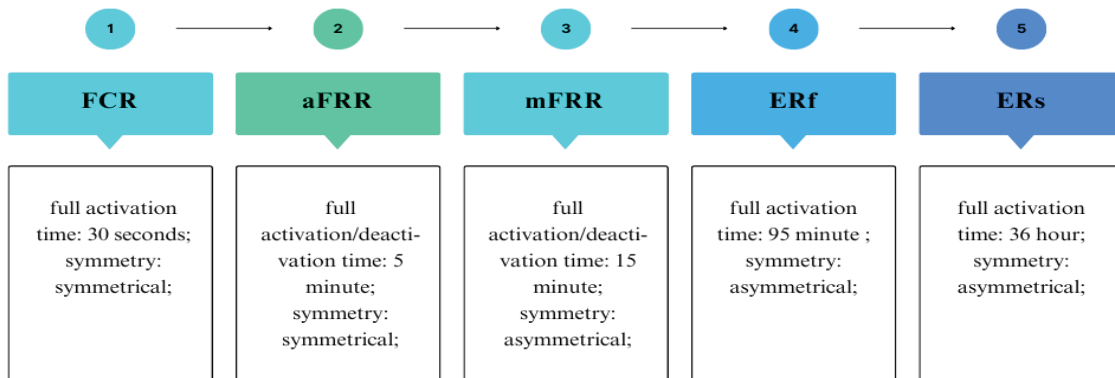
Below, in the picture 4, there is described all important technical and economical parameters for candidate and current PPs located in Georgian power system.



Picture 4: Technical & economical parameters for all PPs in PLEXOS

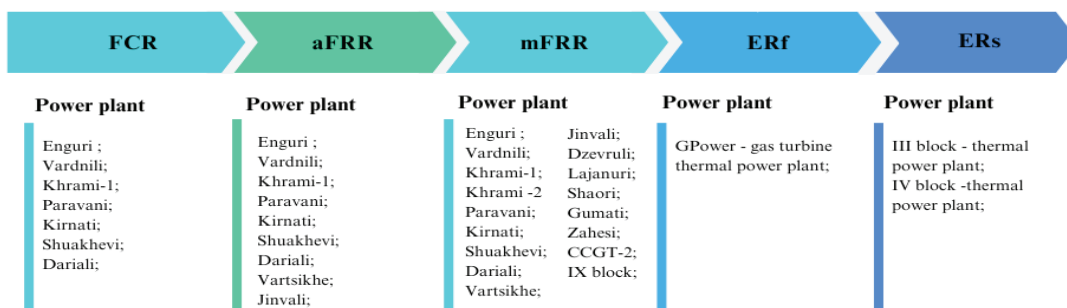
### 3.2.3. Balancing Products

The Electricity Balancing Guideline (EBGL) provides products may be used by the TSO to ensure system reliability. Georgia does not have an obligation to develop standard products provided in the EBGL. However, from market go-live the products will follow the logic of the ENTSO-E standard products due to future compliance requirements.



Picture 5: Georgian balancing products

In the PLEXOS, 5 products are created and assign to the relevant power plant, who has automatic qualification by TSO. Apart from, some power plant has potential in the future to provide several products and this is also considered in the program.



Picture 6: Balancing service provider power plants



### 3.2.4. Reserved capacity determination for the PLEXOS model

TSO will conduct an exercise to determine the yearly reserve requirements for the FCR and FRR product on a weekly basis. This exercise will have following output:

Table 1: Product monthly volumes

	jan	feb	mar	apr	may	jun	jul	aug	sep	oct	nov	dec
MW												
<b>FCR</b>	60	60	60	55	55	55	50	50	55	60	60	60
<b>FRR up</b>	300	300	250	250	250	250	250	250	250	260	270	300
<b>FRR down</b>	280	280	230	200	180	180	180	180	180	230	230	280

The value “Gmax” (largest generator) will provide the primary input for FRR up reserve. During winter, Gmax will be equal to the largest generator (Thermal IX block – 300 MW).

The value “Cmax” (largest consumption center) will be used as primary input for FRR down reserve. The Cmax depends on the size of the largest consumption node.

## 4. RESULTS

In the 4<sup>th</sup> chapter, the results are discussed in two main scenarios. The first scenario is based on a TYNDP and the integration of candidate PPs (hydro, wind, solar) into the system is considered exactly as given in the TYNDP. In the second scenario, hydro, thermal power stays the same as it is provided in the first scenario, but wind and solar are integrated with high power (take into consideration the research made by GSE with the support of European consultant’s consortium DiGSILENT-DMCC-R2B).

### 4.1. System Adequacy

Generation adequacy is a measure of the ability of an electricity system to meet the demand for electricity with an acceptable level of reliability. In PLEXOS, Medium and short-term modules were used. The following issues were calculated: hydro-thermal coordination, weekly/daily/hourly system dispatching, reserves, scheduled and Emergency maintenance, technical limitations consideration (fuel limit, minimum load capacity, power increase and decrease rates, etc.). Indicators of system adequacy in the above scenarios are satisfactory.

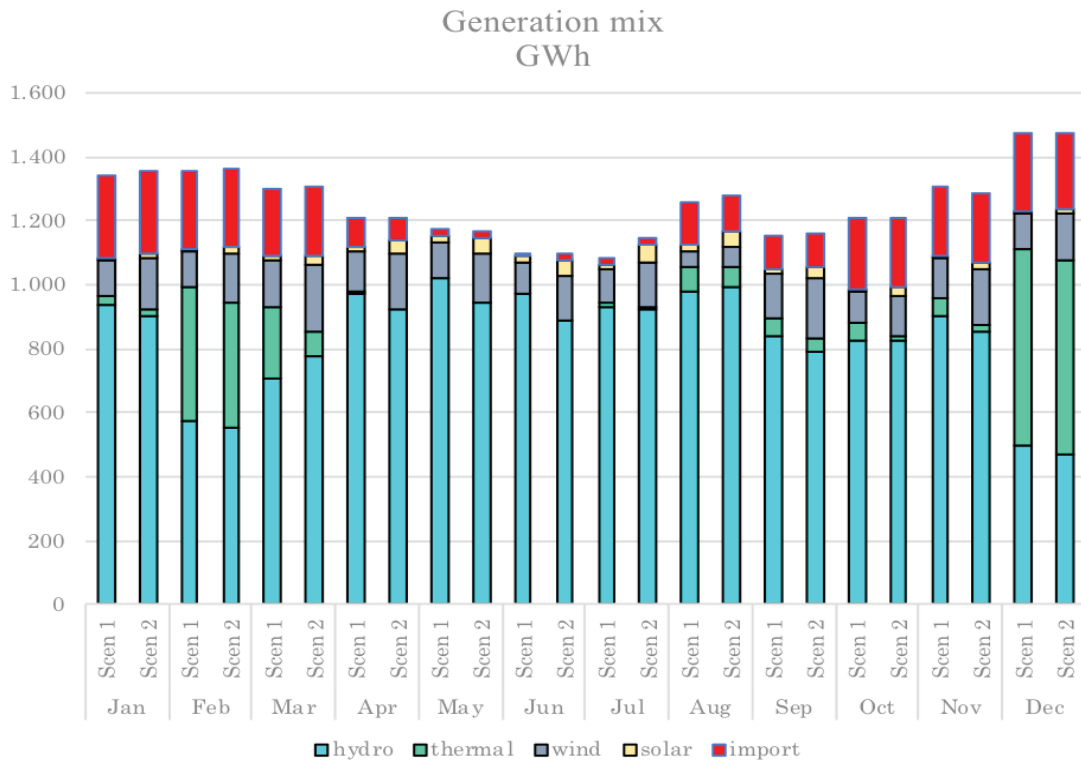
First of all, let’s start analyzing of two different scenarios and their generation mix. Table 2 describes what is generated by each source of PPs for all seasons in 2025.

Table 2: Generation mix by each season

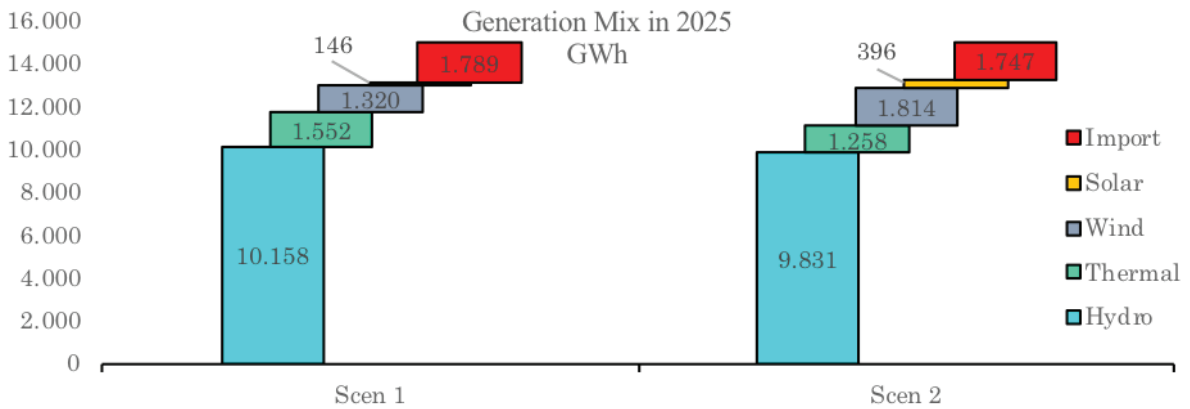
Generation mix										
GWh										
Source	Winter		Spring		Summer		Autumn		Sum	
	Scen 1	Scen 2	Scen 1	Scen 2	Scen 1	Scen 2	Scen 1	Scen 2	Scen 1	Scen 2
<b>Hydro</b>	2015,2	1921,5	2700,2	2639,7	2882,8	2802,3	2560,3	2467,5	10158,4	9830,9
<b>Thermal</b>	1059,5	1029,6	223,0	79,0	89,4	67,1	179,8	82,5	1551,8	1258,3
<b>Wind</b>	329,3	452,8	387,5	534,5	248,5	343,9	355,2	482,6	1320,5	1813,8
<b>Solar</b>	18,6	50,6	42,4	115,0	55,9	151,7	29,0	78,6	145,9	395,9
<b>Import</b>	751,6	735,5	328,7	315,6	164,6	157,2	544,4	538,3	1789,3	1746,7

It can be identified, that hydro generation plays the most important role during the year in both scenarios. In winter period, when water availability decreases to hydro PPs, thermal generation and imported electricity increases to cover electricity consumption. In summer period it is vice versa. For solar and wind generation, logically it increases in summer. For more details, picture 7 focuses on the monthly values of power generation by different sources, including imported energy.



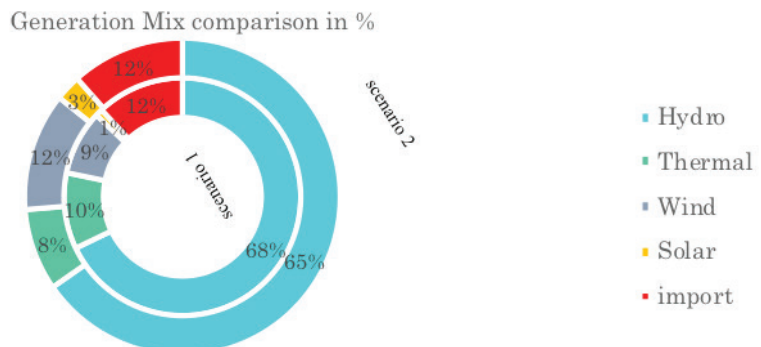


Picture 7: Generation mix of different scenarios by each month



Picture 8: Generation mix of different scenarios in 2025 year

Picture 8 focuses on the total yearly generation in GWh by each technology. As for the picture 9, it gives us % indications.



Picture 9: Generation mix comparison of PLEXOS two scenarios



It can be investigated that in both scenarios hydro sources plays dominant role in the market. In the first scenario hydro generates 68% from the total yearly generation. As for the second scenario, hydro generates 3% less (65%). Thermal generation decreases in the second scenario from 1552 GWh to 1258 GWh. This is caused by the fact that, cheaper solar and wind sources are integrated into the system, which reduces relatively expensive thermal generation. Wind generation in current power system is only 0.8% from the total generation, that increases to 9% and 12% respectively in the PLEXOS scenarios. Solar energy has less generation than wind - 1% and 3%. It has already been decided that from market go-live, importer will participate only on the day ahead market and make price acceptance bid. This issue is considered in the PLEXOS model. That is why import volume is more or less the same amount in both scenarios. This is because in the model, import marginal cost is determined as 0, not to have impact on the market prices. Apart from, it should be mentioned that in the model, network transfer capacity (NTC) is artificially modeled by each month (see table 3 below).

NTC values												
MW												
Month	Jan	Feb	Mar	Apr	May	Jun	Jul	Aug	Sep	Oct	Nov	Dec
Import	350,0	350,0	350,0	350,0	50,0	50,0	50,0	50,0	50,0	350,0	350,0	350,0

Table 3: NTC values of import

Generation adequacy is assessed by energy not served (ENS) parameter, that refers to the amount of energy that is not being used to meet the minimum level of electricity demand required by consumers. This can occur due to a variety of factors, including insufficient generation capacity, transmission constraints, or unexpected outages.

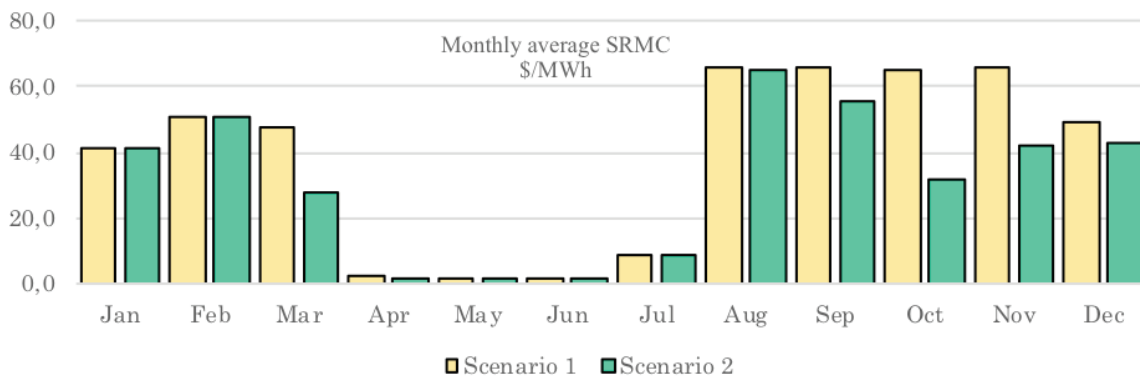
Unserviced energy and unserved energy hours			
ENS ( MWh)		ENS hours	
Scen 1	Scen 2	Scen 1	Scen 2
17 000	7 500	108	42

Table 4: Unserved Energy

Even with careful planning and management, there may be times when the available generation capacity is not sufficient to meet demand. In these cases, energy not served may occur. In the first scenario ENS is more than in the second scenario, that gives us indication that second scenario looks better in terms of adequacy fulfillment, but both of them reference to the load uncovering for some period of time during the year.

### 4.2. Economical factors

In that section short-run marginal cost (SRMC) is assessed for 2 scenarios. SRMC refers to the cost of producing one additional unit of electricity in the short run, which is typically less than a year. The SRMC includes variable costs such as fuel and maintenance expenses. Overall, understanding SRMC is essential for both electricity generators and consumers in determining pricing strategies and optimizing production levels.



Picture 10: Monthly average SRMC



Oral Presentation: Impacts of Variable Renewable Energy on new Wholesale Market in Georgia

In the model, when electricity demand is high, generators charge a higher price that reflects the higher SRMC of producing additional units. In contrast, during times of low demand generators choose to sell their electricity at a lower price that reflects the lower SRMC of producing additional units.

The SRMC can vary depending on the type of generator used to produce electricity. For PLEXOS model, thermal power plants have a higher SRMC than hydro, wind and solar.

In the first scenario yearly average SRMC is 40\$/MWh, as for the second scenario it is 31\$/MWh. This suggests that the integration with more capacity of wind and solar has reduced SRMC.

## 5. CONCLUSION

The results from this paper suggest that the integration of VRE highly effects on the future electricity market and power system. It emphasizes that ENS can have significant economic and environmental impacts. For example, it can lead to increased costs for consumers as power prices rise during periods of high demand. It can also result in increased greenhouse gas emissions as backup generators are brought online to meet demand.

To address ENS, power system operators may implement a range of measures, such as increasing generation capacity, improving transmission infrastructure, or implementing demand-side management programs to reduce peak demand levels.

When energy demand exceeds the available supply, there is a risk of blackouts or brownouts, which can have severe economic and social consequences. To avoid this, power system operators must ensure that there is enough generation capacity available to meet peak demand levels, plus a reserve margin to account for unexpected events.

The integration of wind and solar energy has a significant impact on short-term marginal costs. When these renewable sources are integrated into the energy grid, they displace traditional fossil fuel-based power plants during periods of high wind and solar generation. This results in a decrease in the demand for traditional power plants, which in turn lowers the short-term marginal cost of electricity.

However, the integration of wind and solar energy can also increase short-term marginal costs in certain situations. For example, when there is low wind or solar generation, traditional power plants must increase their output to meet demand, which can result in higher short-term marginal costs.

Overall, the integration of wind and solar energy has a net positive effect on short-term marginal costs. While there may be some instances where costs increase, the overall trend is towards lower costs as renewable energy becomes more prevalent in the energy mix.

## BIBLIOGRAPHY

- [1] [https://www.lawinsider.com/dictionary/energy-not-served-ens#:~:text=energy%20not%20served%20\(ENS%20means,insufficient%20resources%20to%20meet%20demand](https://www.lawinsider.com/dictionary/energy-not-served-ens#:~:text=energy%20not%20served%20(ENS%20means,insufficient%20resources%20to%20meet%20demand)
- [2] Variability of Wind Power and other renewables-management options and strategies, 2008
- [3] International Energy Agency
- [4] Modelling Electricity Generation - Comparing Results: From a Power Systems Model and an Energy Systems Model (Alessandro Chiodia , J.Paul Deaneb , Maurizio Gargiuloc and Brian P Ó Gallachóird, pages 4-5)
- [5] The Economics of Wind and Solar Variability-How the Variability of Wind and Solar Power affects their Marginal Value, Optimal Deployment, and Integration Costs (Dipl.-Volksw. & Mag.phil.Lion Hirth, November 2014, pages 21-22)
- [6] Portfolio Short Run Marginal Cost of Electricity Supply in Half Hour Trading Intervals. (Adam McHugh , 11 January 2008, page 5)
- [7] Ten-Year Network Development Plan of Georgia 2023-2033. (Transmission System Operator JSC "Georgian State Electrosystem". pages 8, 17-18)



# Estimation of Georgian Power System Flexibility and Adequacy

[archil.kokhtashvili@gse.com.ge](mailto:archil.kokhtashvili@gse.com.ge)

**ARCHIL KOKHTASHVILI\*, GURAMI MIRINASHVILI, GIORGI AMUZASHVILI**

*Georgian State Electrosystem (GSE)*

**Georgia**

## SUMMARY

Georgian Power System was planned as a part of big unified system. After country's independence it faces a lack of flexibility which is the main limiting factor for the VRE (Wind and PV) integration. The commercial softwares, for the estimation of the power system flexibility, costs too much, they don't have a satisfactory hydrology model, are too complex, require too big calculation time and human affords. In many cases their results are doubtful and difficult to explain.

This article elaborates a simple approach to estimate the power system flexibility and adequacy level, with consideration of actual power market particularities and detailed charge-discharge models of reservoir power plants of Georgia; The model uses a one-node approach.

Below are listed the calculation steps:

1. Elaboration of the representative future scenarios: combination of demand growth rate, hydrology, geographical distribution of VRE sources and HPP\_Reservoir charge-discharges
2. Calculation of the hourly net load as a difference of load and total non-dispatchable hourly generation (RoR, PV, Wind), for each scenario.
1. Calculation of the total monthly generation. maximum and minimum power outputs of HPP\_Reservoirs are defined by the charge-discharge characteristics.
2. Calculation of the monthly values of load, HPP\_RoR, Wind and PV generations.
3. Determination of the monthly energy interchange as a difference between the monthly demand and all RE generation (including HPP\_Reservoir(s))
4. Calculation of as the monthly interchange as the energy divided on the numbers of hours in the month, as the power of interchange (TPP generation) is assumed as a constant during the month (unless it's impossible to balance the system by the HPP\_Reservoirs).
5. Calculation of the hourly generation of HPP\_Reservoirs as a difference of hourly value of load, total non-dispatchable generation and the interchange. HPP\_Reservoir power output should be fitted in its maximum and minimum capabilities.
6. Calculation of monthly and hourly imports (TPP Generation) and exports and estimation of the adequacy level of the system.

## KEYWORDS

Flexibility, Adequacy, Generation, PV, Wind, RoR, HPP\_Reservoir, Reserve, Charge, Discharge



Oral Presentation: Estimation of Georgian Power System Flexibility and Adequacy

7. Determination of the needed reserves are as a geometrical sum of the biggest infeed and deviations of load and each type non-dispatchable generation.
8. Definition of the positive hourly available reserve is defined as a difference between the maximum of HPP\_Reservoirs and their generated power, plus capacity the of gas turbines; available negative reserve – sum of generated HPP\_Reservoir and TPP (or import) minus sum of the technical minimum of HPP\_Reservoirs and TPP (import)
9. Calculation of the deficits of the positive and negative reserves.
10. Elaboration of the recommendations for the to maximize the VRE integration into Georgian Power System
11. At the final part, determination the mathematical dependence of the reserve deficit durations, Maximum and Minimum MW output and monthly HPP\_Reservoir generation. This dependence has a very close characteristics to the logistic function.

The elaborated model allows to make calculations for the flexibility and adequacy estimation, without any advanced skills of a commercial software or programming language. It also allows to easily change the inputs to recalculate. The results appear in few seconds. The visualization output processing is easy and comfortable.

### ACRONYMS

HPP – Hydro Power Plant

TPP – Thermal Power Plant

VRE – Variable Renewable Energy

RoR – Run of River HPP

CCGT – Combined Cycle Gas Turbine

## 1. INTRODUCTION

Georgian Power System was planned as a part of big unified system and after country's independence it faces a lack of flexibility which is the main limiting factor for the VRE (Wind and PV) integration. At the same time all of the neighboring countries have different power markets and power system planning and operation philosophies. Hence, to access on the fast-acting flexibility of the neighboring countries is impossible. In the other hand the electricity consumption of Georgia is increasing rapidly. In addition, Georgia does not have enough internal fossil fuel sources and imports the fuel, mainly gas, to operate the TPPs. So, to somehow to catch demand growth by the domestic generation, the simplest way is to build VRE power plants, as they need much less time and efforts than HPPs. For this purpose, it's essential to have a possibility to recalculate the acceptable VRE integration limits on a regular base.

The commercial software's costs too much, they don't have a satisfactory hydrology model, are too complex, require too big calculation time and human affords. In many cases their results are doubtful, inadequate and difficult to explain, moreover in some cases with the same inputs, the different commercial software's have a different output. It might happen because of different optimization models or human errors. So, to use the commercial software's for the acceptable VRE limits determination is unfeasible.

Due to the generation deficit, it was decided to increase by 2025, the VRE integration limits in Georgian Power System for wind - up to 700 MW and for solar - up to 500 MW.

According to the previous studies, the VRE integration limits were mainly caused by the flexibility restrictions of Georgian power system.

The purpose of current article is

- To identify the challenges and the possibilities of the system by viewpoint of system flexibility and the reserves. To outline the circumstances that may arise in case of violating such limits and to provide the recommendations addressing the potential challenges.
- To develop a simple method and a tool which allows to make calculations by easy way and minimal efforts
- To define the reserve deficit time dependence on the capability of on the technical maximum and minimum power capacity of the system.

## 2. GEORGIAN POWER SYSTEM [1]

The transmission System (Fig 1) consists with 500 kV (923 km), 400 kV (32 km), 330 kV (21 km), 220 kV (1917 km), and 110 kV (3550 km) OHLs.

The Georgian power system is relatively small system taking into account the size of the country. The installed capacity of Georgian Power System is 4,533 MW, with 3,323 MW HPPs (2,381 MW reservoir and 942 MW RoR), 1,189 MW TPPs and 21 MW Wind.



Figure 1. Transmission System of Georgia

The main source of energy comes from hydro resources, Hydropower covers around 80% of total consumption, but during the dry periods thermal generation has also a big share into the monthly energy balance. There is only one 21 MW wind power plant in the center of Georgia. The operating capacity of biggest generating units are 250 MW, so sometimes one unit covers around 25% of the system load. Georgia has very inconstant demand profile. The difference between peak load and minimum load values is significant. Weather and times of the year has also big influence on consumption. Based on yearly demand profile, highest point of consumption is in winter when it reaches 2350 MW and the lowest point of demand profile is in spring and autumn when demand gets as low as 1100 MW. Although since most of the hydro generation is located in the western part of Georgia and biggest consumption is located in the eastern part of the country, 500kV lines are backbone of system which transmits a large amount of energy. Georgian

electrical grid has following interconnections with neighboring countries:

- Russia – 500kV and 220 KV AC connections
- Turkey – 400kV AC (with DC B2B) connection
- Azerbaijan – 500kV AC and 330kV AC connections
- Armenia – 220kV AC connection

There is theoretical possibility to be synchronously connected with 3 countries. In reality Georgia most of the time works in parallel with Russian or Azerbaijan system. Also, there are some certain periods when Georgian power system operates in an isolated (electrically island) mode.

## 3. INPUTS AND SCENARIOS

For the calculation, the following inputs were taken in account:

- Schedules for the month of water reservoirs charging-discharging





Oral Presentation: Estimation of Georgian Power System Flexibility and Adequacy

- Maximum and minimum capacities of reservoir hydropower plants  $P_{max}$ ,  $P_{min}$  (depending on the level)
- Hourly data
  - consumption forecasts (in MW)
  - records of RoR HPPs (in p.u. =  $P_{ROR_{actual}}/P_{ROR_{nom}}$ )
  - records of PV locations (in p.u. =  $P_{PV_{actual}}/P_{PV_{nom}}$ )
  - records of wind locations (in p.u. =  $P_{WIND_{actual}}/P_{WIND_{nom}}$ )
- Generation mix
  - Reservoir HPPs = 2250 MW (Existing Capacity)
  - RoR HPPs = 1400 MW
  - Wind Power Plants = 700 MW
  - Solar plants = 500 MW

The scenarios were built with the combination of following cases:

- Demand cases
  - 1.5% increase (L1)
  - 4.5% increase (L2)
  - 7.0% increase (L3)
- Hydrology cases
  - Dry (H1)
  - Medium (H2)
  - Wet (H3)
- Discharging cases of Enguri HPP
  - normal (N)
  - intensive (I)
- Geographic distribution cases of Solar PPs
  - 1 location (S1)
  - 3 locations (S2)
  - 10 locations (S3)
- Geographic distribution cases of Wind PPs
  - 1 location (W1)
  - 3 locations (W2)
  - 7 locations (W3)

## 4. SIMULATION TOOL AND METHODOLOGY

The Excel based tool had been elaborated. Each simulation takes several seconds. No special powerful computer or huge human efforts are required. For the big (8760 hour) data processing the matrix functions had been used.

For the simplicity, one node approach is used, so Reservoir HPP, RoR HPP, PV PP, Wind PP are representing the summary characteristics of corresponding types of generation.

Load forecast was elaborated based on linear regression method. For Georgian system, the total load is a function of GDP, population, tourism and electrical vehicles [2].



Hourly net load is the actual load minus hydroelectric, wind and solar (non-dispatchable) generation, (see Fig 1, sample of January month), So, for each 1 to 8760 values

$$P_{NET\_LOAD} = P_{LOAD} - (P_{ROR} + P_{WIND} + P_{SOLAR}) \tag{1}$$

Net load is covered by Reservoir hydroelectric power plants and thermal plants/import (see Fig 2, sample of January month). For 1 to 8760 values

$$P_{LOAD} - (P_{ROR} + P_{WIND} + P_{SOLAR}) = P_{HPP\_R} + P_{TIE} \tag{2}$$

Here, the left side of the equation is the initial information, and the right side is the unknown.

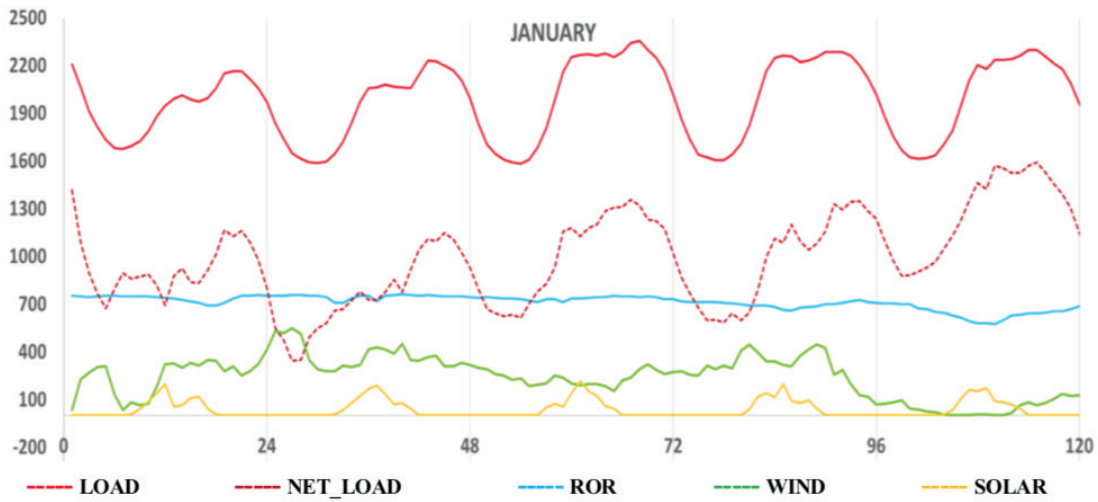


Figure 2. Net Load as Load minus non-dispatchable generation

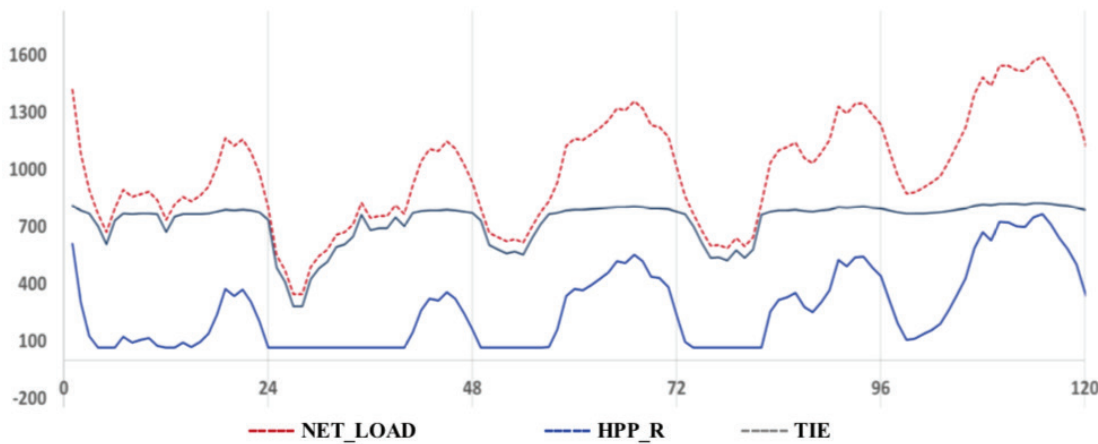


Figure 3. Net Load as sum of HPP\_ Reservoir and TPP&Import&Export

Balancing is done on a monthly basis. The monthly generation of reservoir HPPs, also their maximum and minimum power outputs, are determined from the corresponding charge-discharge schedules, based on the inflow  $Q$  and pressure levels  $H$ , for 1 to 12 values:

$$EM_{HPP_R}, P_{max}, P_{min} = f(H, Q) \tag{3}$$



Oral Presentation: Estimation of Georgian Power System Flexibility and Adequacy

For each HPP\_Reservoir the particular (3) dependence is considered, which is nonlinear and caused by the characteristics of the reservoirs.

Energy consumption, as well as non-dispatchable generations, is determined by the sum of the respective hourly power outputs during the month. So, for each 1 to 12 months:

$$EM_{LOAD} = \sum P_{LOAD}; \quad EM_{ROR} = \sum P_{ROR}; \quad EM_{WIND} = \sum P_{WIND}; \quad EM_{SOLAR} = \sum P_{SOLAR} \quad (4)$$

Thermal plants & import/export monthly energy is defined as the monthly consumption minus the total renewable generation (including Reservoir hydroelectric power stations):

$$EM_{TIE} = EM_{LOAD} - (E_{HPP\_R} + EM_{ROR} + EM_{WIND} + EM_{SOLAR}) \quad (5)$$

Thermal plants & import/export capacity is calculated as the corresponding month's energy  $EM_{TIE}$  divided by  $n$  number of hours per month:

$$P_{TIE} = EM_{TIE}/n \quad (6)$$

At any (1 to 8760) hour, the total power of the Reservoir HPP (as a first approximation) is calculated as the difference between the net consumption and the power of the thermal plant:

$$P_{HPP\_R(1)} = P_{LOAD} - (P_{ROR} + P_{WIND} + P_{SOLAR}) - P_{TIE} \quad (7)$$

In addition, the total capacity of reservoir HPPs is between the total technical maximum and minimum:

$$P_{min} < P_{HPP\_R(1)} < P_{max} \quad (8)$$

Due to this limitation, in some cases the generation of reservoir hydropower plants may be less or more than planned. Therefore, at those hours where it was not limited due to reaching the maximum and minimum. the generation is adjusted by the monthly correction coefficient:

$$k = \sum P_{HPP\_R(1)}; \quad EM_{HPP\_R} \quad (9)$$

Finally, we get the hourly total power output of the reservoir hydroelectric power stations:

$$P_{HPP\_R} = P_{HPP\_R(1)} \cdot k \quad (10)$$

We determine the available values of positive  $R_{(+)}$  and negative  $R_{(-)}$  power reserves, for each (1 to 8760) hour:

$$R_{(+)} = P_{max} - P_{HPP\_R} + P_{GT} \quad (11)$$

$$R_{(-)} = (P_{HPP\_R} - P_{min}) + (P_{TIE} - P_{TIE\_min}) \quad (12)$$

Where gas turbine power plant capacity  $P_{GT} = 110$  MW

For each hour, we determine the amount of both positive and negative reserve deficit. For this, we compare the available reserve values  $R_{(+)}$  and  $R_{(-)}$  with the required reserve value and count the number  $n_{(+)}$  and  $n_{(-)}$  of hours  $T$ , when the reserves are not sufficient:  $R_{(+)} < R$  and  $|R_{(-)}| < R$

$$n_{(+)} = \sum_{T=1}^{8760} T_{R_{(+)} < R} \quad (13)$$

$$n_{(-)} = \sum_{T=1}^{8760} T_{|R_{(-)}| < R} \quad (14)$$



In case of Georgian power system, with acceptable accuracy, the required reserve can be determined with the formula:

R approx sqrt(G\_max^2 + sigma\_LOAD^2 + sigma\_ROR^2 + sigma\_WIND^2 + sigma\_SOLAR^2) (15)

Where

G\_max approx L\_max = maximum value of generation/load unit to be lost in the system. For Georgia this value is nearly 250 MW

sigma\_LOAD, sigma\_ROR, sigma\_WIND, sigma\_SOLAR = are hourly deviations of respectively load, RoR HPPs, Wind and Solar power plants, for 99% of the time.

In case of 17.00 TWh annual consumption, 1400 MW RoR, 700 MW Wind and 500 MW PV (when these two are geographically distributed on 3-3 locations) required spinning reserve R approx 400 MW

"R" assumes FRR (Frequency Restoration Reserves, aFRR - automatic FRR and mFRR - manual FRR)

5. REPRESENTATIVE SCENARIOS AND SIMULATION RESULTS

5.1. Main Scenarios

A 4.5% (L2) increase in consumption, distribution of wind and solar generation in 3-3 locations, normal (non-intensive) discharging of Enguri HPP was selected as the main scenario.

With the above-mentioned scenario, the water-rich H3, average H2 and low-water H1 hydrology were combined and moderate L2H2, optimistic L2H3 and pessimistic L2H1 scenarios were obtained.

Scenario moderate L2H2. Generation-demand is quite asymmetric, the big portion of generation comes on HPP\_Reservoir and HPP\_RoR and because of wet periods they cause big surplus in May, June, July. The wind generation is mostly stable, during the months, the solar is maximum in Jul and minimum is January and December, but because of too small portion, this source does not effect on the generation-consumption balance. The consumption is highest in December and January because of heating consumption, also it's high in July and august because of cooling consumption. The consumption minimal in May and September because of comfortable temperatures and no need for cooling and heating. So, because of energy surplus from May to July there is need of electricity export, when rest mounts are characterized with the deficit of internal energy sources and in these periods, there is a need of electricity import or gas import for the electricity generation (Fig 4)

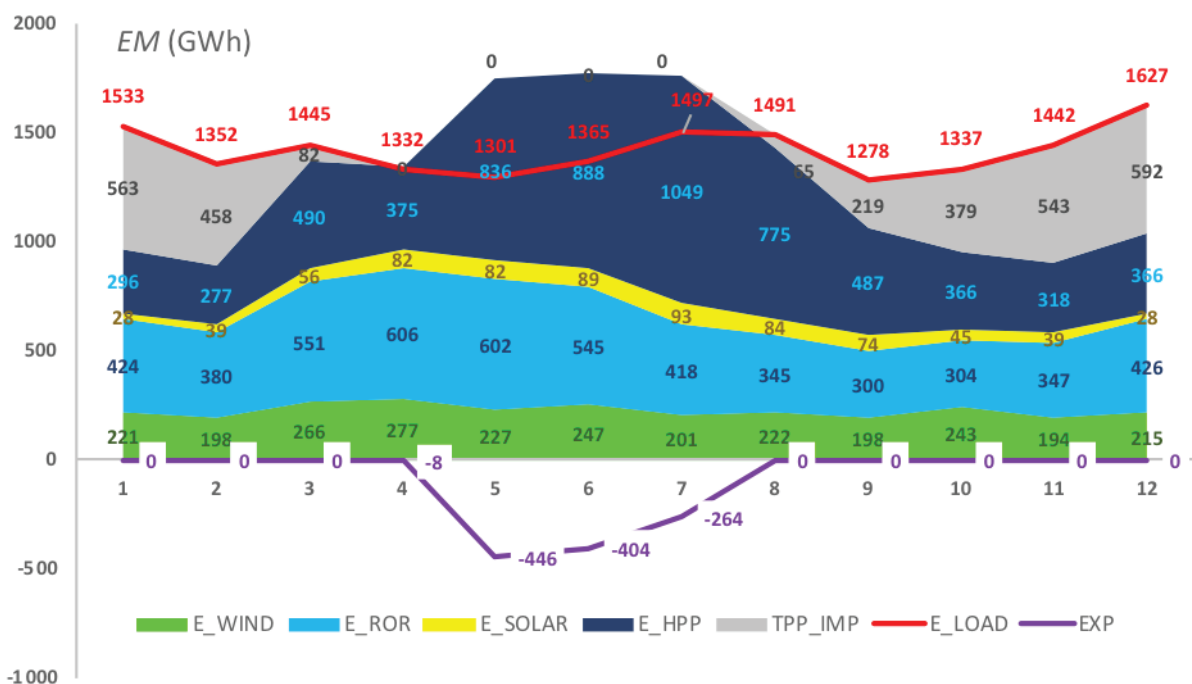


Figure 4. Monthly Energies GWh, Scenario L2H2



Fig 5 shows the daily energy numbers of generation sources, also load, net load, net deficit (TPP generation and import) and surplus (Export). There is clear that daily changing of net load is much significant than for load. This is mainly caused because of wind generation, which itself is very unstable by day-to-day time frame.

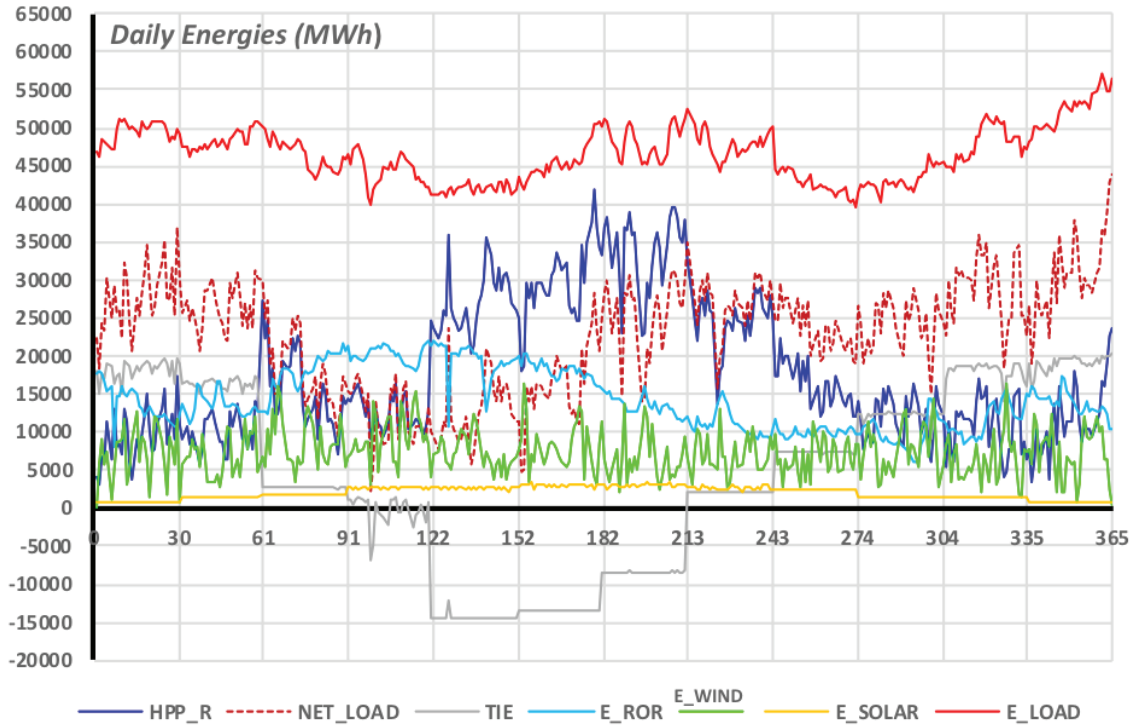


Figure 5. Daily Energies (MWh), Scenario L2H2

Fig 6 shows the daily maximum and minimum load and maximum and minimum net load (MW), it seems that load maximum and load minimum day-to-day change is quite smooth, when the change of minimum and maximum net load is quite significant.

Fig 7 shows the differences of maximum and minimum values (MW) for load and net load, there are many days when these differences for net load is double or more when for load. It means that the stress on the power system flexibility capabilities is increased.

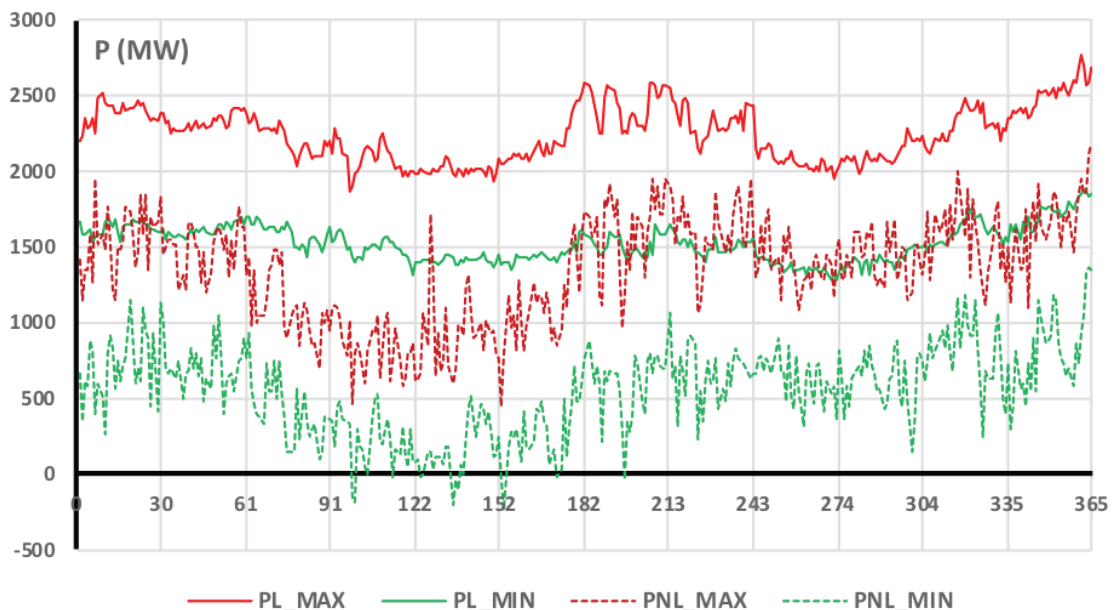


Figure 6. Maximum and Minimum Load and Net Load (MW), Scenario L2H2

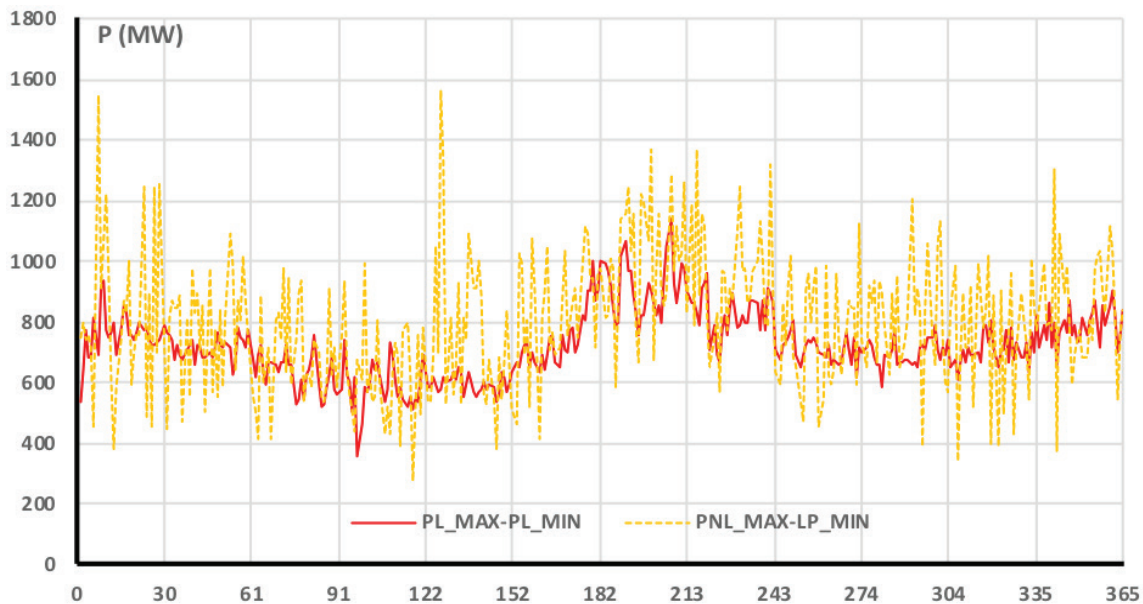


Figure 7. Load\_Max – Load\_Min and Net\_Load\_Max – Net\_Load\_Min, Scenario L2H2

The figures 8, 9 and 10 shows the hourly variation (MW) of HPP\_Reservoir, HPP\_RoR, Wind and Solar generation, as well as hourly variation of load, net load and TIE (TPP, Import, Export) and also values of available positive R(+) and negative R(-) reserves, for January, April and July.

In January month, almost for each hour there is not any deficit of the reserves, it's mainly because, the base load is covered by the TPPs, when the not load variation is covered by the HPP\_Reservoirs. In the April month, there is a significant deficit of the negative R(-) reserves, its mainly because in this month several HPP\_Reservoirs have limited technical minimums, in order to avoid the water spilling due the wet season. In the July month the negative reserves R(-) are mostly in acceptable level, but some hours are deficit of positive reserves R(+), it's because in this month there is not technical minimum problems on HPP\_Reservoirs, as inflows are low, however, there is some challenge with technical maximums Pmax, as the load is increased then in July. There is no TPP operation or imports, because of surplus exports are increased which actually act as additional load, so the Load+Exports are fully covered by HPP\_Reservoir, without support of TPP's.

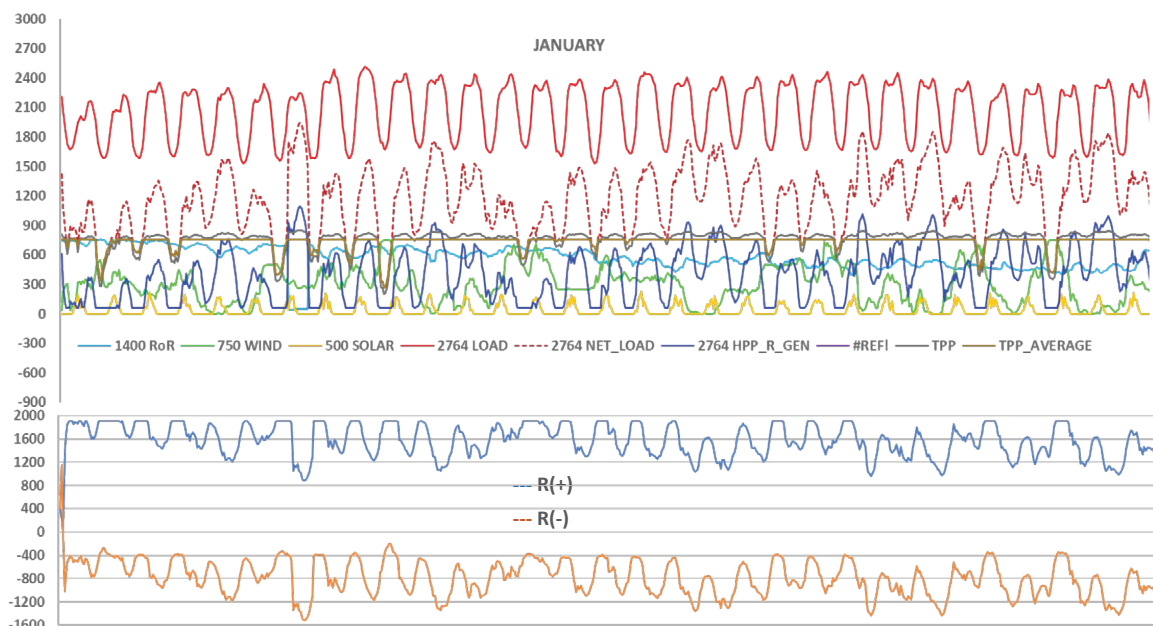


Figure 8. Hourly power values (MW) for January, Scenario L2H2



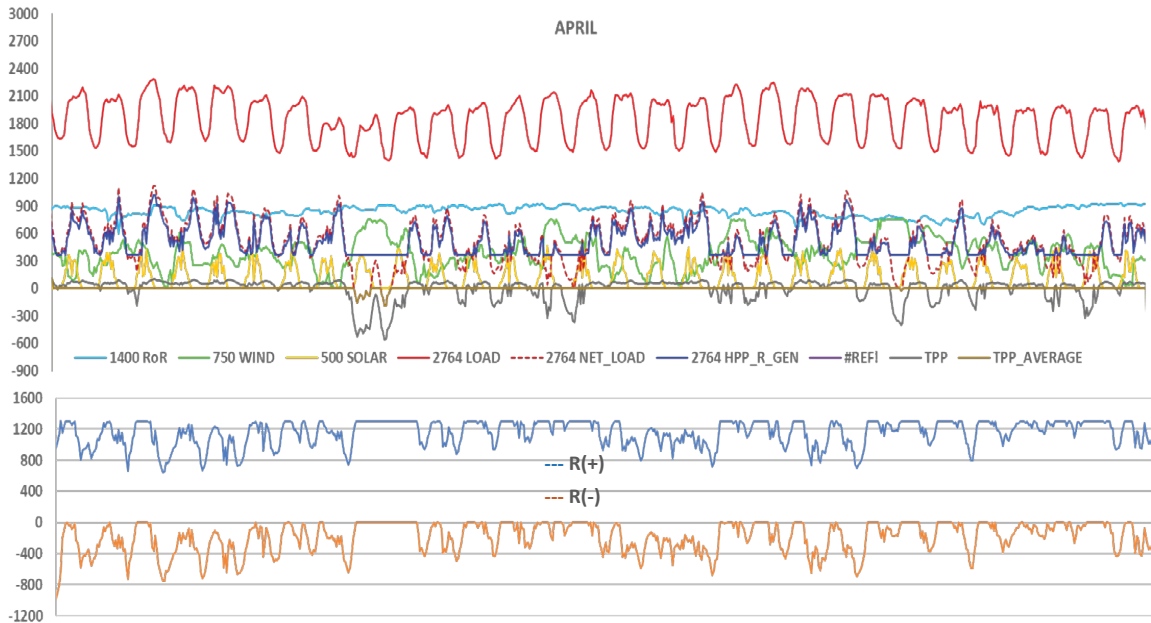


Figure 9. Hourly power values (MW) for April, Scenario L2H2

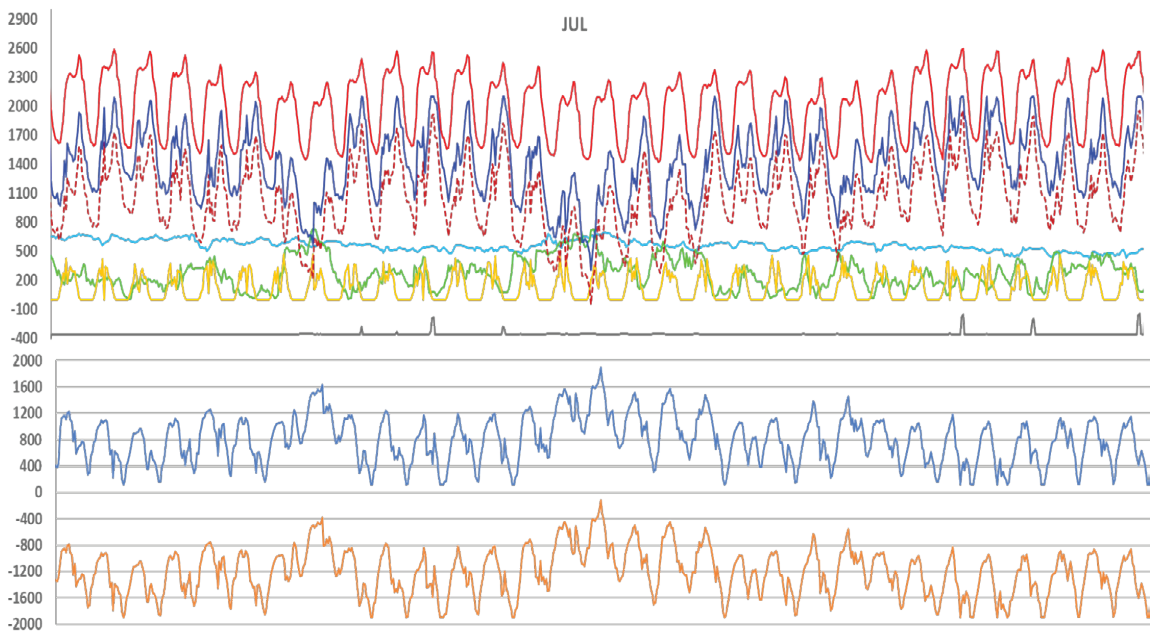


Figure 10. Hourly power values (MW) for July, Scenario L2H2



Scenario pessimistic L2H1

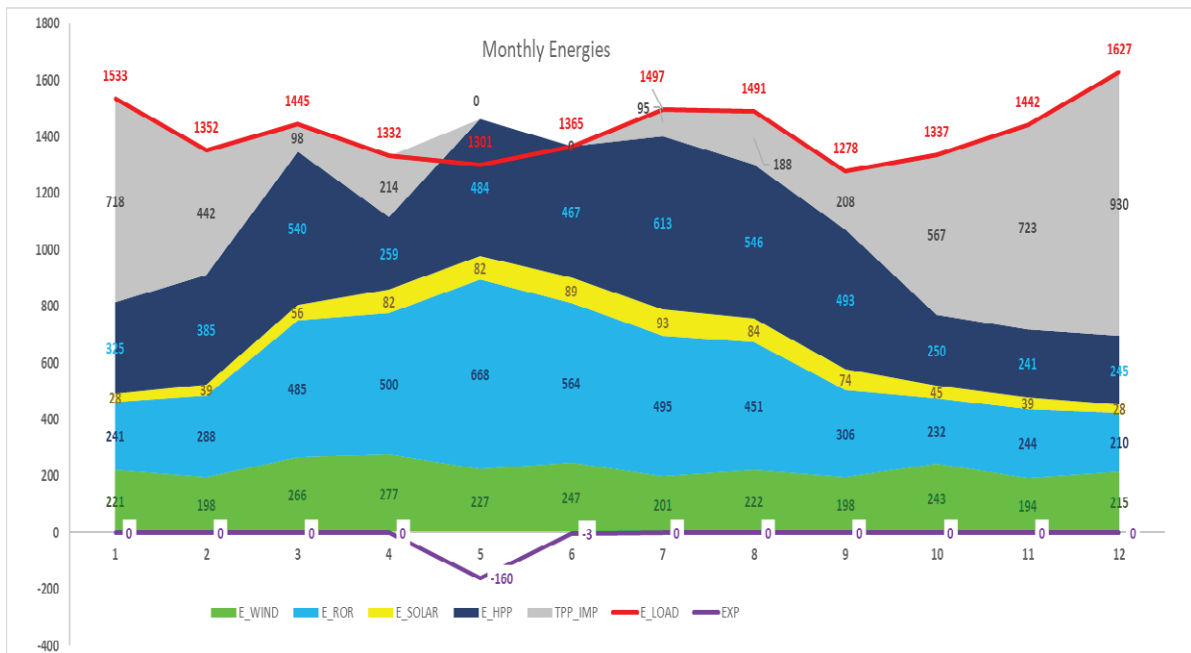


Figure 11. Monthly Energies GWh, Scenario L2H1

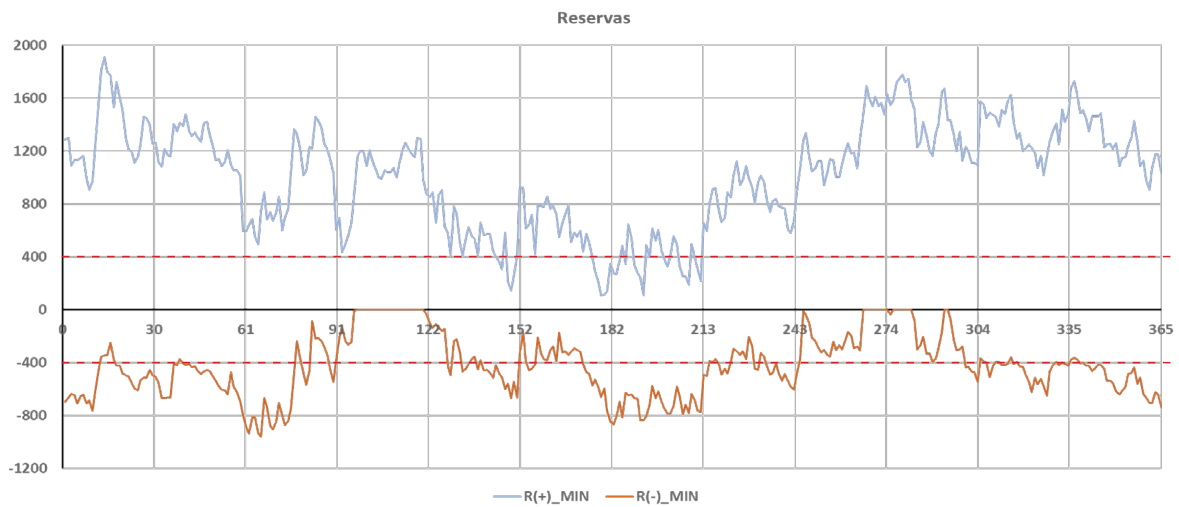


Figure 12. Daily minimal available reserves, Scenario L2H1



Scenario optimistic L2H3

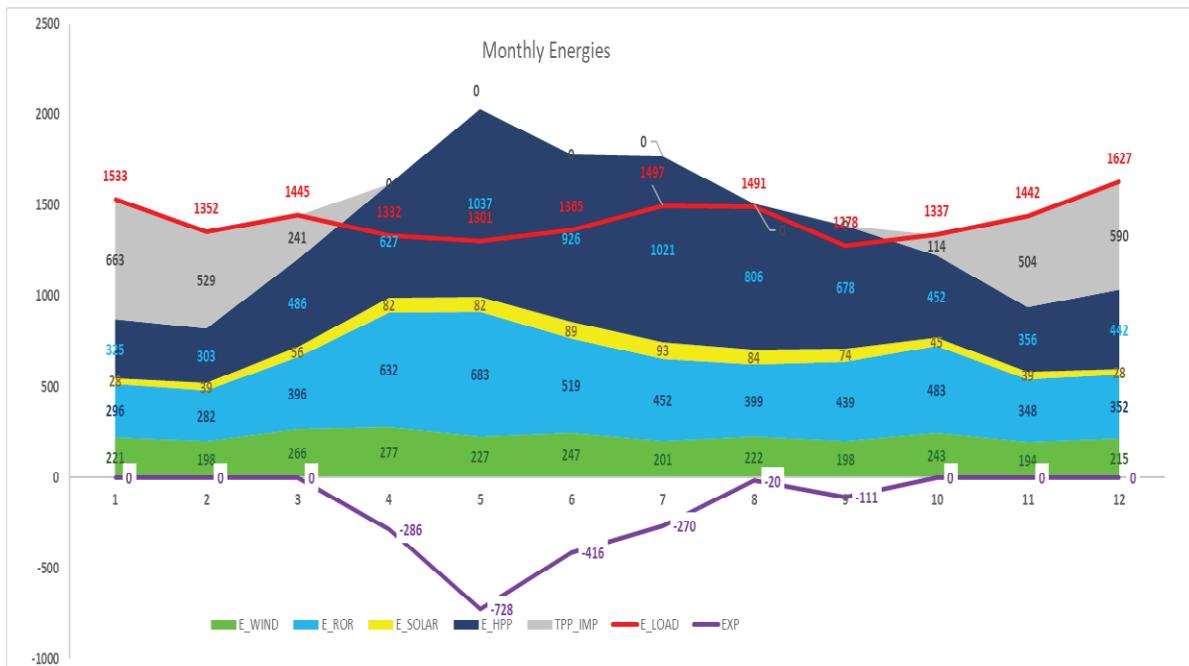


Figure 13. Monthly Energies GWh, Scenario L2H3

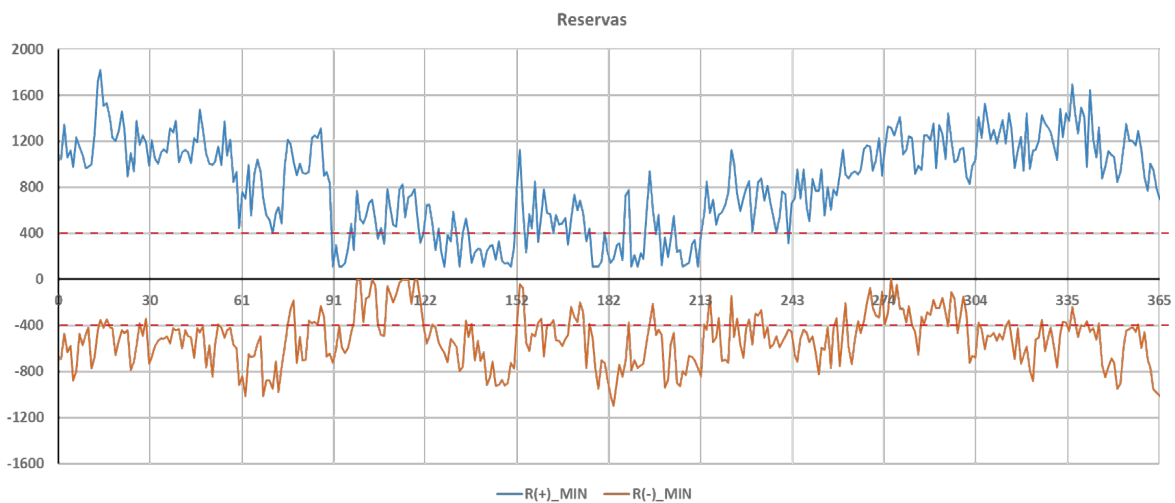


Fig 14. Daily minimal available reserves, Scenario L2H3

Summary of main scenarios:

By viewpoint of system adequacy, The total load, Wind and Solar generation is the same. As expected, the better situation is in Optimistic Hydrology Scenario, where we have biggest HPP\_Reservoir generation and hence TPP generation/Import is minimal. Vice versa, the adequacy is lower in Pessimistic Hydrology Scenario, when HPP\_Reservoir generation is minimal and hence the TPP generation/import is maximal.

By viewpoint of the flexibility, the negative reserve deficit time n(-) is maximal in Pessimistic scenario, moderate - in moderate scenario and minimal in optimistic scenario. The positive reserve deficit is in optimistic scenario, moderate - in moderate scenario and minimal in pessimistic scenario. This is because in case of optimistic scenario there is more HPP\_Reservoir generation and hence more export and the export acts as additional load. So, as we have the unchanged Pmax and Pmin, in case of increased exports it's more difficult to maintain the positive reserves and easier to maintain the negative reserves. Vice versa in case of pessimistic scenario, when system has less exports due the less HPP\_Reservoir generation. So total load is smaller. Hence there is easier to maintain the positive reserves when is more difficult to maintain the negative reserves.



Table 1. Summary results for different hydrology scenarios

SCENARIO	LOAD	HPP_R	ROR	WIND	SOLAR	TPP/IMP	EXP	R_req	n(+)	n(-)
	TWh	TWh	TWh	TWh	TWh	TWh	TWh	MW	Hour	Hour
Moderate L2H2	17.00	6.51	5.26	2.71	0.74	2.90	1.12	400	218	1151
Optimistic L2H3	17.00	7.46	5.28	2.71	0.74	2.64	1.83	400	317	654
Pessimistic L2H1	17.00	4.81	4.68	2.71	0.74	4.18	0.16	400	174	1519

### 5.2. Sensitivity Scenarios

Based on the basic moderate L2H2 scenario, the following sensitivity scenarios were analyzed:

- Scenario L2H2 – T: No renewables are built. The deficit is covered at the expense of thermal power plants/imports
- Scenario L2H2 – RoR: additional 1100 MW of HPP\_RoR are built, in total 2500 MW HPP\_RoR, instead of 750 MW wind and 500 MW solar
- Scenario L2H2-Int: Intensive processing of Enguri HPP is carried out, in conditions of 750 MW wind and 500 MW solar plants

From the table 2, following results are observed:

**Scenario L2H2 – T:** in case of Wind and Solar absence, TPP generation should increase to cover the load. However, the reserve deficits both positive and negative, are reduced, as the TPPs give flexibility to the power system. It should be mentioned, that due the absence of wind and solar sources, the reserve requirements are reduced as well.

**Scenario L2H2 – RoR:** In case, when RoRs are replacing the Wind and Solar, beside the total reserve requirement is decreased than in base scenario, the reserve deficit has almost the same values; However, TPPs generation/Imports are increased and exports are decreased.

**Scenario L2H2-Int:** Nearly the similar results are the same, in case of intensive discharge of Enguri, but in this case beginning from November including March, because of intensive discharge, Enguri HPP have a minimum level of storage so it acts as RoR and provided reserve is close to 0. The rest HPP\_Reservoirs are used to balance the net load and they also unable to provide the reserves.

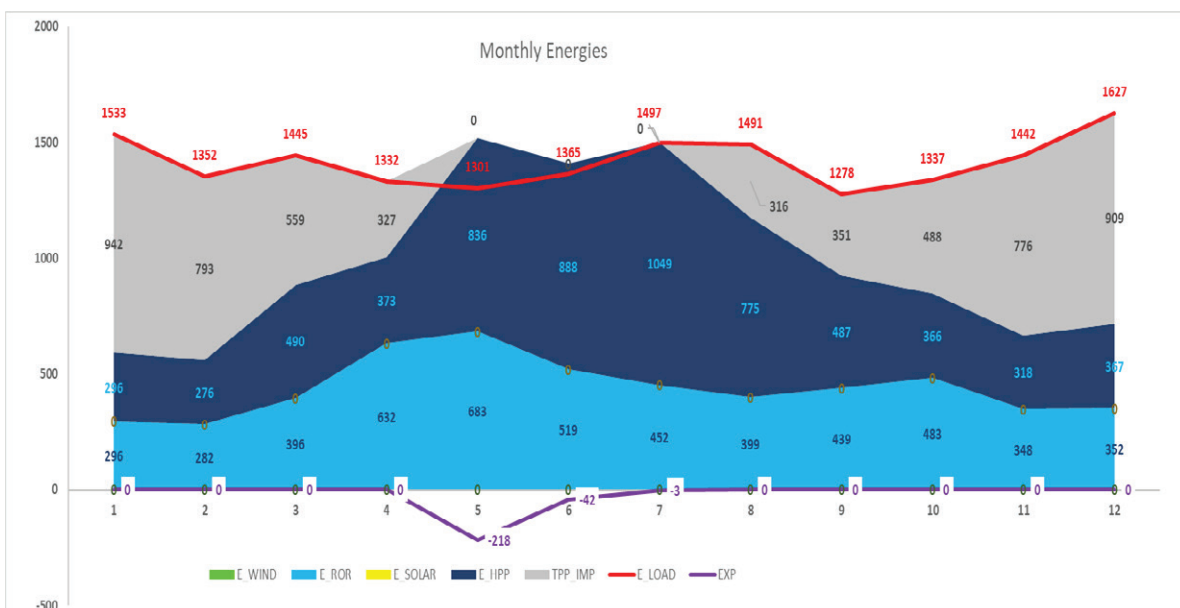


Figure 15. Monthly Energies GWh, Scenario L2H2-T

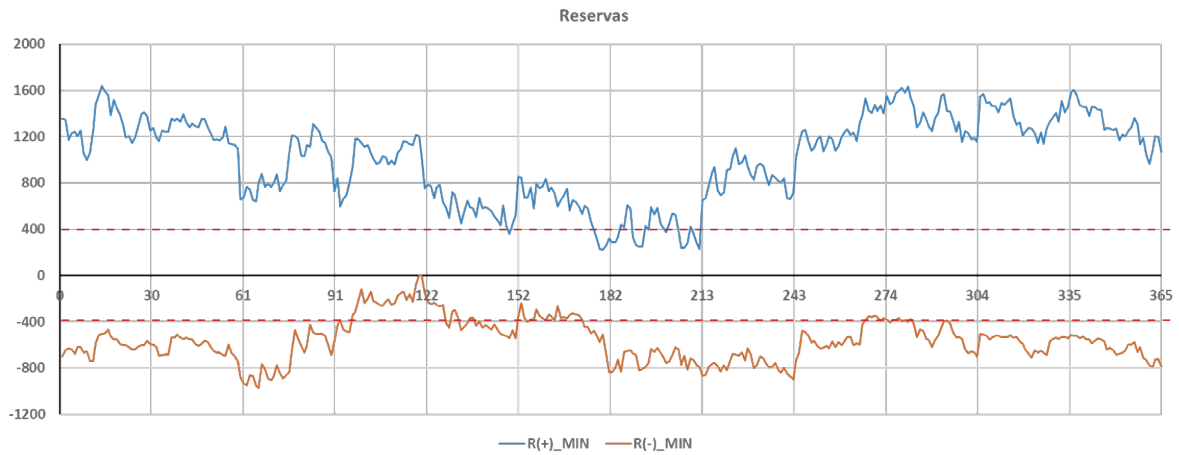


Figure 16. Daily minimal available reserves, Scenario L2H2-T

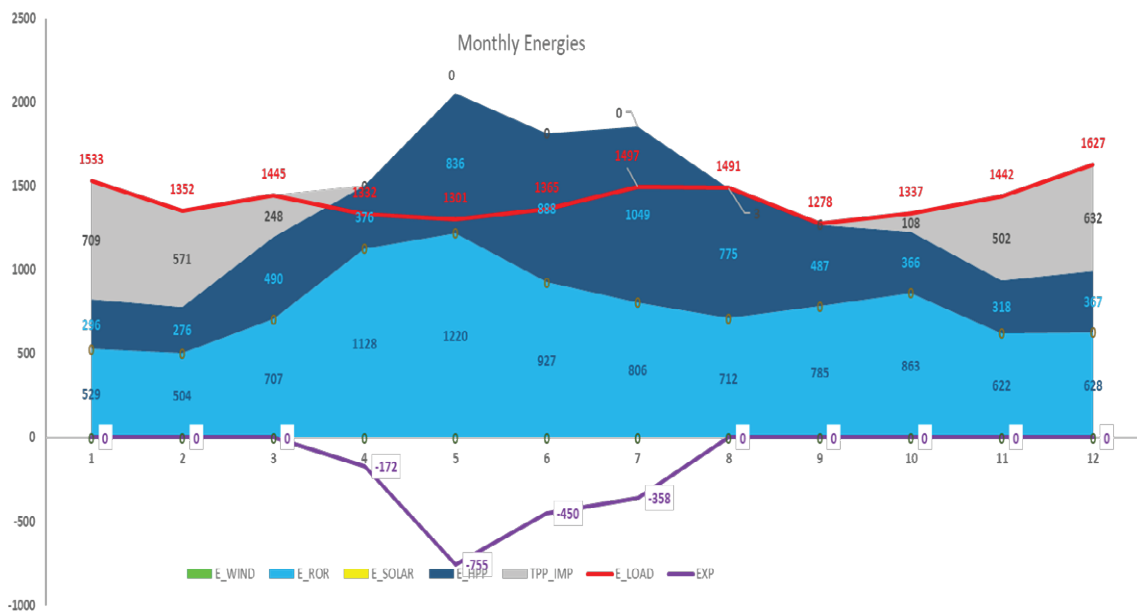


Figure 17. Monthly Energies GWh, Scenario L2H2 - RoR

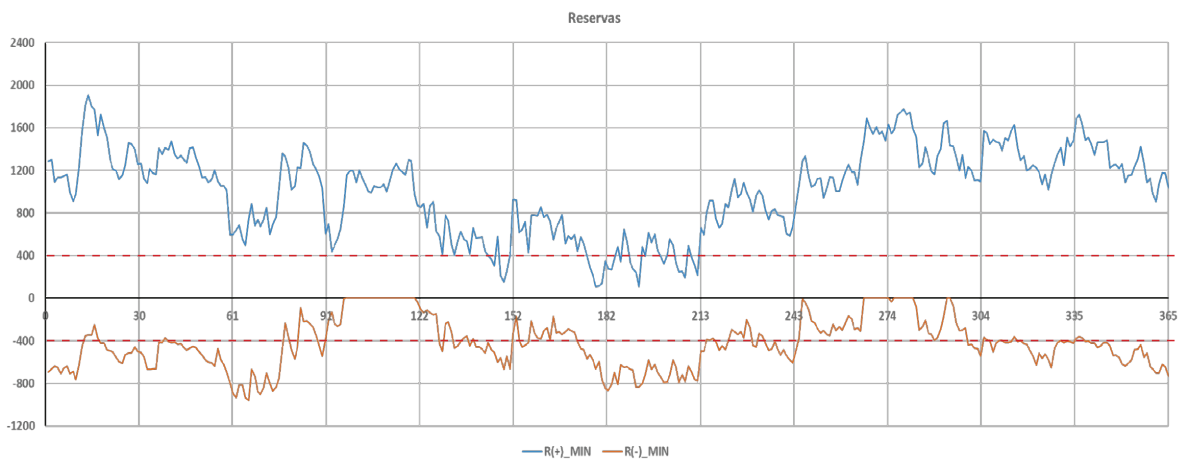


Figure 18. Daily minimal available reserves, Scenario L2H2 - RoR

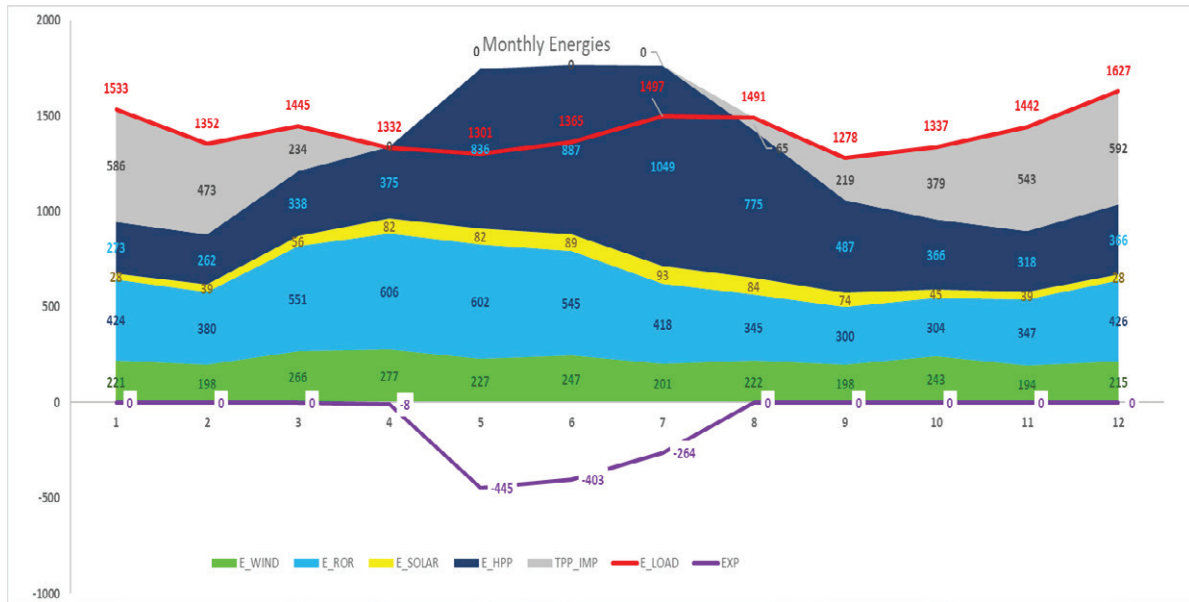


Figure 19. Monthly Energies GWh, Scenario L2H2-Agr

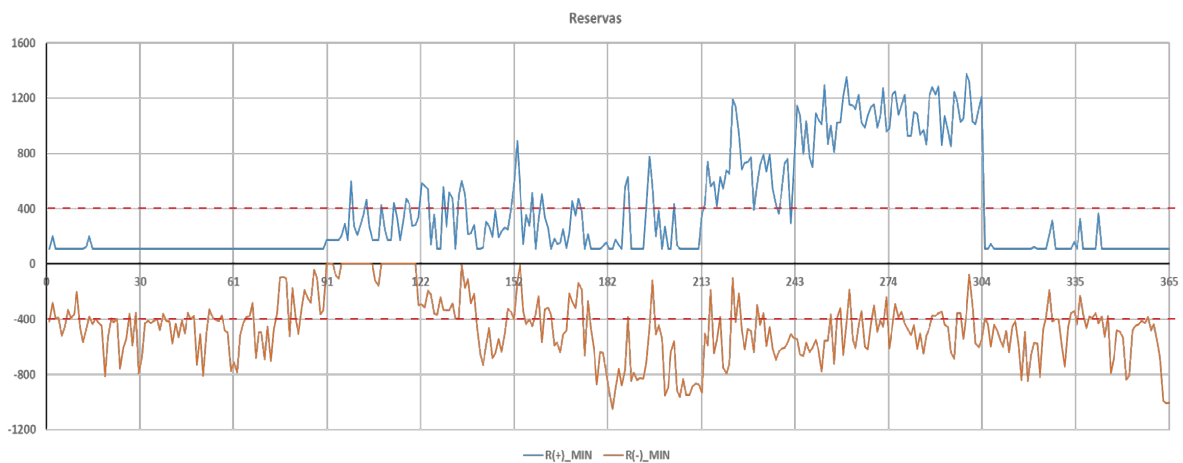


Figure 20. Daily minimal available reserves, Scenario L2H2-Agr

Table 2. Summary of the sensitivity cases in scenario H2H2

SCENARIO	LOAD	HPP_R	ROR	WIND	SOLAR	TPP/IMP	EXP	R_req	n(+)	n(-)
	TWh	TWh	TWh	TWh	TWh	TWh	TWh	MW	Hour	Hour
H2L2 (Base Scenario)	17.00	6.51	5.26	2.71	0.74	2.90	1.12	400	218	1151
H2L2-T	17.00	6.51	5.26	0.00	0.00	5.43	0.21	325	57	200
H2L2 -RoR	17.00	6.51	9.37	0.00	0.00	2.67	1.56	350	121	1167
H2L2 - Int	17.00	6.32	5.26	2.71	0.74	3.09	1.12	400	3492	1109

Summary of sensitivity scenarios:

By viewpoint of system adequacy, H2L2-RoR scenario is the best when the TPP generation/import are up to 2.67 TWh, at the same time H2L2 Base case scenario is close when TPP generation/import is 2.90 TWh. The worst case is H2L2-T scenario when Wind and Solar are replaced by TPPs and there is 5.43 TWh TPP generation/Import.





By viewpoint of the flexibility, the power system has the best performance in case of H2L2-T scenario, where the Wind and Solar Variable generation is replaced by the flexible TPP generation, however this scenario is not attractive by adequacy considerations. The worst case is Enguri Intensive discharging scenario, where the positive reserve deficit is huge - 3492 hours (more than 39% of year), so this scenario with wind and solar is non-dispatchable. The interesting that there is a very small difference between the base case and H2L2 scenario when Wind and solar generation is replaced with additional RoR generation, so, the positive reserve deficit time is relatively high in the base case when the negative reserve deficit is slightly lower in base case scenario. Hence, RoR does not have a big advantage for the power system flexibility relative to the optimal mix of Wind and Solar.

### 6. DETERMINATION OF RESERVE DEFICIT TIME DEPENDENCE ON TECHNICAL MAXIMUM AND MINIMUM POWER AND ENERGY OUTPUT OF HPP\_STORAGES

The approach, developed above, allowed us to elaborate recommendations regarding the different scenarios of VRE integration, the hydrology is too different between scenarios, moreover, several months in more dry year can have more inflows than in wet year. So, now we will try to determine the dependence of reserve shortage time on the energy generated by reservoir HPPs and their technical maximum and minimum power outputs.

For this several let's assume that year consists from the same 12 months (Fig 21). April was chosen as this typical month, as there is a RoR inflow and Wind is too unstable and the stress on the reserves is highest.

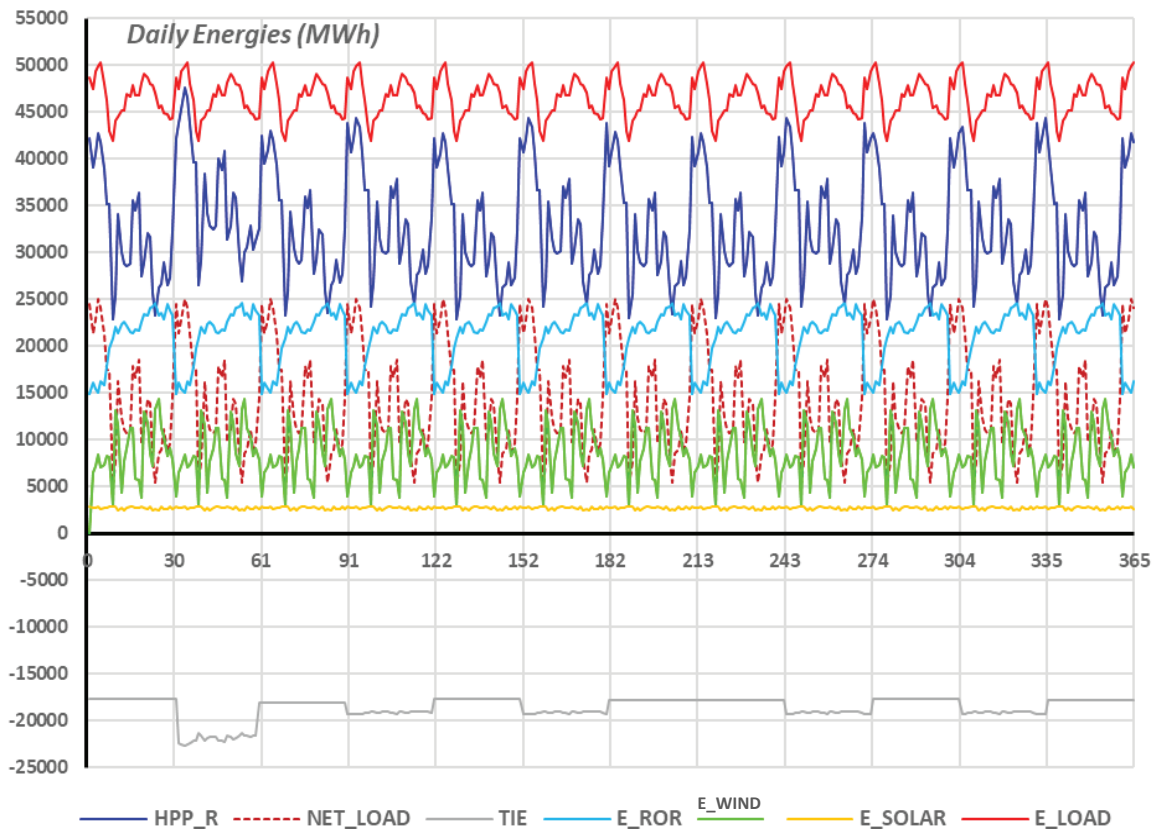


Figure 21. Daily Energies (MWh), Pmax = 2850 MW, Pmin = 0 MW, EM = 1000 MWh

With such assumptions,  $n_{(-)} = f(P_{min})$  and  $n_{(+)} = f(P_{max}, E_M)$  dependences were defined for different monthly generations of HPP\_Reservoir: 370, 500, 600, 700, 800, 900 and 1000 GWh (Fig 22).

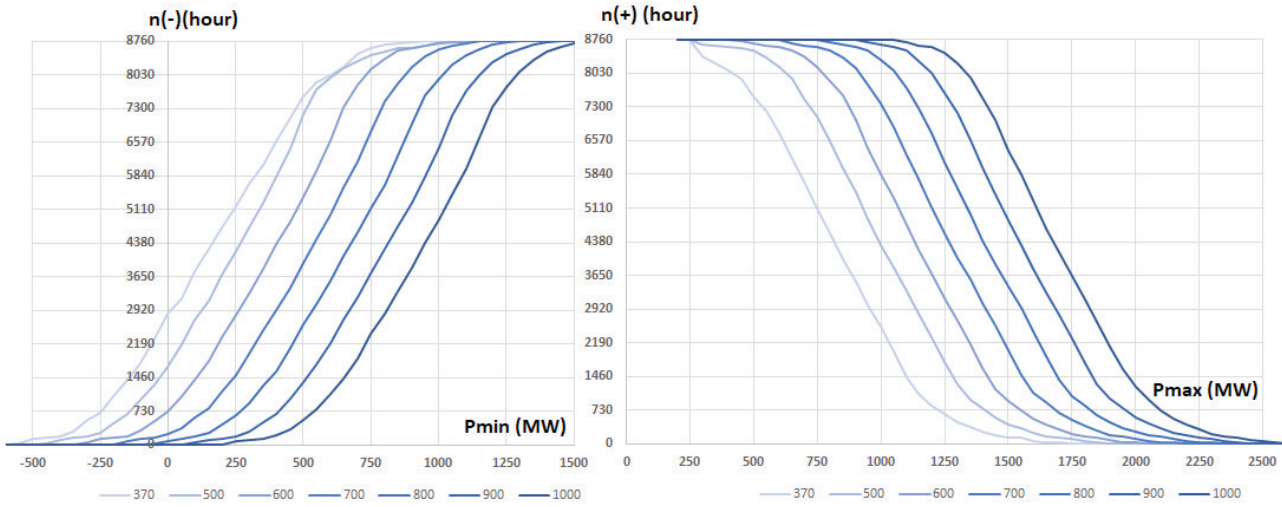


Figure 22.  $n_{(-)} = f(P_{\min}, E_M)$  and  $n_{(+)} = f(P_{\max}, E_M)$

For the algebraic representation of  $n_{(-)} = f(P_{\min}, E_M)$  and  $n_{(+)} = f(P_{\max}, E_M)$  the logistics function [3] had been used:

$$f(x) = \frac{L}{1 + e^{-k(x-x_0)}} \quad (16)$$

where

$x_0$  = the  $x$  value of the sigmoid's midpoint;

$L$  = the supremum of the values of the function

$k$  = the logistic growth rate or steepness of the curve.

In our case

$L$  = number of hours in a year = 8760

For negative reserves:

$k = 0.0059$

$x = P_{\min}$  and  $x_0 = 1.4E_M - 450$

For positive reserves

$k = 0.0059$

$x = P_{\max}$  and  $x_0 = 1.4E_M + 300$

So, the functions  $n_{(-)} = f(P_{\min}, E_M)$  and  $n_{(+)} = f(P_{\max}, E_M)$  have following forms (Fig 23 a, Fig 23 b):

$$n_{(-)} = \frac{8760}{1 + e^{-0.0059(P_{\min} - (1.4E_M - 450))}} \quad (17)$$

$$n_{(+)} = \frac{8760}{1 + e^{0.0059(P_{\max} - (1.4E_M + 300))}} \quad (18)$$

$k$  and  $x_0$  was determined empirically in a way that the points got with these equations were as close to the simulation result points as possible.

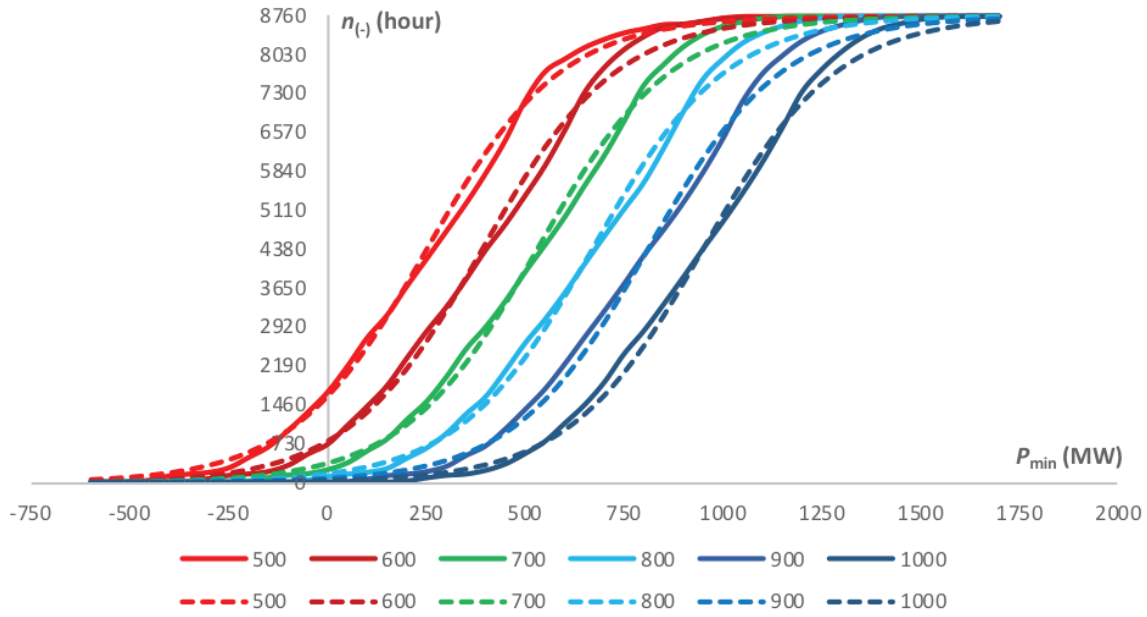


Figure 23 a.  $n_{(-)} = f(P_{min}, E_M)$  simulated values (solid) and logistics equations (dotted)

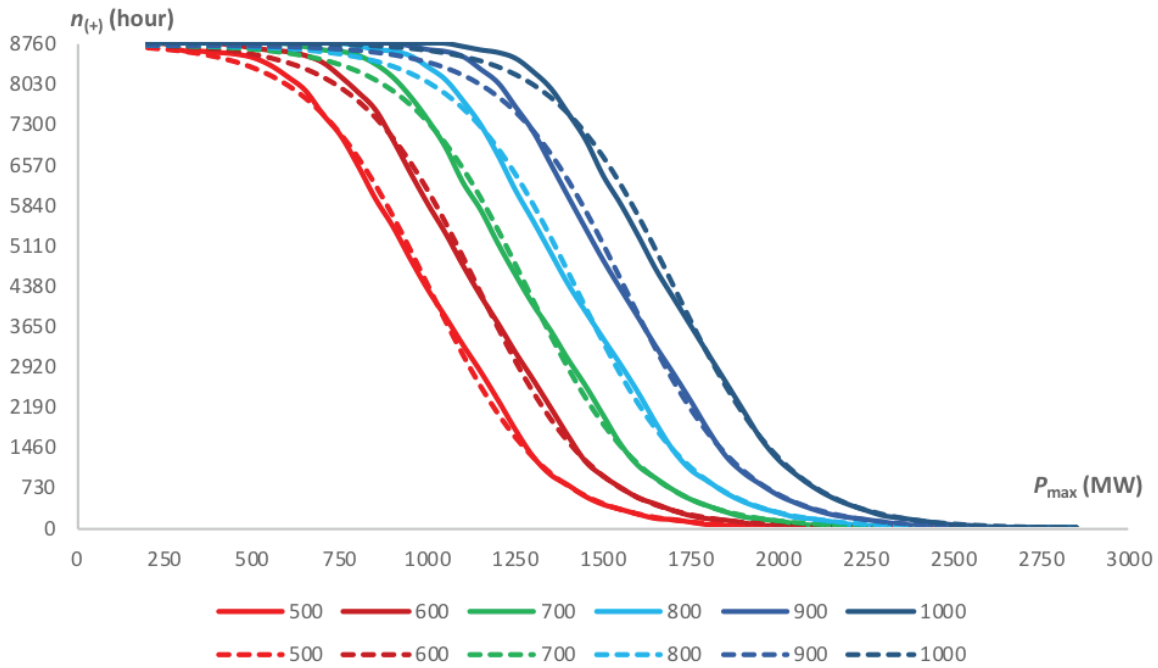


Figure 23 b.  $n_{(+)} = f(P_{max}, E_M)$  simulated values (solid) and logistics equations (dotted)

The equations (17) and (18) allow to define the needed  $P_{min}$  and  $P_{max}$  of the HPP\_Reservoirs, for the given monthly generation  $E_M$  in order not to exceed the given values of the reserve deficits:

$$P_{min} = (1.4E_M - 450) - \ln\left(\frac{8760}{n_{(-)}} - 1\right) / 0.0059 \quad (19)$$

$$P_{max} = (1.4E_M + 300) + \ln\left(\frac{8760}{n_{(+)}} - 1\right) / 0.0059 \quad (20)$$

In reality we have 12 different values of monthly generation  $E_M$ .



For instance, if the acceptable negative and positive reserve deficit time is less than 1% i.e. 87.6 hours and monthly generation of HPP\_Reservoirs is 500 GWh, than

$$P_{\min} = (1.4 \times 500 - 450) - \frac{\ln\left(\frac{8760}{87.6} - 1\right)}{0.0059} \approx -122 \text{ MW}$$

$$P_{\max} = (1.4 \times 500 + 300) + \frac{\ln\left(\frac{8760}{87.6} - 1\right)}{0.0059} \approx 1779 \text{ MW}$$

This means that, in case of 1% acceptable reserve deficit time, the power system should have ability to accumulate 122 MW power and to generate 1779 MW power.

## 7. CONCLUSIONS

1. Intensive discharging of Enguri HPP is not acceptable under conditions of integration of variable renewable sources, as the power system of Georgia, in such case, is non-dispatchable.
2. Due to the increased capacity of variable renewable energy sources, the variability of net consumption increases, which increases the number of reserves required.
3. Wind and solar plants should be geographically dispersed as evenly as possible, at least in 3-3 locations for Georgian power system. As gathering 500 MW of wind and 750 MW of solar at one location, without the geographical distribution, will cause reserve requirement increase from 400 to 550 MW, thus deepening the reserve deficit.
4. To ensure sufficient levels of reserves, a robust and reliable forecasting system for wind, solar and hydrology is needed.
5. The transmission system operator of Georgia should be able to start-stop individual gas turbines of the planned CCGT-3 and CCGT-4 and the existing CCGT-2 to quickly eliminate power shortages. This will actually eliminate the shortfall in positive reserves.
6. More flexible import arrangements with neighboring systems would be recommended, giving the rapid change of exchanges, including the reversing of exports to imports and vice versa.
7. For Georgian power system, it is recommended not to include in the memorandums of understandings, with the wind farms, the responsibility for compensation of the energy not produced, by the transmission system operator, in non-dispatchable conditions.
8. It is recommended to accelerate the projects of hydro storage plants that will remove the challenges of short-term reserves.
9. The deficit of the negative reserve hours increases with increasing of the value of the technical minimum and decreasing of monthly generation of the Reservoir HPPs  $n_{(-)} \downarrow \sim P_{\min} \downarrow, E_M \uparrow$
10. The deficit of the positive reserve hours increases with decreasing of the value of the technical maximums and increasing of monthly generation of the reservoir HPPs  $n_{(+)} \downarrow \sim P_{\max} \uparrow, E_M \downarrow$
11. The reserve deficit hour dependence on the technical maximum and minimum capacities and monthly generation of HPP\_Reservoirs have the saturation characters. It might be represented by the logistics function. This allows to calculate for the given monthly generation of HPP\_Reservoirs and acceptable reserve deficit time, what should be the technical minimum and technical maximum power outputs of the power system.

## BIBLIOGRAPHY

1. Ten-Year Network Development Plan of Georgia 2022-2032 [https://gse.com.ge/sw/static/file/TYNBP\\_GE-2022-2032\\_ENG.pdf](https://gse.com.ge/sw/static/file/TYNBP_GE-2022-2032_ENG.pdf)
2. Medium and long-term generation adequacy 2022-2035; [https://gse.com.ge/sw/static/file/Generation\\_adequacy\\_2022-2035.pdf](https://gse.com.ge/sw/static/file/Generation_adequacy_2022-2035.pdf)
3. [https://en.wikipedia.org/wiki/Logistic\\_function](https://en.wikipedia.org/wiki/Logistic_function)



# A Clustering and Benchmarking Based Monthly Electricity Consumption Analysis for Creating Energy Efficiency Insights to the Utility End-Users

**HAKAN DEMİRER<sup>1\*</sup>, ENGİN YILDIZTEPE<sup>2</sup>, RABİA NUR KALEM<sup>3</sup>, BURAK KESAYAK<sup>3</sup>, DOĞUKAN AYCI<sup>4</sup>, ESMA NUR CELTIKCI<sup>4</sup>**

<sup>1</sup>*Reengen Enerji Teknolojileri A.S.*

<sup>2</sup>*Dokuz Eylul University, Department of Statistics*

<sup>3</sup>*GDZ Elektrik Dagitim A.S.*

<sup>4</sup>*Reengen Enerji Teknolojileri A.S.*

**Türkiye**

## SUMMARY

The “MobileDSM Project” funded by the Turkish Energy Market Regulation Authority (EMRA) and managed by Gdz Elektrik (one of the largest Turkish distribution system operators), aims to improve the electricity end-users’ consumptions in terms of energy efficiency and demand-side flexibility. For this purpose, clustering and benchmarking based algorithms have been used to analyze energy usage performance and create actionable insights for end-users. The scope of the study includes energy consumption analysis (1), clustering users according to their energy consumption behavior using SoftDTW Barycenter method (2) and benchmarking similar user profiles in the same cluster among themselves (3). In addition, an end-user mobile application has been developed that presents the analysis results to users with energy performance indicators, graphical interfaces, and notification mechanisms. In this regard, the project directly addresses improving customer engagement and interaction in demand-side management applications by utilizing meter data with advanced analyses and creating interactive tools.

The study leveraged a substantial dataset comprising monthly electricity readings from fifty thousand subscribers over four years. Despite the challenge of low resolution, due to infrequent smart meter usage in Türkiye, the study supplemented this data with end-user surveys and outdoor air temperature data. This formed the basis for user clustering, employing a questionnaire probing into housing, household characteristics, and appliance usage. An accompanying mobile application provides users with comparative energy performance indicators and consumption alerts, hence promoting energy efficiency in regions with limited smart meter implementation.

## KEYWORDS

Monthly Electricity Consumption Analysis - K-means – Clustering – SoftDTW - Barycenter



**Oral Presentation:** A Clustering and Benchmarking Based Monthly Electricity Consumption Analysis for Creating Energy Efficiency Insights to the Utility End-Users

### 1. INTRODUCTION

In recent times, energy expenditures have seen a dramatic increase, largely instigated by the ongoing energy crisis. Consequently, household users are now facing heightened economic challenges as they strive to balance their need for energy with increasing costs. A telling example is Türkiye, where electricity prices have surged by over 30% in the past year alone [1]. The situation is similarly challenging in Europe, with several countries experiencing a double-digit percentage hike in electricity prices [2]. This crisis has resulted in wide-reaching ramifications, hindering energy accessibility, and exacerbating economic vulnerabilities across Europe and Türkiye studies indicate that almost 10% of households in Türkiye to afford to heat their homes adequately in 2020 [3], while in Europe, energy poverty affects approximately 50 million people [4]. Household users bear significant responsibility for energy consumption. In recent years, residential consumption has accounted for approximately 26-27% of the total energy consumption [5]. This substantial share underscores the critical role households play in energy utilization and the potential impact of energy efficiency measures in this sector.

Energy efficiency applications, therefore, are not just pivotal in managing this crisis but are also fundamental to both economic and environmental sustainability. They hold the promise of mitigating the adverse effects of increasing energy costs, while also reducing the environmental footprint by limiting greenhouse gas emissions. In this context, the “MobileDSM Project,” aims to refine energy consumption practices of electricity end-users through improved energy efficiency and demand-side flexibility. This objective is achieved via the application of clustering and benchmarking-based algorithms for energy usage analysis, user segmentation based on consumption habits, and comparative studies of similar user profiles.

In the project, a literature review was conducted focusing on the analysis of monthly electricity consumption data, segmentation/clustering/benchmarking methods, behavioral energy consumption, and user engagement in Demand-Side Management (DSM). Key resources on user engagement, and electricity consumption data analysis were compiled. The investigated studies cover a broad range of topics, including studies derived from high-frequency data and those analyzing overall load trends. While filtering, special attention was paid to the relevance of the datasets used in the studies to those of the project, the focus on energy efficiency and demand management, and the ability to derive useful conclusions from consumption data. Selected studies were then analyzed regarding their scope, methods, and findings.

First, end-user engagement is an indispensable part of a successful energy efficiency project outside of the technology stack. Many energy efficiency applications fall short in terms of adoption by users. On the other hand, some studies examine this issue with social sciences. In the study by Buchanan et al. [6], the authors examine consumer reactions to in-home energy displays (IHDs) through a qualitative methodology. By conducting interviews and observations with households using IHDs, they aimed to understand the behavioral and cognitive changes induced by these devices. The results of the study revealed that only a minority of users could make lasting consumption changes, pointing to the need for analytic skills and the identification of energy-saving actions as potential areas of improvement. Burchell et al. [7] also used a qualitative approach, utilizing interviews and focus groups to explore how community action and communication can enhance the use of energy consumption feedback. Their findings suggest that starting with local communities and social comparisons can enhance the appeal and engagement of the applications.

Secondly, large datasets play a pivotal role in analyzing user electricity consumption. These datasets often reveal varied consumption profiles, reflecting the fact that electricity usage is influenced by a multitude of parameters. The work of Gouveia et al. [8] is particularly noteworthy. They combined data from smart meters and door-to-door surveys to identify factors that influence residential electricity consumption. Their findings emphasized three key factors: the physical characteristics of the dwelling, the usage of heating/cooling equipment, and the profiles of the building occupants. Additionally, they found a strong correlation between temperature and electricity consumption, further illustrating the complexity of factors shaping energy use.

In order to perform a successful electricity consumption analysis, parameters such as the number of households, outdoor temperature, consumer behavior, etc., that affect residential energy consumption should be considered. On the axis of these variables, consumers exhibit different consumption profiles. Analyzing these consumption patterns is very useful in comparing the clustering of consumers and, thus, their consumption. Many different studies have developed different methodologies on clustering household consumption. Zhou et al. [9] developed a fuzzy clustering process model for monthly electricity consumption modeling. They used an enhanced Fuzzy C-Means (FCM) clustering approach, which differs from Hard Clustering by allowing a data point to belong to multiple groups. The results of this study were promising, with the fuzzy clustering model enabling electricity producers to develop targeted strategies based on consumption patterns and users to gain a better understanding of their energy usage. Oprea et al. [10] conducted a study where they analyzed the relationship between the energy-saving motivations of participants in a smart meter pilot and the tariffs that determine demand management. They applied clustering to create similar consumer groups, including households and small businesses. The results showed that tariff incentives were effective in demand management, but also emphasized the importance of users understanding and aligning these tariffs with their consumption. Yang et al. [11] utilized a k-Shape clustering algorithm





**Oral Presentation:** A Clustering and Benchmarking Based Monthly Electricity Consumption Analysis for Creating Energy Efficiency Insights to the Utility End-Users

to identify building energy consumption patterns. This algorithm was integrated into a Support Vector Regression (SVR) model to enhance energy forecasting accuracy across 10 institutional buildings. The results showed the algorithm's performance surpassing that of Dynamic Time Warping (DTW) clustering, with improved forecasting accuracy for 7 out of 10 buildings. Flor et al. [12] utilized machine learning and spatial analysis to define clusters of residential power load profiles using smart meter data from Ecuador. Their methodology, leveraging recurrent neural networks, yielded short-term load forecasts and uncovered consumption behaviors within specific geographic zones. This led to improved accuracy in predicting energy usage, demonstrating the significant potential of machine learning in energy management. The ENERGY STAR Score [13] provides a methodology that utilizes a combination of weather conditions, building characteristics, and consumption habits to form clusters and carry out trend analysis. A linear regression model is then employed within the clusters to determine the reference parameter value, and scoring is calculated accordingly.

Our research stands out by innovatively in terms of utilizing manual, monthly electricity readings in clustering analysis, contrasting with studies based on more granular smart meter readings. Besides, Soft Dynamic Time Warping (softDTW) methodology is used instead of conventional K-means clustering, supplementing data with user surveys and outdoor temperature readings for improved accuracy. Moreover, we provide individualized energy performance indicators via an energy management mobile app, enhancing user engagement in energy efficiency practices. Hence, our study offers a comprehensive, practical solution, promoting significant advancements in demand-side management strategies and energy efficiency.

The rest of this paper is organized as follows. Section 2 describes the materials and implemented methodologies in the study. Section 3 presents result of clustering and benchmarking studies. Section 4 presents discussion of study. Section 5 concludes the paper.

## 2. METHODOLOGY AND MATERIALS

Various clustering methodologies have been trialed to analyze the energy consumption habits of residential end-users located within the distribution company's region and to present appropriate performance indicators and comparative analyses. This process is aimed at fostering a deeper understanding of energy use patterns and promoting efficient energy practices among consumers.

The study initiated with the data processing of the procured large-scale data. For achieving optimal clustering results, different clustering methodologies were examined. Upon the determination of the preferred method, reference consumption was produced for the resultant clusters. Following this, based on the reference consumption specific to their clusters, performance scorecards were devised for the electricity consumers. This process offered a critical instrument for consumers to assess their energy utilization against a pertinent benchmark, thereby endorsing superior energy management practices.

### 2.1. Data Collection and Data Pre-Processing

For developing electricity consumption analysis models, a sample of 50,000 individuals was created within the region served by Gdz Electricity Distribution Company. Parameters such as income and education levels play a significant role in clustering subscribers. Including all levels and education backgrounds without bias in the regional selection has contributed to determining the cluster. Monthly manual meter readings spanning over four years for approximately 50,000 electricity subscribers were obtained through the distribution company's system. The monthly readings contained in the procured dataset were examined and filtered in light of their low reading frequency, the absence of missing consumption data, and the lack of outliers. This rigorous evaluation ensured a clean and reliable dataset, fostering robust and dependable analysis results. The dataset containing residential subscribers has information on monthly consumption values with time of use breakdowns. The electricity data of the subscribers included in the sampling was utilized for classification, analysis, and comparative analyses.

### 2.2. Methods

In the project's data analysis model determination studies, monthly meter readings and survey responses of electricity subscribers were used to examine their consumption according to the established criteria. The meter readings of a group of approximately 50,000 subscribers were initially compiled. Subsequently, the first study aimed to determine and implement the clustering method best suited for classifying electricity subscribers.

Initially, the Principal Component Analysis (PCA) method was attempted to segregate users into clusters. PCA is a technique employed to reduce the dimensionality of multidimensional data and identify key features. However, upon examining the results, it was concluded that the clustering outcome lacked sufficient consistency. Consequently, a more in-depth literature review was conducted, leading to the use of K-means Clustering and SoftDTW Barycenter methods.



**Oral Presentation:** A Clustering and Benchmarking Based Monthly Electricity Consumption Analysis for Creating Energy Efficiency Insights to the Utility End-Users

K-means Clustering is a widely used clustering method for separating data into similar groups. This method assigns each data point to a cluster according to the closest center and regroups each cluster around the center [14]. The K-means Clustering method allowed for dividing users into five clusters based on their consumption characteristics over the years. SoftDTW Barycenter is a method used to cluster time series data. This method employs a technique called Soft Dynamic Time Warping (SoftDTW) to calculate the distance between time series. The SoftDTW Barycenter method was used to analyze user consumption characteristics more precisely.

To perform a more detailed characterization and interpret clusters compared to randomly selected samples in the created residential clusters, the Barycentre averages of the clusters were taken, and graphs were plotted, attempting to display consumption patterns based on months and seasons [12]. For this purpose, the consumption trends of the clusters shared below were obtained. Each consumption trend was examined, and the seasonality effect was investigated to interpret the increases and decreases in consumption.

A seasonality study was conducted for subscribers belonging to the clusters obtained to verify the seasonality effect on electricity consumption as mentioned in the cluster descriptions. The distribution of electricity consumption at different outdoor temperature values for residences was derived for measuring the seasonality effect. This study particularly benefited from the heating, cooling, and base consumption separation work based on regression analysis, which was detailed in the literature review.

The Piecewise Regression method was used to detect heating and cooling loads in the seasonality analysis. Piecewise Regression is a regression method that uses different regression models between different sections in data sets. This method is used for data sets with different trends in different parts of the data. Piecewise Regression is employed when it is believed that a linear model is appropriate in a specific region of the data but not in other regions. This method separates the data set into distinct clusters and determines a separate regression model for each cluster [15].

Following a comprehensive exploration and selection of suitable clustering methodologies, reference consumption at a monthly level was derived from the averages within each cluster. Essentially, reference consumptions for each cluster were constructed as a mean of monthly electricity usage of the corresponding cluster, with a small fraction of outliers being detected and refined in advance. This procedure laid the foundation for developing performance scorecards for individual electricity consumers, juxtaposed against their respective cluster's reference consumption.

As a result, each user is assigned a reference consumption specific to their cluster. This critical stage offered consumers a tangible benchmark to compare their energy use against, fostering a culture of more efficient energy management practices. The application of these reference consumptions, in conjunction with the individual user's comparison against them, is integral to the mobile app's function of providing sustained feedback and fostering energy efficiency.

### 3. RESULTS

At this stage of the study, time series clustering, normalization, reference consumption generation and performance analysis studies shared in the methodology section were tested and the results were shared.

#### 3.1. Time Series Clustering Analysis

The K-means Clustering and Soft Dynamic Time Warping (SoftDTW) Barycenter methods facilitated the segregation of users into five distinct clusters based on their consumption characteristics, allowing for better data analysis. Figure 1 presents the initial output of the K-means clustering study. Each row of the matrix consisting of graphics represents a different cluster. 5 samples in each row belong to 5 different samples belonging to the related cluster. The electricity consumption trends of five subscribers from each of the five obtained clusters were compared according to electricity usage trends over the years. As seen in the Figure 1, a high degree of similarity was captured in the clustered data. Clusters differentiated between clusters in terms of seasonality and consumption intensity were obtained. However, it was decided that the result obtained should be improved.



Oral Presentation: A Clustering and Benchmarking Based Monthly Electricity Consumption Analysis for Creating Energy Efficiency Insights to the Utility End-Users

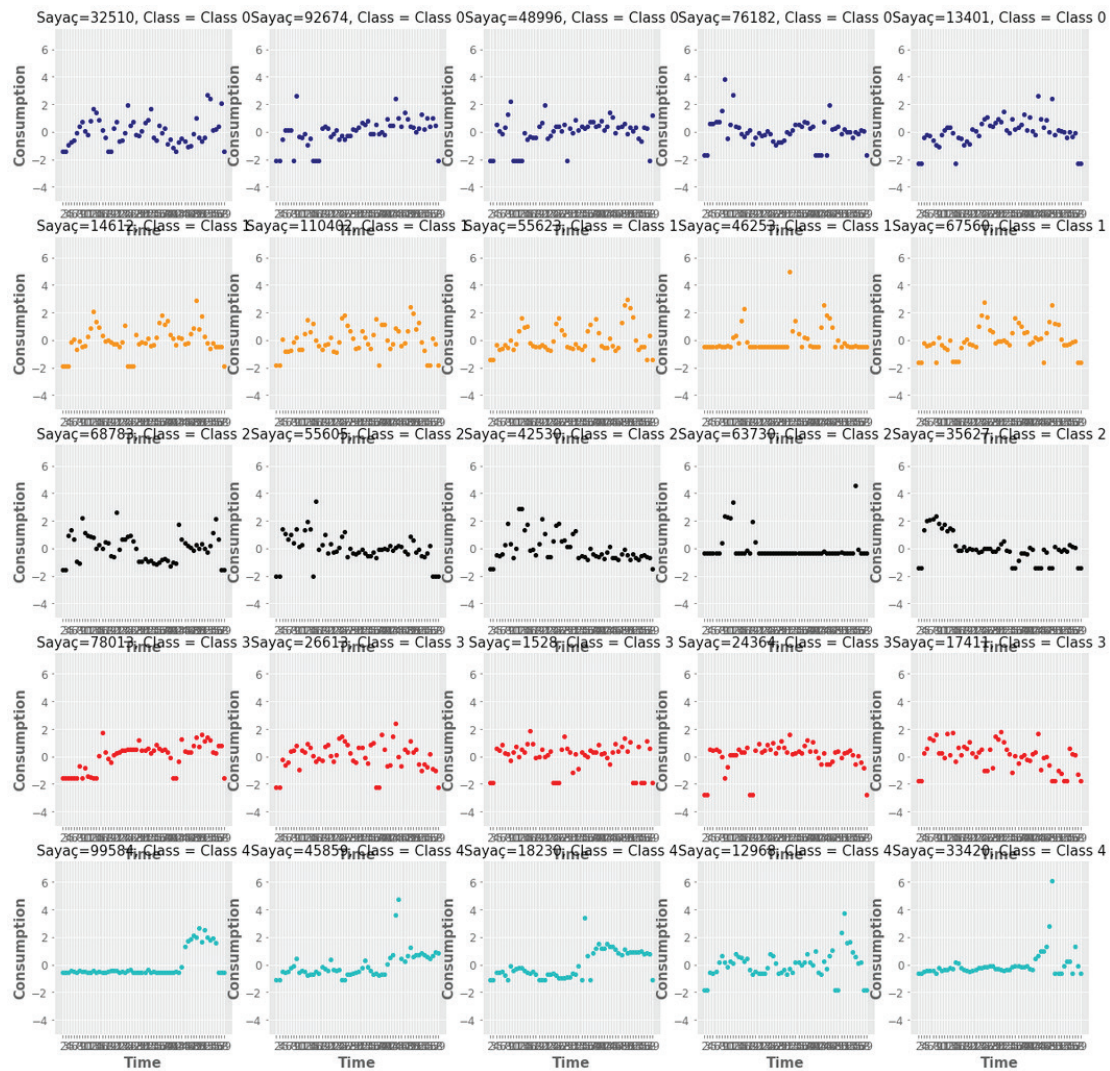


Figure 1. K-Means Clustering Results

In order to perform a more detailed characterization and interpret clusters compared to randomly selected samples in the created residential clusters, the Barycenter averages of the clusters were taken, and graphs were plotted, attempting to display consumption patterns based on months and seasons. Each consumption trend was examined, and the seasonality effect was investigated to interpret the increases and decreases in consumption. The SoftDTW Barycenter method allowed for a more precise analysis of user consumption characteristics, facilitating the identification of different user profiles. In the study conducted, consumers were segmented into five distinct groups through the application of the SoftDTW analysis. The SoftDTW introduces a differentiable loss function, which makes it more adaptable and efficient in handling complex time series data. The primary objective of this segmentation was to identify patterns and trends in energy consumption among different consumer groups. The time series analysis revealed that these groups could be characterized based on several factors.

The results of the Soft-DTW study performed after the K-means study are presented in Figure 2. Firstly, seasonal energy consumption was a significant differentiator among the groups. Some consumers showed a higher energy usage during certain seasons, possibly due to factors such as increased heating during winter or cooling during summer. This seasonal variation in energy consumption can provide valuable insights into the energy needs and usage patterns of different consumer groups. For instance, the corresponding heating and cooling loads in summer and winter are easily seen in Cluster 0 (Fig 2.a) and Cluster 1 (Fig 2.b). Both clusters successfully indicate the seasonality effect. On the other hand, there is no seasonality effect in Cluster 3 (Fig 2.c). This indicates that the residences of Cluster 3 do not use electricity for heating or cooling. In Cluster 4 (Fig 2.d), it is seen that the residences that increase their electricity consumption are grouped within the years. It is predicted that the main reason for this is electrical household appliances such as dryers, which have become widespread in residences. The survey responses we collect from users highly confirm the cluster results.



Oral Presentation: A Clustering and Benchmarking Based Monthly Electricity Consumption Analysis for Creating Energy Efficiency Insights to the Utility End-Users

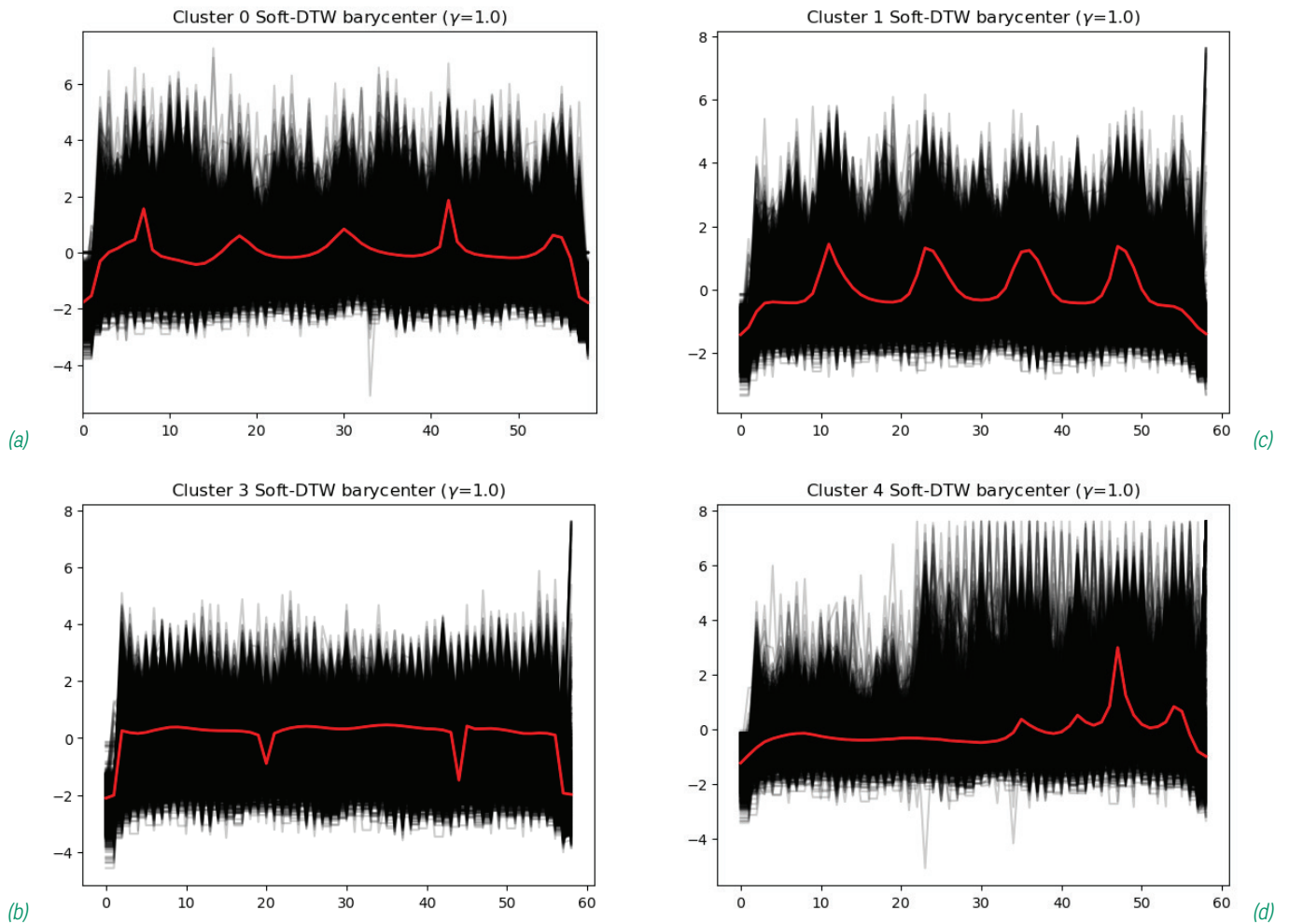


Figure 2. Soft-DTW Barycenter Clustering Results

### 3.2. Piecewise Regression Analysis

As mentioned in the results of the clustering study, seasonal behavior is one of the most distinguishing factors in residential energy consumption trends. The electrical heating and cooling loads of the users could be observed in the trends of the year of the month. In order to better observe the seasonality effect of the study, besides the time series consumption analysis, the temperature consumption distribution was also analyzed.

Piecewise linear regression to delve into the energy consumption patterns of each user throughout the year, in relation to the temperature data of their respective regions. This method is particularly useful when dealing with complex datasets where the relationship between variables is not simply linear, but changes depending on the value of the independent variable. In this case, the temperature data served as the independent variable, while the energy consumption of each user was the dependent variable. By dividing the temperature data into different segments or “pieces” and fitting a separate linear regression model to each segment, a more nuanced understanding of the relationship between temperature and energy consumption was achieved.

This analysis revealed the sensitivity of the consumer to temperature changes and their behavior in different temperature ranges. In Figure 3.a, the number of breakpoints obtained as a result of iteration in determining the breakpoints of the users depending on the temperature distribution is seen. This is a significant aspect of energy consumption analysis, as it helps in understanding how changes in temperature affect energy usage. For instance, during colder months, consumers might use more energy for heating, while during warmer months, the energy usage might increase due to cooling needs. Comparing Figure 3.b and 3.c, it is observed that the consumer represented in Figure 3.b utilizes electricity solely for heating, whereas the consumer depicted in Figure 3.c employs electricity for both heating and cooling. Understanding this temperature sensitivity can provide valuable insights for both consumers and energy providers, aiding in energy conservation for consumers and more accurate energy demand prediction for providers.





Oral Presentation: A Clustering and Benchmarking Based Monthly Electricity Consumption Analysis for Creating Energy Efficiency Insights to the Utility End-Users

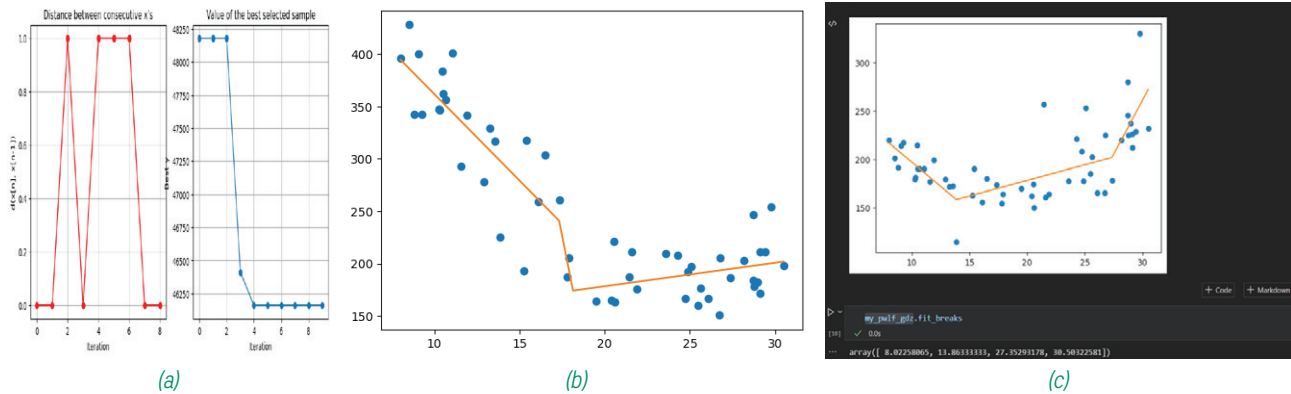


Figure 3. Piecewise linear regression analysis (a) Iteration Results for finding best consumption breakpoints number, (b) Household with electric heating load without cooling load, (c) Household with both electric heating and cooling load

### 3.3. Benchmarking and Energy Performance Analysis

In the calculation of reference consumption, average values from each cluster's time series were utilized. Initially, the z-score standardization method was employed to identify outliers within the same cluster. Subsequently, the monthly average consumption for each cluster was assigned as the reference consumption to each resident within the corresponding cluster. Finally, individual residents' consumption was compared with the assigned reference consumptions, facilitating the ranking and scoring amongst cluster members.

## 4. DISCUSSION

This research presents an innovative approach to energy efficiency awareness by leveraging monthly electricity meter readings, a data resolution that's been traditionally challenging for analysis. The intent was to devise a scalable solution devoid of additional hardware costs, thus appealing to the wider base of distribution system operator energy users. To fortify the low-resolution monthly data, it was enriched with weather information and end-user survey responses. This method has provided electricity users with a convenient and scalable solution to raise awareness of energy efficiency in countries that have not completed the smart meter transformation, such as Türkiye.

In our study focusing on the analysis of monthly electricity meter readings, several clustering methodologies were evaluated. The SoftDTW Barycenter method proved superior, outperforming traditional techniques like K-means. By complementing this method with data enrichment strategies, we obtained insightful user energy consumption behaviors. The SoftDTW Barycenter, a time series data clustering approach, facilitated precise characterization of user profiles. Our methodology allowed for detailed investigation into consumption trends, highlighting seasonality effects on energy usage. This progressive approach to clustering, augmented by our data enrichment strategy, unearthed deeper, more actionable insights into user energy consumption behavior.

Consequent to the clustering, reference consumption patterns were established for each user, enabling the creation of personalized energy performance indicators. These indicators, along with energy-saving suggestions, were shared with users via a specially designed mobile application. The benchmarks provided through this application foster a heightened awareness of energy consumption trends and equip users with the knowledge to implement more efficient energy practices.

## 5. CONCLUSION

This study, strategically structured to avoid additional hardware or complex installations, leveraged a mobile application for uninterrupted and direct user interaction. With a primary focus on analyzing energy consumption patterns, the study used SoftDTW Barycenter-based clustering and benchmarking algorithms to classify users and compare similar profiles within the same cluster. A significant highlight was the creation of distinctive electricity consumer profiles that further revealed the impacts of seasonal consumption variations. The research ingeniously incorporated end-user surveys and outdoor air temperature data to augment monthly electricity readings. The resultant dataset formed the basis of user clustering, leading to the development of a user-friendly mobile application that furnishes energy performance indicators, graphical interfaces, and consumption alerts, thereby fostering energy efficiency and customer engagement.



**Oral Presentation:** A Clustering and Benchmarking Based Monthly Electricity Consumption Analysis for Creating Energy Efficiency Insights to the Utility End-Users

## 6. ACKNOWLEDGEMENT

The authors appreciate the Turkish Energy Market Regulation Authority (EMRA) for their funding of the “MobileDSM Project”, instrumental to this research’s successful completion.

## BIBLIOGRAPHY

- [1] Türkiye Electricity Pricing Report, 2022 [Online]. Available: <https://www.epdk.gov.tr/Detay/Icerik/3-1327/elektrik-faturalarina-esas-tarife-tablolari> [Accessed: May 18, 2023].
- [2] Europe Energy Market Review, 2022 [Online]. Available: [https://energy.ec.europa.eu/data-and-analysis/market-analysis\\_en#electricity-market---recent-developments](https://energy.ec.europa.eu/data-and-analysis/market-analysis_en#electricity-market---recent-developments) [Accessed: May 16, 2023].
- [3] Energy Poverty in Türkiye, 2021 [Online]. Available: <https://www.eppedia.eu/article/202energy-price-crisis-impacts-energy-poverty-turkiye-0> [Accessed: May 18, 2023].
- [4] European Energy Poverty Report, 2022 [Online]. Available: <https://www.odyssee-mure.eu/publications/policy-brief/european-energy-poverty.pdf> [Accessed: May 18, 2023].
- [5] Electricity Distribution Sector Report (TEDAŞ, Türkiye, 2021) [Online]. Available: [https://www.tedas.gov.tr/#!Sektor\\_rapor](https://www.tedas.gov.tr/#!Sektor_rapor) [Accessed: May 18, 2023].
- [6] K. Buchanan, R. Russo, and B. Anderson, “Feeding back about eco-feedback: How do consumers use and respond to energy monitors?” *Energy Policy*, vol. 73, pp. 138-146, 2014.
- [7] K. Burchell, R. Rettie, and T. C. Roberts, “Householder engagement with energy consumption feedback: the role of community action and communications,” in *Energy Policy*, vol. 88, pp. 178-186, 2016.
- [8] Gouveia, João & Seixas, Julia & Luo, Shiming & Bilo, Nuno & Valentim, António. “Understanding electricity consumption patterns in households through data fusion of smart meters and door-to-door surveys” (2015).
- [9] Kaile Zhou et al., “Household monthly electricity consumption pattern mining: A fuzzy clustering-based model and a case study,” *Journal of Cleaner Production*, vol. 141, pp. 900-908, 2017.
- [10] Oprea, S. V., Bucur, C., & Ionescu, R., “Insights into demand-side management with big data analytics in electricity consumers’ behaviour,” *Computers & Electrical Engineering*, vol. 89, 2021.
- [11] Yang, J.; Ning, C.; Zhang, F.; Deb, C.; Cheong, K.W.D.; Lee, S.; Sekhar, C.; Tham, K., “K-Shape clustering algorithm for building energy usage patterns analysis and forecasting model accuracy improvement,” *Energy and Buildings*, vol. 146, 2017.
- [12] Flor, M.; Herraiz, S.; Contreras, I., “Definition of Residential Power Load Profiles Clusters Using Machine Learning and Spatial Analysis,” *Energies*, vol. 14, 6565. <https://doi.org/10.3390/en14206565>, 2021.
- [13] “ENERGY STAR Score,” U.S. Environmental Protection Agency, 2018 [Online]. Available: <https://portfoliomanager.energystar.gov/pdf/reference/ENERGY%20STAR%20Score.pdf> [Accessed: May 16, 2023].
- [14] Papadopoulos, A. I.; Karteris, M. M.; Chalatsis, T.; Vasileiou, M., “The Impact of the Characteristics of the Residential Stock on the Energy Behavior of the Households of the Five Largest EU Consumers,” *Energies*, vol. 11(4), 859. MDPI AG. Retrieved from <https://doi.org/10.3390/en11040859>, 2018.
- [15] Mathieu, J. L.; Price, P. N.; Kiliccote, S.; Piette, M. A., “Quantifying Changes in Building Electricity Use, With Application to Demand Response,” *IEEE Transactions on Smart Grid*, vol. 2(3), pp. 507-518, 2011. doi:10.1109/tsg.2011.2145010.





# The Frequency Stabilization Using Battery Energy Storage System (BESS) in 400 kV Power Systems: a simulation study

[ergin.kayar@teias.gov.tr](mailto:ergin.kayar@teias.gov.tr)

**HAMZA FEZA CARLAK<sup>1</sup>, ERGİN KAYAR<sup>1,2,\*</sup>**

<sup>1</sup>*Department of Electrical and Electronics Engineering, Akdeniz University*

<sup>2</sup>*Western Mediterranean Load Dispatch Directory, TEİAŞ*

**Türkiye**

## SUMMARY

Energy storage systems are one of the most important systems to improve the power system's flexibility, economy, and security. In recent years, with the rapid development of the energy storage industry, the use and applications for versatile and large-scale distributed grids have increased significantly. Power plants must have sufficient installed power capacity to meet the high demand and be continuously operated with adequate ability to meet real-time demand. Battery Energy Storage Systems (BESS) may present a more attractive solution for frequency regulation applications as they show significantly higher potential to provide frequency support services. Within the scope of the study, a feasibility study was carried out in which the Battery Energy Storage System provided frequency support. The instability of power generation and load demand causes severe problems in frequency stability. They effectively balance power generation and load demand since they have fast response characteristics. Various scenarios for frequency support and system load flow analysis were carried out using Dig-SILENT Power Factory software. Several study cases and failure scenarios were simulated in which the architecture of Battery Energy Storage Systems and their utility-scale applications in power systems were examined and tested. Different techniques, such as network frequency adjustment and power flow optimization, were analysed. In addition, particular features have been determined to support the voltage stability in the electrical networks when the Battery Energy Storage System was integrated into the power system. Combining BESS units with optimum power reduces energy loss and improves the voltage stability. Regulating the energy transmission line's active and reactive power simultaneously improves an electrical grid's voltage profile. The results will be compared with the current Turkish electric grid system, and the outputs will be evaluated to improve the interconnected Turkish system.

## KEYWORDS

Battery energy storage systems- distributed systems- frequency control- High Voltage-Interconnected system.



**Oral Presentation:** The Frequency Stabilization Using Battery Energy Storage System (BESS) in 400 kV Power Systems: a simulation study

### 1. INTRODUCTION

In recent years, optimization techniques have been applied to interconnected grid operations and controls for power system analysis worldwide. The main contributions of the applied optimization are reliability, techno-economic research, system stability, and production and consumption losses [1]. Power systems are becoming more complex due to increased load demand and the integration of renewable energy sources [2] [3]. Therefore, power systems optimization has become vital today to ensure the development of interconnected systems [4]. Various optimization issues in power system operations, such as optimal power flow, system stability, economical transmission, and so on, have been addressed and resolved [5]. Energy storage is critical in diversifying energy sources and adding more renewable ones to the market. Using energy storage, it can operate at optimum efficiency while accounting for variations in demand. Energy storage is one of the keyways to improve the power system's flexibility, economy, and security. In recent years, with the rapid development of the battery energy storage industry, its technology has shown features and trends for large-scale integration with multi-purpose collaboration and distributed applications. Using a battery energy storage system (BESS) can be an essential technology to improve the performance of power systems. BESS optimal sizing can reduce power losses, improve the voltage profile, and reduce peak demand in power systems. The BESS can react almost instantly to grid demands but can operate for extended periods with a wide range of storage and power capacities. Due to its technological efficiency, lead-acid chemistry has seen the most widespread use among large-capacity BESS [6]. BESS units are placed in the electrical interconnected network for load levelling, stabilization, load frequency, and voltage control [7].

Several significant problems affect electrical power systems today. Problems include increasing levels of inefficiency, reliability issues, environmental factors, economic development, increased demand, and new resilience requirements [8]. These problems are significant enough to require major changes in power systems planning and operating philosophy [9]. The BESS has proven suitable for dealing with these problems by improving the electricity grid and balancing generation and supply [10]. Integrating BESS into a power system provides enormous benefits. The BESS is well suited to support transmission system operators and overcomes the challenges posed by increasingly distributed, volatile, and uncertain generation from renewable energy sources [11]. Additional energy storage within the grid will allow many more facilities to operate closer to total capacity and reduce energy losses during electricity transmission. Energy storage is essential in diversifying energy sources and adding more renewable energy sources to the market. As a storage unit in power systems, the BESS provides a technological solution to improve power quality, reduce energy costs, reduce emissions, defer investment in transmission and distribution networks, and provide ancillary services to the system [12]. In addition, the BESS can lessen the need for emergency energy reserves. Grid efficiency and reliability can be improved with power quality. Electricity providers must have sufficient installed power capacity to meet peak demand and must continuously operate with adequate ability to meet real-time demand. Meeting these requirements typically means that accommodation is run at 20% above estimated demand, and only an average of 55% of installed generation capacity is used for a year [13].

System inertia is one of the most critical system parameters for the synchronous operation of power systems. The frequency stability of conventional power systems is the task of synchronous generators that respond quickly to any frequency fluctuation by absorbing or transmitting kinetic energy stored in their rotors and turbines to slow down the system's frequency dynamics [14]. Because storage systems respond dynamically and quickly to system frequency deviations, they are an excellent technology for supporting the frequency stability of modern power systems. Among the different technologies proposed for increasing frequency stability, energy storage was adopted in this research [15]. Specifically, this paper aims to model the Battery Energy Storage System to reflect grid-connected operating control strategies. To propose control strategies for voltage control, dynamic stability, and transmission capacity improvement, to compare the simulation and experimental results of the BESS system connected to an interconnected system, and to improve the efficiency and sustainability of the electrical network. To achieve this, it is necessary to develop a dynamic and reliable model for interruptions related to generation failures and sudden drops in load demand concerning the interconnected network and to apply a dynamic analysis capable of assessing the network frequency response [16]. A real-time simulation of the connected network was obtained using Dig-SILENT Power Factory by determining predefined condition scenarios on frequency response distortion occurrences under different BESS capacity ranges of frequency deviations of the network. To check the results, it is examined in two parts: temporary and dynamic models. Their models considered power control in normal operating mode and failure transition and protection segment in abnormal operating mode. The validity of the proposed models is proven according to the results of calculations after introducing the BESS models for simulation fault in a single generator system. The BESS has been fundamentally and widely studied to support frequency stability challenges. Since the BESS offers a fast active power response, the BESS is an excellent choice to compensate for the interconnected network's damaging effects by reducing the power system's oscillations. Based on the BESS development situation analysis, application scenarios such as reduction of power output fluctuations, output on the renewable energy generation side, electricity grid frequency adjustment, and power flow optimization were examined. The studies and implementation status of BESS in recent years were reviewed, and large-scale BESS energy management, operation control methods, and application scenarios were also examined in the study.



Oral Presentation: The Frequency Stabilization Using Battery Energy Storage System (BESS) in 400 kV Power Systems: a simulation study

Considering the abovementioned studies, this study supports the increasing demand level in the current power system. The aim is to keep the system frequency within the limit of 200 mHz of the nominal value to comply with the power quality standards according to the Turkish National Electricity Market. This study's central area of interest is to monitor transient stability in the Turkish electricity grid.

## 2. METHODS AND MODELS

### 2.1. Battery energy storage system technologies

The Battery Energy Storage System can be used in various aspects of the power system. BESS is currently a critical factor for sustainable energy in many countries, especially Europe, America, and Japan. A battery energy storage system consists of two parts. First, a piece of storage that can store/restore energy in an electrochemical process. The second is a rectifier/inverter that can convert the DC voltage in the storage section into the AC voltage required for the grid and vice versa. The rectifier/inverter usually is based on a voltage-sourced converter (VSC) with pulse width modulation (PWM). This way, energy using electrochemical conversion is stored from the grid or restored to the grid [17]. The BESS controls the grid system frequency response while providing auxiliary services such as voltage control, harmonic compensation, or local load protection, mainly when used for system control. When the system frequency is lower than 50 Hz, the BESS provides load flow to the system. On the other hand, BESS draws charge from the system when the system frequency is higher than 50 Hz and controls. It can be concluded that it is a fast and flexible element for the BESS power system. Generally, BESS can be used in various applications such as frequency control, power control, and load balancing since the BESS can provide active power compensation quickly. It has been investigated to determine the commercial and technical feasibility of the Battery Energy Storage System and the applicability of its various functions to the Turkish interconnected system. For example, peak demand response, demand response, and frequency adjustments are examined.

There are mainly 5 separate control sections in BESS control: Frequency controller, Voltage controller, Active Power (P) and Reactive Power (Q) control, Charge controller, and Current control (Figure-1, Figure-2).

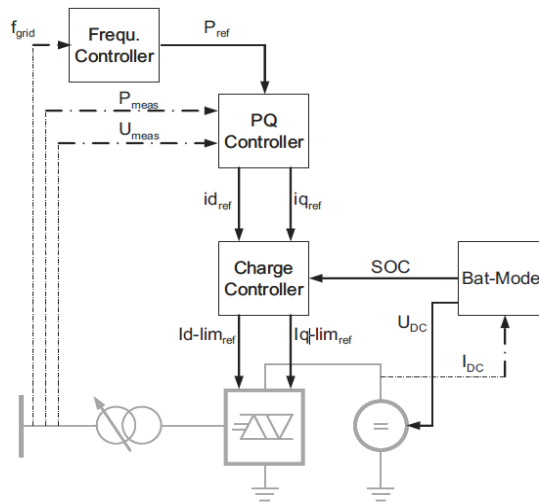


Figure 1. Block diagram of BESS structure

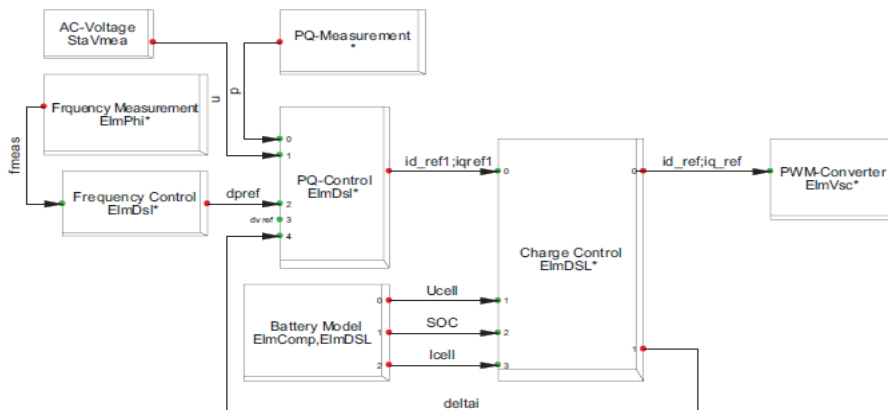


Figure 2. BESS behaviour model



Oral Presentation: The Frequency Stabilization Using Battery Energy Storage System (BESS) in 400 kV Power Systems: a simulation study

The BESS is designed for the behavior model shown in Figure 2. The power control strategy is like that of a PV system. BESS active power control can be achieved by monitoring the reference active current. The reactive power generated by the BESS will also provide voltage support for the busbar connected to the grid. The charge and discharge control module must control the SOC to meet the calculation requirements and ensure the battery’s terminal voltage maintains a linear change. The discharge voltage of a battery is also dependent on the SOC, and the battery should be recharged if the SOC is below a certain level so that the BESS can always control the active power in both ways. The battery voltage nonlinearly depends on the SOC, especially for 0 < SOC < 0.2. The BESS could only consume active power if the battery is not fully loaded (SOC < 1). The BESS could only supply active power if the battery is not discharged (SOC > 0). In this paper, we assume the battery can only work when 0.2 < SOC < 0.9, which means the battery will stop charging when SOC reaches 0.9 and stop discharging when SOC declines to 0.2.

A deterministic approach analyzes power system performance based on a predefined scenario while ignoring uncertainty in system states and parameters [18]. It assumes that all conditions are known and fixed. To ensure the robustness of the analysis, several typical scenarios with constant parameters are considered. The probabilistic method considers the probability distribution for one, some, or all the uncertain parameters and thus more accurately reflects the behavior of the natural system [19]. Probabilistic approaches are well adapted to analyzing systems involving randomness and uncertainty, both essential elements of future power systems [20]. As a result, the probability technique was used in this study to obtain more realistic results.

### 3. RESULTS

Research into modeling and simulating BESS is always one of the hottest topics in the world. The possibilities and scenarios of BESS implementation are also diverse. BESS contributes to the safe and stable operation of the electricity grid and has a positive role in the large-scale integration of this new energy. Various simulations were performed using a computer-aided power system design to verify the control strategy’s effectiveness and determine the BESS’s required size. This study analyzes how system uncertainty impacts the assessment of frequency stability. Compared to deterministic frequency stability analysis, the probabilistic approach to explaining various system uncertainty has led to a more accurate evaluation of frequency stability.

#### 3.1. BESS and Power Systems Modeling

Creating a grid power flow optimization model with a battery energy storage system is the research focus in this area. Many kinds of literature have aimed at energy transmission economics and modeled and solved different energy storage integration systems. This article examines the IEEE 9-bus 400 kV island model. The proposed methodology is first based on the power system model using the island system, a simplified representation of the high-voltage transmission network. The model has 3 synchronous generators with a total system production of 255 MW and loads of 252 MW (Figure-3). Specific changes have also been made to the overall system production to align with these research objectives, representing production uncertainty. A central BESS was installed on Bus-9 (Figure-4).

Total System Summary		Study Case: Gas Outage with BESS			Annex:		/ 1
No. of Substations	0	No. of Busbars	11	No. of Terminals	0	No. of Lines	6
No. of 2-w Trfs.	4	No. of 3-w Trfs.	0	No. of syn. Machines	3	No. of asyn.Machines	0
No. of Loads	4	No. of Shunts/Filters	0	No. of SVS	0		
Generation	= 254,63 MW		-20,06 Mvar		255,42 MVA		
External Infeed	= 0,00 MW		0,00 Mvar		0,00 MVA		
Load P(U)	= 252,00 MW		92,00 Mvar		268,27 MVA		
Load P(Un)	= 252,00 MW		92,00 Mvar		268,27 MVA		
Load P(Un-U)	= 0,00 MW		0,00 Mvar				
Motor Load	= 0,00 MW		0,00 Mvar		0,00 MVA		
Grid Losses	= 2,63 MW		-112,06 Mvar				
Line Charging	=		-140,37 Mvar				
Compensation ind.	=		0,00 Mvar				
Compensation cap.	=		0,00 Mvar				
Installed Capacity	= 374,50 MW						
Spinning Reserve	= 130,37 MW						
Total Power Factor:							
Generation	= 1,00 [-]						
Load/Motor	= 0,94 / 0,00 [-]						

Figure 3. Total system summary



**Oral Presentation:** The Frequency Stabilization Using Battery Energy Storage System (BESS) in 400 kV Power Systems: a simulation study

The system consists of 3 load buses and 3 generator buses with 6 arms. The BESS model is simulated and compared with the power system with and without the BESS connected, considering different distortions such as system performances, phase earth failure, transient line interruption, and load demand increase with various load levels. The effect and improvement of system inertia using fast-response BESS to facilitate increased load levels has been investigated through multiple case studies.

The coordination of the BESS depends on its effect on the power system, its type, and place of installation, as well as on the type and location of failures. Different case studies were examined to understand power system frequency stability and BESS coordination. The case studies are classified as follows:

- Case-1: Single-phase earth failure, three-phase earth failure
- Case-2: Overloaded line interruption during a failure
- Case-3: System overload demand events at various load levels
- Case-4: uncertainty of production load output power

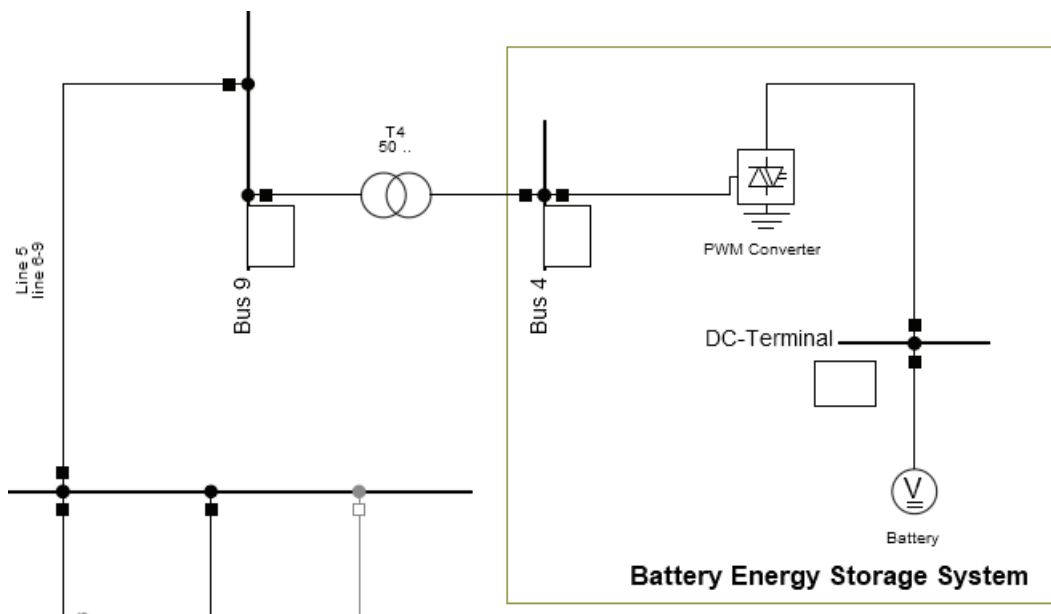


Figure 4. BESS busbar connection diagram

### 3.2. Oscillation Damping and Voltage Control

In conventional high-voltage networks, the voltage is controlled by changing the reactive power flow through different central nodes. The BESS can control both active and reactive power. The performance of the BESS controller has been extensively tested and compared using simulations. For the power flow calculation base-state study (without BESS), the voltage range was 0.89 p.u. and 1.02 p.u. The total reactive power loss was 89.67 MVar (Figure-5). These figures indicate that there is a problem with voltage drop. Figure-6 displays the voltage in p.u. of each busbar in the system after the installation of the BESS on the proposed busbar as a solution to the problem at hand. After power injection into the BESS system, the voltages of the other busbars have changed. When the BESS is installed on busbar 9, it can be observed that the voltage of the additional busbars in the system is considered better than when the BESS is connected to other busbars (Figure-6). Analysis of the power flow for the case study with the BESS showed values in the voltage range of 0.95 p.u and 1.05 p.u. In particular, the voltage level increased, and the total loss in the network was lower than in the primary case.

It was seen that installing the BESS in the correct position and size played an essential role in solving the voltage problem compared to the base situation and improving the overall voltage profile of the system. In addition, it showed that the total loss of the system was reduced. This research was applied in a test case to manage voltage drop and complete loss of active and reactive power and to control optimum power flow. The overview results from the comparison showed the effectiveness of the optimal placement and size of the BESS.



Oral Presentation: The Frequency Stabilization Using Battery Energy Storage System (BESS) in 400 kV Power Systems: a simulation study

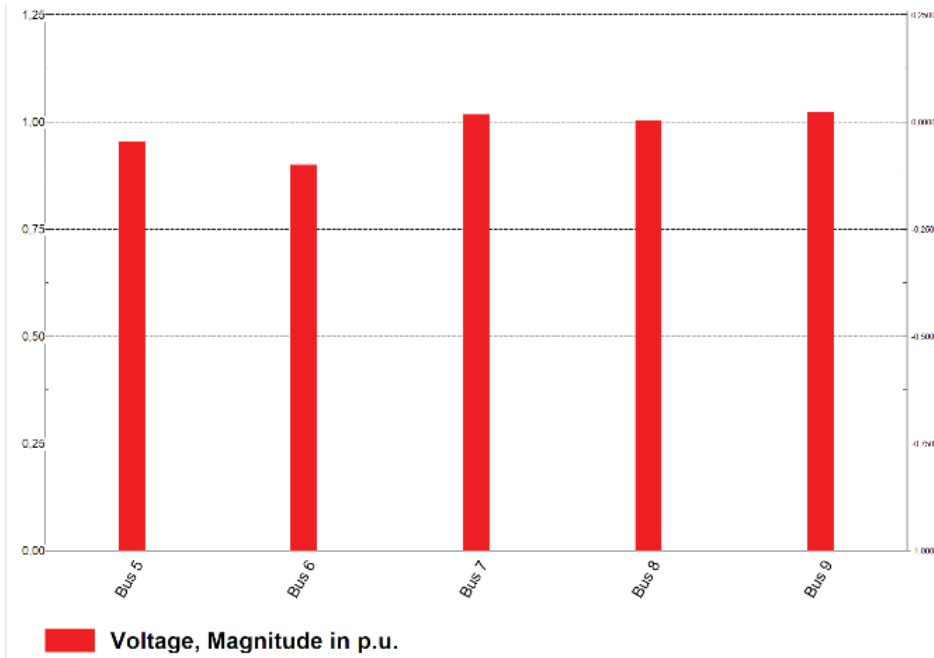


Figure 5. Busbar tensions without BESS

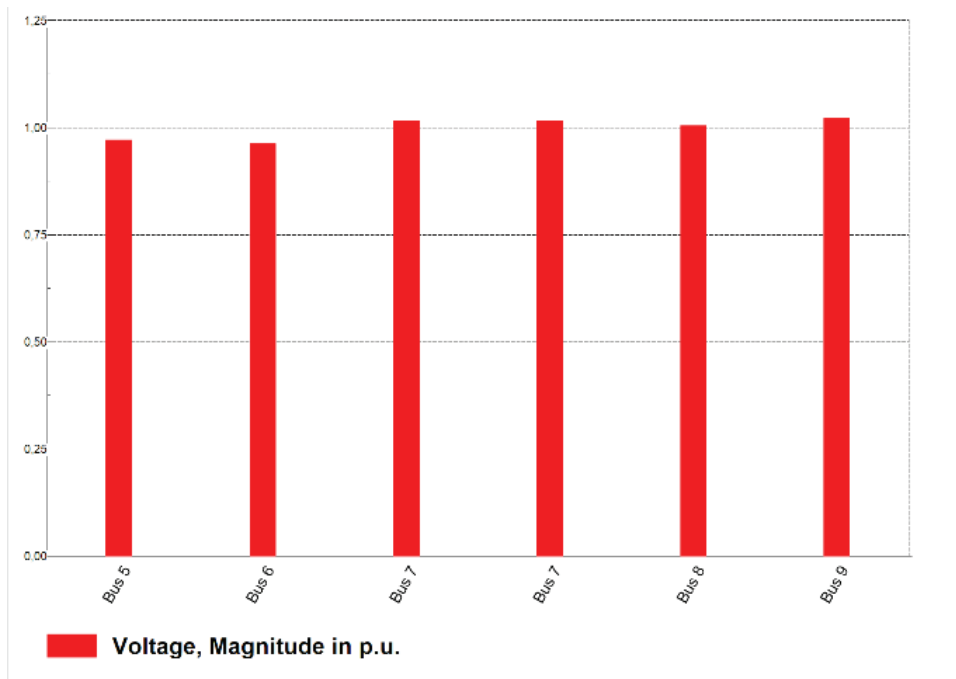


Figure 6. BESS connected busbar tensions

### 3.3. Frequency stability assessment and frequency regulation

Frequency stability can be defined as the power system's ability to maintain the system frequency at an acceptable level, i.e., within the standard operating frequency limit after an emergency. Integrating renewable energy sources greatly influences the power system's inertial and primary frequency responses, especially during contingency formation. Therefore, the transient frequency deviation under power system critical states has been tested. It compares the system frequency stability with and without BESS connected to the power system to support frequency stability in power systems. During a significant breakdown, such as a three-phase failure, the system frequency will drop drastically if the production cannot quickly meet the load demand. This considerable reduction will likely result in more extreme consequences, such as a system crash. Under-frequency load shedding plays a vital role





**Oral Presentation:** The Frequency Stabilization Using Battery Energy Storage System (BESS) in 400 kV Power Systems: a simulation study

in frequency control, and BESS can improve frequency control performance in load shedding. But many deviations may be more balanced in the short term. Since the frequency deviates to values higher than 50,020 Hz, the primary frequency controller must consume power; Since the frequency differs to values below 49.980 Hz, it must provide power. The load supply demand of the power system requires that the system frequency (50 Hz) be kept within the deviation limits of 200 mHz, except in abnormal or exceptional cases. For any loss more significant than the average loss of production, the event is called an emergency, and automatic low-frequency load shedding (UFLS) begins at 48.8 Hz. The UFLS is set to cut off the customer's power demand; If this is triggered, up to 9 phases are used to disconnect up to 60% of the load demand.

### 3.4. The first case, without BESS

In the first phase of the simulation, the power system was operated without the BESS to investigate the frequency response of emergency events. Figure-7 shows the frequency sub-point and its behavior. It is clear from Figure-7 that after the sudden power outage caused by the decommissioning of the gas turbine generator-2, the system frequency has dropped significantly from the average value (50 Hz). The frequency lower point of the system is outside the frequency operating standard. In addition, due to the absence of BESS at this stage, the frequency response is still supported by conventional generators. Therefore, conventional generators need to respond quickly to this unexpected situation to bring the system to a steady state level, as shown in Figure-7. On the other hand, when a more severe load failure occurs in a weak power system, the system frequency rises suddenly within a few seconds due to the low inertia of conventional generators and the delay of the response, which can cause failure. In this study, the power system is interrupted at 60 seconds, representing 20% of the total loads, to simulate a collapse of production in the grid. Before the outage, generators had worked to ensure the grid's stability. However, after the loss of production, as shown in Figure-7, the frequency increases significantly above the average frequency value by a minimum of 47,690 Hz and a maximum of 50,225 Hz. When these results are compared with the network frequency operating standard limits, as shown in Figure-7, it can be observed that the frequency response for the network is violated.

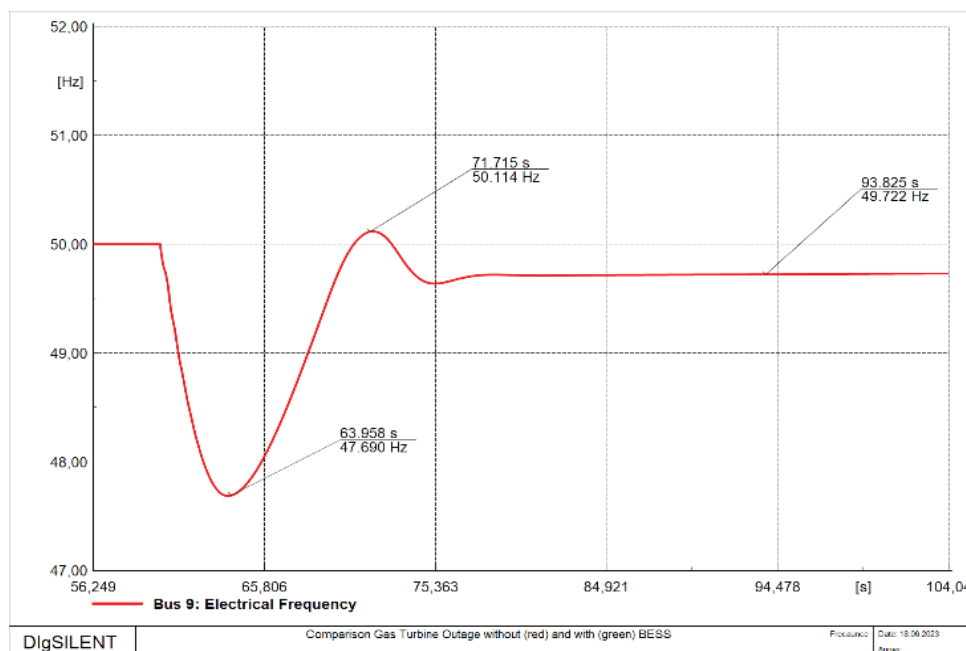


**Figure 7.** Network frequency fluctuation without BESS usage when the gas turbine is out of use.

### 3.5. The second case, with BESS

This study recognizes generator outages and power deficits as important emergency events. Therefore, to avoid this, a BESS is added to the grid to save the power system and eliminate the frequency system disorder of the generator regulators and save more time. Losses can occur during both charging and discharging the BESS. Therefore, in this scenario, the BESS is assumed to provide the same services in a generator emergency that needs upward frequency support to stabilize the frequency power system. Figure-8 shows the BESS frequency responses. As is clear from Figure-8, the BESS is involved in the supportive frequency response during an emergency event. The BESS controller at the optimum time, which helps minimize the frequency fluctuation from the targeted

**Oral Presentation:** The Frequency Stabilization Using Battery Energy Storage System (BESS) in 400 kV Power Systems: a simulation study

frequency, has significantly reduced this fluctuation in a system emergency, as shown in Figure-8. When energy sources lose 20% of the total power system production, the BESS shows the effect of the controller on minimizing frequency distortion. The BESS controller effectively reduced the frequency fluctuation during the system emergency event, as shown in Figure-8. The BESS can reduce high-frequency power surges, reducing the load on the traditional generation involved in inertial response and primary frequency control. It can be achieved by coordinating between the BESS and other production units. The simulation results have shown that system frequency dynamics can be improved with the help of BESS during emergency events. It can be applied to other power networks for which BESS frequency support is designed. However, many other aspects that could significantly improve frequency support in an isolated power system, such as adjusting the controller parameters of the BESS, need further investigation. The BESS device has effectively reduced peak frequency deviations by providing fast active power compensation. Frequency deviations are simulated and compared when the BESS is connected to the power system and the BESS is not. The frequency deviation reaches a maximum peak when the BESS is not connected to the power system.

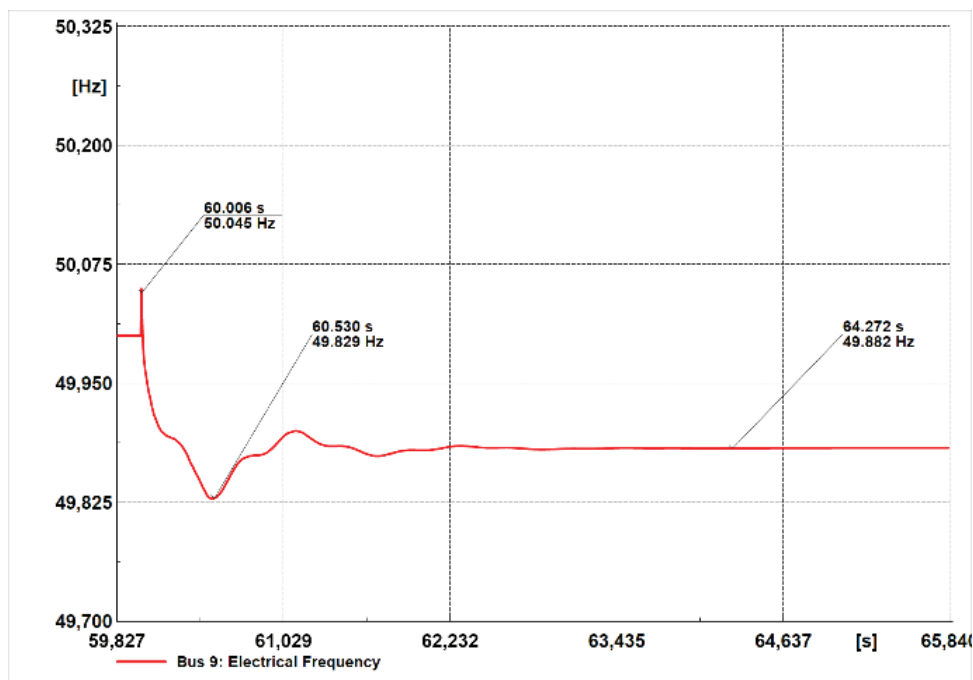


**Figure 8.** Gas turbine frequency fluctuation including BESS unit

## 4. CONCLUSION

Simulation models were used to examine interference between grid-connected BESS and power systems, to develop unified control strategies, and to examine BESS characteristics. The validity of BESS simulation models has also been proven compared to including a single generator system. A complete and accurate BESS model was created. As a result of examining the interaction between grid-connected BESS and power systems, the performance of peak load shifting, power surge smoothing, voltage adjustment, control, improving power quality, and limiting harmonics were analyzed. It demonstrated the advantages of using the BESS inertial controller to reduce the initial drop in the system frequency. It allowed time for low-inertia synchronous generators to provide the frequency response. The impact of the new energy integration process on system power angle stability is more pronounced with the increasing proportion of new energy capacity installed. Large-scale battery energy storage devices have shown the importance of reducing the impact and thus improving the grid capacity of new energy.

The energy storage technology application of the power system, which introduced the development of BESS applications and monitoring technology, was also analyzed in detail from the power supply, power grid, and power distribution sides. The BESS can help improve voltage and frequency levels and is listed as some of the most relevant applications in which the BESS plays an important role. In addition to its application for new power generation and transmission, the BESS has also been found to positively affect the power grid's security, stability, and economic functioning under various related constraints. *It has been shown that using a probabilistic frequency stability analysis approach, which explains the fate of system parameters such as load and generation uncertainty, results in a more accurate frequency stability assessment than the deterministic technique.* The test results show that the optimal placement and size of Battery Energy Storage Systems can be used in effectively solving grid management



**Oral Presentation:** The Frequency Stabilization Using Battery Energy Storage System (BESS) in 400 kV Power Systems: a simulation study

and grid upgrades in electricity transmission network integration. The electric power system has a distinct characteristic wherein power production and consumption should always be in sync without delay. Any disruption in this balance can cause a deviation in system frequency from its set-point value, leading to a decrease in the quality of the power supply. Hence, every power system operator must have enough active power reserves to tackle the worst credible contingency, such as losing the largest generation or transmission facility. The critical contribution of this research can be summarized as investigating the effect of considering different types of system uncertainty on frequency stability evaluation accuracy.

### BIBLIOGRAPHY

- [1] M. P. Haji Abbas and B. Mohammadi-Ivatloo, Optimization of power system problems: methods, algorithms and MATLAB codes, (vol. 262. Springer Nature, 2020).
- [2] J. Wang, X. Qi, F. Ren, G. Zhang, and J. Wang, "Optimal design of hybrid combined cooling, heating and power systems considering the uncertainties of load demands and renewable energy sources," *J. Clean. Prod.*, (vol. 281, pages 53-67, 2021).
- [3] L. Gan, P. Jiang, B. Lev, and X. Zhou, "Balancing of supply and demand of renewable energy power system: A review and bibliometric analysis," *Sustain. Futur.*, (vol. 2, p. 100013, 2020).
- [4] E. Naderi, M. Pourakbari-Kasmaei, and H. Abdi, "An efficient particle swarm optimization algorithm to solve optimal power flow problem integrated with FACTS devices," *Appl. Soft Comput.*, (vol. 80, pages 243-262, 2019).
- [5] Z. Ullah, S. Wang, G. Wu, H. M. Hasanien, M. W. Jabbar, H. S. Qazi, M. Tostado-Véliz, R. A. Turky, M. R. Elkadeem, "Advanced studies for probabilistic optimal power flow in active distribution networks: A scientometric review," *IET Gener. Transm. Distrib.*, (vol. 16, no. 18, pp. 3579-3604, 2022).
- [6] H. S. Chen et al., "Progress in electrical energy storage system: A critical review," *Progr. Natural Sci.*, (vol. 19, pp.291-312, Mar. 10, 2009).
- [7] FO. Alexandre, C. Rachid, B. Antoine, "Sizing and Optimal Operation of Battery Energy Storage System for Peak Shaving Application," (IEEE, Power Tech 2007, pages 621-625)
- [8] T. Yunusov, D. Frame, W. Holderbaum, and B. Potter, "The impact of location and type on the performance of low-voltage network connected battery energy storage systems," *Applied Energy*, (vol. 165, pages. 202 – 213, 2016).
- [9] M. Alizadeh, M. P. Moghaddam, N. Amjady, P. Siano, and M. Sheikh-El-Eslami, "Flexibility in future power systems with high renewable penetration: A review," *Renewable and Sustainable Energy Reviews*, (vol. 57, pp. 1186 – 1193, 2016).
- [10] G. L. Kyriakopoulos and G. Arabatzis, "Electrical energy storage systems in electricity generation: Energy policies, innovative technologies, and regulatory regimes," *Renewable and Sustainable Energy Reviews*, (vol. 56, pp. 1044 – 1067, 2016).
- [11] M. Koller, T. Borsche, A. Ulbig, and G. Andersson, "Review of grid applications with the Zurich 1mw battery energy storage system," *Electric Power Systems Research*, (vol. 120, pp. 128-135, 2015).
- [12] B. Lv and W. Yan, "Coordinated planning model of bess and controllable switches in distribution," *Electronics Letters*, (vol. 50, no. 20, pp. 1479-1480, September 2014).
- [13] R. Lamedica, S. Teodori, G. Carbone, and E. Santini, "An energy management software for smart buildings with fV2Gg and fBESSg," *Sustainable Cities and Society*, (vol. 19, pp. 173 – 183, 2015).
- [14] J. G. Kassakian, W. M. Hogan, R. Schmalensee, and H. D. Jacoby, *The Future of the Electric Grid*. (Boston, MA, USA: MIT Press, 2011).
- [15] D. McConnell, T. Forcey, and M. Sandiford, "Estimating the value of electricity storage in an energy-only wholesale market," *Applied Energy*, (vol. 159, pp. 422 – 432, 2015).
- [16] R.H. Leon, D. Siguenza, D. Sanchez, J. Len, P.J. Ruiz, J. Wu, D. Ortiz, A survey of battery energy storage system (BESS), applications and environmental impacts in power systems, (Proceedings of IEEE Second Ecuador Technical Chapters Meeting, 10.1109/ETCM.2017.8247485, 2017).
- [17] N. K. Medora and A. Kusko. Dynamic Battery Modeling of Lead-Acid Batteries using Manufacturer's Data. (Twenty-Seventh International Telecommunications Conference, INTELEC, 2005).
- [18] J.V. Milanović, Probabilistic stability analysis: the way forward for stability analysis of sustainable power systems, *Philos. Trans. R. Soc. A Math. Phys. Eng. Sci.* 375 (2100) (Jul. 2017), 20160296, <https://doi.org/10.1098/rsta.2016.0296>.
- [19] R. Preece, J.V. Milanović, Assessing the applicability of uncertainty importance measures for power system studies, (*IEEE Trans. Power Syst.* 31 pages 2076-2084 2016).
- [20] K.N. Hasan, R. Preece, J.V. Milanović, Existing approaches and trends in uncertainty modeling and probabilistic stability analysis of power systems with renewable generation, *Renew. Sustain. (Energ. Rev.* 101 pages 168-180 2019).



# Distribution Management System (DMS) Integration in Distribution Network of Kosovo

[turan.kocabayraktar@keds-energy.com](mailto:turan.kocabayraktar@keds-energy.com)

**TURAN KOCABAYRAKTAR\*, DRENUSHA GASHI, VJOLLCA KOMONI**

*Kosovo Electricity Distribution and Supply Company, University of Prishtina*

**Kosovo**

## SUMMARY

Supervisory Control and Data Acquisition (SCADA) consist of multiple computers, user interfaces, and communication networks in order to be able to monitor and control the field processes. This control system integrates hardware and software elements, enabling the different utilities to monitor and control the operational processes remotely while monitoring, collating, and analyzing the data in real-time with correct time tags. A very good part about this system is that it can be combined with other different network management systems. Such a system is Distribution Management System (DMS) that represents a supporting system of the SCADA system and a collection of applications designed for the purpose of monitoring and controlling the electric power distribution network with efficiency and reliability.

Modern systems like Distribution Management System (DMS) are a strategic investment which are necessary for distribution companies that face the challenges of competitive market and levels in increase of data exchange in real time. Based on the new functions developed and given the technology trends the company that manages with distribution network of Kosovo during 2022 has finished with development of DMS system in its distribution network.

The main focus of this paper will be to explain specifically the realization of DMS system, how the system is integrated with the existing SCADA system of Kosovo distribution network, which are the main functions of this system and what are the benefits of having Distribution Management Systems as a part of many other smart grid technologies on the network.

DMS as a system will access real-time data from SCADA system and provide all information based on the functions applied on the control center in an integrated manner, that will help operators to make intelligent and appropriate decisions. Real time load flow solutions in different parts of the distribution network will help dispatchers to verify the grid operating conditions and to take right decisions for resolving problems. Distribution Management System include all the functions from SCADA system coupled with the relevant application functions with support from different real time data and historical data.

The paper will start by giving short information about the electrical distribution network of Kosovo and knowing that the SCADA and DMS systems are interconnected systems, the paper will continue about substation's automation and SCADA realization in the distribution network.

The working principle of the DMS system, auto display builder and DMS main functions as Distribution System Power Flow (DSPF), Distribution System State Estimator (DSSE) that aims to compute an accurate estimate of system loads, Fault Management, Short Circuit Calculation (SCC) will be discussed in more details on another chapter of the paper.

The paper will end by taking a concrete example and by applying the main functions of the DMS system in a feeder of one of the districts of Kosovo distribution network. Paper will show comparison and data analysis based on the results obtained after the application.

## KEYWORDS

SCADA, Distribution Management System (DMS), Automation, Distribution Network, Kosovo



### 1. INTRODUCTION

#### 1.1 Distribution System Automation

It is known that the purpose of distribution system since its creation is basic, to operate on the basis of technical norms and to offer customers a quality and uninterrupted supply of electricity. The challenges to stick to this goal are many, because in recent years this system has been going through the phase of transition from traditionally simple networks to advanced and smart networks. The management of the distribution power system, its maintenance, control and monitoring are the main challenges of the companies that operate with the electric power system.

Every time in electrical substations it is necessary to make measurements, supervision, controls, operations and protective functions. For years these functions have been done manually by system operators, but with recent developments in data communication and digital electronic data processing microprocessors, a variety of new devices and systems are being introduced to automate the energy system. Given these challenges, power systems must be effectively monitored and controlled to take timely action and ensure uninterrupted power supply.

Systems such as SCADA, DMS, OMS, EMS are inevitable in the automation process of many substations the benefits of which are many in terms of control and monitoring of the electrical system. Precisely because of the many benefits, this study is mainly focused on the Distribution Management System (DMS), elaborating the functionality of its applications and the way of use in the distribution network of Kosovo.

#### 1.2. Automation of Kosovo’s substations

The distribution network of Kosovo has gone through many challenges to get in the state where it is right now. Distribution network of Kosovo includes all substation and parts of the medium and low voltage network. Specifically, it includes 35 kV, 20 kV, 10 kV lines with the possibility of switching to 20 kV along with the respective substations. Substations 35/10 kV, 10(20)/0.4 kV, 10/0.4 kV, 6/0.4 kV, 0.4 kV, low voltage lines and thousand individual customer meters are part of this system.

With the development of programmable digital systems, systems mainly based on the use of different microprocessors, all supervisory functions, control functions and protection functions can be combined in a single system, which then makes it even easier to use theirs. For such reasons, the focus of the activities of various operators around the world is the automation of the electricity distribution system, using the latest advances and developments in the field of technology and data communication systems. Such a focus over the years has also been for the company that operates the distribution network in Kosovo, the Kosovo Electricity Distribution and Supply Company (KEDS).

The main digitalization of the network has started with the installation of the SCADA system in the existing network. SCADA system in Kosovo Distribution Network has been completed in period of 3 years, by starting with installations on the field in 2018 and finishing total integration of medium voltage (MV) level in 2020. As a system, SCADA is designed to handle thousands of points captured from multiple sources in the field. Different equipment measuring elements helps in acquiring the data from the field, while the different equipment controlling elements help on implementing the control commands in the field. Typical signals gathered from remote locations include alarms, status, indications, analog values and totalized meter values [1]. The basic SCADA functions installed in the existing network include remote control of field equipment, data acquisition, human- machine interface, historical data analysis, and report writing. SCADA system can support dispatchers, operators, engineers, managers, etc. with tools to predict, control, visualize, optimise the system.

During the implementation of the SCADA system, Kosovo Electricity Distribution and Supply Company managed to implement a similar system that include half of the functions of the Outage Management System (OMS) to monitor the status of network failures (faults). While after the realization of the SCADA system, it was immediately continued with the integration of the DMS system.

SCADA		DMS		OMS	
Operation & Planning		Grid Optimization		Outage Management	
Monitoring	Control	Analyze	Optimize	Track	Restore

Figure 1. SCADA-DMS-OMS in distribution network of Kosovo



## 2. DISTRIBUTION MANAGEMENT SYSTEM IN KOSOVO DISTRIBUTION NETWORK

### 2.1. Distribution Management System (DMS)

DMS applications are used for the optimal management of electrical operation and planning work. A distribution management system (DMS) presents a number of applications that serves to monitor and control the electric power distribution networks efficiently.

### 2.2. DMS Functions

Within DSO of Kosovo, Distribution Management System (DMS) represents a supporting system of SCADA and a collection of applications designed for the purpose of monitoring and controlling the electricity distribution network efficiently and reliably. The two main functions of DMS are:

- Network visualization and support tools
- Individual advanced applications

With the implementation of the SCADA system, the DSO of Kosovo was able to control the feeder up to the circuit breaker point, without having a 10(20)/0.4 [kV] network visualization. In order to have a view of the network (lines, transformers) that supplies customers, DSO decided to implement the DMS system, which provides an end to end integrated view of the entire distribution spectrum. DMS system it was decided to take the basic data from an existing software where all network data were arranged and used for the analysis of distribution systems of electricity. The database of the software fully integrates all the data required for the determination of case studies, single line diagrams of substations or feeders, graphical results and various calculation options and possibilities. To create the right topology, there has been a process of preparing complete data for the electricity network in the software for network modeling in order to convert and integrate this data within the DMS system. Stages of data integration in DMS include: comparison of elements, modeling of elements, interconnection of elements, naming of elements, analysis of elements, exported data preparation, data conversion to SCADA topology, import to DMS system.

#### 2.2.1. Kosovo Distribution Network Visualization in DMS

Most of the distribution network of Kosovo is radial network. Existing SCADA system it is monitoring and controlling in real time more than 1000 MV cubicles of this network.

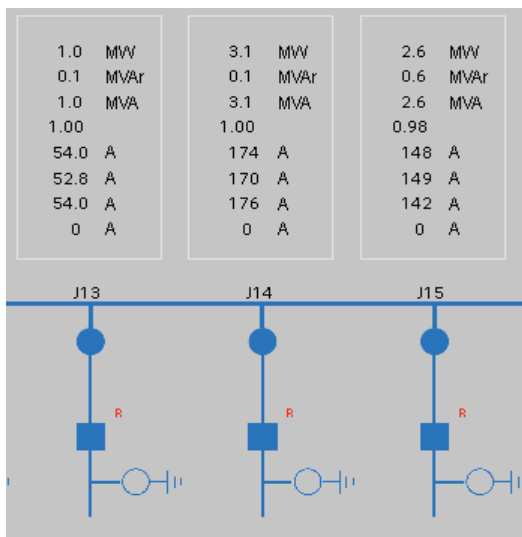


Figure 2. Feeder visualization in SCADA up to CB point

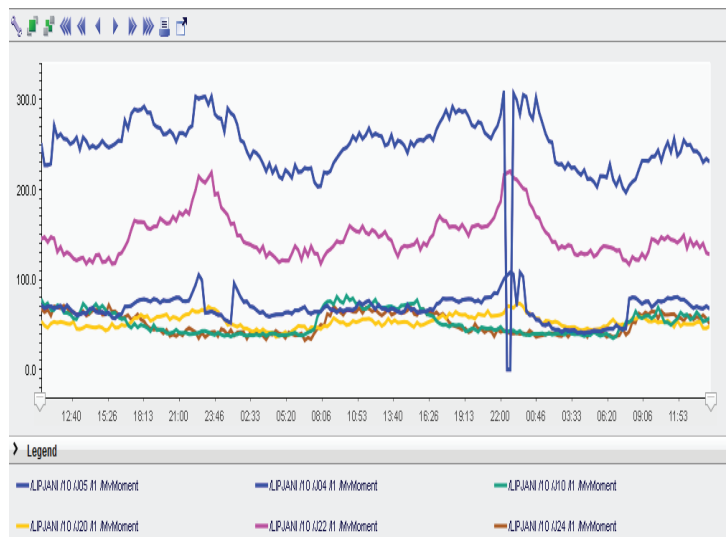


Figure 3. Analog values visualization in SCADA system

Figure 2 represents cubicles in SCADA which are in charge of controlling the distribution of power. Different data like current for each phase, active power in MW, reactive power in MVar, apparent power in MVA can be seen in the front view of single line diagram of respective substation. The system gives the opportunity to read more analog values like line and phase voltages, frequency, power factor etc. In the same time the system offers digital signals that include switch positions, disconnectors and circuit breaker positions in a power system.





While, DMS network visualization it determines distribution network topology based on the connectivity model and the status of switch devices. After network data integration in the DMS, feeder visualization it is provided as an autodisplay builder having in consideration all necessary connection points and network data. It also displays feeder circuit colorization signifying energization status and supplying paths.

The autodisplay builder in the DMS system of Kosovo distribution network has many features that can be used for monitoring and analyses, but the main features of autodisplay builder include:

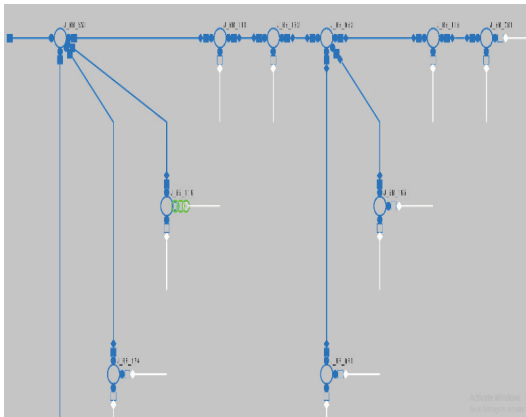


Figure 4. Feeder visualization in DMS

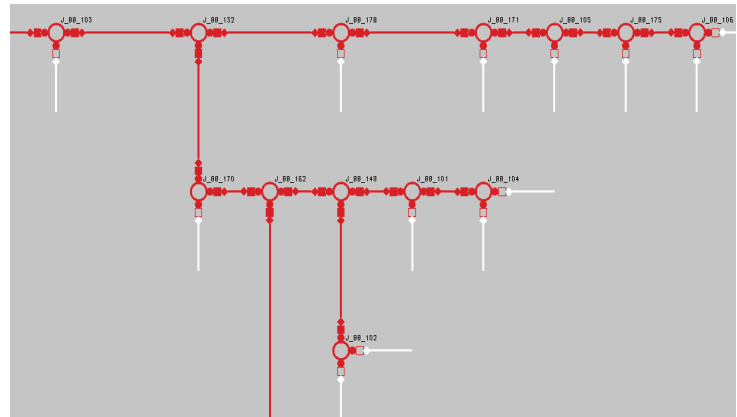


Figure 5. Feeder visualization in DMS

- Determine and show all network elements for the downstream of a selected element
- Determine different elements of the distribution network by name
- Locate and mark supply paths of network elements – visualization of power flow
- Determine energization status of network elements
- Determine and highlight network loops
- Determine and highlight all alternative supply for the feeder
- Color line segments and nodes with voltage magnitudes less than specified values
- Color line segments with loading greater than specified values

Autodisplays are generated automatically and all topological data modifications are instantaneously displayed without any graphical work. When the network is reconfigured, the extensions and coloring of feeders change dynamically.

## 2.2.2. Distribution Management System Functions

In automation systems of distribution network of Kosovo, Distribution Management System (DMS) includes monitoring, analysis, control, optimization and planning tools that all function on a common representation of all distribution network. This system includes all the functions from SCADA coupled with the relevant application functions with support from different real time data and historical data.

Used DMS it is able to represent all elements of the distribution networks, including different conductor types, transformers, loads, switches and monitor the status of these ones by combining real time data and historical ones. In order for the functions to operate properly, DMS requires a lot of analog-digital data which changes quickly. The real data it's obtained from SCADA system while the historical ones (load of transformers) were taken from AMR (automatic meter reading), were analyzed and inserted in the system for proper operation. Demand management and response are being recognized as important drivers for active user participation in the energy market. [2]

The main functionalities of DMS include real-time monitoring and control through the existing system of SCADA and many additional advanced applications, such as:

- Distribution System Power Flow (DSPF)
- Distribution System State Estimator (DSEE)



Oral Presentation: Distribution Management System (DMS) Integration in Distribution Network of Kosovo

- Short-Term Load Scheduler (STLS)
- Fault Management (FM)
- Fault Isolation and Service Restoration (FISR)
- Optimal Feeder Reconfiguration (OFR)
- Short-Circuit Calculation (SCC)
- Volt/VAR Control (VVC)

**Distribution System Power Flow (DSPF)** - When the topology on the system is determined, the network data and specifically load (active and reactive power) are inserted, power flow on the feeder visualization will be enabled. DSPF calculates voltages for all nodes (busbars) and the most important result are flows (active and reactive powers and currents) through lines and transformers, and active and reactive power losses. The DSPF also provides the operators in the main control center (MCC) with calculated line section current and power flow values and node voltage values. The system will alert operators to abnormal conditions out on the feeders and exact points (line, transformers) such as low voltages at different nodes and overloaded line sections. DSPF calculates the network by using the predefined load profiles/curves, without considering the measurement values.

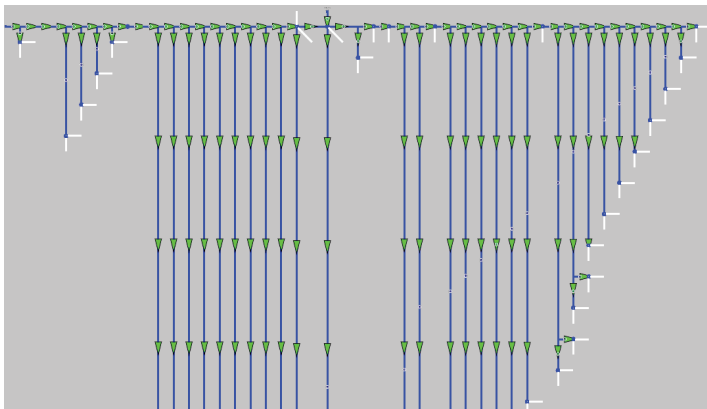


Figure 6. Power flow in feeder

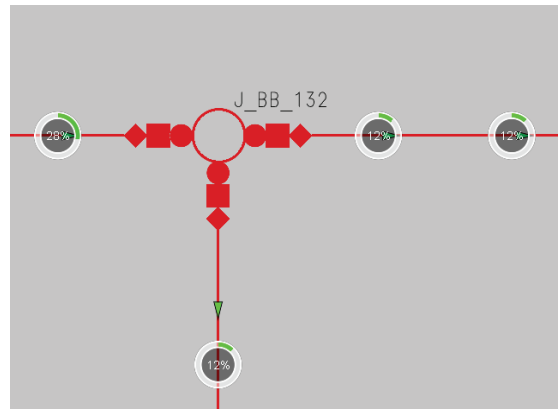


Figure 7. Line section loading

**Distribution System State Estimator (DSSE)** - This DMS function estimates the active and reactive loads of the network using the available measurements, actual topology, the different electrical parameters and a relevant load modeling. DSSE estimates the real-time network operating state using the real measured telemetered values from the SCADA system. DSSE calculates the loads in that way that their values match to the existing measured values and actual network topology obtained from SCADA.

Name	V [kV]	V [p.u.]	Angle [degree]	Cumulative voltage drop [%]
J_BB_036	10.3082	0.98	146.72	2.9217
J_BB_037	10.2974	0.98	146.72	3.0238
J_BB_038	10.4126	0.99	146.82	1.9273
J_BB_040	10.2568	0.98	146.67	3.4111
J_BB_041	10.2544	0.98	146.67	3.4333
J_BB_043	10.2333	0.97	146.65	3.6345
J_BB_044	10.1888	0.97	146.62	4.0582
J_BB_045	10.1759	0.97	146.60	4.1811
J_BB_047	10.1796	0.97	146.60	4.1465
J_BB_048	10.1606	0.97	146.61	4.3269
J_BB_049	10.1588	0.97	146.60	4.3443
J_BB_050	10.1577	0.97	146.60	4.3546

Figure 8. Voltage drop estimation for different busbar points

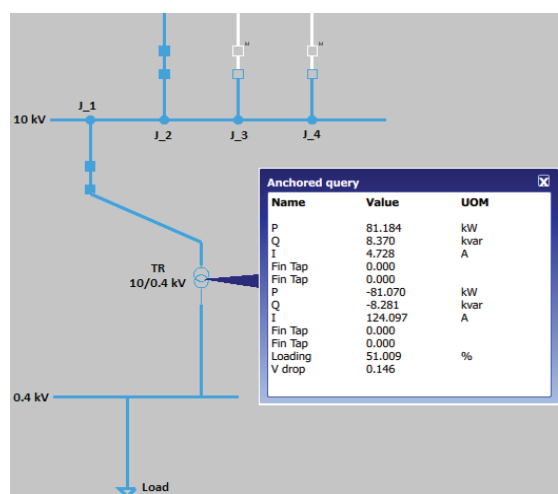


Figure 9. Transformer loading estimation



State estimation holds key to many decisions as it provides many insights into the state of the distribution system. [3]

The purpose of DSSE is to estimate the network state on the base of the available measurements (analog and digital), available load information, and static network data. As a function provides:

- Estimated loads matching measured values using weighting factors for measured values and loads
- Detection of measurements which do not fit to the measurement set

In the case of Kosovo distribution network, the DSSE results are used to monitor the network operating state like transformer loading, voltage profile, busbar, line and transformer violations. Usage of this function helps a lot in operational improvements and network analyses.

**Short-Term Load Scheduler (STLS)** – This DMS function provides active and reactive power values at each load node for a given point in time. STLS maintains scheduled active and reactive power consumption of the power system loads for one week (providing values hourly for each day, holiday and totally week). For example, active power for load *i* and time interval  $t_j$  are calculated after a DSSE run as:

$$P_{i,STLS}(t_{jn}) = f[P_{i,STLS}(t_{jo}), P_{i,DSSE}(t)] = \alpha_{DSSE} * P_{i,DSSE}(t) + (1 - \alpha_{DSSE}) * P_{i,STLS}(t_{jo})$$

$\alpha_{DSSE}$  - Smoothing factor for STLS values updated using DSSE results

$P_{i,STLS}(t_{jn})$  - STLS active power value for load *i* and given hour  $(t_j - 1) < t \leq t_j$  after update

$P_{i,STLS}(t_{jo})$  - STLS active power value for load *i* and given hour  $(t_j - 1) < t \leq t_j$  before update

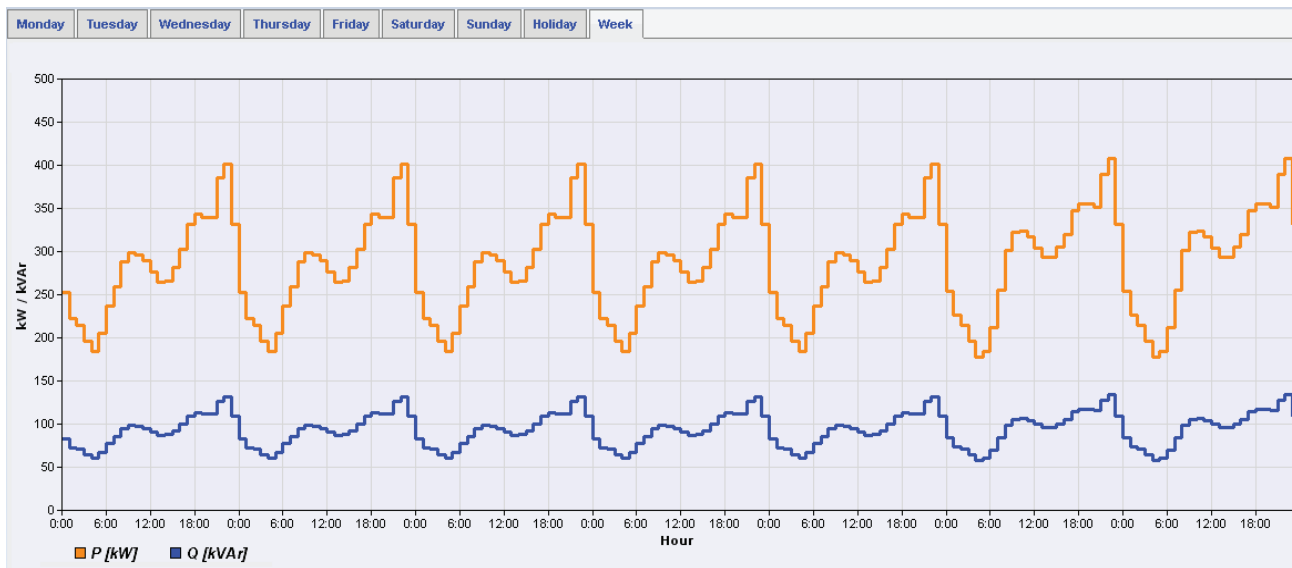


Figure 10. Graphical visualization of Short-Term Load Scheduler (STLS) results for a load node

STLS as a function of DMS updates the active and reactive power consumptions of the power system loads using real-time DSSE results.

**Fault Management (FM)** – Fault management is a challenge for all distribution network operators, as well as for the one in Kosovo. This is because all operators intend to implement different techniques or functions to achieve the minimization of the duration of breakdowns that occur in the network. Automation through the current SCADA system has greatly helped to reduce SAIDI at the level of Kosovo distribution network.

An even greater improvement is expected to be seen with the start of using the fault management function for locating the fault quickly and accurately, as well as applying fault isolation and quick service restoration.

### 3. FEEDER ANALYSIS AND FUNCTION RESULT WITH DMS

From all the functions presented above, below it will be shown a feeder of Kosovo distribution network with all its transformers and results from some DMS functions.



Oral Presentation: Distribution Management System (DMS) Integration in Distribution Network of Kosovo

Table below presents the general data of chosen feeder to present results:

Table 1. Feeder Data - Kosovo DN

Description	Information
Feeder's Substation	35/10 [kV] Substation A
Name	Feeder 1
Type	Radial
Voltage	10 [kV]
Customer Number	2129
Transformer Numbers	14
Line length	3.717 km

Table below gives loading of feeder 1, respectively the Pmax value in [MW] for each month of 2022, where it can be seen that feeder has recorded its highest value in January.

Table 2. Monthly Pmax [MW] recorded value for feeder 1

Feeder	Jan	Feb	Mar	Apr	May	Jun	Jul	Aug	Sep	Oct	Nov	Dec
F-1	2.33	2.11	2.04	1.98	1.71	1.26	1.36	1.58	1.66	1.76	1.89	2.10

Feeder network visualization in software and in DMS will show the configuration and right topology of feeder representing lines, transformers and switches (disconnectors and circuit breakers).

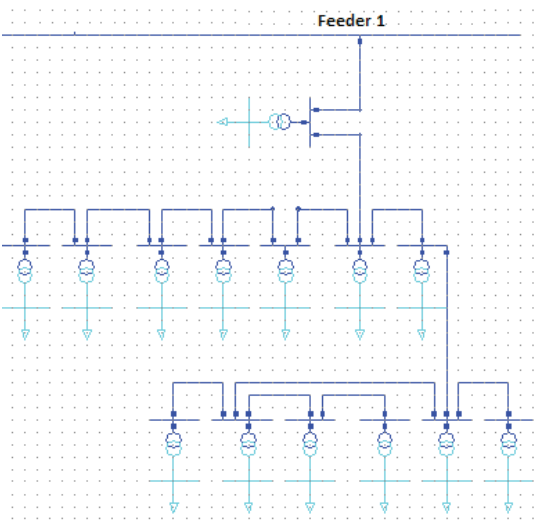


Figure 11. Feeder visualization on software

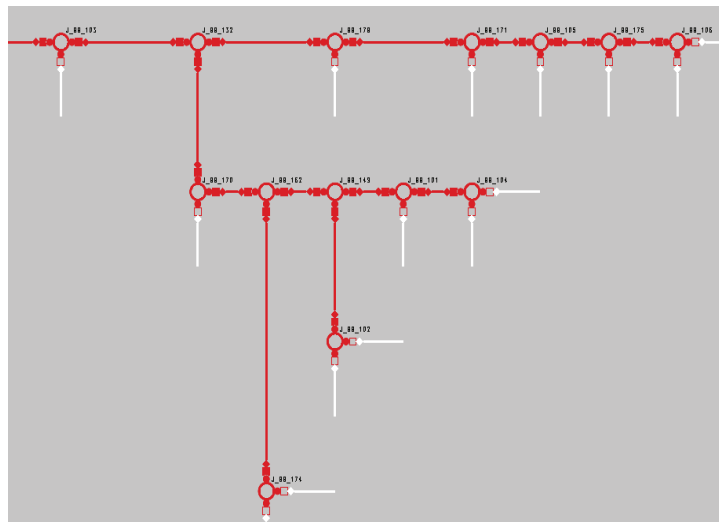


Figure 12. Feeder visualization on DMS

According to state estimation with existing real time measurement data from SCADA and historical data for loading of transformers, the system according to line section will try to estimate loading of each line section.



Power flow and line loading on feeder 1:

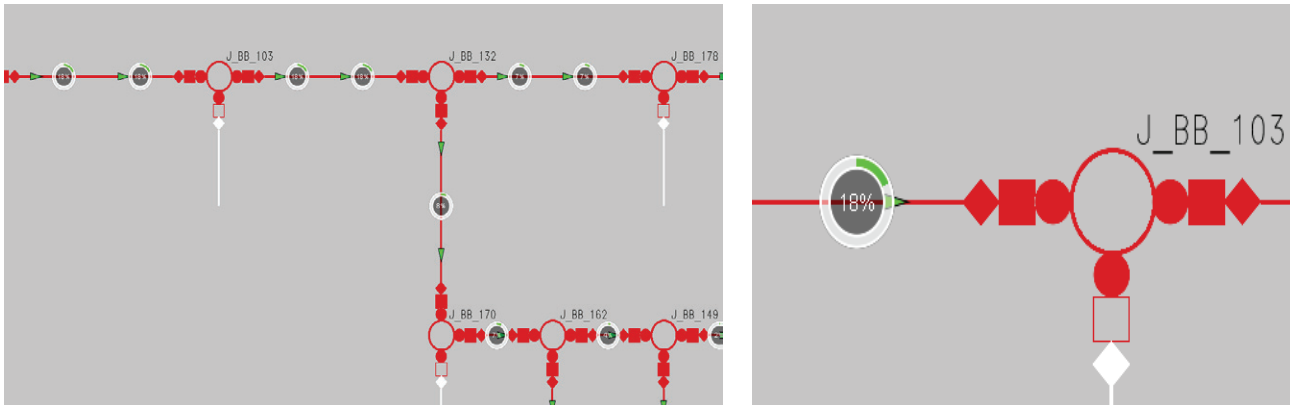


Figure 13. Feeder 1 - Line Loading %

According to main busbar voltage, line parameters and line loading DMS system tries to estimate the voltage in each busbar of transformers. As seen from results since feeder 1 at the time of simulation was not too much loaded also considering that line is not a long line, voltage is within the allowed limits according to Kosovo Distribution Network Grid Code.

Name	V [kV]	V [p.u.]	Angle [degree]	Cumulative voltage drop [%]
J_BB_101	10.3457	NaN	NaN	
J_BB_102	10.4039	0.99	146.80	0.7215
J_BB_103	10.3694	0.99	146.80	0.1669
J_BB_104	10.3713	0.99	146.78	0.4958
J_BB_105	10.3634	0.99	146.78	0.4769
J_BB_106	10.3929	0.99	146.78	0.5521
J_BB_132	10.3609	0.99	146.80	0.2714
J_BB_149	10.3387	0.98	146.78	0.5765
J_BB_162	10.3390	0.98	146.80	0.7876
J_BB_170	10.3390	0.98	146.80	0.7848
J_BB_171	10.3435	0.98	146.79	0.7847
J_BB_174	10.3726	0.99	146.80	0.7422
J_BB_175	10.3963	0.99	146.78	0.4651
J_BB_178	10.3767	0.99	146.80	0.2393
J_BB_154	10.3457	0.99	146.78	0.4254
			146.80	0.7215

Figure 14. Busbar voltage estimation on DMS for feeder 1

DMS will estimate also loading of total feeder. As seen from figure below, it is shown current in [A] and power in [MW] readed in real time from SCADA system. In same time DMS it is estimating the calculated value that is very near with real value, in total of 3.12-3.72% deviation.

Name	Phase	Type	Unit	SCADA value	SCADA adj. sign value	Calculated value	Deviation [%]
	[ALL]	[ALL]	[ALL]				NaN
Feeder 1/I1	ABC	I	A	61.8373	61.8373	63.8307	3.12
Feeder 1/P	ABC	P	MW	1.1492	1.1492	1.1935	3.72

Figure 15. Feeder 1 - SCADA value and DMS calculated value

DMS in same time it will show power flow results for each transformer of feeder by showing active power, reactive power, current and loading in %.

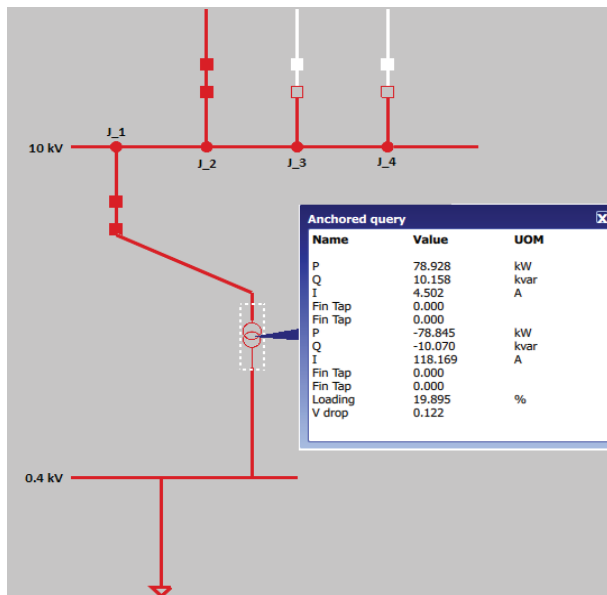


Figure 16. Transformer 1 - Loading

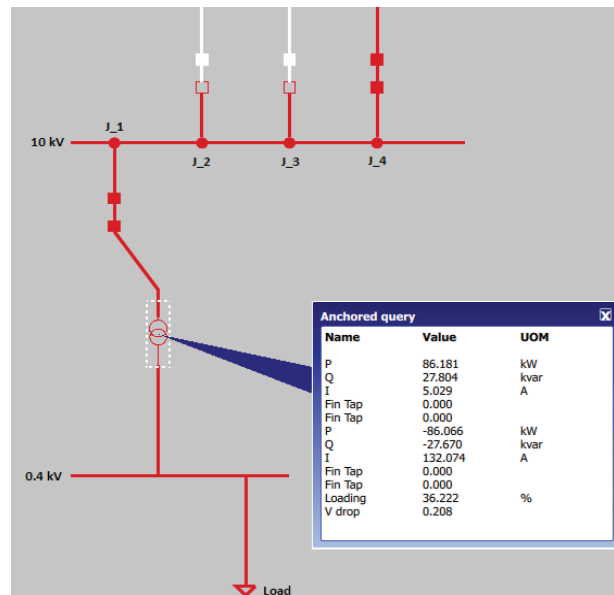


Figure 17. Transformer 2 - Loading

Same like shown at functions above the system for feeder 1 will show short time load scheduler by showing for each load of the feeder hourly for each day active and reactive power value.

## 4. BENEFITS OF DMS INTEGRATION IN KOSOVO DISTRIBUTION NETWORK

DMS as a system will access real-time data from SCADA system and provide all information based on the functions applied on the control center in an integrated manner, that will help operators to make intelligent and appropriate decisions. One of the most important benefit is that real time load flow solutions in different parts of the distribution network will help dispatchers to verify the grid operating conditions and to take right decisions for resolving problems. Both SCADA and DMS include many functions that will help operators to make intelligent and appropriate decisions. Distribution companies implementing distribution management are receiving benefits from many areas such as providing a fast method of improving reliability making the whole operating function more efficient, or simply extending asset life. [4]

The main benefits that Kosovo distribution network will have by using DMS will be:

- Network overview and different analyses possibilities
- Real time load flow solutions
- Reduce the duration of outages
- Improve the speed and accuracy of outage predictions
- Improve the network operational efficiency
- Prevent the network overloads and voltage drop by taking necessary actions
- Network optimization and better investment planning
- Fault identification, isolation and service restoration
- Load management and short-term load forecasting

Advances in digital technology are making true distribution automation a reality. [5]

## 5. CONCLUSION

Power system automation depends on data communication, monitoring and supervisory control. Electricity companies are constantly adopting and incorporating monitoring, control and management with the help of various devices and different systems to provide better services to customers.





Oral Presentation: Distribution Management System (DMS) Integration in Distribution Network of Kosovo

One of the focuses of Kosovo Electricity Distribution and Supply Company activities is the automation of the electricity distribution system, using the latest advances and developments in the field of technology and data communication systems. The integrated DMS system in the distribution network of Kosovo provides and will continue to provide advanced monitoring, different analysis, control, optimization, better planning. By usage of DMS system, the distribution network will be reliable and safe.

### BIBLIOGRAPHY

- [1] S. A. Boyer, SCADA Supervisory Control and Data Acquisition, United States of America: ISA, 2004. [page: 11]
- [2] Yinliang Xu, Wei Zhang, Wenxin Liu, Wen Yu, Distributed Energy Management of Electrical Power System, Canada: IEEE Press, 2021. [page 147]
- [3] Mini S. Thomas & John D. McDonald, Power System SCADA and Smart Grids, CRC Press Taylor & Francis Group, 2015. [page 237]
- [4] James Northcote-Green, Robert Wilson, Control and Automation of Electric Power Distribution Systems, United States of America: Taylor & Francis Group, 2007. [page 1]
- [5] T. Gonen, Electric Power Distribution System Engineering, USA: CRC Press, 2008. [page 21]



# Challenges of Protection System of Kosovo Distribution Network

[nezir.neziri@keds-energy.com](mailto:nezir.neziri@keds-energy.com)

**NEZIR NEZIRI\*, ARTON ALIU, DRENUSHA GASHI**

*Kosovo Electricity Distribution and Supply Company*

**Kosovo**

## SUMMARY

The development of new technologies has affected all areas of the power system by accelerating the development of new equipments in the field of control, monitoring and protection. In accordance with this development, it is important that the appropriate equipments are used in the power system in order to achieve stability and proper functioning of this system.

One of the most important part of the power system is the part of the protection system because it is very important for the system to be protected from various faults that may occur. Protection relays design and manufacture have reached to a new level of advancement where numerical relays have appeared recently with different functions and with different arrangement options. An important point of protection system is selectivity. Selective coordination of relay protection is critical for the reliability of the electrical distribution system.

The purpose of this paper is to present the main challenges of protecting the Kosovo Distribution Network through protection system in two cases:

1. The challenges for protecting a part of distribution network with nondirectional relays
2. The challenges for protecting distribution network with integration of RES

Most of the distribution network in Kosovo is a radial network and the main protection of the system is done with Intelligent Electronic Device (IED). There are different types of relays on the network and of course, depending on the feeder configuration, there are also challenges in parameterizing the relay settings.

For more, because of minimum allowed arrange values, not all relays give the opportunity to arrange parameters in order to achieve the proper selectivity. Also, not all relays sense the direction of the current, despite directional ones. In the directional relay first, it senses the direction of the current for which it has been set whether this is the correct direction for which it has to operate or not.

In order to explain all challenges for protecting a part of distribution network with nondirectional relays, a simulation with ETAP software will be presented in this paper results and all configurations will be shown.

While in the other hand, distributed generation (DG) technology is gaining in popularity in Kosovo due to the increasing demand for energy and the use of cleaner energy. In this case operation, control and protection of distribution system becomes challenging. Integration of DG's in the network it is affecting power quality, system voltage profile, energy security, power flow control, frequency control and above all protection system. To be able to explain the challenges for protecting distribution network with integration of RES, paper will discuss RES in distribution network of Kosovo and the effects of RES in protection system. Also, in this case, the challenges of relay coordination will be discussed through a simulation with software where analysis of effects will be shown.

## KEYWORDS

Relay, Selectivity, Challenges, Directional, Relay Setting, Nondirectional, RES, Distribution Network, Kosovo.



### 1. THE CHALLENGES FOR PROTECTING A PART OF DISTRIBUTION NETWORK WITH NONDIRECTIONAL RELAYS

Nondirectional relays, also known as non-polarized or universal relays, are protective relays used in electrical power systems to detect and respond to abnormal conditions or faults. Unlike directional relays, which consider the direction of current flow or voltage, nondirectional relays operate based on the magnitude or other characteristics of electrical quantities, such as current, voltage, or power.

Here are some key features and characteristics of nondirectional relays:

- **Operation Principle:** Nondirectional relays operate based on the comparison of measured electrical quantities with predetermined thresholds or settings. When the measured quantity exceeds the set threshold, the relay detects the abnormal condition or fault and initiates a protective action.
- **General Protection:** Nondirectional relays provide general protection for power system elements, such as generators, transformers, busbars, and feeders. They are designed to detect a wide range of faults, including short circuits, overcurrent's, overvoltage's, under voltages, and other abnormal conditions.
- **Fault Detection:** Nondirectional relays can detect faults regardless of the direction of fault current flow. They monitor the magnitude of electrical quantities and compare them to the set thresholds. If the measured values exceed the set limits, indicating a fault or abnormal condition, the relay operates to isolate the faulty section of the power system. [6]
- **Flexible Settings:** Nondirectional relays offer flexibility in setting their thresholds and characteristics to meet specific protection requirements. The relay settings can be adjusted to accommodate different system configurations, fault levels, and coordination with other protective devices.
- **Time-Graded Protection:** Nondirectional relays often incorporate time-graded protection, where the relay operates with different time delays based on the severity or location of the fault. This allows for coordinated protection schemes, ensuring the correct relay operates and isolates the fault while minimizing unnecessary tripping of healthy sections.
- **Backup Protection:** Nondirectional relays are commonly used as backup protection, providing an additional layer of protection in case the primary protection devices, such as directional relays, fail or operate incorrectly. [6]

Nondirectional relays play a crucial role in ensuring the safety and stability of electrical power systems by detecting and responding to faults and abnormal conditions. They provide general protection and complement the operation of directional relays and other protective devices in a coordinated protection scheme. [7]

While nondirectional relays have several advantages in distribution systems, they also have a few disadvantages. Here are some potential drawbacks:

- **Lack of Selectivity:** Nondirectional relays may lack selectivity in certain scenarios. Since they do not consider the direction of fault current flow, they may not be able to differentiate between faults occurring at different locations or on different feeders. This can lead to a broader scope of tripping, affecting a larger portion of the distribution system during a fault.
- **Coordination Challenges:** Coordinating nondirectional relays with other protective devices can be more challenging compared to directional relays. Nondirectional relays typically rely on time-graded protection schemes to ensure proper coordination. Setting appropriate time delays for different relays can be complex, especially in systems with varying fault levels and complexities.
- **Increased Fault Clearing Time:** Due to the lack of selectivity and potential coordination challenges, nondirectional relays may result in increased fault clearing time. This can have an impact on the overall system reliability and service continuity, as it takes longer to isolate the faulted section and restore power to healthy sections.
- **Limited Fault Location Information:** Nondirectional relays do not provide precise information about the location of a fault within the distribution system. This can make fault identification and subsequent maintenance and repair processes more time-consuming and challenging.
- **Increased False Tripping Risk:** Nondirectional relays may be more susceptible to false tripping caused by system transients or disturbances. Without considering the direction of fault current flow, they may respond to certain transient conditions that do not pose an actual threat to the system, resulting in unnecessary trips and interruptions. [8]

## 1.1. Simulation of three phase fault using nondirectional relays in distributive network

This paper shows the challenges of protection with nondirectional relays. The connection between two substations substation A (110/35/10 kV) and substation B (35/20 kV) is shown in figure 1. From substation A to substation B there are two supplying feeders of 35 kV that are connected parallel in both busbars of substation. Cable that connects this substation are 3x1x240mm<sup>2</sup> XHE 49-A.

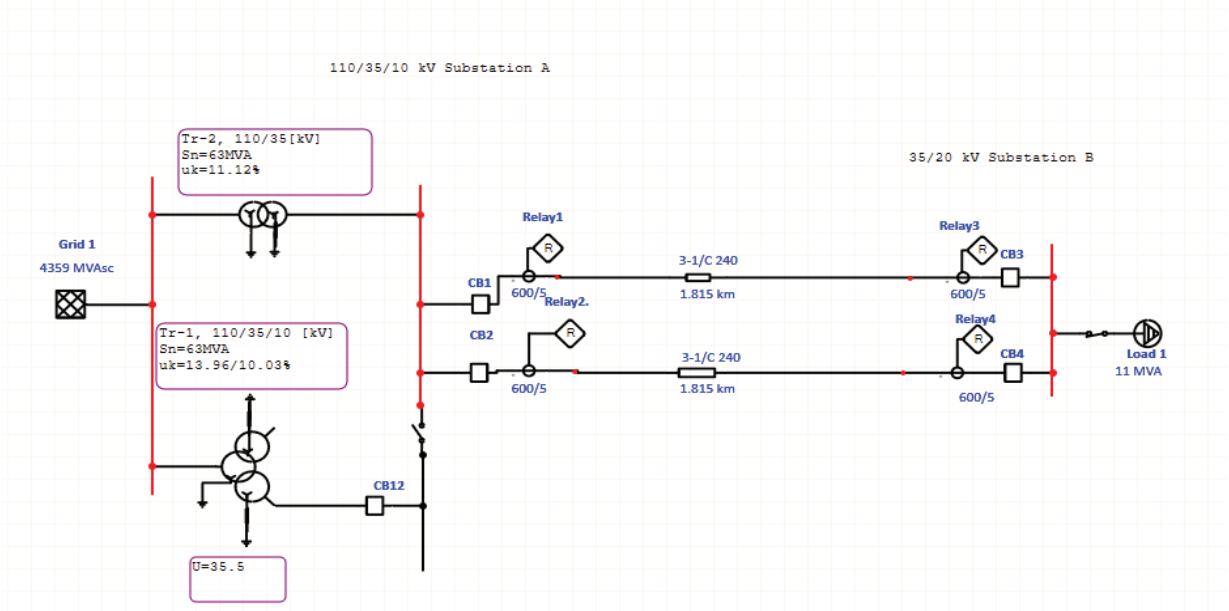


Figure 1. Distribution Network between Substation A and Substation B

The study will be divided in two scenarios depending on the type of relay used: nondirectional relay or directional relay.

The simulation is done with Etap 19 software, where a three-phase fault is simulated in the cable, and the report generated by software shows that which relays in this system are going to trip and the sequence of tripping.

### 1<sup>st</sup> scenario – Nondirectional Relays

In this scenario the parameters for all relays are as follow:

Current transformers in feeders are 600/5 A.

Table 1: Parameters for Relay 1 and Relay 2 - Nondirectional

Function Name	Start Value	Operation Mode	Time Delay
Overcurrent stage 1 (OC1)	0.75 In	IEC Normal Inverse	0.4
Overcurrent stage 2 (OC1)	2.00 In	IEC Definite Time	0.15

Table 2: Parameters for Relay 3 and Relay 4 - Nondirectional

Function Name	Start Value	Operation Mode	Time Delay
Overcurrent stage 1 (OC1)	0.75 In	IEC Normal Inverse	0.35
Overcurrent stage 2 (OC1)	2.00 In	IEC Definite Time	0.05

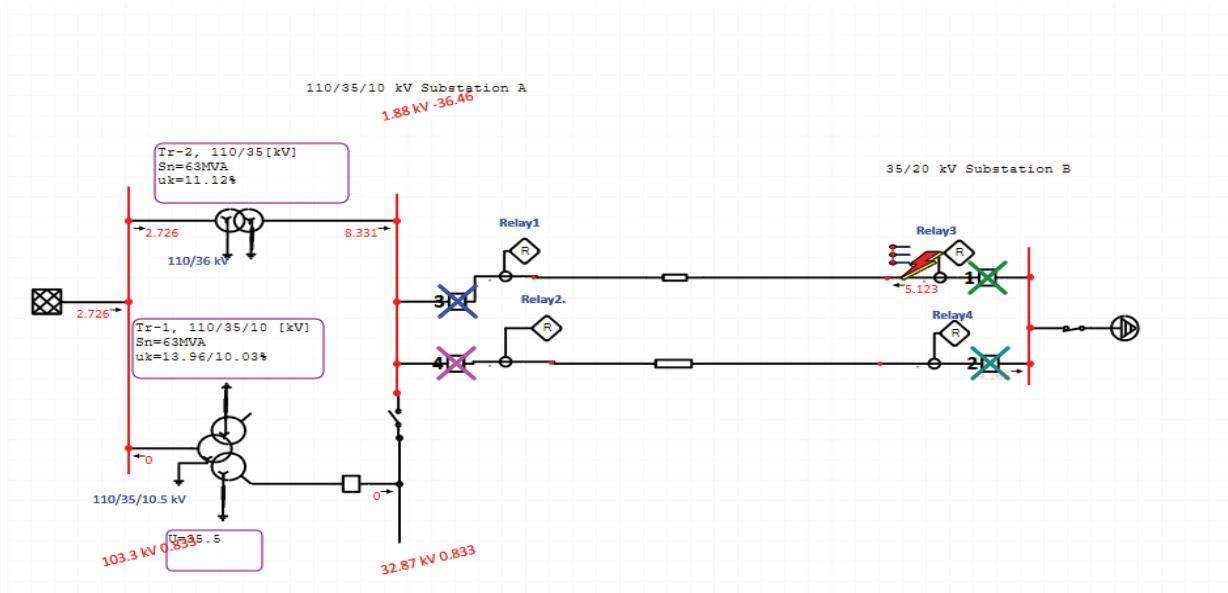


Figure 2. Three Phase Fault simulation on Branch 1 with nondirectional relays

Time (ms)	ID	If (kA)	T1 (ms)	T2 (ms)	Condition
50.0	Relay3	5.123	50.0		Phase - OC1 - 50
50.0	Relay4	4.165	50.0		Phase - OC1 - 50
100	CB3		50.0		Tripped by Relay3 Phase - OC1 - 50
100	CB4		50.0		Tripped by Relay4 Phase - OC1 - 50
150	Relay1	4.165	150		Phase - OC1 - 50
150	Relay2.	4.165	150		Phase - OC1 - 50

Figure 3. Simulation Results: Time of Tripping and Circuit Breaker Opening Time in ETAP Software with nondirectional relays

As it shown in Figure 2 and Figure 3 the sequence of Relay tripping is that Relay 3 and Relay 4 are tripping first and after that Relay 1 and Relay 2 in this case this results in total outage of Substation B even though only one cable has Fault.

While the relays to be in tripping mode they just check the magnitude of Current or Voltage they don't take into consideration the direction of fault, this results in unwanted trips. So, if a fault happens in one of these two cables (no matter the fault) the relays of both feeders will trip due to lack of determining the direction of fault.

Due to parallel working cable is impossible to have full selectivity when fault happens with this type of relays.

### 2<sup>nd</sup> scenario: Directional Relays

In this scenario the parameters for all relays are as follow:

Current transformers in feeders are 600/5 A.

Table 3: Parameters for Relay 1 and Relay 2 - Directional

Function Name	Start Value	Operation Mode	Time Delay	Direction
Overcurrent stage 1 (OC1)	0.75 In	IEC Normal Inverse	0.4	Forward
Overcurrent stage 2 (OC1)	2.00 In	IEC Definite Time	0.15	Forward
Overcurrent stage 3 (OC2)	2.00 In	IEC Definite Time	0.4	Reverse

Table 4: Parameters for Relay 3 and Relay 4 - Directional

Function Name	Start Value	Operation Mode	Time Delay	Direction
Overcurrent stage 1 (OC1)	0.75 In	IEC Normal Inverse	0.35	Reverse
Overcurrent stage 2 (OC1)	2.00 In	IEC Definite Time	0.05	Reverse
Overcurrent stage 3 (OC2)	2.00 In	IEC Definite Time	0.2	Forward

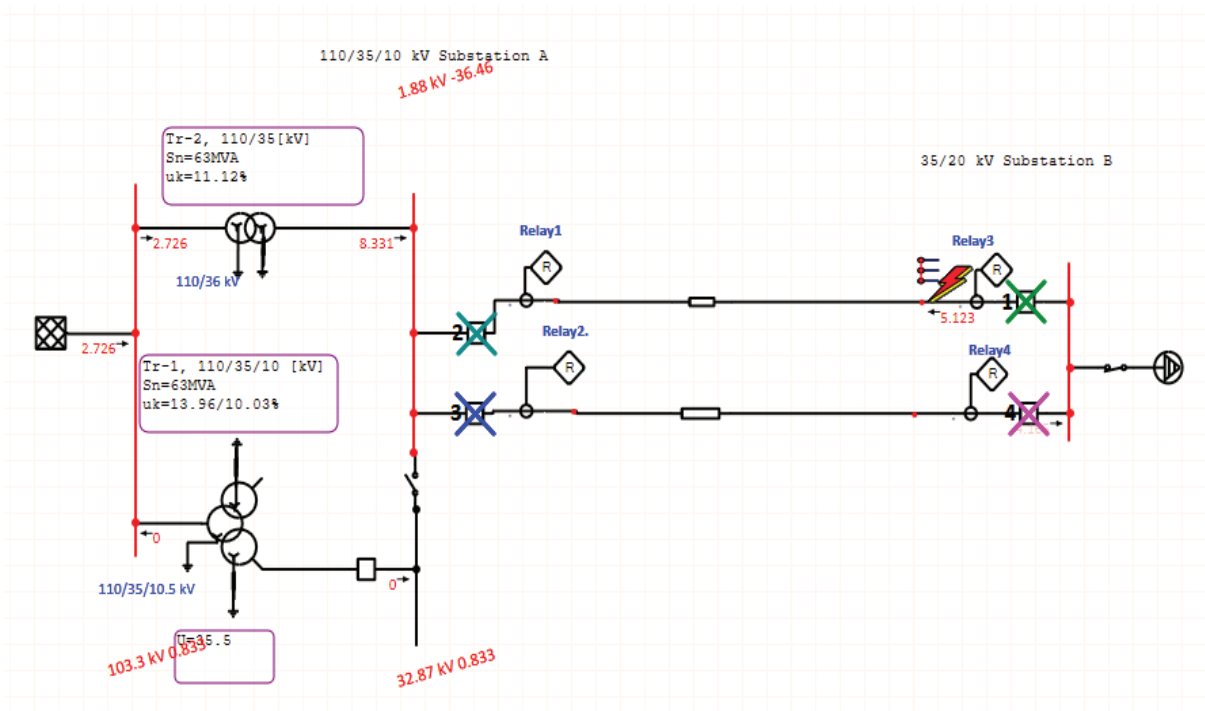


Figure 4. Three Phase Fault simulation on Branch 1 with directional relay

Time (ms)	ID	If (kA)	T1 (ms)	T2 (ms)	Condition
50.0	Relay3	5.123	50.0		Phase - OC1 - 50 - Reverse
100	CB3		50.0		Tripped by Relay3 Phase - OC1 - 50 - Reverse
150	Relay1	4.165	150		Phase - OC1 - 50 - Forward
150	Relay2	4.165	150		Phase - OC1 - 50 - Forward
200	Relay4	4.165	200		Phase - OC2 - 50 - Forward

Figure 5. Simulation Results: Time of Tripping and Circuit Breaker Opening Time in ETAP Software with directional relays

As it shown in Figure 4 and Figure 5 the sequence of Relay tripping is that Relay 3 and Relay 1 are tripping first and after that Relay 4 and Relay 2 in this case this results in isolating the fault on the both ends of cable. With this operation this result in full clearance of fault without effecting any customer on Substation B.

To eliminate the scenario of tripping two supplying 35 kV feeders is necessary to change the relays from nondirectional relays to directional ones. After the relays are changed the same simulation is done and the results are optimal for a parallel supplying feeder. The changed relays are IED with analog inputs 4xI (I1, I2, I3, Io) and 4xU (U1, U2, U3, Uo).





## 2. THE CHALLENGES FOR PROTECTING DISTRIBUTION NETWORK WITH INTEGRATION OF RES

Protecting distribution networks with the integration of Renewable Energy Sources (RES) poses several challenges due to the unique characteristics and intermittent nature of renewable energy generation. Here are some general observations regarding the challenges of protecting distribution networks with RES integration:

- **Voltage and Frequency Variations:** RES, such as solar, hydro and wind power, are subject to fluctuations in output due to weather conditions and other factors. This variability can lead to voltage and frequency variations within the distribution network. Protective devices must be capable of accommodating these fluctuations and ensure the stability and quality of the power supply. [1]
- **Fault Current Contribution:** RES integration can alter the fault current levels within the distribution network. The contribution of renewable energy sources to fault currents needs to be accurately assessed and accounted for in the coordination and operation of protective devices. Failure to account for these contributions can lead to improper coordination and potential damage to equipment.
- **Islanding and Anti-Islanding Protection:** In situations where a distribution network becomes isolated from the main grid but still receives power from RES, islanding can occur. Islanding protection is essential to detect and disconnect the distributed generation sources from the islanded network to prevent safety hazards for maintenance personnel and prevent damage to the equipment during re-energization. [4]
- **Protection Coordination:** RES integration often involves multiple points of generation distributed throughout the network. Coordinating protective devices to ensure selective and rapid fault detection, isolation, and system restoration becomes more complex due to the dispersed nature of generation sources. Coordination challenges arise in determining appropriate settings and time delays to achieve optimal protection without sacrificing selectivity and reliability. [3]
- **Communication and Control:** Integrating RES requires enhanced communication and control systems to enable efficient monitoring, control, and protection of the distributed generation sources. Real-time monitoring of RES output, communication between protective devices, and remote control capabilities are crucial for effective protection and management of the distribution network.
- **Cybersecurity:** With the increased reliance on communication and control systems, cybersecurity becomes a critical concern. Protecting the distribution network from cyber threats and ensuring the integrity of communication and control infrastructure is essential to maintain the reliability and security of the RES-integrated system. [2]

Addressing these challenges requires careful planning, system design, and the selection of appropriate protection and control technologies. Distribution network operators, system planners, and equipment manufacturers are continually working on developing solutions and standards to overcome these challenges and ensure the reliable and secure operation of RES-integrated distribution networks [5]

### 2.1. Impact of Hydropower Plant Generators on Medium Voltage

In this paper the other challenge for protection that will be faced is Voltage Variations, in the region of Prizren in Dragash Municipality the hydro potential for electricity generation is high and that took the attention of investors. So, the hydropower plants are in large quantity with a very high capacity for this region. Municipality of Dragash is small with <35000 population (<10500 costumers), the maximum load is 12 MW and minimum is 5 MW.

Total capacity of hydropower plants is 25.905 MW, that covers the load of Dragash and Zhuri, Zhuri is the biggest village by population in Kosovo. The generated power that is left after consumption returns back to Primary substation of Substation C. All hydropower plants are run of river type.

The generated power is 3-5 times greater than the actual load in peak rainy seasons, while the hydropower plants are run of river type the interest in them is to generate as much as they can while they can. This causes an increase of voltage in 35/10 kV Substation C up to 1.10-1.15 Un, which affects all consumers in this area for overvoltage in low voltage side. The relay protection in this case needs to detect real faults currents/voltage or generated current/voltages from turning on and off of generators.

In the figure 6 is shown the distribution scheme of Prizreni District, with substation and Hydropower plant generators.

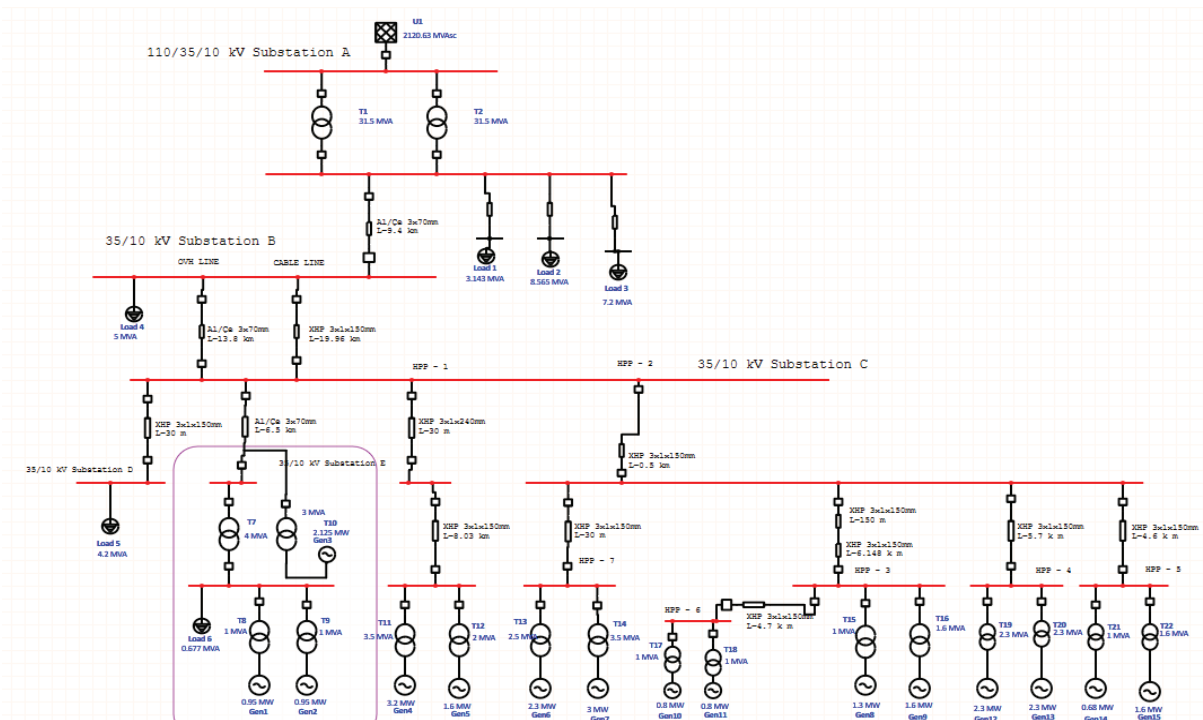


Figure 6. Single Line Diagram of Prizren Region including RES

The simulation is done in Etap 19 software, in this case the power generated is maximum and the load during this season is minimum, so this leaves a high impact in systems stability.

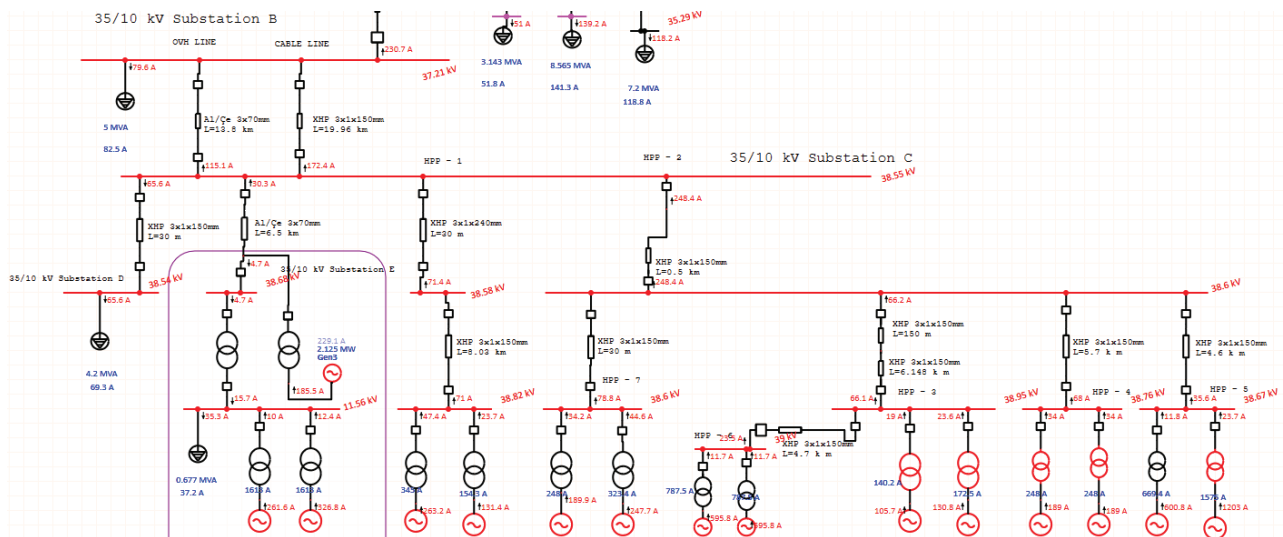


Figure 7. Integration of RES in Distribution Network

When the voltage at Substation C is increased from 35kV to 38.55kV, the impact on the generators can be observed through a simulation conducted using real parameters in ETAP software. This voltage increment will result in several significant effects. Firstly, the increased voltage will cause a proportional increase in the reactive power demand by the generators, requiring the reactive power compensation equipment to respond accordingly. Secondly, the higher voltage level may necessitate adjustments in the generator excitation system to maintain stable voltage levels and prevent potential overvoltage conditions. Additionally, the increased voltage can affect the electrical insulation of the generators, transformers, other equipments in substations, demanding careful evaluation to ensure the equipment's integrity. Overall, the simulation allows for a comprehensive analysis of the impact of the voltage increment on the generators, facilitating informed decision-making and ensuring the reliable operation of Substation C.



### 3. CONCLUSION

In conclusion, the challenges associated with protecting a part of the distribution network using nondirectional relays and integrating renewable energy sources (RES) are significant and require careful consideration.

When it comes to using nondirectional relays, one of the main challenges lies in accurately detecting and distinguishing between faults and normal network conditions. Nondirectional relays do not provide directional information, making it more difficult to identify the precise location of a fault. This can result in longer fault detection times and delays in initiating appropriate protection measures, potentially leading to increased damage to the network.

Moreover, the integration of RES introduces additional complexities to the distribution network protection. Renewable energy sources, such as solar and wind, exhibit inherent variability and intermittency, which can cause fluctuations in power flow and voltage levels. These fluctuations can lead to false relay operations and may require the implementation of specialized protection schemes to address the unique characteristics of RES.

Additionally, the intermittent nature of RES makes fault detection and fault current calculation more challenging. Traditional fault analysis techniques may not be applicable in scenarios where RES contribute a significant portion of the power supply. Furthermore, the bi-directional power flow in distribution networks with RES integration necessitates the development of new protection strategies to ensure the reliable operation of the network under various operating conditions.

In conclusion, protecting a part of the distribution network with nondirectional relays and integrating RES require addressing technical complexities, adapting existing protection schemes, and developing innovative solutions. Overcoming these challenges will be crucial to ensure the reliable and secure operation of distribution networks in the context of evolving energy systems.

### BIBLIOGRAPHY

- [1] Elgallad, E. M., & Braun, M. (2017). Optimal location of protective devices in distribution networks considering renewable energy sources. *Electric Power Systems Research*
- [2] Gómez-Expósito, A., Calleja, A. J., & Martínez-Ramos, J. L. (2016). Challenges and approaches for protection coordination in microgrids. *Renewable and Sustainable Energy Reviews*
- [3] Khamphanchai, W., & Leelarujji, R. (2019). Fault detection and protection coordination in distribution networks with high penetration of distributed generation. *Energies*
- [4] Khodr, H. M., & Mousa, M. H. (2017). Protection coordination techniques for distribution networks with high penetration of renewable energy sources. *Electric Power Systems Research*
- [5] Mansoor, M. K., Alam, M. S., & Hussain, A. (2018). Smart grid protection challenges and solutions: A comprehensive review. *International Journal of Electrical Power & Energy Systems*
- [6] Elgallad, E. M., & Braun, M. (2017). Optimal coordination of directional and nondirectional relays in power systems. *Electric Power Systems Research*
- [7] Teng, J., & Tang, W. (2018). Performance analysis and coordination of directional and nondirectional overcurrent relays for distribution systems. *IET Generation, Transmission & Distribution*
- [8] Mahapatra, K. K., & Giri, V. K. (2019). A review on protective relays in power systems: Classification, challenges, and future trends. *Electric Power Components and Systems*



# Integration of Solar Power Plants in Distribution Network – examples from Bosnia and Herzegovina

s.gruhonjic@epbih.ba

**ŠEILA GRUHONJIĆ, FERHATBEGOVIĆ**

*Monenco*

*Bosnia and Herzegovina*

## SUMMARY

There is an unexpected expansion of requests for integration of Photovoltaic Power Plants (PVPP) into the network of PE “Elektroprivreda” of Bosnia and Herzegovina (PE EP B&H). The commissioning of these renewable sources will led to changes in the control and monitoring of the distribution network. Positive effects include a significant reduction in CO<sub>2</sub> emissions in the production of electricity. This work briefly present the existing methodology used to check the possibility of connecting renewable sources implemented in the EP B&H, Power Utility Tuzla (ED Tuzla). Several examples of defining connection for different required power of PVPPs are presented. In addition to the eliminatory criteria for connection, the energy criteria are also checked by calculating the power flows for the assumed conditions. Significant voltage fluctuations can be expected, so a particular challenge in the new system will be maintaining acceptable voltage values for the end customers.

## KEYWORDS

Distributed generation, photovoltaic (solar) power plants, electrical distribution network



## 1. INTRODUCTION

In recent years, the representation of solar power plants has been constantly increasing. It is predicted that by 2027, production from solar plants will reach more than 20% of the total energy production [1]. According to data solar radiation in the Balkans, Bosnia and Herzegovina has significantly resources of energy from solar radiation, above the European average with extremely favourable seasonal schedule, which gives the possibility for its efficient and long term use [2]. Specifically in the last year, in EP B&H has been an increasing number of requests for connection of solar power plants with powers that usually range from 150 kW up to several MWs. Here is presented the current regulation that is used when checking the possibility of connecting distributed sources to the distribution network in Bosnia and Herzegovina. As examples, the technical possibility of connecting 250 kW solar power plant, 900 kW and 8,8 MW solar power plants to the existing electrical distribution network is presented. The first analysed example was selected from the distribution area where the sum of requests for PVPP's connection exceeded the value of total consumer consumption. The distribution area refers to consumption belonging to one or more supplied transformer stations (TS). The impossibility of connecting to the existing 10 kV network led to the need to form separate medium voltage (MV) feeders for the connection of PVPPs and to request a consent of transmission's company, since this energy, at certain intervals, transferred to the transmission network. For example, the connection of a solar power plant with capacity of 40 MVA which would be built on the abandoned surface mine of the coal mine is also announced. Floating power plants placed on the surface of the lake are also being considered. During the check of the technical connection possibilities, the criteria related to rapid voltage changes, flicker criteria, permitted higher harmonic currents, as well as network energy criteria (permitted voltage changes in the network and thermal load of lines) are checked. This topic is also current in the world and numerous papers can be found that discuss the topic of including solar power plants in distribution network. Combined wind power plants are also an option, and vertical installation of photovoltaic panels is also appearing [3, 4, 5]. In order to avoid more significant voltage fluctuations in the system with production from solar power plants, different methods are being investigated such as frequency regulation methods, reduction of active power, injection of reactive power into the network as well as storage of produced energy. With a significant participation of renewable sources in the electric power system, in order to maintain the balance of production and consumption of electrical energy, in the future, it will be necessary to store electrical energy that is considered the combination of solar and storage systems. Also in the coming period, it can be assumed that specialized energy storage plants will be formed that will replace the existing thermal power plants. These energy storage plants will aim to ensure system stability, peak load coverage and frequency regulation for power system stable operation [6].

## 2. CONNECTION CONDITIONS FOR PVPPS ACCORDING TO CURRENT REGULATION IN EP B&H

The verification the possibility of connecting PVPPs to the existing distribution network is based on the criteria prescribed by the Distribution System Operator (DSO). The technical recommendations for the connection and operation of distributed generation in the EP B&H were updated in accordance with the current events in this area and the latest edition is from September 2022 [7]. In addition to the basic criteria stated in the technical recommendations and the grid code [8], it is also necessary to check the energy criteria concerning that there is no excess of voltage conditions or overloading of the lines and transformers in any permitted operation mode. The basic criteria need to be satisfied for connecting the power plant to distribution network are listed in the following points. Also, for the case of PVPPs connection, the short circuit current criterion does not need to be checked for power plants with inverters, because the inverter currents that supply the short-circuit points is not greater than their rated current.

### 2.1. Permissible power criterion with regard to rapid voltage changes

The voltage change at the point of connection of the distributed power plant when it is switched on or off must not exceed 4% (in the case of connection to the MV network), or 5% (in the case of connection to the LV network). For each generator (group of generators)  $j$  within the power plant  $i$ , the rapid change in voltage at the common connection point need to be estimated according to the expression [7]:

$$\Delta u^{i,j} = k_u^{i,j} (\psi_s^i) \cdot \frac{S_g^{i,j}}{S_{k3}^i} \cdot 100 [\%] \quad (1)$$

If the generator's voltage change factor is not known, to estimate the rapid voltage change, it is necessary to use the expression:

$$\Delta u^{i,j} = k_i^{i,j} \cdot \frac{S_g^{i,j}}{S_{k3}^i} \cdot 100 [\%] \quad (2)$$



where are:

$S_g^{i,j}$  – nominal apparent power of the generator  $j$  in the power plant  $i$ ,

$S_{k3}^i$  – power of (perm. sustain.) three-phase short circuit in the connection point for the power plant  $i$

$k_u^{i,j}(\psi_s^i)$  – the voltage change factor for turning on/off the generator  $j$  in the power plant  $i$  to the angle impedance  $\psi_s^i$  in accordance with the standard IEC 61400-21-1:2019 or the technical guidelines FGW TG3. The generator's voltage change factor is measured for impedance angles 30°, 50°, 70° and 85°, and it is calculated by linear interpolation for other values of the impedance angle.

$\psi_s^i$  – system impedance angle at the common connection point for the power plant  $i$ ,

$k_i^{i,j}$  – current factor of turning on/off the generator  $j$  in the power plant  $i$ , in accordance with the standard DIN VDE V 0124-100 (VDE V 0124-100):2020-06.

Rapid voltage change for the case of simultaneous switching on/off of  $N_i$  generators is calculated as the sum of rapid voltage changes caused by individual switching on/off:

$$\Delta u^i = \sum_{j=1}^N \Delta u^{i,j} \quad (3)$$

In the case when the permitted power criterion is not satisfied during the simultaneous switching on/off of a power plant with several generators, it is possible to switch on/off the generators individually in time intervals determined according to the following expression:

$$\Delta t_{ij} = 23 \cdot (\Delta u^{i,j})^3 \text{ [s]} \quad (4)$$

$\Delta t^{i,j}$  – minimum time between switching on/off generator  $j$  and the next generator within power plant  $i$ .

Examining the criteria of rapid voltage change is no way a substitute and does not exclude the need for the analysis of voltage conditions in critical stationary states (power flow analysis).

## 2.2. Flicker criterion

Flickers are small short term voltage drops which appear as flashing lights. The following limit is set for the long-term flicker intensity caused by power plant  $i$  at the common connection point [7]:

$$P_{lt}^i \leq 0,46 \sqrt{\frac{S_g^i}{\sum_{k=1}^{N_{TS}} S_{dg}^k}} \quad (5)$$

$\sum_{k=1}^{N_{TS}} S_{dg}^k$  is the total approved (apparent) connection power of all  $N_{TS}$  power plants that are (or will be) connected to the same transformer station. This sum should take into account all future connections, but if it is not possible to assume further development of distribution system, it is necessary to adopt that  $\sum_{k=1}^{N_{TS}} S_{dg}^k = S_{TS}$ , where  $S_{TS}$  is the rated apparent power of the transformer to which the power plant is connected. The long-term flicker intensity caused by generator  $j$  in continuous operation within power plant  $i$  is calculated according to the expression:

$$P_{lt}^{i,j} = c_{\psi}^{i,j}(\psi_s^i) \cdot \frac{S_g^{i,j}}{S_{k3}^i} \quad (6)$$

$c_{\psi}^{i,j}(\psi_s^i)$  is the flicker coefficient of generator  $j$  within the power plant  $i$  and connected to the impedance of the angle  $\psi_s^i$ , in accordance with the previously mentioned standards and technical guidelines. The flicker coefficient is measured for impedance angles 30°, 50°, 70° and 85°, and it is calculated by linear interpolation for other values of the impedance angle. The flicker coefficient represents the ability of PVPPs to produce flickers.

## 2.3. Criterion of permitted higher current harmonics

There are regulations that limits produced current harmonics by the PVPPs. The following limit is set for the  $h_{th}$  higher harmonic of the power plant current  $i$  [7]:





$$I_h^i \leq i_h \cdot S_{k3}^i \cdot \sqrt[\alpha_h]{\frac{S_g^i}{\sum_{k=1}^{N_{TS}} S_{dg}^k}} \quad (7)$$

where are:

$i_h$  – allowed total value of the  $h$ -th higher harmonic current for all PVPPs connected to the same transformer station, reduced to the three-phase short circuit power

$\sum_{k=1}^{N_{TS}} S_{dg}^k$  – total approved (apparent) connection power of all  $N_{TS}$  PVPPs that are (or will be) connected to the same transformer station

$\alpha_h$  – exponent for summing higher current harmonics from different sources

The total value of the  $h$ -th higher harmonic of the PVPP current from the  $N_i$  generator is:

$$I_h^i = \sqrt[\alpha_h]{\sum_{j=1}^{N_i} (I_h^{i,j})^{\alpha_h}} \quad (8)$$

$I_h^{i,j}$  – the value of the  $h$ -th harmonic of the current of the generator  $j$  in the power plant  $i$

In TP 17, the permissible values for  $i_h$  [A/MVA] for certain voltage levels are specified. If the harmonic

In addition to the aforementioned criteria, the energy criteria of the network are checked for the selected limit operating conditions:

- Criterion of permitted voltage change in the network,
- Criterion of the permitted thermal loads of lines,
- Criterion of permissible thermal load of the transformer.

When processing the request for connection of higher power, as well as when connecting PVPPs directly to the busbars of the supplied TS 110/x kV (which are under the responsibility of “Elektroprenos”), the criteria specified in the grid code are checked [8]. To check these criteria, the investor should submit all relevant files for the inverters that are planned to be installed. The verification of these criteria depends on the categorization of power plants defined in the aforementioned grid code. Next, several examples of PVPPs connection to the distribution network of PE EP B&H, ED Tuzla will be briefly presented.

### 3. EXAMPLES OF DEFINING TECHNICAL CONNECTION CONDITIONS

During the work on the processing of requests for the connection of new PVPPs, the following representation of the future state of the distribution network was obtained. Several areas have already been recorded where the sum of maximum production becomes greater than the maximum consumption. It considers the sum of the power of smaller power plants distributed in the network, so during operation it will be a great challenge to maintain the voltage conditions and stability of the network. The power range of PVPPs usually ranges from about 20 kW to several MWs. There are also requests for PVPPs connection of a dozen or more MVA forwarded to the Distribution System Operator (DSO). The problem with the connection of larger powers on the distribution 10 kV network can be in the case of the requests to connect powers of several MWs in the depth of the 10 kV network where the short-circuit power is smaller and it is not possible to respond to the requirements of rapid voltage changes. Depending on the situation, the possibility of selective inclusion in certain times intervals is examined here. For example, the requests for connection of 12,5 MW power had to be reduced to the permitted 6 MWs at the nearest point of the 35 kV network. In the event that the investor decided to change the location of the PVPP in order to connect to the busbars of the existing TS 110/35/6 kV, the permitted connection power would be 12 MW. In the following text, the verification of the possibility of connecting three PVPPs of different powers to the distribution network of PE EP B&H, ED Tuzla is briefly presented. The check for aforementioned criteria was done for power factor 1, for the maximum active power of the power plant. Based on energy analyzes and actual system needs, DSO may require power plants to operate at constant power factor, constant reactive power or constant voltage. After checking the criteria mentioned in part 2, there is always a check of the energy parameters. The voltage oscillation and the load of network sections are checked for two limit regimes: the case of maximum consumption and maximum production and the case of minimum consumption and maximum production.

### 3.1. Connection of the PVPP »A«, 250 kW

For the connection of PVPP "A" – 250 kW (2x100 kW+1x50 kW), the possibility of connecting to the 0,4 kV busbars of the existing TS in distribution network was first checked (according to Figure 1). The installation of three inverters with a power of 2x100 kW and 1x50 kW is planned. A rapid voltage change check for variant I is as follows. The three-phase short circuit power at the common connection point (CCP) is:  $S_{k3} = 2264$  kVA and  $\frac{R_S}{X_S} = 1,2748 \rightarrow \psi_s = 38,11^\circ$ . The rapid voltage change in the connection point when switching on and off the PVPP "A", is:

$$\Delta u_{CCP}^{start} = k_i^{inv.start} \cdot \frac{(n \cdot S_{inv})}{S_{k3}^{CCP}} \cdot 100 = 0,025 \cdot \frac{2 \cdot 110}{2264} \cdot 100 + 0,141 \cdot \frac{1 \cdot 55}{2264} \cdot 100 = 0,585 \%,$$

$$\Delta u_{CCP}^{stop} = k_i^{inv.stop} \cdot \frac{(n \cdot S_{inv})}{S_{k3}^{CCP}} \cdot 100 = 1 \cdot \frac{2 \cdot 110}{2264} \cdot 100 + 1,107 \cdot \frac{1 \cdot 55}{2264} \cdot 100 = 12,41 \%$$

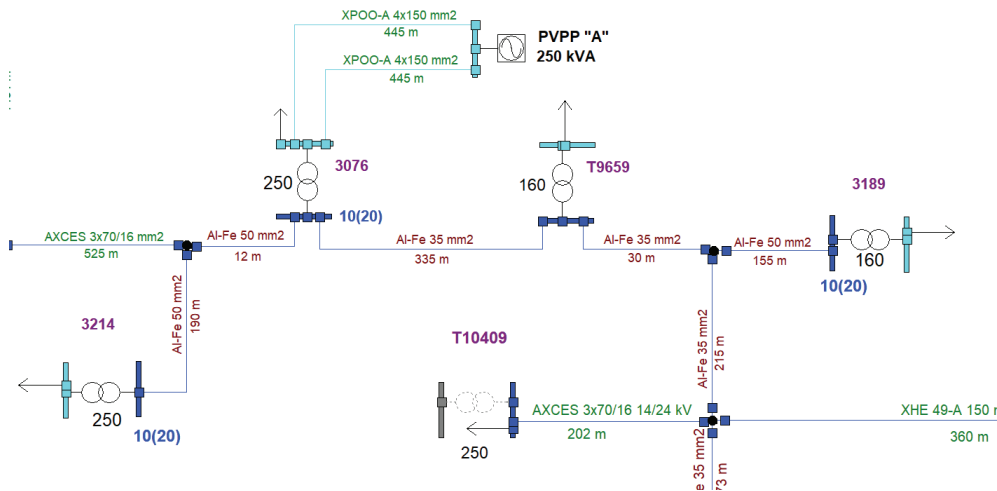


Figure 1: PVPP "A" connection diagram on the existing TS – Variant I

The rapid voltage change caused by the shutdown of the PVPP "A", at  $\cos\varphi_{inv} = 1$  is:  $\Delta u_{CCP}^{stop} = k_i^{inv.stop} \cdot \frac{(n \cdot S_{inv})}{S_{k3}^{CCP}} \cdot \cos(\psi_s - \varphi_{inv}) \cdot 100 = 9,75\%$ . The current factor values  $k_i$  are taken from the manufacturer. It can be seen that criterion of rapid voltage change at the connection point for Variant I is not satisfied since the calculated voltage change is  $\Delta u > 5\%$ . Therefore, Variant II will be analyzed – connection to the new KBTS 10(20)/0,4 kV with a transformer of nominal power 400 kVA (Figure 2).

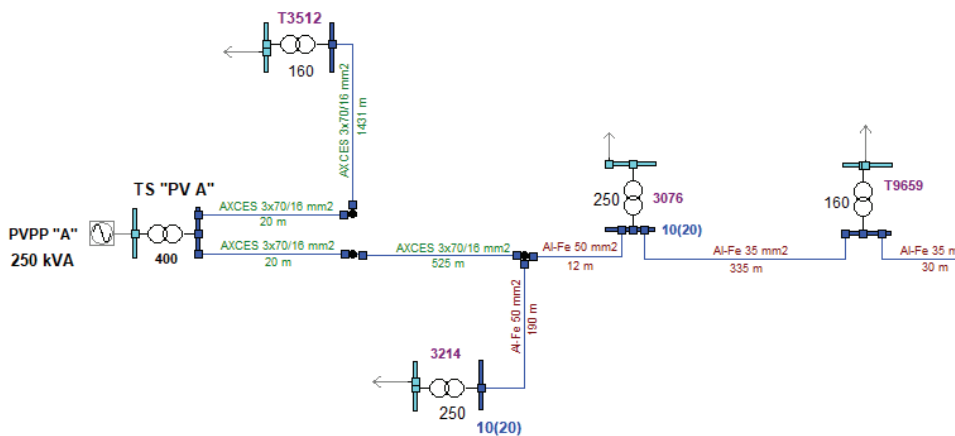


Figure 2: PVPP "A" connection diagram on the 0,4 kV busbars of the new TS, 400 kVA – Variant II

The three-phase short circuit power at the common connection point (0,4 kV side) is:  $S_{k3} = 8784$  kVA and  $\frac{R_S}{X_S} = 0,3787 \rightarrow \psi_s = 69,26^\circ$ . Rapid voltage change when switching on and off PVPP "A" 250 kW, is:



$$\Delta u_{CCP}^{start} = 0,025 \cdot \frac{2 \cdot 110}{8784} \cdot 100 + 0,141 \cdot \frac{1 \cdot 55}{8784} \cdot 100 = 0,151 \%$$

$$\Delta u_{CCP}^{stop} = 1 \cdot \frac{2 \cdot 110}{8784} \cdot 100 + 1,107 \cdot \frac{1 \cdot 55}{8784} \cdot 100 = 3,2 \%$$

Rapid voltage change caused by the shutdown of PVPP “A” at  $\cos\phi_{inv} = 1$  is:  
 $\Delta u_{CCP}^{stop} = 1 \cdot \frac{2 \cdot 110}{8784} \cdot \cos(69,26^\circ - 0^\circ) \cdot 100 + 1,107 \cdot \frac{1 \cdot 55}{2264} \cdot \cos(69,26^\circ - 0^\circ) \cdot 100 = 1,1325\%$ . It can be seen that the criterion of rapid voltage change at the connection point, according to Variant II, satisfied considering that the calculated  $\Delta u < 4\%$ . In most cases, for the connection of PVPPs with a power of 150 kW and more, it turned out that mostly a new TS should be built, and the connection is made on the 0,4 kV buses of TS 10(20)/0,4 kV.

**Flickers:** The permissible value of long-term flicker is defined according to relation (5):  $0,46 \cdot \sqrt{\frac{n_{inv1} \times S_{inv1} + n_{inv2} \times S_{inv2}}{S_{TS}}} = 0,381$

The total long-term flicker intensity of the PVPP “A” (in continuous operation) is:

$$P_{lt}^{FNE} = \sqrt{n_{inv1} \cdot \left(c_{\psi}^{inv1}(\psi_s) \frac{S_{inv1}}{S_{k3}}\right)^2 + n_{inv2} \cdot \left(c_{\psi}^{inv2}(\psi_s) \frac{S_{inv2}}{S_{k3}}\right)^2} = 0,06275 \text{ As } P_{lt}^{FNE} (0,06275) < 0,381$$

the flicker criterion is satisfied for the selected type of photovoltaic inverters to the conceptual design.

**Harmonics:** In accordance with expression (7), the calculation of higher current harmonics was made for the case of connecting PVPP “A” to the 0,4 kV bus of the new TS 10(20)/0,4 kV 400 kVA. The results and limitation are presented in Table 1. The first two columns in the table are the data that correspond to the selected type of inverter for PVPP “A”.

**Table 1:** Higher current harmonics for inverters SUN2000-50KTL-M0 and SUN2000-100KTL-M1

$h$	$I_h^{0,4 \text{ kV}}$ [A]	$I_h^{10 \text{ kV}}$ [A]	$S_k^{0,4 \text{ kV}}$ [MVA]	$i_h^{0,4 \text{ kV}}$ [A/MVA]	$S_k^{10 \text{ kV}}$ [MVA]	$i_h^{10 \text{ kV}}$ [A/MVA]	TP17 0,4 kV [A/MVA]	TP17 10 kV [A/MVA]
2	0,4989	0,0200	8,784	0,0023	63,57	0,0003	0,750	0,0300
3	1,4657	0,0586	8,784	0,0067	63,57	0,0009	3,000	-
4	0,2902	0,0116	8,784	0,0013	63,57	0,0002	0,375	0,0150
5	1,5227	0,0609	8,784	0,0069	63,57	0,0010	1,500	0,0580
6	0,2491	0,0100	8,784	0,0011	63,57	0,0002	0,250	-

By comparing the calculated ( $i_h^{0,4 \text{ kV}}, i_h^{10 \text{ kV}}$ ) and prescribed values according to TP 17 ( $i_h^{0,4 \text{ kV}} < \text{TP17 } 0,4 \text{ kV}$ ) it can be seen that the higher harmonic current criterion is satisfied for the selected type of inverter. The permissible values in [A] should be checked during a test operation (by currents measurement). If the harmonic criterion is not met, the owner of the power plant can install filters for corresponding higher harmonics or connect the power plant to the point with higher value of short circuit power (higher voltage level).

### 3.2. Connection of the PVPP »B«, 900 kW

The assumed connection point of PVPP “B” 900 kW are 10(20) kV busbars of the new TS 10(20)/0,4 kV “PV B” with a transformer of rated power 1000 kVA (Figure 3).

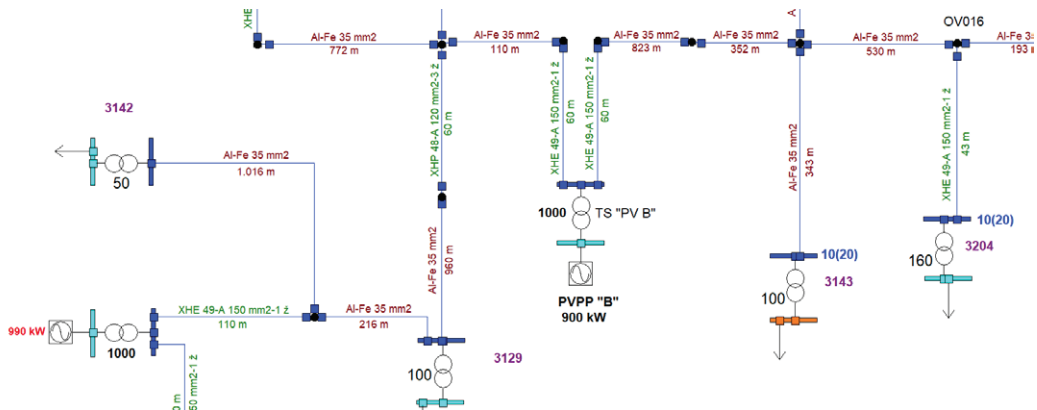


Figure 3: PVPP "B" connection diagram on the 0,4 kV busbars of the new TS 10(20)/0,4 kV, 1000 kVA

The verification of the permitted power criteria with regard to the rapid voltage change is follows. The power of the three-phase short circuit at the connection point is:  $S_{k3} = 36,77$  MVA and  $\frac{R_s}{X_s} = 1,3883 \rightarrow \psi_s = 35,76^\circ$ . The rapid voltage change at the connection point, when switching on and off the PVPP „B“ 900 kW, is:  $\Delta u_{10\text{ kV}}^{start} = k_i^{inv.start} \cdot \frac{(n \cdot S_{inv})}{S_{k3}} \cdot 100 = 0,5 \cdot \frac{9 \cdot 0,11}{36,77} \cdot 100 = 1,35\%$  and  $\Delta u_{10\text{ kV}}^{stop} = k_i^{inv.stop} \cdot \frac{(n \cdot S_{inv})}{S_{k3}} \cdot 100 = 1 \cdot \frac{9 \cdot 0,11}{36,77} \cdot 100 = 2,69\%$ . Therefore, the criterion of rapid voltage change at the connection point is satisfied ( $\Delta u \leq 4\%$ ). The criterion of flicker and permissible values of harmonics is also satisfied. Checking the energy criteria shows an increase in voltage conditions on 0,4 kV busbars above +5%, especially for transformers with a transmission ratio of 10(20)/0,42 kV. In the existing conditions, adequate operation of the automatic regulation in the supplied TS 110/10(20) kV and adjustment of the regulation switch to TS 10(20)/0,42 kV (in a voltage-free state) is available.

### 3.3. Connection of the PVPP »C«, 2x4,4 MW

The planned PVPP "C" with a power of 8,8 MW is located close to the existing TS 110/35/6 kV (connection scheme in Figure 4) and therefore the possibility of connection to the 35 kV bus of this TS was checked.

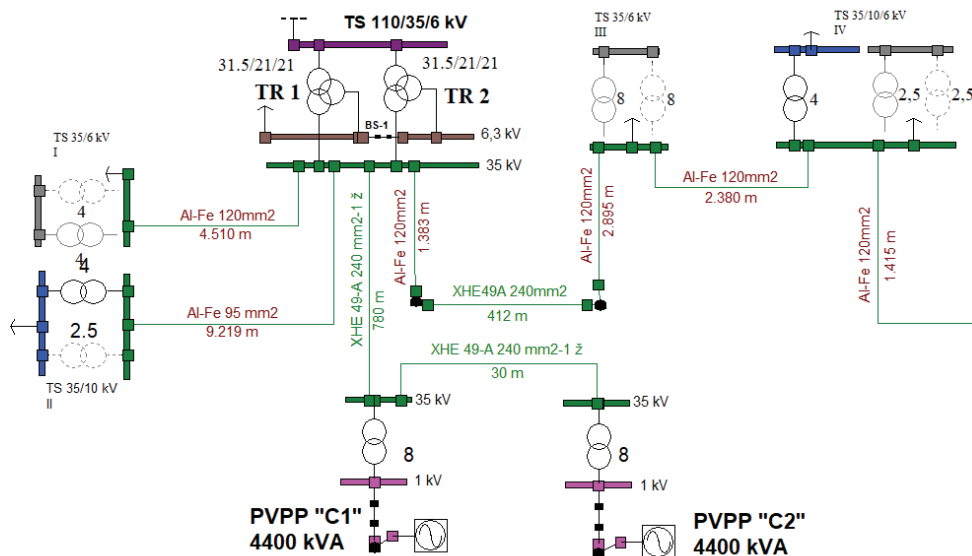


Figure 4: PVPP "C" connection scheme to the 35 kV busbars (on the existing TS)

In the event that both transformers are in operation, three-phase short circuit power is 283,6 MVA and the rapid voltage change is 3,1%. If one transformer is in operation, the power of three-phase short circuit is 158,8 MVA and the rapid voltage change is 5,57%. Therefore, the connection of the PVPP "C" with specified power is possible only with the condition of parallel operation of



transformers. In accordance with the network code [8], for connection to the supplied TS 110/x kV busbars, a dynamic check is performed – passing through the fault state. The considered PVPP “C” belongs to type B production modules: connection point below 110 kV and maximum power up to 10 MW. In terms of stability, production modules have to satisfied the requirements of the ability to pass through a fault condition (fault ride through – FRT), i.e. they have to be able to remain in operation during the occurrence of a fault in the transmission network and continue stable operation after the faults have been removed. The FRT curve expresses the lower limit of the value of the line voltage at the connection point as a function of time before, during and after the fault (symmetrical and asymmetric). Figure 5 shows this type of check for PVPP “C”. The voltage diagram on the MV buses and the active and reactive power of the PVPP “C” are shown.

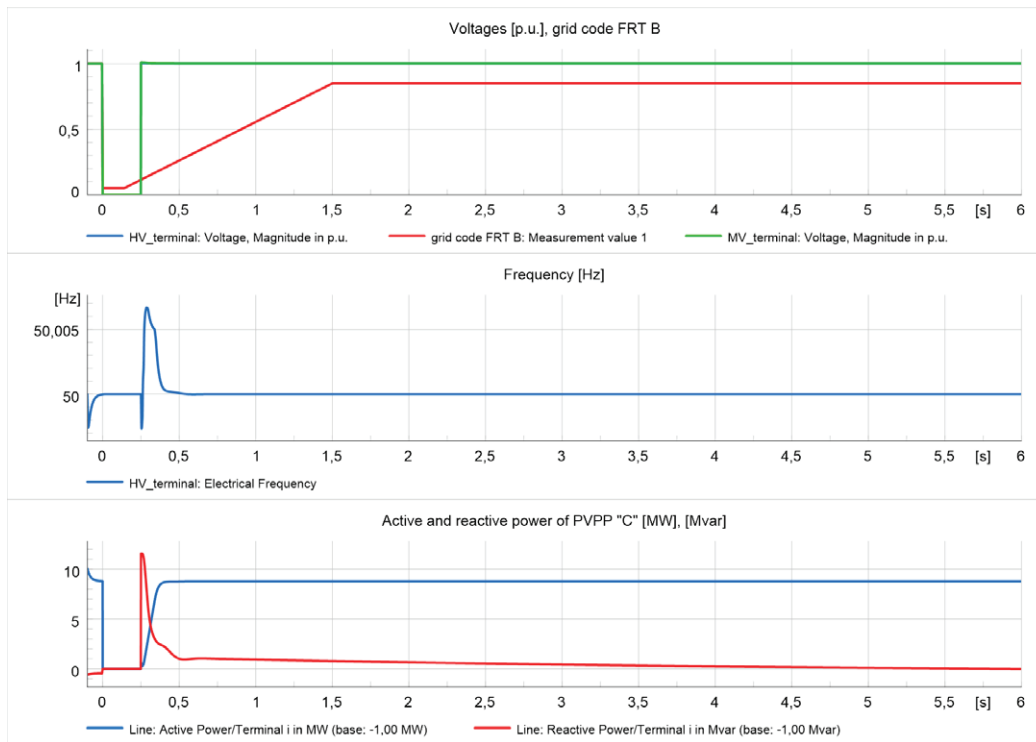


Figure 5: FRT curve for fault duration (three-phase fault) of 250 ms on the 110 kV busbars

For the modeled three-phase fault on the 110 kV busbars of the supplied TS 110/35/6 kV, which is cleared in 0,25 s, the power plant connected to medium voltage remains in operation. The simulation was made for  $\cos\varphi = 1$ . Also, the PVPP need to be able to activate the frequency response of the active power at the frequency threshold and static settings as specified in the grid code [8]. For the frequency threshold of 50,2 Hz and static setting 5%, there is no change in the voltage and active power of the PVPP (Figure 6). The diagrams also show that at the frequency of 51,2 Hz, there is a decrease in active power. For a period less than 2 s, the active power drop is less than 50% of the maximum active power, which is within the limits prescribed in the grid code. Specifically, for the considered PVPP “C”, in 2 sec after the frequency change, the power is 5,78 MW, which is a drop of 34% of the rated power (Figure 6).

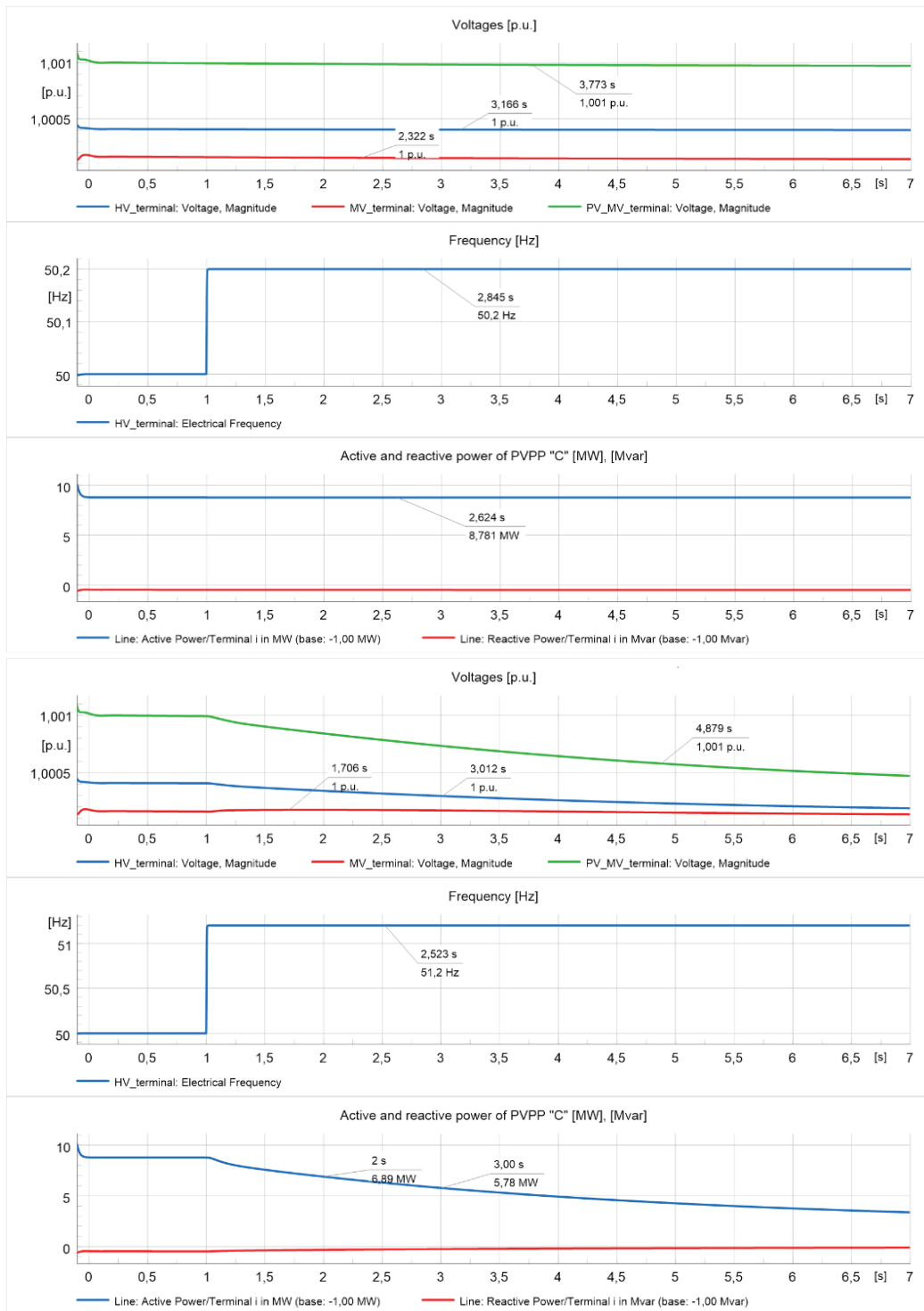


Figure 6: Diagrams of active power and the voltages for frequencies 50,2 Hz and 51,2 Hz

#### 4. FUTURE ACTIVITIES: MORE FLEXIBLE DISTRIBUTION NETWORK

Already now, in some distribution areas, the required connection power exceeds the consumer's load values, so the reverse direction of energy occurs, i.e. energy is transferred to the transmission network. In such cases, the problem in defining the connection conditions can also be the energy criteria in the stationary state. Often, when connecting PVPPs, the voltage conditions are not satisfied. Critical periods are usually the assumed regime of max. production and min. consumption. In this case, the voltage values on the buses above the permissible limits can be obtained in the calculations. The second considered regime is max. consumption





and max. production, and here we have a reduction of the calculated voltages. With a greater influence of distributed generation, the differences in the calculated voltages are quite large. Consequently there is a need to put into operation the voltage regulator on TS 10(20)/0,4 kV and the supplied TS 35/10(20) kV and TS 110/x kV, which allows the existing equipment of the network. It is evident that when planned PVPPs are put into operation, there will be a need to activate more complex methods of voltage management and regulation. By reviewing the available literature, it can be seen various centralized and decentralized regulation methods. Decentralized voltage regulation methods take into account power factor regulation, reactive power compensation, regulation transformers, limitation of power generated from distributed generators, as well as intelligent techniques based on a limited degree of communication between individual parts of the network. These methods do not provide the possibility of voltage regulation at the level of the entire system, but they are reliable depending on the activities undertaken. Centralized methods require high level communication between individual parts of the system, which causes high costs for their implementation. Coordinated methods gives much better results with respects to local strategy, in terms of loss minimization and voltage violation mitigation, but can be applied only in fully supervised and controlled networks [9].

## 5. CONCLUSION

Since 2021, there has been a sudden increase in the number of requests to join the PVPPs in the territory of EP B&H. The existing regulation in B&H, which is used when defining the connection conditions, is briefly presented. Technical recommendations and the network code are subject to constant review and harmonization with the current situation and requirements for the connection of a larger number and larger powers of PVPPs. For higher PVPPs powers, consideration of electrical energy storage is an option. Events in the past year focused on defining the possibility of connecting to the existing network. However, when putting PVPPs into trial and permanent operation, a more detailed approach will be required in terms of network management and voltage regulation, which will be probably lead to significant investments in the network infrastructure.

## BIBLIOGRAPHY

- [1] IRENA Renewables Energy Statistics 2022, downloaded from Renew. Energy Statistics 2022 (irena.org)
- [2] Parsons Brinckerhoff Ltd, branch in Belgrade "The influence of solar power plants on the electric power system in Bosnia and Herzegovina" (elaboration: 287546A Rec 1 December 2014)
- [3] James Reilly, Geza Joos "Integration and Aggregation of Distributed Energy Resources – operating approaches, standards and guidelines" (25th Int. Conf. on Elect. Distribution, Madrid, 3-6 June 2019)
- [4] Nouha Mansouri, Abderezak Lashab, Josep M. Guerrero, Adnen Cherif "Photovoltaic power plants in electrical distribution networks: a review on their impact and solutions" (IET Renew. PG, Special Issue: Power Quality and Protection in RES and Microgrids ISSN 1752-1416, July 2020)
- [5] Sophia Reker, Jens Schneider, Christoph Gerhards, "Integration of vertical solar power plants into a future German energy system" (Smart Energy 7 2022, journal homepage: [www.journals.elsevier.com/smart-energy](http://www.journals.elsevier.com/smart-energy), down. from <https://doi.org/10.1016/j.segy.2022.100083>)
- [6] Xi Lu, Shi Chen, et. all. "Combined solar power and storage as cost-competitive and grid-compatible supply for China's future carbon-neutral electricity system", (PNAS 2021 Vol. 118 No. 42, downloaded from <https://doi.org/10.1073/pnas.210347118> )
- [7] Technical recommendations for the connection and operation of distributed generation – TP 17, PE Elektroprivreda B&H, September 2022
- [8] Grid Code, Independent System Operator in Bosnia and Herzegovina (NOS B&H), November 2021
- [9] V. Ilea, C. Bovo, D. Falabretti et. all. „Voltage Control Methodologies in Active Distribution Networks“ Energies 2020, 13, 3293; doi: 10.3390/en1312393



# Imputation and Forecasting of Energy Consumption data collected by smart meters using Big Data Technologies in the Distribution System Operator

[andrej.somrak@troia.si](mailto:andrej.somrak@troia.si)ANDREJ SOMRAK<sup>1\*</sup>, ROK DOLINŠEK<sup>1</sup>, MAJA SAVINEK<sup>2</sup>, TADEJ ŠINKOVEC<sup>2</sup>, LEON MARUŠA<sup>3</sup><sup>1</sup>Troia d.o.o.<sup>2</sup>Elektro Ljubljana d.d.<sup>3</sup>Elektro Celje d.d.

Slovenia

## SUMMARY

The usage of data from advanced metering systems for advanced analytics, billing purposes, forecasting of energy consumption, and regulatory rules has gained a lot in popularity worldwide in recent years. Besides that, it helps to increase the efficiency and accuracy of the management of electricity (smart) distribution systems. The operation of advanced metering systems creates a large amount of data transmitted from data concentrators or smart meters. It is the largest data source by volume for a DSO. The data is stored in the data lake based on Hadoop distributed architecture. Communication between the smart meters and the data concentrator is via low-voltage wires using frequency signals (PLC). Despite the recent development of smart meters, the problem of missing data is a common problem. It arises due to interference from other devices, unexpected device power-off, and other communication failures. Therefore, we had to develop a methodology to deal with the missing energy consumption data. Due to the regulatory requirements, we could not use the traditional time series imputation methods, and we had to develop a custom solution to deal with the missing data problem. The solution is called the normalised profile of similar days, which is based on the past energy consumption data of the customers. The data is stored in the Kudu database, which enables updating the existing records (upsert). The solution was developed with Apache Spark, specifically the Python API for Apache Spark, called PySpark. Apache Spark is an open-source, distributed processing system used for big data workloads. The energy consumption data is collected at 15-minute intervals, and the solutions consider the cold start problem (when the past data for a customer is unavailable). Imputation of missing data is processed in the following steps: (1) checking the data quality, (2) detecting and removing outliers, (3) detecting the missing data, (4) imputing missing data, and (5) analysing and visualising the results. The implemented solution proved successful regarding precision, processing time, and resource usage and satisfied all regulatory requirements. In the paper, we present the problem of missing energy consumption time series data and existing methods to solve the problem. In more depth, we present our solution, the challenges we had, and the presented solution's advantages, disadvantages, and limitations.

## KEYWORDS

smart meters, DSO, time series, imputation, forecasting, big data, pyspark



**Oral Presentation:** Imputation and Forecasting of Energy Consumption data collected by smart meters using Big Data Technologies in the Distribution System Operator

### 1. INTRODUCTION

The digitalisation of the electrical energy system, driven by energy transformation, smart grids, and advanced metering systems, generates massive data requiring storage, real-time processing, and analysis for decision-making. Traditional data management is insufficient, leading to the adoption of big data and distributed data systems. Digitalisation cannot be imagined without data, which is one of the key foundations of the transition to the digital age. That is helping DSOs on the path to becoming data-driven companies, but only if the data is of high quality.

With the planned changes in the management and development of the distribution network, the integration of renewable energy sources, self-supply, the introduction of electric vehicles and other changes, digital transformation will play a very important role in DSOs. DSOs already collect and store technical data, such as data on electricity infrastructure, spatial data in GIS systems, metering points for billing purposes, electricity consumption and many other parameters of advanced metering devices, and data generated by SCADA and ADMS systems.

Advanced metering systems have experienced a significant surge in popularity on a global scale in recent years. This increased recognition by companies stems from their numerous advantages, resulting in improved efficiency and accuracy in managing electricity distribution systems. The operation of advanced metering systems generates a substantial volume of data, which is transmitted from data concentrators or smart meters to the metering centre. As the metering data comprises time-series data, it necessitates the implementation of specialised techniques for time-series analysis.

In Slovenia, in the upcoming year (2024), there will be changes in the calculation method for the distribution network fee, introducing five blocks with different tariff rates. These blocks will be determined separately for the high and low seasons, as well as for working days and public holidays. The cost of network usage within each block will depend on the network load and the consumer's usage in the previous period.

A novel feature of the upcoming system is the differentiation between contracted and excess power, referring to exceeding the contracted power level. The DSO will determine the contracted power for each consumer based on their connection capacity and historical network usage. This allows the end consumer to modify their contracted power and influence the costs of network usage by monitoring and adjusting their consumption habits. After a two-year transitional period, charges for excess power above the contracted power will be implemented. However, if household consumers modify their contracted power within this transitional period, as determined by the DSO, they will be subject to network fees for excess power starting from January 1st of the following year.

Calculation of the network fees will not be possible if metering time-series data is not properly stored and analysed. Over the past several years, DSOs in Slovenia have been steadily migrating from the traditional electricity grid to a smart grid, resulting in more than 80 % of installed smart meters. The data collected from the smart meters provide granular insights into their physical status, capturing detailed information at intervals as short as 1, 10, or 15 minutes. This includes various registers and meter events that represent different aspects of the grid's condition and performance. In one year, 400 MB of data for a single consumption is generated, which means that, within one year, 40 TB of data is generated per 100.000 customers or measuring points.

This metering data is transmitted over fixed networks, power line communication (PLC), fixed radiofrequency or public networks into three separate proprietary meter data systems. These typically use relational databases and validate the data and the events. Most of the installed smart meters communicate with the concentrator installed in the transformer substation by the PLC. This communication turned out to be very unreliable due to different reasons, such as interference from other devices, unexpected device power-off, and other communication failures. Hence, we devised a methodology outlined in this paper to address the missing energy consumption data issue. Our approach involves imputing the missing values in the time series, and we will provide a detailed description of this methodology in the following sections.

### 2. BIG DATA MANAGEMENT PLATFORM

Maintenance, management, and data storage are complex and extensive work. Analysing and correlating data using traditional client-server and relational database techniques proved impossible, both from a data management and performance perspective. Instead of choosing the traditional Meter Data Management System (MDMS) route, we have opted to develop a more general data management and analytics platform using modern Big Data concepts and industry-proven scalable technologies.

We have developed and implemented a Big Data Management Platform (BDMP) in a DSO. This platform consists of a set of software deployed on a centralised BDMP system. The BDMP facilitates data virtualisation, acting as a connector between diverse data



Oral Presentation: Imputation and Forecasting of Energy Consumption data collected by smart meters using Big Data Technologies in the Distribution System Operator

sources. It combines and transforms key data, leveraging learned data models to uncover valuable information, identify data correlations, and perform statistical calculations tailored to specific business requirements. The BDMP offers a robust platform that empowers end-users with a wide range of analysis capabilities. It incorporates visual elements to explore both historical and real-time streaming data, delivering up-to-the-minute results and fresh insights. The platform ensures integrated management and security, guaranteeing data consistency, high quality, and protection. Users can have confidence in the trustworthiness of the data. Moreover, the BDMP enhances the usability of data for business purposes. It standardises data structures, making them more consistent and easier to comprehend. This enables advanced non-IT users to engage in self-service analytics, leveraging the platform’s capabilities without relying solely on IT support.

BDMP platform is constructed using open-source technology and is designed based on thorough analysis and identified use cases. The goal is to include all the necessary components for a successful implementation. The implemented solution is divided into two main strands: data engineering and data visualisation/data science. The system first captures data from various source systems. It then proceeds to store, aggregate, and process this data, creating unified datasets that can be utilised for further analysis and decision-making. The BDMP platform provides end-users with data visualisation and analytics capabilities to facilitate informed decision-making. This empowers users to explore and interpret the data in a meaningful way. The architectural representation in Figure 1 illustrates a simplified overview of the BDMP platform’s structure.

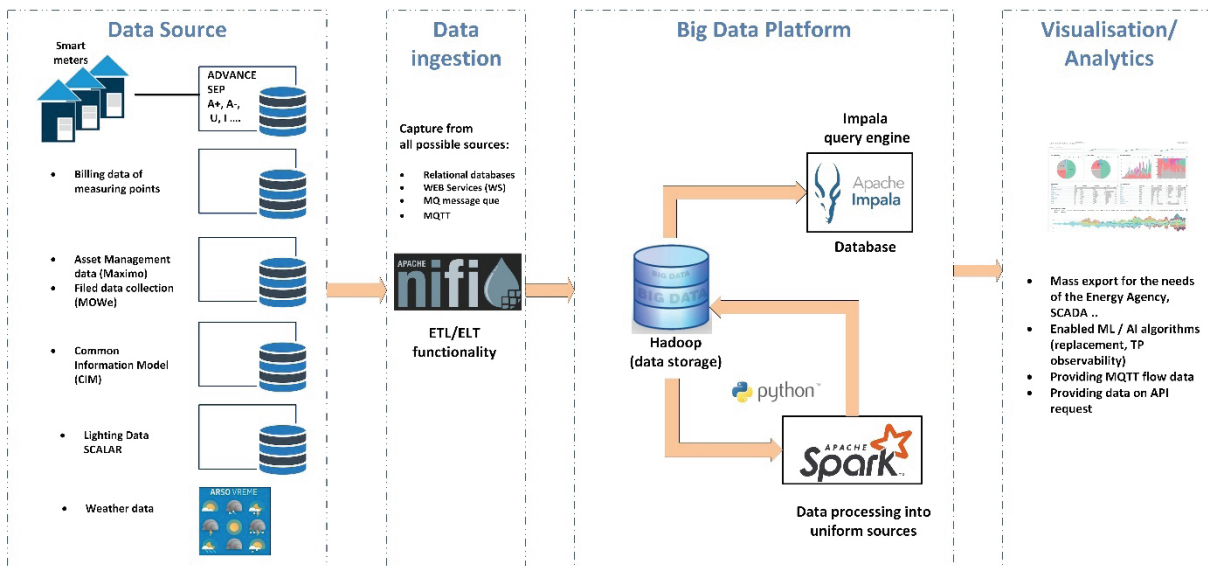


Figure 1. The architecture of the Big Data management and analytics platform

The BDMP provides security, robustness, high mass data processing capability, and is scalable in terms of data volume and extensible, allowing easy extension to use of additional data sources in the future. The entire system is designed to provide a complete process from data capture, processing and visualisation daily, meaning that daily up-to-date status of the network.

This data is ingested into the BDMP through Apache Nifi [1] and Apache Kafka. Apache Kafka is a distributed data store optimised for ingesting and processing streaming data in real time. Apache NiFi supports powerful and scalable directed graphs of data routing, transformation, and system mediation logic. Big Data platform for storage, processing and operation is built on open source technology: (1) Apache Hadoop [2], (2) Apache Impala [3] and (3) pySpark [4]). Apache Hadoop is a collection of open-source software utilities that facilitates using a network of many computers to solve problems involving massive amounts of data and computation. Apache Impala is the open-source, native analytic database for Apache Hadoop. Apache Impala brings scalable parallel database technology to Hadoop, enabling users to issue low-latency SQL queries to data stored in HDFS and Apache HBase without requiring data movement or transformation. The Apache Impala tool provides access to the data via SQL queries for the visualisation tools or ad hoc queries.

The BDMP platform contains a highly distributed HDFS file system that distributes data across data blocks. A highly distributed file system alone is not sufficient for fast data processing, so Apache Spark is used in the platform to improve the performance of the technology through massively parallel processing (MPP).

Data captured from different sources are not always of good quality, do not contain business logic, and are unsuitable for use in different application services and analytics solutions. Therefore, data processing had to be performed first. The data is being



**Oral Presentation:** Imputation and Forecasting of Energy Consumption data collected by smart meters using Big Data Technologies in the Distribution System Operator

cleansed, merged, processed, standardised, aggregated, transformed, recalculated, and prepared as a single source for further analysis using Apache Spark via the Python programming language (PySpark). PySpark is an interface for Apache Spark in Python. It allows you to write Spark applications using Python APIs and provides the PySpark shell for interactively analysing your data in a distributed environment. Spark explicitly manages memory and converts most operations to work directly with binary data. Data processing speed is thus improved with Spark algorithms and data structures that exploit the memory hierarchy with cache computation.

The platform supports capturing and using data regarding grid topology, metering, and events on the infrastructure. A vast amount of data is generated by various systems: advanced metering, SCADA/AMDS, billing, asset management, workforce management, field operations, GIS, CIM topology, weather and lighting data etc. Data is captured from different sources, such as streaming data (sensors, IoT devices, smart meters), relational databases and online sources.

In recent years, metadata and data management have become increasingly important as companies have put data at the heart of digitisation. Data governance enables access to quality and trusted data while complying with legislation, privacy, confidentiality and other data governance policies. To get the most value from data, a data catalogue has been integrated into the BDMP platform. The use of a data catalogue basically allows the management of the metadata of the entire data model dimensioned in BDMP. It also, with additional built-in functions, allows searching and categorising data, browsing the available data and viewing the data all the way from capture to final visualisation. This capability improves the quality and availability of data and enables users to make wider use of data and increase their confidence in the data.

Data governance concerns are addressed through the access layer that allows role-based access control and access auditing (Apache Ranger and Apache Atlas). Apache Atlas provides open metadata management and governance capabilities for organisations to build a catalogue of their data assets, classify and govern them, and provide collaboration capabilities around these data assets for data scientists, analysts and the data governance team. Apache Atlas supports metadata types and instances, data classification, data lineage, and security and data masking. Integration with Apache Ranger enables authorisation/data-masking on data access based on classifications associated with entities in Apache Atlas. Apache Ranger delivers a comprehensive approach to security for a Hadoop cluster. It provides a centralised platform to define, administer and manage security policies consistently across Hadoop components. Using the Apache Ranger console, policies for access to files, folders, databases, tables, or column security administrators are easily managed. These policies can be set for individual users or groups and then enforced consistently across the platform. Apache Ranger was integrated with Active Directory, and by LDAP protocol user groups have been synchronised and access to data and services has been configured according to their authorisations, so we could meet the information security policy of the data classification.

The BDMP platform was also integrated with IBM QRadar for auditing purposes. IBM QRadar is an enterprise security information and event management (SIEM) product. It collects log data from an enterprise, its network devices, host assets and operating systems, applications, vulnerabilities, and user activities and behaviours.

### 3. TIME SERIES DATA

Time series data refers to a sequence of information where each data point is associated with a specific time period. It encompasses measurements or observations made at regular intervals over time, with each time period being equally defined and resulting in a constant frequency. Time series data capture various measurable phenomena and are affected by external factors as well as past values.

Patterns observed in time series data are expected to persist in the future, which makes it valuable for modelling, analysing, and predicting trends and seasonality. Time series analysis has gained significant importance in multiple fields, particularly in finance, weather forecasting, and control systems. Time series data is pervasive and used extensively to make data-driven decisions, anticipate patterns, and enhance product experiences. In finance, time series analysis is highly significant for understanding stock market trends, forecasting asset prices, and managing investment risks. Weather forecasting heavily relies on time series data to analyse historical weather patterns and make predictions about future conditions. Control systems leverage time series data to monitor and optimise processes, ensuring efficient and reliable operations.

The key characteristics of time series data are as follows:

- **Temporal Order:** Time series data is arranged in chronological order, with each observation associated with a specific time stamp. The time intervals between observations are usually fixed or regular.





**Oral Presentation:** Imputation and Forecasting of Energy Consumption data collected by smart meters using Big Data Technologies in the Distribution System Operator

- **Dependence on Previous Observations:** Each data point in a time series is often influenced by previous observations. This dependency can be used to analyse patterns, trends, and relationships within the data.
- **Seasonality and Trends:** Time series data often exhibit recurring patterns known as seasonality, which can occur over daily, weekly, monthly, or yearly cycles. Time series data may also contain long-term trends, indicating overall direction and behaviour.
- **Irregular or Missing Data:** Time series data can sometimes have missing observations or irregular time intervals between measurements. Dealing with missing or irregular data is an important aspect of time series analysis.

Analysing time series data involves various techniques, such as forecasting future values, detecting patterns and trends, identifying seasonality, and understanding the impact of variables on the time series behaviour. Time series analysis can provide valuable insights for decision-making, planning, and understanding the dynamics of a system over time. Time series modelling, analysis, and prediction enable businesses and organisations to leverage collected time series data for pattern recognition and informed decision-making. By studying historical trends, identifying seasonality, and making accurate forecasts, organizations can develop better data-driven products, optimize operations, and improve overall outcomes. Time series data holds immense potential for unlocking insights and driving innovation across a wide range of industries.

#### 4. TIME SERIES DATA IMPUTATION AND FORECASTING

Time series data imputation refers to the process of filling in missing values in a time series dataset. Missing values can occur due to various reasons, such as data collection errors, sensor malfunctions, or incomplete data recording. Imputing missing values is crucial for maintaining the continuity and integrity of the time series data before performing further analysis or forecasting.

There are several methods available for time series data imputation, including:

- **Forward Fill or Backward Fill:** This simple method involves carrying forward the last observed value or backward filling the next observed value to replace missing values. This approach assumes that there are no significant changes between consecutive time points.
- **Mean or Median Imputation:** In this approach, the missing values are replaced with the mean or median of the available data points. This method assumes that the missing values are randomly distributed and do not significantly affect the overall trend or pattern of the time series.
- **Linear Interpolation:** Linear interpolation estimates missing values based on the linear relationship between adjacent data points. It assumes a linear trend between the available data points and fills in the missing values accordingly.
- **Seasonal Imputation:** For time series data exhibiting seasonal patterns, seasonal imputation methods can be used. These methods estimate missing values based on the seasonal component of the time series, taking into account the seasonal patterns observed in the available data.

After imputing missing values, time series forecasting can be performed to predict future values based on historical data. Forecasting techniques for time series data include:

- **Moving Average (MA) or Exponential Smoothing (ES) Methods:** These methods use weighted averages of past observations to forecast future values. Moving Average considers a fixed number of previous observations, while Exponential Smoothing assigns exponentially decreasing weights to older observations.
- **Autoregressive Integrated Moving Average (ARIMA):** ARIMA models incorporate the autoregressive (AR), differencing (I), and moving average (MA) components to capture the trend, seasonality, and random fluctuations in the time series.
- **Seasonal Decomposition of Time Series (STL):** This method decomposes the time series into trend, seasonal, and residual components and models each component separately for forecasting.
- **Machine Learning Models:** Advanced techniques like regression models, support vector machines (SVM), or neural networks can be used for time series forecasting. These models can capture complex relationships and patterns in the data.

The choice of imputation and forecasting methods depends on the specific characteristics of the time series data, the amount of missing data, and the desired level of accuracy or interpretability.

Matrix estimation methods can also be used for time series imputation and forecasting when dealing with multivariate time series data. These methods leverage the relationships and dependencies among multiple variables to fill in missing values and make predictions for future time points.





**Oral Presentation:** Imputation and Forecasting of Energy Consumption data collected by smart meters using Big Data Technologies in the Distribution System Operator

One popular matrix estimation technique is Singular Value Decomposition (SVD). SVD decomposes a matrix into three separate matrices:  $U$ ,  $\Sigma$ , and  $V$ . In the context of time series, the matrix represents the multivariate time series data, where each row corresponds to a time point, and each column corresponds to a variable.

For time series imputation, SVD can be used to estimate missing values by reconstructing the matrix with a reduced rank. The missing values are filled in based on the reconstructed matrix, which captures the underlying patterns and relationships present in the data.

For time series forecasting, SVD can be combined with autoregressive models to capture both the temporal dependencies within each variable and the cross-variable relationships. The SVD decomposition provides a low-rank approximation of the matrix, which can be used to forecast future values based on the observed historical data. The reconstructed matrix can then be transformed back to the original format to obtain the forecasts for each variable.

Other matrix estimation techniques, such as Principal Component Analysis (PCA) and Low-Rank Matrix Completion, can also be utilised for time series imputation and forecasting. These methods aim to exploit the low-rank structure of the data matrix to handle missing values and make accurate predictions.

Matrix estimation methods are particularly useful when dealing with multivariate time series data where the variables are interrelated and share common patterns. However, the effectiveness of these techniques depends on the assumptions made about the underlying data structure and the specific characteristics of the time series being analysed.

It is essential to consider both temporal and spatial dependencies when analysing the electricity metering data. Temporal dependence refers to the seasonality of electricity consumption, while spatial dependence pertains to the proximity of consumers in physical space. For temporal data, there exists temporal autocorrelation when values measured closely together in time exhibit greater similarity than those measured far apart in time [5]. For spatial data, spatial autocorrelation occurs when values measured in close proximity exhibit more similarity than those measured far apart. Understanding the presence of temporal and spatial dependencies is crucial for accurate analysis and modelling of the data. By accounting for these dependencies, we can uncover patterns, trends, and relationships that might be influenced by the time of measurement or physical proximity. Consideration of temporal and spatial autocorrelation enables the development of more robust and accurate forecasting models and facilitates the identification of factors that drive electricity consumption patterns.

## 5. USE CASES BASED ON THE METERING DATA

Metering data, which provides detailed information on energy consumption and usage patterns, can be leveraged for various use cases. Here are some common use cases based on metering data:

- **Predictive Maintenance (Condition-Based Maintenance):** Machine learning algorithms can analyse sensor data from equipment such as transformers and circuit breakers to predict when maintenance is required. This improves reliability and reduces maintenance costs.
- **Load Forecasting:** Machine learning can forecast future energy demand by analysing historical energy consumption data and weather patterns. This enables optimisation of production and distribution, prevents overloads and outages, and facilitates smarter network investments.
- **Generation Forecasting:** Forecasting energy production involves predicting the electricity generated by different energy sources connected to the grid. Accurate forecasting is crucial for maintaining system stability, balancing supply and demand, and managing renewable energy variability.
- **Network Management and Optimization:** Machine learning can optimise the distribution and transmission of electricity, considering factors such as load balancing, congestion management, and asset utilisation.
- **Fault Detection and Outage Management:** Real-time analysis of sensor data and other sources can detect faults, predict outages, and enable corrective actions. This enhances network reliability and minimises downtime.
- **Fraud Detection:** Machine learning helps identify potential cases of energy theft or unauthorised consumption by analysing metering data and detecting suspicious patterns in time series data.
- **Distribution Grid Identification:** Machine learning aids in understanding the characteristics, parameters, and topology of the distribution grid. It enables the prediction of equipment connections based on consumption patterns, facilitating efficient grid planning.



Oral Presentation: Imputation and Forecasting of Energy Consumption data collected by smart meters using Big Data Technologies in the Distribution System Operator

- **Location Selection for Renewable Energy and EV Charging:** AI/ML can determine optimal locations for renewable energy installations and electric vehicle charging stations based on power flow, grid capacity, and profitability.
- **Customer Segmentation:** Analysing customer data allows for the identification of consumption patterns, segmentation of customers, and the development of targeted energy efficiency programs or product offerings.
- **Smart Grid Management:** AI/ML technologies play a crucial role in managing and decentralising energy management in smart grids, enabling more efficient and sustainable energy systems.

## 6. OUR SOLUTION FOR METERING DATA TIME SERIES IMPUTATION

Smart meters report the captured 15-minute measurements to the measurement centre (usually once a day) according to a pre-set schedule. For various reasons, the meters sometimes do not send the data, and missing values occur in the time series of 15-min energy profiles, so these values must be imputed. For that reason, we had to implement the imputation of the missing data in the time series, which will be described in this chapter. We will present the conditions under which missing values are imputed and the methodology according to which they are replaced.

Imputation of missing data is processed in the following steps: (1) checking the data quality, (2) detecting and removing outliers, (3) detecting the missing data, (4) imputing missing data, and (5) analysing and visualising the results.

During the development of the solution, we considered the following factors to ensure its effectiveness:

- **Non-discriminatory and Customer-friendly:** The solution aims to be fair and transparent, providing equal treatment to all customers. It ensures that the information and processes are easy to understand and accessible to customers, promoting a positive customer experience.
- **Scalability and Efficiency:** The solution is designed to be feasible on a wide range of devices and capable of handling a large volume of data efficiently. It takes into account the need to process and analyse data within a reasonable timeframe, ensuring optimal performance even with significant data loads.
- **Legal Compliance:** The solution adheres to applicable laws, regulations, and industry standards. It prioritises data privacy and security, protecting customer information and ensuring compliance with relevant data protection and privacy regulations.

In addition, it had to be considered that DSOs have different information systems for obtaining metering data (Advance or SEP2W), and these are written differently in different data structures.

Data is rewritten as soon as data from the smart meters become available. The data is processed once a day for a 30 days period of data. All the missing data from the previous processing is updated, and existing data remains intact (but checked for any discrepancies from the previous processing). Updating data was made possible by using Kudu tables that allow UPSERT operations (update and insert). Apache Kudu is an open-source column-oriented data store of the Apache Hadoop ecosystem that makes fast analytics on fast and changing data easy.

Application of our solution is used for balance billing (since 1. 1. 2023), calculating distribution network charges (from 1. 1. 2024), and other projects, such as ADMS surrogate curves, demand forecasting, etc.

### 6.1. Key Indicator for the quality of measurement data at the daily level

In the daily replacement process, each missing value is replaced, either with a value of 0 if it is a demonstrable power failure, or by the normalised profile of similar days methodology if it is due to another cause. At the daily level, the quality of the measurement data ( $Kqi\_d$ ) is calculated for each time series according to Equation (1).  $Kqi\_d$  represents the proportion of missing and substituted values over all values expected over a period of one day.

$$Kqi\_d = 100 \cdot \frac{N_d - N_{mer\_d}}{N_d} \quad [\%] \quad (1)$$

$Kqi\_d$	Key indicator for 15-min data quality at daily level [%]
$N_d$	Number of total 15-min intervals at daily level (96 measurements)
$N_{mer\_d}$	Number of actual 15-min values measured at daily level



Oral Presentation: Imputation and Forecasting of Energy Consumption data collected by smart meters using Big Data Technologies in the Distribution System Operator

$Kqi\_d$  is calculated on a daily basis due to the need to monitor data quality on a daily basis. The calculated  $Kqi\_d$  is stored in a special fact table which also stores the  $N_d$  and  $N_{mer\_d}$  values from which  $Kqi\_d$  was calculated.  $Kqi\_d$  is calculated for each daily time series recorded in the meter register belonging to a specific metering point.

In the case that e.g. due to poor meter communication on a certain day, the measurements are not delivered to the measurement centre (we have missing values),  $Kqi\_d < 100\%$  is calculated for that day. At this point, we have three possible scenarios:

- Measurements are never delivered to the measuring centre (meter memory overwrite, meter failure, etc.) - in this case,  $Kqi\_d$  will not change and will not be recalculated.
- The measurements are delivered to the measurement centre once the poor communication has been resolved:
  - If the time stamps of the sent measurements are greater than or equal to the end date of the last accounting period ( $d1$ ), this means that the measurements have not yet been used for accounting. These measurements shall be inserted into the table of measurements, and any superseded values shall be overwritten. In this case,  $Kqi\_d$  is recalculated for the day in question.
  - If the time stamps of the sent measurements are smaller than the end date of the last accounting period ( $d1$ ), this means that the measurements have already been used for the accounting. These measurements are not inserted table of measurements (so we keep the substituted values for these time stamps). In this case,  $Kqi\_d$  is not recalculated for the day in question.

### 6.2. Key Indicator for the quality of metering data at the billing period level

Since the daily values  $N_d$  and  $N_{mer\_d}$  are stored in the table, the quality of the metering data at the billing period level ( $Kqi\_ob$ ) can be calculated by aggregating these values. When the billing is triggered, the quality of the metering data ( $Kqi\_ob$ ) is calculated for the entire billing period for each time series recorded in the meter register belonging to a specific metering point.  $Kqi\_ob$  is calculated according to Equation (2) and represents the proportion of missing and substituted values over all values in the billing period.  $Kqi\_ob$  is calculated from the daily stored values  $N_d$  and  $N_{mer\_d}$ , which are also used to calculate  $Kqi\_d$ . This ensures that also in the calculation of  $Kqi\_ob$ , surrogate values or newly acquired measurements are used where allowed.

$$Kqi\_ob = 100 \cdot \frac{N_{ob} - N_{mer\_ob}}{N_{ob}} = 100 \cdot \frac{\sum_{t=d0}^{d1} N_d - \sum_{t=d0}^{d1} N_{mer\_d}}{\sum_{t=d0}^{d1} N_d} \quad [\%] \quad (2)$$

$Kqi\_ob$	Key indicator for 15-min data quality at accounting period level [%]
$N_{ob}$	Number of total 15-min intervals in the billing period
$N_{mer\_ob}$	Number of 15-min values actually measured during the accounting period
$N_d$	Number of total 15-min intervals at daily level (96 measurements)
$N_{mer\_d}$	Number of actual 15-min values measured at daily level
$d0$	Start date of the current billing period (or end date of the previous accounting period)
$d1$	End date of the current billing period

The calculated  $Kqi\_ob$  is stored in a special table, which also stores the values  $N_{ob} = \sum_{t=d0}^{d1} N_d$  and  $N_{mer\_ob} = \sum_{t=d0}^{d1} N_{mer\_d}$  from which  $Kqi\_ob$  was calculated.  $Kqi\_ob$  is calculated for each time series recorded in the meter register belonging to a specific metering point for a time period of the billing period.

If a time series is considered to have less than 10 % missing values ( $Kqi\_ob < 10\%$ ) during the accounting period, then the measuring point is considered to be eligible for accounting with 15-min measurements recorded. If the missing values are greater than or equal to 10 % ( $Kqi\_ob \geq 10\%$ ), then the measuring point is considered to be eligible for accounting with no 15-min measurements recorded.

### 6.3. Detection and cleaning of values outside the characteristic range (outliers)

In a time series of 15-minute measurements, certain values of the energy profiles are often above the expected values and are not valid. These values are referred to as outliers, and the term meter breakthroughs have become common in DSO jargon. Such values occur for a variety of reasons resulting from the malfunctioning of the smart meter. An example of such values for a given metering point is shown in Figure 2.

Oral Presentation: Imputation and Forecasting of Energy Consumption data collected by smart meters using Big Data Technologies in the Distribution System Operator

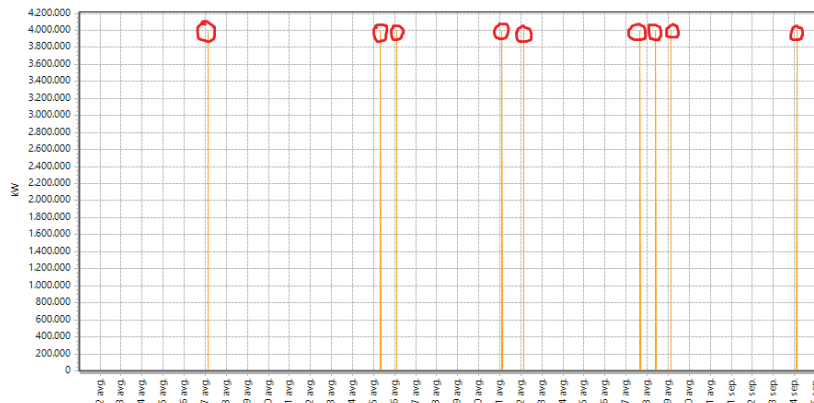


Figure 2: An example of extremely large outliers in smart meter measurements

As we can see, the values in Figure 2 are extremely high, but this is not necessarily true for breakthroughs. There are cases where the breakthroughs take a much smaller value, in which case the missing values appear before them. An example of these breakthroughs is shown in Figure 3.

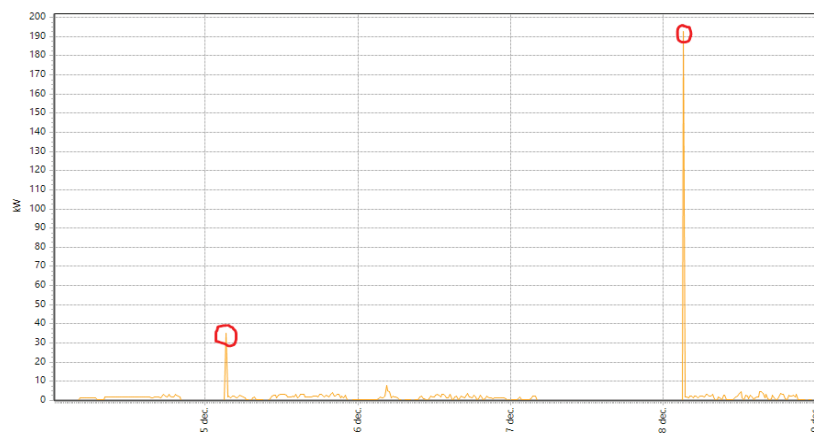


Figure 3: Example of small breakthroughs in smart meter measurements

Taking the breakthroughs into account in the billing of the consumer would result in the billing of higher amounts of energy consumed and the billing of higher excess power ( $Cex_b$ ). As these values are incorrectly recorded, taking them into account in the billing would be detrimental to the consumer, and it is necessary to rectify these values.

The detection of outliers is by using the method of comparing the value with a multiple of the connected power. Since we are looking for a breakthrough detection methodology that can be used regardless of the type of energy profile, we proposed to use the value multiplier method for breakthrough detection, where we label as breakthroughs or out-of-characteristic values all measurements for which the condition in Equation (3) holds. Since the left-hand side of the equation is the 15-min power measurement  $A+(t)$ , we need to multiply it by 4 to get the 15-min power measurement, which can be compared with the connected power on the right-hand side of the equation.

$$4 \cdot A+(t) > 1,2 \cdot Ccn \tag{3}$$

$A+(t)$	Single 15-min energy measurement recorded at 15-min interval t [kWh]
$Ccn$	Connection power of consumer [kW]

The described breakthrough detection is problematic in case of incorrectly recorded connection powers. In case the recorded connection power of a consumer is higher than the actual one, it may happen that the user's ( $Cc_b$ ) will be set too high. Thus the consumer



Oral Presentation: Imputation and Forecasting of Energy Consumption data collected by smart meters using Big Data Technologies in the Distribution System Operator

will be able to achieve higher achieved powers ( $Cm_p$ ) without being billed as overcharged ( $Cex_p$ ). In case the recorded connected power of the system user is much lower than the actual one, it may happen that the consumer will consume energy (profile values will be high), and the algorithm will detect them as outliers, even though the measurements are valid. For this reason, it is essential that DSOs validate and, if necessary, verify the connection powers at the metering points before starting to apply the new network charge. Once the breakthroughs have been detected and properly identified in the metering data, the outliers will be deleted or replaced by missing values, which will be replaced in the next step by substitute values.

#### 6.4. Validation of measurement data and determination of the justification for replacing missing values

For each 15-min interval in the billing period, the energy consumption data coming from the metering centres shall be marked with a status whether it is a measured value or a missing value:

- meter\_data\_status = 0; 15-min value was actually measured by the meter
- meter\_data\_status = 1; 15-min value is missing, no data
- measurement\_data\_status = 2; the 15-min value is replaced by the selected methodology.

Such flagged data is a prerequisite for determining the eligibility of replacing missing values. For the purposes of substitution eligibility, there are two types of data substitution:

- Substitution with a value of 0 kW;
- Replacement with the methodology of normalised profile of similar days methodology.

To justify the substitution of missing values in the 15-min measurements, we first validate the measurements by checking the amount of energy recorded by the 15-min measurements against the difference between the recorded meter states.

The algorithm for determining eligibility for each time series is as follows:

- In the billing period, find all counter states ( $A+_TO$ ) and their timestamps (these time stamps are not aligned to a 15-min interval and are recorded on a per-second granularity);
- Align the time stamps of the counter states to the nearest 15-minute interval;
- For each pair of consecutive counter states ( $A+_TO_{t1}, A+_TO_{t2}$ ):
  - Calculate the difference of the counter states ( $\Delta Ws_{t2-t1}$ ) and record the value as the amount of energy consumed according to Equation (4).

$$\Delta Ws_{t2-t1} = A+_TO_{t2} - A+_TO_{t1} [kWh] \tag{4}$$

$A+_TO_{t1}$	First meter state value [kWh]
$A+_TO_{t2}$	Value of the second (last) meter reading [kWh]
$\Delta Ws_{t2-t1}$	Energy consumed in the period between $t1$ and $t2$ calculated from the difference of the meter readings [kWh]

Next we obtain all 15-min energy measurements ( $A+$ ) between the timestamps ( $t1$  and  $t2$ ) of the successive meter readings and calculate their integral or sum ( $\Delta Wp_{t2-t1}$ ), which also represents the energy consumed in the interval between and  $t_2$ . The sum is calculated by Equation (5).

$$\Delta Wp_{t2-t1} = \sum_{t=t1}^{t2} A+(t) [kWh] \tag{5}$$

$t1$	Time-stamp of the first meter reading aligned to the nearest 15-min interval
$t2$	Time stamp of the second (last) meter reading aligned to the nearest 15-min interval
$A+(t)$	Single 15-min energy measurement recorded at 15-min interval $t$ [kWh]
$\Delta Wp_{t2-t1}$	Energy consumed in the period between $t1$ and $t2$ calculated from the sum of the energy profile [kWh]



Oral Presentation: Imputation and Forecasting of Energy Consumption data collected by smart meters using Big Data Technologies in the Distribution System Operator

Equation (6) calculates the difference ( $diff\_ΔW$ ) between the energies consumed calculated from the difference of the meter readings ( $ΔW_{s_{t2-t1}}$ ) and the sum of the energy profiles ( $ΔW_{p_{t2-t1}}$ ).

$$diff\_ΔW = ΔW_{s_{t2-t1}} - ΔW_{p_{t2-t1}} [kWh] \tag{6}$$

$diff\_ΔW$	Difference in energy consumed calculated from the difference of the meter readings and the sum of the energy profile
$ΔW_{s_{t2-t1}}$	Energy consumed in the period between $t1$ and $t2$ calculated from the difference of the meter readings [kWh]
$ΔW_{p_{t2-t1}}$	Energy consumed between $t1$ and $t2$ calculated from the sum of the energy profile

If  $diff\_ΔW = 0$ , then there were no missing values in the interval between  $t1$  and  $t2$  that are eligible for replacement. Since the original meter readings are recorded with a time granularity of seconds and the energy profiles with a granularity of 15 minutes, the  $diff\_ΔW$  will never be exactly 0. To this end, we simplify that  $diff\_ΔW$  can have a tolerance of 2% of the difference of the meter readings  $ΔW_{s_{t2-t1}}$ .

With this simplification in mind, the following follows:

- If  $diff\_ΔW \leq 0,02 \cdot ΔW_{s_{t2-t1}}$ , the 15-min measurements between two consecutive meter readings are considered to be complete and do not contain any missing values that are eligible for substitution. In case missing values (meter\_data\_status = 1) exist in this interval, they shall be replaced by a value of 0 kW, as these are power failures.
- If  $diff\_ΔW < 0$ , this means an error in the meter measurements. In this case, the cleaning of values outside the characteristic range may not have been performed correctly. These cases have to be analysed individually.
- If  $diff\_ΔW > 0,02 \cdot ΔW_{s_{t2-t1}}$  is valid, the 15-min measurements between two consecutive count conditions are considered to be incomplete and contain missing values that are eligible for replacement. In these cases, substitution is performed according to the normalised profile of similar days methodology.

In determining the eligibility of substitution, it is currently sufficient to consider the condition  $diff\_ΔW > 0.02 \cdot ΔW_{s_{t2-t1}}$  for the choice between 0 kW substitution or substitution by the normalised profile of similar days methodology, as any significant deviation between  $ΔW_{s_{t2-t1}}$  and  $ΔW_{p_{t2-t1}}$  in principle means that energy consumption was present (meter readings were rising), while no 15-min measurements were recorded. Following this logic, any missing value that occurs under the condition  $diff\_ΔW > 0.02 \cdot ΔW_{s_{t2-t1}}$  can be replaced. Once we have determined the eligibility of each 15-min measurement for substitution and cleaned the out-of-range values, we start calculating and applying the substitution values in the time series.

### 6.5. Description of the methodology of the normalized profile of similar days (NPSD)

The NPSD methodology is based on substitution rules in accordance with Article 203 of the SONDSEE (System operating instructions for the electricity distribution system). Using the algorithm described, we have determined the time periods in which data are eligible for substitution, thus obtaining a time series containing only the missing values eligible for substitution under the RNPSD methodology. This time series is taken as input to the RNPSD.

The NPSD algorithm for each time series is as follows. For each pair of consecutive meter readings ( $A+_TO_{t1}$ ,  $A+_TO_{t2}$ ), count the number of complete areas with missing values eligible for replacement ( $n_{ob} = 1,2,3...$ ) and determine the time stamps of the start ( $tz_{ob1}$ ,  $tz_{ob2}$ ,  $tz_{ob3}...$ ) and the end ( $tk_{ob1}$ ,  $tk_{ob2}$ ,  $tk_{ob3}...$ ) of these areas.

For each comprehensive area of missing values eligible for replacement:

- Define the time tag of the beginning of the missing period ( $tz_{ob1}$ ) and the time tag of the end of the missing period ( $tk_{ob2}$ ).
- Find the nearest meter reading ( $A+_TO_{t1}$ ) and its timestamp ( $t_1$ ) before the start of the missing period and find the nearest meter reading ( $A+_TO_{t2}$ ) and its timestamp ( $t_2$ ) after the end of the missing period.
- Align the timestamps of the meter readings to the nearest 15-minute interval;

For each pair of consecutive counter states ( $A+_TO_{t1}$ ,  $A+_TO_{t2}$ ):

- Calculate the difference of the meter readings ( $ΔW_{s_{t2-t1}}$ ) and record the value as the amount of energy consumed according to Equation (7).





Oral Presentation: Imputation and Forecasting of Energy Consumption data collected by smart meters using Big Data Technologies in the Distribution System Operator

$$\Delta W_{S_{t_2-t_1}} = A_{+_T0_{t_2}} - A_{+_T0_{t_1}} \quad [kWh] \quad (7)$$

$\Delta W_{S_{t_2-t_1}}$	Energy consumed in the period between $t_1$ and $t_2$ calculated from the difference of the meter readings [kWh]
$A_{+_T0_{t_1}}$	Value of the first meter reading
$A_{+_T0_{t_2}}$	The value of the second (last) meter reading

Obtain all 15-min meter readings ( $A_+(t)$ ) between the timestamps ( $t_1$  and  $t_2$ ) of the successive meter readings and calculate their integral or sum ( $\Delta W_{P_{t_2-t_1}}$ ), which also represents the energy consumed in the interval between  $t_1$  and  $t_2$ . The sum is calculated using the Equation (8).

$$\Delta W_{P_{t_2-t_1}} = \sum_{t=t_1}^{t_2} A_+(t) \quad [kWh] \quad (8)$$

$t_1$	Time stamp of the first meter reading aligned to the nearest 15-min interval
$t_2$	Time stamp of the second (last) meter reading aligned to the nearest 15-min interval
$A_+(t)$	Single 15-min energy measurement recorded at 15-min interval $t$ [kWh]
$\Delta W_{P_{t_2-t_1}}$	Energy consumed in the period between $t_1$ and $t_2$ calculated from the sum of the energy profile [kWh]

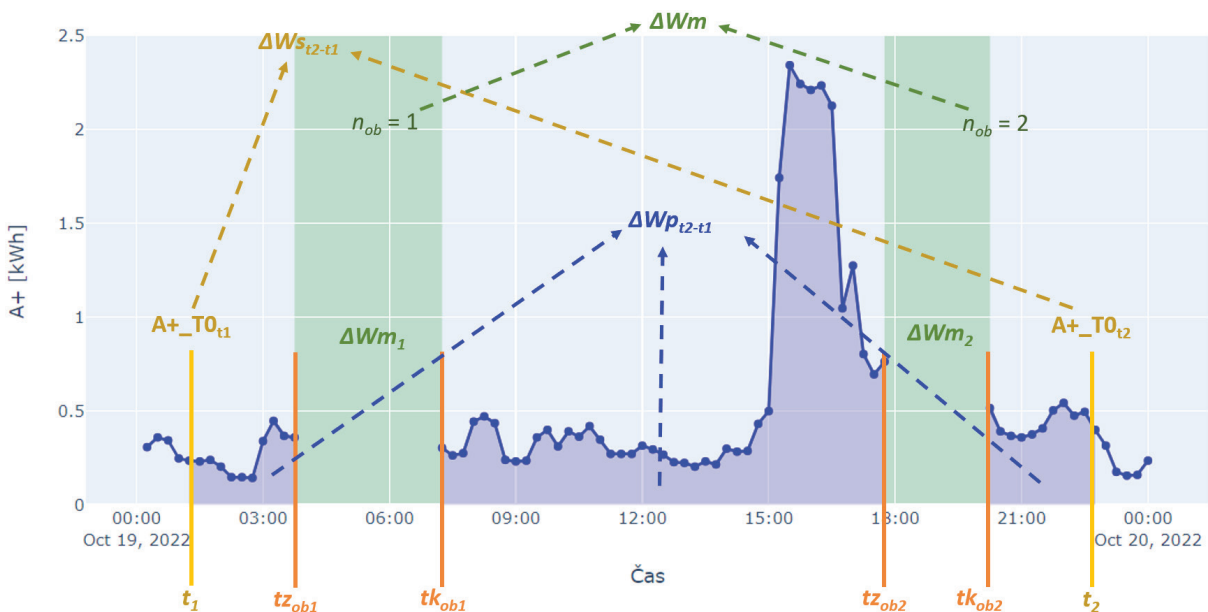


Figure 4: Variable definitions for a day with missing values in the 15-min measurements.

Using Equation (9) we calculate the total energy ( $\Delta W_m$ ) consumed during the missing values (in areas  $n_o = 1, 2, 3, \dots$ ).

$$\Delta W_m = \Delta W_{S_{t_2-t_1}} - \Delta W_{P_{t_2-t_1}} \quad [kWh] \quad (9)$$

$\Delta W_m$	Total energy consumed during missing values [kWh]
$\Delta W_{S_{t_2-t_1}}$	Energy consumed in the period between $t_1$ and $t_2$ calculated from the difference of the meter readings [kWh]
$\Delta W_{P_{t_2-t_1}}$	Energy consumed in the period between $t_1$ and $t_2$ calculated from the sum of the energy profile [kWh]

Oral Presentation: Imputation and Forecasting of Energy Consumption data collected by smart meters using Big Data Technologies in the Distribution System Operator

### 6.6. Condition of selection of the similar day

The similar days with conflicting values are used to obtain values that will be used as references on days where measurements are missing. The following criteria apply for the selection of similar days:

- **Working days:** if the day on which the measurements are missing is a working day, then the working day is the same working day in the previous week, provided that the day was not a public holiday in the previous week.
  - If that day in the previous week was a public holiday, the reference day is the same weekday in the previous two weeks.
- **Saturdays and public holidays on Saturdays:** if the day on which the measurements are missing is a Saturday, then the similar day is the Saturday of the previous week, regardless of whether the day on which the measurements are missing or the similar day of the previous week is an ordinary Saturday or a public holiday.
- **Sundays and public holidays on Saturdays:** if the day on which the measurements are missing is a Sunday, then the similar day is a Sunday in the previous week, whether the day on which the measurements are missing or the similar day of the previous week is an ordinary Sunday or a public holiday.
- **Public holidays in working days:** if the day on which the measurements are missed is a public holiday, but that day is normally a weekday, then the similar day is Saturday of the previous week.

Bear in mind that there may be missing values even on the similar days from which we are trying to impute. For this purpose, we also define auxiliary days for each similar day to be used in case values are also missing on a similar day. As a rule of thumb, for each similar day, we use two auxiliary similar days, each one week back in time. If we have missing values in the primary and all similar days, we will replace the missing values on the day we are replacing them with a value of 0 kWh. Even if a similar day already contains substituted values, these values will still be used in the RNPSD substitution procedure for the current day.

For each similar day, we calculate the energy consumed in that zone ( $\Delta Wa_{n_{obs}}$ ) on a similar day using the Equation (10).

$$\Delta Wa_{n_{obs}} = \sum_{t=tz_{obs_{n_{obs}}}}^{tk_{obs_{n_{obs}}}} A_+(t) \text{ [kWh]}; \quad za \ n_{obs} = 1, 2, \dots, n \tag{10}$$

$\Delta Wa_{n_{obs}}$	Energy consumed in each $n_{obs}$ area where there are 15-min measurements to be used as substitutes for missing 15-min measurements [kWh]
$A_+(t)$	Single 15-min energy measurement recorded at 15-min interval $t$ [kWh]
$tz_{obs_{n_{obs}}}$	$n_{obs}$ area start time-stamp
$tk_{obs_{n_{obs}}}$	$n_{obs}$ area end time-stamp
$n_{obs}$	Comprehensive areas from the similar day containing 15-min measurements to be used as substitutes for missing 15-min measurements

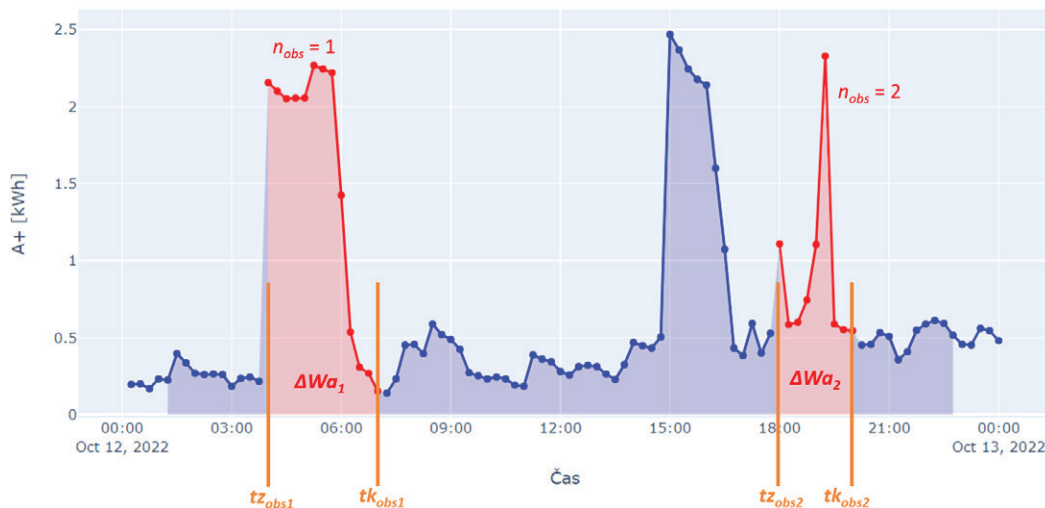


Figure 5: Variable definitions for the solitary day from which the 15-min reference measurements are used

**Oral Presentation:** Imputation and Forecasting of Energy Consumption data collected by smart meters using Big Data Technologies in the Distribution System Operator

Now we divide the 15-min measurements recorded in each similar day  $n_{obs}$  area into shares ( $A+(t)_{delež}$ ) relative to the total energy consumed in that zone  $\Delta Wa_{nobs}$ . In other words, the variable  $A+(t)_{delež}$  share represents the normalised profile for the similar day range. This is calculated by Equation (11).

$$A+(t)_{delež} = 100 \cdot \frac{A+(t)}{\Delta Wa_{nobs}} \quad [\%]; \quad za \quad n_{obs} = 1, 2, \dots, n \quad (11)$$

$A+(t)_{delež}$	Proportion of 15-min energy measurement in interval $t$ to total energy consumed in the $n_{obs}$ range [kWh]
$A+(t)$	Single 15-min energy measurement recorded at 15-min interval $t$ [kWh]
$\Delta Wa_{nobs}$	Energy consumed in each $n_{obs}$ area where there are 15-min measurements to be used as substitutes for missing 15-min measurements [kWh]
$n_{obs}$	Comprehensive areas from the similar day containing 15-min measurements to be used as substitutes for missing 15-min measurements

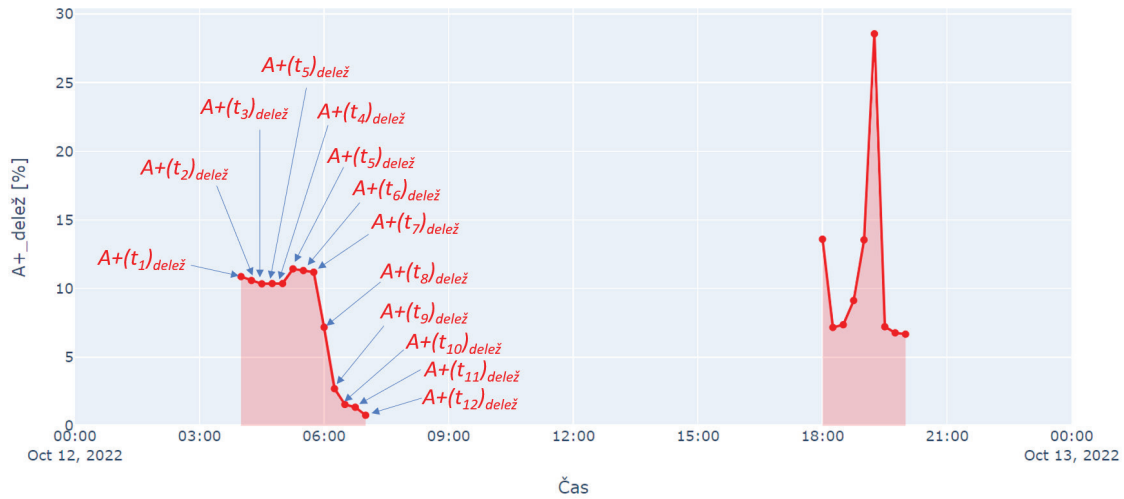


**Figure 6:** Proportions of individual 15-min measurements ( $A+(t)_{delež}$ ) in the  $n_{obs} = 1$  range on a similar day

For the methodology to work for several missing areas within two consecutive counting states, we also need to determine the energy fractions ( $d_{Wa}$ ) between the individual  $n_{obs}$  ranges. The calculation is done using Equation (12).

$$d_{Wa_{nobs}} = 100 \cdot \frac{\Delta Wa_{nobs}}{\sum_{nobs=1}^n \Delta Wa_{nobs}} \quad [\%]; \quad za \quad n_{obs} = 1, 2, \dots, n \quad (12)$$

$d_{Wa_{nobs}}$	Energy fractions $\Delta Wa_{nobs}$ of individual $n_{ob}$ areas in a similar day [%]
$\Delta Wa_{nobs}$	Energy consumed in each $n_{obs}$ region where there are 15-min measurements to be used as substitutes for missing 15-min measurements [kWh]
$n_{obs}$	Comprehensive areas from the similar day containing 15-min measurements to be used as substitutes for missing 15-min measurements
$n$	Number of $n_{obs}$ areas in a similar day

Multiply the energy fractions  $d_{Wa_{nobs}}$  for each  $n_{obs}$  area by the total energy ( $\Delta Wm$ ) for which there are no 15-min measurements recorded in the missing day. This gives the energies ( $\Delta Wm_{nobs}$ ) for each area of missing  $n_{ob}$  measurements, which will be used to raise the normalised profile in each  $n_{ob}$  area. This is always subject to the condition  $n_{ob} = n_{obs}$  since the number of areas from which we use the profiles of a similar day is always equal to the number of areas with missing values in the day we are replacing. The calculation is done using the Equation (13).



Oral Presentation: Imputation and Forecasting of Energy Consumption data collected by smart meters using Big Data Technologies in the Distribution System Operator

$$\Delta Wm_{nob} = \frac{d_{Wa_{nob(s)}}}{100} \cdot \Delta Wm \text{ [kWh]}; \quad za \ n_{ob} = 1, 2, \dots, n \quad (13)$$

$\Delta Wm_{nob}$	Calculated energy consumed in each $n_{ob}$ area with missing 15-min measurements [kWh]
$d_{Wa_{nobs}}$	Energy fractions $\Delta Wa_{nob}$ of individual $n_{ob}$ areas in a similar day [%]
$\Delta Wm$	Total energy consumed during missing values [kWh]
$n_{ob}$	Comprehensive areas with missing values of 15-min measurements eligible for substitution
$n_{obs}$	Comprehensive areas from the similar day containing 15-min measurements to be used as substitutes for missing 15-min measurements
$n$	Number of $n_{ob}$ areas in a missing values day or number of $n_{obs}$ zones in a similar day

For each area, multiply the  $A+(t)_{delež}$  fraction by the energy to raise the normalised profile ( $\Delta Wm_{nob}$ ) to obtain the  $A+(t)_{nadomestek}$ , which represents the 15-min replacement energies. The values are calculated using the Equation (14).

$$A+(t)_{nadomestek} = \frac{A+(t)_{delež}}{100} \cdot \Delta Wm_{nob} \text{ [kWh]}; \quad za \ n_{ob} = 1, 2, \dots, n \quad (14)$$

$A+(t)_{nadomestek}$	Calculated 15-min energy measurement to be used as a replacement for interval $t$ [kWh]
$A+(t)_{delež}$	Proportion of 15-min energy measurement in interval $t$ to total energy consumed in the $n_{obs}$ area [kWh]
$\Delta Wm_{nob}$	Calculated energy consumed in each $n_{ob}$ area with missing 15-min measurements [kWh]
$d_{Wa_{nobs}}$	Energy fractions $\Delta Wa_{nobs}$ between individual $n_{obs}$ areas during a similar day [%]
$\Delta Wm$	Total energy consumed during missing values [kWh]
$n_{ob}$	Comprehensive areas with missing values of 15-min measurements eligible for substitution
$n_{obs}$	Comprehensive areas from the similar day containing 15-min measurements to be used as substitutes for missing 15-min measurements
$n$	število območij $n_{ob}$ v dnevu manjkajočih vrednosti oz. število območij $n_{obs}$ v solednem dnevu Number of $n_{ob}$ areas in a missing values day or number of $n_{obs}$ areas in a similar day

Now we move the  $A+(t)_{nadomestek}$  values from the similar day to the day with the missing values or assign the solitary timestamps to the  $A+(t)_{nadomestek}$  values (change the date to the day of the missing values, do not change the time).

### 6.7. Business rules for value substitution

Replacement of missing values is performed on a daily basis, for as many days as the system allows or as selected according to resources. A daily replacement process is necessary as electricity can be billed on any working day, not only at the end of the month. Mid-month billing can be triggered by a change of supplier, a change of meter, a change of payer, etc. As mentioned above, if the data of a similar day is also missing, two auxiliary similar days, 14 days and 27 days ago, are used for the purpose of replacement.

When substituting with the NPSD methodology, it should be borne in mind that consecutive counter states are not necessarily be recorded on a 15-min period, as counter states are recorded asynchronously at the second level. In order to use the counter states for calculations, they must be aligned to the nearest 15-min time tag. The principle of minimum time distance shall be taken into account. If a counter state is closer in a number of seconds to the next 15-min period than to the previous one, the next period will be used as the state timestamp. If a counter state is closer in a number of seconds to the previous 15-min period than to the next, the previous period shall be used for the state time tag.

Normally, within each day, one daily readout of the counter state is obtained from the meters. In the event that multiple meter readings are obtained within a day, the two readings closest in time to the integral range ( $n_{ob}$ ) containing the missing values shall be used in the substitution.



**Oral Presentation:** Imputation and Forecasting of Energy Consumption data collected by smart meters using Big Data Technologies in the Distribution System Operator

The NPSD value substitution is performed for the following 15-min profiles (time series):

- Consumer's active energy received from the grid (register A+)
- Consumer's active energy delivered to the grid (register A-)
- Consumer's reactive energy of inductive character (register R+)
- Consumer's reactive energy of capacitive character (register R-)

We only use the surrogate values to calculate the amount of energy and to determine the agreed billing power ( $Cc_b$ ) per individual block, which is proposed to the customer by DSO. We do not use the surrogate values to calculate the achieved block power ( $Cm_b$ ) and, therefore, the excess billing power ( $Cex$ ), but in these cases, we only use the actual measurements for billing purposes.

## 7. CONCLUSION

Power engineers today are embracing data analytics as a crucial component of modern industrial systems, driven by advancements in information and communication technologies. Data analytics serves as an additional information layer within traditional electricity transmission and distribution networks, enabling data collection, storage, and analysis. However, the characteristics of data, massive data volumes, and technological challenges present significant hurdles in transitioning to the digital age of electricity, where robust data analytics plays a central role. High-quality, reliable, and trustworthy data is essential for data-driven decision-making.

The operation of advanced metering systems generates a substantial amount of data transmitted from data concentrators or smart meters, making it the primary data source for Distribution System Operators (DSOs). Communication between smart meters and data concentrators occurs through low-voltage wires using frequency signals (PLC). Despite the progress made with smart meters, the issue of missing data remains prevalent due to interference, power disruptions, and communication failures. Consequently, a methodology had to be developed to address this challenge, considering regulatory requirements that limited the use of traditional time series imputation methods.

The developed solution, known as the normalised profile of similar days, is based on past energy consumption data from customers. The imputation of missing data follows a systematic process, including data quality checks, outlier detection and removal, identification of missing data, imputation of missing values, and analysis and visualisation of the results. The application of this solution extends to balance billing, calculation of distribution network charges, as well as other projects like ADMS surrogate curves and demand forecasting. Accurate data imputation is also crucial for machine learning algorithms and models utilising metering time series data, such as energy consumption, production forecasts, and predictive maintenance.

In Slovenia, upcoming changes in 2024 will introduce a new calculation method for the distribution network charges involving five tariff rate blocks. These blocks will be determined separately for high and low seasons, as well as for working days and public holidays. The cost of network usage within each block will depend on the network load and the consumer's usage in the previous period. Notably, the new system will differentiate between contracted and excess power, specifically addressing instances where power levels exceed the contracted limit.

The implemented solution has proven successful in terms of precision, processing time, and resource usage while also meeting regulatory requirements.

The paper presented the challenge of missing energy consumption time series data, and existing methods to address the issue and offers an in-depth presentation of the developed solution, including its advantages, disadvantages, and limitations.

## BIBLIOGRAPHY

- [1] "Apache nifi." <https://nifi.apache.org/> (accessed Jan. 21, 2022).
- [2] "Apache Hadoop," *Apache Hadoop*. <https://hadoop.apache.org/> (accessed Jan. 21, 2022).
- [3] "Apache Impala," *Apache Impala*. <https://impala.apache.org/> (accessed Jan. 21, 2022).
- [4] "PySpark Documentation," *PySpark Documentation*. <https://spark.apache.org/docs/latest/api/python/index.html> (accessed Jan. 21, 2022).
- [5] A. D'Aversa, S. Polimena, G. Pio, and M. Ceci, "Leveraging Spatio-Temporal Autocorrelation to Improve the Forecasting of the Energy Consumption in Smart Grids," in *Discovery Science*, P. Pascal and D. Ienco, Eds., in *Lecture Notes in Computer Science*, vol. 13601. Cham: Springer Nature Switzerland, 2022, pp. 141–156. doi: 10.1007/978-3-031-18840-4\_11.
- [6] M. Savinek and T. Šinkovec, "Vloga napredne analitike v elektroenergetiki," in *15th Conference of Slovenian Electrical Power Engineers*, Laško, Slovenia: Cigre, 2021, p. 5.



# Preparation of a Road Map for DC Transformation of the Turkish Electricity Distribution Grid

[Deniz.Kartal@meramedas.com.tr](mailto:Deniz.Kartal@meramedas.com.tr)

**BURAK ALTUN, HARUN KÖROĞLU, DENİZ KARTAL\***

*Meram Electricity Distribution Co.*

**GÖKHAN ÖNAL, NEGAR DASHTI, OĞUZHAN ÖZÇELİK**

*Lean Power Solutions*

**Türkiye**

## SUMMARY

With the advancement of technology, the needs in power systems have changed. These changes have created technical, economic and operational challenges. With the increasing number of distributed generation sources, DC electricity generation has increased. The DC electricity revolution has started with technological advances such as the increase in the usage areas of battery storage systems due to the decrease in installation costs, the increase in the number of DC consuming devices in residential energy consumption, and the widespread use of electric vehicles. LV DC distribution grids have been recognized as a more efficient alternative to existing AC systems by industry players who are the pioneers of the new era.

In line with the needs of the sector, collective studies are being carried out for the establishment of LV DC electricity distribution grids in Turkey. As set out in the Turkey Smart Grids 2023 vision, pilot zone studies on LV DC distribution grids should be carried out in our country. As the R&D unit under the Business Analysis and R&D Directorate, the researches carried out within the scope of the R&D project "Preparation of a Road Map for DC Transformation of the Turkish Electricity Distribution Grid", which is being carried out under the coordination of ELDER with the support of EMRA, under the coordination of Meram Electricity Distribution Co. and in partnership with TEDAŞ, Yeşilirmak and Başkent Electricity Distribution Companies, are included in this paper.

## KEYWORDS

Smart Grids, LV DC, Distribution Operators, DC Distribution Grids, Power Electronics





### 1. INTRODUCTION

The needs of the energy sector have changed in recent years. Security of supply, economic access to energy and sustainability are the main elements of this need. The technical, economic and operational challenges arising from the changes in power systems with the use of new technologies have led the world’s energy sector players to the trend of smart DC grids.

Various studies on LV DC grids are being carried out by standardization institution around the world. Regarding LV DC distribution grids; power electronics technologies, DC voltage levels that can offer optimum solutions, converter topologies are among the dynamics of the sector. In parallel with these developments, conducting research in accordance with the characteristics of the Turkish electricity distribution grid in order to follow technology trends will enable us to take part in the technology ecosystem.

### 2. PILOT ZONE MODELLING AND AC-DC GRID COMPARISON

The general view of the region modelled on the power system simulation software within the scope of the “Roadmap for DC Transformation of Turkish Electricity Distribution Network” project, which will be discussed in this paper, is given in Figure 1. There is a 20% voltage drop problem on the overhead line shown in red. The total length of this overhead line is 992 meters and most of it consists of Pansy conductor and the characteristics of the power transformer feeding the region are given in Table 1.

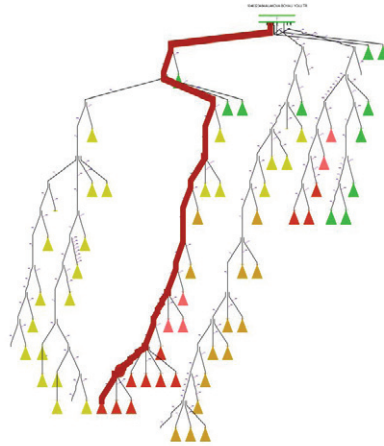


Figure 1: Alakova Boyalı Yolu TR

Table 1: Power Transformer Characteristics

Nominal Voltage	33/0.4 kV
Nominal Power	400 kVA
Connection Group	DYn11
Frequency	50 Hz
Leakage Reactance	%4.6

The maximum power value of the distribution transformer in the Alakova Boyalı Yolu TR region, which is determined as the pilot zone, is 152 kVA for the last three months. Since the power factor is assumed to be 0.95, the active power value is 145 kW. The voltage drop value seen at the end of the line in the model is 314 V. Considering that the voltage drop limit value in Turkey is 5%, 20% voltage drop value is far above the limits. It is suggested that this and more problems can be solved with LV DC networks. [13]

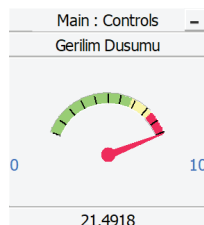


Figure 2: End of line voltage drop in pilot zone %21,4918



Oral Presentation: Preparation of a Road Map for DC Transformation of the Turkish Electricity Distribution Grid

In order to examine the power losses due to line impedance, the active power value seen at the transformer output is taken as the base and the difference between the total power drawn by the loads is considered as loss. The total power value drawn by the loads is given in Figure 3.

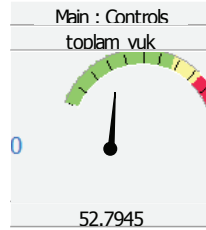


Figure 3: Total Active Power Value Of Loads

The percentage of total active power loss due to line impedance is calculated as 15.38% using Equation 1.

$$\frac{P_{transformer} - P_{load}}{P_{transformer}} \times 100$$

In parallel with this idea, the LV DC Grid Model of the pilot zone was made with the aim of proving that these problems can be solved with the load flow control capability of power electronic converters together with the LV DC grid.

The circuit diagram of the rectifier positioned at the output of the distribution transformer in the power system simulation software is given in Figure 4. The DC output voltage of the rectifier was determined as 1.5 kV. The network topology is determined as "Extended LV DC Distribution" and it is a single pole system. By choosing a unipolar system that does not have the control complexity of the bipolar system, it has been tried to reveal that LV DC networks are more beneficial than LV AC networks in many aspects such as harmonic values and voltage fluctuations even in its simplest form. [13]

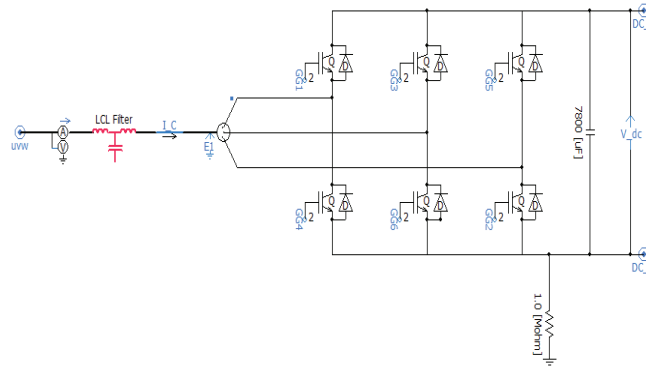


Figure 4: Rectifier circuit for LV DC Grid

The rectifier consists of IGBTs. This converter topology, also called voltage source converter (VSC), has bidirectional power flow capability. The preferred control method is State Vector Control [2] with a switching frequency of 4 kHz. LCL filter is used to reduce the harmonic effects on the grid side of the rectifier. On the DC output side, a 7.8 mF capacitor is preferred to minimize voltage fluctuations and to keep the voltage as constant as possible. As mentioned above, the circuit diagram of the rectifier is given in Figure 4.

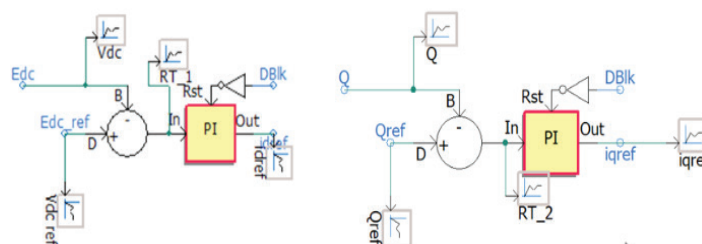


Figure 5: Control Loops



The converter has DC output voltage and reactive power control capabilities. The control loops for these capabilities are given in Figure 5. The DC grid voltage change seen at the rectifier output is given in Figure 6. The converter is activated 0.2 seconds after the simulation starts. Due to PI control, the DC voltage can be adjusted to the desired level in both steady and transient states.

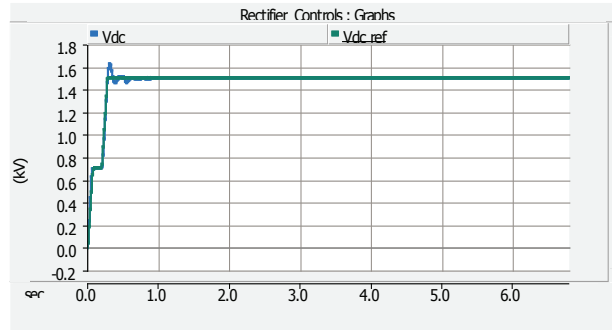


Figure 6: DC Grid Voltage Graph (Steady-State)

The reactive power change on the grid side of the rectifier can be seen in Figure 7. The reactive power reference, which was initially set to 0, was set to 20 MVAR capacitive at the 5th second. This capability of the rectifier can be used to achieve reactive power control in support of the grid. In this way, during an abnormal situation (fault, over-voltage, etc.) in the main AC grid, bidirectional reactive power support can be provided by the DC grid to the main grid.

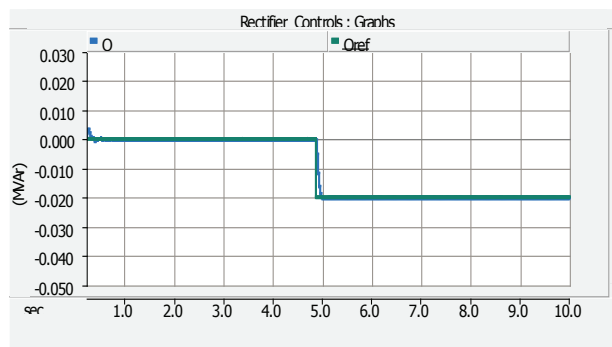


Figure 7: Grid Side Reactive Power Graph

The DC/AC converter, which provides the supply voltage to the users, is modelled with a control method similar to a rectifier. The inverter has output AC voltage and active power control capabilities.

Due to the AC voltage control capability of the inverter, the supply voltage can be kept within the voltage fluctuation limits of the TS EN 50160 standard accepted in our country during load changes. While the supply voltage can be kept within  $400 \pm 1$  V in steady state, it can be kept within  $400 \pm 5\%$  in sudden load changes (50% maximum).

The harmonic effects of power electronic converters on grid voltages and currents were also analysed. The total harmonic distortion values (THD) of the grid side and user supply voltages and currents are given in Figure 8.

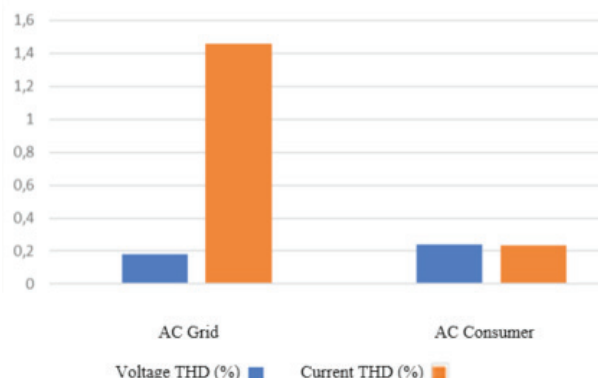


Figure 8: Voltage and Current THD Values



Oral Presentation: Preparation of a Road Map for DC Transformation of the Turkish Electricity Distribution Grid

The total harmonic distortion effect of the rectifier on the grid voltage is 0.18% and the current total harmonic distortion is 1.45%. These values are well below the voltage and current THD limit values specified in TS EN 50160 and IEEE-519 standards and it should be taken into consideration that these values will depend on the grid power and the design of the converter.

In line with the modelling and simulation studies carried out in the pilot region, it has been proven that DC grids are technically more beneficial. Cost-benefit analysis carried out within the scope of the project also studied the investment and depreciation period required for the DC grid transformation of the electricity distribution network. Accordingly, a roadmap for the DC transformation of Turkey's electricity distribution grid was developed and presented in three five-year action plans. The first five-year action plan is described in Chapter 3.

### 3. 15-YEAR ACTION PLAN

#### 3.1. First Five-Year Action Plan

The first five-year action plan of the roadmap aims to commission the LV DC distribution pilot grid. In line with this goal, all actions to be taken in the first five-year action plan have been identified and sub-divided.

##### 3.1.1. Planning, Organization and Budget

It is aimed to identify the institutions and organizations that will take part as stakeholders in the project and to establish their organizational charts. For the pilot zone studies, the relevant budget studies of the project stakeholders need to be realized. These studies should be carried out under the coordination of ELDER in compliance with EMRA regulations. The project should be led by a electricity distribution company and other electricity distribution companies should provide support as project stakeholders. Turkish Electricity Distribution Co. should be invited to these studies as an observer.

##### 3.1.2. Academic Collaborations

Throughout the process, cooperation with universities should be established to support the study academically. In this way, the simulation tools that can obtain optimum output to be used within the scope of the project will be researched at the academic level and their economic analysis methodologies will be revealed.

##### 3.1.3. DC Grid Planning for the Pilot Zone

In order to obtain optimum benefit from the pilot zone studies, it is important to plan the grid. The pilot zone should be selected according to the technical and economic benefits to be gained by the installation of the DC grid. DC voltage level and topology should be selected according to the characteristics and technical requirements of the pilot zone. Technical parameters such as power electronic converter type, number of poles, control methods and modes should be determined in accordance with the voltage level and topology determined within the scope of the First Five-Year Action Plan. Protection and grounding systems that prioritize the safety of people and other living beings and ensure the protection of grid equipment should be designed for the pilot zone application. For remote monitoring and control of all grid equipment, digital equipment complying with international standards should be procured or existing ones should be converted or replaced to meet the relevant technical requirements. The pilot grid should be planned by taking into account the continuous and real-time monitoring of every point of the grid and the storage of this data in a secure system.

##### 3.1.4. Establishment and Commissioning of the Pilot Zone

For the establishment of the pilot zone, optimum selection should be made by interviewing local and foreign producers. Detailed grid analysis should be carried out before the implementation of the pilot zone. Strategies should be determined for malfunctions and interruptions that may occur during the operation of the pilot zone and necessary trainings should be provided to the relevant personnel. In addition, the consumers to be fed from the pilot DC distribution grid should be provided with the necessary information before commissioning. The data to be used in the following stages of the process will be obtained as real data from the field thanks to the pilot zone application.

#### 3.2. SECOND FIVE-YEAR ACTION PLAN

With the start of the pilot zone implementation and data collection within the scope of the First Five-Year Action Plan, the topics to be investigated in the Second Five-Year Action Plan were determined as actions and listed below. The studies to be carried out



Oral Presentation: Preparation of a Road Map for DC Transformation of the Turkish Electricity Distribution Grid

within the scope of the second five-year action plan are aimed at examining innovative technologies, the process of preparing legislation and regulations for LV DC distribution grids, and R&D studies for the domestic production of equipment to be used in LV DC distribution grids with national resources.

### 3.2.1. *Techno-Economic Viability*

It is aimed to prove that LV DC grid offers a more efficient and economical alternative solution compared to LV AC grid, through cost-benefit analysis and techno-economic analysis methods in the light of the data obtained from the pilot zone implementation.

### 3.2.2 *AC-DC Grid Interactions*

It is important for grid planning to examine the effects of the DC grid on the AC grid and the effects of the AC grid on the DC grid and to take the necessary measures to minimize the detected negativities.

### 3.2.3. *Power Quality in DC Systems*

Power quality parameters for the DC grid should be determined, new methods should be investigated, and methods that improve energy continuity should be tested in a pilot zone.

### 3.2.4. *Renewable Energy, Storage Systems and Electric Vehicles*

The optimum connection point and type should be found in order to examine the effects of power plants generating with renewable energy sources and energy storage systems on the DC distribution grid and to ensure their integration. Decision tree algorithms should be created for connection permissibility.

In addition, the effects of electric vehicles and charging stations on the DC distribution grid and new technologies related to the subject should be investigated. Field tests of these technologies, such as providing power to the grid when electric vehicles are not in use, should be carried out in the pilot zone to verify the results obtained. Upon completion of the relevant processes, connection rules should be established and included in the legislation and regulations to be prepared.

### 3.2.5. *Smart Grids*

The DC distribution grid should have a remote monitoring and control mechanism, and every parameter of the grid should be remotely monitored and controlled in real time. For this purpose, the optimum communication protocols that meet the technical requirements should be selected or if an adequate protocol is not available, the existing protocols should be improved.

It is aimed to establish an artificial intelligence-based smart grid infrastructure. In this way, decision-making algorithms should be activated in cases such as malfunctions and interruptions and meet the adequacy of the grid autonomously. Autonomous decision-making algorithms should be created with artificial intelligence to ensure that the grid becomes self-sufficient for the most common situations in failure, interruption and maintenance processes. Demand response methods and real-time monitoring and controllability of all grid parameters from a single point, and Plug&Play grid technologies that will enable the grid to be self-sufficient or adapt to any situation should be investigated.

### 3.2.6. *Green and Sustainable Distribution Grids*

Related research should be conducted for the establishment of a green energy distribution grid. The interaction of the DC grid implemented in the pilot zone with the environment and living things will be examined, and methods to reduce environmental damage in case of malfunctions should be investigated.

### 3.2.7. *Security*

It is necessary to design/select protection and grounding systems suitable for LV DC grid, prioritizing the safety of human and other living beings. Appropriate relays must be determined in order to prevent damage to the grid equipment from the effect that may occur during the fault. For the physical security of the grid, it should be monitored and recorded with camera and/or sensor systems.

### 3.2.8. *Cyber Security*

It is mentioned that the LV DC grid can be remotely monitored and controlled instantaneously, and data on all parameters such as current, voltage, power measurements of the grid are collected and stored. Necessary measures should be taken to ensure that all this valuable information is resistant to cyber-attacks. For this purpose, how the grid reacts to a cyber-attack should be monitored in the pilot zone application and detailed protection methodologies should be researched and tested based on this situation.



Oral Presentation: Preparation of a Road Map for DC Transformation of the Turkish Electricity Distribution Grid

### 3.2.9. Conducting R&D Studies for Domestic Production

With the knowledge and experience gained in the first and second five-year action plan processes, it is aimed to realize the domestic production and design of LV DC distribution grid equipment with national resources. Business models and incentive mechanisms that will provide support to companies that want to carry out R&D studies on this subject should be investigated. In this way, significant contributions can be made to the country's economy by increasing the gross national product by exporting these technologies only from national resources. In addition, by reducing foreign dependency and current account deficit, Turkey can become one of the leading countries in DC distribution grid equipment.

### 3.2.10. National Legislation and Regulations

Relevant national legislation and regulations should be prepared based on all researches, field tests, pilot zone applications and all data obtained on the LV DC Grid. International standardization studies should be examined and all legislation, regulations and standards to be prepared in this context should be prepared in accordance with international standards.

## 3.3. Third Five-Year Action Plan

In the final Third Five-Year Action Plan, the steps to be taken for the transition to the DC grid were determined. Based on the experience and know-how gained during the entire action plan process, the studies to be carried out for the domestic production and design of DC distribution grid equipment for the needs were put forward and the benefits to be provided were evaluated. It is aimed to carry out the commercialization of LV DC distribution grids in this process.

### 3.3.1. Domestic Production Activities

With the completion of the R&D activities under the Second Action Plan, the Third Action Plan aims to start mass production of LV DC distribution grid equipment in Turkey. Thanks to domestic production activities; it is expected that our current account deficit will decrease and gross national product ratios will increase. Turkey is targeted to be a pioneer in introducing domestic and national LV DC grid equipment to the global market.

### 3.3.2. Education

The differences between LV AC grid and LV DC grid should be clearly identified. It is important to inform distribution system operators on this issue and to provide special occupational health and safety trainings. It should also be ensured that all information obtained during the process and the legislation and regulations are transferred to the experts who continue their work on grid planning.

### 3.3.3. Introduction of DC Distribution Grids

The awareness of DC distribution grids should be increased among sector stakeholders, the public and the academic community. All concerns that may arise in this process should be eliminated and trust in DC grids should be ensured. DC grids should be promoted and advertised to the entire academic community, sector stakeholders and the public. At national and international level, the advantages and benefits to be provided with DC grids through workshops, conferences, papers and articles should be clearly explained by the stakeholders responsible for this issue specified in the organization chart.

## 4. CONCLUSION

### 4.1. Commissioning of the First LV DC Distribution Grid

By the end of the Third Action Plan, the techno-economic feasibility of LV DC distribution grids has been demonstrated, the necessary field data and know-how have been obtained through pilot zone studies, R&D studies for local production and design have been completed, and the first real LV DC distribution grid in accordance with comprehensive and detailed national legislation and regulations based on international standards has been commissioned in an operator's area of responsibility.





### BIBLIOGRAPHY

- [1] C. L. Sulzberger, "Triumph of AC - from Pearl Street to Niagara," in *IEEE Power and Energy Magazine*, vol. 1, no. 3, pp. 64-67, May-June 2003, doi: 10.1109/MPAE.2003.1197918.
- [2] TEDAŞ, "2020 Annual Report", Access Date: November 2022
- [3] TEİAŞ, "Electricity Transmission in Numbers", Access Date: November 2022
- [4] EMRA, "2021 Sector Development Report", Access Date: November 2022
- [5] Hitachi Energy, "The Gotland HVDC Link", Accessed November 2022
- [6] J. Yu, K. Smith, M. Urizarbarrena, M. Bebbington, N. Macleod, A. Moon, "Initial Designs For Angle-DC Project: Challenges Converting Existing AC Cable And Overhead Line To DC Operation", [Available Online], Accessed November 2022
- [7] IEC, LVDC: electricity for the 21st century, Accessed November 2022 from
- [8] PD IEC TR 63282:2020, "LVDC systems. Assessment of standard voltages and power quality requirements.", IEC, 2020.
- [9] IEC LVDC SyC Webpage, Accessed November 2022
- [10] NPR 9090:2018 nl, DC Installations for low voltage, Accessed November 2022
- [11] BC Transmission Corporation, "Transmission Technology Roadmap: Pathways to BC's Future Grid", Accessed November 2022
- [12] Pacific Northwest National Laboratory, "Roadmap for Advanced Power System Measurements", Accessed November 2022
- [13] LV DC Distribution Grids and DC Transformation of Turkish Electricity Distribution Grid, CIGRE, Ankara, 2022
- [13] International Energy Agency, "Technology Roadmap - Smart Grids", Accessed November 2022
- [14] Electric Power Research Institute, "Electricity Technology Roadmap", Accessed November 2022
- [15] International Energy Agency, "Technology Roadmap - Energy Storage", Accessed November 2022
- [16] P. Bauer, "Roadmap to DC: From DC Building to a DC Distribution", Accessed November 2022
- [17] Pacific Northwest National Laboratory, "Distribution System Research Roadmap Energy Efficiency and Renewable Energy", Accessed November 2022
- [18] DKE, "Low Voltage DC German Standardization Roadmap Version 2", Accessed November 2022
- [19] Laurens Mackay, Nils H. van der Blij, Laura Ramirez-Elizondo & Pavol Bauer (2017) Toward the Universal DC Distribution System, *Electric Power Components and Systems*, 45:10, 1032-1042, DOI: 10.1080/15325008.2017.1318977
- [20] Hitachi Energy, "Itaipu HVDC", Accessed December 2022.
- [21] TEİAŞ, "Annual activity reports, 2021", Access Date: December 2022.
- [22] A. Praça, H. Arakaki, S.R. Alves, K. Eriksson, J.Graham, G.Biledt, "ITAIPU HVDC TRANSMISSION SYSTEM 10 YEARS OPERATIONAL EXPERIENCE", V SEPOPE, Brasil, 1996.
- [23] J. Graham, A. Kumar, G. Biledt, "HVDC Power Transmission for Remote Hydroelectric Power Plants", CIGRE SC B4 Colloquium on Role of HVDC FACTS and Emerging Technologies in Evolving Power Systems, Bangalore, India, 2005.
- [24] Parag, Y., Sovacool, B. Electricity market design for the prosumer era. *Nat Energy* 1, 16032 (2016). <https://doi-org.divit.library.itu.edu.tr/10.1038/nenergy.2016.32>
- [25] R. Peña et al. 'Doubly Fed Induction Generator Using Back-to-Back PWM Converters and its Application to Variable-Speed Wind-Energy Generation', *IEE Proc. Electrical Power Applications*, Vol. 143, No. 3, May 1996, pp. 231-241.
- [26] TSE, "TS EN 50160 Standard", Ankara, 2011.
- [27] P. Nuutinen et al., "Power Electronic Converters in Low Voltage Direct Current Distribution – Analysis and Implementation", Lappeenranta University of Technology, Doctoral Thesis, 2015.
- [28] P. Nuutinen et al., "Research Site for Low-Voltage Direct Current Distribution in a Utility Network—Structure, Functions, and Operation," in *IEEE Transactions on Smart Grid*, vol. 5, no. 5, pp. 2574–2582, Sept. 2014
- [29] Afamefuna, David & Chung, Il-Yop & Hur, Don & Kim, Ju-Yong & Cho, Jintae. (2014). A Techno-Economic Feasibility Analysis on LVDC Distribution System for Rural Electrification in South Korea. *Journal of Electrical Engineering and Technology*. 9. 1501-1510



# Analysis of Loads During the Summer-Winter Season in Substation (SS) 35/10 kV Gjilani I

[elionaaliu99@gmail.com](mailto:elionaaliu99@gmail.com)

**ELIONA ALIJU, ARTA GRAJÇEVCI**

*KEDS Energy - Kosovo Electricity Distribution and Supply J.S.C*

*Kosovo*

## SUMMARY

In any country, the increase in population in terms of energy affects the increase in the demand for electricity consumption. The existing electric power grid cannot withstand this growth if it is not invested proportionally. The expansion of this network also means an increase in the likelihood of the appearance of various defects in it. Such faults mean overloads, short connections in the network, etc. But what we come up against is the change in supply over time. Due to the busy network, problems arise during the supply periods. In this paper, the main focus falls on the analysis of the loads during the summer-winter season, especially during the winter, at the 35/10 kV Gjilani I Substation. This substation receives its 35 kV supply from the 110/35/10 kV Gjilani 1 Substation, for this reason the analysis of the load flow in the entire district of Gjilan was done by this substation through the advanced SCADA system (System for Remote Control of the Electric Power Network) during the normal summer season, when the loads are below the nominal operating values and during the season winter, when the loads reach the maximum values in the system, which also cause major problems or defects. Such problems are also present at the Low Voltage level of 0.4 kV, but in the case of affecting the Medium Voltage, the Low Voltage is definitely affected as well. For this reason, the focus in this project will be on the analysis of the load at the Medium Voltage level, without neglecting the damage caused to other devices of the Distribution System (on the transformed side of the voltage).

## KEYWORDS

Distribution System, Substation (SS), Medium Voltage, SCADA, load, faults



## 1. INTRODUCTION

The distribution system constitutes one of the basic parts of the Electric Power System, from where consumers receive the primary services of electricity supply. Since it represents the last part of the chain of the complete electrical system, it is exposed to many criticisms from consumers. Other basic parts of entire Electric Power System are generation and transmission.

Despite the fact that many investments in the electric power system are used for the development and improvement of the distribution system, this system has still limited opportunities to use new technologies, as well as defects constantly occur regardless of efforts to eliminate them.

Recent investments in modern technologies in the distribution system aim to increase the quality of electricity supply, thus increasing the reliability and efficiency of the distribution system.

However, considering the connection of consumers, the extension of lines, the internal and external technical problems of the equipment in the distribution system, the various investments cannot always completely eliminate the defects that occur in the system.

Defects in the distribution system, apart from the ones just mentioned, also have a seasonal basis for their occurrence. Precisely in this paper we will present an analysis of the defects in the distribution system depending on the seasonal periods. As a case for analysis, an active output of a substation in the district of Gjilan, which represents one of the seven main districts in Kosovo, will be taken.

## 2. THE STATE OF ELECTRICITY SUPPLY IN THE DISTRICT OF GJILAN

### 2.1. Revision of the Network in District of Gjilan

The district of Gjilan includes four sub-districts: Gjilan-Centre, Viti, Kamenica and Artana. The number of distribution transformers (TS 10/0.4 kV/kV) in the entire district is 958, while only in the sub-district Gjilan-Centre there are 434. Each of these sub-districts has the corresponding 10 kV outputs. Table 1 shows the main data related to all the supply substations of the district of Gjilan.

*Table 1. Data of substations in district of Gjilan (KosovaNET, 2022)*

District	Subdistrict	Substation	SS name	10 kV feeder no.	TS 10/0.4 kV no.
DGL	Gjilan-Center	35/10 kV	Gjilani I	12	83
DGL	Gjilan-Center	35/10 kV	Gjilani II	4	46
DGL	Gjilan-Center	110/35/10 kV	Gjilani 1	11	120
DGL	Gjilan-Center	35/10 kV	Gjilani IV	8	43
DGL	Gjilan-Center	110/10 (20) kV	Gjilani 5	8	123
DGL	Gjilan-Center	35/10 kV	Lladova	4	64
DGL	Viti	35/10 kV	Klllokot	6	116
DGL	Viti	110/35/10 kV	Rrafshina	7	154
DGL	Kamenica	110/10 (20) kV	Kamenica	11	243
DGL	Artana	35/10 kV	Artana	4	55

### 2.2. Substation (SS) 110/35/10 kV Gjilani 1 – The base of the load in Gjilan-Center

This substation is considered as the base load from all other substations in the District. The input voltage of the two transformers in SS 110/35/10 kV Gjilani 1 is provided by the 110 kV line from SS 110/10 kV Prishtina 7, this value is transformed in both transformers,



which operate in parallel with nominal power Sn=31.5 MVA (both with a common capacity of 63 MVA). The KOSTT dispatch center is located inside the substation building. From the center the complete load is controlled through single-pole schemes. The single-pole diagram shows the connection between the various components within an electrical system and helps in schematic visualization of the network. In the schematic, electrical components such as switches, dividers, transformers, grounding, busbars and conductors are shown with schematic symbols.

In the figure 1 is shown the single-pole scheme of SS 110/35/10 kV Gjilani 1. Based on this scheme, we can see that the load drawn by SS 35/10 kV Gjilani I on date 20.04.2023, scheme retrieved from Dispatch Center of KEDS is 12.6 MVA, SS 35/10 kV Artana 0.5 MVA, SS 35/10 kV Gjilani II 6.5 MVA and SS 35/10 kV Gjilani III (within SS 110/35/10 kV Gjilani 1) 10.3 MVA.

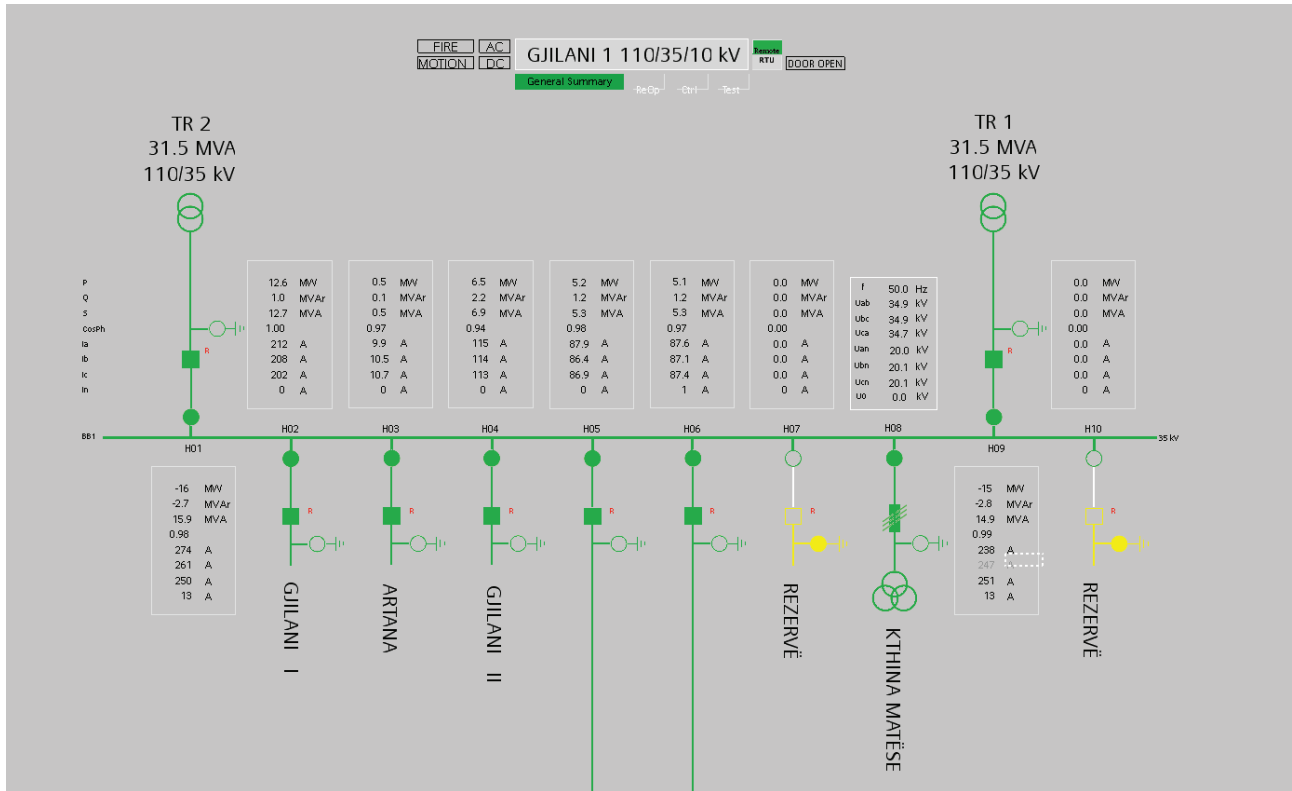


Figure 1. Single-pole scheme of NS 110/35/10 kV Gjilani 1 (SCADA System, 2022)

### 2.3. Analysis of load distribution in SS 35/10 kV Gjilani I

Figure 2 shows a single-pole scheme for NS 35/10 kV/kV Gjilani I, by means of which it is possible to understand where this substation is supplied from, who can supply, what are the feeders, data on the operation of the feeders, how can they be controlled etc. As can be seen, this substation has a total of 11 10 kV feeders, which are traversed by means of 10 kV conductors and each of them has the corresponding branches (not shown in the single-pole diagram). Figure 2 shows all these feeders with operating loads, but the number, name and installation power of the 10/0.4 kV distribution transformers they contain are not shown.

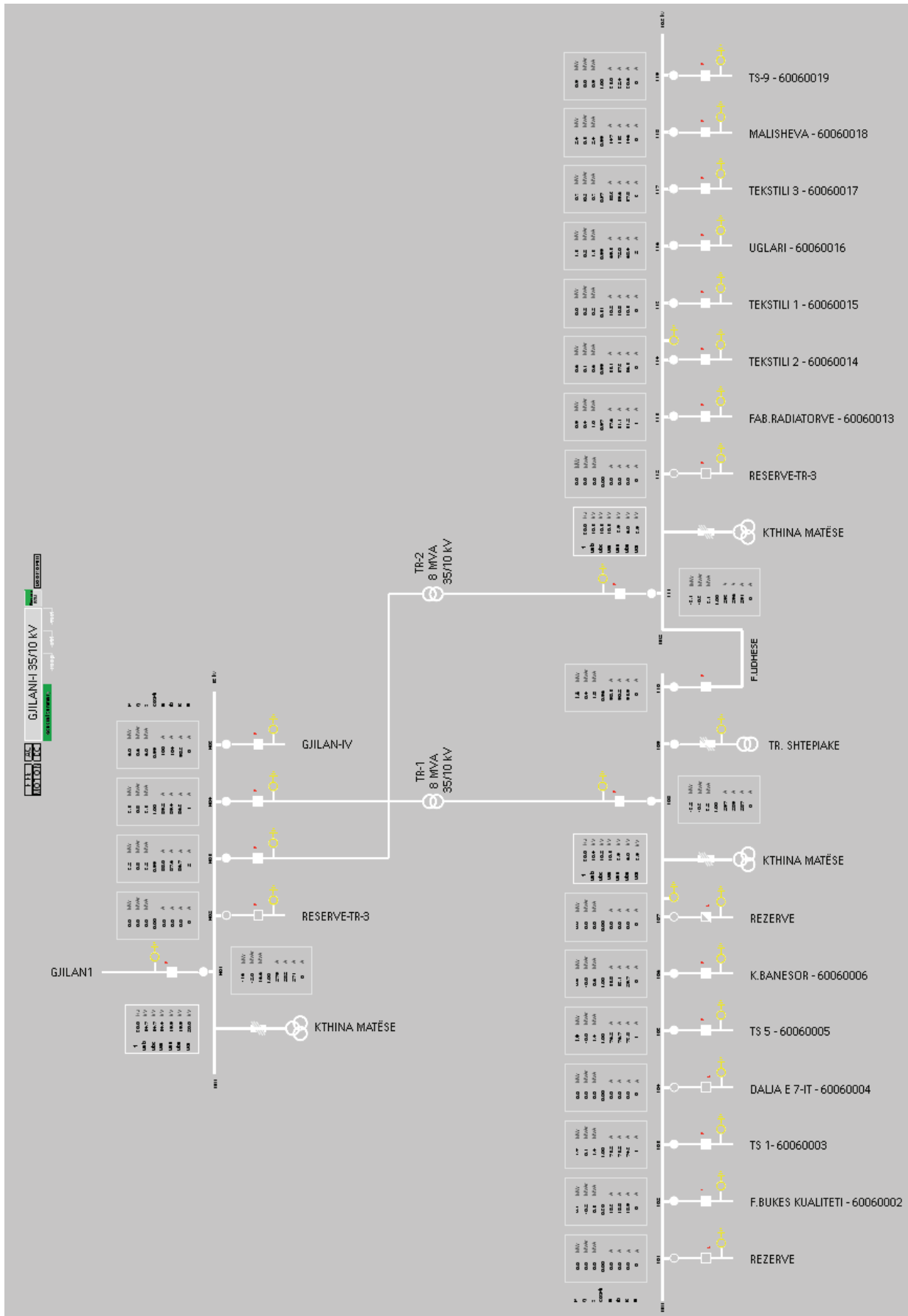


Figure 2. Single-pole scheme of SS 35/10 kV Gjilani I (SCADA System, 2022)



Figure 3 shows the two types of cables that are used for these feeders, i.e. through which the load is distributed:

1. Cable XHE 49 and
2. Conductors Al/Fe.

XHE 49 cable with a section of 120 mm<sup>2</sup> and 150 mm<sup>2</sup> is the cable used in underground cable lines, while Al/Fe conductors with section 25 mm<sup>2</sup>, 35 mm<sup>2</sup>, 50 mm<sup>2</sup> and 70 mm<sup>2</sup> are used for overhead lines.



Figure 3. Types of cables used for 10 kV feeders (UWCABLE Wire&Cable, n.d.)

For the analysis of the network extension and the load flow difference during the summer-winter season, as a concrete case, we have taken the 10 kV Uglari feeder from this Substation.

Figure 4 shows the scheme of this feeder. The four-cornered symbol indicates the 35/10 kV/Gjilani I Substation with a power of 2x8 MVA. This feeder continues with underground cable XHE 49 150 mm<sup>2</sup> about 280 meters from the substation, it is connected to a concrete pole and continues with Al/Fe 70 mm<sup>2</sup> conductor about 1 kilometer to the other concrete pole where we have a branch. This branch goes up to TS Kolektori with power 400 kVA with Al/Fe conductor with section 25 mm<sup>2</sup> to a wooden pole and XHE 49 150 mm<sup>2</sup> cable to the corresponding TS. The feeder continues further with Al/Fe 70 mm<sup>2</sup> and 25 mm<sup>2</sup>, and then we have a branch to the TS Doxht with a power of 250 kVA. The same feeder continues further to the other 10/0.4 kV/kV trafostations at the end of the scheme with the corresponding branches.

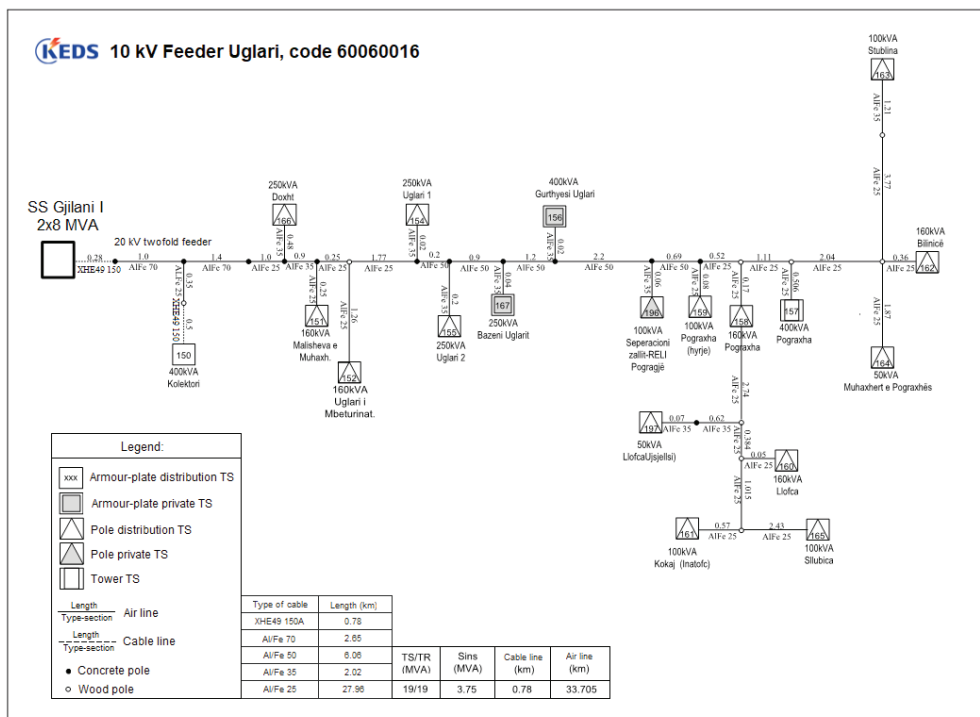


Figure 4. Scheme of 10 kV feeder Uglari, with code: 60060016 (KEDS, 2022)





This feeder supplies 1170 consumers, of which 1097 are household, 57 are commercial, 4 are large consumers and 12 are public lighting. The number of trafostations as can be seen from the diagram is 19, and most of them are pole distribution TS. (KosovaNET, 2022)

The physical extent of this feeder can be seen in KosovaNET as in figure 5. KosovaNET is an advanced program for monitoring all substations with the corresponding feeders, whose data is updated by Network engineers.

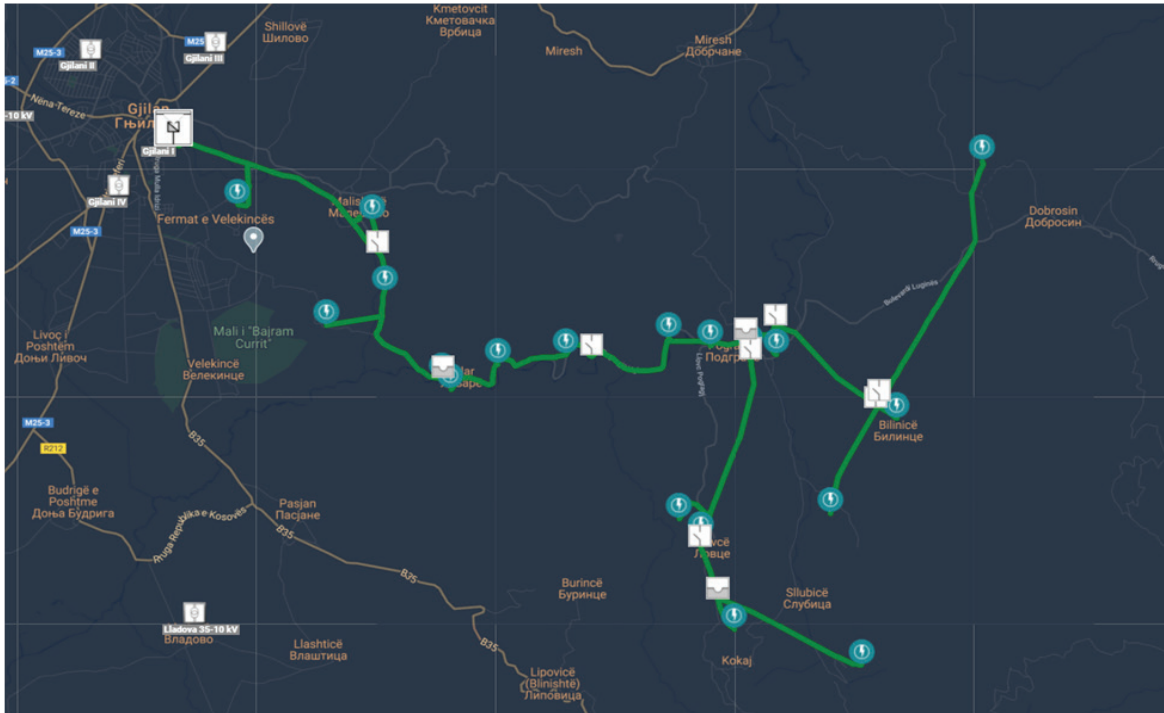


Figure 5. 10 kV feeder Uglari presented in KosovaNET (KosovaNET, 2022)

### 3. LOAD FLOW IN 35/10 KV GJILANI I SUBSTATION

#### 3.1 Differentiation of electricity consumption in the summer-winter season

During different seasons we have an increase or decrease in loads. The peak demands in the summer are usually lower when compared to the peak demands of the winter and the low demands of the summer are low when compared to the low demands of the winter. Demand for electricity tends also to fluctuate over the course of the day, determined by human activity. (Gavin, 2014)

As for differentiation during the summer season, due to the non-use of equipment that consumes excessive kilowatts on the part of electricity consumers, the consumption is low, in which case the loads flow is below the normal values with which a certain feeder operates. Since we have a completely normal load flow situation during this season, then a real analysis has been made of the load flow in the winter season. During the winter season, due to the use of equipment that consumes excessive kilowatts, specifically central heating, then the consumption increases, which in turn increases the loads on the network. But not only central heating, this season also means greater use of other household appliances, such as: other alternative heating, boiler, washing machine, clothes dryer, etc. During this season, the greatest consumption or the peak demand is at 09:00-11:00 in the morning and after 18:00 in the evening. (Fisher, 2022)

#### 3.2 Loads during the winter season in 35/10 kV Gjilani I Substation

Based on chart 1, we can see the differentiation of loads/for a day drew by 35/10 kV Gjilani I Substation at summer-winter season, from where the above are verified. As for only winter season from the analyzed data (extracted from the KEDS SCADA system) for four different dates at different times. The orange line represents Summer's day on 13.07.2022, and the blue line represents Winter's day on 13.12.2022. According to the chart we concluded that on Summer Season the values of loads were within the limits of load distribution, but on Winter Season there were days where these values have exceeded the installed power limit of the substation. Based on the case study on 02.12.2022 this substation drew 13.5 MW, on 13.12.2022 it drew 16.5 MW, on 22.12.2022



it drew 13 MW and on 26.12.2022 it drew 17.3 MW. So the peak on 26.12.2022 was reached due to the low temperatures, which increased consumption of electricity from consumers for different needs.

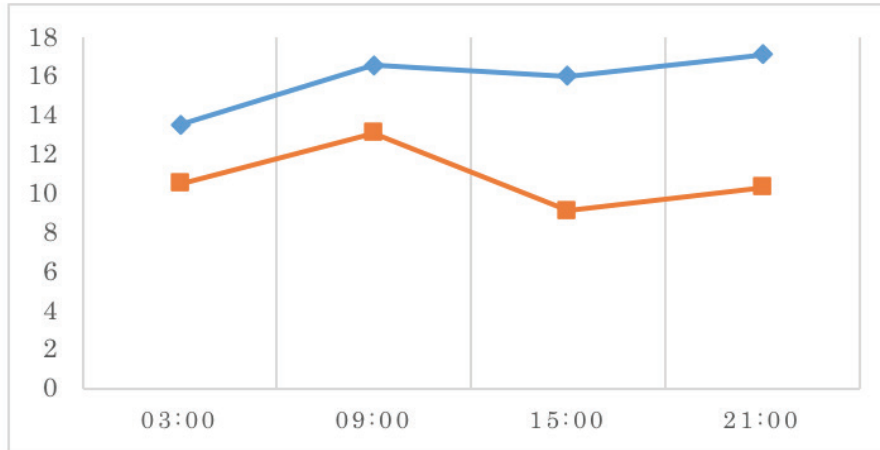


Chart 1. The data analyzed for the summer-winter loads at the 35/10 kV Gjilani I Substation

In figure 7, we can see the loads only distributed at the feeders of this substation on 26.12.2022, concentrated at the busbar where 10 kV Uglari feeder is connected. On the figure we can see that on this day 10 kV feeder Uglari drew 1.7 MW, while in Summer Season it only reaches near 1 MW.

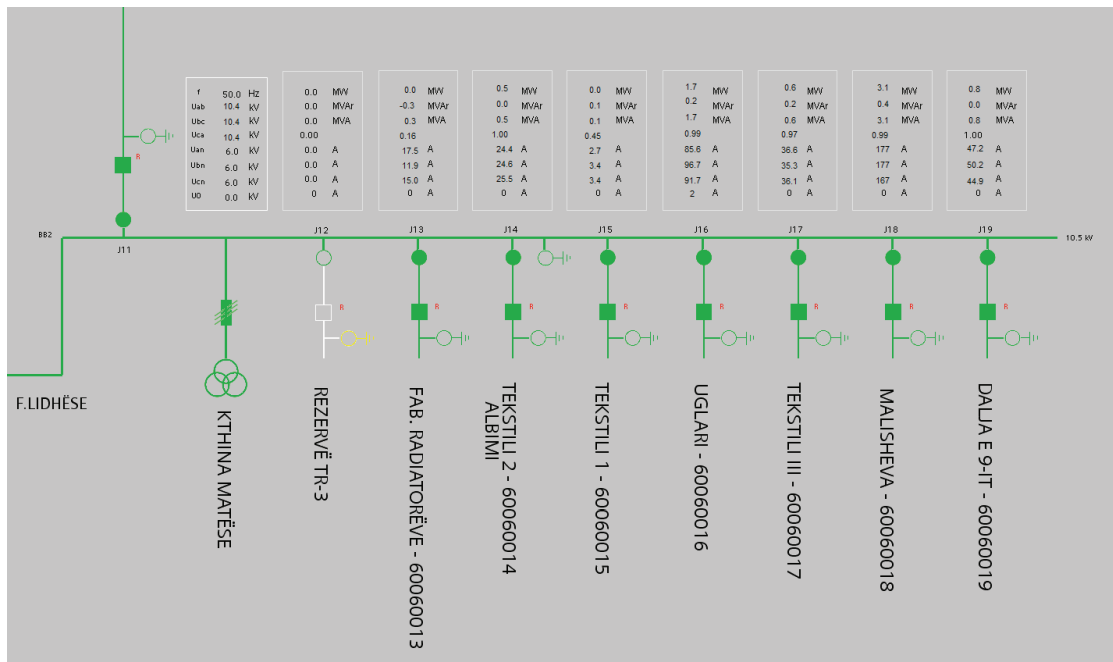


Figure 6. Load flow at 10 kV feeder of 35/10 kV Gjilani I Substation on 26.12.2022 (SCADA System, 2022)

## 4. DEFECTS IN THE NETWORK AS A RESULT OF INCREASED LOADS

### 4.1. Burning of the 10/0.4 kV transformer

Figure 7 shows the burning of the 10/0.4 kV transformer with nominal power  $S_n=630$  kVA at TS 150 Kolektori (from 10 kV feeder Uglari) as a result of overloads in the 0.4 kV network. The 0.4 kV 1000 A switch breaker of this transformer was mechanical (that is, it does not react intermittently in the case of increased loads), so when it was overheated by the load with more than 1000 A, it burned completely. As can be seen, the input cables for the transformer, the output cables for the switch, the switch breaker, the cubicle panel (which are not seen in the figure) etc., were burnt.



**Figure 7.** 10/0.4 kV transformer burnt due to overload

*Note.* Photo of 10/0.4 kV transformer after inspection taken directly from terrain. Own work.

### 4.2. Burning of LV fuses and fuse bases

Figure 8 shows the concrete case in the terrain of the burning of 315 ampere fuses at TS 166 Doxht (from 10 kV feeder Uglari) in the case of increased loads in the winter season. In the presented case, we have the first 0.4 kV output with three phases, the first phase (blackened fuse), the second (cracked, completely burnt), while the third is fine. This happened as a result of the loading of the first two phases by consumers, making bridges in the network.



**Figure 8.** LV fuses blown as a result of overload

*Note.* Photo of LV panel taken from terrain during intervention by changing LV fuse. Own work.



### 4.3 The impact of the connection of consumers without Electricity Consent

Based on 2022, the network of KEDS (Kosovo Electricity Distribution and Supply Company) has been quite at risk. Considering the kW, for which an electricity consumer signs an agreement with KEDS for supply (up to 15 kW), and those that the consumer installs at home after the agreement have a significant difference. Each load in a given field is calculated for use by customers. From these calculations, the electrical network is updated, in which case the 0.4 kV feeders are discharged, other substations are built, so adequate solutions are made so that the consumer is supplied with stable electricity. When the consumer installs more kW than what is agreed upon, and if he has not applied for an Electrical Consent in the case of the intention of increasing the power of the internal installation at home, then the first problem is undoubtedly the consumer himself as in figure 9, and the increase in load on the network is caused, as has happened to many consumers in the country.

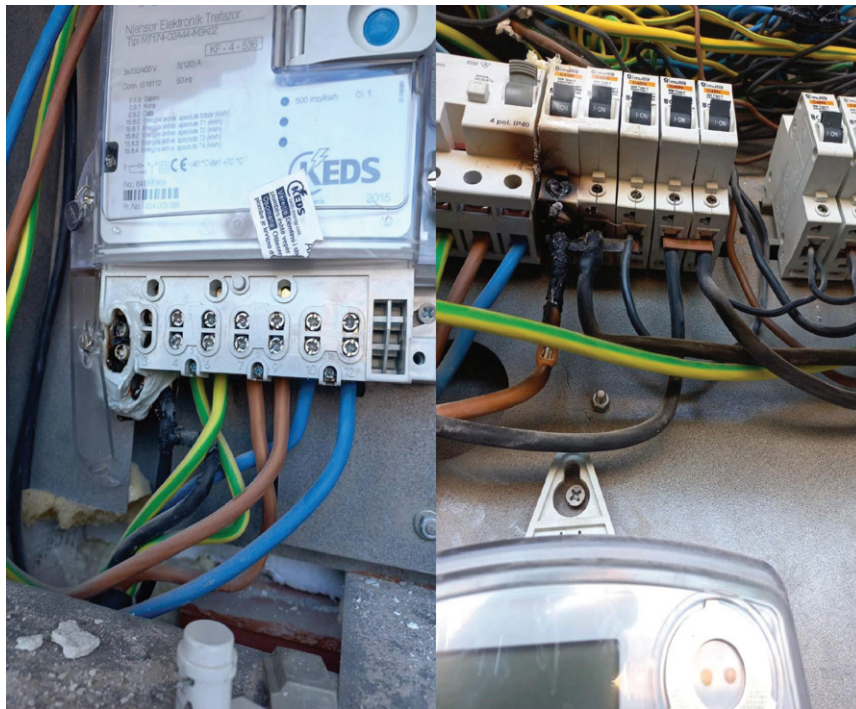


**Figure 9.** Defect as a result of network overload by the customer himself

*Note.* Photo of consumer meter taken from terrain during intervention. Own work.

## 5. CONCLUSION

In this project, we analyzed the distributed load for the supply of electricity consumers in the district of Gjilan. Although the distribution network is quite wide, we have tried to summarize the key points of distribution in this district. In this topic, the complete distributed load in the district of Gjilan is presented, the concrete example NS 35/10 kV Gjilanin I and the 10 kV Uglari feeder of this substation is taken in depth. The load distribution comparison was made focusing on winter loads, since in this season we have an enormous increase in consumption by consumers, where single-pole schemes were used in SCADA (where the load flows in the entire substation are presented).

High population growth in certain areas means more electricity is needed. When the electrical infrastructure in an area is at full capacity, a substation is required to continue providing reliable electricity. It is precisely for this reason that the construction of small substations is required. We have called such distribution substations.

In the municipality of Gjilan, a total of 5 large substations have been built, sufficient for the needs of the citizens. This means that until now it has been achieved quite well that all distribution substations in Gjilan have a sufficient source of supply. From now on, what is more important is the work and the will to fix the breakdowns and realize the projects for the maintenance of the electrical network of the District of Gjilan.





### BIBLIOGRAPHY

- [1] Aliju, E. (2021). *Aspects of measurements, inspections and maintenance at the Substation (SS)35/10 kV Gjilani I* [Unpublished bachelor dissertation]. Prishtinë, Kosovë.
- [2] Fisher, A. (2022). *The role of seasonal demand in all-electric scenario*. PV Magazine.
- [3] Gavin, C. (2014). *Seasonal variations in electricity demand*. Electricity Statistics.
- [4] GoogleEarth. (2022). *GoogleEarth Schemes of Distribution Network*. Gjilan, Kosovë: KEDS.
- [5] KEDS. (2022). *Skemat e daljeve 10 kV nga departamenti i Investimeve*. Prishtinë, Kosovë.
- [6] KosovaNET. (2022). *KosovaNET Schemes of Distribution Network*. Gjilan, Kosovë: KEDS.
- [7] SCADA System. (2022). *SCADA System Single-Line Schemes*. Gjilan, Kosovë: KEDS.
- [8] UWCABLE Wire&Cable. (n.d.). *Standard Al Conductor Steel Reinforces ACSR and underground cable*. Retrieved from <https://www.vwcable.com/product/>



# Under-Frequency Load Shedding Based on Huang's Empirical Model Decomposition Approach for Estimation of $df/dt$ and Artificial Neural Networks

maja.muftic-dedovic@etf.unsa.ba

MAJA MUFTIC DEDOVIC\*, AJDIN ALIHODZIC, ADNAN MUJEZINOVIC, NEDIS DAUTBASIC, ZIJAD BAJRAMOVIC, ADIN MEMIC

University of Sarajevo Faculty of Electrical Engineering

Bosnia and Herzegovina

## SUMMARY

In a power system, the objective is to maintain the frequency as close as possible to system frequency (50 or 60 Hz). To maintain frequency at normal range must be ensured balance between generation and demand. To address this issue, the use of smart load monitoring technology has proven to be an effective solution. It provides valuable insights into the root causes of load shedding, allowing the precise adjustment of electricity consumption to maintain a balanced power system. This paper present the new adaptive under-frequency load shedding. New approach is proposed for UFLS scheme that relies on Huang's Empirical Mode Decomposition estimation of rate of change of frequency (RoCoF). Artificial Neural Networks are used for estimation of the magnitude of generator loss for load shedding. Computer simulation testing are performed on the IEEE 39 bus test system in the DigSILENT PowerFactory power system simulation software and MATLAB platform. Test system has been established to simulate significant disruptions, such as generator outage, in order to improve the load shedding scheme. The results are compared with the conventional UFLS scheme.

## KEYWORDS

Under-frequency load shedding (UFLS), Rate of Change of Frequency (RoCoF), Empirical Mode Decomposition (EMD), Artificial Neural Networks (ANN)





Oral Presentation: Under-Frequency Load Shedding Based on Huang’s Empirical Model Decomposition Approach for Estimation of  $df/dt$  and Artificial Neural Networks

## 1. INTRODUCTION

The study focuses on balancing the frequency in power systems by removing loads equal to the loss of generation. The rate of change of frequency or decline is a result of power imbalance, and the objective is to address this imbalance. The study proposes an Adaptive Under Frequency Load Shedding (AUFLS) algorithm, which involves using slower system simulation software and numerical calculation software. The frequency response data from generator outages in the IEEE 39 bus test system is collected for training an Artificial Neural Network (ANN) model. The ANN model is constructed with 10 hidden layers using the ANN Toolbox in MATLAB. The simulation process involves conducting dynamic simulations, plotting and observing frequency responses, and continuously reading the responses to detect outages. The output of the ANN model, which estimates the loss of generation, is used by the Load Shedding Algorithm to release appropriate loads. The frequency response after implementing AUFLS is compared to the conventional four-stage Under Frequency Load Shedding (UFLS) method. The results show that AUFLS achieves faster and closer restoration to the initial frequency of 50 Hz compared to four-stage UFLS. The IEEE 39 bus test system is used for testing, consisting of 39 buses and 10 generators [1]. The effectiveness of different time samplings for training data is evaluated, and the 0.01 s sampling is determined to be the best. The AUFLS method aims to accurately determine the power imbalance and enable precise load shedding based on the loss of generation. The simulation results demonstrate the superiority of AUFLS in restoring frequency stability. The study concludes that by estimating the loss of generation using frequency response data, the load shedding algorithm can remove the appropriate amount of load, thereby achieving a balance between supply and load and faster frequency restoration after outages.

## 2. APPLIED METHODOLOGY

The methodology applied in the paper can be summarized as follows:

**Step 1. Analysis of Power Imbalance:** The study considers the relationship between electric power ( $P_{ei}$ ) and mechanical turbine power ( $P_{mi}$ ), assuming that electric power represents the load while mechanical turbine power represents the supply. The rate of change of frequency or decline ( $df/dt$ ) can be attributed to power imbalance ( $\Delta P$ ). The objective is to balance the frequency by removing loads equivalent to the loss of generation.

The change of  $i$ -th generator angle frequency is defined by a differential swing equation:

$$\frac{2H_i}{f_n} \frac{df_i}{dt} = \Delta p_i \tag{1}$$

where:  $\Delta p_i$  is the load-generation imbalance,  $H_i$  is the inertia constant,  $f_n$  is nominal frequency and  $f_i$  is the frequency of the  $i$ -th generator [2], [3].

Total power system imbalance, obtained from  $N$  swing equations ( $N$  is number of generators), becomes:

$$\Delta p = \sum_{i=1}^N \Delta p_i = \frac{2 \sum_{i=1}^N H_i}{f_n} \frac{df_c}{dt} \tag{2}$$

where:  $f_c = (\sum_{i=1}^N H_i f_i / \sum_{i=1}^N H_T)$ ,  $H_T$  is the total inertia of system.

Equation (2) describes the movement of the center of inertia [4] and it can be said: although during transient process some generators are retarding at different rates  $df_i/dt$ , the total system is retarding at the constant rate  $df_c/dt$  [2], [3], [4]. The distribution of the overall imbalance  $\Delta p$  in moment  $t^+$  between generators is defined [4]:

$$\Delta p_i = \frac{H_i}{\sum_{j=1}^N H_j} \Delta p \tag{3}$$

and indicates that the total value of the imbalance  $\Delta p$  will be distributed between generators depending on their relative inertia in relation to the total system inertia.

A precise  $df/dt$  estimation enables faster response and shedding of appropriate load levels to restore system stability. Traditional methods often face challenges in capturing the complex dynamics of power systems accurately. This is where Huang’s Empirical Model Decomposition approach coupled with Artificial Neural Networks presents a breakthrough solution.

Huang’s Empirical Model Decomposition (EMD) is a data-driven method used for analysing non-linear and non-stationary signals. It decomposes a signal into a series of intrinsic mode functions (IMFs) that capture different frequency components. By adaptively separating the signal into IMFs based on its local characteristics, EMD enables a more detailed analysis of complex data [5].



**Oral Presentation:** Under-Frequency Load Shedding Based on Huang’s Empirical Model Decomposition Approach for Estimation of  $df/dt$  and Artificial Neural Networks

Huang’s Empirical Mode Decomposition (EMD): EMD decomposes a signal into intrinsic mode functions (IMFs) using the following steps:

- Identify local maxima and minima in the signal.
- Generate the upper  $f_{up}(t)$  and lower envelopes  $f_{low}(t)$  of the signal by interpolating between these extrema.
- Compute the mean of the upper and lower envelopes.  $m_1(t) = (f_{up}(t) + f_{low}(t))/2$
- Subtract the mean from the signal to obtain the first IMF.  $h_1 = f_i(t) - m_1$
- Repeat the process with the residue (original signal minus the first IMF) to obtain subsequent IMFs.

$$f_i(t) = \left(\sum_{j=1}^n c_j(t)\right) + r_n(t) \tag{4}$$

where  $f_i(t)$  represents the angular velocity of the  $i$ -th generator,  $c_j(t)$  are IMFs,  $r_n(t)$  is a residual or low-frequency trend and  $n$  is the total number of IMFs.

Herein we can clearly precise the focus of this research as: to determine fair representation of  $f_c(t)$  with  $r_n(t)$  and to analyze if it can be used for the evaluation of the center of inertia estimation.

**Step 2.** AUFLS Design: The next step involves designing the Adaptive Under Frequency Load Shedding (AUFLS) algorithm. The power system simulation software is used to conduct dynamic simulations, while the numerical calculation software MATLAB is utilized for the Artificial Neural Network (ANN) process. There is a data exchange between these software components. The numerical calculation software requires the frequency response data for constructing the ANN model, while the power system simulation software requires the output of the ANN model as input for the Load Shedding algorithm [6].

**Step 3.** AUFLS Algorithm steps: The AUFLS algorithm is explained in the following steps:

- Prepare the training data by collecting the frequency response data of each generator outage from 9 different dispatch generators in the IEEE 39 bus test system using power system simulation software.
- Construct the ANN model using the training data in the numerical calculation software MATLAB.
- Conduct generator outage simulations using the power system simulation software.
- Plot and observe the frequency response.
- Continuously read the frequency response using the numerical calculation software to detect when the outage occurred and capture the frequency a few seconds later. Test this sample with the ANN model.
- The Load Shedding algorithm in the DigSILENT PowerFactory software reads the output of the ANN model, which estimates the magnitude of loss of generator.
- The AUFLS algorithm releases loads according to the output of the ANN model.
- Plot and observe the frequency response after implementing AUFLS.

**Step 4.** ANN Model and Training: An Artificial Neural Network (ANN) is used to estimate the magnitude of the loss of generator. The ANN MATLAB Toolbox is employed to generate the model. The training data is obtained from the frequency response of 9 dispatch generators. The training method utilizes Bayesian Regularization, and the ANN model consists of 10 hidden layers.

For performance comparison, a conventional four-stage UFLS scheme is developed and tested under the same disturbances. The settings of the conventional four-stage UFLS scheme are determined based on guidelines and common practice [7, 8]. The following Table 1 gives a summary of the conventional four-stage UFLS scheme.

**Table 1.** Conventional four-stage UFLS scheme [9]

Stage	$\Delta p$ (%)	$f_{th}$ (Hz)	$t_d$ (s)
1 <sup>st</sup>	15	59.4	0.2
2 <sup>nd</sup>	10	59.1	0.2
3 <sup>rd</sup>	10	58.8	0.2
4 <sup>th</sup>	5	58.5	0.2



Oral Presentation: Under-Frequency Load Shedding Based on Huang's Empirical Model Decomposition Approach for Estimation of  $df/dt$  and Artificial Neural Networks

### 3. AN ILLUSTRATIVE EXAMPLE USING IEEE 39 BUS TEST SYSTEM

An illustrative example is short-circuit event at 0 s at bus 30, clear short circuit at 0,2 s and then loss of generator G10 (250 MW, 1000 MVA, 16,5 kV). Speed deviation following simulated disturbance is presented in Figure 1. Sampling rate of the signals from Figure 1. is 0.01 second.

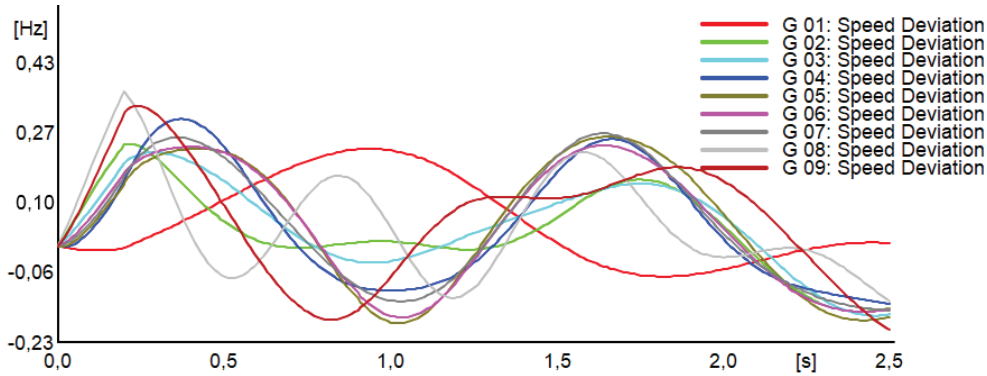


Figure 1. Speed deviation following simulated disturbance

The EMD method, as explained in the previous section, is utilized on the signals shown in Figure 1. The outcomes of this approach are presented in Figure 2 and Figure 3. Figure 2 illustrates the Intrinsic Mode Functions (IMFs) of the G 08: Speed Deviation signal. After applying the EMD method, two IMFs and a residual are obtained. Due to the low sampling frequency, it is evident that the IMFs will reveal low-frequency electromechanical oscillations. On the other hand, the residual represents the overall trend of the analysed signal and can be useful for evaluating the centre of inertia ( $d\omega_c/dt$ ). For this case,  $d\omega/dt = d(res)/dt = -0,07578(\text{Hz/s})$ .

Implementing the same applied procedure to all signals from Figure 1, residuals from the EMD are presented on Figure 3.

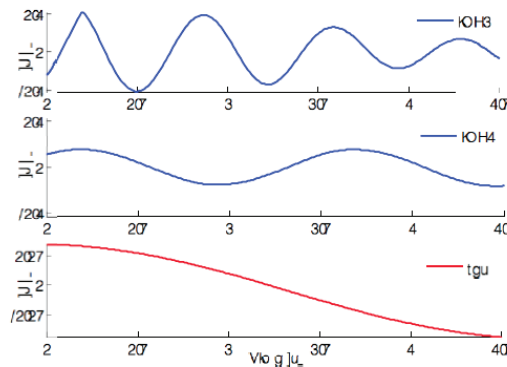


Figure 2. The IMFs from the EMD of G 08: Speed Deviation signal from Figure 1

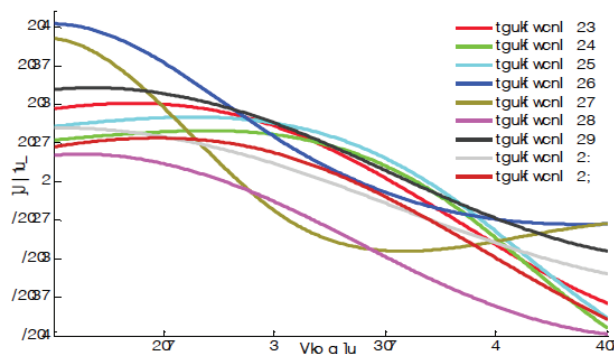


Figure 3. Residuals from the EMD of G 01: Speed Deviation, G 02: Speed Deviation, ... , G 09: Speed Deviation



Oral Presentation: Under-Frequency Load Shedding Based on Huang’s Empirical Model Decomposition Approach for Estimation of  $df/dt$  and Artificial Neural Networks

The EMD estimation results of the generator speed deviations and share of the imbalance impact are presented in Table 2.  $d\omega_i/dt$  are obtained after the EMD approach from residuals given on Figure 3. Results given in Table 2 (Hz/s) represent the mean value on the observed time interval of 2,5 s ( $((x_{i+1} - x_i)/\Delta t), \Delta t = 0.01$  s).

The rate of change of frequency is obtained from the DigSILENT PowerFactory. The RoCoF is calculated using the backward derivative in the PowerFactory with calculation period of 0.01 s on the observed time of 2,5 s.

To be mathematically shown what the influence of deviation in  $df/dt$  on the power is, using equation (5) is calculated  $df_{COI}/dt$  from actual active power deficit that occur after loss of generator 10 in the power system [10].

$$\frac{df_{COI}}{dt} = \frac{P_{def} \cdot f_n}{2 \cdot H_{sys} \cdot S_{sys}} = -0,1 \left[ \frac{Hz}{s} \right] \tag{5}$$

where  $H_{sys} = \frac{1}{S_{sys}} \sum_{i=1}^N H_i \cdot S_i$ ,  $S_{sys} = \sum_{i=1}^N S_i$ ,  $S_{sys} = \sum_{i=1}^N S_i$  is equivalent apparent power of the system [MVA],  $\overline{H_{sys}}$  is equivalent apparent inertia constant of the system [s],  $S_i$  is the rated apparent power of  $i$ -th machine,  $H_i$  is the inertia constant of  $i$ -th machine based on its own rated apparent power,  $P_{def}$  is generation power deficiency 250 [MW],  $f_n$  is nominal frequency [Hz],  $N$  is number of generators in the system.

Table 2. The EMD estimation results of the generators speed deviations and share of the imbalance impact

	EMD
$d\omega_1/dt$ [Hz/s]	-0,1010
$d\omega_2/dt$ [Hz/s]	-0,0814
$d\omega_3/dt$ [Hz/s]	-0,0711
$d\omega_4/dt$ [Hz/s]	-0,0915
$d\omega_5/dt$ [Hz/s]	-0,0932
$d\omega_6/dt$ [Hz/s]	-0,0931
$d\omega_7/dt$ [Hz/s]	-0,0979
$d\omega_8/dt$ [Hz/s]	-0,0757
$d\omega_9/dt$ [Hz/s]	-0,0948
$\Delta p_1$ [MW]	-168,38
$\Delta p_2$ [MW]	-8,2275
$\Delta p_3$ [MW]	-8,4916
$\Delta p_4$ [MW]	-8,7241
$\Delta p_5$ [MW]	-8,0821
$\Delta p_6$ [MW]	-10,809
$\Delta p_7$ [MW]	-8,6214
$\Delta p_8$ [MW]	-6,1384
$\Delta p_9$ [MW]	-10,902
<b>TOTAL [MW]</b>	<b>-238,38</b>

Generator G10 has in actual dispatch active power of 250 MW so total estimated value using EMD approach for estimation of power system imbalance is 238,38 MW, thus representing a quite precise estimation.



Oral Presentation: Under-Frequency Load Shedding Based on Huang’s Empirical Model Decomposition Approach for Estimation of df/dt and Artificial Neural Networks

Table 3 presents the simulated outages of individual generating units in the test system. By applying the EMD approach to the frequency signals, the rate of change of frequency (RoCoF) was calculated for each generator, as well as the Col RoCoF  $df_c/dt$ . The values of  $df_c/dt$  are shown in Table 3. Based on the calculated rate of change of the centre of inertia frequency, imbalances in active power caused by the disturbance of a specific generating unit outage were computed. Table 3 demonstrates that the EMD approach accurately reflects the calculated imbalances in active power.

Table 1. Associated power of generating units,  $df_c/dt$ , and  $\Delta p$  estimated using the EMD method after individual generating unit outages.

Generators	Power (MW)	Col RoCoF (EMD)	$\Delta p$ (MW) EMD
G2	572	-0,183	560,26
G3	650	-0,212	630,94
G4	632	-0,2	605,87
G5	508	-0,162	494,63
G6	650	-0,21	624,22
G7	560	-0,173	529,38
G8	540	-0,166	509,12
G9	830	-0,271	805,84
G10	250	-0,075	238,38

An Artificial Neural Network (ANN) is employed to estimate the magnitude of generator loss. The ANN Toolbox is utilized to create the model. The training data is derived from the frequency response of nine dispatch generators (Figure 4.). Figure 5 illustrates the Col RoCoF (the rate of change of frequency of the center of inertia), which is determined using EMD, according to nine dispatch generators.

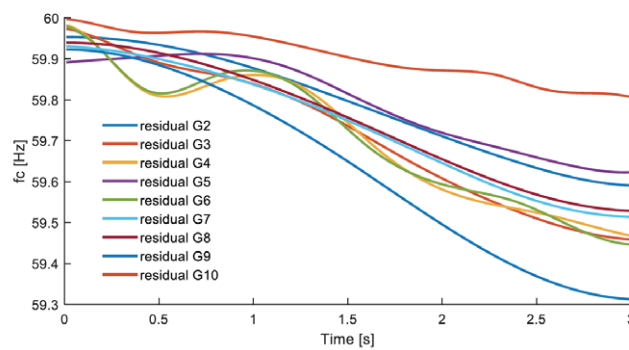


Figure 4. Residuals from the EMD – frequency of centre of inertia of nine dispatch generators

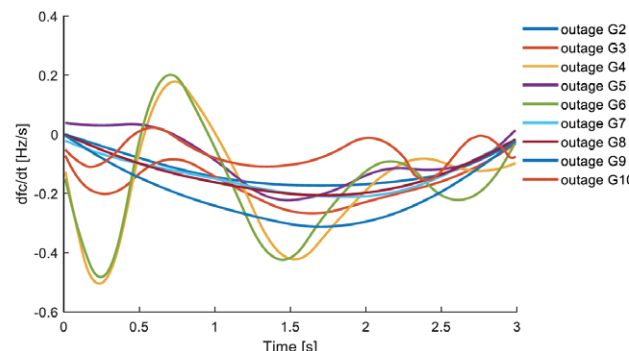


Figure 5. Col RoCoF of nine dispatch generators



**Oral Presentation:** Under-Frequency Load Shedding Based on Huang's Empirical Model Decomposition Approach for Estimation of  $df/dt$  and Artificial Neural Networks

To validate the effectiveness of the AUFLS approach, extensive computer simulations were conducted using IEEE 39 bus test system. This test system is widely accepted benchmarks for power system analysis and provide a realistic environment for evaluating load-shedding schemes. The simulations included scenarios with significant disruptions, such as generator outages, to test the robustness and responsiveness of the AUFLS approach. The results obtained from the simulations were compared against a conventional under-frequency load shedding (UFLS) scheme to assess the performance improvements achieved by the new approach.

## 4. SIMULATION RESULTS

The simulation results, presented in Figure 6 and Figure 7, compare the performance of two load shedding methods: Adaptive Under Frequency Load Shedding (AUFLS) and four-stage Under Frequency Load Shedding. In Figure 6, the frequency response is examined after the outage of generator G4 from the system. Similarly, Figure 7 illustrates the response after the outage of generator G8. The analysis of these figures indicates that AUFLS exhibits a faster and more accurate frequency response following a generator outage compared to traditional UFLS. Figure 6 shows that AUFLS reaches a steady state frequency of 59.976 Hz within 20 seconds, while four-stage UFLS takes 30 seconds to achieve a steady state frequency of 59.871 Hz. Similarly, Figure 9 illustrates that AUFLS restores the frequency to a steady state of 59.984 Hz in 20 seconds, whereas four-stage UFR requires 35 seconds to stabilize at a frequency of 59.731 Hz.

From the Figure 6 and Figure 7 it can be concluded that lower nadir frequency values are achieved by applying AUFLS, which represents a significant advantage of applying AUFLS over the conventional scheme. The nadir frequency according to AUFLS implemented due to outage of generator G4 is 59.361 Hz, while using traditional UFLS nadir frequency is 59.387 Hz. In addition, the nadir frequency according to AUFLS implemented due to outage of generator G8 is 59.354 Hz, while using traditional UFLS nadir frequency is 59.389 Hz.

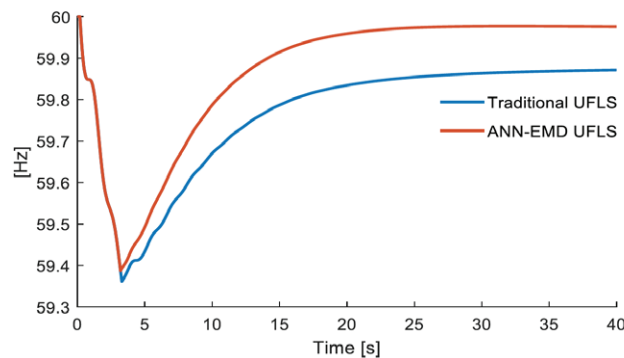


Figure 6. Traditional UFLS and AUFLS (ANN-EMD) due to outage of G4

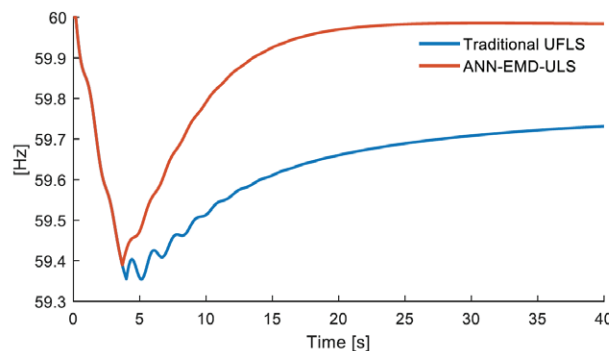


Figure 7. Traditional UFLS and AUFLS (ANN-EMD) due to outage of G8

## CONCLUSION

Under-frequency load shedding is a critical aspect of power system stability, and advancements in estimation techniques can significantly improve the effectiveness of UFLS schemes. The combination of Huang's Empirical Model Decomposition approach and





**Oral Presentation:** Under-Frequency Load Shedding Based on Huang's Empirical Model Decomposition Approach for Estimation of  $df/dt$  and Artificial Neural Networks

Artificial Neural Networks presents a promising solution for accurate and adaptive estimation of  $df/dt$  and magnitude of active power imbalance, enabling optimized load shedding decisions.

By embracing these innovative methodologies, power utilities can enhance the resilience and reliability of their systems, ensuring uninterrupted electricity supply even during challenging conditions. The future of under-frequency load shedding lies in data-driven approaches that leverage the power of machine learning and advanced signal analysis techniques.

### BIBLIOGRAPHY

- [1] Documentation: Description of the 39 Bus New England System. DlgSILENT PowerFactory. DlgSILENT GmbH, Heinrich-Hertz-Str. 9, 72810 Gomaringen, Germany, [www.digsilent.de](http://www.digsilent.de)
- [2] S. Avdakovic, A. Nuhanovic, M. Kusljagic, "An Estimation Rate of Change of Frequency using Wavelet Transform," International Review of Automatic Control, vol. 4, pp. 267-272, 2011.
- [3] P.M. Anderson, A.A. Fouad, "Power System Control and Stability," 2nd ed., Hoboken, NJ: Wiley-IEEE Press, 2002.
- [4] D. Fan, "Synchronized Measurements and Applications During Power System Dynamics," PhD Thesis, Faculty of the Virginia Polytechnic Institute and State University, Blacksburg, Virginia, 2008.
- [5] N.E. Huang, Z. Shen, S.R. Long, M.C. Wu, H.H. Shih, Q. Zheng, N.C. Yen, N. C. Yen, C. C. Tung, H. H. Liu, "The Empirical Mode Decomposition Method and the Hilbert Spectrum for Non-Stationary Time Series Analysis," in Proceedings of the Royal Society of London, pp.903-995, 1998.
- [6] Hartono, J., et al. "Adaptive Underfrequency Load Shedding design based on generation losing estimation using Artificial Neural Network method." IOP Conference Series: Materials Science and Engineering. Vol. 1098. No. 4. IOP Publishing, 2021.
- [7] Lokay, H.E., Burtnyk, V.: Application of Underfrequency Relays for Automatic Load Shedding. Power Apparatus and Systems, IEEE Transactions on Power Apparatus and Systems 87(3), 776-783 (1968).
- [8] Horowitz, S.H., Phadke, A.G.: Power System Relaying. 3rd edn. John Wiley & Sons, (2008).
- [9] PRC-006-SERC-02: Automatic Underfrequency Load Shedding Requirements - NERCipedia." [Online]. Available: <https://nercipedia.com/active-standards/prc-006-serc-02automaticunderfrequency-load-shedding-requirements/>. [Accessed: 28-Jan-2023].
- [10] Dedović, Maja Muftić, and Samir Avdaković. "A new approach for  $df/dt$  and active power imbalance in power system estimation using Huang's Empirical Mode decomposition." International Journal of Electrical Power & Energy Systems 110 (2019): 62-71.



# The Impact of the Connection of Renewable Resources in the Distribution Network - The Case of Hydro Power Plants in Kosovo

[avni.alidemaj@keds-energy.com](mailto:avni.alidemaj@keds-energy.com)

AVNI ALIDEMAJ\*, SIDORELA DODAJ, MARIGONA ZEJNULLAHU, ARIF VITIJA

*Kosovo Electricity Distribution Company – KEDS***Kosovo**

## SUMMARY

For many countries that are still developing, including Kosovo, the challenge of electricity and sufficient energy resources persists. The development of the energy sector is crucial for the well-being of the population, meeting their needs, and advancing the country's progress. The primary objective of the power system is to function according to technical standards and ensure customers receive a reliable and high-quality electricity supply. Renewable energy refers to energy derived from natural sources such as sunlight, wind, rain, tides, waves, and geothermal heat. Among the various types of renewable energy sources, the most commonly utilized ones are wind turbines (for wind energy), solar panels (for solar energy), and hydropower plants (for water energy).

In Kosovo's case, the number of renewable energy sources connected to the electricity grid is steadily increasing, indicating a positive trend for their utilization in the upcoming years. This paper aims to analyze hydropower plants and their integration into the electric power system, where the primary focus is to demonstrate the impact of hydropower plants on the distribution network and present hydropower plants connected to the Dragash region.

## 1. INTRODUCTION

Kosovo relies heavily on its lignite resources to meet its energy demands. However, considering the commitment of the EU Agreement to achieve carbon neutrality in Europe by 2050 and a reduction of up to 40% of greenhouse gas emissions by 2030, Kosovo should also prioritize renewable energy resources. Fortunately, Kosovo possesses numerous renewable resources that offer cost-effective alternatives for the future. It is essential that Kosovo seriously consider and take important steps towards embracing renewable energy.

The integration of hydropower plants into Kosovo's energy system encompasses two primary aspects: connection and operation. Nevertheless, prior to their integration into the electrical grid or the specific connection point, certain modifications need to be implemented in the existing network. These necessary changes are explained below [1], [2]:

**Bidirectional flow of energy** - The existing electricity network of Kosovo must enable the bidirectional flow of energy, that is, from the generator to the consumers and vice versa with the end users who contribute to the electricity supply.

**Creation of efficient mechanisms** - Efficient mechanisms for network management should be created, aimed at reducing peak loads, improving network flexibility, responsiveness and security of supply to cope with increased systemic variability.

## KEYWORDS

Renewable sources - distribution network – impact - hydropower plants - Dragash.



**Oral Presentation:** The Impact of the Connection of Renewable Resources in the Distribution Network - The Case of Hydro Power Plants in Kosovo

**Integration of technologies in the network** – In order to ensure the stability and proper control of the network operation (eg frequency, voltage, etc.) in the presence of a significant part of variable renewable resources, it is necessary that in the existing network advanced technologies are used which enable such a thing.

**Balancing and controlling the power** - The balancing ability of the energy system is one of the main limitations for the integration of hydropower plants in the existing network of Kosovo precisely because of the nature of the uncertainty and volatility of the output power [2], [3].

**Increasing the reserve capacity** - From the point of view of system planning and operation, with the increasing penetration of production from hydropower plants, electricity systems need additional reserve capacity to provide power to the system at times when RE sources are not producing or not producing enough to meet demand.

**Installation of directional protections** - To ensure safe and selective protection, the impact of hydropower plants on the protection systems must be considered in planning the operation of the network by considering the installation of new directional relays as well as the development of new algorithms of directed protection.

**Installation of the SCADA system** - In order to be able to monitor the key parameters from the generation of electricity through hydropower plants such as voltage, currents, frequency, active power, then it is necessary that in all existing power plants and those that will be installed in the future, the SCADA system will be installed.

This paper aims to analyze hydropower plants in Dragash region and their integration into the electric power system, where the primary focus is to demonstrate the impact of these hydropower plants on the distribution network [1], [2].

## 2. MATERIALS AND METHODS

This paper relies on literature and other scientific works related to the subject matter. All the data of the existing condition are obtained from the applications that Kosovo Electricity Distribution Company uses such as: Advance Enterprise and SCADA. Furthermore, simulations of the proposed scenarios were generated using DlgSILENT PowerFactory.

## 3. ANALYSIS AND RESULTS

The region of Dragash is supplied by the substation 35/10 [kV] Dragash. In this substation there are 2 transformers 35/10 [kV] with installed power 2x8 [MVA].

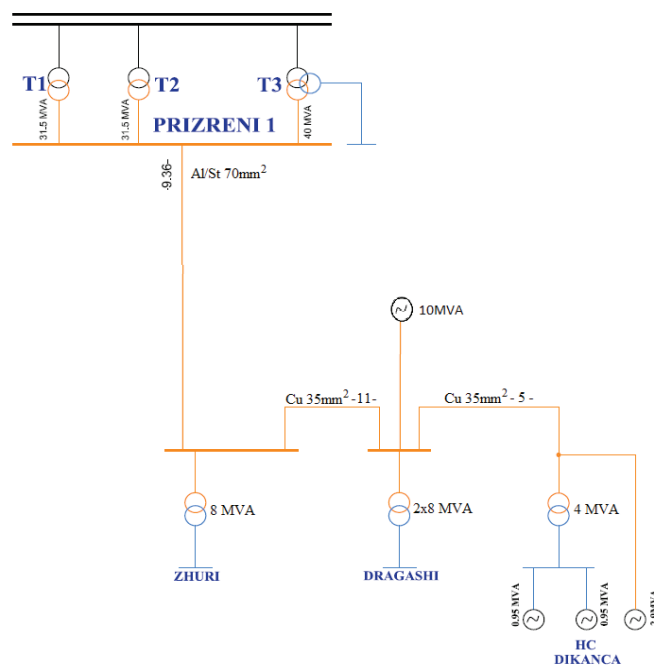


Figure 1. Single-line diagram of 35 [kV] lines in Dragash region (KEDS, 2017).



Oral Presentation: The Impact of the Connection of Renewable Resources in the Distribution Network - The Case of Hydro Power Plants in Kosovo

In this region, there are significant technical losses and voltage drops at both 35 [kV] and 10 [kV] levels. The existing network has surpassed its intended lifespan and is no longer suitable for efficient use. In recent years, there has been considerable interest in the construction of hydropower plants in the region. Unfortunately, the existing line capacities do not allow for the development of any hydro power plants beyond the capacities of these lines [4].

### 3.1. Technical Parameters – Voltage and Losses of Existing Lines

The 35/10 [kV] substations of Zhur, Dragash, and Dikanca face voltage drops during peak load times if they are solely supplied from SS Prizreni 1 110/10 [kV]. The voltage profile of the 35 [kV] lines in the Dragash region is presented in Table 1.

Due to the limitations of the line capacity, line Prizreni - Zhuri it cannot transmit more than 17 [MW], which results in excessive overload. Consequently, the line is mostly operational at 12 [MW] to prevent further strain [5].

Table 1. Technical performance of the lines when generators are not working (KEDS, 2017)

35 [kV] Line	Active Power [MW]	Voltage [kV] 1 <sup>st</sup> SS	Voltage [kV] 2 <sup>nd</sup> SS	Loading of the lines [%]
Prizren 1 - Zhur	17.11	35.06	32.09	142.50
Zhur - Dragash	7.71	32.09	30.16	86.63
Dragash - Dikanca	0.87	30.16	30.07	6.07

The graph below shows the voltage profile of 35kV lines when none of the generators were working.

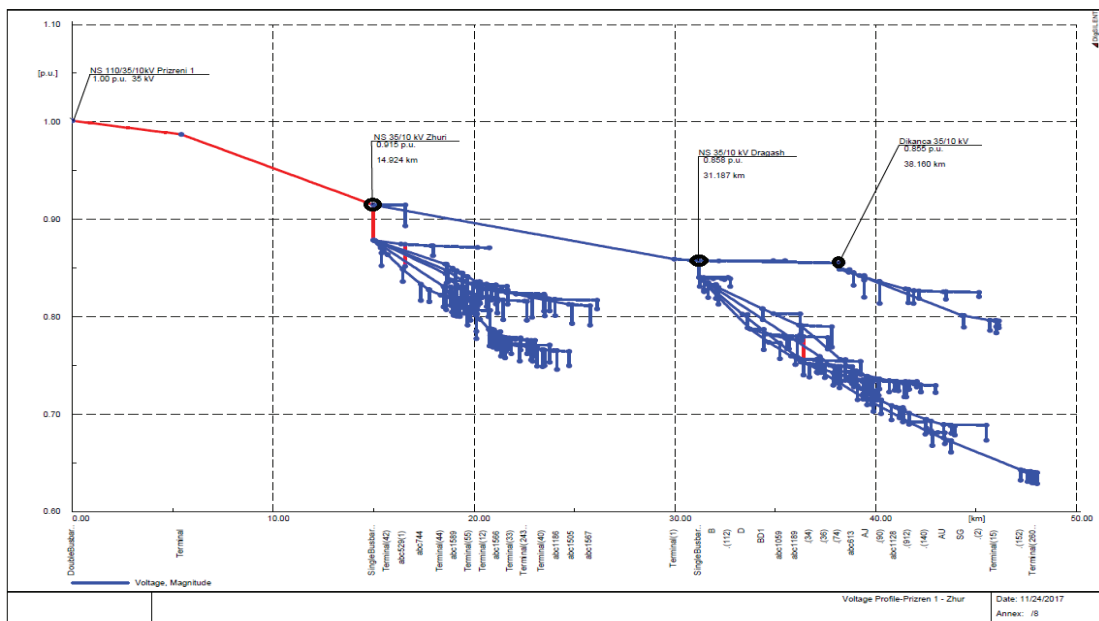


Figure 2. Voltage profile for 35 [kV] lines, 10 [kV] lines and distributed transformers (KEDS, 2017).

### 3.2. Impact of Hydropower plants in Network

The maximum load recorded in the Prizreni 1 - Zhuri line in 2017 was 17.9 [MW], with an average maximum load of approximately simultaneous 15 [MW].

Figure 3 illustrates the load profile of HPPs Eurokos and G3 Dikanca, which are dependent on streamflows. It can be observed that during the spring period (April-May-June), there is an increase in streamflow and energy production from the hydropower plants, with Pmax reaching up to 9.3 [MW]. The average Pmax throughout the year is around 3.3 [MW]. In May 2018, the HPP operated continuously as there were streamflows throughout the entire month. There were only 12 days in the year without hydro generation, and the minimum production recorded was 1.4 [MW] [4], [5].



Oral Presentation: The Impact of the Connection of Renewable Resources in the Distribution Network - The Case of Hydro Power Plants in Kosovo

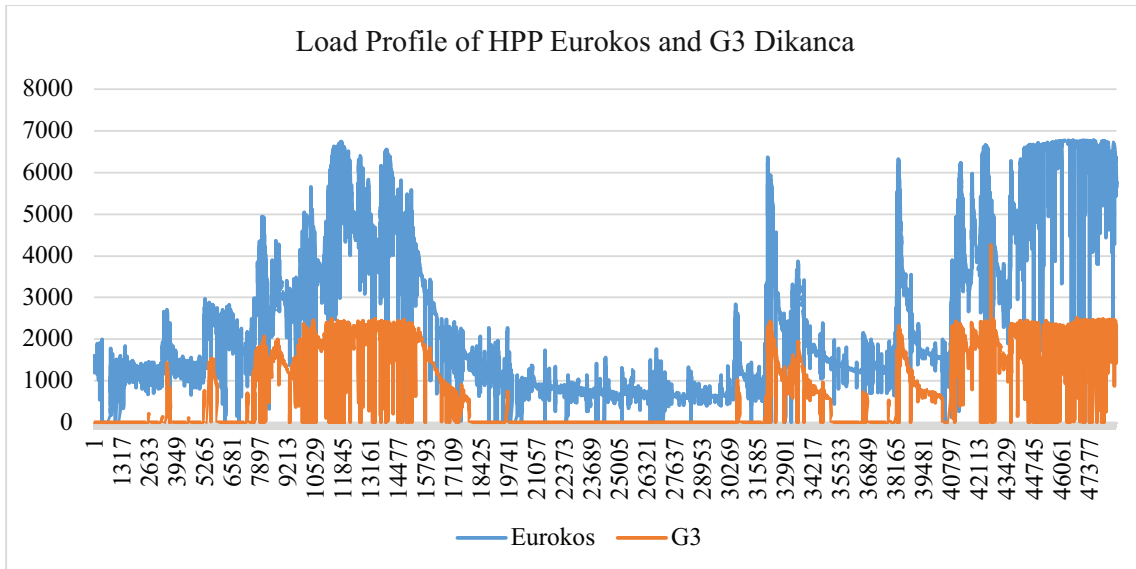
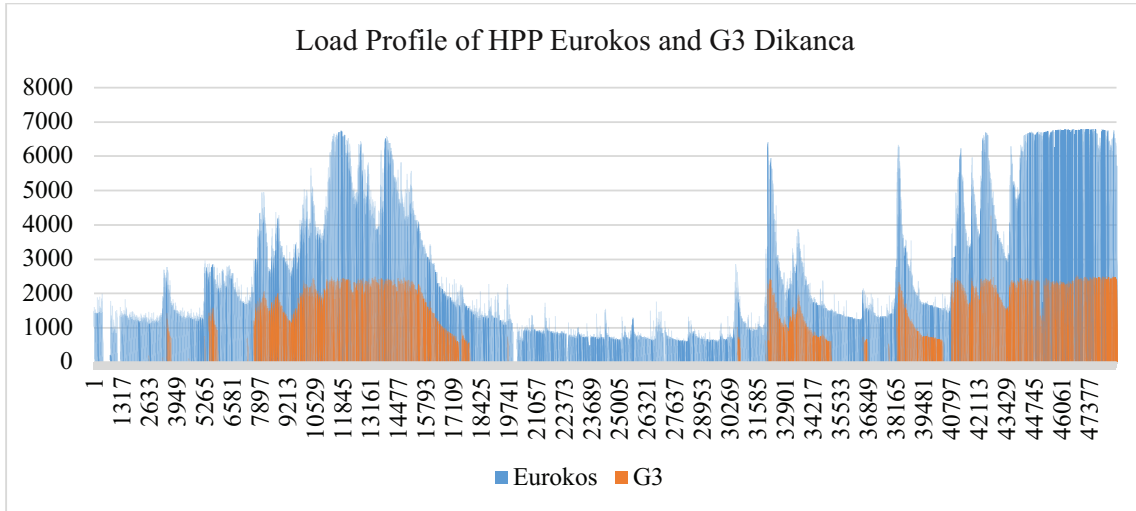


Figure 3. Load profile of Eurokos HPP and G3.

The diagrams below show the electricity consumed from distribution network and generators. The blue area represents the consumption from the KEDS, while the red area represents the energy production from the HPP.

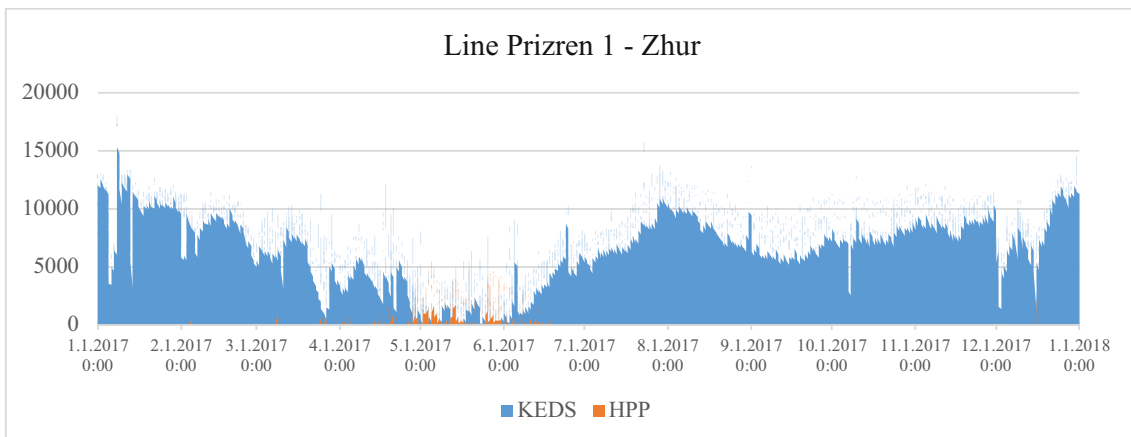


Figure 4. Load profile of KEDS and HPP in the line Prizren 1 - Zhuri



Oral Presentation: The Impact of the Connection of Renewable Resources in the Distribution Network - The Case of Hydro Power Plants in Kosovo

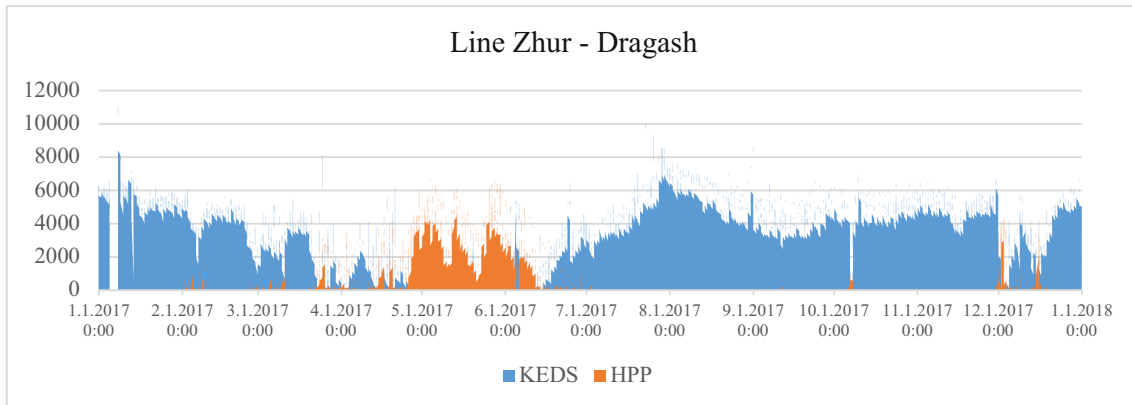


Figure 5. Load profile of KEDS and HPP in the line Zhur - Dragash

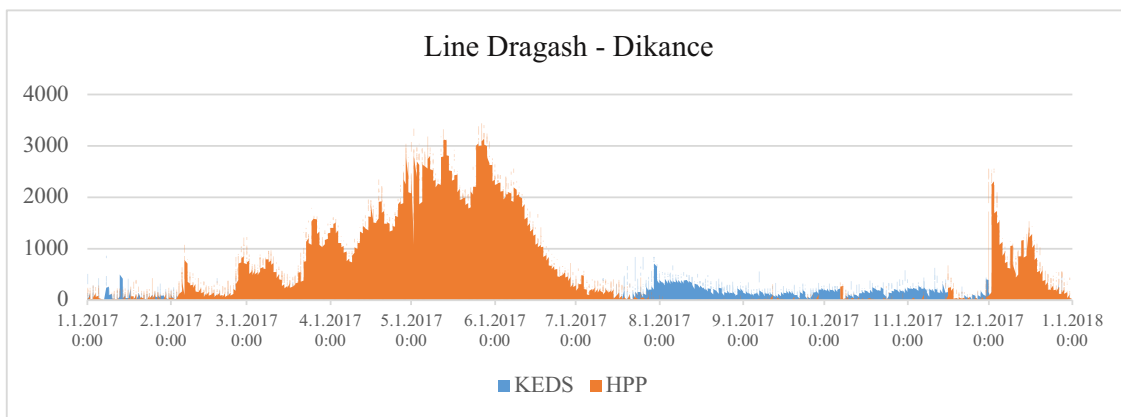


Figure 6. Load profile of KEDS and HPP in the line Dragash - Dikanca.

The diagrams above illustrate that HPPs production is primarily consumed in Dikanca and Dragash, while only a small amount is directed to SS Prizreni 1.

The establishment of a new HPP in Dragash has significantly reduced losses in the 35 [kV] lines. In 2013, losses in the OHL 35 [kV] in the Dragash area exceeded 4000 [MWh]. However, with the construction of the HPPs, particularly during periods of streamflows, these losses have been reduced around 2300 [MWh] [5].

Table 2. Technical losses of the lines 35 [kV], when generators were working

Line	Losses [MWh]
Prizren 1 - Zhur	1331
Zhur - Dragash	582
Dragash - Dikancë	1.58
Transformers	409
<b>Total losses</b>	<b>2,324</b>

As observed in the figure, these substations encounter issues with high voltage levels when consumption is low, typically during night time. Furthermore, all generators have consistently exceeded 10 [MW] throughout 2017. If the generators operate at their full capacity, which exceeds 10 [MW], it will result in overvoltage in the 35/10 [kV] substations. Based on measurements, the following voltage levels can be found in the substations for the worst-case scenarios during low consumption periods in Dragash at night [4].





Oral Presentation: The Impact of the Connection of Renewable Resources in the Distribution Network - The Case of Hydro Power Plants in Kosovo

Table 3. Voltage substations during the night

Time	HPP [MW]	Dragash [kV]	Dikance [kV]	Zhur [kV]
5/7/2018 3:15	8.99	36.40	36.49	35.35
4/28/2018 4:00	8.27	36.39	36.52	35.39
5/14/2018 3:30	8.45	36.38	36.61	35.31
4/27/2018 4:00	8.15	36.38	36.51	35.43
5/7/2018 3:00	9.03	36.38	36.49	35.35
5/16/2018 5:00	9.10	36.37	36.51	35.36
5/13/2018 3:00	8.14	36.37	36.55	35.36
5/10/2018 3:30	8.05	36.37	36.53	35.37
5/7/2018 3:30	8.62	36.37	36.45	35.34
5/4/2018 3:00	8.66	36.36	36.58	35.28
5/11/2018 3:45	8.46	36.36	36.53	35.34
4/27/2018 3:30	8.24	36.36	36.51	35.39
4/28/2018 3:45	8.27	36.36	36.50	35.36
5/7/2018 2:45	9.21	36.36	36.49	35.31
5/6/2018 4:00	9.17	36.35	36.56	35.31
4/26/2018 2:15	8.57	36.35	36.54	35.31
5/10/2018 3:15	8.06	36.35	36.53	35.37

The voltage in the SS Dragash on the 35 [kV] side for the year 2017 is provided below. During the operation of the HPPs, the voltage exceeds 35 [kV]. However, when the HPP generation is reduced and Dragash needs to consume energy from SS Prizreni 1, the voltage drops below 35 [kV]. A temporary choice can be obtained by switching the automatic adjustment t; voltage in Prizren 1 during the night by setting it to values smaller than 36 kV, respectively 35 kV [4], [5].

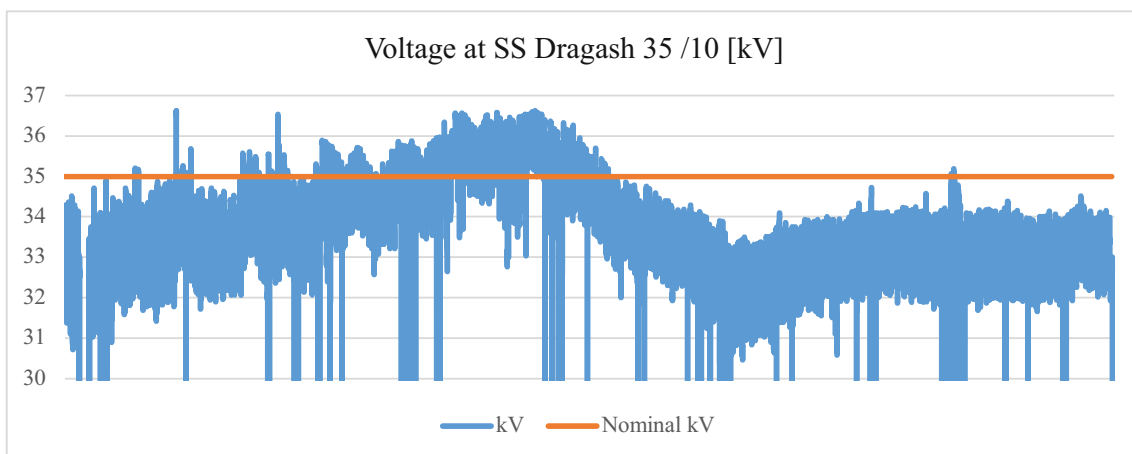


Figure 7. Voltage measurements at 35/10 [kV] Dragash.

### 3.3. Proposed Scenarios

To achieve a favorable solution for the overvoltages resulting from the integration of hydropower plants in the Dragash region, numerous scenarios have been analyzed. Among them, two scenarios are outlined in detail as below.



Oral Presentation: The Impact of the Connection of Renewable Resources in the Distribution Network - The Case of Hydro Power Plants in Kosovo

**Scenario-1: Increased capacity of HPPs to 40 [MW]**

In this scenario, KEDS needs to construct a double 35 [kV] line from Prizreni 1 to Zhuri, Zhuri to Dragash, and Dragash to Dikanca. This is necessary due to the incapacity of the existing line to accommodate the power generation capacity of 40 [MW].

Taking into account the expected increase in HPPs capacity by approximately 10 [MW], the performance of the lines for  $P_{max}$  and  $P_{min}$  will be as shown in Tables 4 and 5 [5], [6].

*Table 4. HPP 40 [MW] during the peak*

Modelling with Generated Power 40 [MW] for HPP - Consumption 17.8 [MW]			
	Prizren 1- Zhur	Zhur- Dragash	Dragash- Dikanca
Losses (MW)	0.335	1.65	0.0032
Loading (%)	49.3	79.95	5.32
Voltage (kV)	35.61	37.56	35.07
Active Power (MW)	-20.36	-27.46	-1.98
Reactive Power (MVar)	-4.66	-6.37	-0.403

*Table 5. HPP 40 [MW] during the night (low consumption)*

Modelling with Generated Power 40 [MW] for HPP - Consumption 4 [MW]			
	Prizren 1- Zhur	Zhur- Dragash	Dragash- Dikanca
Losses (MW)	0.84	2.57	0.054
Loading (%)	27.87	99.76	6.93
Voltage (kV)	36.03	38.30	35.10
Active Power (MW)	-31.8	-34.64	-2.637
Reactive Power (MVar)	-10.22	-9.63	-0.742

**Scenarios 2: Building a new KOSTT substation**

In this scenario, it is necessary to invest in increasing the cross-section of the line between SS Prizreni 1 and SS Zhuri, using an Al/St conductor with a cross-section area of 95mm<sup>2</sup>. Additionally, one more 8 [MVA] transformer should be installed in SS Zhuri and another 8 [MVA] transformer in SS Dragash, as indicated in the table. With these new configurations, SS Zhuri will be supplied from SS Prizreni 1, while SS Dragash and SS Dikanca will be supplied from KOSTT substation and HPPs. If the substation with three voltages is built in Dragash, then the new 8 MVA transformer is not necessary there.

The line between Zhuri and Dragash can serve as an alternative supply, but it will remain mostly open, resulting in all parameters being zero. The modeling is based on a total HPPs capacity of 30 [MW] initially, with an additional 10 [MW] increase to reach a total of 40 [MW] [5], [6].

*Table 6. HPP 30MW with KOSTT new SS*

Modelling with Generated Power 30 [MW] for HPP				
	Prizren 1- Zhur	Zhur- Dragash	KOSTT-Dragash	Dragash- Dikanca
Losses (MW)	0.28	0	0.004	0.027
Loading (%)	48.2	0	45	7.2
Voltage (kV)	33.6	0	35.1	35.08
Active Power (MW)	7.95	0	-19.7	-1.26
Reactive Power (MVar)	2.17	0	-0.85	0.042



Oral Presentation: The Impact of the Connection of Renewable Resources in the Distribution Network - The Case of Hydro Power Plants in Kosovo

Table 7. HPP 40MW with KOSTT new SS

Modelling with Generated Power 40 [MW] for HPP				
	Prizren 1- Zhur	Zhur- Dragash	KOSTT-Dragash	Dragash- Dikanca
Losses (MW)	0.28	0	0.009	0.026
Loading (%)	48.2	0	68.6	7.07
Voltage (kV)	33.6	0	35.1	35.08
Active Power (MW)	7.95	0	-29.6	-1.25
Reactive Power (MVar)	2.17	0	-2.81	0.048

In figure 8 it is shown the single-line diagram of the new configuration after implementing the new KOSTT substation based on Scenario 2.

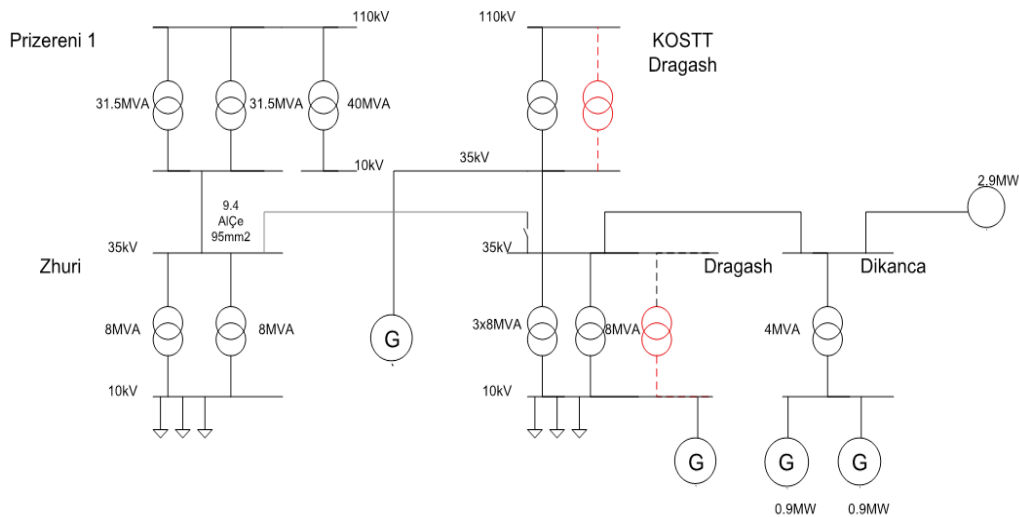


Figure 8. Single-line diagram after new KOSTT SS.

Technical losses

Comparing the losses in the existing situation, the losses are expected to decrease significantly when KEDS makes the necessary investments. Furthermore, if a new KOSTT substation is built, the losses are anticipated to be even lower than with the existing situation [6].

Table 8. Technical losses in different scenarios.

Scenarios	Losses [MWh]
Existing situation	2,324
Double line - 40 [MW] HPP	4,010
KOSTT New Substation - 40 [MW]	969

It is planned to be constructed a new KOSTT substation, for reason such as:

- In comparison to the 35 [kV] line, the 110 [kV] line designated for the new substation is in close proximity to Dragash.
- It will fulfill the N-1 criteria, ensuring a reliable and redundant power supply.



Oral Presentation: The Impact of the Connection of Renewable Resources in the Distribution Network - The Case of Hydro Power Plants in Kosovo

- The implementation of this configuration will result in reduced losses in comparison to alternative scenarios.
- It facilitates the optimization of the power system between Kosovo and Albania.

As the construction of the new substation of KOSTT is still in the planning phase, KEDS has undertaken the implementation of a new underground line connecting the Zhur substation to the Dragash substation.

Single-line diagram of 35 [kV] lines of Dragash region is shown in figure 9 [6].

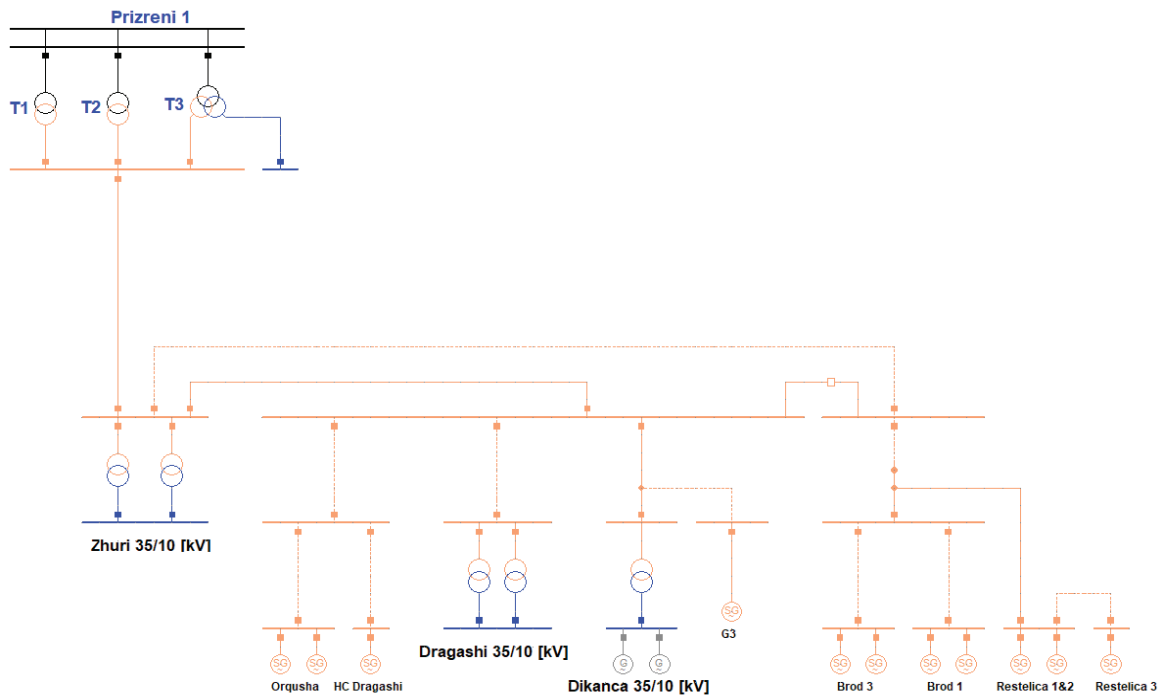


Figure 9. Single-line diagram of 35 [kV] lines of Dragash region (KEDS, 2023).

The hydropower plants connected to SS 35/10 [kV] Dragash are connected to the 35 [kV] side. As such, only the single-line diagram of the 35 [kV] side is presented below.

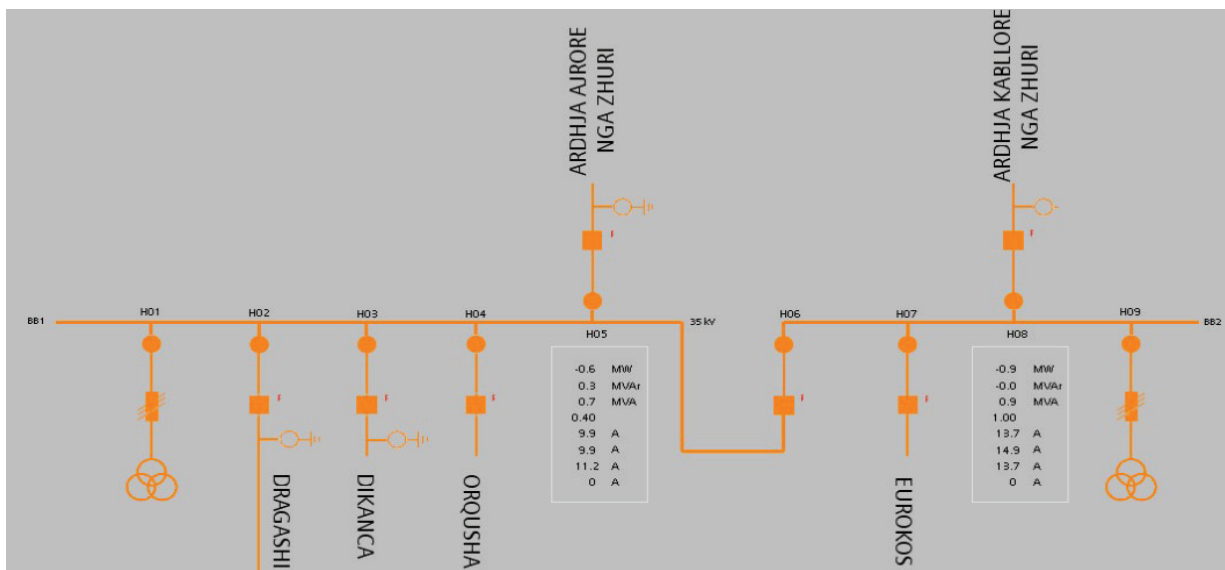


Figure 10. Single-line diagram of the 35 [kV] side of NS 35/10 [kV] Dragash (KEDS, 2023).



**Oral Presentation:** The Impact of the Connection of Renewable Resources in the Distribution Network - The Case of Hydro Power Plants in Kosovo

Therefore, from the single-line diagram of this substation, it can be observed that the 35 [kV] side of this substation comprises of [6]:

- Two measuring openings for the two busbar systems (BB1 and BB2)
- Overhead Incoming from NS 35/10 [kV] Zhuri
- Underground Incoming from NS 35/10 [kV] Zhuri
- Outgoing 35 [kV] that supplies part of NS Dragash
- Outgoing 35 [kV] for NS and HC Dikanca
- Outgoing 35 [kV] for HC Orçusha
- Outgoing 35 [kV] for HC Eurokosi

#### 4. CONCLUSION

From this paper, it can be concluded that the advantages of integrating renewable sources in the electric network are numerous, including: reducing energy losses in the network, increasing the reliability and security of the system, reducing peak demand, reducing pollution, reduction of high harmonics, etc.

From the other side, during low consumption would appear overvoltage's if there are not undertaken additional measures for their elimination through automatic regulation of voltage from place of source (SS 110 kV) mainly during night when we have drop of load.

However, if the fundamental obligation of the operator on customer satisfaction and supply stability is considered, following the parameters required according to the standards, the investments in this part of the system are logical, with this a high priority is given to renewable sources for which all the world is headed in this trend.

This case is also taken for analysis from the other side, where the determination of the priority of renewable resources due to the spatial configuration and load concentrations often exceeds the expectations of profits from this demand and presents obstacles and higher demands for investments in the distribution system outside of reasonableness. technical-economic or relevant optimums.

In some cases, for such support of energy goals with the increase of RES and to move with time, it would also be necessary to receive state donations or grants for certain projects so that the steps of the movement in this direction were even more quickly and realistically achieving effective goals over time.

#### BIBLIOGRAPHY

- [1] Henrik Lund, Renewable energy strategies for sustainable development, 2007.
- [2] Yilmaz Bayar & Mahmut Unsal Sasmaz & Mehmet Hilmi Ozkaya, Impact of Trade and Financial Globalization on Renewable Energy in EU Transition Economies, 2020.
- [3] Energy Strategy of the Republic of Kosovo 2022-203, <https://me.rks-gov.net/en/energy-2/>, March 2023.
- [4] Investment Department of KEDS, Pristina, 2017.
- [5] Metering Department of KEDS, Pristina, 2017.
- [6] Investment Department of KEDS, Pristina, 2023.



**DISTRIBUTION SYSTEMS  
AND SMART GRIDS  
POSTER PRESENTATION**



ELECTRIC MACHINES AND  
POWER ELECTRONICS



ELECTRIC  
TRANSMISSION



AUTOMATION AND  
CONTROL

POWER  
GENERATION



ENERGY  
TRANSITION



DISTRIBUTION SYSTEMS  
AND SMART GRIDS



**11-13 OCTOBER 2023**







# Smart Metering Benefits for Customers and Distribution System

[hamnijete.qorolli@keds-energy.com](mailto:hamnijete.qorolli@keds-energy.com)

**HAMNIJETE QOROLLI, LENDITA SHATRI, ALBANA DEMIRI, MIMOZA BERISHA**

*Engineer in AMR*

*KEDS-Kosovo Electricity Distribution and Supply Company*

**Kosovo**

## SUMMARY

Smart meters displayed measured energy on the LCD, they can also transmit energy values remotely. Except measuring the consumed energy, smart meters can also record other parameters such load and supply parameters, instantaneous values and Pmax values, load profile, voltages, currents, power factor, reactive energy, etc. Also, they have possibilities to register billing values by dividing the amount of energy consumed according to daily and seasonal rates. Smart meters enable two-way communication: between the meter and the central system in different communication modes

KEDS believes that the installation of smart meters offers a high benefit for customers in a way of controlling their rational energy usage, and considering trends and developments it is a necessary project.

Currently KEDS with smart meters had covered all customers at voltage levels 35 kV, 10 kV and 0.4 kV (half indirect connection) and latest have start also to household customers, also all control measurement at voltage level of 35/10 (20) kV and 0.4 kV.

From total customers on KEDS, 13.18 % are with Smart meters, from than 78.5 % are PLC meters.

In this paper, we aim to present the benefits of smart meters to consumers and their impact on improving the quality of service provided by **DSO** -KEDS.

KEDS approved projects for the installation of SMART meters with direct connection, active energy measurement, remote readings with G3 PLC communication at customer side.

In order to achieve good results, the complete replacement of the SS 0.4kV network was done, included: the installation of new poles, changing cables, installing cabinets, etc.

One of the purposes of smart metering Projects with PLC was also reducing the losses, and based on analyses losses will be reduced to the level of 8.86% (technical and commercial), which will be proven with the concrete cases analyzed in the paper.

KEDS uses the system for remote reading of meters, with up to 100 users can operate simultaneously and can support the reading of up to 1 million meters, with the possibility of increasing this number. This system started in 2012 and up to now has installed around 120 thousand meters.

Meters data are readied according to the IEC 62056-53 standard, while access to the meter data's is done according to security levels predetermined by KEDS.

## KEYWORDS

Smart meters, Losses, VPN.



Reading security is based on the security policies of the G3 Alliance, the data are transfer on system through special VPN. Consumer personal information are protected by the Personal Data Protection Law NO. 06/L-082, of Republic of Kosovo, and data on databases are protected with Law on Private Security services no. 04/L-004 of Republic of Kosovo.

Smart metering technology has great potential to achieve cost-effective energy savings where the effective use of electricity is essential in achieving Europe's energy efficiency targets, which are also translated into our laws and regulations national.

However, to make the smart meter project a success, a modernized grid is essential. Considering the unfavorable conditions in Kosovo, the rapid investment in smart meters exposes the country to unaffordable prices for end users, so a slower process is more necessary in Kosovo.

### 1. GENERAL INFORMATION

KEDS has licensed DSO has 7,925 km MV network and 20,574 km LV network, it serves to more than half million active consumers. Household consumers obtain dominant consumption with about 63.27%, followed by commercial consumption with 23.59%, then by industrial consumption with 12.38%, and finally by consumption in public lighting with 0.76%. Compared to the previous year, gross demand decreased by 4.91%, consumption by household consumers decreased by 0.47%, consumption by commercial consumers increased by 4.77%, and industrial consumption decreased by 27.6%. That are connected on different distribution voltage levels [1]. Distribution system in Kosovo operated with MV (35 kV and 10 kV) and LV (0.4 kV), and conform the pricing methodology approved by ERO, tariffs are applied according to respective voltage connection. For clarification purposes, all information and calculations below do not consider data for North Kosovo.

Until now, smart-meters are introduced mainly among MV customers, respectively industrial customers and commercial customers, while the measurement of household customers is mainly done with electronic meters (71 %), electromechanical meters (15 %), and smart meters (14 %).

### 2. DEVELOPMENT OF SMART-METERS THROUGHOUT THE YEARS

On November 2007, DSO as public company initiated a pilot project with smart meters with 2,700 meters. HES system was installed on PC and communication with meters was through GPRS and PLC. Project included 500 half indirect meter and 500 direct meters with GSM/GPRS communication, and 1,700 meters with PLC communication (by using S-FSK modulation), as well as 17 Data Concentrator for PLC communication. It resulted that project with GSM/GPRS communication was very successfully and readings were around 97 % (100 % on areas where telecommunication operator had good signal). However, PLC project on that time was not very success and didn't meet DSO requirements, as reading percentage was very low (up to 70 %), and therefore very difficult to manage.

It should be emphasized that PLC project at that time was not successful because the technology that was used was outdated and the capacity to transmit information back and forth was very low, network conditions were very bad and no investments were done, there were mistake in implementation of the project as PLC meters were not implemented in the whole SS 10/0.4 kV that was selected but partially, and other similar reasons.

On December, 2012 DSO established new Head End System with possibility to read and command 15,000 meters, and with possibility to extend with other 15,000 meters in that time.

On May 2013, when Distribution System was privatized, and KEDS start officially to operate as DSO. there were installed 12,249 Smart meters installed in the field, out of which 5,024 meters belonged to commercial consumers, 1,112 Feeder control meters, and 6,113 control meters in TS 10/04kV. All these meters were managed with existing HES system.

On April 2016 new PLC pilot project started, which included 100 PLC meters and one Data Concentrator, while communication was done through G3 PLC. The purpose of the project was to test the PLC communication and make the balance in 0.4 kV voltage level. In order to achieve good results, a complete replacement of network in this TS was done that included among others: installation of new poles, replacement of existing cable with a new cable and displacement of customer's meters from boxes in the poles.

The topological view of the G3-PLC supports opening phase cleaning and troubleshooting very efficiently, the figure 1 show the topology for two different SS 10/0.4 kV and after investment were good communication quality. The green colour shows the meters are online and good communication quality, the red colour shows the meters lost the communication are bad communication quality.

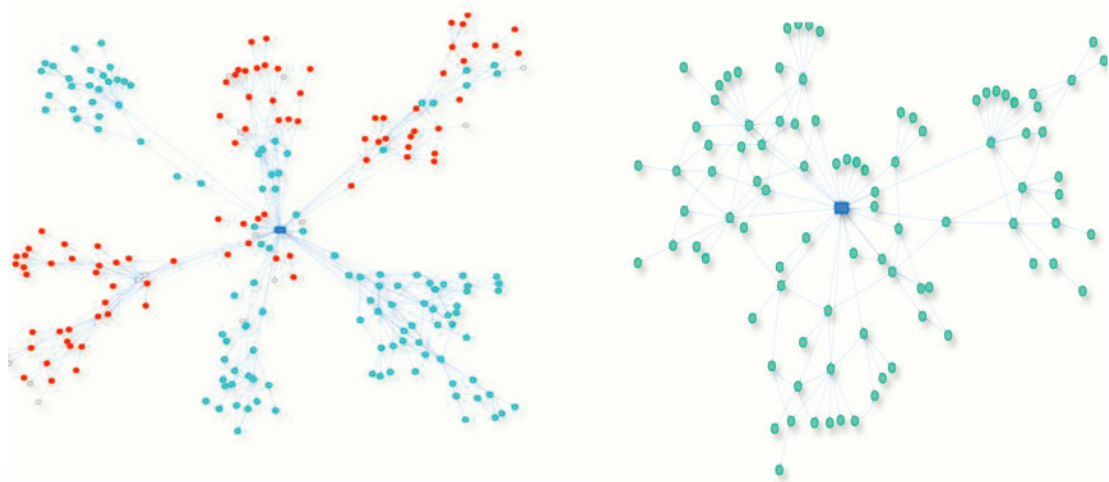


**Figure 1.** PLC communication quality

The project was monitored for one year and based on results it resulted that:

- PLC communication was 99.9% successfully
- Reading with Advance system was also 99.9% successfully.
- Losses have been decreased from 48.95% to 6%
- Reading ratio is increased for 10% 2.2. Practically shown benefits of the sample project

Based on results of PLC project of 2016, on 2017 DSO started with 5 new sample projects, which included around 1,000 customers. The project was selected based on the following conditions:

- The selected area should have high losses,
- Network should be radial,
- Have easy and faster access to the meter in any time.

After teams in the DSO have analysed all potential areas, the implementation of the project was agreed to be = developed in below written regions:

- District of Gjakova TS 10/04 kV Llozicë-Zogajt, Llozicë-Foniqt and school Llozicë,
- District of Pristina TS 10/04 kV Kalabrija 4,
- District of Prizreni TS 10/04 kV Caparci,
- District of Mitrovica TS 10/04 kV Hamza B,
- District of Peja TS 10/04 kV small Jabllanica.

Analyses are done for all project together based on regular Balance calculation procedure. Energy on entrance is calculated from readings of meters on SS 10/0.4 kV, Energy billed is sum of energy of all costumers that are supply from these SS 10/0.4 kV. Difference between Energy in entrance (kWh) and Energy billed (kWh) remain as Energy lost (kWh).

Same calculation is done for SS 10/0.4 kV before and after PLC project for a time period one year. Period when PLC project was during process is not included on calculation because during this implementation phase was faced with several problems, like customer's side problems, supply verification for several costumers, etc.

Yearly results shown that:

- energy entering into the transformer decreased for 20%
- losses decreased from 35% to 11%
- billing increased for 11%.

Respectively, load has decreased for 1,352 MWh, billing has increased for 502 kWh and losses decreased for 1,854 MWh.



**Table I.** Analyse of losses for projects PLC of period 2017/2019

	Before PLC	After PLC	After/Before
Energy in entrance (MWh)	6,873	5,521	-20%
Energy billed (MWh)	4,434	4,936	11%
Energy lost (MWh)	2,439	585	
Energy lost (%)	35	11	
Number of customers	849	873	

DSO expectation for PLC projects was achieved and good results for these five transformers are maintained successfully. As prove, another analysis is done similar as previews analyse but this time period after PLC is three year after finishing project, and analyses are done for each project.

**Table II.** Analyse of losses for projects PLC of period 2017/2022

	Before PLC	After PLC	After/Before
Energy in entrance (MWh)	6,873	6,447	-6%
Energy billed (MWh)	4,434	6,013	36%
Energy lost (MWh)	2,439	434	
Energy lost (%)	35	7	
Number of customers	849	967	

Results shown that:

- energy entering into the transformer decreased for 6%
- losses decreased from 35% to 7%
- billing increased for 36%.

Respectively, load has decreased for 426 MWh, billing has increased for 1,579 MWh and losses decreased for 2,005 MWh.

Same result is presented also in graphical form.

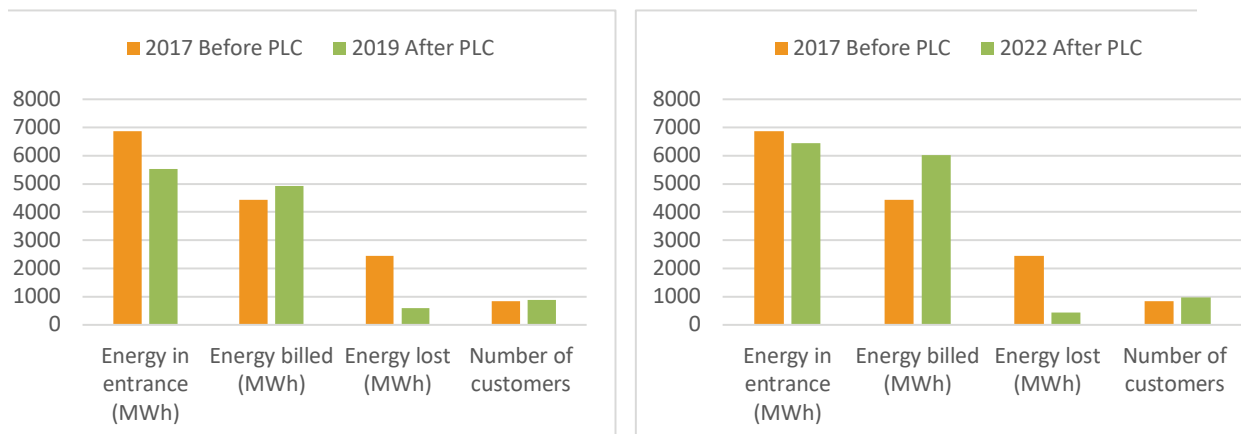


**Figure 2.** Load and loss graph



### 3. DSO PLC PROJECTS

As is mentioned in the abstract of this paper modernisation of the grid is essentially, but unfavorable conditions in Kosova, and operating status of DSO not allowed to made a massive implementation of PLC project, even the results was even better than was expect. From 2016 till end of year 2022 are mounted 73,525 PLC meters, spread in all territory of Kosova.

Table III. PLC meters per year

Meter /end of Year	2016	2017	2018	2019	2020	2021	2022
PLC	98	3,938	21,664	39,742	54,024	65,984	73,525

PLC projects are developed on 900 SS 10/0.4kV from they: finished 508 SS, ongoing 290 SS and not finished 111 SS.

AT all these PLC projects, in addition to meter installation, also network improvements were needed, such as:

- change of poles,
- new substation 10/0.4kV (when the system requires additional substation due to voltage drop),
- replacing the wire in 0.4 kV with cable,
- change of cabinet in 10/0.4 kV TS,
- removal of the old network,
- displacement meters (meter installation in poles, displacement of meters from consumer in cabinet, replacement of mechanical meters with electronic meter, and installation of PLC meters).

For 180 SS the projects together were analysed carefully for 12 months, and a before and after analysis was performed. project together based on regular balance calculation procedure. Energy on entrance is calculated from readings of meters on SS 10/0.4 kV, energy billed is sum of energy of all costumers that are supply from these SS 10/0.4 kV. Difference between energy in entrance (MWh) and energy billed (MWh) remain as lost energy (MWh). For each project energy is yearly average, values are present as sum of all yearly averages.

Table IV. Analyse of losses for projects PLC for 180 SS of period 2017/2022

	Before PLC Project	After PLC Project	After/Before (%)
TS Energy (MWh)	136,221	117,834	-13
Billing (MWh)	77,597	110,668	43
Losses (MWh)	58,624	7,166	
Losses %	43	6	
Nb. of consumers	15,567	18,238	
Comparative period	12		

Results shows that:

- energy entering into the transformer decreased for 13%,
- losses decreased from 43% to 6%,
- billing increased for 43%.

Respectively, load has decreased for 18,386 MWh, billing has increased for 33,071 MWh and losses decreased for 51,457 MWh.

Results are presented also graphically as bellow.



Figure 2. Graph of energy and energy losses

Analyses are done to get result for benefit per costumer. Average benefit per losses is losses is dividing per number of costumers. Per one-year customer losses are decrease from 312 kWh to 33 kWh, means that benefit per customer is 279 kWh per month.

Table V. Average benefit per consumer

Average	Before	After	After minus before	(After minus before)/before
TS Energy (kWh)	63,065	54,553	-8,512	-0.13
Billing (kWh)	35,924	51,235	15,311	0.43
Losses (kWh)	27,141	3,318	-23,823	-0.88
Losses %	43	6		
Number of consumers	87	101		
Loses for consumer	312	33		
Benefit Per Customer	279			
Number of SS 10/0.4	180	255		
Comparative period	12			

PLC investment as is presents in the Abstract has wide benefits, some of them are listed:

- decrease of energy at the entrance of substations, since after war in Ukraine there is world energy crises it will help DSO to decrease the consumption,
- decrease of losses (easy monitoring of energy flow)

For all PLC projects is sum benefit per year and comparing with yearly DSO Losses the impact of PLC is very successful.

Table VI. PLC Benefit in total losses

Year	2018	2019	2020	2021	2022
DSO Losses%	22.6	20.36	19.68	18.48	16.79
PLC Benefit in total losses %	0.23	0.49	0.96	1.19	1.29





Poster Presentation: Smart Metering Benefits for Costumers and Distribution System

- Decrease of errors in reading (more accurate billing),
- Elimination of eventual errors related to meters (decrease of customer complaints),
- Decrease of time for reading and billing (reading is done from HES, automatic billing in the reader only must print bill and to deliver to customer),
- Since PLC meters has regular daily reading costumers can check their daily consumption, actually through application E-kesco that is IOS and Android app and all customers can install in their phones. This will help customers to analyse their consumption manage better consume. (E-kesco).

## 4. DATA SECURITY

PLC communication that is used in DSO is done through different security levels. Smart meter supports reading of any instantaneous register. Additionally, meter configuration (set, action service) is possible for all COSEM objects, but limited to agreed meter security system Each G3-PLC meter needs to have:

- G3-PLC Alliance certificate,
- DLMS/COSEM certificate from DLMS User Association.

Data Concentrator reading all G3-PLC Meters with communication by using integrated S-FSK modulation and OFDM, enable two-way communication: between the meter and the central system in different communication modes and access to data only to authorized persons with different security levels (access control). Data transfer from DC to the system using VPN virtual private network which protects and secures information, applies cryptographic protection, implements IP security with a guaranteed integrity [figure 3]. Data storage on a special server with enough capacity and space storage - access to data only to authorized persons.

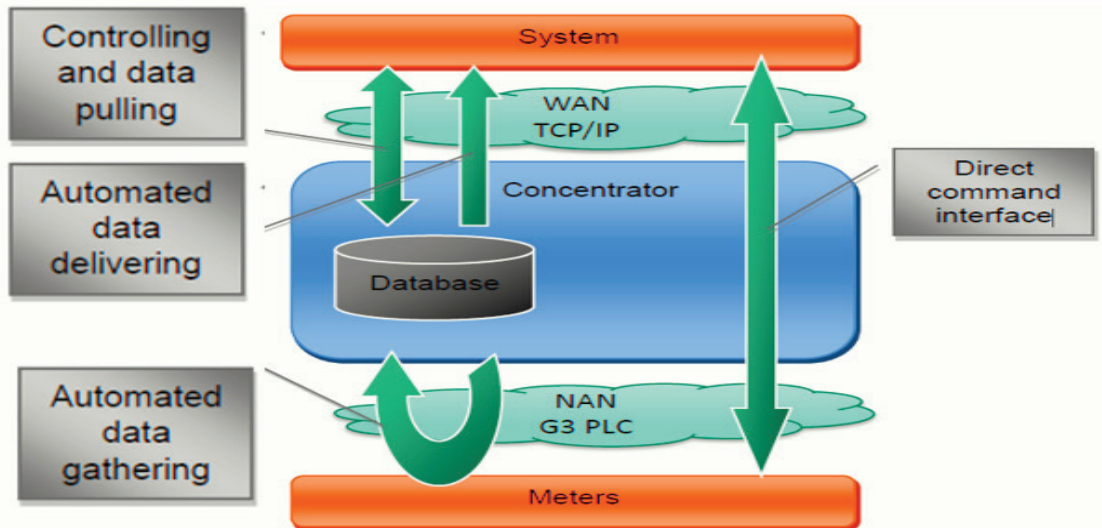


Figure 3. PLC communication [5]

Costumer datas are saved by policies on KEDS IT and are protected with Law on Private Security services no. 04/L-004 of Republic of Kosovo.

Cyber security is done based on procedure KEDS-AIT-HIB-ASC-01 that is approved from standards ISO 9001, ISO 14001.

## 5. CONCLUSIONS

Smart-meters are revolutionizing electricity industry all around the world. Moreover, smart-meters are ensuring that problems and issues are mitigating. As practically shown smart meters not only mitigate enormous and faulty meter readings, but they are key-players in fighting frauds faced by consumers.



EU and national level regulation, based on the needs of network modernization and energy efficiency, are the primary drivers for smart metering in Europe. Kosovo on the other hand by transposing EU legislation has also put electricity development and smart-metering in its top agenda.

With the deregulation of the market, as a major driver for new and innovative smart metering services are and with the unbundling, DSO will have to learn new ways to speak with their customers. It will require a more active presence in the market, as well as upfront investments especially in terms of upgrading their IT system, digitalization of data, and also win customer trust. One smart way of doing all this possible is unquestionably becoming digital through smart-meters.

Nevertheless, to make smart-meter project a success, a modernized network is necessity. Considering still the non-favourable conditions in Kosovo investing rapidly in smart-meters is exposing the country towards unaffordable end-user prices, hence a more stable a slower process is a must in Kosovo.

The future path is surely smart-metering, however for the project to be truly feasible and deliver the potential benefits to all stakeholders, particularly customers, it must be financially viable. With the assistance a potential funding sources and the collaboration of all stakeholders the project of smart-meters would become a financially attractive proposition. Nevertheless, as explain even in the event that it is not possible to secure any source of grant funding, the project may still be feasible but there are increased risks associated as will definitively impact the affordability of the end-users.

DSO believes that the installation of smart meters provides a number of benefits and savings to customers supports personal energy management. Considering the trends and developments it is a must project, however in order the project to be feasible financially and in term of implementation, it should grant and reasonable implementation phase, as PLC communication is in the low voltage network and is free of charge, network is fully available for advanced metering applications.

## BIBLIOGRAPHY

- [1] Annual Report 2022 ERO Kosova
- [2] KEDS-AIT-HIB-ASC-01
- [3] Law on Private Security services no. 04/L-004 of Republic of Kosovo.
- [4] John R. Vacca (ed.) - Computer and information security handbook-Morgan Kaufmann (2017)
- [5] G3 PLC Basics
- [6] E450 S4 - ZMX\_User Manual



# The Impact of Wind Farm Parks on Mitigation of Energy Crisis (2022) in Kosovo's Power System

[rexhep.selimi@kostt.com](mailto:rexhep.selimi@kostt.com)

**REXHEP SELIMI\*, GAZMEND KABASHI**

*Kosovo Transmission, System and Market Operator - KOSTT*

**Kosovo**

## SUMMARY

Due to low investment in South European Countries in new generation capacities, the effect of the high price increase of electricity and gas was very critical for the security of supply and the financial stability of all chains of the energy sector. Kosovo Power System in 2021 and 2022 has faced similar problems due to a gap in the generation to meet the demand during high load regimes.

The main purpose of the paper is to present the assessment of the impact of RES/Wind Parks in reducing import costs during the energy crisis in Kosovo's Power System in 2022. Although the installed capacity of the total Wind Parks is about 15% of the total production by thermal power plants (TPPs), which is mainly based on lignite, the impact of generating energy from Wind Farms has mitigated the cost of daily imports, mainly during the days when energy prices during the peak in the European markets were very high.

The comparison between the cost of energy produced by RES and the cost of energy imported from European exchanges to cover energy demands shows how great the influence of RES is in mitigating the energy crisis in cases like that of Kosovo's Power System.

Results show that Kosovo should focus on increasing investments in the installation of new RES capacities (wind and solar) to achieve faster energy diversification and transition, without overlooking the fact that the need for energy is constantly increasing. Furthermore, new investment on Energy Storage System and smart grids should follow to mitigate the intermittent RES integration in Kosovo Power System.

## KEYWORDS

Wind Park – RES – energy – mitigate – energy prices – transition



## 1. INTRODUCTION

### 1.1. Overview of the Kosovo's Power System

Most of the main generating units in Kosovo's power system are old non-conventional lignite-based capacities, such as Thermal Power Plants (TPPs), built during the 1960s and 1970s. These existing generation capacities currently comprise about 75% (around 900 MW) of all internal energy production throughout the year. Only 11% (around 132 MW) of total energy generation was produced by the Hydro Power Plants (HPPs) connected in transmission and in distribution network. Energy production produced by the newest wind park farm, commissioned during the last four years is around 12% (around 138 MW), while only 2% (around 20 MW) from small Solar Parks and prosumers based on PV which are installed in the distribution network.

The Kosovo's transmission network operates with high voltage transmission level 400 kV, 220 kV, and 110 kV while the distribution network operates with medium voltage (35 kV, 20 kV and 10 kV) and low voltage network (0.4 kV).

### 1.2. Actual Structure of the Generation Units

The existing structure of all generation units connected to Kosovo's transmission system during 2022 was as follows:

- Net generation capacity by thermal power plants (TPP) was approx. 900 MW
- Net generation capacity by hydropower plants (HPP) was approx. 67 MW
- Net generation capacity by wind farm parks (WFP) was approx. 138 MW
- Net generation capacity by solar parks (SP) was 0 MW.

This distribution reflects the installed capacity of each type of power generation unit connected to the transmission system in Kosovo during the specified period.

### 1.3. The Investments and Plans on New Renewables Sources

In the last four years, Kosovo has made significant progress in the integration of wind power plants (WPPs) into its transmission network. Two main wind power plants have been connected at the 110 kV network level, with a combined installed capacity of 138 MW.

The first investment in renewable sources for connection to the transmission network occurred in 2018 with the installation of WFP Kitka, which has a capacity of 32.4 MW. Following that, in 2021, the second investment in a renewable source was commissioned in autumn. WPP Selaci, with a total installed capacity of 105 MW, became operational.

However, it is important to note that currently, there are no solar plants connected to Kosovo's transmission network. According to the Energy Strategy of Kosovo, the plan is to install approximately 1500 MW of solar power in the power system by 2030. This highlights the country's commitment to decarbonization and transitioning to cleaner energy sources[3].

These developments signify Kosovo's efforts to diversify its energy mix and reduce reliance on fossil fuels. By integrating renewable energy sources into its transmission network, Kosovo aims to contribute to decarbonization goals and promote a more sustainable and environmentally friendly energy sector.

In addition to the integration of wind farm plants, Kosovo is also making strides in other areas of renewable energy development. The country has recognized the importance of diversifying its energy sources and reducing its dependency on fossil fuels.

Kosovo has set ambitious targets outlined in its Energy Strategy, aiming to increase the share of renewables in its energy mix. These targets include increasing the installed capacity of renewable energy sources, such as wind and solar, to contribute to the overall energy production. The development of renewable energy projects aligns with Kosovo's commitment to decarbonization and transitioning to a more sustainable energy system. By investing in clean energy technologies, Kosovo aims to reduce greenhouse gas emissions, improve air quality, and promote sustainable economic growth.

Furthermore, the integration of renewable energy sources not only contributes to environmental benefits but also enhances energy security. Diversifying the energy mix with renewables reduces reliance on imported energy and enhances the resilience of the energy sector. To support the transition to renewable energy, Kosovo is also focusing on policy and regulatory frameworks, attracting investments in the renewable sector, and fostering collaboration with international partners and organizations.

Overall, Kosovo's efforts in renewable energy development, including wind power plants and future plans for solar energy, demonstrate its commitment to a sustainable energy future and align with global efforts to combat climate change and promote a greener economy.



## 2. ENERGY CRISIS DURING 2022

The global energy crisis began as a result of the COVID-19 pandemic in 2021 to continue enormously way during 2022. During the year 2022, the effects of the energy crisis were felt throughout Europe. The crisis was caused by a variety of economic factors, including the rapid post-pandemic economic rebound that outpaced energy supply, and escalated into a widespread global energy crisis following the Russian invasion of Ukraine. Additionally, the start of the war in Ukraine (February 24, 2022) and the sanctions against Russia led to a big limitation in the supply of gas from Russia to European countries. As a consequence, was a significant increase in the price of gas per cubic meter in Europe. This increase then caused an enormity rise in the cost of energy production from gas-fired power plants in Europe. Therefore, the increase in gas prices in European countries throughout the year 2022 was one of the main drivers of the movement and rise in energy prices in some international markets. Average weekly energy prices during 2022 according to the Hungarian stock exchange HUPX are shown in Figure 1.

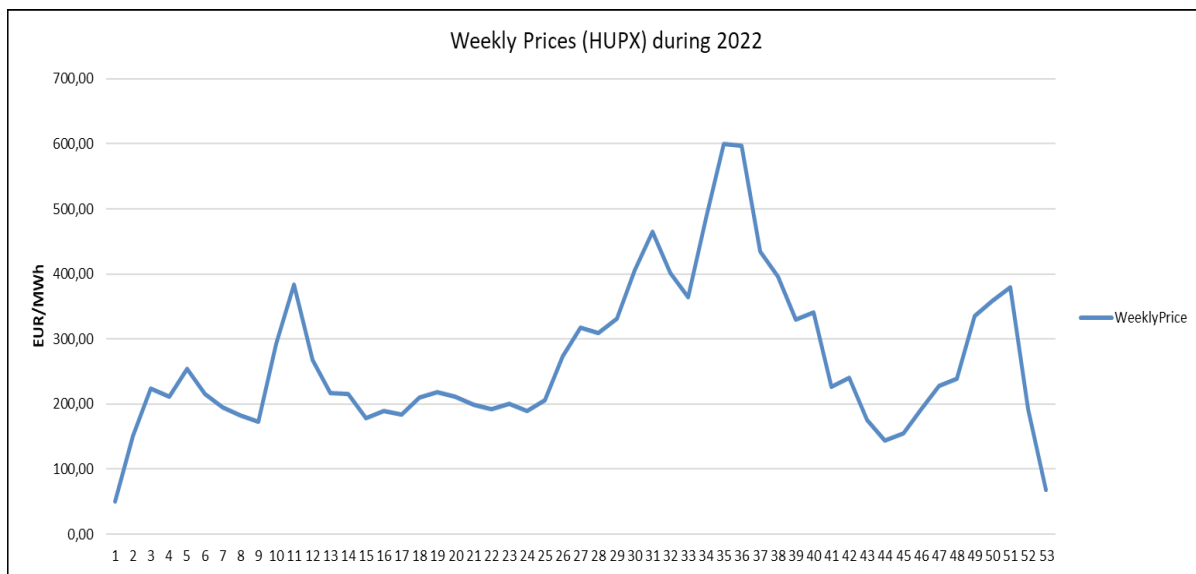


Figure 1. Average weekly energy prices during 2022 by HUPX [1]

Based on the significant and continuous movement and rise in energy prices in some of the international markets, and the need to import a portion of the energy to meet the demand for regular electricity supply, during the year 2022 Kosovo faced an energy crisis. This crisis was particularly evident during the winter season when the demand for energy was highest, while domestic production was unable to cover the entire consumption of demand of the power system. Comparing of average weekly energy prices by HUPX and by Feed-in Tariff prices (for Wind Farm Parks) during 2022 is shown as below through Figure 2 .

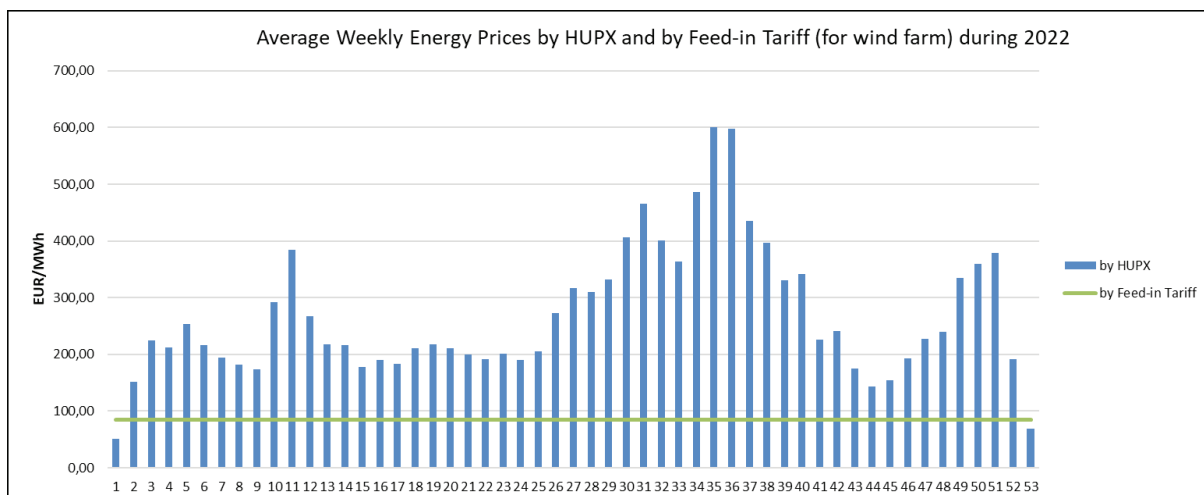


Figure 2. Average Weekly Energy Prices by HUPX and Feed-in Tariff during 2022 [2], [4]



Overall, the energy crisis in Kosovo in 2022 highlighted the urgent need for comprehensive energy planning, infrastructure development, and diversification of energy sources to ensure a reliable, affordable, and sustainable energy supply for the country.

The data from 2022 reveals that the import demand for meeting Kosovo's domestic energy needs was approximately 14.3% higher than the value of local production. This indicates a significant reliance on imported energy to fulfill the country's energy requirements. However, the high cost of imported energy has further exacerbated the situation, primarily due to the volatile and elevated prices observed in international energy markets. To visualize the dynamics of domestic energy consumption, total generation, and import in 2022, Figure 3 provides a graphical representation. This diagram illustrates the proportions and relationships between these factors, offering a comprehensive overview of the energy landscape during that year.

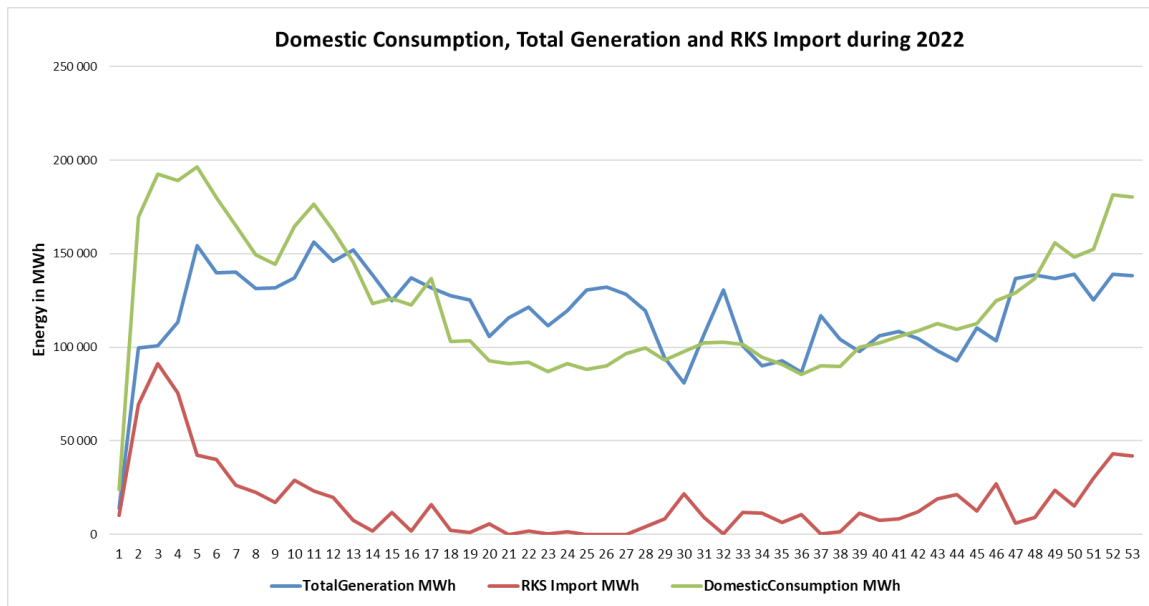


Figure 3. Domestic Consumption, Total Generation and RKS Import during 2022 [2]

The data from 2022 highlights the imbalance between domestic energy production and the demand for energy in Kosovo. The import demand for meeting internal energy needs was significantly higher, amounting to approximately 14.3% more than the value of local production. This indicates a heavy reliance on imported energy sources to bridge the energy gap and meet the country's requirements.

However, the reliance on imports came at a cost. The high and unstable price of energy in international markets worsened the situation, further straining the energy sector in Kosovo. The increased cost of imported energy added financial pressure and challenges to the energy supply chain, impacting both consumers and the overall economy. To gain a clearer understanding of the energy landscape during 2022, Figure 3 presents a diagram depicting domestic energy consumption, total generation, and import. This visual representation helps to illustrate the proportions and relationships between these factors, providing valuable insights into the energy dynamics and the import dependency of Kosovo during that period.

### 2.1. The Electricity Balance of Kosovo Power System (2022)

The majority of domestic electricity production during the year 2022 was primarily covered by thermal power plants at a rate of 81%, followed by wind farm parks at approx. 5%, while only 1.5% came from hydropower plants. The remaining portion of the energy used for domestic needs was covered by imports, which accounted for around 12.5% of the total.

The participation of energy sources in domestic production and imports for internal needs has been presented in the form of percentages. Figure 4 visually represents the participation of these sources in domestic production and imports in the form of a graph or diagram. Table 1 contains information regarding the participation of thermal power plants, wind farms, hydroelectric power plants, and imports in electricity production.





Table 1. Participation [2]

Yearly Data for 2022	Participation	
	GWh	%
TPP	5 798	80.97
WFP	363	5.07
HPP	107	1.49
RKS Import	893	12.47
Consumption	7 161	-

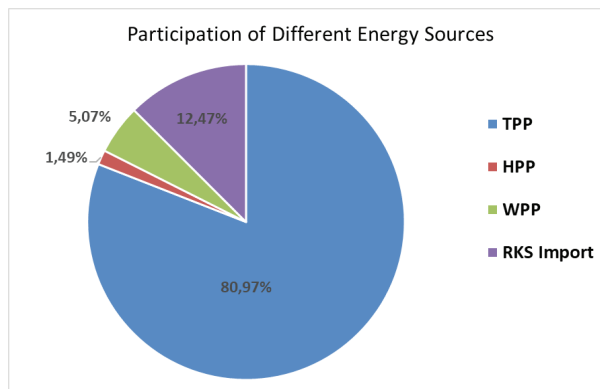


Figure 4. Participation of Sources [2]

### 3. THE CALCULATION OF THE IMPACT OF WIND FARM PARKS

#### 3.1. Calculation Methodology

The methodology for calculating the impact of wind farms on the alleviating of the energy crisis is based on the following key factors and steps:

- the total energy generation from wind farms during the specific period (2022) must be determined. This information is usually obtained from power generation reports.
- the total energy generated by the wind farm parks in megawatt-hours (MWh) during the specified period (2022) must be calculated.
- the Feed-in Tariff price for wind energy must be determined. In this case, the price according to the Feed-in Tariff in Kosovo is 85.00 EUR/MWh [4].
- it is necessary to multiply the total energy generation from the wind farm parks with the price of the Feed-in Tariff per megawatt-hour. This will then give the total revenue generated from wind power generation.
- the price of imported energy should be obtained in our case from the Hungarian Energy Exchange (HUPX) for the same period. This data can be obtained from energy market reports or exchange price lists[1].
- at the end, the financial income generated by wind energy production (calculated acc. step 4) should be compared with the cost of importing the same amount of energy based on HUPX prices. This will then provide a clear understanding of the impact of wind farms on the energy crisis, as it is estimated that wind energy production offers a more cost-effective solution compared to importing energy.

The specific calculations and data required may vary depending on the context and availability of information. Therefore, it is important to ensure the accuracy and relevance of the data used in the calculations to obtain reliable results.

Based on the above steps, the calculation of the cost of energy produced by the wind parks for 2022 according to the Feed-In Tariff prices and the calculation of the cost of imported energy according to the prices of the Hungarian stock exchange HUPX for the same time and period it is shown in below figure.

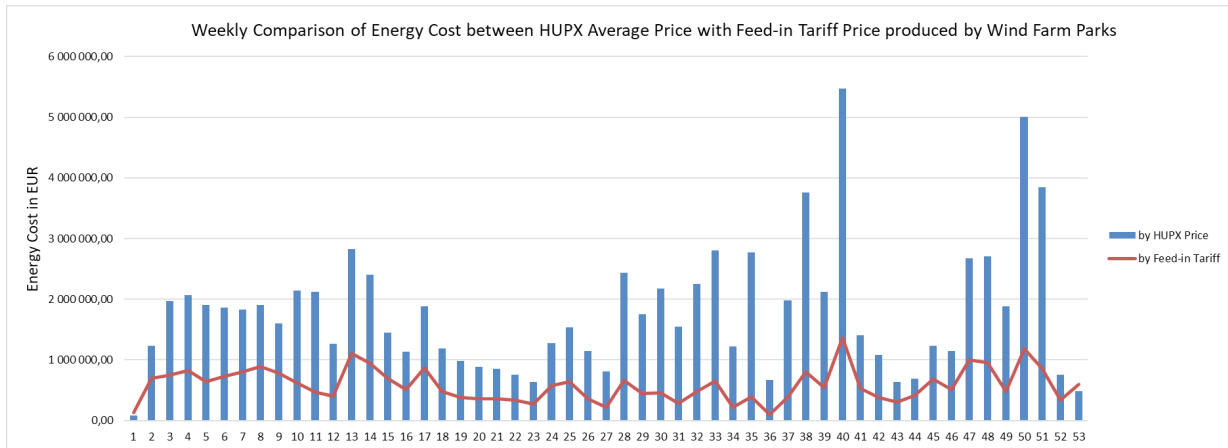


Figure 4. Weekly Comparison of Energy Cost between HUPX Average Price with Feed-in Tariff Price produced by Wind Farm Parks during 2022

By comparing the data based on costs per MWh, it is evident the significant positive impact that wind parks have had during the energy crisis in Kosovo in 2022, as well as the reduction in the cost of imported energy. The methodology used to calculate the cost reveals that the total annual energy produced by the wind farm parks is around twice as cheap compared to purchasing the same amount of energy from international markets, such as HUPX.

Additionally, this cost comparison highlights the cost-effectiveness and economic benefits of relying on wind energy from domestic sources, such as wind farm parks, rather than heavily depending on imported energy. By leveraging the renewable energy potential of wind parks, Kosovo can enhance its energy security, reduce reliance on expensive imports, and contribute to a more sustainable and self-sufficient energy system. The positive impact of wind parks extends beyond the financial aspect, as they also contribute to environmental preservation by reducing greenhouse gas emissions and promoting clean energy generation.

#### 4. MITIGATION OF THE ENERGY CRISIS IN KOSOVO BY THE WIND PARKS

The wind farm parks in Kosovo played a significant role in mitigating the energy crisis by contributing to the electricity generation and reducing the dependency on imported energy. With a total installed capacity of 138 MW, these wind farms provided a substantial amount of clean and renewable energy to the power system. During the energy crisis, when the demand for electricity was high and domestic production was insufficient, the wind farm parks helped bridge the supply-demand gap. By harnessing the power of wind, which is a free and abundant resource, the cost of generating electricity from wind energy was relatively lower compared to importing energy from international markets

Table 2. Contribution of Wind Parks to reducing of import costs during 2022

Energy Production by WFPs in 2022	Income of WFPs	Cost of Imports based on HUPX's prices (if there were no Wind Farm Parks)	Savings and Impact
	a	b	c=b-a
GWh	M€uro	M€uro	M€uro
363	30.85	92.71	61.86

The wind farm parks played a crucial role in mitigating the energy crisis in Kosovo. Here are some ways in which they contributed to alleviating the crisis:

- Increased local energy generation: The wind farm parks significantly increased the local energy generation capacity in Kosovo. By harnessing the power of wind, these parks produced a substantial amount of electricity, reducing the dependency on imported energy sources.
- Diversification of energy sources: Prior to the establishment of wind farm parks, Kosovo relied heavily on imported energy, which made the country vulnerable to supply disruptions and price fluctuations. The introduction of wind energy as a domestic source diversified the energy mix, reducing reliance on imports and enhancing energy security.



- **Cost-effective energy production:** Wind energy production from the wind farm parks proved to be a cost-effective solution compared to importing energy from international markets. The methodology used to calculate costs demonstrated that the total annual energy produced by the wind farm parks was significantly cheaper than purchasing the same amount of energy from abroad.
- **Reduced pressure on the power system:** The additional energy generated by wind farm parks helped alleviate the strain on the power system during times of high demand, such as the winter season. By supplementing the local energy supply, the parks contributed to meeting the energy needs of the population and businesses, reducing the risk of blackouts or energy shortages.
- **Environmental benefits:** Wind energy is a clean and renewable source of power, producing minimal greenhouse gas emissions. The operation of wind farm parks in Kosovo contributed to reducing the carbon footprint and promoting sustainable development.

Overall, the wind farm parks played a significant role in mitigating the energy crisis in Kosovo by increasing local energy generation, diversifying energy sources, reducing costs, relieving pressure on the power system, and providing environmental benefits.

## 5. CONCLUSION

In conclusion, the wind farm parks in Kosovo played a crucial role in mitigating the energy crisis that occurred in the country. Their contribution was significant in several aspects. Firstly, the wind farm parks increased the local energy supply, reducing the reliance on imported energy and improving energy self-sufficiency. Secondly, they provided a stable and reliable source of power, helping to alleviate the uncertainties and fluctuations associated with imported energy. Additionally, wind energy production proved to be cost-effective, offering a cheaper alternative to purchasing energy from international markets. The presence of wind farm parks also reduced the strain on the power system, particularly during times of high demand, and contributed to a more environmentally sustainable energy sector by reducing greenhouse gas emissions. Overall, the wind farm parks played a pivotal role in ensuring a reliable, affordable, and sustainable energy supply for Kosovo during the energy crisis. Additionally, the energy crisis in Kosovo in 2022 brought attention to the following aspects:

- **Energy Efficiency Measures:** The crisis underscored the importance of implementing energy efficiency measures across various sectors. Improving energy efficiency in buildings, industries, and transportation can help reduce energy consumption, decrease dependence on imports, and mitigate the impact of future energy crises.
- **Increasing of Renewable Energy Investments:** The need to diversify the energy mix and reduce reliance on imported energy sources was highlighted. Kosovo has significant potential for renewable energy, particularly in wind, solar, and less on hydropower. Encouraging investments in renewable energy infrastructure can enhance energy security, reduce emissions, and create opportunities for local economic development.
- **Energy Storage Solutions:** The energy crisis emphasized the importance of developing energy storage systems. Energy storage technologies, such as batteries or pumped hydro storage, can help store excess energy during times of high production and release it during peak demand, providing stability to the energy grid and reducing the need for imported energy.
- **Cross-Border Energy Cooperation:** The crisis highlighted the potential benefits of regional energy cooperation and integration. Collaborating with neighbouring countries in energy projects, establishing interconnections, and sharing energy resources can enhance energy security, increase resilience, and create opportunities for joint infrastructure development.
- **Public Awareness and Engagement:** The energy crisis raised awareness among the public about the importance of energy conservation, responsible energy consumption, and the need for a sustainable energy future. It created an opportunity for engaging citizens, raising their energy literacy, and encouraging their participation in energy-saving practices and renewable energy initiatives.

Addressing these aspects and implementing comprehensive energy policies and strategies can help Kosovo build a resilient and sustainable energy sector, reduce vulnerability to future energy crises, and pave the way for a greener and more secure energy future.

In summary, the wind farm parks in Kosovo played a vital role in mitigating the energy crisis by increasing energy supply, improving self-sufficiency, providing a stable and reliable energy source, reducing costs, relieving strain on the power system, and delivering environmental benefits.



Poster Presentation: The Impact of Wind Farm Parks on Mitigation of Energy Crisis (2022) in Kosovo's Power System

### 6. BIBLIOGRAPHY

- [1] Hungarian Power Exchange (HUPX) – Average energy data prices, 2022
- [2] Data for domestic consumption, domestic production and RKS Import (for the needs of Kosovo), Transmission, System and Market Operator – KOSTT, 2022
- [3] Kosovo's Energy Strategy, Ministry of Economy, Government of Republic of Kosovo, 2023
- [4] Energy Regulatory Office, Home | ZRRE (ero-ks.org), 2023
- [5] Transmission Network Development Plan, KOSTT, 2023 - 2032
- [6] Annual Energy Balance, KOSTT, 2022
- [7] Kosovo Agency of Statistics, <https://ask.rks-gov.net/en/kosovo-agency-of-statistics/add-news/statistical-yearbook-of-the-republic-of-kosovo-2022>



# Prevention of High Voltage Network Disturbance Propagation By On-Line Monitoring and Diagnostic of Relay Protection

[Alexey.nebera@kontron.sl](mailto:Alexey.nebera@kontron.sl)

**ALEXEY NEBERA\***, JANEZ ZAKONJSJEK

*Kontron Smart Energy*

**PROF. BOŠTJAN POLAJŽER**

*University of Maribor, FERi Gorazd Hrovat*

**Slovenia**

## SUMMARY

Proper operation of relay protection is a necessary precondition for Power system reliability. Malfunction of relay protection is one of the main contributors to extended network outages. Protection engineers make a lot of effort to establish and maintain sensitivity, selectivity and reliability of protection systems, but due to the big number of substations and protection devices each of them can be checked and serviced only once in a few years. Until then almost any failure in a protection device and its external circuits usually remains hidden and pose a risk of malfunction and bigger network disturbance. Meanwhile modern numerical relays provide variety of communication possibilities and monitoring information, but most of this data, are still not regularly collected and analyzed in the Power systems.

Authors are describing a new on-line protection monitoring and diagnostic system, a real time simulation-based testbed for its testing in high voltage networks and the results of the testing.

## KEYWORDS

Power system – Relay protection – Mis operation – Malfunction – Monitoring – Diagnostics



Poster Presentation: Prevention of High Voltage Network Disturbance Propagation By On-Line Monitoring and Diagnostic of Relay Protection

### 1. INTRODUCTION

After a whole lot of scientific, engineering and organization efforts to develop, design, install and maintain relay protection in power systems, it is very important to get an objective measure of its actual performance in real-life conditions. This measure can be derived from accurate statistics about its proper operations and malfunctions. One of the best sources about relay protection performance in large interconnected power systems can be found in NERC "State of reliability" reports, published each year. As stated in 2022 report [1]: "When designed and implemented properly, automated tools can enhance the reliable and secure use of new technologies and concepts that become available. On the other hand, maintaining, prudently replacing, and upgrading bulk power system control system assets can lead to protection and control system Misoperation. Misoperation can initiate more frequent and/or more widespread outages."

As can be seen on the Figure 1 below, an average rate of protection misoperations for major US power system lies mostly in the range of 6-8% and in some cases can reach 11% of total amount of operations. This is quite a substantial amount of protection malfunctioning which requires further analysis. Main causes of protection misoperation in 2021 with corresponding percentage are shown on the Figure 2. As stated in the report, the top causes of misoperations over the past five years have consistently been Incorrect Settings and Relay Failures/Malfunctions which reflects both the growing complexity of modern power systems and microprocessor based protection IEDs.

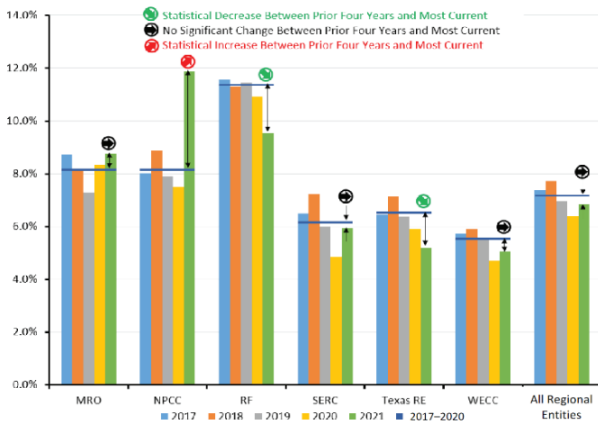


Figure 1: Changes and trends in annual Misoperation rate cause code

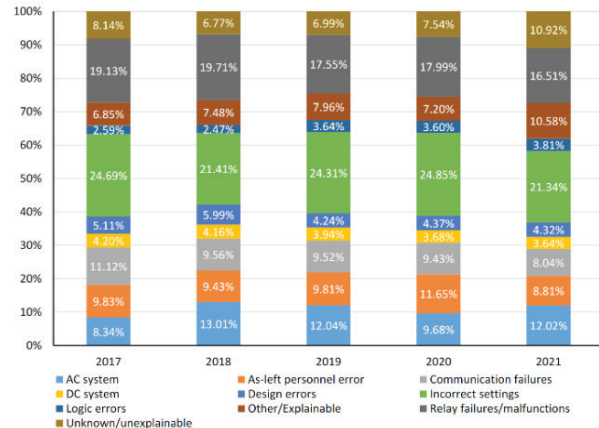


Figure 2: Misoperation by cause code

During misoperation analysis it can be also noted that Human error is one of potential causes for misoperations. Human error is involved in about 40% of all misoperations and manifests itself in:

- As-left personnel error – test switches left open, wiring errors not associated with incorrect drawings, carrier grounds left in place, settings placed in the wrong relay, or settings left in the relay that do not match engineering intended and approved settings
- Design errors – incorrect schematics or equipment application
- Incorrect settings – inaccurate or insufficient modeling, calculation errors
- Logic errors – programming errors in custom user logic, wrong assignment or mapping of signals.

Thus, it can be seen that growing complexity of power systems and their protection requires more efforts to improve reliability and avoid extended outages due to protection malfunctioning. On the other hand, power system personnel in real life are always limited in time and can itself be a source of potential reliability threats. In the meantime, modern protection IEDs are able to provide a lot of measurement and diagnostic information which is not used to a full extent nowadays since it's just impossible to do manually without automated monitoring and analysis systems.

### 2. AUTOMATED PROTECTION MONITORING AND DIAGNOSTICS

A distinctive aspect of relay protection is a big average time between operations – from none to few operations a year depending on equipment type and voltage level. This gives us enough time to discover potential failure and act upon it, if there is a regular information exchange between protection devices and protection engineers' office.

Let's consider the protection misoperation causes shown above, along with data allowing to identify the problem.





Poster Presentation: Prevention of High Voltage Network Disturbance Propagation By On-Line Monitoring and Diagnostic of Relay Protection

**Table I:** Information available to identify protection problems

Misoperation cause	Available information	Ways of retrieval
AC system	Analog measurements of voltage and current sensed by protection IEDs. Measurements from more than one IED located on the same bay or busbar can be compared to identify significant mismatch.	<ol style="list-style-type: none"> <li>1) Live RMS values via IEC 60870-5-103, 104 or IEC 61850-8-1 MMS messages</li> <li>2) Live sampled values via IEC 61850-9-2 or 61869-9 streams</li> <li>3) Sampled values in disturbance record files</li> </ol>
As-left personnel error	Protection IED configuration info: <ul style="list-style-type: none"> <li>• Protection functions state (on/off)</li> <li>• Operational switching key position on the protection cubicle or panel</li> </ul> Analog measurements of voltage and current Approved settings vs actual protection configuration files comparison	Discrete signals via IEC protocols or relay contacts As for AC system above <ol style="list-style-type: none"> <li>1) File retrieval by IEC 61850-8-1 MMS messages</li> <li>2) File retrieval by a protection IED manufacturer engineering software</li> </ol>
Communication failures	Communication channels state	Discrete signals via IEC protocols
DC System	Availability of DC supply	Discrete signals via IEC protocols or relay contacts
Design errors	Disturbance record files including analog as well as protection start and trip signals	File retrieval by IEC 61850-8-1 MMS messages
Incorrect settings	Approved settings vs actual protection configuration files comparison Disturbance record files including analog as well as protection start and trip signals	<ol style="list-style-type: none"> <li>1) File retrieval by IEC 61850-8-1 MMS messages</li> <li>2) File retrieval by a protection IED manufacturer engineering software</li> </ol>
Logic errors	Disturbance record files including analog as well as protection start and trip signals	File retrieval by IEC 61850-8-1 MMS messages
Relay failures/malfunctions	Self-diagnostic signals	Discrete signals via IEC protocols
Other/Explainable		
Unknown/Unexplainable		

As can be seen from the table above, most of device and its circuits failures can be explicitly detected based on information available in modern protection IEDs. It should be noted that partially monitoring functions can be implemented even for electromechanical devices as long as disturbance records in a digital form are regularly available from standalone fault recorders.

Other problem types require additional consideration:

- Design errors, Incorrect settings and Logic errors are usually hardly identifiable in a normal state of a power system just by looking on any information provided by a protection IED. However, they can be detected by studying protection start signals during disturbances. As there are more protection starting events than actual tripping, start signals rarely got carefully studied by protection engineers<sup>1</sup> and often not configured in disturbance records. More dangerous errors will manifest themselves in starting faults or excessive starts, thus providing a valuable insight and possibility to prevent protection misoperation<sup>2</sup>.
- Unknown/Unexplainable causes – the very existence of this group reflects a lack of information, as well as inevitable time and resource limitations of protection departments with low automated ways of disturbance information gathering and analysis. Authors believe that properly implemented protection monitoring and diagnostic system will allow to significantly decrease amount of unknown causes of protection malfunctions.

<sup>1</sup> It is interesting to note that the definition of protection malfunction or misoperation is only related to protection tripping events, thus protection start signals not followed by a trip are much less investigated and reported.

<sup>2</sup> Evaluation of start signals for a protection with many stages require accurate modelling of a power system disturbances as well as protection functional and logical blocks



**Poster Presentation:** Prevention of High Voltage Network Disturbance Propagation By On-Line Monitoring and Diagnostic of Relay Protection

Besides the task of information extraction from remote protection devices and other potential data sources like standalone fault recorders, protection manufacturers engineering software and SCADA systems are additional important aspects to be considered.

To extract the full potential of protection monitoring and diagnostic system (PMD), maximum of usual routine analysis operations should be done automatically, including:

- synchronization and stitching of disturbance records from various devices and/or periods of the disturbance (fault and auto-reclosing)

- fault location and fault type determination

- evaluation of actual protection operation based on network topology and event tree analysis

- analysis of self-diagnostic signals and evaluation of hardware and software IED state and conditions of power supply, secondary circuits and communication networks

- protection configuration checking by automatic comparison of actual settings (a file received from an IED directly or via a manufacturers engineering software workstation) with a reference settings file initially prepared for configuration

Ability of consistent automated analysis provision for different types of protection device manufacturers, versions etc. relies upon a careful information model of underlying power system and protection devices with all their circuits, functions and signals. To minimize initial configuration efforts as well as subsequent updates of PMD information model it is worth to implement an integration functions with Network Model Management or SCADA/EMS/DMS systems. This exchange needs to support IEC Common Information Model (CIM) standards to allow automated import of power system topology and parameters to PMD. On the other hand, protection IED data retrieval should support IEC 61850 standard series as the most widely used now and in the observable future. Since neither CIM nor 61850 fully cover all the details of protection information modelling, PMD needs to map both standard worlds and maintain additional information extensions to implement its functions.

An automated protection monitoring and diagnostics system implementing the features described above has been developed by Kontron Smart Energy and tested together with Slovenian TSO ELES and Maribor University.

### 3. TESTING OF PMD

The PMD system was tested during March 2023 at the Faculty of Electrical Engineering and Computer Science (FERI) of Maribor University on the RTDS (Real Time Digital Simulator) testbed. A 220-kV power line between substations Podlog (Slovenia) and Obersielach (Austria) was simulated together with corresponding equivalent impedances and generating facilities on both line ends. The whole testbed as shown on Figure 3, included two main parts:

- 1) Substation level, located in Maribor university (FERI) where part of ELES high voltage network is represented by the RTDS simulator.
- 2) Control center level represented by Kontron Smart Energy infrastructure in Kranj.

Two monitored protection devices IED 1 and IED 2 on Figure 5 represented by Siemens 7SD522 line current differential and distance protection were connected over current and voltage amplifiers as well as binary signals (tripping and breaker closing commands) transducers to the RTDS.

Protection IEDs are controlling circuit breakers on both ends of the simulated power line and have two communication channels:

- to a local computer with Siemens DIGSI engineering software used to configure and control these IEDs
- to a PMD server in Kontron's Smart Energy cloud infrastructure located on the control center level.

A number of different system operating conditions together with different fault types and impedances within and outside of protected power line has been simulated in real time, which caused corresponding operation of protection IEDs.

During the testing an automated PMD data retrieval via IEC 61850-8-1 as well as analysis functions listed above were confirmed to be successfully working.



Poster Presentation: Prevention of High Voltage Network Disturbance Propagation By On-Line Monitoring and Diagnostic of Relay Protection

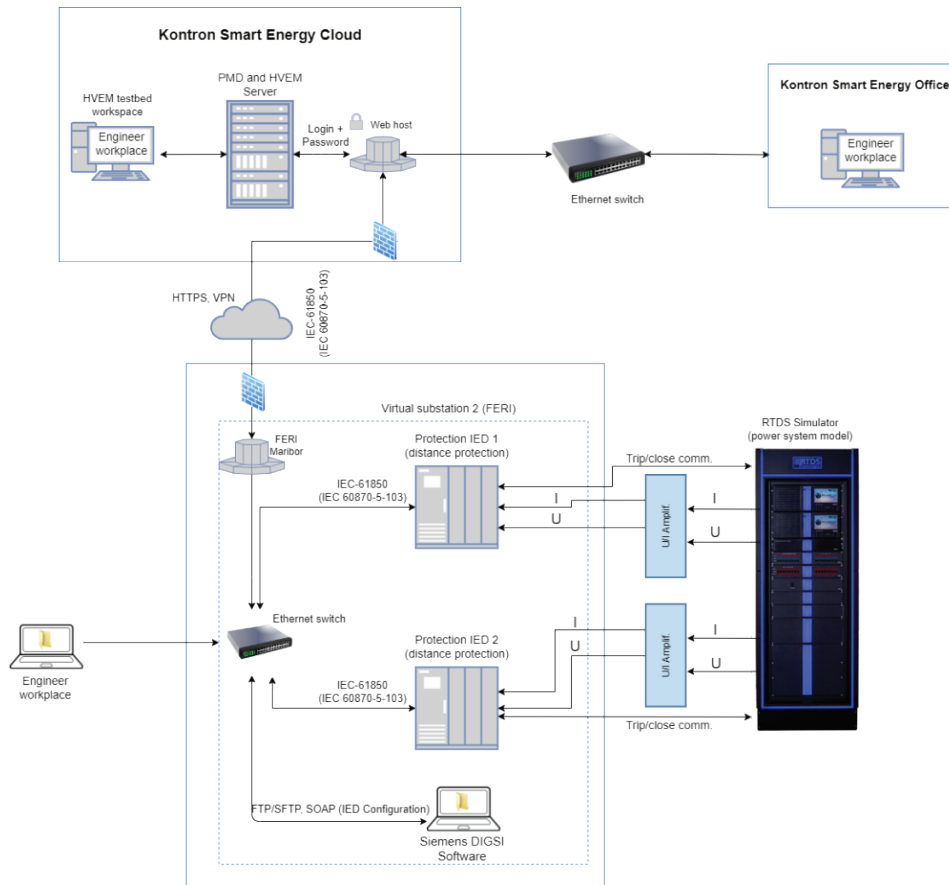


Figure 3: PMD testbed architecture

It is worth to note that successful operation of relay protection in isolating a fault in power system is only possible in conjunction with associated high voltage equipment, namely instrument transformers and circuit breakers. Problems in instrument transformers and their secondary circuits may cause inaccuracies or inability of relay protection to sense a fault, while failures of circuit breakers lead to the fault extension in time and geography.

That is why a follow-up testing was implemented, based on disturbance records gathered on the Maribor FERI testbed and devoted to a possibility of circuit breaker (CB) monitoring.

As shown on Figure 4, various parts of a fault clearing time during a CB opening can be estimated based on a disturbance record analog and discrete signals if they are properly configured. The most important ones are 1) the arcing time directly influencing the CB commutation life and 2) the inherent opening time reflecting the state of CB drive.

## 4. CONCLUSION AND FUTURE WORK

After detailed analysis of all available results is possible to conclude, that application of automated protection monitoring and diagnostics system along with high voltage equipment monitoring functions would contribute to more efficient work of TSO/DSO specialists. Some of the findings are listed below:

- 1) Automatic collection of disturbance records within a very short time after a certain event (fault) occurred in the observed power system. It is possible to automatically receive disturbance information in matter of minutes, when all disturbance records, related to the same event, can be collected from different substations within the PMD system and prepared for further automatic analysis. Manual activities as used today may require for this work many hours or even days.
- 2) Initial analysis of disturbance records from several involved substations and preparation of basic report may take by PMD system between 10 minutes up to a couple of hours, when a big number of power facilities is included. Manual work, as performed today, takes usually at least few hours for simple events and up to couple of days for more complex faults.



Poster Presentation: Prevention of High Voltage Network Disturbance Propagation By On-Line Monitoring and Diagnostic of Relay Protection

- 3) ETA (Event Tree Analysis) within PMD system may take in most cases half an hour for rather complex event but may need much shorter time for single fault in power system. Such analysis may take even a couple of days when competent specialist needs to make it manually.
- 4) Automatic collection of binary signals, related to self-supervision of protection IEDs contributes definitely to higher availability of complete secondary system as well to its more reliable operation.
- 5) General practice in current situation is to manually download and analyse only disturbance records from IEDs which reacted to certain events by a tripping command. This is related to very high work load in protection departments which makes it practically impossible to study not only tripped IEDs, but also IEDs which have started but not tripped due to their time parameters. Implementation of the PMD system makes it possible to download disturbance records and study also the responses of IEDs which initiated only starting signals.
- 6) Estimation of circuit breaker time components during the opening (and closing if possible) operation, including arcing time or phase-to-phase time difference, allows evaluate the impact of operations on the circuit breaker lifetime.
- 7) Both protection monitoring and CB as well as instrument transformer monitoring functions develop a solid base for the potential change towards Condition Based Maintenance with corresponding economic benefits for power system companies.

Future development of the presented system can be considered in the next directions:

- Pilot project implementation on the high voltage substations to:
  - estimate the real-life system performance
  - gather detailed statistics of protection operations and technical state changes
  - develop and test an optimal system architecture reflecting cybersecurity needs.
- Functional extension including more detailed:
  - protection starting signal analysis with corresponding modelling
  - monitoring of circuit breakers and instrument transformers based on real time measurements in addition to disturbance records
  - secondary equipment monitoring, including the collection of self-diagnostic signals from communication equipment involved in protection operations in addition to the signals from protection IEDs.

## BIBLIOGRAPHY

- [1] NERC: State of Reliability, August 2022. Assessment of 2021 Bulk Power System Performance. July 2022
- [2] The Risk of Hidden Failures to the United States Electrical Grid and Potential for Mitigation. Arthur K. Barnes, Adam Mate, and Jose E. Tabarez. IEEE/PES 53RD North American Power Symposium, November 2021.
- [3] Fukui C., Kawakami J. An expert system for fault section estimation using information from protective relaying and circuit breakers // IEEE Trans. on Power Delivery. Vol. 1. Oct. 1986. P. 83-90.
- [4] Kezunovic M., Spasojevic P., Fromen C.W., Sevcik D. An expert system for substation event analysis // IEEE Trans. on Power Delivery. Vol. 8. Oct. 1993. P. 1942-1949.
- [5] D. C. Elizondo et al. Hidden Failures in Protection Systems and their Impact on Wide-Area Disturbances. In Proc. of the 2001 IEEE Power Engineering Society Winter Meeting, Feb. 2001.
- [6] Informational analysis of processes in electrical power systems / Y. Liamets, Y. Romanov, D. Zinoviev, J. Zakonjšek, G. Nudelman // Proc. 15th Int. Conf. Power System Protection. – Bled, Slovenia, 2006. – P. 87-96.
- [7] IEEE Power System Relaying Committee WGK15, Centralized Substation Protection and Control, December 2015.
- [8] Lyamets Yu.Ya., Efimov E.B., Nudelman G.S., Zakonshek Ya. / Principle of information perfection of a relay protection // Elektrotehnika (Russian Electrical Engineering). 2001. # 2. P. 12-17.
- [9] Standard PRC-004-6 — Protection System Misoperation Identification and Correction. NERC
- [10] BH K/O CIGRE u elektronskoj formi na e-mail adresu (office@bhkcigre.ba). Referat se dostavlja u MS Word (.doc) formatu.
- [11] Zhang N., Kezunovic M. / Verifying the Protection System Operation Using an Advanced Fault Analysis Tool Combined with the Event Tree Analysis // Northern American Symposium (NAPS), 2004.
- [12] S. H. Horowitz et al. Boosting Immunity to Blackouts. IEEE Power Energy Mag., 1(5):47-53, Sep. 2003 pages after title page must start from this line, i.e. 1" (2.5 cm) margin from the top (Times or Helvetica, size 11 or 12). Pages will be automatically numbered.



# A Novel Method for Short Circuit Calculation

giorgi.arziani@parvusgroup.ge

GIORGI ARZIANI\*, NANA TURKIA, TEMUR PIPIA, VAKHTANG BANTSADZE, TEONA ELIZARASHVILI

Parvus Consulting, Georgian Technical University

Georgia

## SUMMARY

A wide range of software tools is available worldwide for modeling and simulating electrical power systems. These software programs are often multi-domain, enabling comprehensive analysis of power systems from various perspectives within a single environment. They encompass several common study areas, such as load flow, short circuits, RMS (Root Mean Square), EMT (Electromagnetic Transients), power quality, quasi-dynamics, and many others. While these software tools are highly sophisticated, a significant limitation is the lack of flexibility in their short circuit calculation modules.

Typically, most of the existing software tools can only analyze a single type of short circuit at a time, without the ability to handle simultaneous and diverse types of short circuits. The complexity and computational resources required for investigating multiple, especially asymmetric, short circuits occurring at different nodes exceed the capabilities of these tools.

To address this gap, the article proposes a novel method for calculating the parameters of an electrical system's emergency mode in the event of multiple simultaneous faults, including both series and shunt faults. The proposed approach is designed to handle various accidents that can be identical or completely different in nature. It introduces unified equations that establish connections between emergency mode parameters when different types of faults occur. This concept presented in the article enables the calculation of both symmetrical and asymmetrical short circuits.

By adopting this new method, power system analysts and engineers gain the capability to accurately determine the parameters of emergency operation during multiple fault scenarios. Whether the faults are similar or distinct, the proposed approach provides a systematic framework to compute the relevant parameters. It eliminates the limitation of existing software tools and allows for the analysis of complex situations involving simultaneous and diverse short circuits.

With the ability to handle a broader range of short circuit scenarios, engineers can better assess the performance and stability of electrical power systems. This methodology opens up opportunities for more comprehensive studies, enabling the evaluation of system behavior under various fault conditions. The proposed approach enhances the understanding of emergency mode operation and contributes to the development of more reliable and resilient power systems.

## KEYWORDS

Short circuit calculation, asymmetric faults, symmetrical components.



## INTRODUCTION

In order to calculate the parameters of asymmetric electrical modes, authors developed a methodology based on the principles outlined in [1]. Approach involved implementing a direct current model, where single-phase transverse faults were represented as ideal current sources with magnitudes equal to the corresponding short-circuit currents. Similarly, single-phase series faults were represented as ideal voltage sources with magnitudes equal to the voltage at the points of phase break.

To determine the values of these currents, the authors employed equations that incorporated coefficients obtained through measurements of the relevant parameters in the initial mode of the direct current model. This approach made possible to maintain the circuit representation unchanged when considering different combinations of single-phase faults. This was achieved due to the infinitely large internal resistance of the ideal current sources and the zero internal resistance of the voltage sources.

The authors developed a method for calculating simultaneous asymmetrical faults, which includes single-phase and two-phase faults, entailing phase-to-phase faults. This approach utilizes matrix algebra and topological analysis methods. To ensure uniform calculations, three-phase faults were represented as a superposition of single-phase faults. This technique allowed for consistent boundary conditions and unchanged circuit parameters to be applied to any type of fault.

Unified equations connecting the active parameters of electric mode are given below.

$$\begin{bmatrix} MY_d M^T & M Y_d \\ Y_d M^T & Y_d \end{bmatrix} \begin{bmatrix} U_{nod} \\ E_{br} \end{bmatrix} = \begin{bmatrix} I_{nod} \\ I_{br} \end{bmatrix} \quad \text{otherwise} \quad \begin{matrix} M Y_d M^T U_{nod} + & M Y_d E_{br} = & I_{nod} \\ Y_d M^T U_{nod} + & Y_d E_{br} = & I_{br} \end{matrix} \quad (1)$$

Where:  $U_{nod}$ ,  $I_{nod}$  – matrixes of nodal voltages and currents,  $E_{br}$  – matrix of voltage source within the branches,  $I_{br}$  – matrix of currents in the branches,  $Y_d$  – diagonal matrix of conductivity of branches,  $M$  – the first matrix of incidence for the initial scheme,  $E$  – identity matrix order  $K$ , where  $K$  – is the number of branches in the initial circuit.

$$M' Y_d M'^T = \begin{bmatrix} M \\ E \end{bmatrix} Y_d [M^T E^T] = \begin{bmatrix} M Y_d M^T & M Y_d \\ Y_d M^T & Y_d \end{bmatrix}$$

The system of equations (1) connects 4 basic parameters of the electric mode: node voltages, branch voltages, node currents and branch currents. Based on known and unknown parameters, a system of equations of the corresponding modes is established.

Therefore, with the help of these equations we can describe both normal and emergency modes. For instance, the case when only nodal currents are known, and we are looking for nodal voltage, is a particular case of unified equations, the so-called nodal voltage equation.

$$[M Y_d M^T] U_{nod} = I_{nod}$$

Where  $Y_{nod} = M Y_d M^T$  – matrix of proper and reciprocal conduction of the nodes of a scheme.

To describe emergency modes (short circuits and open-phase faults) we need to transform the general equations (1) in a way that mode parameters to be found are node currents  $I_{nod}$  and voltages included in the branches  $E_{br}$ , and parameters which are given are node voltages  $U_{nod}$  and currents in the branches  $I_{br}$ . Consequently, we will get a system of equation, describing the electrical regime at optional combination of series and shunt faults:

$$\begin{matrix} [M Y_d M^T]^{-1} I_{nod} - [M Y_d M^T]^{-1} [M Y_d] E_{br} = U_{nod} \\ [Y_d M^T] [M Y_d M^T]^{-1} I_{nod} + [Y_d - [Y_d M^T] [M Y_d M^T]^{-1} [M Y_d]] E_{br} = I_{br}, \end{matrix}$$

in a particular case, when only transverse fault occurs, the equations (inverse to the nodal voltages equations) take the form:  $U_{nod} = [M Y_d M^T]^{-1} I_{nod} = Z_{nod} I_{nod}$

where  $Z_{nod} = [M Y_d M^T]^{-1}$  – matrix of proper and reciprocal impedance of the nodes of a scheme.

$I_{nod}$  vector-matrix of nodal currents, the unknown currents of the short circuit.

To carry out calculations of the mode parameters at simultaneous short circuits, it is convenient to use not the equation of nodal voltages, but its inverse form, since the elements of the matrix of nodal resistances (intrinsic and mutual resistances of the nodes), calculated by inverting the nodal conductance matrix, contain information about the entire circuit and do not depend on the number of simultaneous faults.





Based on the fact that symmetric components of asymmetric emergency current circulate within just the circuits of the respective sequence, the dependences between the currents and voltages existing within the symmetric systems are also fair within the separate sequence circuits. Accordingly, the relationships between the currents and voltages in the individual circuits of the sequence, provided that the currents of the special phases (in the case of a single-phase short circuit) are brought to the phase A through the shift operator, can be described using the node equations. So, for the currents and voltages in all sequence circuits, in case of one-phase short circuit, the following matrix equations can be written:

$$\begin{bmatrix} Z'_{11} & Z'_{1i} & Z'_{1j} & Z'_{1k} & Z'_{1n} \\ Z'_{i1} & Z'_{ii} & Z'_{ij} & Z'_{ik} & Z'_{in} \\ Z'_{j1} & Z'_{ji} & Z'_{jj} & Z'_{jk} & Z'_{jn} \\ Z'_{k1} & Z'_{ki} & Z'_{kj} & Z'_{kk} & Z'_{kn} \\ Z'_{n1} & Z'_{ni} & Z'_{nj} & Z'_{nk} & Z'_{nn} \end{bmatrix} \cdot \begin{bmatrix} 0 \\ I'_{iA} \\ aI'_{jB} \\ a^2 I'_{kC} \\ 0 \end{bmatrix} = \begin{bmatrix} U'_1 \\ U_{iA} - U'_{iA} \\ aU_{jB} - aU'_{jB} \\ a^2 U_{kC} - a^2 U'_{kC} \\ U'_n \end{bmatrix}; \quad (2)$$

$$\begin{bmatrix} Z''_{11} & Z''_{1i} & Z''_{1j} & Z''_{1k} & Z''_{1n} \\ Z''_{i1} & Z''_{ii} & Z''_{ij} & Z''_{ik} & Z''_{in} \\ Z''_{j1} & Z''_{ji} & Z''_{jj} & Z''_{jk} & Z''_{jn} \\ Z''_{k1} & Z''_{ki} & Z''_{kj} & Z''_{kk} & Z''_{kn} \\ Z''_{n1} & Z''_{ni} & Z''_{nj} & Z''_{nk} & Z''_{nn} \end{bmatrix} \cdot \begin{bmatrix} 0 \\ I''_{iA} \\ a^2 I''_{jB} \\ aI''_{kC} \\ 0 \end{bmatrix} = \begin{bmatrix} U''_1 \\ -U''_{iA} \\ -a^2 U''_{jB} \\ -aU''_{kC} \\ U''_n \end{bmatrix}$$

$$\begin{bmatrix} Z^0_{11} & Z^0_{1i} & Z^0_{1j} & Z^0_{1k} & Z^0_{1n} \\ Z^0_{i1} & Z^0_{ii} & Z^0_{ij} & Z^0_{ik} & Z^0_{in} \\ Z^0_{j1} & Z^0_{ji} & Z^0_{jj} & Z^0_{jk} & Z^0_{jn} \\ Z^0_{k1} & Z^0_{ki} & Z^0_{kj} & Z^0_{kk} & Z^0_{kn} \\ Z^0_{n1} & Z^0_{ni} & Z^0_{nj} & Z^0_{nk} & Z^0_{nn} \end{bmatrix} \cdot \begin{bmatrix} 0 \\ I^0_{iA} \\ I^0_{jB} \\ I^0_{kC} \\ 0 \end{bmatrix} = \begin{bmatrix} U^0_1 \\ -U^0_{iA} \\ -U^0_{jB} \\ -U^0_{kC} \\ U^0_n \end{bmatrix}$$

In this case when the phase A is damaged in node i and the phase B - in node j and phase C - in node K. Matrix elements in the equations (2) are the matrix elements of intrinsic and mutual resistances within the circuits of positive, negative and zero sequence.

As a result of multiplying the matrixes in the equation (2), the equation interconnecting emergency currents and voltages within the circuits of three components is obtained:

$$\begin{cases} Z'_{ii} I'_{iA} + Z'_{ij} a I'_{jB} + Z'_{ik} a^2 I'_{kC} = U_{iA} - U'_{iA} \\ Z'_{ji} I'_{iA} + Z'_{jj} a I'_{jB} + Z'_{jk} a^2 I'_{kC} = a U_{jB} - a U'_{jB} \\ Z'_{ki} I'_{iA} + Z'_{kj} a I'_{jB} + Z'_{kk} a^2 I'_{kC} = a^2 U_{kC} - a^2 U'_{kC} \end{cases}$$

From the mentioned equations the second will be multiplied by a2, and the third - by a:

$$\begin{cases} Z'_{ii} I'_{iA} + Z'_{ij} a I'_{jB} + Z'_{ik} a^2 I'_{kC} = U_{iA} - U'_{iA} \\ Z'_{ji} I'_{iA} a^2 + Z'_{jj} I'_{jB} + Z'_{jk} I'_{kC} a = U_{jB} - U'_{jB} \\ Z'_{ki} I'_{iA} a + Z'_{kj} a^2 I'_{jB} + Z'_{kk} I'_{kC} = U_{kC} - U'_{kC} \end{cases} \quad (3)$$



Similarly, we write the equations for the currents and voltages of the negative and zero sequence components:

$$\begin{cases} Z''_{ii}I''_{iA} + Z''_{ij}a^2I''_{jB} + Z''_{ik}aI''_{kC} = -U''_{iA} \\ Z''_{ji}aI''_{iA} + Z''_{jj}I''_{jB} + Z''_{jk}a^2I''_{kC} = -U''_{jB} \\ Z''_{ki}a^2I''_{iA} + Z''_{kj}aI''_{jB} + Z''_{kk}I''_{kC} = -U''_{kC} \end{cases} \quad \begin{cases} Z^0_{ii}I^0_{iA} + Z^0_{ij}I^0_{jB} + Z^0_{ik}I^0_{kC} = -U^0_{iA} \\ Z^0_{ji}I^0_{iA} + Z^0_{jj}I^0_{jB} + Z^0_{jk}I^0_{kC} = -U^0_{jB} \\ Z^0_{ki}I^0_{iA} + Z^0_{kj}I^0_{jB} + Z^0_{kk}I^0_{kC} = -U^0_{kC} \end{cases} \quad (4)$$

In conclusion, it may be noted that in the case of single-phase short circuits, when formulating equations of fault currents in the circuits of the positive, negative and zero sequence components, the phase currents in the nodes are expressed by means of phases of interest (faulty phase) and the phase shift operator.

If we summarize the equations for nodes i, j, k made by the circuits of the positive, negative and zero sequences (3), (4), taking into the account the boundary conditions of the single-phase short circuit (5), will get the equation (6):

$$I' = I'' = I^0 \quad \text{and} \quad U' + U'' + U^0 = 0. \quad (5)$$

We got the equation system the solution of which provides the value of the currents of the positive (negative or zero) sequence at the damage points, i.e., in the nodes i, j, k. Tripled values of these currents are phase values of emergency currents.

$$\begin{cases} (Z'_{ii} + Z''_{ii} + Z^0_{ii})I'_{iA} + (aZ'_{ij} + a^2Z''_{ij} + Z^0_{ij})I'_{jB} + (a^2Z'_{ik} + aZ''_{ik} + Z^0_{ik})I'_{kC} = U_{iA} \\ (a^2Z'_{ji} + aZ''_{ji} + Z^0_{ji})I'_{iA} + (Z'_{jj} + Z''_{jj} + Z^0_{jj})I'_{jB} + (aZ'_{jk} + a^2Z''_{jk} + Z^0_{jk})I'_{kC} = U_{jB} = a^2U_{jA} \\ (aZ'_{ki} + a^2Z''_{ki} + Z^0_{ki})I'_{iA} + (a^2Z'_{kj} + aZ''_{kj} + Z^0_{kj})I'_{jB} + (Z'_{kk} + Z''_{kk} + Z^0_{kk})I'_{kC} = U_{kC} = aU_{kA} \end{cases} \quad (6)$$

For circuits of positive, negative and zero sequences, matrixes of proper and mutual resistances of nodes are calculated in advance. Then proper and mutual resistances corresponding to short-circuit nodes are selected from these matrixes. If the equation is written for the node i, then the intrinsic resistance of this node and the mutual resistance of the nodes i and j of similar damaged phases will be the sum of the respective intrinsic and mutual resistances within the circuits of all sequences:

$$Z'_{ii} + Z''_{ii} + Z^0_{ii} = Z_{iisov} \quad \text{and} \quad Z'_{ij} + Z''_{ij} + Z^0_{ij} = Z_{ijsov}$$

if the damaged phase in the node j leads damaged phase in the node i:

$$a^2Z'_{ij} + aZ''_{ij} + Z^0_{ij} = Z_{ijop}$$

if the damaged phase in the node j lags behind damaged phase in the node i:

$$aZ'_{ij} + a^2Z''_{ij} + Z^0_{ij} = Z_{ijol}$$

Similar to equation (6), it is possible to compose equations for an arbitrary number of simultaneous short circuits on the ground in different phases.

For calculation unification purposes, all types of asymmetric short circuits should be considered as the results of superposition of one-phase short circuit. For instance, three-phase short circuit is considered as the superposition of three one-phase short circuits:

$$Z_{ii} = Z_{jj} = Z_{kk} = Z_{ij} = Z_{ik} = Z_{kj} \quad (7)$$

then the solution will give the value of the one third of the phase currents (current values in sequence schemes) in the node i, if it is the node of the short circuit. Same happens with two-phase short circuit to ground – it is considered as the superposition of two one-phase short circuit. The equations considering the condition (7) will have the following form:



$$\left. \begin{aligned} (Z'_{ii} + Z''_{ii} + Z^0_{ii})I'_{iB} + (aZ'_{ii} + a^2Z''_{ii} + Z^0_{ii})I'_{iC} &= a^2U_{iA} \\ (a^2Z'_{ii} + aZ''_{ii} + Z^0_{ii})I'_{iB} + (Z'_{ii} + Z''_{ii} + Z^0_{ii})I'_{iC} &= aU_{iA} \end{aligned} \right\} \quad (8)$$

Therefore, we considered all types of asymmetric short circuits to earth as a superposition of single-phase short circuits. By taking into account the selection of phases of interest (faulty phase), we compiled the corresponding equations. In order to include phase-to-phase short circuits in these equations, additional conditions that are a consequence of such circumstances (for instance when one phase for example phase B, switches to another phase C) had to be considered.

Thus, we consider the phase-to-phase short-circuit to be a two-phase short-circuit to ground, taking into account the additional condition. Two-phase earth faults are two simultaneous single-phase earth faults in the supernodes i and j (with their subsequent merging). In node i there is a single-phase short-circuit with a special phase B, and in node j - single-phase short-circuit with special phase C.

And given the connection of phases B and C we will have special phase currents in the positive sequence circuit  $I'_{JB} = aI'_{JC}$  and in the negative sequence circuit -  $I''_{JB} = aI''_{JC}$ .

The equations of the node i (special phase B) for the circuit of the positive, negative and zero sequences will have the following form:

$$\left. \begin{aligned} Z'_{ii}I'_{iB} + aZ'_{ij}I'_{jC} &= U_{iB} - U'_{iB} \\ Z''_{ii}I''_{iB} + aZ''_{ij}I''_{jC} &= -U''_{iB} \\ Z^0_{ii}I^0_{iB} + Z^0_{ij}I^0_{jC} &= -U^0_{iB} \end{aligned} \right\} \quad (9)$$

Summation of the equations (9) in conjunction with equations (5) and (7) provides:

$$(Z'_{ii} + Z''_{ii} + Z^0_{ii})I'_{iB} + (aZ'_{ij} + aZ''_{ij} + Z^0_{ij})I'_{jC} = U_{iB} = a^2U_{iA} \quad (10)$$

The equation for the node j according to the circuits of all successions would be:

$$\left. \begin{aligned} Z'_{jj}aI'_{Cj} + Z'_{ji}I'_{Bi} &= aU_{Cj} - aU'_{Cj} \\ Z''_{jj}aI''_{Cj} + Z''_{ji}I''_{Bi} &= -aU''_{Cj} \\ Z^0_{jj}I^0_{Cj} + Z^0_{ji}I^0_{Bi} &= -U^0_{Cj} \end{aligned} \right\} \quad (11)$$

Summation of the equations (11), taking into the consideration (5), after multiplying the first and the second equations of the system (11) by  $a^2$  defines the equation for the node j

$$(Z'_{jj} + Z''_{jj} + Z^0_{jj})I'_{jC} + (a^2Z'_{ji} + a^2Z''_{ji} + Z^0_{ji})I'_{iB} = U_{jC} = aU_{jA}$$

taking into account the condition of merging of super nodes at two-phase and three-phase short circuits (7), let's rewrite the obtained equations for node j.

Consequently, we will get the equation system describing interphase short circuit:

$$\left. \begin{aligned} (Z'_{jj} + Z''_{jj} + Z^0_{jj})I'_{jB} + (aZ'_{jj} + aZ''_{jj} + Z^0_{jj})I'_{jC} &= a^2U_{jA} \\ (a^2Z'_{jj} + a^2Z''_{jj} + Z^0_{jj})I'_{jB} + (Z'_{jj} + Z''_{jj} + Z^0_{jj})I'_{jC} &= aU_{jA} \end{aligned} \right\} \quad (12)$$

Solution of (12) gives the one third of the value of phase currents in the short circuit between the phases B and C.

Consider a single-phase short circuit in node i with a two-phase short circuit between phases B and C in node j.

Figure 1 represents the model of the currents at the short circuit points with ideal current sources in the circuits of the positive, negative and zero sequences (Fig.1).

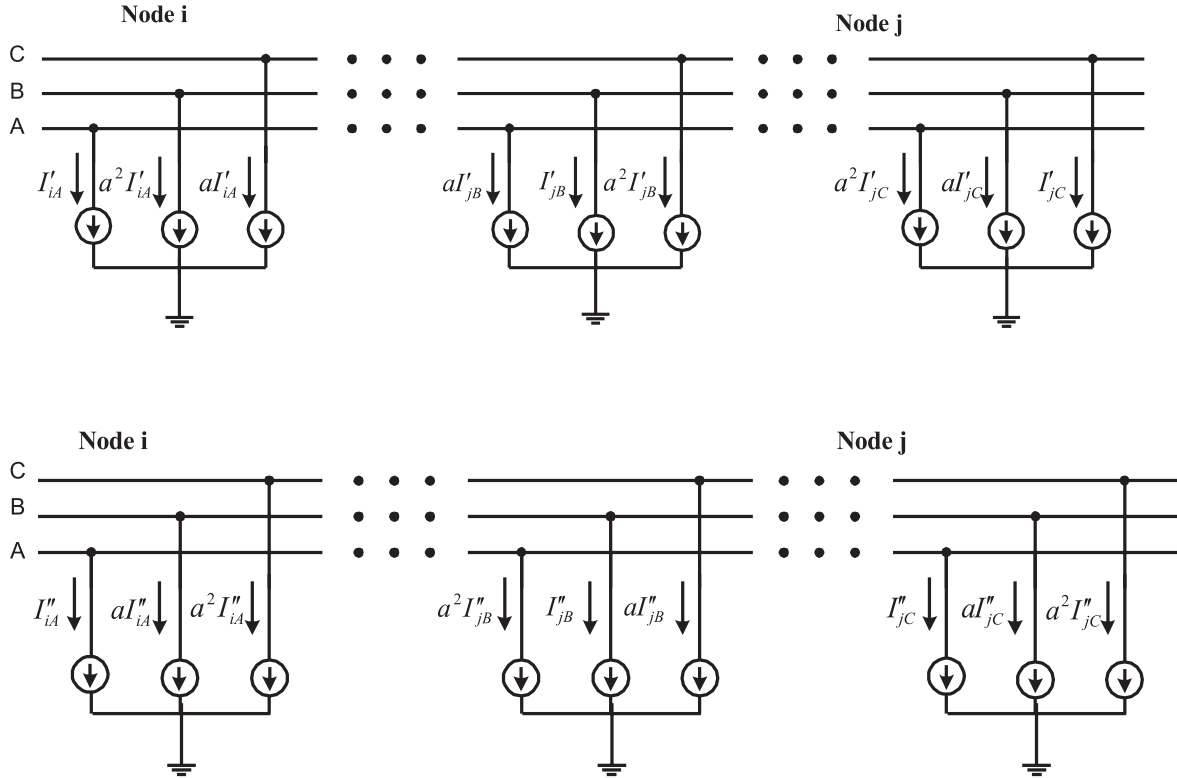


Figure 1

The equations describing the dependence between the currents in the circuits of the positive, negative and zero sequences for the node i where phase A is closed, will have the following form:

$$\begin{cases} Z'_{ii} I'_{iA} + Z'_{ij} a I'_{jB} + Z'_{ij} a^2 I'_{jC} = U_{iA} - U'_{iA} \\ Z''_{ii} I''_{iA} + Z''_{ij} a^2 I''_{jB} + Z''_{ij} I''_{jC} = -U''_{iA} \\ Z^0_{ii} I^0_{iA} + Z^0_{ij} I^0_{jB} + Z^0_{ij} I^0_{jC} = -U^0_{iA} \end{cases} \quad (13)$$

Summation of the equations (13) considering the boundary conditions of the one-phase short circuit will give:

$$(Z'_{ii} + Z''_{ii} + Z^0_{ii}) I'_{iA} + (a Z'_{ij} + a^2 Z''_{ij} + Z^0_{ij}) I'_{jB} + (a^2 Z'_{ij} + Z''_{ij} + Z^0_{ij}) I'_{jC} = U_{iA} \quad (14)$$

Similarly, for the node j, where the phase B is closed, will obtain:

$$\begin{cases} Z'_{ji} a^2 I'_{iA} + Z'_{jj} I'_{jB} + Z'_{jj} a I'_{jC} = U_{jB} - U'_{jB} \\ Z''_{ji} a I''_{iA} + Z''_{jj} I''_{jB} + Z''_{jj} a I''_{jC} = -U''_{jB} \\ Z^0_{ji} I^0_{iA} + Z^0_{jj} I^0_{jB} + Z^0_{jj} I^0_{jC} = -U^0_{jB} \end{cases} \quad (15)$$

$$a^2 Z'_{ji} + a Z''_{ji} + Z^0_{ji} I'_{iA} + Z'_{jj} + Z''_{jj} + Z^0_{jj} I'_{jB} + a Z'_{jj} + a Z''_{jj} + Z^0_{jj} I'_{jC} = U_{jB} \quad (16)$$

For the node j, where the phase C is closed, will obtain:

$$\begin{cases} Z'_{ji} a I'_{iA} + Z'_{jj} a^2 I'_{jB} + Z'_{jj} I'_{jC} = U_{jC} - U'_{jC} \\ Z''_{ji} a^2 I''_{iA} + Z''_{jj} a I''_{jB} + Z''_{jj} a^2 I''_{jC} = -a^2 U''_{jC} \\ Z^0_{ji} I^0_{iA} + Z^0_{jj} I^0_{jB} + Z^0_{jj} I^0_{jC} = -U^0_{jC} \end{cases} \quad (17)$$

$$aZ'_{ji} + Z''_{ji} + Z^0_{ji} I'_{iA} + a^2 Z'_{jj} + a^2 Z''_{jj} + Z^0_{jj} I'_{jB} + Z'_{jj} + Z''_{jj} + Z^0_{jj} I'_{jC} = U_{jC}$$

The system of equations to determine the sought unknowns will have the following form:

$$\begin{cases} (Z'_{ii} + Z''_{ii} + Z^0_{ii}) I'_{iA} + (aZ'_{ij} + a^2 Z''_{ij} + Z^0_{ij}) I'_{jB} + (a^2 Z'_{ij} + Z''_{ij} + Z^0_{ij}) I'_{jC} = U_{iA} \\ (a^2 Z'_{ji} + aZ''_{ji} + Z^0_{ji}) I'_{iA} + (Z'_{jj} + Z''_{jj} + Z^0_{jj}) I'_{jB} + (aZ'_{jj} + aZ''_{jj} + Z^0_{jj}) I'_{jC} = a^2 U_{jA} \\ (aZ'_{ji} + Z''_{ji} + Z^0_{ji}) I'_{iA} + (a^2 Z'_{jj} + a^2 Z''_{jj} + Z^0_{jj}) I'_{jB} + (Z'_{jj} + Z''_{jj} + Z^0_{jj}) I'_{jC} = aU_{jA} \\ I^F_{iA} = 3I'_{iA}, \quad I^F_{jB} = 3I'_{jB}, \quad I^F_{jC} = 3I'_{jC} \end{cases} \quad (18)$$

The equations (19) determining the sought value  $I'_{iB}$ ,  $I'_{jB}$ ,  $I'_{jC}$ , when the phase B is closed in the node i and the phases B and C in the node j are closed between each other (fig. 2) are obtained in a similar way.

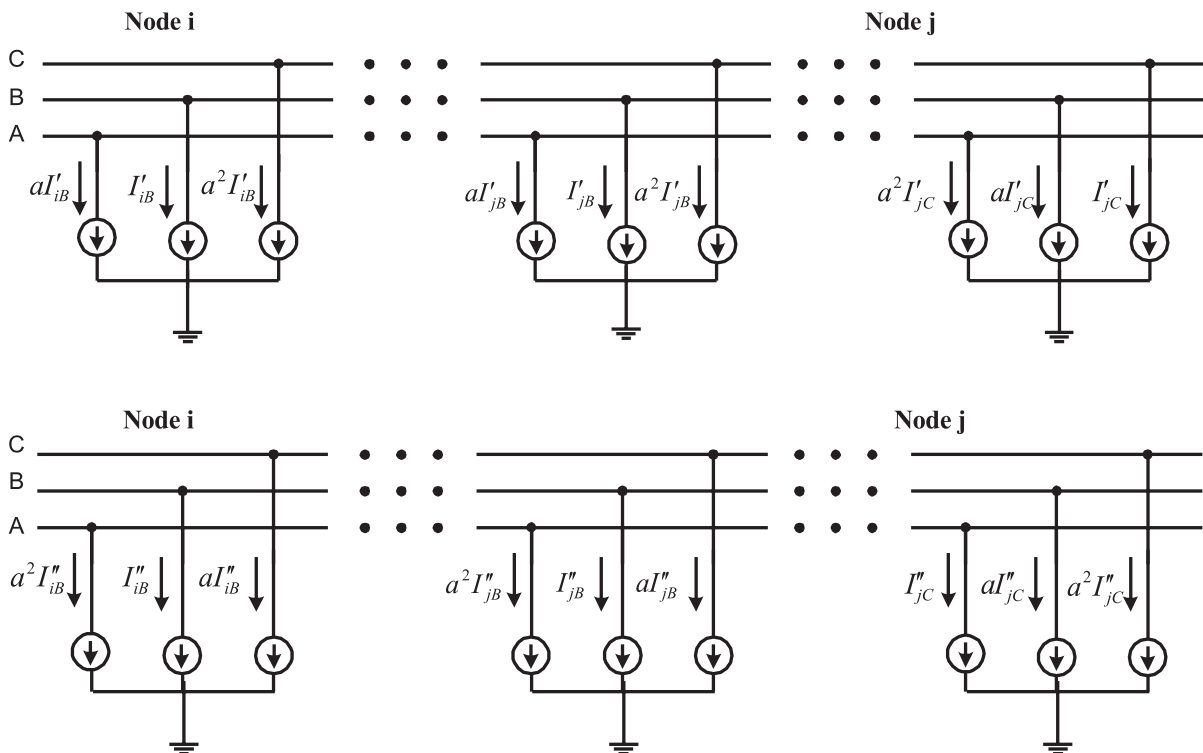


Figure 2

$$\begin{cases} (Z'_{ii} + Z''_{ii} + Z^0_{ii}) I'_{iB} + (Z'_{ij} + Z''_{ij} + Z^0_{ij}) I'_{jB} + (aZ'_{ij} + aZ''_{ij} + Z^0_{ij}) I'_{jC} = a^2 U_{iA} \\ (Z'_{ji} + Z''_{ji} + Z^0_{ji}) I'_{iB} + (Z'_{jj} + Z''_{jj} + Z^0_{jj}) I'_{jB} + (aZ'_{jj} + aZ''_{jj} + Z^0_{jj}) I'_{jC} = a^2 U_{iA} \\ (a^2 Z'_{ji} + a^2 Z''_{ji} + Z^0_{ji}) I'_{iB} + (a^2 Z'_{jj} + a^2 Z''_{jj} + Z^0_{jj}) I'_{jB} + (Z'_{jj} + Z''_{jj} + Z^0_{jj}) I'_{jC} = aU_{jA} \end{cases} \quad (19)$$

The equations for the case when the phase C is closed in the node i and the phases B and C are closed between each other in the node j (fig. 3) are obtained in a similar way

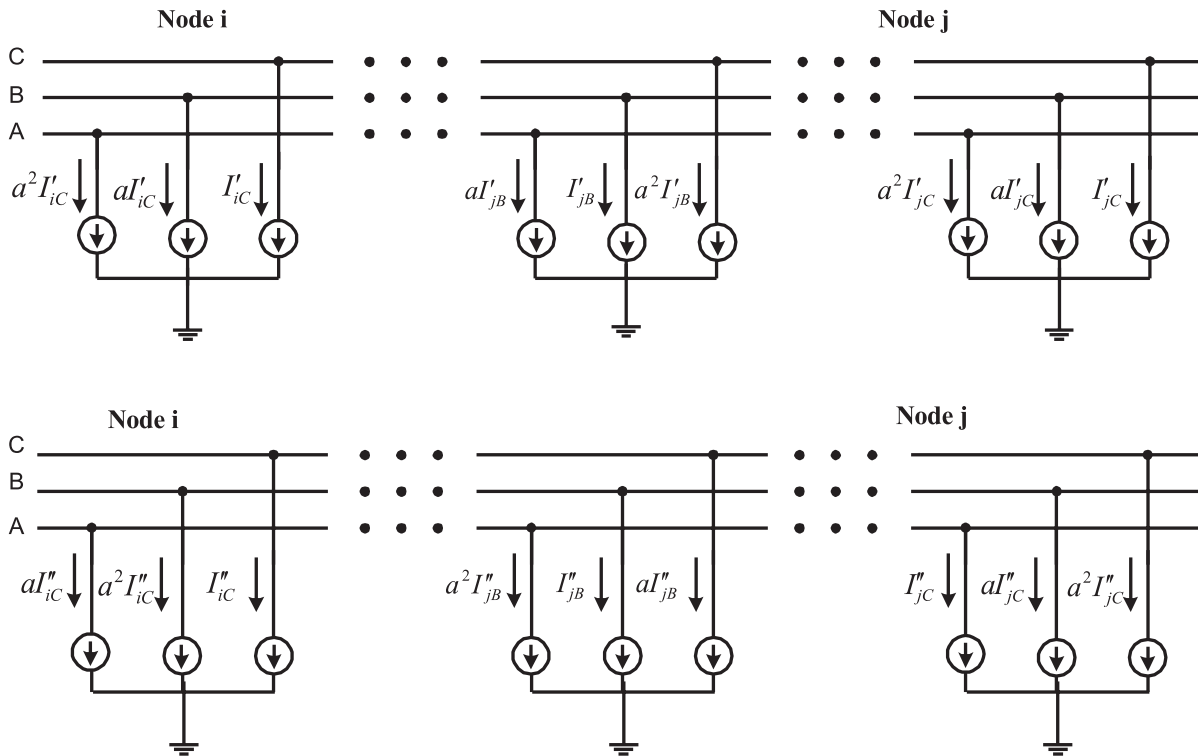


Figure 3

We calculated various combinations of simultaneous asymmetric short circuits, but as the most illustrative example exemplifying the reliability of calculations according to the proposed method, we chose the case of phase-to-phase short circuit in node j at three-phase short circuit in node i.

So, the equations are made for five one-phase short circuits - two one-phase short circuits in the node j and three one-phase short circuits in the node i (20).

## CONCLUSION

The proposed algorithm treats all types of short circuits as combinations of single-phase cases, applying appropriate criteria for single-phase fault boundaries. This approach allows for representing three-phase, two-phase to ground, and phase-to-phase short circuits as single-phase faults, with the inclusion of additional conditions.

One advantage of using the inverse form of nodal voltage equations in this method is that it accommodates any number of unknown variables. There is no need to recalculate the initial matrix. Instead, the corresponding individual and mutual impedances of the emergency nodes are selected from the inverse matrix of nodal conductance (derived from the matrix of nodal impedances). As a result, any number of simultaneous short circuits can be expressed as a superposition of single-phase short circuits.

Furthermore, the authors have employed the same analytical method to handle unbalanced load conditions, which will be discussed in their subsequent paper.

## BIBLIOGRAPHY

1. G. Kostanian. Representation of complex asymmetric faults on a DC model. News of higher educational institutions, №2, 1960.
2. N. Turkia. Unified equation of condition of electrical power systems. Electronic Journal EOL, issue 2, April, 2010.
3. N Turkia, V. Bantsadze. Equations for asymmetrical short circuit. "Energy". Tbilisi 2008. N3 (47).





# An Innovative Metric for Evaluating Operational Resilience of the High-Voltage Grid

[simone.talomo@terna.it](mailto:simone.talomo@terna.it) / [luigi.calcara@uniroma1.it](mailto:luigi.calcara@uniroma1.it)

C. VERGINE<sup>1</sup>, E.M. CARLINI<sup>1</sup>, G. BIASIOTTI<sup>1</sup>, S. TALOMO<sup>1</sup>, L. CALCARA<sup>2</sup>, M. POMPILI<sup>2</sup>

<sup>1</sup>Terna Rete Italia

<sup>2</sup>University of Roma "La Sapienza"

Italia

## SUMMARY

For the High Voltage (HV) electrical grids, concepts and applications related to resilience have become quite common. Both power utilities and grid system operators have emphasized more on resilience during planning, designing, and operating phases, so that power system can adapt to or recover from natural disasters, cyber-attacks, or cascading failures, maintaining their functionality.

To measure power system resilience both qualitative and quantitative metrics are often used. Normally, quantitative indicators are based on single outages curves giving an estimation of the extent of the damage to the system before the recovery. These curves assume shapes normally known as resilient triangle or trapezoid. The integrals of the energy not supplied are strictly correlated with the power system resilience. In this framework, indicators as degree and duration of degradation, rate of restoration and overall performance are normally used.

During extreme negative events, a major importance is assumed by operational resilience, which refers to the ability of an organization to maintain its core functions and continue to deliver its critical services during and after a disruptive event. It includes IT systems, infrastructure, processes, people, and supply chains. It aims to minimize disruptions' impact and ensure that the organization can recover quickly.

In the present paper, an innovative metric for operational resilience evaluation is presented and discussed. This index, reported in the paper as H or SiRI (Site Resilience Index), is based on a function that considers data of Energy Not Supplied (ENS), maximum Power (Pmax) and infrastructural reliability of different HV substations. Main advantages of this innovative index are:

- i) to consider both of the magnitude of the event and the characteristics of the affected portion of the grid in terms of reliability and power consumption;
- ii) to allow the evaluation of operational resilience of each HV substation (point of delivery), making possible comparisons;
- iii) to allow the evaluation of the impact of an outage of a part of the electrical grid, both at regional and/or at national level, making possible comparisons and evaluations of more urgent improvements (both infrastructural and related to operational resilience).

## KEYWORDS

Electrical Resilience, resilience index, operational resilience, innovative metric.



## 1. INTRODUCTION

Many of the external threats to the electrical system can be associated with adverse weather conditions or with wildlife and vegetation that may come in contact with its infrastructural components.

Thunderstorms, strong winds, wet-snow and other negative weather conditions are certainly the most common and potentially serious natural threat to the electrical system. In more recent years, also cyber attacks are becoming more frequent and dangerous.

Only in 2022 the world suffered more record-breaking floods, droughts, heavy snowfalls, typhoons, and heatwaves that caused widespread human and economic destruction. From these events, as an example, it is possible to mention the floods in Pakistan and South Asia (June), heatwave in South and Central Asia (May), heatwave and drought in China (June-August), heatwave in Europe (July), floods in Malaysia (February), tropical storms and typhoons in the Philippines (October), hurricane Ian in the United States (September), Sandstorms in the Middle East (May), etc.

Surely, the most common and potentially serious extreme weather threats to the High Voltage (HV) electrical systems are winter storm, strong winds and heat waves. Obviously, the components of a power system such as transformer, overhead line (OHL), power cable, substation, etc., can be affected differently by natural threats. In general, winter storm may result in the damage of transmission towers, short circuits of OHL conductors and snow/ice sleeve accretion on conductors with increasing of the conductor sag in the span. Normally, heat waves have negative impacts on underground power cables (especially for the distribution system) and, in case of extremely high temperature, also on OHL.

Electrical transmission network has been built over time based on regulations and standards that have set reference values for weather events. However, there is no guarantee that the electrical grid is able to withstand the meteorological stresses under extreme weather conditions which have become more frequent in recent years, due to the climate changes, and that exceed design values.

Due to the growing frequency of natural disasters, cyber-attacks, and other disturbances to the power system, the concept of resilience has gained increased importance in recent years.

It is the task of the electrical operators (TSOs and DSOs) to try to limit the effects of this climatic disorder by implementing mitigating actions and increasing the resilience of the electrical system.

These implementations may concern both infrastructural or operational reinforcements.

In this paper, are shown an overview of the key factors that contribute to the operational resilience of HV electrical grids and propose an operational resilience index that can be used to assess and monitor their performance when facing extreme negative events.

### 1.1. A possible index for evaluating the operational resilience

A lesson learned process is often in place in order to increase power system resilience on the basis of the historical impacts of High Impact Low Frequency (HILF) events.

In this paper a new operational resilience index (H) has been evaluated by examining historical information related to high voltage outages caused by extreme weather events as strong wind and snow. The use of historical data approach provides valuable insights into the frequency and severity of past disruptions and can help to identify trends and patterns that can inform future planning and preparedness efforts.

In order to evaluate this index, it is necessary to consider the Energy Not Supplied (ENS) which is an estimate of the amount of energy that was not supplied to end users connected to the HV substation due to any possible outage. The calculation of ENS requires knowledge of the load demand and the duration of the outage event. Load demand refers to the amount of energy required during a specific time period and the duration of the outage event is the time period during which the electrical grid was unable to supply energy to the HV substation end users.

Other benchmarks used in the present study are the maximum power ( $P_{max}$ ) absorbed by the considered HV substations and their reliabilities.

Starting from these parameters, it is possible to perceive a new resilience index (H) able to evaluate the ability to withstand from negative events (i.e. snow/ice and wind) for each HV substation or portion of the electrical grid. These resilience indexes can be estimated as:

$$H = \frac{ENS_{net} \cdot Reliability}{P_{max}} \text{ [hours]}$$



where:

$ENS_{net}$ : is the energy not supplied [MWh] on a given time period (i.e. yearly);

*Reliability*: is the probability that the event considered does not occur in a given time and it is equal to  $1-\lambda$ , in which  $\lambda$ : is the failure rate of a particular component or system and can be calculated as  $1/PBT$ . PBT is the payback time, i.e. the average number of years between two failures of the same type due to the occurrence of a certain type of event;

$P_{max}$ : is the maximum power absorbed by the considered HV substations [MW].

The PayBack Time (PBT) considered in this study is referred to High Voltage OverHead Lines (OHL) and substations for snow and wind events and takes into account the probability of occurrence of these extreme meteorological phenomena, that are the responsible of the largest contribution to the not served energy (ENS) in the Italian electrical grid, in the future.

To evaluate the new index for operational resilience, in this paper have been analysed the major negative events occurred in the considered HV substations of 3 different geographical Regions of Italy during the period 2017-2021. More in detail, it has been considered the North-East part of Italy distinguishing the three regions: Friuli-Venezia-Giulia, Trentino-Alto-Adige and Veneto.

As an example, in Fig. 1 are reported the Energy Not Served (ENS), the average maximum power ( $P_{max}$ ) and the trends of the operational resilience index (H) of all local HV substations for the period 2017-2021 calculated for the region Trentino-Alto-Adige. From this figure it is possible to note some HV substations (HV substations 2, 15 and 26) with higher values of H than others, considering as reference the HV substation ability to withstand to adverse weather events limited to snow and wind. This is mainly related to the following aspects:

- i) low infrastructural resilience of such HV substations as estimated on the basis of the payback time (PBT); obviously low PBT values correspond to low HV substation reliability values (e.g. in the case of a radial connection of the substation to the HV grid);
- ii) high impact of ENS of the HV substations in comparison with the  $P_{max}$  of the same HV substation.

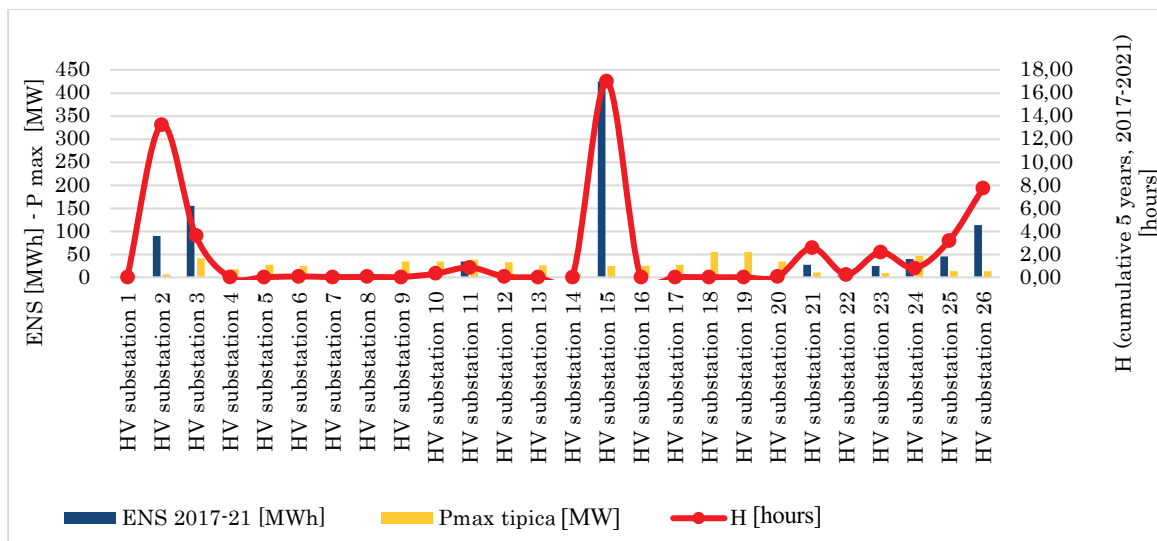


Figure 1. Operational resilience index (H), Energy Not Served (ENS) and average maximum power (Pmax) trends of HV substations for the period 2017-2021 due to adverse weather events (snow/ice and wind) calculated for the region Trentino-Alto-Adige

Always for the case of Trentino-Alto-Adige region, in Fig. 2 is reported the representation over the years (2017-2021) of the operational resilience index (H) for each HV substation following all the considered negative events. From this figure may be immediately perceived the impact of the dramatic events that occurred during October-November 2018 (peak of the graph: higher value of the H index) and also known as Vaia event. Vaia was a severe storm that affected the Alpine region of northern Italy, including the Trentino-Alto-Adige region. The storm brought heavy rainfall and strong winds, resulting in significant damage to forests and infrastructure, including the HV electrical grid.

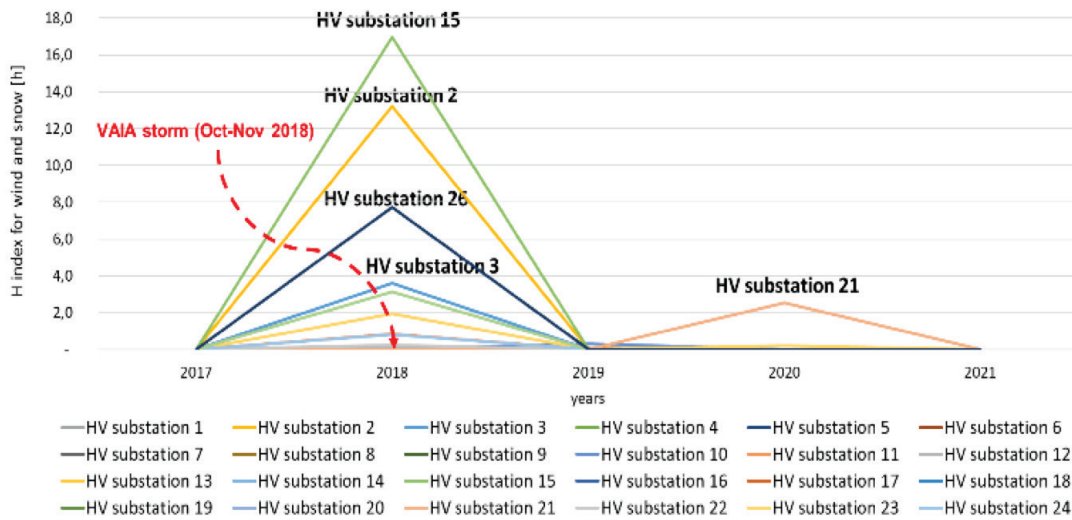


Figure 2. Representation over the years (2017-2021) of the operational resilience indicator (H) for each HV substation following all the events for the Trentino-Alto-Adige region

As reported above, the operational resilience index (H) is given by the products of 2 terms, namely ENS and Reliability/Pmax. This product identifies a family of hyperbolae (in red) on the plan Reliability/Pmax and ENS. This means that for each combination of Reliability/Pmax and ENS values, there is a corresponding point on the hyperbola that represents the operational resilience index (H) for that system. By plotting these hyperbolae on a graph, it is possible then to visualize the relationship between ENS, Reliability/Pmax, and operational resilience, and to compare the operational resilience of different HV substations or different power systems. In Fig. 3 is reported the case of the behaviour of the Trentino-Alto-Adige region HV substations during the past events of the years 2017-2021. The hyperbolae are shown in red on the graph, indicating the area of acceptable operational resilience levels. As the ENS increases or the Reliability/Pmax decreases, the system moves closer to the edge of the acceptable range (i.e.  $H < 1$  or  $H < 3$  evaluated over the period 2017-2021), indicating lower levels of operational resilience. By analyzing the shape and position of the hyperbolae, it is possible to identify areas of the graph where improvements to the power system could lead to significant increases in operational resilience. In particular, most critical sites in terms of energy and infrastructure are located on the left side of the plan, since they are characterized by high values of the power consumption and low values of infrastructural reliability. For these sites, grid reinforcement interventions should be preferred. Instead, for HV substations on the right side of the plan, operational resilience assumes a strategic value, representing the most valuable measure against these types of extreme natural events.

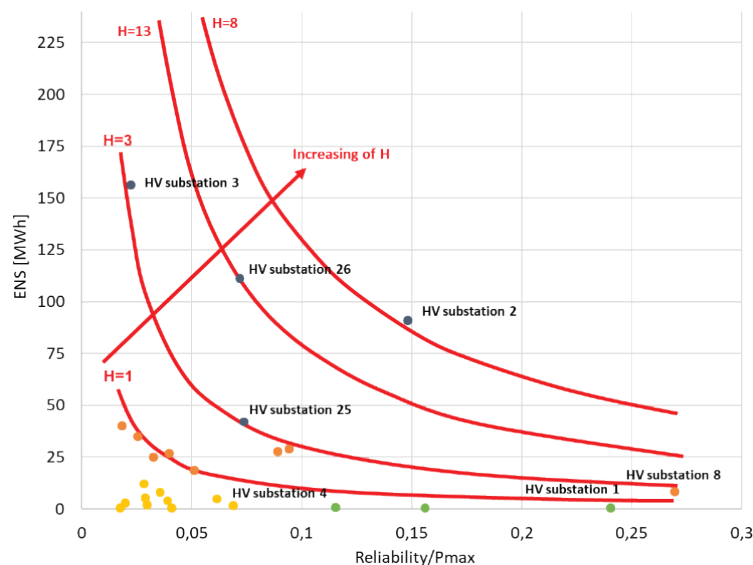


Figure 3. Representation of a family of hyperbolises on the plan Reliability/Pmax and ENS to identify the resilience indicator H for different HV substations of Trentino-Alto-Adige region (events of 2017-2021). Note: H is evaluated over the period 2017-2021.



It is also useful, with the necessary approximations, to carry out an analysis of the calculation of the operational resilience index (H) considering not only the snow-wind events, but also all the other possible causes of HV substation outage, such as example: electrical, operating, mechanical causes, accidental damage, etc. In the regulatory field, several causes of unavailability (service interruptions) have been codified, classifying them into categories: insufficient resources, force majeure, external causes, other causes and planned outages.

By comparing the H values referred to snow and wind, or to all the causes of energy unavailability in general, similar results could be obtained demonstrating how the HV substations connected almost entirely by OHLs to the HV grid are mainly subject to interruptions due to meteorological causes (direct or indirect).

It may be interesting then, still for the Trentino-Alto-Adige region taken as an example, to extend the present analysis by reconsidering all the aforementioned causes of unavailability of the HV substations. In making this, however, it is necessary to know the payback time for each component and for the various types of stresses to which they are subjected. These values are not easy to estimate.

Furthermore, the H indicator obviously can refer not only to a region but also to several regions, or to a territorial area, or to the entire HV national grid. This may allow the indicator to also have local or overall performance significance, giving also priorities in the reinforcement actions of the electrical grid.

Analysing the “most critical” average H resilience indexes, based on the hypotheses formulated, this leads to believe that the actions to be implemented are very different, since it is possible to estimate infrastructural strengthening interventions for some HV substations or other operational actions able to increase the overall reliability of the considered portion of the electrical grid.

## 2. CONCLUSION

The resilience of high voltage electrical grids is a critical issue in ensuring the reliability of energy supply, particularly in the face of extreme weather conditions also due to ongoing climate changes. As the electrical system is subject to constant variations in demand, generation capacity and operational conditions, it is important to develop metrics that accurately estimate the system's ability to adapt to changing conditions.

Many studies and actions have been aimed at improving the infrastructural resilience of the electrical grid and its components (substations, OHLs, etc.); nevertheless, appreciable advantages can be also obtained by improvement of the operational resilience, which refers to the ability of an organization to maintain its core functions and continue to deliver its critical services during and after a disruptive event. It includes IT systems, infrastructure, processes, people, and supply chains. It aims to minimize disruptions' impact and ensure that the organization can recover quickly.

In this paper an innovative operational resilience index (H) has been proposed to make possible to evaluate both the actual capability of the electrical grid to withstand in case of adverse events and scheduling corrective actions to increase the resilience of the system. By monitoring this index, it is possible to identify specific areas where reinforcement actions to be implemented may have priority to reduce the risk of electrical outages.

Analysing the “most critical” H resilience indexes, based on the hypotheses formulated, this leads to believe that the actions to be implemented may be very different, in function of the nominal power of the involved HV substations ranging from infrastructural strengthening actions to other operational activities able to increase the overall resilience of the considered portion of the electrical grid.

## BIBLIOGRAPHY

- [1] CIGRE C2 Technical Brochure, “Operational strategies and preparedness for system operational resilience, 2021
- [2] E. Ciapessoni, S. Massucco, D. Cirio, M. Sforza, A. Pitto, P. Marcacci, “Model based resilience assessment and threats mitigation: a sensitivity based approach”, IEEE, 2018 AEIT International Annual Conference
- [3] L. Calcarà, A. Di Pietro, S. Giovanazzi, M. Pollino, M. Pompili, “Towards the Resilience Assessment of Electric Distribution System to Earthquakes and Adverse Meteorological Conditions”, IEEE, 2018 AEIT International Annual Conference
- [4] P. Faggian, G. Decimi, “An Updated Investigation about Climate-Change Hazards that might Impact Electric Infrastructures”, IEEE, 2019 AEIT International Annual Conference
- [5] E. M. Carlini, S. Favuzza, S. E. Giangreco, F. Massaro, C. Quaciari, “Uprating an Overhead Line. Italian TSO Applications to Increase System N-1 Security”, International Conference on Renewable Energy Research and Applications, 2013
- [6] L. Campisano, P. Ferretti, S. Neri, C. Quaciari, M. Pierno, E. M. Carlini, “Tools and strategies for managing critical grid situations and extreme weather events”, IEEE, 2020 AEIT International Annual Conference



Poster Presentation: An Innovative Metric for Evaluating Operational Resilience of the High-Voltage Grid

- [7] [https://www.ipcc.ch/site/assets/uploads/2018/02/WGIIAR5-AnnexII\\_FINAL.pdf](https://www.ipcc.ch/site/assets/uploads/2018/02/WGIIAR5-AnnexII_FINAL.pdf)
- [8] <https://www.eco-business.com/news/10-devastating-extreme-weather-events-in-2022/>
- [9] "Innovation in the Power Systems Industry", CIGRE Science&Engineering Vol. 18, June 2020
- [10] The effects of high winds on transmission lines, A.M. Loredo-Souza!,\*, 1, A.G. Davenport
- [11] E. Bompard, T. Huang, Y. Wu, and M. Cremenescu, "Classification and trend analysis of threats origins to the security of power system," Electrical Power & Energy Sytems, 2013.





# Smart Grid Project GreenSwitch

goran.levacic@hops.hr / simon.tot@eles.si / mate.lasic@hops.hr

**GORAN LEVAČIĆ<sup>1</sup>, MATE LASIĆ<sup>1</sup>**

<sup>1</sup>*Croatian Transmission System Operator Plc.*

*Croatia*

**SIMON TOT,**

*ELES, d.o.o.*

*Slovenia*

## SUMMARY

GreenSwitch, one of five smart grid projects included in the smart grid PCI list, is a cross-border regional project between Austria, Croatia and Slovenia. The project does not start from zero, it leverages the results, acquired experience, and cooperation from previous smart grid project - SINCRO.GRID.

The project is characterized by an innovative and efficient incorporation of new technologies and advanced functionalities for the cross-sectoral and cross-border enhancement of the power system infrastructure resulting in higher network hosting capacity, efficient integration of new types of network users, optimization of future investments, and improvement of security of supply and quality of service in Austria, Croatia and Slovenia. Project partners will invest in primary infrastructure and introduce various technologies, platforms, and functionalities to develop smart grids.

Main goals of the project comprise increasing possibilities to integrate more RES in the electricity networks, coupling electricity, transport and heating sectors, as well as increasing security of power supply in countries already involved in the integrated EU electricity market.

In order to achieve these goals, high investment costs are required, since existing economic frameworks imply that full project costs cannot be justified through network tariff increases, unless other necessary investments are deferred. Therefore, project is submitted and selected for co-financing from the European Commission's CEF fund (Connecting Europe Facilities), with support of €73.1 million (what equals to 50% of total project budget).

The geographical scope of the GreenSwitch project covers the area of Austria, Croatia and Slovenia, but it is expected that the project will significantly contribute to the decarbonization efforts in the wider central European region. The expected result will be a grid that is better prepared for the expected large additional loads and renewable energy sources.

Paper gives an overview of the project goals, work packages and description of main technologies and techniques.

## KEYWORDS

smart grid, regional cooperation, synergy, power system, TSO, DSO, flexibility, RES, new technologies, PCI, CEF



## 1. INTRODUCTION

This paper gives an overview on the project GreenSwitch, one of five smart grid projects included in the PCI list and supported by CEF funds. It is a cross-border project between Austria, Croatia and Slovenia. The GreenSwitch project upgrades the results of previous successful smart grid project (SINCRO.GRID, finished in 2022) with additional cross border capacity and optimization of grid operation while expanding to lower voltage levels. Also, in scope of project, a new technologies will be introduced, and the grid will be better prepared for expected large amounts of new network users and RES.

## 2. ABOUT THE PROJECT

The project will last six years (start in 2023 and commissioning in December 2028) and is divided into six phases, each lasting one year. The first five phases cover most of the “hardware” installations, while the last phase focuses on the finalization of complex algorithms that will include the existing and new active elements into the day-to-day operation of TSOs and DSOs, distribution companies and retailers, taking into consideration cross-border optimization. Each TSO and DSO will be responsible for implementing investments and functionalities in their network.

The main goals [1] of the GreenSwitch project are to optimize grid investment and to enable the integration of an increasing quantity of dispersed resources. Other goals of the project include;

- increase hosting capacity for distributed renewable sources,
- optimize grid investment,
- improve observability of the distribution network,
- increase cross-border capacity,
- efficiently integrate new loads,
- improve supply quality,
- coordinate flexibility in procurement and supply,
- make optimal use of the infrastructure.

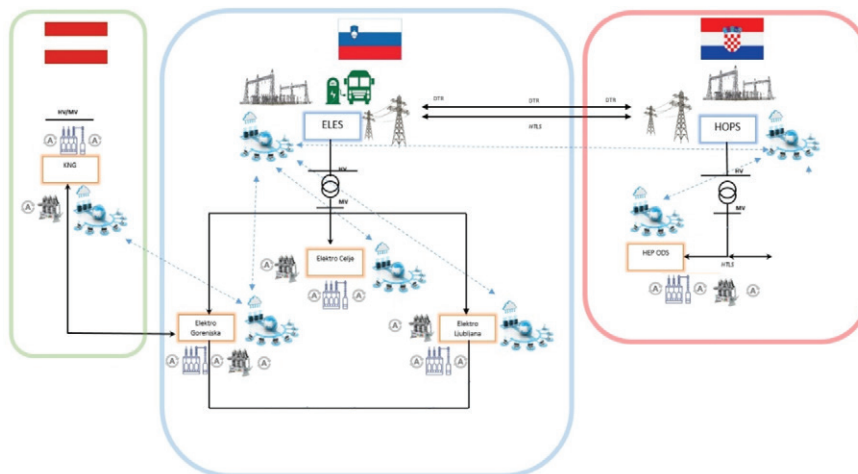


Figure 1: GreenSwitch project scheme

## 3. CONSORTIUM

Project consortium [1,2] comprises from TSOs (Slovenian ELES acting as the project coordinator and Croatian HOPS) and DSOs (Slovenian Elektro Celje, Elektro Ljubljana and Elektro Gorenjska; Croatian HEP-ODS; and Austrian Kaernten Netz). Transmission and distribution system and network operators in the GreenSwitch project have a long history of cooperation both at cross border level between TSO-TSO and DSO-DSO as well as within each country as a TSO-DSO cooperation. ELES and HOPS has daily relations with their respective DSOs (Elektro Celje, Elektro Gorenjska and Elektro Ljubljana in Slovenia and HEP-ODS in Croatia).

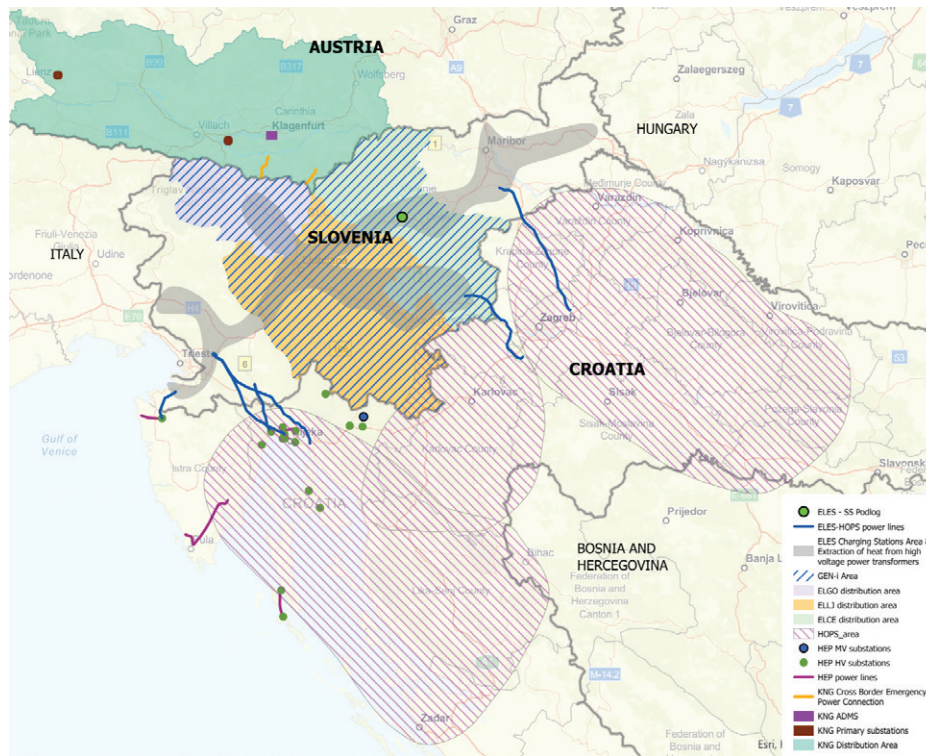


Figure 2: Geographical scope of the GreenSwitch project

## 4. PCI STATUS AND CEF FUNDING PROCESS

Generally, smart grid projects play a key role in implementing digital communication technologies across the EU to efficiently integrate large amounts of electricity generated from RES, connecting all users for an effective demand response. These projects also contribute to reducing greenhouse gas emissions. They are therefore firstly subject to be awarded the Project of Common Interest (PCI) status, which means that they can benefit from fast track EU financial assistance in the form of grants for studies and works under Connecting Europe Facility Energy programme (CEF Energy).

Smart grids deployment has been identified in the TEN-E Regulation [3,4] as one of the 12 trans-European energy infrastructure priority corridors and thematic areas. The PCIs were introduced in 2013 and are updated every two years as the projects and the energy system evolve. The Commission submits the list of projects to the European Parliament and to the Council.

Firstly, GreenSwitch project has been shortlisted on the meeting of the TEN-E Thematic Group for Smart Grids for 5<sup>th</sup> Projects of Common Interest list [5] in June 2021, and finally listed on 5<sup>th</sup> PCI list in November, 2021, under Priority Thematic Area Smart Grids Deployment. Also, GreenSwitch together with five another electricity and four gas smart grid projects have been proposed for the EU's first list of projects of common interest (6<sup>th</sup> PCI) and projects of mutual interest (PMI). The new category of PMIs was introduced in the revised TEN-E regulation as projects between the EU and third countries to further promote the integration of renewables and other clean energy technologies to support EU emissions reductions. All the projects finally selected are able to benefit from streamlined permitting, environmental assessment and regulatory procedures and are eligible for financial support from the EU's Connecting Europe Facility.

The Connecting Europe Facility (CEF) [6] for Energy is the EU funding programme to implement the Trans-European Networks for Energy policy. Today, CEF Programme Sectors are divided on Energy, Transport and Digital. CEF Energy aims at supporting investments in building new cross-border energy infrastructure in Europe or rehabilitating and upgrading the existing one.

At the end of 2022, it has been finally confirmed that smart grid project GreenSwitch will receive €73,1 million, as one of eight cross-border energy infrastructure projects that are awarded from the EU's CEF fund [8].

The total project costs encompass investment costs that are required for the procurement and implementation of equipment, costs for management and coordination of the project and operation costs arising during the period of use of the assets.



Figure 3 gives an overview of the total budget per partners (€146,2 million).

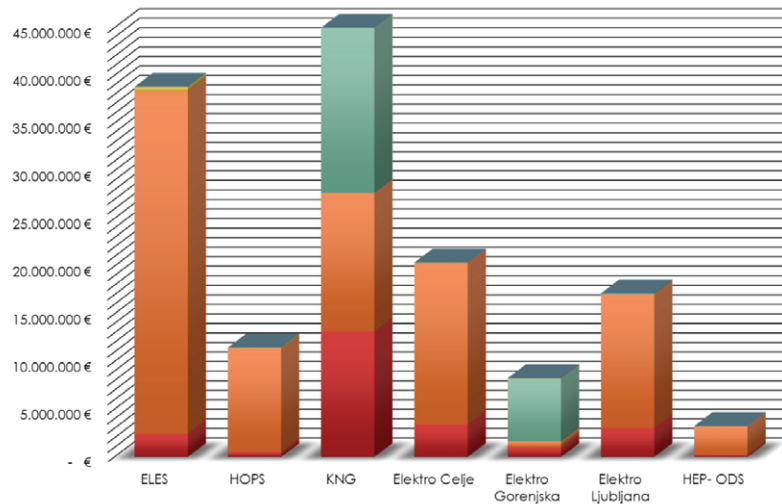


Figure 3: Overview of total budget per partners

A detailed cost benefit analysis (CBA) was performed [7], which demonstrated that the GreenSwitch project generates significant system wide benefits, and as such, the Project should be undertaken.

In short, the financial profitability of an investment is assessed by estimating the financial net present value and the financial rate of return of the investment (FNPV and FRR). These indicators compare investment costs to net revenues and measure the extent to which the project's net revenues are able to repay the investment, regardless of the sources of financing.

The high investment costs of the project for the current economic frameworks in Croatia, Slovenia and Austria, imply that the full costs of the project cannot be justified by increasing the network tariff, unless other necessary investments are postponed. At the end, CBA proved contribution of this comprehensive project to the transition of a low emission economy, and from that reason, it was decided to continue with the project deployment and submission for funding.

## 5. TECHNOLOGIES AND MAIN COMPONENTS OF THE PROJECT

In general, the project work packages (WPs) are divided into four main categories [1,2];

- WP1 - Project management and coordination,
- WP2 - Increasing efficiency in operation and controllability of the transmission network in HR and SI,
- WP3 - Integration of new network users and cross-sectoral coupling,
- WP4 - Increasing the efficiency of the distribution network, security of supply, cross-border and capacity for RES in AT, HR and SI.

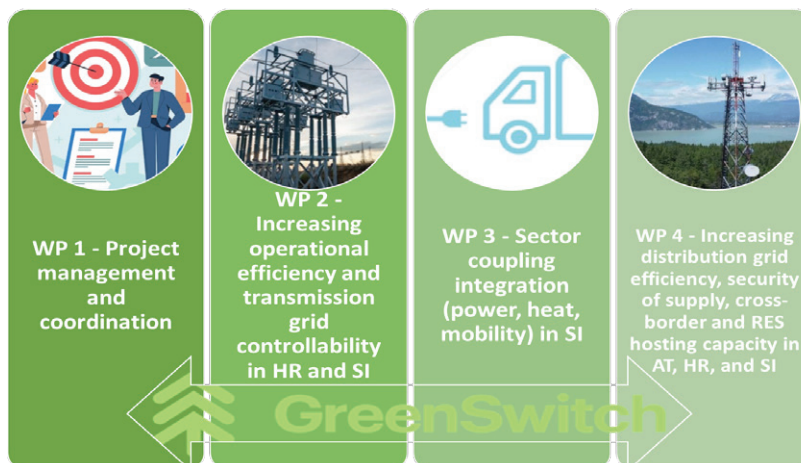


Figure 4: Work packages



The chapter continues with brief description of the each work packages (WP) and related activities.

First WP [1,2], called Project management and coordination is joint activity for all partners in project, and consists of planning, management and monitoring of the work packages and tasks, execution and documentation of meetings and regular conference calls with all participants, monitoring of the progress and impact of the project, completion of specified deliverables and milestone, reporting to CINEA in accordance with the project time plan and representation of the project towards stakeholders at international level.

Second WP [1,2], refers to TSOs from Croatia (HOPS) and Slovenia (ELES). Goal of this WP is to: optimize new network investments, optimize the existing infrastructure and efficiently incorporate new technologies and advanced functionalities and to support and accelerate RES integration. The activity consists of installation of power control systems (PST and SSSC), together with accompanying primary, protection and control equipment in Croatia and Slovenia.

The installation of phase shifting transformer (PST) in Croatia includes 110 kV line bay with the associated primary and secondary equipment for connection to the 110 kV network. PST will be installed in the substation 110/35 kV Gračac (in the line bay of OHL 110 kV Gračac-Obrovac) which will be managed through optimization functions (for better utilization of lines and/or minimizing losses in grid) as a part of Optimal Power Flow Platform (OPFP). This is an important activity to support integration of RES in Croatian region of Dalmatia with the highest RES potential (both WPPs and PVs).

A PSTs are specialised type of transformer that are typically used to control the flow of active power on three-phase electric transmission networks. It does so by regulating the voltage phase angle difference between two nodes of the system.

Furthermore, the above mentioned OPFP platform extends the goal to integration of different power system resources (TSO assets and 3rd party assets such as dispatchable and non-dispatchable RES along with energy storage technologies) under an advanced control system with optimization-based techniques for different target functions: loss minimization, congestion management and security constrained redispatch, as it is shown of figure 5.

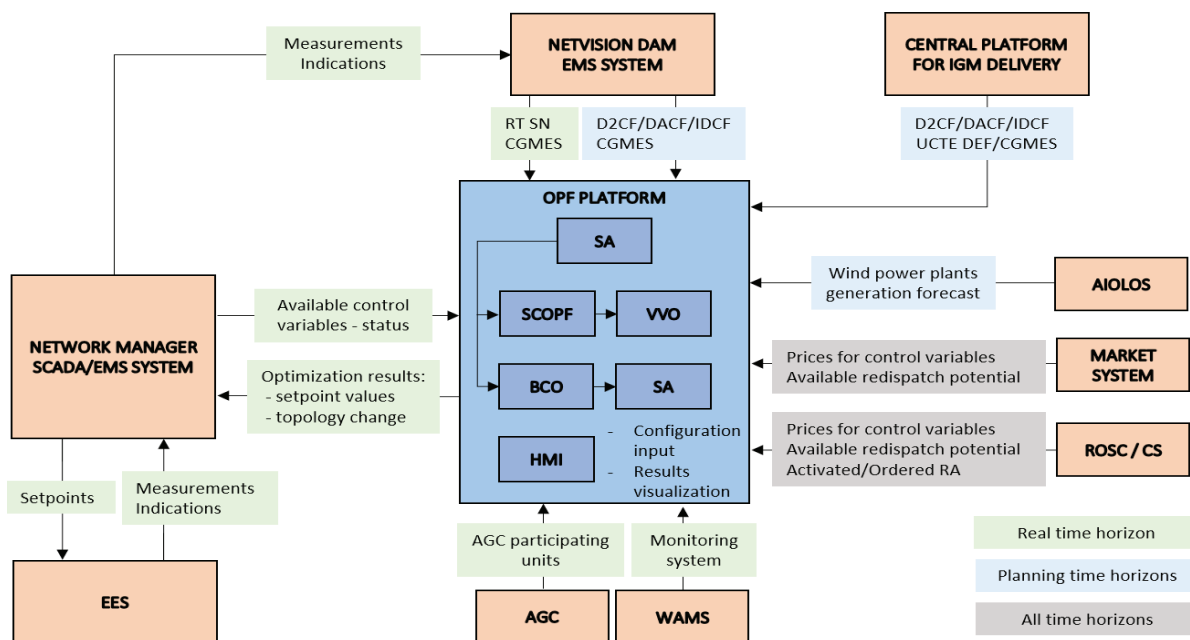


Figure 5: Optimal Power Flow Platform

In order to additionally support RES integration in the most promising RES potential area of south Croatia, along with improving security of supply on the islands which is of utmost importance in this touristic highly developed area, High Temperature Low Sag Conductors (HTLS) will be installed (replace existing conductor) on the OHL 220 kV Senj-Brinje, with total length of 15.5 km.

In Slovenia, the activity consists of installing the static synchronous series compensator (SSSC) on the 220 kV voltage level in substation Podlog and accompanying primary, protection and control equipment, which will continuously regulate the Power Control System. The installation of SSSC devices in the Podlog substation includes a 220 kV switchgear (two bays – possibility connection on power line Obersilach or Beričevo) with the associated primary and secondary equipment for connection to the 220 kV network. The





**Poster Presentation:** The Impact of the Connection of Renewable Resources in the Distribution Network - The Case of Hydro Power Plants in Kosovo

220 kV bay equipment consists of HV substation equipment (circuit breakers, disconnectors, instrument transformers, and surge arrestors), HV connections, cable connections, auxiliary control equipment (protection, measuring, operations).

SSSC consists of power electronics technology that injects a controllable voltage (leading or lagging) into a circuit, either manually or automated, and it is used for dynamic power flow control in a system. Example of mobile SSSC device is shown in figure 6.



*Figure 6: Mobile SSSC device installed in substation*

The task also covers developing DTR system on cross-border lines between Slovenia and Croatia as well as on power transformers on 400 kV and MV level: expanding existing DTR system on cross borderlines with Slovenia and power transformers in three primary substations (400/220/110 kV). The activity consists of deploying DTR system to allow for real-time monitoring of local conditions on the overhead lines and primary substations (400/220/110 kV), thus enabling better and safer grid utilization. Weather stations will be installed on all power lines and substations (400/220/110 kV).

Third WP [1,2] called Integration of new network users and cross-sectoral coupling refers to ELES, and its main goal is to improve cross-sector integration using waste heat from the transformer and investing in the preparation of infrastructure for grid connection for heavy duty charging station in Slovenia.

ELES is planning to invest in technology to using heat from many high voltage power transformers to heat water and then use it for heating in the local and district heating systems. 11 transformers will be equipped by technology to extract waste heat. This innovative action demonstrates how dependence on the heating by using imported gas may be gradually decreased. Principal idea is shown on figure 7.

ELES is also planning to invest in commercially available high-power infrastructure on frequent traffic locations that enable simultaneous fast charging of at least 50 busses or heavy-duty vehicles with the charging power of between 1-4 MW per vehicle. The task will establish new connection points to the 110 kV/20kV/0.4 kV network for guaranteed fast charging of commercial vehicles, with the possibility of expanding to private stations, ensuring the optimal use of local energy sources, established and used micro resilient grid schemes in connection with chargers.

Cross sector integration on the field of mobility and heating in this project represents a rarely seen example of smart technology implementation into the power system. Today, gasoline stations are typically located in areas where stronger grid connections have not been planned. This goes especially for highways, where connections at current gas stations are far too weak to handle mass fast-charging once this type of e-vehicles will be widespread (estimated around 2030) but it is also expected that heavy-duty and fast-charging stations will increase deployment of electric cars in Slovenia.





Poster Presentation: The Impact of the Connection of Renewable Resources in the Distribution Network - The Case of Hydro Power Plants in Kosovo

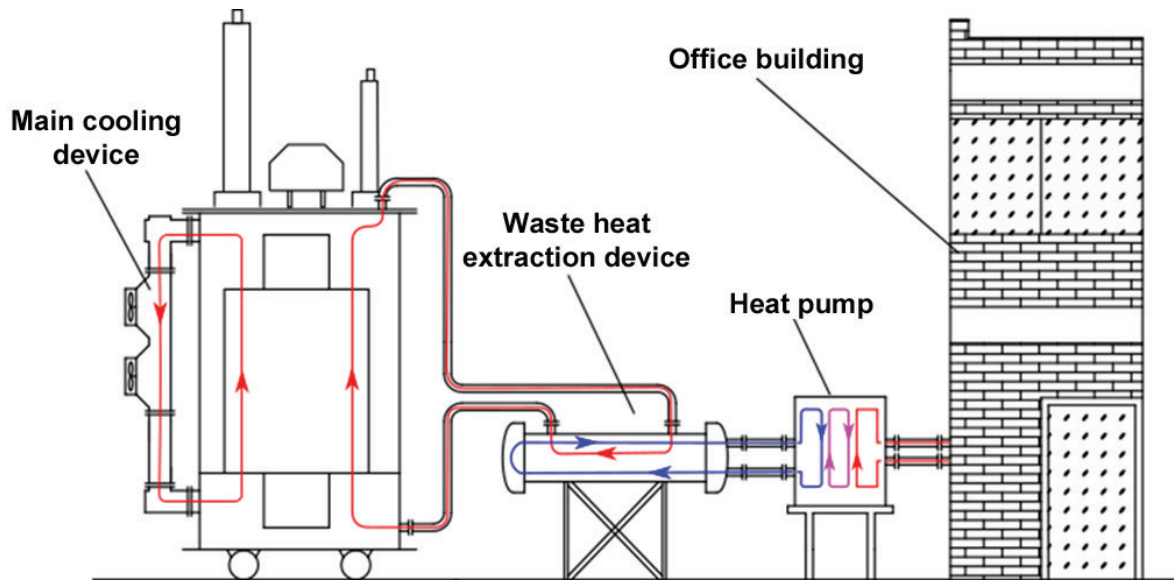


Figure 7: Waste heat extraction from substation transformers

At the end, fourth WP [1,2] is devoted to increasing efficiency of the distribution network, security of supply, cross-border and capacity for RES in AT, HR and SI. This WP refers to DSOs involved in the project: Elektro Ljubljana, Elektro Gorenjska, Elektro Celje, HEP Operator distribucijskog sustava and KNG-Kärnten Netz.

DSOs are facing the challenge of not being able to keep up with the grid upgrades to follow all the connections of new loads and distributed generation. New, smart functionalities are commonly seen as the only way out for a timely and sufficient increase of the hosting capacity of the existing grid and improving the security and quality of supply while reducing the need for costly and lengthy investments in primary equipment. Briefly, DSO activities consist of:

- Automation and upgrading of seven primary HV/MV stations 2 in AT, 2 in SI and 3 in HR;
- Automation of MV/LV secondary stations: 60 in AT and 331 in SI;
- Upgrade of ADMS in AT and SI;
- Installation of HTLS conductors on MV OHLs in HR (approximately 12 km);
- Modernization of ICT networks: - 70 km of optical cables in AT, 15 km of optical cables in SI - 219 network nodes, 11,000 meters/modems, 3 base stations and 3,192 meters in SI;
- Closing of MV loops: 150 km in AT and 204 km in SI;
- Interconnections: 1 new and 1 upgraded MV reserve line between SI and AT;
- Installation of 4 MV shunt reactors in HR.

To balance reactive power that is generated in the long MV cable systems, as the result of the capacitance between the ground and the line itself, HEP-ODS is planning to install shunt reactors in the four primary and secondary substations.

The project activity also consists of building new and upgrading existing secondary substations (MV/LV) with automatization and control equipment on various locations in Carinthia (Austria) and Slovenia. These improvements in the distribution networks are the integral parts of successful operation and implementation of an advanced distribution management system (ADMS) and therefore contribute to increasing the security of supply.

## 6. WIDER PROJECT IMPACT

Results and outcomes of this regional and multi-sectoral project offers large benefits and other positive externalities to the improvement of EU market liquidity and power system resilience, macro-regional operational security and technological innovation with replication potential.



**Poster Presentation:** The Impact of the Connection of Renewable Resources in the Distribution Network - The Case of Hydro Power Plants in Kosovo

The GreenSwitch project contributes to the regional coordination and serves as an example of good cooperation between neighbouring countries. This project delivers synergetic technology building blocks which meet general research and innovation specifications under EU umbrella. It has the potential for replication of the deployed solutions through the system operators of other SEE and CEE countries with similar challenges.

This project also contributes to achieving the goals and objectives of the Paris Agreement as well as the 2030 climate and energy targets and EU long-term decarbonisation objective. It also fits in the European Green Deal that has further emphasized the key enabling role of energy infrastructure in the transition to a climate neutral economy. Investments in the scope of the GreenSwitch project are aligned with goals of the EU that the market should remove existing barriers to cross-border trade and encourage investments into supporting infrastructure, for example, more flexible generation, interconnection, and demand response.

At the end the GreenSwitch project fits into the REPowerEU Plan through its support and contribution to the acceleration of the diversification of energy supplies and the roll-out of renewable energy, which are needed to replace fossil fuels in homes, industry and power generation.

## 7. CONCLUSION

Nowadays, network users are facing electricity cost increase due to higher RES integration costs and unstable market prices. In case that such project costs are going to be fully covered through the national network tariffs, network users would be overexposed to high network costs, decreasing overall socio-economic welfare. Combined with actual extremely high electricity market prices, this would become additional pressure on the final electricity price. Considering that regulatory authorities tend to avoid a large increase in transmission and distribution fees, it was found that additional funds are needed to realize such project and make it financially sustainable.

At the end of 2021, the project was listed on the 5<sup>th</sup> PCI list in the field of smart grids. The project was, therefore, eligible to apply for funds through the EU funding instrument Connecting Europe Facility, and the consortium prepared the proposal.

In the evaluation process, the European Commission assessed that GreenSwitch would significantly contribute to solving the challenges associated with the green transition and granted the consortium 50% co-funding of the investment.

At the end, the project consortium and the CINEA - European Climate, Infrastructure and Environment Executive Agency signed the grant agreement for the GreenSwitch project under the #cefenergy programme.

The GreenSwitch project will enable faster green transition of the energy sector, better integration of renewable energy sources and more efficient use of the existing energy infrastructure.

## BIBLIOGRAPHY

- [1] GreenSwitch - Project of Common Interest Business Plan, EIHP, 2022
- [2] <https://www.greenswitchproject.eu/>
- [3] Regulation (EU) No 347/2013 Of The European Parliament And Of The Council, 2013
- [4] Regulation (EU) 2022/869 Of The European Parliament And Of The Council, 2022
- [5] Commission Delegated Regulation (EU) 2022/564 of 19 November 2021 amending Regulation (EU) No 347/2013 of the European Parliament and of the Council as regards the Union list of projects of common interest
- [6] <https://wayback.archive-it.org/12090/20221207150821/https://ec.europa.eu/inea/connecting-europe-facility/cef-energy>
- [7] GreenSwitch - Project of Common Interest, Cost Benefit Analysis, EIHP, 2022
- [8] <https://www.smart-energy.com/regional-news/europe-uk/greenswitch-smart-grid-project-to-receive-e73-million/>



# The Caterpillar and the Butterfly the Experience of Italian Engineering

M. CELOZZI, R. GOMEZ, R. RENDINA, G. SANTAGOSTINO, G. SARACENO, G. SIMIOLI

TEN – TransMed Engineering Network

Italia

## SUMMARY

“The caterpillar and the butterfly” is a fairy tale for children with morals for adults [1], which induces to build the future without ever giving up.

For start, we recall Henry Kissinger’s advice: “Identify where you are. Pitilessly.”

The global energy crisis, triggered by the invasion of Ukraine and Chinese threats, has given a strong impetus to the transition of Western countries towards sustainable development models, not only from an environmental, but also social, industrial and geopolitical point of view.

### Nothing will be as before.

This document is developed along four lines:

1. Grids development
2. The European energy context
3. Technological challenges
4. The Hypergrid project

The answer to the crisis is the replacement of fossil energy sources with renewable sources to produce electricity, so it is necessary to “electrify” energy consumption using new technologies, such as hybrid systems in direct current and alternating current, where Italy has significant experience, integrating electrotechnical, electronic, environmental and mechanical engineering skills, with an impact on the organization of engineering activities.

The development of the new **power generation park is the driver of the grids design**, for:

- **the increasing the distance between the new renewable generation centers and the consumption centers**, so that the transmission network (bulk-transmission) resumes its original role as **enabling platform** for the **new energy market and the use of remote energy sources**,
- **the electricity consumption growth**, notably distributed (residential, transport), **still in an initial stage** due to the difficulties of developing distribution networks, infrastructures and energy end-use devices (like e-vehicles, heat pumps, induction hobs).

To respond to this evolution, the Hypergrid Project is born, developed by the **Grid Planning Department** of **TERNA** (the Italian electricity TSO-Transmission System Operator) with expertise, vision of future scenarios and synthesis of design choices, combining innovation and development. A project of Euro-Mediterranean significance, involving all Italian engineering.

**Doubling renewable production by 2030**, with an increase of 70 GW compared to 32 GW installed in Italy in 2019, is an **epochal challenge**, requiring **specific design skills**, technological, organizational, regulatory, market and industrial policy.

The **North Sea and the Mediterranean Projects will be the two pillars** of the new European energy system, **to enhance the opportunities of the Sea through a flexible, transnational and intersectoral** approach and with the **Italian experience** contribution.



### ACKNOWLEDGEMENTS

The authors are grateful to Enrico **Enrico Maria Carlini**, Terna's Director of Network Planning, **Giuseppe Tomassetti**, Vice President of FIRE - Italian Federation for the Rational Use of Energy, and **Domenico Villacci**, Director of the EnSiEL Consortium for their valuable contributions to the discussion in the preparation of this report.

### Lo sviluppo delle reti

As a first step, we try to follow Henry Kissinger's advice: "Identify where you are. Pitilessly." [2]

The international energy context moves towards decarbonization scenarios in which **electricity will play a key role**.

In electrical engineering, the HVDC (High Voltage Direct Current) is a system for the transmission of electricity in direct current, instead of in alternate current.

The development of **electricity grids** is based on new **transmission** technologies and, above all, their availability in the times that separate us from the target 2030 (65% of renewable electricity production) and 2050, planning the objectives according to the order of priority.

The **priority objectives** concern **flexibility and control of "transmission", a scarce and critical resource at global level**. [3]

The **vision** of the future scenarios drives the selection of the reference scenario and the related **enabling technologies (Strategy)** to schedule the investments (**Planning**).

The development of the transmission network achieves the integration of **resources upstream** (generation park and interconnections) **and downstream** (distribution networks), reconciling the intermittent generation (wind and photovoltaic) with a flexible demand (interruptible supplies, self-consumption, mixed units of generation and consumption, energy communities), through storage technologies (hydroelectric and electrochemical, daily and seasonal) and appropriate logic of regulation and control of network parameters (voltage and frequency) compliant with operational security and the emergence of new (private) energy markets.

**Safety and sustainability** are the **drivers of development**, which must bridge the emerging gap between the expected duration of investment and technological obsolescence.

**International organizations have set climate targets for reducing the environmental impact of energy transformations** [4], and many countries have set minimum targets for electricity generation from renewable sources, as in Europe.

**The capacity and geographical distribution of the power-generating modules guide the planning of the future network, to continue to ensure the security and quality of service constraints**.

The main **technical constraint** is the **inertia of the** electrical system [5,6], which defines the sensitivity of the system, i.e. the magnitude of electrical frequency variations in the face of network disturbances [7].

The lower the **inertia of the system**, the faster the **perturbations propagate**.

Large **interconnected electrical systems** generally have high inertia, so large frequency deviations from the nominal value are rare and limited. Frequency deviations in **small isolated** electrical systems, or weakly connected to larger systems, tend to produce **oscillatory phenomena** that can result in the interruption of the electrical service.

The increase in **synchronous generation** [8] in a generation park increases the inertial response of the system, but the vice versa does not apply with the increase of generators powered by renewable sources, having different **electromechanical characteristics**: the replacement of synchronous generation with solar and wind generation can degrade **the inertial response of the system**, with a consequent increase in the speed of variation and greater frequency excursions, due to the **reduced ability of the system to react to disturbances**.

In small isolated systems, such as Sardinia or some countries on the southern shore of the Mediterranean, these phenomena are worrying due to the low inertia of the system, due to the low level of interconnection and mesh of the network; this forces TSOs to modify their frequency and voltage control strategies, to increase the penetration of generation from renewable sources [9].

Network constraints depend on **the structural characteristics and generation mix of the system**.



### The European energy context

The global energy system is undergoing an unprecedented transition in **Europe** aimed at achieving the sustainability goals of the **Green Deal**, the shared holistic view of the energy system evolution.

The key element of the Green Deal is the “decarbonization” of the energy sector **by 2050** [10], with the **doubling of electricity consumption, the distributed generation and the digitalization of processes**, which change the **energy flows between the different voltage levels**.

The **renewal of the electricity generation park** is already underway, with the partial replacement of **fossil fuel and nuclear generation** with plants powered by renewable sources or more efficient gas-fired power plants, generally installed in **different locations than the replaced plants**.

In Europe increasing production from renewable sources has been under way for decades, but a strong acceleration is necessary to achieve the 2050 targets.

**Solar PV and wind are the cornerstones of the European REPowerEU energy plan** [11], a €300 billion plan based on the **Green Deal** (grants and loans), introduced by the EU in May 2022 to eliminate imports of fossil fuels from Russia by 2030.

#### Photovoltaic – European goal doubling production by 2025 and increasing capacity by 600 GW by 2050

The development potential from PV is enormous, but it involves a high consumption of land (about 1 hectare for each MW installed), so it is foreseeable a development of the PV generation installed on the roofs, considering the high European population density [12,13].

At the same time, distributed generation systems and electrochemical storage will spread. (BESS [14]), now available for **utility scale** applications, integrated with gas-fired combined cycle plants, to build quick-response backup units [15], and **small size** (energy communities, electric vehicle fleets).

The growing economic competitiveness of PV plants will boost investment in the coming years.

According to the IEA [16], in 2021 **PV production increased to a record level (179 TWh, plus 22% compared to 2020), exceeding 1,000 TWh: the second largest absolute growth after wind**.

Solar PV power generation in the Net Zero Scenario, 2010-2030

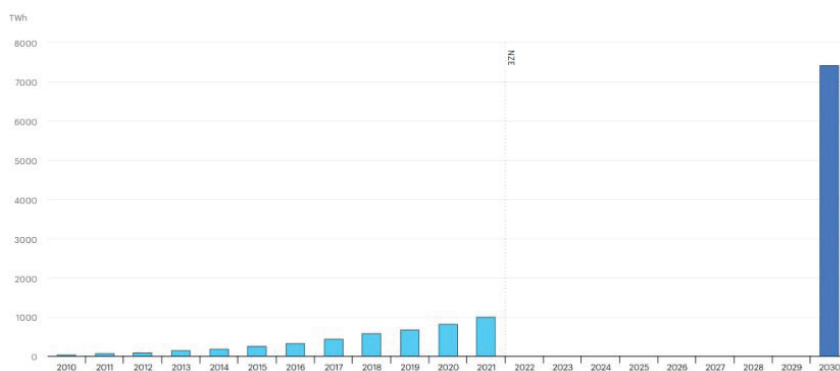


Figure 1 Energia elettrica prodotta da PV a livello globale (fonte IEA 2022)-

Photovoltaic production has continued to grow, despite the **pandemic** (reduction in exports of Chinese components to Western countries) and **increases in raw material prices**, and in 2021 a **record annual increase in generation capacity** was achieved (almost 190 GW). However, to be in line with the Net Zero scenario, annual PV generation in 2030 is expected to reach around 7,400 TWh, continuing to grow at a rate similar to the average annual increase over the past five years.

In the past two years, higher fuel and electricity prices have made **distributed PV** an attractive alternative to consumers.

The **generation “utility-scale”** [17] remains the most competitive form of PV power generation, but the construction of large power plants is hampered by the lack of suitable sites (land consumption, impact on the landscape).

To achieve the objectives of the Net Zero scenario, an annual increase of solar PV capacity of about 600 GW/y from now to 2030 at a global level would be necessary.



Poster Presentation: The Caterpillar and the Butterfly the Experience of Italian Engineering

The shares of the **two development models** (distributed production and utility scale) will depend on the characteristics of each country (orography, latitude, incentives, industrial development, licensing processes).

As far as technology is concerned, polycrystalline silicon remains the dominant technology for photovoltaic modules, with a market share of over 95%. The transition to monocrystalline silicon (wafer) layers accelerated growth in 2021 and increased the efficiency of cell application (PERC [18]) is rapidly expanding, with a market share expected over the next few years of almost 75%. The new cells even more efficient (come TOPCon [19]) have experienced an expansion of about 20% of the market in 2021 alone.

Distributed **generation systems** play an increasingly important role in the growth of PV electricity generation.

In 2021, “utility-scale” PV plants accounted for over 50% of the global increase in production capacity, followed by small-scale plants in the residential (28%) and commercial and industrial (19%) sectors. On the contrary, the increase in the capacity of utility-scale plants was reduced in 2021. However, to reach the Net Zero (Zero Net CO2 Emissions) target by 2050, an average annual PV generation growth of 25% per year would be needed in the 2022-2030 period, which requires a more ambitious industrial policy for the management of the intermittence of renewable generation, the integration in the electricity grid, the reduction of licensing and regulatory obstacles, the increased security of supply of critical raw materials and industrial production of PV modules and components for basic electronics (chips). This is especially true in emerging and developing countries, whose latitudes are more productive than solar power plants.

### Wind - European target 300 GW of offshore wind by 2050

The offshore wind generation will play a decisive role in Northern Europe, where the low depths and the prevailing constant winds ensure competitive costs and high factors of use (order of 4,000 h/y of operation at equivalent power), greater social acceptability compared to onshore wind, while having a significant impact on existing networks and regulatory systems [20].

The **EU's offshore wind development goal** is to integrate **300 GW** of capacity into the energy system **by 2050**, but there are detailed estimates of a potential for offshore wind in the North Sea of **between 500 and 700 GW**.

The **magnitude of this target** implies new challenges for the European electricity system, including a review of the **electricity market model**. We can no longer ignore the different structural characteristics of the new market, where the remuneration comes more from services than from energy, far from the assumptions of the old model. The regulatory frameworks developed for onshore applications will have to consider the integration of the **largest offshore wind power park**, the deep renewal of the energy system with a **structural change** in the supply and demand of electricity, i.e., a new market model [21].

### Renewables and Grid Development

European projects for the development of renewable sources are developed along two main lines, **wind and photovoltaic**, respectively in the North and South of Europe. They are projects with a **strong impact on the transmission** infrastructure, which must evolve simultaneously with the development of the generation park.

#### The North Sea project.

The experience gained with the **North Sea Project (NSWPH -North Sea Wind Power Hub)** will be important for the development of the entire European energy system and the Mediterranean Project: the two cornerstones of the new European energy system.

So far, offshore applications in the North Sea have mainly concentrated on “**single use**” (or dedicated) **solutions**, with radial connections from offshore wind farms (OWF) to interconnected market areas. In the future, these solutions will still exist, but **multiterminal architecture systems** will grow, connecting **offshore installations to market areas**, more than to individual countries, integrating onshore and offshore generation resources (“hybrid offshore”).

**Multipurpose solutions**, which include intersectoral generation parks (gas and electricity), and in the future could also include Power-to-X offshore installations, to convert electricity into other energy carriers, to allow **storage and use** even in sectors where it is more difficult to use electricity directly, using renewable energy products (hydrogen, ammonia, liquid and gaseous synthetic fuels, chemicals) to replace fossil fuels in areas where this is not yet possible.

Northern Europe, having large offshore wind resources [22], has promoted and integrated the development of these projects, with a first organizational model (**Consortium Development**) that can be usefully reproduced even in the Mediterranean.





Poster Presentation: The Caterpillar and the Butterfly the Experience of Italian Engineering

The aim is to set up a **coordination framework of initiatives** from all Northern European countries to activate the enormous potential of **offshore wind power in the North Sea**. The initial program provides 180 GW of installed power by 2050. A transnational, cross-sectoral and integrated “hub- and-spokes” approach represents a radical change from previous, predominantly national and disjointed projects.

NSWPH integrates offshore and onshore wind generation into continental interconnected transportation systems, to implement **flexible, long-term, supranational programmes for the development of projects of common interest**.

A new perspective which exploits the **opportunities of the Sea**: multilateral international co- operation enables the development of trans-sectoral gas and electricity projects, which are essential for the implementation of large-scale projects.

### The “hub-and-spokes” architecture

The NSWPH project consists of the **transition from “near shore” connections** (proximity, AC radial) to **offshore connections** (DC multi-terminal).

Traditionally, separate electric connections have been used to **connect wind farms to individual countries and then connect countries**. In the new project, the **multi-terminal electrical connections connect the wind farms** (onshore and offshore) with **market areas** that can include multiple countries, **by integrating generation and transmission functions**.

The “hub-and-spokes” model is a structured scheme with a core (hub) and peripheral components connected to it (radii), applied in the most disparate domains (aeronautics, information technology, medicine).

In the case of wind power, the hub is the offshore wind farm, with radial connections to various interconnected market areas.

The hub can be **physical, virtual** (with a centralized multi-center structure), **hybrid** (combined offshore and onshore wind connections) or **multi-terminal** (linking multiple platforms and/or market areas).

To develop the project, the NSWPH Consortium was set up to coordinate research and development activities, foster the interaction of all stakeholders (public and private) and enhance the experience gained in previous projects. The three **Consortium Partners** are the companies interested in building the hub, namely **Gasunie** (the gas TSO in the Netherlands and part of northern Germany), **TenneT** (the electricity TSO in the Netherlands and part of northern Germany), **Energinet** (the gas and electricity TSO in Denmark).

The Consortium consists of **four task forces**:

1. **MARKET AND REGULATION** (coordinated by **Energinet**) for defining the **market model**, with a **supranational approach to market zones connected to the hub**.
2. **STAKEHOLDER MANAGEMENT AND COMMUNICATION** (coordinated by **TenneT**) for sharing **key project assumptions between key stakeholders**, including **developers, TSOs, policy institutions and regulators**.
3. **ENERGY SYSTEMS** (coordinated by **Gasunie**) for defining the **design criteria for the infrastructures** to be built and **mapping the energy flows** between the production islands and the market areas.
4. **TECHNICAL CONCEPTS** (coordinated by **TenneT**), for (i) defining the **terms of references of the main elements of the system** and (ii) verifying the **technological feasibility of the possible development scenarios, to pave the way for the first pilot project**. Activities include **pre-FEED engineering analysis** (preliminary Front-End Engineering Design).

### Technological challenges

Electricity networks play a strategic role in the **security** (supply chains) and **sustainability** (penetration of renewables) of Europe’s new energy system.

Emerging technologies, in addition to **active power** generation, allow solar systems to generate **reactive power**, contributing to the security and stability of operation of the networks (frequency and voltage regulation and response times to perturbations).

The **new hardware and software technologies** for the management of the inverters (“grid- converter”), that connect renewable power plants to the grid, are already applied in the European, North American and Australian networks, and technological innovation will be essential to improve their competitiveness. [23]



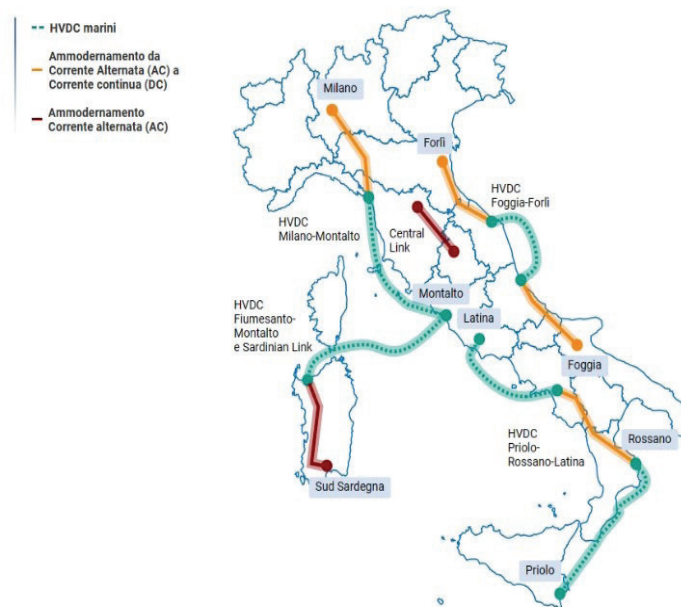
## DC technology is at the core of tomorrow's changing energy systems.

The achievement of the objectives of European energy policy requires the **integration of PV and wind production in the electricity system**, for which the **technology of DC is enabling**, in symbiosis with existing networks and devices in AC.

**Terna's Hypergrid project** summarizes and integrates a development story initiated by ENEL, in the constant search for efficiency, security and innovation that drives the progress of the entire Italian electricity sector, and Italian engineering companies have integrated engineering skills [24] that are the advanced know-how of the energy transition.

## The Hypergrid project

The new **Terna Development Plan** covers the whole spectrum of opportunities offered by technological innovation in the electricity sector and outlines the lines of **energy system development**, in complementarity with the **SNAM Development Plan** (the Italian Gas TSO), will allow Italy to **enhance its strategic geographical position**, to realize a **Mediterranean Project** and to strengthen its **role as energy hub of Europe in the Mediterranean**, intersectoral and supranational. The **Mediterranean Project** is the southern frontier of Europe, as the **North Sea Project** is the northern frontier.



The **Hypergrid network is a direct current system that links and integrates all other development projects**, already planned or underway, either national or international.

### The national dimension includes:

- the **Tyrrhenian Link**, HVDC connection of about 970 kilometers long and 1000 MW capacity, which is the essential infrastructure to strengthen the exchange capacity **between Southern Italy**, where the availability of solar and wind is greater, **and Northern Italy**, where most of the domestic electricity consumption is located. The total plan previews **two branches**: EAST (Sicily - Peninsula) and WEST (Sicily - Sardinia).
- the **Adriatic Link**, a 250 km power line consisting of **two submarine cables** which will connect Abruzzo to the Marche region. The work will allow an increase of about **1,000 MW of exchange capacity** between the **two most critical Italian market zones**, Central- South and Central-North, with positive effects of competitiveness and reduction of electricity costs.
- the Hypergrid system**, which includes five new DC backbones, which allow **to double the internal transport capacity** along the South - North direction of the Italian electricity system, **from the current 16 GW to over 30 GW**.



### The international dimension includes:

- In the **North**, **three new power lines** (Italy-France, Italy-Switzerland and Italy-Austria) to reinforce transmission capacity along the northern electricity frontier **for optimum integration of the European electricity market**.



Poster Presentation: The Caterpillar and the Butterfly the Experience of Italian Engineering

- In the **South**, enhancing **Mediterranean interconnections**:
- **eastward**, doubling the transmission capacity of the **Italy-Greece (+500 MW)** and **Italy - Montenegro (+600 MW)** interconnectors.
- **southwards**, with the **EIMed Project**, 600 MW electricity connection between Italy and Tunisia, opening the **North Africa - Europe electricity corridor** and **enabling the Euro- Mediterranean integration of electricity systems throughout the Maghreb**. Confirming the importance of the link, the project was included in the list of **European "Projects of Common Interest" (PCI)** and, in December 2022, received funding from the **"Connecting European Facility" (CEF)** which manages the European Fund for the Development of Community Energy Infrastructure.

### The technologies

The **Hypergrid project** exploits **all the opportunities offered by new technologies** to **increase transport capacity, reduce environmental impact** (electromagnetic pollution, impact on the territory and land consumption, reuse existing assets and decommissioning sites) and **increase energy efficiency** (lower investment costs and network losses compared to the AC solution).

The Hypergrid architecture is strongly **innovative** for the **high level of integration of multi- terminal systems in DC and AC**, thanks to the installation of **switches in direct current (DCCB)** in all conversion stations that allow **meshing of the network into DC and interoperability with the AC network**.

For a long time, first in ENEL and then in Terna, **a backbone in DC reinforcement of the South North of the Italian network** had been suggested: today Terna has collected, relaunched and updated all the ideas of recent years. The result: **a visionary and revolutionary design of the new network**, with international resonance.

### DC and AC power lines

The integration of **HVDC** (very high voltage direct current) and **HVAC** (very high voltage alternate current) plants required the **forecast analysis** of power flows on the network, with the development of models of the different components in different operating configurations, and software for network and market simulations, which allowed **to manage the complexity of the choices**, according to the pre-set standards of security and robustness of the transmission network.

A network structure among the most advanced in the world, if not the most advanced.

The feasibility needs of the project (time and costs), imposed by the European objectives, led to the choice of **converting existing AC lines into DC lines**, an intuition transformed into a successful project, especially in a "long" electricity system like the Italian one, poorly meshed because of the orography from the Apennines, and in which consumption is concentrated in the North of the country and renewable resources are largely located in the South and in the Islands, where the availability of primary energy is greater and the constraints imposed by the population density and territorial vocations are lesser.

The use of DC technology allows **to convey, address and control the energy flows on the network**, as well as manage events that can cause the propagation of disturbances on interconnected networks: in this sense the direct current **"connects by separating"**, because it allows to connect different systems, avoiding risks to the stability of connected systems.

The **length of the lines in direct current** (over **2500 km** between **overhead and submarine power lines**), connected in an innovative way (**multiterminal and ring links**), represent a very challenging goal, but compliant with the Italian experience.

### AC power lines- transmission towers for so called "five-phase" lines.

The **correlation between electric and magnetic fields at very low frequency** (ELF - Extremely Low Frequency) and **human health** is one of the most critical issues of the social acceptability of power lines, with a negative impact on network planning and penetration of renewable sources.

Terna has developed a new generation of towers, so-called **"5 Phase"** (picture on the left), able to reduce the electromagnetic fields of power lines, thanks to the optimized spatial arrangement of conductors, which are 5 and no longer 3, applicable for transmission (400 kV) and sub-transmission lines (150 kV).





### Other instruments to assist the development of renewable sources.

In 2022, Terna conducted a preliminary study to evaluate the areas available in Italy for the installation of new onshore wind and solar power plants. This analysis shows that about 80% of RES connection requests in VHV/HV fall completely or partially in areas **not subject to regulatory constraints**.

On top of that, Terna has developed a navigation portal [25] that allows stakeholders and operators to view information on the geographical location and authorization status of new photovoltaic and wind, onshore and offshore, in Italy. A **digital platform** essential for the **coordinated development** of networks, renewable and storage facilities, and for **planning new infrastructures** in the most suitable areas to host them.

### Findings

The Hypergrid project is a successful overall project, not only of Terna but of the entire Italian system, to achieve **national and regional objectives of common interest** for the **integration of Euro- Mediterranean energy systems**.

The **transition** to sustainable development models implies a **profound change**, from production processes to the lifestyles of citizens, which is achieved in medium-long times.

**A transition to be planned**, from the **vision** of the development model to be aimed at, to the reference energy scenario (**Strategic Plan**) in which to frame projects (**National Recovery and Resilience Plan**), with objectives that interact functionally and temporally, which should be **updated as the global and European context evolves**.

The **vision**, shared at European level with the Green Deal, must be **expressed in a way that is consistent with the energy and economic systems of the various countries**, in order of priority:

- **in the short term (2030)**, using **proven** (photovoltaic and wind) **technologies that are commercially available** [26]
- **in the medium term (2040)**, applying technologies currently in the R&D phase, such as hydrogen [27], with a certain amount of accuracy to manage uncertainties (risk allocation) [28]
- **long-term (2050)**, such as **Nuclear Fusion**, with objectives defined with **easy scheduling and updating**, based on the progress of the activities, for the greater uncertainties they present, in terms of time, cost and performance.

The **North Sea Project** and the **Mediterranean Project** are the two cornerstones of the new **European energy system**, which enhances the opportunities of the Sea with a **flexible, transnational and intersectoral approach**, in which Italy has the experience to contribute in industrial, technological, organizational and institutional terms.

### BIBLIOGRAPHY

- [1] The fable tells of the caterpillar that dreamed of flying and eventually turned into a butterfly, because, with commitment and courage, no mountain is too high to climb. <https://leggimiancora.altervista.org/storia-un-bruco-voleva-scalare-montagna/>
- [2] The Economist - 17 maggio 2023 - "Henry Kissinger explains how to avoid world war three". [https://www.economist.com/briefing/2023/05/17/henry-kissinger-explains-how-to-avoid-world-war-three?utm\\_campaign=r.the-economist-this-week&utm\\_medium=email.internal-newsletter.np&utm\\_source=salesforce-marketing-cloud&utm\\_term=20230519&utm\\_content=ed-picks-article-link-2&etear=nl\\_weekly\\_2&utm\\_campaign=r.the-economist-this-week&utm\\_medium=email.internal-newsletter.np&utm\\_source=salesforce-marketing-cloud&utm\\_term=5/19/2023&utm\\_id=1602490](https://www.economist.com/briefing/2023/05/17/henry-kissinger-explains-how-to-avoid-world-war-three?utm_campaign=r.the-economist-this-week&utm_medium=email.internal-newsletter.np&utm_source=salesforce-marketing-cloud&utm_term=20230519&utm_content=ed-picks-article-link-2&etear=nl_weekly_2&utm_campaign=r.the-economist-this-week&utm_medium=email.internal-newsletter.np&utm_source=salesforce-marketing-cloud&utm_term=5/19/2023&utm_id=1602490)
- [3] In Western Europe and the USA, not to mention countries with high economic growth rates, where transmission infrastructure is enabling social and economic development.
- [4] Limits to the production of carbon dioxide (CO<sub>2</sub>), taken as an indicator of sustainability.
- [5] ENTSO E - Frequency Stability Evaluation Criteria for the Synchronous Zone of Continental Europe - file:///C:/Users/MichelangeloCelozzi/AppData/Local/Temp/MicrosoftEdgeDownloads/a4d2a016-377e-4a38-abd4-e57a985a29f6/RGCE\_SPD\_frequency\_stability\_criteria\_v10.pdf
- [6] NREL Technical Report /TP-6A20-73856 - May 2020- Inertia and the Power Grid: A Guide Without the Spin - <https://www.nrel.gov/news/program/2020/inertia-and-the-power-grid-a-guide-without-the-spin.html#.ZF-rXa8b500.mailto>
- [7] Due to imbalances in demand - power supply on the grid or outages, such as loss of grid elements for disconnection of power lines or power plants.
- [8] The synchronous generator or alternator is an electrical machine that converts the mechanical power of a primary motor to electrical power in alternating current at a certain voltage and frequency.
- [9] For example, Ireland has a low level of interconnection and a rapid increase in wind generation, so it has had to change the transmission and distribution system codes for wind energy. The main risks concern the specific requirements for frequency, voltage and fault recovery, being a small system, with a peak load of the order of 6100 MW, with relatively low inertia. In England, the TSO National Grid has developed an innovative system for real-time estimation of network inertia.



Poster Presentation: The Caterpillar and the Butterfly the Experience of Italian Engineering

- [10] **Source IEA- International Energy Agency.** Global electricity demand increases by 5,900 terawatt hours (TWh) under the declared policy scenario and by over 7,000 TWh under the pledged scenario by 2030. In emerging markets and developing economies, population growth and growing cooling demand contribute to increased electricity demand. Electricity represents an increasingly large proportion of final energy consumption in all economies. Global electricity demand in 2050 will be more than 75% higher than today in the declared policy scenario and 150% in the Net Zero Emissions by 2050 (NZE) scenario. <https://www.iea.org/reports/world-energy-outlook-2022/outlook-for-electricity>
- [11] <https://www.pmi.it/economia/green-economy/384905/repowereu-fondi-e-incentivi-per-la-svolta-green.html#un-piano-per-il-fotovoltaico>
- [12] "Integration of Utility Distributed Energy Resource Management System and Aggregators for Evolving Distribution System Operators" – by Luka Strezoski, Member, Harsha Padullaparti, Fei Ding, Murali Baggu - JOURNAL OF MODERN POWER SYSTEMS AND CLEAN ENERGY, VOL. 10, NO. 2, March 2022
- [13] Federated Architecture for Secure and Transactive Distributed Energy Resource Management - Solutions (FAST-DERMS) System Architecture and Reference Implementation - January 2022 <https://www.nrel.gov/docs/fy22osti/81566.pdf>
- [14] Battery Electricity Storage System
- [15] Fast-reserve unit.
- [16] <https://www.iea.org/reports/solar-pv>
- [17] Size greater than 1 MW, generally installed on the ground, that supplies the grid with energy, paid for by power purchase agreement.
- [18] **PERC** (Passivated Emitter and Rear Cell) technology is a type of cell structure that contains the silicon layer, which is very different from that used in the last 30 years.
- [19] The **TOPCon** technology is the new generation of PERC and, like its predecessor, can be added to traditionally produced cells; it involves the addition of an ultra-thin layer of silicon dioxide (SiO<sub>2</sub>) and a layer of polycrystalline silicon doped with phosphorus. Compared to PERC, it doesn't add big extra costs, it increases efficiency compared to just over 22%, even if it doesn't reach the levels of the most advanced technologies (which can reach 27%, like HJT cell technology).
- [20] Investigating Power System Primary and Secondary Reserve Interaction under High Wind Power Penetration - Yingchen Zhang, Jin Tan, Ibrahim Krad, Rui Yang, and Vahan Gevorgian - National Renewable Energy Laboratory - Erik Ela Electric Power Research Institute - <https://www.nrel.gov/docs/fy17osti/64637.pdf>
- [21] The market rules based on the Sistem Marginal Price, with the role of price maker played by gas and with modest penetration of renewable sources will inevitably be reviewed, evaluating, in the light of recent and ongoing experience, decoupling of markets and a more innovative market model of services rather than energy raw materials. The concept of the energy market as a commodity market is waning.
- [22] ENTSO-E Position on Offshore Development - [https://eepublicdownloads.azureedge.net/clean-documents/Publications/Position%20papers%20and%20reports/2021/entso-e\\_pp\\_Offshore\\_Development\\_01\\_200528.pdf](https://eepublicdownloads.azureedge.net/clean-documents/Publications/Position%20papers%20and%20reports/2021/entso-e_pp_Offshore_Development_01_200528.pdf)
- [23] The emerging technology in this field is represented by **SSSC devices** (synchronous static compensators in series) to regulate the power and energy flows on alternating current networks, which allow to maximize the use of existing lines..
- [24] Network Analysis, Feasibility Studies, Development Plans (power park, interconnections, networks), Plant Design (generation and storage units, transmission and distribution lines and stations, in AC, DC and hybrid AC-DC systems, grid converter control systems).
- [25] <https://www.terna.it/it/sistema-elettrico/rete/econnexion>
- [26] Availability of components and systems, design, construction and maintenance services, including "end-of-life" activities (decommissioning).
- [27] Source Agora – press communication May 4<sup>th</sup> 2023: Breaking free from fossil gas -A new path to a climate-neutral Europe. <https://www.agora-energiawende.de/en/publications/breaking-free-from-fossil-gas-1/>
- [28] Performance and completion risks involve regulatory, capital and market risks.





SCAN ME



# 4<sup>th</sup> SEERC CONFERENCE İSTANBUL

11-12  
OCTOBER 2023



[www.seercturkiye2023.com](http://www.seercturkiye2023.com)



<https://www.linkedin.com/company/cigre-seerc/>